

State-of-the-Art Reactor Consequence Analyses Project

Uncertainty Analysis of the Unmitigated Long-Term Station Blackout of the Peach Bottom Atomic Power Station

AVAILABILITY OF REFERENCE MATERIALS IN NRC PUBLICATIONS

NRC Reference Material

As of November 1999, you may electronically access NUREG-series publications and other NRC records at NRC's Library at www.nrc.gov/reading-rm.html. Publicly released records include, to name a few, NUREG-series publications; *Federal Register* notices; applicant, licensee, and vendor documents and correspondence; NRC correspondence and internal memoranda; bulletins and information notices; inspection and investigative reports; licensee event reports; and Commission papers and their attachments.

NRC publications in the NUREG series, NRC regulations, and Title 10, "Energy," in the *Code of Federal Regulations* may also be purchased from one of these two sources.

1. The Superintendent of Documents

U.S. Government Publishing Office
Mail Stop IDCC
Washington, DC 20402-0001
Internet: bookstore.gpo.gov
Telephone: (202) 512-1800
Fax: (202) 512-2104

2. The National Technical Information Service

5301 Shawnee Rd., Alexandria, VA 22312-0002
www.ntis.gov
1-800-553-6847 or, locally, (703) 605-6000

A single copy of each NRC draft report for comment is available free, to the extent of supply, upon written request as follows:

Address: U.S. Nuclear Regulatory Commission

Office of Administration
Publications Branch
Washington, DC 20555-0001
E-mail: distribution.resource@nrc.gov
Facsimile: (301) 415-2289

Some publications in the NUREG series that are posted at NRC's Web site address www.nrc.gov/reading-rm/doc-collections/nuregs are updated periodically and may differ from the last printed version. Although references to material found on a Web site bear the date the material was accessed, the material available on the date cited may subsequently be removed from the site.

Non-NRC Reference Material

Documents available from public and special technical libraries include all open literature items, such as books, journal articles, transactions, *Federal Register* notices, Federal and State legislation, and congressional reports. Such documents as theses, dissertations, foreign reports and translations, and non-NRC conference proceedings may be purchased from their sponsoring organization.

Copies of industry codes and standards used in a substantive manner in the NRC regulatory process are maintained at—

The NRC Technical Library

Two White Flint North
11545 Rockville Pike
Rockville, MD 20852-2738

These standards are available in the library for reference use by the public. Codes and standards are usually copyrighted and may be purchased from the originating organization or, if they are American National Standards, from—

American National Standards Institute

11 West 42nd Street
New York, NY 10036-8002
www.ansi.org
(212) 642-4900

Legally binding regulatory requirements are stated only in laws; NRC regulations; licenses, including technical specifications; or orders, not in NUREG-series publications. The views expressed in contractor-prepared publications in this series are not necessarily those of the NRC.

The NUREG series comprises (1) technical and administrative reports and books prepared by the staff (NUREG-XXXX) or agency contractors (NUREG/CR-XXXX), (2) proceedings of conferences (NUREG/CP-XXXX), (3) reports resulting from international agreements (NUREG/IA-XXXX), (4) brochures (NUREG/BR-XXXX), and (5) compilations of legal decisions and orders of the Commission and Atomic and Safety Licensing Boards and of Directors' decisions under Section 2.206 of NRC's regulations (NUREG-0750).

DISCLAIMER: This report was prepared as an account of work sponsored by an agency of the U.S. Government. Neither the U.S. Government nor any agency thereof, nor any employee, makes any warranty, expressed or implied, or assumes any legal liability or responsibility for any third party's use, or the results of such use, of any information, apparatus, product, or process disclosed in this publication, or represents that its use by such third party would not infringe privately owned rights.

State-of-the-Art Reactor Consequence Analyses Project

Uncertainty Analysis of the Unmitigated Long-Term Station Blackout of the Peach Bottom Atomic Power Station

Manuscript Completed: September 2015
Date Published: May 2016

Prepared by:
P. Mattie, R. Gauntt, K. Ross, N. Bixler, D. Osborn,
C. Sallaberry, and J. Jones

Sandia National Laboratories
Severe Accident Analysis Dept. 6232
Albuquerque, NM 87185-0748

T. Ghosh, NRC Technical Lead

NRC Job Code N6306

Office of Nuclear Regulatory Research

Sandia National Laboratories is a multi-program laboratory managed and operated by Sandia Corporation, a wholly owned subsidiary of Lockheed Martin Corporation, for the U.S. Department of Energy's National Nuclear Security Administration under contact DE-AC04-94AL85000.

ABSTRACT

This document describes the U.S. Nuclear Regulatory Commission's (NRC's) uncertainty analysis of the accident progression, radiological releases, and offsite consequences for the State-of-the-Art Reactor Consequence Analyses (SOARCA) unmitigated long-term station blackout (LTSBO) severe accident scenario at the Peach Bottom Atomic Power Station. The objective of the SOARCA Uncertainty Analysis is to evaluate the robustness of the SOARCA deterministic results and conclusions documented in NUREG-1935, and to develop insight into the overall sensitivity of the SOARCA results to uncertainty in key modeling inputs. As this is a first-of-a-kind analysis in its integrated look at uncertainties in the MELCOR accident progression and the MELCOR Accident Consequence Code System, Version 2 (MACCS) offsite consequence analyses, an additional objective is to demonstrate uncertainty analysis methodology that could be used in future source term, consequence, and Level 3 probabilistic risk assessment studies.

This work assessed key MELCOR and MACCS modeling uncertainties in an integrated fashion to quantify the relative importance of each uncertain input (included in the analysis) on potential accident consequences. A detailed uncertainty analysis was performed for a single-accident scenario at the Peach Bottom pilot plant. Not all possible uncertain input parameters were included in the analysis. Rather, a set of key parameters was carefully chosen to capture important influences on release and consequence results. 21 MELCOR parameters and 350 MACCS parameters (representing 20 parameter groups) were included in the integrated analysis. The uncertainty in these parameters was propagated to consequence results in a two-step Monte Carlo simulation with a total of 865 realizations. This quantitative uncertainty analysis provides measures of the effects for each of the selected uncertain parameters both individually and through interaction with other parameters, through the use of four regression methods. Phenomenological insights are also qualitatively described and corroborated through the analysis of individual Monte Carlo realizations that show different accident progression, release, and consequence behavior.

Sampling the chosen input parameters in this uncertainty analysis revealed three groupings of similar accident progression sequences within the Peach Bottom unmitigated LTSBO scenario: (1) early stochastic failure of the cycling safety-relief valve (SRV), which was the SOARCA estimate scenario in NUREG-1935; (2) thermal failure of the SRV without main steam line (MSL) creep rupture; and (3) thermal failure of the SRV with MSL creep rupture. Even with the sequences that could lead to higher source terms, the results corroborated the SOARCA results and conclusions in NUREG-1935; the projected consequences are still much smaller than previous studies (the 1982 Siting Study in particular) calculated, and the projected early fatality risk is essentially zero.

For the release magnitude (source term) and timing, the regression methods rank the SRV stochastic failure probability, chemical forms of cesium and iodine, station battery duration, SRV open area fraction (after thermal failure), and drywell liner melt-through area as the most important parameters. For the conditional, mean (average over weather variability), individual latent cancer fatality risk, the regression methods rank the MACCS dry deposition velocity, the MELCOR SRV stochastic failure probability, and the MACCS residual cancer risk factor as the most important input parameters.

FOREWORD

The U.S. Nuclear Regulatory Commission (NRC) initiated the State-of-the-Art Reactor Consequence Analyses (SOARCA) project to develop current realistic evaluations of the offsite radiological health consequences for potential severe reactor accidents for two pilot plants—the Peach Bottom Atomic Power Station, a boiling-water reactor (BWR) in Pennsylvania, and the Surry Power Station, a pressurized-water reactor in Virginia. The SOARCA project evaluated plant improvements and changes not reflected in earlier NRC publications from 1975-1990.

This report describes the NRC's first integrated uncertainty analysis (UA) for the SOARCA project that was directed by the NRC and conducted by Sandia National Laboratories. This UA evaluates the SOARCA unmitigated long-term station blackout (LTSBO) severe accident scenario for Peach Bottom. The analysis used the existing SOARCA models implemented in the MELCOR code for accident progression and release analysis, the MACCS code for offsite consequence analysis, and a representative set of important uncertain parameters. The UA used expert judgment supplemented with limited external peer review to select a set of parameters and to define distributions of values representing the state-of-knowledge for each parameter. The uncertainty in these parameters was then propagated to release and offsite radiological health consequence results (individual latent cancer fatality risk and individual early fatality risk) using a two-step Monte Carlo simulation process. The analysis used a variety of techniques to examine the results including regression analyses, study of select individual Monte Carlo samples, scatter plots, and supplemental separate sensitivity analyses. This UA corroborates the conclusions from the SOARCA study that (1) the public health consequences from severe nuclear accidents modeled are smaller than previously calculated; (2) delayed releases calculated provide more time for emergency response actions such as evacuation and, hence, the long-term dominates health effect risks; and (3) negligible early fatality risk is projected.

The results and insights from this UA are expected to be useful for ongoing and future work such as informing the technical bases for post-Fukushima regulatory activities and the NRC's Site Level 3 Probabilistic Risk Assessment (PRA) project. This study adds to the body of knowledge created by earlier uncertainty analyses (such as those conducted in conjunction with NUREG-1150, "Severe Accident Risks: An Assessment for Five U.S. Nuclear Power Plants") as well as the SOARCA project through the generation of over 800 variations of how an LTSBO scenario may evolve in a BWR such as Peach Bottom. This study has already informed some NRC activities such as the projected spread of consequence results in the UA supporting SECY-12-0157, "Consideration of Additional Requirements for Containment Venting Systems for Boiling Water Reactors with Mark I and Mark II Containments," and SECY-15-0085, "Evaluations of the Containment Protection and Release Reduction for Mark I and Mark II Boiling Water Reactor Rulemaking Activities." Other envisioned uses of this work are to help identify key sources of model uncertainty (per NUREG-1855, "Guidance of the Treatment of Uncertainties Associated with PRAs in Risk-Informed Decision Making," guidance on treatment of uncertainty) for the Level 2 portion of PRA studies for BWR Mark I plants and the Level 3 portion of PRA studies for light-water reactors. The results also identify areas where improving our state-of-knowledge or our state-of-modeling capabilities could significantly reduce uncertainties in the accident scenario studied.

Examples of these results and insights are improving our knowledge of BWR safety-relief valve behavior under severe accident conditions and improving our knowledge and modeling of offsite radionuclide deposition velocities. This analysis also confirms the importance of using more advanced regression techniques, such as recursive partition analysis, for identifying important inputs (and their joint influences on outcomes) in complex uncertain systems.

TABLE OF CONTENTS

<u>Section</u>	<u>Page</u>
ABSTRACT	iii
FOREWORD.....	v
TABLE OF CONTENTS	vii
LIST OF FIGURES.....	xi
LIST OF TABLES	xxi
EXECUTIVE SUMMARY	xxvii
ACKNOWLEDGMENTS	xxxv
ACRONYMS	xxxvii
1. INTRODUCTION	1-1
1.1 Background of the SOARCA Project.....	1-1
1.2 SOARCA Comparison and Contrast with Fukushima Accidents.....	1-3
1.3 Objectives of the Uncertainty Analysis	1-7
1.4 Uncertainty Analysis Report Outline.....	1-10
2. UNCERTAINTY ANALYSIS APPROACH.....	2-1
2.1 Accident Scenario Selection.....	2-1
2.2 Selection of Uncertain Parameters.....	2-2
2.3 Treatment of Uncertainty.....	2-4
3. DESCRIPTION OF ANALYSES.....	3-1
3.1 Software Used.....	3-1
3.1.1 MELCOR	3-1
3.1.2 MELMACCS	3-1
3.1.3 MACCS	3-1
3.2 Code Integration.....	3-2
3.3 Probabilistic Model Calculation for Uncertainty Analysis.....	3-3
3.3.1 Source Term Uncertainty Calculations	3-3
3.3.2 Consequence Analysis Calculations.....	3-4
3.4 Uncertainty and Sensitivity Analysis.....	3-4
3.4.1 Uncertainty Analysis: Purpose and Results Generated.....	3-4
3.4.2 Sensitivity Analysis: Purpose and Results Generated.....	3-6
4. UNCERTAIN INPUT PARAMETERS AND DISTRIBUTIONS	4-1
4.1 Source Term Model Uncertainty (MELCOR Inputs)	4-1

4.1.1	Sequence Issues.....	4-2
4.1.2	In-Vessel Accident Progression Issues	4-6
4.1.3	Ex-Vessel Accident Progression Issues	4-19
4.1.4	Containment Behavior Issues.....	4-24
4.1.5	Chemical Forms of Iodine and Cesium.....	4-35
4.1.6	Aerosol Deposition	4-39
4.2	Consequence Model Uncertainty (MACCS Inputs)	4-45
4.2.1	Wet Deposition Model (CWASH1).....	4-46
4.2.2	Dry Deposition Velocities (VEDPOS)	4-48
4.2.3	Shielding Factors (CSFACT, GSHFAC, PROTIN).....	4-51
4.2.4	Early Health Effects (EFFACA, EFFACB, EFFTHR)	4-54
4.2.5	Latent Health Effects (GSHFAC, DDREFA, Inhalation Dose Coefficients, CFRISK)	4-57
4.2.6	Dispersion (CYSIGA, CZSIGA)	4-68
4.2.7	Hot Spot and Normal Relocation (DOSNRM, TIMNRM, DOSHOT, TIMHOT)	4-71
4.2.8	Evacuation Delay (DLTEVA)	4-74
4.2.9	Evacuation Speed (ESPEED)	4-77
4.3	Other Phenomena Considered.....	4-79
4.3.1	Source Term Model	4-80
4.3.2	Consequence Model.....	4-83
5.	STATISTICAL CONVERGENCE.....	5-1
5.1	Source Term Model (MELCOR)	5-1
5.1.1	Statistical Convergence Testing (Probabilistic Base Case)	5-1
5.2	Consequence Model	5-8
5.2.1	Statistical Convergence Testing - Probabilistic Base Case	5-8
6.	SOARCA MODEL PARAMETER UNCERTAINTY AND SENSITIVITY ANALYSES	6-1
6.1	Source Term Parameter Uncertainty Analysis	6-1
6.1.1	Fraction of Iodine Released to the Environment.....	6-2
6.1.2	Fraction of Cesium Released from the Core Inventory.....	6-11
6.1.3	Hydrogen Production.....	6-19
6.1.4	Analysis of Important Phenomena and Single Realizations	6-22
6.2	Offsite Consequence.....	6-55
6.2.1	Latent Cancer Fatality Risk	6-56

6.2.2	Early Fatality Risk.....	6-64
6.2.3	Regression Analysis.....	6-70
6.2.4	Analysis of Single Realizations.....	6-86
6.3	Summary of Phenomena Important to Uncertainty in Analysis Results ...	6-106
6.3.1	Source Term Analysis	6-106
6.3.2	Consequence Analysis.....	6-107
6.4	Separate Sensitivity Studies.....	6-109
6.4.1	Manual Control of the Safety Relief Valve (Operator Actions).....	6-109
6.4.2	Sensitivity of Fission Product Release to Reactor Lower Head Penetration Failures.....	6-113
6.4.3	Dose Truncation Uncertainty Sensitivity Analyses.....	6-116
6.4.4	Habitability Criterion	6-139
6.4.5	Weather Sampling Effects	6-154
7.	SUMMARY OF RESULTS AND CONCLUSIONS.....	7-1
7.1	Source Term Analyses.....	7-1
7.2	Consequence Analyses.....	7-4
7.2.1	Regression Summary for LCF Risks	7-6
7.2.2	Regression Summary for Early-Fatality Risk.....	7-7
7.2.3	Regression Summary of LCF Risk using Dose Truncation.....	7-8
7.2.4	Habitability Sensitivity Study Summary	7-11
7.2.5	Weather Effects Summary.....	7-11
7.2.6	Single Realization Summary	7-13
7.2.7	Importance Summary	7-15
7.3	Use of Multiple Regression Techniques.....	7-16
7.4	Conclusions.....	7-17
8.	REFERENCES	8-1
APPENDIX A	PROBABILISTIC ANALYSIS METHODOLOGY	A-1
APPENDIX B	SOFTWARE USED AND CODE INTEGRATION	B-1
APPENDIX C	MODEL VERIFICATION AND CONVERGENCE.....	C-1
APPENDIX D	PEER REVIEW/ACRS COMMENT RESOLUTION REPORT	D-1
APPENDIX E	ADDITIONAL INFORMATION AND ANALYSES IN RESPONSE TO ACRS QUESTIONS.....	E-1
APPENDIX F	GLOSSARY OF UNCERTAINTY ANALYSIS TERMS	F-1

LIST OF FIGURES

<u>Figure</u>	<u>Page</u>
Figure 1-1	Comparison of Peach Bottom Long Term Station Blackout RPV Pressure (left) and Fukushima Unit 3 accident (right, [3]) 1-3
Figure 1-2	Comparison of Peach Bottom Long Term Station Blackout RPV Pressure (left) and Fukushima Unit 2 accident (right, [3]) 1-4
Figure 1-3	Comparison of Peach Bottom STSBO Term Station Blackout hydrogen distribution (left) and MELCOR-predicted Fukushima Unit 1 hydrogen conditions (right, [3]) 1-6
Figure 1-4	SOARCA Uncertainty Analysis Information Flow Diagram..... 1-9
Figure 2.3-1	Typical complementary cumulative distribution function (CCDF) of consequence..... 2-6
Figure 3.2-1	Diagram of the information flow of the SOARCA Uncertainty Analysis..... 3-3
Figure 3.4-1	Time-dependent results reflecting uncertainty due to lack of knowledge (epistemic) 3-5
Figure 3.4-2	Distribution of results presented as a complementary cumulative distribution function for a selected time 3-6
Figure 4.1-1	Cumulative distribution function of safety relief valve failure to close valve cycle (λ = per demand failure probability ($1/\lambda$ = number of SRV demands))..... 4-4
Figure 4.1-2	Cumulative distribution function of duration of direct current power 4-5
Figure 4.1-3	Depiction of the fuel rod degradation 4-7
Figure 4.1-4	Cumulative distribution function of zircaloy melt breakout temperature..... 4-8
Figure 4.1-5	Cumulative distribution function of molten clad drainage rate 4-9
Figure 4.1-6	Cumulative distribution function of criteria for thermal seizure of safety relief valve due to heating after onset of core damage 4-11
Figure 4.1-7	Cumulative distribution function of safety relief valve open area fraction after thermal seizure..... 4-12
Figure 4.1-8	Cumulative distribution function of main steam line creep rupture area..... 4-13
Figure 4.1-9	Probability density function of fuel failure criterion alternatives (transformation of intact fuel to particulate debris) 4-15
Figure 4.1-10	Fuel failure criterion functions 4-15
Figure 4.1-11	Cumulative distribution of radial debris relocation time constants: (a) solid debris and (b) liquid debris 4-17
Figure 4.1-12	Drywell floor regions..... 4-20
Figure 4.1-13	Cumulative distribution function debris overflow head as a function of debris at specified fixed temperatures: (a) T-solidus/no-flow head at 1420 K and (b) T-liquidus at 1670 K 4-23
Figure 4.1-14	Cumulative distribution function of flow area resulting from drywell liner failure 4-25
Figure 4.1-15	Cumulative distribution function of hydrogen ignition criteria (where flammable) 4-26

Figure 4.1-16	Cumulative distribution function of railroad door open fraction due to over-pressure failure in reactor building: (a) inner door and (b) outer door	4-28
Figure 4.1-17	Drywell head flange connection details	4-30
Figure 4.1-18	Force balance on drywell head	4-31
Figure 4.1-19	Drywell head flange gap area versus pressure	4-34
Figure 4.1-20	Probability density function for five alternative combinations for MELCOR model radionuclide classes 2, 4, 16, and 17 (I_2 , CsI, CsOH, and Cs_2MoO_4)	4-38
Figure 4.1-21	Cumulative distribution function of particle density.....	4-44
Figure 4.2-1	Cumulative distribution function for the linear coefficient (CWASH1) in the MACCS wet deposition model	4-47
Figure 4.2-2	Cumulative distribution functions of dry deposition velocities for MACCS aerosol bins/aerosol mass median diameters	4-49
Figure 4.2-3	Cumulative distribution for shielding factors.....	4-52
Figure 4.2-4	Cumulative distribution functions of three early health effects: (a) hematopoietic system, (b) pulmonary system, and (c) gastrointestinal system	4-55
Figure 4.2-5	Cumulative distribution functions for the groundshine shielding factors, GSHFAC, for the three types of activity.....	4-58
Figure 4.2-6	The probability density for DDREFA applied in the uncertainty analysis for breast and all other cancers [49, Figure 10].....	4-59
Figure 4.2-7	The cumulative distribution for DDREFA applied in the uncertainty analysis for breast and other cancers	4-61
Figure 4.2-8	Cumulative distribution functions for latent health effects: mortality risk coefficients (CFRISK) for each of the organs included in the SOARCA analysis.....	4-67
Figure 4.2-9	Cumulative distribution functions of linear (a) crosswind dispersion coefficients, $a(m)$ and (b) vertical dispersion coefficients, $a(m)$	4-70
Figure 4.2-10	Cumulative distribution functions of hotspot and normal (a) relocation doses and (b) relocation times	4-73
Figure 4.2-11	Cumulative distribution functions of evacuation delay.....	4-76
Figure 4.2-12	Cumulative distribution functions of evacuation speed.....	4-78
Figure 4.3-1	Creep rupture parameter distribution	4-81
Figure 5.1-1	Results of three replicates and $q = 0.95$ confidence interval (using bootstrap resampling) over selected statistics for released fraction of Cesium: (a) mean, (b) median, (c) quantile $q = 0.05$ and (d) quantile $q = 0.95$	5-4
Figure 5.1-2	Results of three replicates and $q = 0.95$ confidence interval (using bootstrap resampling) over selected statistics for released fraction of Iodine: (a) mean, (b) median, (c) quantile $q = 0.05$ and (d) quantile $q = 0.95$	5-6
Figure 5.2-1	Conditional, mean, individual LCF risk (per event) for all distances with the LNT dose model for emergency and long-term phases ranked from highest to lowest LCF risk result	5-10

Figure 5.2-2	Complementary cumulative distribution function for conditional, mean, individual LCF risk (per event) for the MACCS Convergence Analysis for specified circular areas.....	5-11
Figure 5.2-3	Complementary cumulative distribution function for conditional, mean, individual early-fatality risk (per event) for the MACCS Convergence Analysis for specified circular areas.....	5-13
Figure 5.2-4	Complementary cumulative distribution function and statistical values for conditional, mean, individual LCF risk (per event) within a 10-mile radius for the MACCS Convergence Analysis.....	5-17
Figure 5.2-5	Complementary cumulative distribution function and statistical values for conditional, mean, individual LCF risk (per event) within a 20-mile radius for the MACCS Convergence Analysis.....	5-18
Figure 5.2-6	Complementary cumulative distribution function and statistical values for conditional, mean, individual LCF risk (per event) within a 30-mile radius for the MACCS Convergence Analysis.....	5-19
Figure 5.2-7	Complementary cumulative distribution function and statistical values for conditional, mean, individual LCF risk (per event) within a 40-mile radius for the MACCS Convergence Analysis.....	5-20
Figure 5.2-8	Complementary cumulative distribution function and statistical values for conditional, mean, individual LCF risk (per event) within a 50-mile radius for the MACCS Convergence Analysis.....	5-21
Figure 5.2-9	Complementary cumulative distribution function and statistical values for conditional, mean, individual early-fatality risk (per event) within a 1.3-mile radius for the MACCS Convergence Analysis.....	5-25
Figure 5.2-10	Complementary cumulative distribution function and statistical values for conditional, mean, individual early-fatality risk (per event) within a 2-mile radius for the MACCS Convergence Analysis.....	5-26
Figure 5.2-11	Complementary cumulative distribution function and statistical values for conditional, mean, individual early-fatality risk (per event) within a 2.5-mile radius for the MACCS Convergence Analysis.....	5-27
Figure 5.2-12	Complementary cumulative distribution function and statistical values for conditional, mean, individual early-fatality risk (per event) within a 3-mile radius for the MACCS Convergence Analysis.....	5-28
Figure 5.2-13	Complementary cumulative distribution function and statistical values for conditional, mean, individual early-fatality risk (per event) within a 3.5-mile radius for the MACCS Convergence Analysis.....	5-29
Figure 6.1-1	Time-dependent fraction of iodine core inventory released to the environment for the first 48 hours for combined (865) results for the Peach Bottom Unmitigated LTSBO.....	6-2

Figure 6.1-2	Cumulative distribution function of fraction of iodine core inventory released to the environment at 48 hours based on all combined (i.e., 865) results, with 95% confidence interval over mean, median and quantiles $q = 0.05$ and $q = 0.95$ for the Peach Bottom Unmitigated LTSBO	6-3
Figure 6.1-3	Cumulative distribution function of SRVOAFRAC with samples where main steam line creep rupture occur indicated for Replicate 1 for the Peach Bottom Unmitigated LTSBO.....	6-5
Figure 6.1-4	Time-dependent fraction of the cesium core inventory released to the environment over the first 48 hours for combined (865) results for the Peach Bottom Unmitigated LTSBO.....	6-12
Figure 6.1-5	Cumulative distribution function of fraction of cesium core inventory released to the environment after 48 hours based on all combined (i.e., 865) results, with 95% confidence interval over mean, median and quantiles $q = 0.05$ and $q = 0.95$ for the Peach Bottom Unmitigated LTSBO	6-13
Figure 6.1-6	Time-dependent fraction (a) and cumulative distribution function (b) of in-vessel hydrogen production over 48 hours based on combined (i.e., 865) results, with 95% confidence interval over mean, median and quantiles $q = 0.05$ and $q = 0.95$ for the Peach Bottom Unmitigated LTSBO	6-20
Figure 6.1-7	Distribution for the fraction of cesium core inventory released to the environment for Replicate 1 of the source term uncertainty analysis of the SOARCA Peach Bottom unmitigated LTSBO scenario	6-23
Figure 6.1-8	Single realizations selected for detailed analysis from Replicate 1 of the Peach Bottom unmitigated LTSBO, fraction of cesium core inventory released to the environment for (a) SRV stochastic failures, (b) SRV thermal failures, and (c) MSL creep ruptures.....	6-24
Figure 6.1-9	SRV open area fraction after thermal seizure Peach Bottom unmitigated LTSBO Replicate 1: (a) cumulative distribution function and (b) fraction of cesium core inventory released to the environment. Samples with MSL creep ruptures are identified	6-31
Figure 6.1-10	Reactor and containment pressure and water level for Realization 62 of the Peach Bottom unmitigated LTSBO Replicate 1, an MSL creep rupture.....	6-32
Figure 6.1-11	Fraction of cesium core inventory released to the environment for Peach Bottom unmitigated LTSBO Replicate 1: (a) SRV stochastic failures, (b) SRV thermal failures, and (c) MSL creep ruptures. Realizations are identified that have cesium core inventory initialized as CsOH	6-33
Figure 6.1-12	Time dependent relocation of core material from the RPV to the reactor cavity for Realization 268 of the Peach Bottom unmitigated LTSBO Replicate 1, an SRV thermal seizure failure	6-35
Figure 6.1-13	In-vessel hydrogen production for Realization 268 of the Peach Bottom unmitigated LTSBO Replicate 1, an SRV thermal seizure failure	6-36

Figure 6.1-14	Cumulative distribution function for the flow area resulting from drywell liner failure for Peach Bottom unmitigated LTSBO Replicate 1 with samples identified that have a surge of water from the wetwell during depressurization of the drywell	6-37
Figure 6.1-15	Water level in containment for Realization 170 of the Peach Bottom unmitigated LTSBO Replicate 1, an SRV Stochastic failure	6-38
Figure 6.1-16	Fraction of cesium core inventory released to the environment for Peach Bottom unmitigated LTSBO Replicate 1: (a) SRV stochastic failures, (b) SRV thermal failures, and (c) MSL creep ruptures. The realizations are identified that have closed railroad doors.....	6-39
Figure 6.1-17	Fraction of cesium core inventory released to the environment for the updated deterministic SOARCA Peach Bottom unmitigated LTSBO case documented in Section 5.1.1.1 for two scales on the ordinate: (a) 0 to 1.0 and (b) 0 to 0.20.....	6-41
Figure 6.1-18	Fraction of cesium core inventory released to the environment for Realization 18 of Replicate 1 for two scales on the ordinate: (a) 0 to 1.0 and (b) 0 to 0.20	6-44
Figure 6.1-19	Fraction of cesium core inventory released to the environment for Realization 51 of Replicate 1 for two scales on the ordinate: (a) 0 to 1.0 and (b) 0 to 0.02	6-45
Figure 6.1-20	Fraction of cesium core inventory released to the environment for Realization 52 of Replicate 1 for two scales on the ordinate: (a) 0 to 1.0 and (b) 0 to 0.2	6-46
Figure 6.1-21	Fraction of cesium core inventory released to the environment for Realization 62 of Replicate 1 for two scales on the ordinate: (a) 0 to 1.0 and (b) 0 to 0.2	6-47
Figure 6.1-22	Fraction of cesium core inventory released to the environment for Realization 63 of Replicate 1 for two scales on the ordinate: (a) 0 to 1.0 and (b) 0 to 0.2	6-48
Figure 6.1-23	Fraction of cesium core inventory released to the environment for Realization 86 of Replicate 1 for two scales on the ordinate: (a) 0 to 1.0 and (b) 0 to 0.2	6-49
Figure 6.1-24	Fraction of cesium core inventory released to the environment for Realization 90 of Replicate 1 for two scales on the ordinate: (a) 0 to 1.0 and (b) 0 to 0.2	6-50
Figure 6.1-25	Fraction of cesium core inventory released to the environment for Realization 122 of Replicate 1 for two scales on the ordinate: (a) 0 to 1.0 and (b) 0 to 0.2	6-51
Figure 6.1-26	Fraction of cesium core inventory released to the environment for Realization 134 of Replicate 1 for two scales on the ordinate: (a) 0 to 1.0 and (b) 0 to 0.2	6-52
Figure 6.1-27	Fraction of cesium core inventory released to the environment for Realization 170 of Replicate 1 for two scales on the ordinate: (a) 0 to 1.0 and (b) 0 to 0.2	6-53

Figure 6.1-28	Fraction of cesium core inventory released to the environment for Realization 268 of Replicate 1 for two scales on the ordinate: (a) 0 to 1.0 and (b) 0 to 0.2	6-54
Figure 6.2-1	Complementary cumulative distribution function and statistical values for conditional, mean, individual LCF risk (per event) within a 10-mile radius	6-58
Figure 6.2-2	Complementary cumulative distribution function and statistical values for conditional, mean, individual LCF risk (per event) within a 20-mile radius	6-59
Figure 6.2-3	Complementary cumulative distribution function and statistical values for conditional, mean, individual LCF risk (per event) within a 30-mile radius	6-60
Figure 6.2-4	Complementary cumulative distribution function and statistical values for conditional, mean, individual LCF risk (per event) within a 40-mile radius	6-61
Figure 6.2-5	Complementary cumulative distribution function and statistical values for conditional, mean, individual LCF risk (per event) within a 50-mile radius	6-62
Figure 6.2-6	Complementary cumulative distribution function for conditional, mean, individual LCF risk (per event) within a 10-mile and 20-mile radius for 'overall' and 'long-term phase' LCF risk	6-63
Figure 6.2-7	Complementary cumulative distribution function for conditional, mean, individual LCF risk (per event) within a 10-mile and 20-mile radius for 'overall' and 'emergency phase' LCF risk.....	6-63
Figure 6.2-8	Complementary cumulative distribution function and statistical values for conditional, mean, individual early-fatality risk (per event) within a 1.3-mile radius	6-67
Figure 6.2-9	Complementary cumulative distribution function and statistical values for conditional, mean, individual early-fatality risk (per event) within a 2-mile radius	6-68
Figure 6.2-10	Complementary cumulative distribution function and statistical values for conditional, mean, individual early-fatality risk (per event) within a 2.5-mile radius	6-68
Figure 6.2-11	Complementary cumulative distribution function and statistical values for conditional, mean, individual early-fatality risk (per event) within a 3-mile radius	6-69
Figure 6.2-12	Complementary cumulative distribution function and statistical values for conditional, mean, individual early-fatality risk (per event) within a 3.5-mile radius	6-69
Figure 6.2-13	Conditional, mean, individual LCF risk (per event) for MELCOR Replicate 1 single realizations for the 10-mile circular area	6-89
Figure 6.2-14	Conditional, mean, individual LCF risk (per event) for MELCOR Replicate 1 single realizations for the 20-mile circular area	6-90
Figure 6.2-15	Conditional, mean, individual LCF risk (per event) for MELCOR Replicate 1 single realizations for the 30-mile circular area	6-91
Figure 6.2-16	Conditional, mean, individual LCF risk (per event) for MELCOR Replicate 1 single realizations for the 40-mile circular area	6-91

Figure 6.2-17	Conditional, mean, individual LCF risk (per event) for MELCOR Replicate 1 single realizations for the 50-mile circular area	6-92
Figure 6.2-18	MELCOR Replicate 2 Realization 291 reactor and containment pressure response	6-96
Figure 6.2-19	MELCOR Replicate 3 Realization 046 reactor and containment pressure response	6-96
Figure 6.2-20	MELCOR Replicate 3 Realization 267 reactor and containment pressure response	6-97
Figure 6.2-21	Conditional, mean, individual LCF risk (per event) MACCS Uncertainty Analysis single realizations for the 10-mile circular area.....	6-99
Figure 6.2-22	Conditional, mean, individual LCF risk (per event) MACCS Uncertainty Analysis single realizations for the 20-mile circular area.....	6-100
Figure 6.2-23	Conditional, mean, individual LCF risk (per event) MACCS Uncertainty Analysis single realizations for the 30-mile circular area.....	6-101
Figure 6.2-24	Conditional, mean, individual LCF risk (per event) MACCS Uncertainty Analysis single realizations for the 40-mile circular area.....	6-101
Figure 6.2-25	Conditional, mean, individual LCF risk (per event) MACCS Uncertainty Analysis single realizations for the 50-mile circular area.....	6-102
Figure 6.2-26	Conditional, mean, individual early-fatality risk (per event) MACCS Uncertainty Analysis single realizations for specified circular areas	6-103
Figure 6.4-1	Environmental iodine release fraction for UA SOARCA sensitivity cases for the manual control of the SRV.....	6-112
Figure 6.4-2	Environmental cesium release fraction for UA SOARCA sensitivity cases for the manual control of the SRV.....	6-113
Figure 6.4-3	Cesium distribution in a high-release case of the Lower Head Penetration Model Sensitivity Study.....	6-116
Figure 6.4-4	Habitability criterion comparison of conditional, mean, individual LCF risk (per event) for specified circular areas for the LNT dose-response model	6-142
Figure 6.4-5	Habitability criterion comparison of conditional, mean, individual LCF risk (per event) for the 10-mile circular area for the LNT dose-response model.....	6-143
Figure 6.4-6	Habitability criterion comparison of conditional, mean, individual LCF risk (per event) for the 20-mile circular area for the LNT dose-response model.....	6-144
Figure 6.4-7	Habitability criterion comparison of conditional, mean, individual LCF risk (per event) for the 30-mile circular area for the LNT dose-response model.....	6-144
Figure 6.4-8	Habitability criterion comparison of conditional, mean, individual LCF risk (per event) for the 40-mile circular area for the LNT dose-response model.....	6-145

Figure 6.4-9	Habitability criterion comparison of conditional, mean, individual LCF risk (per event) for the 50-mile circular area for the LNT dose-response model.....	6-145
Figure 6.4-10	Habitability criterion comparison of conditional, mean, individual LCF risk (per event) for the 10-mile circular area for the USBGR dose-response model.....	6-148
Figure 6.4-11	Habitability criterion comparison of conditional, mean, individual LCF risk (per event) for the 20-mile circular area for the USBGR dose-response model.....	6-148
Figure 6.4-12	Habitability criterion comparison of conditional, mean, individual LCF risk (per event) for the 30-mile circular area for the USBGR dose-response model.....	6-149
Figure 6.4-13	Habitability criterion comparison of conditional, mean, individual LCF risk (per event) for the 40-mile circular area for the USBGR dose-response model.....	6-149
Figure 6.4-14	Habitability criterion comparison of conditional, mean, individual LCF risk (per event) for the 50-mile circular area for the USBGR dose-response model.....	6-150
Figure 6.4-15	Habitability criterion comparison of conditional, mean, individual LCF risk (per event) for the 10-mile circular area for the HPS dose-response model.....	6-152
Figure 6.4-16	Habitability criterion comparison of conditional, mean, individual LCF risk (per event) for the 20-mile circular area for the HPS dose-response model.....	6-152
Figure 6.4-17	Habitability criterion comparison of conditional, mean, individual LCF risk (per event) for the 30-mile circular area for the HPS dose-response model.....	6-153
Figure 6.4-18	Habitability criterion comparison of conditional, mean, individual LCF risk (per event) for the 40-mile circular area for the HPS dose-response model.....	6-153
Figure 6.4-19	Habitability criterion comparison of conditional, mean, individual LCF risk (per event) for the 50-mile circular area for the HPS dose-response model.....	6-154
Figure 6.4-20	Example wind rose diagram.....	6-156
Figure 6.4-21	Peach Bottom wind rose and atmospheric stability chart, year 2006	6-158
Figure 6.4-22	Weather sampling comparison of the conditional, mean, individual LCF risk (per event) using the LNT dose-response model within specified circular areas	6-160
Figure 6.4-23	Weather sampling comparison of the conditional, mean, individual LCF risk (per event) using the USBGR dose-response model within specified circular areas	6-161
Figure 6.4-24	Weather sampling comparison of the conditional, mean, individual LCF risk (per event) using the HPS dose-response model within specified circular areas	6-162
Figure 6.4-25	CCDF of conditional, mean, individual LCF risk (per event) within the 10-mile circular area for aleatory weather uncertainty and the MACCS CAP17 analysis.....	6-165

Figure 6.4-26	CCDF of conditional, mean, individual LCF risk (per event) within the 20-mile circular area for aleatory weather uncertainty and the MACCS CAP17 analysis.....	6-166
Figure 6.4-27	CCDF of conditional, mean, individual LCF risk (per event) within the 30-mile circular area for aleatory weather uncertainty and the MACCS CAP17 analysis.....	6-167
Figure 6.4-28	CCDF of conditional, mean, individual LCF risk (per event) within the 40-mile circular area for aleatory weather uncertainty and the MACCS CAP17 analysis.....	6-167
Figure 6.4-29	CCDF of conditional, mean, individual LCF risk (per event) within the 50-mile circular area for aleatory weather uncertainty and the MACCS CAP17 analysis.....	6-168
Figure 6.4-30	CCDF of conditional, mean, individual LCF risk (per event) within the 10-mile circular area for aleatory weather uncertainty for the LNT, USBGR, and HPS dose-response models using the SOARCA uncertainty analysis base case source term	6-171
Figure 6.4-31	CCDF of conditional, mean, individual LCF risk (per event) within the 20-mile circular area for aleatory weather uncertainty for the LNT, USBGR, and HPS dose-response models using the SOARCA uncertainty analysis base case source term	6-172
Figure 6.4-32	CCDF of conditional, mean, individual LCF risk (per event) within the 30-mile circular area for aleatory weather uncertainty for the LNT, USBGR, and HPS dose-response models using the SOARCA uncertainty analysis base case source term	6-173
Figure 6.4-33	CCDF of conditional, mean, individual LCF risk (per event) within the 40-mile circular area for aleatory weather uncertainty for the LNT, USBGR, and HPS dose-response models using the SOARCA uncertainty analysis base case source term	6-174
Figure 6.4-34	CCDF of conditional, mean, individual LCF risk (per event) within the 50-mile circular area for aleatory weather uncertainty for the LNT, USBGR, and HPS dose-response models using the SOARCA uncertainty analysis base case source term	6-175
Figure 6.4-35	CCDF of conditional, mean, individual LCF risk (per event) within the 10-mile circular area for aleatory weather uncertainty using the USBGR dose-response model and the MACCS CAP15 analysis.....	6-176
Figure 6.4-36	CCDF of conditional, mean, individual LCF risk (per event) within the 20-mile circular area for aleatory weather uncertainty using the USBGR dose-response model and the MACCS CAP15 analysis.....	6-177
Figure 6.4-37	CCDF of conditional, mean, individual LCF risk (per event) within the 30-mile circular area for aleatory weather uncertainty using the USBGR dose-response model and the MACCS CAP15 analysis.....	6-178
Figure 6.4-38	CCDF of conditional, mean, individual LCF risk (per event) within the 40-mile circular area for aleatory weather uncertainty using the USBGR dose-response model and the MACCS CAP15 analysis.....	6-179

Figure 6.4-39	CCDF of conditional, mean, individual LCF risk (per event) within the 50-mile circular area for aleatory weather uncertainty using the USBGR dose-response model and the MACCS CAP15 analysis.....	6-180
Figure 6.4-40	CCDF of conditional, mean, individual LCF risk (per event) within the 10-mile circular area for aleatory weather uncertainty using the HPS dose-response model and the MACCS CAP16 analysis ...	6-182
Figure 6.4-41	CCDF of conditional, mean, individual LCF risk (per event) within the 20-mile circular area for aleatory weather uncertainty using the HPS dose-response model and the MACCS CAP16 analysis. ..	6-183
Figure 6.4-42	CCDF of conditional, mean, individual LCF risk (per event) within the 30-mile circular area for aleatory weather uncertainty using the HPS dose-response model and the MACCS CAP16 analysis ...	6-184
Figure 6.4-43	CCDF of conditional, mean, individual LCF risk (per event) within the 40-mile circular area for aleatory weather uncertainty using the HPS dose-response model and the MACCS CAP16 analysis ...	6-185
Figure 6.4-44	CCDF of conditional, mean, individual LCF risk (per event) within the 50-mile circular area for aleatory weather uncertainty using the HPS dose-response model and the MACCS CAP16 analysis. ..	6-186

LIST OF TABLES

<u>Table</u>	<u>Page</u>
Table 2.2-1	SOARCA uncertain parameter groups 2-4
Table 4.1-1	MELCOR uncertain parameters—sequences issues 4-5
Table 4.1-2	Time versus temperature relationship for intact fuel rod collapse 4-8
Table 4.1-3	MELCOR uncertain parameters—In-Vessel accident progression issues..... 4-18
Table 4.1-4	Concrete composition 4-21
Table 4.1-5	MELCOR uncertain parameters—Ex-vessel accident progression issues..... 4-24
Table 4.1-6	MELCOR uncertain parameters—containment behavior issues 4-35
Table 4.1-7	MELCOR uncertain parameters for chemical forms of iodine and cesium..... 4-39
Table 4.1-8	Densities of several radionuclide compounds 4-41
Table 4.1-9	Released radionuclide masses and weighting factors from SOARCA Peach Bottom Unmitigated LTSBO Case 4-42
Table 4.1-10	Totals and density ranges 4-43
Table 4.1-11	MELCOR uncertain parameters—aerosol deposition 4-44
Table 4.2-1	MACCS uncertain parameters—wet deposition model 4-47
Table 4.2-2	MACCS uncertain parameters—dry deposition velocities..... 4-50
Table 4.2-3a	MACCS uncertain parameters—cloudshine shielding factors..... 4-52
Table 4.2-3b	MACCS uncertain parameters—groundshine shielding factors 4-53
Table 4.2-3c	MACCS uncertain parameters—inhalation protection factors 4-53
Table 4.2-4	MACCS uncertain parameters—early health effects..... 4-56
Table 4.2-5	MACCS uncertain parameters—multiplier for groundshine dose coefficients 4-57
Table 4.2-6	Piecewise uniform distributions for the combined uncertainty in groundshine shielding factors (GSHFAC) including multiplier..... 4-58
Table 4.2-7	Piecewise uniform distributions for DDREFA 4-62
Table 4.2-8	MACCS uncertain parameters—geometric mean (i.e., median values, which were also used in the SOARCA analyses) for inhalation dose coefficients (Gy/Bq) [49]..... 4-63
Table 4.2-9	MACCS uncertain parameters—geometric standard deviations for inhalation dose coefficients (i.e., σ [49])..... 4-65
Table 4.2-10	Crosswalk between reference type from Tables 4.2-8 and 4.2-9 and WINMACCS organ doses 4-66
Table 4.2-11	Age-averaged cancer mortality risk estimates and uncertainties for low-dose, low-LET uniform irradiation of the body [49] 4-68
Table 4.2-12	MACCS uncertain parameters—inputs for log-normal dispersion parameters distributions..... 4-69
Table 4.2-13	MACCS uncertain parameters—dispersion 4-71
Table 4.2-14	MACCS uncertain parameters—relocation doses and times 4-74
Table 4.2-15	MACCS uncertain parameters—evacuation delay 4-76
Table 4.2-16	MACCS uncertain parameters—evacuation speed..... 4-79
Table 4.3-1	A worst-case scenario of SRV-1 set point drift time estimates 4-83

Table 5.1-1	Success rates of MELCOR simulations for STP08, STP09, and STP10	5-1
Table 5.1-2	MELCOR error summary for STP08, STP09, STP10.....	5-2
Table 5.2-1	Conditional, mean, individual LCF risk (per event) basic statistics for the LNT dose model at specified circular areas	5-8
Table 5.2-2	Conditional, mean, Individual LCF risk (per event) basic from the SOARCA UA base case for the LNT dose model at specified circular areas	5-9
Table 5.2-3	Conditional, mean, individual early-fatality risk (per event) for the Surry ISLOCA Scenario	5-12
Table 5.2-4	Conditional, mean, individual early-fatality risk (per event) basic statistics	5-12
Table 5.2-5	Radionuclide specific contribution to overall 'effective' inhalation dose	5-14
Table 5.2-6	Combined conditional, mean, individual LCF risk (per event) average statistics for the MACCS statistical convergence test for specified circular areas	5-15
Table 5.2-7	Combined conditional, mean, individual LCF risk (per event) standard error statistics for the MACCS statistical convergence test for specified circular areas	5-16
Table 5.2-8	Combined conditional, mean, individual LCF risk (per event) lower bounding case statistics for the MACCS statistical convergence test for specified circular areas	5-16
Table 5.2-9	Combined conditional, mean, individual LCF risk (per event) upper bounding cases statistics for the MACCS statistical convergence test for specified circular areas	5-16
Table 5.2-10	Correlation matrix for the MELCOR STP08 Uncertainty Model Source Term MACCS Analysis for the conditional, mean, individual LCF risk (per event) for specified circular areas.....	5-22
Table 5.2-11	Correlation matrix for the MELCOR STP09 Uncertainty Model Source Term MACCS Analysis for the conditional, mean, individual LCF risk (per event) for specified circular areas.....	5-22
Table 5.2-12	Correlation matrix for the MELCOR STP10 Uncertainty Model Source Term MACCS Analysis for the conditional, mean, individual LCF risk (per event) for specified circular areas.....	5-22
Table 5.2-13	Combined conditional, mean, individual early-fatality risk (per event) average statistics for the MACCS statistical convergence test for specified circular areas	5-23
Table 5.2-14	Combined conditional, mean, individual early-fatality risk (per event) standard error statistics for the MACCS statistical convergence test for specified circular areas	5-24
Table 5.2-15	Combined conditional, mean, individual early-fatality risk (per event) lower bounding case statistics for the MACCS statistical convergence test for specified circular areas	5-24
Table 5.2-16	Combined conditional, mean, individual early-fatality risk (per event) upper bounding cases statistics for the MACCS statistical convergence test for specified circular areas	5-24

Table 5.2-17	Correlation matrix for the MELCOR STP08 Uncertainty Model Source Term MACCS Analysis for the conditional, mean, individual early-fatality risk (per event) for specified circular areas	5-30
Table 5.2-18	Correlation matrix for the MELCOR STP09 Uncertainty Model Source Term MACCS Analysis for the conditional, mean, individual early-fatality risk (per event) for specified circular areas	5-30
Table 5.2-19	Correlation matrix for the MELCOR STP10 Uncertainty Model Source Term MACCS Analysis for the conditional, mean, individual early-fatality risk (per event) for specified circular areas	5-30
Table 6.1-1	Regression analysis of fraction of iodine released after 48 Hours.....	6-6
Table 6.1-2	Regression analyses of fraction of iodine released after 48 hours for realizations leading to SRV stochastic failures.....	6-7
Table 6.1-3	Regression analyses of fraction of iodine released after 48 hours for realizations leading to SRV thermal failures without MSL creep rupture.....	6-8
Table 6.1-4	Regression analyses of fraction of iodine released after 48 hours for realization leading to SRV thermal failure and MSL creep rupture.....	6-9
Table 6.1-5	Regression analyses over time when the fraction reaches 0.001 of the iodine inventory released over the first 48 Hours	6-11
Table 6.1-6	Regression analyses of fraction of cesium released over 48 hours ...	6-15
Table 6.1-7	Regression analyses of fraction of cesium released over 48 hours for realizations leading to SRV stochastic failure	6-16
Table 6.1-8	Regression analyses of fraction of cesium released over 48 hours for realizations leading to SRV thermal failure without MSL creep rupture.....	6-18
Table 6.1-9	Regression analyses of fraction of cesium released over 48 hours for realizations leading to SRV thermal failure and MSL creep rupture.....	6-19
Table 6.1-10	Regression analysis of hydrogen production.	6-22
Table 6.1-11	Sampled parameter values for Replicate 1 (STP08) for selected individual realizations	6-25
Table 6.1-12	Timing of events, key occurrences/attributes, and environmental releases for selected individual realizations of the Peach Bottom unmitigated LTSBO Replicate 1 (STP08).....	6-27
Table 6.2-1	MACCS probabilistic analyses	6-56
Table 6.2-2	Conditional, mean, individual LCF risk (per event) average statistics for the MACCS Uncertainty Analysis for five circular areas (using all three source term replicates)	6-56
Table 6.2-3	Correlation matrix of the conditional, mean, individual LCF risk (per event) for the MACCS Uncertainty Analysis for specified circular areas (using all three source term replicates).....	6-64
Table 6.2-4	Conditional, mean, individual early-fatality risk (per event) for the Surry ISLOCA Scenario	6-65
Table 6.2-5	Conditional, mean, individual early-fatality risk (per event) average statistics for the composite MACCS Uncertainty Analysis for specified circular areas (using all three source term replicates) ...	6-66

Table 6.2-6	Correlation matrix for the MACCS Uncertainty Analysis for the conditional, mean, individual early-fatality risk (per event) for specified circular areas (using all three source term replicates).....	6-70
Table 6.2-7	Conditional, mean, individual LCF risk (per event) regression of the MACCS Uncertainty Analysis for the 10-mile circular area	6-72
Table 6.2-8	Conditional, mean, individual LCF risk (per event) regression of the MACCS Uncertainty Analysis for the 20-mile circular area	6-73
Table 6.2-9	Conditional, mean, individual LCF risk (per event) regression of the MACCS Uncertainty Analysis for the 30-mile circular area	6-74
Table 6.2-10	Conditional, mean, individual LCF risk (per event) regression of the MACCS Uncertainty Analysis for the 40-mile circular area	6-75
Table 6.2-11	Conditional, mean, individual LCF risk (per event) regression of the MACCS Uncertainty Analysis for the 50-mile circular area	6-76
Table 6.2-12	Conditional, mean, individual early-fatality risk (per event) regression of the MACCS Uncertainty Analysis for the 1.3-mile circular area	6-80
Table 6.2-13	Conditional, mean, individual early-fatality risk (per event) regression of the MACCS Uncertainty Analysis for the 2-mile circular area	6-81
Table 6.2-14	Conditional, mean, individual early-fatality risk (per event) regression of the MACCS Uncertainty Analysis for the 2.5-mile circular area	6-83
Table 6.2-15	Conditional, mean, individual early-fatality risk (per event) regression of the MACCS Uncertainty Analysis for the 3-mile circular area	6-84
Table 6.2-16	Conditional, mean, individual early-fatality risk (per event) regression of the MACCS Uncertainty Analysis for the 3.5-mile circular area	6-85
Table 6.2-17	Brief source term description for the single realizations selected from Replicate 1 (STP08) MELCOR Analyses.....	6-87
Table 6.2-18	Conditional, mean, individual early-fatality risk (per event) for the MELCOR Replicate 1 single realization nonzero realizations for specified circular areas	6-93
Table 6.2-19	Timing of key events for MELCOR source terms selected from the three replicates for the MACCS single realization analysis.....	6-95
Table 6.2-20	Brief source term description for the MELCOR source terms selected from the three replicates for the CAP17 MACCS Uncertainty Analysis of single realizations	6-97
Table 6.2-21	Conditional, mean, individual LCF risk (per event) for the MACCS Uncertainty Analysis single realizations for specified circular areas for MELCOR source terms selected from the three replicates.....	6-98
Table 6.2-22	Conditional, mean, individual early-fatality risk (per event) for the MACCS single realizations for specified circular areas.....	6-102
Table 6.2-23	Conditional, mean, individual early-fatality risk (per event) for the MACCS single realizations for specified circular areas beyond 10 miles.....	6-104

Table 6.4-1	Timing of key events for Peach Bottom Unmitigated LTSBO, manual SRV operation action at 0.5 hr, 1.0 hr, 2.0 hr and 3.0 hr.....	6-110
Table 6.4-2	Conditional, mean, individual LCF risk (per event) average statistics for the Dose Truncation Sensitivity Analysis at specified Radial Distances	6-117
Table 6.4-3	Conditional, mean, individual LCF risk (per event) regression of MACCS sensitivity LNT model at the 10-mile circular area.....	6-119
Table 6.4-4	Conditional, mean, individual LCF risk (per event) regression of MACCS sensitivity LNT model at the 20-mile circular area.....	6-120
Table 6.4-5	Conditional, mean, individual LCF risk (per event) regression of MACCS sensitivity LNT model at the 30-mile circular area.....	6-121
Table 6.4-6	Conditional, mean, individual LCF risk (per event) regression of MACCS sensitivity LNT model at the 40-mile circular area.....	6-122
Table 6.4-7	Conditional, mean, individual LCF Risk (per event) regression of MACCS sensitivity LNT model at the 50-mile circular area.....	6-123
Table 6.4-8	Conditional, mean, individual LCF Risk (per event) regression of MACCS sensitivity USBGR model at the 10-mile circular area.....	6-126
Table 6.4-9	Conditional, mean, individual LCF risk (per event) regression of MACCS sensitivity USBGR model at the 20-mile circular area.....	6-127
Table 6.4-10	Conditional, mean, individual LCF risk (per event) regression of MACCS sensitivity USBGR model at the 30-mile circular area.....	6-128
Table 6.4-11	Conditional, mean, individual LCF risk (per event) regression of MACCS sensitivity USBGR model at the 40-mile circular area.....	6-129
Table 6.4-12	Conditional, mean, individual LCF risk (per event) regression of MACCS sensitivity USBGR model at the 50-mile circular area.....	6-130
Table 6.4-13	Conditional, mean, individual LCF risk (per event) regression of MACCS sensitivity HPS model at the 10-mile circular area	6-134
Table 6.4-14	Conditional, mean, individual LCF risk (per event) regression of MACCS sensitivity HPS model at the 20-mile circular area	6-135
Table 6.4-15	Conditional, mean, individual LCF risk (per event) regression of MACCS sensitivity HPS model at the 30-mile circular area	6-136
Table 6.4-16	Conditional, mean, individual LCF risk (per event) regression of MACCS sensitivity HPS model at the 40-mile circular area	6-137
Table 6.4-17	Conditional, mean, individual LCF risk (per event) regression of MACCS sensitivity HPS model at the 50-mile circular area	6-138
Table 6.4-18	Habitability criterion comparison of conditional, mean, individual LCF risk (per event) for LNT dose-response model	6-142
Table 6.4-19	Percentage change in conditional, mean, individual LCF risk (per event) for the LNT dose-response model from variations in habitability criterion (reduction/increase (-/+))	6-143
Table 6.4-20	Habitability criterion comparison of conditional, mean, individual LCF risk (per event) for USBGR dose-response model	6-147
Table 6.4-21	Percentage change in conditional, mean, individual LCF risk (per event) for the USBGR dose-response model from variations in habitability criterion (reduction/increase (-/+))	6-147
Table 6.4-22	Habitability criterion comparison of conditional, mean, individual LCF risk (per event) for HPS dose-response model.....	6-151

Table 6.4-23	Percentage change in conditional, mean, individual LCF risk (per event) for the HPS dose-response model from variations in habitability criterion (reduction/increase (-/+))	6-151
Table 6.4-24	Weather sampling inputs for Peach Bottom	6-157
Table 6.4-25	Statistical summary of raw meteorological data	6-158
Table 6.4-26	Weather sampling comparison of the conditional, mean, individual LCF risk (per event) using the LNT dose-response mode.....	6-159
Table 6.4-27	Weather sampling comparison of the conditional, mean, individual LCF risk (per event) using the USBGR dose-response model.....	6-160
Table 6.4-28	Weather sampling comparison of the conditional, mean, individual LCF risk (per event) using the HPS dose-response model	6-161
Table 6.4-29	Brief source term description for the single realizations selected from Replicate 1 (STP08) MELCOR Analyses for the aleatory weather uncertainty analyses.....	6-163
Table 6.4-30	MACCS aleatory uncertainty analyses conditional mean, individual LCF risk (per event) comparison of source terms to the conditional, mean, individual LCF risk (per event) CCDF of the MACCS CAP17 analysis for specified circular areas.....	6-164
Table 6.4-31	The MACCS CAP17 analysis conditional, mean, individual LCF risk (per event) of the source terms for specified circular areas.....	6-164
Table 6.4-32	Conditional, mean, individual LCF risk (per event) ratio for the MACCS aleatory uncertainty analyses and the MACCS CAP17 analysis for specified circular areas	6-168
Table 6.4-33	MACCS aleatory uncertainty analyses median LCF risk per event comparison of source terms to the CCDF of the MACCS CAP14 analysis (LNT) for specified circular areas	6-169
Table 6.4-34	MACCS aleatory uncertainty analyses median LCF risk per event comparison of source terms to the CCDF of the MACCS CAP15 analysis (USBGR) for specified circular areas	6-170
Table 6.4-35	MACCS aleatory uncertainty analyses median LCF risk per event comparison of source terms to the CCDF of the MACCS CAP16 analysis (HPS) for specified circular areas.....	6-170
Table 6.4-36	MACCS aleatory uncertainty analyses percent contribution of the emergency phase for the conditional, mean, individual LCF risk (per event) using the LNT dose-response model for specified circular areas	6-170
Table 6.4-37	Conditional, mean, individual LCF risk (per event) ratio for the MACCS aleatory uncertainty analyses using the USBGR dose-response model and the MACCS CAP15 analysis for specified circular areas	6-181
Table 6.4-38	Conditional, mean, Individual LCF risk (per event) ratio for the MACCS aleatory uncertainty analyses using the HPS dose-response model and the MACCS CAP16 analysis for specified circular areas	6-187

EXECUTIVE SUMMARY

The U.S. Nuclear Regulatory Commission (NRC), the nuclear power industry, and the international nuclear energy research community have devoted considerable research over the last several decades to examining severe reactor accident phenomena and offsite consequences. The NRC initiated the State-of-the-Art Reactor Consequence Analyses (SOARCA) project to leverage this research and develop current estimates of the offsite radiological health consequences for potential severe reactor accidents for two pilot plants: the Peach Bottom Atomic Power Station, a boiling-water reactor (BWR) in Pennsylvania and the Surry Power Station, a pressurized-water reactor in Virginia. By applying modern analysis tools and techniques, the SOARCA project developed a body of knowledge regarding the realistic outcomes of select severe nuclear reactor accidents. To accomplish this objective, the SOARCA project's integrated modeling of accident progression and offsite consequences used both state-of-the-art computational analysis tools (the MELCOR code and the MELCOR Accident Consequence Code System [MACCS]) and best modeling practices drawn from the collective wisdom of the severe accident analysis community. The SOARCA project is documented in NUREG-1935, "State-of-the-Art Reactor Consequence Analyses (SOARCA) Report" (2012), NUREG/CR-7110, "State-of-the-Art Reactor Consequence Analyses (SOARCA) Project Volume 1: Peach Bottom Integrated Analysis" and "State-of-the-Art Reactor Consequence Analyses (SOARCA) Project Volume 2: Surry Integrated Analysis" (2013).

This document describes the NRC's uncertainty analysis of the SOARCA unmitigated long-term station blackout (LTSBO) severe accident scenario for the Peach Bottom Atomic Power Station. The objective of this uncertainty analysis is to evaluate the robustness of the SOARCA project's deterministic results and conclusions, and to develop insight into the overall sensitivity of the SOARCA results to uncertainty in key modeling input parameters. As this is a first-of-a-kind analysis in its integrated look at uncertainties in MELCOR severe accident progression and MACCS offsite consequence analyses, an additional objective is to demonstrate an uncertainty analysis methodology that could be used in future combined Level 1/2/3 consequence and probabilistic risk assessment (PRA) studies.

Approach

The SOARCA offsite consequence results presented in NUREG-1935 incorporated only the aleatory uncertainty associated with weather conditions at the time of the accident. The reported offsite consequence values represent the average (mean) value obtained from a large number of random (aleatory) weather trials. The weather uncertainty is handled the same way in this uncertainty analysis. In addition, the impact of state-of-knowledge (epistemic) uncertainty in the input parameters is explored in detail by randomly sampling distributions for model parameters that are considered to be potentially important. Assessing key MELCOR and MACCS parameter uncertainties in an integrated fashion helps form an understanding of the relative importance of each uncertain input on the potential consequences.

This analysis uses the existing SOARCA models and software. In other words, the uncertainty stemming from the choice of conceptual models and model implementation is not explicitly explored, nor is completeness uncertainty. In addition, not all possible uncertain input parameters were included in the analysis. Rather, a set of key parameters was carefully chosen by NRC staff and severe accident experts at Sandia National Laboratories to capture important influences on the potential release of radioactive material to the environment and on offsite health consequences.

A detailed uncertainty analysis was performed for a single accident scenario rather than for all seven of the SOARCA scenarios documented in NUREG-1935. The SOARCA Peach Bottom BWR unmitigated LTSBO scenario was analyzed. While a single scenario cannot provide a complete exploration for all possible effects of uncertainties in analyses for the two SOARCA pilot plants, it can be used to provide initial insights into the overall sensitivity of SOARCA results and conclusions to input uncertainty. In addition, since station blackouts are an important class of events for BWRs in general, the phenomenological insights gained on severe accident progression and radionuclide releases may prove useful for BWRs in general.

Through expert judgment and iteration after interim reviews by the independent SOARCA peer review panel¹ and the NRC's Advisory Committee on Reactor Safeguards, 21 key MELCOR parameters and 20 key MACCS parameter groups were identified for inclusion in the uncertainty analysis, and distributions were defined for each parameter. The 20 MACCS parameter groups were comprised of 350 individual parameters, many of which were fully correlated to form a parameter group. For example, there were many individual organ-specific and radionuclide-specific dose conversion factors, which were considered one group of parameters.

The MELCOR uncertain parameters were selected to capture:

- accident sequence issues,
- accident progression issues within the reactor vessel,
- accident progression issues outside the reactor vessel,
- containment behavior issues, and
- fission product release, transport, and deposition upon plant structures.

These broad areas span the severe accident progression over time, ranging from minor sequence variations as affected by safety relief valve (SRV) behavior and battery duration, to uncertainties in the core damage and melt progressions. Other parameters more specific to fission product transport include deposition and settling processes, and chemical speciation of cesium and iodine which affects both release and transport within plant structures.

The parameters selected from the MACCS consequence model were those that affect individual latent cancer fatality (LCF) risk and individual early fatality risk, due to:

- cloudshine during radiological plume passage,
- groundshine from deposited radionuclides, and
- inhalation during plume passage and following plume passage from resuspension of deposited radionuclides.

Parameters related to emergency response were also varied. Although there is high confidence in emergency response actions, an emergency is a dynamic event with uncertainties in elements of the response. The following three emergency planning parameter sets were selected:

- hotspot and normal relocation criteria,
- evacuation delay, and

¹ The peer review panel did not review the final distributions.

- evacuation speed.

Several of the distributions for non-site-specific MACCS parameters selected for this analysis were based on past expert elicitation data. The United States and the Commission of European Communities conducted a series of expert elicitations in the 1990's to obtain distributions for uncertain variables used in health consequence analyses related to accidental releases of nuclear material. The distributions reflect degrees of belief for non-site specific parameters that are uncertain and are likely to have a significant or moderate influence on the results.

This uncertainty analysis uses a two-step Monte Carlo simulation. Simple random sampling was chosen for MELCOR calculations as some of the results do not converge. 865 of the 900² MELCOR realizations ran to completion. From these complete MELCOR realizations, a family of source term results were produced. Latin hypercube sampling was chosen for MACCS, with a sample size of 865 to match the number of source terms. The MACCS results are presented as individual LCF risk and individual early fatality risk, averaged over the aleatory uncertainty stemming from weather.

Four regression techniques were used in this analysis to estimate the importance of the input parameters with respect to the uncertainty in source terms and consequences: linear rank regression, quadratic regression, recursive partitioning, and multivariate adaptive regression splines (MARS). This analysis provides measures of the effects of the selected uncertain parameters both individually and in interaction with other parameters, and helps:

- Identify which of these uncertain important parameters and phenomena are driving the variability in model results.
- Verify and validate the SOARCA model through exploration of unexpected or non-physical phenomena in the distributions of results.
- Provide an assessment of linear and non-linear regression techniques and the overall uncertainty analysis approach.
- Provide a technical basis for future work.

Results

Performing the source term calculations of the Peach Bottom unmitigated LTSBO uncertainty analysis revealed three groupings of similar accident progression sequences within the Peach Bottom unmitigated LTSBO scenario: (1) early stochastic failure of the cycling SRV, which was the deterministic SOARCA scenario in NUREG-1935; (2) thermal failure of the SRV without main steam line (MSL) creep rupture; and (3) thermal failure of the SRV with MSL creep rupture. The three sequence groups exhibited differences in release magnitude, with MSL failure generally leading to the largest environmental releases. The majority of samples in this uncertainty analysis resulted in larger iodine and cesium releases than the SOARCA project calculated because early stochastic failure of the cycling SRV generally leads to smaller releases. The accident progression path depended on the values sampled for a couple of key

² The other 35 samples that did not run to completion were due to numerical convergence challenges, and not because of any problems with extending the MELCOR model into a larger parameter value domain.

uncertain variables: the SRV stochastic failure rate (the rate at which the SRV fails to close on demand, thereby remaining fully open), and the SRV open area fraction if the SRV fails thermally. The data supporting the input distributions of these two variables is sparse. Similarly, there was considerable uncertainty in the selection of appropriate distributions for other important variables, such as the size of the opening that results from core melt contacting and failing the drywell liner. This uncertainty analysis was most useful in uncovering important influences, and defining the plausible range in accident progression and consequences given uncertainty in the input parameters studied. The relative likelihood of different results within the range, on the other hand, still retains considerable uncertainty given the scarcity of relevant data to support the definition of some key input distributions.

Several influences were found to strongly affect the magnitude and timing of fission product releases to the environment, as summarized below. Most notably, with respect to the magnitude of the source term (the magnitude of cesium and/or iodine releases), the following were found to be influential:

- whether the SRV sticks open before or after the onset of core damage, with higher releases if after core damage, and the SRV open area if the SRV fails thermally rather than stochastically,
- whether MSL creep rupture occurs (largely determined by the two SRV factors above), with higher releases if MSL failure occurs due to fission products being vented straight to the drywell and thus bypassing wetwell scrubbing,
- the amount of cesium chemisorbed (if any) from cesium hydroxide (CsOH) into the stainless steel of reactor pressure vessel (RPV) internals; more chemisorption results in less cesium release to the environment for high-temperature scenarios such as MSL creep rupture,
- whether core debris relocates from the RPV to the reactor cavity all at once or over an extended period of time with relocation all at once leading to lower releases to the environment,
- the degree of oxidation, primarily fuel-cladding oxidation, occurring within the vessel with greater oxidation resulting in larger releases, and
- whether a surge of water from the wetwell up onto the drywell floor occurs at drywell liner melt-through (which depends on the sampled value of the drywell liner open area), with the development of a wetwell water surge leading to larger releases.

With respect to release timing, the strongest influences identified were:

- when the reactor core isolation cooling (RCIC) system fails (determined solely by the time taken to exhaust the station batteries),
- when the SRV fails to reseal, and
- what the open fraction of the SRV is when it fails to reseal if it fails thermally.

Figure ES-1 shows the fraction of the iodine core inventory released to the environment over time, for the 865 samples. For contrast, note the SST1 source term from the 1982 Siting Study (NUREG/CR-2239, "Technical Guidance for Siting Criteria Development") assumed an environmental iodine release starting at 1.5 hours, and steadily rising to a final value of 0.45 by

3 hours (as noted in NUREG-1935 for the SOARCA project). The earliest releases in this uncertainty analysis began after 10 hours, with average (mean) and 95th percentile iodine releases a factor of 10 and 4 smaller, respectively.

Figure ES-2 shows the fraction of cesium core inventory released to the environment over time, for the 865 samples. For contrast, the SST1 source term from the 1982 Siting Study assumed a cesium release starting at 1.5 hours and steadily rising to a final value of 0.67 by 3 hours. The earliest releases in this uncertainty analysis began after 10 hours, with average (mean) and 95th percentile cesium releases a factor of 30 and 7 smaller, respectively.

Table ES-1 shows the distribution of results for the conditional, mean, individual LCF risk using the linear-no-threshold dose-response model. For contrast, the 10-mile LCF risk recalculated for the SST1 source term in NUREG-1935 was more than an order of magnitude higher than the 95th percentile from this uncertainty analysis.

For the conditional, mean, individual LCF risk, within different circular areas (within 10- to 50-mile radii around the plant), the different regression techniques explain 40-85% of the variance in the results, with the recursive partitioning analysis consistently capturing the most variance.

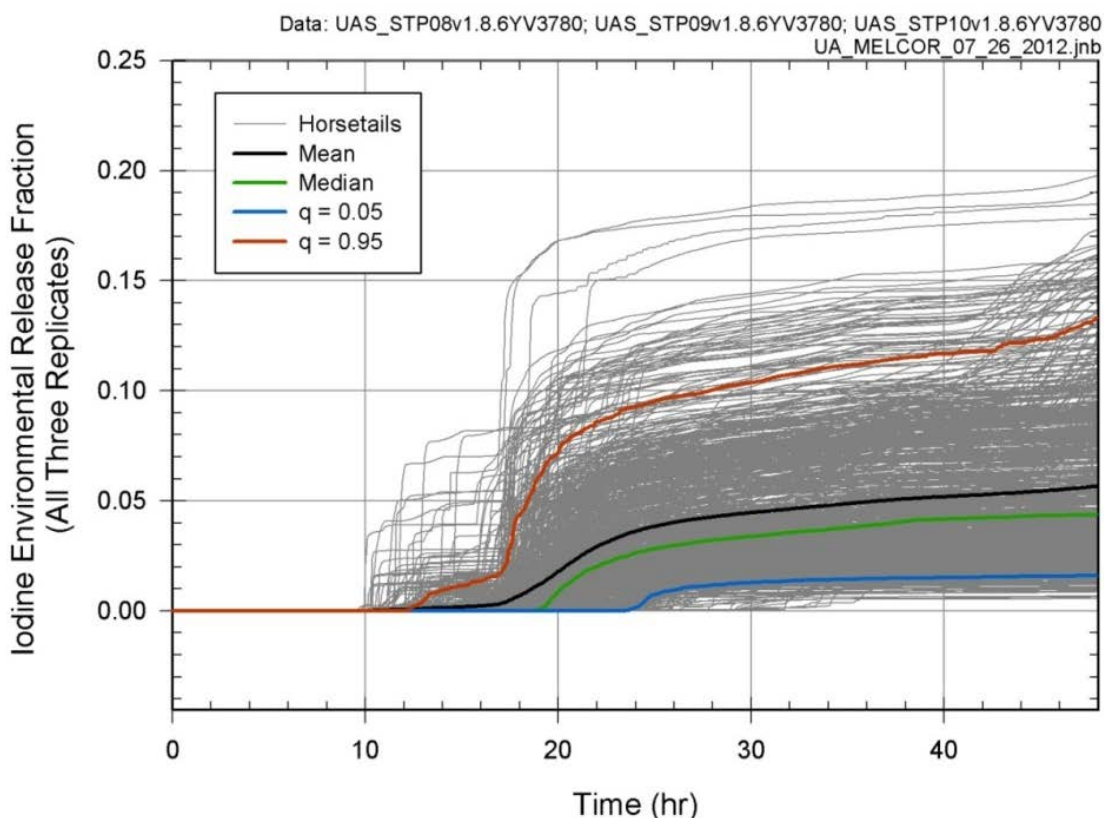


Figure ES-1 Time-dependent fraction of iodine core inventory released to the environment for the first 48 hours for combined (865) results for the Peach Bottom Unmitigated LTSBO

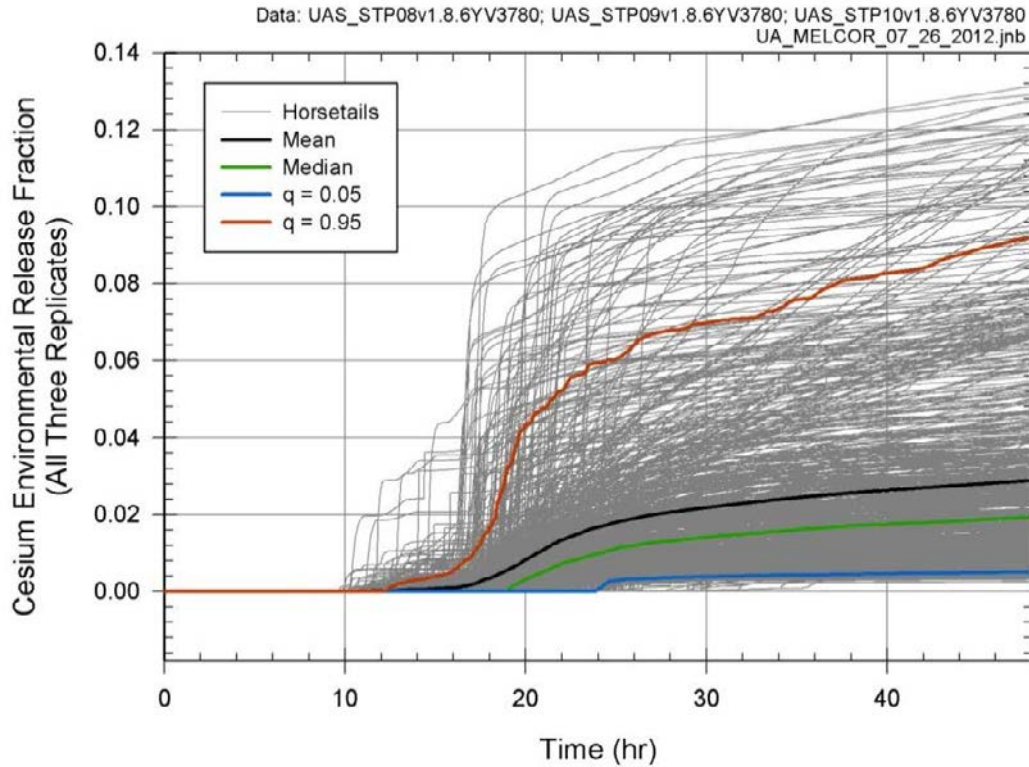


Figure ES-2 Time-dependent fraction of cesium core inventory released to the environment for the first 48 hours for combined (865) results for the Peach Bottom Unmitigated LTSBO

Table ES-1 Conditional³, mean⁴, individual LCF risk (per event) averaged statistics of the MACCS uncertainty analysis for circular areas around the plant, considering all 865 MELCOR/MACCS samples with the linear-no-threshold dose-response model.

	0-10 miles	0-50 miles
5th percentile	3×10^{-5}	2×10^{-5}
Median	1×10^{-4}	7×10^{-5}
Mean	2×10^{-4}	1×10^{-4}
95th percentile	4×10^{-4}	3×10^{-4}
SOARCA UA Base Case	9×10^{-5}	3×10^{-5}

³ Note that the scenario frequency is $\sim 3 \times 10^{-6}$ per reactor-year as documented in NUREG-1935.

⁴ The 'mean' within this context is in reference to the expected value over sampled weather conditions representing a year of meteorological data and over the entire residential population within a circular region. This is also applicable for early-fatality risk results.

All regression methods consistently rank the following parameters as the most important input variables for LCF risk:

- The MACCS dry deposition velocity,
- The MELCOR SRV stochastic failure rate, and
- The MACCS risk factor for cancer fatality for the 'residual' organ⁵.

The following additional variables also consistently showed some level of importance at all circular areas in at least one of the regression methods:

- The MELCOR fuel failure criterion,
- The MELCOR drywell liner melt-through open area,
- The MACCS dose and dose-rate effectiveness factor for the 'residual' organ.

These six variables alone account for 25%-75% of the variance in individual LCF risk results using the different regression methods. In other words, of the hundreds of variables included in this uncertainty analysis, a handful of variables drove most of the uncertainty in the consequence results. The MELCOR variables included those that were responsible for much of the variance in the source term (environmental releases). The MACCS dry deposition velocity describes how fast radionuclides deposit on the ground, and groundshine is the major contributor to long-term doses. While wet deposition (during precipitation events) more rapidly deposits radionuclides on the ground, the wet deposition parameters are not as important because precipitation occurs only ~7% of the time at the Peach Bottom site. The MACCS risk factor for cancer together with the dose and dose-rate effectiveness factor determine the potential lethality of a given dose assuming the linear-no-threshold dose response model.

Conclusions

In explaining the variations in possible source terms and consequences, the use of more advanced non-linear regression techniques proved to be advantageous because they capture interaction effects and non-monotonic effects missed by the linear rank regression technique. Interaction effects among variables and non-monotonic effects are common in complex systems, such as nuclear power plant systems and environmental factors during and after a severe accident. Furthermore, the use of select single-realization analyses (analyzing the MELCOR and MACCS results of one Monte Carlo sample) in this uncertainty analysis proved useful in validating the results of the statistical regression analyses through phenomenological explanations.

The uncertainty analysis documented in this NUREG/CR corroborates the SOARCA project (NUREG-1935) conclusions with the following:

- Public health consequences from severe nuclear accident scenarios modeled are smaller than those projected in NUREG/CR-2239.
- The delay in releases calculated provide more time for emergency response actions (such as evacuating or sheltering).

⁵ The 'residual' organ is represented by the pancreas and is used to define all latent cancers not specifically accounted for in the MACCS model. The pancreas is chosen to be a representative soft tissue.

- “Essentially zero” absolute early fatality risk is projected:
 - The mean absolute early fatality risk is on the order of 10^{-12} per reactor-year⁶ within one mile of the plant boundary, and even this minute risk is based on less than 13% of 865 samples having a non-zero calculated risk; 87% had zero (no) risk.
- The long-term phase dominates the overall health effect risk within the 10-mile emergency planning zone (EPZ) because the emergency response is expected to be effective prior to the onset of environmental release. More than half the time, the long-term phase is the larger contributor to overall health effect risk beyond the EPZ.
- A major determinant of source term magnitude is whether the SRV sticks open before or after the onset of core damage. Compounding this effect is whether or not MSL creep rupture occurs, which leads to higher environmental releases and consequences.
- Health-effect risks don’t vary as much as the source terms (environmental releases) because people are not allowed to return until doses are below the habitability criterion.
- This analysis confirms the known importance of some phenomena (e.g., the dry deposition velocity in MACCS), and reveals some new phenomenological insights (e.g., the importance of the drywell liner melt-through area in MELCOR).
- The use of multiple regression techniques provides better explanatory power of which input parameters are most important to uncertainty in the results.

⁶ Estimated risks below 10^{-7} per reactor-year should be viewed with caution because of the potential impact of events not studied within the analyses, and the inherent uncertainty in very small calculated numbers.

ACKNOWLEDGMENTS

The contributions from the following individuals in preparing this document are gratefully acknowledged:

Jon Barr	U.S. Nuclear Regulatory Commission	
Richard Chang	U.S. Nuclear Regulatory Commission	
Edward Fuller	U.S. Nuclear Regulatory Commission	
S. Tina Ghosh	U.S. Nuclear Regulatory Commission	Document Co-lead
Jason Schaperow	U.S. Nuclear Regulatory Commission	

Nathan E. Bixler	Sandia National Laboratories	
Jeffrey N. Cardoni	Sandia National Laboratories	
Randall O. Gauntt	Sandia National Laboratories	
Andrew S. Goldmann	Sandia National Laboratories	
Jon C. Helton	Sandia National Laboratories	
Joseph A. Jones	Sandia National Laboratories	
Donald A. Kalinich	Sandia National Laboratories	
Patrick D. Mattie	Sandia National Laboratories	Document Co-lead
Douglas M. Osborn	Sandia National Laboratories	
Kyle W. Ross	Sandia National Laboratories	
Cedric J. Sallaberry	Sandia National Laboratories	
Mike F. Young	Sandia National Laboratories	

Mark T. Leonard	Dycoda, LLC
Deborah Phipps	Nuclear Regulatory Support Services

ACRONYMS

BEIR	Biological Effects of Ionizing Radiation
BWR	boiling-water reactor
CC	correlation coefficient
CCDF	complementary cumulative distribution function
CDF	cumulative distribution function
DC	direct current
DCF	dose conversion factor
DDREFA	dose and dose rate effectiveness factor
EPDM	ethylene propylene diene methylene
EOP	emergency operating procedure
EPA	Environmental Protection Agency
EPZ	emergency planning zone
ETE	evacuation time estimate
FTC	failure to close
GUI	graphical user interface
HPCI	high-pressure coolant injection system
HPS	Health Physics Society
ICRP	International Commission on Radiological Protection
IPE	Individual Plant Examination
ISLOCA	Interfacing System Loss-of-Coolant-Accident
LHS	Latin hypercube sampling
LET	linear energy transfer
LNT	linear no threshold
LOCA	loss-of-coolant accident
LTSBO	long-term station blackout
MACCS	MELCOR Accident Consequence Code System
MSL	main steam line
MCCI	molten core-concrete interactions

NA	Not Applicable
NCRP	National Council on Radiation Protection and Measurements
NPP	nuclear power plant
NRC	U.S. Nuclear Regulatory Commission
OROs	Offsite Response Organizations
PAGs	Protective Action Guidelines
PCC	partial correlation coefficient
PDF	Probability Density Function
PIRT	Phenomena Identification and Ranking Table
PRA	Probabilistic Risk Assessment
PRCC	partial rank correlation coefficient
PWR	pressurized-water reactor
RCIC	reactor core isolation cooling
RCS	reactor coolant system
RPV	reactor pressure vessel
SAE	Site Area Emergency
SAMG	Severe Accident Management Guideline
SBO	station blackout
SGTR	steam generator tube rupture
SNL	Sandia National Laboratories
SOARCA	State-of-the-Art Reactor Consequence Analyses
SRC	standardized regression coefficient
SRRC	standardized rank regression coefficients
SRV	safety relief valve
SSE	sum of square error
STSBO	short-term station blackout
USBGR	U.S. background

1. INTRODUCTION

This document describes the U.S. Nuclear Regulatory Commission's (NRC's) uncertainty analysis of the accident progression, radiological releases, and offsite consequences for the State-of-the-Art Reactor Consequence Analyses (SOARCA) unmitigated long-term station blackout (LTSBO) severe accident scenario at the Peach Bottom Atomic Power Station.

The SOARCA project [1] estimated the outcomes of postulated severe accident scenarios which could result in release of radioactive material from a nuclear power plant (NPP) into the environment. The SOARCA report [1] documents the outcomes of severe reactor accidents using an internally-consistent, integrated model of accident progression and offsite consequences. The SOARCA model is based on current best practices that are used to estimate offsite consequences of important classes of events. SOARCA couples the deterministic "current-state-of-knowledge estimate" modeling of accident progression (i.e., reactor and containment thermal-hydraulic and fission product response), embodied in the MELCOR code with modeling of offsite consequences in the MELCOR Accident Consequence Code System (MACCS). This uncertainty analysis presents the results of an analysis of epistemic uncertainty associated with the accident progression and offsite consequence modeling.

1.1 Background of the SOARCA Project

The evaluation of accident phenomena and offsite consequences of severe reactor accidents has been the subject of considerable research by the NRC, the nuclear power industry, and the international nuclear energy research community. Recently, with NRC guidance and as part of plant security assessments, updated analyses of severe accident progression and offsite consequences were completed [1]. These analyses were detailed in terms of the fidelity of the representation of facilities and emergency response, realistic in terms of phenomenological models and procedures, and integrated in terms of the coupling between accident progression and offsite consequence models.

The results of these previous studies confirmed and quantified what was suspected but not well quantified: that some past studies were sufficiently conservative to the point that predictions were not useful in characterizing results. The calculation of risk attributable to severe reactor accidents should consider realistic estimates of the more likely outcomes and should incorporate both the many improvements to NPPs and improved understanding of severe accident behavior. Moreover, improvements in plant design and construction, better understanding of accidents and their consequences, and realistic modeling should be appropriately communicated.

In addition to the improved understanding and calculational capabilities that have resulted from these studies, many influential changes have occurred in the training of operating personnel and the increased use of plant-specific capabilities. These changes include the following:

- The transition from event-based to symptom-based emergency operating procedures (EOPs) for the boiling-water reactor (BWR) and pressurized-water reactor (PWR) designs.
- The performance and maintenance of plant-specific probabilistic risk assessments (PRAs) that include a spectrum of accident scenarios.
- The implementation of plant-specific, full-scope control room simulators to train operators.

- An industry wide, owners-group-specific guidance, and plant-specific implementation of the severe accident management guidelines (SAMGs).
- Additional safety enhancements, described in Title 10, Section 50.54(hh) of the Code of Federal Regulations (10CFR50.54(hh)). These enhancements are intended to be used to maintain or restore core cooling, containment integrity, and spent fuel pool cooling capabilities under the conditions associated with the loss of large areas of the plant due to explosions or fire and include strategies for use in the following areas: (i) firefighting; (ii) operations to mitigate fuel damage; and (iii) actions to minimize radiological release. Successful implementation of this equipment and associated procedures could possibly: (i) prevent core damage or (ii) delay or prevent radiological release, which is reflected in the SOARCA scenarios.
- Improved understanding of the underlying phenomena that result in influential processes such as the following:
 - in-vessel steam explosions
 - Mark I containment drywell shell attack
 - dominant chemical forms for fission products
 - direct containment heating
 - hot-leg creep rupture
 - reactor pressure vessel (RPV) failure and molten core-concrete interactions (MCCI).

Additional changes in plant operation have occurred over time, including the following:

- power uprates
- higher core burnups.

The SOARCA project, conducted by the NRC and Sandia National Laboratories (SNL), was a research effort to realistically estimate the outcomes of postulated severe accident scenarios that might cause a NPP to release radioactive material into the environment.

SOARCA [1] conducted an in-depth analysis of two operating NPPs: Peach Bottom, a BWR, and Surry, a PWR. SOARCA used computer modeling techniques to understand how a reactor might behave under severe accident conditions, and how a release of radioactive material from the plant might impact the public. Specifically, SOARCA used MELCOR (i.e., an integral severe accident analysis code) to model the severe accident scenarios within the plant, and MACCS (i.e., a radiological consequence assessment code) to model the offsite health consequences for atmospheric releases of radioactive material.

In determining realistic consequences of postulated severe accidents, SOARCA relied on many years of previous national and international reactor safety research. The NRC, the U.S. Department of Energy, the nuclear power industry, and international nuclear safety organizations have extensively researched plant responses to hypothetical scenarios that could damage the reactor core or the containment. This research has significantly improved the NRC's ability to analyze and predict how nuclear plant systems are likely to respond to severe accidents, and how accidents progress. In addition, NPP owners have continually improved safety by enhancing their plant designs, emergency procedures, inspection programs, and operator training. Plant owners and local governments have also refined and improved emergency preparedness to further protect the public in the highly unlikely event of a severe accident. Finally, the NRC has incorporated insights from health physics organizations and employed both the linear-no-threshold model and alternate linear-with-threshold (dose truncation) dose-response models for analyzing health effects.

SOARCA incorporated the accumulated research and plant operations and design enhancements to integrated computer models. These models consider onsite and offsite actions, including the implementation of mitigation measures and protective actions for the public such as evacuation and sheltering that may prevent or mitigate accident consequences. These SOARCA calculations, results, and conclusions are documented in NUREG-1935, "State-of-the-Art Reactor Consequence Analyses (SOARCA) Report" [1], and NUREG/CR-7110, Volume 1, "State-of-the-Art Reactor Consequence Analyses Project Volume 1: Peach Bottom Integrated Analysis" for the Peach Bottom pilot plant [2].

1.2 SOARCA Comparison and Contrast with Fukushima Accidents

The SOARCA analyses [2] of station blackout accidents in Peach Bottom were performed several years before the accidents at Fukushima occurred and as such, were anticipatory of the real-world events that occurred in the three accidents at Fukushima as evident from comparisons highlighted in the following. The Fukushima accidents were all variants of either the long-term or short-term station blackout scenarios identified in the SOARCA Peach Bottom study. The SOARCA study summary report (NUREG-1935) includes an appendix comparing a few key aspects of the Fukushima accidents to the SOARCA scenarios. The following are some informative contrasts and comparisons between the Peach Bottom station blackout analyses and observations from the Fukushima accidents and MELCOR analyses of these accidents performed more recently [3]. Shown below on Figure 1-1 is the RPV pressure predicted by MELCOR for the Peach Bottom LTSBO (left) compared with the observed and predicted pressure response for the Fukushima Unit 3 accident (right). Both sequences are considered "long-term" owing to the availability of direct current (DC) power at the start of the accident. At a glance, both pressure signatures show similar overall characteristics starting with RPV at the safety relief valve (SRV) setpoint with reactor core isolation cooling (RCIC) operating, a period of RPV depressurization before loss of turbine-driven injection to the RPV, a period where the RPV returns to the SRV setpoint and a final stage where RPV depressurization takes place as core damage ensues.

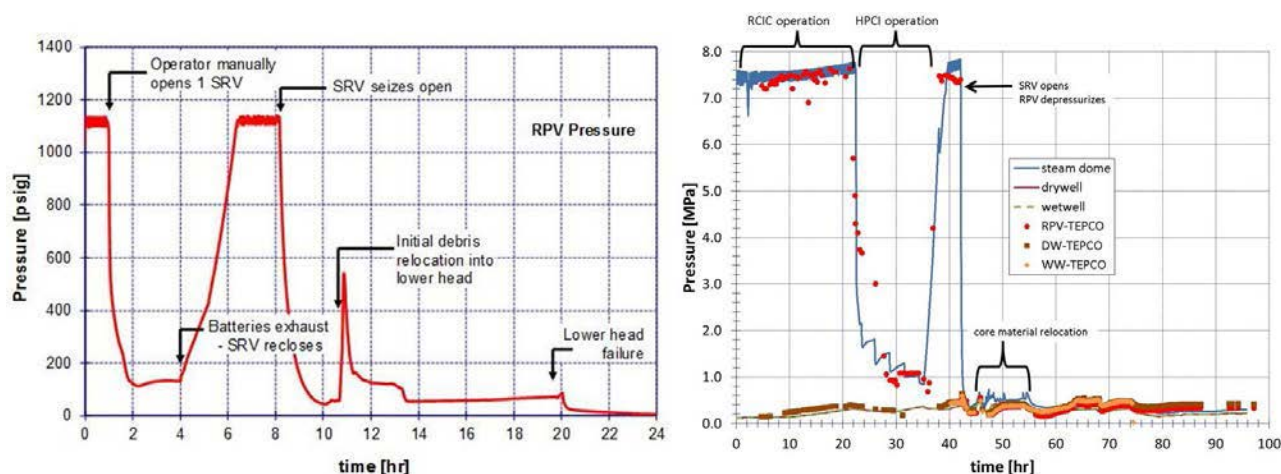


Figure 1-1 Comparison of Peach Bottom Long Term Station Blackout RPV Pressure (left) and Fukushima Unit 3 accident (right, [3])

The overall signatures of the accidents are strikingly similar, where differences are due to differences in the accident management actions taken in the simulated SOARCA analyses and the real-world event. Firstly, in the SOARCA LTSBO after approximately one hour the operators are assumed to open an SRV to drop the RPV pressure as RCIC maintains water level in the core using the available DC power to power the SRV and regulate water level, following EOPs.

In contrast, in Fukushima Unit 3, the RPV remains at the SRV setpoint for more than 20 hours as the RCIC system operates, and it is not until the operators engage the high-pressure coolant injection system (HPCI) following RCIC shutdown that the RPV pressure is reduced. In the SOARCA LTSBO, battery depletion leads to SRV closure and a return to the SRV setpoint along with an assumed loss of RCIC function, similar to when the HPCI system in Fukushima Unit 3 shuts down and terminates the steam draw from the Unit 3 RPV. In the SOARCA LTSBO, after returning to full RPV pressure with SRV's cycling, one SRV is assumed to seize open causing RPV depressurization and concurrent water level loss and core damage. In Fukushima Unit 3, the RPV also depressurizes after cycling for a while as water level loss and core damage is likely occurring due to HPCI shut down. This depressurization in Fukushima Unit 3 has been assumed due to operator actions taken to allow low pressure water injection, an action not modeled in the SOARCA LTSBO owing to battery depletion and no additional assumed operator actions. Both signatures exhibit features of core degradation after this. It is notable that only 4 hours of battery life was assumed with no remedial actions taken to restore DC power in the SOARCA analysis, whereas in the Fukushima Unit 3 sequence of events, operators refresh batteries to allow ongoing emergency operations to continue.

The same SOARCA LTSBO pressure signature is shown below in Figure 1-2 compared with the Fukushima Unit 2 accident. Both accidents begin similarly with RPV pressure at the SRV setpoint and RCIC running. For the first approximately 40 minutes in the Fukushima Unit 2 accident, DC power is available to regulate water level, but after the arrival of the tsunami, all DC power is lost and RCIC operation proceeds without level information or ability to regulate RCIC operation. In the SOARCA model for Peach Bottom, such loss of DC power would result in RCIC flooding water into the steam line and an assumed failure of the RCIC pump. However, while it is currently believed that steam line flooding did occur in Fukushima Unit 2 due to unregulated RCIC operation, it is also apparent that RCIC failure did not follow as a result of this flooding. Instead, the two-phase flow of steam and water through the RCIC turbine is thought to have produced the RPV depressurization below the SRV setpoint that was observed between about 5 hours and through the time of apparent RCIC failure at about 67 hours. As in the Unit 3 accident, assumed operator depressurization following RCIC failure and water level loss is observed followed by emergency procedures for low pressure water injection and some degree of core damage. The SOARCA analyses generally and conservatively did not model such extended EOPs.

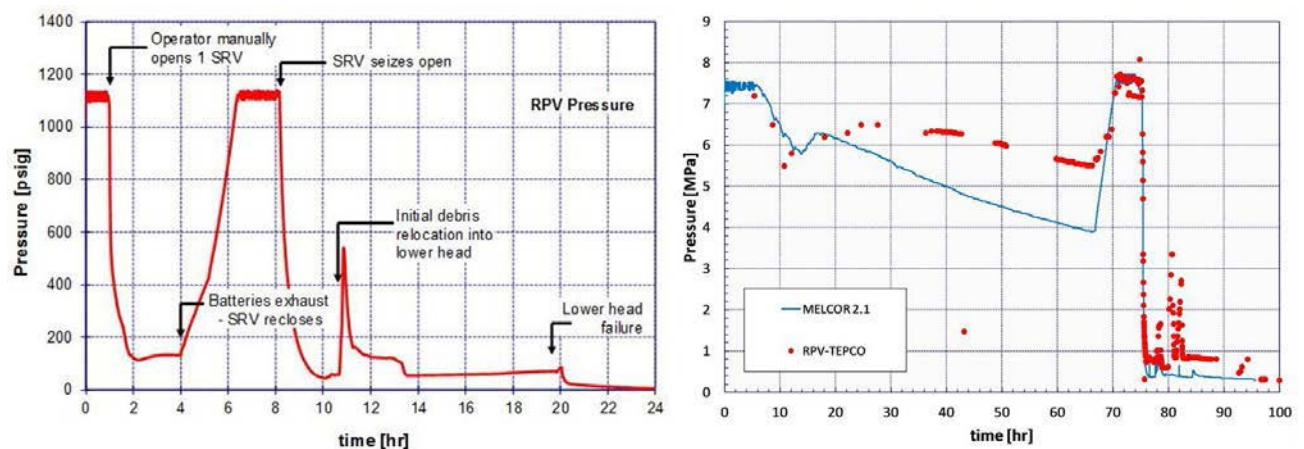


Figure 1-2 Comparison of Peach Bottom Long Term Station Blackout RPV Pressure (left) and Fukushima Unit 2 accident (right, [3])

These comparisons⁷ highlight some of the common system responses modeled by the MELCOR code for the Peach Bottom station blackout analyses and consistently observed in the Fukushima real-world events. The main differences being due to unappreciated extended operability of RCIC turbine operation and additional EOP measure for engaging low pressure water injection following manual RPV depressurization. Accident details such as those observed at Fukushima can of course be modeled by the MELCOR-SOARCA methodology.

Another difference observed between SOARCA Peach Bottom station blackout (SBO) analyses and the Fukushima accidents is with respect to containment failure mode and hydrogen behavior. The SOARCA analyses of Peach Bottom, a significantly larger reactor compared with the Fukushima reactors, consistently predicted drywell liner failure following vessel lower head failure and release of core material to the drywell cavity, caused by contact between core materials and the steel liner of the containment. This resulted in containment depressurization and release of hydrogen to the torus room at a low elevation in the reactor building.

In contrast, at least for Fukushima Unit 1, such liner failure was not predicted by MELCOR analyses and instead a long-term pressurization of the drywell/wetwell containment was predicted, eventually producing gross leakage at the drywell head flange, releasing hydrogen to the refueling bay at the highest elevation of the reactor building. Evidence (i.e., protracted high containment pressure and video of the hydrogen explosion) from the Fukushima Unit 1 observations supports this modeling prediction. Shown below in Figure 1-3 are hydrogen/steam concentrations that are predicted by MELCOR for the Peach Bottom short-term station blackout (STSBO) (left) and Fukushima Unit 1 (right). Because of the predicted drywell liner failure and resulting release of hydrogen in the torus room, a sequence of hydrogen burns are predicted for the torus room as flammable conditions are encountered. In contrast, the predicted conditions for the refueling bay in Fukushima Unit 1 suggest that inert conditions were maintained due to high steam concentrations, in spite of continuous leakage of hydrogen into the refueling bay through the leaking drywell head flange between 15 and 24 hours into the accident. Flammable conditions are not predicted until after 24 hours when containment venting and cessation of water injection leads to a decrease in steam leakage to the refueling bay, whereupon a large hydrogen explosion was observed to have taken place at about 25 hours.

⁷ While other phenomena, such as recirculation pump seal leakage and lower head penetration failure, have been proposed, they are not modeled in [3.] Gauntt, R.O., et al., SAND2012-6173, "Fukushima Daiichi Accident Study (Status as of April 2012)," Sandia National Laboratories, Albuquerque, NM, 2012.. Future modeling efforts and eventual information from decommissioning of the Fukushima reactors themselves may shed light on the relative importance of these phenomena.

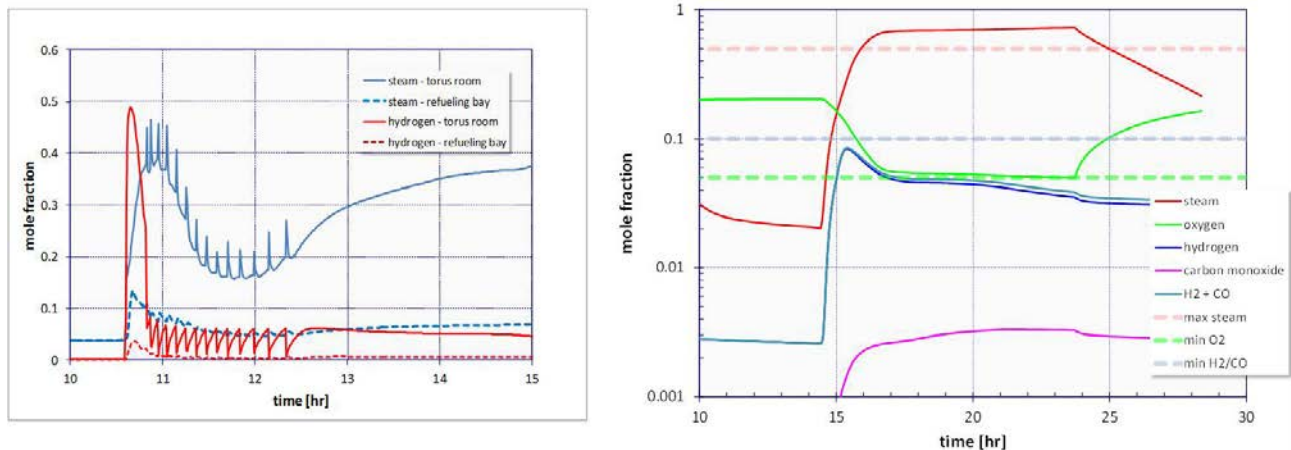


Figure 1-3 Comparison of Peach Bottom STSBO Term Station Blackout hydrogen distribution (left) and MELCOR-predicted Fukushima Unit 1 hydrogen conditions (right, [3])

These comparisons illustrate remarkable consistency in accident sequence progression and overall system response between MELCOR-SOARCA modeling and real-world observations from Fukushima. Differences in the signatures are generally understood and due to differences in operator actions as well as better-than-expected durability of the RCIC turbine driven steam system in the Fukushima accidents. The modeled and observed differences in hydrogen release (i.e., drywell liner failure versus drywell head flange leakage from over-pressurization) are apparently due to modeled differences in corium behavior in the cavity, perhaps attributable to the comparatively larger Peach Bottom core which may have a higher potential to flow and contact the steel liner. The real-world observations from Fukushima are consistent with phenomenology and system responses modeled by MELCOR, and give confidence to the overall findings in the SOARCA studies. In time, additional evidence from the Fukushima reactors will likely shed additional light on other important issues identified in this uncertainty study with respect to potential steam line rupture or SRV seizure occurring under high temperature severe accident conditions that may further inform and clarify MELCOR modeling practices in future severe accident studies.

Recent work [91] has also been conducted in which a comparative assessment of how MELCOR and MAAP5 model in-vessel core damage progression, from onset of core damage to breach of the RPV lower head. The objective of the comparative assessment was the identification of the principal modeling assumptions within the two codes leading to identified simulation differences. Key differences in the modeling assumptions were:

- MAAP5 does not explicitly consider the radial relocation of particulate or molten material during this early phase of core degradation; it is assumed that downward motion of core debris is the primary mode of relocation.
- The two codes use different fuel-failure time-at-temperature failure relationships.
- Particulate debris bed geometries are treated in significantly different manners.
- MAAP5 and MELCOR have different models for the slumping of molten material/debris slumping into the lower plenum.

- The MAAP5 and MELCOR models of lower plenum core debris are conceptually quite different.

1.3 Objectives of the Uncertainty Analysis

The purpose of SOARCA is to evaluate the consequences of postulated severe reactor accident scenarios that might cause a NPP to release radioactive material into the environment. Toward that end, the objective of the SOARCA Uncertainty Analysis is to evaluate the robustness of the SOARCA deterministic results and conclusions, and to develop insight into the overall sensitivity of the SOARCA results to uncertainty in key modeling inputs. As this is a first-of-a-kind analysis in its integrated look at uncertainties in MELCOR accident progression and MACCS offsite consequence analyses, an additional objective is to demonstrate uncertainty analysis methodology that could be used in future source term, consequence, and Level 3 PRA studies. Figure 1-4 provides a general information flow diagram of the uncertainty analysis highlighting specific sections that may be of interest to the reader.

SOARCA included sensitivity studies to examine issues associated with accident progression, mitigation, and offsite consequences for the accident scenarios of interest. The objective of these sensitivity studies was to examine specific issues and ensure the robustness of the conclusions documented in NUREG-1935 [1]. Single sensitivity studies, however, do not form a complete picture of the uncertainty associated with accident progression and offsite consequence modeling. Such a picture requires a more comprehensive and integrated evaluation of modeling uncertainties.

In general terms, the SOARCA offsite consequence results presented in NUREG-1935 [1] incorporated only the uncertainty associated with weather conditions at the time of the accident scenario considered. The reported offsite consequence values represent the expected (i.e., mean, the arithmetic average) value of the probability distribution obtained from a large number of aleatory weather trials. The weather uncertainty is handled the same way in this uncertainty analysis. In addition, the impact of epistemic model parameter uncertainty (the focus of this analysis) is explored in detail by randomly sampling distributions for key model parameters that are considered to have a potentially important impact on the offsite consequences. The objective of this uncertainty analysis is to develop insight into the overall sensitivity of the SOARCA results and conclusions to the combined integrated uncertainty in accident progression (MELCOR) and offsite health effects (MACCS). Assessing key MELCOR and MACCS modeling uncertainties in an integrated fashion, yields an understanding of the relative importance of each uncertain input on the potential consequences.

NRC guidance documents (i.e., Regulatory Guide 1.174 and NUREG-1855) discuss three types of epistemic uncertainty: parameter, model, and completeness. Neither completeness uncertainty nor model uncertainty are not treated in this study. This analysis leverages the existing SOARCA models and software, along with a representative set of key parameters. In other words, the uncertainty stemming from the choice of conceptual models and model implementation is not explicitly explored. The integrated uncertainty analysis is supplemented with limited sensitivity analyses which explore some model uncertainties. In addition, not all possible uncertain input parameters were included in the analysis. Rather, a set of key parameters was carefully chosen to capture important influences on release and consequence results.

A detailed uncertainty analysis was performed for a single-accident scenario rather than all seven of the SOARCA scenarios documented in NUREG-1935 [1]. This work does not include uncertainty in the scenario frequency. The SOARCA Peach Bottom BWR Pilot Plant

Unmitigated LTSBO scenario [2] is analyzed. While one scenario cannot provide a complete exploration of all possible effects of uncertainties in analyses for the two SOARCA pilot plants, it can be used to provide initial insights into the overall sensitivity of SOARCA results and conclusions to input uncertainty. In addition, since station blackouts (SBOs) are an important class of events for BWRs in general, the phenomenological insights gained on accident progression and radionuclide releases may prove useful for BWRs in general. (A second uncertainty analysis is currently underway for one of the SOARCA Surry PWR pilot plant scenarios.)

Section 2.0 outlines the uncertainty analysis approach used to meet the two primary objectives of this analysis: (1) identify the uncertainty in the input parameters used in the SOARCA deterministic analysis and (2) to develop insight into the overall sensitivity of the SOARCA results and conclusions to uncertainty in key modeling inputs by assessing MELCOR and MACCS modeling uncertainties in an integrated fashion to quantify the relative importance of each uncertain input on the potential consequences.

.

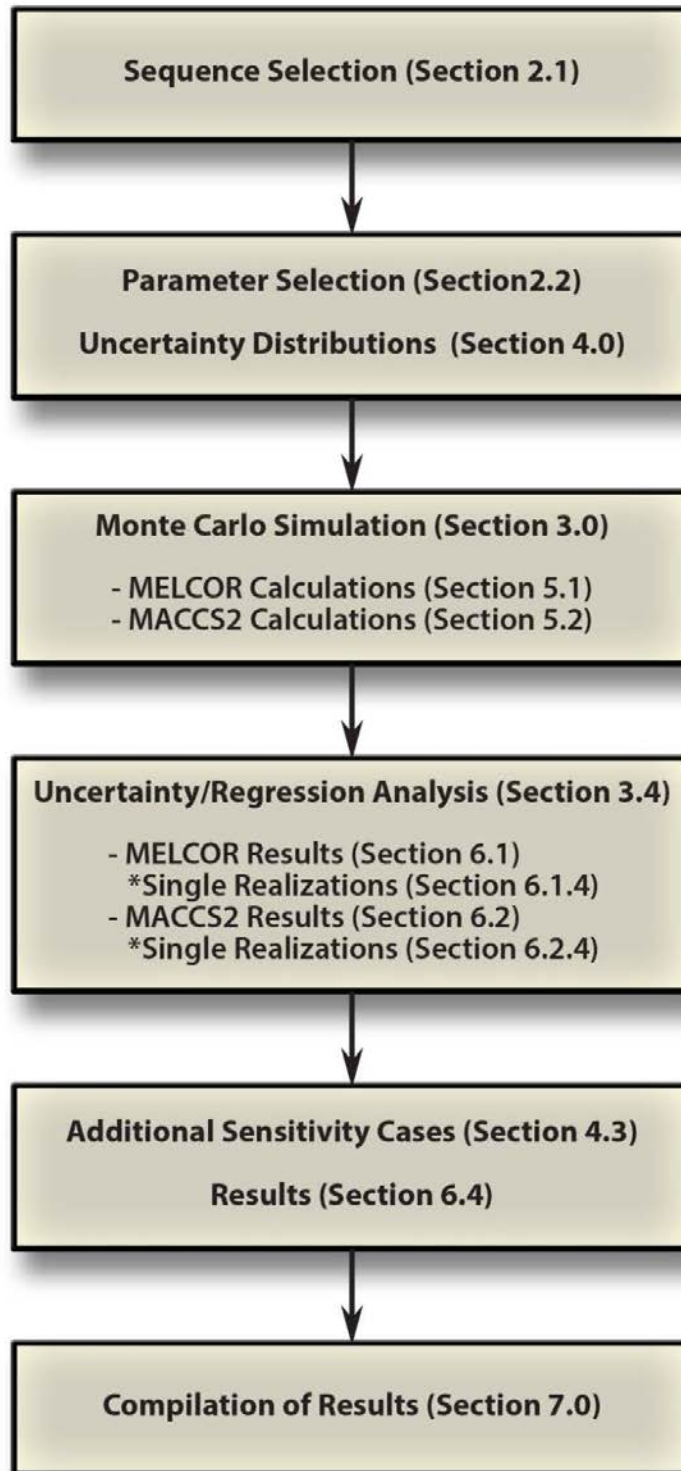


Figure 1-4 SOARCA Uncertainty Analysis Information Flow Diagram

1.4 Uncertainty Analysis Report Outline

Section 2 presents a description of the uncertainty analysis approach including the SOARCA probabilistic analysis methodology. Section 3 includes a description of the probabilistic analysis structure, process and software used. Section 4 describes the uncertainty input parameters for MELCOR and MACCS, respective distributions and technical bases. Section 5 documents the Peach Bottom unmitigated LTSBO “base case” results used in this analysis. In addition, Section 5 includes a demonstration of the convergence of the probabilistic results used in the parameter sensitivity and uncertainty analysis. Section 6 presents the results of parameter sensitivity and uncertainty analysis for source term releases and offsite consequences. Section 7 is a summary of the results and conclusions. Section 8 provides a list of references used in this report.

Appendix A includes a detailed mathematical description of the probabilistic analysis methodology described in Section 2.0 and the parameter sensitivity uncertainty analysis techniques used in Section 6.0. Appendix B includes a detailed description of the software used for the source term and consequence analyses and code integration used for the probabilistic analyses as described in Sections 2.0 and 3.0. Appendix C contains an analysis documenting changes to the SOARCA model and codes necessary for convergence of the probabilistic analysis. Appendix D includes and the SOARCA Uncertainty Analysis team’s responses to individual and group comments contained in the two PRC memoranda on the uncertainty analysis and the ACRS’ final letter on the SOARCA project. Appendix E contains additional information and analyses developed in response to questions from the ACRS for this uncertainty analysis. Appendix F contains a glossary of uncertainty analysis terms, as they are used in this study.

2. UNCERTAINTY ANALYSIS APPROACH

2.1 Accident Scenario Selection

An accident sequence begins with the occurrence of an initiating event (e.g., a loss of offsite power, a loss-of-coolant accident (LOCA), or an earthquake) that perturbs the operation of the NPP. The initiating event challenges the plant's control and safety systems, whose failure might cause damage to the reactor fuel and result in the release of radioactive material. Because a NPP has numerous diverse and redundant safety systems, many different accident sequences are possible depending on the type of initiating event that occurs, which equipment subsequently fails, and the nature of the operator actions involved, as described in the SOARCA study [1, 2]. Individual accident sequences can be grouped into accident scenarios that represent functionally similar sequences. The SOARCA project analyzed a handful of important scenarios in detail. The scenario selection process for the SOARCA project is described in NUREG-1935 [1]. Three accident scenarios were chosen for analysis for Peach Bottom (the BWR pilot plant) and four accident scenarios were selected for Surry (the PWR pilot plant) [1].

The process for selecting a SOARCA scenario for this uncertainty analysis considered both the magnitude and timing of the offsite radionuclide release, which have major impacts on both early and latent cancer fatality risks. The examination of candidate scenarios considered both the timing of core damage and the timing of containment failure.

SBOs are an important class of events for NPPs, especially BWRs, which pointed to both Peach Bottom LTSBO and STSBO scenarios as good candidates. Although the uncertainty analysis was already under way by March 2011, the events at the Fukushima Daiichi plant re-confirmed the interest in SBOs for BWRs. The STSBO has a more prompt radiological release and a slightly larger release compared to LTSBO over the same interval of time. Although it was a more prompt release (i.e., 8 hours versus 20 hours), the STSBO release was delayed beyond the time needed for successful evacuation. In addition, the STSBO frequency is assessed to be approximately an order of magnitude lower than the LTSBO (i.e., $\sim 3 \times 10^{-7}$ per reactor-year (STSBO) versus $\sim 3 \times 10^{-6}$ per reactor-year (LTSBO)). The NUREG-1935 [1] analysis indicated the absolute risk is smaller for the STSBO than for the LTSBO. The same trends apply for the Surry scenarios where the lower-frequency scenarios (the Surry interfacing systems loss of coolant accident (ISLOCA) or the Surry steam generator tube rupture (SGTR)) may have greater conditional risk but absolute risk is assessed to be smaller than or equivalent to other higher-frequency scenarios.

Another factor that influenced the choice of the LTSBO was the ability to explore the impact of parameters that are not evaluated in the STSBO. For example, only the LTSBO could assess the importance of battery life. Additionally, the performance of the SRV as it impacts the main steam line (MSL) failure was an important sensitivity study identified by the peer review committee, assessed in the SOARCA project, and found to be important for the LTSBO scenario. Similarly, choosing the *unmitigated* LTSBO scenario allowed the exploration of the effect of a wider set of physical phenomena and parameters on releases and consequences, since the *mitigated* LTSBO scenario was assessed to have no core damage in the SOARCA project (the unmitigated and mitigated scenarios are defined in the SOARCA project summary report, NUREG-1935 [1]). While it would be interesting to explore the effect of modeling uncertainties on the mitigated scenario results as well, it is expected that human actions – decisions by the Technical Support Center and actions implemented by plant operators – would be a dominant contributor to uncertainties. As with the SOARCA project, a formal human reliability analysis was outside the scope of this uncertainty analysis, making the choice of the mitigated scenario less useful.

As in NUREG/CR-7110 Volume 1, an expected national level response to a severe NPP accident provides a basis for truncating the release no later than 48 hours after the accident begins. Note that past studies, including PRAs such as NUREG-1150, typically truncated releases after 24 hours.

Mitigative actions during an accident are intended to:

- prevent the accident from progressing;
- terminate core damage if it begins;
- maintain the integrity of the containment as long as possible; and
- minimize the effects of offsite releases.

A response to a LTSBO would begin with the onsite emergency response organization and would expand as needed to include utility corporate resources, State and local resources, and resources available from the Federal government, should these be necessary. It is most likely that plant personnel would attempt to mitigate the accident before core melt, but if their efforts were unsuccessful the national level response would provide resources to support mitigation of the source term.

In summary, the Peach Bottom Unmitigated LTSBO was selected based on the rationale that: (1) SBOs are an important class of events for NPPs and BWRs in particular, and the March 2011 Fukushima Daiichi accident further renewed interest in SBOs and (2) the choice of unmitigated LTSBO also allows the exploration of important phenomena and parameters that do not have a part in the Peach Bottom STSBO or Peach Bottom mitigated LTSBO.

2.2 Selection of Uncertain Parameters

A core team of senior staff members from SNL and the NRC was formed with special expertise in probability and statistics, uncertainty analysis, MELCOR modeling, and MACCS consequence analysis. This SOARCA Uncertainty Analysis team collectively has decades of experience with different aspects of severe accident phenomena, accident progression, consequence modeling, and uncertainty analysis methodology. The team also includes the developers of the SOARCA project MELCOR and MACCS models for Peach Bottom (i.e., those who are most familiar with how the influence of various phenomena are captured in the specific Peach Bottom Unmitigated LTSBO models). Furthermore, the team gained additional preliminary insight into the important influences of particular phenomena and parameters through a host of sensitivity studies conducted as part of the SOARCA project itself (many of these sensitivity studies are documented in NUREG/CR-7110 Vol. 1 [2]). In addition to the core team, selected subject matter experts (SMEs) provided support on an as-needed basis and facilitated the reviews of data, parameters, distributions, and their technical bases. The approach to parameter selection focuses on available data and relies on expert judgment, informally using methods used in a more formalized phenomena identification and ranking table (PIRT) process. Expert judgment was used to identify the important phenomena and select parameters. The phenomena and related parameters were not ranked; rather, a consensus approach was utilized to include as many as practicable. An additional difference between the approach used here and a formal PIRT process (or expert elicitation) is that the interim discussions and products were not rigorously documented in this uncertainty analysis. Rather, this NUREG/CR report alone is intended to capture important aspects of the rationale for inclusion of parameters and development of distributions.

The selection of uncertain parameters was a multi-year iterative process. At multiple points in the process, the selected phenomena, parameters, and distributions were technically reviewed

internally at the NRC and SNL. The technical reviews focused on: (1) confirming that the parameter representations appropriately reflect major sources of uncertainty, and (2) ensuring model parameter representations (i.e., probability distributions) are reasonable and have a defensible technical basis. After each review, the selection and technical bases were updated.

In addition, the uncertainty analysis benefited from two interim reviews by the SOARCA Peer Review Committee (PRC) (in addition to the benefit of having feedback from the peer reviewers as part of the overall SOARCA project). Though the uncertainty analysis was outside the original scope of the SOARCA Peer Review charter, the SOARCA team presented the overall UA methodology and approach, and initial selection of parameters and distributions in two separate meetings with the PRC, after each of which the PRC provided feedback via guidance memoranda. In addition, the team held a final teleconference with the PRC on the team's resolutions to peer reviewers' comments on the uncertainty analysis. The peer review is documented in Appendix D, which includes the SOARCA Uncertainty Analysis team's peer review comment resolution report for the two PRC memoranda on the uncertainty analysis. Examples of improvements to this analysis in response to peer reviewer comments include the revision of several parameter distributions, a more careful evaluation of MELCOR parameters that should be correlated, the final selection of weather treatment, and enhanced documentation in this NUREG/CR report.

This uncertainty analysis also benefitted from an interim review by the NRC's Advisory Committee on Reactor Safeguards (ACRS). The uncertainty analysis team presented the uncertainty analysis methodology and overall approach, parameter selection and distributions, and preliminary insights based on MELCOR results, to the ACRS. In its final letter to the Commission on the SOARCA project, the ACRS provided some comments on the uncertainty analysis. Appendix D includes the uncertainty analysis team's responses to uncertainty analysis comments the ACRS' final letter on the SOARCA project. In addition to enhancing the documentation of the uncertainty analysis (in this NUREG/CR report) and the addition of Section 4.3, one notable addition in response to ACRS comments was the inclusion of a sensitivity study for an alternate lower head failure location (see section 6.4.3). Appendix F also includes additional information and analyses developed in response to ACRS comments of this uncertainty analysis, for example on the relative and combined contributions of aleatory (weather) and epistemic MELCOR and MACCS parameter uncertainties, and the convergence of MACCS results.

For this uncertainty analysis, a set of 21 epistemic MELCOR parameters, 20 independent MACCS epistemic parameters, and one MACCS aleatory parameter were selected. A discussion of the importance of and distributions for each selected parameter is provided in Sections 4.1 and 4.2 for the MELCOR and MACCS parameters, respectively. Table 2.2-1 lists all of the uncertain parameters (or parameter groups) in this analysis. Some of the MACCS parameters listed in Table 2.2-1 actually represent a parameter group that contains multiple individual parameters. The MACCS parameters are further defined in Section 4.2, which details the unique epistemic distributions and a set of random aleatory weather trials.

Limitations of the codes and availability of models and or data limited the ability to evaluate some potentially important phenomena in this analysis. Some of these potentially important phenomena and related parameters were evaluated in separate sensitivity studies instead, or discussed qualitatively (see Sections 4.3 and 6.4).

Table 2.2-1 SOARCA uncertain parameter groups

MELCOR	MACCS
Epistemic Uncertainty	Epistemic Uncertainty
<i>Sequence Issues</i>	<i>Deposition</i>
SRV stochastic failure to reclose (SRVLAM)	Wet deposition model (CWASH1)
Battery Duration (BATTDUR)	Dry deposition velocities (VEDPOS)
<i>In-Vessel Accident Progression Parameters</i>	<i>Shielding Factors</i>
Zircaloy melt breakout temperature (SC1131(2))	Shielding factors (CSFACT, GSHFAC, PROTIN)
Molten clad drainage rate (SC141(2))	<i>Early Health Effects</i>
SRV thermal seizure criterion (SRVFAILT)	Early health effects (EFFACA, EFFACB, EFFTHR)
SRV open area fraction (SRVOAFRAC)	<i>Latent health effects</i>
Main Steam line creep rupture area fraction (SLCRFRAC)	Dose and dose rate effectiveness factor (DDREFA)
Fuel failure criterion (FFC)	Mortality risk coefficient (CFRISK)
Radial debris relocation time constants (RDMTC, RDSTC)	Inhalation dose coefficients (radionuclide specific)
<i>Ex-Vessel Accident Progression Parameters</i>	<i>Dispersion Parameters</i>
Debris lateral relocation – cavity spillover and spreading rate (DHEADSOL, DHEADLIQ)	Crosswind dispersion coefficients (CYSIGA)
<i>Containment Behavior Parameters</i>	Vertical dispersion coefficients (CZSIGA)
Drywell liner failure flow area (FL904A)	<i>Relocation Parameters</i>
Hydrogen ignition criteria (H2IGNC)	Hotspot relocation (DOSHOT, TIMHOT)
Railroad door open fraction (RRIDRFAC, RRODRFAC)	Normal relocation (DOSNRM, TIMNRM)
Drywell head flange leakage (K, E, δ)	<i>Evacuation Parameters</i>
<i>Chemical Forms of Iodine and Cesium</i>	Evacuation delay (DLTEVA)
Iodine and Cesium fraction (CHEMFORM)	Evacuation speed (ESPEED)
<i>Aerosol Deposition</i>	Aleatory Uncertainty
Particle Density (RHONOM)	<i>Weather Trials</i>

2.3 Treatment of Uncertainty

In the design and implementation of analyses for complex systems, it is useful to distinguish between two types of uncertainty: aleatory uncertainty and epistemic uncertainty [4, 5, and 6]. It is also important to note that some parameters may have both aleatory and epistemic attributes, but are treated as epistemic for analytic convenience.

Aleatory uncertainty arises from an inherent randomness in the properties or behavior of the system under study. For example, the weather conditions at the time of a reactor accident are inherently random with respect to our ability to predict the future. Other potential examples include the variability in the properties of a population of system components and the variability in the possible future environmental conditions to which a system component could be exposed. Alternative designations for aleatory uncertainty include variability, stochastic, irreducible and type A.

Epistemic uncertainty derives from a lack of knowledge about the appropriate value to use for a quantity that is assumed to have a fixed value in the context of a particular analysis. For example, the pressure at which a given reactor containment would fail for a specified set of pressurization conditions is fixed but not amenable to being unambiguously defined. Other possible examples include minimum voltage required for the operation of a system and the maximum temperature that a system can withstand before failing. Alternative designations for epistemic uncertainty include state of knowledge, subjective, reducible and type B.

The analysis of a complex system typically involves answering the following three questions about the system and one additional question about the analysis itself:

1. What can happen?
2. How likely is it to happen?
3. What are the consequences if it happens?
4. How much confidence exists in the answers to the first three questions?

The answers to questions one and two involve the characterization of aleatory uncertainty, and the answer to question four involves the characterization and assessment of epistemic uncertainty, which is the objective of this analysis. The answer to question three typically involves numerical modeling of the system conditional on specific realizations of aleatory and epistemic uncertainty. The posing and answering of questions one through three gives rise to what is often referred to as the Kaplan/Garrick ordered triplet representation for risk [6].

While not arbitrary, the definitions of aleatory and epistemic uncertainty do depend in a fundamental way on the system under study. This is the concept relating to the “inner weather loop” approach (described below) in evaluating the uncertainty in the SOARCA consequence calculations.

In the modeling system used to generate the SOARCA results [1], weather is treated as an aleatory parameter. Each SOARCA calculation represents the mean offsite consequence for a given accident sequence calculated from a large number of weather trials. In this way, the SOARCA calculation seeks an answer to the question, “What is the expected consequence of a given accident scenario, like a LTSBO, at the Peach Bottom Atomic Power Station?” (i.e., expected outcome over all aleatory sequences— “inner weather loop” approach”) as opposed to, “What is the expected consequence of a given accident scenario during a snow storm in February at the Peach Bottom Atomic Power Station?” (i.e., results conditional on a specific weather trial). While it is certainly feasible to obtain a reasonable estimate of the consequences of a LTSBO at Peach Bottom during any given weather scenario (“outer weather loop” approach), this would not be a useful result, since it is not known what the weather conditions might be during such an event and no amount of additional information and research will serve to reduce that uncertainty.

The SOARCA consequences, including weather uncertainty, are illustrated on Figure 2.3-1. A single source term release, S_{BE} , dependent upon the estimated input, $x_{i, BE}$, was used as input to a consequence analysis dependent upon the estimated input, $y_{i, BE}$. The result is a distribution of consequences conditional on the estimated values (i.e., Question 3 above), over the weather variability (i.e., Question 1 and Question 2 above). The mean value, $||H||$, is the mean consequence over the weather variability. However, to address question four (i.e., “How much confidence exists in the answer to the first three questions?”), a series of analyses must be conducted that quantify the effects of epistemic uncertainty in the system over all possible weather conditions. These concepts are detailed in a mathematical description of the probabilistic analysis in Appendix A.

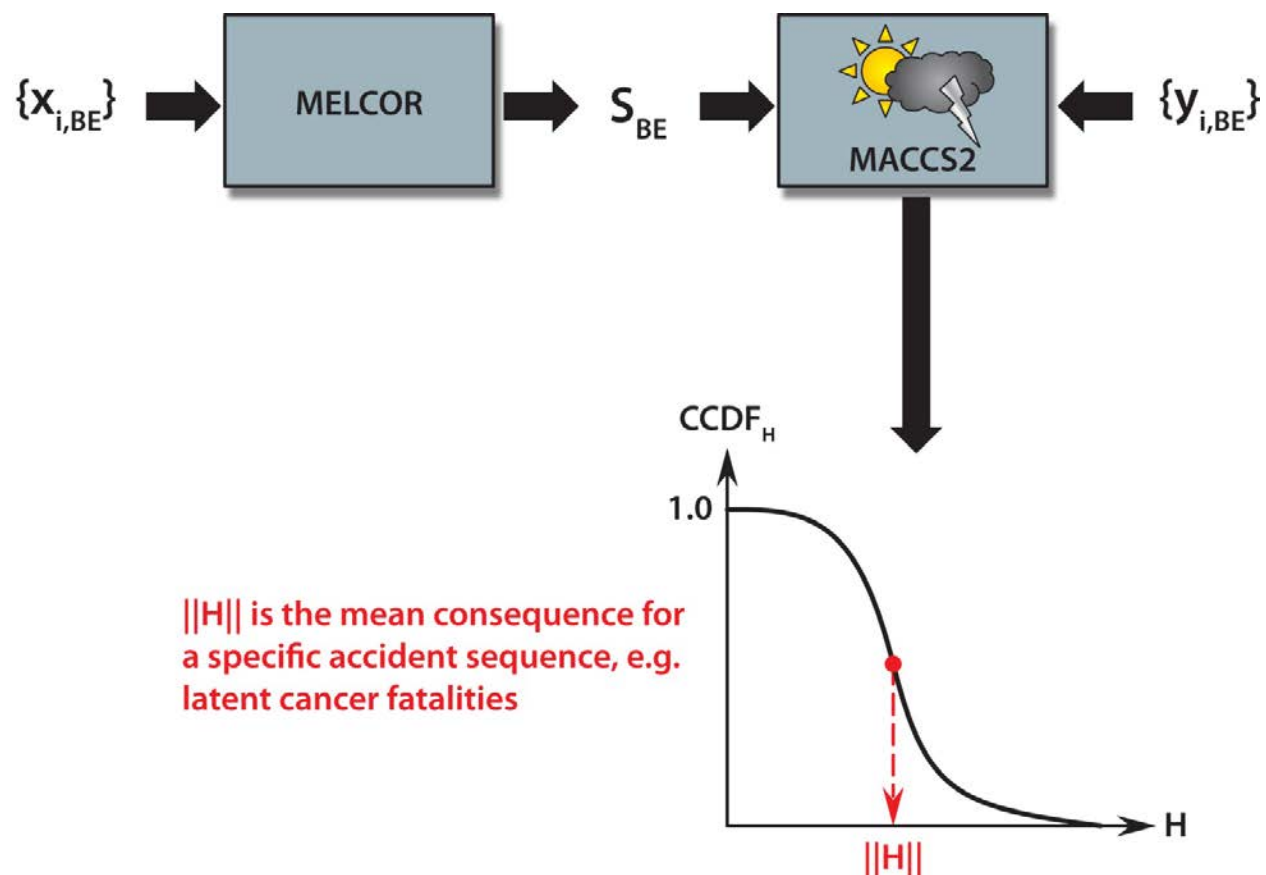


Figure 2.3-1 Typical complementary cumulative distribution function (CCDF) of consequence

3. DESCRIPTION OF ANALYSES

3.1 Software Used

This section briefly discusses the codes used in the integrated probabilistic analyses, including an overview of the integrated analysis and probabilistic calculations used for the parameter uncertainty and sensitivity analysis. To better understand the uses of computer codes that are listed in this section, a brief overview of the software used to calculate the source term and consequence analysis is included in Appendix B. In addition, Appendix B documents the detailed process: the inputs and outputs, information flow, and order of operation for each code used to conduct the integrated probabilistic analysis.

3.1.1 MELCOR

MELCOR is a computer code that models the progression of severe accidents in PWRs and BWRs [7]. MELCOR 1.8.6 YV3780 was used to generate the probabilistic source terms used for the parameter uncertainty and sensitivity analysis documented in Section 6.0 of this report. MELCOR 1.8.6 YR549 was used for the SOARCA Peach Bottom unmitigated LTSBO analysis presented in NUREG 1935 [1] and NUREG/CR 7110, Volume 1 [2]. MELCOR 1.8.6 YV3780 was used for the Surry pilot plant documented in NUREG 1935 [1]. A comparison between the two codes for the Peach Bottom unmitigated LTSBO analysis presented in NUREG 1935 [1] and NUREG/CR 7110, Volume 1 [2], and this uncertainty analysis, is presented in Appendix C.

3.1.2 MELMACCS

MELMACCS compiles MELCOR outputs for transition into a WinMACCS/MACCS (MELCOR Accident Consequence Code System) input [8]. The MELMACCS software is a Windows based program that creates a MACCS radionuclide file from the MELCOR output plot file. The MELCOR plot files contain large amounts of data, only some of which is needed for MACCS calculations. The MELMACCS software provides an interface between MELCOR and MACCS to integrate the required data.

When the SOARCA scenarios, including the Peach Bottom LTSBO scenario in NUREG/CR-7110 [2], were developed, the MELCOR output was converted to a MACCS radionuclide input file using MELMACCS Version 1.5.1. To ensure proper source term continuity between MELCOR and MACCS, a comparison of MELCOR source terms was conducted using MELMACCS Version 1.7.0 and MELMACCS Version 1.5.1 as documented in Appendix C.

3.1.3 MACCS

MACCS [9] can estimate the consequences associated with a release of radioactive material into the environment. Detailed descriptions of the capabilities of the software used in this analysis can be found in Appendix B and the referenced user's manuals [7-9].

The original Peach Bottom Unmitigated LTSBO WinMACCS/MACCS simulation in Section 5.1 of NUREG/CR-7110 Volume 1 [2] was conducted in November 2010. Since this study, MACCS code changes have caused the numerical results for the Peach Bottom LTSBO scenario used in this study to change. These changes have resulted in changes to the conditional, mean (over weather variability), individual LCF risk.

The updates in the MACCS graphic user interface from the version used in NUREG/CR-7110 Volume 1, WinMACCS Version 3.6.2, to the version used for this work, WinMACCS Version 3.6.4, deal with expanding the uncertainty engine. The older version of WinMACCS was not capable of handling the number of MACCS uncertainty distributions required for this study. Also, Version 3.6.2 did not allow certain dose conversion factors (DCFs) to be treated as uncertain. The newest version of WinMACCS, Version 3.6.4, has corrected these problems.

The updates to MACCS from the version used in NUREG/CR-7110 Volume 1, MACCS Version 2.5.0.0, to the version used for this work, MACCS Version 2.5.0.9 deal with the following:

- Provide file locations on MACCS cyclical files (e.g., MELMACCS source term files) to provide enhances traceability between inputs and results,
- Lower plume density limit (PLMDEN) consistent with the MACCS User Manual [9],
- Change to a FORTRAN compiler compatible with the Windows 7 operating system, and
- Correction of the NRC Regulatory Guide 1.145 plume meander model [10], which is not used in the SOARCA scenarios.

A comparison between the two codes for the Peach Bottom unmitigated LTSBO analysis presented in NUREG 1935 [1] and NUREG/CR 7110, Volume 1 [2] is presented in Appendix C.

3.2 Code Integration

A description of the elements and processes (e.g., codes and files) used to implement the integrated probabilistic analysis is provided in this section. Figure 3.2-1 shows the information flow of the SOARCA Uncertainty Analysis. A description of each item on Figure 3.2-1 is described in Appendix B.

- Uncertain MELCOR and MACCS parameters are sampled
- MELCOR is run for each set of its sampled values
- MACCS is run for each set of its sampled values in conjunction with the associated MELCOR source term outputs

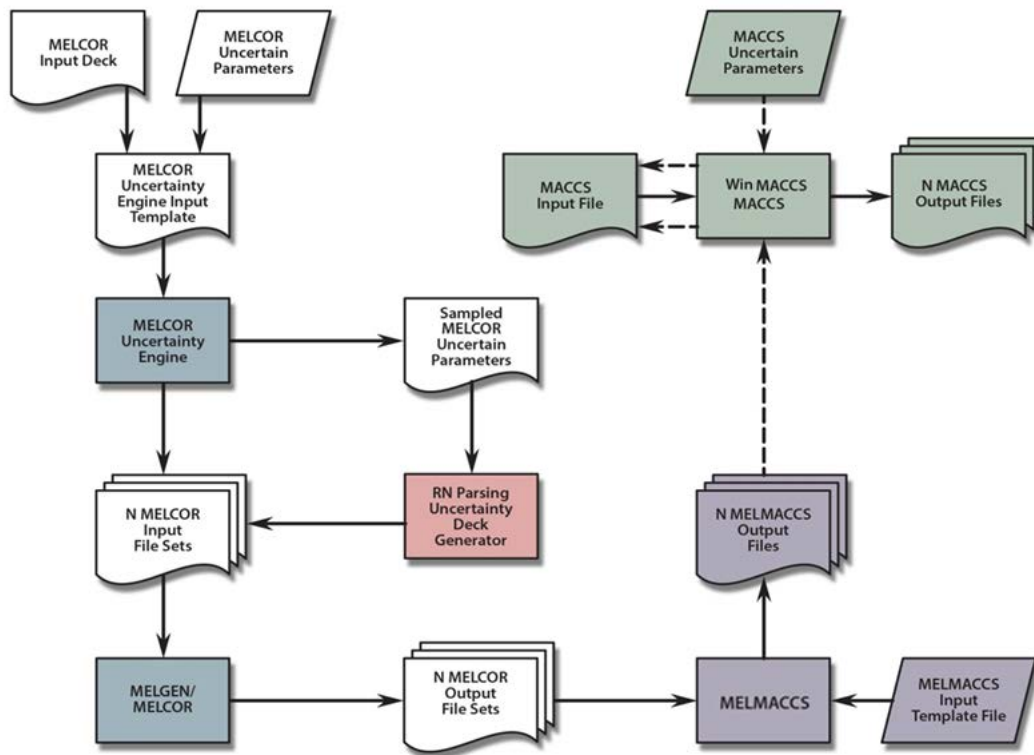


Figure 3.2-1 Diagram of the information flow of the SOARCA Uncertainty Analysis

3.3 Probabilistic Model Calculation for Uncertainty Analysis

This section outlines the calculation of the simulated source term releases and offsite consequences documented in Section 5.0 and used in the uncertainty analysis presented in Section 6.0. Appendix A presents the formal derivations for the calculation.

3.3.1 Source Term Uncertainty Calculations

Probability distributions for the selected uncertainty parameters are documented in Section 4.1 for the source term model calculations. In concept, the probability distributions of analysis outcomes over the uncertainty are defined by integrals over the sample space defined by the uncertain analysis inputs. In practice, such integrals are too complex and are approximated with sampling-based procedures. Latin hypercube sampling (LHS) is usually preferred over simple random sampling (SRS) for its potential of producing more stable results using fewer samples. However, SRS was chosen for MELCOR calculations as some of the results do not converge (addressed in Section 5.1.2). If LHS were employed, distributions of analysis outcomes with non-convergence issues would need to account for an input sample set with stratification that was incomplete. Using the MELCOR uncertainty engine, three replicate sample sets using an initial size of 300 using SRS have been generated for the group of 21 epistemic parameter distributions, using a different random seed for each replicate set. Each sample set was used to produce a unique distribution of analysis outcomes using MELCOR. Model calculation progresses as described in Section 3.2. A family of source term results is produced that forms the basis for analysis of the uncertainty in the system. As SRS has been used to generate all three samples, it is valid to assemble results from the three separate runs into one sample of larger size.

3.3.2 Consequence Analysis Calculations

Probability distributions for selected MACCS parameters are documented in Section 4.2 for the offsite consequence model calculations. Using the LHS technique in the WinMACCS GUI, a sample of size matching the number of converged results for each of the three source term replicates has been generated for the set of 596 epistemically uncertain inputs specific to MACCS calculation (i.e., all 865 MELCOR source terms have 596 epistemically uncertain inputs). For each of the three considered sets, each sample element was paired with a single result of the population generated from the source term (MELCOR) analysis. The stratification used within LHS to propagate uncertainty in MACCS calculations does not easily allow assembling the results from the three separate replicates into a valid larger sample set as can be done with SRS. Consequently, a fourth analysis has been performed with an LHS sample set equal to the total number of converged source term results for all three replicates combined.

For each epistemic sample, aleatory uncertainty about the weather was taken into account by generating 984 weather trials. Calculations were performed for each of these weather trials to construct a family of CCDFs for the corresponding LHS sample set. Model calculation progresses as described in Section 3.2. A family of consequence results is thus produced that form the basis for analysis of the uncertainty in the system.

3.4 Uncertainty and Sensitivity Analysis

In the last step of a probabilistic approach, results are statistically analyzed (via uncertainty analysis) and influence of input parameter uncertainty over the variance of the output is assessed (via sensitivity analysis). Such analyses help to draw insights with respect to the results. Many techniques have been developed to perform such analyses (several are presented in Helton et. al. [11]). The method specifically used in this analysis is presented in detail in Appendix A.2.

3.4.1 Uncertainty Analysis: Purpose and Results Generated

Uncertainty analysis refers to the determination of the uncertainty in analysis results that derives from uncertainty in analysis inputs. This corresponds essentially to a statistical analysis of the output set. Most of the results presented in Section 6 are based on uncertainty analysis, as statistics over a range of possible results will give more insights than results from a single realization.

Source term results from MELCOR provide several estimates at each timestep representing the (epistemic) uncertainty due to lack of knowledge in the result of interest. These estimates can be displayed as time-dependent results as shown in the example on Figure 3.4-1).

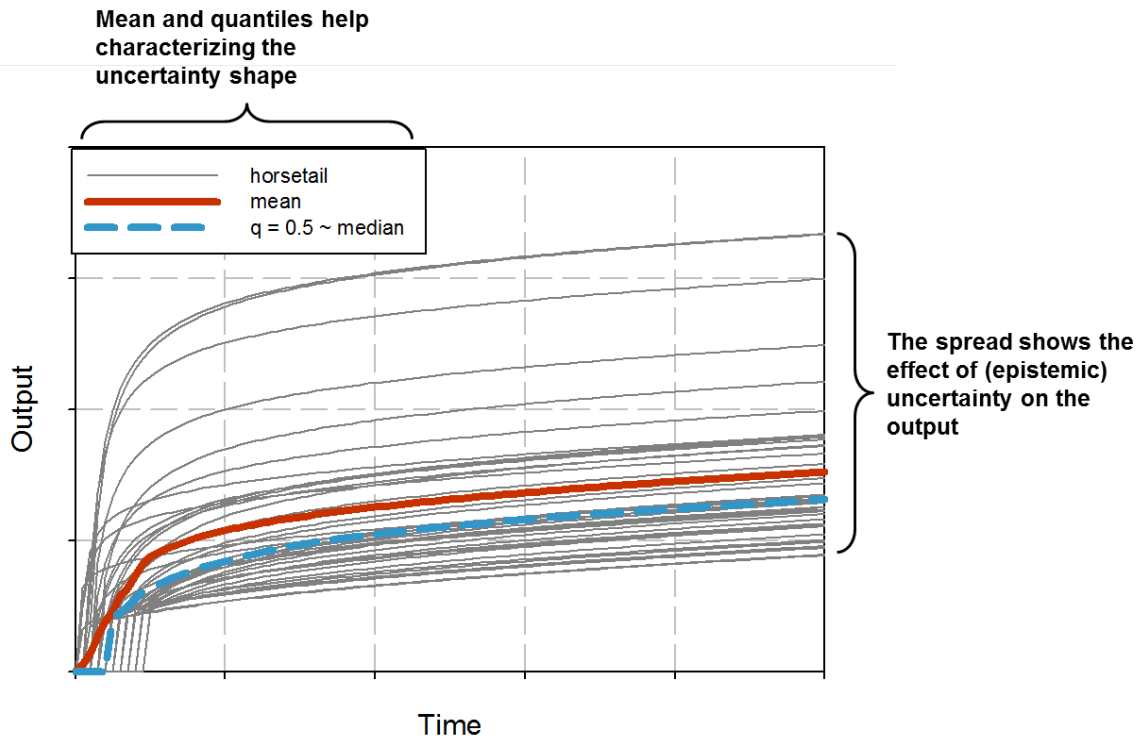


Figure 3.4-1 Time-dependent results reflecting uncertainty due to lack of knowledge (epistemic)

Often, statistics such as mean and quantiles are included in order to give a better visualization of this uncertainty and a graphical summary of the uncertainty. The quantiles selected for this analysis are $q = 0.05$, $q = 0.5$ (median) and $q = 0.95$.

While the preceding representation shows the time dependence of the results, it does not show the shape of a distribution of results. A cumulative distribution function (CDF) or complementary cumulative distribution function (CCDF) of the sampled result at a selected timestep can be more informative. An example is displayed on Figure 3.4-2. The x-axis represents the distribution of possible results and is generated by sorting (from smallest to largest) all the results from the sample of size N at the selected time (for time-dependent results). The y-axis represents the likelihood of being lower or equal (for CDF) or higher (for CCDF) than the value read on the x-axis. When SRS or LHS is used, the likelihood of the outcome is estimated a weight of $1/N$ and increasing the y-value from this weight, starting from zero (for CDF) or decreasing by this weight starting from one (for CCDF). The mean can be added on the curve (as a dot for instance) to the CDF or CCDF. Quantiles can be read directly by finding the corresponding y-value to the graph, or displayed (for a selected quantile) as a dot over the curve.

In risk analysis, it is traditional to plot CCDFs rather than CDFs as they answer the question “how likely it is to have such value or higher”.

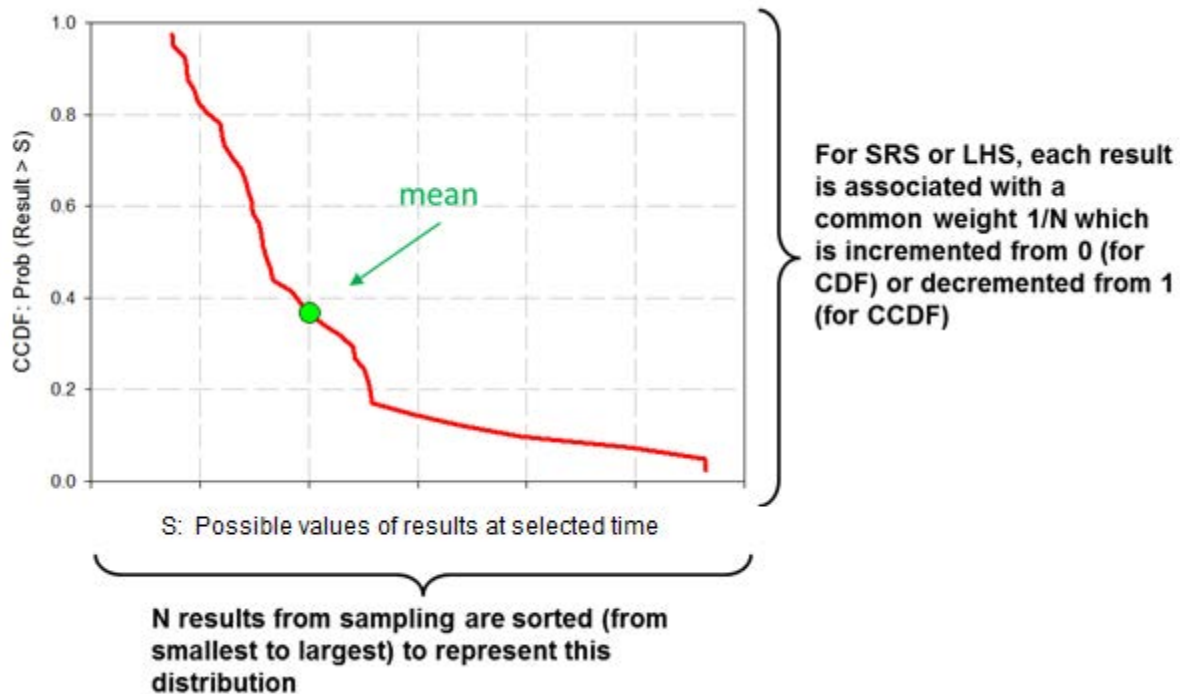


Figure 3.4-2 Distribution of results presented as a complementary cumulative distribution function for a selected time

MACCS results incorporate both aleatory (via consideration of 984 potential weather histories) and epistemic (input parameter) uncertainty. The results presented in Sections 5 and 6 correspond to probability of latent cancer fatality and early fatality. These probabilities are averaged over aleatory uncertainty (weather histories) and therefore represent expected (mean) values over aleatory uncertainty. As a consequence, only the spread and effect of epistemic uncertainty will be displayed, using figures similar to Figure 3.4-1 and 3.4-2.

When low probabilities are estimated, the accuracy of the estimate and its stability may be questionable. The stability of results depends on the selected numerical method (e.g., SRS or LHS) and the parameters used with the method (e.g., sample size, choice of input parameters). Stability of the results used in this analysis is assessed in Section 5 using confidence intervals.

3.4.2 Sensitivity Analysis: Purpose and Results Generated

Sensitivity analysis refers to the determination of the contributions of individual uncertain analysis inputs to the uncertainty in analysis results. Rank regression, quadratic regression, recursive partitioning, and multivariate adaptive regression splines (MARS) are the four regression techniques used in this analysis to estimate the importance of the input parameters in the uncertainty of the output in consideration. A short description of each technique follows. A more detailed description of the techniques (with examples) can be found in [12] and [13].

Rank regression

Rank regression technique consists of using a rank transformation over the input and output variables in consideration. The smallest value of a variable is given a rank of one, the next a rank of two and so on up to the largest value having a rank of nS (i.e. sample size). A stepwise

linear regression is then applied to the rank-transformed data. The model is linear and additive, in the following form:

$$Y = a_0 + a_1X_1 + a_2X_2 + \cdots + a_nX_n + \varepsilon = a_0 + \sum_{i=1}^n a_iX_i + \varepsilon$$

The stepwise approach starts with trying to find the best fit with only one parameter (testing all possible input parameters), then builds up from this by selecting the best fit with two parameters conditional on keeping the first parameter and so on. An alpha value is selected as a criterion below which to stop adding parameters. Rank regression is effective in capturing monotonic (increasing or decreasing) relationships between inputs and outputs. Its non-parametric aspect makes it less sensitive to outliers. This technique is limited to additive models (no conjoint influences are considered) and may perform poorly on non-monotonic relationships.

Three metrics are included for each input variable in the section of the table used to display rank regression results. R^2_{inc} gives the cumulative coefficient of determination of the regression model for the variable including all variables in the table identified before. $R^2_{cont.}$ gives the gain in R^2 due only to the variable. Finally, standardized rank regression coefficients (SRRC) display the result of rank regression coefficients, standardized to take out the unit influence. The rank regression coefficient is an indication of the strength of the influence: an absolute value close to zero means no influence while an absolute value of one represents a very strong influence. The rank regression coefficient also indicates the direction (positive or negative) of the influence of this input variable on the considered output. A negative sign represents negative influence: high values of the input lead to low values of the output and low values of the input lead to high values of the output. A positive sign represents positive influence: high values of input lead to high values of the output and low values of the input lead to low value of the output.

This is a traditional method used in many past analyses, such as NUREG-1150.

Quadratic regression

Quadratic regression technique applies the same approach as linear regression, including individual input variables, the square of these variables and second order multiplicative interaction terms. The prediction model is of the form:

$$Y = a_0 + \sum_{i=1}^n a_iX_i + \sum_{i=1}^n b_iX_i^2 + \sum_{i=1}^n \sum_{j=i+1}^n c_iX_iX_j + \varepsilon$$

Quadratic regression is not completely additive as it can capture second order interactions. It can also capture the parabolic influence measured by the square of variables in the regression model. However, a complex relationship between variables and the output, like asymptotic behavior, may still be hard to capture with this technique and the method remains parametric which makes it sensitive to outliers. As quadratic regression can capture non-monotonic relationships, additional sets of metrics are displayed in the table of regression results from this method. S_i represents the first order sensitivity index and informs on how much of the variance of the selected output is explained by the input parameter in consideration by itself. This index is similar to the $R^2_{cont.}$ presented above for the rank regression technique and it is acceptable to compare the two metrics. The second metric, labeled T_i represents the total order sensitivity index and indicates how much of the variance of the selected output is explained by the input parameter alone and how much by its interaction with the other uncertain parameters. It has no equivalent in the rank regression model (as the additive model does not capture conjoint

influences). The difference between T_i and S_i gives an estimate of the conjoint influence for this input on the output considered. Finally, a p-value is displayed as third metric, representing the probability that the hypothesis $T_i = 0$ is true, meaning that the parameter has no influence at all. A p-value equal or close to zero indicates that the hypothesis is false and therefore, the influence is likely to be true in the mathematical sense. It can still be unrealistic physically and due to the particularity of the sample. A p-value equal or close to one indicates a relationship that is not real and is due to a spurious correlation.

Recursive partitioning

Recursive partitioning regression is also known as a regression tree. A regression tree splits the data into subgroups in each of which the values are relatively homogeneous in. The regression function is constructed using the sample mean of each subgroup. This approach, results in a piecewise constant function over the input space in consideration. Recursive partitioning handles conjoint influences. The predictive model is:

$$Y = \sum_{s=1}^{nP} (d_s I_s(X_i))_{i=1,\dots,n} + \varepsilon$$

The same metrics used for quadratic regression are used for recursive partitioning, that is to say the first order sensitivity indices (S_i), total order sensitivity indices (T_i) and p-values.

Multivariate Adaptive Regression Splines (MARS)

MARS is a combination of (linear) spline regression, stepwise model fitting and recursive partitioning. A regression with a single input starts with a mean only model and adds basis functions in a stepwise manner adding the overall linear trend first. A second model using linear regression via least squares is fit to the data. This model is then added to the basis functions in a way that reduces the sum of square error (SSE) between observation and prediction. A fourth basis function is then added to minimize the SSE again. This process is repeated until M basis functions have been added.

At this point, the MARS procedure will try to simplify the model using stepwise deletion of basis functions, while keeping the y-intercept and linear trend. The M-2 candidate leading to the smallest increase of SSE will be selected. This deletion will be applied until regressed to the original linear model.

Stepwise addition and deletion leads to the building of two different M-2 different models. The “best” model is chosen using a generalized cross validation (GCV) score which corresponds to a SSE normalized by the number of basis functions considered. With multiple inputs, the basis functions will consider main effects and multiple-way interactions. The options used for this analysis consider only two-way interactions to avoid the exponential cost of considering more interactions. MARS are presented using the same metrics as quadratic regression and recursive partitioning in the summary tables.

4. UNCERTAIN INPUT PARAMETERS AND DISTRIBUTIONS

Sections 4.1 and 4.2 provide the technical basis and justification for parameters included as uncertain inputs for the SOARCA Peach Bottom unmitigated LTSBO Uncertainty Analysis. The uncertain parameters and their distributions were identified/characterized through an informal elicitation of subject matter experts. The subject matter experts were asked to define distributions for the parameters which they considered most important in describing the uncertainty around the SOARCA analysis. In addition, the uncertain parameters and distributions were presented to and evaluated by the independent SOARCA peer review panel. The SOARCA Peer Review Panel agreed with the basic methods and provided comments on the selected parameters and distributions. The parameters and distributions were revised to address these concerns. A discussion of the uncertain parameters and distributions are contained in Sections 4.1 and 4.2 for the source term model and consequence model parameters uncertainty, respectively.

The general approach taken in defining the scope of the SOARCA uncertainty quantification is to attain a balanced depth and breadth of coverage so as to obtain contributions from uncertainty across the spectrum of phenomena operative in the analyses without excessive detail dedicated to any particular regime of phenomenon. Both MELCOR and MACCS permit extensive access to parameters that may be uncertain, but for practical reasons, a judiciously selected subset of possible uncertain parameters is proposed that covers the range of phenomena across the stages of a severe accident.

A variety of distribution shapes are chosen to reflect experts' degree of belief in different values for the uncertain parameters. This uncertainty study began with parameter values anchored to the estimates used in the SOARCA study. The team then took a consensus approach to constructing distributions around the SOARCA estimates. For those parameters where the team assessed that values other than the SOARCA estimate were less likely, a probability density function was chosen to reflect a peak at the mode – for example, a triangular or normal shape. If the parameters' range spanned multiple orders of magnitude, a log scale was chosen for the distribution. Or if the parameter was thought to be equally likely to be x times the SOARCA estimate or $1/x$ times the SOARCA estimate, a log scale was chosen. In some cases, as described in Section 4.2, the distributions are based on a prior expert elicitation, or a methodology described in FGR-13 for health effect parameters.

4.1 Source Term Model Uncertainty (MELCOR Inputs)

The MELCOR uncertain parameters are selected to cover the following issues and phenomenological areas:

- sequence issues
- in-vessel accident progression issues
- ex-vessel accident progression issues
- containment behavior issues
- fission product release, transport, and deposition

These broad areas span the temporal domain of the severe accident progression ranging from minor sequence variations as affected by SRV behavior, to uncertainties in the core damage and melt progressions, especially those affecting rate of core degradation and amount of hydrogen generation. Hydrogen production provides an indication of fission product release from the fuel, since hydrogen generation is an indicator of cladding oxidation which is an indicator that fuel temperatures are rising above 1500 K. This is the temperature range where thermally driven release of the volatile fission products, cesium, iodine, and tellurium, occurs.

Source term release behavior in terms of the rate and total amount released in-vessel is strongly coupled to in-vessel melt progression behavior owing to the strong temperature dependence of fission product release. The onset of volatile fission product release is set by the time that fuel is heated to a temperature above about 1500 K (about 1227°C), and this is tightly coupled to cladding oxidation rate. Total release of both volatile and less volatile species is affected by the time at which fuel remains at elevated temperatures and the state of the fuel (rods or debris). Therefore, many of the parameters that affect cladding oxidation and hydrogen generation also affect fission product release. Other parameters more specific to fission product transport include deposition processes (e.g., chemisorption or hygroscopicity) and settling processes (agglomeration shape factors for example). Speciation of cesium and iodine affects the volatility of cesium and consequently affects both release and revaporization. The parameters selected in the study were considered in terms of both melt progression and fission product release and transport. This includes important phenomena taking place following vessel lower head melt-through such as melt attack of the drywell liner, containment behavior issues, such as uncertainty in onset of drywell head flange leakage, and uncertainties in radioactive aerosol transport mechanics. The selection of uncertain parameters ensures a commensurate representation of uncertainties in the major phases of the accident evolution. Each uncertain parameter, together with the rationale for the range and shape of the uncertainty distribution are described in the following sections. All other MELCOR parameters not discussed in this section (e.g., eutectic liquefaction temperature for ZrO_2/UO_2) remain the original point estimates used in NUREG/CR-7110, Volume 1.

Additional discussions on certain MELCOR parameters presented are discussed in Appendix E.

4.1.1 Sequence Issues

Uncertainty in safety relief valve stochastic failure to reclose (SRVLAM)

One concern regarding the timing of the accident sequence is when the depressurization of the reactor coolant system (RCS) occurs. As part of the SOARCA project, the RCS depressurizes resulting from the failure of a SRV. The MELCOR model is setup to cause the SRVs to open at predetermined pressures and specified flow rates. The SRVs will close when pressure drops below 96 percent (%) of their opening pressure. This model sets the SRVs to fail to close based on a per-demand failure probability.

The SOARCA value was cited in the Peach Bottom Individual Plant Examination (IPE) of $\lambda = 3.7 \times 10^{-3}$ per demand [2] or $1/\lambda = 270$ valve cycles. In addition, the Peach Bottom IPE considered a failure rate per-demand probability multiplied by a factor of eight to account for the fact that the valve was operating under extreme environmental conditions (e.g., $\lambda = 2.96 \times 10^{-2}$ per demand or approximately 34 valve cycles).

Recent assessments of component reliability in nuclear systems suggest an SRV failure to close (FTC) frequency may be smaller than the SOARCA value cited in the Peach Bottom IPE. An NRC analysis of industry-average data for SRV FTC performance was documented in two reports: NUREG/CR-6928 [14] and NUREG/CR-7037 [15]. NUREG/CR-6928 computed an estimated per demand failure probability e described in Table 5-1 (SRV FTC - SRV failure to close) with a mean value of $\lambda = 7.95 \times 10^{-4}$ per demand (1,258 cycles) with 5th and 95th percentile values of 3.13×10^{-6} and 3.05×10^{-3} per demand, respectively. NUREG/CR-7037 provides updated failure data for BWR SRVs, depending on their operating mode. The operating mode of interest for SOARCA is the “pressure mode,” where the SRVs are actuated via a pilot sensing port that is internal to the valve (not the air actuator). NUREG/CR-7037 reports a mean value of $\lambda = 1.39 \times 10^{-2}$ /demand (72 cycles) with 5th and 95th percentile values of 4.43×10^{-5} and 5.39×10^{-2} /demand, respectively [15, Table B-7]. However, when all the data

are considered, the NUREG/CR-7037 approach computed a mean value of $\lambda = 7.07 \times 10^{-4}/\text{demand}$ (1,414 cycles) with 5th and 95th percentile values of 2.75×10^{-6} and $2.7 \times 10^{-3}/\text{demand}$, respectively [15, Table B-7], very similar to the reported value from NUREG/CR-6928.

Significant reductions in the observed rate of spurious valve opening were achieved by various modifications to the Target Rock SRV through a BWR Owner's Group initiative coordinated under Generic Safety issue B-55. The extent to which these modifications would also affect the expected failure rates of SRV FTC is not known. However, this might contribute to the difference in the current (NRC) estimated failure rates of SRV FTC and the older (circa 1990) failure rate reflected in the Peach Bottom IPE.

It should be noted, however, that the failure rate reflected in the generic data base and the value obtained from the Peach Bottom IPE are conceptually different from the situation modeled here. In simple terms, the rate at which an SRV fails to reclose is calculated by dividing the number of observed valve failures (to reclose) by the number of valve demands. This ratio, therefore, reflects the conditional probability that a valve would fail to reclose, given a successful demand to open. However, the failure events that represent the numerator of this ratio occurred after only a few valve cycles. The precise number is difficult to determine from the raw data documented in the NUREG/CRs. However, it is clear that valve failure data after numerous cycles are extremely rare (perhaps non-existent) primarily because events involving numerous, continuous valve cycling are not observed. It is, therefore, debatable whether the failure rate used to calculate the (low) probability of failure to reclose after a few cycles should be extrapolated to estimate the (higher) probability of failure after a large number of cycles. Other unknown failure mechanisms would likely overwhelm those that lie behind the nominal failure rate. This qualitative observation is consistent with the opinion expressed by members of the peer review panel that the valve failure rates obtained from the PRA database are too low (e.g., predict a high number of cycles before failure). However, it should be noted that comments provided by the licensee on the NUREG/CR-7110, Volume 1 indicated the early failure rate reported in their IPE was not based on plant-specific performance data, and they have since replaced this value with the industry value reported in NUREG/CR-6928.

A beta distribution, listed in Table 4.1-1, and used for this analysis was fit for the mean value from the Peach Bottom IPE (the SOARCA value) using the methodology in NUREG/CR-7037. For comparison, Figure 4.1-1 plots the CDF for the Peach Bottom IPE derived beta distributions with the NUREG/CR distributions. Qualitatively, the Peach Bottom IPE derived distribution falls within the middle of the set of CDFs. Quantitatively, it is clear from the SOARCA results values above 5×10^{-2} and below 9×10^{-4} per demand will either fail before the batteries are depleted or after SRV will fail from thermal seizure and/or main steam line creep rupture, respectively. The Peach Bottom IPE derived beta distribution covers the range of values that are needed to define the parametric relationship between the probability that the SRV will fail to close and the severe accident.

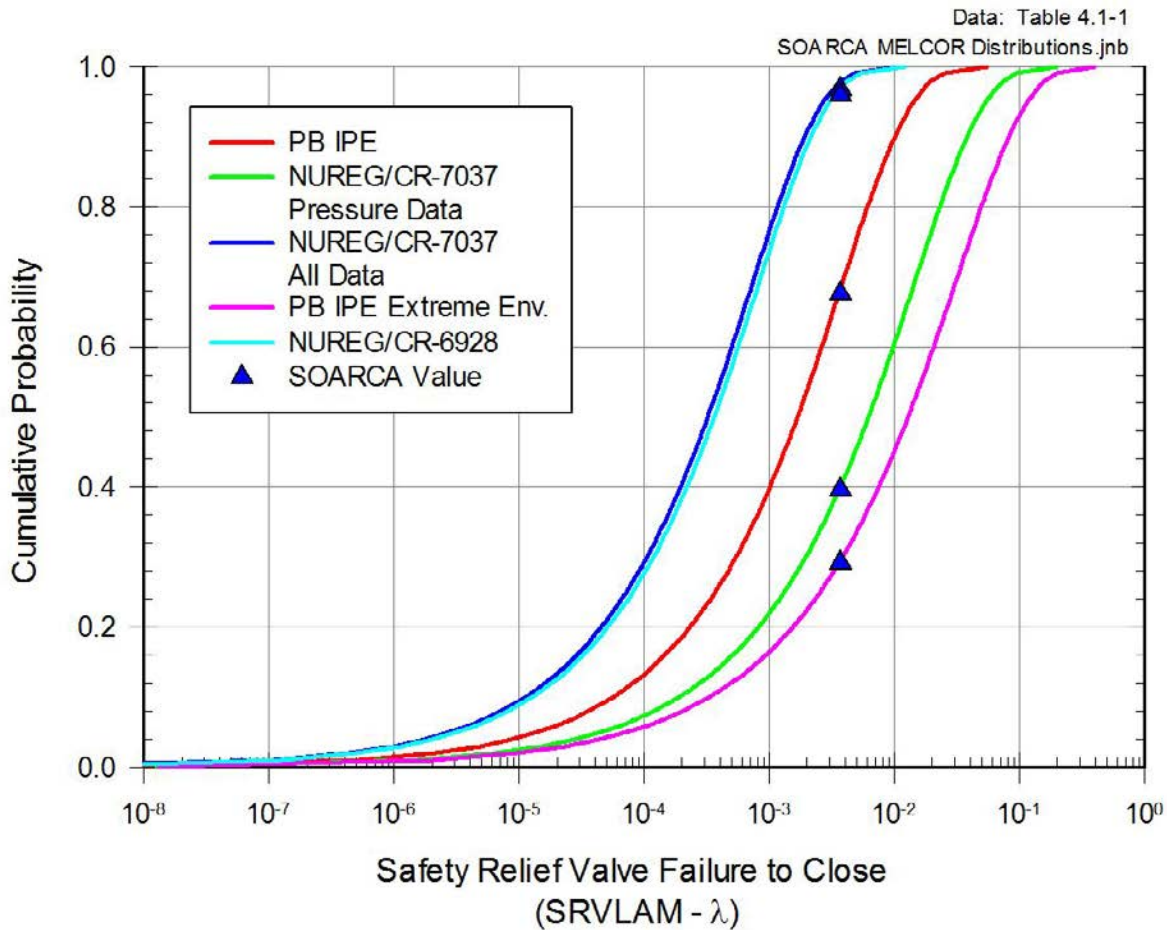


Figure 4.1-1 Cumulative distribution function of safety relief valve failure to close valve cycle (λ = per demand failure probability ($1/\lambda$ = number of SRV demands))

Duration of direct current power (BATTDUR)

DC power is maintained by DC batteries during a SBO. The DC batteries are used to provide power to the DC electrical buses for minimum electrical loading to monitor instrumentation in the control room. Without DC power, none of the control room instrumentation is available, and thus, there is no indication of plant status. Uncertainty in the duration of DC power is influenced by the efficiency of operator actions to shed non-essential loads and the age of the batteries. A log triangular distribution was selected for BATTDUR with a mode of 4.0 hours, the value used in the deterministic SOARCA analysis, and 2.0 and 8.0 hours for the lower and upper bounds, respectively (Figure 4.1-2 and Table 4.1-1).

The licensee's PRA uses a value of two hours, which is the minimum duration required by plant technical specifications and represents the worst possible condition. The licensee's engineering judgment is that batteries can last four hours with effective DC load shedding. The upper bound of eight hours was selected because the licensee recommended a lower value than what was selected in the past studies (i.e., NUREG-1150 [16]) which assumed 10 to 12 hour battery life with sufficient load shedding) as there is concern with the ability or requirements necessary to demonstrate a capacity for that long.

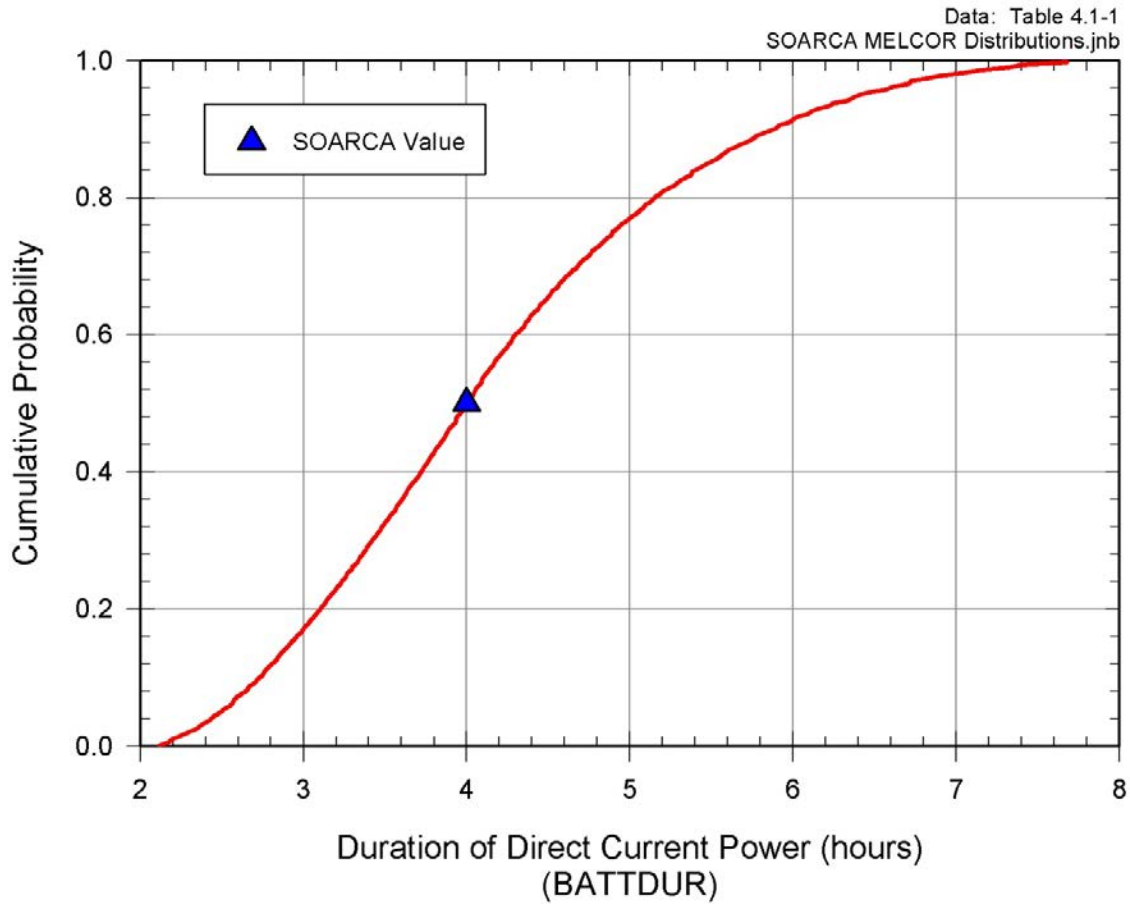


Figure 4.1-2 Cumulative distribution function of duration of direct current power

Table 4.1-1 MELCOR uncertain parameters—sequences issues

Parameter	Distribution
SRVLAM: lambda for SRV stochastic failure to reclose (per demand)	Beta distribution Mean = 3.7×10^{-3} Alpha = 0.494 Beta = 133.2 LB = 0.0 UB = 1.0
	SOARCA estimate: 3.7×10^{-3}
BATTDUR: Duration of direct current power (hours)	Log Triangle distribution LB = 2.0 hr. Mode = 4.0 hr. UB = 8.0 hr.
	SOARCA estimate: 4.0 hrs.

4.1.2 In-Vessel Accident Progression Issues

Zircaloy melt breakout temperature (SC1131(2))

The core melt progression modeling options have been set to be consistent with current best-practices guidelines, which are generally default models [17]. As the fuel temperature increases, an oxide shell forms on the outer surface of the fuel cladding. Since the oxide shell has a higher melting temperature than the unoxidized zircaloy inside the fuel rod, the zircaloy on the interior of the cladding will become molten once the temperature rises above the melting temperature (Figure 4.1-3). This zircaloy melt breakout temperature represents the uncertain properties that determine the conditions at which oxidized clad mechanically fails, releasing molten unoxidized zircaloy. This initiates the downward drainage of molten zircaloy on a ring-by-ring basis in the MELCOR analysis. Based on prior work on in-vessel melt progression [18], this parameter is expected to be among the more important uncertain parameters. As described in the previous studies [18], at the "breakout temperature" oxidizing molten zircaloy is relocated to cooler regions at a time when the oxidation rate is at its peak value. Fuel temperatures are increasing rapidly ($\sim 10\text{K/s}$) at this time, hydrogen generation is locally at a maximum, and fission product release rates are large. The relocation of the oxidizing melt has the effect of terminating the intense local fuel heating, since the chemical heating source has relocated to a cooler region of the vessel. This should affect release rate for volatile fission products and total localized releases of low-volatile species. The lower bound value is the zircaloy melting temperature of 2100 K. The value of 2100 K also corresponds to fragile outer oxide shells that are incapable of retaining molten zircaloy. The upper bound value is based on likely rod collapse temperature occurring within 15 minutes. The upper value of 2540 K, was selected in the original hydrogen uncertainty study [18] based on qualitative consideration of the $\alpha\text{-Zr(O)}$ phase diagram and observations/analyses of the Phebus experiments [19-23]. The mode is the value used in the deterministic SOARCA analysis (Figure 4.1-4 and Table 4.1-3). The selection of a triangle distribution suggests that a most probable value for the uncertain parameter is recommended (mode), with decreasing likelihood for values away from the most probable. This is in contrast to a range-bounded uniform distribution, where it is implied that any value lying within a range is equally probable.

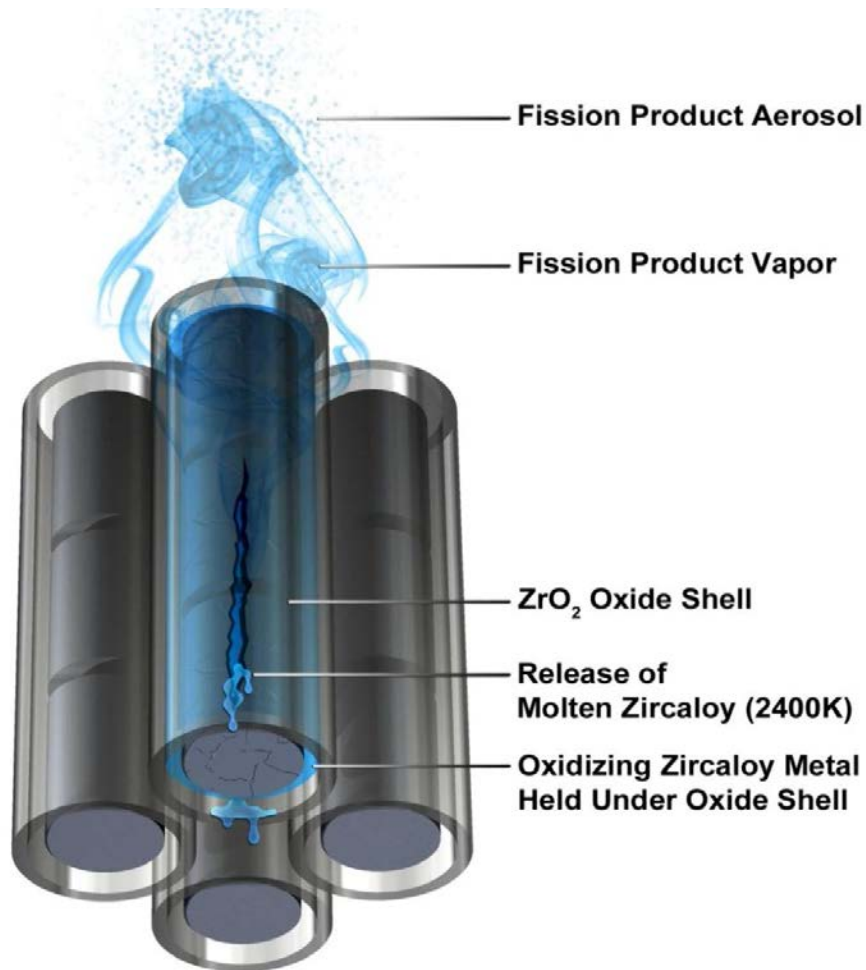


Figure 4.1-3 Depiction of the fuel rod degradation

Based on observations from Phebus tests [19-23], MELCOR includes a molten zircaloy breakout model of the loss of structural integrity of the oxidized zircaloy. Following the relocation of the molten Zircaloy, the oxidation ceases and the fuel rods remain intact based on the thermal response of the system which is largely governed by decay heat loss and perhaps relocating molten material from above. Subsequently, the fuel rods are only supported by a relatively thin oxide structure that can weaken at high temperatures. The calculated failure mechanisms include:

- failure due to melting the oxidized shell, or
- failure of the supporting fuel rods (collapse of the fuel rods will result in fracture of the melt-retaining oxide shell), and
- a time-at-temperature model that calculates the failure of the oxidized zircaloy shell holding the fuel rods.

The time-at-temperature model includes a thermal-mechanical weakening of the oxide shell as a function of temperature. As the temperature rises above zircaloy melting temperature (i.e., represented as 2098 K in MELCOR) towards 2500 K, a thermal lifetime function linearly accrues cladding damage and predicts time to local thermal-mechanical failure (Table 4.1-2).

Table 4.1-2 Time versus temperature relationship for intact fuel rod collapse

Temperature	Time to Failure
2000 K	Infinite
2090 K	10 days
2100 K	10 hours
2500 K	1 hour
2600 K	5 minutes
2700 K	30 seconds

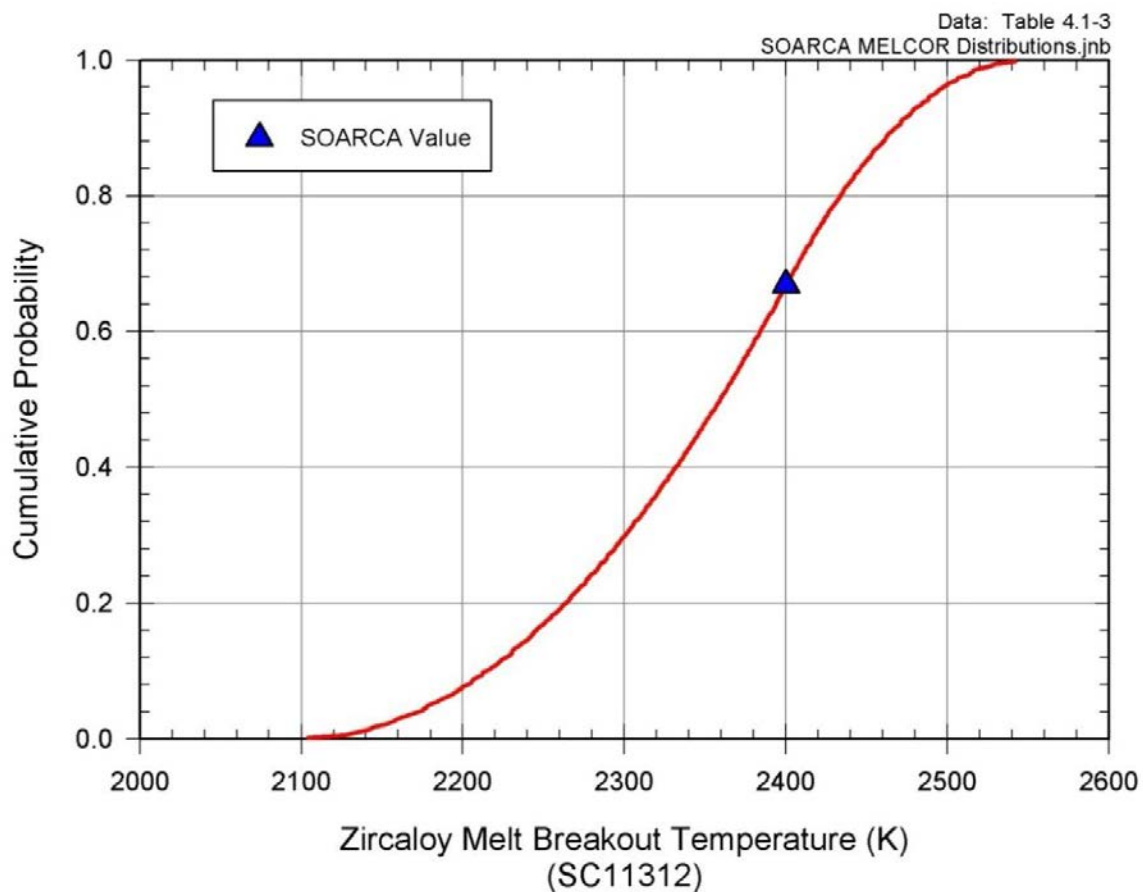


Figure 4.1-4 Cumulative distribution function of zircaloy melt breakout temperature

Molten clad drainage rate (SC1141(2))

Time constant for heat transfer to substrate material versus downward molten flow is another factor that influences uncertainty in the source term release model. The molten clad drainage rate impacts material relocation from the top of active fuel to the bottom of active fuel. This parameter (SC11412) represents effective downward flow rate of the molten fuel, balancing heat transfer and freezing on substrate against vertical momentum and, therefore, affects the overall melt progression behavior. It is one of the few MELCOR melt progression parameters

available for variation. A log triangular distribution is used for the molten clad drainage rate (SC1141(2)) with a mode of 0.2 kg/m-s used in the deterministic SOARCA analysis, and 0.1 and 1.0 kg/m-s respectively for the lower and upper bounds (Figure 4.1-5 and Table 4.1-3). The selection of a triangular distribution suggests that a most probable value for the uncertain parameter is recommended (mode), with decreasing likelihood for values away from the most probable.

The lower and upper bounds of the distribution represent an order of magnitude of uncertainty. This was selected based upon previous studies [18] to ensure the behavior was appropriately captured in the uncertainty in this parameter.

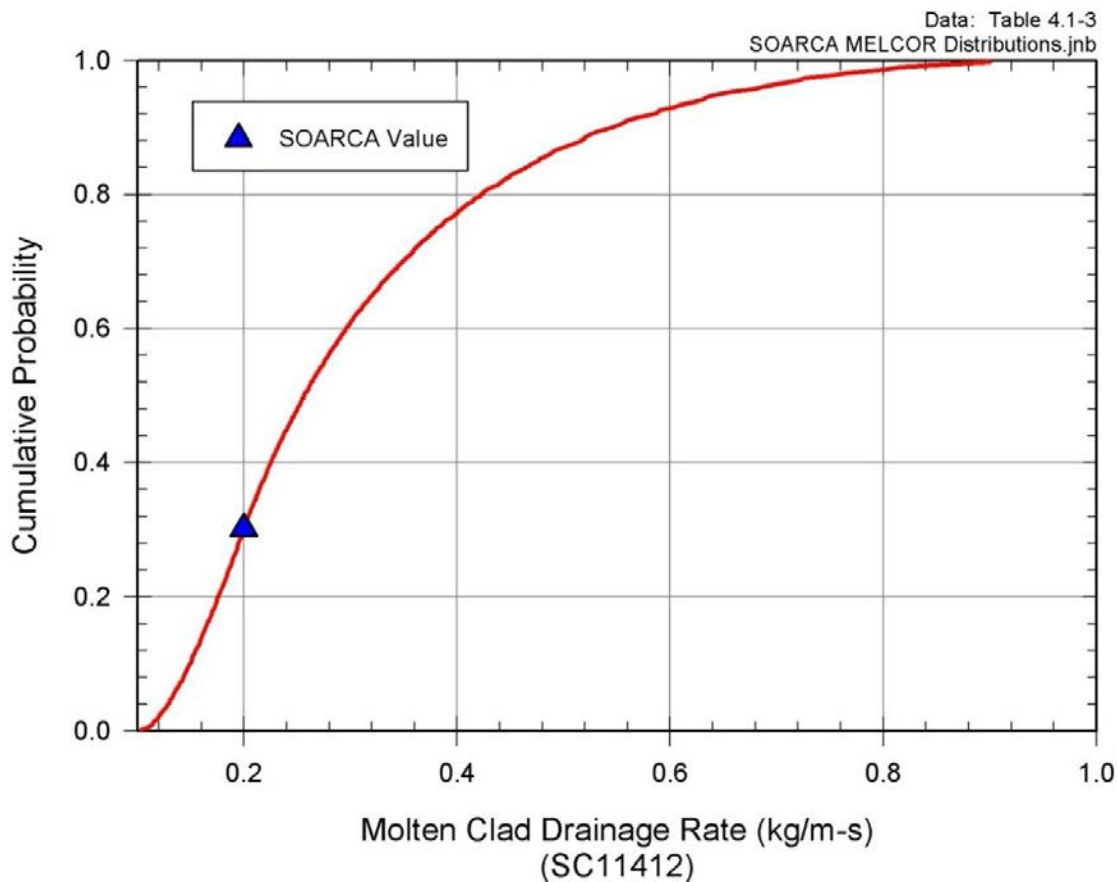


Figure 4.1-5 Cumulative distribution function of molten clad drainage rate

Criteria for thermal seizure of safety relief valve due to heating after onset of core damage [SRVFAILT]

One concern regarding the timing of the accident sequence is the depressurization of the RCS. As part of the SOARCA project, the RCS depressurizes resulting from the failure of a SRV to close. In the MELCOR SOARCA, model SRVs open at predetermined pressures and specified flow rates. The SRVs will close when pressure drops below 96% of their opening pressure. In addition, to the stochastic failure to close (SRVLAM), the SRVs fail to close by thermal seizure if a specified temperature limit is exceeded [2].

For the gas exposure time during open cycles, heat conduction within a valve, and expansion of valve components, the MELCOR model estimates the thermal response of a representative valve internal component (perhaps the valve stem) as a solid steel cylinder, heated by the gas

discharged through the valve when open. The valve is assumed to seize in the open position (failure to reclose) on the first cycle above a specified component temperature. Model uncertainty in valve thermal response, expansion, and seizure is represented by the component temperature limit for thermal seizure. For the uncertainty analysis, a beta distribution was selected with the mean at 900 K, which is the value used in the deterministic SOARCA analysis [2], and 811 K and 1143 K selected for the lower and upper bounds respectively (Figure 4.1-6 and Table 4.1-3).

An evaluation of thermal seizure of the SRV was included in NUREG/CR-7110, Volume 1, Sections 4.4.1 and 4.4.2. An initial criterion for high-temperature valve failure was based on manufacturers' information describing the strength of stainless steel, published by the Stainless Steel Information Center (www.ssina.com/composition/temperature.html). Softening or loss of strength of stainless steel (300 series) was described to start to occur at "about 1000°F" (811 K). This data provides the lower bound for the distribution. The NUREG/CR-7110 evaluation included differential thermal expansion, effects of temperature gradients, and material deformation as the basis for the SOARCA value of 900 K used in the uncertainty analysis as the mean of the distribution. A supplemental analysis conducted by the U.S. NRC [24], independently validated the findings in the NUREG/CR-7110 report for Peach Bottom. The letter report evaluated the two analyses presented in NUREG/CR-7110 Volume 1 that address thermal effects on valve reliability and performance. In the first analysis, thermal expansion is calculated due to differences in properties between the valve guide and stem materials, and an additional term is added that addresses the fact that the stem experiences a greater heat-up than the larger valve body. The result of these calculations presented in the NUREG/CR-7110 report gives a total stem to guide gap reduction over time corresponding to a MSL temperature of 811 K, which was close to the range of times and MSL temperatures calculated independently by Rathbun, 2011 [24].

In the second thermal analysis included in NUREG/CR-7110, the effect of strength degradation of the valve stem material is analyzed. Based on strength reduction at elevated temperatures, an estimate of 900 K is estimated as the temperature at which the stainless steel stem will degrade to the point where the valve will fail. The 900 K valve stem temperature corresponds to a MSL temperature of approximately 950 K. No direct comparison with the 900 K material failure criterion in NUREG/CR-7110 Volume 1 was made in the Rathbun [24] analyses. However, the corresponding steam line temperature of 950 K was somewhat higher than the highest steam line temperature at failure (900 K) calculated in the Rathbun report [24]. This temperature difference has been encompassed within the standard deviation of the distribution for thermal seizure temperature used in the uncertainty analysis.

Sensitivity studies in NUREG/CR-7110 Volume 1 [2], determined that valve stem temperatures greater than 1175 K satisfied the conditions necessary for MSL creep rupture. The temperature at which material deformation occurs is lower than the value used in the early SOARCA calculations (i.e., 1000 K) [2]. This value was selected primarily to reflect the 'service temperature' for stainless steel components, as reported by the steel industry trade association. A review of vendor literature on material properties of 304 stainless steel clearly indicates the maximum service temperature of approximately 870°C (~1143 K) is based on the scaling properties (or resistance to corrosion) of 300 series stainless steel, rather than its mechanical properties. Given that material deformation would be expected at the hot working temperature of 304 stainless steel, between 1149-1260°C [25], an upper bound limit for plastic deformation is based on the vendor recommended service temperature of 1143 K. This upper bound is further supported by Rathbun [24] analyses that suggest failure by thermal expansion of moving valve components would occur at temperatures below 870°C (~1143 K).

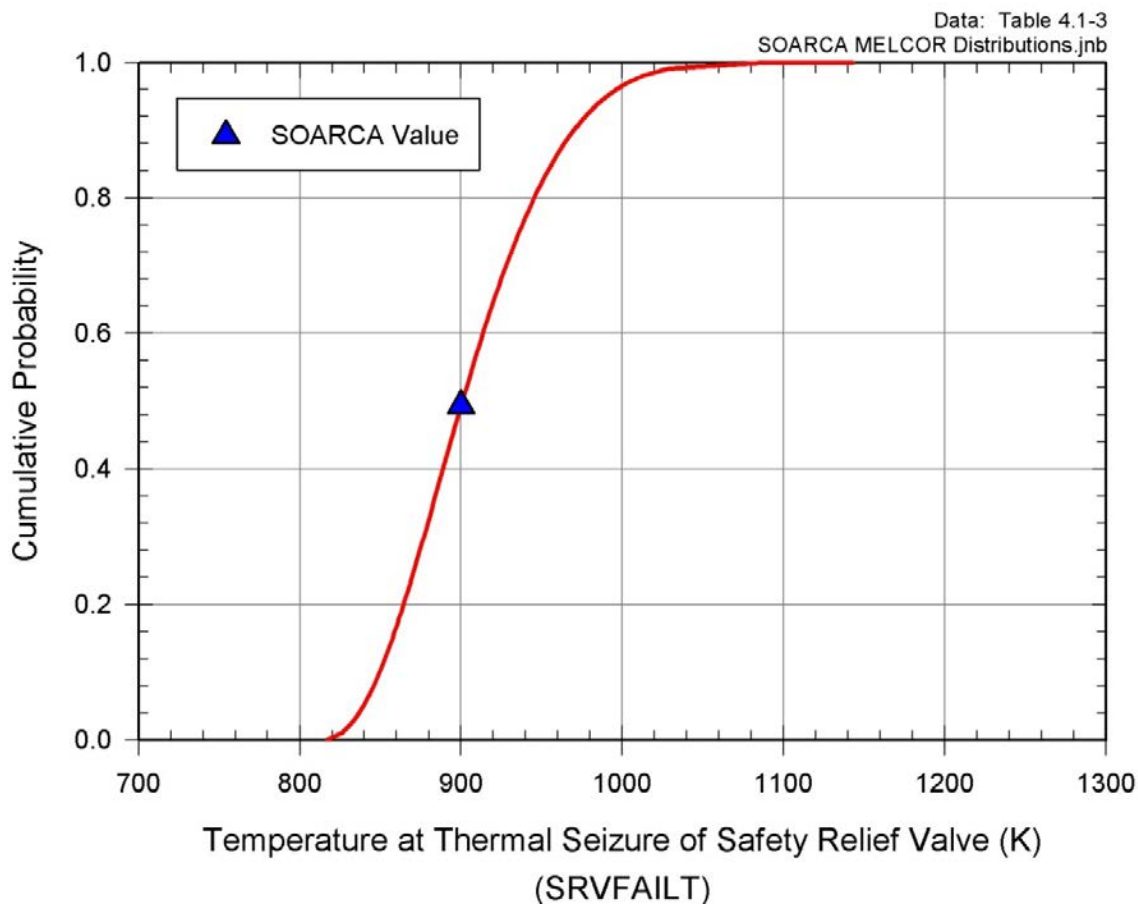


Figure 4.1-6 Cumulative distribution function of criteria for thermal seizure of safety relief valve due to heating after onset of core damage

Safety relief valve open area fraction after thermal seizure (SRVOAFRAC)

The timing of the accident sequence is dependent upon when the depressurization of the RCS occurs. The RCS depressurizes because of failure of a SRV to close. During normal operations, the SRVs open at predetermined pressures and specified flow rates. The SRVs will close when pressure drops below 96% of their opening pressure unless the SRVs fail to close based on high temperature conditions within the SRV as described in the previous section. However, thermal expansion of the SRV would occur primarily during periods of gas flow (open cycles), although penetration (conduction) of heat transferred to inner surfaces would occur over a longer period of time (valve open or closed). This behavior leads to uncertainty in the valve position immediately prior to seizure and to the final stem position after seizure and thus the open area for releases from the SRV. In addition, sensitivity studies in NUREG/CR-7110 Volume 1, determined that a valve open fraction of 10% of the nominal flow area satisfied the conditions necessary for MSL creep rupture.

A fraction of 1.0 was used as the value in the deterministic SOARCA analysis [2]. Since there is no data available to predict the uncertainty within the SRV position at the time the SRV sticks open from thermal seizure, a triangle distribution between 0.1 and 1.0 (fully open) with a mode of 1.0 was investigated to measure the potential effects of this event on accident progression and source term releases (Figure 4.1-7 and Table 4.1-3). This distribution was selected to skew to higher values because the geometry of the SRV is such that it does not have to vertically traverse much of its shaft length before reaching an open area close to fully open.

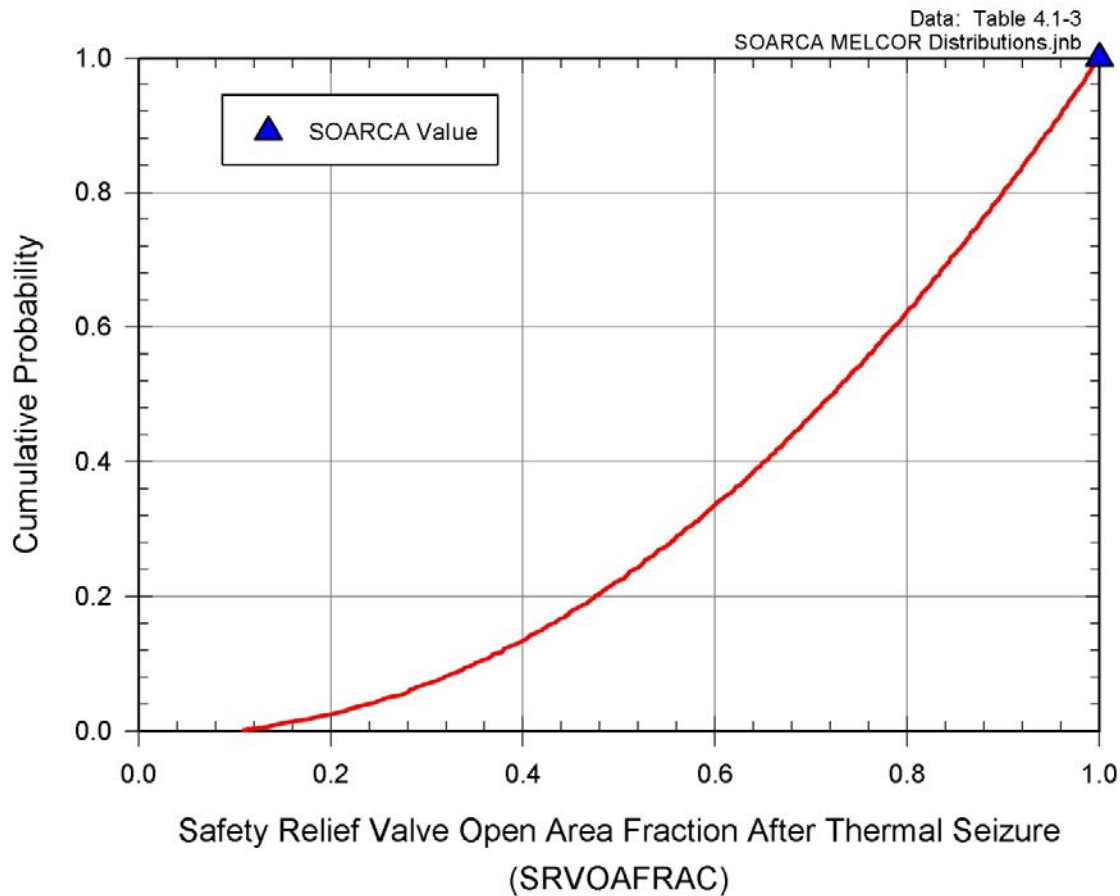


Figure 4.1-7 Cumulative distribution function of safety relief valve open area fraction after thermal seizure

Main steam line creep rupture area fraction (SLCRFRAC)

Creep rupture is monitored at two locations (i.e., MSL nozzle and MSL piping). This parameter represents the size of the opening that would be generated at either location if creep failure occurs. The potential for creep failure is calculated using a standard Larson-Miller (L-M) formulation, identical in structure to the one used in MELCOR PWR calculations of hot leg and pressurizer surge line failure. Uncertainties in the L-M model itself are not considered here, in part, due to the observation from past calculations that the transition from zero damage to creep appears to occur too fast for reasonable variations in the L-M parameter to have a significant effect on the time that creep failure occurs.

Factors that contribute to uncertainty in the size of the opening generated by creep rupture of a BWR MSL include: the possibility of pre-existing flaws in weld locations, upper RPV and steam line circulation flow patterns, multi-dimensional effects of heat transfer to MSL piping, and the impact of pipe restraints on piping mechanical response.

The MELCOR model preserves the total flow area of the MSL, but partitions this area between the intact pipe and the rupture opening. Therefore, a rupture open fraction of 1.0 closes flow through the MSL, and replaces it with an opening to the drywell with an equivalent area. A value of 0.5 partitions the MSL flow equally between the intact pipe flow path and the rupture flow path. Therefore, the creep rupture open fraction is the numerical complement of the MSL open fraction. Sensitivity studies in NUREG/CR-7110 Volume 1, using the SOARCA Peach

Bottom case, involving creep rupture of the MSL assumed the structural response of the MSL is a fully offset, guillotine break of one MSL (i.e., open fraction of 1.0). This was considered a conservative assumption because the large break area maximizes the hydrodynamic load to the containment pressure boundary and facilitates fission product transport from the RCS. Alternative credible responses, such as a smaller crack or fissure in the MSL were not considered in these sensitivity calculations. A piecewise uniform distribution between 0.0 and 1.0 is used in this analysis to measure the potential effects of this event on accident progression and source term releases (Figure 4.1-8 and Table 4.1-3). This distribution was selected based upon expert judgment and Peer Review feedback, and based on findings of experimental work and analysis for PWR hot leg creep rupture [26]. Some expert judgment was used to adapt the PWR hot leg analysis to the BWR MSL and generate the distribution shape, which was the numerical way of reflecting the study's conclusion of a strong bias toward a full-open area.

Note, the intent of the distribution is to open the MSL to the containment through an area equivalent to the full cross-sectional area of the pipe for 85% of the realizations. However, the means through which the MSL rupture is accomplished in the MELCOR model (i.e., adjusting the flow area of three junctions) leads to an effective break area equal to the full area of the pipe for any value of SLCFRAC greater than or equal to 0.5. So, the MSL will actually open fully to containment 96% of the time in this analysis, which is slightly more than was intended.

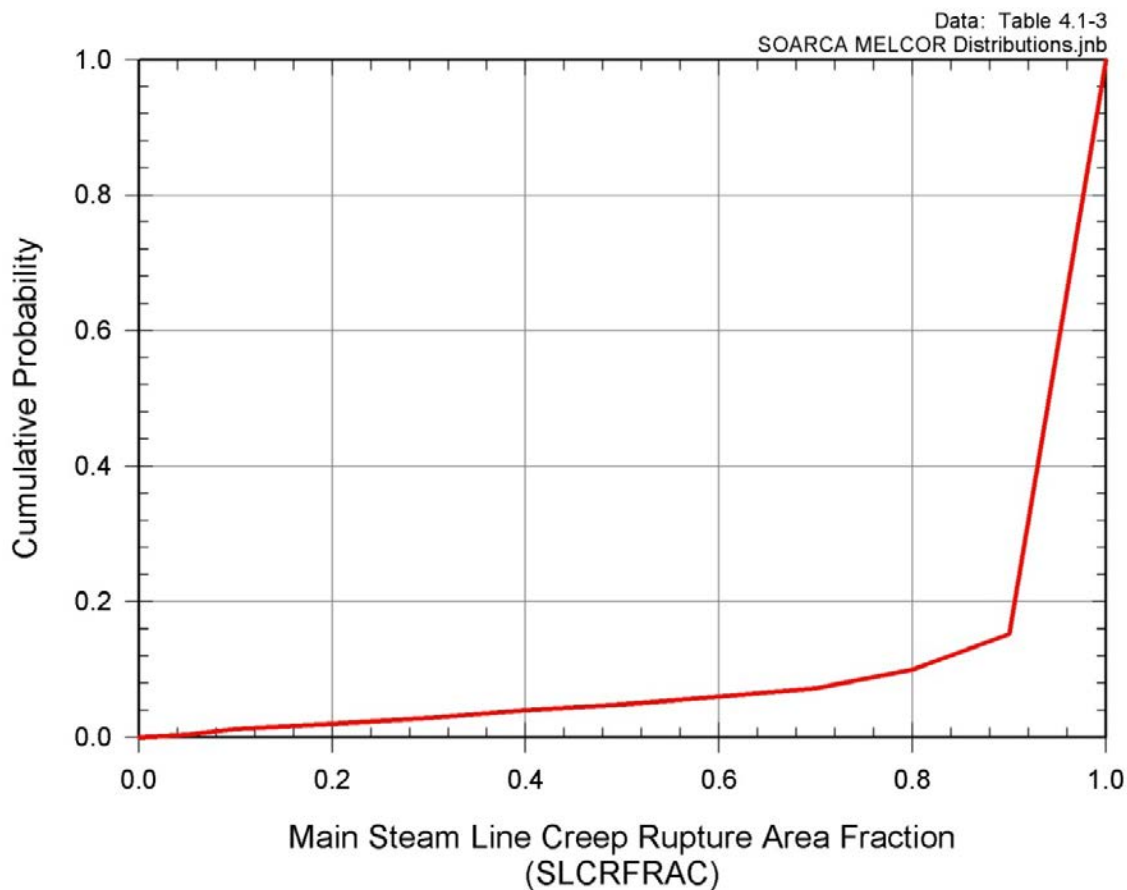


Figure 4.1-8 Cumulative distribution function of main steam line creep rupture area

Fuel failure criterion (transformation of intact fuel to particulate debris) (FFC)

MELCOR lacks a deterministic model for evaluating fuel mechanical response to the effects of clad oxidation, material interactions (i.e., eutectic formation), zircaloy melting, fuel swelling and other processes that occur at very high temperatures. In lieu of detailed models in these areas a simple temperature-based criterion is used to define the threshold beyond which normal ("intact") fuel rod geometry can no longer be maintained, and the core materials at a particular location collapse into particulate debris. The temperature-based criterion incorporates uncertainties in numerous physico-chemical processes that affect fuel rod integrity. The "time-at-temperature" criterion is the time endurance of the upright, cylindrical configuration of fuel rod bundles which decreases with increasing temperature. A temperature-based 'cumulative damage' criterion is used in the MELCOR model to define the remaining lifetime of normal fuel rod geometry (Table 4.1-2). The alternative functions represent shifts in temperature of +/- 100 K and fuel endurance times of +/- factor of 2.0 (Figure 4.1-9, Figure 4.1-10 and Table 4.1-3). The fuel failure criterion distribution is qualitative in nature, but based on observations from testing such as Phebus facility tests [19-23], accounting for scale effects (small bundles are inherently more stable and less fragile than full length fuel assemblies). This approach is considered the best effort at evaluating the importance of this uncertain parameter. In part the nature of the treatment (time at temperature) is intended to avoid non-physical cliff-edge effects that are observed during a calculation when fuel temperatures are predicted to hover just below a failure temperature.

Alternative one is derived from the SOARCA estimate by reducing its temperatures by 100 K and dividing its time intervals by two. Alternative two is derived from the SOARCA estimate by increasing its temperatures by 100 K and multiplying its time intervals by two. The code/model then uses the selected table to determine, based on the fuel temperature, the reduction in fuel lifetime; and when fuel lifetime is exceeded, the fuel is failed.

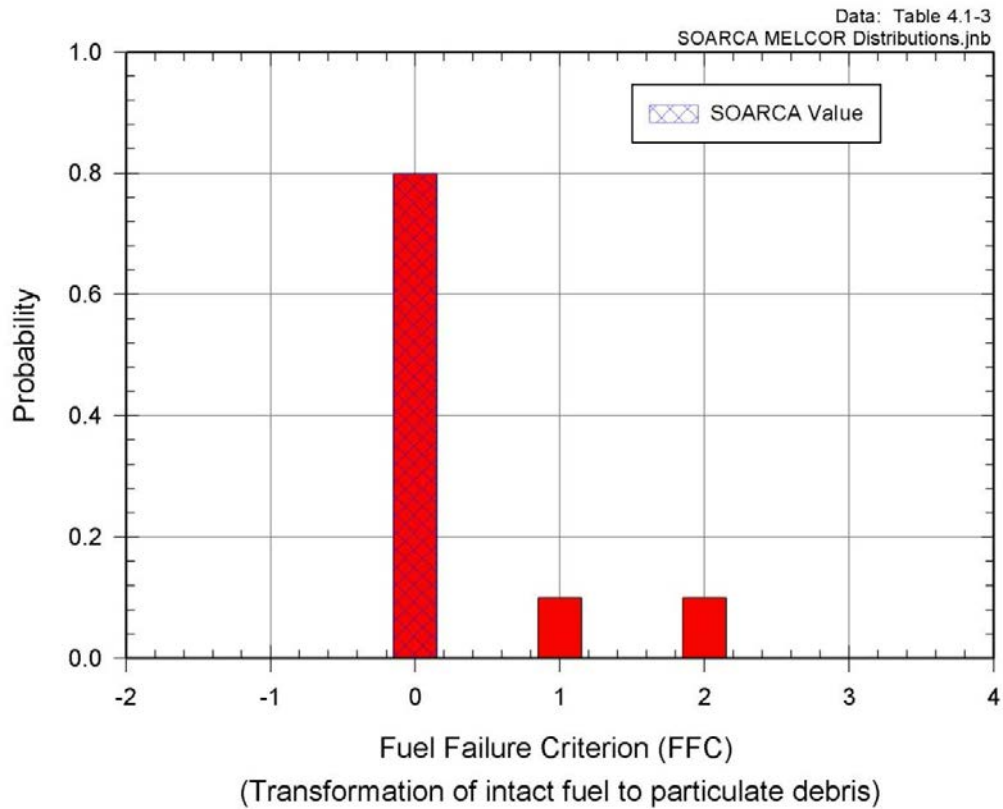


Figure 4.1-9 Probability density function of fuel failure criterion alternatives (transformation of intact fuel to particulate debris)

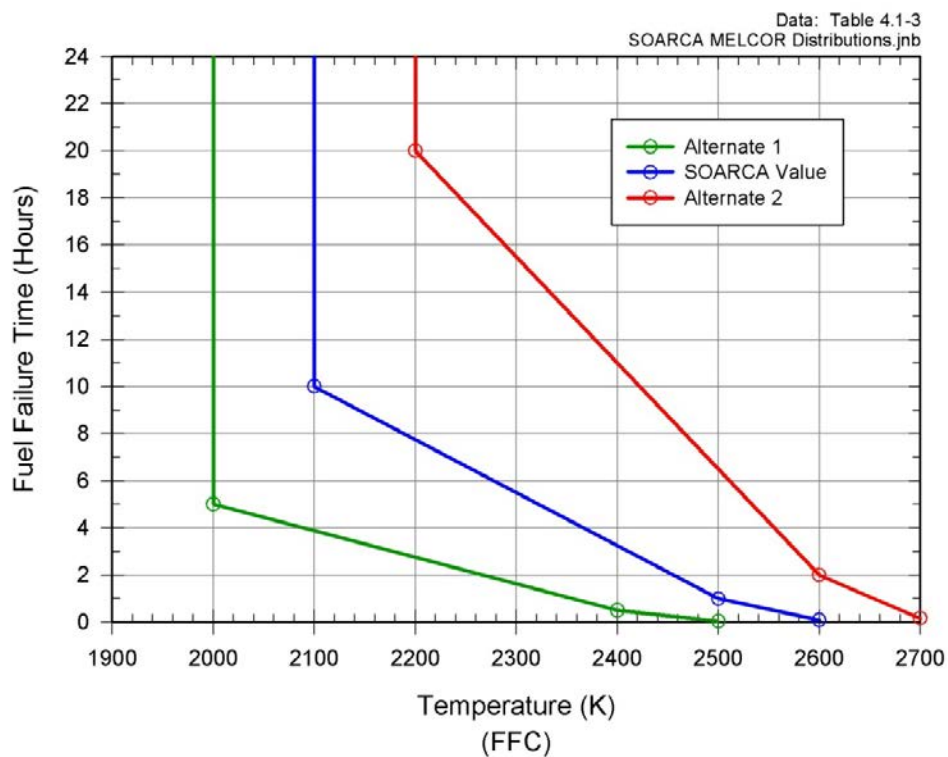


Figure 4.1-10 Fuel failure criterion functions

Radial debris relocation time constants (RDMTC, RDSTC)

The relocation time constant controls the rate of movement of radial molten (RDMTC) and solid debris (RDSTC) to the center of the core, and thus the time it takes the debris to move to the lower plenum. This specific parameter is used as a surrogate for the broad uncertainty of debris relocation rate into water in the lower head. This, in turn, affects the potential for debris coolability in the lower head (faster relocation rates decrease coolability; slower rates improve coolability). Debris relocation in MELCOR occurs when the lower core plate in a ring yields. Molten material and particulate debris from the ring immediately moves towards the center of the core and fall into the lower head. The rate at which this debris and debris from adjacent rings relocates into the lower head is determined by the radial relocation time constant. Thus, adjustments in this parameter affect the overall rate at which debris enters the lower head after support plate failure (Figure 4.1-11 (a and b) and Table 4.1-3).

This parameter is only one of a few MELCOR parameters which can be modified to influence large scale movement, and thus is a key parameter to core melt progression and ultimately source term releases. The distributions are based on expert judgment and are not based on any specific data as no data exists for radial debris relocation. Additionally, the radial debris relocation time constant influences the axial debris relocation. Like the fuel failure criterion discussed previously, this parameter is qualitative and is a surrogate for more complex relocation processes. Phebus facility tests [19-23] offer no insights here as the scale of the testing is too small to provide insights. The parameter ensures that debris does not pile up within single radial rings in an unphysical manner. The exact rate of effective relocation is not known. The values used are felt to bound possible behavior of leveling of materials that may be solid debris, partly molten two phase debris or fully molten.

Exponential time constants for molten debris relocation and solid particulate debris relocation control the rate of relocation of core material. For the uncertainty analysis, a log triangular distribution was selected for both the molten and solid radial relocation time constants. For solid debris, the mode = 360 s, which is the value used in the deterministic SOARCA analysis, and 180 and 720 s are selected for the lower and upper bounds respectively (Figure 4.1-11a and Table 4.1-3). A factor of two variation in the SOARCA value was used to investigate the sensitivity of the analysis results to uncertainty in this parameter. For molten debris the mode = 60 s, which is the value used in the deterministic SOARCA analysis, and 30 s and 120 s are selected for the lower and upper bounds respectively (Figure 4.1-11b and Table 4.1-3).

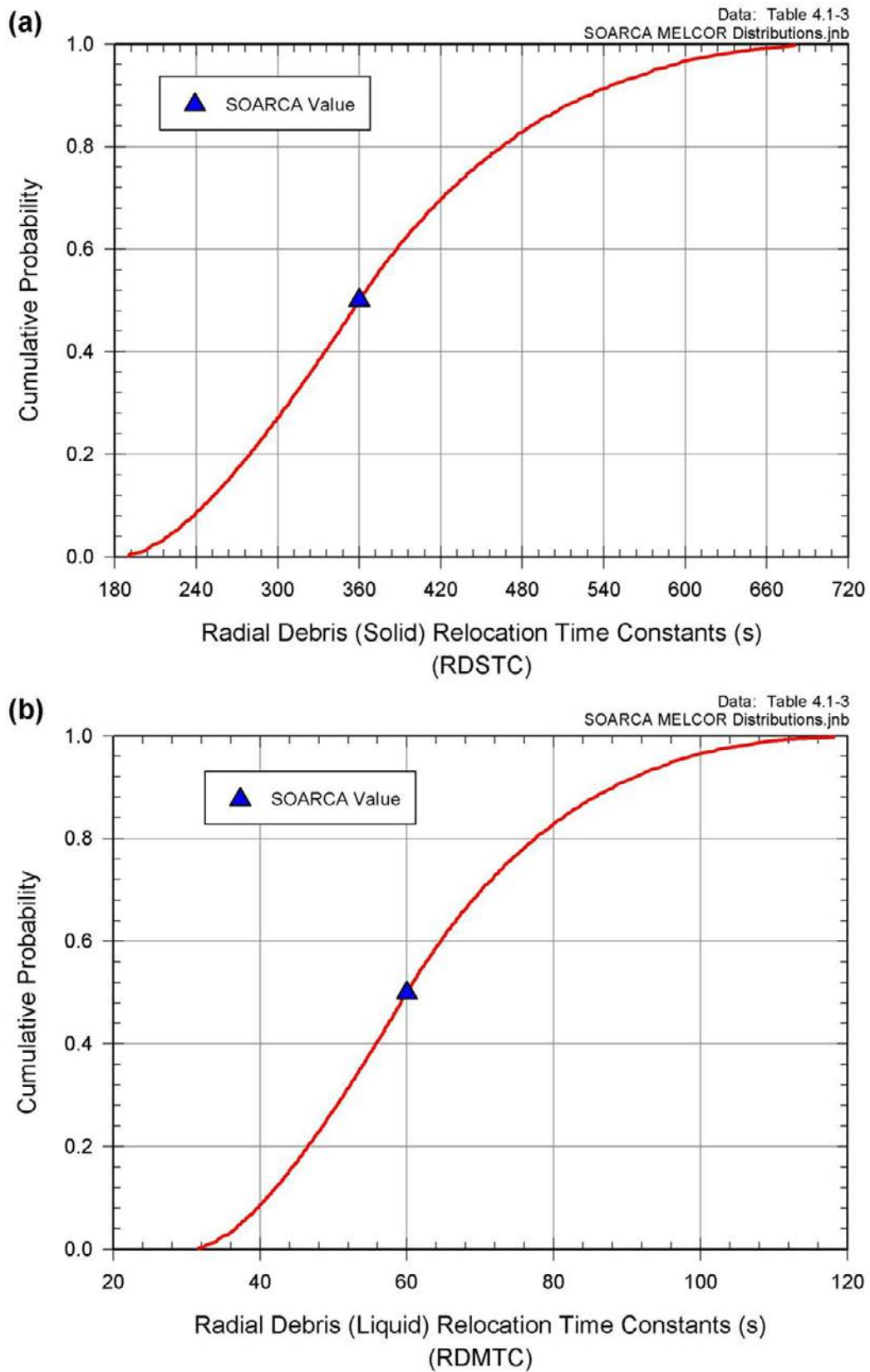


Figure 4.1-11 Cumulative distribution of radial debris relocation time constants:
(a) solid debris and (b) liquid debris

Table 4.1-3 MELCOR uncertain parameters—In-Vessel accident progression issues

Parameter	Distribution
SC1131(2): Zircaloy melt breakout temperature (k))	Triangle distribution LB = 2098 K mode = 2400 K UB = 2550 K
	SOARCA estimate = 2400 K
SC1141(2): Molten clad drainage rate (kg/m-s)	Log Triangle distribution LB = 0.1 kg/m-s mode = 0.2 kg/m-s UB = 1.0 kg/m-s
	SOARCA estimate = 0.2 kg/m-s
SRVFAILT: Criteria for thermal seizure of SRV due to heating after onset of core damage (K)	Beta distribution Mean = 900 K Alpha = 2.72 Beta = 6.79 LB = 811 K UB = 1143 K
	SOARCA estimate = 900 K
SRVOAFRAC: SRV open area fraction after thermal seizure	Log Uniform distribution LB = 0.05 UB = 1.0
	SOARCA estimate = 1.0
SLCRFRAC: Main steam line creep rupture area fraction	Piecewise Uniform distribution weight SLCRFRAC 0.5 5.00×10^{-2} 0.5 1.00×10^{-1} 1 2.00×10^{-1} 1 3.00×10^{-1} 1 4.00×10^{-1} 1 5.00×10^{-1} 1 6.00×10^{-1} 1 7.00×10^{-1} 3 8.00×10^{-1} 5 9.00×10^{-1} 85 1.00
	SOARCA estimate = 1.0
FFC: Fuel failure criterion (transformation of intact fuel to particulate debris)	Discrete distribution SOARCA model = 0.8 alternate-1 = 0.1 alternate-2 = 0.1

Table 4.1-3 MELCOR uncertain parameters—In-Vessel accident progression issues (continued)

Parameters	Distribution										
FFC: Fuel failure criterion function (SOARCA value)	Discrete distribution <table> <tr> <th>T [K]</th><th>Time [s]</th></tr> <tr> <td>2090.0</td><td>6.00×10^{31}</td></tr> <tr> <td>2100.0</td><td>3.60×10^4</td></tr> <tr> <td>2500.0</td><td>3.60×10^3</td></tr> <tr> <td>2600.0</td><td>3.00×10^2</td></tr> </table>	T [K]	Time [s]	2090.0	6.00×10^{31}	2100.0	3.60×10^4	2500.0	3.60×10^3	2600.0	3.00×10^2
T [K]	Time [s]										
2090.0	6.00×10^{31}										
2100.0	3.60×10^4										
2500.0	3.60×10^3										
2600.0	3.00×10^2										
FFC: Fuel failure criterion function (Alternative one)	Discrete distribution <table> <tr> <th>T [K]</th><th>Time [s]</th></tr> <tr> <td>1990.0</td><td>6.00×10^{31}</td></tr> <tr> <td>2000.0</td><td>1.80×10^4</td></tr> <tr> <td>2400.0</td><td>1.80×10^3</td></tr> <tr> <td>2500.0</td><td>1.50×10^2</td></tr> </table>	T [K]	Time [s]	1990.0	6.00×10^{31}	2000.0	1.80×10^4	2400.0	1.80×10^3	2500.0	1.50×10^2
T [K]	Time [s]										
1990.0	6.00×10^{31}										
2000.0	1.80×10^4										
2400.0	1.80×10^3										
2500.0	1.50×10^2										
FFC: Fuel failure criterion function (Alternative two)	Discrete distribution <table> <tr> <th>T [K]</th><th>Time [s]</th></tr> <tr> <td>2190.0</td><td>6.00×10^{31}</td></tr> <tr> <td>2200.0</td><td>7.20×10^4</td></tr> <tr> <td>2600.0</td><td>7.20×10^3</td></tr> <tr> <td>2700.0</td><td>6.00×10^2</td></tr> </table>	T [K]	Time [s]	2190.0	6.00×10^{31}	2200.0	7.20×10^4	2600.0	7.20×10^3	2700.0	6.00×10^2
T [K]	Time [s]										
2190.0	6.00×10^{31}										
2200.0	7.20×10^4										
2600.0	7.20×10^3										
2700.0	6.00×10^2										
RDSTC: Radial debris relocation time constant (Solid debris)	Log Triangle distribution LB = 180 s mode = 360 s UB = 720 s SOARCA estimate = 360 s										
RDMTC: Radial debris relocation time constant (Molten debris)	Log Triangle distribution LB = 30 s mode = 60 s UB = 120 s SOARCA estimate = 60 s										

4.1.3 Ex-Vessel Accident Progression Issues

Debris lateral relocation— cavity spillover criteria and spreading rate (DHEADLIQ, DHEADSOL)

The dominant mechanism of containment failure in accident sequences involving the drywell floor, such as the LTSBO, is thermal failure (melting) of the drywell liner following contact with molten core debris (i.e., drywell liner melt-through). Containment failure by this mechanism occurs after debris is released from the reactor vessel lower head and flows out of the reactor pedestal onto the main drywell floor. If a sufficiently large quantity of debris accumulates in the pedestal, it can flow out of the pedestal through a large doorway in the concrete pedestal wall. If the debris temperatures remain sufficiently high as it spreads across the drywell floor and contacts the drywell liner, the liner would melt and fail. The precise conditions under which core debris would flow out of the pedestal and across the drywell floor are uncertain. These uncertainties are adequately captured by assuming debris mobility and the potential for liner failure are represented by two key parameters: debris mass (i.e., static head) necessary for lateral flow and debris temperature (which characterizes debris rheological properties and internal energy available to challenge the liner).

The drywell floor is subdivided into three regions for the purposes of modeling molten-core/concrete interactions in the MELCOR model. The first region, which receives core debris exiting the reactor vessel, corresponds to the reactor pedestal floor and sump areas (CAV 0). Debris that accumulates in CAV 0 can flow out through a doorway in the pedestal wall⁸ to a second region representing a 90-degree sector of the drywell floor (CAV 1). If debris accumulates in this region to a sufficient depth, it can spread further around the annular drywell floor into the third region (CAV2). This discrete representation of debris spreading is illustrated on Figure 4.1-12.

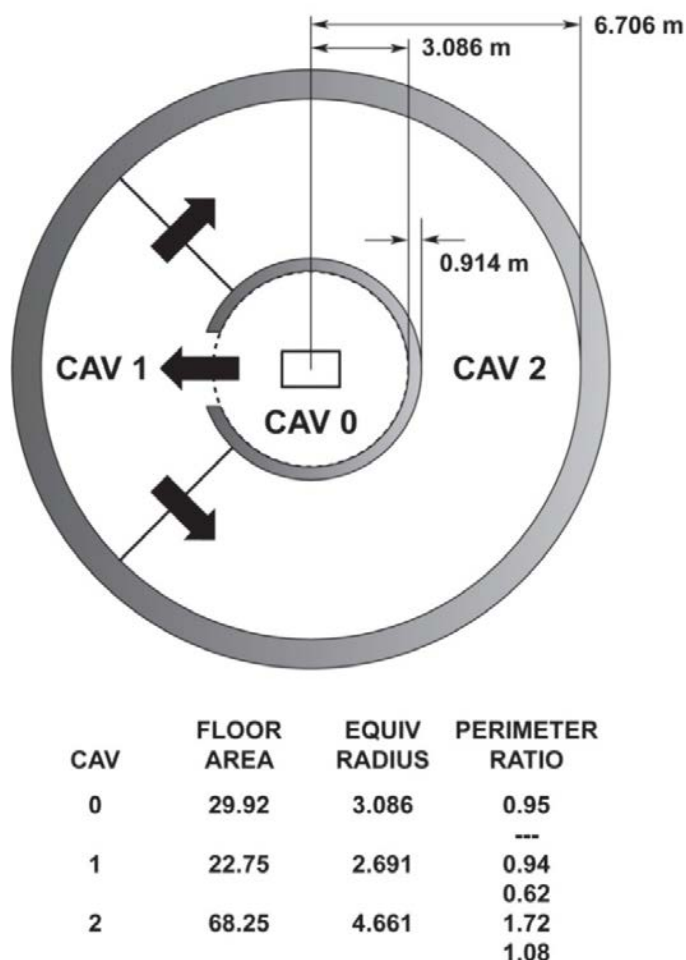


Figure 4.1-12 Drywell floor regions

⁸ Although the drawing provided by the licensee seems to indicate the presence of a swing-door in the personnel opening at the base of the reactor pedestal, the analysis described here assumes this door does not actually exist. Years of research on the issue of drywell liner melt-through never acknowledged the presence of a door (e.g., NUREG/CR-5423 and NUREG/CR-6025). It is noted in the introduction to NUREG/CR-5423 that the geometry of the Peach Bottom configuration was used as the template for the analysis. The flow of debris from the pedestal onto the outer drywell floor would not be impeded in any way by an obstacle in the concrete 'doorway' in the pedestal wall. As a result, the current SOARCA analysis applied the same rationale and assumed molten debris would freely flow from the pedestal onto the drywell floor.

A MELCOR model control function monitors the debris elevation and temperature within each drywell floor region, each of which must satisfy user-defined threshold values for debris to move from one region to its neighbor. More specifically, when debris in a cavity is at or above the liquidus temperature of concrete, all material that exceeds a predefined elevation above the floor/debris surface in the adjoining cavity is relocated (i.e., 6 inches for CAV 0 to CAV 1 and 4 inches for CAV 1 to CAV 2). When debris in a cavity is at or below the solidus temperature of concrete, no flow is permitted. Between these two debris temperatures, restricted debris flow is permitted by increasing the required elevation difference in debris between the two cavities (i.e., more debris *head* required to flow).

Another MELCOR model control function manages the debris spreading radius across the drywell floor within CAVs 1 and 2. Debris entering CAV 1 and CAV 2 is not immediately permitted to cover the entire surface area of the cavity floor. The maximum allowable debris spreading radius is defined as a function of time. If the debris temperature is at or above the concrete's liquidus temperature, then the maximum transit velocity of the debris front to the cavity wall is calculated (e.g., NUREG/CR-7110 Volume 1, Peach Bottom SOARCA results are 10 minutes to transverse CAV 1 and 30 minutes to transverse CAV 2). When the debris temperature is at or below the concrete solidus temperature, the debris front is assumed to be frozen, and lateral movement is precluded (i.e., debris velocity is 0 meters per second). A linear interpolation is performed to determine the debris front velocity at temperatures between these two values.

Full mixing of all debris into a single mixed layer is assumed in each of these debris regions. The concrete composition represented in the MELCOR model is listed in Table 4.1-4. The drywell floor concrete composition includes 13.5% rebar.

Table 4.1-4 Concrete composition

Species	Mass Fraction
Al ₂ O ₃	0.0091
Fe ₂ O ₃	0.0063
CaO	0.3383
MgO	0.0044
CO ₂	0.2060
SiO ₂	0.3645
H ₂ O _{evap}	0.0449
H ₂ O _{chem}	0.0265

The debris lateral relocation criteria determines if and when hot debris contacts the drywell liner. There are two principal contributors: (1) Debris (differential) height and temperature required for "spill-over" from the pedestal to the quadrant of drywell floor adjacent to the pedestal doorway (i.e., CAV 0 to CAV 1), and (2) debris velocity as it flows across drywell floor (from the pedestal doorway to the liner). This is calculated by control functions discussed above assuming a minimum transit time from the pedestal to the drywell liner (i.e., CAV 1) of 10 minutes if T(debris) > liquidus temperature. The velocity is zero when T(debris) < solidus temperature. The control functions do a linear interpolation between these two temperatures. The assumed maximum flow velocity is fixed. It is assumed that lateral debris mobility (i.e., spill-over from the pedestal to the drywell floor) is a function of debris temperature and the differential head

(i.e., depth) of debris inside relative to the material outside the pedestal doorway. For simplicity, it is assumed the temperatures at which debris begins to move and the value at which the debris' lateral velocity is at maximum are fixed. These values are used in the baseline model (i.e., the solidus and liquidus, respectively). To represent the uncertainty in debris mobility, uncertainty in the heights of debris at those temperatures necessary for lateral movement are used (Figure 4.1-13 (a and b) and Table 4.1-5). The two parameters are considered to be perfectly correlated in this analysis to avoid non-physical behavior in which the debris height at the liquidus temperature is greater than the debris height at the solidus temperature.

The mode of the solidus (0.5 m), the value used in the deterministic SOARCA analysis [2], represents the height at which solid particulate debris would 'tumble' laterally. The upper and lower bounds of the distribution provide an order of magnitude range about the mode.

For the liquidus mode (6-inches), the value used in the deterministic SOARCA analysis [2] for CAV 0, was determined from sample distributions documented in NUREG/CR-5423 [27]. Note that NUREG/CR-5423 only provides sample distributions for cases with water on the drywell floor, which is not the case for this sequence. However, the upper and lower bounds span a distribution for debris depth from the experimental results discussed in NUREG/CR-5423.

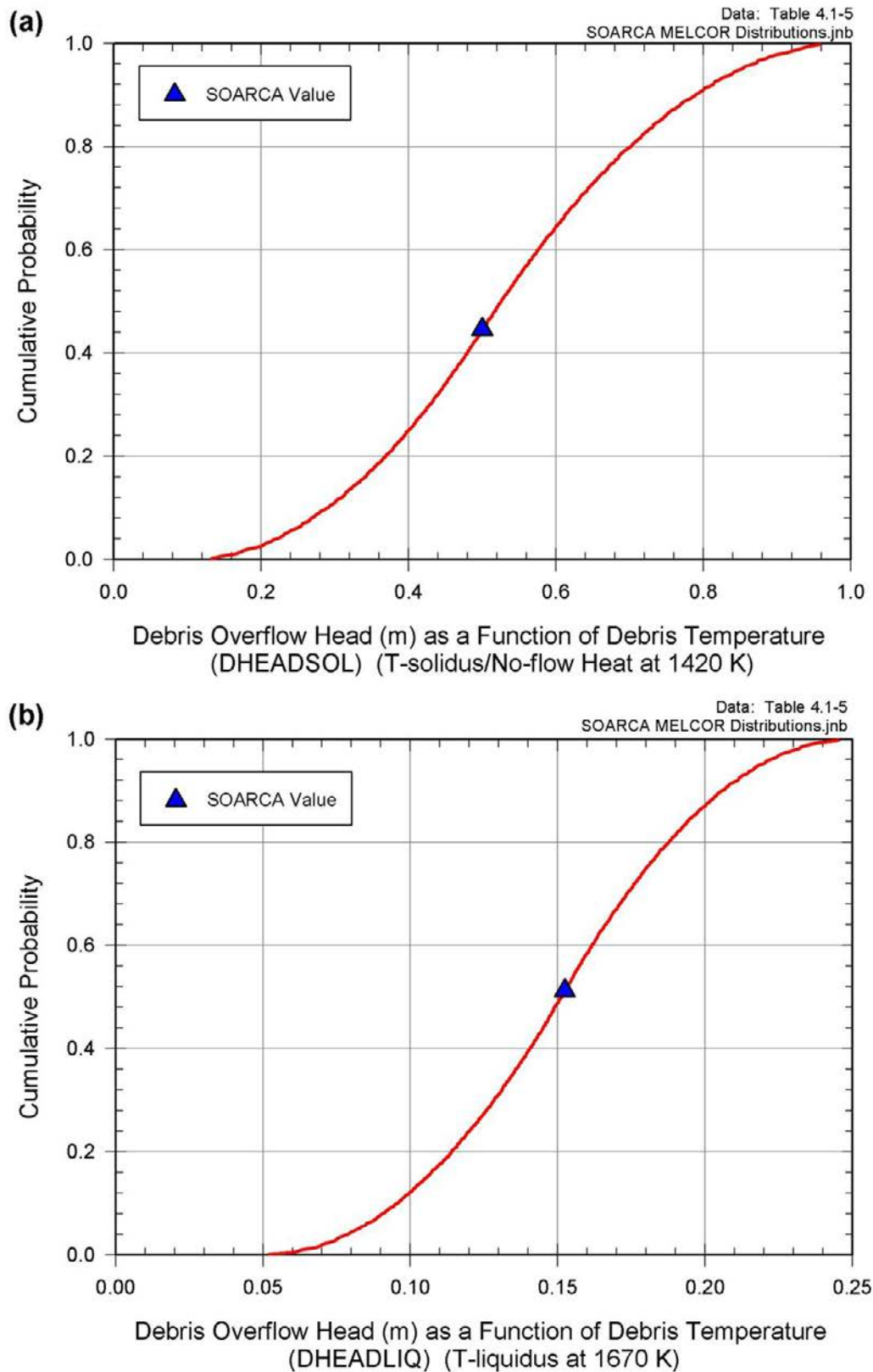


Figure 4.1-13 Cumulative distribution function debris overflow head as a function of debris at specified fixed temperatures: (a) T-solidus/no-flow head at 1420 K and (b) T-liquidus at 1670 K

Table 4.1-5 MELCOR uncertain parameters—Ex-vessel accident progression issues

Parameter	Distribution
DHEADSOL: Debris overflow head (m) as a function of debris at specified fixed temperature (T-solidus/no-flow head at 1420 K)	Triangle distribution LB = 0.1 m Mode = 0.5 m UB = 1.0 m Correlation (T-liquidus at 1670 K) = 1
	SOARCA estimate = 0.5 m
DHEADLIQ: Debris overflow head (m) as a function of debris at specified fixed temperature (T-liquidus at 1670 K)	Triangle distribution LB = 0.05 m Mode = 0.1524 m UB = 0.25 m Correlation (T-solidus at 1420 K) = 1
	SOARCA estimate = 0.1524 m

4.1.4 Containment Behavior Issues

Flow area resulting from drywell liner failure (FL904A)

If debris flows out of the reactor pedestal and spreads across the drywell floor, as described above, and contacts the outer wall of the drywell, the steel liner will fail. This failure opens a release pathway to the lower reactor building. Heat transfer between the steel liner and molten core debris is not explicitly calculated in the MELCOR model, due to limitations of the CAV Package, which addresses ex-vessel model debris behavior. The model assumes an opening in the drywell liner occurs 15 minutes after debris first contacts the drywell wall. This time delay represents an average of estimates for failure time discussed in NUREG/CR-5423 [27] for situations in which the drywell floor is not covered with water.

The failure area affects drywell atmosphere discharge rate to the reactor building or post-failure 'residence time'. The flow area is determined by debris temperature, debris depth against the liner, and the possibility of debris plugging part of the opening in the liner. A log-uniform distribution was selected for the uncertainty analysis (Figure 4.1-14 and Table 4.1-6).

The lower bound ($0.05 \text{ m}^2 \approx 10\text{-inch diameter hole}$) of the distribution is a factor of two less than the SOARCA estimates for drywell liner failure. The lower bound is also the minimum observed critical zone determined for a damage index profile at 1143°C (2090°F) in NUREG/CR-6025 [21]. The upper bound ($1.0 \text{ m}^2 \approx 44\text{-inch diameter hole}$) is determined as a sufficient flow area to provide containment depressurization within the matter of seconds. Additionally, the upper bound is 14% greater than the maximum observed critical zone (0.88 m^2) determined for a damage index profile at 1260°C (2300°F) in NUREG/CR-6025, and ensures the upper bound uncertainty of this parameter is fully captured.

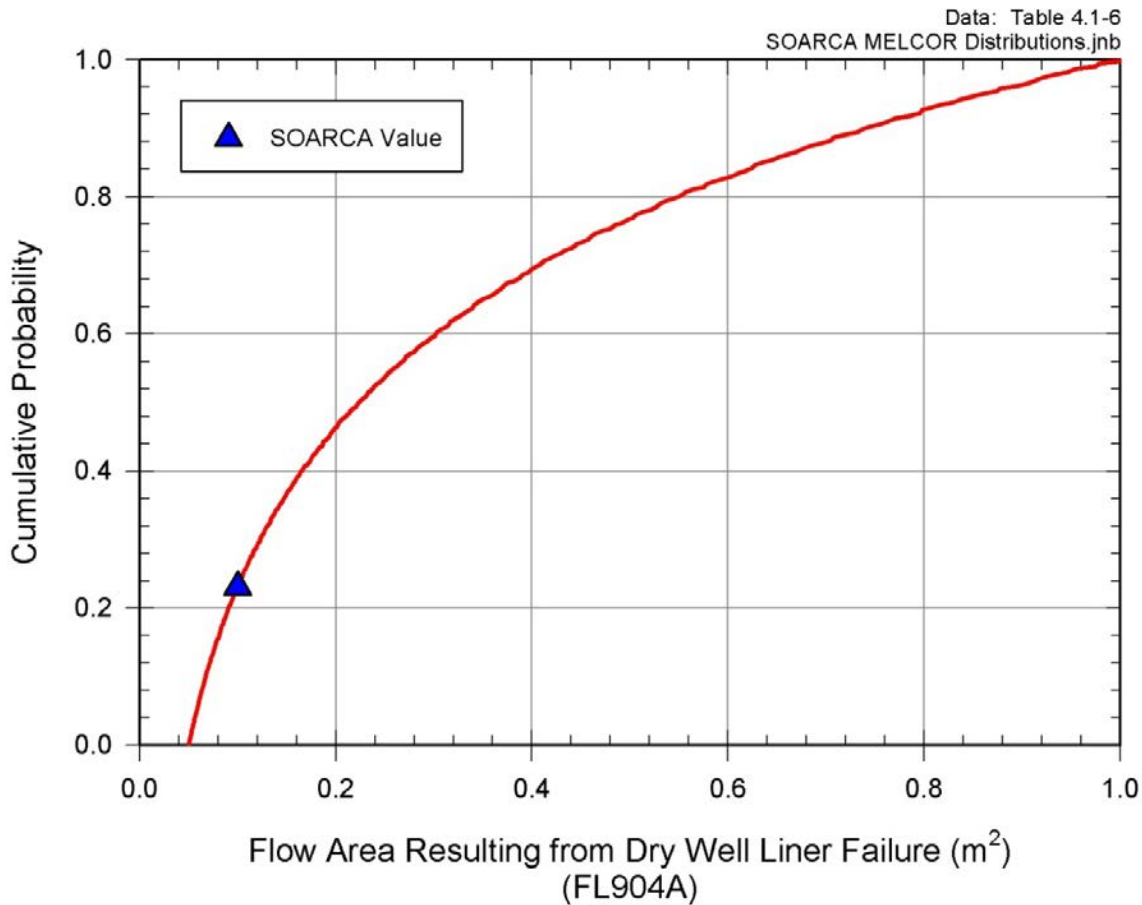


Figure 4.1-14 Cumulative distribution function of flow area resulting from drywell liner failure

Hydrogen ignition criteria (where flammable) (H2IGNC)

An ignition source for hydrogen combustion in the reactor building is unclear during a SBO. Since there are no electrically energized components in the reactor building during a SBO, the most likely ignition source will be a hot surface. Default ignition parameters were used in the SOARCA calculations for NUREG/CR-7110 Volume I. However, the accumulation of hydrogen due to an absence of an electrical ignition source is credible.

The ignition of hydrogen from a hot surface is caused by local heating of the hydrogen-oxygen mixture to a point where there is a sufficiently large volume of the mixture reaching the auto ignition. There are other factors which affect the auto ignition temperature such as [28, 29, and 30]:

- mixture concentrations,
- ambient temperature,
- size and shape of the hot surface,
- degree of confinement around the surface,
- the strength of convection currents across the surface, and
- the surface material.

For auto ignition on hot surfaces, a temperature range of 500-1265°C has been observed for hydrogen-air and hydrogen-oxygen mixtures [28, 31-33]. Work using very small hot surfaces suggests that mixtures as low as 10% to 15% hydrogen are most easily ignited [31, 33]. However for hydrogen-oxygen mixtures, research indicates a weak dependence on hydrogen concentrations from 20% to 94% [32]. Additionally experiments have shown that for a range of hydrogen concentrations from 4% to 94%, the minimum ignition temperature for a hydrogen-oxygen mixture on a hot surface occurs for a 20% hydrogen concentration [32]. For the uncertainty analysis, a triangular distribution was selected for both the hydrogen ignition criteria with the mode at 0.1 mole fraction, the value used in the deterministic SOARCA analysis [2], while 0.05 and 0.20 mole fraction were selected for the lower and upper bounds respectively (Figure 4.1-15 and Table 4.1-6).

The lower bound of the distribution is the lower flammability limit for a hydrogen-air mixture. The upper bound is based on research into hydrogen auto ignition from hot surfaces for a hydrogen-oxygen mixture [32].

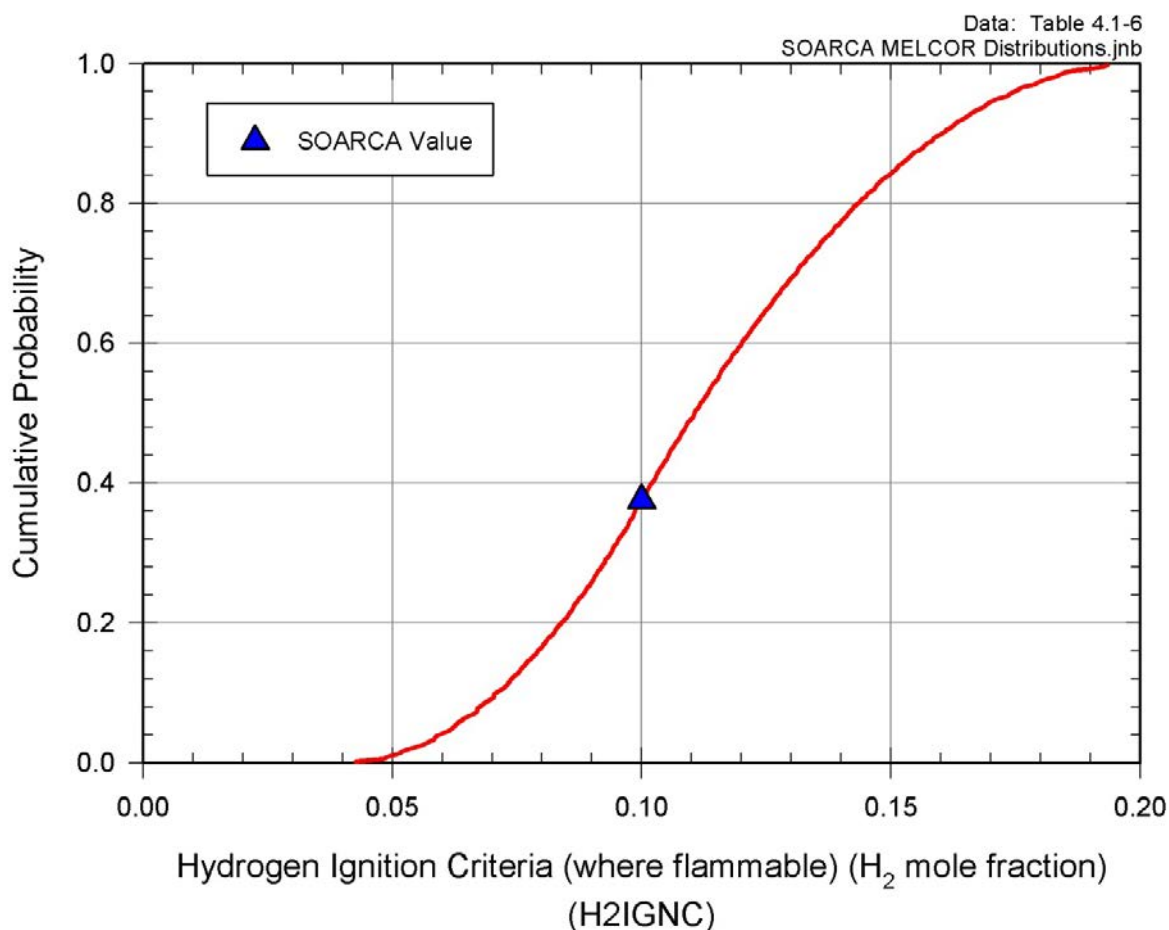


Figure 4.1-15 Cumulative distribution function of hydrogen ignition criteria (where flammable)

Railroad door open fraction due to over-pressure failure in reactor building (RRIDRAC, RRODFRAC)

The mechanical response of the large doors at each end of the equipment tunnel into the reactor building affects air infiltration and the establishment of a "chimney effect" through the building. This, in turn, greatly reduces the aerosol residence time and the building decontamination factor. The MELCOR model calculates aerosol transport and deposition in the reactor building, and thus the effective decontamination factor is explicitly calculated as a function of time.

In NUREG/CR-7110 Volume 1, the doors are assumed to fail with a 50% open fraction as an estimate if the local internal building pressure is 0.62 psi greater than the environment [34]. Smaller open areas are credible and might reduce the airflow and increase residence time. The large equipment access doors on the 135-ft level of the reactor building area are assumed to be relatively weak when subjected to modest internal pressure loads.

Past calculations [2] have shown that hydrogen combustion leads to a nearly immediate opening of the refueling bay blow-out panels and the railroad doorway at grade level. Blow-out panels into the turbine building and personnel access doorways out of the reactor building might also open. However, the dominant flow path for fission products to the environment is through the refueling bay blowout panels⁹. These past calculations have shown that failure by buckling is rather certain during a hydrogen burn. However, the open area that results from this failure is not known.

The distributions selected for this analysis are based on expert judgment and are not based on any specific data (e.g., Fukushima accident) as no data exists for railroad door open area. This parameter is only one of a few MELCOR parameters which can be modified to influence the dominant flow path for fission products to the environment, and is thus a key parameter for the analysis of source term releases. For the uncertainty analysis, uniform distributions were selected for both the inner and outer railroad door open area fractions due to overpressure failure in the reactor building. For both the railroad inner door and outer door, open area fractions 0.05 and 0.75 were selected for the lower and upper bounds respectively (Figure 4.1-16 (a and b) and Table 4.1-6).

⁹ A stable flow of air is calculated to enter the building through the open railroad doorway, rise upward through the open equipment hatches from grade level to the refueling bay and exit the building to the environment through the open blow-out panels.

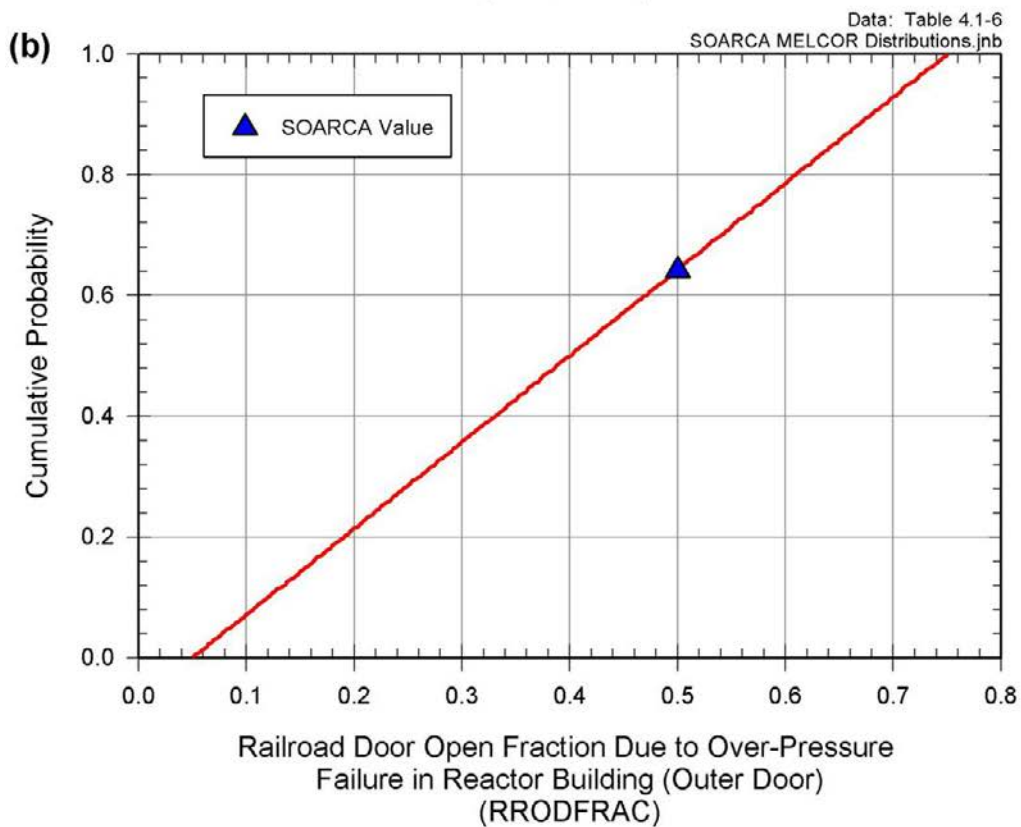
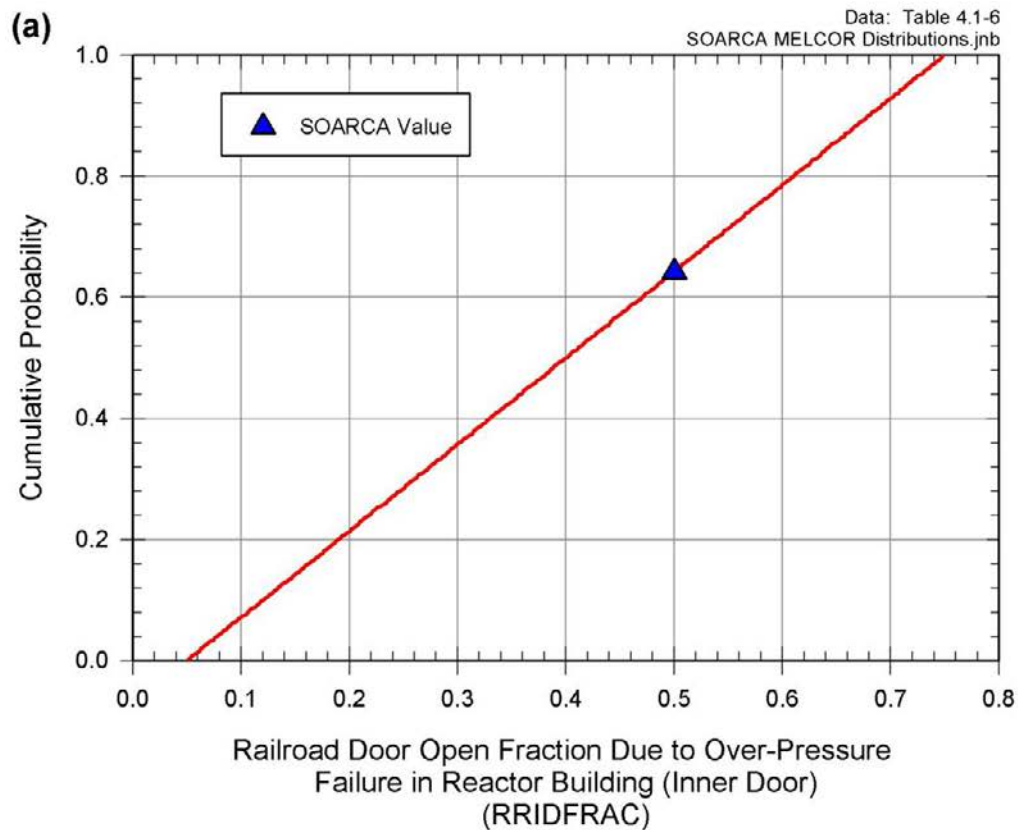


Figure 4.1-16 Cumulative distribution function of railroad door open fraction due to over-pressure failure in reactor building: (a) inner door and (b) outer door

Drywell Head Flange Leakage (K , E , and δ)

Peach Bottom has a Mark I containment that consists of a drywell and a toroidal shaped wetwell, which is half full of water (i.e., the pressure suppression pool). The drywell has the shape of an inverted light bulb. The drywell head is removed during refueling to gain access to the reactor vessel. The drywell head flange is connected to the drywell shell with 68 bolts of 2 ½ inch diameter (Figure 4.1-17). The flanged connection also has two ¾ inch wide and ½ inch thick ethylene propylene diene methylene (EPDM) gaskets. The torque on the 2 ½ inch diameter bolts range from 817 to 887 foot pounds (ft-lb) [21, 22]. An average bolt torque of 850 ft. lb. was used in this study.

The 68 drywell head flange bolts (Figure 4.1-17) are pre-tensioned during reassembly of the head. This pre-tension also compresses the EPDM gaskets in the head flange. During an accident condition, the containment vessel may be pressurized internally. The internal pressure would counteract the pre-stress in the bolts. At a certain internal pressure, all of the pre-stressing force from the bolts would be eliminated, and the EPDM gaskets would be decompressed. Further increase in the internal pressure would result in leakage at the flanged connection.

The EPDM gasket manufacturers recommend a maximum squeeze (compression) of 30% for a static seal joint. The gaskets recover about 15% of the total thickness after the compressive load is removed from the flange. However, engineering observations are that the gaskets for the drywell head flange are squeezed to 50% to have a metal to metal contact to ensure no leakage at a design pressure of 56 psig. In addition, the gaskets are exposed to constant temperature and radiation, which contribute to early degradation. For this reason, the gaskets are replaced during each reassembly of the reactor vessel head. Based on this information and actual observations, the Peach Bottom licensee engineers recommended a gasket recovery of 0.03 inch.

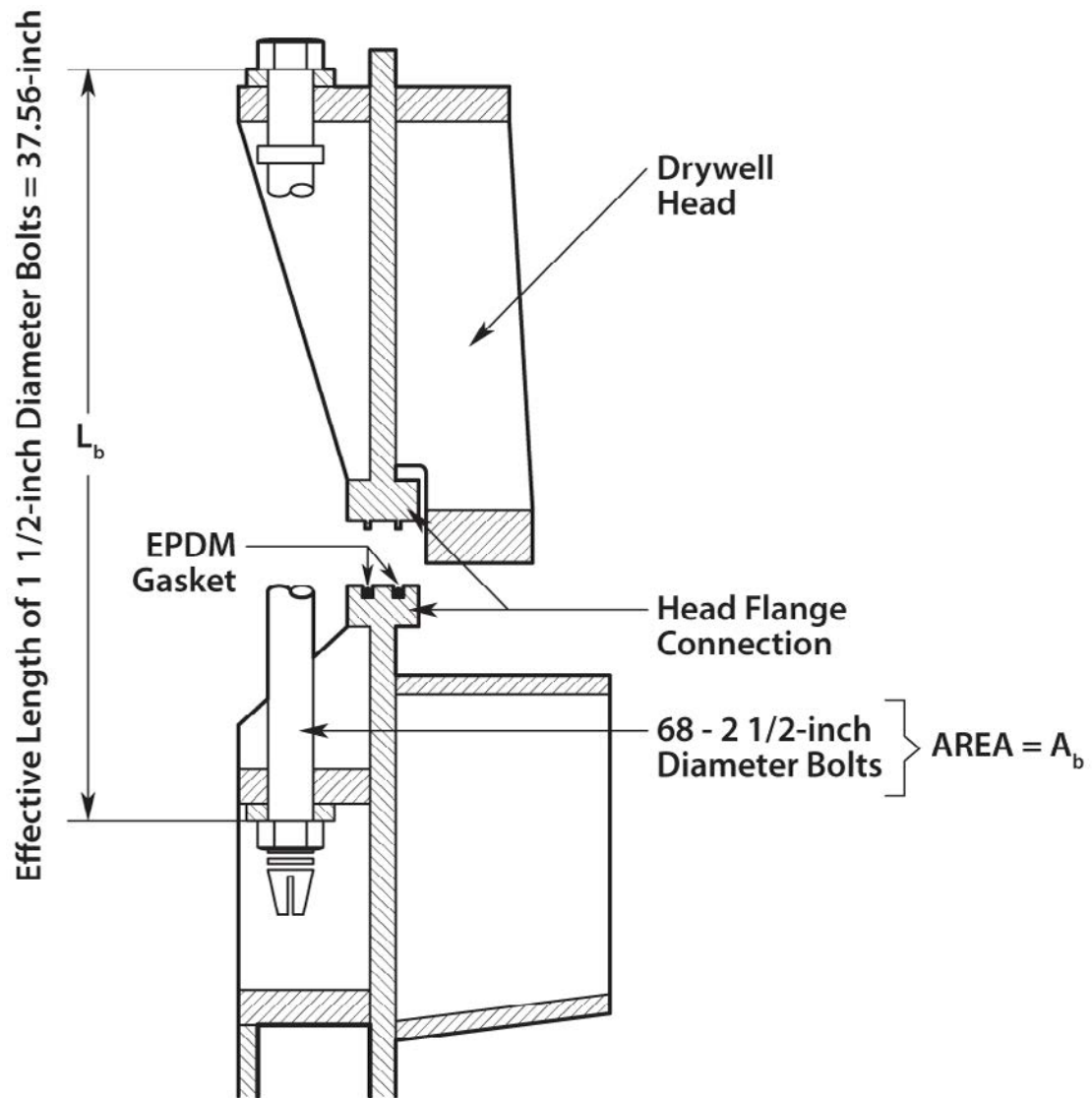


Figure 4.1-17 Drywell head flange connection details

Figure 4.1-18 shows the force balance on the drywell head given drywell pressure high enough that the head is not resting on the drywell flange.

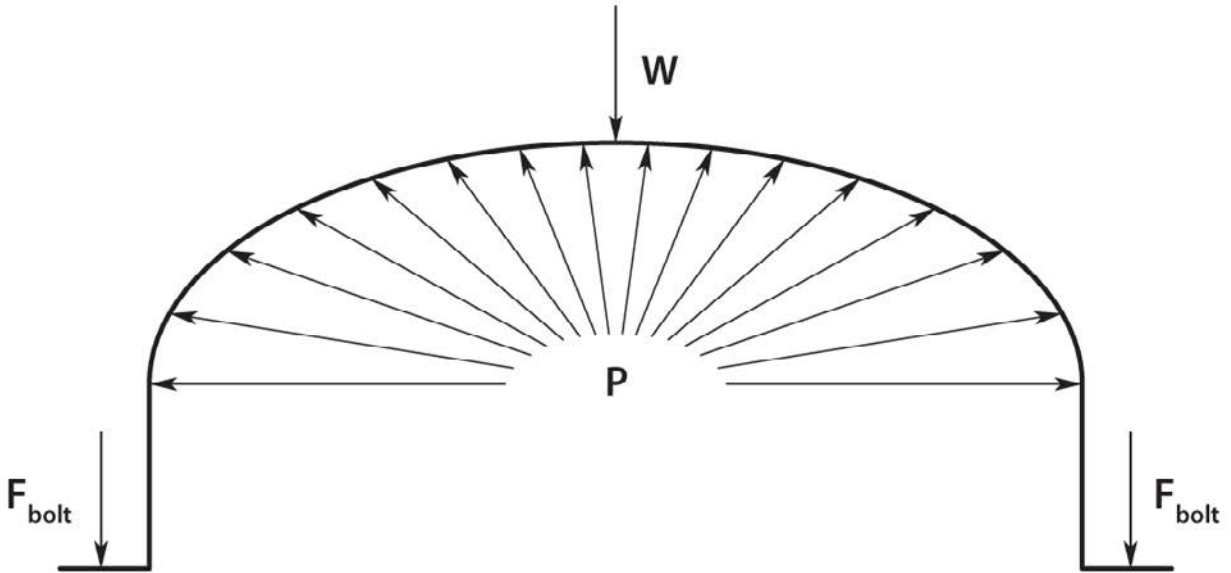


Figure 4.1-18 Force balance on drywell head

The force balance is given by:

$$W + N \cdot F_{bolt} = P \cdot A_{head} \quad \text{Equation 4.1-1}$$

where,

W is the weight of the head (130,000 lb.)

N is the number of bolts (68)

F_{bolt} is the force attributable to each bolt

P is the pressure in the drywell

A_{head} is the projected area of the head

The projected area of the head is given by:

$$A_{head} = \pi \cdot R_{head}^2 \quad \text{Equation 4.1-2}$$

R_{head} in Equation 4.1-2 is the internal radius of the drywell at the head flange (194 in). F_{bolt} has two components expressed as:

$$F_{bolt} = F_{bolt_{pre}} + F_{bolt_{press}} \quad \text{Equation 4.1-3}$$

$F_{bolt_{pre}}$ is the force associated with the pre-tensioning of the head bolt during assembly and is given by [35]:

$$F_{bolt_{pre}} = \frac{T}{K \cdot d_{bolt}} \quad \text{Equation 4.1-4}$$

where,

T is the torque applied to the bolt during assembly (850 ft-lb)

K is the torque coefficient (0.08 SOARCA estimate)

d_{bolt} is the nominal diameter of the bolt (2.5 in)

$F_{bolt,press}$ is the force associated with the tension developed in the head bolt in response to the pressure force developed as drywell pressure increases. This force is given by:

$$F_{bolt,press} = E \cdot \frac{\Delta L_{bolt}}{L_{bolt}} \cdot A_{tensile} \quad \text{Equation 4.1-5}$$

where,

E is the modulus of elasticity of the bolt (28,000,000 psi SOARCA estimate)

ΔL_{bolt} is the elongation of the bolt

L_{bolt} is the length of the bolt (37.56 between the head and the nut)

$A_{tensile}$ is the tensile area of the bolt (4.00 in for a bolt of 2.5 in nominal size)

Substituting Equations 2, 3, 4, and 5 into Equation 1 yields:

$$W + N \left(\frac{T}{K \cdot d} + E \cdot \frac{\Delta L_{bolt}}{L_{bolt}} \cdot A_{tensile} \right) = P \cdot \pi \cdot R_{head}^2 \quad \text{Equation 4.1-6}$$

Solving for bolt elongation gives:

$$\Delta L_{bolt} = \frac{L_{bolt}}{E \cdot A_{tensile}} \left(\frac{P \cdot \pi \cdot R_{head}^2 - W}{N} - \frac{T}{K \cdot d_{bolt}} \right) \quad \text{Equation 4.1-7}$$

The height of the circumferential gap opened by lifting the drywell head is given by:

$$L_{gap} = \Delta L_{bolt} - \delta_{gasket} \quad \text{Equation 4.1-8}$$

Where δ_{gasket} is the rebound thickness of the gasket (i.e., the increase in thickness that the gasket would experience once the compressive force on it was removed; 0.03 is the SOARCA estimate). The associated area of the gap is:

$$A_{gap} = L_{gap} \cdot 2 \cdot \pi \cdot R_{head} \quad \text{Equation 4.1-9}$$

Substituting Equation 8 into Equation 9 gives:

$$A_{gap} = (\Delta L_{bolt} - \delta_{gasket}) 2 \cdot \pi \cdot R_{head} \quad \text{Equation 4.1-10}$$

The parameters in the above equations considered uncertain (Table 4.1-6) are the modulus of elasticity (E) of the drywell head bolts, the torque coefficient associated with the pre-tensioning of the head bolts (K), and the rebound thickness of the drywell head gasket (δ_{gasket}). A uniform distribution between 26,600,000 psi and 29,400,000 psi was investigated to measure the potential effects of uncertainty in E . A triangular distribution was selected for K with mode 0.08 and 0.029 and 0.57 lower and upper bounds, respectively. A uniform distribution between 0.026 in and 0.034 in was investigated to measure the potential effects of uncertainty in δ .

The choice of the uniform distribution on E reflects the fact that E for steel varies somewhat with temperature and that the temperature of the bolts is not directly determined in the MELCOR calculations. The bounds chosen for the distribution on E reflect:

1. The observation that mid-height drywell temperature reaches 227°C in the SOARCA estimate calculation.
2. The assumption that the drywell head flange bolts are carbon steel.
3. That the modulus of elasticity of carbon steel varies between 29,300,000 psi at 21°C and 27,300,000 psi at 260°C.

The bounds on E are 5% to either side of the SOARCA estimate which covers the foreseeable variation in E due to temperature in the LTSBO scenario.

The mode adopted for K is the SOARCA estimate value identified in work accomplished by NRC personnel in their SOARCA-related evaluation of Peach Bottom Nuclear Power Station containment strength. The lower and upper bounds imposed on the distribution for K were determined from the relation [35]:

$$K = \left(\frac{d_m}{2d} \right) \left(\frac{\tan \psi + \mu \sec \alpha}{1 - \mu \tan \psi \sec \alpha} \right) + 0.625 \mu_c \quad \text{Equation 4.1-11}$$

where,

d_m is the mean diameter of the bolt
 d is the nominal size of the bolt
 Ψ is the helix angle of the thread

$$\Psi = \tan^{-1} \left(\frac{1/\# \text{ of threads per inch}}{\pi d_m} \right) \quad \text{Equation 4.1-12}$$

μ is the coefficient of thread friction
 α is half the thread angle
 μ_c is the coefficient of collar friction

For a 2.5-inch nominal size bolt assuming American National (Unified) Screw Thread UNC Class 2A:

$d_m = 2.3294$ in (nominally)
 $d = 2.4850$ in (nominally)
 $\#$ of threads per inch = 4
 $\Psi = 0.03415$ rad (= 1.96°)
 $\alpha = 0.5236$ rad (= 30°)

Friction coefficients μ and μ_c were taken to fall within the range between 0.029 and 0.57 applicable to steel (greasy or dry) sliding on steel [36].

Substituting values into Equation 4.1-11 yields a lower bound on K of 0.050 for $\mu = \mu_c = 0.029$ and an upper bound on K of 0.688 for $\mu = \mu_c = 0.57$.

The uniform choice of the distribution on δ_{gasket} reflects there not being information about the rebound thickness of the gasket other than the value recommended by informed Peach Bottom engineers (as described above). The bounds on the distribution are simply 15% to either side of

the SOARCA estimate rounded to two significant figures. These bounds are though large enough to identify the importance of the uncertainty in the rebound thickness of the drywell head flange gasket.

Equation 4.1-9 (i.e., A_{gap} versus P), is plotted on Figure 4.1-19 for three different combinations of the uncertain parameters E , K , and δ_{gasket} . One of the combinations utilizes the SOARCA estimate values of the parameters ($E = 28,000,000$ psi, $K = 0.08$, $\delta_{\text{gasket}} = 0.03$ in), another uses the values that would give the smallest gap area ($E = 29,400,000$ psi, $K = 0.050$, $\delta_{\text{gasket}} = 0.034$ in), and the remaining combination uses the values that would give the largest gap area ($E = 26,600,000$ psi, $K = 0.688$, $\delta_{\text{gasket}} = 0.026$ in).

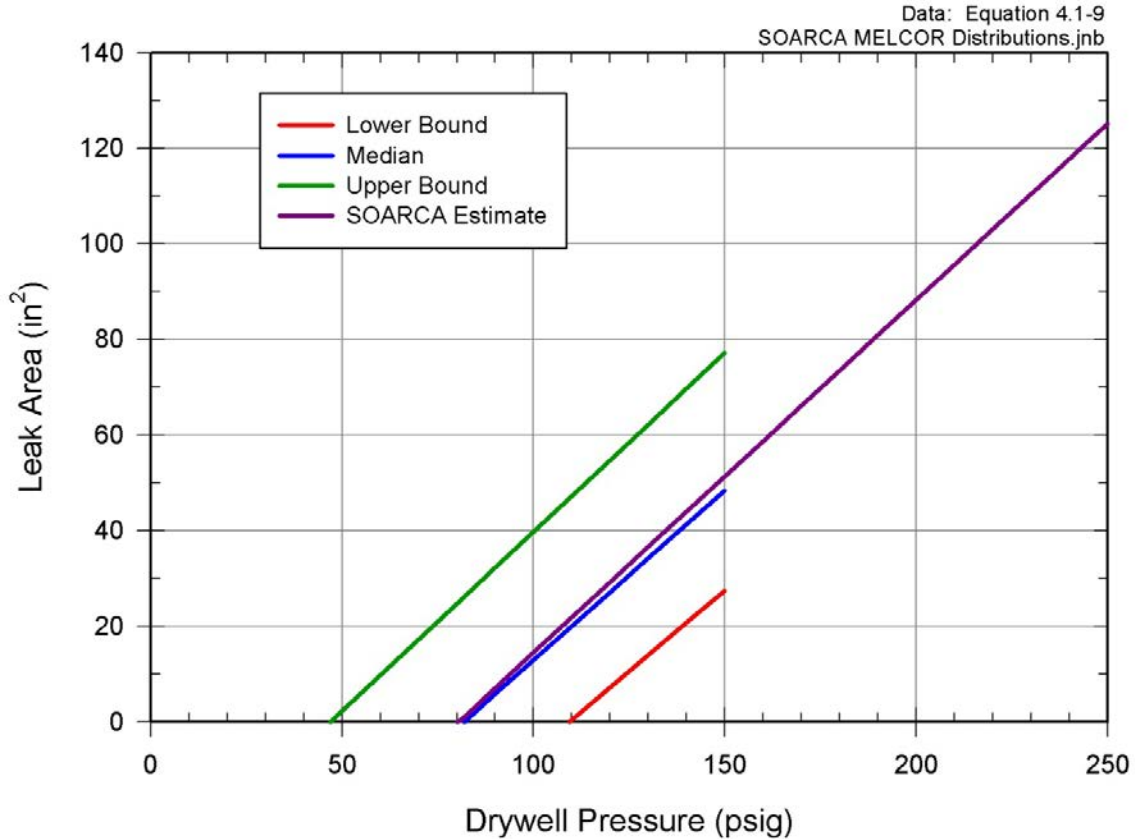


Figure 4.1-19 Drywell head flange gap area versus pressure

Uncertainty parameters K , E , and δ are introduced to the MELCOR modeling as terms in algebraic relationships formed by the following control functions:

$$CF88011 = 1 \cdot \frac{\text{time} \cdot 0.0 + 7030714.0}{\text{time} \cdot 0.0 + K} + 0.0 \quad \text{Equation 4.1-13}$$

$$CF88017 = 5.4365 \cdot \frac{CF88015 \cdot 1.0 + 0.0}{\text{time} \cdot 0.0 + E} + 0.0 \quad \text{Equation 4.1-14}$$

$$CF88019 = 1.0 \cdot (1.0 \cdot CF88017 + 0.0 + 0.0 \cdot \text{time} - \delta) + 0.0 \quad \text{Equation 4.1-15}$$

where E is in Pascals and δ is in meters.

Table 4.1-6 MELCOR uncertain parameters—containment behavior issues

Parameter	Distribution
FL904A: Flow area resulting from drywell liner failure (m ²)	Log Uniform distribution LB = 0.05 m ² UB = 1.0 m ²
	SOARCA estimate = 0.1 m ²
H2IGNC: Hydrogen ignition criteria (where flammable) (H ₂ mole fraction)	Triangle distribution LB = 0.04 mode = 0.10 UB = 0.20
	SOARCA estimate = 0.10
RRIDFRAC: Railroad inner door open fraction due to over-pressure failure in reactor building	Uniform distribution LB = 0.05 UB = 0.75
	SOARCA estimate = 0.5
RRODFRAC: Railroad outer door open fraction due to over-pressure failure in reactor building	Uniform distribution LB = 0.05 UB = 0.75
	SOARCA estimate = 0.5
E: Modulus of elasticity of the drywell head bolts (psi)	Uniform distribution LB = 26.6 × 10 ⁶ UB = 29.4 × 10 ⁶
K: Torque coefficient associated with the pre-tensioning of the head bolts	Triangle distribution Mode=0.08 LB = 0.029 UB = 0.57
δ: Rebound thickness of the drywell head (inches)	Uniform distribution LB = 0.026 UB = 0.034

4.1.5 Chemical Forms of Iodine and Cesium

Chemical forms of iodine and cesium (I₂, CH₃I, CsI, CsOH, and Cs₂MoO₄) (CHEMFORM)

The predominant speciation of cesium described in NUREG/CR-7110 Volume 1 was based on detailed chemical analysis of the deposition and transport of the volatile fission products in the Phebus facility tests [19-23]. The chemical analysis revealed molybdenum combined with cesium and formed cesium molybdate. Prior to NUREG/CR-7110 Volume 1, the default predominant chemical form of cesium was cesium hydroxide. Consistent with past studies, NUREG/CR-7110 Volume 1 assumed all released iodine combines with cesium. However, the Phebus facility tests show that gaseous iodine is found within containment [19-23].

The presence of gaseous iodine remains an uncertain source term issue, especially with respect to long-term radioactive release mitigation issues after the comparatively much larger airborne aerosol radioactivity has settled from the atmosphere. Mechanistic modeling of gaseous iodine behavior is a technology still under development with important international research programs to determine the dynamic behavior of iodine chemistry with respect to paints, wetted surfaces, buffered and unbuffered water pools undergoing radiolysis, and gas phase chemistry. The SOARCA estimate treatment under the best practices recommendation was deemed sufficient for the mean effects addressed in NUREG/CR-7110 Volume 1. Uncertainty in the gaseous iodine fraction to the total iodine released was identified as a key parameter and selected for evaluation of the sensitivity of SOARCA results.

Partitioning the initial core inventory of cesium and iodine among certain allowable chemical forms (for release and transport) is managed within MELCOR input files that define the initial spatial mass distribution of each chemical species and its associated decay heat. Changes to the mass fractions assumed for a particular chemical group directly affect the mass fractions of other chemical groups, and hundreds of individual input records within the MELCOR model for Peach Bottom. Due to the complexity of this general modeling uncertainty, five alternative sets of MELCOR input files are used to span the range of plausible combinations of chemical forms of key radionuclide groups. Fixed partition fractions are used to preserve mass balances.

The fraction of gaseous iodine for each of the five alternatives was determined using Phebus experimental results (see Table 4.1-7). The following provides discussion for the development of the five alternative combinations with regards to gaseous iodine release to containment.

- (1) Combination 1: From the Phebus FTP0 experiment [19], $3\% \pm 1.1\%$ of the initial iodine inventory was found in containment during 3.75 to 3.81 hours following the first zircaloy oxidation phase. After this timeframe, the gaseous iodine concentration in containment drops to $0.32\% \pm 0.16\%$ of the initial iodine inventory. This is due to steam condensation on the painted condenser and adsorption process on other containment surfaces, or both. Since it is uncertain as to when in the accident progression containment will fail, the averaged peak gaseous iodine fraction (3%) is assumed.
- (2) Combination 2: From the Phebus FTP1 experiment [20], $0.2\% \pm 0.045\%$ of the initial iodine inventory was found in containment following the first zircaloy oxidation phase. After the second zircaloy oxidation phase, the gaseous iodine concentration in containment drops to $0.07\% \pm 0.016\%$ of the initial iodine inventory. This is due to similar reasons described in the FTP0 experiment. Since it is uncertain as to when in the accident progression containment will fail, the averaged peak gaseous iodine fraction (0.2%) is assumed.
- (3) Combination 3: From the Phebus FTP2 experiment [22], 0.298% of the initial iodine inventory was found in containment. However, unlike the two previous experiments, the maximum gaseous iodine concentration occurs during the second oxidation phase of zircaloy. The minimum gaseous iodine concentration of 0.011% occurs during the main zircaloy oxidation phase. Since it is uncertain as to when in the accident progression containment will fail, the peak gaseous iodine fraction (0.298%) is assumed.
- (4) Combination 4: From the Phebus FTP3 experiment [23], 7.57% of the initial iodine inventory was found in containment. This peak gaseous iodine concentration occurred just after the first zircaloy oxidation phase. The minimum gaseous iodine concentration of 0.28% occurs prior to the first zircaloy oxidation phase. Since it is uncertain as to when in the accident progression containment will fail, the peak gaseous iodine fraction (7.57%) is assumed.

- (5) Combination 5: From the Phebus experiments [19, 20, 22, and 23], an averaged peak gaseous iodine of 2.77% of the initial iodine inventory was assumed.

Each of the five alternative combinations of the four chemical groups has a probability of occurrence defined by a discrete distribution (Figure 4.1-20 and Table 4.1-7). Each of the five alternatives partitions the radionuclide mass of iodine and cesium between four radionuclide classes in the MELCOR model (radionuclide classes: 2 (CsOH), 4 (I₂), 16 (CsI), and 17 (Cs₂MoO₄), Table 4.1-7). The physical properties of methyl iodide are not currently defined for a radionuclide class in the MELCOR model. Therefore, input for a new class and the associated mass balance arithmetic in the core inventory would be necessary to model this form of iodine. This was considered beyond the scope of this analysis and CH₃I is neglected.

The peak gaseous iodine amounts recorded in the four different Phebus experiments are fundamental in defining the five speciation combinations of cesium and iodine considered in the distributions. A combination is devoted to each of the four recorded amounts and a 5th combination was formed by averaging the four recorded amounts of iodine together. Equal weighting in the parameter sampling was given to all but the Combination #5 which was weighted four times greater than the other combinations reflecting that it was jointly formed from the iodine recorded in the four experiments.

With gaseous iodine (fraction of initial core inventory) defined for the five combinations, enough cesium was defined as CsI to involve all of the iodine not defined as gaseous (i.e., most all of the iodine). The remaining cesium was defined in the different combinations to be either in the form of all CsOH, all Cs₂MoO₄, or half CsOH and half Cs₂MoO₄, to represent uncertainty in cesium speciation. In five every eight realizations (Combinations #3 and #5), the remaining cesium is all Cs₂MoO₄. In two of every eight realizations (Combinations #2 and #4), the remaining cesium is half CsOH and half Cs₂MoO₄, representing the possibility of a mixed speciation. In one of every eight realizations (Combination #1), the remaining cesium is all CsOH, representing the former conventional assumption. Note that in all cases, including the SOARCA case, 1% of the initial cesium inventory is defined to be elemental cesium residing in the fuel-cladding gap.

With respect to cesium speciation, Combinations #3 and #5 closely match the SOARCA calculation. In the sampling of the chemical form of iodine and cesium, Combination #3 results once in every eight realizations while Combination #5 results four times in every eight realizations. Thus, in five of every eight realizations, the cesium speciation closely resembles the cesium speciation in the SOARCA calculation. However, there is no specific speciation combination that matches the iodine and cesium speciation of the SOARCA calculation identically. Combination #3 comes closest with the smallest fraction of gaseous iodine (~0.3%) and 100% Cs₂MoO₄. Recall, SOARCA did not include any gaseous iodine.

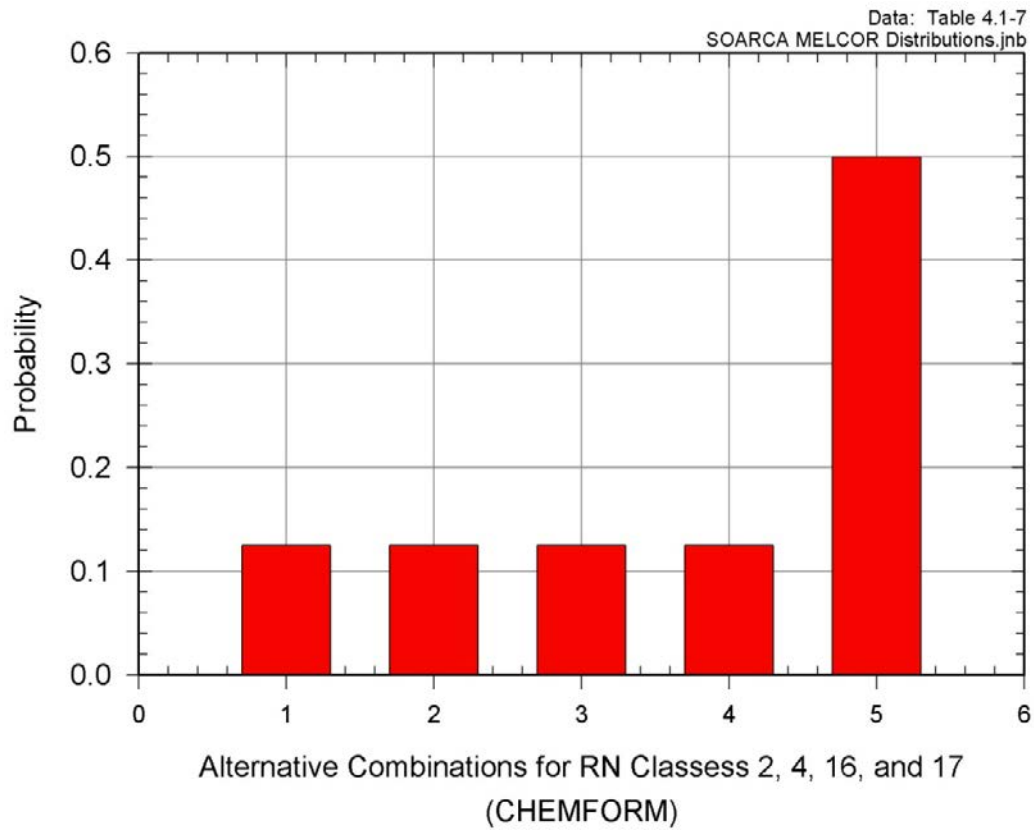


Figure 4.1-20 Probability density function for five alternative combinations for MELCOR model radionuclide classes 2, 4, 16, and 17 (I_2 , CsI , $CsOH$, and Cs_2MoO_4)

Table 4.1-7 MELCOR uncertain parameters for chemical forms of iodine and cesium.

Parameter			Distribution			
CHEMFORM: Five alternative combinations of RN classes 2, 4, 16, and 17 (CsOH, I ₂ , CsI, and Cs ₂ MoO ₄)			Discrete distribution			
			Combination #1 = 0.125			
			Combination #2 = 0.125			
			Combination #3 = 0.125			
			Combination #4 = 0.125			
			Combination #5 = 0.500			
Five Alternatives			Species (MELCOR RN Class)			
		CsOH (2)	I ₂ (4)	CsI (16)	Cs ₂ MoO ₄ (17)	
Combination #1	fraction iodine	--	0.03	0.97	--	
	fraction cesium ^a	1	--	--	0	
Combination #2	fraction iodine	--	0.002	0.998		
	fraction cesium	0.525 ^b	--	--	0.475	
Combination #3	fraction iodine	--	0.00298	0.99702	--	
	fraction cesium	0	--	--	1	
Combination #4	fraction iodine	--	0.0757	0.9243	--	
	fraction cesium	0.525 ^b	--	--	0.475	
Combination #5	fraction iodine	--	0.0277	0.9723	--	
	fraction cesium	0	--	--	1	
SOARCA estimate	Fraction iodine	--	0.0	1.0	--	
	Fraction cesium	0.05 ^b	--	--	0.95	

^a This represents the distribution of 'residual' cesium which is the mass of cesium remaining after first reacting with the amount of iodine assumed to form CsI.

^b The MELCOR model used in SOARCA always assumes 5.0% of the cesium is CsOH in the fuel gap. This parameter was not varied.

4.1.6 Aerosol Deposition

Dynamic and Agglomeration Shape Factors

When two or more aerosol particles collide, they can combine to form a larger particle. This process is known as agglomeration or coagulation. MELCOR code includes four agglomeration processes: Brownian diffusion, differential gravitational settling, and turbulent agglomeration by shear and inertial forces.

Except when they include significant amounts of liquid, aerosol particles are not usually assumed to be spherical, and the effective aerosol densities may be significantly less than the bulk density of the materials of which the aerosols are composed. In aerosol codes, these effects may be taken into account by using the agglomeration shape factor and the dynamic shape factor. The shape factors are used to represent the effect of a non-spherical shape upon aerosol collision cross sections and aerosol-atmosphere drag forces, respectively. Values of the shape factors correspond to dense aerosol of spherical shape (i.e., near 1.0 or unity), while porous spherical agglomerates lead, in theory, to values somewhat greater than unity. Highly irregular aerosols and agglomerates can have shape factors substantially greater than unity, often with the agglomeration and dynamic shape factors being quite unequal.

Given experimental data for aerosol shapes and densities applicable to light water reactor accidents, shape factors could in principle, be derived. Because this is not practical, empirical values are obtained by fitting code calculations to the results of aerosol experiments. The distributions used for this work can provide sensitivity to aerosol composition and to atmospheric conditions, especially to relative humidity. Humid conditions tend to produce more nearly spherical aerosols due to condensation of water onto aerosol agglomerates. Only limited information is available concerning the dependence of shape factors upon the relevant parameters (e.g., particle characteristics and atmospheric conditions [37]), and these parameters are themselves quite uncertain under accident conditions. Most experiments used in validating aerosol deposition are ideal aerosols comprised of known compositions (e.g., NaCl, CsOH, or polystyrene). The experiments are characterized in terms of aerodynamic diameters, which is the diameter that the true particle would apparently be if the assumed density was unity. Nuclear aerosol particles are difficult to define in terms of true density and diameter, so we vary shape factor and density to account for these unknowns.

For this work, it is assumed that hygroscopic effects during the accident sequence will induce some condensation of moisture on the aerosol particles causing the particles to tend towards being spherical and limit the degree of non-spherical shapes (i.e., 1.0 which is a perfectly spherical aerosol particle).

Particle Density (RHONOM)

Of the natural depletion processes used in MELCOR, gravitational deposition is often the dominant mechanism for large control volumes such as those typically used to simulate containment. A major uncertainty within gravitational deposition is the particle density.

Aerosol particles can become wet and when particles agglomerate, the resulting agglomerate is not fully dense with respect to the particle's assumed spherical shape. In its original context, "wet" implies "with water" from steam condensation in the containment environment. This can be generalized to also reflect that some components of the aerosol are possibly molten. The primary aerosol particles are condensation aerosol particles, probably in the sub-micrometer size range. Agglomeration of the smaller particles "grows" their size, but they may or may not be molten. Hence, the aerosol that escapes the RCS may not be spherical as previously molten drops, but rather, chain agglomerates of smaller particles or "puffy" agglomerations that are approximately spherical, but not fully dense. The agglomerate particles are clusters of smaller particles that have stuck together by collisions. The smaller particles comprising the agglomerate are presumed spherical but there are small spaces between the agglomerated particles. For this reason the agglomerate particle cannot be fully dense owing to the inherent porosity of the agglomerate. The aerosol shape factor and density are individual parameters in MELCOR, however, in a review by Brockmann [38] it is stated that the density usually is considered as the actual material density, and the shape factor is used to account for the porosity of the aerosol particle, thus correcting the aerodynamic diameter used in collision and settling terms. The suggested range of packing efficiency α , or ratio of apparent density to

material density, is 0.18 to 0.5. The apparent size is derived as follows: given a particle mass M , the diameter at the apparent density ρ is related to that at the real density ρ_o by:

$$M = \rho \frac{\pi}{6} D^3 = \rho_o \frac{\pi}{6} D_o^3$$

Equation 4.1-16

or

$$\alpha = \frac{\rho}{\rho_o} = \left(\frac{D_o}{D} \right)^{1/3}$$

Equation 4.1-17

Thus the shape factor, defined as the ratio of apparent volumetric diameter to fully dense diameter, would vary as $\sim \alpha^{-1/3}$. The suggested range for the shape factor is 1 to 3, although, if we use the suggested range for α , we only get a variation of 1 to 1.4. Another factor is whether the aerosols are considered to be dry or wet. Wet aerosols are those that absorb water in a humid environment, generally when the humidity is >80%. This is a consideration in containments, not so much inside a RPV. Wet aerosols would be more spherical and have a density closer to that of water (i.e., a value of 1.0).

The above suggests that density and shape factor are not entirely independent variables, and what should actually be varied is the packing efficiency. In particular, for a given density ratio, α , the shape factor ratio is $\alpha^{-1/3}$. Varying the density ratio and shape factor ratio in this manner should produce results that are consistent with a relationship between shape factor and density, in theory.

Expanding on this, the aerosols of interest in reactor accidents are cesium, iodine, and to some extent strontium, because of its biological effects, relatively long half-life, and volatility, meaning greater release. In the version of MAEROS (the aerosol package) used in MELCOR, the radionuclide density for all radionuclide classes is represented by a single value. Table 4.1-8 lists some material densities of representative aerosols of interest.

Table 4.1-8 Densities of several radionuclide compounds

Radionuclide aerosol compound	Density (kg/m ³)
CsOH	3675
Cs ₂ MoO ₄	4410
Sr(OH) ₂	3670
SrO	4700
I ₂	4930
CsI	4150

As can be seen, the material density range of interest is about 3700-4900 kg/m³. Using the above suggested range for packing efficiency, this gives a range of apparent density of about 660-2460 kg/m³. The default density used in MELCOR and the SOARCA analysis is 1000 kg/m³, with a shape factor of 1.0, so this seems to be a reasonable distribution of values, with the packing efficiency factor being absorbed in the density value.

Aerosol Deposition Uncertainty

For the uncertainty analysis, an average actual material density can be derived in the following way. Table 4.1-9 below gives the released mass for the different radionuclide classes in a MELCOR run for the SOARCA Peach Bottom Unmitigated LTSBO case (the classes for boron, water, and concrete are omitted). Also given are the radionuclide class name, an assumed chemical form for the aerosol, and the density. The column labeled “weighting factor” is the released class mass divided by the density, or

$$w_i = \frac{m_i}{\rho_i}$$

Equation 4.1-18

for the i^{th} class. This factor represents the volume of the released radionuclide, and, if we assume that the radionuclide was originally released as a vapor and condensed into the smallest aerosol size bin, this is proportional to the initial number density of the aerosol for the class. These factors are then summed and the inverse multiplied by the total released mass to get an average material density for the aerosols, as

$$\rho_{avg} = \frac{M}{\sum w_i}$$

Equation 4.1-19

Table 4.1-9 Released radionuclide masses and weighting factors from SOARCA Peach Bottom Unmitigated LTSBO Case

RN Class	RN Class Name	Chemical Form	Released Mass (kg)	Density (kg/m ³)	Weighting Factor (m ³)
1	Xe	Xe	5.32×10^2		
2	Cs	CsOH	1.71×10^1	3,675	4.64×10^{-3}
3	Ba	BaO	6.67×10^0	5,720	1.17×10^{-3}
4	I	I ₂	5.61×10^{-3}	4,930	1.14×10^{-6}
5	Te	TeO ₂	5.49×10^1	5,680	9.66×10^{-3}
6	Ru	RuO ₂	1.23×10^1	6,970	1.77×10^{-3}
7	Mo	MoO ₂	4.38×10^0	6,470	6.77×10^{-4}
8	Ce	CeO ₂	3.89×10^0	7,215	5.40×10^{-4}
9	La	La ₂ O ₃	1.11×10^{-1}	6,510	1.70×10^{-5}
10	U	UO ₂	6.04×10^2	10,960	5.51×10^{-2}
11	Cd	CdO	6.14×10^0	8,150	7.54×10^{-4}
12	Ag	SnO ₂	8.31×10^0	6,950	1.20×10^{-3}
16	CsI	CsI	4.07×10^1	4,510	9.03×10^{-3}
17	CsM	Cs ₂ MoO ₄	4.60×10^2	4,410	1.04×10^{-1}
18	Sn metal	SnO ₂	6.69×10^2	6,950	9.62×10^{-2}

Note: Chemical forms and densities from Wikipedia and MELCOR RN-RM

Table 4.1-10 gives the totals, not including the noble gas class, with and without the tin metal (released from zircaloy cladding) for the weights, average densities, and minimum and maximum effective densities using the suggested range for the packing efficiency, 0.18-0.5.

Table 4.1-10 Totals and density ranges

Totals	Released mass (kg)	Sum of weights (m³)	Average density (kg/m³)	Minimum density (kg/m³)	Maximum density (kg/m³)
Without class 18	1.22×10^3	1.89×10^{-1}	6.45×10^3	1.16×10^3	3.23×10^3
With class 18	1.89×10^3	2.85×10^{-1}	6.62×10^3	1.19×10^3	3.31×10^3

The range of densities in Table 4.1-10 can be used for the uncertainty range. It should be noted that there is a large variation in the amount of UO₂ and tin metal released, depending on variations in the accident scenario; the range between minimum and maximum densities should be increased to account for this uncertainty. The value of χ should be close to 1.0, since the effect of packing efficiency is now absorbed into the apparent density – the maximum noted in Hinds [39], for a string of five spheres, is 1.2. Kissane also notes that there is no evidence in experiments on reactor accident scenarios for anything but a spherical agglomeration as the usual shape of an aerosol particle [37].

The average material density of the particulate released to the environment in the SOARCA LTSBO MELCOR calculation (6,450 kg/m³) served as the basis for the sampling of particle density in the calculations. Packing factors of 0.18 minus 25% variance (= 0.135) and 0.5 plus 25% variance (= 0.626) were applied to the average from the SOARCA calculation to define the lower and upper bounds of the sampling as 870 kg/m³ and 4,037 kg/m³, respectively. A triangular distribution was invoked with mode equal to the MELCOR default density (and SOARCA value) of 1,000 kg/m³ lending somewhat of a bias toward smaller densities in the sampling. At first, the aerosol dynamic shape factor was also identified as an uncertain parameter for sampling, but there was a worry about simultaneous varying both variables potentially leading to the modeling of unphysical conditions. After further deliberation and consultation with experts, the team concluded that assuming a shape factor of 1 (perfectly spherical) and varying RHONOM should capture the effects of uncertainty stemming from both these related parameters.

In this analysis, it is assumed that Chi and Gamma = 1.0, and the particle density has a triangular distribution of [870, 1,000, 4,037] kg/m³ for the min, mode, max (Figure 4.1-21 and Table 4.1-11). The density distribution is based on the average effective density range (1.16×10^3 to 3.23×10^3) representative of the mass fractions for the various radionuclide classes released as aerosols as calculated for the SOARCA case, with a 25% variance on the min and max to account for variation over the range of uncertainty in the MELCOR in-vessel parameters which will yield a range in the amount of the heavier radionuclide classes and tin, which are in turn dependent on the amount of core damage and peak temperatures in the RPV.

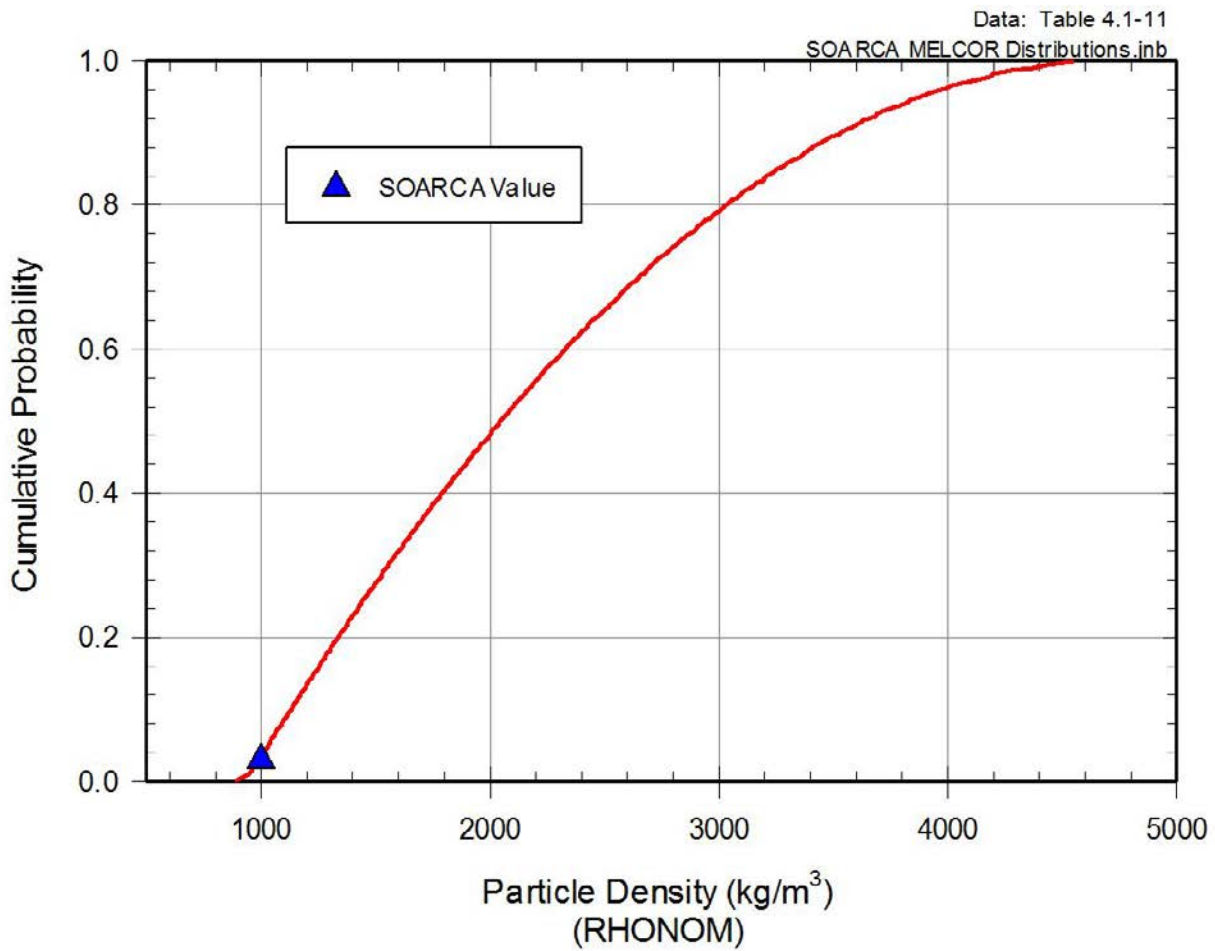


Figure 4.1-21 Cumulative distribution function of particle density

Table 4.1-11 MELCOR uncertain parameters—aerosol deposition

Parameter	Distribution
RHONOM: Particle Density	Triangular distribution LB = 870 kg/m ³ Mode = 1,000 kg/m ³ UB = 4,730 kg/m ³

4.2 Consequence Model Uncertainty (MACCS Inputs)

The MACCS consequence model (Version 2.5.0.0) is used in the SOARCA analysis to calculate offsite doses and their effect on members of the public. Epistemic uncertainty was considered for the principal phenomena in MACCS, including atmospheric transport using a straight-line Gaussian plume model of short-term and long-term dose accumulation through several pathways including: cloudshine, groundshine, and inhalation. The ingestion pathway was not treated in the SOARCA analyses because uncontaminated food and water supplies are abundant within the United States and it is unlikely that the public would eat radioactively contaminated food [40]. The parameter uncertainty in the MACCS consequence model will impact the following doses included in the SOARCA reported risk metrics:

- cloudshine during plume passage
- groundshine during the emergency and long-term phases from deposited aerosols
- inhalation during plume passage and following plume passage from resuspension of deposited aerosols. Resuspension is treated during both the emergency and long-term phases.

Development of the emergency planning related uncertainty parameters for MACCS input required establishing an emergency response timeline. The timeline includes actions described in the onsite and offsite emergency response plans. The emergency response plans are tested and exercised often and there is a high confidence in the interactions between onsite and offsite agencies. Research of existing evacuations provided information regarding movement of the public in response to an emergency and has shown that emergency response actions are routinely implemented and successful [41, 42]. Although there is high confidence in response actions, an emergency response is a dynamic event with uncertainties in elements of the response.

All of the emergency planning parameters used in MACCS were reviewed to determine the most appropriate parameters for the uncertainty analysis. The following three¹⁰ emergency planning parameter sets were selected:

- Hotspot and normal relocation,
- evacuation delay, and
- evacuation speed.

In addition, the SOARCA estimate offsite consequence results presented in the SOARCA study include the aleatory uncertainty associated with weather conditions at the time of the accident scenario. These SOARCA estimate offsite consequence values represent the expected (mean) value of the probability distribution obtained from a large number of weather trials. The uncertainty analysis is consistent with the weather-sampling strategy adopted for SOARCA and uses the same non-uniform weather-binning approach in MACCS used in the SOARCA calculation [1]. Weather binning is an approach used in MACCS to categorize similar sets of

¹⁰ The habitability criterion is also considered to be an important potentially uncertain parameter, but will not be included as part of the integrated uncertainty analysis. A separate discussion is included in Section 4.3 on the influence of the habitability criterion.

weather data based on wind speed, stability class, and the occurrence of precipitation. For the non-uniform weather sampling strategy approach for SOARCA, the number of trials selected from each bin is the maximum of 12 trials and 10% of the number of trials in the bin. Some bins contain fewer than 12 trials. In those cases, all of the trials within the bin are used for sampling. This strategy results in roughly 1,000 weather trials for the Peach Bottom accident scenario.

Several of the parameter distributions selected for this analysis are based on expert elicitation data captured in the report, *Synthesis of Distributions Representing Important Non-Site-Specific Parameters in Off-Site Consequence Analysis* [43]. The United States and the Commission of European Communities conducted a series of expert elicitations to obtain distributions for uncertain variables used in health consequence analyses related to accidental release of nuclear material [43]. The distributions reflect degrees of belief for non-site specific parameters that are uncertain and are likely to have significant or moderate influence on the results. The referenced report presents the effort to develop ranges of values and degrees of belief that fairly represent the divergent opinions of the experts while maintaining the resulting parameters within physical limits, specifically with the MACCS code in mind. The methodology used a resampling of the experts' values and was based on the assumption of equal weights of the experts' opinions. All other MACCS parameters not discussed in this section (e.g., emergency planning parameters) remain the original point estimates used in NUREG/CR-7110, Volume 1.

Additional discussions on certain MACCS parameters presented are discussed in Appendix E.

4.2.1 Wet Deposition Model (CWASH1)

Wet deposition is an important phenomenon that strongly affects atmospheric transport. Under heavy rains, wet deposition is very effective and rapidly depletes the plume. This process can produce concentrated deposits on the ground and create what is often referred to as a hot spot (i.e., an area of higher radioactivity than the surrounding areas). While rain occurs less than 10% of the time at Peach Bottom and for most of the U.S., it can significantly affect consequence calculations when it does occur. For this reason, uncertainty in the wet deposition model is considered in this uncertainty analysis. Table 4.2-1 provides the parameters describing the distribution for one of the parameters in the MACCS wet deposition model; the median value of the distribution was the value used in the deterministic SOARCA analysis [2]. The second parameter in the model, CWASH2, is fixed at a value of 0.664. The basis for this distribution comes from expert elicitation data [44], as further evaluated in *Synthesis of Distributions Representing Important Non-Site-Specific Parameters in Off-Site Consequence Analysis* [43]. The cumulative distribution for the wet deposition model coefficient is shown on Figure 4.2-1 and the values are provided in Table 4.2-1.

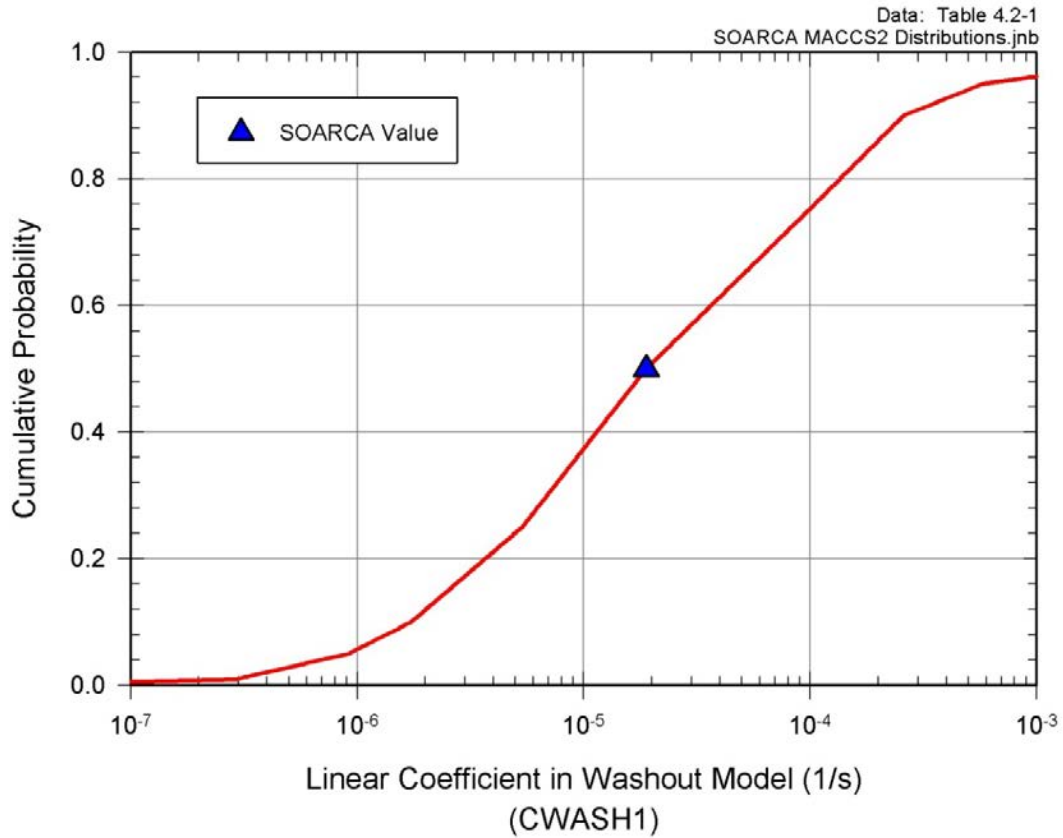


Figure 4.2-1 Cumulative distribution function for the linear coefficient (CWASH1) in the MACCS wet deposition model

Table 4.2-1 MACCS uncertain parameters—wet deposition model

CWASH1: Linear coefficient in wet deposition model	Percentile	CWASH1 [1/s]
Piecewise log-uniform distribution	0	2.73×10^{-8}
	1	2.92×10^{-7}
	5	9.13×10^{-7}
	10	1.73×10^{-6}
	25	5.36×10^{-6}
	50	1.89×10^{-5}
	75	9.84×10^{-5}
	90	2.59×10^{-4}
	95	5.79×10^{-4}
	99	3.78×10^{-3}
	100	1.14×10^{-2}
SOARCA estimate		1.89×10^{-5}

4.2.2 Dry Deposition Velocities (VDEPOS)

Dry deposition is the only mechanism for deposition onto the ground for more than 90% of the hours of the year at Peach Bottom (i.e., the hours during which rainfall does not occur). The term dry deposition involves a variety of mechanisms that cause aerosols to deposit, including gravitational settling, impaction onto terrain irregularities, including buildings and other manmade structures, and Brownian diffusion. Dry deposition is a much slower process than wet deposition, but occurs continuously, whereas, wet deposition occurs intermittently. Dry deposition is characterized in MACCS with a set of deposition velocities corresponding to a set of aerosol size bins. Larger values of dry deposition velocity result in larger long-term doses at shorter distances and smaller doses at longer distances; the converse is also true that smaller values of dry deposition velocity result in smaller long-term doses at shorter distances and larger doses at longer distances. The distributions for dry deposition velocity are based on expert elicitation data [44] and the expert data are evaluated in *Synthesis of Distributions Representing Important Non-Site-Specific Parameters in Off-Site Consequence Analysis* [43]. The values¹¹ used in this analysis are based on a mean annual wind speed of 2.2 m/s and a surface roughness length of 10 cm. The cumulative distributions for the dry deposition velocities are shown on Figure 4.2-2 and the values are provided in Table 4.2-2.

In revisiting the dry deposition velocities from the expert elicitation, some of the upper ranges of the distributions appear too high to be supported by physical understanding. Furthermore, in reviewing the original expert elicitation data, in some cases only one outlier expert's beliefs are responsible for the upper 10% of the distribution. However, in this study, surface roughness was not included as an uncertain parameter (see discussion under Section 4.3.5). Varying the dry deposition velocity accounts for the net effects had both VDEPOS and surface roughness been varied simultaneously. As noted in the MACCS SOARCA best practices document (NUREG/CR-7009 [93]) and the SOARCA detailed analyses documented in NUREG/CR-7110 Volume 1 [2], surface roughness somewhat greater than 10 cm may be more representative of the Peach Bottom site. As such, the higher deposition velocities sampled account for the net effect of the potential higher surface roughness.

¹¹ Subsequent to completing the UA calculations, the team discovered that there was an incorrect implementation of the expert elicitation data resulting in the wrong curves for some particle size bins, most notably bins 9 and 10 (the largest particle sizes). However, the effect of this incorrect implementation is judged not to be important, especially since there is relatively little mass within these bins.

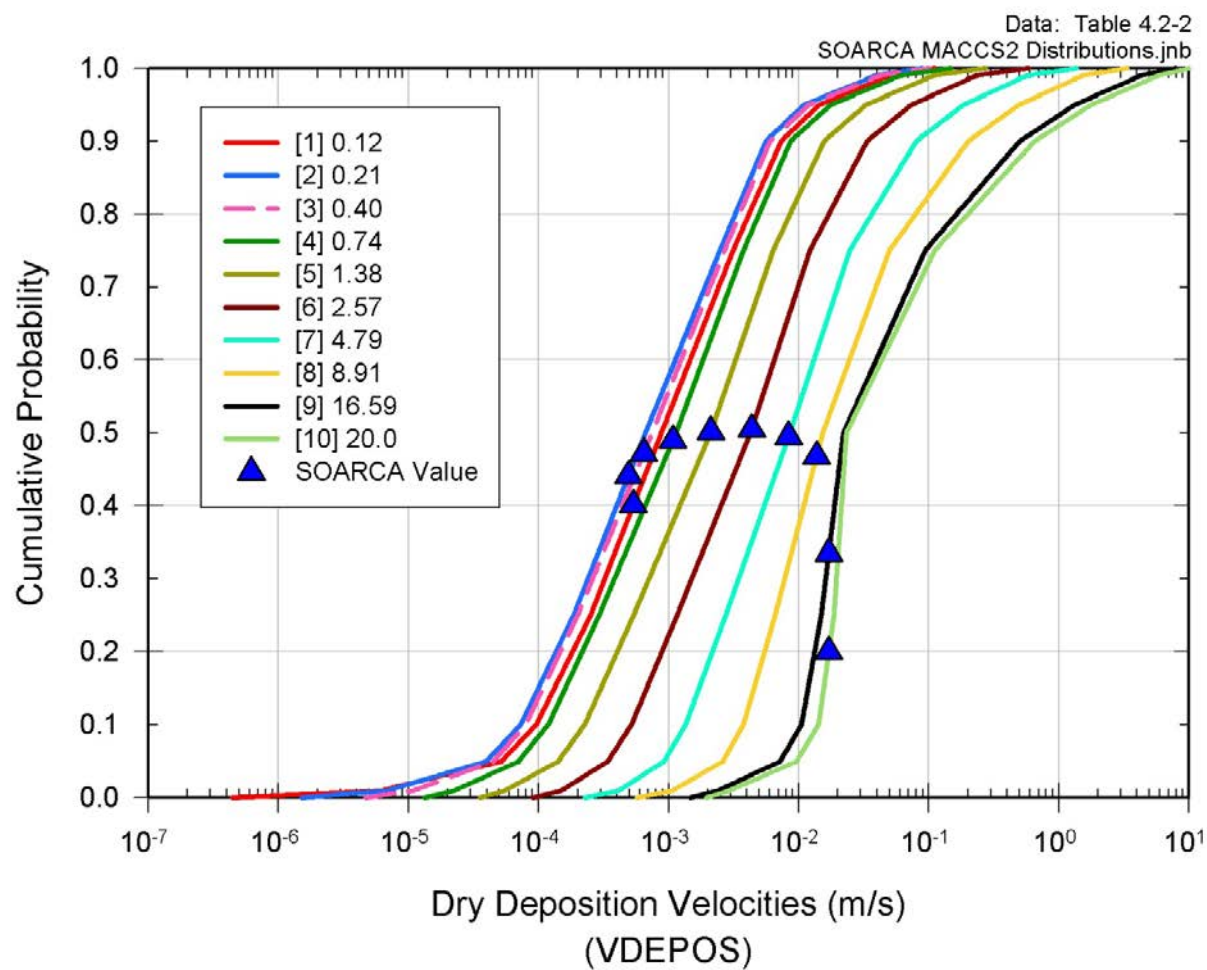


Figure 4.2-2 Cumulative distribution functions of dry deposition velocities for MACCS aerosol bins/aerosol mass median diameters

Table 4.2-2 MACCS uncertain parameters—dry deposition velocities

Dry Deposition Velocities VDEPOS (1 to 10) [m/s] Piecewise Log-Uniform Distribution																				
Aerosol Bin/Aerosol Mass Median Diameter (micrometers)																				
Percentile	1	0.12	2	0.21	3	0.40	4	0.74	5	1.38	6	2.57	7	4.79	8	8.91	9	16.59	10	20.00
0	4.44 × 10 ⁻⁷		1.52 × 10 ⁻⁶		4.71 × 10 ⁻⁶		1.34 × 10 ⁻⁵		3.56 × 10 ⁻⁵		9.11 × 10 ⁻⁵		2.28 × 10 ⁻⁴		5.73 × 10 ⁻⁴		1.47 × 10 ⁻³		1.96 × 10 ⁻³	
1	6.25 × 10 ⁻⁶		7.00 × 10 ⁻⁶		1.10 × 10 ⁻⁵		2.27 × 10 ⁻⁵		5.57 × 10 ⁻⁵		1.51 × 10 ⁻⁴		4.18 × 10 ⁻⁴		1.08 × 10 ⁻³		2.42 × 10 ⁻³		2.96 × 10 ⁻³	
5	5.20 × 10 ⁻⁵		3.99 × 10 ⁻⁵		4.52 × 10 ⁻⁵		7.05 × 10 ⁻⁵		1.42 × 10 ⁻⁴		3.42 × 10 ⁻⁴		9.25 × 10 ⁻⁴		2.62 × 10 ⁻³		7.22 × 10 ⁻³		9.66 × 10 ⁻³	
10	9.60 × 10 ⁻⁵		7.30 × 10 ⁻⁵		7.99 × 10 ⁻⁵		1.19 × 10 ⁻⁴		2.26 × 10 ⁻⁴		5.19 × 10 ⁻⁴		1.35 × 10 ⁻³		3.76 × 10 ⁻³		1.05 × 10 ⁻²		1.42 × 10 ⁻²	
25	2.51 × 10 ⁻⁴		1.86 × 10 ⁻⁴		2.00 × 10 ⁻⁴		2.92 × 10 ⁻⁴		5.38 × 10 ⁻⁴		1.16 × 10 ⁻³		2.75 × 10 ⁻³		6.59 × 10 ⁻³		1.49 × 10 ⁻²		1.87 × 10 ⁻²	
50	8.80 × 10 ⁻⁴		6.63 × 10 ⁻⁴		7.47 × 10 ⁻⁴		1.14 × 10 ⁻³		2.10 × 10 ⁻³		4.26 × 10 ⁻³		8.56 × 10 ⁻³		1.53 × 10 ⁻²		2.21 × 10 ⁻²		2.33 × 10 ⁻²	
75	3.13 × 10 ⁻³		2.48 × 10 ⁻³		2.69 × 10 ⁻³		3.76 × 10 ⁻³		6.36 × 10 ⁻³		1.22 × 10 ⁻²		2.47 × 10 ⁻²		4.98 × 10 ⁻²		9.39 × 10 ⁻²		1.11 × 10 ⁻¹	
90	7.35 × 10 ⁻³		5.60 × 10 ⁻³		6.03 × 10 ⁻³		8.67 × 10 ⁻³		1.57 × 10 ⁻²		3.36 × 10 ⁻²		8.03 × 10 ⁻²		2.02 × 10 ⁻¹		5.03 × 10 ⁻¹		6.55 × 10 ⁻¹	
95	1.45 × 10 ⁻²		1.11 × 10 ⁻²		1.21 × 10 ⁻²		1.78 × 10 ⁻²		3.32 × 10 ⁻²		7.42 × 10 ⁻²		1.87 × 10 ⁻¹		5.00 × 10 ⁻¹		1.34 × 10 ⁰		1.79 × 10 ⁰	
99	4.99 × 10 ⁻²		3.92 × 10 ⁻²		4.25 × 10 ⁻²		6.06 × 10 ⁻²		1.09 × 10 ⁻¹		2.33 × 10 ⁻¹		5.72 × 10 ⁻¹		1.53 × 10 ⁰		4.28 × 10 ⁰		5.84 × 10 ⁰	
100	1.11 × 10 ⁻¹		8.92 × 10 ⁻²		1.00 × 10 ⁻¹		1.48 × 10 ⁻¹		2.72 × 10 ⁻¹		5.83 × 10 ⁻¹		1.37 × 10 ⁰		3.35 × 10 ⁰		7.95 × 10 ⁰		1.00 × 10 ¹	
SOARCA Estimate	5.35 × 10 ⁻⁴		4.91 × 10 ⁻⁴		6.43 × 10 ⁻⁴		1.08 × 10 ⁻³		2.12 × 10 ⁻³		4.34 × 10 ⁻³		8.37 × 10 ⁻³		1.37 × 10 ⁻²		1.70 × 10 ⁻²		1.70 × 10 ⁻²	

Note: VDEPOS is perfectly rank correlated across aerosol sizes. Rank order correlation is the most commonly used method of computing a correlation coefficient using the rank order of the sampled values between two variables, rather than the absolute value sampled from the distribution.

4.2.3 Shielding Factors (CSFACT, GSHFAC, PROTIN)

In MACCS, shielding and protection factors are specified for each dose pathway and directly affect the dose received by individuals at each location. The shielding factors are used as multipliers on the dose that a person would receive if there were no shielding or protection. Thus, a shielding factor of one represents the limiting case of a person receiving the full dose (i.e., standing outdoors and completely unprotected from exposure); a shielding factor of zero represents the limiting case of complete shielding from the exposure. The shielding factors used in the MACCS calculation are clearly important because the doses received are directly proportional to these factors.

The values used in this uncertainty analysis for groundshine and inhalation are derived from expert elicitation data [45] by Gregory et al. [46]. Heames et al. [47] further evaluated the expert data to also derive distributions for cloudshine. Three types of activity, normal, sheltering, and evacuation, are evaluated for each dose pathway, resulting in nine sets of shielding factors, which are provided in Tables 4.2-3a, b, and c. Figure 4.2-3 shows a graphical representation of the Table 4.2-3 data. In this context, normal activity refers to a combination of activities that are averaged over a week and over the population, including being indoors at home, commuting, being indoors at work, and being outdoors. These values are used in the uncertainty analysis with the further assumption that the distributions for normal activity and sheltering are correlated with a rank correlation coefficient (RCC) of 0.75. This correlation should be applied for normal and sheltering activities for each of the pathways. There is no correlation between the three pathways. Each parameter (CSFACT, GSHFAC, PROTIN) can be specified for each of the six cohorts in WinMACCS (see Section 6.1 and 6.3.1 in Reference 1 for further discussions on the six cohorts). In the SOARCA analysis, the distributions listed in Tables 4.2-3a, b, and c are used in the WinMACCS file. In the SOARCA study [1], shielding values for Cohorts 1, 2, 3, 5, and 6 are identical. Cohort 4 is special facilities, which has different shielding values in the SOARCA study. For this study, a single distribution was sampled and applied to all of the cohorts. A rank linear coefficient of 0.75 is associated for normal and sheltering activities for all cohorts.

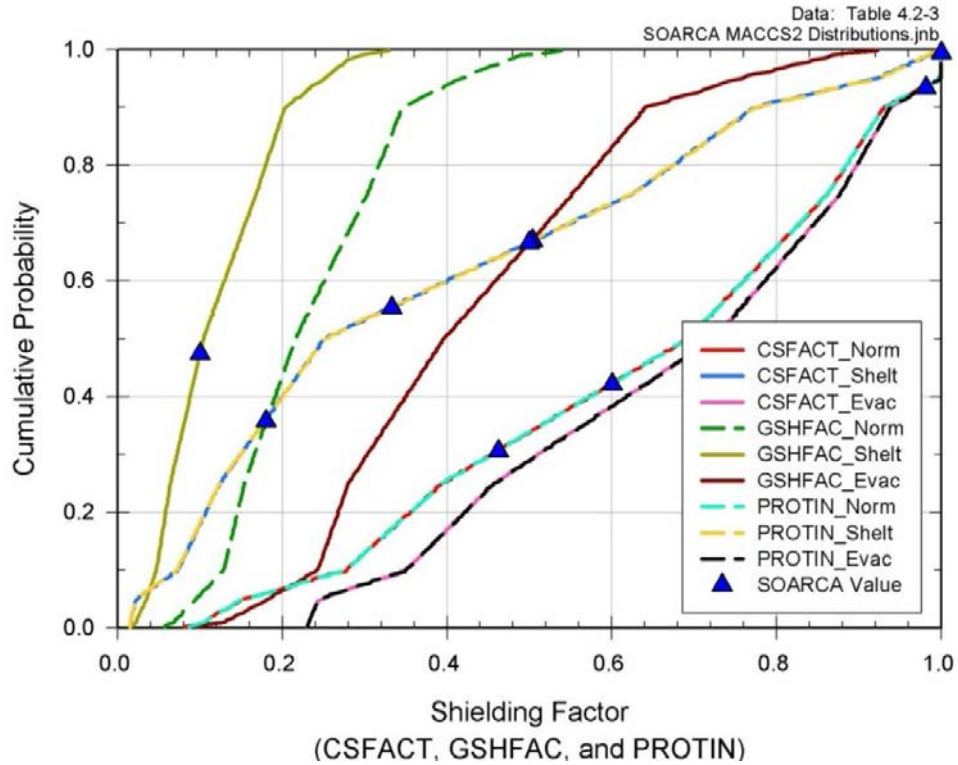


Figure 4.2-3 Cumulative distribution for shielding factors

Table 4.2-3a MACCS uncertain parameters—cloudshine shielding factors

CSFACT Piecewise Uniform Distribution			
Percentile	Normal	Sheltering	Evacuation
0%	0.076	0.015	0.230
1%	0.104	0.016	0.232
5%	0.152	0.022	0.244
15%	0.277	0.073	0.350
25%	0.394	0.124	0.457
50%	0.692	0.251	0.724
75%	0.862	0.624	0.877
85%	0.930	0.773	0.938
95%	0.999	0.922	0.999
99%	0.9999	0.984	0.9999
100%	1.000	1.000	1.000
SOARCA Estimate	0.6	0.5	1.0

Table 4.2-3b MACCS uncertain parameters—groundshine shielding factors

GSHFAC Piecewise Uniform Distribution			
Percentile	Normal	Sheltering	Evacuation
0%	0.053	0.015	0.083
1%	0.068	0.022	0.128
5%	0.095	0.035	0.182
15%	0.129	0.047	0.243
25%	0.154	0.064	0.280
50%	0.216	0.104	0.396
75%	0.303	0.168	0.552
85%	0.346	0.203	0.641
95%	0.417	0.250	0.755
99%	0.489	0.288	0.870
100%	0.548	0.331	0.935
SOARCA Estimate	0.18	0.1	0.5

Table 4.2-3c MACCS uncertain parameters—inhalation protection factors

PROTIN Piecewise Uniform Distribution			
Percentile	Normal	Sheltering	Evacuation
0%	0.076	0.015	0.230
1%	0.104	0.016	0.232
5%	0.152	0.022	0.244
15%	0.277	0.072	0.350
25%	0.394	0.124	0.457
50%	0.692	0.251	0.724
75%	0.862	0.624	0.877
85%	0.930	0.773	0.938
95%	0.999	0.922	0.999
99%	0.9999	0.984	0.9999
100%	1.000	1.000	1.000
SOARCA Estimate	0.46	0.33	0.98

4.2.4 Early Health Effects (EFFACA, EFFACB, EFFTHR)

The uncertain characteristics associated with estimation of four types of early health effects are derived from expert elicitation data [48] and evaluated by Bixler et al. [43]. Three of these early health effects are potentially fatal: the hematopoietic (acute dose to the red bone marrow), gastrointestinal (acute dose to the stomach), and pulmonary (acute dose to the lungs) syndromes. The fourth, pneumonitis is generally nonfatal, and was not included in the SOARCA calculation. The parameter distributions and SOARCA values associated with these three potentially fatal early health effects are shown on Figure 4.2-4 and also in Table 4.2-4. Correlations between the coefficients are applied as indicated in the footnote to the table.

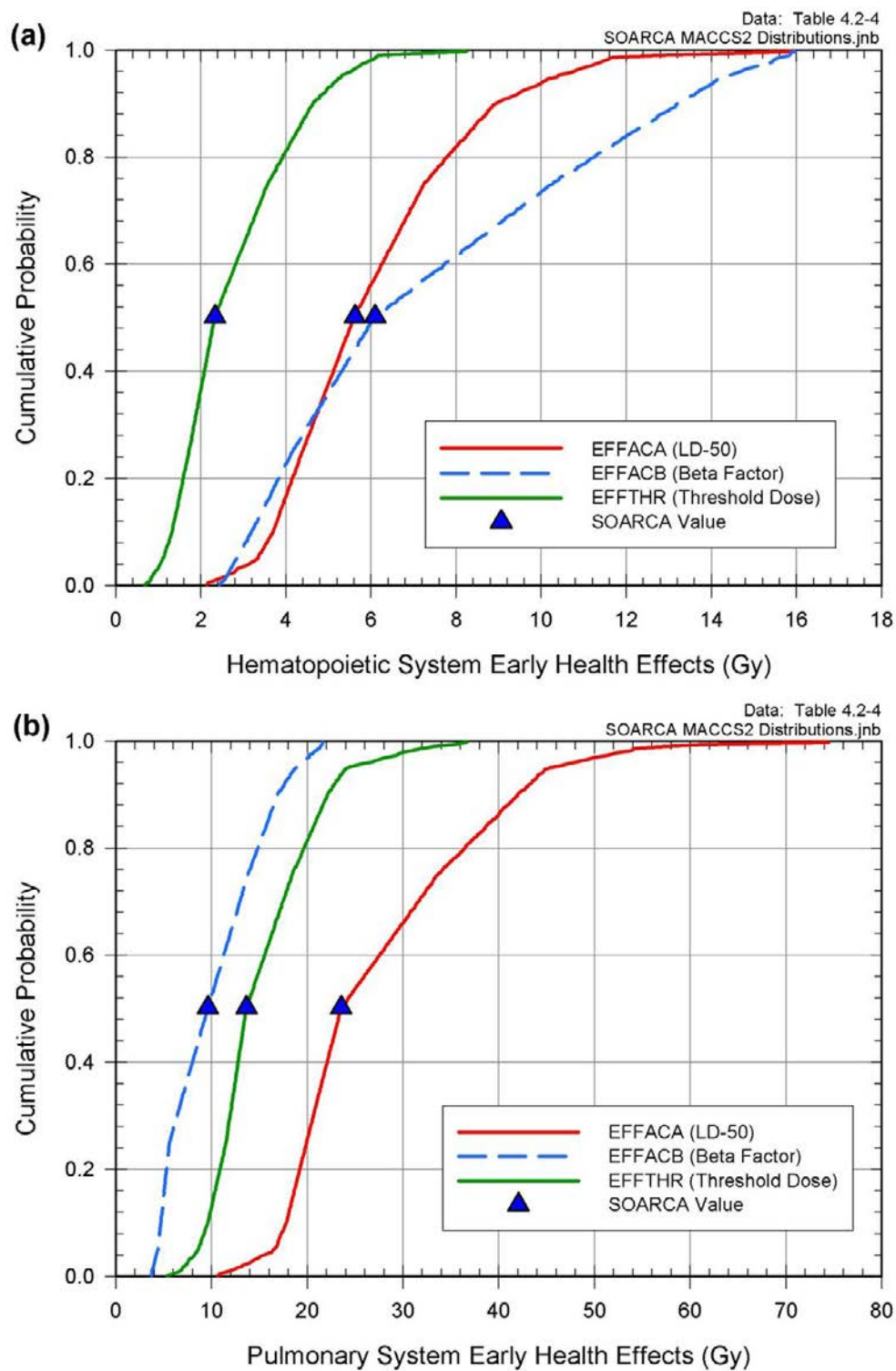


Figure 4.2-4 Cumulative distribution functions of three early health effects:
(a) hematopoietic system, (b) pulmonary system, and (c) gastrointestinal system

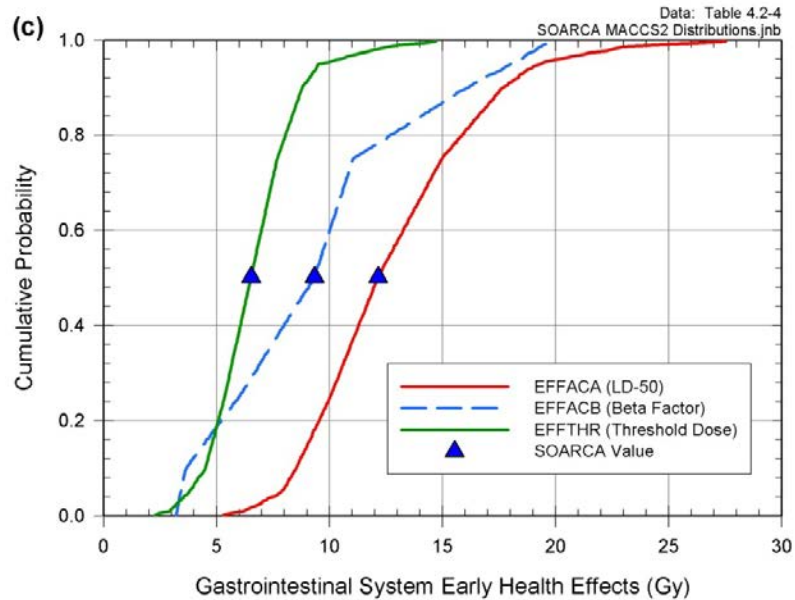


Figure 4.2-4 Cumulative distribution functions of three early health effects: (a) hematopoietic system, (b) pulmonary system, and (c) gastrointestinal system (continued)

Table 4.2-4 MACCS uncertain parameters—early health effects

Early Health Effects Continuous Linear Distribution									
	Hematopoietic S.			Pulmonary S.			Gastrointestinal S.		
Percentile	LD-50 EFFACA [Gy]	Beta EFFACB [-]	Threshold EFFTHR [Gy]	LD-50 EFFACA [Gy]	Beta EFFACB [-]	Threshold EFFTHR [Gy]	LD-50 EFFACA [Gy]	Beta EFFACB [-]	Threshold EFFTHR [Gy]
0	2.00	2.39	0.667	10.0	3.7	5.3	4.80	3.21	2.000
1	2.41	2.54	0.803	12.0	3.8	6.7	6.18	3.25	2.932
5	3.32	2.83	1.113	16.6	4.4	8.6	7.88	3.41	3.773
10	3.69	3.19	1.316	17.8	4.7	9.6	8.51	3.64	4.499
25	4.38	4.15	1.716	19.9	5.6	11.5	10.02	5.99	5.351
50	5.59	6.07	2.319	23.5	9.6	13.6	12.12	9.31	6.516
75	7.24	10.23	3.560	33.6	13.8	18.4	14.94	11.04	7.671
90	8.89	13.22	4.629	42.0	16.9	22.1	17.65	16.01	8.784
95	10.32	14.28	5.256	45.0	18.7	24.0	19.14	18.03	9.522
99	11.84	15.82	6.188	55.7	21.4	32.4	23.35	19.52	12.962
100	16.50	15.99	8.550	76.5	21.7	37.5	30.00	19.94	15.000
SOARCA Estimate	5.6	6.1	2.32	23.5	9.6	13.6	12.1	9.3	6.5

Note: For each health effect, D-50 or LD-50 is correlated with the Threshold for the same health effect using a 0.99 rank correlation coefficient.

4.2.5 Latent Health Effects (GSHFAC, DDREFA, Inhalation Dose Coefficients, CFRISK)

The uncertain characteristics associated with the estimation of latent health effects are derived from work performed by Keith Eckerman [49]. The two most important exposure pathways are groundshine and inhalation. Groundshine is especially important for the long-term phase where the only operable exposure pathways correspond to radioactive aerosols that have deposited onto the ground. This leads to three potential exposure pathways: groundshine, inhalation of resuspended aerosols, and ingestion. Doses from ingestion have not been treated in the SOARCA work and are not included in the uncertainty analysis because the supply of clean food and water would be more than adequate so that the population in an affected area would not need to consume contaminated food and water.

Groundshine (GSHFAC)

Uncertainty in groundshine doses has two components: uncertainty in the amount of shielding between an individual and the source of the groundshine (GSHFAC) and uncertainty in the energy deposited within a human organ for a specified incident radiation. Distributions representing the uncertainty in the groundshine shielding factors (GSHFAC) are presented in Table 4.2-3b. Additional uncertainties of the deposition of radiation in individual organs stem from age, height, and weight variations of the population.

To simplify the implementation of uncertainty in the energy deposited within a human organ for a specified incident radiation, Eckerman [49] recommends apply the same uncertainty distribution for all radionuclides and for all organs. The distribution is a triangular one with a minimum of 0.5, a peak (mode) of 0.8, and a maximum of 1.5. Furthermore, Eckerman suggests that the uncertainty in groundshine dose coefficients is highly correlated. As a result, it makes sense to combine the uncertainty in the groundshine shielding factor and the uncertainty in the dose coefficients into a single uncertainty factor, which can be implemented as an overall uncertainty in the groundshine shielding factor (GSHFAC) in WinMACCS. The uncertainties in the groundshine shielding factor and in the groundshine dose coefficients should be treated as being uncorrelated.

The parameters for the triangular distribution used to represent uncertainty in the dose coefficients for groundshine radiation are presented in Table 4.2-5. Piecewise uniform distributions for the uncertainty is for the combined scale factor for shielding and resultant dose are listed in Table 4.2-6, implemented as an overall uncertainty in the groundshine shielding factors (GSHFAC), are presented on Figure 4.2-5. The resulting rank correlation for the combined groundshine shielding factors should be implemented using 0.76 for normal and sheltering, 0.2 for normal and evacuation, and 0.15 for sheltering and evacuation.

Table 4.2-5 MACCS uncertain parameters—multiplier for groundshine dose coefficients

Multiplier on dose coefficients for groundshine pathway for all organs	Triangle distribution LB = 0.5 mode = 0.8 UB = 1.5
--	---

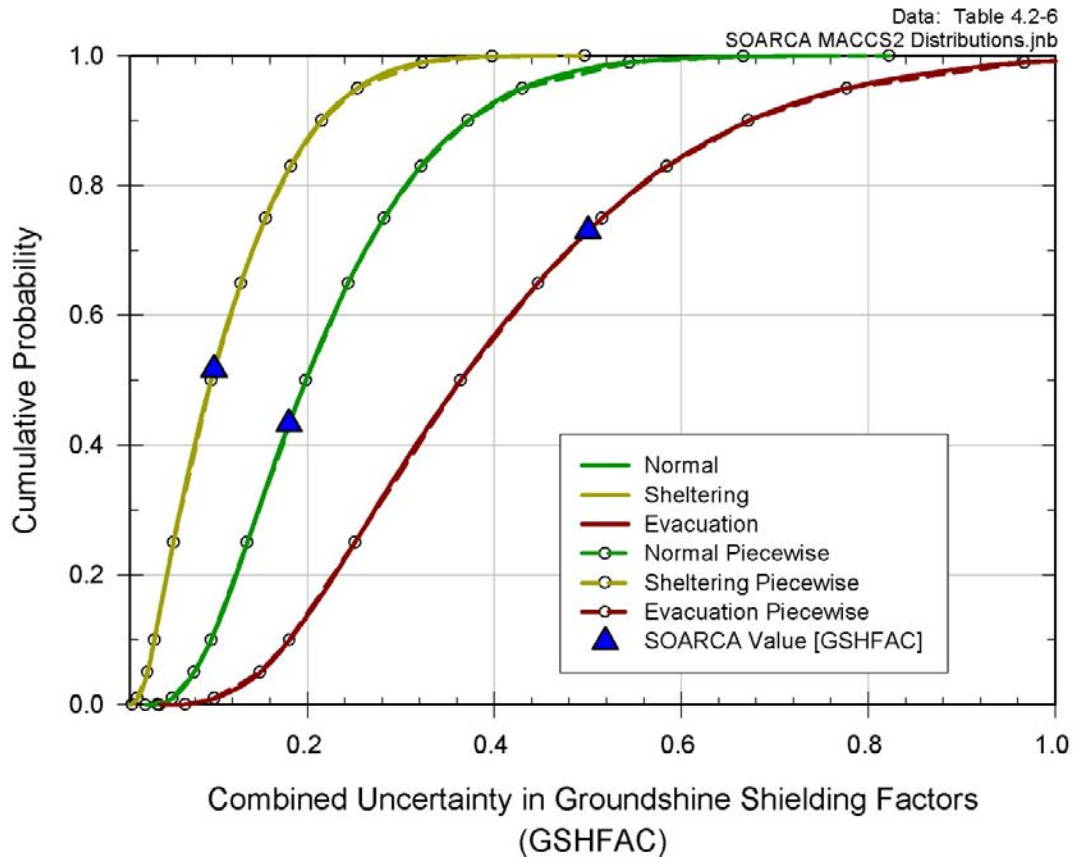


Figure 4.2-5 Cumulative distribution functions for the groundshine shielding factors, GSHFAC, for the three types of activity

Table 4.2-6 Piecewise uniform distributions for the combined uncertainty in groundshine shielding factors (GSHFAC) including multiplier

Quantile	GSHFAC Normal	GSHFAC Sheltering	GSHFAC Evacuation
0	0.0265	0.0075	0.0415
0.001	0.0394	0.0120	0.0692
0.01	0.0552	0.0179	0.1001
0.05	0.0784	0.0286	0.1491
0.1	0.0967	0.0361	0.1804
0.25	0.1354	0.0563	0.2504
0.5	0.1979	0.0969	0.3635
0.65	0.2433	0.1288	0.4464
0.75	0.2816	0.1549	0.5146
0.83	0.3211	0.1818	0.5843
0.9	0.3719	0.2148	0.6717
0.95	0.4297	0.2533	0.7768
0.99	0.5441	0.3226	0.9665
0.999	0.6660	0.3975	1.1555 (1.0) ^a
1	0.8220	0.4965	1.4025 (1.0) ^a

^a The piecewise distribution was limited to a maximum value of 1.0, equal to the upper bound for GSHFAC in MACCS.

Dose and Dose Rate Effectiveness Factor (DDREFA)

An additional parameter that affects the calculation of latent health effects is the dose and dose rate effectiveness factor (DDREFA). This factor uses Biological Effects of Ionizing Radiation (BEIR) V risk factors for estimating health effects to account for observed differences between low and high dose rates. In MACCS, doses received during the emergency phase are divided by DDREFA when they are less than 0.2 Gy (20 rad) in the calculation of latent health effects; they are not divided by DDREFA when emergency-phase doses exceed 0.2 Gy. Doses received during the long-term phase are generally controlled by the habitability criterion to be well below 0.2 Gy, so these doses are always divided by DDREFA in the calculation of latent health effects.

Eckerman [49] recommends that the uncertainty in DDREFA be treated with the following functional form [49]. For breast cancer, the probability density function is equal to:

$$f(x) = e^{-(x-1)}, 1 < x \leq 3 \quad \text{Equation 4.2-1}$$

For other types of cancer:

$$f(x) = 0.5, 1 < x \leq 2 \text{ and } f(x) = 0.5 e^{-(x-2)}, 2 < x \leq 8 \quad \text{Equation 4.2-2}$$

Where x is the value of DDREFA and $f(x)$ is the probability associated with a value of DDREFA, Figure 4.2-6. Eckerman [49] further recommends that high linear energy transfer (LET) radiation be assigned a DDREFA of unity with no uncertainty, but the distinction between low and high LET radiation to an organ cannot be accommodated within the MACCS framework so the above functions are applied to all types of radiation. The values of DDREFA for the various organs are to be treated as uncorrelated.

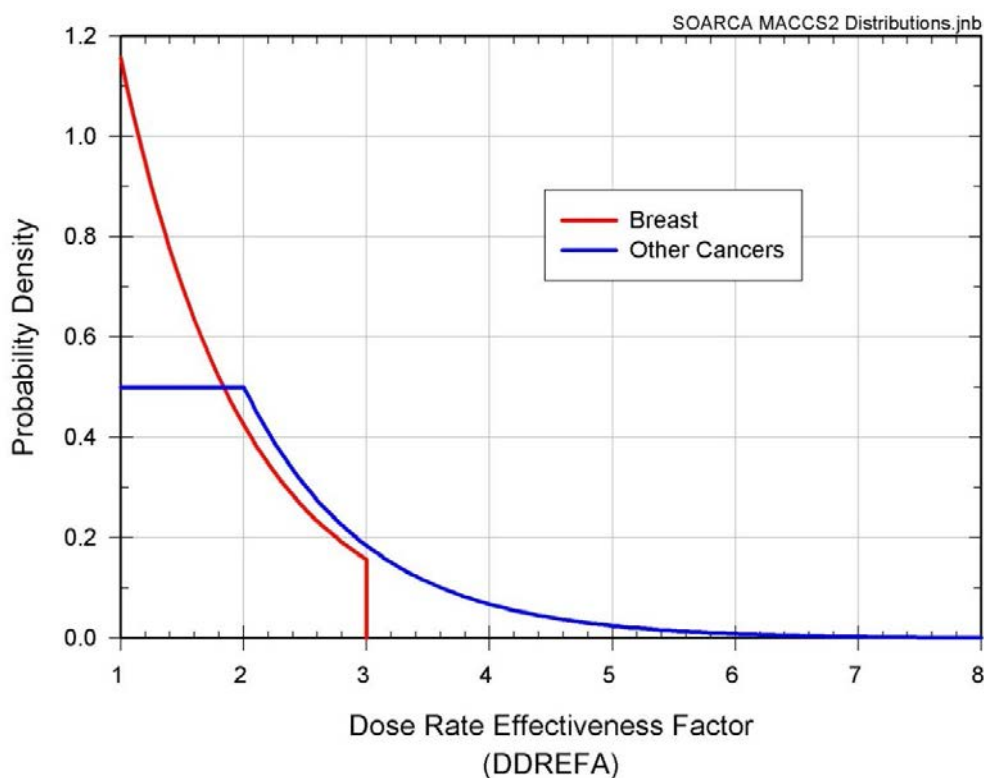


Figure 4.2-6 The probability density for DDREFA applied in the uncertainty analysis for breast and all other cancers [49, Figure 10]

To implement the uncertainty in DDREFA, the probability density functions (PDFs) in Equation 4.2-1 and Equation 4.2-2 are integrated over the range of DDREFA values. The resulting CDF is segmented into equally spaced quantiles to construct the piecewise uniform distributions provided in Table 4.2-7.

As a truncation has been recommended and applied to the original exponential distributions, the resulting density functions do not integrate to one over their interval of definition. Therefore, they need to be normalized in order to be appropriately defined.

Normalization of equation 4.2-1:

$$F = \int_1^3 e^{-(x-1)} dx = e \int_1^3 e^{-x} dx = e[-e^{-x}]_1^3 = 1 - \frac{1}{e^2} = t1 \sim 0.864665$$

The normalized PDF is then

$$f(x) = \frac{1}{t1} e^{-(x-1)}, \text{ with } t1 = 1 - \frac{1}{e^2} \text{ and } 1 < x \leq 3$$

The resulting CDF is

$$Fa(x) = \frac{1}{t1} \int_1^x e^{-(s-1)} ds = \frac{e}{t1} \int_1^x e^{-s} ds = \frac{e}{t1} [-e^{-s}]_1^x = \frac{1}{t1} \left(1 - \frac{1}{e^{s-1}}\right), 1 < x \leq 3 \quad \text{Equation 4.2-3}$$

Normalization of equation 4.2-2:

$$F1 = \int_1^2 0.5 dx = [0.5x]_1^2 = 0.5$$

$$F2 = \int_2^8 e^{-(x-2)} dx = e^2 \int_2^8 e^{-x} dx = e^2 [-e^{-x}]_2^8 = \left(1 - \frac{1}{e^6}\right) = t2 \sim 0.997521$$

The normalized PDF is then

$$f(x) = 0.5, \quad 1 < x \leq 2$$

$$f(x) = 0.5 \frac{1}{t2} e^{-(x-2)}, \text{ with } t2 = \left(1 - \frac{1}{e^6}\right) \text{ and } 2 < x \leq 8$$

The resulting CDF is

$$Fb(x) = 0.5(x - 1), \quad 1 < x \leq 2$$

$$Fb(x) = 0.5 + 0.5 \frac{1}{t2} \int_2^x e^{-(s-2)} ds = 0.5 + 0.5 \frac{e^2}{t2} \int_2^x e^{-s} ds = 0.5 + 0.5 \frac{e^2}{t2} [-e^{-s}]_2^x = 0.5 + 0.5 \frac{1}{t2} \left(1 - \frac{1}{e^{s-2}}\right), 2 < x \leq 8 \quad \text{Equation 4.2-4}$$

$Fa(x)$ (Equation 4.2-3) and $Fb(x)$ (Equation 4.2-4) represent the CDF for the truncated distributions. In other words, they allow the estimation of a quantile, given a value of x . In order to approximate them with piecewise uniform distribution, it is simpler to work with the inverse functions of Fa and Fb , and estimate the values of $F_a^{-1}(q)$ and $F_b^{-1}(q)$ for a quantile q .

The inverse function for $Fa(x)$ is:

$$F_a^{-1}(q) = \ln\left(\frac{e}{1-t_1 \cdot q}\right), \text{ with } t_1 = 1 - \frac{1}{e^2} \text{ and } 0 \leq q \leq 1 \quad \text{Equation 4.2-5}$$

While the inverse of $Fb(x)$ is equal to:

$$F_b^{-1}(q) = 2q + 1, \text{ with } 0 \leq q \leq 0.5$$

$$F_b^{-1}(q) = \ln\left(\frac{e^2}{1-2t_2[q-0.5]}\right), \text{ with } t_2 = 1 - \frac{1}{e^6} \text{ and } 0.5 \leq q \leq 1 \quad \text{Equation 4.2-6}$$

The resulting CDFs are displayed on Figure 4.2-7 for DDREFA Equation 4.2-3 and Equation 4.2-4. The resulting piecewise uniform distributions constructed from the CDFs are listed in Table 4.2-7.

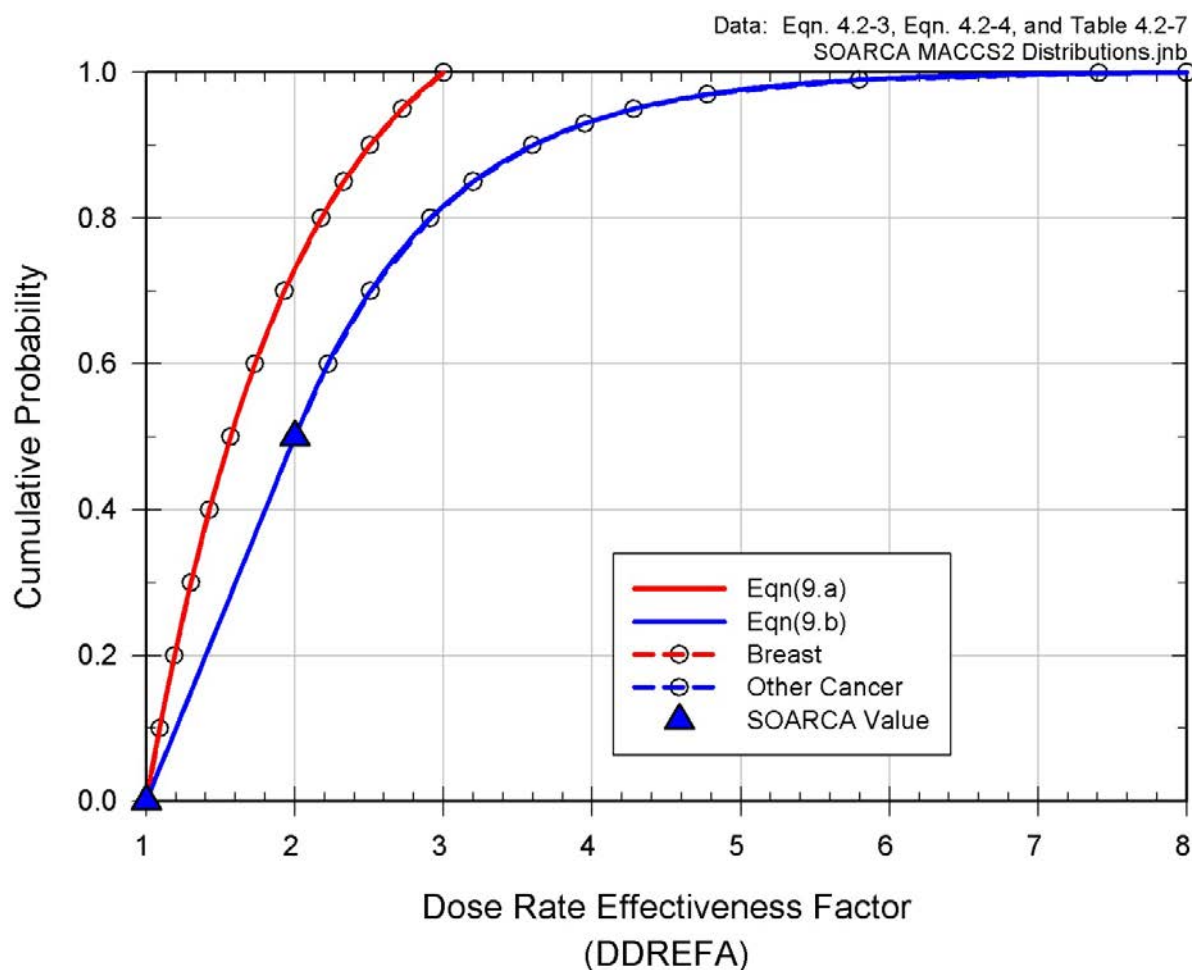


Figure 4.2-7 The cumulative distribution for DDREFA applied in the uncertainty analysis for breast and other cancers

Table 4.2-7 Piecewise uniform distributions for DDREFA

(Equation 4.2-5)		(Equation 4.2-6)	
Quantile	DDREFA	Quantile	DDREFA
0.0000	1.000	0.0000	1.0000
0.1000	1.0904	0.5000	2.0000
0.2000	1.1899	0.6000	2.2225
0.3000	1.3003	0.7000	2.5092
0.4000	1.4244	0.8000	2.9126
0.5000	1.5662	0.8500	3.1982
0.6000	1.7315	0.9000	3.5996
0.7000	1.9295	0.9300	3.9510
0.8000	2.1768	0.9500	4.2805
0.8500	2.3279	0.9700	4.7753
0.9000	2.5060	0.9900	5.7974
0.9500	2.7228	0.9990	7.4095
1.0000	3.0000	1.0000	8.000
SOARCA Estimate	1.0	SOARCA Estimate	2.0

Inhalation Dose Coefficients

For the dose coefficients related to the inhalation pathway, Eckerman [49] recommends that the coefficients be treated as truncated log normal with the geometric means and standard deviations provided in Tables 4.2-8 and 4.2-9, respectively. The geometric means are the same as the median values used in the SOARCA analysis. A truncation at ± 3 sigma is applied to each distribution. The 3 sigma truncation represents a truncation at quantile 0.00135 (~0.1 percentile) and 0.99865 (~99.9 percentile). In the LHS software used by the WinMACCS framework, the truncation is made by normalizing any quantile generated in the probability space [0,1] into the truncation space [0.00135; 0.99865].

For an individual radionuclide, the dose coefficients are treated as correlated with a coefficient of one for all of the organs except the lung; the lung is to be correlated with a coefficient of negative one with all of the other organs. The logic behind this is that the inhaled radionuclides may spend more or less time in the lungs, depending on the chemical form of the radionuclide and its solubility. After departing from the lung, the radionuclide is carried through the blood stream to other systemic tissues. The longer the time spent in the lungs, the greater the dose there and the less the dose to the other systemic tissues; the shorter the time spent in the lungs, the smaller the dose there and the greater the dose to the other systemic tissues. Table 4.2-10 lists WinMACCS corresponding tissues correlated to the organ dose coefficients from the reference report, Eckerman [49]. In addition, the effective dose coefficient (ICRP60ED in WinMACCS) is not uncertain in this analysis.

Table 4.2-8 MACCS uncertain parameters—geometric mean (i.e., median values, which were also used in the SOARCA analyses) for inhalation dose coefficients (Gy/Bq) [49]

Nuclide	Type	Leukemia	Bone	Breast	Lung	Thyroid	Liver	Colon	Residual	Effective
Co-58	S	7.16×10^{-10}	5.26×10^{-10}	1.32×10^{-9}	1.27×10^{-8}	5.18×10^{-10}	1.06×10^{-9}	8.26×10^{-10}	9.27×10^{-10}	2.12×10^{-9}
Co-60	S	1.24×10^{-8}	9.36×10^{-9}	2.48×10^{-8}	1.83×10^{-7}	9.89×10^{-9}	1.98×10^{-8}	4.50×10^{-9}	1.63×10^{-8}	3.08×10^{-8}
Rb-86	F	1.43×10^{-9}	2.82×10^{-9}	7.32×10^{-10}	7.69×10^{-10}	7.46×10^{-10}	7.46×10^{-10}	1.28×10^{-9}	7.52×10^{-10}	9.37×10^{-10}
Rb-88	F	1.74×10^{-12}	1.86×10^{-12}	1.65×10^{-12}	3.14×10^{-11}	1.74×10^{-12}	1.66×10^{-12}	1.75×10^{-12}	1.96×10^{-12}	1.62×10^{-11}
Sr-89	F	4.33×10^{-9}	5.40×10^{-9}	1.77×10^{-10}	2.03×10^{-10}	1.78×10^{-10}	1.78×10^{-10}	2.26×10^{-9}	1.78×10^{-10}	1.01×10^{-9}
Sr-90	F	1.62×10^{-7}	3.69×10^{-7}	5.97×10^{-10}	6.19×10^{-10}	5.97×10^{-10}	5.97×10^{-10}	3.22×10^{-9}	5.97×10^{-10}	2.40×10^{-8}
Sr-91	F	1.31×10^{-10}	1.35×10^{-10}	2.07×10^{-11}	5.18×10^{-11}	2.64×10^{-11}	2.54×10^{-11}	4.64×10^{-10}	2.88×10^{-11}	1.57×10^{-10}
Sr-92	F	6.10×10^{-11}	8.89×10^{-11}	1.29×10^{-11}	3.70×10^{-11}	1.55×10^{-11}	1.49×10^{-11}	3.13×10^{-10}	1.76×10^{-11}	9.83×10^{-11}
Y-90	S	1.22×10^{-12}	1.22×10^{-12}	4.23×10^{-14}	7.85×10^{-9}	4.23×10^{-14}	1.20×10^{-12}	4.44×10^{-9}	4.23×10^{-14}	1.50×10^{-9}
Y-91	S	6.44×10^{-11}	6.42×10^{-11}	5.21×10^{-12}	6.97×10^{-8}	2.83×10^{-12}	6.43×10^{-11}	4.64×10^{-9}	3.93×10^{-12}	8.96×10^{-9}
Y-91m	S	9.41×10^{-13}	7.25×10^{-13}	8.01×10^{-13}	5.00×10^{-11}	6.78×10^{-13}	8.97×10^{-13}	5.26×10^{-12}	2.03×10^{-12}	1.14×10^{-11}
Y-92	S	1.83×10^{-12}	1.27×10^{-12}	1.43×10^{-12}	6.95×10^{-10}	1.09×10^{-12}	1.75×10^{-12}	4.94×10^{-10}	2.49×10^{-12}	1.77×10^{-10}
Y-93	S	1.77×10^{-12}	1.29×10^{-12}	1.27×10^{-12}	1.62×10^{-9}	8.99×10^{-13}	1.66×10^{-12}	1.63×10^{-9}	1.75×10^{-12}	4.22×10^{-10}
Zr-95	M	2.43×10^{-9}	1.26×10^{-8}	1.21×10^{-9}	3.07×10^{-8}	6.50×10^{-10}	1.05×10^{-9}	1.62×10^{-9}	1.05×10^{-9}	4.79×10^{-9}
Zr-97	M	7.77×10^{-11}	6.43×10^{-11}	3.78×10^{-11}	3.43×10^{-9}	2.77×10^{-11}	4.39×10^{-11}	2.81×10^{-9}	4.69×10^{-11}	9.23×10^{-10}
Nb-95	S	3.39×10^{-10}	2.49×10^{-10}	5.86×10^{-10}	1.19×10^{-8}	2.35×10^{-10}	4.94×10^{-10}	7.02×10^{-10}	4.23×10^{-10}	1.76×10^{-9}
Nb-97	S	1.63×10^{-12}	1.20×10^{-12}	1.39×10^{-12}	1.65×10^{-10}	1.14×10^{-12}	1.56×10^{-12}	2.44×10^{-11}	3.26×10^{-12}	4.52×10^{-11}
Mo-99	S	2.07×10^{-11}	2.12×10^{-11}	2.17×10^{-11}	6.02×10^{-9}	1.09×10^{-11}	2.74×10^{-11}	2.00×10^{-9}	2.06×10^{-11}	9.95×10^{-10}
Tc-99m	M	1.65×10^{-12}	2.32×10^{-12}	1.16×10^{-12}	7.60×10^{-11}	5.45×10^{-12}	1.66×10^{-12}	1.84×10^{-11}	2.30×10^{-12}	1.93×10^{-11}
Ru-103	S	2.36×10^{-10}	1.73×10^{-10}	4.06×10^{-10}	2.21×10^{-8}	1.64×10^{-10}	3.32×10^{-10}	1.08×10^{-9}	3.02×10^{-10}	2.96×10^{-9}
Ru-105	S	7.95×10^{-12}	5.59×10^{-12}	6.05×10^{-12}	7.99×10^{-10}	4.50×10^{-12}	7.41×10^{-12}	2.96×10^{-10}	1.02×10^{-11}	1.80×10^{-10}
Ru-106	S	6.70×10^{-10}	5.44×10^{-10}	1.12×10^{-9}	5.35×10^{-7}	5.43×10^{-10}	9.28×10^{-10}	1.28×10^{-8}	8.44×10^{-10}	6.62×10^{-8}
Rh-103m	S	1.32×10^{-15}	3.04×10^{-15}	1.64×10^{-15}	1.76×10^{-11}	7.05×10^{-16}	2.70×10^{-15}	9.37×10^{-13}	5.60×10^{-15}	2.73×10^{-12}
Rh-105	S	4.64×10^{-12}	3.87×10^{-12}	4.18×10^{-12}	2.31×10^{-9}	2.64×10^{-12}	4.49×10^{-12}	5.62×10^{-10}	4.61×10^{-12}	3.54×10^{-10}
Te-127	M	1.71×10^{-12}	1.74×10^{-12}	7.84×10^{-13}	7.50×10^{-10}	2.81×10^{-12}	8.01×10^{-13}	2.51×10^{-10}	8.20×10^{-13}	1.27×10^{-10}
Te-127m	M	2.31×10^{-9}	9.03×10^{-9}	5.84×10^{-11}	5.62×10^{-8}	8.62×10^{-10}	5.88×10^{-11}	1.91×10^{-9}	4.89×10^{-11}	7.43×10^{-9}
Te-129	M	3.51×10^{-13}	3.58×10^{-13}	3.00×10^{-13}	1.48×10^{-10}	3.53×10^{-13}	3.19×10^{-13}	2.06×10^{-11}	4.78×10^{-13}	3.70×10^{-11}
Te-129m	M	1.17×10^{-9}	2.71×10^{-9}	9.12×10^{-11}	4.83×10^{-8}	1.01×10^{-9}	8.69×10^{-11}	4.00×10^{-9}	8.02×10^{-11}	6.56×10^{-9}
Te-131	M	5.25×10^{-13}	5.36×10^{-13}	5.46×10^{-13}	9.37×10^{-11}	4.79×10^{-11}	5.37×10^{-13}	5.10×10^{-12}	1.06×10^{-12}	2.86×10^{-11}
Te-131m	M	8.85×10^{-11}	1.17×10^{-10}	7.11×10^{-11}	4.65×10^{-9}	2.69×10^{-9}	7.44×10^{-11}	1.46×10^{-9}	7.59×10^{-11}	1.07×10^{-9}
Te-132	M	2.22×10^{-10}	2.87×10^{-10}	2.30×10^{-10}	1.01×10^{-8}	4.36×10^{-9}	2.21×10^{-10}	3.34×10^{-9}	2.08×10^{-10}	2.06×10^{-9}

Table 4.2-8 MACCS uncertain parameters—geometric mean (i.e., median values, which were also used in the SOARCA analyses) for inhalation dose coefficients (Gy/Bq) [49] (continued)

Nuclide	Type	Leukemia	Bone	Breast	Lung	Thyroid	Liver	Colon	Residual	Effective
I-131	F	3.71×10^{-11}	4.89×10^{-11}	2.12×10^{-11}	5.98×10^{-11}	1.47×10^{-7}	1.67×10^{-11}	2.54×10^{-11}	1.82×10^{-11}	7.41×10^{-9}
I-132	F	1.16×10^{-11}	1.23×10^{-11}	8.59×10^{-12}	3.64×10^{-11}	1.36×10^{-9}	9.91×10^{-12}	1.18×10^{-11}	1.45×10^{-11}	9.39×10^{-11}
I-133	F	1.85×10^{-11}	2.00×10^{-11}	1.37×10^{-11}	4.24×10^{-11}	2.84×10^{-8}	1.38×10^{-11}	2.09×10^{-11}	1.57×10^{-11}	1.47×10^{-9}
I-134	F	5.51×10^{-12}	5.82×10^{-12}	4.40×10^{-12}	2.99×10^{-11}	2.59×10^{-10}	5.00×10^{-12}	5.39×10^{-12}	8.27×10^{-12}	4.52×10^{-11}
I-135	F	1.69×10^{-11}	1.84×10^{-11}	1.26×10^{-11}	4.04×10^{-11}	5.76×10^{-9}	1.35×10^{-11}	1.74×10^{-11}	1.73×10^{-11}	3.23×10^{-10}
Cs-134	F	6.37×10^{-9}	6.81×10^{-9}	4.81×10^{-9}	6.02×10^{-9}	6.34×10^{-9}	6.73×10^{-9}	7.20×10^{-9}	7.40×10^{-9}	6.71×10^{-9}
Cs-136	F	9.89×10^{-10}	1.12×10^{-9}	7.37×10^{-10}	9.68×10^{-10}	1.01×10^{-9}	1.05×10^{-9}	1.15×10^{-9}	1.17×10^{-9}	1.24×10^{-9}
Cs-137	F	4.47×10^{-9}	4.69×10^{-9}	3.82×10^{-9}	4.35×10^{-9}	4.46×10^{-9}	4.62×10^{-9}	5.22×10^{-9}	4.90×10^{-9}	4.69×10^{-9}
Ba-139	F	1.17×10^{-11}	1.20×10^{-11}	1.67×10^{-12}	2.91×10^{-11}	1.71×10^{-12}	1.73×10^{-12}	1.12×10^{-10}	1.81×10^{-12}	3.39×10^{-11}
Ba-140	F	1.46×10^{-9}	2.07×10^{-9}	8.97×10^{-11}	1.55×10^{-10}	1.21×10^{-10}	1.28×10^{-10}	5.45×10^{-9}	1.66×10^{-10}	1.03×10^{-9}
La-140	M	1.35×10^{-10}	9.67×10^{-11}	1.10×10^{-10}	3.96×10^{-9}	6.60×10^{-11}	3.23×10^{-10}	2.51×10^{-9}	1.23×10^{-10}	1.08×10^{-9}
La-141	M	3.07×10^{-12}	1.21×10^{-11}	1.33×10^{-12}	6.64×10^{-10}	1.13×10^{-12}	1.94×10^{-11}	3.67×10^{-10}	1.56×10^{-12}	1.47×10^{-10}
La-142	M	7.85×10^{-12}	6.06×10^{-12}	6.75×10^{-12}	2.45×10^{-10}	5.81×10^{-12}	9.79×10^{-12}	8.08×10^{-11}	1.34×10^{-11}	8.99×10^{-11}
Ce-141	S	3.71×10^{-11}	1.08×10^{-10}	5.97×10^{-11}	2.97×10^{-8}	2.26×10^{-11}	8.18×10^{-11}	1.29×10^{-9}	4.65×10^{-11}	3.76×10^{-9}
Ce-143	S	1.45×10^{-11}	1.38×10^{-11}	1.27×10^{-11}	4.98×10^{-9}	6.72×10^{-12}	1.64×10^{-11}	1.73×10^{-9}	1.38×10^{-11}	8.34×10^{-10}
Ce-144	S	1.19×10^{-9}	2.06×10^{-9}	2.74×10^{-10}	4.24×10^{-7}	1.44×10^{-10}	5.87×10^{-9}	1.14×10^{-8}	2.16×10^{-10}	5.29×10^{-8}
Pr-143	S	2.01×10^{-12}	2.01×10^{-12}	1.29×10^{-14}	1.82×10^{-8}	1.29×10^{-14}	1.60×10^{-11}	2.08×10^{-9}	1.29×10^{-14}	2.45×10^{-9}
Pr-144	S	1.58×10^{-14}	1.39×10^{-14}	1.71×10^{-14}	5.66×10^{-11}	1.58×10^{-14}	1.61×10^{-14}	1.28×10^{-12}	3.86×10^{-14}	1.83×10^{-11}
Nd-147	S	3.42×10^{-11}	9.92×10^{-11}	4.33×10^{-11}	1.80×10^{-8}	1.65×10^{-11}	6.26×10^{-11}	1.82×10^{-9}	3.35×10^{-11}	2.41×10^{-9}
Np-239	M	3.46×10^{-11}	5.16×10^{-10}	1.29×10^{-11}	6.35×10^{-9}	8.24×10^{-12}	3.34×10^{-11}	1.18×10^{-9}	1.46×10^{-11}	9.36×10^{-10}
Pu-238	S	4.14×10^{-7}	1.62×10^{-4}	1.38×10^{-7}	9.34×10^{-5}	2.77×10^{-7}	3.43×10^{-5}	2.88×10^{-7}	2.77×10^{-7}	1.61×10^{-5}
Pu-239	S	4.57×10^{-7}	1.84×10^{-4}	1.59×10^{-7}	8.76×10^{-5}	3.18×10^{-7}	3.91×10^{-5}	3.29×10^{-7}	3.18×10^{-7}	1.61×10^{-5}
Pu-240	S	4.58×10^{-7}	1.84×10^{-4}	1.59×10^{-7}	8.78×10^{-5}	3.18×10^{-7}	3.91×10^{-5}	3.29×10^{-7}	3.18×10^{-7}	1.61×10^{-5}
Pu-241	S	9.30×10^{-9}	4.08×10^{-6}	3.57×10^{-9}	4.58×10^{-7}	7.11×10^{-9}	8.60×10^{-7}	7.18×10^{-9}	7.12×10^{-9}	1.75×10^{-7}
Am-241	M	2.94×10^{-6}	1.70×10^{-3}	1.44×10^{-6}	3.72×10^{-5}	2.88×10^{-6}	1.05×10^{-4}	2.89×10^{-6}	2.88×10^{-6}	4.17×10^{-5}
Cm-242	M	9.32×10^{-8}	2.73×10^{-5}	1.73×10^{-8}	3.54×10^{-5}	3.47×10^{-8}	7.14×10^{-6}	4.39×10^{-8}	3.47×10^{-8}	5.22×10^{-6}
Cm-244	M	1.94×10^{-6}	9.22×10^{-4}	6.42×10^{-7}	3.93×10^{-5}	1.28×10^{-6}	7.53×10^{-5}	1.29×10^{-6}	1.28×10^{-6}	2.66×10^{-5}

Notes F = fast dissolution and high level of absorption to blood; M = an intermediate rate of dissolution and level of absorption to blood; and S = slow rate of dissolution and low level of absorption to blood. The fractional rate of absorption (d-1) assigned to the default types are: Type F = 100, Type M = $10.0 \exp(-100 t) + 0.005 \exp(-0.005 t)$, and Type S = $0.1 \exp(-100 t) + 1.0 \times 10^{-4} \exp(-0.0001 t)$ where t is the time (days) since deposition in the lung.

Table 4.2-9 MACCS uncertain parameters—geometric standard deviations for inhalation dose coefficients (i.e., $\sigma[49]$)

Nuclide	Type	Lung	Leukemia	Bone	Breast	Thyroid	Liver	Colon	Residual
Co-58	S	1.5	1.5	1.5	1.5	1.5	1.5	1.5	1.5
Co-60	S	1.5	1.5	1.5	1.5	1.5	1.5	1.5	1.5
Rb-86	F	2.51	1.5	1.5	1.5	1.5	1.5	1.5	1.5
Rb-88	F	1.5	1.5	1.5	1.5	1.5	2.56	1.5	1.5
Sr-89	F	5.4	1.5	1.5	1.5	1.5	1.5	1.5	1.5
Sr-90	F	5.15	1.5	1.5	1.5	1.5	2.74	1.5	1.5
Sr-91	F	3.03	1.5	1.5	1.5	1.5	1.5	1.5	1.5
Sr-92	F	2.88	1.56	1.76	1.5	1.5	1.5	1.5	1.5
Y-90	S	1.5	2.05	1.5	1.61	1.61	2.33	1.5	1.61
Y-91	S	1.5	4.51	3.25	1.5	1.65	4.95	1.5	1.5
Y-91m	S	1.5	1.5	1.5	1.5	1.5	1.5	1.5	1.5
Y-92	S	1.5	1.5	1.5	1.5	1.5	1.5	1.5	1.5
Y-93	S	1.5	1.5	1.5	1.5	1.5	1.5	1.5	1.5
Zr-95	M	1.5	1.5	1.5	1.5	1.5	1.88	1.5	1.5
Zr-97	M	1.5	1.5	1.5	1.5	1.5	1.5	1.5	1.5
Nb-95	S	1.5	1.5	1.5	1.5	1.5	1.5	1.5	1.5
Nb-97	S	1.5	1.5	1.5	1.5	1.5	1.5	1.5	1.5
Mo-99	S	1.5	1.61	2.05	1.5	1.5	3.05	3	1.5
Tc-99m	M	1.5	1.5	1.5	1.5	2.22	1.5	1.5	1.5
Ru-103	S	1.5	1.5	1.5	1.5	1.5	1.5	1.5	1.5
Ru-105	S	1.5	1.5	1.5	1.5	1.5	1.5	1.5	1.5
Ru-106	S	1.5	2.04	2.49	1.5	1.5	1.88	1.5	1.5
Rh-103m	S	1.5	1.5	1.5	1.5	1.5	1.5	3.08	1.5
Rh-105	S	1.5	1.5	1.5	1.5	1.5	1.5	1.5	1.5
Te-127	M	1.5	1.5	1.5	1.5	1.5	1.5	1.5	1.5
Te-127m	M	1.5	3.55	5.72	1.5	3.03	7.38	1.5	1.5
Te-129	M	1.5	1.5	1.5	1.5	1.5	1.5	1.5	1.5
Te-129m	M	1.5	3.2	4.24	1.5	2.68	4.48	1.5	1.5
Te-131	M	1.5	1.5	1.5	1.5	1.5	1.5	1.5	1.5
Te-131m	M	1.5	1.5	1.5	1.5	1.5	1.5	1.5	1.5
Te-132	M	1.5	1.5	1.5	1.5	1.5	1.5	1.5	1.5
I-131	F	6.54	1.5	1.5	1.5	1.5	1.5	2.74	1.5
I-132	F	1.87	1.5	1.5	1.5	2.64	1.5	1.5	1.5
I-133	F	4.22	1.5	1.5	1.5	1.54	1.5	2.75	1.5
I-134	F	1.5	1.5	1.5	1.5	3.49	1.5	1.5	1.5
I-135	F	2.67	1.5	1.5	1.5	1.97	1.5	1.86	1.5
Cs-134	F	1.5	1.5	1.5	1.5	1.5	1.5	1.5	1.5
Cs-136	F	2.04	1.5	1.5	1.5	1.5	1.5	1.5	1.5

Table 4.2-9 MACCS uncertain parameters—geometric standard deviations for inhalation dose coefficients (i.e., σ [49] (continued))

Nuclide	Type	Lung	Leukemia	Bone	Breast	Thyroid	Liver	Colon	Residual
Cs-137	F	1.55	1.5	1.5	1.5	1.5	1.5	1.5	1.5
Ba-139	F	1.72	4.25	3.31	2.25	2.47	2.09	1.5	1.85
Ba-140	F	6.28	1.5	1.5	1.5	1.5	3.68	1.5	1.5
La-140	M	1.5	1.5	1.5	1.5	1.5	1.5	1.5	1.5
La-141	M	1.5	1.5	1.5	1.5	1.5	1.5	1.5	1.5
La-142	M	1.5	1.5	1.5	1.5	1.5	1.5	1.5	1.5
Ce-141	S	1.5	1.5	1.6	1.5	1.5	1.5	1.5	1.5
Ce-143	S	1.5	1.5	1.5	1.5	1.5	1.5	1.5	1.5
Ce-144	S	1.5	4.57	3.39	1.5	1.5	3.32	1.5	1.5
Pr-143	S	1.5	3.88	2.39	5.49	5.49	2.24	1.5	5.49
Pr-144	S	1.5	1.5	1.5	1.5	1.5	1.5	1.5	1.5
Nd-147	S	1.5	1.5	1.84	1.5	1.5	1.5	1.5	1.5
Np-239	M	1.5	1.5	1.5	1.5	1.5	1.5	1.5	1.5
Pu-238	S	1.5	4.32	2.97	3.15	3.15	3.1	3.17	3.15
Pu-239	S	1.5	4.32	2.95	3.13	3.14	3.08	3.16	3.13
Pu-240	S	1.5	4.32	2.95	3.14	3.14	3.08	3.16	3.14
Pu-241	S	1.84	4.29	2.77	2.96	2.97	2.92	2.99	2.96
Am-241	M	1.5	1.78	1.5	1.5	1.5	1.5	1.5	1.5
Cm-242	M	1.5	1.51	1.5	1.5	1.5	1.5	1.5	1.5
Cm-244	M	1.5	1.71	1.5	1.5	1.5	1.5	1.5	1.5

Notes F = fast dissolution and high level of absorption to blood; M = an intermediate rate of dissolution and level of absorption to blood; and S = slow rate of dissolution and low level of absorption to blood. The fractional rate of absorption ($d-1$) assigned to the default types are; Type F = 100, Type M = $10.0 e^{-(100 t)} + 0.005 e^{-(0.005 t)}$, and Type S = $0.1 e^{-(100 t)} + 1.0 \times 10^{-4} e^{-(0.0001 t)}$ where t is the time (days) since deposition in the lung.

Table 4.2-10 Crosswalk between reference type from Tables 4.2-8 and 4.2-9 and WINMACCS organ doses

Tables 4.2-8 and 4.2-9 (from [49])	WinMACCS Organ List
Leukemia	Red Marrow
Bone	Bone Surface
Breast	Breast
Lung	Lung
Thyroid	Thyroid
Liver	Liver
Effective	ICRP60ED
Residual	Bladder Wall (representing the pancreas)
Colon	Lower LI
not included	Stomach ^a

^a Not used in the calculation of latent cancer fatalities for SOARCA estimate.

Mortality Risk Coefficient (CFRISK)

Eckerman [49] also provides estimates of the uncertainty in the mortality risk coefficients (CFRISK) for each of the organs included in the SOARCA analyses for latent health effects. The distributions are log normal and are assumed to be uncorrelated. Table 4.2-11 provides the geometric mean and geometric standard deviation for each truncated log normal distribution. Figure 4.2-8 shows a graphical representation of the data presented in Table 4.2-11. A truncation at ± 3 sigma is applied to each distribution. The three sigma truncation represents a truncation at quantile 0.00135 (~0.1 percentile) and 0.99865 (~99.9 percentile). In the LHS software used by the WinMACCS framework, the truncation is made by normalizing any quantile generated in the probability space [0, 1] into the truncation space [0.00135; 0.99865].

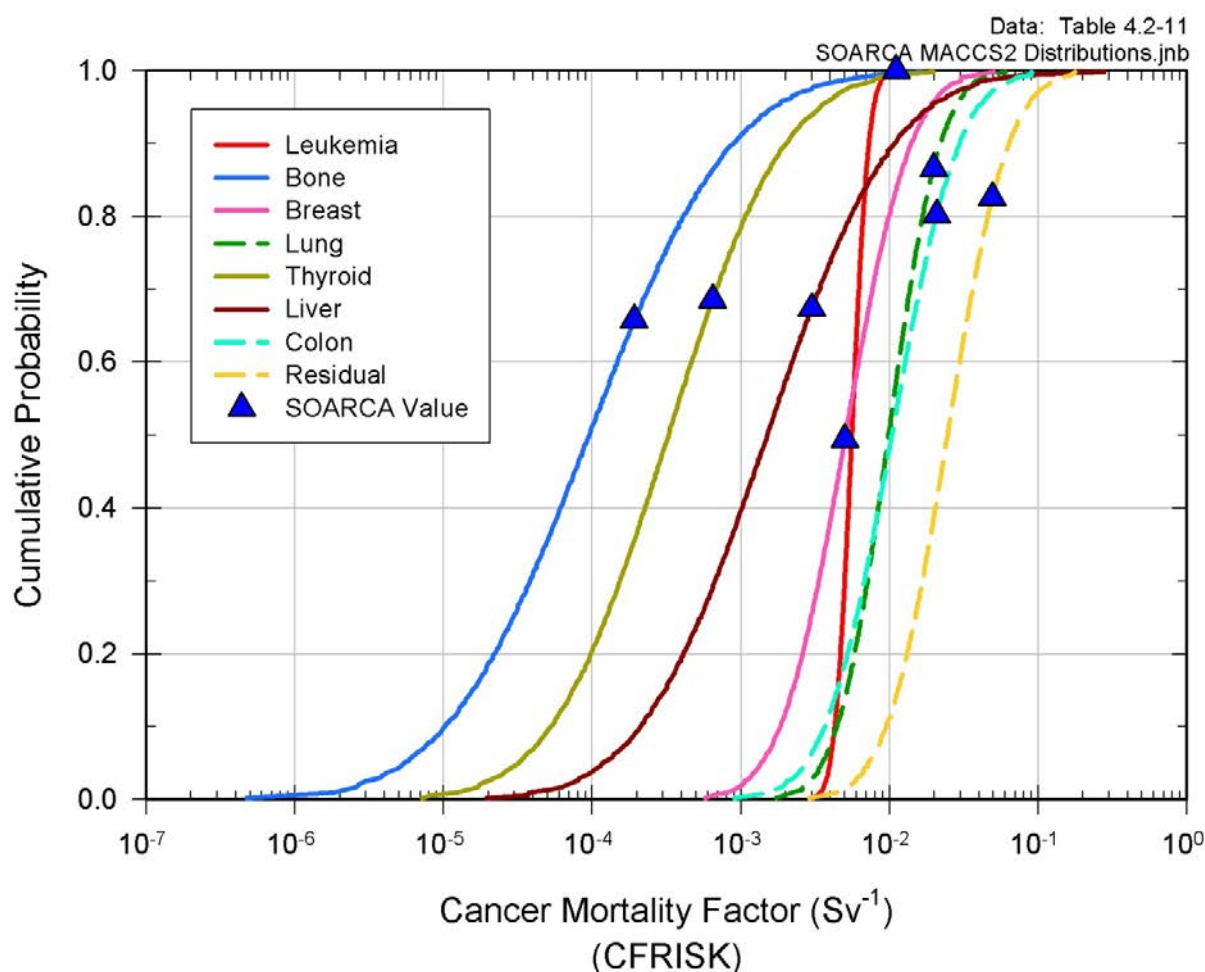


Figure 4.2-8 Cumulative distribution functions for latent health effects: mortality risk coefficients (CFRISK) for each of the organs included in the SOARCA analysis

Table 4.2-11 Age-averaged cancer mortality risk estimates and uncertainties for low-dose, low-LET uniform irradiation of the body [49]

Site	Mortality Risk Coefficient (CFRISK)		
	Mean(Sv^{-1}) ^a	Standard Deviation ^b	SOARCA Estimate
Leukemia	5.57×10^{-3}	$\text{Ln}(1.23)$	1.11×10^{-2}
Bone	9.50×10^{-5}	$\text{Ln}(5.70)$	1.90×10^{-4}
Breast	5.06×10^{-3}	$\text{Ln}(2.21)$	5.06×10^{-3}
Lung	9.88×10^{-3}	$\text{Ln}(1.87)$	1.98×10^{-2}
Thyroid	3.24×10^{-4}	$\text{Ln}(4.15)$	6.48×10^{-4}
Liver	1.50×10^{-3}	$\text{Ln}(4.65)$	3.00×10^{-3}
Colon	1.04×10^{-2}	$\text{Ln}(2.26)$	2.08×10^{-2}
Residual	2.46×10^{-2}	$\text{Ln}(2.10)$	4.93×10^{-2}
Total	5.75×10^{-2}		

Note: ^a Geometric mean of the log normal distribution, which is also the median of the distribution. ^b $\text{Ln}(\sigma)$ where σ is the geometric standard deviation of the log normal distribution.

4.2.6 Dispersion (CYSIGA, CZSIGA)

Dispersion directly affects doses to members of the population and resulting health effects. Thus, the dispersion parameters used to estimate atmospheric dispersion are important to the outcome of the calculation. However, in terms of predicted health effects, these parameters tend to have a non-linear effect when using the linear, no-threshold (LNT) dose-response model for estimating latent health effects because more dispersion simply means lower individual dose to a greater population. However, dispersion has a greater effect when using dose truncation because a smaller dose to an individual can reduce a finite risk to zero.

Initially, the authors considered basing the distributions for dispersion on expert data [44] as evaluated in *Synthesis of Distributions Representing Important Non-Site-Specific Parameters in Off-Site Consequence Analysis* [43]. However, after a review of the data, it became clear that this would not be appropriate. The expert elicitation evaluated the uncertainty in a single weather instance over a short period of time. The intended use of the uncertainty analysis, though, is to apply the uncertainty to a whole year of weather data. Doing this would imply that the uncertainty in the dispersion for a single hour of weather is fully correlated with the uncertainty for all hours of the year. This would be an extremely poor assumption; a better assumption would be that uncertainty in a single hour of weather data is completely uncorrelated with other hours of weather data. Thus, because of the way the uncertainty in dispersion is being implemented in this analysis, expert judgment is used to estimate the range of uncertainty in dispersion. A previous study compared mean results over a year of weather for four different computer codes using different approaches for modeling a plume [50] and found that the variation in the results was within a factor of two. Here, we assume that this factor of two is the uncertainty in the Gaussian plume model. Because ground-level concentrations in the near field are proportional to the product of the horizontal and vertical dispersion parameters, the product of the two is assumed to range from 0.5 to 2.0 times the nominal values at the 5th and 95th percentiles of a log-normal distribution, respectively. Furthermore, the

uncertainty is apportioned evenly between the two parameters, so both σ_y and σ_z are assumed to be 0.707 and 1.414 times their nominal values at the 5th and 95th percentiles, respectively. Because dispersion in the two dimensions are related physically, they are taken to be fully correlated. Likewise, the dispersion coefficients for each of the stability classes are fully correlated. Tables 4.2-12 and 4.2-13 show log-normal inputs for the CYSIGA and CZSIGA parameters. Figure 4.2-9 shows a graphical representation of the data presented in Tables 4.2-12 and 4.2-13.

Table 4.2-12 MACCS uncertain parameters—inputs for log-normal dispersion parameters distributions

	Linear, Crosswind Dispersion Coefficients (CYSIGA)				Linear, Vertical Dispersion Coefficients (CZSIGA)			
	Stability Class				Stability Class			
	A/B [m]	C [m]	D [m]	E/F [m]	A/B [m]	C [m]	D [m]	E/F [m]
Nominal (50 th quantile Ref. 36)	0.7507	0.4063	0.2779	0.2158	0.0361	0.2036	0.2636	0.2463
5 th	0.37535	0.20315	0.13895	0.1079	0.01805	0.1018	0.1318	0.12315
95 th	1.5014	0.8126	0.5558	0.4316	0.0722	0.4072	0.5272	0.4926

Note: A factor of 2 between 50th and 95th as well as between 5th and 50th quantile is equivalent to a factor of $\ln(2)$ in log-transformed data

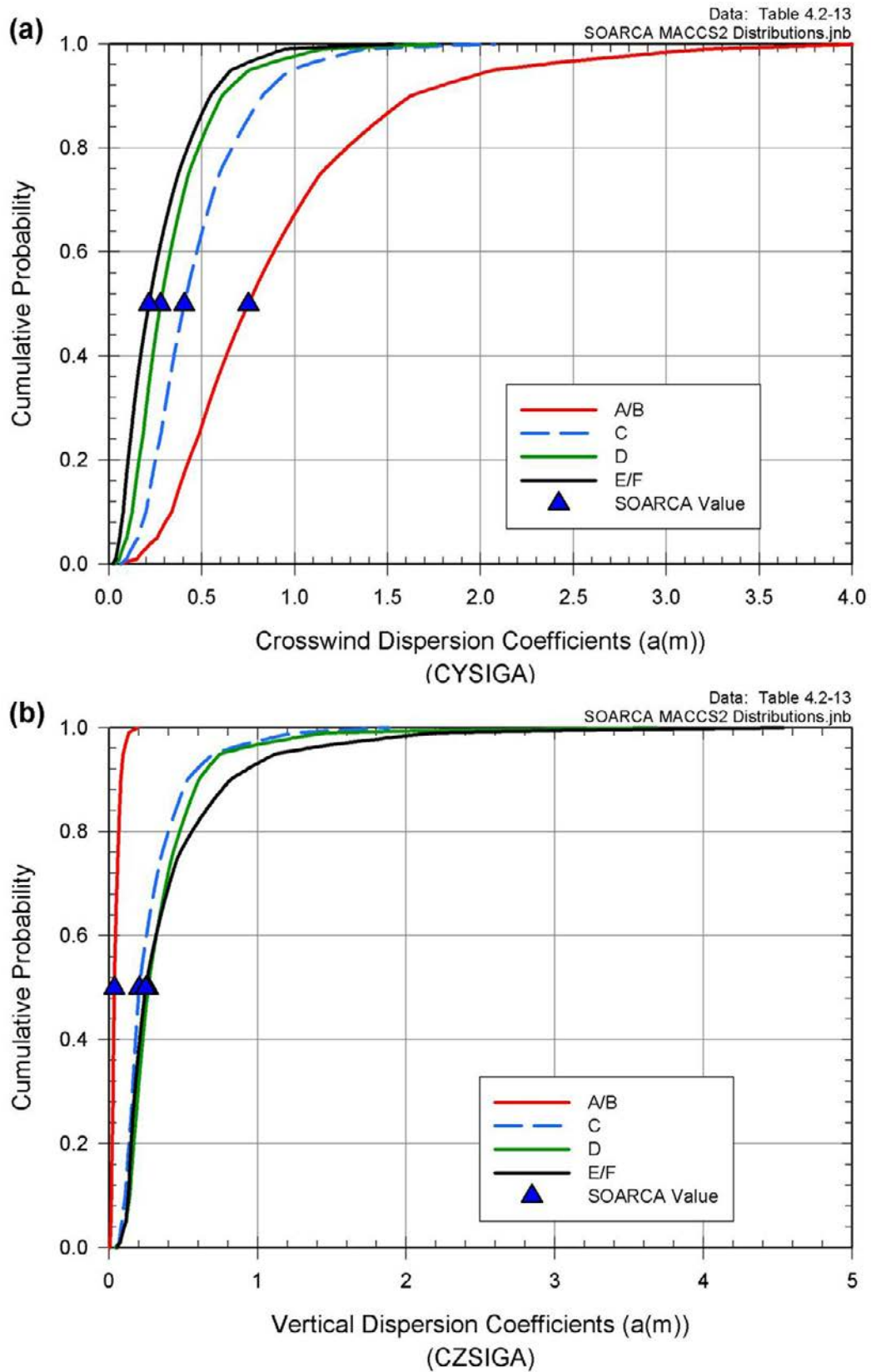


Figure 4.2-9 Cumulative distribution functions of linear (a) crosswind dispersion coefficients, $a(m)$ and (b) vertical dispersion coefficients, $a(m)$

Table 4.2-13 MACCS uncertain parameters—dispersion

Linear, Crosswind Dispersion Coefficients, a(m) (CYSIGA)	Percentile	Stability Class			
		A/B [m]	C [m]	D [m]	E/F [m]
Piecewise log-uniform distribution	0	0.0650	0.0631	0.0341	0.0212
	1	0.2817	0.1524	0.1043	0.0810
	5	0.3754	0.2032	0.1390	0.1079
	10	0.4374	0.2368	0.1619	0.1258
	25	0.5650	0.3058	0.2091	0.1624
	50	0.7507	0.4063	0.2779	0.2158
	75	0.9975	0.5399	0.3693	0.2867
	90	1.2883	0.6972	0.4769	0.3703
	95	1.5014	0.8126	0.5558	0.4316
	99	2.0009	1.0829	0.7407	0.5752
	100	4.0698	2.0763	1.7618	1.5307
SOARCA Values		0.7507	0.4063	0.2779	0.2158
Linear, Vertical Dispersion Coefficients, a(m) (CZSIGA)	Percentile	Stability Class			
		A/B [m]	C [m]	D [m]	E/F [m]
Piecewise log-uniform distribution	0	0.0056	0.0487	0.0421	0.0533
	1	0.0135	0.0764	0.0989	0.0924
	5	0.0181	0.1018	0.1318	0.1232
	10	0.0210	0.1186	0.1536	0.1435
	25	0.0272	0.1532	0.1984	0.1854
	50	0.0361	0.2036	0.2636	0.2463
	75	0.0480	0.2705	0.3503	0.3273
	90	0.0620	0.3494	0.4524	0.4227
	95	0.0722	0.4072	0.5272	0.4926
	99	0.0962	0.5427	0.7026	0.6565
	100	0.1951	1.8861	3.6880	4.5386
SOARCA Values		0.0361	0.2036	0.2636	0.2463

Note: CYSIGA and CZSIGA are perfectly rank correlated with each other and across the stability classes.

4.2.7 Hot Spot and Normal Relocation (DOSNRM, TIMNRM, DOSHOT, TIMHOT)

Protective actions that may be implemented in response to a severe accident and radiological release include evacuation and sheltering of individuals who reside in the emergency planning zone (EPZ). In addition to these protective actions, there are effective dose thresholds that are established to ensure members of the public are relocated from elevated dose areas that exceed U.S. Environmental Protection Agency (EPA) protective action guides (PAGs). When these thresholds are exceeded, offsite response organizations (OROs) will relocate individuals from the affected areas. This application is typically considered for residents beyond the EPZ where the effective dose exceeds protective action criteria but also applies to residents who refused to follow the initial evacuation orders. It is assumed these individuals will evacuate when they understand a release has in fact occurred and they are informed they are located in

high dose areas. The OROs determine the affected areas based on dose projections using State, utility, and Federal agency computer models together with dose measurements taken in the field. The use of multiple dose models combined with field measurements and the need for response organizations to mobilize to relocate affected residents provides opportunity for variations in dose predictions and response time which makes these parameters good candidates for the uncertainty analysis.

Hot-spot relocation and normal relocation models are included in the MACCS code to reflect this relocation activity performed by OROs. Hot-spot and normal relocation models are based on effective dose models using the total effective dose commitment projected to be received by an individual who remained in place for the entire emergency-phase period while engaging in normal activity. The pathways used for calculating the total effective dose commitment are cloudshine, groundshine, direct inhalation, and resuspension inhalation. The reference time for the relocation dose criterion is plume arrival. Any individuals relocated due to hot spots are removed from the problem for the duration of the emergency phase and receive no additional dose during this phase [9].

Hot-spot and normal dose information would be available shortly before or concurrent with the release to the environment which occurs at about 20 hours for the LTSBO. Dose projections would be available earlier, however, over a 20 hour period, wind shifts and changing accident conditions may not support projections for use in relocation much earlier.

Relocation is a process that requires identification of the affected areas, notification of residents within those areas, and movement of the public out of the affected areas. The time values represent the average time expected to implement these actions. The baseline for hot-spot relocation criteria is 12 hours after plume arrival if the total effective lifetime dose commitment for the weeklong emergency phase is projected to exceed 0.05 Sv (5 rem). The 5 rem value is the upper limit of the EPA PAGs [51]. A single time value was selected and applied to all of the accident scenarios evaluated for the Peach Bottom plant. The relocation time considers that response agencies would have competing priorities early in the event. The hot-spot time values will be varied from 6 hours to 18 hours in this uncertainty analysis to reflect the possibility that relocations could begin early based on dose projections or may be delayed while responders address other priorities (Figure 4.2-10b and Table 4.2-14). A lower bound of 1 rem and an upper bound of 10 rem will be used for the effective dose (Figure 4.2-10a and Table 4.2-14).

For normal relocation, individuals are relocated 24 hours after plume arrival if the total effective lifetime dose commitment for the weeklong emergency phase is projected to exceed 0.005 Sv (0.5 rem). The relocation time was established because response agencies would evacuate the hot-spot areas prior to focusing on the normal relocation areas. Also, there is less urgency in relocating these individuals because, similar to hotspot relocation, the 0.5 rem projected value represents the effective cumulative dose for the entire early phase and through relocation the individuals would be moved long before the end of the early phase. Typically, the EPA PAGs of 1 rem is used for normal relocation; however, 0.5 rem was used in the Peach Bottom analysis because local officials had expressed this as the value likely to be established for habitability. The normal relocation time values will be varied from 12 hours to 36 hours in this uncertainty analysis to reflect the possibility that relocations could begin early based on projected dose or may be delayed while responders address other priorities (Figure 4.2-10b and Table 4.2-14). A lower bound of 0.1 rem and an upper bound of 1 rem will be used for the effective dose (Figure 4.2-10a and Table 4.2-14).

The hot-spot and normal relocation values used in NUREG-1150 were 50 rem and 25 rem respectively [16]. The values used in SOARCA were established to better align with site specific response expectations and EPA PAGs.

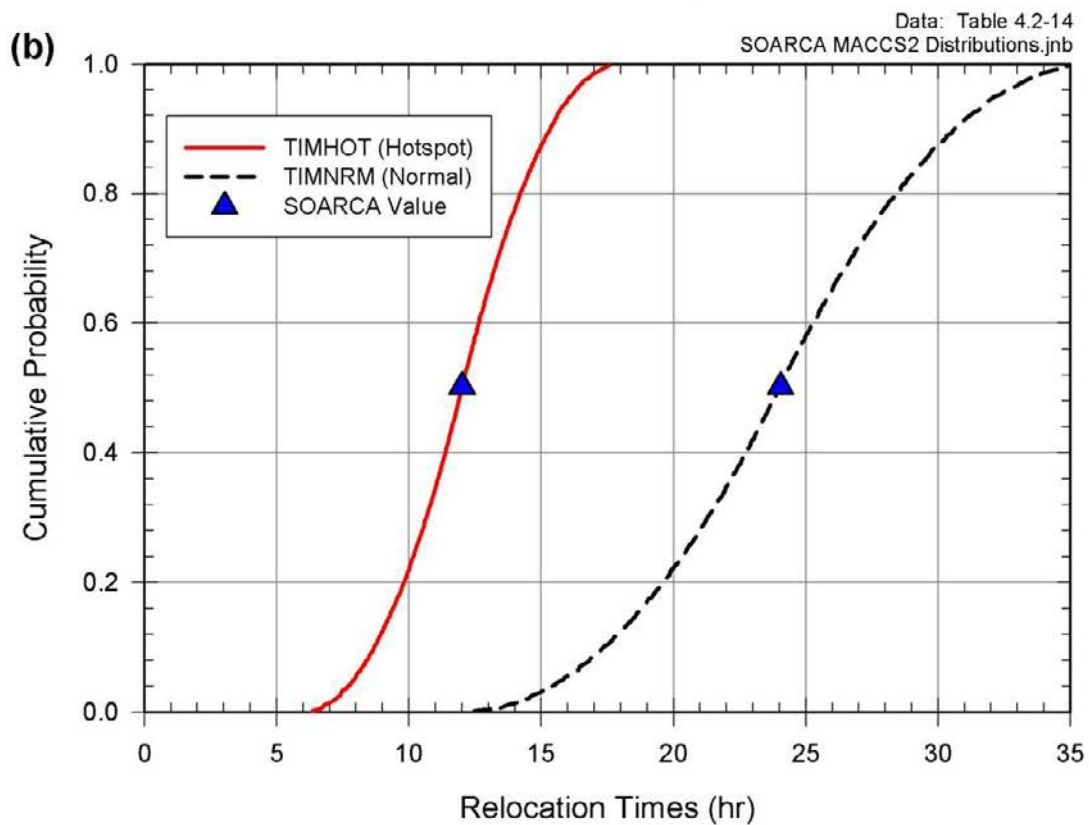
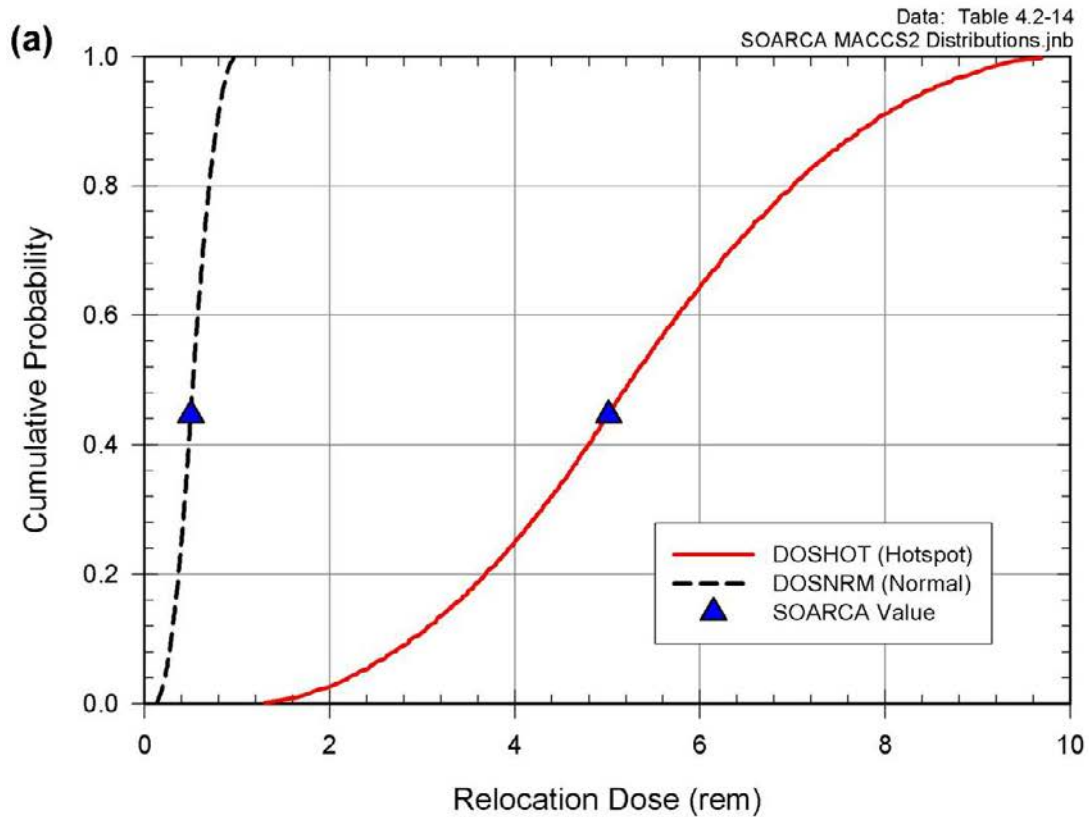


Figure 4.2-10 Cumulative distribution functions of hotspot and normal (a) relocation doses and (b) relocation times

Table 4.2-14 MACCS uncertain parameters—relocation doses and times

Parameter	Triangular Distribution
DOSHOT: Hot-spot relocation – dose SOARCA estimate: 5 rem	LB = 1.0 rem UB = 10.0 rem Mode = 5.0 rem
TIMHOT: Hot-spot relocation – time SOARCA estimate: 12 hours	LB = 6.0 hr. UB = 18 hr. Mode = 12 hr.
DOSNRM: Normal relocation – dose SOARCA estimate: 0.5 rem	LB = 0.1 rem UB = 1.0 rem Mode = 0.5 rem
TIMNRM: Normal relocation – time SOARCA estimate: 24 hours	LB = 12.0 hr. UB = 36.0 hr. Mode = 24 hr.

Note: Relocation times are perfectly rank correlated. Relocation doses are perfectly rank correlated.

4.2.8 Evacuation Delay (DLTEVA)

Evacuation delay defines the duration of the sheltering period that occurs before evacuation of residents begins [9]. Delay to evacuation might be affected by a delay in response to the evacuation order, a need to wait for the return of commuters, a need to wait for public transportation, a need to shut down operations prior to leaving work, etc. Research shows that delay is not uniform with most of the evacuees experiencing a smaller delay (e.g., 90% of the public evacuates in about 60% of the response time) [52, 53]. There is high confidence in the alert and notification system to warn the public within the specified time; however, response of the public is a function of the time to receive the notification and the time to prepare to evacuate [54]. Because people are located throughout the EPZ and have different response timing, this variable was considered a good candidate for the uncertainty analysis.

The DLTEVA parameter is applied at the cohort level and the uncertainty analysis will sample on each of the cohorts (Figure 4.2-11 and Table 4.2-15). Cohorts 1 and 2 represent the 0-10 mile public and 10-20 mile shadow respectively, and the baseline DLTEVA value is one hour. This value is supported by the ORNL 6615 study, which provided empirical data showing that most of the public is mobilized in about an hour [54]. The lower bound is established as 0.0 hr which would indicate there is no delay after the public becomes aware of the emergency. The lower bound was set based on results of a focus group survey of residents of EPZs that indicate some people may evacuate immediately upon receipt of an evacuation order [55]. The upper bound was selected as four hours to account for the need to gather family members, pack, and prepare to evacuate. Cohort 2 is the shadow evacuation which is aligned with the evacuation of Cohort 1.

Cohort 3 represents the schools and the 0-10 mile shadow evacuation. A baseline value of 45 minutes was used because schools are notified early and are prepared to evacuate when the official order is issued. The 0-10 mile shadow has the same response characteristics because this cohort has been defined in SOARCA as evacuating when the schools evacuate. The 0-10 mile shadow evacuates spontaneously (prior to receiving an evacuation order) when the

emergency is communicated to the residents of the EPZ via the sirens and emergency evacuation system messaging for the site area emergency (SAE). Shadow evacuation of the public has been observed to occur quickly for industrial accidents [41]. For the uncertainty analysis, the lower bound for this cohort was set at 0.25 hr, which is 15 minutes after site declares the SAE. The Pennsylvania emergency management plan explains that evacuation can be implemented for an SAE or a general emergency. Therefore, there could be conditions in which the State might evacuate the schools early, and if the evacuation were to occur in the morning at the beginning of school or in the afternoon at the end of school, buses would be positioned to begin the evacuation promptly. The early warning for schools provides time for buses to mobilize and be at the school if an evacuation were to be ordered. Evacuation drills at schools demonstrate the ability to prepare and move students quickly. The upper bound of four hours was established to account for potential delay in notification, communication with drivers, delay in travel due to weather or other impediments, etc.

Cohort 4 represents special facilities and was modeled in the baseline as evacuating later in the event at 4.25 hours. Special facilities often take longer as a whole than the general public. These facilities actually evacuate individually following facility specific evacuation plans and are not typically dependent upon one another for support [55]. Therefore, in practice, some facilities begin earlier in the event and some begin later. For this uncertainty analysis, the lower bound was set at 0.0 hr because facilities may have onsite transportation resources and could prepare to evacuate promptly. The upper bound was set at six hours to represent a delay in availability of transportation resources, communication with drivers, delay in travel due to weather, or other impediments. Since the site is located near larger cities such as Lancaster, Pennsylvania, and Baltimore, Maryland it is expected there are ample regional resources, should these be needed. Six hours is estimated to be a maximum time that it would take to coordinate regional resources.

Cohort 5 is the evacuation tail, which by definition begins evacuating at the end of the general public evacuation. The baseline value of 4.25 hours was based on the site specific evacuation time estimate (ETE) study which showed that 90% of the population had completed the evacuation in 4.25 hours. The values for the uncertainty analysis are established based on the ETE by adding four hours to the Cohort 1 distribution. This equates to Cohort 5 values of four hours for the lower bound and eight hours for the upper bound.

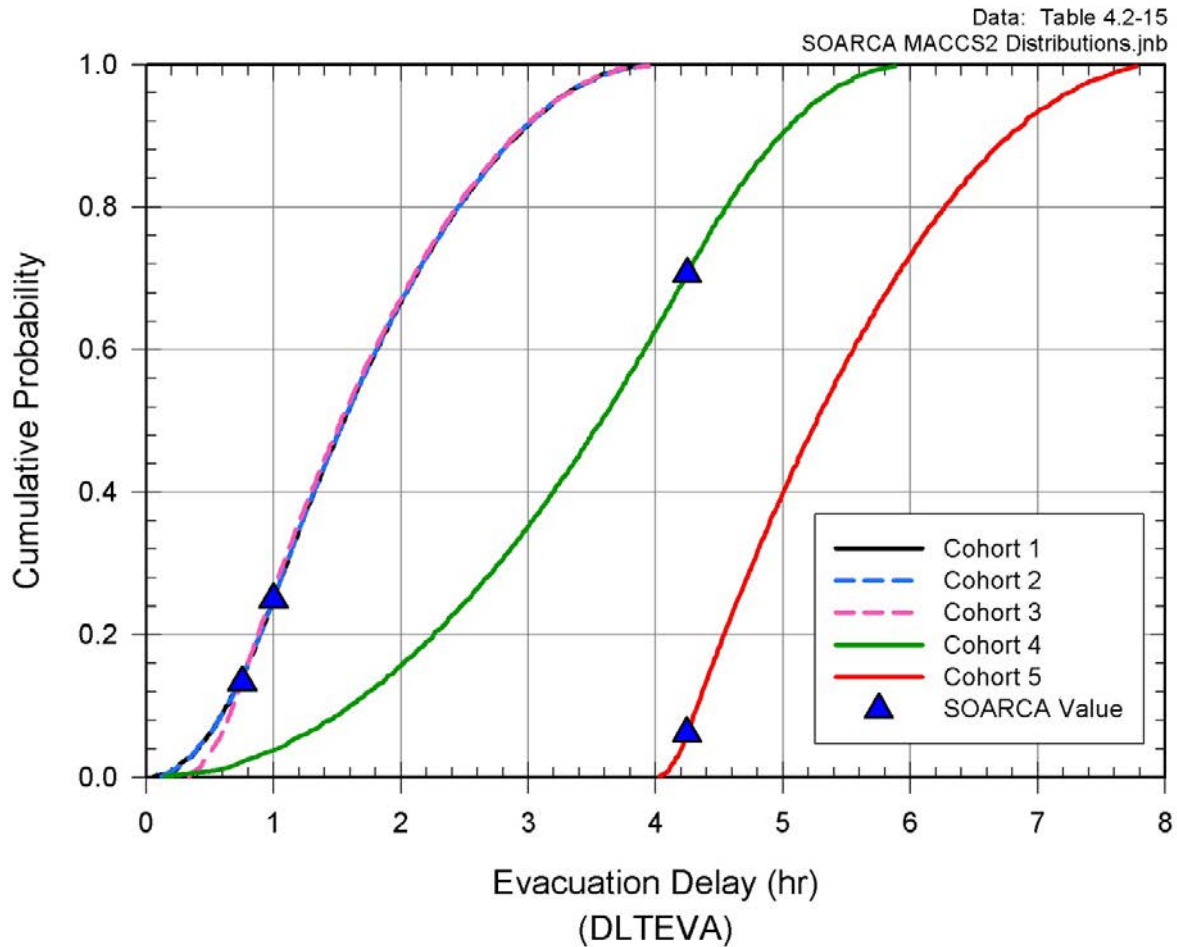


Figure 4.2-11 Cumulative distribution functions of evacuation delay

Table 4.2-15 MACCS uncertain parameters—evacuation delay

DLTEVA		
Parameter	SOARCA Estimate/Mode	Triangular Distribution
Evacuation delay – cohort 1 (0-10 mile Public)	1.0	LB = 0.0 hr. UB = 4.0 hr.
Evacuation delay – cohort 2 (10-20 mile Shadow)	1.0	LB = 0.0 hr. UB = 4.0 hr.
Evacuation delay – cohort 3 (Schools/Shadow)	0.75	LB = 0.25 hr. UB = 4.0 hr.
Evacuation delay – cohort 4 (Special Facilities)	4.25	LB = 0.0 hr. UB = 6.0 hr.
Evacuation delay –cohort 5 (Evacuation Tail)	4.25	LB = 4.0 hr. UB = 8.0 hr.

Note: Evacuation delays are sampled independently for each cohort and for each radial ring.

4.2.9 Evacuation Speed (ESPEED)

Evacuation speed represents the travel speed of evacuees as they evacuate the EPZ. To model evacuation with WinMACCS, evacuees are loaded onto the roadway network at a specified time and a single speed is used. However, evacuations typically occur as a distribution in which the cumulative percent of the public evacuating the area increases over time until all members of the public have evacuated [53]. Evacuations are typically represented as a curve of the number of people evacuated that is relatively steep at the beginning and tends to decrease over time as the last members of the public exit the area. This distribution curve is relatively steep for shorter duration evacuations from areas the size of an EPZ, and the distribution curve is less steep for longer duration evacuations typical of those for hurricanes which may begin days in advance of landfall. The point at which the curve tends to flatten occurs when approximately 90% of the population has evacuated. The last 10% of the population is called the evacuation tail [53]. The ESPEED parameter is applied at the cohort level and the uncertainty analysis will sample on each of the cohorts (Figure 4.2-12 and Table 4.2-16). For the uncertainty analysis the distributions are applied to the mid-phase for all of the cohorts.

For cohorts 1 and 2 which represent the 0-10 mile public and 10-20 mile shadow respectively, the baseline speed was 3 mph. The slow speed is established to account for the model loading all members of the public cohort at one time. In reality, the evacuees would load the network over a longer period of time and travel a little faster. The 10-20 mile shadow would be expected to have a higher speed, but was limited to 3 mph because of the way the general public is integrated with this cohort [1]. This speed value was developed using information from the site specific ETE. The lower bound is established as 1.0 mph which would indicate there are impediments to the evacuation causing travel to be considerably slower. The upper bound was selected as 10 mph which would indicate that minimal traffic congestion occurs.

Cohort 3 represents the schools and the 0-10 mile shadow evacuation. A baseline speed of 20 mph was used because schools are notified directly and early. The schools contribute the first evacuating vehicles on the roadway and their vehicles enter the transportation network before congestion from the general public begins. The 0-10 mile shadow has the same response characteristics as the schools, leaving almost immediately. A lower bound was set at 10.0 mph to account for unexpected travel delays due to impediments such as weather. The upper bound of 30 mph was established based on the roadway network posted speeds. Most of the roadways within the EPZ have posted speeds greater than 30 mph and many roadways have 50 or 55 mph speed limits. The average travel speed on a roadway is always less than the posted speed because of traffic control requiring stops and starts.

Cohort 4 (special facilities) was modeled in the baseline as starting evacuation later in the event, near the end of the peak traffic congestion. As discussed earlier, in practice some facilities move earlier in the event and some move later. The lower bound was set at 1.0 mph to represent facilities that have entered the roadway at the peak congestion period when speeds are the slowest. The upper bound was set at 30 mph to represent sufficient resources to support prompt evacuation of these facilities or for those facilities evacuating very late when speeds have increased.

Cohort 5 (evacuation tail) begins evacuation at the end of the general public evacuation. Although their initial speed is the same as the general public, the roadways begin to clear and the tail has overall faster exiting speeds. The SOARCA values of 3 mph for the early phase and 20 mph for the middle phase considers that these are the last vehicles on the roadway entering when congestion is at the peak and as congestion clears, the cohorts speed increases. The

lower bound and mode of the triangular distribution was set at 3 mph because by definition, the tail enters the roadway after 90% of the public has evacuated, therefore they are at the end of the peak congestion and the speed at this point could be 1 mph for Cohort 1. The upper bound of 30 mph represents roadways that are relatively free of congestion once the majority of vehicles have left the area [53].

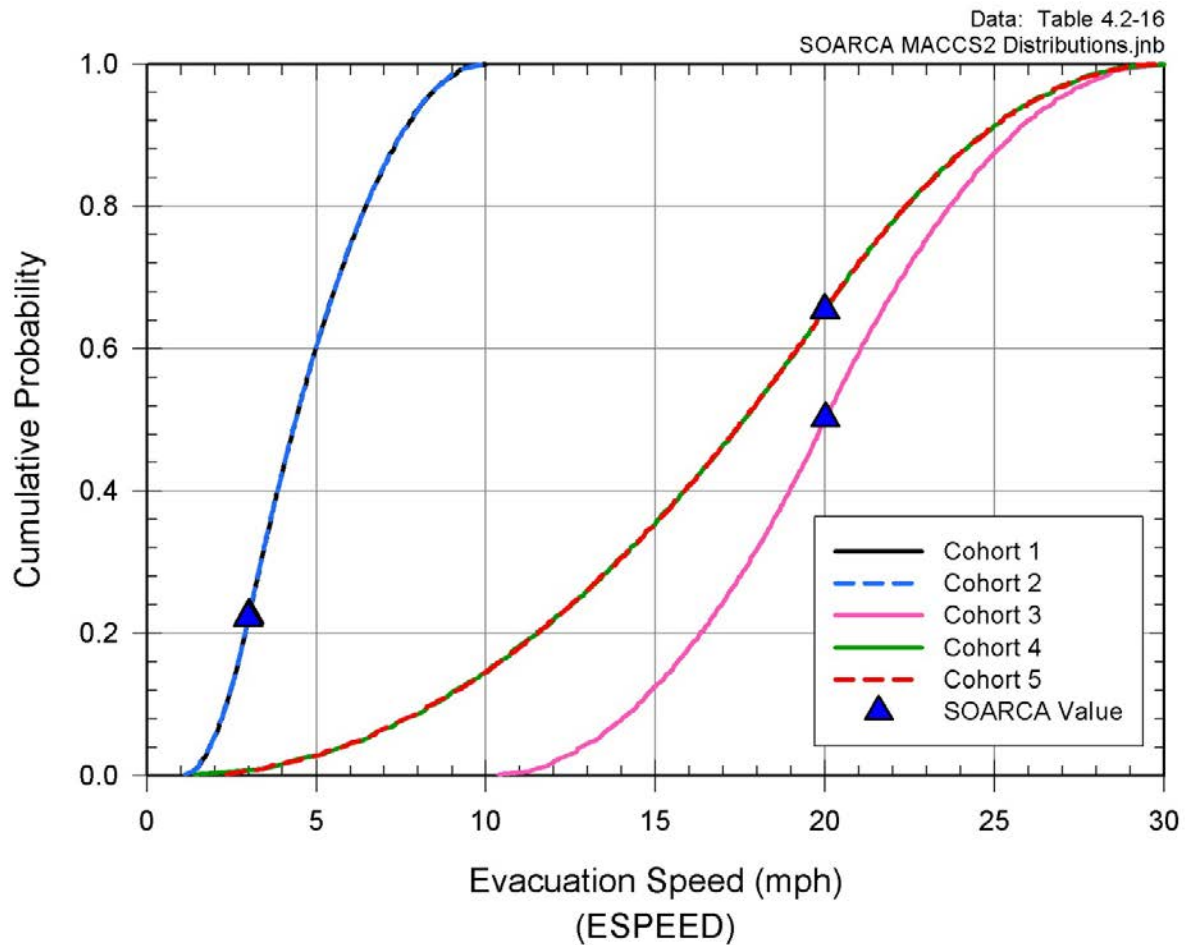


Figure 4.2-12 Cumulative distribution functions of evacuation speed

Table 4.2-16 MACCS uncertain parameters—evacuation speed

ESPEED		
Parameter	SOARCA Estimate/Mode	Distribution
Evacuation speed – cohort 1 (0-10 mile Public)	3 mph	Triangular LB = 1.0 UB = 10.0 Mode = 3.0
Evacuation speed – cohort 2 (10-20 mile Shadow)	3 mph	Triangular LB = 1.0 UB = 10.0 Mode = 3.0
Evacuation speed – cohort 3 (Schools/Shadow)	20 mph	Triangular LB = 10.0 UB = 30.0 Mode = 20
Evacuation speed— cohort 4 (Special Facilities)	20 mph	Triangular LB = 1.0 UB = 30.0 Mode = 20
Evacuation speed – cohort 5 (Evacuation Tail)	20 mph	Triangular LB = 1.0 UB = 30.0 Mode = 20

Note: Evacuation speeds are perfectly rank correlated between cohorts.

4.3 Other Phenomena Considered

In some cases, it is desirable to investigate the influence of phenomena that are considered important, but cannot be easily accessed by replacing point estimates with distributions for available input parameters. The integrated cases in this study can determine the influence on selected results only over the parameters and range of inputs defined in Section 4.1 and Section 4.2. Exclusion of specific phenomena from this study does not indicate whether or not they are important, rather in some cases it is driven by the lack of knowledge as to how to incorporate uncertainty in these phenomena. In other cases, the models and codes used in this study have not been parameterized such that uncertainty in these potentially important phenomena can be quantified. In some cases, to measure the effects of other potentially important phenomena, alternative sensitivity study can be employed using approaches specific to the phenomena being investigated. These approaches include one-off analysis, targeted modeling scenarios, and sensitivity cases that are tailored to the analysis to help quantify the effects. Other cases would require significant code changes to explore the phenomena of interest.

The following section discusses several potentially important phenomena identified during the parameter selection and review process, as well as those raised during ACRS and peer reviews. While this list is not intended to be all inclusive rather, it is an attempt to qualitatively and quantitatively, when possible, assess the potential importance of a few select phenomena identified by expert judgment.

4.3.1 Source Term Model

4.3.1.1 Early Event Operator Actions

As pointed out during the peer review of the selected parameters and distributions listed in Section 4.1 and Section 4.2, as well as by ACRS committee members, there is generally an uncertainty in the timing of operator actions. It is clear that the operator actions by default, through the assumption of in-action, define the unmitigated LTSBO scenario. However, the larger uncertainty in operator actions includes either the potential for operators to (i) take unexpected actions, (ii) take actions out of order depending upon the severity of the accident, (iii) experience degradation of specific performance abilities due to stress and other factors, or (iv) all of the above. Globally, these issues are beyond the scope of this study and the selected unmitigated LTSBO scenario.

The SOARCA Peach Bottom unmitigated response LTSBO scenario includes some operator actions. It is generally accepted that even for an unmitigated response scenario, early in the event, some minimal operator actions will be expected to occur. Two operator actions were credited in the unmitigated LTSBO calculation¹². First, operators are assumed to open one SRV to begin a controlled depressurization of the reactor vessel approximately one hour after the initiating event. This action is prescribed in station emergency procedures to prevent excessive cycles on the SRV. The target reactor vessel pressure is at or above 125 psi, which would permit continued operation of RCIC or HPCI, if necessary. Five SRVs associated with the automatic depressurization system would be available for this operation. These SRVs are provided with accumulators that provide a back-up pneumatic supply for operation of the valves upon loss of the Instrument Nitrogen System. Second, operators are assumed to take manual control of RCIC approximately two hours after the initiating event. This involves remote (i.e., from the control room) manipulation of the position of the steam throttle valve at the inlet to the RCIC turbine to reduce and control turbine speed. This action reduces and stabilizes coolant flow from the RCIC pump to maintain the reactor vessel level within a prescribed range. In addition, there are a general series of actions that shed loads on emergency buses to extend the battery lifetime. The effectiveness of those actions is captured in the uncertain distribution for battery life included in the uncertainty analysis.

It is clear that without the expected actions occurring that the RPV would pressurize and the RPV would be overfilled by which the RCIC which would then automatically turn off. This would accelerate the accident and subsequent releases to the environment. The first operator action, opening the SRV to begin a controlled depressurization of the RPV, uses a designated MELCOR control function (i.e., CF094) to actuate the SRV. After a predetermined time (e.g., one hour after the initiating event) the designated control function actuates SRV-1 to open to begin the cool down. However, the second operator action, taking manual control of RCIC approximately two hours after the initiating event, does not have designated control functions within MELCOR. The MELCOR control functions used when RCIC is initiated are the same as those used when manual control is assumed to occur. To create a separate suite of control functions specifically for manual control of RCIC would require a significant change to the Peach Bottom MELCOR deck. Thus, the second operator action is not analyzed. The uncertain in the

¹² The action times used in NUREG/CR-7110 Volume 1 were based on 'table-top' exercises among NRC staff and licensee personnel, in which the anticipated accident sequence timeline was reviewed to characterize a reasonable time at which action would be taken.

time of the operator action, opening the SRV to begin a controlled depressurization of the RPV, in terms of this analysis is considered as scenario uncertainty, and as such, delays in this operator action are evaluated in this study in a series of sensitivity analyses presented in Section 6.4.1, rather than incorporated into the integrated uncertainty analysis.

4.3.1.2 Timing of Lower Head Failure

During the peer review and ACRS meetings, the single mode of lower head failure used for SOARCA (i.e., gross creep rupture of the lower head) was discussed. To better clarify this single mode of lower head failure, the uncertainty analysis took into consideration variations in the Larson-Miller creep parameters, and whether small penetration/drain line failures would affect the overall timing of lower head failure.

Larson-Miller Creep Parameters

Initial investigations into lower head failure were considered by varying the Larson-Miller creep rupture parameter in MELCOR. Current dynamic PRA work [56] indicates that applying a distribution to the MELCOR Larson-Miller creep rupture parameter (i.e., LM-Creep (t)) shown on Figure 4.3-1, will only result in approximately a 20 minute change in the timing of lower head failure between the 5th and 95th percentiles. This change in timing will not affect the overall accident progression, nor will it noticeably change the environmental source term. Based on these analyses, it was determined that Larson-Miller creep rupture parameter uncertainty would not be investigated for this work.

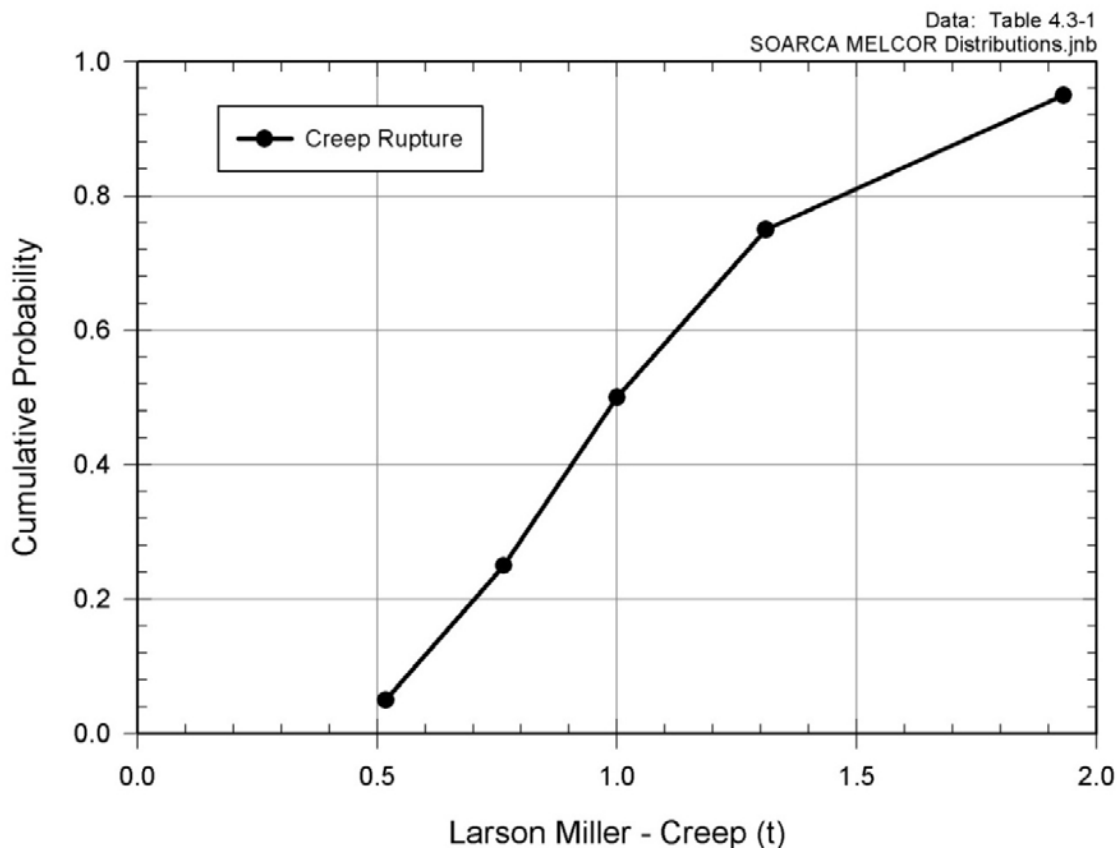


Figure 4.3-1 Creep rupture parameter distribution

Small Penetrations/Drain Line

Detailed analysis of the MELCOR source code and ongoing MELCOR studies associated with U.S. Department of Energy and NRC post Fukushima analysis, have determined two issues regarding small penetrations and drain line lower head failure modes. The first issue involves a computational work-around developed for MELCOR to model corium flow through the lower head failure. Due to numerical limitations of computers when MELCOR Version 1.8.6 was released, a limit of 10% was applied to the amount of molten corium in the lower RPV prior to flow through the lower head failure. The 10% molten material limit was required for corium within the RPV to go ex-vessel independent of whether the lower head had failed. This allowed the MELCOR code to conduct a simulation within a relatively fast time (e.g., weeks instead of months for a single MELCOR simulation). Since numerical limitations are no longer an issue with current technology, MELCOR Version 2.1 has removed this limitation. However, in order to maintain a certain amount of continuity between the analysis done in NUREG/CR-7110 Volume 1 and this work, MELCOR Version 1.8.6 is used.

The second issue involves the progression of a small lower head failure into a large failure. A sensitivity study for small lower head penetration failures is presented in section 6.4.2.

4.3.1.3 SRV Set Point Drift

With regard to the sequence issues, specifically the SRV stochastic failure rate, it was noted during an ACRS subcommittee review meeting that during as-found testing after outages, the SRVs were found to typically fail to activate at the set point pressure by plus three percent of acceptance criteria. For the Peach Bottom Unmitigated LTSBO MELCOR model, SRV-1 begins to open at 1,100 psig, and the valve is full open at 103% of the set point. As the pressure decreases, SRV-1 begins to close at 1,100 psig, and the valve is fully closed at 97% of the set point. It is assumed the set point drift is due to corrosion bonding of the SRV valve seat and disk. The corrosion bonding will cause the SRV lifting set point to increase. For the purpose of this discussion, an increase in the SRV set point for set point drift is assumed at 103% (1,133 psig), 110% (1,210 psig), and 120% (1,320) of the SRV-1 set point. However, it is assumed that the corrosion bonding will not raise the reseating set point since the bonding between the valve seat and disk will not affect the reseating pressure set point. Thus the reseating pressure value is assumed to remain constant (i.e., full closed at 97% of the initial set point of 1,100 psig).

Based on the Peach Bottom Unmitigated LTSBO MELCOR model, SRV-1 opens approximately six seconds into the event. The next SRV-1 cycle opening occurs approximately 30 seconds and continues to cycle at approximately 20 second intervals until the cooldown occurs at approximately 55 minutes into the scenario. Table 4.3-1 shows the estimated timing of the SRV-1 cycles due to set point drift when compared to the SRV-1 original set point. The results presented in Table 4.3-1 assume the pressure at which SRV-1 closes remains constant (i.e., fully closed at 97% of the original set point of 1,100 psig). It should also be noted that even if the SRV-1 set point was to drift upwards, the subsequent SRVs, 10 additional SRVs, could lift at their designed pressures which are lower than the 10% and 20% set point drift pressure limits. However for this discussion, it is assumed that all SRVs will have the same percentage of upward set point drift.

Table 4.3-1 A worst-case scenario of SRV-1 set point drift time estimates

	Original Set point	103% Set point	110% Set point	120% Set point
1 st SRV-1 cycle	6 seconds	8 seconds	14 seconds	22 seconds
2 nd SRV-1 cycle	30 seconds	47 seconds	144 seconds	282 seconds
3 rd SRV-1 cycle	48 seconds	71 seconds	222 seconds	440 seconds
SRV-1 failure (270 cycles)	8.2 hours	10 hours	27 hours	52 hours

The simplified analysis of the potential effects on the timing of SRV stochastic FTC assume a worst case scenario, one in which all of the SRVs experience set point drift in a positive direction (e.g., higher pressure required to open the valve) and this occurs at each demand.

In this worst case scenario a delay in the SRV stochastic FTC, in the LTSBO scenario will cause an increase RPV temperatures (i.e., the RPV is in a water/steam saturated condition during SRV cycling) from approximately 295°C to approximately 300 to 310°C during the SRV cycling period. With the increased time for the SRV remaining open during the blowdown, there could be potential for uncovering the core. With a longer SRV cycling, SRV-1 will intermittently release radionuclides during cycling to the wetwell, and if a sufficient delay occurs, SRV-1 will experience a thermal failure due to the high temperature gases exiting the RPV to the wetwell or the MSL will creep rupture. Either of these conditions will result in a delay of the overall melt sequence of the Peach Bottom Unmitigated LTSBO shown in Table 5-1 of NUREG/CR-7110 Volume 1. However, the longer the time delay in failure of the SRV will result in a larger environmental release. This important phenomenon, the delay in SRV FTC, is the same whether due to the potential for set point drift or an increase in the number of demands for SRV FTC. This phenomenon is already captured in the uncertainty analysis with the uncertainty in the number of SRV demands before FTC (i.e., SRVLAM). Any delays, either by SRV set point drift or the increased number of demands before FTC, will increase the likelihood of the SRV thermal failure or MSL creep rupture accident sequences.

The as-found testing measurements occur over one or a few lifts, whereas the Peach Bottom Unmitigated LTSBO scenario would experience tens to hundreds of demands before a FTC. More realistically, the very first few demands would likely break the corrosion bonding and the valve would perform as expected. The cumulative delay in timing would be minutes not hours before the sampled number of cycles at which SRV FTC occurred.

4.3.2 Consequence Model

An evaluation of the sensitivity to the size of the evacuation zone and evacuation start time, the effect of seismic activity on emergency response, surface roughness, and the importance of chemical classes was completed in NUREG/CR-7110 Volumes 1 & 2, and is summarized below. Two additional sensitivity analyses were performed to support this uncertainty analysis: One on the habitability criterion and a second to quantify the uncertainty that results from performing a finite set of weather trials.

4.3.2.1 Size of the Evacuation Zone and Evacuation Start Time

In NUREG/CR-7110 Volume 1 Section 7.3.3 [2], an analysis provides consequence estimates for the unmitigated Peach Bottom STSBO scenario without RCIC blackstart¹³. This calculation considered evacuation of a 10-mile circular area surrounding the plant. Three additional calculations were performed in NUREG/CR-7110 Volume 1 to assess variations in the protective actions:

- (1). evacuation of a 16-mile circular area
- (2). evacuation of a 20-mile circular area
- (3). delayed Evacuation of a 10-mile circular area

Results show expanding the size of the evacuation zone decreases the latent cancer fatality risk beyond the 10-mile radius for the unmitigated STSBO without RCIC blackstart; however, the risk within 10 miles increases with this change. This is because evacuating a larger area increases the time to evacuate the 10-mile region due to increased traffic congestion. For circular areas with greater than a 20-mile radius, the risk reduction associated with increasing the size of the evacuation zone is slight.

4.3.2.2 Evaluation of the Effect of Seismic Activity on Emergency Response

In NUREG/CR-7110 Volume 1 Section 7.3.4 [2], an analysis provides consequence estimates that include the effects of the seismic event on public evacuation. These consequence estimates were developed for the unmitigated Peach Bottom STSBO without RCIC blackstart scenario. Even though this has a lower frequency and lower absolute risk than the LTSBO scenario, this scenario was chosen because it had the earliest release of the Peach Bottom scenarios and was believed to be the most likely to show an increase in risk. Seismic effects on emergency response are site-specific and at Peach Bottom, the seismic analysis showed limited damage to the roadways and infrastructure. For Peach Bottom, the results demonstrated no substantial effect on health consequences at Peach Bottom. Although sirens fail, alternative notification is adequate and a larger shadow evacuation is expected as a result of the earthquake. The bridges and roadways that fail within the EPZ are not significant for evacuation; an adequate road network remains, and evacuation speeds are unchanged.

4.3.2.3 Surface Roughness

The SOARCA analyses used a surface roughness length that represents a typical value for the US, which is 10 cm. This value was used in past studies [16, 57] and has become a de facto value for many consequence analyses. However, this value of surface roughness is not necessarily the best choice for all regions of the country. In NUREG/CR-7110 Volume 1 Section 7.3.7 [2], an examination of a more site-specific value of surface roughness as a sensitivity study was completed to determine whether this parameter is significant for estimated risk.

The effect of increased surface roughness is twofold:

- It increases vertical mixing of the plume and
- It increases deposition velocities for all aerosol sizes.

¹³ Blackstart of the RCIC system refers to starting RCIC without any ac or dc control power.

Both effects were treated in this sensitivity study. A general observation based on this sensitivity study is that the specific choice of surface roughness has a modest effect on LNT predictions of risk; it has a larger effect, but less than a factor of two for the dose truncation models. (See discussion under Section 4.2.2.)

4.3.2.4 Importance of Chemical Classes

Each isotope present in the core of a nuclear reactor contributes to the overall risk from an accident; however, the release of some isotopes contributes to risk much more than others. There are three reasons some isotopes are more important than others:

- abundance of an isotope in the inventory in the core at the beginning of an accident,
- release fraction of an isotope into the atmosphere, and
- the dose conversion factors for an isotope, which depends strongly on the type and energy of the radiation produced, the half-life of the isotope, and for internal pathways, the biokinetics of the isotope.

There are 69 isotopes in the treatment of consequences considered in the MACCS analysis for SOARCA. These isotopes are grouped into a set of nine chemical classes in the MELCOR analyses that generated the source terms used in the SOARCA analyses. Since release fractions are calculated by MELCOR at the level of chemical classes, it is both reasonable and useful to examine how these same chemical classes influence the evaluation of risk.

In NUREG/CR-7110 Volume 1 Section 7.3.8 [2], an evaluation of the contribution of a chemical class was performed in which MACCS calculations were conducted with all but that one chemical class. The effect of that chemical class is then calculated by taking the difference between the risk when all chemical classes are included and the risk for all but that one chemical class (i.e., setting the release fractions for that chemical class to zero).

The relative importance of each chemical class was evaluated for all three accident sequences for Peach Bottom: the unmitigated LTSBO, the STSBO with RCIC blackstart, and the unmitigated STSBO without RCIC blackstart. Results were also calculated for each of the three dose-response models which are the following:

1. LNT dose-response model;
2. Linear with threshold dose-response model with US average natural background dose rate combined with average annual, medical dose as a dose truncation level (USBGR), which is 620 mrem/yr; and
3. Linear with threshold dose-response model using a dose truncation level based on the Health Physics Society's (HPS) position statement that there is a dose below which, due to uncertainties, a quantified risk should not be assigned, which is 5 rem/yr with a lifetime limit of 10 rem.

Each accident scenario for each dose-response model at specified circular areas produced different results.

4.3.2.5 Habitability

Habitability is the consequence model parameter that is used to establish the dose level at which residents are allowed to return to their homes. Habitability applies to everyone, not just evacuees. Whereas most states adhere to the EPA guidelines for habitability, the state of Pennsylvania has its own, stricter, habitability criterion guideline. The Pennsylvania guideline was used for the Peach Bottom analysis in the SOARCA project.

In Section 6.4.4, five habitability sensitivity analyses are presented for the current State of Pennsylvania guideline, EPA guidelines, the criterion implemented in NUREG-1150, and International Commission of Radiological Protection (ICRP) recommendations.

4.3.2.6 Weather Uncertainty

The atmospheric transport models implemented in MACCS require hourly readings of wind speed, wind direction, atmospheric stability, and precipitation as input for each weather sequence examined. In addition, four values of daytime and nighttime mixing height (i.e., height of the capping inversion layer), one for each season of the year, are also specified.

For SOARCA, a structured Monte-Carlo sampling method was employed for weather sampling. This was done by random selection of a user-specified number of weather sequences (i.e., start times) from the set of sequences assigned to each user-specified weather category. This begins by sorting an annual weather file according to user specified criteria. Each MACCS analysis uses a user-specified random seed. This random seed was kept constant for all MACCS analysis and thus the same weather trials from the same meteorological data file were selected for all of the analyses.

Section 6.4.5 discusses a sensitivity study conducted to determine the overall effect of using all 8760 hours of weather data (i.e., one year of hourly weather data) for each of the dose-response models (LNT, USBGR, and HPS), versus the trials used in SOARCA. In SOARCA, the aleatory uncertainties due to weather were characterized in terms of mean values. However, a CCDF of aleatory uncertainties can be obtained using a single MACCS analysis for each source term. A set of sensitivity analyses to evaluate the aleatory weather uncertainty using the SOARCA weather sampling technique is also presented in Section 6.4.5 for the LNT, USBGR, and HPS dose-response models.

5. STATISTICAL CONVERGENCE

5.1 Source Term Model (MELCOR)

The results presented in this uncertainty analysis (Section 6.0) were generated with an updated version of the MELCOR SOARCA Peach Bottom unmitigated LTSBO model that included all of the changes discussed in Appendix C. The updated version addresses issues identified during the development of the probabilistic analysis that impacted the ability to achieve probabilistic model convergence.

5.1.1 Statistical Convergence Testing (Probabilistic Base Case)

Statistical convergence testing demonstrates that a sufficient number of stochastic realizations have been generated to achieve a numerically converged mean, including: (1) determining confidence intervals (based on the successful MELCOR calculations) around the mean and percentiles for the combined case and each replicate; and (2) demonstrating numerical accuracy of the mean by comparing the results of the three sets of 300 realizations with a combined 900 realizations.

The three replicate sets (STP08, STP09, and STP10) each consist of 300 distinct MELCOR simulations. A successful MELCOR calculation is defined by the simulation progressing to 48 hours after scram, which is the truncation time of each calculation. Each replicate exhibits a unique success rate from the MELCOR code, as shown in Table 5.1-1. The success rates from MELCOR for STP08, STP09, and STP10 are 94.7%, 96.7%, and 97.0%, respectively. Thus about 4% of the total MELCOR simulations do not successfully reach 48 hours.

Table 5.1-1 Success rates of MELCOR simulations for STP08, STP09, and STP10

Replicate	Rep. #	Number of successful simulations	Number of aborted simulations	Success rate
STP08	1	284	16	94.7%
STP09	2	290	10	96.7%
STP10	3	291	9	97.0%
Total		865	35	96.1%

The 35 simulations that were not run to completion were caused primarily by non-convergence issues detected in the MELCOR code, related to the time-step scheme used to progress the system transient via the governing equations in MELCOR. Occasional non-convergence issues are to be expected when executing hundreds of MELCOR simulations, especially for uncertainty analyses in which variations in model input alter the progression of the core and vessel degradation, which are the most computationally intensive portions of the simulation. These detected non-convergent simulations should not be confused with run-time errors, which occur when the code fails due to unexpected reasons; run-time errors do not catch the code fault and thus cannot report the nature of the error to the user.

Most of the MELCOR failures are due to thermal-hydraulic convergence issues in the core region during core material relocation. Table 5.1-2 provides a summary of the MELCOR errors encountered by the 35 failed simulations. MELCOR convergence issues can usually be resolved by restarting the simulation before the onset of instabilities that lead to the fatal errors,

and continuing the transient using smaller time-steps as specified by the refined user input. However, manual restarts were not attempted for the 35 failed simulations. The replicates were executed on a computer cluster in an automated fashion, and the 865 successful simulations were deemed to be a sufficient sample size for the statistical analyses.

Table 5.1-2 MELCOR error summary for STP08, STP09, STP10

Error description	Number of occurrences
Thermal-hydraulic convergence error in core region	24
Core materials eutectics error (component mass less than zero)	3
Cavity convergence error	3
Radionuclide package: conductivity calculation error for gas mixture	2
Core geometry error: surface area calculation during core relocation	1
Core debris temperature convergence error in lower plenum	1
Core temperature convergence error during core relocation	1
Total	35

A regression analysis has been performed as described in Section 3.4.2 using all 900 input sets on an indicator function that was set to one if the realization converged and equal to zero if it did not. The resulting regressions show no significant correlation between any input variable and the indicator function, giving more confidence that disregarding the non-convergent realizations should not affect the parameter uncertainty analyses presented in Section 6.0. The only correlation found was with the (unsampled) parameter RRDOOR, which indicates whether railroad doors are open (=1) or closed (=0). This correlation is not surprising as most (~88%) of the converged realizations lead to open railroad doors. 30 of the 35 non-converged results happen in the core calculation *before* the railroad doors have a chance to open and does not affect the railroad doors. Therefore, this correlation between railroad doors and convergence is a numerical artifact and does not reflect any bias in the distributions.

Statistical convergence was evaluated by a replicated sampling procedure. Three independent Monte Carlo sample sets of epistemic uncertain parameters were generated using 300 samples each. As explained in Section 3.4, the simple random sampling (SRS) procedure was preferred to LHS as it preserves validity of the sample even in a case of unfinished realizations, as long as the failed realizations do not bias the results. Each sample was used to generate three estimates of mean fraction of cesium and iodine core inventory released to the environment. Other statistics (median, quantiles values $q = 0.05$ and $q = 0.95$) were also estimated to test for convergence of the output distributions in a more general context. Since all three replicates have been generated with SRS, it is appropriate to combine them and estimate confidence intervals over the mean and selected quantiles using a bootstrap approach, as described below.

To estimate convergence of these statistics, a bootstrap resampling technique was used to generate 1,000 sample sets, each of size 300, from the pool of 865 results available (the non-convergent results were subtracted from the total of 900 runs). From the generated distributions of statistics, a mean value and 0.90 confidence interval (using quantiles $q = 5\%$ and $q = 95\%$) have been estimated. The results are displayed on Figure 5.1-1 (cesium) and Figure 5.1-2 (iodine) for mean and median as well as 5th and 95th percentiles. The true value of the mean and quantiles displayed will be within the confidence interval with a confidence of 95%.

Comparison of these estimates, and the associated distributions of uncertainty, showed that the three independent sample sets produced statistically similar values, as well as similar distributions of uncertainty in the results. The 95th percentile results are more spread out, but remain in an appropriate range (within 20% of the bootstrap mean). A sample size of 300 was, therefore, considered adequate within the scope of the current analysis.

The results of the analysis are statistically converged. Moreover, the similarity between the three replicates demonstrates that performance could be evaluated using any one of the replicates. However, considering that greater accuracy will be obtained by using a larger sample size, and due to the fact that results will be segregated into three failure modes for independent analysis (SRV stochastic, SRV Thermal and MSL Creep rupture), a combined sample was used for the uncertainty analysis presented in Section 6 of this report.

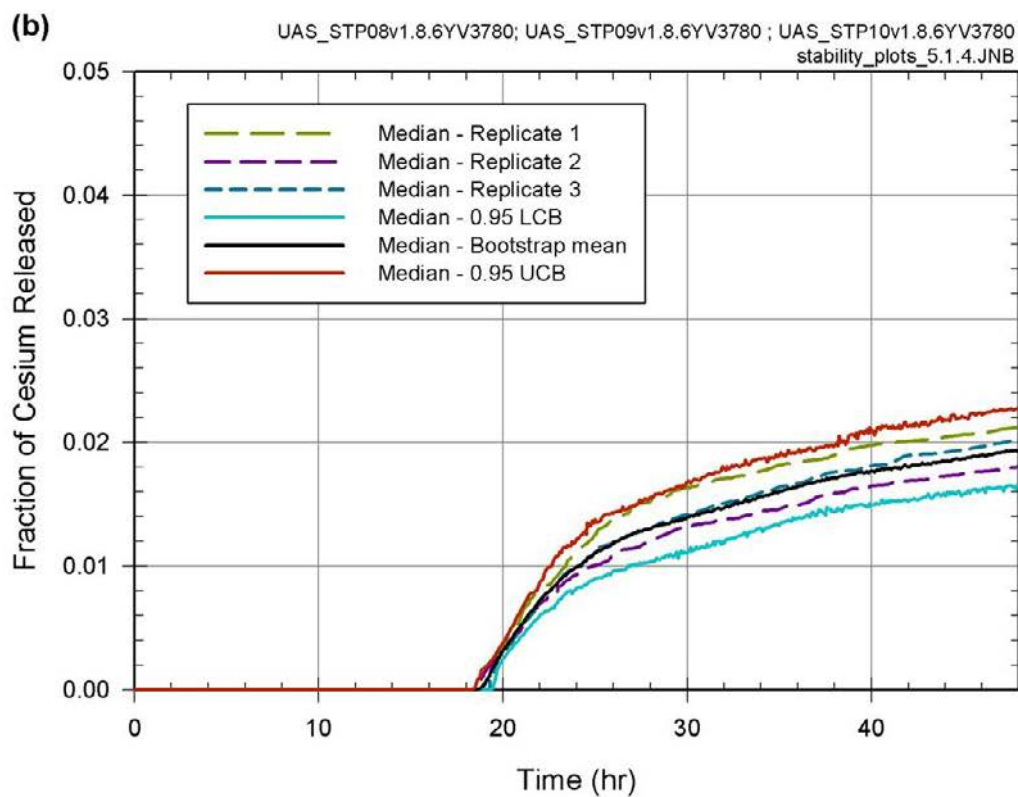
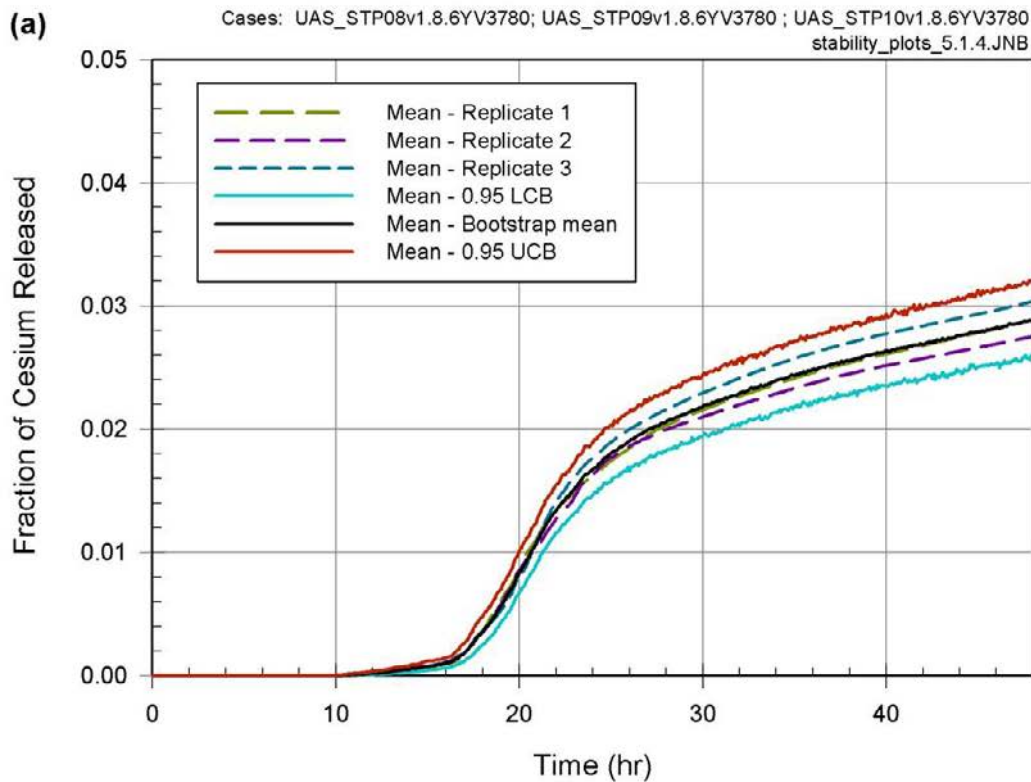


Figure 5.1-1 Results of three replicates and $q = 0.95$ confidence interval (using bootstrap resampling) over selected statistics for released fraction of Cesium: (a) mean, (b) median, (c) quantile $q = 0.05$ and (d) quantile $q = 0.95$

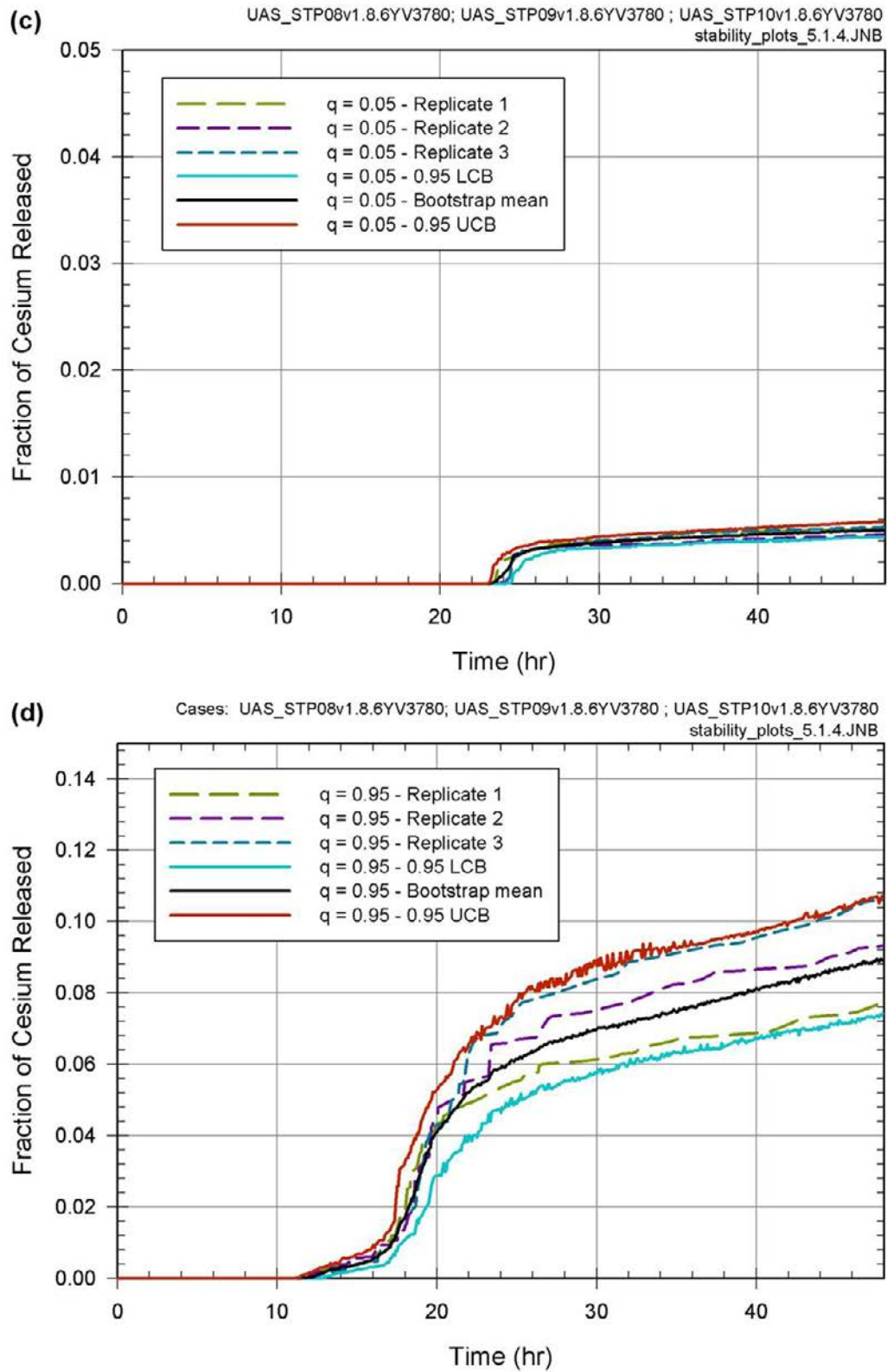


Figure 5.1-1 Results of three replicates and $q = 0.95$ confidence interval (using bootstrap resampling) over selected statistics for released fraction of Cesium: (a) mean, (b) median, (c) quantile $q = 0.05$ and (d) quantile $q = 0.95$ (continued)

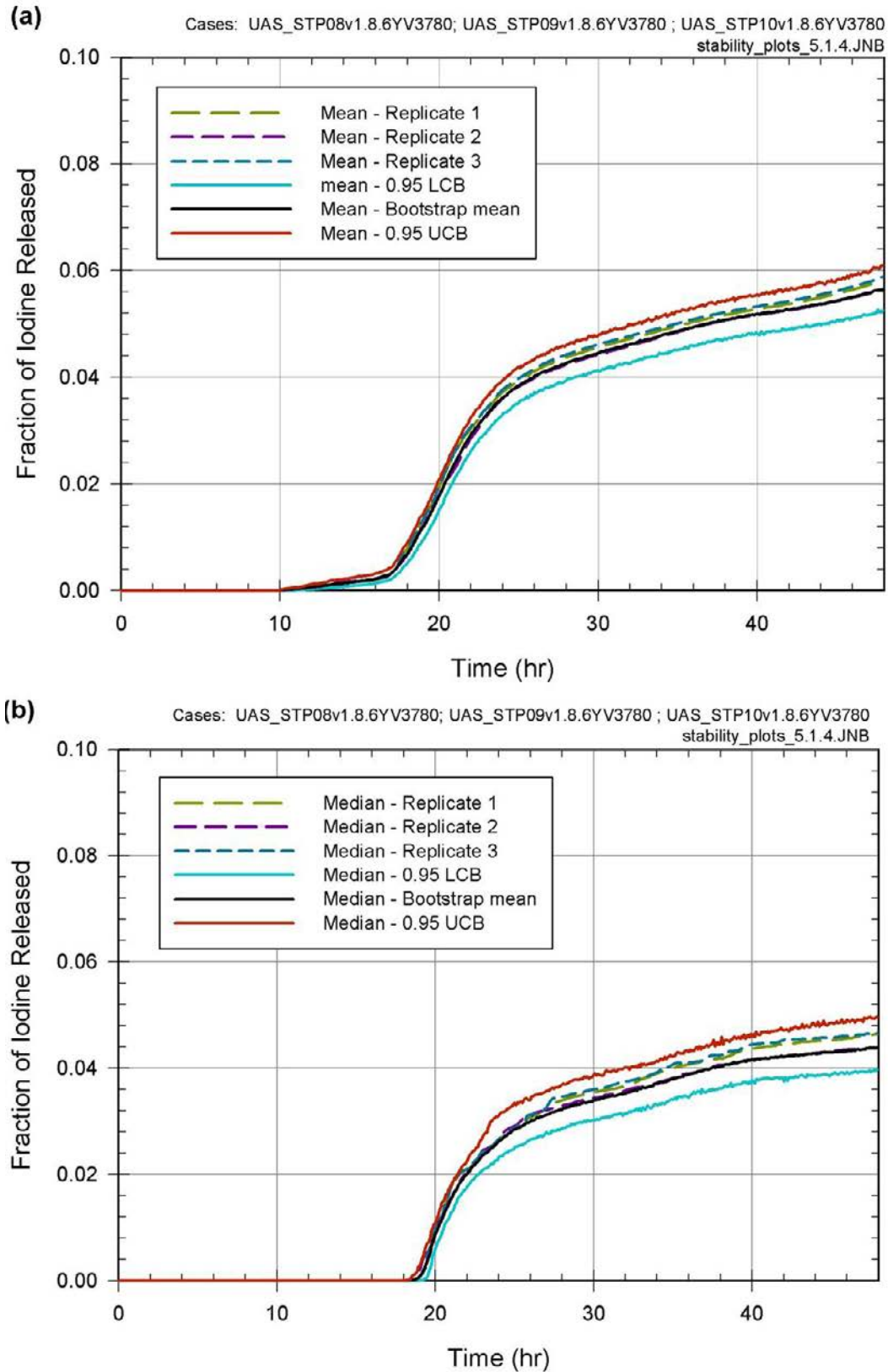


Figure 5.1-2 Results of three replicates and $q = 0.95$ confidence interval (using bootstrap resampling) over selected statistics for released fraction of iodine: (a) mean, (b) median, (c) quantile $q = 0.05$ and (d) quantile $q = 0.95$

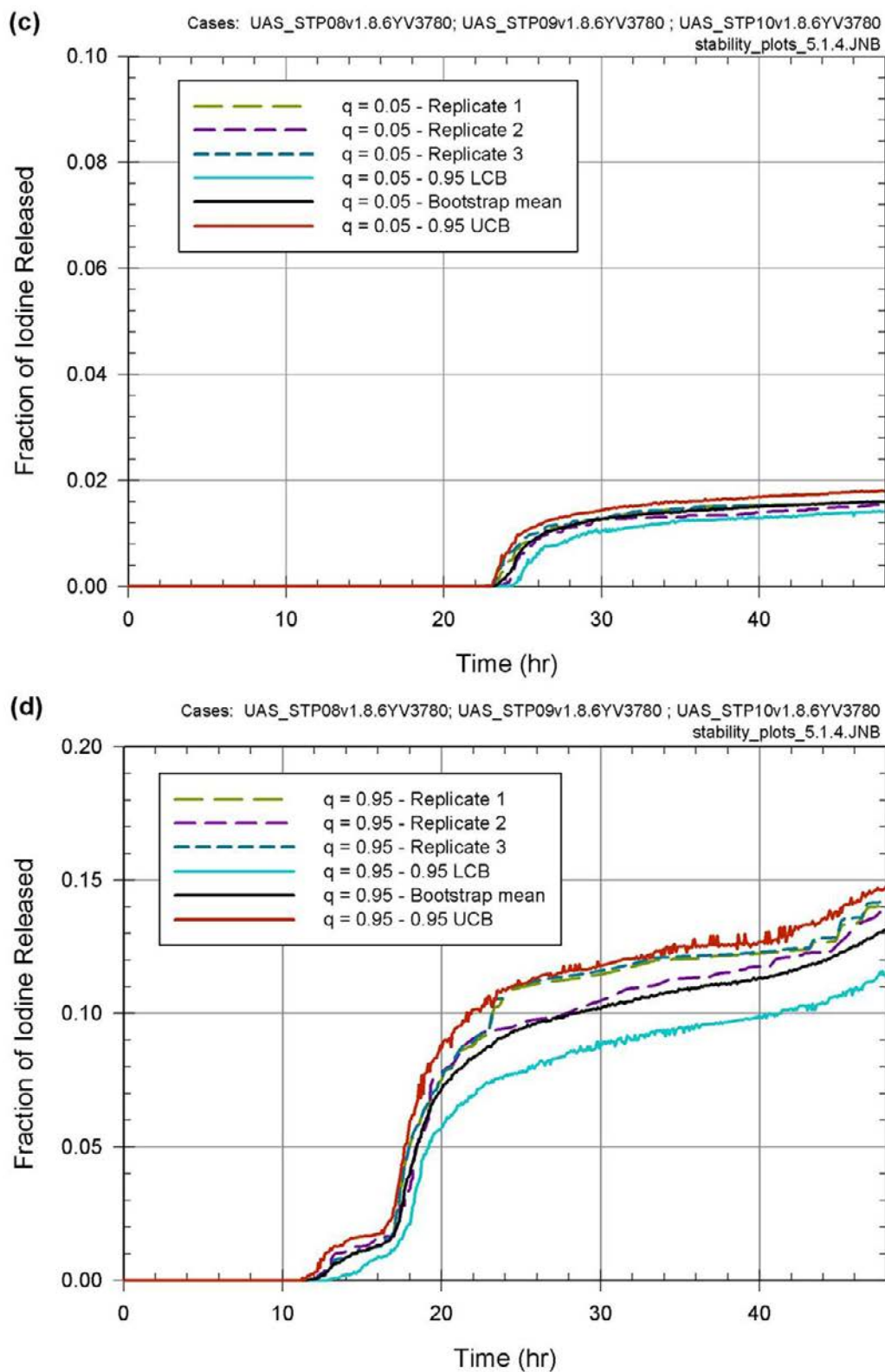


Figure 5.1-2 Results of three replicates and $q = 0.95$ confidence interval (using bootstrap resampling) over selected statistics for released fraction of iodine: (a) mean, (b) median, (c) quantile $q = 0.05$ and (d) quantile $q = 0.95$ (continued)

5.2 Consequence Model

SOARCA uncertainty analysis results presented in Section 6.0 include the updated SOARCA source term presented in Section 5.1 and documented in Appendix C combined with the current version of WinMACCS/MACCS as discussed in Section 3.1.3 and documented in Appendix C.

5.2.1 Statistical Convergence Testing - Probabilistic Base Case

This section discusses the LCF risks per event and the early-fatality risks per event using all the MACCS uncertainty parameters discussed in Section 4.2 with the 284 MELCOR source terms STP08, the first of the three replicates of the uncertainty model. This section also discusses the reduction in inhalation dose conversion factors previously discussed in Section 4.2.5. The convergence testing of MACCS was determined with a reduced LHS statistical sampling technique using all three MELCOR source terms developed from Section 5.1.1 (i.e., MELCOR results from the three replicates of the uncertainty model). All results discussed in this section use the LNT dose-response model. Uncertainty analyses of the dose truncation models are discussed in Section 6.4.3.

5.2.1.1 Latent Cancer Fatality Risk

To investigate the uncertain parameters discussed in Section 4.2, an initial MACCS analysis was conducted using all 598 uncertain input variables. A MACCS cyclical file set was created for the 284 MELCOR source terms developed from the work discussed in Section 5.1.1 (i.e., STP08, the MELCOR results from the first of the three replicates of the uncertainty model). In this section, the risk tables represent rounded values obtained from the full data sets. The plots were developed from the full data sets and slight differences may be noticed due to this rounding.

Table 5.2-1 displays the basic statistics for the conditional, mean, individual LCF risk (per event) for the LNT dose model. The maximum LCF risk results shown in Table 5.2-1 are not the same for the 10-mile (i.e., MELCOR source term Realization 133) and the 20-mile (i.e., MELCOR source term Realization 77) circular areas. None of the circular areas have the same ordered sequence from largest to smallest LCF risk per event results.

Table 5.2-1 Conditional, mean, individual LCF risk (per event) basic statistics for the LNT dose model at specified circular areas

	0-10 miles	0-20 miles	0-30 miles	0-40 miles	0-50 miles
Mean	1.7×10^{-4}	2.7×10^{-4}	1.9×10^{-4}	1.2×10^{-4}	1.0×10^{-4}
Standard Error	7.7×10^{-6}	1.6×10^{-5}	1.1×10^{-5}	7.1×10^{-6}	5.7×10^{-6}
Median	1.4×10^{-4}	2.1×10^{-4}	1.5×10^{-4}	9.3×10^{-5}	7.7×10^{-5}
Mode	1.2×10^{-4}	1.2×10^{-4}	1.1×10^{-4}	1.2×10^{-4}	1.0×10^{-4}
Standard Deviation	1.3×10^{-4}	2.7×10^{-4}	1.9×10^{-4}	1.2×10^{-4}	9.6×10^{-5}
Sample Variance	1.7×10^{-8}	7.5×10^{-8}	3.7×10^{-8}	1.4×10^{-8}	9.2×10^{-9}
Minimum	1.3×10^{-5}	1.7×10^{-5}	1.2×10^{-5}	7.4×10^{-6}	6.1×10^{-6}
Maximum	8.6×10^{-4}	3.1×10^{-3}	2.2×10^{-3}	1.3×10^{-3}	1.1×10^{-3}
Confidence Level (95.0%)	1.5×10^{-5}	3.2×10^{-5}	2.2×10^{-5}	1.4×10^{-5}	1.1×10^{-5}

Table 5.2-2 shows where the results for the SOARCA uncertainty analysis base case source term determined in Appendix C with respect to the results within the distribution of this probabilistic case for conditional, mean, individual LCF risk (per event) for the LNT dose-response model. From Table 5.2-2, the risk for the 10-mile circular area corresponds to a higher percentile compared to the other SOARCA uncertainty analysis base case circular areas due to the influence of the uncertain evacuation parameters on the relative timing of evacuation compared with the release.

Figure 5.2-1 shows the results for each of the conditional, mean, individual LCF risk (per event) for all 284 MELCOR source terms in STP08 with 598 uncertain MACCS input variables. The rank order for each specified circular area on Figure 5.2-1 is ranked from the highest LCF risk result to the lowest result. None of the specified circular areas have the same ordered sequence. The black dots represent the SOARCA uncertainty analysis base case results. The overall LCF risk for any circular area is small. The highest absolute LCF risk is 1.0×10^{-8} pry (i.e., recall the Peach Bottom LTSBO core damage frequency is 3×10^{-6} pry) at 20 miles.

Table 5.2-2 Conditional, mean, Individual LCF risk (per event) basic from the SOARCA UA base case for the LNT dose model at specified circular areas

SOARCA UA Base Case radius of circular area (mi)	Conditional, mean, individual LCF risk (per event) for the LNT dose model	Percentile
10	9.0×10^{-5}	30 th
20	8.3×10^{-5}	12 th
30	5.8×10^{-5}	12 th
40	3.7×10^{-5}	11 th
50	3.0×10^{-5}	11 th

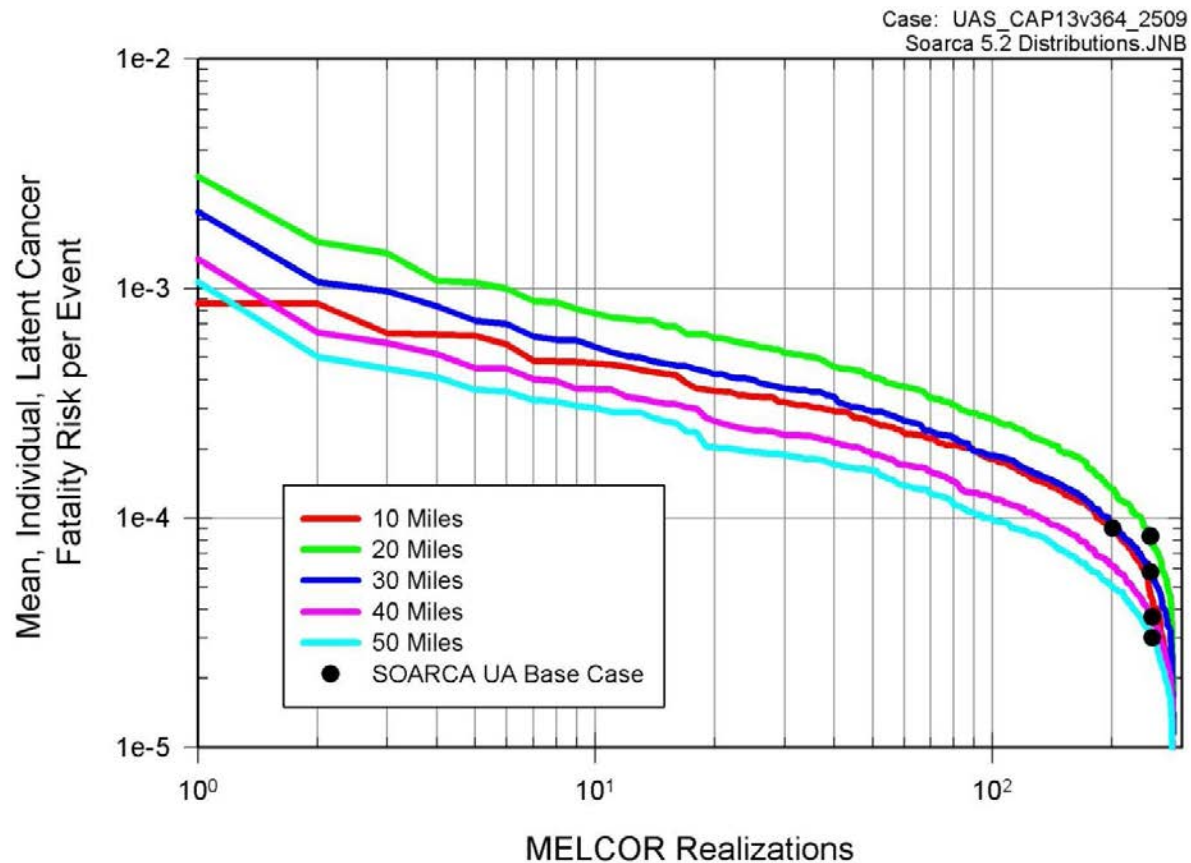


Figure 5.2-1 Conditional, mean, individual LCF risk (per event) for all distances with the LNT dose model for emergency and long-term phases ranked from highest to lowest LCF risk result

Figure 5.2-2 shows the CCDF for the conditional mean, individual LCF risk (per event) contribution for both emergency and long-term phases for the specified circular areas. Since most people evacuate (99.5%) within the 10-mile EPZ, the LCF risk results from the long-term exposure are mostly based on the return criteria. For larger circular areas, the majority of the LCF risk is contributed from the emergency-phase for approximately 165 MELCOR realizations (i.e., the emergency-phase LCF risk accounts for $\geq 50\%$ of the overall LCF risk) but this number decreases with circular area (i.e., from 166 MELCOR realizations at 20 miles to 136 MELCOR realizations at 50 miles have the emergency phase LCF risk account for $\geq 50\%$ of the overall LCF risk).

On Figure 5.2-2, the x-axis represents the distribution of possible LCF risk per event results within the 10-mile circular area and is generated by sorting (from smallest to largest) all the LCF risk results from the sample of size 'N' (i.e., $N=284$ samples for Figure 5.2-2). On Figure 5.2-2, the y-axis represents the likelihood of being higher or equal than the value read on the x-axis. When LHS is used, the likelihood of the outcome is estimated by a weight of $1/N$ and decreasing the y-value by this weight starting from one. The mean can be added on the curve (i.e., a dot for Figure 5.2-2) to the CCDF. Quantiles can be read directly by finding the corresponding y-value to the graph, or displayed for a selected quantile as a dot over the curve.

In risk analysis, it is traditional to plot CCDFs rather than CDFs as a CCDF answers the question, "How likely it is to have such value or higher?"

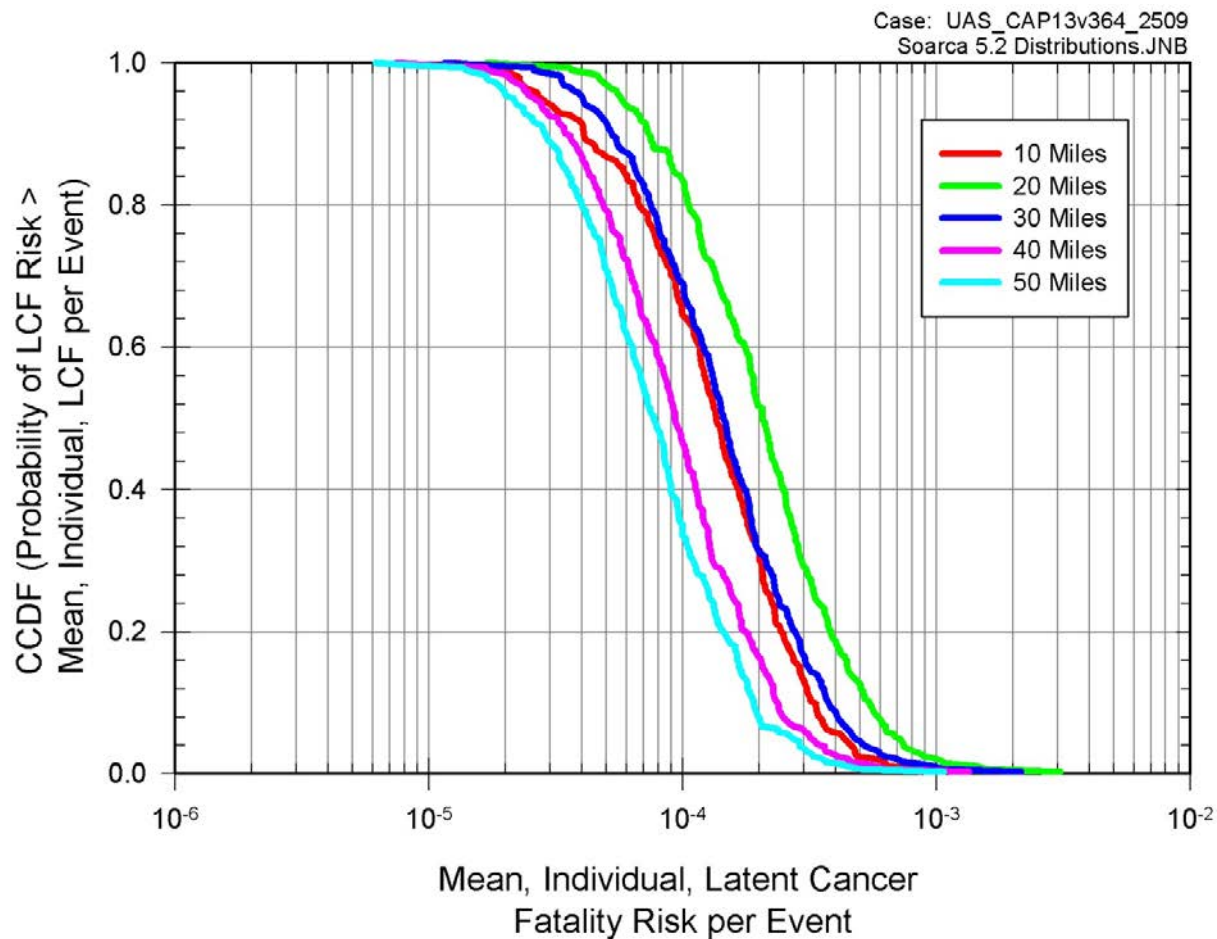


Figure 5.2-2 Complementary cumulative distribution function for conditional, mean, individual LCF risk (per event) for the MACCS Convergence Analysis for specified circular areas

5.2.1.2 Early-Fatality Risk

The NRC quantitative health objective (QHO) [58, 59] for prompt fatalities (5×10^{-7} pry) is generally interpreted as the absolute risk within one mile of the exclusion area boundary (EAB), so that distance is used as a useful indicator in this study as well. The only SOARCA scenario for which the risk of early fatalities is not zero is the Surry ISLOCA (i.e., discussed in NUREG/CR-7110 Volume 2, Section 7.3.5). For Surry, the EAB is 0.35 miles from the reactor building from which release occurs, so the outer boundary of the one-mile zone is at 1.35 miles. The closest MACCS grid boundary to 1.35 miles used in the ISLOCA calculations is at 1.3 miles. Using the risk at 1.3 miles is considered a reasonable approximation to the risk within one mile of the EAB. Table 5.2-3 shows the conditional, mean, mean early-fatality risk (per event) for the Surry ISLOCA scenario. The core damage frequency for this event is 3×10^{-8} pry. Thus, the absolute early-fatality risk within one mile of the EAB is 4.5×10^{-14} pry.

Table 5.2-3 Conditional, mean, individual early-fatality risk (per event) for the Surry ISLOCA Scenario

Radius of circular area (mi)	Early-fatality risk (per event)
1.3	1.5×10^{-6}
2.0	6.4×10^{-7}
2.5	4.0×10^{-7}

For Peach Bottom, the EAB is 0.5 mile from the reactor building from which release occurs, so the outer boundary of this one mile zone is at 1.5 miles. The closest MACCS grid boundary to 1.5 miles used in this set of calculations is at 1.3 miles. Evaluating the risk within 1.3 miles is considered a reasonable, but slightly conservative, approximation to the risk within 1 mile of the EAB. In the SOARCA study, the Peach Bottom LTSBO scenario has a conditional, mean, individual early-fatality risk (per event) of 0.00 (NUREG/CR-7110 Volume 1, Section 7.3.1).

Table 5.2-4 displays the basic statistics for the conditional, mean, individual early-fatality risk (per event) at specified circular areas for the 284 MELCOR source terms developed from the discussion in Section 5.1 (i.e., the MELCOR STP08 uncertainty model). The realization with the peak MACCS results shown in Table 5.2-4 is the same for the 1.3-mile to 2.5-mile circular areas (i.e., MELCOR STP08 source term Realization 238). The 3-mile to 10-mile circular areas have the same peak MACCS result (i.e., MELCOR STP08 source term Realization 91). The 10-mile distance has only two scenarios where early fatalities occur (i.e., MELCOR STP08 source term Realization 91 and 134). In each of these realizations, there is a specific weather trial corresponding to the peak dose which produces the early-fatality risk at the 10-mile circular area.

Table 5.2-4 Conditional, mean, individual early-fatality risk (per event) basic statistics

	1.3 miles	2 miles	2.5 miles	3 miles	3.5 miles	5 miles	7 miles	10 miles
Mean	4.6×10^{-7}	1.6×10^{-7}	8.3×10^{-8}	5.8×10^{-8}	2.4×10^{-8}	5.7×10^{-9}	2.4×10^{-9}	1.0×10^{-9}
Standard Error	1.5×10^{-7}	5.0×10^{-8}	3.3×10^{-8}	2.3×10^{-8}	1.1×10^{-8}	3.8×10^{-9}	1.8×10^{-9}	7.9×10^{-10}
Median	0	0	0	0	0	0	0	0
Mode	0	0	0	0	0	0	0	0
Standard Deviation	2.5×10^{-6}	8.4×10^{-7}	5.5×10^{-7}	3.9×10^{-7}	1.8×10^{-7}	6.4×10^{-8}	3.0×10^{-8}	1.3×10^{-8}
Sample Variance	6.2×10^{-12}	7.1×10^{-13}	3.0×10^{-13}	1.5×10^{-13}	3.4×10^{-14}	4.1×10^{-15}	9.3×10^{-16}	1.8×10^{-16}
Minimum	0	0	0	0	0	0	0	0
Maximum	3.2×10^{-5}	9.9×10^{-6}	6.1×10^{-6}	4.3×10^{-6}	2.7×10^{-6}	1.0×10^{-6}	4.7×10^{-7}	2.1×10^{-7}
Confidence Level (95%)	2.9×10^{-7}	9.8×10^{-8}	6.4×10^{-8}	4.5×10^{-8}	2.1×10^{-8}	7.5×10^{-9}	3.6×10^{-9}	1.6×10^{-9}

From Table 5.2-4 the grand mean, individual early-fatality per event (i.e., the mean value of the conditional, mean, individual early-fatality risk (per event)) for the 1.3-mile circular area is less than the SOARCA ISLOCA result. The maximum early-fatality risk per event result for the 1.3-mile circular area is on the same order of magnitude to the SOARCA Uncertainty Analysis Base Case mean LCF risk per event result (i.e., 9.0×10^{-5} LCF risk per event – Appendix C) at 10 miles.

Figure 5.2-3 provides the CCDF results for the conditional, mean, individual early-fatality risk (per event) for specified circular areas. Figure 5.2-3 shows only those early-fatality risks that are nonzero. The 7-mile and 10-mile circular area have only two nonzero early-fatality risk. The early-fatality risk for any circular area is small. The highest absolute early-fatality risk is 9.7×10^{-11} pry (i.e., recall the Peach Bottom LTSBO core damage frequency is 3×10^{-6} pry) at 1.3 miles. There are approximately 265 MACCS realizations less than 1.0×10^{-6} early-fatality risk per event for all circular areas. There are approximately 250 MACCS realizations which have a zero early-fatality risk at all distances (i.e., ~88% of all MACCS realizations result in a zero early-fatality risk per event at all specified circular areas). There is no early-fatality risk for the cohorts that evacuate.

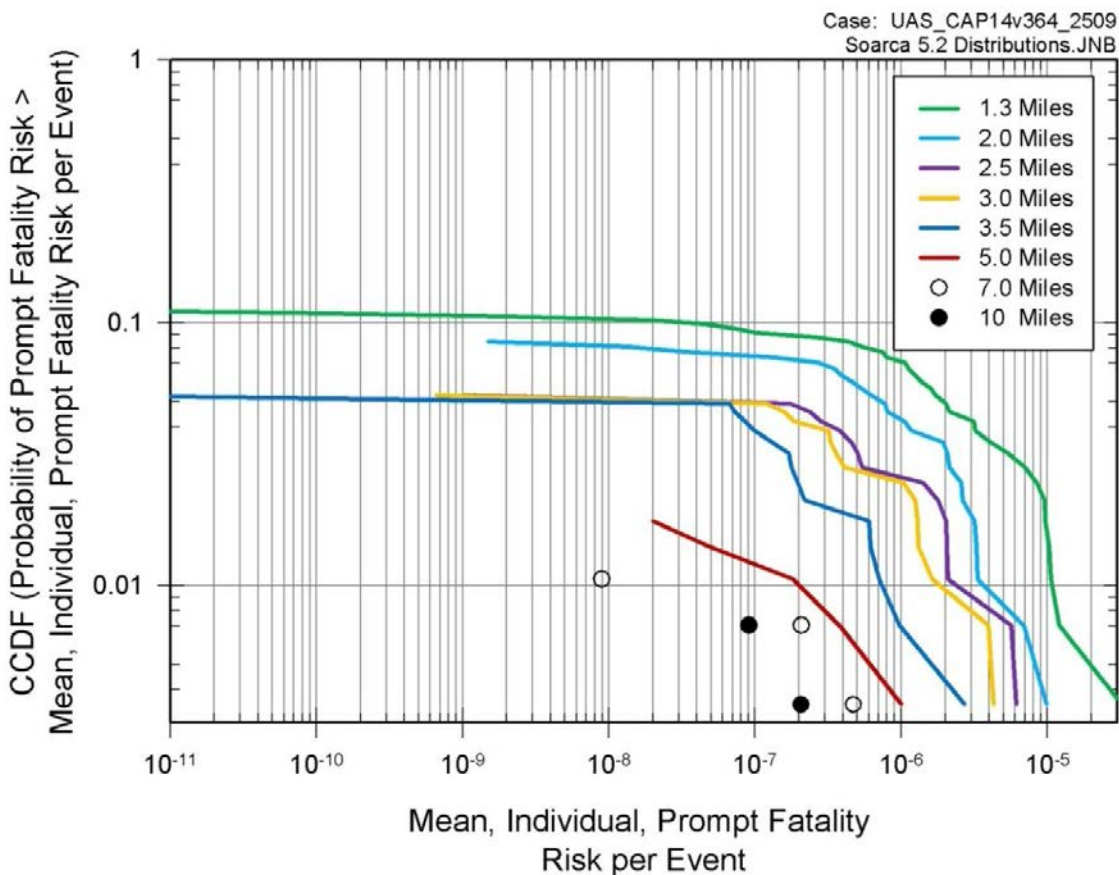


Figure 5.2-3 Complementary cumulative distribution function for conditional, mean, individual early-fatality risk (per event) for the MACCS Convergence Analysis for specified circular areas

Originally, 58 radionuclides that were treated in this analysis were selected to have uncertainty distributions for their long-term inhalation DCFs (see Section 4.2.5). However, it was determined that nearly half of the uncertainty resulted from a subset of 27 radionuclides. This reduces the set of uncertain parameters from 598 input variables to 350 input variables, not including the source term input parameters calculated by MELCOR.

The reduction from 58 to 27 radionuclides was determined by selecting the radionuclides that collectively contribute at least 99% of the 'effective' long-term inhalation dose based on the first replicate MELCOR source terms developed from the discussion in Section 5.1 (i.e., the STP08 uncertainty model – Replicate 1) nearest the mean for LCF risk (Replicate 1 Realization 58 and Replicate 1 Realization 214), and the MELCOR source term for the SOARCA estimate. Based

on this analysis, it was determined that the MELCOR source term Replicate 1 Realization 58 from the MELCOR STP08 uncertainty model provided the best estimate of the radionuclides that contributed to at least 99% of the 'effective' inhalation dose. The radionuclides from the other source terms (i.e., Replicate 1 Realizations 214 and the SOARCA estimate) which were not included accounted for less than 2% of the 'effective' long-term inhalation dose for their respective source terms. Based on this reduction, the other 31 radionuclides had their respective long-term inhalation DCFs converted back to their default values used in NUREG/CR-7110 Volume 1. Table 5.2-5 shows the 27 radionuclides used for the probabilistic analyses discussed later in this section and in Section 6.0, and their 'effective' long-term inhalation dose contribution for the Replicate 1 Realization 58 source term.

Table 5.2-5 Radionuclide specific contribution to overall 'effective' inhalation dose

Nuclide	'Effective' Inhalation Dose Contribution
I-131	34.600%
I-133	14.475%
I-135	8.782%
Te-132	8.607%
Ce-144	6.099%
Sr-90	3.641%
Ba-140	3.303%
Pu-238	3.005%
Sr-89	1.952%
Pu-241	1.861%
Cs-134	1.571%
Np-239	1.446%
Nb-95	1.326%
Cs-137	1.138%
Te-129m	0.880%
Mo-99	0.808%
Zr-95	0.805%
I-132	0.647%
Ce-141	0.609%
Pu-239	0.605%
Te-131m	0.557%
I-134	0.508%
Pu-240	0.501%
Cm-242	0.425%
Sr-91	0.383%
Te-127m	0.278%
Sr-92	0.252%
Total	99.062%

5.2.1.3 MACCS Statistical Convergence – LCF Risk

In order to determine the overall statistical convergence of the MACCS results using the reduced set input variables, the three separate MELCOR uncertainty source terms discussed in Section 5.1 were used in separate MACCS uncertainty analyses to determine the CCDFs for the conditional, mean, individual LCF risk (per event). The three uncertainly MELCOR analyses produced 284 (STP08), 290 (STP09), and 291 (STP10) source terms, respectively. Each of these MELCOR source term sets were analyzed separately in MACCS using the same LHS sampling technique and the same sampled aleatory weather trials. However, since there are a different number of source terms for each MELCOR source term group, the LHS sampling is independent between the three MACCS analyses even with the same sampled aleatory weather trials. The STP08 MELCOR source term was analyzed and resulted in the MACCS CAP14 model. The STP09 MELCOR source term was analyzed and resulted in the MACCS CAP18 model. The STP10 MELCOR source term was analyzed and resulted in the MACCS CAP19 model.

Tables 5.2-6 through 5.2-9 show the conditional, mean, individual LCF risk (per event) average, standard error, lower bounding case and upper bounding case statistics for the three MACCS analyses combined at each specified circular area. Each statistic was determined over the epistemic uncertainties samples in the MACCS LHS uncertainty inputs using mean results over the weather trials representing aleatory uncertainty. A t-distribution was used to generate centered 95% confidence intervals (based on the lower 2.5 and upper 97.5th percentiles). Values for mean and selected quantiles have been displayed on the graph along with confidence intervals. The small number of replicates (3) used for the t-distribution generate large confidence intervals (reflecting the variability in the three replicates), and the position of the corresponding statistics provides a more reasonable indicator of stability in results. As a comparison, Table 5.2-6 also has the SOARCA Uncertainty Analysis base case conditional, mean, individual LCF risk (per event) results from Table C.2-1.

Table 5.2-6 Combined conditional, mean, individual LCF risk (per event) average statistics for the MACCS statistical convergence test for specified circular areas

	0-10 miles	0-20 miles	0-30 miles	0-40 miles	0-50 miles
Mean	1.6x10 ⁻⁴	2.9x10 ⁻⁴	2.0x10 ⁻⁴	1.3x10 ⁻⁴	1.1x10 ⁻⁴
Median	1.3x10 ⁻⁴	1.9x10 ⁻⁴	1.4x10 ⁻⁴	8.8x10 ⁻⁵	7.2x10 ⁻⁵
5th percentile	3.1x10 ⁻⁵	5.1x10 ⁻⁵	3.5x10 ⁻⁵	2.2x10 ⁻⁵	1.8x10 ⁻⁵
95th percentile	4.0x10 ⁻⁴	7.8x10 ⁻⁴	5.6x10 ⁻⁴	3.6x10 ⁻⁴	3.0x10 ⁻⁴
SOARCA UA Base Case	9.0x10 ⁻⁵	8.3x10 ⁻⁵	5.8x10 ⁻⁵	3.7x10 ⁻⁵	3.0x10 ⁻⁵

Table 5.2-7 Combined conditional, mean, individual LCF risk (per event) standard error statistics for the MACCS statistical convergence test for specified circular areas

	0-10 miles	0-20 miles	0-30 miles	0-40 miles	0-50 miles
Mean	4.4×10^{-6}	1.1×10^{-5}	7.2×10^{-6}	3.7×10^{-6}	2.7×10^{-6}
Median	4.5×10^{-6}	3.0×10^{-6}	2.8×10^{-6}	2.7×10^{-6}	2.6×10^{-6}
5 th percentile	4.5×10^{-6}	7.2×10^{-6}	5.5×10^{-6}	3.8×10^{-6}	2.9×10^{-6}
95 th percentile	1.5×10^{-5}	5.2×10^{-5}	3.5×10^{-5}	2.5×10^{-5}	3.0×10^{-5}

Table 5.2-8 Combined conditional, mean, individual LCF risk (per event) lower bounding case statistics for the MACCS statistical convergence test for specified circular areas

	0-10 miles	0-20 miles	0-30 miles	0-40 miles	0-50 miles
Mean	1.4×10^{-4}	3.4×10^{-4}	2.4×10^{-4}	1.5×10^{-4}	1.2×10^{-4}
Median	1.1×10^{-4}	2.0×10^{-4}	1.5×10^{-4}	9.9×10^{-5}	8.3×10^{-5}
5 th percentile	1.2×10^{-5}	8.2×10^{-5}	5.8×10^{-5}	3.9×10^{-5}	3.1×10^{-5}
95 th percentile	3.3×10^{-4}	1.0×10^{-3}	7.1×10^{-4}	4.7×10^{-4}	4.3×10^{-4}

Table 5.2-9 Combined conditional, mean, individual LCF risk (per event) upper bounding cases statistics for the MACCS statistical convergence test for specified circular areas

	0-10 miles	0-20 miles	0-30 miles	0-40 miles	0-50 miles
Mean	1.8×10^{-4}	3.4×10^{-4}	2.4×10^{-4}	1.5×10^{-4}	1.2×10^{-4}
Median	1.5×10^{-4}	2.0×10^{-4}	1.5×10^{-4}	9.9×10^{-5}	8.3×10^{-5}
5 th percentile	5.1×10^{-5}	8.2×10^{-5}	5.8×10^{-5}	3.9×10^{-5}	3.1×10^{-5}
95 th percentile	4.6×10^{-4}	1.0×10^{-3}	7.1×10^{-4}	4.7×10^{-4}	4.3×10^{-4}

As shown on Figure 5.2-4, the CCDFs for the three MACCS analyses for the conditional, mean, individual LCF risk (per event) are very similar and in good agreement for each analysis for the 10-mile EPZ. Also, Figure 5.2-4 shows a relatively small uncertainty within the 95th confidence interval between each analysis.

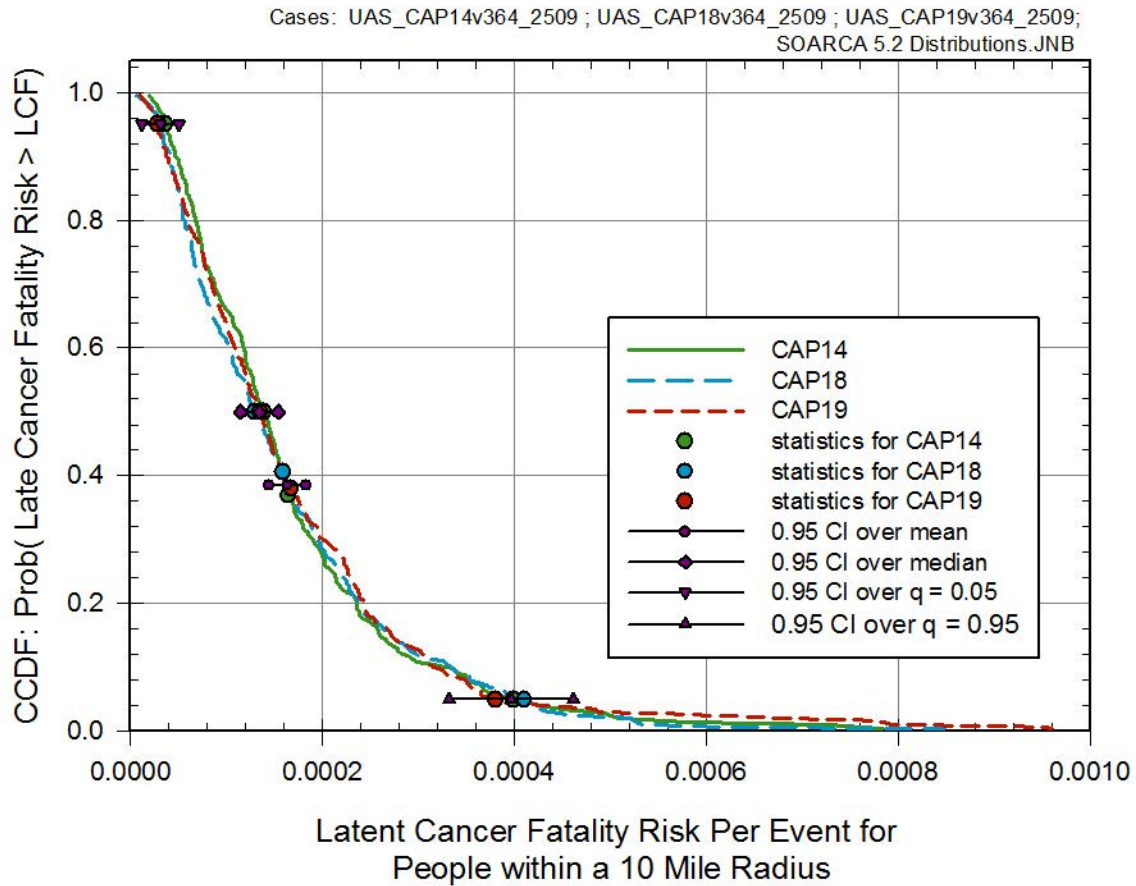


Figure 5.2-4 Complementary cumulative distribution function and statistical values for conditional, mean, individual LCF risk (per event) within a 10-mile radius for the MACCS Convergence Analysis

As shown on Figure 5.2-5, the CCDFs for the three MACCS analyses for conditional, mean, individual LCF risk (per event) are very similar and are in good agreement between each analysis for the 20-mile circular area. Also, Figure 5.2-5 shows a relatively small uncertainty within the 95th confidence interval between each analysis.

The CCDFs for the three MACCS analyses for the conditional, mean, individual LCF risk (per event) for the 30-mile, 40-mile, and 50-mile circular areas are shown on Figure 5.2-6 through Figure 5.2-8, respectively. The 30-mile, 40-mile and 50-mile circular areas show similar statistical results to those shown on Figure 5.2-5 for the MACCS convergence analysis for the 20 mile radius statistical data.

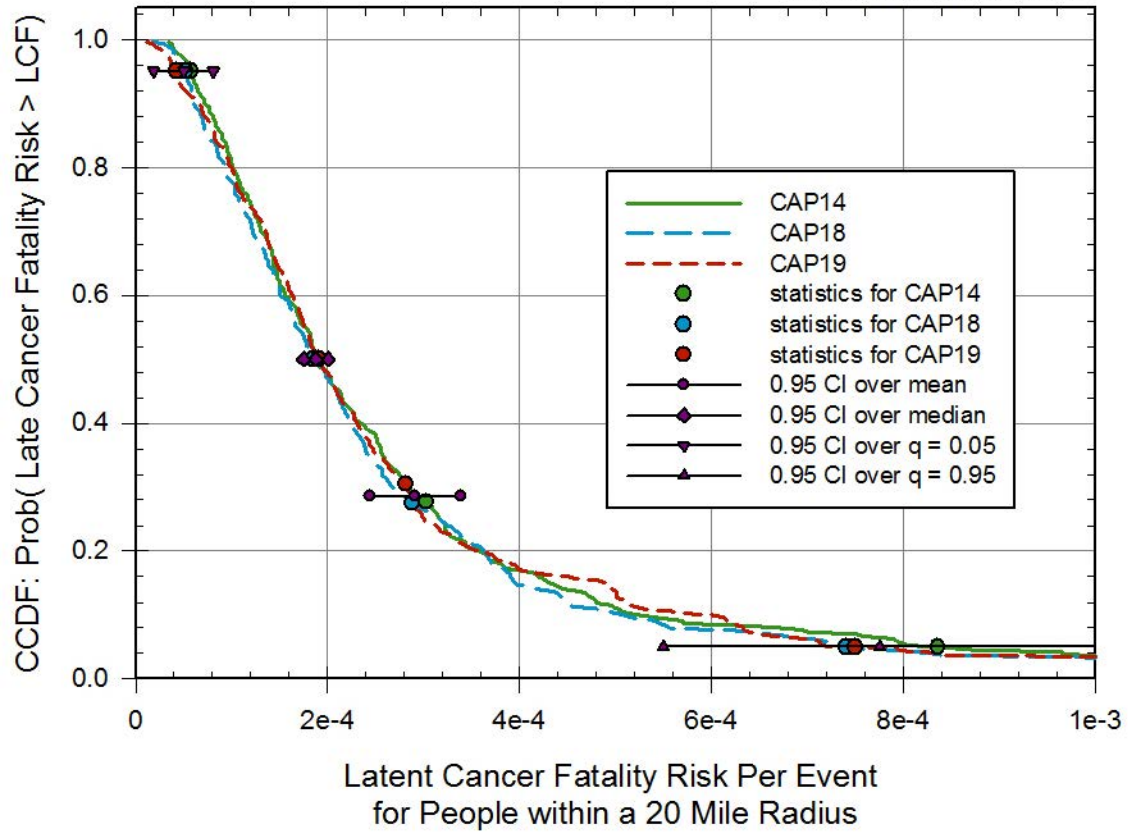


Figure 5.2-5 Complementary cumulative distribution function and statistical values for conditional, mean, individual LCF risk (per event) within a 20-mile radius for the MACCS Convergence Analysis

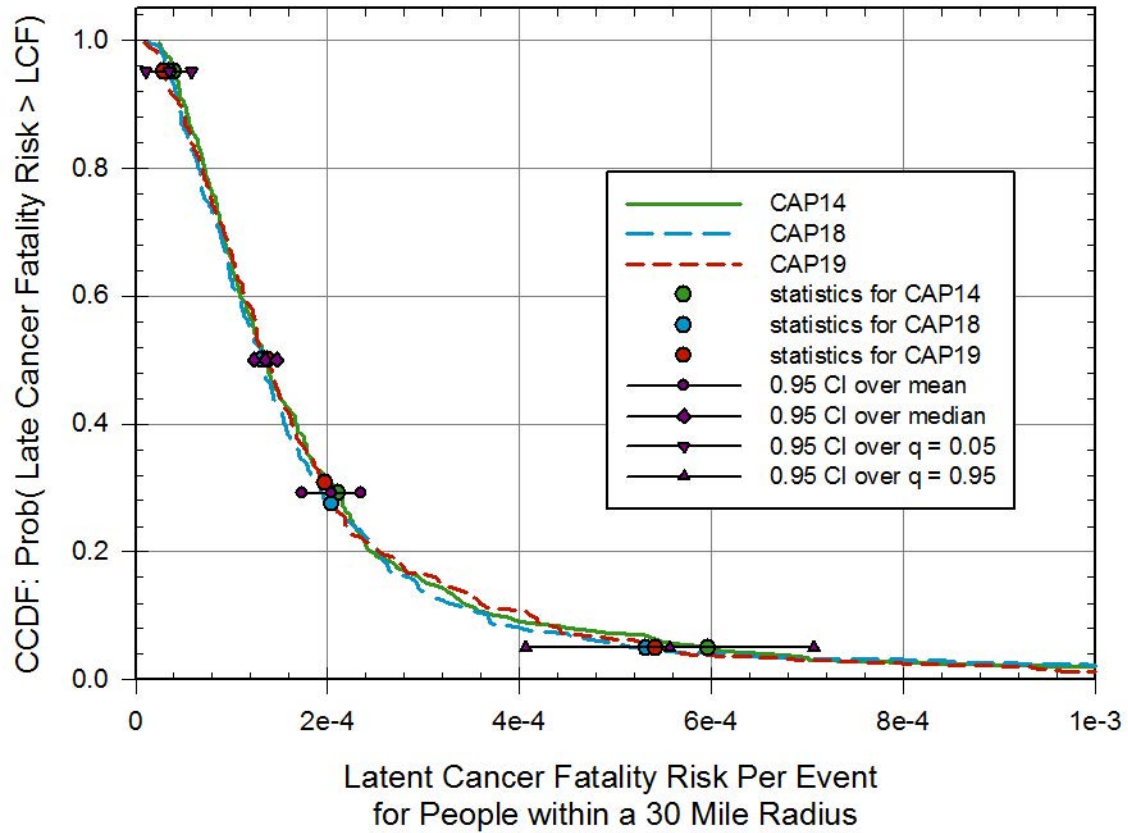


Figure 5.2-6 Complementary cumulative distribution function and statistical values for conditional, mean, individual LCF risk (per event) within a 30-mile radius for the MACCS Convergence Analysis

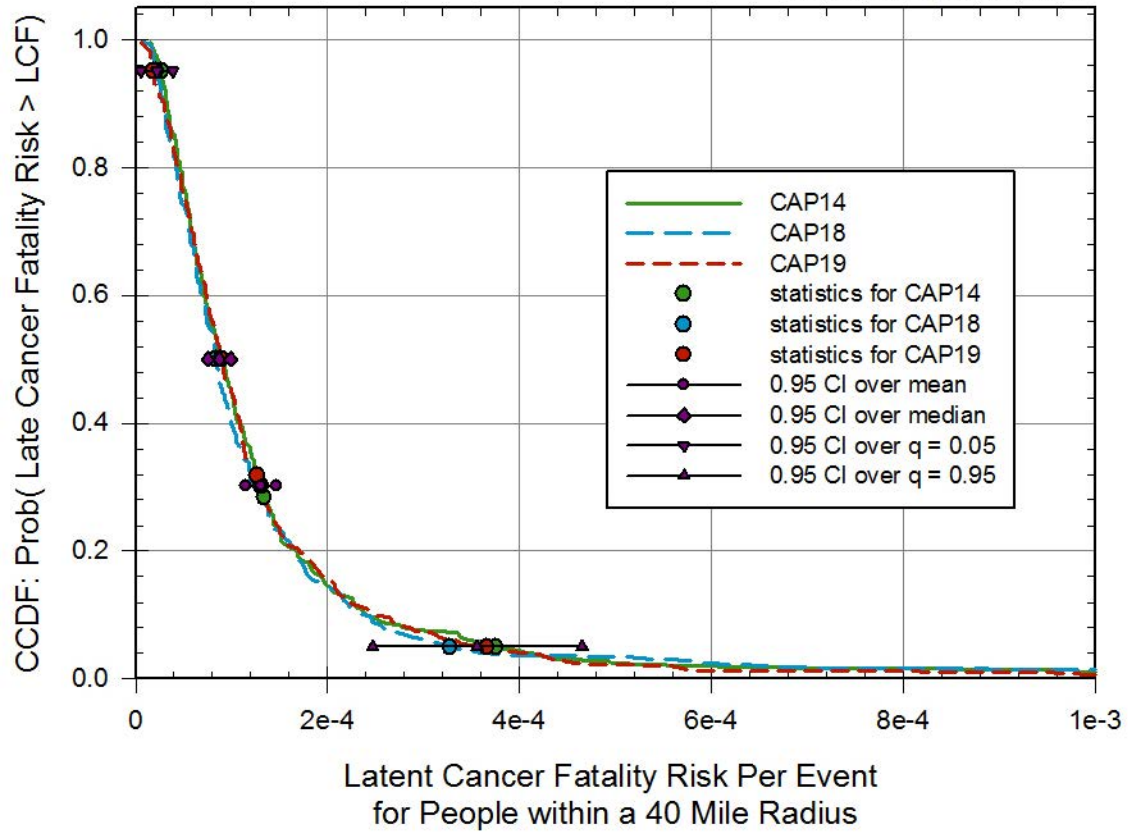


Figure 5.2-7 Complementary cumulative distribution function and statistical values for conditional, mean, individual LCF risk (per event) within a 40-mile radius for the MACCS Convergence Analysis

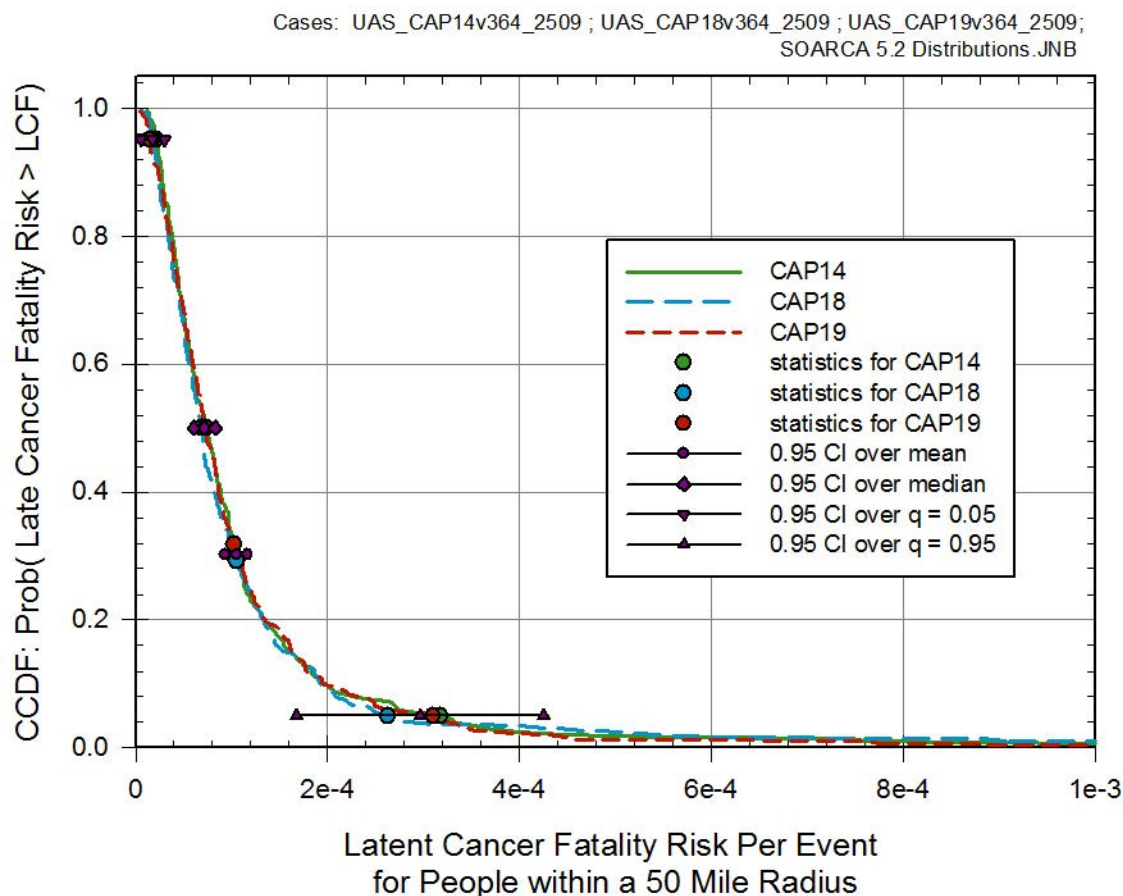


Figure 5.2-8 Complementary cumulative distribution function and statistical values for conditional, mean, individual LCF risk (per event) within a 50-mile radius for the MACCS Convergence Analysis

Tables 5.2-10 through 5.2-12 show the correlation matrix for all three MACCS analyses for the conditional, mean, individual LCF risk (per event) at specified circular areas. These tables indicate how strongly these MACCS results are correlated amongst each other when the radial distances change. The closer the correlation value is to 1.0, the more similar are the results. As an example, Table 5.2-10 indicates that while the conditional, mean, individual LCF risk (per event) for a radial distance of 10 miles is different than other radials distance (i.e., first row, correlation coefficient ranging from 0.31 to 0.42), the other radial distances lead to pretty similar results (i.e., coefficients of correlation greater than 0.99).

The correlation matrix between each of the circular areas outside the EPZ to the EPZ distance (i.e., 10 miles) shows that evacuation uncertainty parameters have a noticeable effect on the correlation. Additionally, the evacuation parameters affect the correlation in a similar fashion for all three MACCS analyses. At circular areas beyond the EPZ (i.e., 10 miles), the results are strongly correlated with regards to their respective MACCS input parameters. This is expected since there are no MACCS input parameters that would change and affect the correlation of a specific circular area beyond the EPZ with another circular area beyond the EPZ.

Table 5.2-10 Correlation matrix for the MELCOR STP08 Uncertainty Model Source Term MACCS Analysis for the conditional, mean, individual LCF risk (per event) for specified circular areas

	0-10 miles	0-20 miles	0-30 miles	0-40 miles	0-50 miles
0-10 miles	1	0.31	0.34	0.39	0.42
0-20 miles		1	0.998	0.993	0.99
0-30 miles			1	0.998	0.994
0-40 miles				1	0.999
0-50 miles					1

Table 5.2-11 Correlation matrix for the MELCOR STP09 Uncertainty Model Source Term MACCS Analysis for the conditional, mean, individual LCF risk (per event) for specified circular areas

	0-10 miles	0-20 miles	0-30 miles	0-40 miles	0-50 miles
0-10 miles	1	0.29	0.30	0.36	0.39
0-20 miles		1	0.998	0.99	0.98
0-30 miles			1	0.997	0.99
0-40 miles				1	0.999
0-50 miles					1

Table 5.2-12 Correlation matrix for the MELCOR STP10 Uncertainty Model Source Term MACCS Analysis for the conditional, mean, individual LCF risk (per event) for specified circular areas

	0-10 miles	0-20 miles	0-30 miles	0-40 miles	0-50 miles
0-10 miles	1	0.55	0.57	0.63	0.66
0-20 miles		1	0.998	0.99	0.98
0-30 miles			1	0.995	0.99
0-40 miles				1	0.999
0-50 miles					1

Based on these analyses, the conditional, mean, individual LCF risk (per event) are determined to be well converged for this uncertainty analysis. These analyses further verify the overall statistical convergence of the MACCS code when applying epistemic (e.g., radionuclide inhalation DCFs) and aleatory (e.g., weather trials) uncertainties.

5.2.1.4 MACCS Statistical Convergence – Early-Fatality Risk

To determine the overall statistical convergence of the MACCS results using the reduced set of input variables, the three separate sets of MELCOR source terms discussed in Section 5.1 were used in separate MACCS uncertainty analyses to determine the CCDFs for the conditional, mean, individual early-fatality risk (per event). The three MELCOR analyses produced 284 (STP08), 290 (STP09), and 291 (STP10) source terms, respectively. Each of these MELCOR source term sets were analyzed separately in MACCS using the same LHS sampling technique

and the same sampled aleatory weather trials. However, since there are a different number of source terms for each MELCOR source term group, the LHS sampling is independent between the three MACCS analyses even with the sampled aleatory weather trials. The STP08 MELCOR source term was analyzed and resulted in the MACCS CAP14 model. The STP09 MELCOR source term was analyzed and resulted in the MACCS CAP18 model. The STP10 MELCOR source term was analyzed and resulted in the MACCS CAP19 model.

Unlike the SOARCA analyses in NUREG/CR-7110 Volume 1 and Volume 2, early-fatality risk was observed beyond 2.5 miles (see Table 5.2-3). 0.9% of the 865 scenarios investigated (i.e., CAP14, CAP18, and CAP19) resulted in nonzero early-fatality risk out to 10 miles. A small number of realizations result in a large enough source term release that in combination with specific weather trials produce nonzero early-fatality risks out to the boundary of the EPZ. A more detailed discussion of the specific combination of inputs that produce early-fatality risks out to 10 miles is provided in Section 6.2.4.

Tables 5.2-13 through 5.2-16 show the conditional, mean, individual early-fatality risk (per event) mean, median, 75th percentile, and 95th percentile statistics which combined the results for all three MACCS analyses for each specified circular area. Each statistic was determined from the samples in the MACCS uncertainty inputs. A t-distribution was used to determine the 75th percentile and 95th confidence intervals. The 75th percentile was selected as a lower bounding case in this analysis since all results less than the 75th percentile are zero. At 2.5 miles and beyond in Table 5.2-13 the mean result is greater than the 95th percentile. This is due to the small number of nonzero data points (i.e., less than 5%) available at these distances and indicates an extremely skewed distribution. It is possible that the smallest nonzero values will be lower than the average of all values. In theory, a distribution can be skewed enough so that the mean is greater than the 95th percentile. An instance of this is an exponential of a value sample from a log-normal distribution. The mean will be higher than the 99th percentile, because it will be driven by those very rare but really high values. This is the same thing that happens here for early-fatality risk beyond 3.5 miles.

Table 5.2-13 Combined conditional, mean, individual early-fatality risk (per event) average statistics for the MACCS statistical convergence test for specified circular areas

	0-1.3 miles	0-2 miles	0-2.5 miles	0-3 miles	0-3.5 miles	0-5 miles	0-7 miles	0-10 miles
Mean	4.1x10 ⁻⁷	1.5x10 ⁻⁷	9.0x10 ⁻⁸	5.4x10 ⁻⁸	2.7x10 ⁻⁸	8.4x10 ⁻⁹	3.4x10 ⁻⁹	1.4x10 ⁻⁹
Median	0.0	0.0	0.0	0.0	0.0	0.0	0.0	0.0
75 th percentile	0.0	0.0	0.0	0.0	0.0	0.0	0.0	0.0
95 th percentile	3.3x10 ⁻⁶	5.4x10 ⁻⁷	6.3x10 ⁻⁸	9.2x10 ⁻⁹	0.0	0.0	0.0	0.0

Table 5.2-14 Combined conditional, mean, individual early-fatality risk (per event) standard error statistics for the MACCS statistical convergence test for specified circular areas

	0-1.3 miles	0-2 miles	0-2.5 miles	0-3 miles	0-3.5 miles	0-5 miles	0-7 miles	0-10 miles
Mean	1.2×10^{-7}	4.8×10^{-8}	4.3×10^{-8}	3.3×10^{-8}	2.4×10^{-8}	9.0×10^{-9}	3.9×10^{-9}	1.9×10^{-9}
Median	0.0	0.0	0.0	0.0	0.0	0.0	0.0	0.0
75 th percentile	0.0	0.0	0.0	0.0	0.0	0.0	0.0	0.0
95 th percentile	1.2×10^{-6}	4.7×10^{-8}	1.8×10^{-8}	6.2×10^{-9}	0.0	0.0	0.0	0.0

Table 5.2-15 Combined conditional, mean, individual early-fatality risk (per event) lower bounding case statistics for the MACCS statistical convergence test for specified circular areas

	0-1.3 miles	0-2 miles	0-2.5 miles	0-3 miles	0-3.5 miles	0-5 miles	0-7 miles	0-10 miles
Mean	0.0	0.0	0.0	0.0	0.0	0.0	0.0	0.0
Median	0.0	0.0	0.0	0.0	0.0	0.0	0.0	0.0
75 th percentile	0.0	0.0	0.0	0.0	0.0	0.0	0.0	0.0
95 th percentile	0.0	0.0	0.0	0.0	0.0	0.0	0.0	0.0

Table 5.2-16 Combined conditional, mean, individual early-fatality risk (per event) upper bounding cases statistics for the MACCS statistical convergence test for specified circular areas

	0-1.3 miles	0-2 miles	0-2.5 miles	0-3 miles	0-3.5 miles	0-5 miles	0-7 miles	0-10 miles
Mean	9.4×10^{-7}	3.6×10^{-7}	2.8×10^{-7}	2.0×10^{-7}	1.3×10^{-7}	4.7×10^{-8}	2.0×10^{-8}	9.7×10^{-9}
Median	0.0	0.0	0.0	0.0	0.0	0.0	0.0	0.0
75 th percentile	0.0	0.0	0.0	0.0	0.0	0.0	0.0	0.0
95 th percentile	8.4×10^{-6}	7.4×10^{-7}	1.4×10^{-7}	3.6×10^{-8}	0.0	0.0	0.0	0.0

As shown on Figure 5.2-9, the CCDFs for the three MACCS analysis for the conditional, mean, individual early-fatality risk (per event) are very similar and are in good agreement between each analysis for the 1.3-mile circular area (i.e., within 1 mile of EAB). Also, Figure 5.2-9 shows an uncertainty within the 95th confidence interval that is zero to $\sim 8.0 \times 10^{-6}$ between each analysis. This large confidence level is a result of the limited number of early-fatality risks greater than zero. Only 10% to 13% of the results for the three analyses resulted in a nonzero

early-fatality risk at any distance. The highest absolute early-fatality risk is 6.7×10^{-11} pry (i.e., recall the Peach Bottom LTSBO core damage frequency is 3×10^{-6} pry) at 1.3 miles from the CAP19 MACCS model.

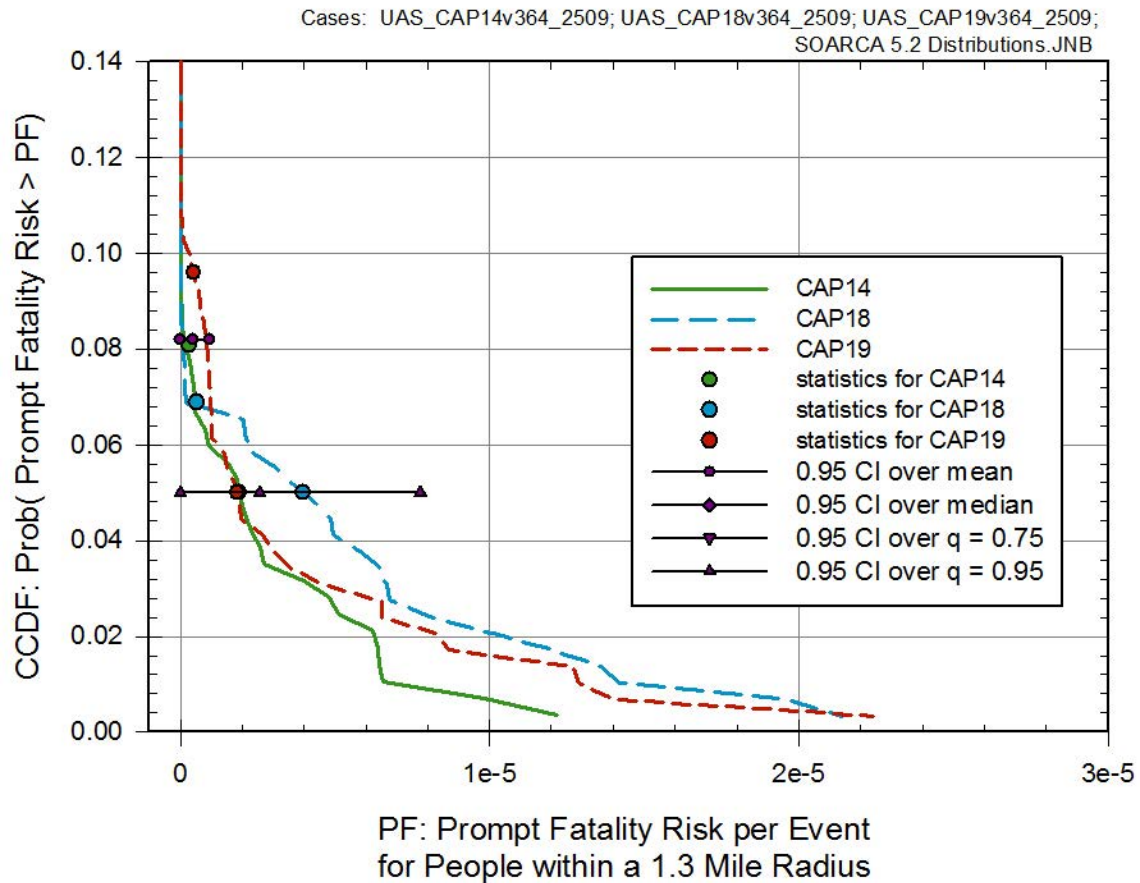


Figure 5.2-9 Complementary cumulative distribution function and statistical values for conditional, mean, individual early-fatality risk (per event) within a 1.3-mile radius for the MACCS Convergence Analysis

Figures 5.2-10 through 5.2-13 show the CCDFs for the conditional, mean, individual early-fatality risk (per event) for the 2-mile, 2.5-mile, 3-mile, and 3.5-mile circular areas, respectively. The results are similar to those on Figure 5.2-10, however, the number of early-fatality risk results greater than zero for each subsequent circular area decreases. As a result the data for a nonzero early-fatality risk decreases from a maximum of 12% of the total data at 1.3 miles (CAP19) to a maximum of 4.5% of the realizations at 3.5 miles (CAP18). Beyond the 3.5-mile circular area, the realizations with nonzero early-fatality risk drops below 3% of the total data and provides no discernible graphical information.

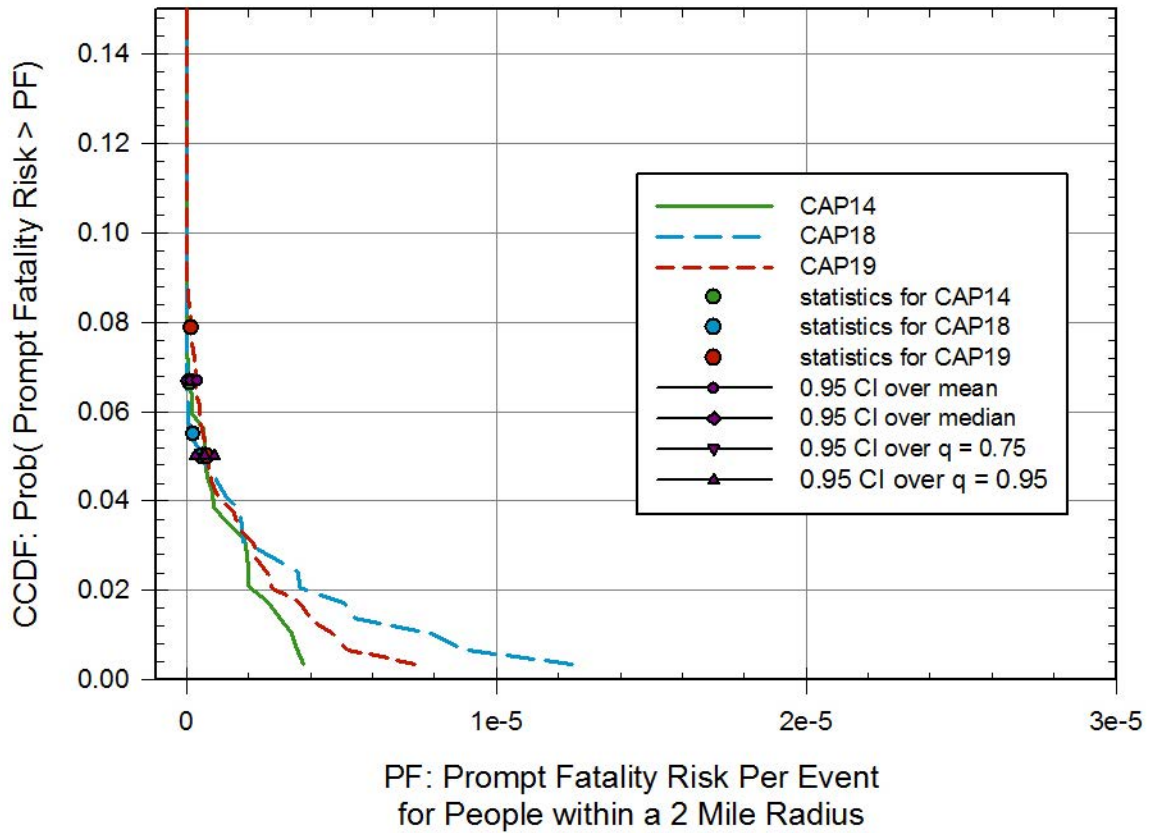


Figure 5.2-10 Complementary cumulative distribution function and statistical values for conditional, mean, individual early-fatality risk (per event) within a 2-mile radius for the MACCS Convergence Analysis

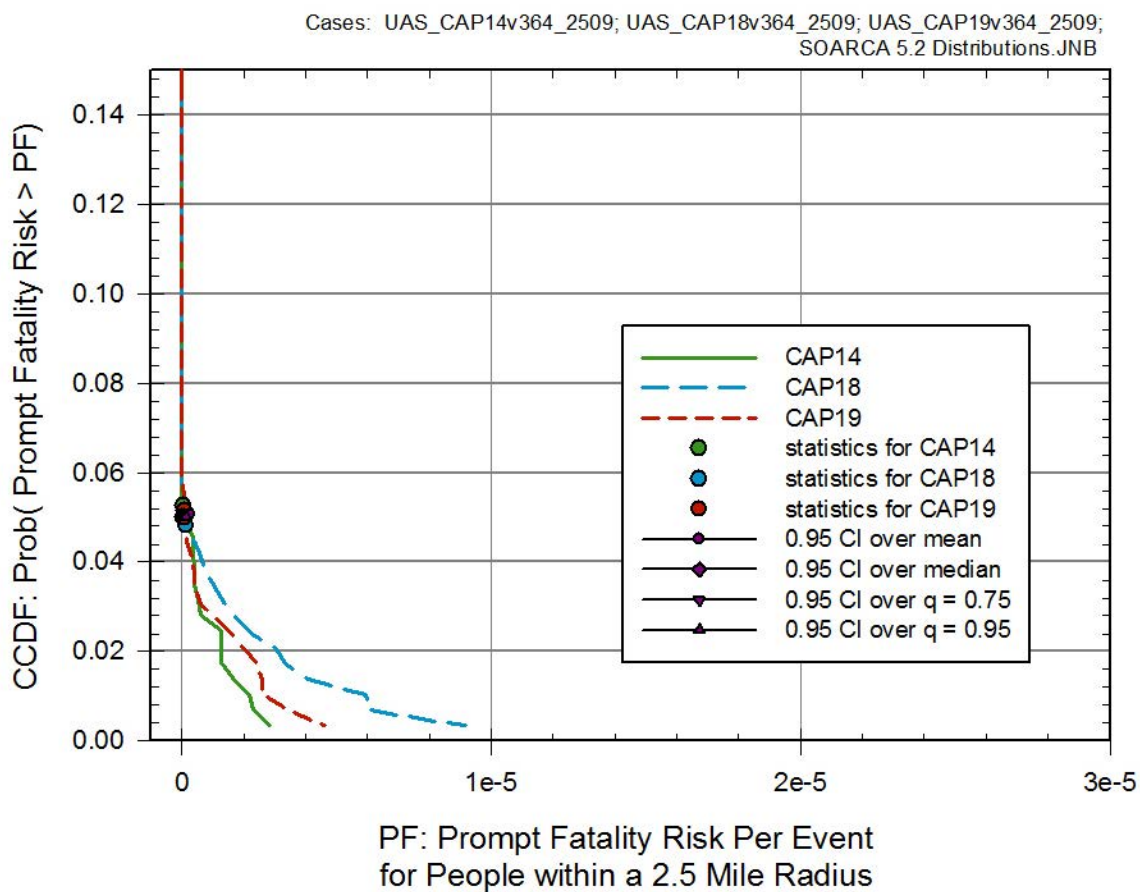


Figure 5.2-11 Complementary cumulative distribution function and statistical values for conditional, mean, individual early-fatality risk (per event) within a 2.5-mile radius for the MACCS Convergence Analysis

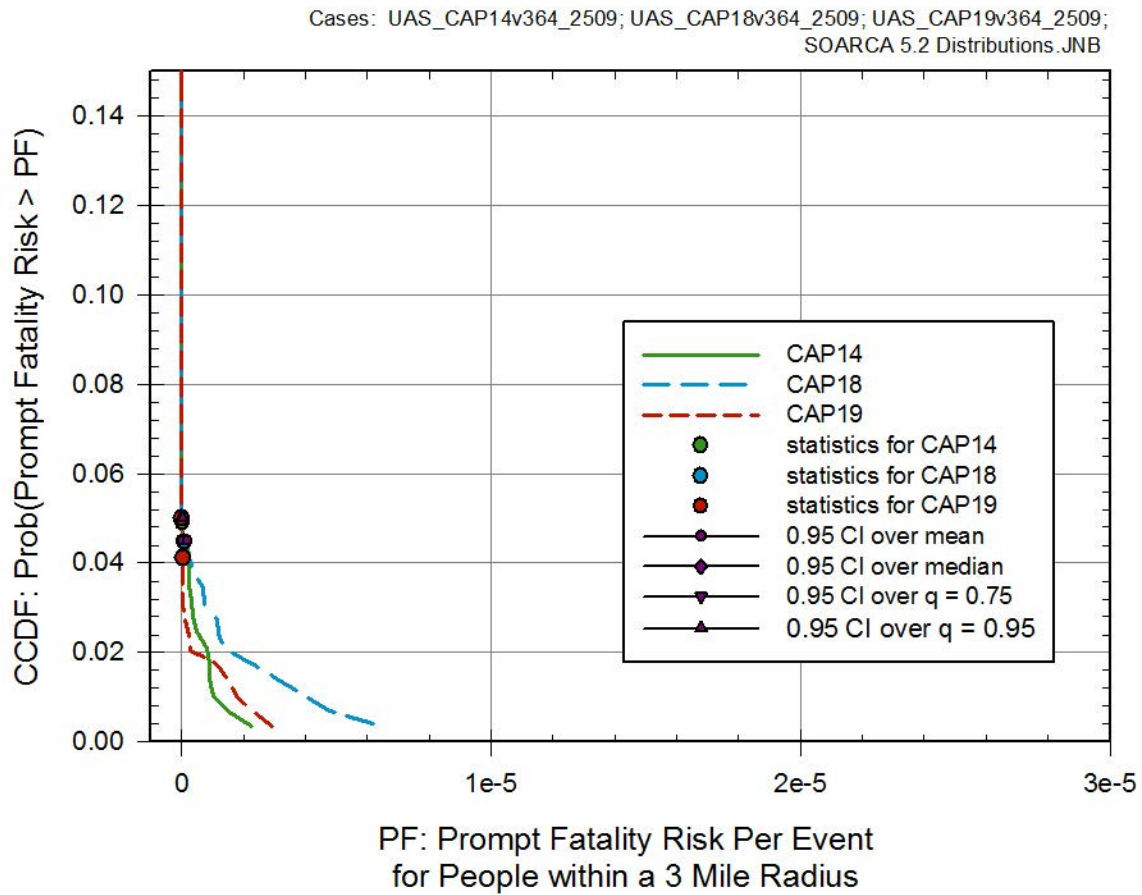


Figure 5.2-12 Complementary cumulative distribution function and statistical values for conditional, mean, individual early-fatality risk (per event) within a 3-mile radius for the MACCS Convergence Analysis

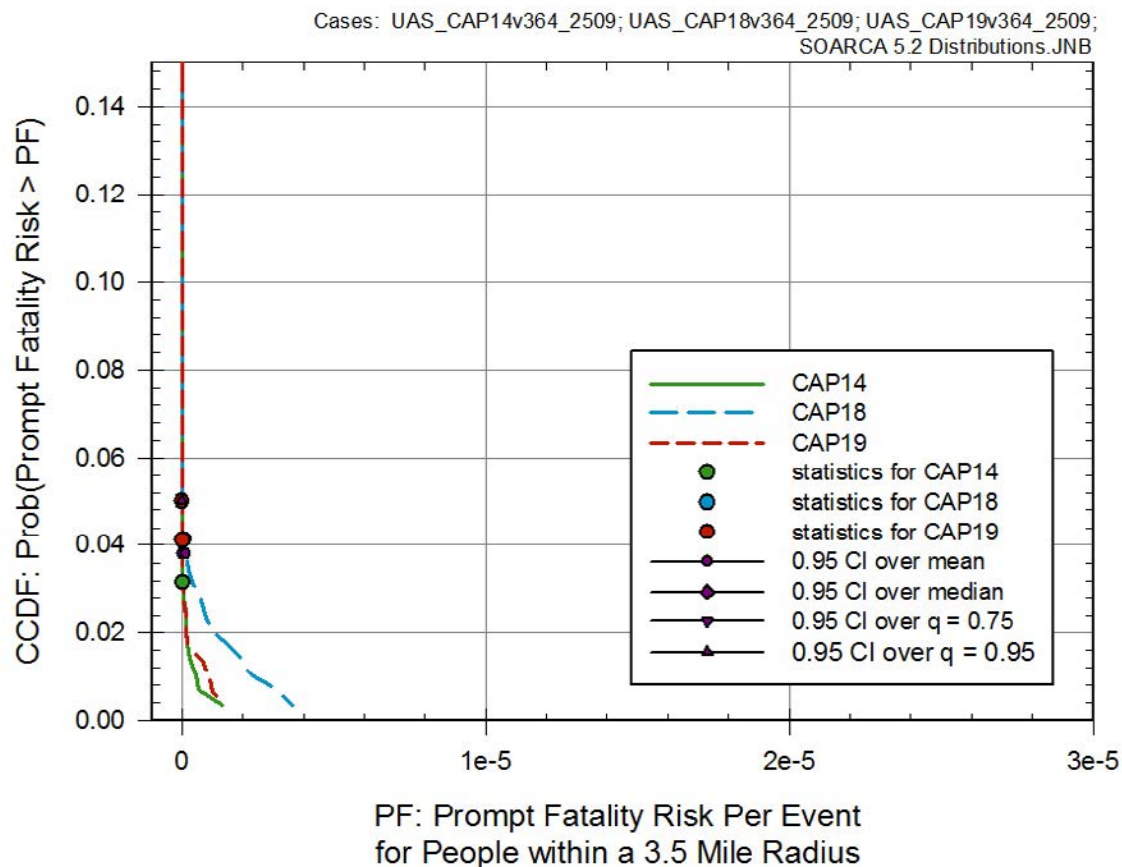


Figure 5.2-13 Complementary cumulative distribution function and statistical values for conditional, mean, individual early-fatality risk (per event) within a 3.5-mile radius for the MACCS Convergence Analysis

Tables 5.2-17 through 5.2-19 show the correlation matrix for the three MACCS analyses for the conditional, mean, individual early-fatality risk (per event) at specified circular areas. The correlation data applies to both zero and nonzero early-fatality risk results. The correlation between the closer circular areas and the further circular areas is poor due to the small number of realizations for which a nonzero early-fatality risk is observed beyond 3 miles. This is most noticeable in Table 5.2-17 for the 10-mile correlation. At this location 1% of the total realizations result in a nonzero early-fatality risk which is about the same percentage as the other two uncertainty cases. However in Table 5.2-18, these nonzero early fatality realizations at 10 miles account for 40% of the top 3% of the nonzero early fatality realizations at 1.3 miles. Thus the correlation at 10 miles is not that dependent on the lower circular areas since it is weighted heavily towards the higher end of the early-fatality risks.

Table 5.2-17 Correlation matrix for the MELCOR STP08 Uncertainty Model Source Term MACCS Analysis for the conditional, mean, individual early-fatality risk (per event) for specified circular areas

	0-1.3 miles	0-2 miles	0-2.5 miles	0-3 miles	0-3.5 miles	0-5 miles	0-7 miles	0-10 miles
0-1.3 miles	1	0.84	0.68	0.72	0.37	0.28	0.22	0.22
0-2 miles		1	0.88	0.77	0.51	0.45	0.40	0.40
0-2.5 miles			1	0.90	0.67	0.61	0.56	0.56
0-3 miles				1	0.79	0.74	0.68	0.68
0-3.5 miles					1	0.94	0.88	0.88
0-5 miles						1	0.94	0.94
0-7 miles							1	1
0-10 miles								1

Table 5.2-18 Correlation matrix for the MELCOR STP09 Uncertainty Model Source Term MACCS Analysis for the conditional, mean, individual early-fatality risk (per event) for specified circular areas

	0-1.3 miles	0-2 miles	0-2.5 miles	0-3 miles	0-3.5 miles	0-5 miles	0-7 miles	0-10 miles
0-1.3 miles	1	0.93	0.92	0.85	0.84	0.78	0.57	0.53
0-2 miles		1	0.992	0.95	0.94	0.88	0.63	0.60
0-2.5 miles			1	0.97	0.96	0.91	0.66	0.63
0-3 miles				1	0.994	0.95	0.72	0.68
0-3.5 miles					1	0.98	0.77	0.73
0-5 miles						1	0.87	0.85
0-7 miles							1	0.99
0-10 miles								1

Table 5.2-19 Correlation matrix for the MELCOR STP10 Uncertainty Model Source Term MACCS Analysis for the conditional, mean, individual early-fatality risk (per event) for specified circular areas

	0-1.3 miles	0-2 miles	0-2.5 miles	0-3 miles	0-3.5 miles	0-5 miles	0-7 miles	0-10 miles
0-1.3 miles	1	0.84	0.92	0.75	0.46	0.45	0.39	0.34
0-2 miles		1	0.83	0.80	0.56	0.56	0.48	0.40
0-2.5 miles			1	0.87	0.64	0.64	0.55	0.44
0-3 miles				1	0.76	0.76	0.66	0.51
0-3.5 miles					1	0.991	0.85	0.64
0-5 miles						1	0.86	0.63
0-7 miles							1	0.75
0-10 miles								1

Based on these analyses, the conditional, mean, individual early-fatality risk (per event) are determined to be well converged for this uncertainty analysis. These analyses further verify the overall statistical convergence of the MACCS code when applying epistemic (e.g., radionuclide inhalation DCFs) and aleatory (e.g., weather trials) uncertainties.

6. SOARCA MODEL PARAMETER UNCERTAINTY AND SENSITIVITY ANALYSES

This section presents uncertainty and sensitivity analysis results for the unmitigated LTSBO severe accident scenario at the Peach Bottom Atomic Power Station. Uncertainty analyses determine the variability in analysis results that derives from uncertainty in analysis inputs. Sensitivity analyses determine the contribution to the variability in analysis results that derives from individual analysis inputs. This section is divided into four parts. The first two sections present the uncertainty and sensitivity analysis results for the probabilistic source term and consequence analysis in Sections 6.1 and 6.2, respectively. The procedures used to generate these results are described in Appendix A while the independent and dependent variables under consideration are listed in Section 4.0.

In addition, within each section is an analysis of single realizations selected from the probabilistic sample set. These detailed analyses provide a unique insight into the coupling of various processes and a comprehensive explanation detailing how the key phenomena in the various components of the complex system under varying physical-chemical-thermal-mechanical conditions provides confidence in the measure of the key uncertainty in the analysis results.

Section 6.3 presents a summary of the key parameters. Section 6.4 presents a series of sensitivity cases to target phenomena that could not be directly captured in the parametric study and regression analyses. As discussed in Section 4.3, several of the issues and sensitivity cases in Section 6.4 lack the technical basis to develop meaningful distributions of the uncertainty or the capability of the codes to directly assess the phenomena is absent. Collectively the results of the parametric parameter uncertainty analysis, single realizations, and selected sensitivity calculations, provide a quantitative measure of the impact of key uncertainty within a complex modeling system.

6.1 Source Term Parameter Uncertainty Analysis

For the uncertainty analysis, time-varying fractions of the corresponding radionuclide inventory released over the first 48 hours for all results from the three replicates combined were used (as discussed in Section 5.1.1), as well as the representative statistics (mean, median and quantiles $q=0.05$ and 0.95). A CDF of the uncertainty at the selected time of 48 hours after the incident is also presented, with the inclusion of a 95% confidence interval (CI) over the previously mentioned statistics, based on a q-bootstrap estimation, as described below.

All three sample sets for the three replicates were generated using a simple random sampling (SRS) technique. Therefore, it is valid to use the combined sample set for this uncertainty analysis. Moreover, bootstrap samples (selection of realizations n times from the original sample with replacement) of similar size can be generated to estimate mean and selected quantiles (median, $q=0.05$ and $q=0.95$). Five thousand such samples have been generated to construct distributions over the mean and selected quantiles. Quantiles 0.025 and 0.975 in each distribution have been selected to represent a 95% CI.

A sensitivity analysis was also performed at the selected time of 48 hours for both the combined population of results and for each of the three individual replicates. Rank regression, quadratic regression, recursive partitioning, and multivariate adaptive regression splines (MARS) are the four regression techniques selected for the regression analysis. While the first regression technique gives direct indices of importance of the input parameters, the last three techniques are used to construct a surrogate model. Sobol variance decomposition is then applied on the surrogate model to estimate the importance of the input parameters in the uncertainty of the

output in consideration. A simplified description of the techniques is presented in Section 3.4.2, while a more detailed description can be found in Storlie et al [12, 13]. Each of these methods uses an alpha cut off (representing the probability that a value is due to spurious correlation) equal to 0.02. Moreover, the maximum number of displayed variables is set to 15 since most of the influence will be negligible beyond the first 15 uncertain parameters.

6.1.1 Fraction of Iodine Released to the Environment

The time-dependent graph of fraction of iodine released over the first 48 hours (Figure 6.1-1) shows releases starting after 10 hours and tending to plateau within the following 8 hours for some realizations and a second pulse (happening this time for most of the realizations) around 18 hours after the event. The highest releases correspond to the realizations with thermal SRV failure leading to creep rupture for reasons identified in Section 6.1.4. The distribution of results is slightly skewed to the right (positive skew) as to the relative position of the mean compared to the median. But considering that a linear scale is used, the skewness is relatively small. The expected value and median are around 5% of the fraction of iodine released. The 95th percentile stands between 10% and 15%, while the maximum (over 865 samples) does not go beyond 20%.

A CDF representation at 48 hours is displayed on Figure 6.1-2. 95% confidence intervals over all considered statistics show convergence for 5th percentile, median and mean. The 95th percentile shows more variability (which is expected considering that, for a sample of size 865, the highest 43 results define its position), but it remains reasonable, within 10% of the estimate value, leading to an accuracy of plus or minus 1% of iodine release with 95% confidence.

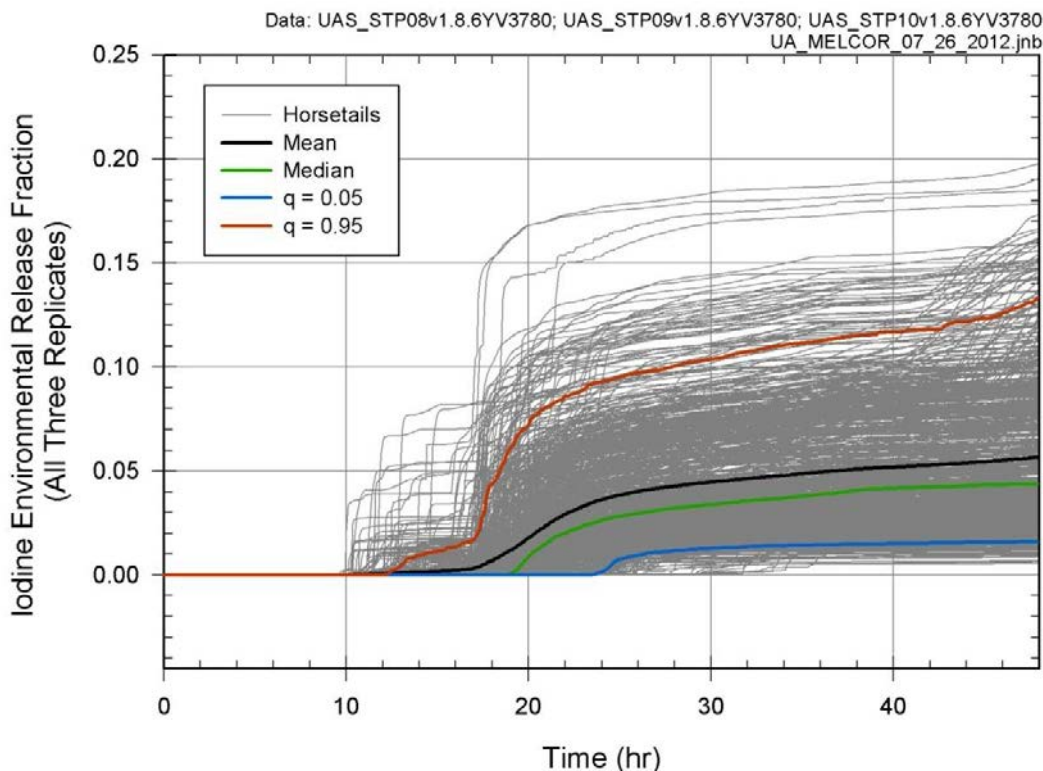


Figure 6.1-1 Time-dependent fraction of iodine core inventory released to the environment for the first 48 hours for combined (865) results for the Peach Bottom Unmitigated LTSBO

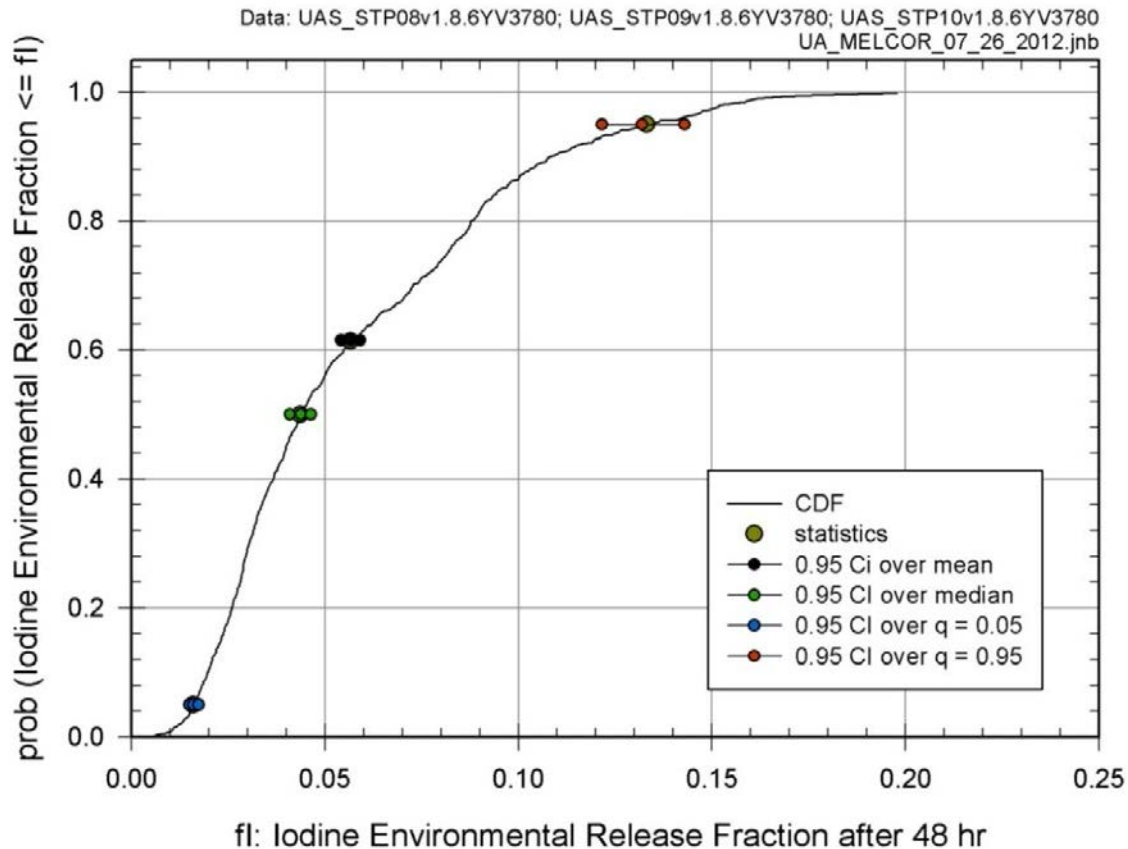


Figure 6.1-2 Cumulative distribution function of fraction of iodine core inventory released to the environment at 48 hours based on all combined (i.e., 865) results, with 95% confidence interval over mean, median and quantiles $q = 0.05$ and $q = 0.95$ for the Peach Bottom Unmitigated LTSBO

Table 6.1-1 presents the results of four regression analyses applied to the fraction of the iodine core inventory released to the environment over 48 hours. The coefficient of determination for all four regression models are fairly high, ranging from 0.69 (for rank regression) to 0.93 (for recursive partitioning).

All regression methods rank the uncertainty in lambda in SRV stochastic failure to reclose (SRVLAM, defined in Section 4.1.1) as the most significant parameter. It explains about half of the variability in the fraction of iodine released on average by itself. In conjunction with other parameters, the three non-additive techniques (i.e., quadratic regression, recursive partitioning and MARS) indicate that SRVLAM may explain up to 70% of the variance. The influences that variations in this parameter have on accident progression and releases to the environment are discussed at length in Section 6.1.4.

The methods also agree that the second most important parameter is chemical form of iodine and cesium (CHEMFORM, defined in Section 4.1.5) which explains an additional 10% of the variance. Quadratic and recursive partitioning tend to identify some conjoint influence (i.e., carried on by two or more uncertain input parameters in combination) which is not captured using MARS. While the conjoint effect is small, it may not have been captured by MARS because CHEMFORM has a discrete distribution (integer from 1 to 5 representing 5 different chemical states) and the spline regression has difficulties when dealing with discrete variables.

In considering the dependence of iodine release on CHEMFORM, it is important to note that the different combinations of chemical form in the uncertainty analysis vary in the amount of elemental (gaseous) iodine initialized in the core. Important with respect to gaseous iodine in the calculations is that it is scrubbed very effectively when introduced to the wetwell pool, and that unless scrubbed in the pool, releases to the environment. Therefore, for gaseous iodine to release to the environment, it must bypass the wetwell pool. In the base uncertainty case, all of the elemental iodine is released from the core before reactor lower head failure and is swept to the wetwell through the stuck-open SRV. The iodine is efficiently scrubbed by the wetwell pool such that 99.8% of the original core inventory is retained in the pool. In other calculations, a MSL rupture interrupts the sweeping of gaseous iodine to the wetwell introducing it to the drywell instead where it is readily available to escape containment through the drywell head flange or a drywell liner melt-through. In still other calculations, not all of the iodine releases from the core (or core debris) before lower head failure and so too introduces to the drywell where it is available to escape through the drywell head flange or a drywell liner melt-through.

Flow area resulting from drywell liner failure (FL904A, described in Section 4.1.4) and SRV open area fraction after thermal seizure (SRVOAFRAC, defined in Section 4.1.2) both explain about 5% of the variance. SRVOAFRAC seems, however, to have a greater conjoint influence than FL904A. As recursive partitioning associates a higher T_i value than quadratic and MARS, it seems that SRVOAFRAC projects its influence in conjunction with one or multiple other parameters. The dependence of FL904A reflects the larger fission product releases associated with contaminated water surging up from the wetwell given larger values of this parameter as described in Section 6.1.4. The conjoint influence noted for SRVOAFRAC reflects the importance of this parameter with respect to whether a MSL rupture occurs. MSL ruptures consistently resulted in larger releases but SRVOAFRAC alone does not determine whether or not a MSL rupture occurs.

Yet, as SRVOAFRAC is considered not as important by rank regression (only 2% of the variance explained), it is likely that SRVOAFRAC has a nonlinear/non-monotonic effect. Since the significance was determined by quadratic regression, it is likely that the shape of influence is parabolic (with one area of the distribution leading to the highest or lowest value set). This nonlinear effect is demonstrated on Figure 6.1-3. Samples of SRVOAFRAC for Replicate 1 (without a SRV stochastic failure) indicate that at values below approximately 0.7, main steam line rupture and associated higher source term releases will occur.

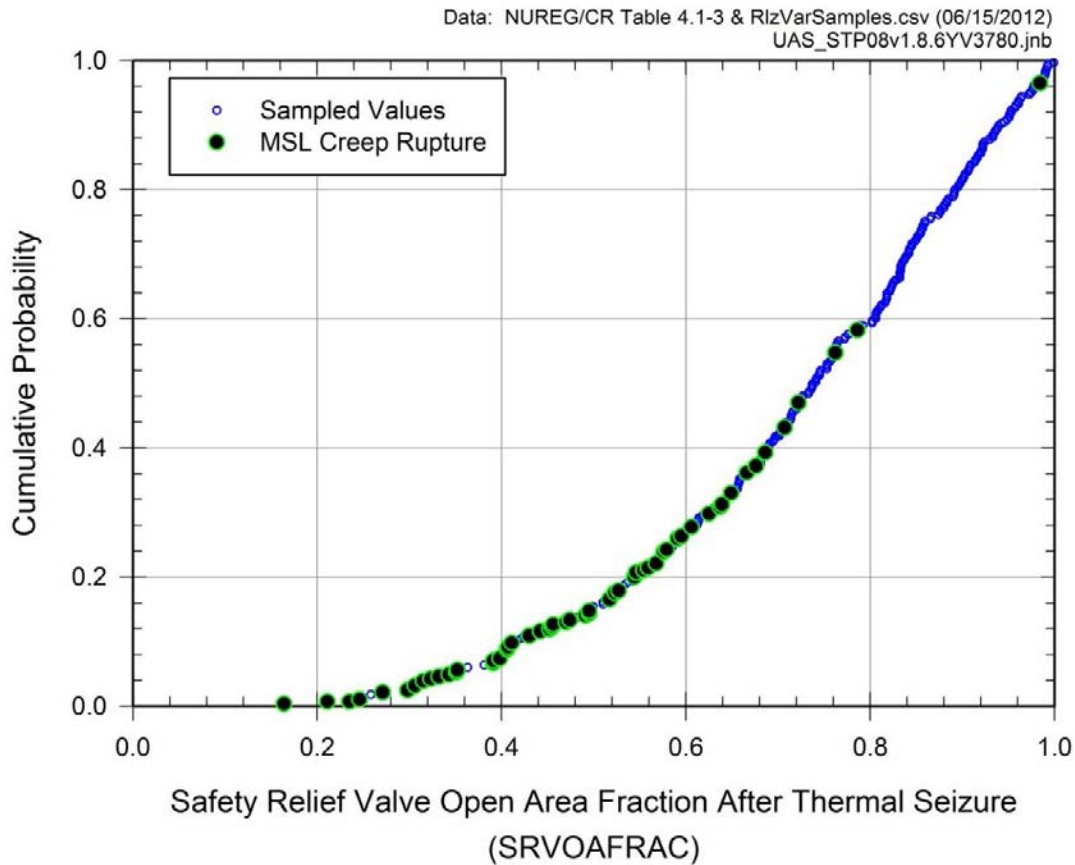


Figure 6.1-3 Cumulative distribution function of SRVOAFRAC with samples where main steam line creep rupture occur indicated for Replicate 1 for the Peach Bottom Unmitigated LTSBO

These four input parameters (SRVLAM, CHEMFORM, SRVOAFRAC and FL904A) explain at least 70% of the variability in each regression analysis. It is likely, considering the regression techniques capture different effects that these parameters actually explain about 80% of the variability. The phenomenological effects of these parameters are discussed in Section 6.1.4.

Other parameters were not as important and have a negligible influence. Amongst the remaining parameters, the only one worth noting is the criteria for thermal seizure of the SRV due to heating after onset of core damage (SRVFAILT, defined in Section 4.1.2), which has a small influence (around 2 or 3%) according to all three non-monotonic techniques.

Table 6.1-1 Regression analysis of fraction of iodine released after 48 Hours

	Rank Regression			Quadratic			Recursive Partitioning			MARS		
Final R ²	0.69			0.76			0.93			0.80		
Input name	R ² inc.	R ² cont.	SRRC	S _i	T _i	p-val	S _i	T _i	p-val	S _i	T _i	p-val
SRVLAM	0.49	0.49	-0.72	0.46	0.68	0.00	0.55	0.78	0.00	0.64	0.70	0.00
CHEMFORM	0.58	0.09	0.30	0.10	0.16	0.00	0.07	0.22	0.00	0.09	0.12	0.00
FL904A	0.64	0.06	0.26	0.05	0.06	0.22	0.02	0.12	0.00	0.05	0.08	0.00
RRDOOR	0.67	0.03	0.28	0.01	0.06	0.03	0.04	0.07	0.00	---	---	---
SRVOAFRAC	0.69	0.02	-0.12	0.06	0.13	0.00	0.05	0.20	0.00	0.06	0.16	0.00
FFC	0.69	0.00	0.06	0.03	0.03	0.17	---	---	---	0.02	0.00	1.00
RRIDFRAC	0.69	0.00	0.03	---	---	---	---	---	---	0.00	0.02	0.09
KBOLT	0.69	0.00	-0.04	0.04	0.00	1.00	0.00	0.00	1.00	---	---	---
BATTDUR	---	---	---	0.00	0.08	0.00	0.00	0.04	0.06	0.00	0.00	1.00
RHONOM	---	---	---	0.00	0.06	0.01	---	---	---	---	---	---
H2IGNC	---	---	---	0.00	0.04	0.02	0.00	0.00	0.41	0.02	0.01	0.17
DGASKET	---	---	---	0.00	0.02	0.23	0.01	0.00	1.00	---	---	---
SLCRFRAC	---	---	---	0.02	0.01	0.47	---	---	---	0.00	0.00	1.00
SRVFAILT	---	---	---	0.03	0.00	1.00	0.03	0.07	0.00	0.00	0.02	0.18
SC1131_2	---	---	---	0.04	0.00	1.00	0.00	0.06	0.00	0.00	0.02	0.05
DHEADSOL	---	---	---	0.00	0.00	1.00	0.00	0.04	0.00	0.01	0.00	1.00
SC1141_2	---	---	---	---	---	---	0.00	0.03	0.12	0.01	0.00	1.00
RDSTC	---	---	---	---	---	---	0.00	0.01	0.26	0.00	0.00	1.00
RRODFRAC	---	---	---	---	---	---	0.00	0.00	1.00	0.01	0.01	0.28
	---	---	---	---	---	---	---	---	---	---	---	---

SRVLAM and SRVOAFRAC combined influences separate the realizations into three groups, each representing a distinct mode of venting the RPV during much of the core degradation. These groups are: SRV stochastic failure (with about ½ of the realizations), SRV thermal failure without MSL creep rupture (representing ~1/3 of the realizations), and SRV thermal failure with MSL creep rupture (for ~1/6 of the realizations). The importance of these parameters is large as their values strongly influence the releases of iodine (and other fission products) to the environment. To better understand the driving variables for each of these three failure groups, separate analyses have been performed for each of them. Table 6.1-2 presents the results of regression analysis for environmental iodine release fraction after 48 hours for the realizations leading to SRV stochastic failure. Regressions are fairly good with R² values ranging from 0.7 to 0.9.

The most influential parameters are FL904A and SRVLAM. The negative SRRC for SRVLAM comes from the fact that an earlier stochastic SRV failure results in a decrease in the amount of iodine released to the environment. As described at length in Section 6.1.4, earlier SRV failures result in less core oxidation and less late revaporization of fission products off reactor vessel internals. Since most of the iodine released to the environment in the uncertainty calculations can be traced to material revaporized late off of reactor internals, earlier SRV failures result in smaller releases to the environment. In the worst case, a long period of SRV valve cycling

promotes a main steam line creep rupture characteristically leading to large releases to the environment. These two variables explain together between 50% and 70% of the variance. CHEMFORM, the third most influential parameter, explains about 10% of the variance. The influence of other parameters is low compared to the influence of these three parameters and not necessarily consistent amongst techniques.

Table 6.1-2 Regression analyses of fraction of iodine released after 48 hours for realizations leading to SRV stochastic failures

	Rank Regression			Quadratic			Recursive Partitioning			MARS		
Final R ²	0.69			0.71			0.91			0.80		
Input name	R ² inc.	R ² cont.	SRRC	S _i	T _i	p-val	S _i	T _i	p-val	S _i	T _i	p-val
FL904A	0.31	0.31	0.53	0.20	0.24	0.00	0.24	0.37	0.00	0.27	0.24	0.00
SRVLAM	0.54	0.23	-0.52	0.30	0.33	0.00	0.36	0.61	0.00	0.56	0.57	0.00
CHEMFORM	0.61	0.07	0.28	0.10	0.12	0.06	0.07	0.21	0.00	0.11	0.06	0.16
RRDOOR	0.63	0.02	0.43	0.06	0.15	0.01	0.00	0.03	0.03	---	---	---
BATTDUR	0.65	0.02	0.16	0.01	0.00	1.00	0.01	0.14	0.00	0.03	0.01	0.77
FFC	0.66	0.00	0.10	0.00	0.06	0.15	---	---	---	0.00	0.00	1.00
RRIDFRAC	0.66	0.01	0.08	---	---	---	---	---	---	0.02	0.05	0.01
RHONOM	0.67	0.00	-0.07	0.00	0.11	0.00	0.00	0.00	1.00	---	---	---
DGASKET	0.67	0.00	0.05	0.00	0.06	0.09	---	---	---	---	---	---
H2IGNC	0.67	0.00	0.04	---	---	---	---	---	---	0.01	0.00	1.00
KBOLT	---	---	---	0.02	0.05	0.07	0.00	0.04	0.09	---	---	---
RDSTC	---	---	---	0.03	0.01	0.50	0.00	0.00	1.00	0.00	0.00	1.00
DHEADSOL	---	---	---	0.04	0.01	0.62	0.01	0.07	0.00	0.00	0.10	0.00
SRVFAILT	---	---	---	0.00	0.03	0.72	0.04	0.00	1.00	0.02	0.02	0.20
SC1131_2	---	---	---	0.03	0.00	1.00	0.01	0.05	0.02	0.00	0.00	1.00
SC1141_2	---	---	---	0.02	0.00	1.00	0.01	0.04	0.15	0.04	0.03	0.12
SRVOAFRAC	---	---	---	0.00	0.00	1.00	0.00	0.00	1.00	0.00	0.06	0.01
EBOLT	---	---	---	---	---	---	0.02	0.03	0.16	---	---	---
RRODFRAC	---	---	---	---	---	---	0.02	0.00	1.00	0.03	0.00	0.46
SLCRFRAC	---	---	---	---	---	---	---	---	---	0.00	0.03	0.14

The regression analyses for environmental iodine release fraction for SRV thermal failure without MSL creep rupture leads to a high R² for all techniques (between 0.78 and 0.90), as shown in Table 6.1-3. All methods agree that CHEMFORM is the most important parameter in explaining between 40% and 50% of the variance. Second, explaining another 20% is the condition of the railroad doors, closed or blown open by an overpressure in the reactor building. When the railroad doors blow open, a buoyant draft establishes in the reactor building where air enters low through the doors and exits high out opened blowout panels or failed roofing in the refueling bay. The draft efficiently carries aerosols released from containment out into the environment. Note that the RRDOOR is not a sampled parameter. Its status is determined by the course of a calculation. RRDOOR assumes the value of one if the doors are blown open and the value of zero if they remain closed. The non-detection of RRDOOR effect by MARS is

not surprising as MARS has some difficulties with discrete variables. FL904A comes in third with 15% more of the variance explained. The other parameters have negligible influence.

Table 6.1-3 Regression analyses of fraction of iodine released after 48 hours for realizations leading to SRV thermal failures without MSL creep rupture

	Rank Regression			Quadratic			Recursive Partitioning			MARS		
Final R ²	0.78			0.89			0.90			0.84		
Input name	R ² inc.	R ² cont.	SRRC	S _i	T _i	p-val	S _i	T _i	p-val	S _i	T _i	p-val
CHEMFORM	0.42	0.42	0.68	0.49	0.53	0.00	0.49	0.56	0.00	0.59	0.58	0.00
RRDOOR	0.59	0.18	0.63	0.16	0.22	0.01	0.25	0.24	0.00	---	---	---
FL904A	0.74	0.14	0.38	0.15	0.13	0.04	0.17	0.21	0.00	0.14	0.17	0.00
FFC	0.75	0.02	0.17	0.02	0.04	0.11	0.00	0.01	0.30	0.05	0.02	0.37
KBOLT	0.76	0.01	-0.08	0.00	0.00	1.00	0.03	0.03	0.33	---	---	---
SC1131_2	0.77	0.01	0.10	0.05	0.07	0.02	0.01	0.00	1.00	0.05	0.02	0.16
DHEADSOL	0.77	0.00	-0.07	0.03	0.02	0.33	0.01	0.00	1.00	0.01	0.02	0.05
RRIDFRAC	0.77	0.00	-0.05	0.00	0.00	1.00	0.03	0.02	0.06	0.00	0.00	1.00
RHONOM	0.78	0.00	-0.05	0.00	0.00	1.00	0.00	0.03	0.06	---	---	---
BATTDUR	---	---	---	0.05	0.08	0.03	---	---	---	0.01	0.03	0.06
SLCRFRAC	---	---	---	0.01	0.06	0.18	---	---	---	0.00	0.04	0.00
RDSTC	---	---	---	0.00	0.01	0.48	0.01	0.00	1.00	0.00	0.03	0.04
SRVFAILT	---	---	---	0.02	0.00	0.63	0.00	0.01	0.36	0.00	0.01	0.31
DGASKET	---	---	---	---	---	---	0.05	0.05	0.02	---	---	---
RRODFRAC	---	---	---	---	---	---	0.00	0.02	0.15	0.00	0.02	0.06
SC1141_2	---	---	---	---	---	---	0.03	0.00	0.51	0.00	0.00	1.00
H2IGNC	---	---	---	---	---	---	---	---	---	0.00	0.02	0.10
SRVOAFRAC	---	---	---	---	---	---	---	---	---	0.00	0.00	0.55
SRVLAM	---	---	---	---	---	---	---	---	---	0.00	0.00	1.00
	---	---	---	---	---	---	---	---	---	---	---	---

SRV thermal failure with MSL creep rupture is the last segregated group. Results of the analysis on this group for environmental iodine release are presented in Table 6.1-4. R² values are reasonably high for all regression techniques (from 0.7 to 1), suggesting that the important parameters are accurately estimated. CHEMFORM is the most important parameter explaining between 33% and 50% of the variance. Second, is RRDOOR, explaining another 10% (except for MARS). At third and found by all techniques, zircaloy melt breakout temperature (SC1131-2, defined in Section 4.1.2) explains about 5% of the variance by itself and about 15% in conjunction with other parameters. Besides these three parameters, methods seem to disagree on what are the next important parameters.

The importance of CHEMFORM stems from more or less elemental (gaseous) iodine being initialized in the core dependent upon the sampled value of this variable. A MSL rupture allows some of the iodine to enter the drywell instead of being vented to the wetwell (through the stuck-open SRV) where it would be efficiently scrubbed in the wetwell pool. Once in the drywell,

the gaseous iodine is readily available to escape containment through the drywell head flange or a drywell liner melt-through.

RRDOOR is important to iodine release in cases of MSL rupture in the same way as described earlier in this section.

The importance of zircaloy melt breakout temperature (SC1131-2) is explained by the effect this parameter has on oxidation. Larger breakout temperatures lead to greater oxidation. Greater oxidation leads to greater heat generation and earlier MSL rupture. Earlier MSL rupture allows more gaseous iodine to enter the drywell instead of being vented to the wetwell (through the stuck-open SRV) where it would be efficiently scrubbed in the wetwell pool. Once in the drywell, the gaseous iodine is readily available to escape containment through the drywell head flange or a drywell liner melt-through.

Table 6.1-4 Regression analyses of fraction of iodine released after 48 hours for realization leading to SRV thermal failure and MSL creep rupture

	Rank Regression			Quadratic			Recursive Partitioning			MARS		
Final R ²	0.70			0.99			0.82			0.76		
Input name	R ² inc.	R ² cont.	SRRC	S _i	T _i	p-val	S _i	T _i	p-val	S _i	T _i	p-val
CHEMFORM	0.33	0.33	0.52	0.12	0.27	0.16	0.48	0.69	0.00	0.41	0.40	0.00
RRDOOR	0.45	0.12	0.39	0.06	0.14	0.01	0.02	0.10	0.11	---	---	---
SLCRFRAC	0.50	0.05	0.25	0.01	0.21	0.31	---	---	---	0.02	0.00	1.00
BATTDUR	0.56	0.06	-0.28	0.02	0.06	0.16	0.02	0.18	0.00	0.18	0.17	0.00
SC1131_2	0.60	0.04	0.16	0.05	0.14	0.05	0.04	0.12	0.02	0.06	0.09	0.00
FL904A	0.62	0.02	0.12	0.04	0.16	0.04	0.00	0.03	0.12	0.02	0.00	0.68
SRVOAFRAC	0.63	0.01	-0.15	0.00	0.16	0.03	0.02	0.10	0.23	0.09	0.08	0.04
SRVFAILT	0.65	0.02	0.13	0.04	0.07	0.15	0.03	0.02	0.36	0.09	0.14	0.01
KBOLT	0.66	0.01	-0.11	0.00	0.14	0.02	---	---	---	---	---	---
RHONOM	0.67	0.01	-0.11	0.00	0.04	0.43	---	---	---	---	---	---
FFC	0.68	0.02	0.16	0.00	0.00	1.00	---	---	---	0.02	0.03	0.05
DGASKET	0.69	0.01	-0.09	---	---	---	0.00	0.03	0.24	---	---	---
RRODFRAC	0.70	0.01	-0.08	0.00	0.00	1.00	0.00	0.05	0.13	0.01	0.04	0.01
SC1141_2	---	---	---	0.02	0.08	0.14	0.05	0.07	0.05	0.00	0.05	0.00
H2IGNC	---	---	---	0.00	0.06	0.20	---	---	---	0.00	0.07	0.00
RRIDFRAC	---	---	---	0.06	0.00	1.00	0.00	0.04	0.11	0.00	0.00	1.00
EBOLT	---	---	---	---	---	---	0.00	0.05	0.08	---	---	---
DHEADSOL	---	---	---	---	---	---	0.00	0.03	0.16	0.00	0.04	0.01
SRVLAM	---	---	---	---	---	---	0.02	0.00	1.00	0.01	0.00	1.00
RDSTC	---	---	---	---	---	---	---	---	---	0.00	0.00	1.00

6.1.1.1 Timing of Initial Iodine Released to the Environment

In order to better understand what affects the timing of radionuclide release, the time when the fraction of iodine released to the environment reaches 0.001 (i.e., 0.1% of the iodine inventory) has been analyzed using the same four techniques. This metric served as an indication of when fission product releases to the environment were first nonzero.

Table 6.1-5 shows the regression analyses over time when the fraction of the iodine inventory released to the environment reaches 0.001. Rank regression leads to a relatively small R^2 (0.42), while all three other techniques range from 0.67 to 0.87. This difference indicates that some conjoint and non-monotonic influences are probably involved in the variance of release timing. Battery duration (BATTDUR) is the most influential parameter, explaining 30% of the variance. The non-additive techniques, with conjoint influence, explain as much as 40%. SRVOAFRAC is the second most influential parameter, but once again the difference between R^2 contribution (purely monotonic) and S_i (capturing non-monotonic) indicates that its effect is probably non-monotonic. SRVOAFRAC also seems to have conjoint influence as the total sensitivity indices (T_i) are between 0.3 and 0.45. And, equally important according to the three non-monotonic techniques, but considered as negligible by rank regression, is SRVLAM, with S_i values between 0.1 and 0.2 and T_i values around 0.4. The influence of SRVLAM and SRVOAFRAC explains the difference in R^2 between rank regression and the three other regressions. All the remaining uncertain parameters seem to have negligible influence.

Battery duration (BATTDUR) has an obvious influence on release timing in that RCIC functions to keep the reactor cool as long as DC power is available. It isn't until DC power is lost that the operators lose control of RCIC and its water delivery increases overfilling the vessel and flooding the steam lines. The drive turbine on the RCIC pump is assumed to fail when the steam lines flood.

The number of cycles to SRV failure ($1/\text{SRVLAM}$) and the open fraction of an SRV after thermal seizure (SRVOFRAC) are important to release timing because they are important to whether or not a MSL rupture occurs. When a MSL rupture occurs, containment over pressurizes and leaks past the drywell head flange. This results in an early release.

Table 6.1-5 Regression analyses over time when the fraction reaches 0.001 of the iodine inventory released over the first 48 Hours

	Rank Regression			Quadratic			Recursive Partitioning			MARS		
Final R ²	0.42			0.67			0.87			0.68		
Input	R ² inc.	R ² cont.	SRRC	S _i	T _i	p-val	S _i	T _i	p-val	S _i	T _i	p-val
BATTDUR	0.32	0.32	0.52	0.32	0.41	0.00	0.30	0.43	0.00	0.39	0.43	0
SRVOAFRAC	0.40	0.08	0.29	0.13	0.27	0.00	0.20	0.46	0.00	0.22	0.36	0
FFC	0.41	0.01	0.13	0.00	0.03	0.23	0.01	0.04	0.02	0.00	0.00	0.55
RRDOOR	0.42	0.00	0.13	0.00	0.20	0.00	0.00	0.00	1.00	---	---	---
CHEMFORM	0.42	0.00	0.04	0.01	0.00	1.00	---	---	---	0.00	0.00	1
SRVFAILT	0.42	0.00	-0.06	0.01	0.00	1.00	0.00	0.00	1.00	0.00	0.03	0.11
FL904A	0.42	0.00	-0.05	0.02	0.05	0.05	0.00	0.00	0.54	0.05	0.02	0.17
SRVLAM	0.42	0.00	0.04	0.12	0.39	0.00	0.21	0.41	0.00	0.18	0.39	0
SC1141_2	---	---	---	0.04	0.09	0.00	0.03	0.03	0.07	0.00	0.00	1
DGASKET	---	---	---	0.01	0.08	0.01	0.00	0.00	1.00	---	---	---
H2IGNC	---	---	---	0.02	0.02	0.28	0.00	0.02	0.23	0.00	0.01	0.4
RHONOM	---	---	---	0.00	0.02	0.29	0.00	0.09	0.00	---	---	---
SC1131_2	---	---	---	0.02	0.02	0.35	0.00	0.03	0.05	0.01	0.00	1
SLCRFRAC	---	---	---	0.00	0.00	1.00	---	---	---	0.01	0.06	0
RRIDFRAC	---	---	---	0.00	0.00	1.00	0.00	0.00	1.00	0.01	0.00	1
RRODFRAC	---	---	---	---	---	---	0.03	0.00	0.61	0.00	0.00	1
EBOLT	---	---	---	---	---	---	0.04	0.00	1.00	---	---	---
DHEADSOL	---	---	---	---	---	---	---	---	---	0.00	0.06	0
RDSTC	---	---	---	---	---	---	---	---	---	0.01	0.00	0.4

6.1.2 Fraction of Cesium Released from the Core Inventory

The time dependent fraction of the cesium core inventory released to the environment presents the same characteristics as seen for iodine releases (Figure 6.1-4). The release fractions are smaller than for iodine, ranging from 2% to 3% of the inventory for median and mean respectively, and reaching 9% for the 95th percentile. Figure 6.1-5 displays the CDF of the results at 48 hours. Confidence intervals confirm that the statistics are fairly converged, with the 95th percentile result having a 95% CI within plus or minus 1% of inventory released.

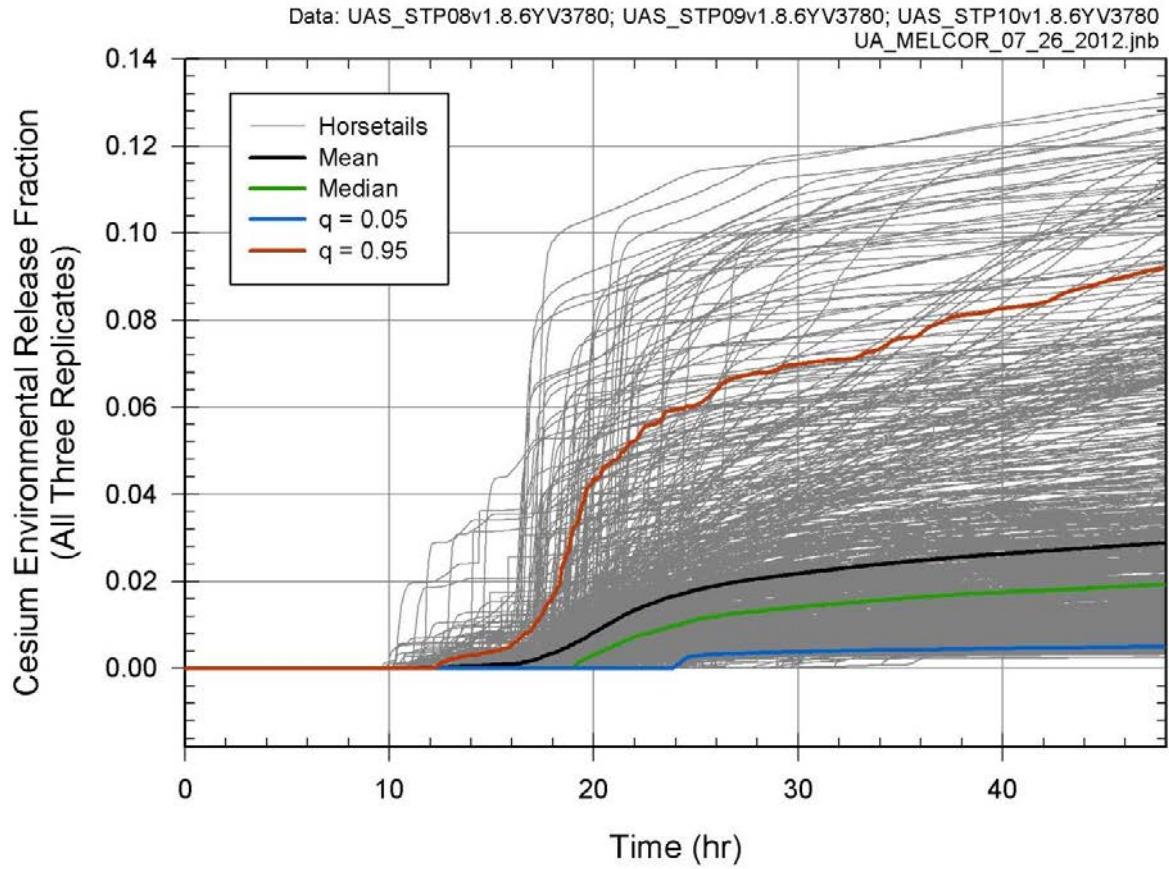


Figure 6.1-4 Time-dependent fraction of the cesium core inventory released to the environment over the first 48 hours for combined (865) results for the Peach Bottom Unmitigated LTSBO

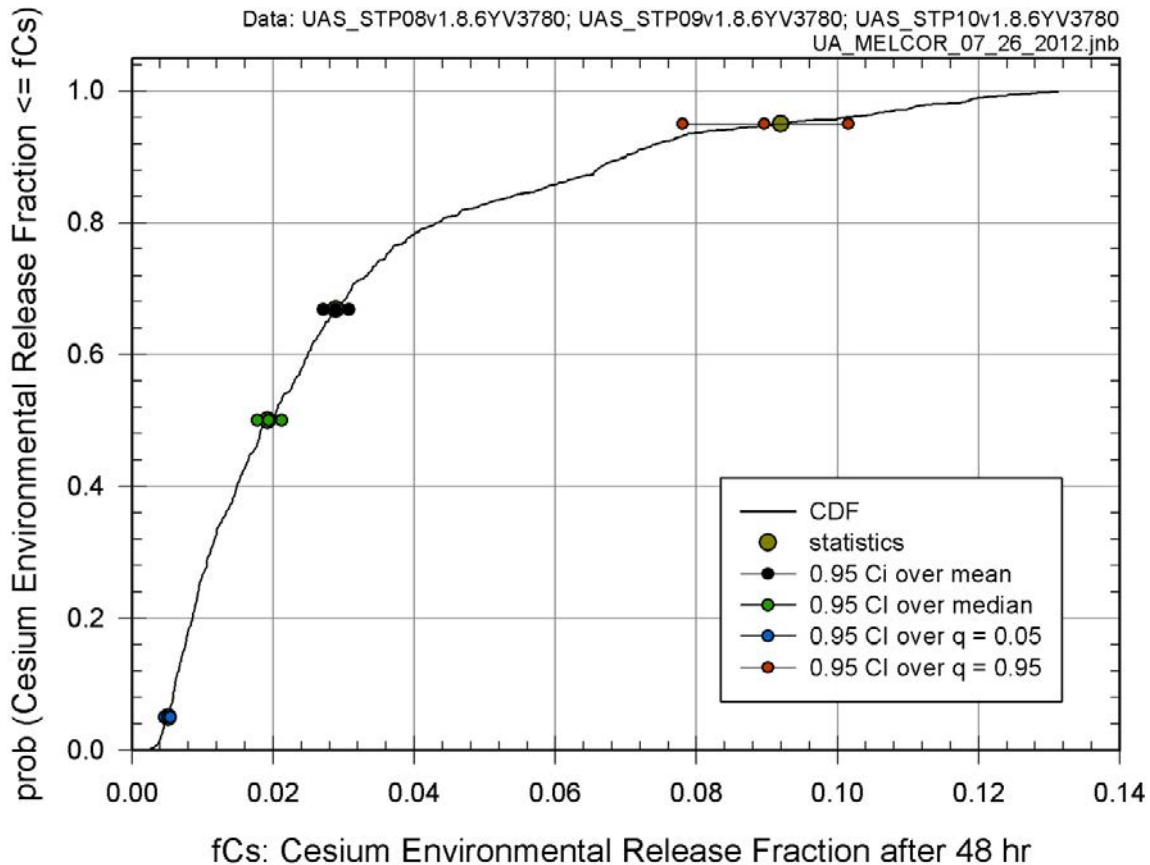


Figure 6.1-5 Cumulative distribution function of fraction of cesium core inventory released to the environment after 48 hours based on all combined (i.e., 865) results, with 95% confidence interval over mean, median and quantiles $q = 0.05$ and $q = 0.95$ for the Peach Bottom Unmitigated LTSBO

Table 6.1-6 presents the results of the four regression analyses applied to the fraction of the cesium core inventory released to the environment over 48 hours. R^2 are not as good as for fraction of iodine released, as three of them range between 0.6 and 0.66 of the variance explained and only recursive partitioning seems to find a better match with 0.9 of the variance explained. As for fraction of the cesium core inventory released to the environment, the most important parameter is SRVLAM, explaining again about half of the variance by itself. All three non-additive techniques agree that SRVLAM explain 10% to 20% more of the variance with conjoint influence of the other uncertain parameters. The next most important parameter is SRVOAFRAC for all three non-monotonic regressions, explaining 7% to 12% of the variance by itself and between 19% and 33% with conjoint influence of the other uncertain parameters. The regression results also indicate that FL904A, the fuel failure criterion on the transformation of intact fuel into particulate debris (FFC, described in Section 4.1.2) and RRDOOR explain between 2% and 5% of the uncertainty depending on the techniques. The influence of RRDOOR is not captured, as expected, by MARS.

Finally, three parameters (CHEMFORM, SC1131_2, and RRIDFRAC) seem to explain a very small amount of variance in the fraction of cesium released (around 1% each). For CHEMFORM, both quadratic and recursive partitioning suggest that it may have an effect in conjunction with other variables. This makes sense physically as chemisorption, the phenomenon behind the influence of CHEMFORM, is only strong at the relatively higher core

degradation temperatures consistent with SRV thermal with or without MSL creep rupture (as described in Section 6.1.4). The regression analyses confirms that CHEMFORM is the most important parameter when only MSL creep rupture cases are considered, explaining between 30% and 50% of the variance (see Table 6.1-9). This kind of specific influence is better captured with tree analysis (which is the basis for recursive partitioning). This explains why only recursive partitioning captures fully this influence, leading to a higher R^2 value.

The different influences that variations in SRVLAM have on releases to the environment are discussed at length in Section 6.1.4. The largest influence with respect to cesium release affects the slow revaporization of material off of reactor internals; longer times to SRV failure leading to more revaporization. The revaporization comes after reactor lower head failure and after drywell liner melt-through. The cesium migrates from the reactor vessel condensing to aerosol and exits the drywell through the breach in the liner.

As in the case with iodine, the conjoint influence noted for SRVOAFRAC reflects the importance of this parameter with respect to whether a MSL rupture occurs. MSL ruptures consistently resulted in larger releases of cesium but SRVOAFRAC alone does not determine whether or not a MSL rupture occurs. MSL ruptures result in higher releases because, for a period of time before lower head failure, the reactor vents to the drywell rather than to the wetwell. Scrubbing by the wetwell is not realized during this time and the cesium introduced to the drywell is available to leak to the environment.

The dependence of FL904A reflects the fission product releases associated with contaminated water surging up from the wetwell given larger values of this parameter as described in Section 6.1.4. The water pools on the drywell floor, in contact with the core debris relocated from the reactor, and eventually boils away, releasing its content of radionuclides including cesium. Larger values of FL904A (larger drywell breaches from liner melt-through) support the surging of water up from the wetwell.

FFC is important to cesium release in that it affects how long fuel remains standing. The longer fuel remains standing the longer oxidation of fuel cladding persists. Persistent oxidation drives continued revaporization of cesium deposits off of reactor internals late (i.e., after reactor lower head failure). The revaporized cesium migrates from the reactor to the drywell condensing to aerosol and escapes containment through the drywell liner melt-through. Conjoint influence of FFC and SC1131_2 (zirconium melt breakout temperature) is suspected as longer standing fuel and delayed draining away of zircaloy would combine to give the most persistent oxidation.

RRDOOR (railroad doors open/closed) is important to cesium release in the same way as it is important to iodine release in that open doors promote the development of a buoyant draft in the reactor building.

In conclusion, more of the variance is explained by recursive partitioning than by the other methods, considering that MARS misses the influence of the discrete variable RRDOOR, while rank regression misses the non-monotonic influence of SRVOAFRAC, which also seems to be underestimated by the quadratic regression. The regression analyses combined indicate that eight input parameters (SRVLAM, SRVOAFRAC, FL904A, FFC, RRDOOR, CHEMFORM, SC1131_2, and RRIDFRAC) explain between 70% and 75% of the variance, the last three accounting for a relatively small contribution to the overall variance in the results. The effect of CHEMFORM is more important than suspected by regression techniques other than recursive partitioning by which the total variance explained is probably closer to 85% to 90%. Once again, amongst the remaining parameters, only SRVFAILT seems to have a small influence, but at best on the order of 1%.

Table 6.1-6 Regression analyses of fraction of cesium released over 48 hours

	Rank Regression			Quadratic			Recursive Partitioning			MARS		
Final R ²	0.61			0.64			0.90			0.66		
Input name	R ² inc.	R ² cont.	SRRC	S _i	T _i	p-val	S _i	T _i	p-val	S _i	T _i	p-val
SRVLAM	0.50	0.50	-0.72	0.39	0.64	0.00	0.43	0.70	0.00	0.57	0.68	0.00
FL904A	0.53	0.03	0.19	0.01	0.04	0.12	0.06	0.02	0.44	0.00	0.03	0.10
FFC	0.55	0.02	0.19	0.04	0.05	0.31	0.02	0.10	0.00	0.01	0.08	0.00
RRDOOR	0.58	0.03	0.33	0.02	0.10	0.00	0.02	0.03	0.19	---	---	---
SRVOAFRAC	0.59	0.02	-0.13	0.07	0.19	0.00	0.11	0.33	0.00	0.12	0.27	0.00
CHEMFORM	0.60	0.01	0.09	0.00	0.08	0.38	0.01	0.18	0.00	0.02	0.00	0.87
SC1131_2	0.60	0.01	-0.07	0.02	0.01	0.63	0.00	0.07	0.00	0.00	0.04	0.01
RRIDFRAC	0.61	0.00	0.06	0.05	0.00	1.00	0.00	0.01	0.57	0.01	0.03	0.07
BATTDUR	0.61	0.00	0.04	0.03	0.02	0.49	0.00	0.02	0.47	0.00	0.01	0.53
RRODFRAC	---	---	---	0.01	0.04	0.15	0.00	0.03	0.16	0.00	0.00	1.00
SRVFAILT	---	---	---	0.04	0.03	0.27	0.00	0.04	0.11	0.01	0.00	1.00
DGASKET	---	---	---	0.00	0.03	0.27	0.00	0.06	0.02	---	---	---
H2IGNC	---	---	---	0.03	0.02	0.34	---	---	---	0.01	0.00	1.00
SC1141_2	---	---	---	0.05	0.01	0.52	0.00	0.08	0.00	0.00	0.00	1.00
SLCRFRAC	---	---	---	0.00	0.01	0.66	---	---	---	0.00	0.02	0.06
EBOLT	---	---	---	---	---	---	0.00	0.03	0.02	---	---	---
RHONOM	---	---	---	---	---	---	0.03	0.02	0.40	0.00	0.03	0.05
RDSTC	---	---	---	---	---	---	---	---	---	0.00	0.00	1.00
DHEADSOL	---	---	---	---	---	---	---	---	---	---	---	---

In order to understand the driving factors for cesium release to the environment, the realizations have been segregated according to the three different modes of RPV depressurization (SRV stochastic, SRV thermal, and MSL creep ruptures) and analyzed through the same techniques. Table 6.1-7 presents the results of regression analyses for the environmental cesium release fraction over 48 hours for the realizations leading to only an SRV stochastic failure. Regressions are not as good as for iodine: R² values are ranging from 0.4 to 0.5 for three regression techniques, with only Recursive partitioning R² reaching 0.8.

Similarly to the regression for iodine, FL904A is the most important parameter explaining about 20% of the variance. CHEMFORM is in the second position, explaining about 10% of the variance. The effect of SRVLAM is not as strong here for rank regression and quadratic regression (respectively 5% and 10%) but recursive partitioning identifies it as one of the most important parameters (while MARS agrees with recursive partitioning, its low R² value requires caution in interpreting results from variance decomposition). Another important parameter is FFC: results from quadratic regression, recursive partitioning and MARS attribute this parameter and influence varying between 15% and 20% of the variance by itself and up to 50% conjointly. Its effect is likely non-monotonic considering it is predicted as unimportant by rank regression. As described in Section 4.1.2, FFC is an indicator function whose value varies from one to three. The value of one represents the nominal case and the numbers two and three represent shifts in temperature of 100 K and in fuel endurance of time with a factor of ½ and 2

respectively (creating optimistic and pessimistic conditions). Such characterization creates by default an asymmetry in the influence of the parameter. The influence of the remaining parameters is low.

The importance of FL904A is explained by the significant amount of cesium made available for release as a consequence of wetwell water surging up onto the drywell floor as described in the previous section. The importance of CHEMFORM stems from cesium hydroxide being generally more transportable than cesium molybdate due to its higher vapor pressure (i.e., due to it being more readily evaporable). Dependent on the CHEMFORM choice, more or less cesium is initialized as cesium hydroxide. The fact that SRVLAM is important in the subset of cases that experience SRV stochastic failure, given that it is the sole sampled parameter that determines whether a case is in the subset, identifies that the timing of the stochastic failure (not just whether a stochastic failure happens) is important to cesium release to the environment. FFC is important due to its impact on core oxidation as described earlier in this section.

Table 6.1-7 Regression analyses of fraction of cesium released over 48 hours for realizations leading to SRV stochastic failure

	Rank Regression			Quadratic			Recursive Partitioning			MARS		
Final R ²	0.47			0.51			0.80			0.39		
Input name	R ² inc.	R ² cont.	SRRC	S _i	T _i	p-val	S _i	T _i	p-val	S _i	T _i	p-val
FL904A	0.22	0.22	0.47	0.14	0.21	0.04	0.16	0.40	0.00	0.22	0.19	0.04
CHEMFORM	0.28	0.06	0.24	0.07	0.00	0.95	0.07	0.07	0.81	0.02	0.09	0.02
SRVLAM	0.34	0.05	-0.25	0.10	0.17	0.02	0.19	0.20	0.03	0.38	0.45	0.00
FFC	0.34	0.00	0.07	0.18	0.51	0.00	0.14	0.43	0.00	0.23	0.36	0.00
RRDOOR	0.37	0.03	0.44	0.02	0.16	0.01	0.00	0.00	1.00	---	---	---
SC1131_2	0.40	0.03	-0.15	0.02	0.09	0.08	0.04	0.12	0.00	0.02	0.00	1.00
SC1141_2	0.41	0.01	0.10	0.00	0.10	0.02	0.00	0.11	0.01	0.00	0.02	0.30
BATTDUR	0.42	0.01	0.09	0.05	0.02	0.46	0.00	0.03	0.24	0.00	0.15	0.00
RRIDFRAC	0.42	0.01	0.09	---	---	---	---	---	---	0.00	0.07	0.02
DHEADSOL	0.43	0.01	-0.07	---	---	---	0.00	0.01	0.65	0.00	0.00	1.00
EBOLT	0.43	0.00	-0.06	0.02	0.10	0.05	0.00	0.08	0.00	---	---	---
RRODFRAC	---	---	---	0.00	0.06	0.10	0.02	0.02	0.37	0.01	0.00	1.00
SRVOAFRAC	---	---	---	0.02	0.07	0.20	---	---	---	0.02	0.02	0.29
RHONOM	---	---	---	0.00	0.00	1.00	0.00	0.07	0.06	---	---	---
KBOLT	---	---	---	---	---	---	0.00	0.03	0.23	---	---	---
RDSTC	---	---	---	---	---	---	0.00	0.00	1.00	0.01	0.00	1.00
DGASKET	---	---	---	---	---	---	0.00	0.00	1.00	---	---	---
SRVFAILT	---	---	---	---	---	---	---	---	---	0.00	0.09	0.00
SLCRFRAC	---	---	---	---	---	---	---	---	---	0.00	0.06	0.04
H2IGNC	---	---	---	---	---	---	---	---	---	0.00	0.00	1.00

Once again the regression analyses for environmental cesium release fraction for SRV thermal failures without MSL creep rupture do not lead to an R^2 as high as for iodine (between 0.4 and 0.70), but are better than for SRV stochastic failures as can be shown in Table 6.1-8.

CHEMFORM, RRDOOR and FFC are the top three parameters explaining about 40% of the uncertainty for all regressions techniques. Considering that MARS does not identify RRDOOR influences, but may be better estimating other parametric influences, the total variance explained by these three parameters is probably closer to 50% to 60%. In fourth position, SRVOAFRAC seems to explain an additional 5% to 15% of the uncertainty. It is reasonable to consider that, with MARS missing the effect of RRDOOR and Rank regression missing non-monotonic and conjoint influences, these four parameters explain about 70% of the uncertainty. The influence of the remaining parameters is relatively low and each of them should explain no more than 2 to 3% of the variance.

CHEMFORM is important in the subset of cases that experience a thermal SRV failure for a different reason than in the subset of cases that experience stochastic SRV failure. The greater oxidation taking place during core degradation at the higher pressures and temperatures resulting from the SRV cycling successfully for a longer period of time is fundamentally important here. The greater oxidation drives reactor temperatures high enough to be supportive of the chemisorption of cesium from cesium hydroxide into stainless steel. The chemisorption permanently captures cesium in the reactor vessel. RRDOOR and FFC are important as described in the previous section and earlier in this section, respectively.

Table 6.1-8 Regression analyses of fraction of cesium released over 48 hours for realizations leading to SRV thermal failure without MSL creep rupture

	Rank Regression			Quadratic			Recursive Partitioning			MARS		
Final R ²	0.51			0.71			0.74			0.38		
Input name	R ² inc.	R ² cont.	SRRC	S _i	T _i	p-val	S _i	T _i	p-val	S _i	T _i	p-val
RRDOOR	0.20	0.20	0.75	0.12	0.10	0.05	0.20	0.38	0.00	---	---	---
CHEMFORM	0.31	0.12	0.38	0.09	0.24	0.00	0.06	0.10	0.07	0.20	0.17	0.06
FFC	0.37	0.05	0.40	0.09	0.20	0.01	0.13	0.25	0.00	0.25	0.26	0.00
SRVOAFRAC	0.40	0.03	-0.20	0.09	0.02	0.67	0.08	0.28	0.01	0.15	0.13	0.04
FL904A	0.44	0.04	0.21	---	---	---	0.02	0.17	0.05	0.00	0.00	1.00
SC1131_2	0.45	0.01	-0.11	0.04	0.10	0.06	0.01	0.09	0.30	0.04	0.04	0.36
RHONOM	0.45	0.01	-0.07	0.01	0.00	1.00	0.00	0.11	0.02	---	---	---
RRODFRAC	0.46	0.01	-0.09	0.00	0.06	0.16	0.00	0.06	0.24	0.00	0.02	0.13
SC1141_2	0.46	0.00	0.06	0.00	0.04	0.48	0.00	0.00	1.00	0.00	0.00	0.43
SRVLAM	---	---	---	0.00	0.16	0.01	0.02	0.00	1.00	0.00	0.00	1.00
EBOLT	---	---	---	0.00	0.07	0.11	---	---	---	---	---	---
BATTDUR	---	---	---	0.03	0.06	0.13	0.00	0.13	0.00	0.01	0.05	0.04
DHEADSOL	---	---	---	0.02	0.05	0.15	---	---	---	0.04	0.00	0.55
RRIDFRAC	---	---	---	0.00	0.04	0.35	---	---	---	0.00	0.02	0.08
SLCRFRAC	---	---	---	0.00	0.17	0.43	---	---	---	0.00	0.02	0.15
SRVFAILT	---	---	---	0.00	0.04	0.46	0.02	0.13	0.02	0.04	0.01	0.47
KBOLT	---	---	---	---	---	---	0.00	0.13	0.01	---	---	---
H2IGNC	---	---	---	---	---	---	0.00	0.04	0.20	0.00	0.03	0.09
DGASKET	---	---	---	---	---	---	0.00	0.01	0.66	---	---	---
RDSTC	---	---	---	---	---	---	---	---	---	0.02	0.00	1.00

The regression results for the fraction of cesium released to the environment considering only realizations exhibiting SRV thermal failure with MSL creep rupture are presented in Table 6.1-9. R² values are high for all regression techniques (from 0.6 to 0.9), as they were for the analysis of iodine release. CHEMFORM is the most important parameter explaining between 33% and 50% of the uncertainty. Second, is RRDOOR explaining another 20% (except for MARS) of the uncertainty. SRVOAFRAC and BATTDUR explain between 5% and 10% more of the uncertainty. The remaining parameters have a small effect compared to these four.

CHEMFORM is important to the MSL rupture cases in the same way as it is to the SRV thermal failure cases; that being through the phenomenon of chemisorption. Chemisorption of cesium is most prevalent in the MSL rupture cases because they experience successful SRV cycling for the longest period of time. RRDOOR is important as described in the previous section.

That SRVOFRAC explains a significant amount of the uncertainty in the subset of calculations that experience a MSL rupture is interesting. As described in Section 6.1.4, the value of this variable is the key to whether or not a MSL rupture occurs. That it shows to be important in the MSL-rupture subset of calculations means that its influence goes beyond determining whether a

rupture occurs. The SRV (that seizes open) is downstream of the MSL rupture. Therefore, it seems the further influence of SRVOFRAC on cesium release must come before MSL rupture.

BATTDUR being important to the magnitude of cesium release is non-intuitive. That this variable would affect release timing is intuitive but not that it would affect release magnitude. The reason BATTDUR is showing to be important to magnitude is that cesium release in a significant number of calculations is not over at 48 hrs. The shift in release history dependent upon BATTDUR, and the generally greater release magnitudes in MSL rupture cases, affects the reported cumulative release at 48 hrs.

Table 6.1-9 Regression analyses of fraction of cesium released over 48 hours for realizations leading to SRV thermal failure and MSL creep rupture

	Rank Regression			Quadratic			Recursive Partitioning			MARS		
Final R ²	0.67			0.74			0.91			0.64		
Input name	R ² inc.	R ² cont.	SRRC	S _i	T _i	p-val	S _i	T _i	p-val	S _i	T _i	p-val
CHEMFORM	0.32	0.32	0.56	0.43	0.48	0.00	0.33	0.57	0.00	0.52	0.51	0.00
RRDOOR	0.50	0.18	0.63	0.24	0.26	0.00	0.18	0.27	0.00	---	---	---
SRVOAFRAC	0.56	0.06	-0.27	0.03	0.10	0.06	0.05	0.22	0.00	0.11	0.12	0.00
BATTDUR	0.62	0.05	0.23	0.06	0.03	0.52	0.04	0.18	0.00	0.03	0.06	0.35
SLCRFRAC	0.63	0.01	0.20	0.05	0.08	0.33	0.00	0.03	0.00	0.02	0.00	1.00
RRIDFRAC	0.64	0.01	0.11	---	---	---	0.00	0.07	0.03	0.01	0.05	0.01
SRVFAILT	0.66	0.02	0.12	0.07	0.04	0.26	0.00	0.03	0.06	0.03	0.00	1.00
FL904A	0.66	0.01	0.09	---	---	---	0.01	0.01	0.58	0.00	0.03	0.03
SRVLAM	0.67	0.01	-0.09	0.00	0.10	0.04	---	---	---	0.04	0.04	0.30
RRODFRAC	---	---	---	0.00	0.00	1.00	---	---	---	0.01	0.00	1.00
DGASKET	---	---	---	---	---	---	0.02	0.09	0.00	---	---	---
DHEADSOL	---	---	---	---	---	---	0.01	0.05	0.01	0.03	0.05	0.01
SC1131_2	---	---	---	---	---	---	0.04	0.10	0.04	0.00	0.00	0.49
EBOLT	---	---	---	---	---	---	0.00	0.03	0.13	---	---	---
H2IGNC	---	---	---	---	---	---	0.01	0.00	1.00	0.00	0.05	0.02
SC1141_2	---	---	---	---	---	---	0.02	0.00	1.00	0.00	0.00	1.00
FFC	---	---	---	---	---	---	---	---	---	0.00	0.00	1.00
RDSTC	---	---	---	---	---	---	---	---	---	0.00	0.00	1.00

6.1.3 Hydrogen Production

As described in Section 4.1, in-vessel hydrogen production can be associated with fission product release to the environment, and, in its own right, hydrogen production is crucial considering the severe damage potential hydrogen poses to a reactor building should it burn. The amount of hydrogen generated in-vessel through 48 hours is considered in the following analysis. A CDF of the hydrogen production at 48 hours is displayed on Figure 6.1-6. Confidence Intervals show that the results are fairly well-converged, even at the 95th percentile.

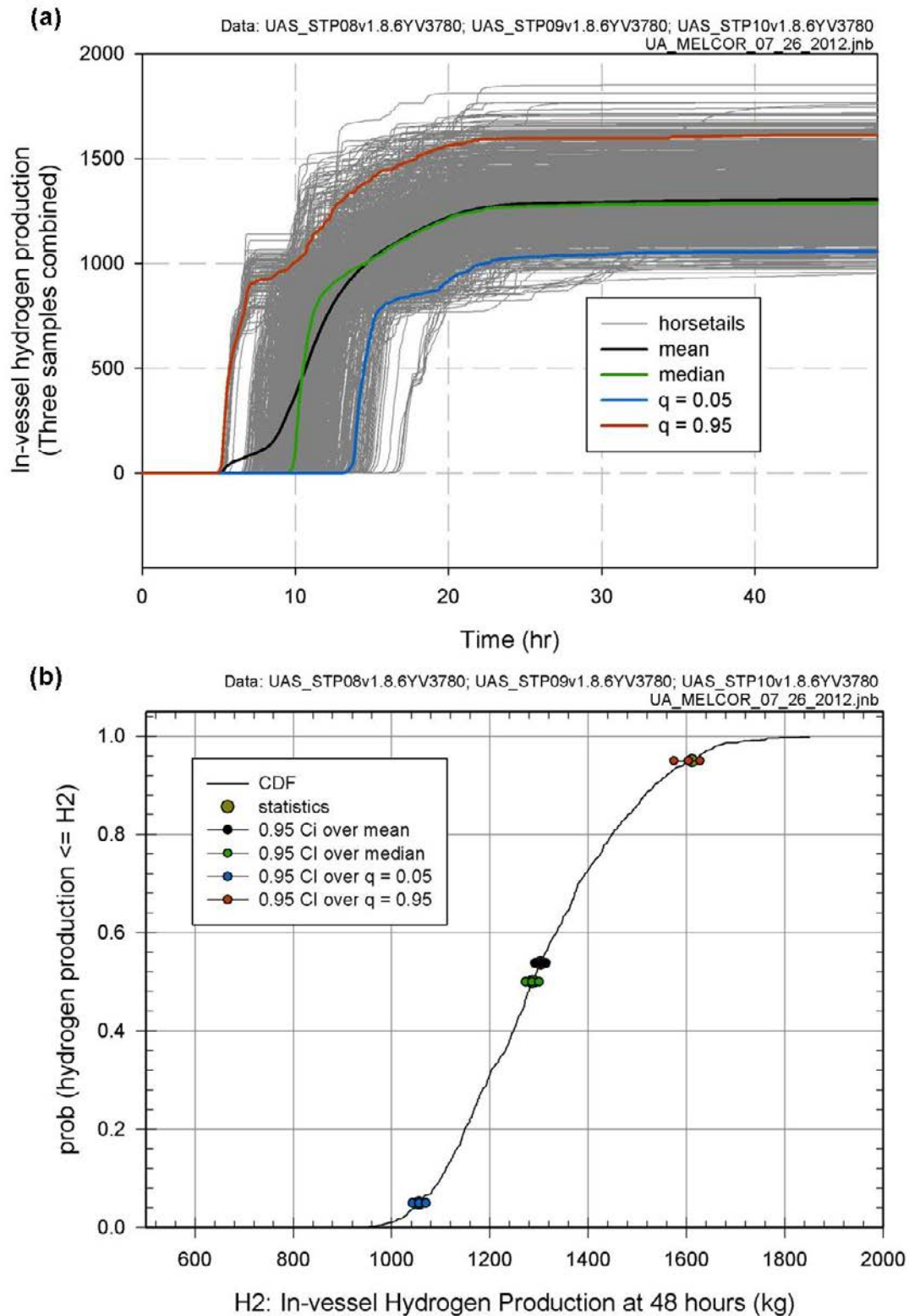


Figure 6.1-6 Time-dependent fraction (a) and cumulative distribution function (b) of in-vessel hydrogen production over 48 hours based on combined (i.e., 865) results, with 95% confidence interval over mean, median and quantiles $q = 0.05$ and $q = 0.95$ for the Peach Bottom Unmitigated LTSBO

Table 6.1-10 shows the regression analysis for hydrogen production. SRVLAM is the most important parameter explaining between 40% and 66% of the variance, depending on the regression technique. All regressions found SRVLAM accounts for at least 50% of the uncertainty by itself, with at least 15% more in conjunction with other parameters. SC1131_2 appears to be the second most influential uncertainty with a contribution between 14% and 25% to the variance, followed by SC1141_2 with a contribution between 1% and 5%. All the other parameters seem to have negligible influence or questionable results (i.e., are only found in some regressions and associated with high p-values). As described in section 6.1.2, FFC and SC1131_2 are expected to have a conjoint influence on hydrogen production. While it seems that the quadratic regression captures this influence, MARS seems to attribute it mostly to SC1131_2 solely, while recursive partitioning recognizes some conjoint influence for SC1131_2 but fail to attribute it to FFC. This lack of accuracy is not surprising considering that the conjoint influence is partly hidden by the strong influence of SRVLAM, and by the particular structure of FFC (indicator function) that makes its influence detection more difficult.

Principally important to hydrogen generation is how much core degradation occurs at high pressure (i.e., SRV set-point pressure). More core degradation at high pressure relates to more hydrogen generation from oxidation. The most important parameter affecting the amount of core damage occurring at high pressure is SRVLAM. If the SRV (the lowest set-point SRV) sticks open early, e.g., before the onset of core damage, no core degradation takes place at high pressure and so relatively little hydrogen is produced. If the SRV sticks open late (e.g., 1.25 hours after the onset of core damage,) substantial core degradation takes place at high pressure and a relatively large amount of hydrogen is produced.

SC1141_2 is important to hydrogen production, as mentioned in the previous section, in that it determines how long un-oxidized molten zirconium is held behind an oxidized cladding shell. The longer the zirconium is held the longer oxidation takes place and the more hydrogen produced.

Table 6.1-10 Regression analysis of hydrogen production.

	Rank Regression			Quadratic			Recursive Partitioning			MARS		
Final R ²	0.55			0.63			0.88			0.65		
Input name	R ² inc.	R ² cont.	SRRC	S _i	T _i	p-val	S _i	T _i	p-val	S _i	T _i	p-val
SRVLAM	0.39	0.39	-0.64	0.48	0.65	0.00	0.50	0.70	0.00	0.66	0.75	0.00
SC1131_2	0.53	0.14	0.37	0.19	0.29	0.00	0.17	0.33	0.00	0.25	0.26	0.00
SC1141_2	0.54	0.01	-0.11	0.03	0.08	0.01	0.03	0.14	0.00	0.05	0.05	0.03
RDSTC	0.54	0.01	0.07	0.02	0.00	0.73	0.02	0.04	0.10	0.00	0.02	0.18
CHEMFORM	0.55	0.00	0.04	0.01	0.09	0.00	---	---	---	0.03	0.01	0.19
BATTDUR	0.55	0.00	0.06	0.00	0.00	1.00	---	---	---	0.00	0.02	0.04
SRVFAILT	0.55	0.00	0.05	0.03	0.07	0.01	0.02	0.00	1.00	0.00	0.00	1.00
DGASKET	0.55	0.00	0.04	---	---	---	0.04	0.00	1.00	---	---	---
EBOLT	0.55	0.00	0.03	0.01	0.00	1.00	0.01	0.00	1.00	---	---	---
RRIDFRAC	0.55	0.00	0.03	---	---	---	0.00	0.04	0.04	0.01	0.00	1.00
SRVOAFRAC	---	---	---	0.00	0.09	0.00	0.06	0.04	0.02	0.00	0.00	1.00
FFC	---	---	---	0.00	0.05	0.05	---	---	---	0.02	0.00	0.53
H2IGNC	---	---	---	0.00	0.02	0.46	0.00	0.04	0.02	0.03	0.00	1.00
RRDOOR	---	---	---	0.04	0.02	0.54	---	---	---	---	---	---
RHONOM	---	---	---	0.04	0.01	0.66	0.04	0.06	0.00	---	---	---
KBOLT	---	---	---	0.00	0.00	1.00	0.00	0.02	0.36	---	---	---
RRODFRAC	---	---	---	0.00	0.00	1.00	0.02	0.00	0.62	0.01	0.01	0.32
SLCRFRAC	---	---	---	---	---	---	0.02	0.03	0.00	0.03	0.00	0.40
DHEADSOL	---	---	---	---	---	---	0.04	0.03	0.18	0.00	0.01	0.12
FL904A	---	---	---	---	---	---	---	---	---	0.02	0.00	1.00

6.1.4 Analysis of Important Phenomena and Single Realizations

Analysis of single realizations provides a specific insight into the physical phenomena controlling the variability in the source term release results. A comprehensive explanation detailing how the release is affected by various components of the complex model of the reactor system and associated uncertain parameters for each failure modes (SRV Stochastic, SRV thermal, and MSL creep ruptures) under varying physical-chemical-thermal-mechanical conditions provides confidence that the various processes are working as expected and insight to the phenomena that are driving the results. This in turn defines the phenomenology driven by the key uncertain parameters identified in the parameter uncertainty analyses presented in earlier sections of this document.

Individual realizations from Replicate 1 were selected for investigation in greater detail to identify the phenomena affecting their cesium releases to the environment. The distribution of the fraction of the cesium inventory released to the environment for Replicate 1 is shown on

Figure 6.1-7, along with selected statistics (median and 5th and 95th percentiles). For comparison with Replicate 1 results, Figure 6.1-7, and Figure 6.1-8(a) include the SOARCA Peach Bottom unmitigated LTSBO scenario for the case where a stochastic failure of the SRV occurs. Figure 6.1-7 also includes the SOARCA Peach Bottom sensitivity case with an MSL creep rupture.

Representative single realizations were selected for each of the three failure modes. These realizations, selected for detailed analysis, are representative of the overall distribution of the results for all replicate sets. The realizations were also selected to be representative of the distribution of results over each group of the three failure scenarios (Stochastic SRV failures, Thermal SRV failures, and Thermal SRV failures with MSL creep rupture occurring). Figure 6.1-8 shows, on a linear scale, the distribution of results for each of the failure modes as well as the realizations selected. The individual analysis includes realizations that represent outliers, median and low (5th percentile) and high (95th percentile) behavior. Collectively these single realizations describe the phenomena driven by the key uncertainties in the complex system. Table 6.1-11 lists the sampled parameter values for the single realizations selected for the detailed analysis. Table 6.1-12 presents key event timings, key occurrences/attributes, and cesium and iodine releases to the environment for the selected realizations.

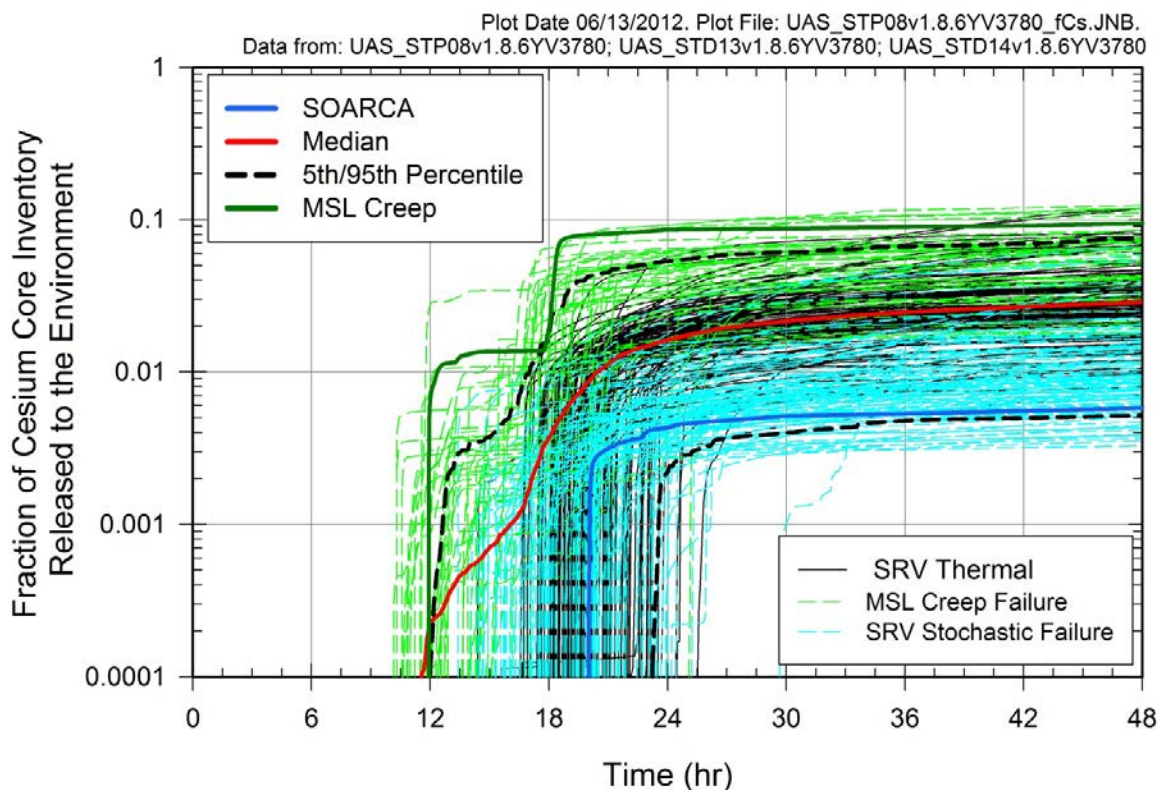


Figure 6.1-7 Distribution for the fraction of cesium core inventory released to the environment for Replicate 1 of the source term uncertainty analysis of the SOARCA Peach Bottom unmitigated LTSBO scenario

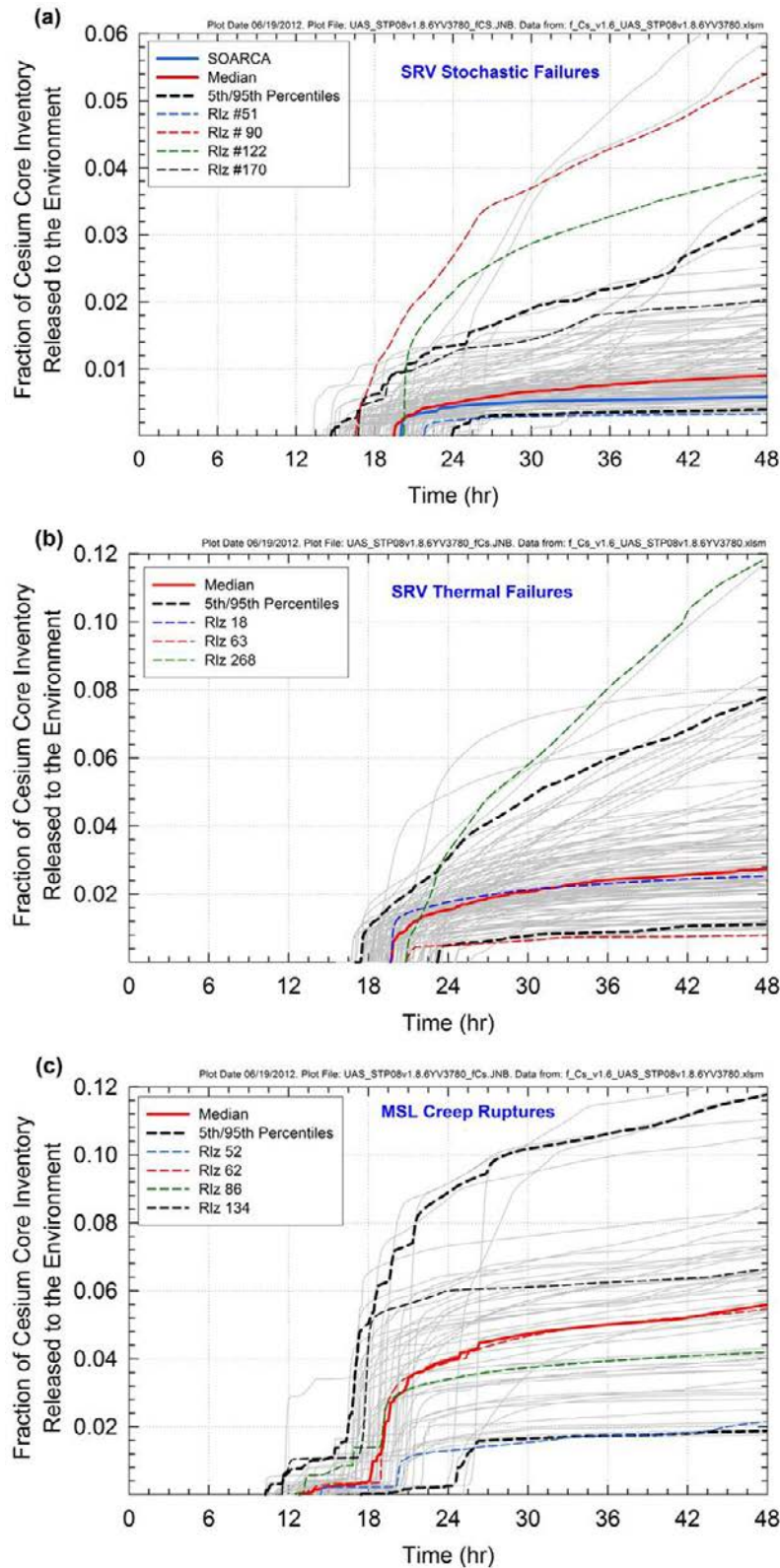


Figure 6.1-8

Single realizations selected for detailed analysis from Replicate 1 of the Peach Bottom unmitigated LTSBO, fraction of cesium core inventory released to the environment for (a) SRV stochastic failures, (b) SRV thermal failures, and (c) MSL creep ruptures

Table 6.1-11 Sampled parameter values for Replicate 1 (STP08) for selected individual realizations

Parameter	SOARCA	18	51	52	62	63	86	90	122	134	170	268
SRV failure to reclose (SRVLAM) per demand	3.70E-03	7.90E-05	4.45E-03	9.42E-04	2.14E-04	2.02E-03	9.90E-04	2.41E-03	2.16E-03	1.78E-04	3.97E-03	1.01E-03
Battery duration (BATTDUR) hrs	4.00E+00	4.14E+00	5.11E+00	4.76E+00	3.79E+00	4.66E+00	3.72E+00	2.19E+00	4.26E+00	3.74E+00	2.86E+00	4.58E+00
Zircaloy melt breakout temperature (SC1131(2)) K	2.40E+03	2.26E+03	2.37E+03	2.41E+03	2.42E+03	2.39E+03	2.16E+03	2.34E+03	2.41E+03	2.48E+03	2.36E+03	2.35E+03
Molten clad drainage rate (SC1141(2)) kg/m-s	2.00E-01	4.56E-01	2.79E-01	2.19E-01	5.70E-01	2.71E-01	3.92E-01	2.20E-01	2.90E-01	1.60E-01	5.57E-01	2.27E-01
SRV thermal failure criterion (SRVFAILT) K	9.00E+02	8.38E+02	9.50E+02	9.18E+02	8.72E+02	8.57E+02	8.63E+02	9.29E+02	9.26E+02	8.99E+02	9.66E+02	8.86E+02
SRV open fraction (SRVOAFRAC) unitless	1.00E+00	6.87E-01	5.46E-01	3.23E-01	3.91E-01	7.53E-01	2.46E-01	7.08E-01	5.23E-01	1.64E-01	9.42E-01	5.98E-01
MSL creep rupture area (SLCRFRAC) unitless	0.00E+00	0.00E+00	0.00E+00	0.00E+00	0.00E+00	0.00E+00	4.00E-01	0.00E+00	1.00E-01	0.00E+00	5.00E-01	8.00E-01
Fuel failure criterion (FFC) unitless	0.00E+00	1.00E+00	1.00E+00	1.00E+00	3.00E+00	3.00E+00	1.00E+00	3.00E+00	1.00E+00	1.00E+00	1.00E+00	1.00E+00
Solid debris radial relocation (RDSTC) s	3.60E+02	3.10E+02	4.72E+02	2.35E+02	2.82E+02	2.50E+02	2.83E+02	3.04E+02	3.91E+02	4.13E+02	3.62E+02	3.11E+02
Molten debris radial relocation (RDMTC) s	6.00E+01	5.31E+01	8.12E+01	4.09E+01	4.73E+01	4.19E+01	4.77E+01	5.21E+01	6.75E+01	7.11E+01	6.17E+01	5.31E+01
Debris height for solid core-concrete (DHEADSOL) m	5.00E-01	5.56E-01	6.06E-01	5.95E-01	4.02E-01	7.02E-01	6.41E-01	5.57E-01	5.73E-01	8.73E-01	7.06E-01	6.48E-01

Table 6.1-11 Sampled parameter values for Replicate 1 (STP08) for selected individual realizations (continued)

Parameter	SOARCA	18	51	52	62	63	86	90	122	134	170	268
Debris height for molten core-concrete debris (DHEADLIQ) m	1.52E-01	1.47E-01	1.57E-01	1.56E-01	1.16E-01	1.84E-01	1.66E-01	1.47E-01	1.51E-01	2.24E-01	1.85E-01	1.67E-01
DW liner melt-thru area (FL904A) m2	1.00E-01	1.49E-01	1.38E-01	5.30E-02	1.88E-01	5.28E-02	1.42E-01	6.83E-01	1.99E-01	7.38E-02	9.07E-01	7.55E-02
H ₂ ignition criterion (H2IGNC) mole fraction	1.00E-01	1.41E-01	1.08E-01	5.47E-02	9.45E-02	1.43E-01	5.25E-02	7.16E-02	1.51E-01	1.02E-01	9.03E-02	9.75E-02
Inner RR door open fraction (RRIDFRAC) unitless	5.00E-01	6.90E-01	1.69E-01	2.69E-01	1.82E-01	4.21E-01	2.32E-01	2.74E-01	4.01E-01	1.44E-01	3.34E-01	5.94E-01
Outer RR door open fraction (RRODFRAC) unitless	5.00E-01	1.28E-01	1.32E-01	3.17E-01	4.08E-01	2.58E-01	6.74E-01	1.36E-01	5.90E-01	2.60E-01	3.64E-01	2.83E-01
Chemical form of I and Cs (CHEMFORM) unitless	5.00E+00	3.00E+00	3.00E+00	1.00E+00	5.00E+00	1.00E+00	4.00E+00	5.00E+00	5.00E+00	5.00E+00	1.00E+00	5.00E+00
Aerosol particle density (RHONOM) kg/m3	1.00E+03	4.01E+03	1.20E+03	1.62E+03	1.51E+03	2.10E+03	1.74E+03	3.31E+03	3.20E+03	3.48E+03	2.15E+03	2.72E+03
DW head bolt torque coeff. (KBOLT) unitless	8.00E-02	2.03E-01	3.52E-01	1.59E-01	1.34E-01	2.31E-01	2.42E-01	2.36E-01	3.88E-01	1.16E-01	2.17E-01	2.82E-01
DW head bolt modulus of elasticity (EBOLT) psi	1.93E+11	2.01E+11	1.86E+11	2.00E+11	2.00E+11	2.01E+11	1.93E+11	1.86E+11	1.91E+11	1.95E+11	2.00E+11	1.88E+11
DW head gasket rebound thickness (DGASKET) inch	7.62E-04	6.80E-04	7.02E-04	8.39E-04	8.48E-04	7.08E-04	7.87E-04	6.66E-04	7.69E-04	7.20E-04	7.26E-04	7.42E-04

Table 6.1-12 Timing of events, key occurrences/attributes, and environmental releases for selected individual realizations of the Peach Bottom unmitigated LTSBO Replicate 1 (STP08)

Event	Timing by realization (hr)											
	SOARCA	18	51	52	62	63	86	90	122	134	170	268
100 °F/hr cooldown initiated (SRV opened, RCIC throttled)	1.00	1.00	1.00	1.00	1.00	1.00	1.00	1.00	1.00	1.00	1.00	1.00
SRV closes on battery depletion	4.00	4.10	5.10	4.80	3.80	4.70	3.70	2.20	4.30	3.70	2.90	4.60
RCIC turbine floods failing RCIC	5.19	5.34	6.36	6.00	4.97	5.89	4.91	2.99	5.46	4.92	4.08	5.80
SRV fails to close due to excessive cycling	8.19	NA	9.07	NA	NA	NA	NA	8.17	11.67	NA	6.60	NA
Downcomer level drops to TAF	8.40	9.23	9.46	10.09	8.76	9.95	8.68	6.84	9.39	8.70	6.87	9.82
First fuel-cladding gap release	9.12	10.32	10.35	11.24	9.83	11.09	9.75	7.80	10.49	9.76	7.59	10.95
SRV fails to close due to the excessive temperature	NA	11.51	NA	12.59	10.99	12.34	10.95	NA	NA	11.01	NA	12.23
MSL creep rupture	NA	NA	NA	14.43	13.59	NA	12.48	NA	NA	11.51	NA	NA
First large scale relocation of core debris to lower plenum	10.69	13.50	11.92	14.26	13.47	14.09	13.01	9.77	12.46	11.77	8.85	13.11
RPV lower head failure	19.76	19.49	21.54	19.96	18.91	20.60	18.84	16.38	20.01	17.06	16.51	20.59
Drywell head flange leakage begins	19.87	14.87	13.61	14.44	13.61	15.00	12.48	10.54	14.54	11.51	16.52	15.94
Reactor building fails due to overpressure	19.92	16.20	21.60	14.44	13.61	15.90	12.48	16.46	15.79	11.52	16.55	20.66
Wetwell rupture (above waterline)	NA	NA	NA	14.44	NA	NA	NA	NA	NA	11.52	NA	NA
Drywell liner melt-through	20.00	19.72	21.78	20.19	19.14	20.83	19.07	16.61	20.24	17.29	16.76	20.82
H ₂ burns initiate in reactor building grossly damaging the building	20.01	19.74	21.68	14.44	18.98	20.85	13.16	16.57	20.26	11.52	16.78	20.76
Key occurrences/attributes	Value by realization											
	SOARCA	18	51	52	62	63	86	90	122	134	170	268
Elapsed time between SRV sticking open and onset of core damage (hr)	0.94	-1.18	1.28	-1.36	-1.16	-1.25	-1.20	-0.37	-1.18	-1.25	0.99	-1.28
Elapsed time between onset of core damage and MSL creep rupture (hr)	NA	NA	NA	3.19	3.76	NA	2.73	NA	NA	1.75	NA	NA
In-vessel H ₂ production (kg)	1,083	1,307	1,203	1,640	1,444	1,343	1,257	1,534	1,362	1,200	1,221	1,472
Surge of water from wetwell up onto drywell floor at liner melt-thru (Yes/No)	N	N	N	N	Y	N	N	Y	Y	N	Y	N
Railroad Doors blow open (Yes/No)	Y	Y	N	Y	Y	Y	Y	Y	Y	Y	Y	Y

Table 6.1-12 **Timing of events, key occurrences/attributes, and environmental releases for selected individual realizations of the Peach Bottom unmitigated LTSBO Replicate 1 (STP08) (continued)**

Releases to the environment	Value by realization											
	SOARCA	18	51	52	62	63	86	90	122	134	170	268
I release to environment > 0.1% (hr)	20.1	19.8	14.3	12.7	14.3	24.0	15.8	21.8	14.7	22.5	19.8	20.9
Cs release to environment by 48 hr (fraction)	0.005	0.025	0.003	0.021	0.055	0.008	0.042	0.054	0.039	0.066	0.020	0.119
I release to environment by 48 hr (fraction)	0.025	0.070	0.017	0.131	0.160	0.005	0.023	0.045	0.136	0.039	0.067	0.090

6.1.4.1 Identification of Important Phenomena

Several influences were found to strongly affect the amount of cesium released to the environment. The influences were (not necessarily in order of importance):

- (1). Whether the sticking open of the SRV (the lowest setpoint SRV) occurs before or after the onset of core damage
- (2). Whether an MSL creep rupture occurs
- (3). The elapsed time between the onset of core damage and MSL creep rupture (if an MSL creep rupture occurs)
- (4). The amount of cesium chemisorbed from CsOH into the stainless steel of RPV internals
- (5). Whether core debris relocates from the RPV to the reactor cavity all at once or over an extended period of time
- (6). The degree of oxidation, primarily zircaloy oxidation, occurring in-vessel (identified by the amount of in-vessel hydrogen production)
- (7). Whether a surge of water from the wetwell up onto the drywell floor occurs at drywell liner melt-through
- (8). Whether an overpressure rupture of the wetwell occurs
- (9). Whether the reactor building railroad doors are blown open by a hydrogen deflagration.

A discussion of each of these influences and their impact on cesium released follows.

SRV Failure Timing

Whether the SRV sticks open before or after core damage relates directly to the amount of cesium released from the core that is deposited in the wetwell. When the SRV is open, the RPV is vented to the wetwell pool. Fission products carried by the gas flow venting from the RPV are largely scrubbed by the pool. The earlier the SRV sticks open in the core degradation process, the more fission products are carried to the wetwell rather than deposited in the RPV. If the SRV sticks open before the onset of core damage, the venting of released fission products directly to the wetwell is maximized.

MSL Rupture

Whether an MSL rupture occurs also relates directly to the amount of cesium released from the core that is deposited in the wetwell. If an MSL creep rupture occurs, the path by which fission products carry through the stuck-open SRV to the wetwell pool is bypassed as gas venting from the RPV flows straight to the drywell. Instead of first being scrubbed by the wetwell pool, the fission products are introduced directly to the drywell, and then possibly to the environment via leakage through the drywell head flange or a drywell liner melt-through.

The elapsed time between the onset of core damage and MSL rupture similarly relates to the amount of cesium deposited in the wetwell. The more time that elapses between the onset of core damage and an MSL rupture the more time there is for gas flows venting from the RPV to carry fission products through the stuck-open SRV to the wetwell.

Key to whether an MSL creep rupture occurs is the uncertain parameter of SRV open fraction following the sticking open of an overheated SRV. Smaller stuck-open areas relieve steam more slowly and so lead to higher pressures. Higher pressures result in elevated stresses in the MSL piping which combine with elevated temperatures to accumulate creep damage over time that can lead to an MSL rupture. Figure 6.1-9 shows the relationship, for all the realizations in Replicate 1 experiencing SRV thermal failure, between (1) SRV open area fraction and occurrence of MSL creep rupture, and (2) the fraction of cesium core inventory released to the environment with and without MSL rupture, in plots a and b, respectively.

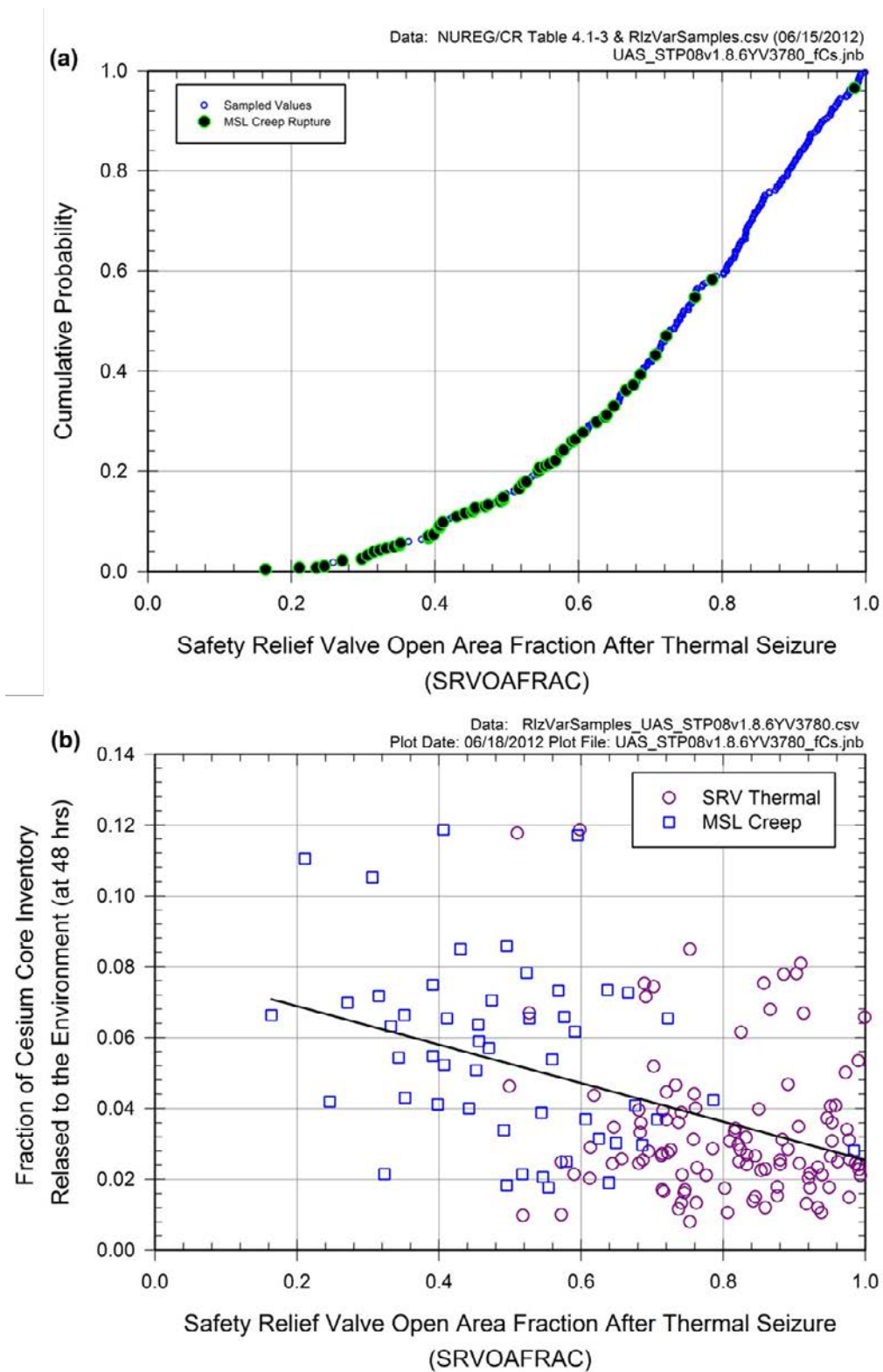


Figure 6.1-9 SRV open area fraction after thermal seizure Peach Bottom unmitigated LTSBO Replicate 1: (a) cumulative distribution function and (b) fraction of cesium core inventory released to the environment. Samples with MSL creep ruptures are identified

Figure 6.1-10 shows reactor and containment pressure and water level for Realization 62 of Replicate 1, a realization that experienced thermal seizure of the SRV followed by an MSL creep rupture. The realization was selected since its plot is near the lower 5th percentile of the distribution of MSL creep rupture results. Interesting is that the rupture occurs after the RPV has depressurized following the sticking open of the SRV. The re-pressurization resulting from a large scale relocation of core debris to the (flooded) RPV lower plenum, and the associated energetic steam production, triggers the creep rupture. This is typical of the realizations that experienced an MSL creep rupture.

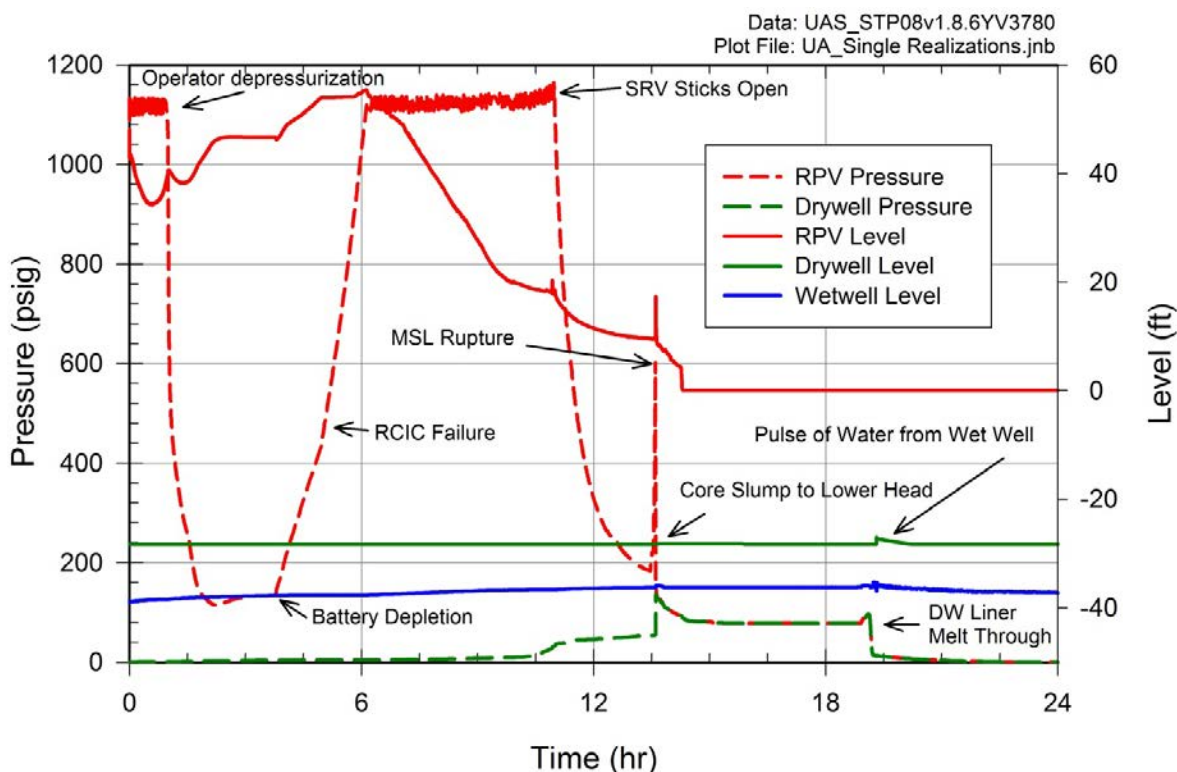


Figure 6.1-10 Reactor and containment pressure and water level for Realization 62 of the Peach Bottom unmitigated LTSBO Replicate 1, an MSL creep rupture

Chemisorption

The amount of cesium chemisorbed from CsOH into the stainless steel of reactor internals relates to the amount of cesium permanently deposited in the RPV in the MELCOR calculations. This influence is only pertinent for the realizations that have all or some of the reactor core cesium inventory initialized as CsOH (MELCOR treats the chemisorption of cesium from CsI but realizations in the uncertainty analysis did not experience chemisorption from CsI). The chemisorption was more robust in the realizations that experienced higher RPV temperatures and it very strongly influenced the amount of cesium released to the environment as evidenced on Figure 6.1-11. The chemisorption often involved greater than half of the initial core inventory of cesium. Important to the chemisorption influence is that CsOH is a more readily evaporable form of cesium and so a more transportable form. Without chemisorption of cesium from CsOH, cesium being prevalent as CsOH (as opposed to Cs_2MoO_4) would tend to heighten the release of cesium to the environment.

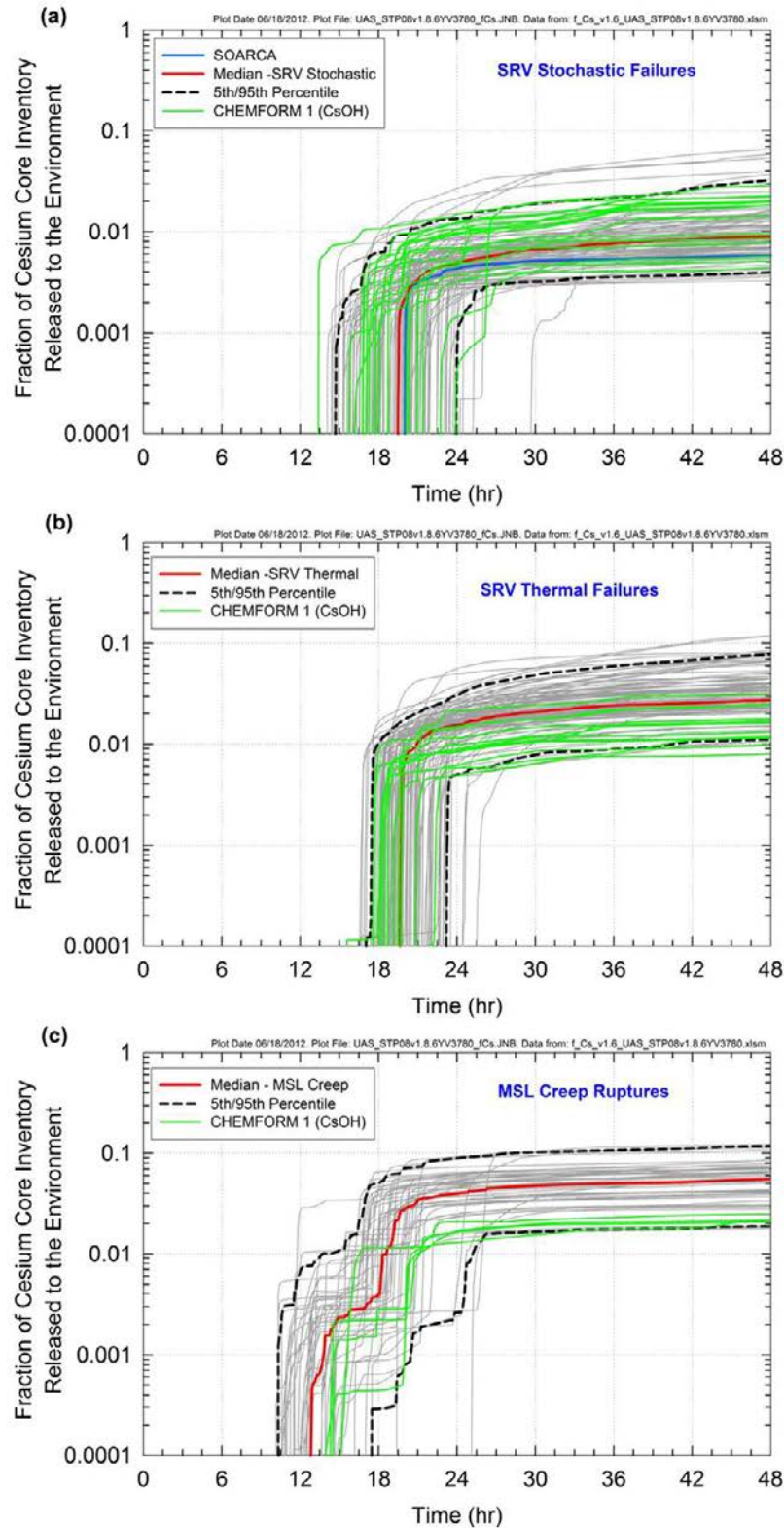


Figure 6.1-11 Fraction of cesium core inventory released to the environment for Peach Bottom unmitigated LTSBO Replicate 1: (a) SRV stochastic failures, (b) SRV thermal failures, and (c) MSL creep ruptures. Realizations are identified that have cesium core inventory initialized as CsOH

Speed of Debris Relocation to the Reactor Cavity and In-Vessel Hydrogen Production

Most all of the cesium that releases to the environment by 48 hours in the realizations of the uncertainty analysis does so by the following sequential steps:

- (1). Releasing from the dismantling core as CsOH, CsI, or Cs₂MoO₄ vapor.
- (2). Condensing into aerosols.
- (3). Gravitational settling onto reactor internals.
- (4). Re-vaporizing after RPV lower head failure steadily over approximately the next day.
- (5). Re-condensing into aerosols that are carried out a breach in the drywell liner resulting from core debris contacting the liner and melting through it.

Key to the re-vaporization of aerosols settled on reactor internals is the temperature of the internals; the hotter the temperature the greater the re-vaporization. Whether core debris relocates from the RPV to the reactor cavity all at once or over an extended period of time relates to the strength and duration of energy sources in the RPV after lower head failure. In the realizations where not all of the initial core material relocates from the RPV at once, decay heat and oxidation persist in the RPV. These persistent energy sources heat the reactor internals and drive the re-vaporization. The degree of oxidation occurring in-vessel relates to how hot reactor internals can potentially become due to the oxidation of (primarily) fuel canisters and cladding; the greater the degree of oxidation the greater the energy deposition in reactor internals.

Figure 6.1-12 shows the time history of the relocation of core material from the RPV to the reactor cavity for Realization 268 of Replicate 1. This realization was selected in the distribution of SRV thermal seizure results that shows outlier behavior (upper 99th percentile). In this realization the relocation of core material doesn't happen all at once, but rather gradually over time. For comparison, Figure 6.1-12 includes the time history of the relocation of core material from the RPV to the reactor cavity for the updated deterministic SOARCA Peach Bottom unmitigated LTSBO case documented in Section 5.1.1.1. The more gradual relocation of material in Realization 268 relative to the SOARCA case (UA base case) results in extended oxidation and therefore extended and heightened heat generation in the RPV. The extended and heightened heat generation efficiently re-vaporizes deposits of cesium from reactor internals resulting in a relatively very large release of cesium to the environment.

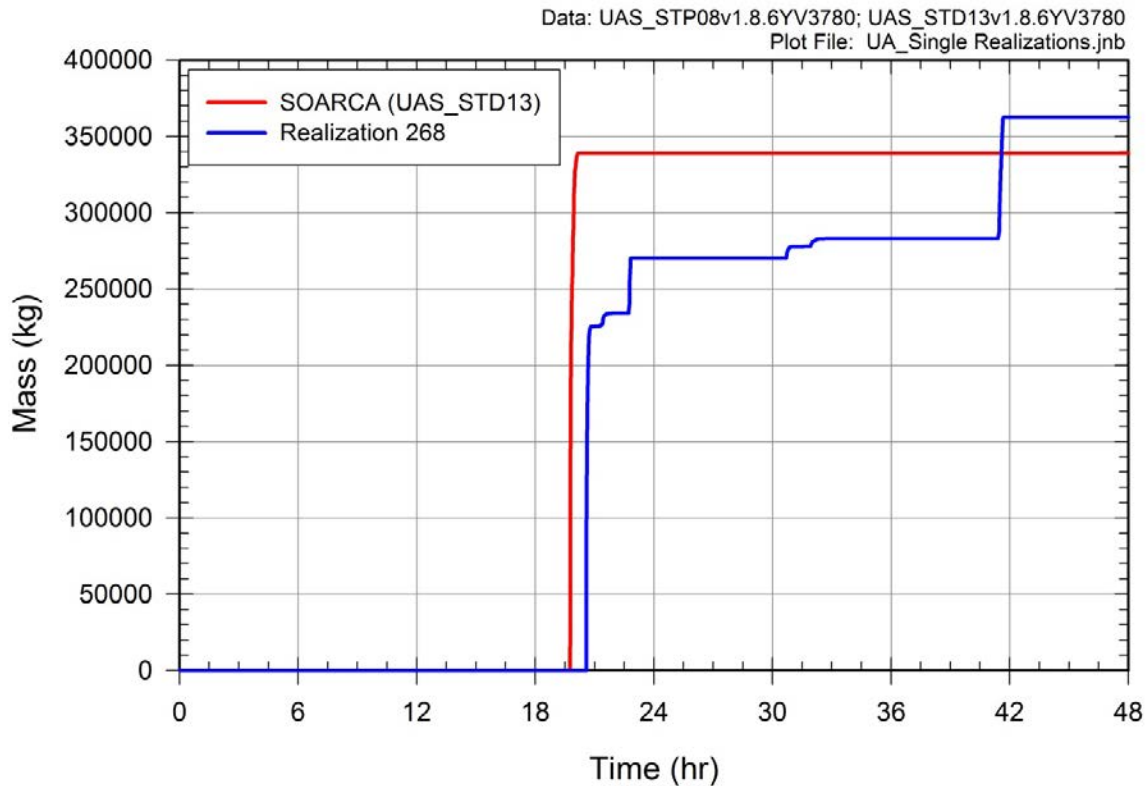


Figure 6.1-12 Time dependent relocation of core material from the RPV to the reactor cavity for Realization 268 of the Peach Bottom unmitigated LTSBO Replicate 1, an SRV thermal seizure failure

Figure 6.1-13 shows the in-vessel hydrogen production associated for Realization 268 of Replicate 1 of the Peach Bottom unmitigated LTSBO scenario and for comparison includes the time history from the updated deterministic SOARCA Peach Bottom unmitigated LTSBO case (UA base case) documented in Section 5.1.1.1.

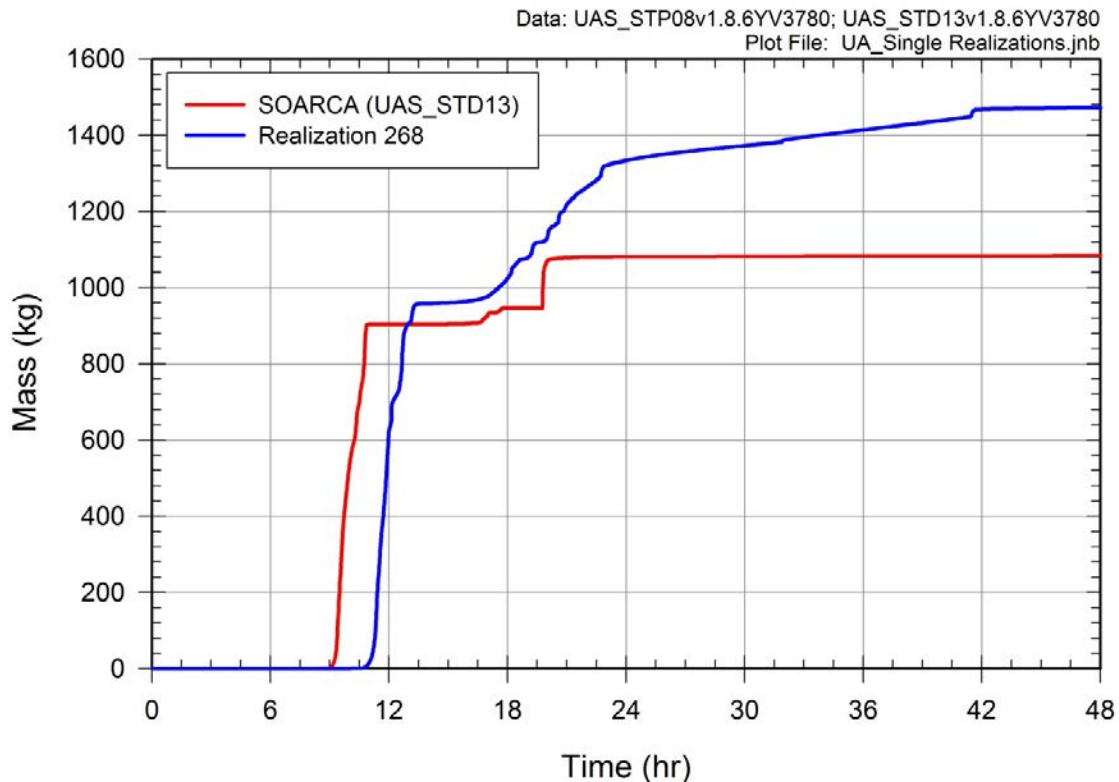


Figure 6.1-13 In-vessel hydrogen production for Realization 268 of the Peach Bottom unmitigated LTSBO Replicate 1, an SRV thermal seizure failure

Water Surging from the Wetwell

Whether a surge of water from the wetwell up onto the drywell floor occurs relates to amounts of cesium that deposit in the wetwell pool but fail to be confined there. In a large number of the realizations, a surge of water from the wetwell up onto the drywell floor occurs when the containment depressurizes in response to a breach developing in the drywell liner due to core debris contacting the liner and melting through it. The wetwell pool is saturated at the time and susceptible to flashing given a depressurization. The vacuum breakers between the wetwell and the drywell are overwhelmed and contaminated water from the wetwell surges up onto the drywell floor. Most of the water moves out the liner breach but some of it pools above the core debris on the drywell floor. The pool subsequently evaporates introducing its inventory of fission products to the atmosphere and structures of the drywell where they are available for release to the environment. (Note that the flow path representing the liner breach in the MELCOR model is a 6-cm high horizontal slot with its lowest point 0.41 m off the drywell floor.)

There is a correlation between the uncertainty in the drywell liner breach size and whether a surge of water from the wetwell occurs as evidenced in Figure 6.1-14. Larger sizes cause stronger containment depressurizations and hence larger potentials for water to surge from the wetwell.

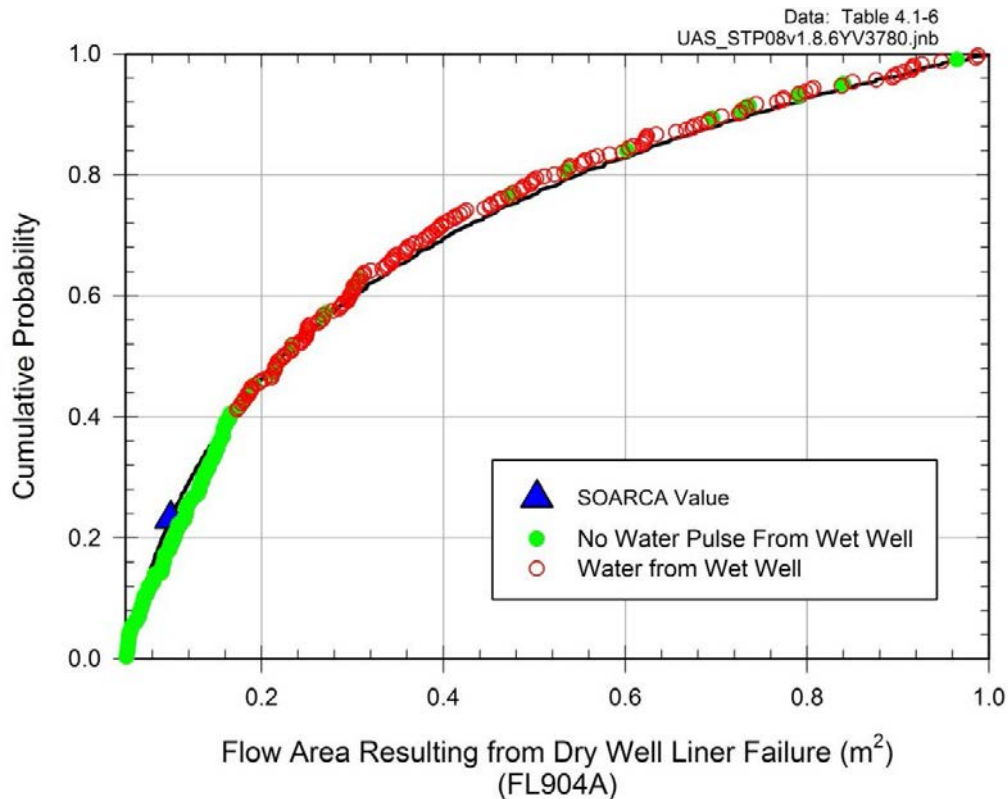


Figure 6.1-14 Cumulative distribution function for the flow area resulting from drywell liner failure for Peach Bottom unmitigated LTSBO Replicate 1 with samples identified that have a surge of water from the wetwell during depressurization of the drywell

Figure 6.1-15 shows water level in containment for Realization 170 of Replicate 1, a realization where a surge of water from the wetwell up onto the drywell floor occurs in response to the containment depressurizing when core debris contacts the drywell liner and melts through it. This realization was selected from the set of SRV stochastic failure cases whose behavior is similar to the upper 95th percentile of the distribution. The small sumps in the reactor cavity and outside the reactor pedestal are not accounted for in this figure. Note that most of the water that surges up from the wetwell moves out of the drywell and into the reactor building through the breach in the drywell liner. The water that pools on the drywell floor is atop core debris and so evaporates releasing its content of fission products to the drywell.

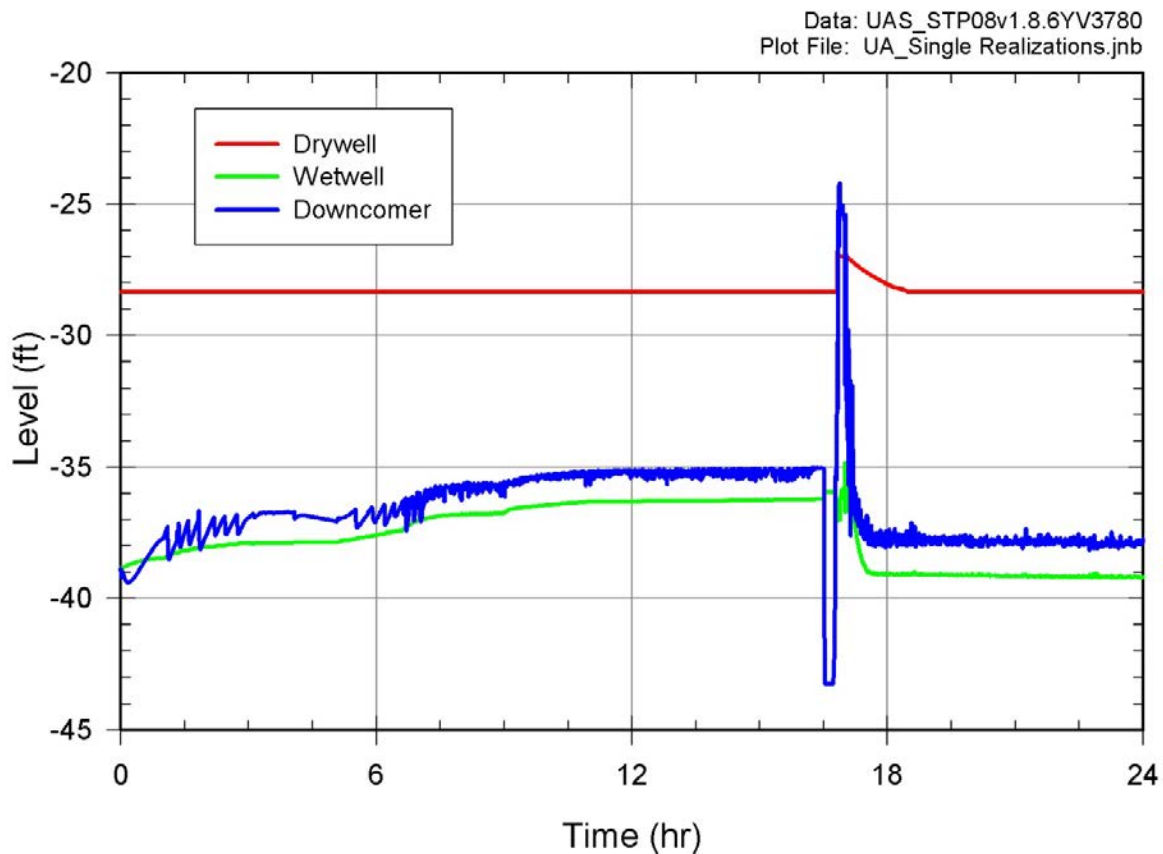


Figure 6.1-15 Water level in containment for Realization 170 of the Peach Bottom unmitigated LTSBO Replicate 1, an SRV Stochastic failure

Overpressure Rupture of the Wetwell

Whether an overpressure rupture of the wetwell occurs pertains to a containment failure whereby a breach occurs in the wetwell above waterline due to overpressure. The breach actually has beneficial impact as it results in a venting of containment through the wetwell pool. The pool scrubs fission products from the venting gas flows as they make their way to the breach.

Compromising of the Railroad Doors

In most of the calculations, the Railroad Doors in the lower reactor building were blown open by a hydrogen deflagration. This resulted in a thermal updraft developing in the reactor building that adversely impacted fission product settling.

The effect can be seen on Figure 6.1-16 for all three of the failure modes.

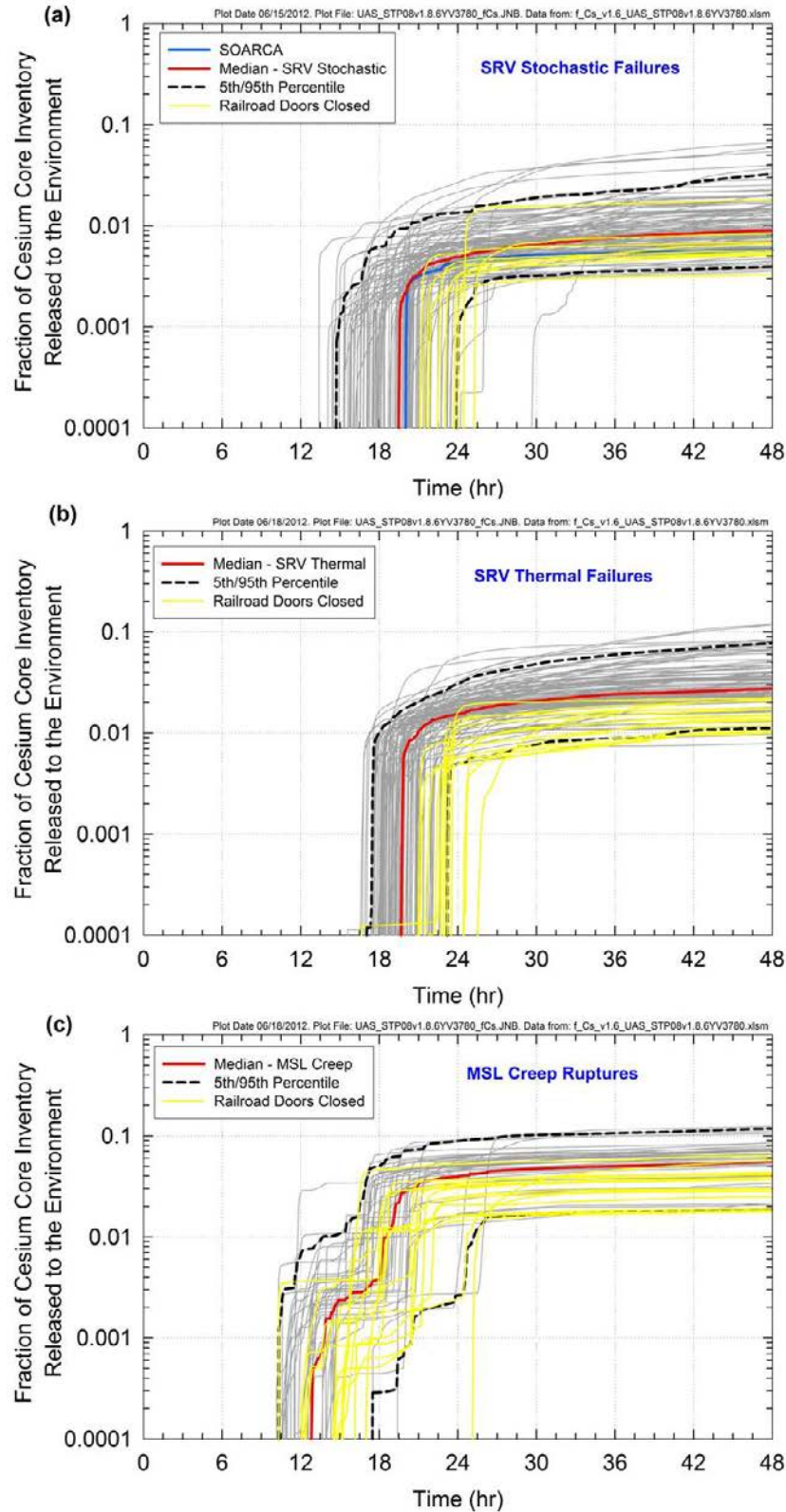


Figure 6.1-16 Fraction of cesium core inventory released to the environment for Peach Bottom unmitigated LTSBO Replicate 1: (a) SRV stochastic failures, (b) SRV thermal failures, and (c) MSL creep ruptures. The realizations are identified that have closed railroad doors

6.1.4.2 Analysis of Single Realizations

For comparison with the individual single realizations, Figure 6.1-17 includes the time dependent distribution of cesium throughout the reactor system from the updated deterministic SOARCA Peach Bottom unmitigated LTSBO case documented in Appendix C. The distribution of cesium throughout the reactor system for selected individual realizations from Replicate 1 of the Peach Bottom unmitigated LTSBO (the realizations of Tables 6.1-11 and 6.1-12), is presented in Figures 6.1-18 through 6.1-28. The figures present pairs of plots showing two scales for each realization. Noteworthy influences specific to each realization are discussed below. In reviewing the figures, the information in Tables 6.1-11 and 6.1-12 should be considered realizing that the minimum, median, and maximum values of hydrogen generation in Replicate 1 of the Peach Bottom unmitigated LTSBO results were 954.5 kg, 1,305.5 kg, and 1,850.0 kg, respectively. Similarly, realize that the minimum, median, and maximum values of fractional cesium release to the environment were 0.003, 0.021, and 0.124, respectively.

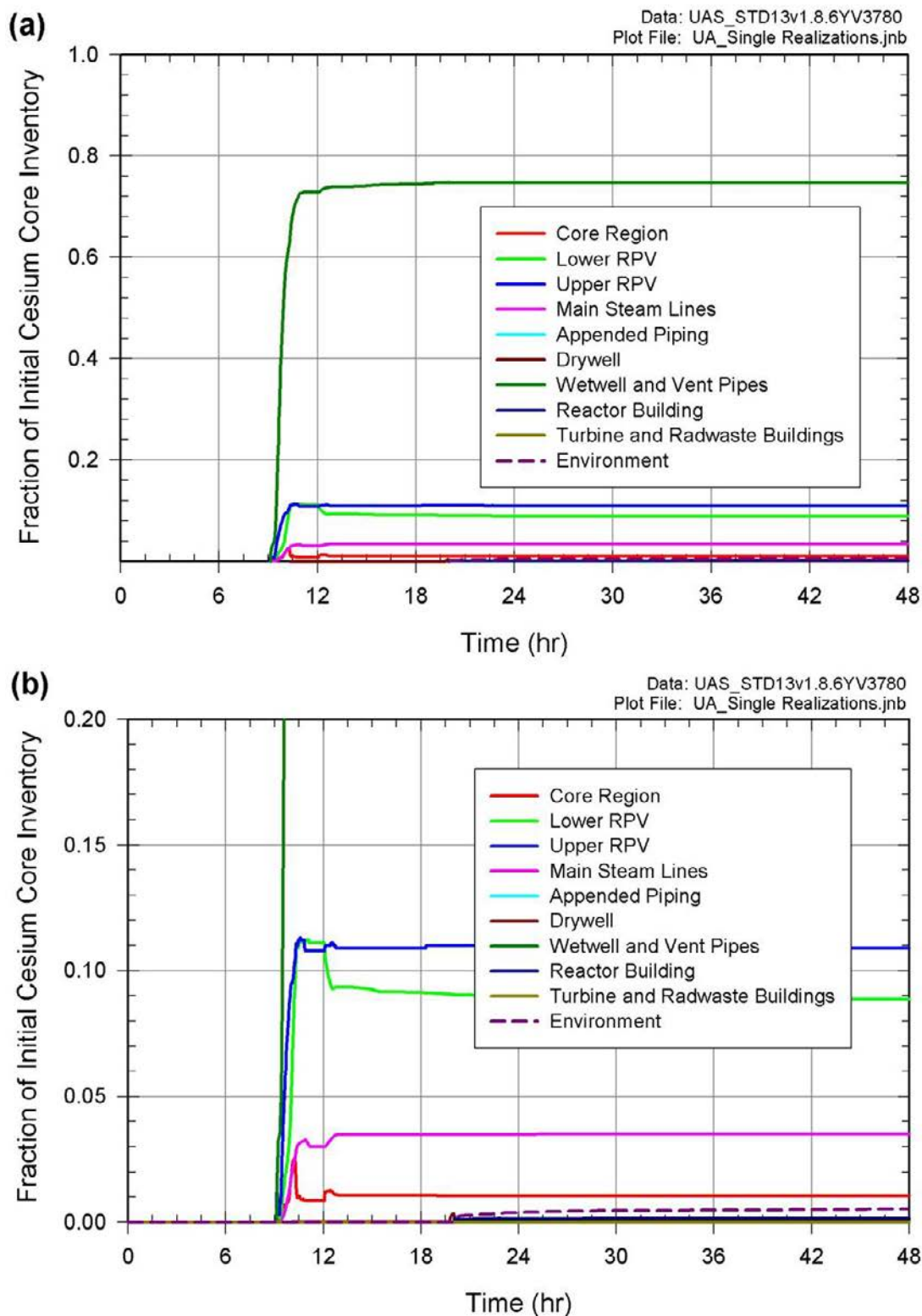


Figure 6.1-17 Fraction of cesium core inventory released to the environment for the updated deterministic SOARCA Peach Bottom unmitigated LTSBO case documented in Section 5.1.1.1 for two scales on the ordinate: (a) 0 to 1.0 and (b) 0 to 0.20

Figure 6.1-18: Realization 18 falls near the median behavior in the distribution of SRV thermal seizure results for Replicate 1 exhibiting an approximately median release of cesium to the environment relative to the collective results of Replicate 1. Nothing really stands out in the progression of this scenario relative to the SOARCA Uncertainty Analysis calculation or the Uncertainty Analysis realizations in general. The realization shows median in-vessel hydrogen production and did not see a surge of water from the wetwell up onto the drywell floor.

Figure 6.1-19: Realization 51 falls near the 5th percentile behavior in the distribution of SRV stochastic failures exhibiting the lowest cesium release of all the Replicate 1 realizations and a release lower than the SOARCA Uncertainty Analysis base case calculation. Contributing to the low cesium release in this realization is that the SRV fails open before the onset of core damage, in-vessel hydrogen production is lower than median, no surge of water from the wetwell up onto the drywell floor occurs, and that the Railroad Doors do not blow open.

Figure 6.1-20: Realization 52 falls near the 5th percentile of the distribution of MSL creep ruptures exhibiting a median cesium release. Factors in this realization that would tend to suppress the release are strong chemisorption, a long elapsed time between the onset of core damage and MSL creep rupture, a wetwell rupture, and no surge of water from the wetwell up onto the drywell floor. Factors that would tend to heighten the release are high in-vessel hydrogen production and a MSL creep rupture.

Figure 6.1-21: Realization 62 falls near the median of the distribution of MSL creep ruptures experiencing a high cesium release. There are several factors in this realization that would tend to heighten the release, namely: high in-vessel hydrogen production, no cesium in the form of CsOH and so no chemisorption, an MSL creep rupture, and a surge of water from the wetwell up onto the drywell floor. A factor that would tend to suppress the release is that a relatively long period of time elapsed between the onset of core damage and the MSL creep rupture.

Figure 6.1-22: Realization 63 falls near the 5th percentile of the distribution of SRV thermal seizure failures exhibiting a low cesium release to the environment. The strong factor identified as contributing to the low release in this realization is high chemisorption.

Figure 6.1-23: Realization 86 falls near the median of the distribution of MSL creep ruptures exhibiting a high cesium release. Factors here that would tend to suppress the release are significant chemisorption and no surge of water from the wetwell up onto the drywell floor. Factors that would tend to heighten release are MSL creep rupture and a short time between the onset of core damage and the MSL creep rupture

Figure 6.1-24: Realization 90 is a very high outlier in the distribution of SRV stochastic failures exhibiting a high cesium release to the environment. This realization exhibits high in-vessel hydrogen production and a more gradual relocation of core material from the RPV to the reactor cavity (over something like a day rather than all at once). Both of these factors, in a related fashion, would tend to increase the cesium release. Tending to suppress the release is that no surge of water from the wetwell up onto the drywell floor occurred.

Figure 6.1-25: Realization 122 is another high outlier in the distribution of SRV stochastic failures showing cesium release to the environment on the high side. There do not seem to be any remarkable factors contributing to the release in this realization but in-vessel hydrogen production is higher than median and there was a surge of water from the wetwell up onto the drywell floor. In this realization, core damage occurs prior to SRV failure.

Figure 6.1-26: Realization 134 is a high outlier in the distribution of MSL creep ruptures showing a high cesium release. Contributors to the release are no CsOH being initialized in the core so no chemisorption taking place, a MSL creep rupture occurring, a short elapsed time between the onset of core damage and the MSL creep rupture, and core material relocation from the RPV over 8 hours (as opposed to all at once). Detractors from the release are low in-vessel hydrogen production, a wetwell rupture, and no surge of water from the wetwell up onto the drywell floor

Figure 6.1-27: Realization 170 falls near the 95th percentile of the distribution of SRV stochastic failures relating to an approximately median cesium release. Contributing to the release is that all the cesium initialized in the core is in the form of CsOH but that only a modest amount of cesium is chemisorbed into the stainless steel of reactor internals. CsOH is a more readily evaporable form of cesium, and therefore, a more transportable form. Given little chemisorption of cesium from CsOH in this realization, cesium being initialized as CsOH would tend to heighten the release of cesium to the environment. Also contributing to the release is that a surge of water from the wetwell up onto the drywell floor occurs. Detracting from the cesium release in this realization is that the SRV fails open before the onset of core damage and that in-vessel hydrogen production is on the low side.

Figure 6.1-28: Realization 268 is a high outlier in the distribution of SRV thermal seizure failures exhibiting a high release of cesium to the environment. It had the highest cesium release of the select realizations. The factor accounting for the high release is the spreading over an extended period of time of the relocation of core material from the RPV to the reactor cavity (as opposed to a relocation that happens all at once). The extended residence time of core material in the RPV, results in continued oxidation (of primarily fuel cladding). The continued heat generation associated with the continued oxidation drives off (evaporates) cesium deposited on reactor vessel internals earlier in the core degradation process. The cesium aerosolizes and transports out of the vessel through the breached lower head and out of the drywell to the reactor building through the melt-through in the drywell liner.

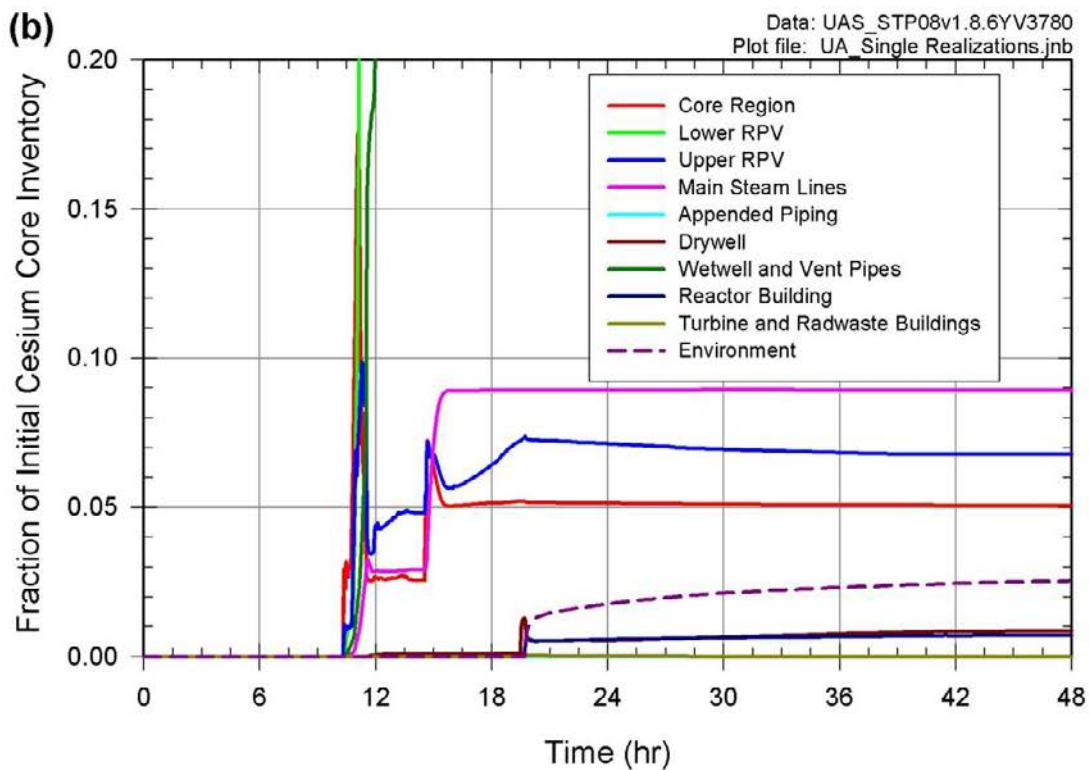
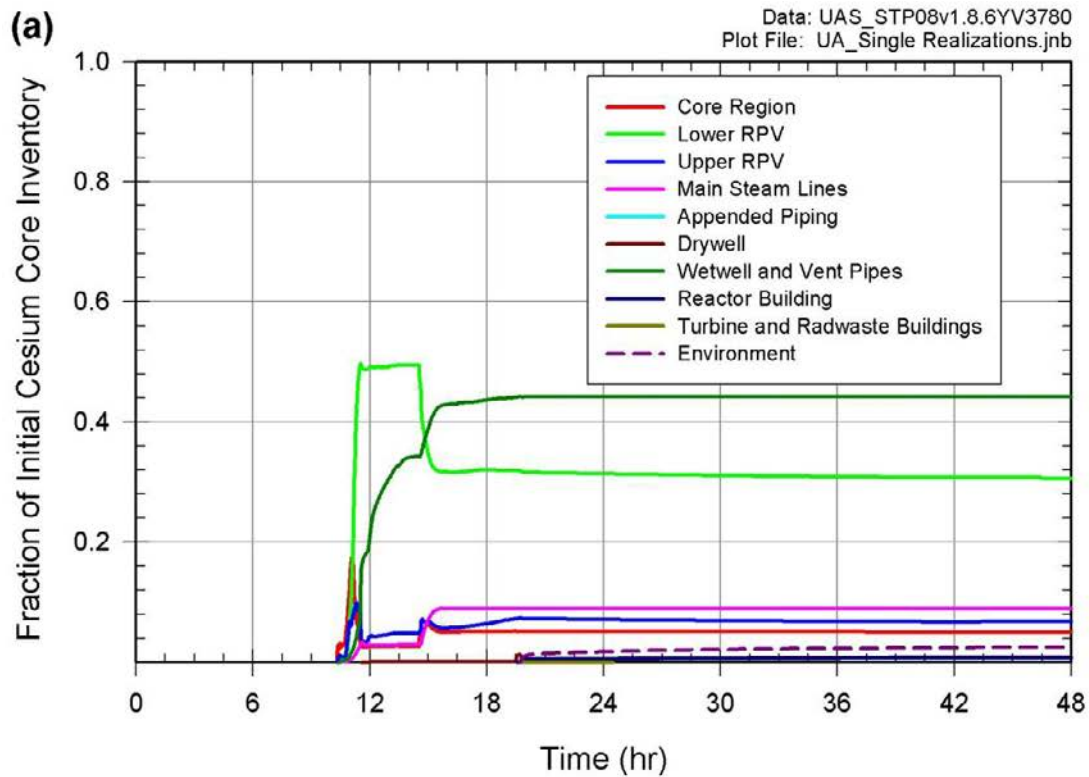


Figure 6.1-18 Fraction of cesium core inventory released to the environment for Realization 18 of Replicate 1 for two scales on the ordinate: (a) 0 to 1.0 and (b) 0 to 0.20

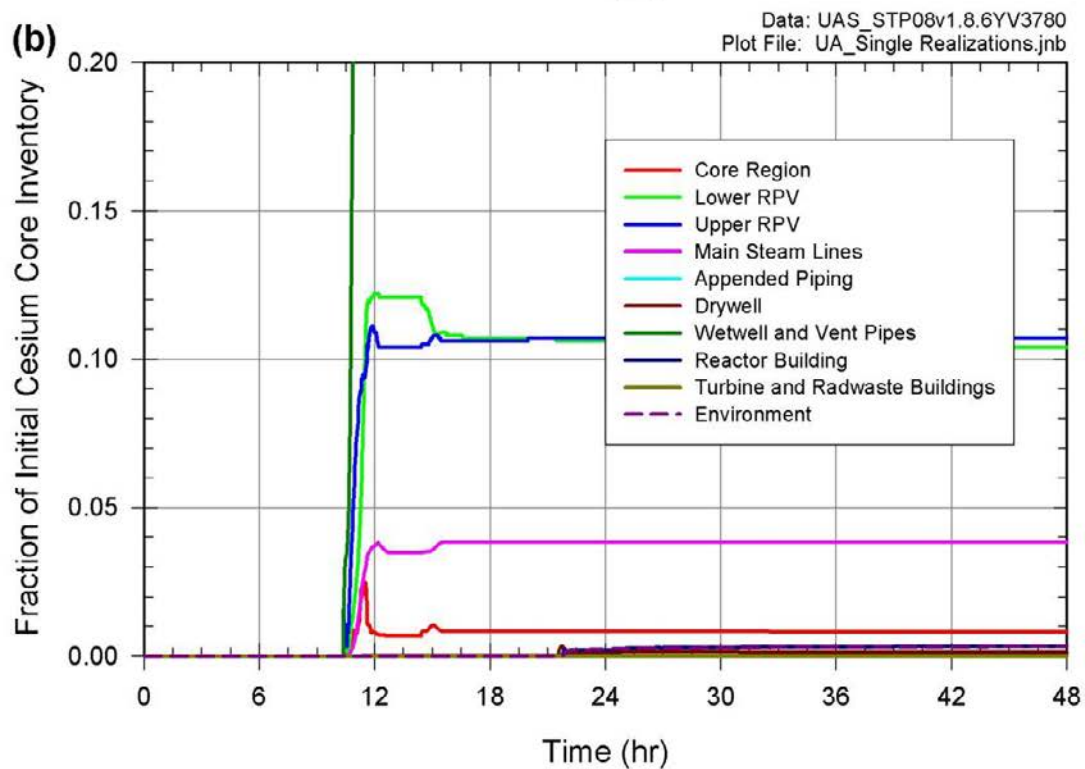
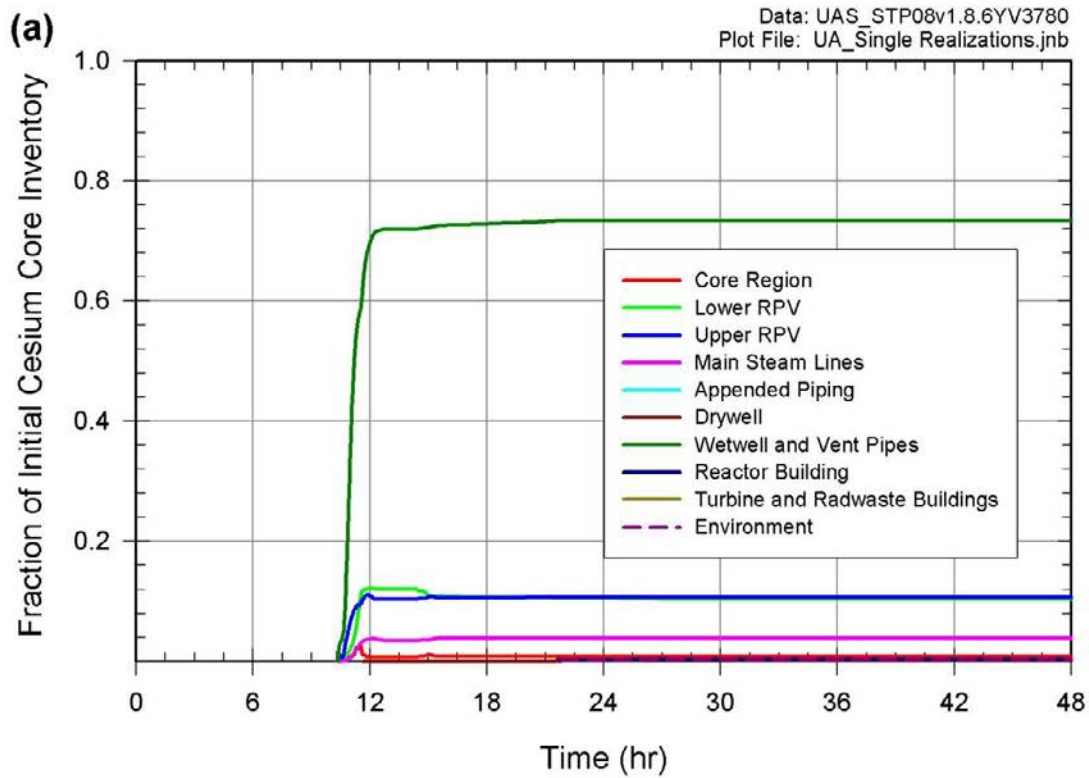


Figure 6.1-19 Fraction of cesium core inventory released to the environment for Realization 51 of Replicate 1 for two scales on the ordinate: (a) 0 to 1.0 and (b) 0 to 0.02

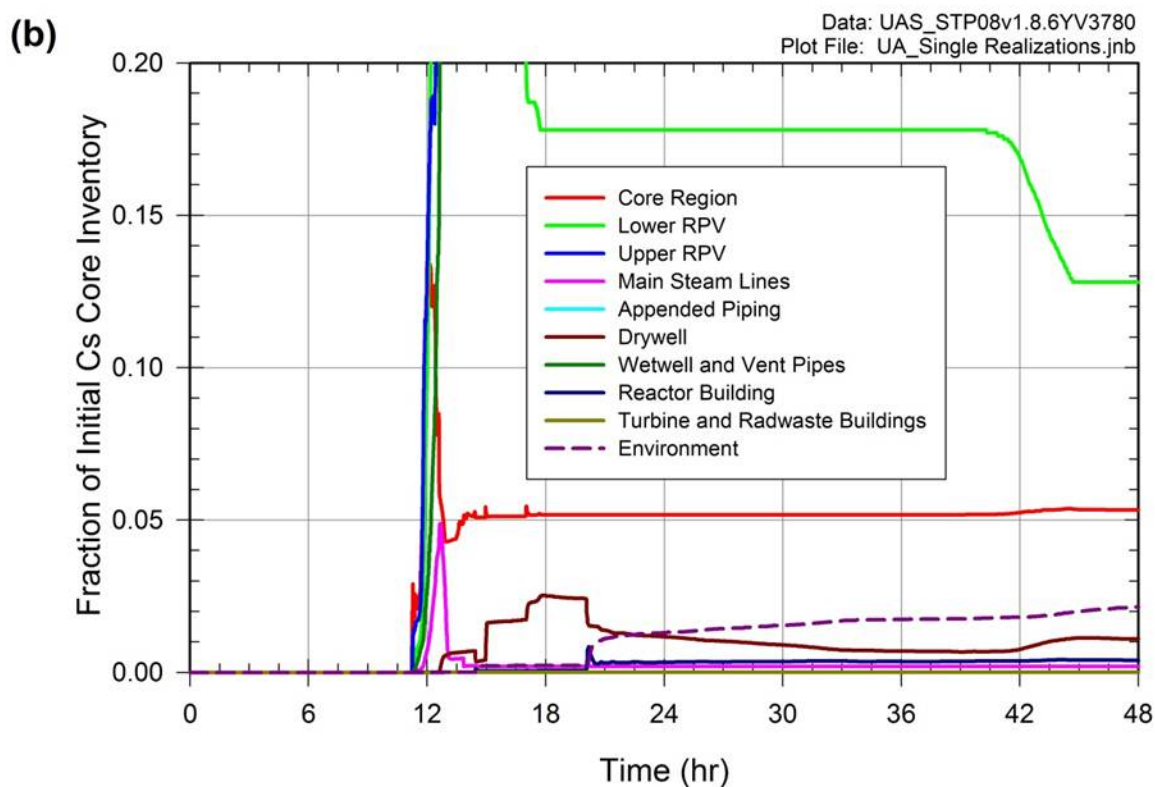
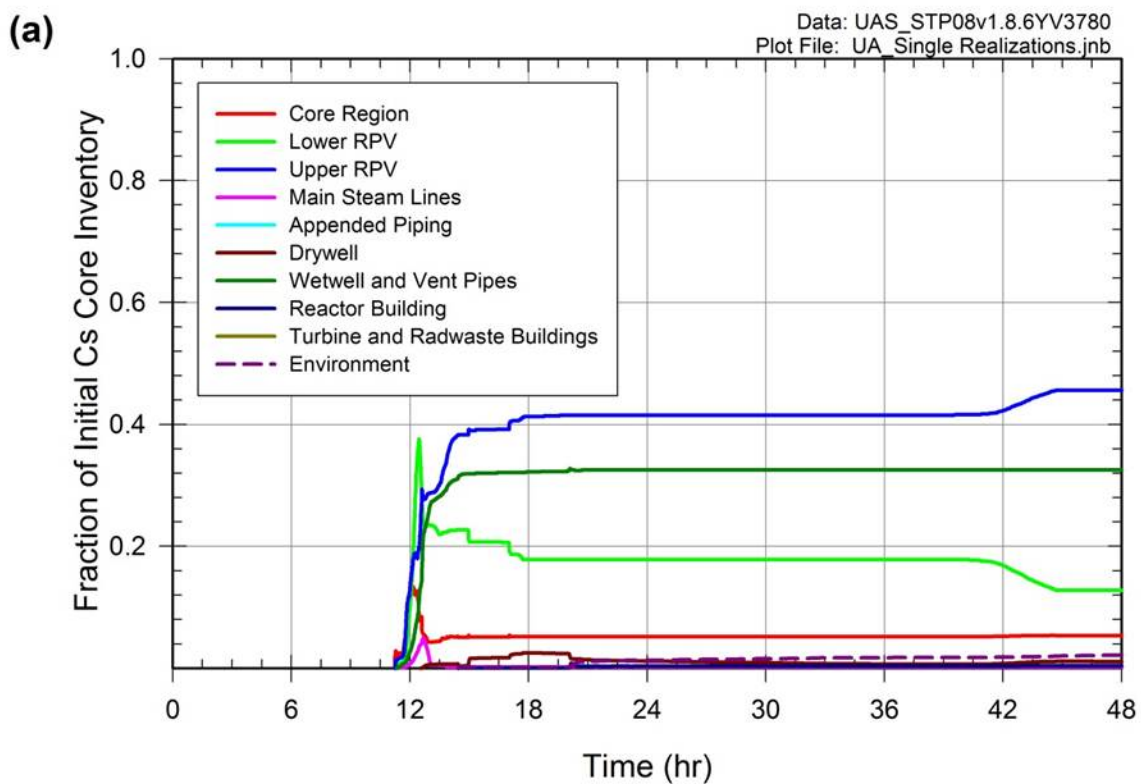


Figure 6.1-20 Fraction of cesium core inventory released to the environment for Realization 52 of Replicate 1 for two scales on the ordinate: (a) 0 to 1.0 and (b) 0 to 0.2

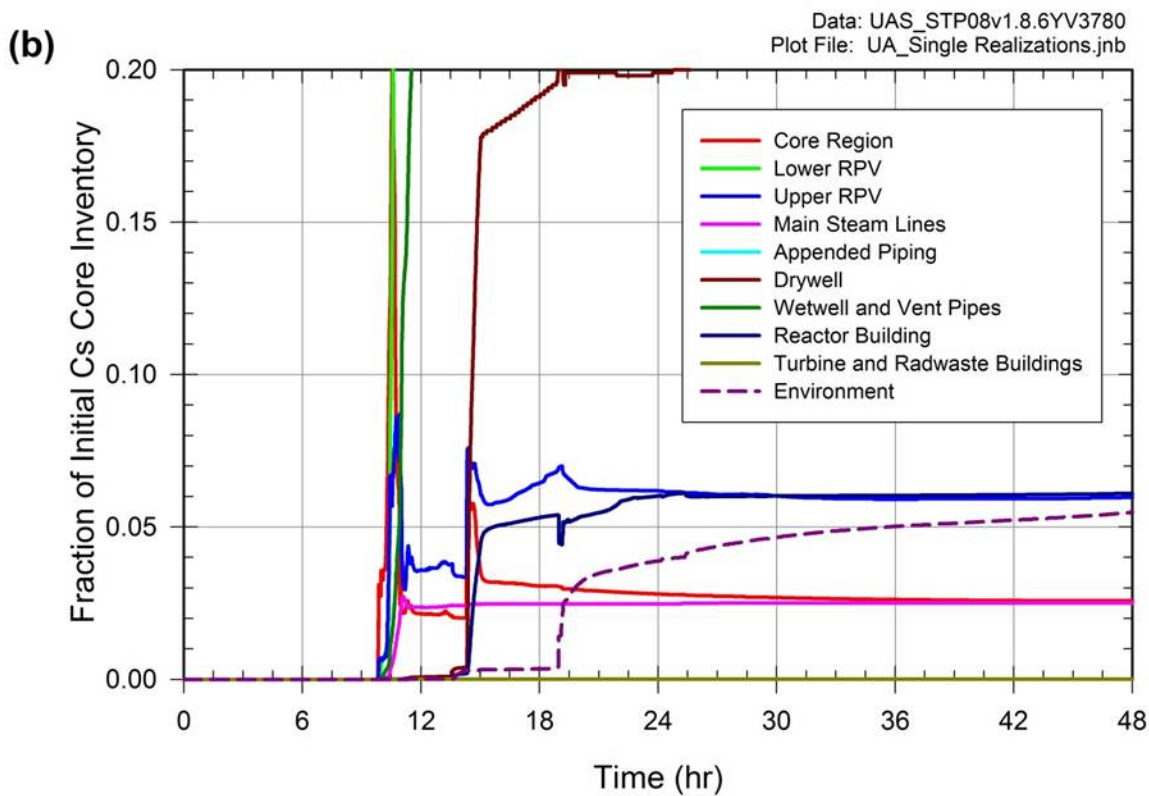
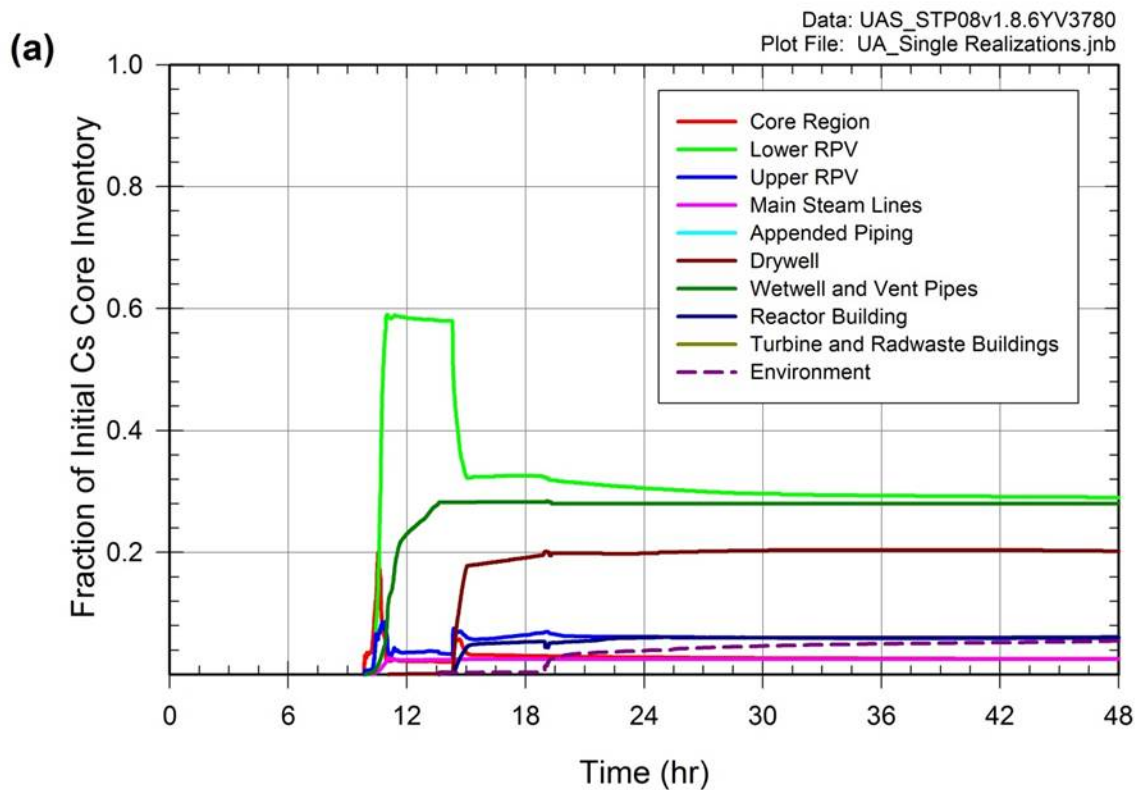


Figure 6.1-21 Fraction of cesium core inventory released to the environment for Realization 62 of Replicate 1 for two scales on the ordinate: (a) 0 to 1.0 and (b) 0 to 0.2

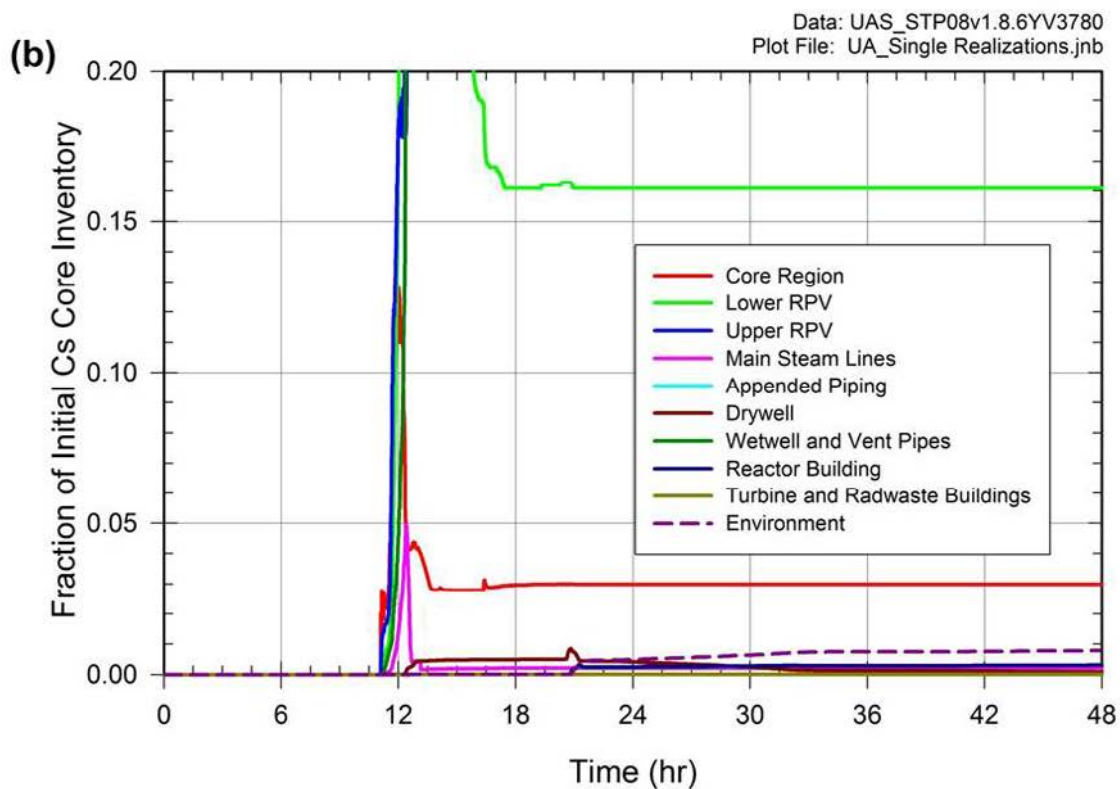
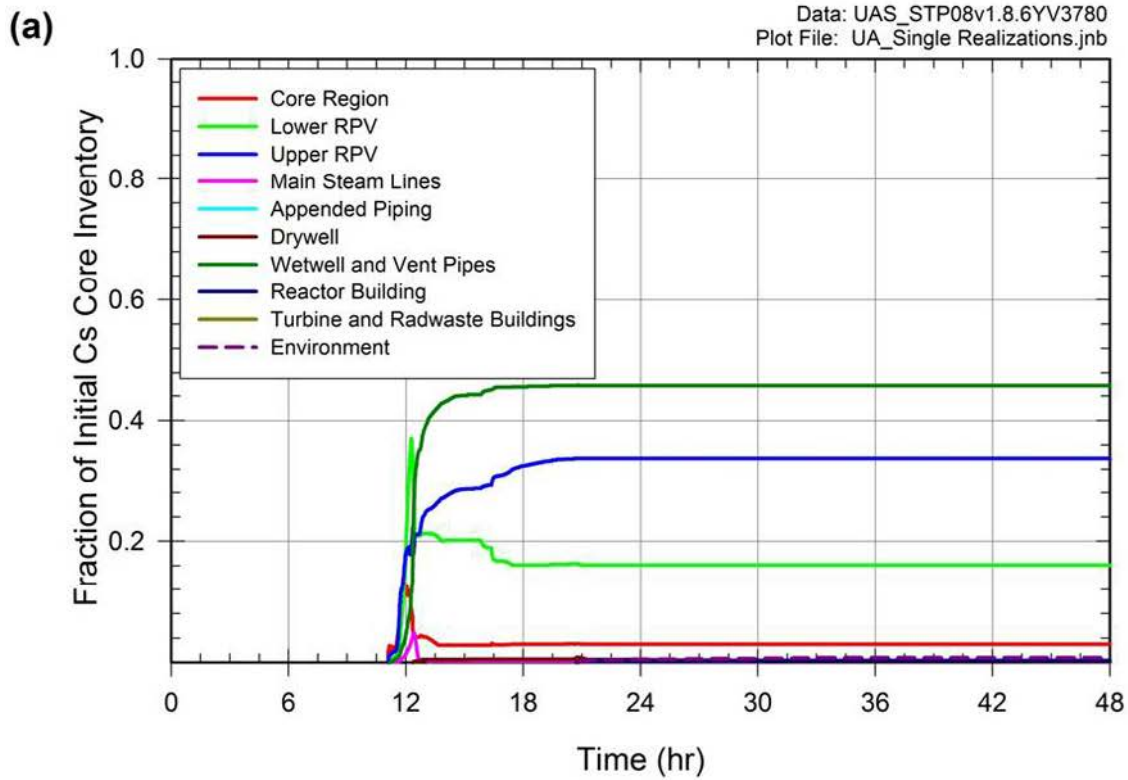


Figure 6.1-22 Fraction of cesium core inventory released to the environment for Realization 63 of Replicate 1 for two scales on the ordinate: (a) 0 to 1.0 and (b) 0 to 0.2

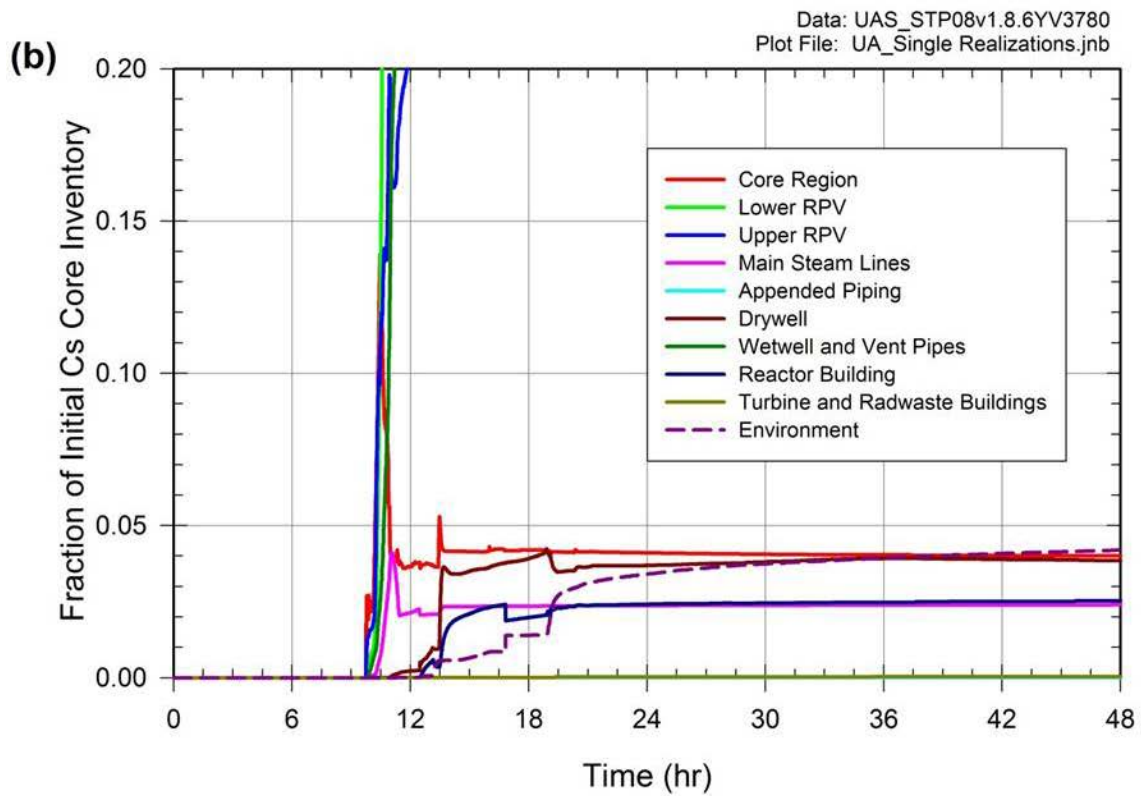
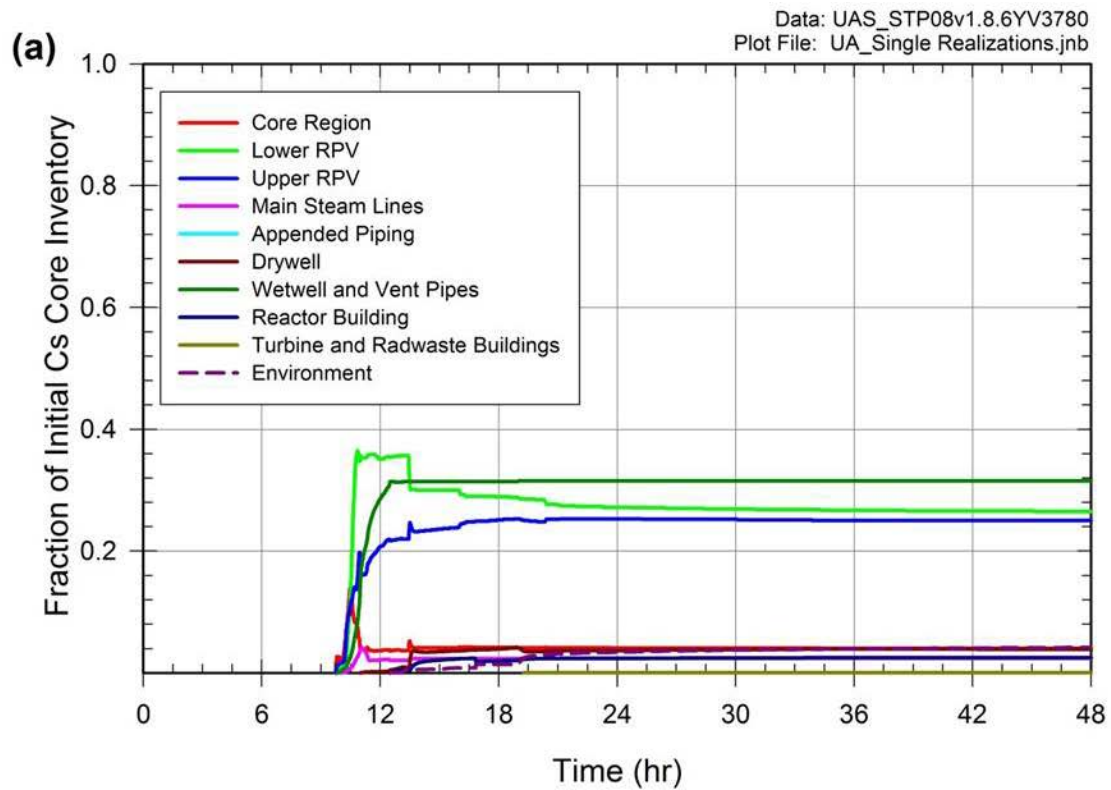


Figure 6.1-23 Fraction of cesium core inventory released to the environment for Realization 86 of Replicate 1 for two scales on the ordinate: (a) 0 to 1.0 and (b) 0 to 0.2

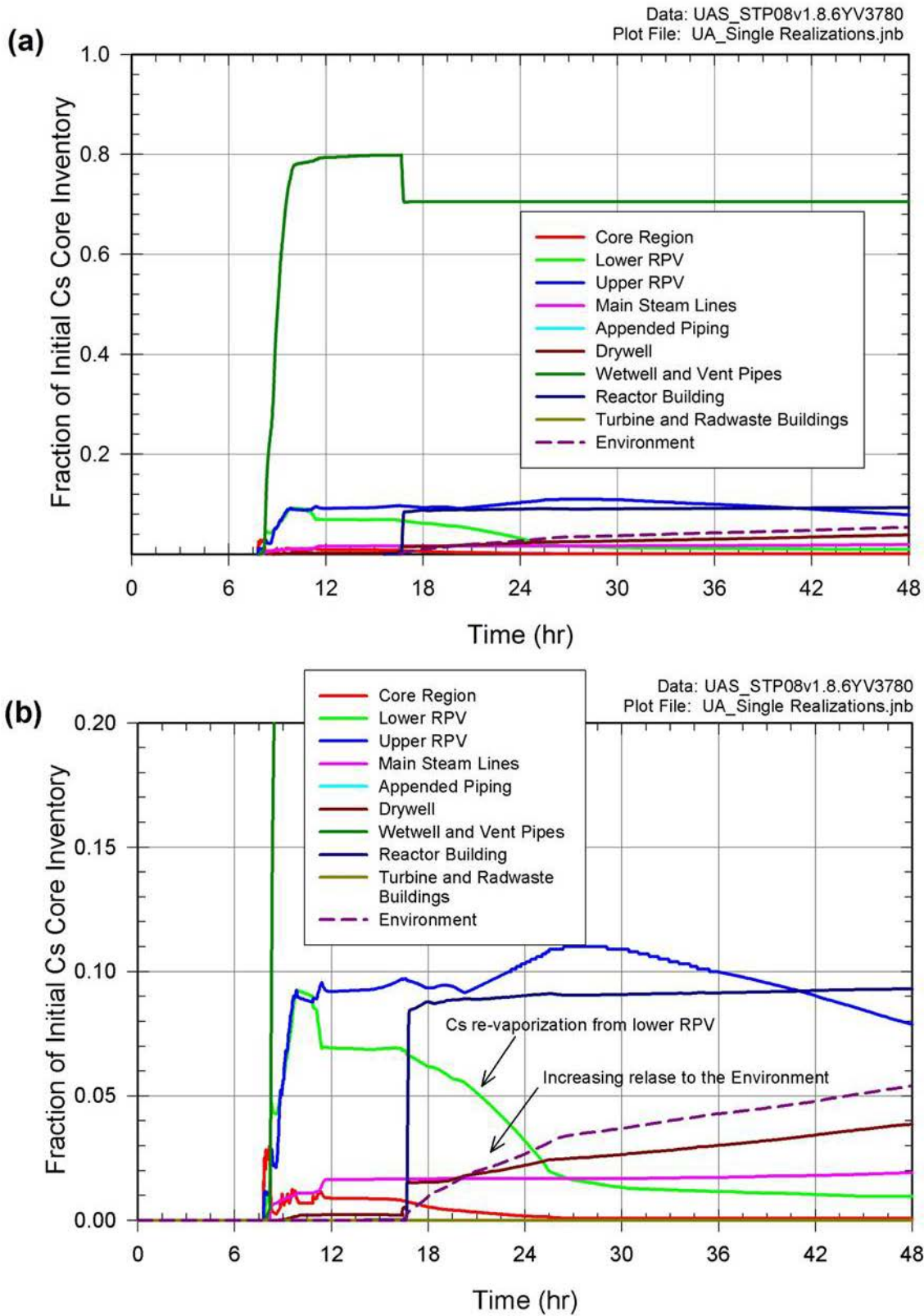


Figure 6.1-24 Fraction of cesium core inventory released to the environment for Realization 90 of Replicate 1 for two scales on the ordinate: (a) 0 to 1.0 and (b) 0 to 0.2

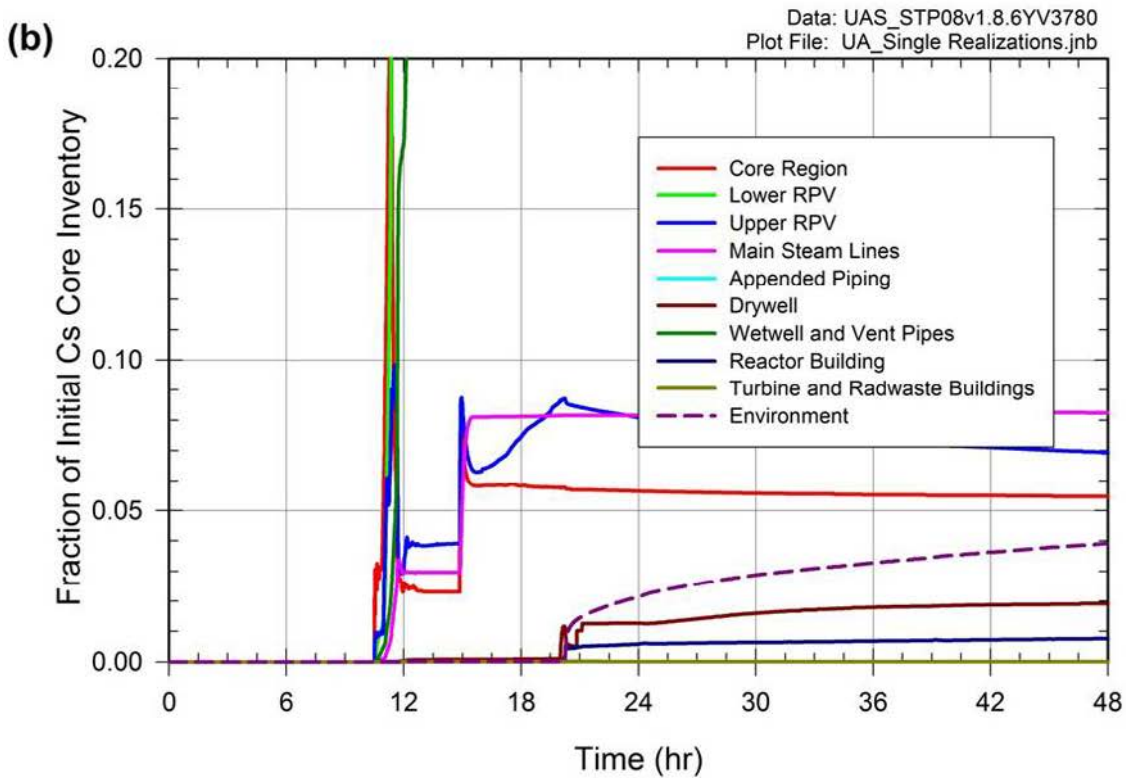
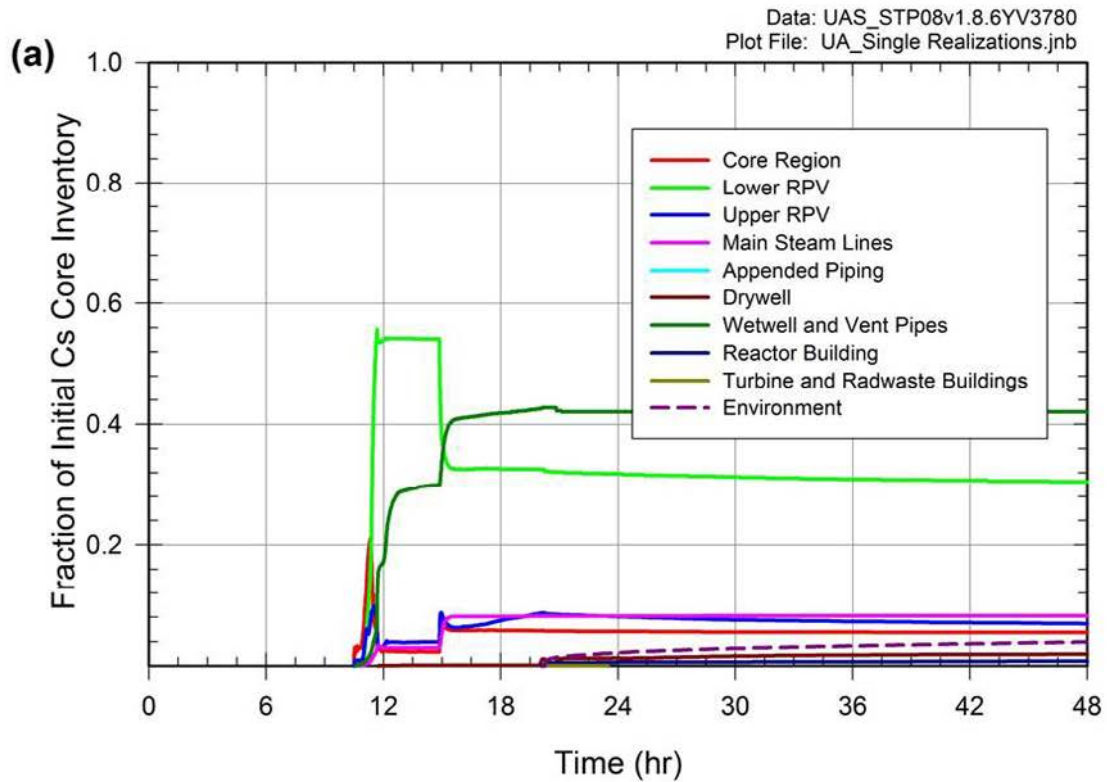


Figure 6.1-25 Fraction of cesium core inventory released to the environment for Realization 122 of Replicate 1 for two scales on the ordinate: (a) 0 to 1.0 and (b) 0 to 0.2

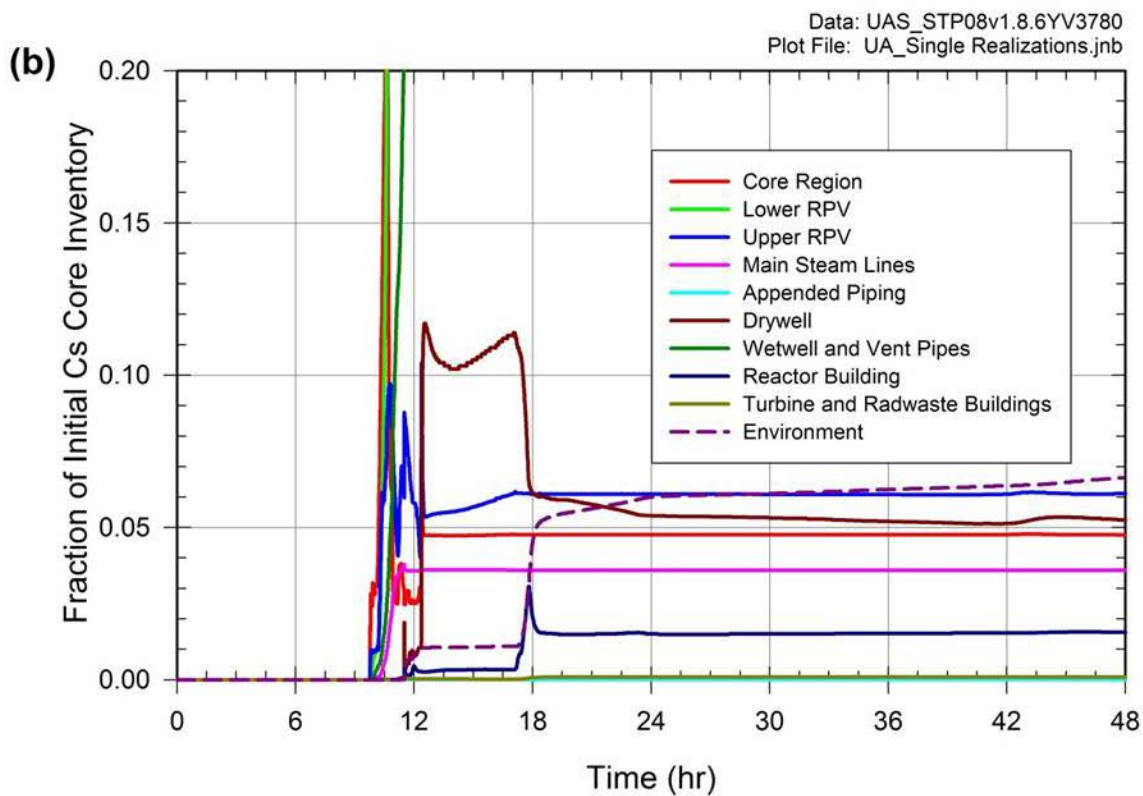
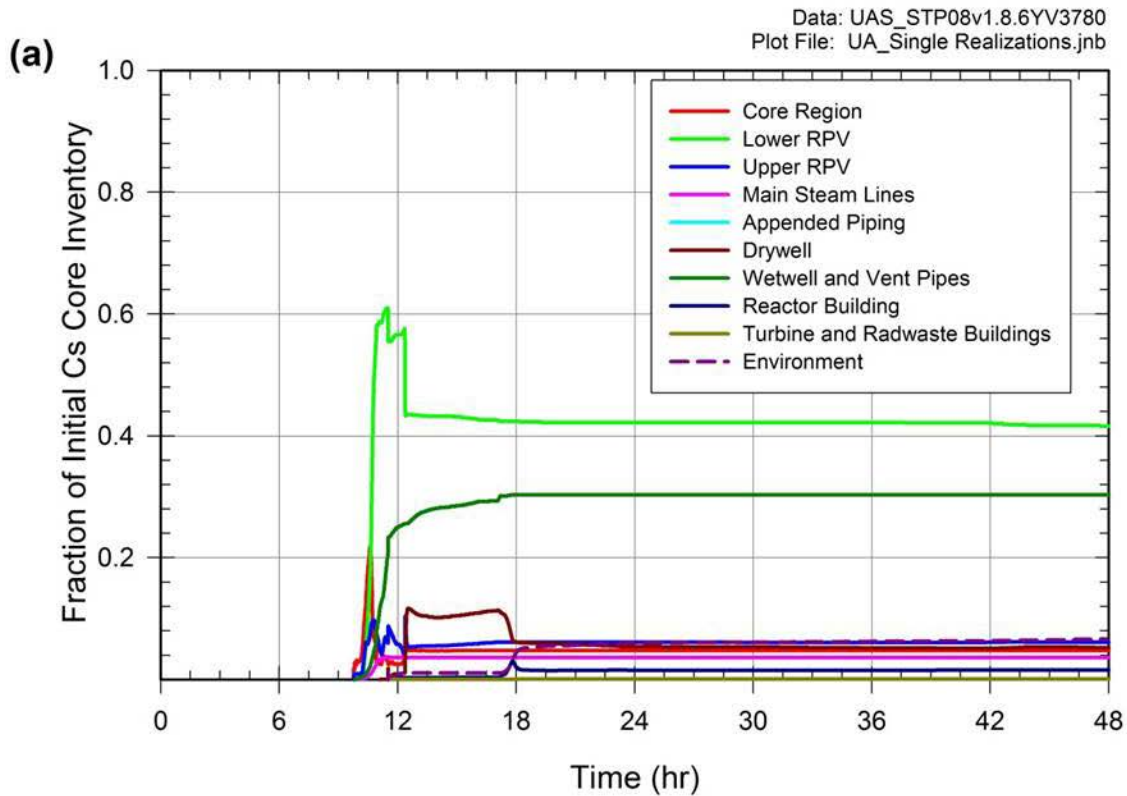


Figure 6.1-26 Fraction of cesium core inventory released to the environment for Realization 134 of Replicate 1 for two scales on the ordinate: (a) 0 to 1.0 and (b) 0 to 0.2

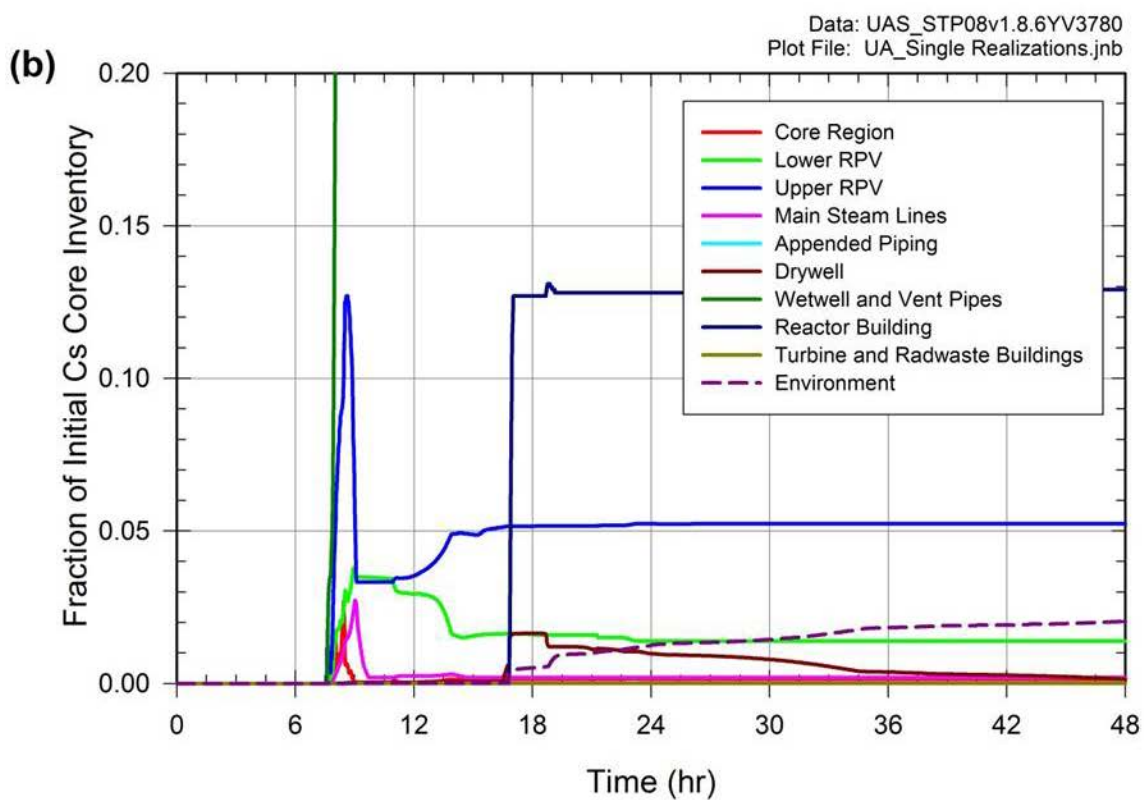
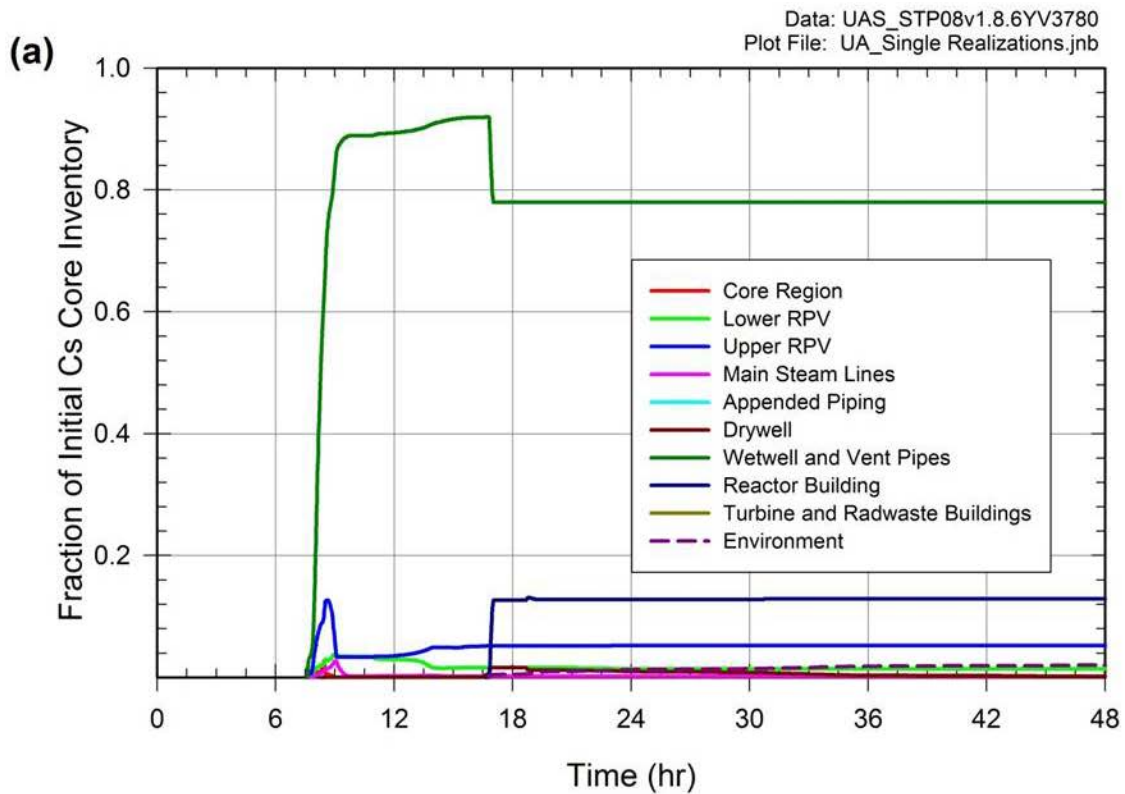


Figure 6.1-27 Fraction of cesium core inventory released to the environment for Realization 170 of Replicate 1 for two scales on the ordinate: (a) 0 to 1.0 and (b) 0 to 0.2

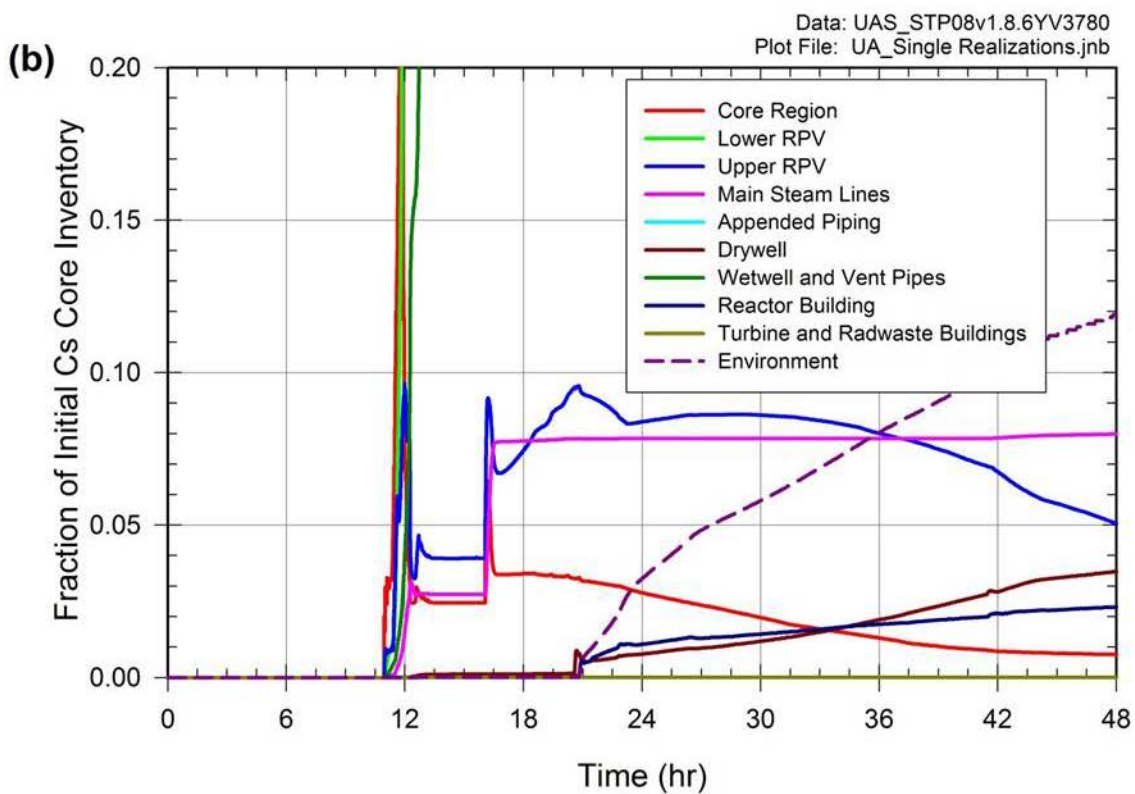
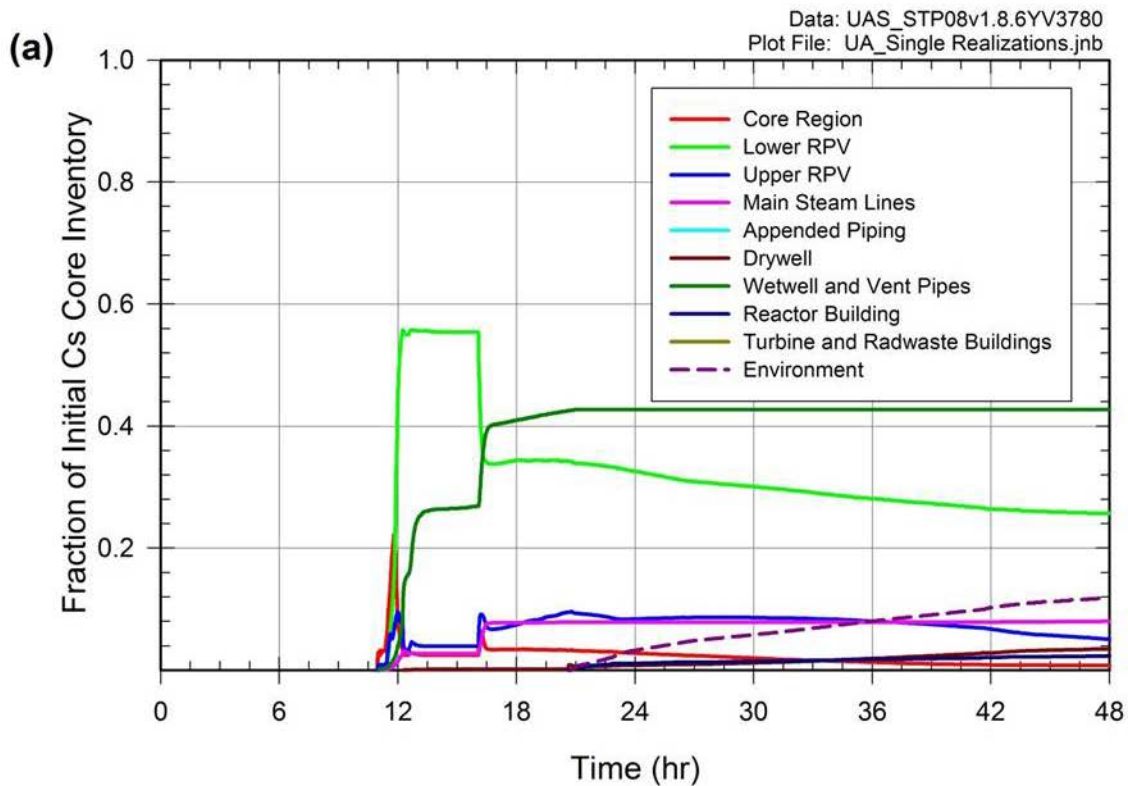


Figure 6.1-28 Fraction of cesium core inventory released to the environment for Realization 268 of Replicate 1 for two scales on the ordinate: (a) 0 to 1.0 and (b) 0 to 0.2

6.2 Offsite Consequence

The results of the consequence analyses are presented in terms of risk to the public for each of the probabilistic source terms analyzed using the Peach Bottom unmitigated LTSBO MELCOR model for the uncertainty analysis presented in Section 6.1. All results are presented as conditional risk. Absolute risk is discussed in certain instances within the text (see NUREG-1935 [1], Section 5.8, for a more full discussion of risk metrics reported). The conditional risks assume that the accident occurs and show the risks to individuals as a result of the accident (i.e., latent cancer fatality (LCF) risk per event or early-fatality risk per event). The absolute risk is the product of the core damage frequency for the accident sequence and the conditional risk for that sequence. The absolute risk is the likelihood of incurring a latent fatal cancer or early fatality for an average individual living within a specified radius of the plant per year of plant operation (i.e., LCF risk per reactor year (prr) or early-fatality risk pryr).

The reported risk metrics, LCF and early-fatality risks to residents in circular regions surrounding the plant, are averaged over the entire residential population within each circular region. The risk values represent the predicted number of fatalities divided by the population for the selected dose response model. These risk metrics account for the distribution of the population within the circular region and for the interplay between the population distribution and the wind rose probabilities.

The three separate replicates representing the uncertainty in the MELCOR source terms, as discussed in Section 5.1.1, were combined and used in a single MACCS uncertainty analysis to determine the conditional, mean, individual LCF risk (per event) and early-fatality risk per event CCDFs. The reported risk is the mean risk over possible variations in weather using the weather sampling strategy developed for SOARCA. The three MELCOR replicate analyses produced 284 (Replicate 1), 290 (Replicate 2), and 291 (Replicate 3) MELCOR source terms, respectively. Each MELCOR source term replicate was analyzed individually with a single WinMACCS run using LHS sampling and include the 350 MACCS uncertain input variables. In addition, a WinMACCS run created a set of 865 MACCS realizations, each paired with one of the MELCOR source terms from all three replicates. Table 6.2-1 identifies the nomenclature for the MACCS probabilistic analyses and corresponding MELCOR source terms.

This section discusses the LCF risks per event and the early-fatality risks per event. All the cases use the MACCS uncertainty parameters (i.e., 350 uncertain input parameters) discussed in Section 5.2.1. This section also discusses the consequence analyses for the MELCOR single realizations discussed in Section 6.1.4, and the three MACCS realizations that resulted in an early-fatality risk out to 10 miles. The single realization analysis provides insight into the important phenomena driven by the uncertainty in the input parameters and source terms.

Table 6.2-1 MACCS probabilistic analyses

MACCS Analysis	Description	MELCOR Source Terms
UAS_CAP14v364_2509	CAP14. MACCS analysis for MELCOR Replicate #1, LNT Dose Response model.	UAS_STP08v1.8.6YV3780
UAS_CAP18v364_2509	CAP18. MACCS analysis for MELCOR Replicate #2, LNT Dose Response model.	UAS_STP09v1.8.6YV3780
UAS_CAP19v364_2509	CAP19. MACCS analysis for MELCOR Replicate #3, LNT Dose Response model.	UAS_STP10v1.8.6YV3780
UAS_CAP17v364_2509	CAP17. MACCS analysis for combined MELCOR Replicates #1, #2, & #3, LNT Dose Response model.	UAS_STP08v1.8.6YV3780; UAS_STP09v1.8.6YV3780; UAS_STP10v1.8.6YV3780

The risk results presented in this section use only the LNT dose-response model. Uncertainty analyses using dose truncation models are discussed in Section 6.4.4.

In this section, the risk tables represent rounded values obtained from the full data sets. The plots were developed from the full data sets and slight differences may be noticed due to rounding of the tabulated values.

6.2.1 Latent Cancer Fatality Risk

Table 6.2-2 shows statistical results for conditional, mean, individual LCF risk (per event) from the MACCS uncertainty analysis at each specified circular area for the analysis using all three MELCOR source term replicates combined (CAP17). Each statistic was estimated to evaluate the epistemic uncertainties resulting from the uncertain inputs to MACCS and MELCOR (through the source term). A t-distribution was used to determine the 5th and 95th percentiles.

Table 6.2-2 Conditional, mean, individual LCF risk (per event) average statistics for the MACCS Uncertainty Analysis for five circular areas (using all three source term replicates)

	0-10 miles	0-20 miles	0-30 miles	0-40 miles	0-50 miles
Mean	1.7x10 ⁻⁴	2.8x10 ⁻⁴	2.0x10 ⁻⁴	1.3x10 ⁻⁴	1.0x10 ⁻⁴
Median	1.3x10 ⁻⁴	1.9x10 ⁻⁴	1.3x10 ⁻⁴	8.7x10 ⁻⁵	7.1x10 ⁻⁵
5th percentile	3.1x10 ⁻⁵	4.9x10 ⁻⁵	3.4x10 ⁻⁵	2.2x10 ⁻⁵	1.9x10 ⁻⁵
95th percentile	4.2x10 ⁻⁴	7.7x10 ⁻⁴	5.3x10 ⁻⁴	3.4x10 ⁻⁴	2.7x10 ⁻⁴

For this work, the emergency phase is defined as the first seven days following the initial release to the environment. The long-term phase is defined as the time following the emergency phase (i.e., there is no intermediate phase). The long-term phase risk (i.e., the LCF risk contribution beyond the emergency phase) dominates the total risks (i.e., 100% of all realizations have a long-term risk contribution that is greater than 50% of the total risk) within the EPZ for the uncertainty analysis when the LNT dose-response assumption is made. No realization resulted in an emergency phase risk contribution greater than 48% of the total risk. The emergency phase risk within the EPZ is entirely to the 0.5% of the population who are assumed not to evacuate. These results further emphasize the benefits of evacuating the EPZ.

The long-term risks are controlled by the habitability (return) criterion, which is the dose rate at which residents are allowed to return to their homes following the emergency phase. For Peach Bottom, the habitability criterion is an annual dose rate of 500 mrem/yr¹⁴. For comparison, only 55% of all realizations have a long-term risk contribution greater than 50% of the total risk within a 20-mile radius (i.e., 45% of the realizations have an emergency phase risk greater than 50% of the total risk). Since only hotspot and normal relocation are modeled beyond the EPZ (in addition to a 20% shadow evacuation in the 10-20 mile ring), it is possible for residents beyond 10 miles to incur larger doses during plume passage in the emergency phase before the hotspot or normal relocation occurs. It should be noted that earlier ad hoc evacuation would be expected to occur in the case of an anticipated large release (see for example, NUREG-2161 [92], "Consequence Study of a Beyond Design-Basis Earthquake Affecting the Spent Fuel Pool for a U.S. Mark I Boiling Water Reactor," Section 7.1.4) but an ad hoc evacuation model was not within the scope of this uncertainty study.

Figures 6.2-1 to 6.2-5 show the CCDFs for the conditional, mean, individual LCF risk (per event) for the composite MACCS uncertainty analysis (CAP17) within five concentric circular areas from the plant. Also noted on the figures are the mean, median, 5th and 95th quantiles (percentiles) for the conditional LCF risk distributions using each of the three MELCOR replicate results (i.e., CAP 14, CAP18, and CAP19 results described in Section 5.2.1.3). The composite CCDFs (for CAP17) are very similar and are in good agreement with the three uncertainty analyses corresponding to the three sets of MELCOR results (i.e., CAP14, CAP18, and CAP19). This indicates that incorporation of all 865 MELCOR source terms into a single MACCS uncertainty analysis is reasonably well converged compared with smaller samples using the MELCOR Replicates 1, 2, and 3 (i.e., compare Table 5.2-6 with Table 6.2-2).

On Figure 6.2-1 to Figure 6.2-5, the x-axis represents the distribution of possible LCF risk per event results within the 10-mile circular area and is generated by sorting (from smallest to largest) all the LCF risk results from the sample of size 'N' (i.e., N=865 samples for Figure 6.2-1). On Figure 6.2-1, the y-axis represents the likelihood of being higher than or equal to the value read on the x-axis. The likelihood of the outcome is estimated by a weight of 1/N and decreasing the y-value by this weight starting from one. The mean (arithmetic average) is added to each CCDF curve. Quantiles (q) can be read directly by finding the corresponding y-value to the graph, and are displayed for the 5th, 50th (median), and 95th quantiles as dots over the curve.

In risk analysis, it is traditional to plot CCDFs rather than CDFs as a CCDF answers the question, "How likely it is to have such value or higher?"

¹⁴ In accordance with Pennsylvania State Guidelines.

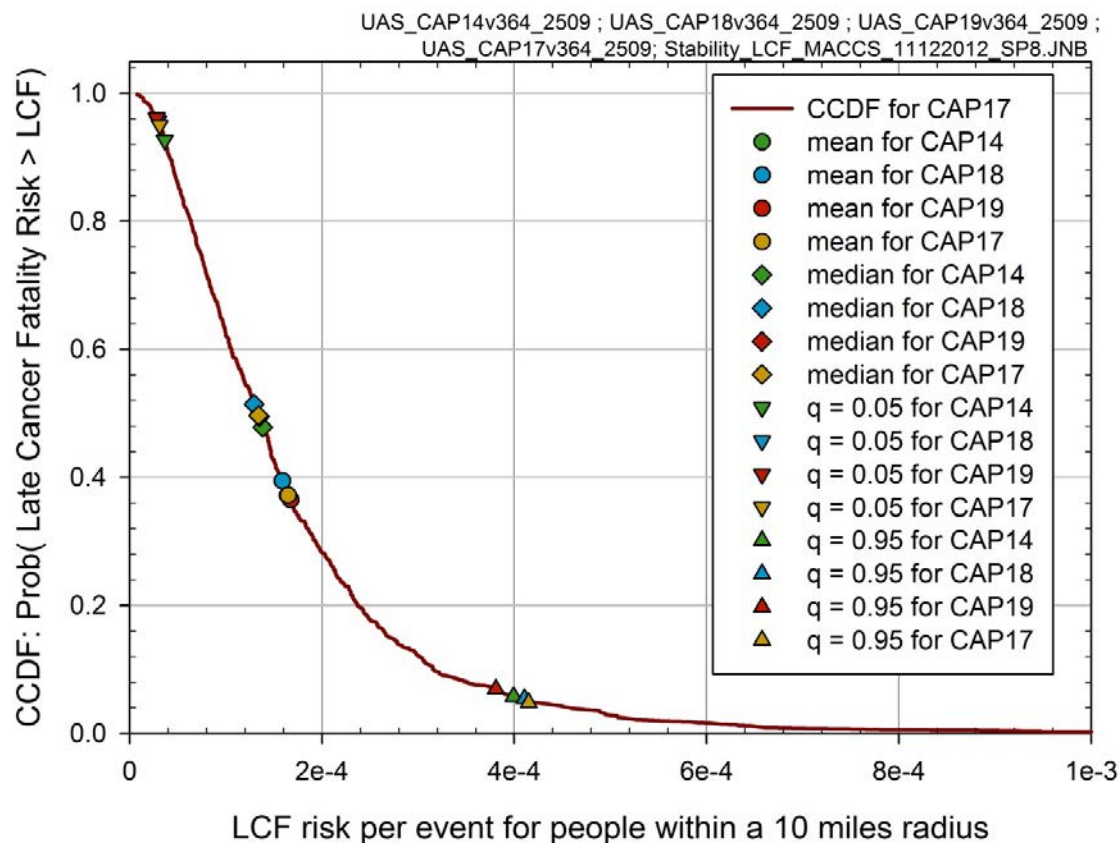


Figure 6.2-1 Complementary cumulative distribution function and statistical values for conditional, mean, individual LCF risk (per event) within a 10-mile radius

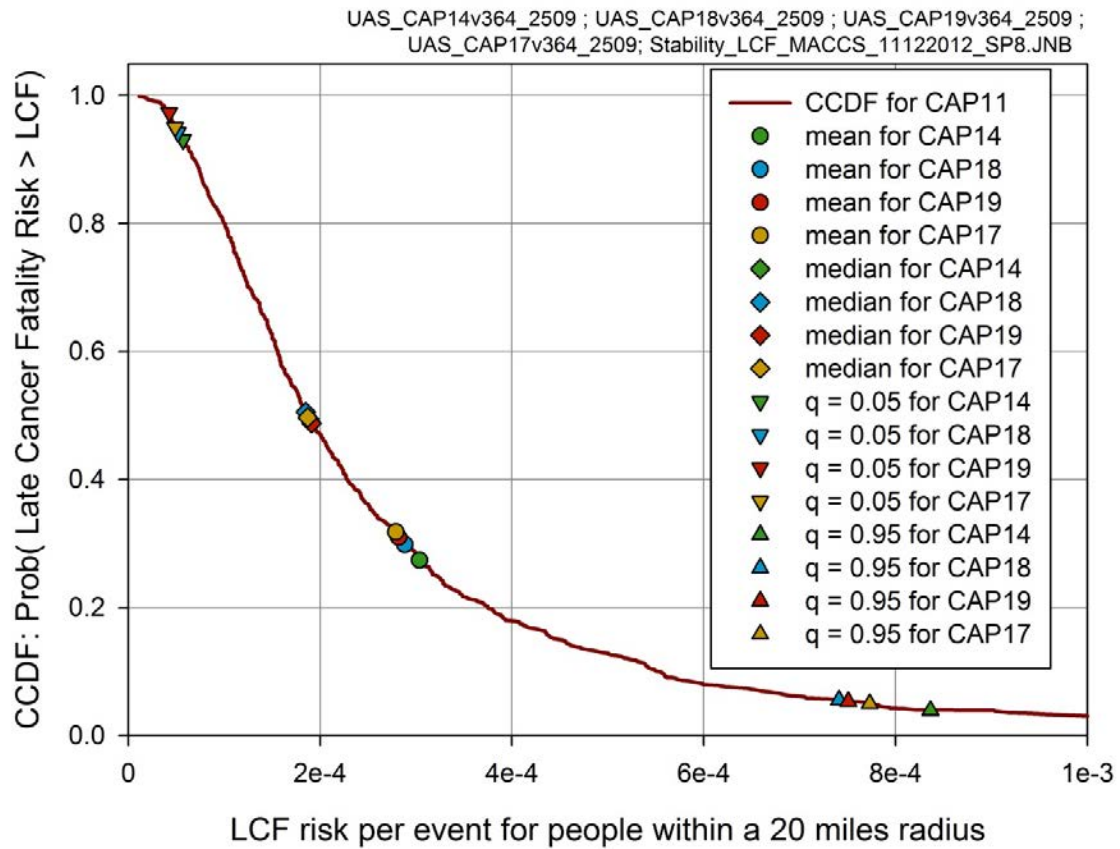


Figure 6.2-2 Complementary cumulative distribution function and statistical values for conditional, mean, individual LCF risk (per event) within a 20-mile radius

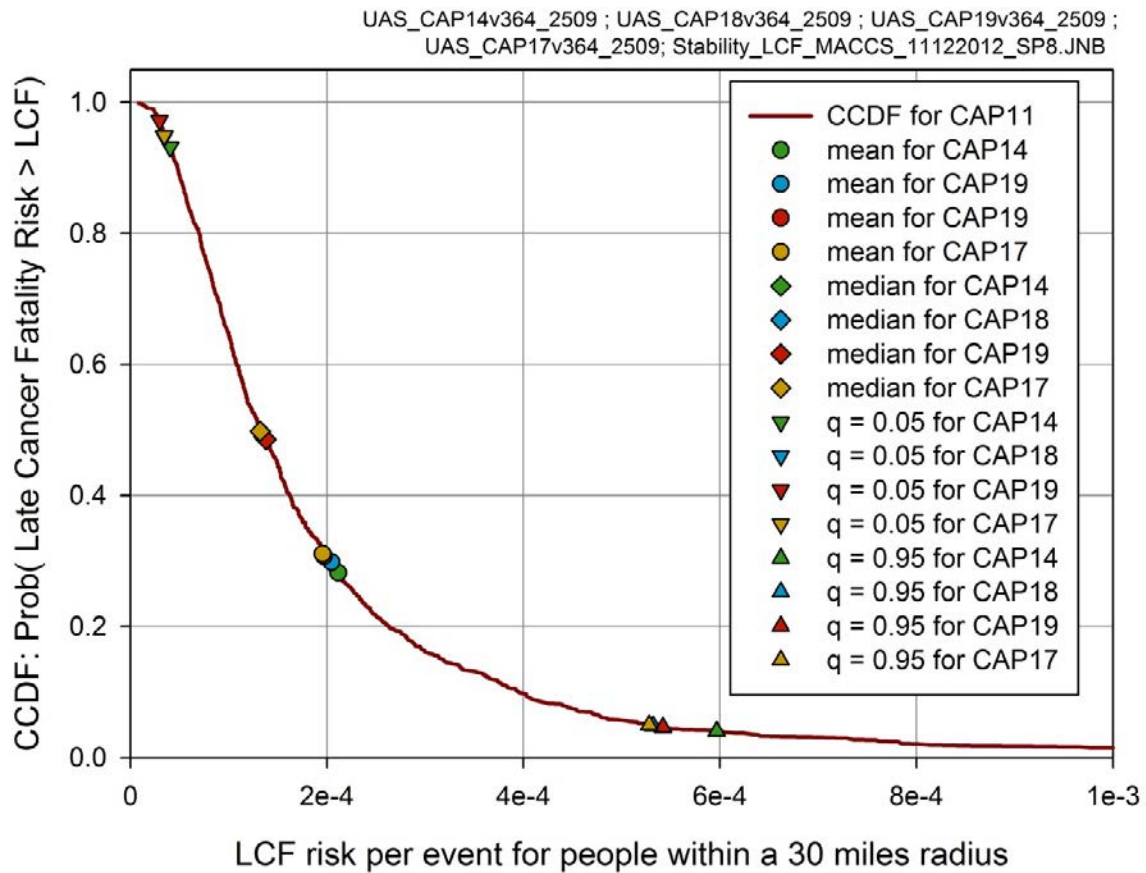


Figure 6.2-3 Complementary cumulative distribution function and statistical values for conditional, mean, individual LCF risk (per event) within a 30-mile radius

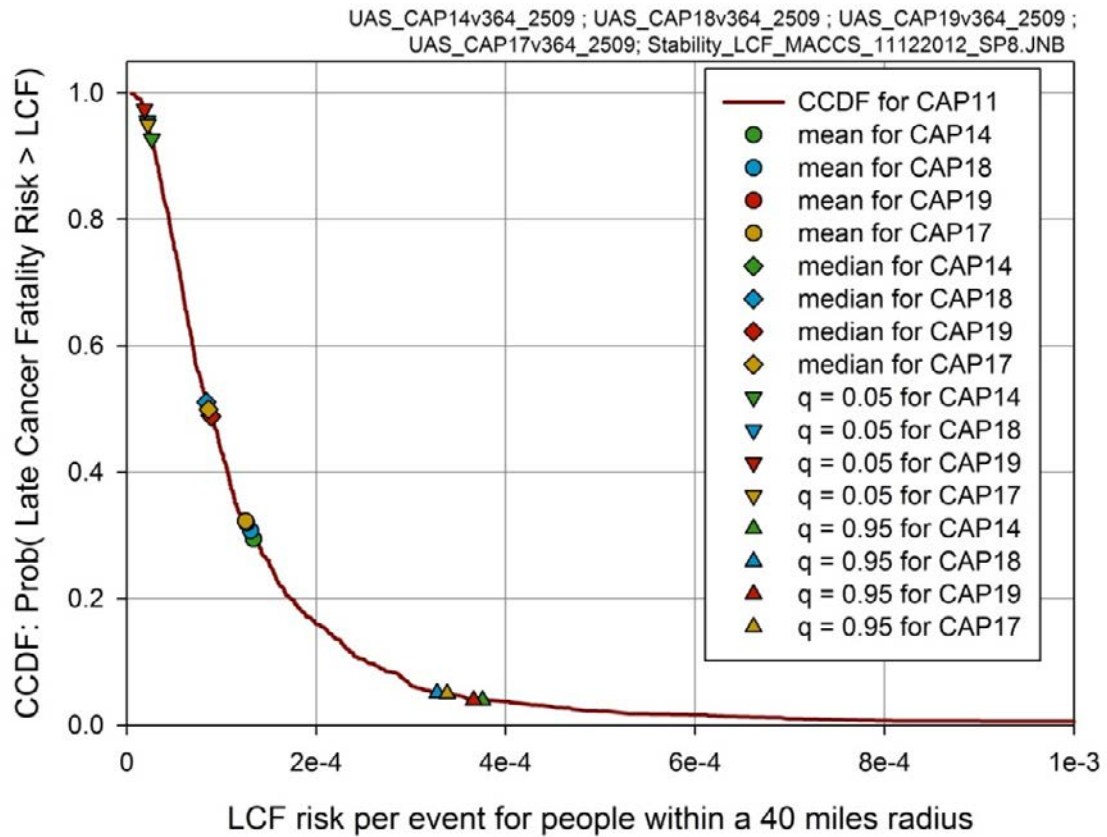


Figure 6.2-4 Complementary cumulative distribution function and statistical values for conditional, mean, individual LCF risk (per event) within a 40-mile radius

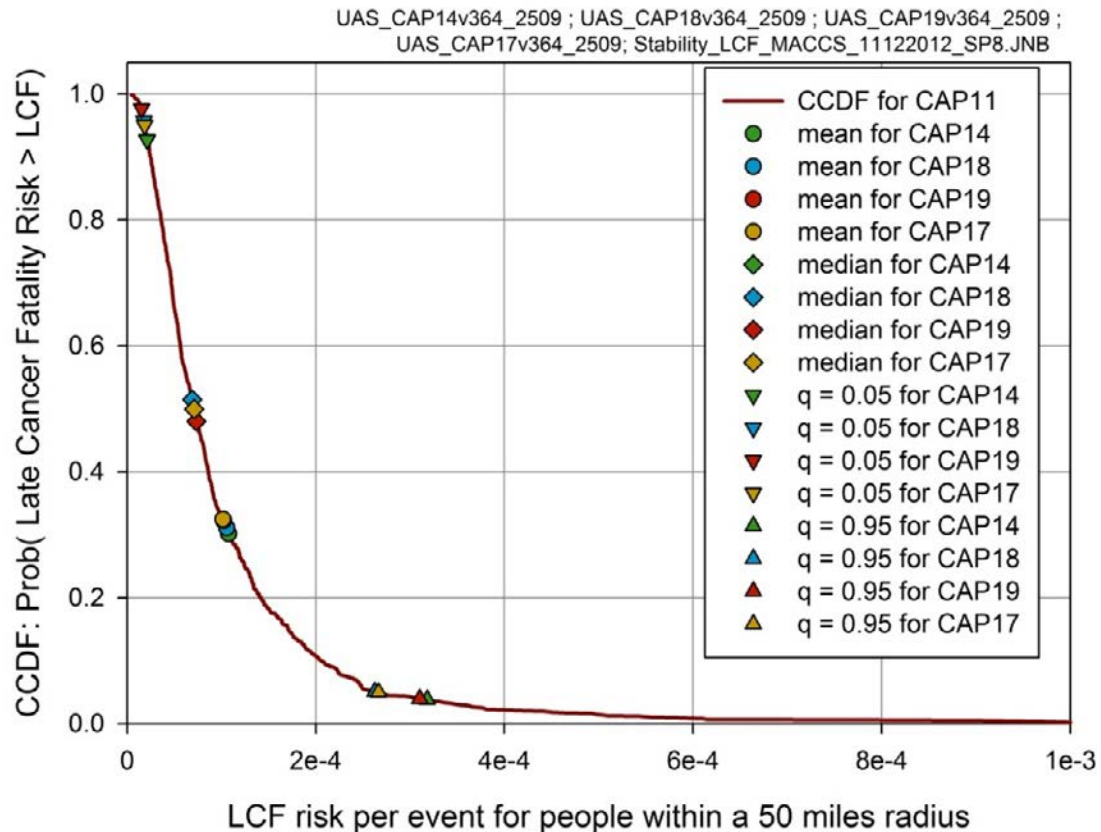


Figure 6.2-5 Complementary cumulative distribution function and statistical values for conditional, mean, individual LCF risk (per event) within a 50-mile radius

When the 10-mile and 20-mile circular area statistics are compared, there is larger influence of the emergency phase for the 20-mile region compared to the 10-mile region, for which nearly all of the population evacuated. This comparison is shown on Figure 6.2-6 for the contribution to LCF risk from the long-term phase, and Figure 6.2-7 for the contribution of the LCF risk from the emergency phase. This indicates that variations in doses during the emergency phase are greater than variations in dose during the long-term phase. As noted above, ad hoc evacuation modeling beyond the 10-mile EPZ was not included in this uncertainty study.

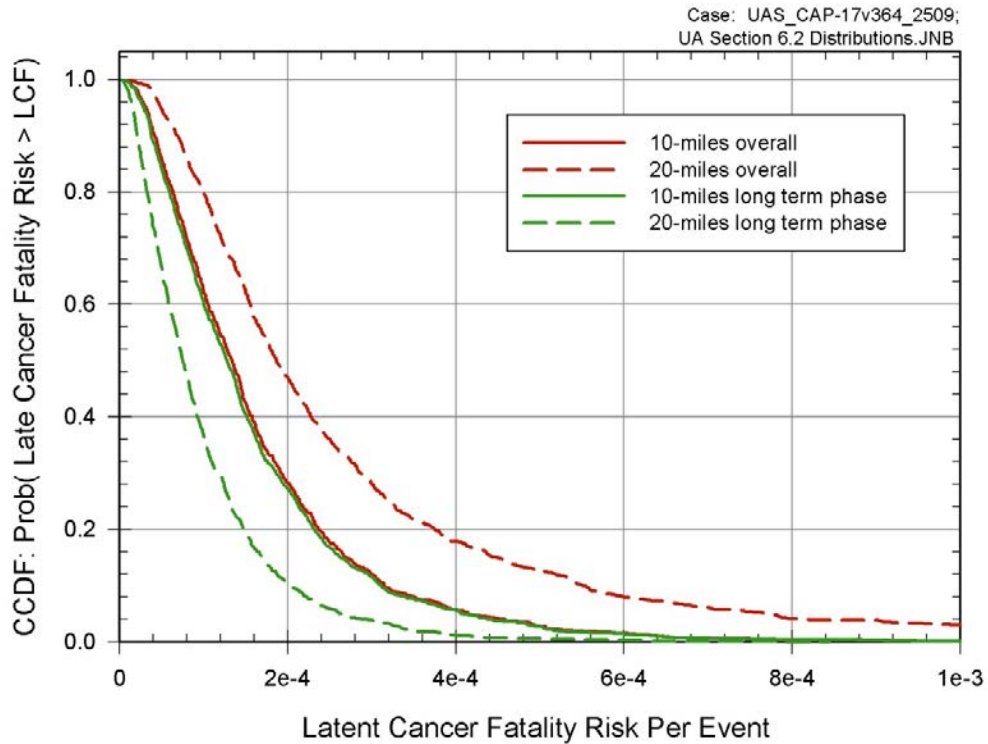


Figure 6.2-6 Complementary cumulative distribution function for conditional, mean, individual LCF risk (per event) within a 10-mile and 20-mile radius for 'overall' and 'long-term phase' LCF risk

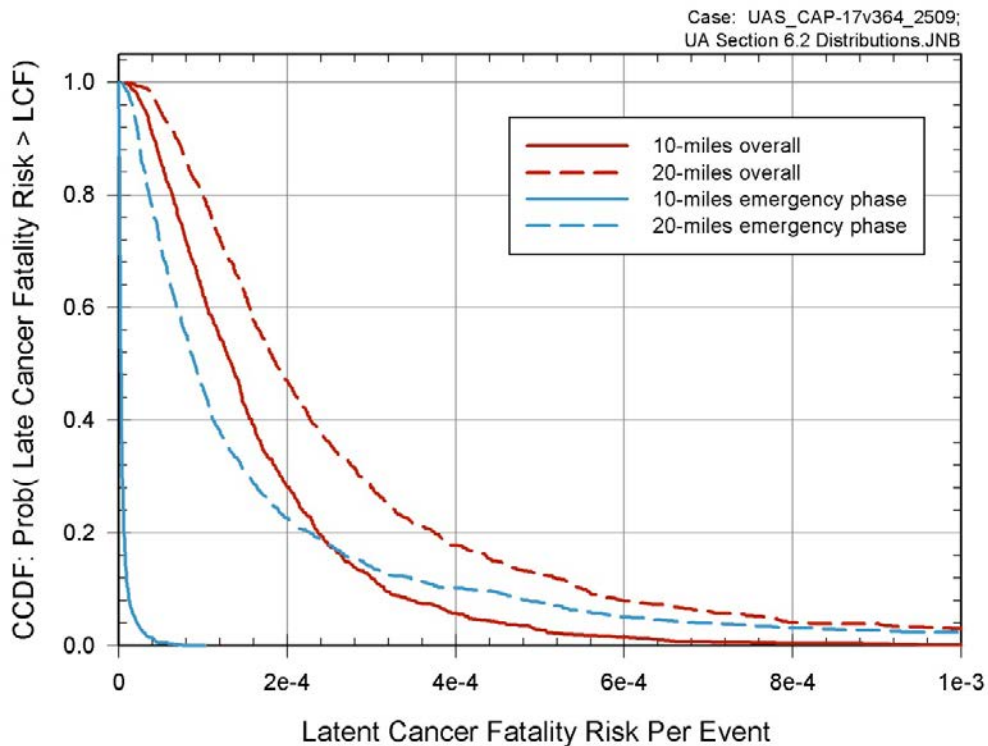


Figure 6.2-7 Complementary cumulative distribution function for conditional, mean, individual LCF risk (per event) within a 10-mile and 20-mile radius for 'overall' and 'emergency phase' LCF risk

Table 6.2-3 shows the correlation matrix for the MACCS Uncertainty Analysis for the conditional, mean, individual LCF risk (per event) at the specified circular areas. This table indicates how strongly the MACCS results are correlated amongst each other when the radial distances change. The closer the correlation value is to 1.0, the more similar are the results. Table 6.2-3 indicates that while the conditional, mean, individual LCF risk (per event) for a radial distance of 10 miles is different than other radials distance (i.e., first row, correlation coefficient ranging from 0.41 to 0.55), the other radial distances lead to pretty similar results (i.e., coefficients of correlation greater than 0.98). The correlation between all the circular areas outside the EPZ to the EPZ distance (i.e., 10 miles) shows that evacuation has a pronounced effect on the correlation. This is because residents within the EPZ, with the exception of the 0.5% who are assumed not to evacuate, evacuate ahead of the release and therefore receive no dose during the emergency phase. The majority of the residents outside the EPZ do receive a dose during the emergency phase. All circular areas beyond the EPZ (i.e., 10 miles) are very well correlated with regards to their respective MACCS input parameters. This is expected since there are no MACCS input parameters that would significantly affect one region differently than another. One minor exception is that 20% of the residents between 10 and 20 miles from the site are assumed to be part of the shadow evacuation. Otherwise, all residents outside of the EPZ are assumed to behave the same way.

Table 6.2-3 Correlation matrix of the conditional, mean, individual LCF risk (per event) for the MACCS Uncertainty Analysis for specified circular areas (using all three source term replicates)

	0-10 miles	0-20 miles	0-30 miles	0-40 miles	0-50 miles
0-10 miles	1	0.41	0.44	0.51	0.55
0-20 miles		1	0.998	0.99	0.98
0-30 miles			1	0.996	0.99
0-40 miles				1	0.998
0-50 miles					1

6.2.2 Early Fatality Risk

The only nonzero early-fatality risk result calculated in the original SOARCA project was for the Surry ISLOCA scenario (NUREG/CR-7110 Volume 2, Section 7.3.5). For Surry, the exclusion area boundary (EAB) is 0.35 miles from the reactor building from which release occurs, so one mile from the EAB is at 1.35 miles. The closest MACCS grid boundary to 1.35 miles used in the ISLOCA calculations is at 1.3 miles. Table 6.2-4 shows the conditional, mean, individual early-fatality risk (per event) for the Surry ISLOCA scenario. The core damage frequency for this event is 3×10^{-8} pry. Thus the absolute early-fatality risk within one mile of the EAB is 4.5×10^{-14} pry.

Table 6.2-4 Conditional, mean, individual early-fatality risk (per event) for the Surry ISLOCA Scenario

Radius of circular area (mi)	Early-fatality risk (per event)
1.3	1.5×10^{-6}
2	6.4×10^{-7}
2.5	4.0×10^{-7}

For Peach Bottom, the EAB is 0.5 mile from the reactor building from which a release occurs, so the outer boundary of this one mile zone is at 1.5 miles. The closest MACCS grid boundary to 1.5 miles used in this set of calculations is at 1.3 miles. The Peach Bottom LTSBO scenario has a conditional, mean, individual early-fatality risk (per event) of 0.00 (NUREG/CR-7110 Volume 1, Section 7.3.1).

In this uncertainty analysis, the early-fatality risks are zero for 87% of all realizations at all specified circular areas. This is because the release fractions are too low to produce doses large enough to exceed the dose thresholds for early fatalities, even for the 0.5% of the population that are modeled as refusing to evacuate. The largest value of the mean, acute exposure for the closest resident (i.e., 1.6 to 2.1 kilometers from the plant) for many of these replicates is about 0.3 gray (Gy) to the red bone marrow, which is usually the most sensitive organ for early fatalities, but the minimum acute exposure that can cause a early fatality is about 2.3 Gy to the red bone marrow. The calculated exposures for these scenarios are all below this threshold.

Unlike the SOARCA analyses in NUREG/CR-7110 Volume 1 and Volume 2, a nonzero early-fatality risk was calculated beyond 2.5 miles (see Table 6.2-4). 11% of the 865 MACCS realizations investigated resulted in a nonzero early-fatality risk per event out to 1.3 miles. 1.3% of the realizations result in a early-fatality risk at 2 miles but not at 1.3 miles due to specific sampled weather trial conditions, including wind directions, and the nearest location of residents in that direction. 0.3% of the 865 realizations that resulted in a nonzero early-fatality risk per event out to 10 miles. In other words, a select few realizations (three) result in a large enough source term that when combined with specific weather trials in the MACCS calculation result in early-fatality risks out to the boundary of the EPZ. A more detailed discussion of this is provided in Section 6.2.4.

Table 6.2-5 shows statistical results for conditional, mean, individual early-fatality risk (per event) from the MACCS Uncertainty Analysis at the specified circular areas. Each statistic was estimated to evaluate the epistemic uncertainties resulting from the uncertain inputs. Since at most radial distances there were insufficient results to calculate the 75th and 95th percentiles directly, a t-distribution was used to estimate the 75th and 95th percentiles.

At 2.5 miles and beyond in Table 6.2-5 the mean result is greater than the 95th percentile. This is due to the few number of nonzero early-fatality risks (i.e., less than 5% of the realizations) at these distances. A distribution can be skewed enough so that the mean is greater than the 95th percentile. For these cases the mean may be higher than the 99th percentile, because it is driven by just a few nonzero values within a population comprised overwhelming of zeros. This is the case here for early-fatality risk beyond 2.5 miles.

Table 6.2-5 Conditional, mean, individual early-fatality risk (per event) average statistics for the composite MACCS Uncertainty Analysis for specified circular areas (using all three source term replicates)

	0-1.3 miles	0-2 miles	0-2.5 miles	0-3 miles	0-3.5 miles	0-5 miles	0-7 miles	0-10 miles
Mean	4.5×10^{-7}	1.8×10^{-7}	8.9×10^{-8}	6.4×10^{-8}	3.5×10^{-8}	1.4×10^{-8}	8.3×10^{-9}	4.8×10^{-9}
Median	0.0	0.0	0.0	0.0	0.0	0.0	0.0	0.0
75 th percentile	0.0	0.0	0.0	0.0	0.0	0.0	0.0	0.0
95 th percentile	1.9×10^{-6}	7.4×10^{-7}	3.5×10^{-8}	5.3×10^{-10}	0.0	0.0	0.0	0.0

As shown on Figure 6.2-8, the CCDF for the composite MACCS uncertainty analysis (CAP17) for the conditional, mean, individual early-fatality risk (per event) are very similar and are in good agreement when compared with the three uncertainty analyses conducted for MACCS convergence (i.e., CAP14, CAP18, and CAP19 results described in Section 5.2.1) at the 1.3-mile circular area (i.e., within 1 mile of EAB). Also, Figure 6.2-8 shows a change within the 95th percentile interval between the MACCS Uncertainty Analysis and the MACCS convergence analyses. This is a result of the limited number of early-fatality risks greater than zero. Only 11% of the total data of the MACCS results for the MACCS Uncertainty Analysis resulted in a nonzero early-fatality risk. However, the slight difference between the means indicates that the incorporation of all 865 MELCOR source terms into a single MACCS uncertainty analysis does not result in any significant change to the overall statistics with respect to the MACCS uncertainty inputs (i.e., compare Table 5.2-13 with Table 6.2-5).

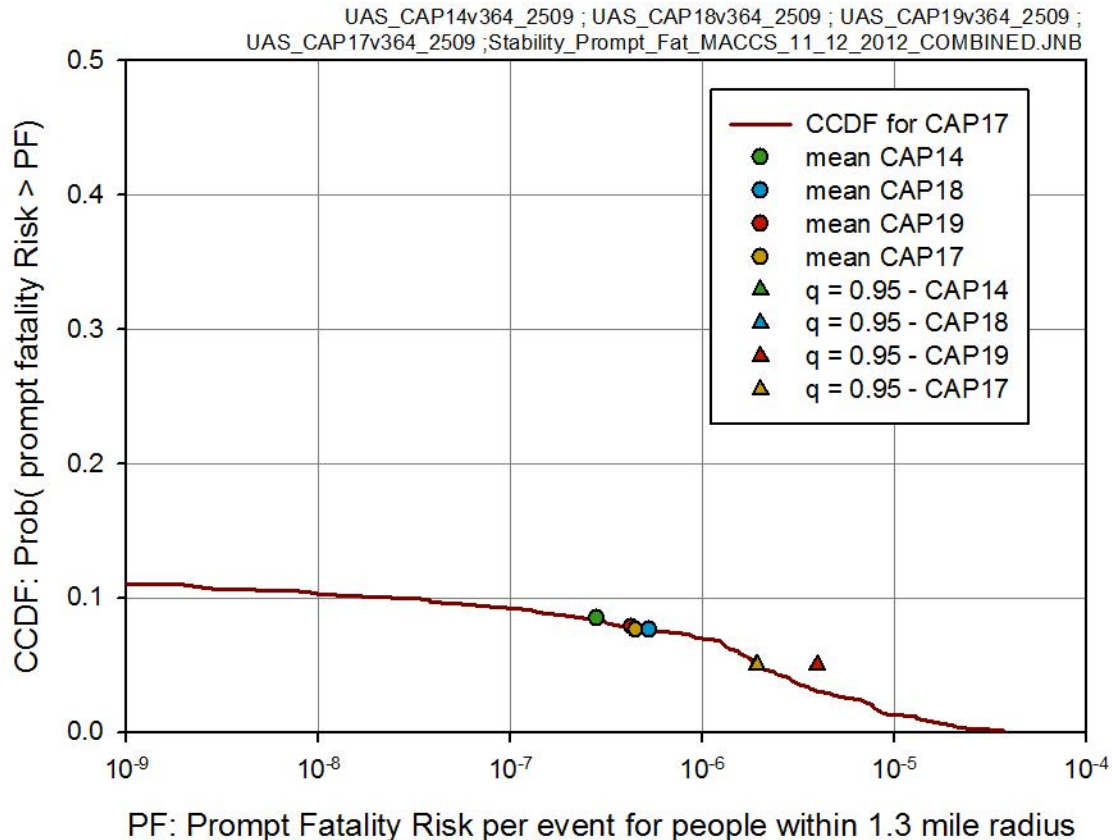


Figure 6.2-8 Complementary cumulative distribution function and statistical values for conditional, mean, individual early-fatality risk (per event) within a 1.3-mile radius

Figures 6.2-9 through 6.2-12 show the CCDFs for the composite MACCS Uncertainty Analysis (CAP 17) for the conditional, mean, individual early-fatality risk (per event) for the 2-, 2.5-, 3-, and 3.5-mile circular areas, respectively. These figures also show the mean and 95th quantiles from the three replicate/convergence analyses (CAP 14, 18, 19) for comparison. The results are similar to those discussed on Figure 6.2-8; however, the percent of early-fatality risk results greater than zero for each subsequent circular area decreases. The nonzero early-fatality risk results decreases from 11% of the total early-fatality risk results at 1.3 miles to 4% of the total early-fatality risk results at 3.5 miles. Beyond the 3.5 mile circular area, the source terms that generate nonzero early-fatality risks drop below 2% and the plots convey little useful information. For distances beyond 2.5 miles, the 95th percentile statistics are not well converged (i.e., greater than an order of magnitude difference). Even at a 2-mile radius, the 95th percentiles differ up to 70%. This is expected, given the small fraction of nonzero results in the total population of results.

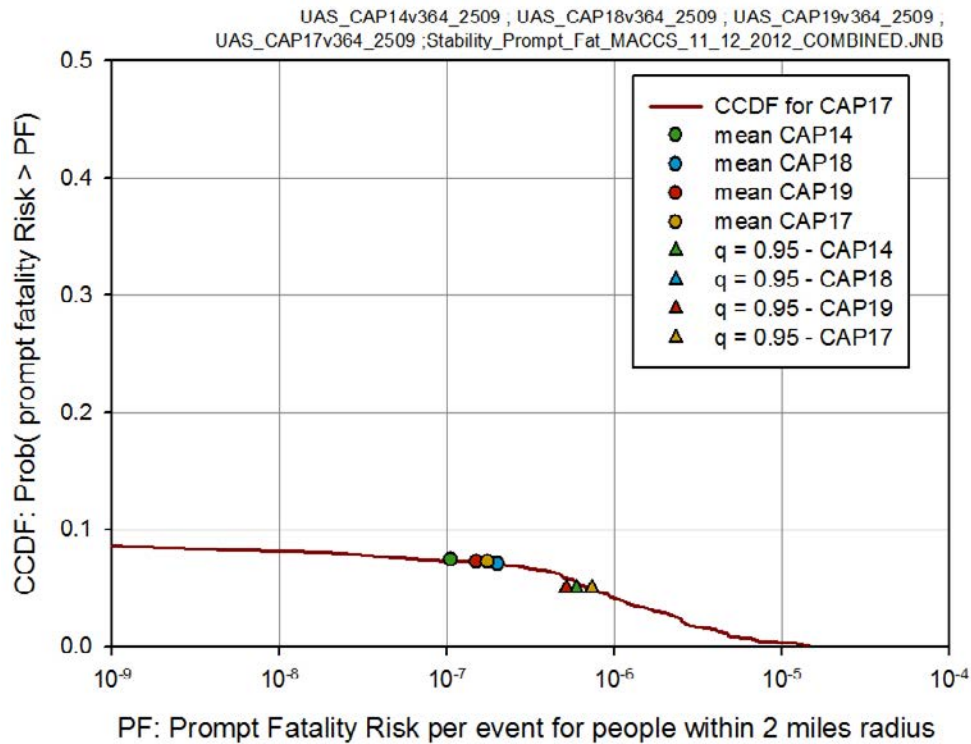


Figure 6.2-9 Complementary cumulative distribution function and statistical values for conditional, mean, individual early-fatality risk (per event) within a 2-mile radius

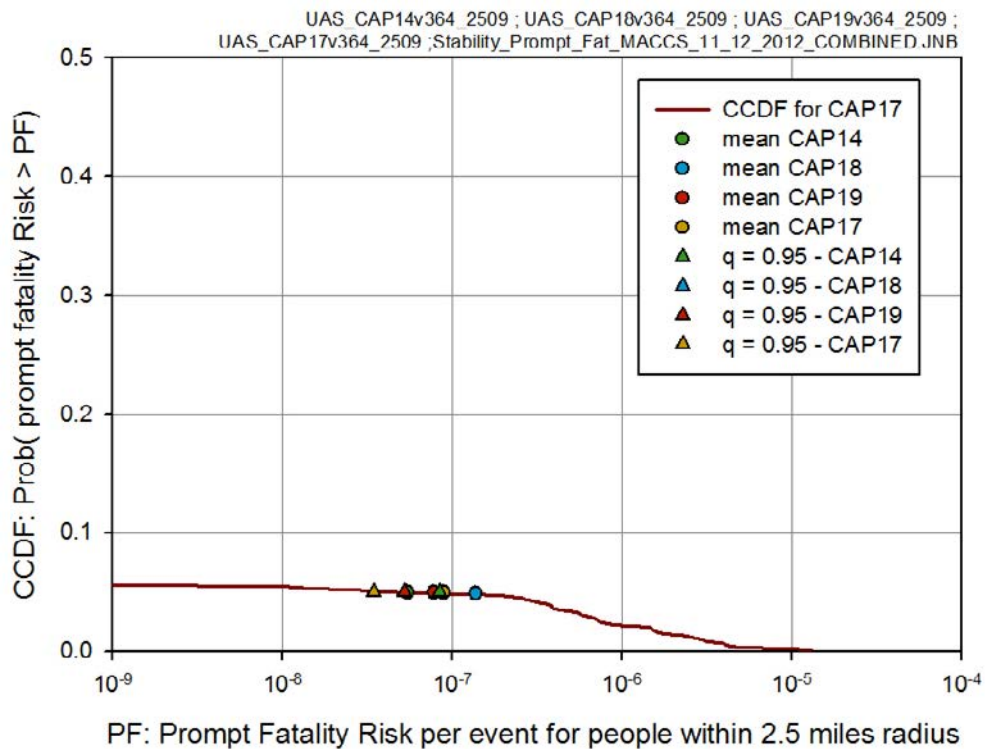


Figure 6.2-10 Complementary cumulative distribution function and statistical values for conditional, mean, individual early-fatality risk (per event) within a 2.5-mile radius

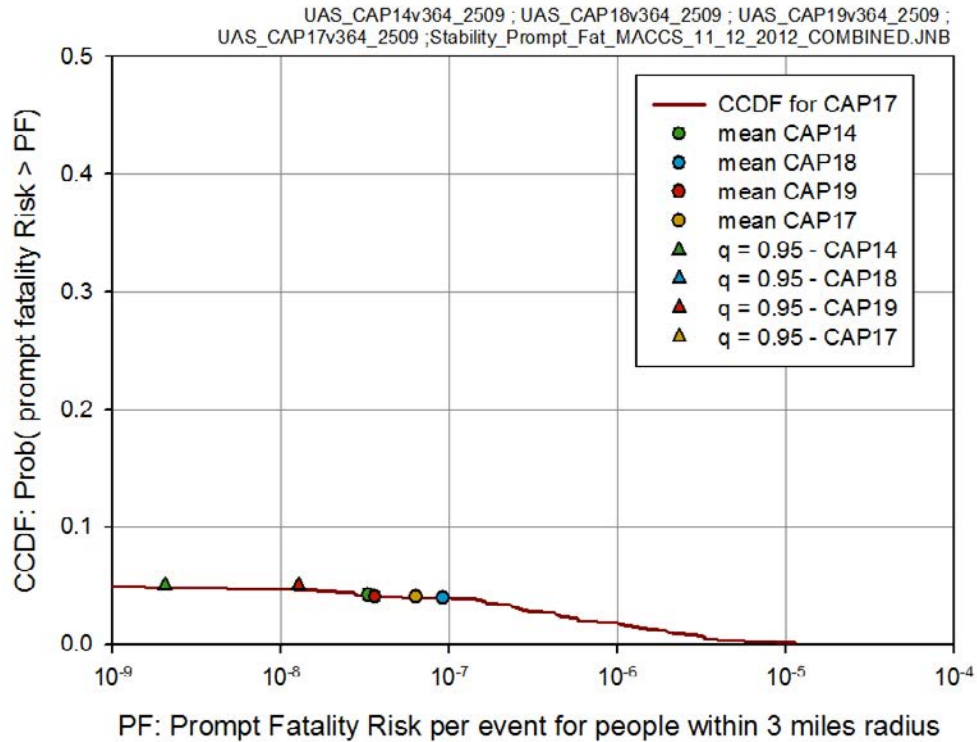


Figure 6.2-11 Complementary cumulative distribution function and statistical values for conditional, mean, individual early-fatality risk (per event) within a 3-mile radius

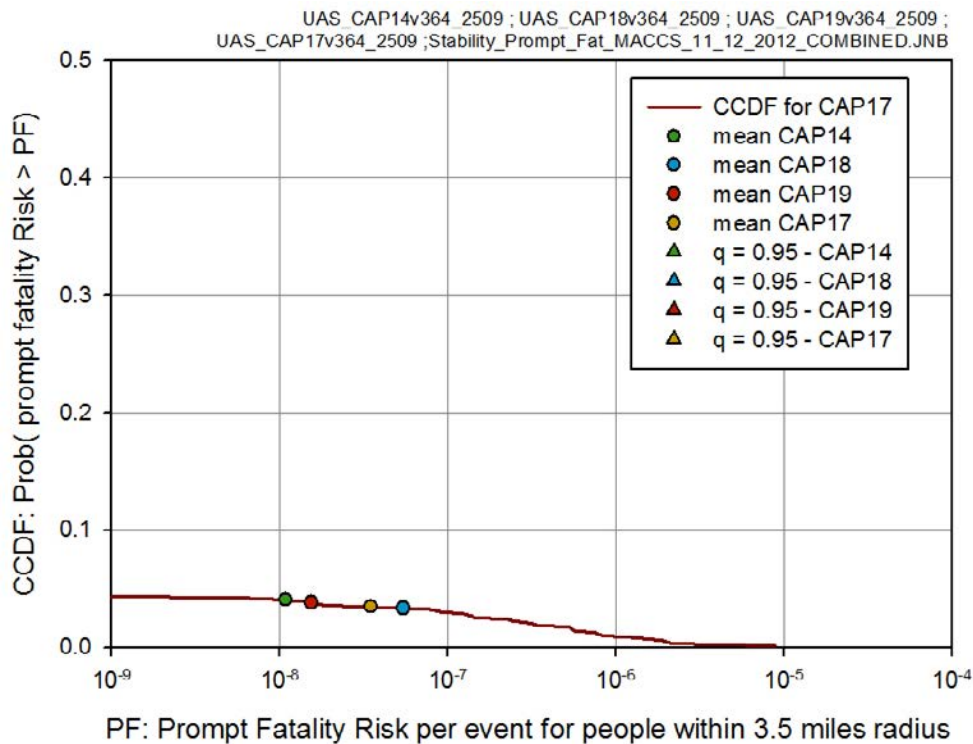


Figure 6.2-12 Complementary cumulative distribution function and statistical values for conditional, mean, individual early-fatality risk (per event) within a 3.5-mile radius

Table 6.2-6 shows the correlation matrix for the MACCS uncertainty analysis for the conditional, mean, individual early-fatality risk (per event) at specified circular areas. The correlation data only applies to nonzero early-fatality risk results. There is poorer correlation between the closer circular areas and the further circular areas due to the small number of replicates where a nonzero early-fatality risk is observed beyond five miles. Only 1% of the MACCS realizations result in a nonzero early-fatality risk at the 7-mile circular area. These 7-mile early-fatality risk realizations are amongst the top 2% of the realizations (4 realizations total) that result in a nonzero early-fatality risk at the 1.3-mile circular area. Thus the risk at seven miles is not strongly correlated with the shorter distances since it is heavily weighted towards the higher end of the early-fatality risks. Similarly, the realizations at 10 miles that result in a nonzero early-fatality risk are amongst the top 2% of the realizations that result in a nonzero early-fatality risk at 1.3 miles. The 5-mile, 7-mile, and 10-mile circular area early fatality risks are strongly correlated with each other. Three of the top four of the realizations that result in a nonzero early-fatality risk at the 7-mile circular area also result in a nonzero early-fatality risk at the 10-mile circular area. These three nonzero early-fatality risk at the 10-mile circular area are further discussed in Section 6.2.4.

Table 6.2-6 Correlation matrix for the MACCS Uncertainty Analysis for the conditional, mean, individual early-fatality risk (per event) for specified circular areas (using all three source term replicates)

	0-1.3 miles	0-2 miles	0-2.5 miles	0-3 miles	0-3.5 miles	0-5 miles	0-7 miles	0-10 miles
0-1.3 miles	1	0.93	0.68	0.74	0.54	0.42	0.34	0.26
0-2 miles		1	0.85	0.90	0.77	0.67	0.59	0.50
0-2.5 miles			1	0.93	0.94	0.85	0.77	0.68
0-3 miles				1	0.93	0.87	0.81	0.73
0-3.5 miles					1	0.96	0.91	0.85
0-5 miles						1	0.99	0.95
0-7 miles							1	0.99
0-10 miles								1

6.2.3 Regression Analysis

As part of the statistical analysis of the MACCS Uncertainty Analysis, a series of regression methods were applied to determine which input parameters most affect LCF risk and early-fatality risk. The four regression methods used were rank regression, quadratic regression, recursive partitioning, and MARS, as described in section 3.4.2.

6.2.3.1 Regression Analysis from Latent Cancer Fatality Risk

Tables 6.2-7 through 6.2-11 show the results of the regression methods used to correlate the conditional, mean, individual LCF risk (per event) results from the MACCS uncertainty analysis (CAP17) for the 10-mile, 20-mile, 30-mile, 40-mile, and 50-mile circular areas, respectively. The tables are a general indication of input parameter influence on the results. Rank regression often underestimates the true influence of a parameter since it captures only a monotonic

relationship (see discussion in Section 3.4.2). A slightly non-monotonic relationship results in a smaller R^2 than when the relationship is purely monotonic.

The tables are ordered by input variables with the highest rank regression results, and then are further grouped according to the type of input parameter (i.e., MACCS or MELCOR variables). The final R^2 determination for all four regression models are fairly high at the five specified circular areas and range from 0.42 for MARS at 30 miles (Table 6.2-9) to 0.85 for recursive partitioning at 10 miles (Table 6.2-7).

All regression methods for the specified circular areas consistently rank the following parameters, respectively, as the most important input variables:

- The MACCS dry deposition velocity (VDEPOS),
- The MELCOR safety relief valve (SRV) stochastic failure probability (SRVLAM), and
- The MACCS risk factor for cancer fatalities for the residual organ (CFRISK–Residual). The residual organ is represented by the pancreas and is used to define all latent cancers not specifically accounted for in the MACCS model. The pancreas is chosen to be a representative soft tissue.

Additional variables also consistently show some level of importance at all circular areas in at least one of the regression methods. These additional input variables include the following:

- The MELCOR fuel failure criterion,
- The MELCOR drywell liner melt-through open area flow path (FL904A),
- The MACCS dose and dose-rate effectiveness factor for the residual organ (DDREFA-Residual).

These six variables (VDEPOS, SRVLAM, fuel failure criterion, FL904A, CFRISK-residual, and DDREFA-residual) account for 26%-75% of the variance for the different circular areas using the different regression methods. Other input parameters indicate some importance within certain circular areas but not within other circular areas.

Thus, the most important variable, VDEPOS, appears at the top of the tables followed by the consistently important MELCOR variables, (i.e., SRVLAM, fuel failure criterion, and FL904A), the LCF risk parameters for residual cancers (i.e., CFRISK-residual and DDREFA-residual), and finally other LCF risk parameters, dose conversion factors for inhalation, and MELCOR parameters (e.g., rail road doors open or closed – RRDOOR) that appear in only some of the tables.

The MACCS dry deposition velocity (VDEPOS) is expected to be important to LCF risk because the long-term dose with the LNT model is driven by dry deposition velocity since long-term dose results mainly from groundshine. Wet deposition also contributes to groundshine dose, but its contribution is smaller on average due to the fact that rain only occurs about 7% of the time at Peach Bottom. A larger value of dry deposition velocity results in larger long-term doses at shorter distances and smaller doses at longer distances. This explains why the correlation coefficient is positive at 10 miles and negative beyond 10 miles for the rank regression analysis. As discussed in further detail in Section 4.2.2, dry deposition is characterized in MACCS with a set of deposition velocities corresponding to a set of aerosol size bins. All of the deposition velocities are correlated, so VDEPOS indicates the deposition velocity for each of the aerosol bins. Currently, MACCS uses a fixed deposition velocity that is independent of wind speed and other conditions (whereas in reality, deposition velocity would vary with wind speed and surface roughness).

Table 6.2-7 Conditional, mean, individual LCF risk (per event) regression of the MACCS Uncertainty Analysis for the 10-mile circular area

	Rank Regression			Quadratic			Recursive Partitioning			MARS		
Final R ²	0.73			0.76			0.85			0.72		
Input	R ² inc.	R ² cont.	SRRC	S _i	T _i	p-val	S _i	T _i	p-val	S _i	T _i	p-val
VDEPOS	0.31	0.31	0.56	0.15	0.28	0	0.22	0.53	0	0.33	0.37	0
SRVLAM	0.43	0.12	-0.35	0.07	0.21	0	0.16	0.35	0	0.12	0.12	0.02
Fuel failure criterion	0.44	0.01	0.15	0.01	0.03	0.55	---	---	---	0.07	0.13	0
FL904A	0.45	0.01	0.12	---	---	---	---	---	---	0	0	1
BATTDUR	---	---	---	---	---	---	0	0.01	0.55	0	0	1
CFRISK Residual	0.54	0.09	0.31	0.16	0.27	0	0.15	0.48	0	0.18	0.25	0
DDREFA Residual	0.57	0.03	-0.18	0.03	0.19	0	0.01	0.05	0.05	0.05	0.16	0
GSHFAC Normal	0.63	0.06	0.24	0.05	0.22	0	---	---	---	0.04	0.09	0.01
CFRISK Colon	0.66	0.03	0.17	0.03	0.20	0	0	0.04	0.33	0.07	0.08	0.05
DDREFA Colon	0.67	0.01	-0.08	0.03	0.02	0.4	---	---	---	---	---	---
CFRISK Lung	0.70	0.03	0.17	0.03	0	1	0	0.10	0.11	0.05	0.02	0.35
DDREFA Lung	0.71	0.01	-0.08	---	---	---	0.01	0.05	0.09	0	0	1
CFRISK Breast	0.72	0.01	0.10	0	0.03	0.44	0	0	1	0.04	0.08	0
CYSIGA	0.73	0.01	0.09	0.01	0.11	0	---	---	---	---	---	---
CWASH1	0.74	0.01	0.07	---	---	---	0	0	1	---	---	---
CFRISK Liver	0.75	0.01	0.07	0.03	0	1	---	---	---	---	---	---
GSHFAC Evacuation	---	---	---	0	0.11	0	0.02	0	1	---	---	---
Cm-242 Inhalation	---	---	---	0	0.08	0.01	---	---	---	0	0	1
Ce-144 Inhalation	---	---	---	0	0	1	---	---	---	---	---	---
Sr-91 Inhalation	---	---	---	---	---	---	0	0.07	0.03	---	---	---
RDSTC	---	---	---	---	---	---	0.04	0.05	0.09	---	---	---
GSHFAC Sheltering	---	---	---	---	---	---	0.04	0.05	0.11	0.01	0	1
I-134 Inhalation	---	---	---	---	---	---	0	0	1	---	---	---
Pu-238 Inhalation	---	---	---	---	---	---	---	---	---	0.03	0	1

Note: Parameters are grouped by importance and relationship (e.g. MELCOR parameters). Light shading indicates parameters with low importance. The dark shading and no shading represent 'groupings' of parameters (e.g., source term influence from MELCOR inputs or latent cancer risk associated for a specific target organ).

Table 6.2-8 Conditional, mean, individual LCF risk (per event) regression of the MACCS Uncertainty Analysis for the 20-mile circular area

	Rank Regression			Quadratic			Recursive Partitioning			MARS		
Final R ²	0.50			0.61			0.64			0.44		
Input	R ² inc.	R ² cont.	SRRC	S _i	T _i	p-val	S _i	T _i	p-val	S _i	T _i	p-val
VDEPOS	0.17	0.17	-0.41	0.12	0.26	0	0.12	0.47	0	0.22	0.40	0
SRVLAM	0.25	0.08	0.28	0.12	0.21	0	0.11	0.24	0.05	0.19	0.31	0
BATTDUR	0.28	0.03	0.26	---	---	---	---	---	---	0.05	0.06	0.04
Fuel failure criterion	0.30	0.02	0.13	0	0.10	0	---	---	---	0.02	0	1
FL904A	0.31	0.01	-0.11	0	0.01	0.67	0.02	0.07	0.15	0.02	0	1
CFRISK Residual	0.38	0.07	0.28	0.11	0.07	0.55	0.04	0.16	0.03	0.14	0.12	0.06
DDREFA Residual	0.40	0.02	0.16	0.01	0	1	0.07	0.08	0.02	0.04	0	1
Cm-242 Inhalation	0.43	0.03	0.18	0.01	0.07	0.04	0.02	0.04	0.10	0	0.06	0.14
CFRISK Breast	0.45	0.02	0.13	---	---	---	0	0.08	0.01	0.02	0.10	0
CFRISK Lung	0.47	0.02	-0.14	0.04	0.23	0	0.04	0.34	0	0.07	0.24	0
DDREFA Lung	0.48	0.01	-0.09	---	---	---	---	---	---	0	0	1
RRDOOR	0.50	0.02	-0.08	0.02	0.06	0.21	---	---	---	---	---	---
I-134 Inhalation	0.52	0.02	-0.08	0.05	0	1	---	---	---	---	---	---
CFRISK Liver	0.53	0.01	0.08	---	---	---	0	0.01	0.61	---	---	---
GSHFAC Evacuation	0.54	0.01	0.08	0.01	0.12	0.01	0.07	0.18	0	---	---	---
RDSTC	---	---	---	0.01	0.20	0	0.01	0.14	0	---	---	---
Sr-91 Inhalation	---	---	---	0	0.09	0	0.01	0.04	0.15	---	---	---
Ba-140 Inhalation	---	---	---	0	0	1	---	---	---	---	---	---
Sr-90 Inhalation	---	---	---	0	0	1	---	---	---	---	---	---
DDREFA Colon	---	---	---	---	---	---	0	0.15	0	---	---	---
CFRISK Colon	---	---	---	---	---	---	0	0.06	0.06	0	0	1
RRIDFRAC	---	---	---	---	---	---	0	0	1	---	---	---
GSHFAC Sheltering	---	---	---	---	---	---	---	---	---	0	0.08	0.02
GSHFAC Normal	---	---	---	---	---	---	---	---	---	0	0	0.48

Table 6.2-9 Conditional, mean, individual LCF risk (per event) regression of the MACCS Uncertainty Analysis for the 30-mile circular area

	Rank Regression			Quadratic			Recursive Partitioning			MARS		
Final R ²	0.51			0.59			0.64			0.42		
Input	R ² inc.	R ² cont.	SRRC	S _i	T _i	p-val	S _i	T _i	p-val	S _i	T _i	p-val
VDEPOS	0.17	0.17	-0.43	0.13	0.23	0	0.20	0.49	0	0.22	0.29	0
SRVLAM	0.25	0.08	0.28	0.20	0.26	0	0.05	0.34	0	0.15	0.30	0
BATTDUR	0.28	0.03	0.26	---	---	---	---	---	---	0	0.03	0.33
Fuel failure criterion	0.31	0.03	0.18	0.02	0.13	0	0.02	0	1	0.01	0.06	0.21
FL904A	0.32	0.01	-0.12	0.01	0.08	0.02	0	0.18	0	0	0	1
CFRISK Residual	0.38	0.06	0.27	0.11	0.16	0	0	0.12	0	0.12	0.15	0.02
DDREFA Residual	0.40	0.02	0.16	0.07	0.11	0	---	---	---	0.04	0.06	0.12
CFRISK Colon	0.42	0.02	0.14	0.01	0.06	0.04	0	0.08	0.05	0.01	0.07	0
CFRISK Breast	0.44	0.02	0.13	---	---	---	---	---	---	0	0.05	0.04
Cm-242 Inhalation	0.46	0.02	-0.13	0.06	0.18	0	0.04	0.43	0	0.18	0.22	0
RRDOOR	0.48	0.02	-0.08	0	0	1	0	0.09	0.09	---	---	---
DDREFA Lung	0.50	0.02	-0.09	---	---	---	---	---	---	0	0	1
RRIDFRAC	0.51	0.01	0.09	---	---	---	---	---	---	---	---	---
Ba-140 Inhalation	0.52	0.01	-0.07	0	0	1	---	---	---	---	---	---
Sr-90 Inhalation	0.53	0.01	0.07	---	---	---	0	0.01	0.44	---	---	---
GSHFAC Evacuation	---	---	---	0.02	0.12	0	---	---	---	---	---	---
CYSIGA	---	---	---	0.00	0.09	0	---	---	---	---	---	---
I-134 Inhalation	---	---	---	0.01	0.06	0.03	0.02	0.03	0.20	---	---	---
CFRISK Lung	---	---	---	0.03	0.06	0.12	0	0.12	0	0	0.01	0.29
DDREFA Bone	---	---	---	0	0	1	0	0.11	0	---	---	---
GSHFAC Normal	---	---	---	---	---	---	0	0.03	0.40	0.01	0	1
RDSTC	---	---	---	---	---	---	0.01	0	1	---	---	---
CFRISK Liver	---	---	---	---	---	---	0.03	0	1	---	---	---
GSHFAC Sheltering	---	---	---	---	---	---	---	---	---	0.03	0.03	0.25
Pu-238 Inhalation	---	---	---	---	---	---	---	---	---	0	0	1

Table 6.2-10 Conditional, mean, individual LCF risk (per event) regression of the MACCS Uncertainty Analysis for the 40-mile circular area

	Rank Regression			Quadratic			Recursive Partitioning			MARS		
Final R ²	0.52			0.57			0.67			0.50		
Input	R ² inc.	R ² cont.	SRRC	S _i	T _i	p-val	S _i	T _i	p-val	S _i	T _i	p-val
VDEPOS	0.18	0.18	-0.43	0.10	0.21	0	0.12	0.52	0	0.23	0.24	0
SRVLAM	0.25	0.07	0.27	0.12	0.28	0	0.16	0.39	0	0.14	0.33	0
Fuel failure criterion	0.28	0.03	0.19	0.01	0.02	0.80	0.05	0.16	0	0.02	0.08	0.06
BATTDUR	0.31	0.03	0.16	---	---	---	0	0.04	0.24	0.01	0.12	0
FL904A	0.32	0.01	-0.13	0.03	0.10	0	0.03	0	0.83	0.05	0.06	0.04
CFRISK Residual	0.37	0.05	0.25	0.04	0.15	0	---	---	---	0.10	0.14	0.02
DDREFA Residual	0.40	0.03	0.16	0.08	0	0.94	0	0	1	0.06	0.10	0.03
DDREFA Lung	0.43	0.03	0.27	0	0	1	---	---	---	0.05	0	1
CFRISK Lung	0.45	0.02	-0.13	0.06	0.25	0	0.04	0.38	0	0.06	0.29	0
CFRISK Colon	0.48	0.03	0.16	---	---	---	---	---	---	0.03	0	1
RRDOOR	0.50	0.02	-0.07	0	0.06	0.21	---	---	---	---	---	---
CFRISK Breast	0.52	0.02	-0.09	0	0	1	0	0	1	0	0	1
I-134 Inhalation	0.53	0.01	-0.08	---	---	---	0.01	0	1	---	---	---
Ce-144 Inhalation	0.54	0.01	0.10	---	---	---	0.05	0	1	---	---	---
CYSIGA	0.55	0.01	0.07	---	---	---	---	---	---	---	---	---
GSHFAC Normal	---	---	---	0.01	0.11	0	0	0.03	0.37	0	0	1
GSHFAC Evacuation	---	---	---	0.07	0.08	0.01	---	---	---	---	---	---
Ba-140 Inhalation	---	---	---	0	0.07	0.03	0	0	1	---	---	---
Sr-91 Inhalation	---	---	---	0	0.05	0.06	---	---	---	---	---	---
Cm-242 Inhalation	---	---	---	0.02	0.04	0.39	0	0.17	0	0.01	0	1
GSHFAC Sheltering	---	---	---	---	---	---	0	0.14	0	0.02	0.05	0.02
Pu-238 Inhalation	---	---	---	---	---	---	0.01	0.02	0.38	0.02	0.06	0.01

Table 6.2-11 Conditional, mean, individual LCF risk (per event) regression of the MACCS Uncertainty Analysis for the 50-mile circular area

	Rank Regression			Quadratic			Recursive Partitioning			MARS		
Final R ²	0.52			0.57			0.71			0.54		
Input	R ² inc.	R ² cont.	SRRC	S _i	T _i	p-val	S _i	T _i	p-val	S _i	T _i	p-val
VDEPOS	0.18	0.18	-0.43	0.09	0.18	0	0.16	0.46	0	0.19	0.39	0
SRVLAM	0.25	0.07	0.26	0.12	0.31	0	0.05	0.29	0	0.05	0.16	0.06
Fuel failure criteria	0.45	0.03	0.16	---	---	---	0	0.05	0.07	0	0.01	0.38
FL904A	0.48	0.02	-0.14	0.04	0.08	0	0.05	0.28	0	0.02	0	1
BATTDUR	---	---	---	0.03	0.02	0.46	---	---	---	0	0.01	0.34
DDREFA Residual	0.30	0.05	0.24	0.05	0.09	0.07	---	---	---	0.09	0.09	0.29
CFRISK Residual	---	---	---	0	0.04	0.33	0	0.12	0	0.02	0.01	0.37
GSHFAC Normal	0.34	0.04	0.18	---	---	---	0	0.03	0.45	0.06	0.05	0.14
CFRISK Lung	0.37	0.03	0.19	0.01	0.12	0.01	0.04	0.22	0	0.03	0.07	0.28
DDREFA Lung	0.40	0.03	0.26	0	0.13	0	---	---	---	0.02	0.11	0
GSHFAC Evacuation	0.43	0.03	0.16	0.06	0.15	0	0.01	0.23	0	0.04	0.08	0
Cm-242 Inhalation	0.47	0.02	-0.13	0.09	0.19	0	0.05	0.40	0	0.11	0.22	0
Ce-144 Inhalation	0.50	0.02	0.10	---	---	---	---	---	---	---	---	---
CFRISK Breast	0.51	0.02	-0.09	0.02	0	1	0.03	0	1	0	0.03	0.08
I-134 Inhalation	0.51	0.02	-0.08	0.02	0.06	0.19	---	---	---	---	---	---
Sr-91 Inhalation	0.52	0.01	0.07	---	---	---	0.02	0.05	0.09	---	---	---
RRDOOR	0.52	0.00	0.06	---	---	---	---	---	---	---	---	---
DDREFA Bone	---	---	---	0.01	0.06	0.07	---	---	---	---	---	---
Sr-90 Inhalation	---	---	---	0.03	0	0.6	0.01	0	1	---	---	---
DDREFA Colon	---	---	---	0	0	1	---	---	---	---	---	---
CFRISK Colon	---	---	---	---	---	---	0	0.09	0.21	0	0.05	0.02
GSHFAC Sheltering	---	---	---	---	---	---	0	0	1	---	---	---
Pu-238 Inhalation	---	---	---	---	---	---	---	---	---	0	0.09	0

The MELCOR input variables (SRVLAM, fuel failure criterion, and FL904A) account for at least 7% of the variance with a T_i of 0.16 using the MARS analysis to at most at most 24% of the variance using the recursive partitioning analysis at the specified circular areas for all regression methods. Based on this uncertainty analysis, these three variables ultimately correlate with most of the uncertainty contribution of the source term to LCF risk. As discussed in Section 6.1.1 and Section 6.1.2, these MELCOR input variables account for most of the variance in iodine and cesium release fractions and hence are expected to be important. The MELCOR regression analyses indicate CHEMFORM and SRV open area fraction (SRVOAFRAC) to also be important to release magnitude but these two variables, on the other hand, do not appear as variables of most importance to LCF risk.

Within 10 miles, SRVLAM is negatively correlated with LCF risk in the rank regression analysis. This is because longer SRV valve cycling (lower failure rate) is more likely to result in a main steam line creep rupture, a higher degree of core degradation, and greater releases. The larger releases lead to greater LCF risk mainly from long-term doses since the 10-mile area is evacuated with the exception of the assumed 0.5% of the population that refuses to evacuate.

Beyond 10 miles, SRVLAM is positively correlated in the rank regression analysis. Further statistical regression and sensitivity studies are required to understand the negative correlation beyond 10 miles. A possible explanation is the different dependence on SRVLAM of the release fractions for the chemical classes that results in emergency phase dose versus long-term phase dose.

The remaining two of the six most important variables in the regression analysis, CFRISK-residual, and DDREFA-residual, account for at most 23% of the variance using the MARS analysis at the specified circular areas. The T_i values indicate greater influence in conjunction with other variables. As discussed in Section 4.2.5, the mortality risk coefficients (CFRISK) for each of the organs included in the SOARCA analyses for latent health effects are assumed to be uncorrelated. The dose and dose rate effectiveness factor (DDREFA) is based on BEIR V risk factors for estimating health effects to account for observed differences between low and high dose rates. Doses received during the emergency phase are divided by DDREFA when they are less than 0.2 Gy (20 rad) in the calculation of latent health effects; they are not divided by DDREFA when emergency-phase doses exceed 0.2 Gy. Doses received during the long-term phase are generally controlled by the habitability criterion to be well below 0.2 Gy, so these doses are always divided by DDREFA in the calculation of latent health effects. Since DDREFA is in the denominator, it is negatively correlated with LCF risk.

The MACCS latent cancer parameters CFRISK-residual and DDREFA-residual are used for estimating residual cancers not related to the seven organ-specific cancers that were used in SOARCA:

- Leukemia,
- bone cancer,
- breast cancer,
- lung cancer,
- thyroid cancer,
- liver cancer, and
- colon cancer

It is understandable that the CFRISK and DDREFA factors for the “residual” category would be important, because they account for multiple organs, and their respective CFRISK uncertainty distributions, that are not modeled separately.

In a previous study [60], the amount of shielding between an individual and the source of groundshine, the groundshine shielding factor (GSHFAC), was determined to be an important variable. However, it is found to be of lesser importance in this study. The long-term GSHFAC was directly correlated with the emergency-phase GSHFAC during normal activities for the non-evacuated residents (GSHFAC-Normal). Tables 6.2-7 through 6.2-11 show GSHFAC-Normal as an important variable at the 10- and 50-mile circular areas (i.e., 0-11% of the variance for all regression methods). The 20-, 30-, and 40-mile circular areas show GSHFAC-Normal as variable of much lower importance. The 20-mile, 30-mile, and 40-mile circular areas show a larger contribution of the emergency phase (i.e., an average of 44-55% of the overall LCF risk is contributed by the emergency phase), than the 10-mile and 50-mile circular areas (i.e., an average of 5-40% of the overall LCF risk contributed to the emergency phase).

Unlike the previous study, this uncertainty analysis has varied source terms, a more detailed evacuation model, and approximately 300 more MACCS uncertainty variables.

6.2.3.2 Regression Analysis for Early-fatality Risk

Tables 6.2-12 through 6.2-16 show the regression results obtained for conditional, mean, individual early-fatality risk (per event) for the MACCS Uncertainty Analysis (i.e., CAP17) for the 1.3-mile, 2-mile, 2.5-mile, 3-mile, and 3.5-mile circular areas, respectively. Since less than 2.5% of all the MACCS Uncertainty Analysis realizations resulted in a nonzero early-fatality risk for the 5-mile, 7-mile, and 10-mile circular areas, they are not included in the regression analysis results due to unreliable statistics regarding variable importance.

The tables are a general indication of input parameter influence on the results. Rank regression is often an underestimate the true influence of a parameter since it captures only a monotonic relationship. A slightly non-monotonic relationship results in a smaller R^2 than when the relationship is purely monotonic. The tables are ordered by input variables with the highest rank for all regression results, and then are further grouped according to the type of input parameter (i.e., MACCS or MELCOR variables). There are two noticeable groupings when the important variables are examined. Those within 2 miles, Table 6.2-12 and Table 6.2-13, show the final R^2 for the non-rank regression models are fairly high and range from 0.58 for MARS (Table 6.2-13) to 0.75 for recursive partitioning (Table 6.2-12). The rank regression shows that monotonic relationship for all variables are poor.

For the circular areas less than 2 miles, the non-rank regression methods consistently rank the MACCS wet deposition model (CWASH1), the MELCOR SRV stochastic failure probability (SRVLAM), the MELCOR SRV open area fraction (SRVOAFRAC), the MACCS early health effects threshold and beta (shape) factor for red bone marrow (EFFTHR-Red Marrow and EFFACB-Red Marrow), and the MACCS linear, crosswind dispersion coefficient (CYSIGA), in order, as the most important input variables.

Additional variables also consistently show some level of importance for circular areas less than 2 miles. These additional input variables include the following:

- The MACCS amount of shielding between an individual and the source of groundshine during normal activities for the non-evacuated residents (GSHFRAC-Normal),
- The MACCS evacuation delay for Cohort 5 (DELTVA-Cohort 5), and
- The MELCOR DC station battery duration (BATTDUR)

These nine variables (CWASH1, SRVLAM, SRVOAFRAC, EFFTHR-red marrow, EFFACB-red marrow, CYSIGA, GSHFRAC-normal, DELTVA-cohort 5, and BATTDUR) account for at least 24% of the variance for the quadratic regression, at least 46% of the variance for the recursive partitioning, and at least 30% of the variance for MARS.

Other input parameters show a low importance at certain circular areas but not for other circular areas. Thus, the most important variable, CWASH1, appears at the top of Table 6.2-12 and Table 6.2-13 followed by the consistently important MELCOR variables, SRVLAM and SRVOAFRAC, and then the other five important variables, and finally a set of parameters not consistently seen in all the tables.

The MACCS wet deposition parameter (CWASH1) accounts for at least 4% of the variance with a T_i of 0.78 using the MARS analysis to at most 29% of the variance with a T_i of 0.76 using the quadratic regression analysis for circular areas less than 2 miles for all non-ranked regression methods and is the most important input variable. Also, CWASH1 consistently has the highest rank for interactions with other input variables (T_i). As discussed in detail in Section 4.2.1, the wet deposition model shows that under heavy rains, wet deposition is very effective and rapidly depletes the plume. This process can produce concentrated deposits on the ground and create what is often referred to as a hot spot (i.e., an area of higher radioactivity than the surrounding areas). As seen in the non-ranked regression analysis, rain and its interactions with other input variables (e.g., see the T_i for recursive partition in Table 6.2-12) can significantly affect consequence calculations when it does occur. However, the early-fatality risk is more highly correlated with crosswind dispersion (CYSIGA) beyond 2 miles (see Table 6.2-14). The crosswind dispersion parameter defines how narrow the plume is while it travels, with a narrower plume allowing higher radionuclide concentrations to reach individuals farther from the plant.

The crosswind dispersion coefficient (CYSIGA), early health effects threshold for red bone marrow (EFFTHR-Red Marrow), and other important variables also show a large non-monotonic interaction with other input variables. While the overall R^2 contribution from these input variables is low, their interactions with other variables do justify their consideration to early-fatality risk. The red bone marrow is usually the most sensitive organ for early fatalities. EFFTHR-red marrow and EFFACB-red marrow (discussed below) are important because the hematopoietic syndrome has the lowest threshold for an early fatality.

Table 6.2-12 Conditional, mean, individual early-fatality risk (per event) regression of the MACCS Uncertainty Analysis for the 1.3-mile circular area

	Rank Regression			Quadratic			Recursive Partitioning			MARS		
Final R ²	0.26			0.67			0.75			0.64		
Input	R ² inc.	R ² cont.	SRRC	S _i	T _i	p-val	S _i	T _i	p-val	S _i	T _i	p-val
CWASH1	0.03	0.03	0.10	0.12	0.88	0	0.29	0.77	0	0.11	0.94	0
SRVLAM	0.07	0.04	-0.10	0	0.03	0.56	0.15	0.60	0	0.01	0.17	0.19
SRVOAFRAC	0.10	0.03	-0.09	0.01	0.20	0.13	0.02	0.15	0.12	0.04	0.23	0.14
BATTDUR	---	---	---	---	---	---	0	0.29	0	---	---	---
GSHFAC Normal	0.12	0.02	0.08	0.01	0.60	0	0	0	1	0.01	0.13	0.59
EFFTHR Red Marrow	0.18	0.06	-0.14	0.01	0	1	0	0	1	0	0.04	0.43
EFFACB Red Marrow	0.19	0.01	-0.05	---	---	---	---	---	---	0	0.39	0
CYSIGA	0.22	0.03	-0.09	0	0	1	0.01	0.39	0	0.02	0.39	0
DLTEVA Cohort 5	0.23	0.01	0.01	0.01	0	1	---	---	---	0	0.13	0.30
ESPEED	---	---	---	0.01	0.52	0	0	0.22	0	0	0	1
PROTIN Sheltering	---	---	---	0	0.29	0	0	0.28	0	0	0	1
EFFTHR Stomach	---	---	---	0.01	0.32	0	---	---	---	---	---	---
DLTEVA Cohort 3	0.25	0.02	-0.10	0.01	0.18	0.07	---	---	---	0	0.29	0.01
PROTIN Normal	0.26	0.01	0.06	---	---	---	---	---	---	0.03	0.12	0.45
RRIDFRAC	0.27	0.01	0.04	---	---	---	---	---	---	---	---	---
SC1131_2	0.28	0.01	0.03	---	---	---	---	---	---	0.01	0.27	0.03
DLTEVA Cohort 4	0.28	0.00	0.03	0	0	1	0.02	0	1	---	---	---
GSHFAC Sheltering	---	---	---	0	0.07	0.42	0	0	1	0	0	1
CZSIGA	---	---	---	---	---	---	0.01	0	1	---	---	---
DLTEVA Cohort 2	---	---	---	---	---	---	0	0	1	---	---	---

Table 6.2-13 Conditional, mean, individual early-fatality risk (per event) regression of the MACCS Uncertainty Analysis for the 2-mile circular area

	Rank Regression			Quadratic			Recursive Partitioning			MARS		
Final R ²	0.24			0.62			0.63			0.58		
Input	R ² inc.	R ² cont.	SRRC	S _i	T _i	p-val	S _i	T _i	p-val	S _i	T _i	p-val
CWASH1	0.03	0.03	0.08	0.29	0.76	0	0.15	0.60	0	0.04	0.78	0
SRVLAM	0.07	0.04	-0.10	0.01	0.41	0	0	0.10	0.35	0.01	0.28	0.07
SRVOAFRAC	0.10	0.03	-0.09	0.01	0	1	0.06	0.53	0	0.06	0	1
BATTDUR	0.10	0	-0.03	0	0.13	0.09	0	0.05	0.32	---	---	---
EFFTHR Red Marrow	0.15	0.05	-0.12	0	0.18	0.13	0.01	0.52	0	0.02	0.47	0
EFFACB Red Marrow	0.16	0.01	0.04	---	---	---	---	---	---	0.01	0	1
CYSIGA	0.18	0.02	0.07	0	0.40	0	---	---	---	0.04	0.48	0
DLTEVA Cohort 5	0.19	0.01	-0.07	0.02	0	1	0.07	0.15	0.17	0	0	1
GSHFAC Normal	0.21	0.02	0.06	---	---	---	---	---	---	0.01	0.12	0.27
PROTIN Sheltering	0.22	0.01	0.05	---	---	---	---	---	---	0	0	1
PROTIN Normal	0.23	0.01	-0.04	---	---	---	---	---	---	0	0	1
DLTEVA Cohort 3	0.24	0.01	-0.04	0.02	0.03	0.34	0	0.01	0.58	0	0.39	0
SC1131_2	0.25	0.01	0.04	0	0.15	0.15	---	---	---	0	0.06	0.37
DLTEVA Cohort 4	0.26	0.01	0.03	---	---	---	---	---	---	---	---	---
RRIDFRAC	---	---	---	0	0.07	0.41	---	---	---	---	---	---
ESPEED	---	---	---	0	0	1	---	---	---	0	0	1
RRDOOR	---	---	---	---	---	---	0	0.15	0.06	---	---	---
CZSIGA	---	---	---	---	---	---	0.01	0	1	---	---	---
GSHFAC Sheltering	---	---	---	---	---	---	---	---	---	0.01	0.07	0.55

For the circular areas greater than two miles but less than five miles (Table 6.2-14 through Table 6.2-16), the regression methods consistently rank the following as the most important input variables:

- MACCS crosswind dispersion coefficient (CYSIGA),
- The early health effects threshold risk for red bone marrow (EFFTHR-Red Marrow),

- The early health effects beta (shape) factor for red bone marrow (EFFACB-Red Marrow),
- The MELCOR SRV stochastic failure probability (SRVLAM), and
- The MELCOR SRV open area fraction (SRVOAFRAC).

However, additional variables also consistently show some level of importance for circular areas greater than two miles. These additional input variables include the following:

- The MACCS inhalation protection factor during sheltering activities for non-evacuated residents (PROTIN-Sheltering),
- The MELCOR DC station battery duration (BATTDUR), and
- The MELCOR railroad inner door open fraction (RRIDFRAC).

The final R^2 for non-rank regression models is reasonable for circular areas between 2.5 to 3.5 miles. They range from 0.44 for recursive partitioning at 3.5 miles (Table 6.2-16) to 0.82 for MARS at 3.5 miles (Table 6.2-16). These eight variables (CYSIGA, EFFTHR-red marrow, EFFACB-red marrow, SRVLAM, SRVOAFRAC, PROTIN-sheltering, BATTDUR, and RRIDFRAC) account for at least 12% of the variance (Final R^2 value) for the quadratic regression analysis, at least 96% of the variance for the recursive partitioning analysis, and at least 21% of the variance for the MARS analysis.

Other input parameters show a low importance at certain circular areas but not for other circular areas. Thus, the most important variable, CYSIGA, appears at or near the top of Table 6.2-14 through Table 6.2-16 (Table 6.2-14 has PROTIN-sheltering as the most important variable) followed by EFFTHR-red marrow and EFFACB-red marrow, the consistently important MELCOR variables, SRVLAM, SRVOAFRAC, BATTDUR, and RRIDFRAC, and then the other important variables, and finally those parameters not consistently seen in all of the tables.

The MACCS crosswind dispersion coefficient (CYSIGA) parameter accounts for at least 0% of the variance with a T_i of 0.16 using the quadratic regression analysis to at most 81% of the variance with a T_i of 0.25 using the recursive partitioning regression analysis for circular areas from 2.5 to 3.5 miles for all non-ranked regression methods and is the most important input variable. Also, CYSIGA consistently has one of the highest ranks for interactions with other input variables (T_i). As discussed in greater detail in Section 4.2.6, crosswind dispersion directly affects peak concentrations, and thus it affects early doses to members of the population and resulting early health effects.

Table 6.2-14 Conditional, mean, individual early-fatality risk (per event) regression of the MACCS Uncertainty Analysis for the 2.5-mile circular area

	Rank Regression			Quadratic			Recursive Partitioning			MARS		
Final R ²	0.18			0.52			0.50			0.66		
Input	R ² inc.	R ² cont.	SRRC	S _i	T _i	p-val	S _i	T _i	p-val	S _i	T _i	p-val
PROTIN Sheltering	0.01	0.01	0.04	0.28	0.78	0	0.28	0.41	0	0.10	0.74	0
CYSIGA	0.02	0.01	-0.04	0.05	0.21	0.03	0.17	0.28	0.01	0	0	1
SRVLAM	0.05	0.03	-0.06	0	0	1	0.01	0.31	0	0	0.12	0.28
SRVOAFRAC	0.07	0.02	-0.07	0.01	0	1	0.03	0	1	0.03	0.35	0.01
BATTDUR	0.07	0	0.02	---	---	---	---	---	---	---	---	---
RRIDFRAC	0.08	0.01	0.02	0	0.17	0.11	---	---	---	---	---	---
EFFTHR Red Marrow	0.14	0.06	-0.10	0	0	1	0.03	0.42	0	0.01	0.65	0
EFFACB Red Marrow	0.14	0	0.02	0	0.41	0	---	---	---	0	0	1
CWASH1	0.15	0.01	0.05	0	0.36	0	---	---	---	0	0	1
DLTEVA Cohort 3	0.17	0.02	-0.01	---	---	---	---	---	---	0.02	0.41	0
PROTIN Normal	0.18	0.01	-0.03	0.01	0	1	0	0	1	0	0.48	0
GSHFAC Normal	0.18	0	-0.03	0.03	0.01	0.51	---	---	---	0	0.31	0.01
DLTEVA Cohort 5	0.19	0.01	0.02	0	0.20	0.08	0	0.02	0.43	0.01	0.15	0.15
SC1131_2	0.19	0	-0.02	---	---	---	---	---	---	0	0.15	0.22
DLTEVA Cohort 3	---	---	---	0	0.35	0	0.01	0	1	---	---	---
DHEADSOL	---	---	---	0.01	0	1	---	---	---	---	---	---
DLTEVA Cohort 4	---	---	---	---	---	---	0.01	0.50	0	---	---	---
VDEPOS	---	---	---	---	---	---	0	0.12	0.06	---	---	---
ESPEED	---	---	---	---	---	---	---	---	---	0	0.18	0.19
GSHFAC Sheltering	---	---	---	---	---	---	---	---	---	0	0	1

Table 6.2-15 Conditional, mean, individual early-fatality risk (per event) regression of the MACCS Uncertainty Analysis for the 3-mile circular area

	Rank Regression			Quadratic			Recursive Partitioning			MARS		
Final R ²	0.16			0.52			0.51			0.59		
Input	R ² inc.	R ² cont.	SRRC	S _i	T _i	p-val	S _i	T _i	p-val	S _i	T _i	p-val
CYSIGA	0.01	0.01	-0.04	0	0.51	0	0.30	0.21	0.24	0	0	1
EFFTHR Red Marrow	0.07	0.06	-0.09	0.03	0	1	0.02	0	0.87	0.14	0.82	0
EFFACB Red Marrow	0.08	0.01	0.03	0	0.30	0	---	---	---	0.02	0.35	0
SRVOAFRAC	0.10	0.02	-0.05	0.01	0.11	0.36	0	0.15	0.06	0	0.50	0
SRVLAM	0.12	0.02	-0.05	0	0.35	0	0	0.52	0	0	0	1
BATTDUR	---	---	---	0.02	0.10	0.42	---	---	---	---	---	---
RRIDFRAC	0.13	0.01	0.03	0	0.71	0	0.17	0.44	0	---	---	---
DLTEVA Cohort 3	0.15	0.02	-0.0	0.03	0.46	0	---	---	---	0.03	0.09	0.28
CWASH1	0.16	0.01	0.04	0.01	0.31	0.01	---	---	---	0.02	0	1
DLTEVA Cohort 5	0.16	0	-0.03	0	0.07	0.38	0.01	0	1	0.01	0	1
GSHFAC Normal	0.16	0	-0.03	0	0.21	0.03	---	---	---	0	0	1
GSHFAC Sheltering	0.17	0.01	0.03	---	---	---	---	---	---	0	0.01	0.59
PROTIN Normal	0.18	0.01	0.03	---	---	---	---	---	---	0	0	1
PROTIN Sheltering	0.18	0	-0.02	---	---	---	---	---	---	0	0	1
SC1131_2	0.18	0	-0.02	---	---	---	---	---	---	0	0	1
CZSIGA	---	---	---	0	0.39	0	---	---	---	---	---	---
EFFTHR Stomach	---	---	---	0.05	0.06	0.58	---	---	---	---	---	---
ESPEED	---	---	---	0	0	1	---	---	---	0	0	1

Table 6.2-16 Conditional, mean, individual early-fatality risk (per event) regression of the MACCS Uncertainty Analysis for the 3.5-mile circular area

	Rank Regression			Quadratic			Recursive Partitioning			MARS		
Final R ²	0.16			0.50			0.44			0.82		
Input	R ² inc.	R ² cont.	SRRC	S _i	T _i	p-val	S _i	T _i	p-val	S _i	T _i	p-val
CYSIGA	0.01	0.01	-0.04	0	0.16	0.04	0.81	0.25	0.27	0	0	1
EFFTHR Red Marrow	0.07	0.06	-0.08	0.05	0.22	0.06	0.03	0.27	0.10	0.06	0.58	0
EFFACB Red Marrow	0.07	0	-0.02	---	---	---	---	---	---	0	0.13	0.19
SRVLAM	0.09	0.02	-0.05	---	---	---	0	0.13	0.15	0	0.11	0.34
SRVOAFRAC	0.10	0.01	-0.04	0.02	0	1	0	0.36	0	0	0.55	0
BATTDUR	---	---	---	---	---	---	0.02	0.16	0.07	---	---	---
DLTEVA Cohort 5	0.11	0.01	0.02	0.07	0.38	0	0.05	0.17	0.15	0.01	0	1
CWASH1	0.12	0.01	0.03	---	---	---	---	---	---	0	0.37	0
GSHFAC Normal	0.13	0.01	-0.03	---	---	---	0	0.18	0.02	0	0	1
PROTIN Normal	0.14	0.01	0.03	0	0.23	0.	---	---	---	0	0	1
DLTEVA Cohort 3	0.16	0.02	0.04	0	0.14	0.13	0.04	0.23	0	0.01	0	1
ESPEED	0.16	0	0.02	---	---	---	---	---	---	0.01	0.38	0
SC1131_2	0.16	0	0.02	0	0.25	0	---	---	---	0.05	0.71	0
GSHFAC Sheltering	0.16	0	-0.02	0.01	0.19	0.01	---	---	---	0.01	0.40	0
DHEADSOL	---	---	---	0	0.25	0	---	---	---	---	---	---
CZSIGA	---	---	---	0.02	0.29	0	---	---	---	---	---	---
VDEPOS	---	---	---	0	0.09	0.20	0.01	0	1	---	---	---
DLTEVA Cohort 4	---	---	---	0.01	0	1	---	---	---	---	---	---
PROTIN Sheltering	---	---	---	---	---	---	0	0	1	0	0	1

The MELCOR input variables (SRVLAM, SRVOAFRAC, BATTDUR, and RRIDFRAC) account for at least 0% of the variance with a T_i of 0.5 using the MARS analysis to at most 17% of the variance with a T_i of 0.52 using the recursive partitioning regression analysis for circular areas greater than 2 miles for all non-ranked regression methods and are the second most important group of input variables. As discussed in Section 6.1.1 and Section 6.1.2, these MELCOR input variables account for the majority of the variance for iodine and cesium release fractions and timing.

The early health effects threshold risk for red bone marrow (EFFTHR-Red Marrow) and the early health effects beta (shape) factor for red bone marrow (EFFACB-Red Marrow) inputs account for at least 0% of the variance with a T_i of 0.41 using the quadratic regression analysis to at most 16% of the variance with a T_i of 0.82 using the MARS analysis for circular areas of 2.5 to 3.5 miles for all non-ranked regression methods and are the third most important group of input variables. Also, EFFTHR-red marrow and EFFACB-red marrow consistently show interactions with other input variables. As discussed in greater detail in Section 4.2.4, EFFTHR-red marrow and EFFACB-red marrow are important because the hematopoietic syndrome has the lowest threshold for an early fatality.

The amount of shielding between an individual and the source of groundshine for sheltering activities for the non-evacuees (GSHRAC-sheltering), the wet deposition parameter (CWASH1), and a few other important variables also show a significant non-monotonic interaction with other input variables. While the overall R^2 contribution from these input variables is low, with the exception of PROTIN-sheltering at the 2.5-mile circular area, their interactions with other variables do justify their consideration for early-fatality risk.

In the case of PROTIN-sheltering within the 2.5-mile circular area (i.e. see Table 6.2-14), this variable has the largest overall non-monotonic variance (i.e., 15-56% of the variance for the regression methods considered) and the highest rank for interactions with other input variables (T_i). Since this MACCS input variable does not consistently appear as an important variable at other distances, it is considered to be a minor overall variable.

6.2.4 Analysis of Single Realizations

Select individual realizations from the uncertainty analysis were further investigated in greater detail to identify the influences affecting the predicted consequences. The cases investigated are broken into two groups, the MELCOR single realizations discussed in Section 6.1.4, and the MACCS Uncertainty Analysis single realizations that resulted in a nonzero early-fatality risk per event at the 10-mile circular area. These analyses were conducted from the results from the MACCS Uncertainty Analysis.

6.2.4.1 MELCOR Single Realizations Consequence Analysis

As discussed in Section 6.1.4, the MELCOR single realizations were selected to illustrate the influences affecting the cesium released to the environment. Table 6.2-17 provides a brief source term description for each MELCOR single realization and associated release timing. The SOARCA estimate and SOARCA uncertainty analysis base case source term descriptions are also included to provide a comparison. These individual realizations were selected from the MACCS Uncertainty Analysis. Based on these results, a comparison of the consequence impacts was conducted.

Table 6.2-17 Brief source term description for the single realizations selected from Replicate 1 (STP08) MELCOR Analyses

Scenario	Integral Release Fractions by Chemical Group									Atmospheric Release Timing	
	Xe	Cs	Ba	I	Te	Ru	Mo	Ce	La	Start (hr)	End (hr)
SOARCA Estimate	0.978	0.005	0.006	0.020	0.022	0	0.001	0	0	20	48
SOARCA UA Base Case	0.981	0.005	0.010	0.025	0.019	0	0	0	0	19.9	48
RLZ018	0.927	0.024	0.019	0.069	0.042	0	0.003	0	0	16.2	48
RLZ051	0.733	0.003	0.010	0.015	0.013	0	0	0	0	17.4	48
RLZ052	0.955	0.021	0.165	0.082	0.056	0	0	0.023	0.001	14.3	48
RLZ062	0.995	0.055	0.014	0.104	0.089	0	0.012	0	0	13.6	48
RLZ063	0.984	0.008	0.015	0.021	0.013	0	0	0.001	0	15.9	48
RLZ086	0.865	0.041	0.040	0.082	0.093	0.001	0.008	0.002	0	12.5	48
RLZ090	0.875	0.053	0.013	0.064	0.029	0	0.013	0	0	14.8	48
RLZ122	0.906	0.038	0.035	0.086	0.046	0	0.007	0.003	0	15.8	48
RLZ134	0.762	0.064	0.147	0.146	0.119	0	0.014	0.020	0	10.8	48
RLZ170	0.985	0.020	0.022	0.031	0.027	0	0	0.001	0	16.6	48
RLZ268	0.797	0.118	0.015	0.073	0.046	0	0.031	0.001	0	18	48

For this work, the early (emergency) phase is defined as the first seven days following the initial release to the environment. The long-term phase is defined as the time following the emergency phase (i.e., there is no intermediate phase). Figure 6.2-13 shows the conditional, mean, individual LCF risk (per event) for all the selected MELCOR single realizations within the EPZ for the emergency phase risk contribution (red) and the long-term phase risk contribution (blue). The red dots on Figure 6.2-11 are the fraction of cesium in the core released into the environment and the orange dots are the fraction of cerium in the core released to the environment. Of the LCF risks presented, Realization 52 of Replicate 1 shows the highest contribution to LCF risk from the early phase. This is due to the LCF risk contribution to the red bone marrow being appreciably higher than the other single realizations in part due to the following:

- The mortality risk coefficient (CFRISK) for red bone marrow is 0-40% higher than other single realizations analyzed,
- The linear, crosswind dispersion coefficient (CYSIGA) is 25-80% lower than other single realizations analyzed, and
- The relatively large release of the barium and cerium groups (i.e., see Table 6.2-17).

Realization 170 of Replicate 1 shows the highest contribution to LCF risk from the long-term phase. This is due to the LCF risk contribution to the lungs being appreciably higher than the other single realizations in part due to the following:

- The mortality risk coefficient (CFRISK) for lungs is 0-85% higher than other single realizations analyzed,
- The crosswind dispersion coefficient (CYSIGA) is 5-70% lower than other single realizations analyzed,
- The vertical dispersion coefficient (CZSIGA) is 5-70% lower than other single realizations analyzed,
- The Pu-240 inhalation dose conversion factor for the lungs is 0-70% higher than other single realizations analyzed,
- The Ce-144 inhalation dose conversion factor for the lungs is 5-60% higher than other single realizations analyzed, and
- The largest contribution to long-term inhalation dose is from the cerium group. Of the more important isotopes in the cerium group for long-term inhalation doses are Pu-238, which has a 87.7 year half-life; Pu-241, which has a 14.4 year half-life; and Ce-144, which has a 285-day half-life.

When the fraction of cesium released to the environment is compared for all single realizations analyzed, there is no direct relationship to the LCF risk in the long-term phase. However, when the cesium and cerium release fractions are both considered, a better relationship to long-term risk does appear. This can be seen on Figure 6.2-13.

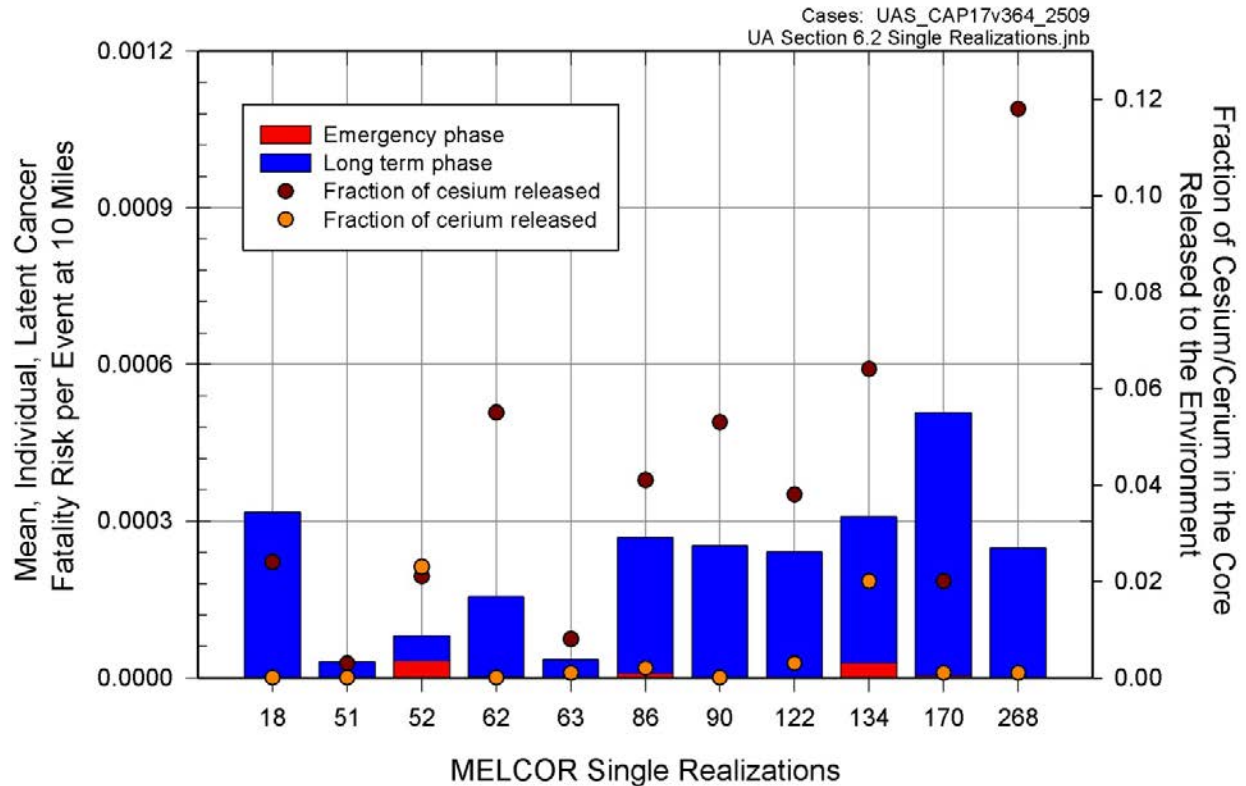


Figure 6.2-13 Conditional, mean, individual LCF risk (per event) for MELCOR Replicate 1 single realizations for the 10-mile circular area

Figure 6.2-14 shows the conditional, mean, individual LCF risk (per event) for the selected realizations from Replicate 1 of the MELCOR analyses within the 20-mile circular area for the emergency phase risk contribution (red) and the long-term phase risk contribution (blue). The red dots on Figure 6.2-14 are the fraction of cesium in the core released into the environment and the orange dots are the fraction of cerium in the core released to the environment. The LCF risk results show emergency phase LCF risk and long-term phase LCF risk are dependent on the same input variables discussed for the Figure 6.2-13 results, and those dominated by the emergency phase LCF risk (e.g., Realization 52 and Realization 134) further emphasize the advantage of emergency phase evacuation within the EPZ (i.e., compare Figure 6.2-13 with Figure 6.2-14).

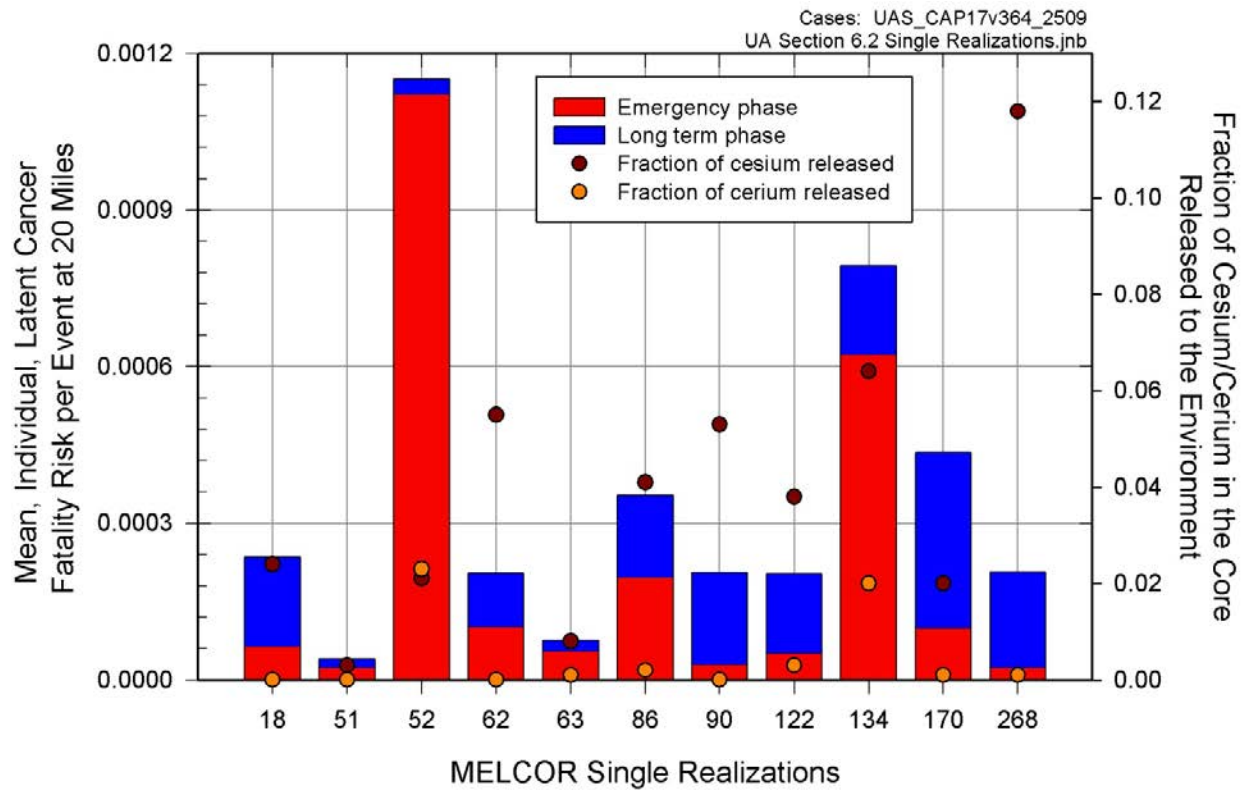


Figure 6.2-14 Conditional, mean, individual LCF risk (per event) for MELCOR Replicate 1 single realizations for the 20-mile circular area

Figures 6.2-15 through 6.2-17 show the conditional, mean, individual LCF risk (per event) results for the selected realizations from Replicate1 of MELCOR analyses for the 30-mile, 40-mile, and 50-mile circular areas respectively. These figures show similar trends to those shown on Figure 6.2-14.

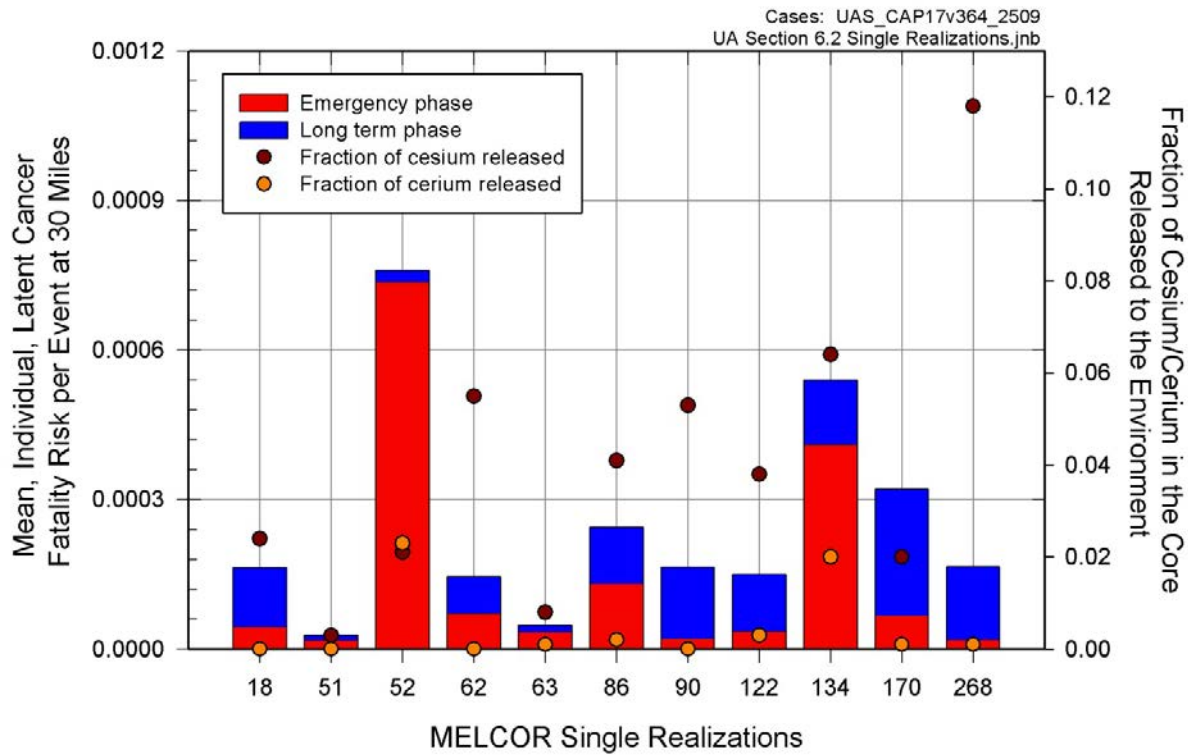


Figure 6.2-15 Conditional, mean, individual LCF risk (per event) for MELCOR Replicate 1 single realizations for the 30-mile circular area

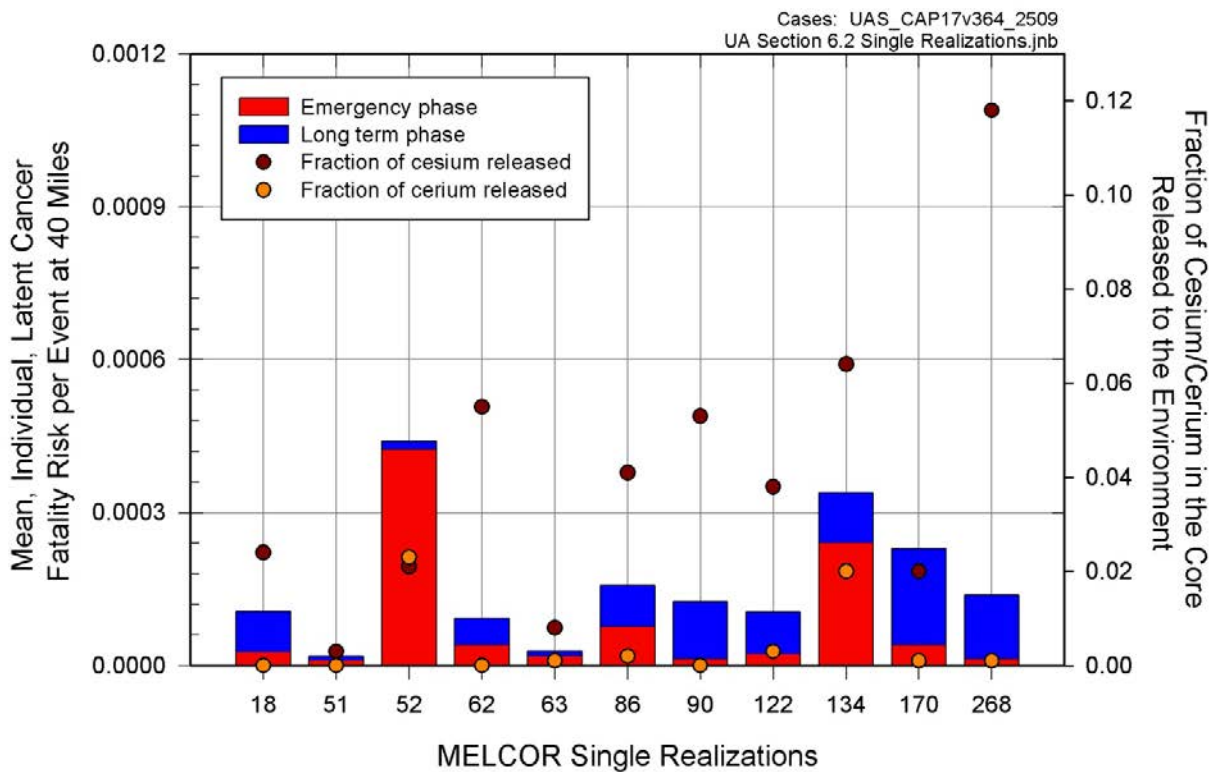


Figure 6.2-16 Conditional, mean, individual LCF risk (per event) for MELCOR Replicate 1 single realizations for the 40-mile circular area

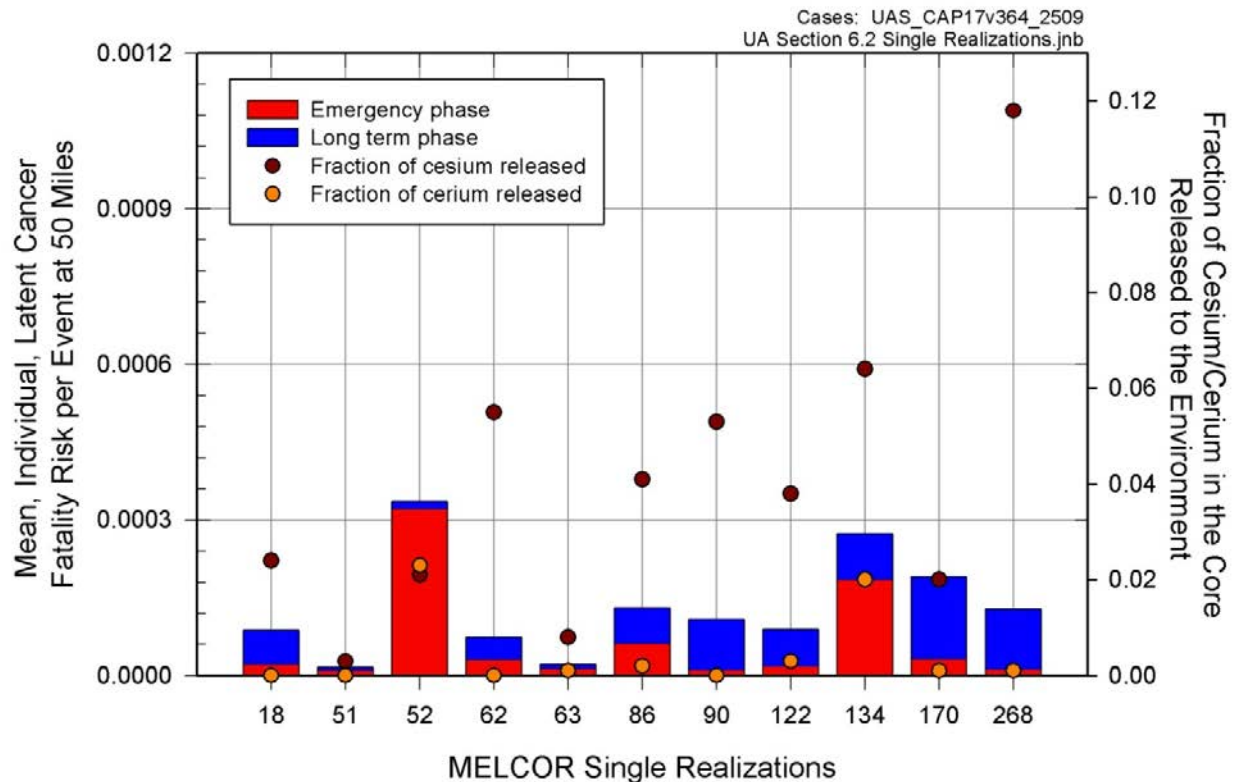


Figure 6.2-17 Conditional, mean, individual LCF risk (per event) for MELCOR Replicate 1 single realizations for the 50-mile circular area

The early-fatality risks are zero for all single realizations at the specified circular areas except for two realizations. Both Realizations 52 and 134 have nonzero early-fatality risks. This is because the release fractions are too low to produce doses large enough to exceed the dose thresholds for early fatalities, even for the 0.5% of the population that are modeled as refusing to evacuate. With the exception of Realizations 52 and 134, the largest value of the mean, acute exposure for the closest resident (i.e., 1.6 to 2.1 kilometers from the plant) for these realizations is about 0.56 Gy to the red bone marrow, which is the most sensitive organ for early fatalities, but the minimum acute exposure that can cause a early fatality is about 2.3 Gy to the red bone marrow. The calculated exposures for these realizations are nearly an order of magnitude below this threshold.

Table 6.2-18 shows the conditional, mean, individual early-fatality risk (per event) for only the MELCOR single realizations selected from Replicate 1 which has a nonzero result for specified circular areas. Realization 52 has early-fatality risks that are larger than the SOARCA Surry ISLOCA results (i.e., see Table 6.2-4) and extend to the 5-mile circular area. The only early-fatality risks are for the cohort that is assumed not to evacuate.

For the Realization 52 early-fatality risk at 1.3 miles, only 5% of all weather trials resulted in a nonzero early-fatality risk. At two miles this increases to 10% of all weather trials. It peaks at 2.5 miles, where approximately 15% of all weather trials results in a nonzero early-fatality risk. Beyond this distance, the number of weather trials that produce a nonzero early-fatality risk decreases. These weather trials estimate an early-fatality risk according to their associated wind direction, wind speed, and stability class combined with a population located in that specific wind direction.

Table 6.2-18 Conditional, mean, individual early-fatality risk (per event) for the MELCOR Replicate 1 single realization nonzero realizations for specified circular areas

	1.3 miles	2 miles	2.5 miles	3 miles	3.5 miles	5 miles
RLZ52	4.0×10^{-6}	1.3×10^{-6}	8.5×10^{-7}	5.8×10^{-7}	3.2×10^{-7}	8.7×10^{-8}
RLZ134	1.3×10^{-6}	5.0×10^{-7}	3.1×10^{-7}	0.0	0.0	0.0

When Realization 52 was further examined, it was determined that the crosswind dispersion coefficient (CYSIGA) parameter was 25-80% lower than the other single realizations analyzed. This results in a higher concentration of radionuclides within the plume (and persisting at further distances) and subsequently results in a greater inhalation dose.

For Realization 52, the early-fatality risk is a result of population exceeding the red bone marrow threshold. The threshold dose for red bone marrow (EFFTHR-Red Marrow) is 0-75% lower and the beta (shape) factor for red bone marrow (EFFTHR-Red Marrow and EFFACB-Red Marrow) is 20-80% higher than the other single realizations analyzed. This reduces the dose to the red bone marrow that can cause a early fatality.

When the fraction of cesium in the core released to the environment is compared for all realizations, there is no relationship to with the early-fatality risk, as expected. Early fatality risk is driven by inhalation and direct exposure during the emergency phase, where iodine (and perhaps the cerium group) would be most important. Realization 134 had the highest iodine release fraction at 14.6%, and the release began at 10.8 hours.

6.2.4.2 MACCS Single Realization Consequence Analysis

During the MACCS Uncertainty Analysis, it was discovered that three of the 865 realizations have a conditional, mean, individual early-fatality risk (per event) greater than zero out to the 10-mile circular area. Since this was not expected, a further investigation into these realizations was conducted. The three realizations of interest are the following: Replicate 2 Realization 291, Replicate 3 Realization 46, and Replicate 3 Realization 267. None of these realizations were selected for the MELCOR single realization analysis discussed in Section 6.1.4. In order to better understand these realizations, a time table of the accident sequence is provided in Table 6.2-19. Figures 6.2-18 through 6.2-20 provide the reactor and containment pressure responses for Replicate 2 Realization 291 (RLZ291), Replicate 3 Realization 46 (RLZ046), and Replicate 3 Realization 267 (RLZ267), respectively.

As documented in Section 6.1.4, there are five factors found to strongly affect the amount of radionuclides released to the environment, namely:

- (1). whether the SRV fails open before or after the onset of core damage,
- (2). whether a main steam line creep rupture occurs,
- (3). the elapsed time between the onset of core damage and main steam line creep rupture,
- (4). whether a surge of water from the wetwell goes up onto the drywell floor at drywell liner melt through, and
- (5). whether an overpressure rupture of the wetwell occurs.

The first factor identified relates directly to when the SRV fails open, and the RPV is vented to the wetwell pool through the failed SRV. Fission products carried by the gas flow venting from the RPV are largely scrubbed by the wetwell pool. The earlier the SRV fails open in the core degradation process, the more fission products are carried to the wetwell rather than deposited in the RPV. If the SRV fails open before the onset of core damage, the venting of released fission products directly to the wetwell is maximized.

The second influence identified is if a main steam line creep rupture occurs. The path through the failed open SRV to the wetwell pool is bypassed after main steam line failure and gases and aerosols from the RPV flow straight to the drywell. From the drywell, fission products are released to the environment via leakage/failure through the drywell head flange, containment failure due to drywell liner melt through, or containment failure due to wetwell rupture above the waterline. All of these release paths avoid fission product scrubbing by the suppression pool.

The third factor similarly relates to the amount of radionuclides deposited in the wetwell. The more time that elapses between the onset of core damage and a main steam line creep rupture the more time there is for gases venting from the RPV to carry fission products through the failed open SRV to the wetwell.

The fourth factor relates to amount of radionuclides that deposit in the suppression pool but fail to be contained there. A surge of water from the wetwell goes up onto the drywell floor when the containment depressurizes in response to debris contacting the drywell liner and melting through it if the hole in the drywell liner is large enough. The suppression pool is saturated at the time and is susceptible to flashing in response to depressurization. The vacuum breakers between the wetwell and the drywell are overwhelmed and contaminated water from the wetwell surges up onto the drywell floor. The water encounters the core debris on the drywell floor and evaporates which introduces fission products into the atmosphere and structures of the drywell where they become available for release into the environment.

The last factor is a containment failure due to a wetwell rupture above the waterline. The breach actually has beneficial impact as it results in the venting of containment through the wetwell. The suppression pool provides some scrubbing of fission products from the venting gas flowing just above the suppression pool as the fission products make their way through the breach.

None of the single realizations have a stochastic SRV failure. For all cases the accident scenario is a SRV thermal failure followed by a main steam line creep rupture and ultimate containment failure due to wetwell rupture above the water line and drywell head flange failure.

Table 6.2-19 Timing of key events for MELCOR source terms selected from the three replicates for the MACCS single realization analysis

Event	Single Realization (time in hours unless noted otherwise)		
	Replicate 2 RLZ291	Replicate 3 RLZ046	Replicate 3 RLZ267
Station blackout loss of all onsite and offsite AC power	0.0	0.0	0.0
Low-level 2 and RCIC actuation signal	10 minutes	10 minutes	10 minutes
Operators manually open SRV to depressurize the reactor vessel	1.0	1.0	1.0
RPV pressure first drops below LPI setpoint (400 psig)	1.2	1.2	1.2
Battery depletion leads immediate SRV re-closure	3.0	2.3	3.0
RCIC steam line floods with water RCIC flow terminates	4.8	3.2	4.2
Downcomer water level reaches top of active fuel	8.5	6.9	7.7
First hydrogen production	8.7	7.2	8.0
First fuel cladding gap release	9.6	8.1	9.0
SRV sticks open because of high temperature cycling	10.8	9.1	9.9
SRV sticks open because of excessive cycling	-	-	-
Main steam line creep rupture	11.5	10.8	10.7
Drywell head flange leakage begins	11.5	10.8	10.7
Containment failure due to wetwell rupture above the waterline	11.5	10.8	10.7
First hydrogen burns initiated in reactor building	11.5	10.8	10.7
Refueling bay to environment blowout panels open	11.5	10.8	10.7
Equipment Lock Door at 135-ft fails due to overpressure	11.5	10.8	10.7
Door to environment through railroad access opens because of overpressure	11.5	10.8	10.7
Refueling bay roof fails due to overpressure	11.5	10.8	10.7
Time iodine release to environment exceeds 0.1% of initial core inventory	11.5	11.0	10.7
Lower head dries out	12.1	11.2	11.9
Lower head failure	16.7	16.0	16.8
Drywell shell melt-through initiated	17.0	16.2	17.0
Calculation terminated	48.0	48.0	48.0

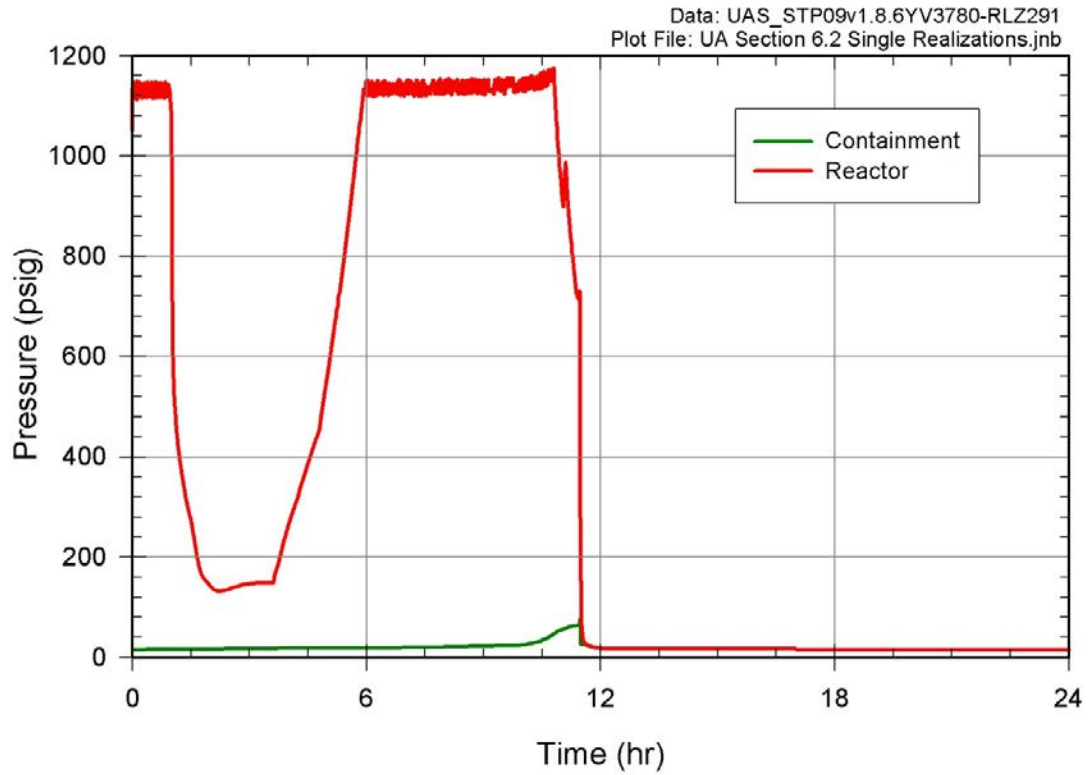


Figure 6.2-18 MELCOR Replicate 2 Realization 291 reactor and containment pressure response

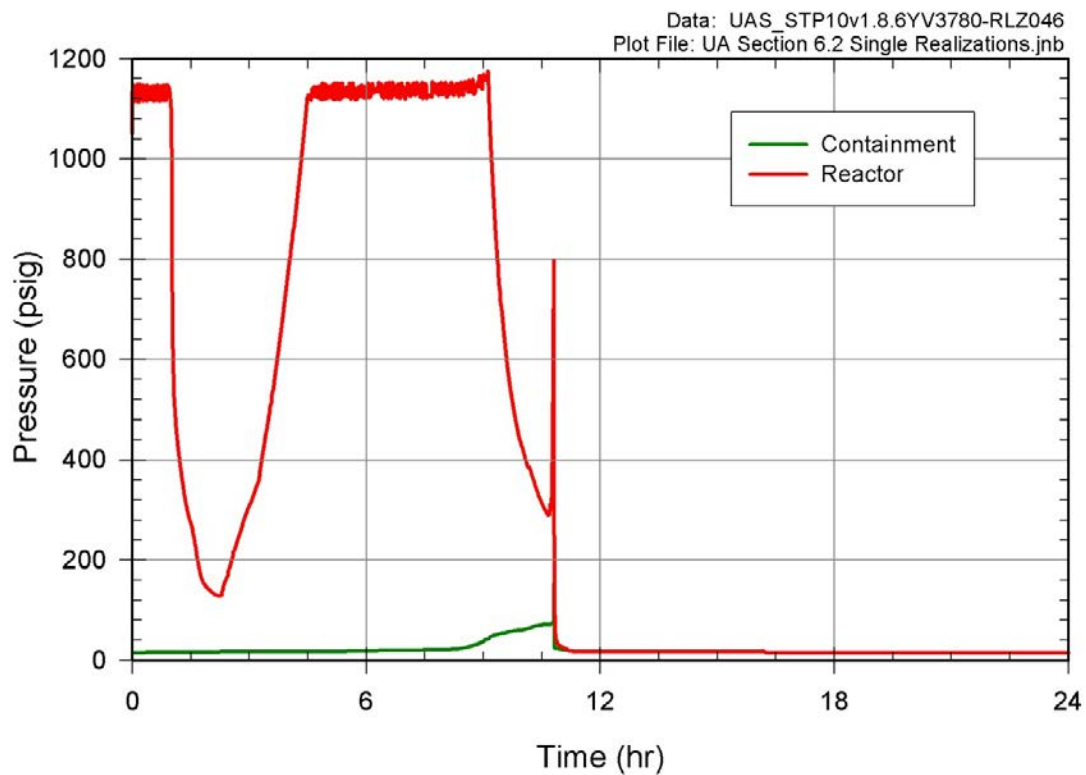


Figure 6.2-19 MELCOR Replicate 3 Realization 046 reactor and containment pressure response

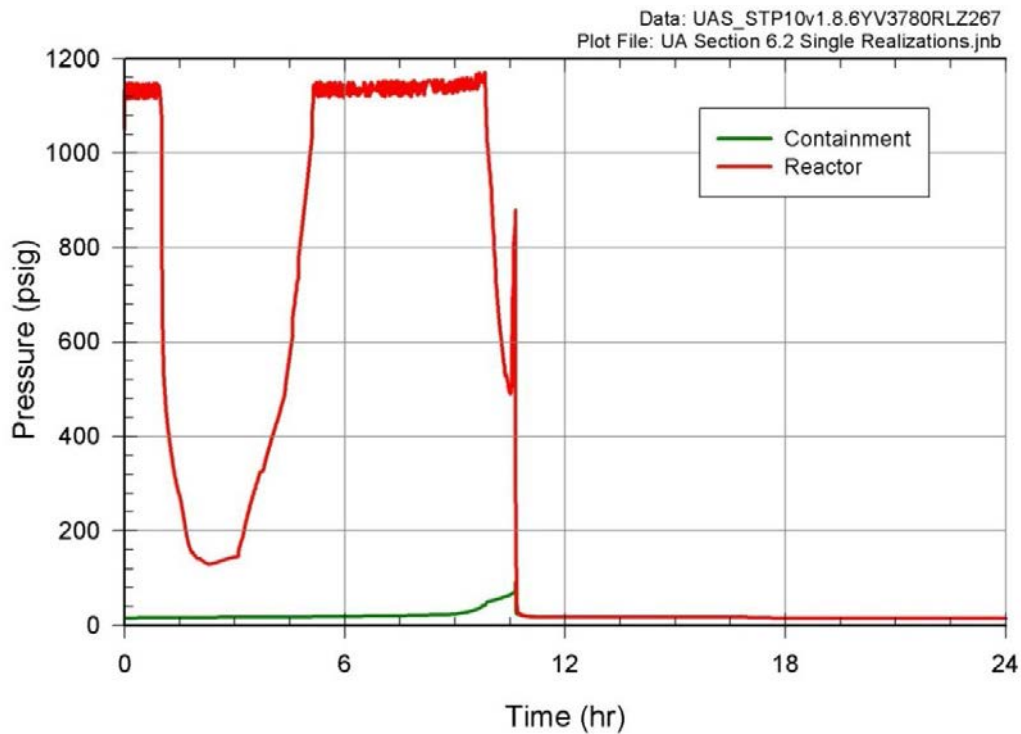


Figure 6.2-20 MELCOR Replicate 3 Realization 267 reactor and containment pressure response

The single realizations were selected to identify the influences affecting the conditional, mean, individual early-fatality risk (per event) results. Table 6.2-20 provides a brief source term description for each MACCS single realization and subsequent release timing. The SOARCA estimate and SOARCA uncertainty analysis base case source term descriptions are also included to provide a comparison. The three individual realizations were selected from the MACCS Uncertainty Analysis. Based on these results, a comparison of the environmental impacts was conducted.

Table 6.2-20 Brief source term description for the MELCOR source terms selected from the three replicates for the CAP17 MACCS Uncertainty Analysis of single realizations

Scenario	Integral Release Fractions by Chemical Group									Atmospheric Release Timing	
	Xe	Cs	Ba	I	Te	Ru	Mo	Ce	La	Start (hr)	End (hr)
SOARCA Estimate	0.978	0.005	0.006	0.020	0.022	0	0.001	0	0	20	48
SOARCA UA Base Case	0.981	0.005	0.010	0.025	0.019	0	0	0	0	19.9	48
Replicate 2 RLZ291	0.792	0.085	0.134	0.160	0.132	0	0.019	0.012	0	11.5	48
Replicate 3 RLZ046	0.672	0.099	0.170	0.109	0.097	0	0.025	0.023	0.001	10.8	48
Replicate 3 RLZ267	0.876	0.102	0.178	0.139	0.125	0	0.024	0.031	0.001	10.7	48

Table 6.2-21 shows the conditional, mean, individual LCF risk (per event) for the MACCS Uncertainty Analysis single realizations for the specified circular areas. All LCF risks are above the 95th percentile of the MACCS Uncertainty Analysis (i.e., see Table 6.2-2) for all replicates except for the 10-mile, circular area for all replicates, which are about the median.

Table 6.2-21 Conditional, mean, individual LCF risk (per event) for the MACCS Uncertainty Analysis single realizations for specified circular areas for MELCOR source terms selected from the three replicates

	RLZ291	RLZ046	RLZ267
10 miles	1.3×10^{-4}	1.5×10^{-4}	1.2×10^{-4}
20 miles	1.5×10^{-3}	3.3×10^{-3}	1.5×10^{-3}
30 miles	1.2×10^{-3}	2.3×10^{-3}	1.1×10^{-3}
40 miles	7.7×10^{-4}	1.3×10^{-3}	6.6×10^{-4}
50 miles	6.1×10^{-4}	1.0×10^{-3}	5.1×10^{-4}

Figure 6.2-21 shows the conditional, mean, individual LCF risk (per event) for the MACCS Uncertainty Analysis realizations within the EPZ for the emergency phase risk contribution (red) and the long-term phase risk contribution (blue). Of the LCF risks presented, the Replicate 3 Realization 46 shows the highest contribution to LCF risk from the early phase. This is due to the LCF risk contribution to the red bone marrow and lungs and is influenced by the following input parameters:

- The mortality risk coefficient (CFRISK) for red bone marrow is 5-20% higher than the other realizations analyzed,
- The vertical dispersion coefficient (CZSIGA) is 35-80% lower than the other realizations analyzed,
- The Ce-141 long-term inhalation dose conversion factor for the lungs is 15-30% higher than the other realizations analyzed,
- The Cs-134 long-term inhalation dose conversion factor for the red bone marrow is 35% to 50% higher than the other realizations analyzed,
- The Pu-238 long-term inhalation dose conversion factor for red bone marrow is 5-95% higher than other realizations analyzed,
- The Pu-240 long-term inhalation dose conversion factor for the lungs is 10-75% higher than the other realizations analyzed,
- The Pu-241 long-term inhalation dose conversion factor for the lungs is 10-35% higher than the other realizations analyzed,
- The Te-129m long-term inhalation dose conversion factor for the lungs is 5-35% higher than the other realizations analyzed,
- The Sr-90 long-term inhalation dose conversion factor for the red bone marrow is 5-35% higher than the other realizations analyzed, and,

- The relatively large releases of the cesium, barium, cerium, and iodine groups (i.e., see Table 6.2-20).
- The relatively earlier start of release (see Table 6.2-20), 10.7-11.5 hours versus ~20 hours for the SOARCA estimate and the UA base case.

Replicate 2 Realization 291 has the highest contribution to LCF risk from the long-term phase. This is due to the LCF risk contribution to the breast is higher than the other two realizations analyzed in part due to the following:

- The mortality risk coefficient (CFRISK) for the breast is 10-65% higher than the other realizations analyzed,
- The crosswind dispersion coefficient (CYSIGA) is 10-85% lower than the other realizations analyzed,
- The long-term groundshine shielding factor (LGSHFRAC) is 45-75% higher (i.e., 1 = No shielding protection) than the other realizations analyzed,
- The Pu-240 long-term inhalation dose conversion factor for the breast is 10-95% higher than the other realizations analyzed and,
- The Pu-241 long-term inhalation dose conversion factor for the breast is 65-80% higher than the other realizations analyzed.

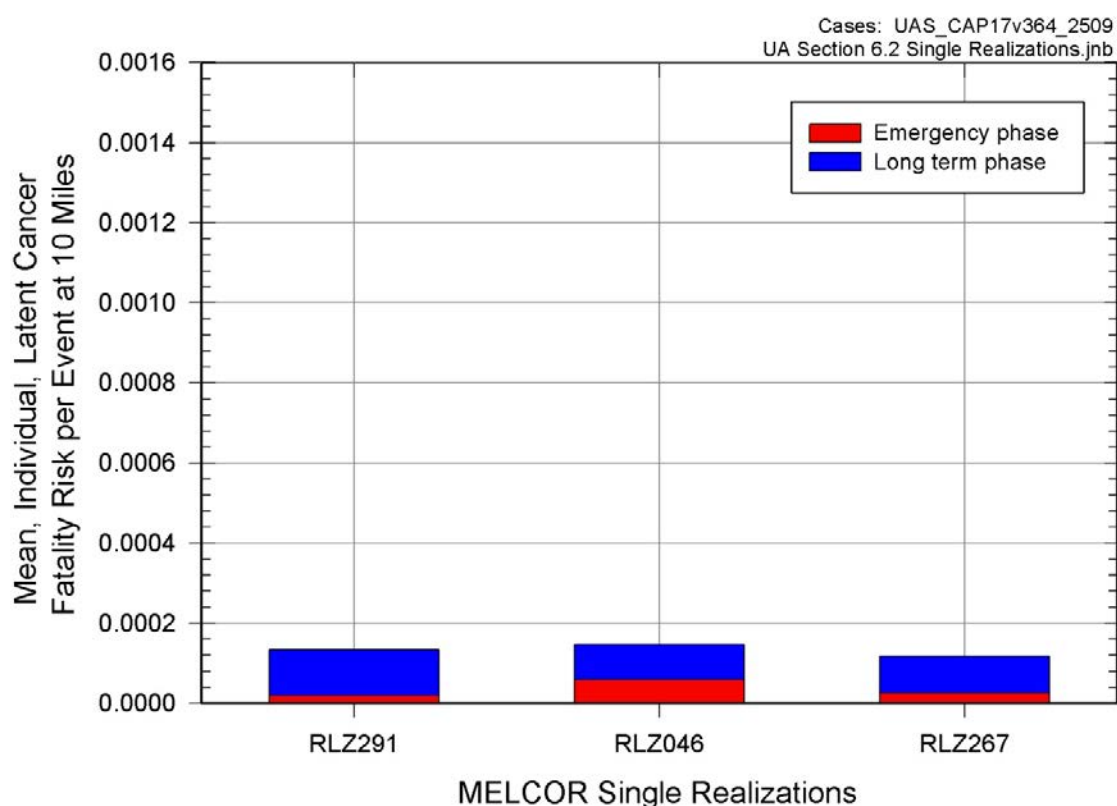


Figure 6.2-21 Conditional, mean, individual LCF risk (per event) MACCS Uncertainty Analysis single realizations for the 10-mile circular area

Figure 6.2-22 shows the conditional, mean, individual LCF risk (per event) for the MACCS Uncertainty Analysis single realizations within the 20-mile circular area for the emergency phase risk contribution (red) and the long-term phase risk contribution (blue). The LCF risk results show that the emergency phase LCF risk and long-term phase LCF risk are dependent on the same input variables discussed for the Figure 6.2-21 results, and those are dominated by the emergency phase risk.

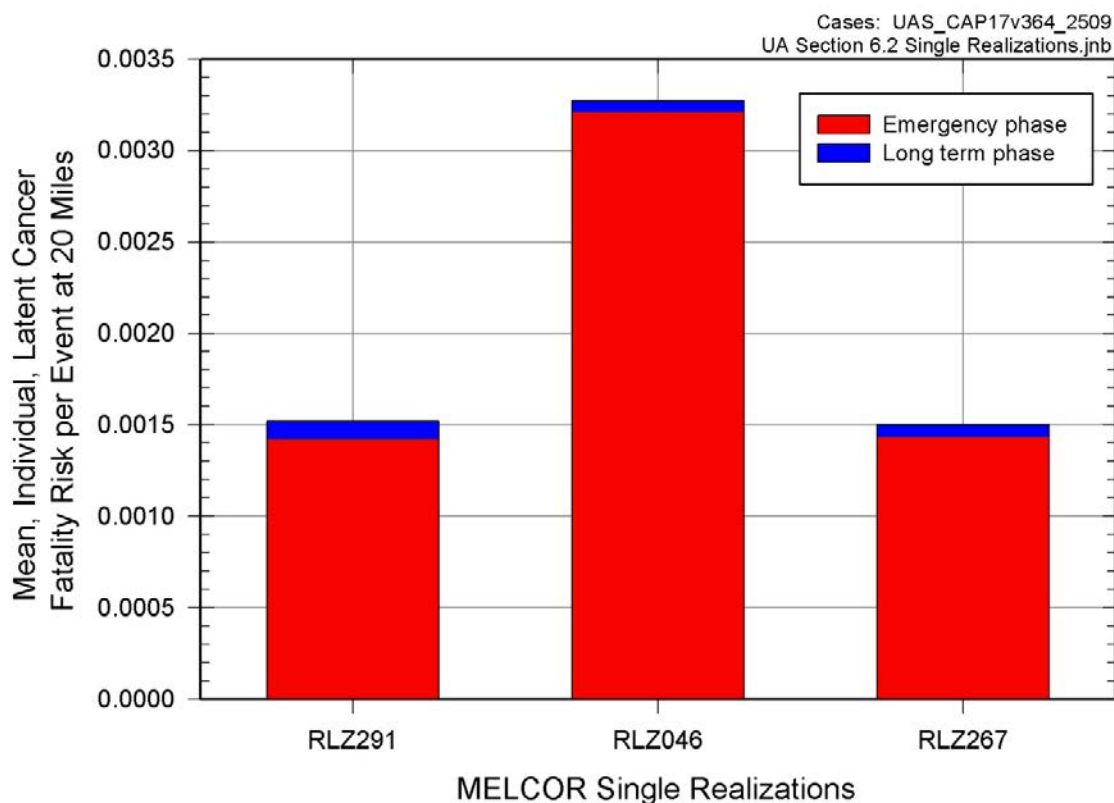


Figure 6.2-22 Conditional, mean, individual LCF risk (per event) MACCS Uncertainty Analysis single realizations for the 20-mile circular area

Figures 6.2-23 through 6.2-25 show the conditional, mean, individual LCF risk (per event) MACCS Uncertainty Analysis single realization results for the 30-mile, 40-mile, and 50-mile circular areas respectively. These figures show similar trends to those shown on Figure 6.2-23.

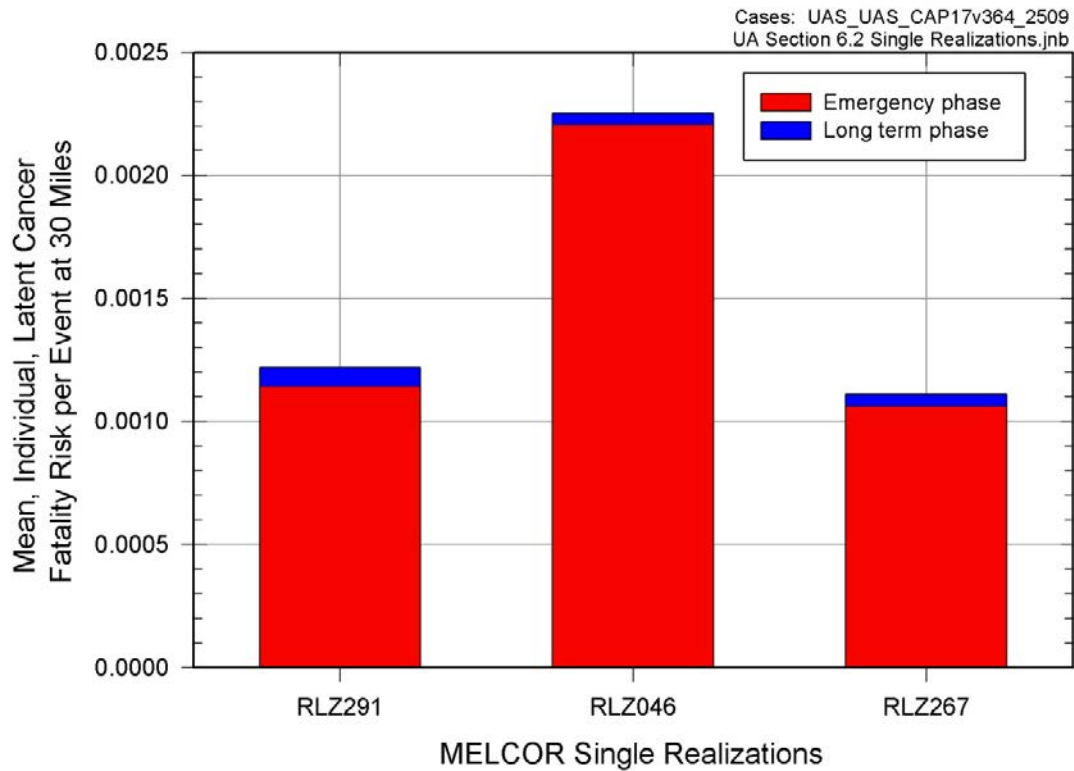


Figure 6.2-23 Conditional, mean, individual LCF risk (per event) MACCS Uncertainty Analysis single realizations for the 30-mile circular area

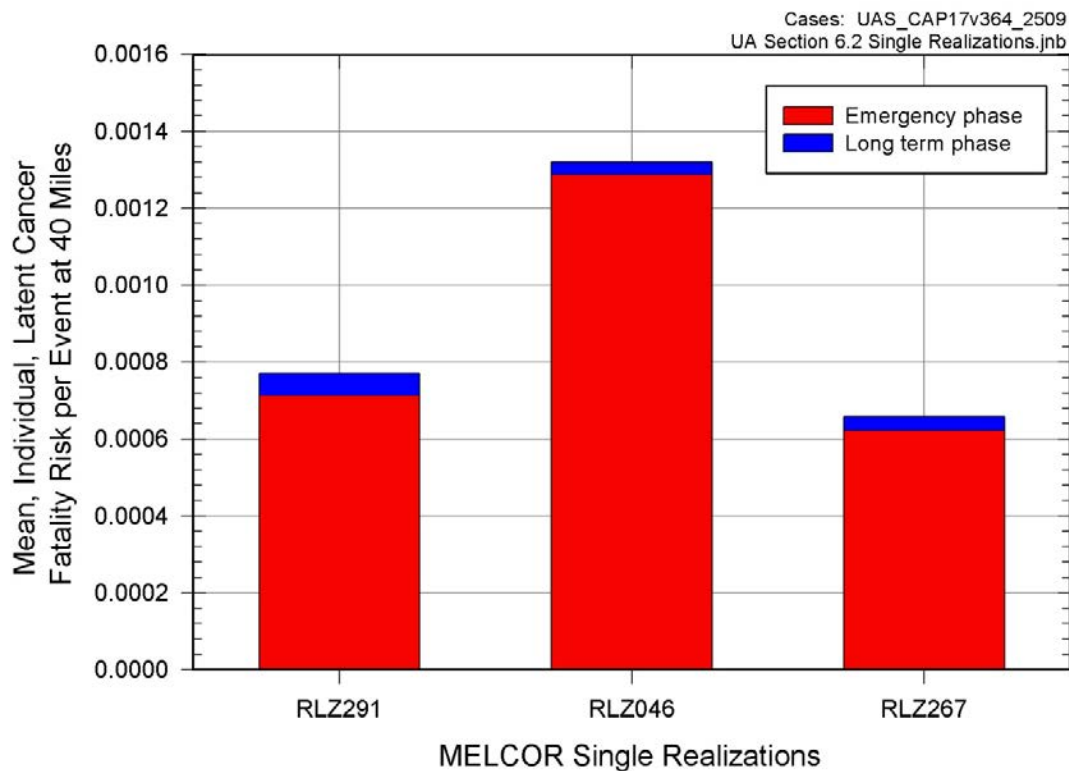


Figure 6.2-24 Conditional, mean, individual LCF risk (per event) MACCS Uncertainty Analysis single realizations for the 40-mile circular area

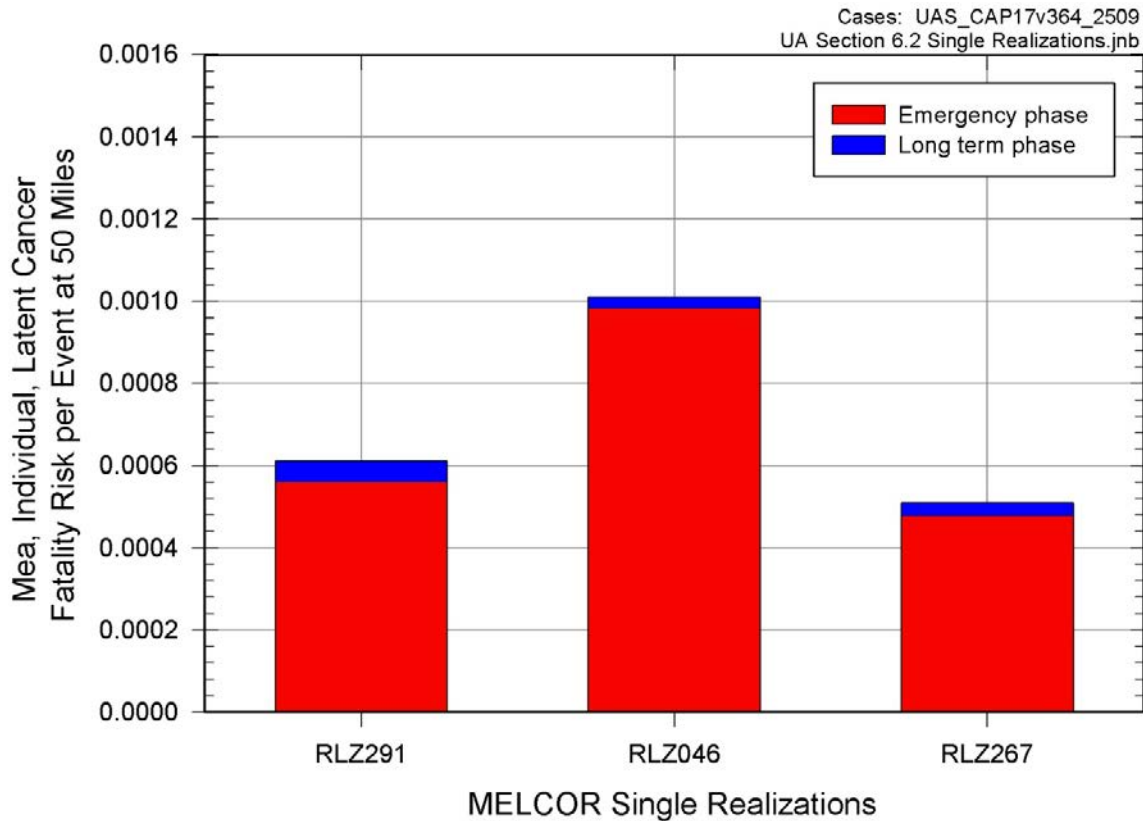


Figure 6.2-25 Conditional, mean, individual LCF risk (per event) MACCS Uncertainty Analysis single realizations for the 50-mile circular area

Table 6.2-22 and Figure 6.2-26 show the conditional, mean, individual early-fatality risk (per event) for the MACCS Uncertainty Analysis single realizations for specified circular areas. All early-fatality risks are above the mean and the 95th percentile of the MACCS Uncertainty Analysis for specified circular areas (i.e., see Table 6.2-5).

Table 6.2-22 Conditional, mean, individual early-fatality risk (per event) for the MACCS single realizations for specified circular areas

	RLZ291	RLZ046	RLZ267
1.3 miles	1.8×10^{-5}	8.1×10^{-6}	6.9×10^{-6}
2 miles	1.5×10^{-5}	4.7×10^{-6}	4.8×10^{-6}
2.5 miles	1.3×10^{-5}	4.0×10^{-6}	3.9×10^{-6}
3 miles	1.1×10^{-5}	3.1×10^{-6}	3.3×10^{-6}
3.5 miles	8.9×10^{-6}	2.0×10^{-6}	2.2×10^{-6}
5 miles	5.8×10^{-6}	7.8×10^{-7}	1.0×10^{-6}
7 miles	4.8×10^{-6}	4.2×10^{-7}	5.7×10^{-7}
10 miles	3.7×10^{-6}	1.9×10^{-7}	2.9×10^{-7}

For Replicate 2 Realization 291 early-fatality risk at the 1.3-mile circular area, only 10 of the all-weather trials resulted in a nonzero early-fatality risk. From the 2-mile to 10-mile circular areas this increases to 50% or greater of all-weather trials. This is due to increasing populations beyond 1.3 miles and a tighter plume allows a persistent concentration out to further distances. For Replicate 3 Realization 46 early-fatality risk at the 1.3-mile circular area, only 5% of all weather trials resulted in a nonzero early-fatality risk. From the 2-mile to 10-mile circular areas, 10% of all weather trials result in a nonzero early-fatality risk. For Replicate 3 Realization 267 early-fatality risk at the 1.3-mile to 10-mile circular areas, 10% of all weather trials result in a nonzero early-fatality risk.

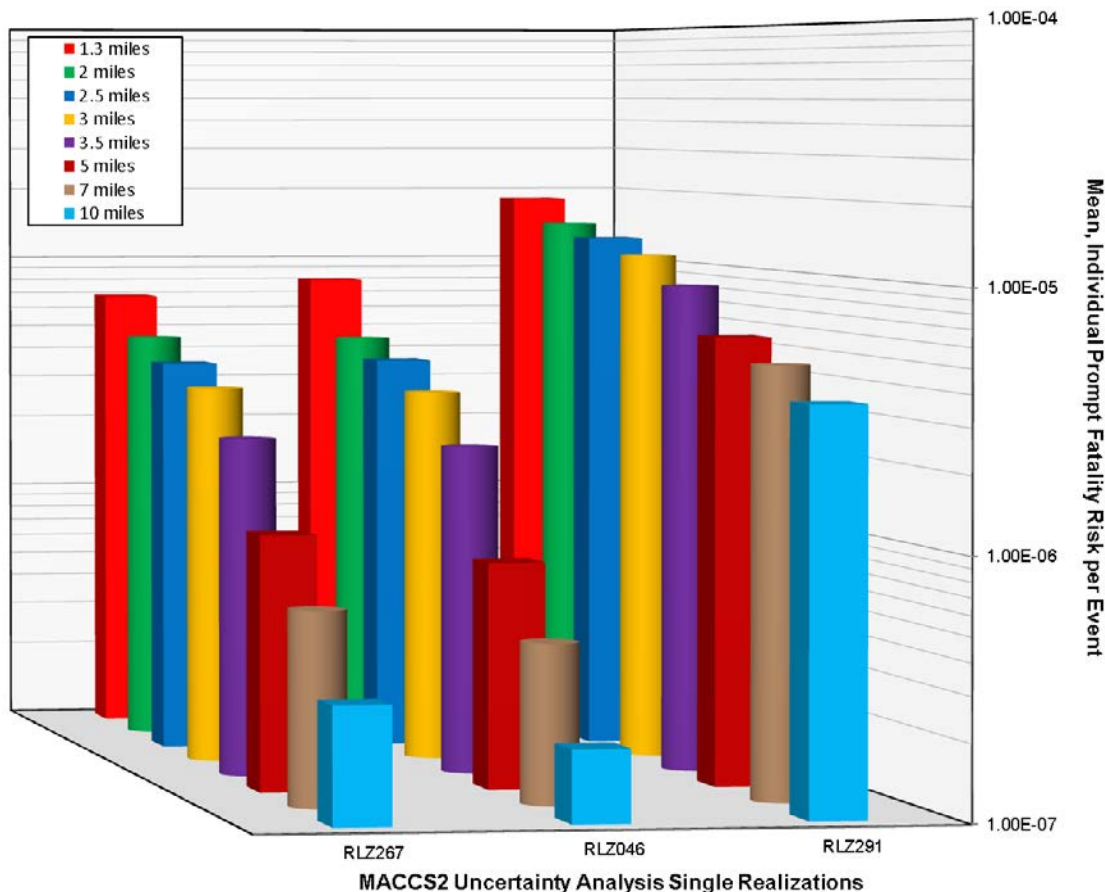


Figure 6.2-26 Conditional, mean, individual early-fatality risk (per event) MACCS Uncertainty Analysis single realizations for specified circular areas

Of the realizations listed in Table 6.2-22, Replicate 2 Realization 291 produced the highest early-fatality risks per event at the specified circular areas. When Replicate 2 Realization 291 was further examined, it determined that the crosswind dispersion coefficient (CYSIGA) is 10% to 85% lower than all other realizations analyzed. Also the vertical dispersion coefficients (CZSIGA) are 15% to 55% lower than all other realizations analyzed. This results in a higher concentration of radionuclides within the plume and in a greater inhalation dose.

For Replicate 2 Realization 291, the early-fatality risk is a result of population exceeding the red bone marrow exposure limit. This is due in part to the early-fatality risk contribution for the red bone marrow from following input parameters:

- The early health effects threshold risk for red bone marrow (EFFTHR-Red Marrow) is 40% to 80% lower and the beta (shape) factor for red bone marrow (EFFACB-Red Marrow) is 5% to 15% higher than the other realizations analyzed. This reduces the dose to the red bone marrow that can cause a early fatality.
- The cloudshine shielding factor for sheltering (CSFACT - sheltering) is 75% to 85% higher (i.e., 1 = No shielding protection) than the other realizations analyzed,
- The crosswind dispersion coefficient (CYSIGA) is 10% to 90% lower than the other realizations analyzed,
- The vertical dispersion coefficient (CZSIGA) is 10% to 55% lower than the other realizations analyzed,
- The peak dose to the red bone marrow within a 10 mile circular area is 60% to 70% higher than the other realizations analyzed, and
- The relatively large releases of the iodine and tellurium groups compared to the other realizations analyzed (i.e., see Table 6.2-19).

Beyond the 10-mile circular area for Replicate 3 Realization 46 and Replicate 3 Realization 267, there is no early-fatality risk for any weather trial (i.e., the conditional, mean, individual early-fatality risk (per event) = 0.00). For these two realizations, the weather trials produced an early-fatality risk due to their associated wind direction, wind speed, and stability class combined with the proximity of residents in the specified wind.

For Replicate 2 Realization 291, there is a nonzero early-fatality risk beyond the 10-mile circular area and can be seen in Table 6.2-23. The noticeable increase in early-fatality risk beyond the 10-mile circular area is due to the population beyond 10 mile does not evacuate, except for those in the 10-20 mile shadow evacuation for Cohort 2. As a result, the early fatality risk beyond 10 miles increases by two orders of magnitude.

From Table 6.2-23, the peak, conditional, mean, individual early-fatality risk is 1.4×10^{-4} per event at 13 miles. The core damage frequency for the unmitigated LTSBO event is $\sim 3 \times 10^{-6}$ pry. Thus the absolute early-fatality risk within 13 miles of the plant is $\sim 4 \times 10^{-10}$ pry. In this one realization (out of 865), 50% or greater of all-weather trials result in a nonzero early fatality risk out to 30 miles.

Table 6.2-23 Conditional, mean, individual early-fatality risk (per event) for the MACCS single realizations for specified circular areas beyond 10 miles

	RLZ291	RLZ046	RLZ267
10 miles	3.7×10^{-6}	1.9×10^{-7}	2.9×10^{-7}
13 miles	1.4×10^{-4}	0.0	0.0
16 miles	1.3×10^{-4}	0.0	0.0
20 miles	1.1×10^{-4}	0.0	0.0
25 miles	8.4×10^{-5}	0.0	0.0
30 miles	5.4×10^{-5}	0.0	0.0
40 miles	0.0	0.0	0.0

While the early fatality risk results for Replicate 2 Realization 291 are extreme, further investigation into the parameters that affected these results does not indicate the source term as a main cause. Instead, the MACCS parameters previously discussed for Replicate 2 Realization 291, which have a higher early-fatality risk contribution for the red bone marrow, are also contributing to the early fatality risk beyond 10 miles. Specifically the following variables are at the extreme ends (the end which results in higher early fatality risk) of their respective distributions:

- The EFFTHR for red bone marrow is near the 1st percentile of the distribution,
- The EFFACB for red bone marrow is near the 10th percentile of the distribution,
- The CSFACT for sheltering is near the 80th percentile of the distribution,
- The CYSIGA is near the 5th percentile of the distribution,
- The CZSIGA is near the 5th percentile of the distribution and,
- The source term is near the 95th percentile of the distribution.

6.3 Summary of Phenomena Important to Uncertainty in Analysis Results

6.3.1 Source Term Analysis

Four outputs were selected from the source term results estimated via MELCOR to be analyzed using regression techniques. These outputs are the fraction of iodine released to the environment, time it took to release 0.1% of the iodine inventory (i.e., a release fraction of 0.001), environmental fraction of cesium released, and the in-vessel hydrogen production. One of the most important parameters, both for amount of radionuclide release and hydrogen production is the uncertainty in lambda for the SRV stochastic failure to reclose (SRVLAM – described in Section 4.1.1) which sets the expected number of cycles occurring before the safety valve fails to reclose. It has a strong negative monotonic influence (indicating that low values of lambda leads to higher releases) as indicated by SRRC results. This affects results because longer SRV valve cycling will cause a thermal seizure of the SRV and potential main steam line creep rupture, in both cases yielding a higher degree of core degradation. This ultimately leads to a larger source term release to the environment. Other regressions techniques indicate that it also has non-monotonic and conjoint influence. The conjoint influence is partly shared with the SRV open area fraction after thermal seizure (SRVOAFRAC – see section 4.1.2) whose effect appears to be non-monotonic (rank regression captures only a small fraction of its influence) for the radionuclide fractional releases. As discussed in Section 6.1.4, SRVOAFRAC is an important determinant to whether a MSL creep rupture occurs. Smaller stuck-open areas relieve steam more slowly and so lead to protracted higher pressures. Higher pressures result in elevated stresses in the MSL piping which combine with elevated temperatures to accumulate creep damage over time that can lead to an MSL rupture. Combined, these parameters control the type of failure (SRV stochastic, SRV thermal seizure or SRV thermal seizure with MSL creep rupture). The importance of failure mode clearly visible on Figure 6.1-7 shows the major role of SRVLAM.

The independent regression analyses for each of the failure modes (SRV stochastic, SRV thermal seizure or SRV thermal seizure with MSL creep rupture) identified additional important parameters and phenomena, as presented in Section 6.1.4. For realizations with only a stochastic SRV failure, fractional releases of iodine and cesium are also sensitive to drywell liner failure flow area (FL904A). There is a correlation between the uncertainty in the drywell liner breach size and whether a surge of water from the wetwell occurs as displayed for the cesium releases on Figure 6.1-11. Larger breach sizes cause stronger containment depressurizations. The water encounters the core debris on the drywell floor and evaporates introducing its inventory of fission products to the atmosphere and structures of the drywell where they are available for release to the environment. Due to the larger releases in case of thermal seizure of the SRV, with or without an MSL creep rupture, the influence of FL904A is negligible for these failure modes. Finally, the chemical form of iodine and cesium, separated by the discrete input variable CHEMFORM, can be added to the list of the influential parameters for iodine and cesium release fractions for all three failure modes. The influence relates to the amount of iodine in iodine gas fraction and the cesium permanently deposited in the RPV via chemisorption of cesium from CsOH onto the stainless steel of reactor internals. This influence is only pertinent for the realizations that have all or some of the reactor core cesium inventory present as CsOH. The chemisorption was more extensive in realizations that experienced higher RPV temperatures, which very strongly influenced the amount of cesium released to the environment as displayed on Figure 6.1-10. Other important phenomena that are identified to a lesser degree in the analyses includes the occurrence of a thermal updraft that develops in the reactor building if the railroad doors are blown open by a hydrogen deflagration (RRDOORS).

The sensitivity analysis for hydrogen production identifies (after SRVLAM) the Zircaloy melt breakout temperature (SC1131_2 described in section 4.1.2) and, to a lesser extent Molten clad drainage rate (SC1141_2 section 4.1.2) as important parameters. The effect of SC1131_2 on the hydrogen production is as expected (as indicated in its description in section 4.1.2). The effect of SC1141_2 is also not surprising as it affects the overall melt progression behavior (and is one of the few melt progression parameter available for uncertainty analysis).

The duration of battery (BATTDUR) does not seem to affect (or only in a marginal way) the amount of radionuclide released or hydrogen production. However, it has a large effect on the time the release will start as seen in the regression over the time it takes to release 10^{-3} of the iodine inventory (Table 6.1-5). BATTDUR explains between 30% and 40% of the uncertainty.

6.3.2 Consequence Analysis

The results generated by MACCS, conditional, mean, individual latent cancer fatality (LCF) risk (per event) and conditional, mean, individual early-fatality risk (per event), have been evaluated using regression techniques. These MACCS analyses are based on the linear no-threshold dose-response model. Influential parameters are presented in two groups: (1) the input parameters inherited from the source term regression (i.e., MELCOR input parameters), and (2) MACCS specific inputs.

The analysis of conditional, mean, individual LCF risk (per event) produces consistent results for the most influential parameters at all circular areas considered (i.e., 10-mile, 20-mile, 30-mile, 40-mile and 50-mile). Since the MELCOR source terms are used as inputs for the MACCS code, it is not surprising that three of the MELCOR parameters (i.e., SRVLAM, fuel failure criterion, and FL904A) appear as important in the regression analysis of MACCS LCF risk results.

For MACCS specific parameters, the most important variable is the dry deposition velocity (VDEPOS) which accounts for at least 9% of the variance with a T_i of 0.18 using the quadratic regression analysis to at most 33% of the variance with a T_i of 0.37 using the MARS analysis for LCF risk depending on the technique used and the distance evaluated, and the median value accounts for around 17% of the variance. Thus VDEPOS is slightly more influential on the variance than the MELCOR input group. The VDEPOS uncertainty distribution is described in Section 4.2.2.

Two other consistently important MACCS parameters are the mortality risk coefficient for residual cancers (CFRISK-residual) and the dose and dose rate effectiveness factor for residual cancer (DDREFA – residual). These two parameters account for at least 0% of the variance with a T_i of 0.12 using the recursive partitioning regression analysis to at most 23% of the variance with a T_i of 0.25 using the MARS analysis for LCF risk depending on the technique used and the distance evaluated, and the median value accounts for around 12% of the variance. The CFRISK and DDREFA uncertainty distributions are described in Section 4.2.5.

The regression analysis for conditional, mean, individual early-fatality risk (per event) shows some variation in the most important parameters depending on the distance. As with LCF risk, MELCOR input parameters (i.e., SRVLAM, SRVOAFRAC, and BATTDUR) are identified as important parameters. However, FL904A is not identified as an important input parameter. BATTDUR makes sense here since release timing is important for early fatality risk. This group accounts for at least 0% of the variance with a T_i of 0.5 using the MARS analysis to at most 17% of the variance with a T_i of 0.6 using the recursive partitioning regression analysis for early-fatality risk depending on the technique used and the circular area evaluated. The median value is around 7% of the variance at shorter distances (i.e., 1.3-mile and 2-mile circular areas)

and falls to 3% of the variance when the distance increases (i.e., 2.5-mile, 3-mile, and 3.5-mile circular areas).

At short distances (i.e., 1.3-mile and 2-mile circular areas) the most important MACCS input parameter is the wet deposition parameter (CWASH1) with mostly non-monotonic and conjoint influence and is identified with all three non-additive and non-monotonic regressions techniques. This variable explains at least 4% of the variance with a T_i of 0.78 using the MARS analysis to at most 29% of the variance with a T_i of 0.76 using the quadratic regression analysis for early-fatality risk depending on the technique used and the circular area evaluated, and the median value is around 12% of the variance at the shorter distances. This influence at short distance is expected since wet deposition is very effective and rapidly depletes the plume. The CWASH1 uncertainty distribution is described in Section 4.2.1.

At longer distances (i.e., 2.5-mile, 3-mile, and 3.5-mile circular areas), the variation in early-fatality risk is more heavily influenced by horizontal dispersion than by the washout coefficient. For these distances, the crosswind dispersion coefficient (CYSIGA) becomes the most important parameter with CWASH1 becoming of marginal importance. This variable explains at least 0% of the variance with a T_i of 0.16 using the quadratic regression analysis to at most 81% of the variance with a T_i of 0.25 using the recursive partitioning regression analysis for early-fatality risk depending on the technique used and the circular area evaluated, and the median value is around 1% of the variance at the longer distances. The CYSIGA uncertainty distribution is described in Section 4.2.6.

Parameters consistently important, but not as important as CWASH1 within 2 miles and not as important as CYSIGA beyond 2 miles, are the early fatality threshold for red bone marrow (EFFTHR–Red Marrow) and the early health effects beta (shape) factor for red bone marrow (EFFACB–Red Marrow). At longer distances (i.e., 2.5-mile, 3-mile, and 3.5-mile circular areas), these two variables account for at least 0% of the variance with a T_i of 0.41 using the quadratic regression analysis to at most 16% of the variance with a T_i of 0.82 using the MARS analysis for early-fatality risk depending on the technique used and the circular area evaluated, and are the third most important group of input variables. The median value is around 4% of the variance at the longer distances. Also, EFFTHR-red marrow and EFFACB-red marrow consistently show interactions with other input variables. The EFFTHR-red marrow and EFFACB-red marrow uncertainty distributions are described in Section 4.2.4.

6.4 Separate Sensitivity Studies

Some sensitivity studies were conducted as part of the original SOARCA project. These are documented in NUREG-1935 [1] and NUREG/CR-7110 Volume 1 [2]. During the course of conducting this uncertainty analysis, other sensitivity studies were suggested by UA team members, or external reviewers such as the SOARCA peer review panel and the NRC ACRS. The separate sensitivity studies conducted in conjunction with this UA are documented in this section.

6.4.1 Manual Control of the Safety Relief Valve (Operator Actions)

A sensitivity study was carried out to determine the effect of manual operation of the SRV. For this study, the SOARCA uncertainty analysis unmitigated LTSBO scenario was used. The SOARCA uncertainty analysis base case is the current estimate SOARCA case with the updates described in Appendix C. The updates include temporal convergence adjustments, near equilibrium model turned off, the use of CHEMFORM #5, bottom elevation of separator control volume modification, addition of check valve in the vacuum breaker line (FL904A water from wetwell relationship) modification, and addition of FL904A open area growth rate. MELCOR 1.8.6 Version YV3780 was employed for the subsequent cases.

The study varied the manual opening time of a single SRV. In order to depressurize the reactor vessel in a controlled manner, operators can manually open a SRV, as described in the station emergency procedures, in order to prevent excessive cycling of the SRVs (NUREG/CR-7110 Volume I [2]). The base case opened the SRV at 1.0 hours after the initiating event. The three variations on the base case open the SRV at 0.5 hours, 2.0 hours, and 3.0 hours. Finally, a bounding case is run with no manual SRV opening in order to quantify the effects of excessive SRV cycling.

Table 6.4-1 lists the timing of key events for the base case of manual SRV operation at 0.5 hours, 1.0 hours, 2.0 hours, and 3.0 hours. The only case that differs significantly from the base case (SRV open at 1.0 hour) is the case with SRV opening at 0.5 hours. By opening the SRV a half hour earlier than the base case, most key events occur about four hours earlier than the base case; i.e. the accident progression is accelerated with earlier SRV opening. However, this effect is probably being caused by an unrealistic change in the RCIC operation. Manually opening the SRV at 0.5 hours causes the RPV pressure to drop below the RCIC turbine trip pressure (75 psig), which terminates the RCIC injection into the feedwater lines three hours before the base case. In reality, the operators would not allow the steam line pressure to drop so low to trip the RCIC. With manual SRV operation at 2.0 hours, most of the key events are in close agreement to the base 1.0 hour case; however, some events occur about 1 hour later than the base case. Similarly, with manual SRV operation at 3.0 hours, the timings of most important events are close to the 1.0 hour case, and some events in the 3.0 hour case occurring slightly later (~1.5 hr).

Table 6.4-1 Timing of key events for Peach Bottom Unmitigated LTSBO, manual SRV operation action at 0.5 hr, 1.0 hr, 2.0 hr and 3.0 hr

Event	LTSBO with 4 hr DC power (time in hours unless noted otherwise)				
	UA SOARCA MELCOR 1.8.6 Version YV3780, SRV Manual Operation at 1.0 hr	UA SOARCA MELCOR 1.8.6 Version YV3780, SRV Manual Operation at 0.5 hr	UA SOARCA MELCOR 1.8.6 Version YV3780, SRV Manual Operation at 2.0 hr	UA SOARCA MELCOR 1.8.6 Version YV3780, SRV Manual Operation at 3.0 hr	UA SOARCA MELCOR 1.8.6 Version YV3780, No SRV Manual operation
Station blackout loss of all onsite and offsite AC power, reactor scram	0.00	0.00	0.00	0.00	0.00
Low-level 2 and RCIC actuation signal	0.17	0.17	0.17	0.17	0.17
Operators manually open SRV to depressurize the reactor vessel	1.0	0.50	2.0	3.0	NA
RPV pressure first drops below LPI setpoint (400 psig)	1.2	0.77	2.3	3.3	4.9
Battery depletion leads immediate SRV re-closure	4.0	4.0	4.0	4.0	4.0
RCIC trip due to low steam line pressure (75 psig)	--	2.1	--	--	--
RCIC steam line floods with water RCIC flow terminates	5.2	--	5.3	4.8	--
SRV sticks open because of excessive cycling	8.2	6.4	7.9	7.5	4.6
Downcomer water level reaches top of active fuel	8.4	0.71	8.2	8.1	5.0
First hydrogen production	8.6	4.4	8.4	8.4	5.4
First fuel-cladding gap release	9.1	5.3	9.0	9.1	6.2
First channel box failure	9.4	5.7	9.4	9.4	6.5
Reactor vessel water level reaches bottom of core support plate	9.4	6.7	9.3	9.0	6.6
First localized failure of core support plate	10.7	7.5	10.6	10.8	8.4
First core cell collapse because of time at temperature	10.0	6.2	9.9	10.0	7.0
Beginning of large-scale relocation of core debris to lower plenum	10.7	7.5	10.6	10.8	8.4
Lower head dries out	12.1	9.2	12.5	13.4	10.2

Table 6.4-1 Timing of key events for Peach Bottom Unmitigated LTSBO, manual SRV operation action at 0.5 hr, 1.0 hr, 2.0 hr and 3.0 hr (continued)

Event	LTSBO with 4 hr DC power (time in hours unless noted otherwise)				
	UA SOARCA MELCOR 1.8.6 Version YV3780, SRV Manual Operation at 1.0 hr	UA SOARCA MELCOR 1.8.6 Version YV3780, SRV Manual Operation at 0.5 hr	UA SOARCA MELCOR 1.8.6 Version YV3780, SRV Manual Operation at 2.0 hr	UA SOARCA MELCOR 1.8.6 Version YV3780, SRV Manual Operation at 3.0 hr	UA SOARCA MELCOR 1.8.6 Version YV3780, No SRV Manual Operation
Ring 5 CRGT column collapse	16.1	12.6	16.6	17.6	12.9
Ring 3 CRGT column collapse	16.9	13.4	17.2	18.4	12.9
Ring 4 CRGT column collapse	17.0	13.5	16.7	18.8	12.9
Ring 1 CRGT column collapse	17.4	12.7	17.4	17.4	16.7
Ring 2 CRGT column collapse	17.5	12.6	18.6	18.8	12.9
Lower head failure	19.8	15.9	20.9	21.2	17.5
Drywell head flange leakage begins	19.9	15.9	20.9	19.7	17.5
Hydrogen burns initiated in drywell enclosure region of reactor building	19.9	15.9	21.0	20.0	17.5
Refueling bay to environment blowout panels open	19.9	15.9	21.0	21.3	17.5
Hydrogen burns initiated in reactor building refueling bay	20.1	16.2	21.2	21.4	17.8
Drywell shell melt-through initiated and drywell head flange re-closure	20.0	16.1	21.2	21.5	17.8
Hydrogen burns initiated in lower reactor building	20.0	16.1	21.2	21.5	17.8
Door to environment through railroad access opens because of overpressure	20.0	16.1	21.2	21.5	17.8
Equipment Lock Door at 135-ft fails due to overpressure	20.0	16.1	21.2	21.5	17.8
Time iodine release to environment exceeds 1% of initial core inventory	22.8	16.2	21.3	21.6	20.9
Calculation terminated	48.0	48.0	48.0	48.0	48.0

As a metric for comparison, cesium and iodine release to the environment are used to compare the environmental release. For this comparison the only release pathways considered (i.e., refueling bay blowout panels and the equipment lock door at 135 feet above ground level) are those which would be carried over into the MACCS analysis.

As shown on Figure 6.4-1, the initial iodine release to the environment is highest (8.7×10^{-2}), and occurs about four hours earlier, for the case with manual operation at 0.5 hours compared to the base case of 1.0 hour. This can be attributed to the earlier uncovering of the core and ultimately earlier lower head and containment failure, due to the early loss of RCIC injection (i.e., turbine tripped on low pressure). Similarly, when no manual SRV operation action was taken, RCIC operation was negatively impacted due to excessive SRV cycling and ultimately the failure of the SRV in the open position. The higher iodine release in this case is due to revaporization from hotter internal structures. Manual SRV operation at 2.0 hours and 3.0 hours, along with the case with no SRV opening, results exhibit similar release fractions to the base case of 1.0 hour; the final iodine release fractions for these cases are between 2.5×10^{-2} and 4.0×10^{-2} . The same trends exist for the cesium release fractions to the environment, as shown on Figure 6.4-2. Manual opening of the SRV at 0.5 hours results in the greatest release of cesium to the environment (4.1×10^{-2}). The other cases have lower release fractions between 6×10^{-3} to 9×10^{-3} .

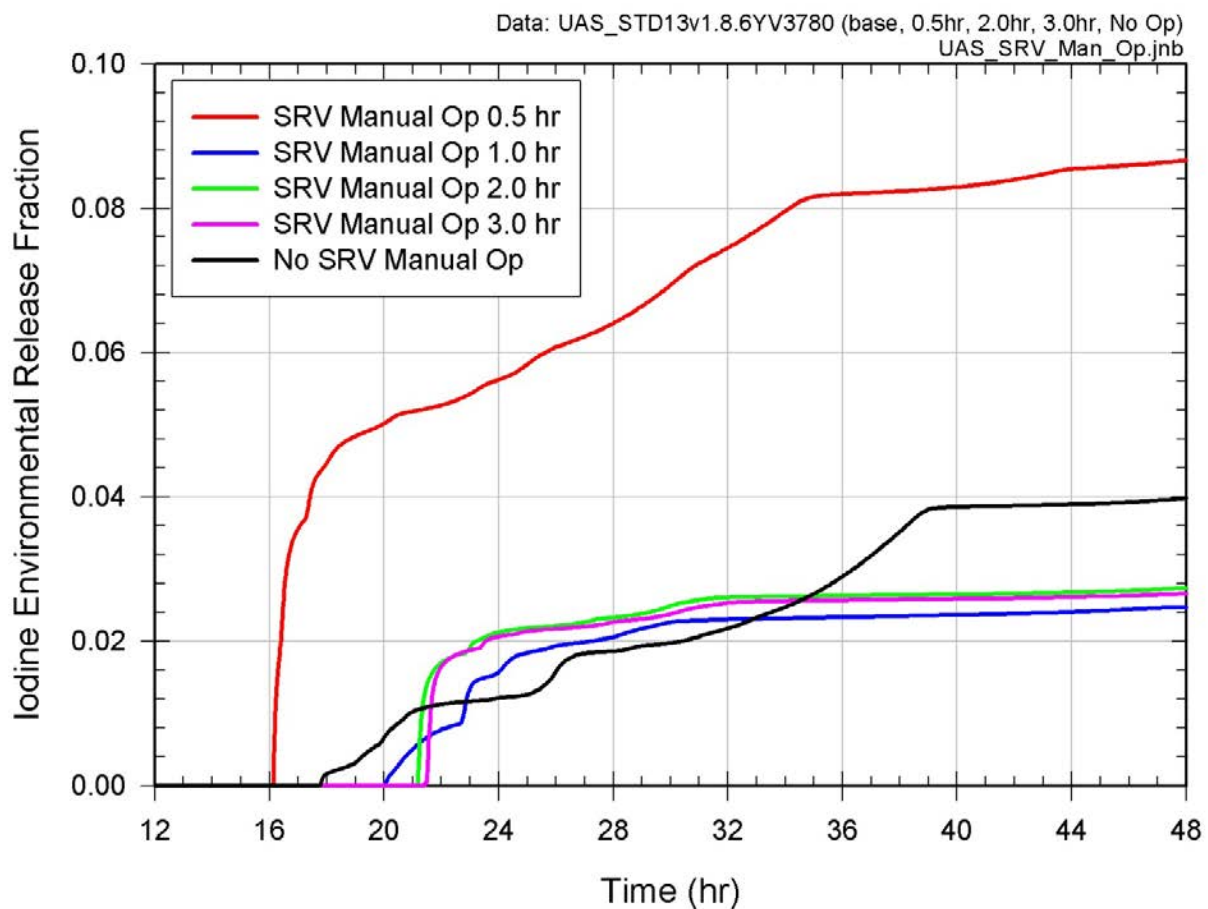


Figure 6.4-1 Environmental iodine release fraction for UA SOARCA sensitivity cases for the manual control of the SRV

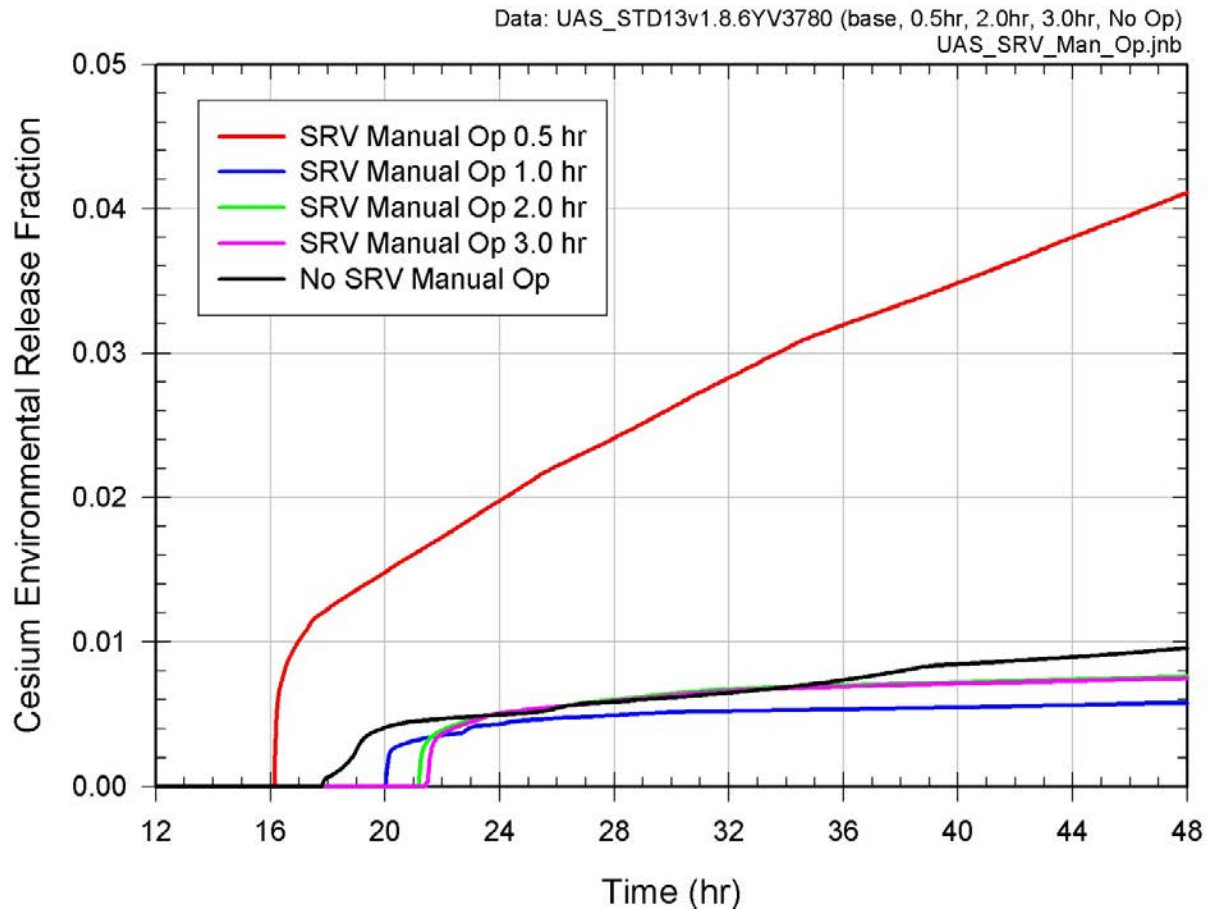


Figure 6.4-2 Environmental cesium release fraction for UA SOARCA sensitivity cases for the manual control of the SRV

Based on the results of the sensitivity study, early manual operation (opening at 0.5 hours) of the SRVs would lead to larger environmental consequences. The early opening of the SRV depressurizes the reactor below 75 psig, which trips the RCIC system since it is a steam driven system. This action terminates the RCIC injection into the feedwater lines (suction is from the condensate storage tank), leading to less core makeup water being delivered to the reactor.

6.4.2 Sensitivity of Fission Product Release to Reactor Lower Head Penetration Failures

In response to a concern raised in an ACRS review letter [94], a sensitivity study was carried out late in the uncertainty analysis to investigate the dependence of fission product releases to the environment on the mode of RPV lower head failure. The concern was with respect to whether the MELCOR release predictions for the LTSBO scenario would change if lower head penetration failures were considered as a means of core debris relocating from the RPV to the reactor cavity. RPV lower head failure in the SOARCA estimate calculations, and in the subject uncertainty calculations, was considered to only occur by gross “creep” failure. The sensitivity study was carried out by varying certain input parameters of the available MELCOR penetration model, acknowledging that the model is parametric in nature with known limitations. Cesium release to the environment was the metric considered.

The melt ejection model in MELCOR for penetrations is designed to model the failure of a penetration and melt ejection through it at high pressure. It includes an ablation model, which is a simplified version of one developed from the Hi-Pressure Melt Streaming (HIPS) tests [61]. Although the HIPS tests were high pressure ejection tests, the ablation model is based on user-specified heat transfer coefficients and an energy balance and so is probably applicable to low pressure scenarios (such as the SOARCA LTSBO). Important with respect to the capability of the penetration model is that it lacks provisions for calculating molten material flow through an instrument guide tube or predicting the plugging of an open penetration by freezing melt.

The penetration model sensitivity study focused primarily on the number of penetrations that might fail. The Peach Bottom lower head has penetrations that accommodate control blades and instrument tubes. Additionally, the head accommodates a drain line at its lowest point. The ACRS concern is most specific to the failure of the penetration accommodating the drain line, pointing out that it may be the most vulnerable penetration [62]. Peach Bottom has 55 instrument tubes. The sensitivity study involved a set of 50 MELCOR calculations in which a varying number of penetrations, representative of 1.5-inch diameter instrument tube penetrations, was represented. The penetrations were defined in groups of between 1 and 11 penetrations for each of the 5 radial rings of the active core nodalization. The calculations were run to 48 hours. The resulting open area in the lower head in the calculations, given that penetrations in some rings failed while penetrations in other rings didn't, varied between 0.0024 m² and 0.0423 m² averaging 0.01487 m². This relates to the area of between 2.2 and 38.4 instrument tubes averaging the area of 13.5 instrument tubes. The smaller areas of this range are thought to account for the drain line vulnerability identified by the ACRS.

Two other parameters were varied (sampled) in the MELCOR calculations in addition to the number of penetrations represented. These parameters were the heat transfer coefficient between the penetrations and core debris and the temperature at which a penetration would fail. The heat transfer coefficient was varied between half and twice the MELCOR default value of 1,000 W/m²-K while the failure temperature was varied between 1,500 K and 1,700 K.

Of the 50 MELCOR calculations, seven failed to complete and two progressed to a gross creep failure of the lower head. In all but three of the calculations, core debris migrated to and melted through the drywell liner. Penetration failures generally occurred 3 hours before the gross lower head failure in the base uncertainty calculation. This timing difference was relatively insensitive to variations in the sampled input parameters. Relocation of core debris to the reactor cavity through penetrations generally began within 6 minutes of the first penetration failure once appreciable molten material resided near the penetration. The penetrations did not ablate significantly. Fractional releases of cesium to the environment showed the statistics:

- Min: 0.0063
- Mean: 0.0372
- Median: 0.0418
- Max: 0.0701

Comparing these statistics to the fractional cesium release of 0.0052 in the base uncertainty calculation, which did not consider the possibility of penetration failures, suggests a marked increase in release if penetration failures are considered. Characteristics of the sensitivity calculations fundamental to their cesium releases were:

- Calculations experiencing greater and extended degrees of cladding/steel oxidation within the reactor vessel, as evidenced by in-vessel hydrogen production, exhibited larger releases of cesium to the environment. The releases can be traced to late revaporization of material deposited on reactor internals during core degradation as evidenced in Figure 6.4-3 for one of the high-release calculations. On this figure, the increasing cesium in the environment mirrors the decreasing cesium on “Lower RPV” structures. The revaporization is driven by the heat generation associated with the greater and extended degrees of oxidation in the high-release calculations¹⁵.
- Calculations experiencing greater degrees of oxidation saw large amounts of core debris remaining in the vessel for a protracted period of time.
- Calculations seeing a protracted residence of large amounts of core debris in the vessel experienced a middling number of penetration failures, i.e., not a small number of failures and not a large number of failures, but a medium number of failures. This dependence is intuitive as a small number of failed penetrations would not relieve enough core debris to preclude a gross lower head failure and a large number of failed penetrations would allow debris to fall readily from the vessel.

The penetration model sensitivity study suggests that it may be important to consider lower head penetration failures when modeling severe accidents in a BWR. The influence on relative cesium release to the environment is potentially large. In considering the results of the study, however, it may be entirely important that the penetration modeling available in MELCOR lacks provisions for calculating the plugging of an open penetration by freezing melt. If this phenomenon were accounted for, penetration failures might be immaterial in that the associated openings readily reclose promoting an eventual gross failure of the lower head. Such plugging was observed to have occurred in the Three Mile Island Unit 2 accident where metallic debris was found refrozen inside instrument tubes outside of the RPV.

See Appendix E, section E.10.2, for additional information.

¹⁵ Since cesium is specified as cesium molybdate here, there is no potential chemisorption of cesium hydroxide.

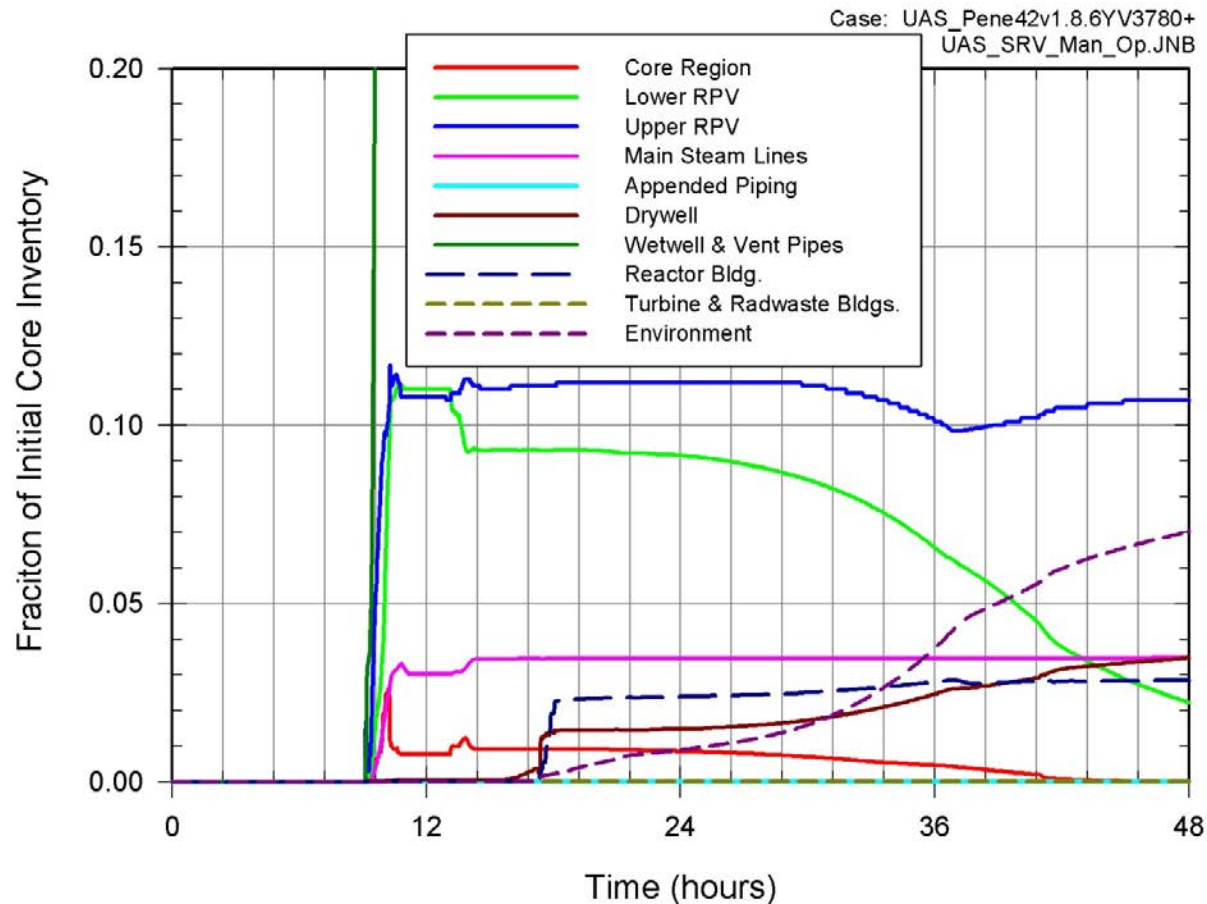


Figure 6.4-3 Cesium distribution in a high-release case of the Lower Head Penetration Model Sensitivity Study

6.4.3 Dose Truncation Uncertainty Sensitivity Analyses

An uncertainty sensitivity study was conducted on the alternate dose response models used in the SOARCA project. Risk results for this sensitivity study are presented for three dose-response models which are the following:

1. LNT dose response model;
2. Linear-with-threshold dose response model, using a truncation level of the US average natural background dose rate combined with average annual, medical dose as a dose truncation level (USBGR), which is 620 mrem/yr; and
3. Linear-with-threshold model using a dose truncation level based on the HPS position statement that there is a dose below which, due to uncertainties, a quantified risk should not be assigned, which is 5 rem/yr with a lifetime limit of 10 rem.

The USBGR and HPS dose response models were applied to the MACCS CAP14 uncertainty model discussed in Section 5.2.1, which used the LNT dose-response model for the MELCOR Replicate 1 source terms. of the same four regression methods, as used in the integrated UA, were applied to determine which input parameters affect the estimated LCF risk: rank regression, quadratic regression, recursive partitioning, and MARS. See Section 3.4.2 for a description of these methods.

Table 6.4-2 provides the basic statistical results related to LCF risk of the MELCOR Replicate 1 source terms sensitivity analysis (i.e., MACCS uncertainty model CAP14 used the LNT dose model, the CAP15 uncertainty model used the USBGR dose model, and the CAP16 uncertainty model used the HPS dose model) for the 10-mile and 50-mile radius circular areas. It should be noted that the habitability criterion is assumed to be 500 mrem/yr. This dose rate is below the USBGR and HPS truncation levels; therefore, most of the doses received during the long-term phase are below the dose truncation limit and are not counted toward health effects when using this criterion. Thus, most of the risks associated with the USBGR and HPS truncation levels are from doses received during the first year. The emergency and long-term phases are not easily separated in the first year for purposes of evaluating the annual dose threshold.

Table 6.4-2 Conditional, mean, individual LCF risk (per event) average statistics for the Dose Truncation Sensitivity Analysis at specified Radial Distances

	LNT 0-10 miles	USBGR 0-10 miles	HPS 0-10 miles	LNT 0-50 miles	USBGR 0-50 miles	HPS 0-50 miles
Mean	1.6×10^{-4}	5.2×10^{-6}	5.4×10^{-6}	1.1×10^{-4}	4.6×10^{-5}	4.2×10^{-5}
Median	1.4×10^{-4}	2.3×10^{-6}	2.3×10^{-6}	7.4×10^{-5}	1.7×10^{-5}	9.1×10^{-6}
5th percentile	3.7×10^{-5}	4.3×10^{-7}	2.3×10^{-7}	2.2×10^{-5}	2.4×10^{-6}	7.4×10^{-8}
95th percentile	4.0×10^{-4}	1.8×10^{-5}	1.9×10^{-5}	3.0×10^{-4}	1.6×10^{-4}	1.6×10^{-4}

6.4.3.1 Latent Cancer Fatality Regression Analysis

Tables 6.4-2 through 6.4-16 show the results of regression analyses used to evaluate the sensitivity of the conditional, mean, individual LCF risk (per event) results for the MACCS sensitivity uncertainty analysis for the MELCOR Replicate 1 source terms (i.e., MACCS uncertainty model CAP14 used the LNT dose model, the CAP15 uncertainty model used the USBGR dose model, and the CAP16 uncertainty model used the HPS dose model) for the 10-mile, 20-mile, 30-mile, 40-mile, and 50-mile radius circular areas, respectively. The tables represent input parameter influence on the results of the uncertainty analysis. Rank regression is often an underestimate of the true influence of a parameter since it captures only a monotonic relationship. A slightly non-monotonic relationship results in a smaller R^2 than when the relationship is purely monotonic.

The tables are ordered by input variables with the highest rank regression results, and then are further grouped according to the type of input parameter (i.e., MACCS or MELCOR variables). The final R^2 determination for all four regression models range from good to high confidence for all dose models for the five circular areas and range from 0.47 for the rank regression analysis to 0.92 for the quadratic regression analysis.

Since the dose truncation models only affect the LCF risk results, early-fatality risk is not reported in this sensitivity study.

6.4.3.1.1 Linear No Threshold Dose-Response Model

Tables 6.4-2 through 6.4-6 show the results of the regression analyses used to evaluate the sensitivity of the conditional, mean, individual LCF risk (per event) results for the MACCS sensitivity uncertainty analysis for the MELCOR Replicate 1 source terms using the LNT dose model (i.e., MACCS uncertainty model CAP14) for the 10-mile, 20-mile, 30-mile, 40-mile, and 50-mile circular areas, respectively. For the LNT dose-response model, the regression

analyses at the five circular areas consistently rank the MACCS dry deposition velocity (VDEPOS) and the MELCOR SRV stochastic failure probability (SRVLAM) as the most important input variables.

Additional variables also consistently show some level of importance at all circular areas. These additional input variables include the following:

- The MELCOR fuel failure criterion, and
- The MELCOR SRV open area fraction (SRVOAFRAC),
- The MELCOR drywell liner melt-through open area flow path (FL904A), and
- The MACCS residual dose and dose-rate effectiveness factor (DDREFA–Residual)

These four variables (VDEPOS, SRVLAM, SRVOAFRAC, and fuel failure criterion,) account for at least 30% of the variance for the five circular areas for the rank regression analysis, at least 3% of the variance for the five circular areas for the quadratic regression analysis, at least 12% of the variance for the five circular areas for the recursive partitioning analysis, and at least 10% of the variance for the five circular areas for the MARS analysis.

Table 6.4-3 Conditional, mean, individual LCF risk (per event) regression of MACCS sensitivity LNT model at the 10-mile circular area

	Rank Regression			Quadratic			Recursive Partitioning			MARS		
Final R ²	0.71			0.89			0.83			0.81		
Input	R ² inc.	R ² cont.	SRRC	S _i	T _i	p-val	S _i	T _i	p-val	S _i	T _i	p-val
VDEPOS	0.25	0.25	0.63	0.10	0.11	0.6	0.15	0.44	0	0.12	0.28	0
SRVLAM	0.37	0.12	-0.33	0.05	0	1	0.01	0.21	0	0.01	0.34	0
Fuel failure criterion	0.41	0.04	0.21	0.05	0	1	---	---	---	0	0.01	0.6
SRVOAFRAC	0.43	0.02	-0.08	---	---	---	0	0.08	0.04	0	0	1
CHEMFORM	---	---	---	0.03	0.19	0.05	---	---	---	---	---	---
CFRISK Residual	0.51	0.08	0.24	0.01	0.27	0	0.14	0.34	0	0.10	0.33	0
DDREFA Residual	0.53	0.02	-0.14	0	0.12	0.03	0.03	0.02	0.18	---	---	---
GSHFAC Normal	0.60	0.07	0.22	0.02	0	1	0	0.10	0.01	---	---	---
CFRISK Colon	0.65	0.05	0.23	0.07	0.25	0	0.05	0.28	0	0.02	0.05	0.56
CFRISK Lung	0.69	0.04	0.17	0.01	0.06	0.26	0	0.17	0.01	0.02	0.37	0
ESPEED	0.71	0.02	-0.10	0.05	0.05	0.18	0.03	0.07	0.05	0.02	0	1
CFRISK Breast	0.73	0.02	0.11	0.05	0.04	0.47	0	0	1	---	---	---
DLTEVA Cohort 5	0.74	0.01	-0.09	0	0.11	0.05	0	0	1	0.03	0.26	0.01
Pu-239 Inhalation	0.75	0.01	0.10	---	---	---	---	---	---	---	---	---
CZSIGA	0.76	0.01	-0.09	---	---	---	---	---	---	---	---	---
Te-127m Inhalation	---	---	---	0.05	0.03	0.55	---	---	---	---	---	---
CYSIGA	---	---	---	0	0	1	0.01	0.02	0.46	0.01	0.17	0.08
Nb-95 Inhalation	---	---	---	---	---	---	0	0.07	0	0.03	0	1
Zr-95 Inhalation	---	---	---	---	---	---	---	---	---	0.03	0	1
I-132 Inhalation	---	---	---	---	---	---	---	---	---	0	0	1

Note: Parameters are grouped by importance and relationship (e.g. MELCOR parameters). Light shading indicates parameters with low importance. The dark shading and no shading represent 'groupings' of parameters (e.g., source term influence from MELCOR inputs or latent cancer risk associated for a specific target organ).

Other input parameters have a low importance at certain circular areas but not at other circular areas. Thus, the most important variable, VDEPOS, appears at the top of the tables followed by the consistently important MELCOR variables (i.e., SRVLAM, fuel failure criterion, and SRVOAFRAC), the LCF risk parameters for residual cancers (CFRISK-residual and DDREFA-residual), and finally those LCF risk parameters, dose conversion factors for inhalation, and MELCOR parameters (e.g., CHEMFORM) not consistently ranked as important variables at the five circular areas.

The two most important MELCOR input variables are the same as those in the MACCS Uncertainty Analysis regression analyses discussed in Section 6.2.3. Since this is a smaller subset of the MACCS uncertainty analysis and still ranks very similar important parameters, this sensitivity analysis provides additional confidence in the regression analysis for parameters considered to be important.

Table 6.4-4 Conditional, mean, individual LCF risk (per event) regression of MACCS sensitivity LNT model at the 20-mile circular area

	Rank Regression			Quadratic			Recursive Partitioning			MARS		
Final R ²	0.48			0.92			0.67			0.82		
Input	R ² inc.	R ² cont.	SRRC	S _i	T _i	p-val	S _i	T _i	p-val	S _i	T _i	p-val
VDEPOS	0.22	0.22	0.35*	0.07	0.21	0.76	0.36	0.72	0	0.09	0.66	0
SRVLAM	0.33	0.11	-0.31	0	0.01	0.37	0.05	0	1	0	0.33	0.01
CHEMFORM	0.34	0.01	0.06	0	0.57	0	---	---	---	---	---	---
Fuel failure criterion	---	---	---	0	0.15	0.04	---	---	---	0.01	0.73	0
SRVOAFRAC	---	---	---	---	---	---	---	---	---	0	0.51	0
CFRISK Colon	0.37	0.03	0.15	0	0	1	0	0	1	0	0.39	0.02
DLTEVA Cohort 1	0.40	0.03	-0.13	0	0.01	0.64	0	0.20	0.01	---	---	---
Nb-95 Inhalation	0.42	0.02	0.15	0	0.10	0.50	0	0.05	0.08	0.01	0.35	0
CFRISK Lung	0.44	0.02	-0.11	---	---	---	---	---	---	0	0.48	0
Pu-239 Inhalation	0.46	0.02	-0.13	---	---	---	---	---	---	---	---	---
CYSIGA	0.48	0.02	0.11	0.02	0.08	0.05	0.02	0	1	0	0.58	0
ESPEED	0.49	0.01	0.12	0.01	0.05	0.37	0	0.02	0.54	0.03	0.66	0
Zr-95 Inhalation	0.51	0.02	-0.09	---	---	---	0	0.24	0	0.01	0	1
Sr-91 Inhalation	0.52	0.01	-0.10	0.01	0.19	0.01	---	---	---	---	---	---
CFRISK Breast	---	---	---	0.03	0.11	0.03	---	---	---	---	---	---
I-132 Inhalation	---	---	---	0	0.08	0.19	---	---	---	0.03	0.30	0.03
DLTEVA Cohort 5	---	---	---	0.02	0.01	0.81	0	0	1	0.07	0.42	0
Sr-90 Inhalation	---	---	---	---	---	---	0	0.22	0	---	---	---
Pu-241 Inhalation	---	---	---	---	---	---	0	0.21	0	---	---	---
CFRISK Residual	---	---	---	---	---	---	0.04	0	1	0	0.40	0

* The SRRC for VDEPOS is a sum of positive and negative SRRC values for four VDEPOS particle size bins.

Table 6.4-5 Conditional, mean, individual LCF risk (per event) regression of MACCS sensitivity LNT model at the 30-mile circular area

	Rank Regression			Quadratic			Recursive Partitioning			MARS		
Final R ²	0.49			0.92			0.68			0.64		
Input	R ² inc.	R ² cont.	SRRC	S _i	T _i	p-val	S _i	T _i	p-val	S _i	T _i	p-val
VDEPOS	0.20	0.20	0.37*	0.01	0.40	0	0.22	0.71	0	0.43	0.58	0
SRVLAM	0.31	0.11	-0.35	0.02	0.18	0.01	0.03	0.03	0.62	0.02	0.01	0.66
CHEMFORM	0.32	0.01	0.07	0.01	0.50	0	0.01	0.02	0.12	---	---	---
Fuel failure criterion	---	---	---	0	0	1	---	---	---	0	0	1
SRVOAFRAC	---	---	---	---	---	---	---	---	---	0.01	0.17	0.01
Zr-95 Inhalation	0.38	0.06	0.23	0.02	0	1	0.03	0.09	0.10	0	0	1
CFRISK Residual	0.42	0.04	0.14	0	0	1	0	0	1	0.02	0	1
DDREFA Residual	---	---	---	0.01	0.07	0.30	---	---	---	---	---	---
Sr-91 Inhalation	0.44	0.02	0.09	---	---	---	0	0	1	---	---	---
CFRISK Colon	0.46	0.02	0.16	0.07	0.47	0	---	---	---	0	0	1
GSHFAC	0.48	0.02	-0.13	---	---	---	0.05	0.57	0	---	---	---
ESPEED	0.50	0.02	0.12	0.02	0.30	0	0.01	0	1	0.03	0.31	0.02
CFRISK Lung	0.53	0.03	-0.10	---	---	---	0.06	0.09	0.14	0.03	0.41	0
CYSIGA	0.54	0.01	-0.10	---	---	---	0	0	1	0	0.12	0.02
DLTEVA Cohort 1	---	---	---	0	0.33	0	---	---	---	---	---	---
I-132 Inhalation	---	---	---	0.04	0.26	0.01	0	0	1	0	0	1
DLTEVA Cohort 5	---	---	---	0.01	0	1	---	---	---	0.01	0.19	0.05
CFRISK Breast	---	---	---	0	0	1	---	---	---	---	---	---
Sr-90 Inhalation	---	---	---	0	0	1	---	---	---	---	---	---
Te-127m Inhalation	---	---	---	---	---	---	0	0.07	0.07	---	---	---
Nb-95 Inhalation	---	---	---	---	---	---	---	---	---	0	0.06	0.26

* The SRRC for VDEPOS is a sum of positive and negative SRRC values for five VDEPOS particle size bins.

Table 6.4-6 Conditional, mean, individual LCF risk (per event) regression of MACCS sensitivity LNT model at the 40-mile circular area

	Rank Regression			Quadratic			Recursive Partitioning			MARS		
Final R ²	0.47			0.88			0.70			0.69		
Input	R ² inc.	R ² cont.	SRRC	S _i	T _i	p-val	S _i	T _i	p-val	S _i	T _i	p-val
VDEPOS	0.14	0.14	-0.04*	0.04	0.13	0.22	0.28	0.64	0	0.28	0.71	0
SRVLAM	0.26	0.12	-0.34	0	0.14	0.08	0.02	0.15	0.09	0.03	0	1
SRVOAFRAC	0.30	0.04	0.16	---	---	---	---	---	---	0.03	0.06	0.27
CHEMFORM	---	---	---	---	---	---	0	0	1	---	---	---
Fuel failure criterion	---	---	---	---	---	---	---	---	---	0	0	1
Zr-95 Inhalation	0.36	0.06	0.20	0.02	0.33	0	0	0.09	0.09	0	0	0.63
I-132 Inhalation	0.39	0.03	-0.10	---	---	---	0	0	1	---	---	---
Nb-95 Inhalation	0.42	0.03	0.11	---	---	---	---	---	---	0.04	0.12	0.09
Pu-239 Inhalation	0.44	0.02	0.09	0	0.59	0	---	---	---	---	---	---
Sr-91 Inhalation	0.46	0.02	-0.11	0.02	0.00	1	---	---	---	---	---	---
CFRISK Colon	0.48	0.02	0.15	0.15	0.55	0	0.01	0.18	0	0	0.14	0.04
Sr-92 Inhalation	0.50	0.02	0.07	---	---	---	0.03	0	1	---	---	---
CFRISK Lung	0.51	0.01	-0.08	---	---	---	0.01	0.13	0.03	0.04	0.24	0.01
CFRISK Breast	0.52	0.01	-0.11	---	---	---	---	---	---	---	---	---
CYSIGA	---	---	---	0.06	0.49	0	0	0.21	0	0.03	0.19	0.04
ESPEED	---	---	---	0	0.26	0	0	0.04	0.15	0	0.14	0.05
DLTEVA Cohort 1	---	---	---	0.04	0.32	0	0.01	0	1	---	---	---
DDREFA Residual	---	---	---	0.02	0.03	0.56	---	---	---	---	---	---
CFRISK Residual	---	---	---	---	---	---	---	---	---	0.01	0.09	0.09
Pu-241 Inhalation	---	---	---	0.01	0	1	---	---	---	---	---	---
CZSIGA	---	---	---	---	---	---	0	0.05	0.09	---	---	---
GSHFAC	---	---	---	---	---	---	0	0	1	---	---	---
I-132 Inhalation	---	---	---	---	---	---	---	---	---	0.06	0.10	0.07
DLTEVA Cohort 5	---	---	---	---	---	---	---	---	---	0.01	0.07	0.19

* The SRRC for VDEPOS is a sum of positive and negative SRRC values for four VDEPOS particle size bins.

Table 6.4-7 Conditional, mean, individual LCF Risk (per event) regression of MACCS sensitivity LNT model at the 50-mile circular area

	Rank Regression			Quadratic			Recursive Partitioning			MARS		
Final R ²	0.47			0.92			0.71			0.75		
Input	R ² inc.	R ² cont.	SRRC	S _i	T _i	p-val	S _i	T _i	p-val	S _i	T _i	p-val
VDEPOS	0.17	0.17	0.30*	0	0.21	0.01	0.12	0.45	0	0.07	0.11	0.08
SRVLAM	0.29	0.12	-0.33	---	---	---	0	0.14	0.08	0.05	0.36	0.03
Fuel failure criterion	0.30	0.01	0.08	0	0.21	0.50	---	---	---	0	0.37	0
SRVOAFRAC	0.31	0.01	-0.14	0.04	0.21	0.03	0.12	0.58	0	0.14	0.63	0
ESPEED	0.36	0.05	0.20	0.03	0.25	0	0	0	1	0.04	0	1
CFRISK Residual	0.40	0.04	0.11	0.02	0	1	0.06	0.12	0.21	0	0	1
DDREFA Residual	---	---	---	---	---	---	0	0.08	0.07	---	---	---
Sr-91 Inhalation	0.42	0.02	-0.11	0	0.06	0.25	0	0.08	0.08	---	---	---
CYSIGA	0.44	0.02	-0.01**	0.01	0.03	0.58	0	0	1	0	0	1
CFRISK Colon	0.46	0.02	0.15	0	0.42	0	0	0.03	0.23	0	0.02	0.35
DLTEVA Cohort 5	0.49	0.03	-0.11	---	---	---	0.05	0	1	0	0.16	0.02
GSHFAC	0.50	0.01	-0.12	---	---	---	---	---	---	---	---	---
Pu-241 Inhalation	0.51	0.01	0.08	---	---	---	---	---	---	---	---	---
CZSIGA	---	---	---	0	0.15	0.05	---	---	---	---	---	---
Sr-90 Inhalation	---	---	---	0.01	0.05	0.22	---	---	---	---	---	---
DLTEVA Cohort 1	---	---	---	0	0	1	---	---	---	---	---	---
Nb-95 Inhalation	---	---	---	0.04	0	1	---	---	---	0.02	0	1
Zr-95 Inhalation	---	---	---	---	---	---	0	0.01	0.46	0	0	1
I-132 Inhalation	---	---	---	---	---	---	0	0	1	0	0.15	0.03
CFRISK Lung	---	---	---	---	---	---	0.03	0	1	0.02	0.21	0.15
Sr-92 Inhalation	---	---	---	---	---	---	0	0	1	---	---	---

* The SRRC for VDEPOS is a sum of positive and negative SRRC values for three VDEPOS particle size bins.

** The SRRC for CYSIGA is a sum of positive and negative SRRC values for two CYSIGA stability classes.

The MACCS dry deposition velocity (VDEPOS) parameter accounts for at least 0% of the variance with a T_i of 0.21 using the quadratic regression analysis to at most 43% of the variance with a T_i of 0.58 using the MARS analysis at the five circular areas for all regression methods and is the most important input variable. As discussed in more detail in Section 4.2.2, dry deposition is characterized in MACCS with a set of deposition velocities corresponding to a set of aerosol size bins.

The MELCOR input variables (SRVLAM, fuel failure criterion, and SRVOAFRAC) accounts for at least 0% of the variance with a T_i of 0.57 using the quadratic regression analysis to at most 19% of the variance with a T_i of 0.63 using the MARS analysis at the five circular areas for all regression methods. As discussed in Section 6.1.1 and Section 6.1.2, the MELCOR input variables SRVLAM and SRVOAFRAC account for the majority of the variance for iodine and cesium release. CHEMFORM does appear as a variable of importance but is not consistently throughout all distances. The FL904A is not shown to be an important parameter in the MELCOR regression analysis discussed in Section 6.1. This discrepancy may be due to the smaller sample size used for this sensitivity study.

6.4.3.1.2 USBGR Dose-Response Model

Tables 6.4-7 through 6.4-11 show the results of the regression analyses used to evaluate the sensitivity of the conditional, mean, individual LCF risk (per event) results for the MACCS sensitivity uncertainty analysis for the MELCOR Replicate 1 source terms using the USBGR dose truncation model (i.e., MACCS uncertainty model CAP15) for the 10-mile, 20-mile, 30-mile, 40-mile, and 50-mile circular areas, respectively. For the USBGR dose-response model, the regression analyses at the five circular areas consistently rank the MACCS inhalation protection factor for normal activity (PROTIN-Normal) and the lung lifetime risk factor for cancer death (CFRISK-Lung) as the most important input variables.

Additional variables also consistently show some level of importance at all circular areas. These additional input variables include the following:

- The MELCOR SRV stochastic failure probability (SRVLAM),
- The MELCOR SRV open area fraction (SRVOAFRAC), and
- The MELCOR DC station battery duration (BATTDUR)

These five variables (PROTIN-Normal, CFRISK-Lung, SRVLAM, SRVOAFRAC, and BATTDUR) account for at least 40% of the variance at the five circular areas for the rank regression analysis, at least 1% of the variance for the five circular areas for the quadratic regression analysis, at least 2% of the variance for the five circular areas for the recursive partitioning analysis, and at least 0% of the variance for the five circular areas for the MARS analysis.

Other input parameters have a low importance at certain circular areas but not at other circular areas. Thus, the most important variables, PROTIN-Normal and CFRISK-Lung, appear at the top of the tables followed by the consistently important MELCOR variables (i.e., SRVLAM, SRVOAFRAC, and BATTDUR), and finally those LCF risk parameters, dose conversion factors for inhalation, and MELCOR parameters (e.g., fuel failure criterion) not consistently ranked as important variables at the five circular areas.

The important MELCOR input variables are similar as those in the MACCS Uncertainty Analysis regression analyses discussed in Section 6.2.3. However, the MACCS input variables are not the same. The most important MACCS input parameters using the USBGR dose truncation model are those associated with doses received in the first year and not ones associated with the long-term phase risk beyond the first year.

For Peach Bottom, the habitability criterion is an annual dose rate of 500 mrem/yr. This dose rate is below the USBGR truncation level (620 mrem/yr); therefore, most of the doses received during the long-term phase are below the dose truncation limit and are not counted toward health effects when using this criterion. Thus, most of the risks associated with the USBGR truncation level are from doses received during the first year. The emergency and long-term

phases are not easily separated in the first year for purposes of evaluating the annual dose threshold.

To better understand this explanation, it is important to understand the differences between exposure periods, commitment periods, and the periods of time when doses are actually received. For external dose pathways, the time over which doses are received is concurrent with the exposure period. External dose pathways include cloudshine and groundshine.

The exposure period for internal pathways, inhalation and ingestion, is the period of time when the inhalation or ingestion occurs; however, doses continue to be received over a person's entire lifetime following the exposure. A person's lifetime is obviously variable, depending upon the age of the person at the time of exposure, among other things. The period of time over which doses are received from an internal pathway is accounted for in the construction of dose conversion factors by integrating the doses over a finite period called a dose commitment period, which is usually taken to be 50 years when calculating internal-pathway dose conversion factors for adults. The implicit assumption is that the average adult lives for an additional 50 years following the exposure, which is most likely a conservative assumption.

Table 6.4-8 Conditional, mean, individual LCF Risk (per event) regression of MACCS sensitivity USBGR model at the 10-mile circular area

	Rank Regression			Quadratic			Recursive Partitioning			MARS		
Final R ²	0.54			0.90			0.61			0.80		
Input	R ² inc.	R ² cont.	SRRC	S _i	T _i	p-val	S _i	T _i	p-val	S _i	T _i	p-val
CFRISK Lung	0.14	0.14	0.33	0.04	0.25	0.03	0.03	0.04	0.32	0.15	0.49	0.01
PROTIN Normal	0.27	0.13	0.38	0.07	0	1	0	0	1	0	0.11	0.15
SRVLAM	0.38	0.11	-0.29	0	0.06	0.34	0.04	0.60	0	0.01	0.23	0.04
BATTDUR	0.42	0.04	-0.16	0	0.01	0.66	0.02	0.09	0.15	0.01	0.05	0.31
SRVOAFRAC	0.44	0.02	-0.17	0.08	0.17	0.17	0.24	0.74	0	0.09	0.56	0
Fuel Failure Criterion	0.44	0	0.06	---	---	---	---	---	---	---	---	---
Te-127m Inhalation	0.47	0.03	0.14	0.11	0	1	0	0.16	0	0	0.29	0.08
TIMHOT	0.49	0.02	0.14	0	0.23	0.01	0.04	0.08	0.06	---	---	---
SC1131_2	0.51	0.02	0.10	0	0	1	---	---	---	0	0	1
ESPEED Cohort 5	0.52	0.01	-0.13	---	---	---	0.04	0	1	0	0	1
Cs-137 Inhalation	0.53	0.01	-0.11	---	---	---	0.02	0	1	0	0	1
SLCRFRAC	0.54	0.01	-0.13	0.02	0.46	0.07	---	---	---	---	---	---
Ba-140 Inhalation	0.55	0.01	-0.09	---	---	---	---	---	---	0	0.19	0.08
I-133 Inhalation	0.56	0.01	0.08	---	---	---	0.01	0	1	---	---	---
Sr-90 Inhalation	0.57	0.01	0.08	---	---	---	---	---	---	---	---	---
DLTEVA Cohort 4	---	---	---	0.08	0.27	0	---	---	---	---	---	---
CFRISK Thyroid	---	---	---	0.06	0.45	0.01	0.01	0.05	0.52	0.03	0.12	0.12
RHONOM	---	---	---	0	0.04	0.20	---	---	---	---	---	---
Sr-92 Inhalation	---	---	---	0	0.03	0.44	---	---	---	0.02	0.09	0.15
Pu-239 Inhalation	---	---	---	0.07	0.05	0.60	0.05	0.24	0.01	---	---	---
SC1141_2	---	---	---	0.02	0	1	---	---	---	---	---	---
Ce-141 Inhalation	---	---	---	---	---	---	0.02	0.05	0.13	---	---	---
DLTEVA Cohort 3	---	---	---	---	---	---	0.05	0.02	0.46	---	---	---
DLTEVA Cohort 1	---	---	---	---	---	---	0	0	1	---	---	---
SC1141_2	---	---	---	---	---	---	---	---	---	0	0	1
CSFACT Evacuation	---	---	---	---	---	---	---	---	---	0	0	1

Table 6.4-9 Conditional, mean, individual LCF risk (per event) regression of MACCS sensitivity USBGR model at the 20-mile circular area

	Rank Regression			Quadratic			Recursive Partitioning			MARS		
Final R ²	0.55			0.84			0.64			0.69		
Input	R ² inc.	R ² cont.	SRRC	S _i	T _i	p-val	S _i	T _i	p-val	S _i	T _i	p-val
CFRISK Lung	0.12	0.12	0.33	0.07	0.34	0	0.01	0	1	0	0.81	0
PROTIN Normal	0.23	0.11	0.37	0.01	0	1	0	0	1	0	0.40	0.01
SRVLAM	0.34	0.11	-0.33	---	---	---	0	0.22	0	0	0	1
SRVOAFRAC	0.40	0.06	-0.26	0	0	1	0.01	0.06	0.11	0	0.02	0.52
BATTDUR	0.42	0.02	0.13	0	0.21	0	---	---	---	0	0	1
DLTEVA Cohort 4	0.46	0.04	0.17	---	---	---	---	---	---	---	---	---
Ba-140 Inhalation	0.48	0.02	-0.12	0.03	0.22	0	0.01	0.06	0.10	0.02	0.50	0
ESPEED	0.50	0.02	-0.12	---	---	---	0.02	0	1	0	0.50	0.01
SC1131_2	0.51	0.01	-0.13	0.09	0.10	0.55	0.21	0.79	0	0	0.96	0
CSFACT Evacuation	0.52	0.01	0.08	0.03	0.21	0	0.03	0.07	0.11	0	0.17	0.11
Zr-95 Inhalation	0.53	0.01	-0.11	0	0.12	0	0	0.47	0	---	---	---
Te-127m Inhalation	0.55	0.02	-0.11	0.05	0	1	---	---	---	0.01	0.30	0.08
SLCRFRAC	0.57	0.02	0.12	0	0.21	0	---	---	---	---	---	---
Sr-92 Inhalation	0.58	0.01	0.09	0.02	0.04	0.30	0.05	0.06	0.16	0	0.43	0
Cs-137 Inhalation	0.59	0.01	-0.07	---	---	---	0	0	1	0	0	1
Ce-141 Inhalation	---	---	---	0.01	0.21	0	0.01	0	1	---	---	---
CFRISK Thyroid	---	---	---	0	0.24	0	---	---	---	0.01	0	1
DLTEVA Cohort 3	---	---	---	0	0.06	0.05	---	---	---	---	---	---
Pu-239 Inhalation	---	---	---	---	---	---	0.07	0.23	0	---	---	---
SC1141_2	---	---	---	---	---	---	---	---	---	0	0.42	0.01

Table 6.4-10 Conditional, mean, individual LCF risk (per event) regression of MACCS sensitivity USBGR model at the 30-mile circular area

	Rank Regression			Quadratic			Recursive Partitioning			MARS		
Final R ²	0.55			0.87			0.65			0.57		
Input	R ² inc.	R ² cont.	SRRC	S _i	T _i	p-val	S _i	T _i	p-val	S _i	T _i	p-val
CFRISK Lung	0.11	0.11	0.32	0	0.28	0	0.02	0	1	0.07	0.57	0
PROTIN Normal	0.22	0.11	0.37	0.03	0.12	0	0.04	0	1	0	0	1
SRVLAM	0.33	0.11	-0.33	---	---	---	0.02	0.23	0.01	0	0	1
SRVOAFRAC	0.40	0.07	-0.28	0.05	0.05	0.15	0.01	0.29	0	0	0.11	0.12
BATTDUR	---	---	---	0	0.07	0.06	---	---	---	0	0.08	0.12
I-133 Inhalation	0.44	0.04	0.18	---	---	---	---	---	---	---	---	---
SC1131_2	0.46	0.02	-0.14	0.04	0.18	0.01	---	---	---	0.02	0	1
CSFACT Evacuation	0.48	0.02	-0.12	---	---	---	0.04	0	1	0	0.11	0.19
SC1141_2	0.49	0.01	0.12	0.06	0.05	0.38	---	---	---	0.21	0.20	0.12
ESPEED	0.50	0.01	-0.12	0.05	0.21	0	0.20	0.80	0	0.26	0.83	0
Te-127m Inhalation	0.51	0.01	-0.12	---	---	---	---	---	---	0	0.17	0.07
DLTEVA Cohort 3	0.52	0.01	-0.11	0.01	0.08	0.07	0.03	0.53	0	---	---	---
TIMHOT	0.54	0.02	0.11	0	0.10	0	---	---	---	---	---	---
CFRISK Thyroid	0.56	0.02	0.08	0.04	0.08	0.28	---	---	---	0.01	0.21	0.01
Cs-137 Inhalation	0.57	0.01	-0.08	---	---	---	---	---	---	0	0	1
Ce-141 Inhalation	0.58	0.01	0.08	0.01	0.17	0	0.02	0	1	---	---	---
Sr-92 Inhalation	---	---	---	0.06	0.21	0	0.01	0.15	0.03	0.01	0.19	0.01
Ba-140 Inhalation	---	---	---	0.04	0.13	0.01	0.06	0.20	0.01	0.01	0.22	0.01
Pu-239 Inhalation	---	---	---	0	0.04	0.28	---	---	---	---	---	---
Zr-95 Inhalation	---	---	---	---	---	---	0	0.27	0	---	---	---
RHONOM	---	---	---	---	---	---	0	0	1	---	---	---

Table 6.4-11 Conditional, mean, individual LCF risk (per event) regression of MACCS sensitivity USBGR model at the 40-mile circular area

	Rank Regression			Quadratic			Recursive Partitioning			MARS		
Final R ²	0.55			0.86			0.65			0.77		
Input	R ² inc.	R ² cont.	SRRC	S _i	T _i	p-val	S _i	T _i	p-val	S _i	T _i	p-val
PROTIN Normal	0.11	0.11	0.38	0	0.07	0.07	0.07	0.02	0.67	0.01	0.14	0.23
CFRISK Lung	0.21	0.10	0.31	0.01	0.32	0	0	0.11	0.11	0	0.55	0
SRVLAM	0.33	0.12	-0.34	---	---	---	0	0	1	0	0.27	0
SRVOAFRAC	0.40	0.07	-0.26	0	0	1	0	0	1	0.01	0	1
BATTDUR	0.42	0.02	-0.12	---	---	---	0	0	1	0	0.28	0
Fuel failure criterion	---	---	---	0	0.07	0.12	0.10	0	1	---	---	---
Ce-141 Inhalation	0.46	0.04	0.18	---	---	---	---	---	---	---	---	---
SC1131_2	0.48	0.02	-0.14	---	---	---	---	---	---	0	0	1
Cs-137 Inhalation	0.50	0.02	-0.01	0.11	0.29	0	0.29	0.78	0	0.10	0.84	0
CSFACT Evacuation	0.51	0.01	0.11	0	0.16	0	---	---	---	0.04	0	1
Te-127m Inhalation	0.52	0.01	-0.11	---	---	---	0.02	0	1	0	0.36	0
ESPEED	0.54	0.02	-0.08	---	---	---	---	---	---	0.04	0.02	0.52
SLCRFRAC	0.56	0.02	-0.10	---	---	---	0.05	0.51	0	---	---	---
TIMHOT	0.57	0.01	0.11	0	0.04	0.58	---	---	---	---	---	---
DLTEVA Cohort 4	0.58	0.01	0.08	0.01	0.21	0	0	0.18	0	---	---	---
Pu-239 Inhalation	---	---	---	0.05	0.10	0.02	---	---	---	---	---	---
Sr-92 Inhalation	---	---	---	0.02	0.11	0.08	0	0.17	0.02	0.01	0	1
DLTEVA Cohort 1	---	---	---	0.02	0	0.52	---	---	---	---	---	---
Ba-140 Inhalation	---	---	---	0.03	0.03	0.66	0	0.02	0.39	0.01	0	1
CFRISK Thyroid	---	---	---	0.01	0.03	0.70	---	---	---	0.02	0	1
SC1141_2	---	---	---	0.03	0	0.77	---	---	---	0	0.15	0.06
Sr-90 Inhalation	---	---	---	0	0	1	0	0	1	---	---	---
Zr-95 Inhalation	---	---	---	---	---	---	0.02	0.12	0.03	---	---	---
I-133 Inhalation	---	---	---	---	---	---	0.02	0	0.52	---	---	---

Table 6.4-12 Conditional, mean, individual LCF risk (per event) regression of MACCS sensitivity USBGR model at the 50-mile circular area.

	Rank Regression			Quadratic			Recursive Partitioning			MARS		
Final R ²	0.55			0.86			0.64			0.81		
Input	R ² inc.	R ² cont.	SRRC	S _i	T _i	p-val	S _i	T _i	p-val	S _i	T _i	p-val
CFRISK Lung	0.10	0.10	0.29	0	0.36	0	0.02	0.12	0.09	0.05	0	1
PROTIN Normal	0.21	0.11	0.37	0	0.02	0.56	0.04	0	1	0	0.44	0.01
SRVLAM	0.33	0.12	-0.35	0.02	0.03	0.66	0	0	1	0.01	0	1
SRVOAFRAC	0.40	0.07	-0.25	0	0	1	0.06	0	1	0.02	0	1
BATTDUR	0.44	0.04	-0.11	---	---	---	0	0.18	0.01	0.06	0	1
Fuel failure criterion	---	---	---	0.02	0.08	0	0.02	0.08	0.24	---	---	---
SC1131_2	0.47	0.03	-0.14	---	---	---	---	---	---	0.02	0.14	0.24
Ce-141 Inhalation	0.48	0.01	0.22	---	---	---	---	---	---	---	---	---
Ba-140 Inhalation	0.49	0.01	0.12	0.01	0.03	0.62	---	---	---	0	0	1
Cs-137 Inhalation	0.50	0.01	-0.12	0.08	0.32	0	0.12	0.72	0	0.32	0.84	0
ESPEED	0.51	0.01	-0.08	---	---	---	---	---	---	0.02	0.06	0.42
Te-127m Inhalation	0.52	0.01	-0.11	---	---	---	0	0	0.41	0	0.16	0.14
CSFACT Evacuation	0.54	0.02	0.12	0.02	0.11	0.05	---	---	---	0	0.26	0.05
SLCRFRAC	0.56	0.02	-0.11	---	---	---	0.12	0.36	0	---	---	---
Sr-90 Inhalation	0.57	0.01	-0.08	---	---	---	0	0	1	---	---	---
Zr-95 Inhalation	0.58	0.01	0.12	---	---	---	---	---	---	---	---	---
DLTEVA Cohort 4	---	---	---	0	0.22	0	0	0.33	0	---	---	---
CFRISK Thyroid	---	---	---	0	0.17	0	---	---	---	0	0.21	0.07
Sr-92 Inhalation	---	---	---	0.03	0.12	0.03	0	0.01	0.61	0	0.43	0
DLTEVA Cohort 1	---	---	---	0.03	0.07	0.04	0.06	0.16	0.01	---	---	---
SC1141_2	---	---	---	0.01	0.09	0.07	---	---	---	0	0.28	0.01
Pu-239 Inhalation	---	---	---	0	0	1	---	---	---	---	---	---
I-133 Inhalation	---	---	---	---	---	---	0	0.16	0.02	---	---	---
TIMHOT	---	---	---	---	---	---	0	0.07	0.09	---	---	---

Since ingestion doses are taken to be negligible in SOARCA, inhalation is the only internal pathway that is treated. A significant portion of the exposures during the emergency phase are from inhalation. As explained above, these exposures are assumed to lead to doses over the commitment period, which is the next 50 years following the exposure. However, depending on the isotope inhaled, the doses received may diminish rapidly and become negligible for most of the dose commitment period.

Most of the exposures during the long-term phase are from groundshine, and a small fraction is from inhalation of resuspended aerosols. Since groundshine is an external pathway, doses received are concurrent with the exposure period, which is also taken to be 50 years in the SOARCA study. On the other hand, exposures from inhalation of resuspended material during each year of the long-term phase contribute to doses received over the subsequent 50-year commitment period.

Doses received in the first year thus correspond to:

- all of the dose from external exposure during the emergency phase,
- most of the dose from internal exposure during the emergency phase,
- all of the dose from external exposure during the first year of the long-term phase, and
- most of the dose from internal exposure during the first year of the long-term phase.

Doses received in the second and subsequent years correspond to:

- a fraction of the dose from internal exposure during all previous years plus most of the dose from internal exposure during that year, and
- all of the dose from external exposure during that year.

Following a single exposure, internal doses decrease more slowly from one year to the next when the isotopic half-life is relatively long (i.e., on the order of a year or longer) and the solubility of the dominant chemical form of the isotope is low so that the removal rate from the human body is low (i.e., the biological half-life is long). A good example is ^{90}Sr , for which the second-year effective dose from inhalation is 60% of the first-year dose. The isotopic half-life is 29 years, so most of the reduction from year one to year two results from the biological half-life. The internal doses decrease more rapidly from one year to the next when either the isotopic half life is short or when the solubility of the dominant chemical form of the isotope is high so that the human body tends to excrete it rapidly. A good example of this is ^{131}I , for which the second-year effective dose from inhalation is essentially zero. This isotope has a short isotopic half-life (i.e., 8 days) and a short biological half-life because of its high solubility. For comparison, the second-year effective dose from inhalation for ^{137}Cs is about 10% of the first-year dose, so it is intermediate between the previous examples.

Because the internal doses from inhalation diminish with time, most of the doses in the second and subsequent years are from the exposures during that year. But these doses are limited by the habitability criterion to be less than 500 mrem in any year. The 500 mrem limit is for all dose pathways, except ingestion, in this case groundshine and inhalation from resuspended aerosols. The inhalation dose used in this criterion is a committed dose (i.e., it accounts for doses received over the next 50 years). Because the annual doses allowed by the habitability criterion are less than the USBGR truncation level, nearly all of the risk is from doses received during the first year. These doses include most of emergency phase doses and a fraction of the long-term phase doses.

The MACCS lung lifetime risk factor for cancer death (CFRISK-Lung) input accounts for at least 0% of the variance with a T_i of 0.11 using the recursive partitioning regression analysis to at most 15% of the variance with a T_i of 0.49 using the MARS analysis at the five circular areas for all regression methods, and is one of the most important variables. As discussed in Section 4.2.5, the mortality risk coefficients (CFRISK) for each of the organs included in the SOARCA analyses for latent health effects are assumed to be uncorrelated.

The MACCS inhalation protection factor for normal activity (PROTIN–Normal) input accounts for at least 0% of the variance with a T_i of 0.02 using the quadratic regression analysis to at most 13% of the variance with a SRRC of 0.38 using the rank regression analysis at the five circular areas for all regression methods and is one of the most important input variable. As discussed in further detail in Section 4.2.3, protection factors are specified for each dose pathway and directly affect the doses received by individuals at each location. The protection factors are used as multipliers on the dose that a person would receive if there were no protection. In this context, normal activity refers to a combination of activities that are averaged over a week and over the population, including being indoors at home, commuting, being indoors at work, and being outdoors. These values are used in the uncertainty analysis making the further assumption that the distributions for normal activity and sheltering are correlated with a rank correlation coefficient of 0.75.

The MELCOR input variables (SRVLAM, SRVOAFRAC, and BATTDUR) account for at least 0% of the variance with a T_i of 0.02 using the MARS analysis to at most 30% of the variance with a T_i of 0.74 using the recursive partitioning regression analysis at the five circular areas for all regression methods. As discussed in Section 6.1.1 and Section 6.1.2, the MELCOR input variables SRVLAM, and SRVOAFRAC, account for the majority of the variance for iodine and cesium release. Fuel failure criterion, FL904A, and CHEMFORM do not consistently appear as variables of importance.

6.4.3.1.3 HPS Dose-Response Model

Tables 6.4-12 through 6.4-16 show the results of the regression analyses used to evaluate the sensitivity of the conditional, mean, individual LCF risk (per event) results for the MACCS sensitivity uncertainty analysis for the MELCOR Replicate 1 source terms using the HPS dose truncation model (i.e., MACCS uncertainty model CAP16) for the 10-mile, 20-mile, 30-mile, 40-mile, and 50-mile circular areas, respectively. For the HPS dose-response model, the regression analyses at the five circular areas consistently rank the MACCS lung lifetime risk factor for cancer death (CFRISK-Lung) and the inhalation protection factor for normal activity (PROTIN–Normal) and the MELCOR SRV stochastic failure probability (SRVLAM) as the most important input variables.

Additional variables also consistently show some level of importance at all circular areas. These additional input variables include the following:

- The MELCOR SRV open area fraction (SRVOAFRAC),
- The MELCOR DC station battery duration (BATTDUR), and
- The MELCOR fuel failure criterion

These six variables (CFRISK-Lung, PROTIN-Normal, SRVLAM, SRVOAFRAC, BATTDUR, and fuel failure criterion) account for at least 39% of the variance at the five circular areas for the rank regression analysis, at least 10% of the variance at the five circular areas for the quadratic regression analysis, at least 2% of the variance at the five circular areas for the recursive

partitioning analysis, and at least 21% of the variance at the five circular areas for the MARS analysis.

Other input parameters have a low importance at certain circular areas but not at other circular areas. Thus, the most important variables, PROTIN-Normal and CFRISK-Lung, appear at the top of the tables followed by the consistently important MELCOR variables (i.e., SRVLAM, SRVOAFRAC, BATTDUR, and fuel failure criterion), and finally those LCF risk parameters, dose conversion factors for inhalation, and MELCOR parameters (e.g., SC1131_2) not consistently ranked as important variables at the five circular areas.

Overall, the input variables of importance are the same as those for the USBGR dose truncation model. The explanations provided for USBGR dose truncation model MACCS also apply to the HPS dose truncation model.

The MACCS lung lifetime risk factor for cancer death (CFRISK-Lung) input accounts for at least 0% of the variance with a T_i of 0.04 using the recursive partitioning regression analysis to at most 12% of the variance with a SRRC of 0.34 using the rank regression analysis at the five circular areas for all regression methods, and is one of the most important variables. As discussed in Section 4.2.5, the mortality risk coefficients (CFRISK) for each of the organs included in the SOARCA analyses for latent health effects are assumed to be uncorrelated.

The MACCS inhalation protection factor for normal activity (PROTIN-Normal) parameter accounts for 0% of the variance with a T_i of 0.09 using the recursive partitioning regression analysis to at most 20% of the variance with a T_i of 0.82 using the MARS analysis at the five circular areas for all regression methods and is the most important input variable. As discussed in more detail in Section 4.2.3, protection factors are specified for each dose pathway and directly affect the doses received by individuals at each location. The protection factors are used as multipliers on the dose that a person would receive if there were no protection. In this context, normal activity refers to a combination of activities that are averaged over a week and over the population, including being indoors at home, commuting, being indoors at work, and being outdoors. These values are used in the uncertainty analysis making the further assumption that the distributions for normal activity and sheltering are correlated with a rank correlation coefficient of 0.75.

The MELCOR input variables (SRVLAM, SRVOAFRAC, BATTDUR, and fuel failure criterion) account for 0% of the variance with a T_i of 0.28 using the MARS analysis to at most 48% of the variance with a T_i of 1.0 using the MARS analysis at the five circular areas for all regression methods. As discussed in Section 6.1.1 and Section 6.1.2, the MELCOR input variables SRVLAM and SRVOAFRAC account for the majority of the variance for iodine and cesium release fractions. FL904A and CHEMFORM do not appear as variables of importance.

Table 6.4-13 Conditional, mean, individual LCF risk (per event) regression of MACCS sensitivity HPS model at the 10-mile circular area

	Rank Regression			Quadratic			Recursive Partitioning			MARS		
Final R ²	0.52			0.92			0.62			0.59		
Input	R ² inc.	R ² cont.	SRRC	S _i	T _i	p-val	S _i	T _i	p-val	S _i	T _i	p-val
CFRISK Lung	0.12	0.12	0.31	0.04	0.33	0	0	0.09	0.04	0.06	0.32	0.04
PROTIN Normal	0.25	0.13	0.39	0.03	0.08	0.22	0.02	0	1	0.04	0	1
SRVLAM	0.37	0.12	-0.30	---	---	---	0.06	0.53	0	0.02	0.25	0.03
BATTDUR	0.41	0.04	-0.14	---	---	---	0.01	0	1	0	0.15	0.09
SRVOAFRAC	0.44	0.03	-0.16	0.04	0	1	0.23	0.73	0	0.28	0.73	0
Fuel failure criterion	0.44	0	0.06	0	0	1	---	---	---	---	---	---
Te-127m Inhalation	0.47	0.03	0.14	0.02	0.21	0.04	---	---	---	0.01	0	1
Ce-141 Inhalation	0.49	0.02	0.11	0.02	0	1	---	---	---	---	---	---
SC1131_2	0.50	0.01	0.08	---	---	---	---	---	---	0	0	1
Sr-92 Inhalation	0.51	0.01	0.08	0.01	0.32	0.01	0.04	0.18	0.02	0.03	0	1
ESPEED	0.52	0.01	-0.10	---	---	---	---	---	---	0.01	0	1
Cs-137 Inhalation	0.53	0.01	-0.10	0.07	0	1	0	0	1	0.04	0	1
Ba-140 Inhalation	0.54	0.01	-0.09	---	---	---	0	0.07	0.05	---	---	---
RHONOM	0.55	0.01	0.08	0	0.05	0.53	---	---	---	---	---	---
SLCRFRAC	0.56	0.01	-0.12	0	0.34	0.18	---	---	---	---	---	---
Pw-239 Inhalation	---	---	---	0.01	0.22	0.03	---	---	---	---	---	---
DLTEVA Cohort 3	---	---	---	0.02	0.16	0.03	0.05	0.01	0.67	---	---	---
CFRISK Thyroid	---	---	---	0.01	0	1	0	0.26	0.02	0	0.16	0.02
CSFACT Evacuation	---	---	---	0	0	1	---	---	---	0	0.25	0.02
VDEPOS	---	---	---	---	---	---	0	0.15	0	0	0	1
SC1141_2	---	---	---	---	---	---	---	---	---	0.01	0.19	0.01

Table 6.4-14 Conditional, mean, individual LCF risk (per event) regression of MACCS sensitivity HPS model at the 20-mile circular area

	Rank Regression			Quadratic			Recursive Partitioning			MARS		
Final R ²	0.55			0.80			0.67			0.69		
Input	R ² inc.	R ² cont.	SRRC	S _i	T _i	p-val	S _i	T _i	p-val	S _i	T _i	p-val
PROTIN Normal	0.08	0.08	0.25	0.07	0.43	0	0.04	0.02	0.56	0.13	0.31	0.04
CFRISK Lung	0.18	0.10	0.36	0.01	0	1	0.06	0.06	0.19	0	0.27	0
SRVOAFRAC	0.30	0.12	-0.31	---	---	---	0.02	0.23	0.04	0.04	0.21	0
SRVLAM	0.40	0.10	-0.30	0.01	0.01	0.51	---	---	---	0.02	0	1
BATTDUR	0.41	0.01	0.10	0.01	0.12	0	0	0.18	0.01	0.04	0	1
Fuel failure criterion	0.41	0	0.07	---	---	---	---	---	---	---	---	---
Ba-140 Inhalation	0.45	0.04	-0.16	0.04	0.05	0.38	0.02	0.10	0.20	---	---	---
Sr-92 Inhalation	0.48	0.03	-0.15	0.05	0	1	0	0.21	0	0.02	0.13	0.06
CFRISK Thyroid	0.50	0.02	0.10	---	---	---	---	---	---	0	0.14	0.01
RHONOM	0.52	0.02	0.12	0.04	0.07	0.49	---	---	---	---	---	---
SC1141_2	0.53	0.01	-0.10	0.01	0	1	---	---	---	0.03	0	1
SC1131_2	0.54	0.01	-0.12	0.11	0.32	0	0.83	0.78	0	0.32	0.79	0
VDEPOS	0.56	0.02	0.10	0	0.15	0	0	0	1	0.01	0.12	0.12
Pu-239 Inhalation	0.57	0.01	0.11	0.02	0	1	---	---	---	---	---	---
Sr-90 Inhalation	0.57	0	-0.06	0.01	0.08	0.07	0.05	0.03	0.45	---	---	---
ESPEED	---	---	---	0	0.20	0	---	---	---	0	0	1
Cs-137 Inhalation	---	---	---	0.01	0.04	0.29	0	0.10	0.07	0.01	0.22	0.01
SLCRFRAC	---	---	---	0	0.05	0.48	---	---	---	---	---	---
Ce-141 Inhalation	---	---	---	---	---	---	0.04	0	1	---	---	---
DLTEVA Cohort 4	---	---	---	---	---	---	0	0	1	---	---	---
Te-127m Inhalation	---	---	---	---	---	---	0.05	0	1	0.02	0	1
CSFACT Evacuation	---	---	---	---	---	---	---	---	---	0	0.19	0.02

Table 6.4-15 Conditional, mean, individual LCF risk (per event) regression of MACCS sensitivity HPS model at the 30-mile circular area

	Rank Regression			Quadratic			Recursive Partitioning			MARS		
Final R ²	0.56			0.82			0.70			0.76		
Input	R ² inc.	R ² cont.	SRRC	S _i	T _i	p-val	S _i	T _i	p-val	S _i	T _i	p-val
PROTIN Normal	0.07	0.07	0.23	0.04	0.21	0	0.02	0.22	0.02	0.20	0.82	0
CFRISK Lung	0.19	0.12	0.34	0	0.10	0	0	0.04	0.24	0.01	0.25	0.03
SRVLAM	0.28	0.09	-0.31	0.05	0.11	0.01	---	---	---	0	0.08	0.47
SRVOAFRAC	0.39	0.11	-0.31	---	---	---	0.01	0	1	0	0	1
Fuel failure criterion	0.40	0.01	0.12	---	---	---	---	---	---	---	---	---
BATTDUR	---	---	---	0.02	0.01	0.83	---	---	---	0	0.28	0.01
Ba-140 Inhalation	0.42	0.02	0.11	0.09	0.20	0	0.13	0.16	0.49	---	---	---
Sr-92 Inhalation	0.43	0.01	-0.12	0.12	0.26	0	0.28	0.64	0	0.05	0.49	0.01
RHONOM	0.47	0.04	-0.15	---	---	---	---	---	---	---	---	---
SC1131_2	0.50	0.03	-0.17	---	---	---	0.01	0.01	0.25	0	0	1
CFRISK Thyroid	0.52	0.02	0.10	0	0.12	0.02	0	0.04	0.14	0.02	0	1
SC1141_2	0.53	0.01	-0.09	---	---	---	---	---	---	0.03	0	1
ESPEED	0.54	0.01	0.10	---	---	---	0.02	0.16	0	0.03	0	1
Ce-141 Inhalation	0.56	0.02	0.10	0.02	0.18	0	0	0	1	---	---	---
SLCRFRAC	0.56	0	-0.06	0.05	0	1	0.01	0.41	0	---	---	---
CSFACT Evacuation	---	---	---	0.01	0.14	0	0	0	1	0	0.16	0.04
Cs-137 Inhalation	---	---	---	0	0.10	0.01	---	---	---	0.01	0.33	0
DLTEVA Cohort 3	---	---	---	0	0.05	0.48	---	---	---	---	---	---
Sr-90 Inhalation	---	---	---	0	0	1	---	---	---	---	---	---
DLTEVA Cohort 4	---	---	---	---	---	---	0	0.12	0.01	---	---	---
VDEPOS	---	---	---	---	---	---	0	0.04	0.65	0	0.31	0
DLTEVA Cohort 1	---	---	---	---	---	---	0	0	1	---	---	---
Te-127m Inhalation	---	---	---	---	---	---	---	---	---	0	0	1

Table 6.4-16 Conditional, mean, individual LCF risk (per event) regression of MACCS sensitivity HPS model at the 40-mile circular area

	Rank Regression			Quadratic			Recursive Partitioning			MARS		
Final R ²	0.56			0.80			0.70			0.85		
Input	R ² inc.	R ² cont.	SRRC	S _i	T _i	p-val	S _i	T _i	p-val	S _i	T _i	p-val
PROTIN Normal	0.10	0.10	-0.33	0.04	0.05	0.45	---	---	---	0	0.23	0.11
CFRISK Lung	0.22	0.12	0.33	0	0	1	0	0.10	0.01	0	0	1
SRVOAFRAC	0.33	0.11	-0.32	---	---	---	0.02	0	1	0	0	1
SRVLAM	0.39	0.06	0.22	0.06	0.27	0	0.01	0.12	0.15	0.21	1	0
Fuel failure criterion	---	---	---	0	0.09	0	---	---	---	---	---	---
BATTDUR	---	---	---	0.01	0.07	0.17	---	---	---	0	0.42	0
Ba-140 Inhalation	0.41	0.02	0.12	0.03	0.22	0	0.20	0.26	0.13	---	---	---
Sr-92 Inhalation	0.42	0.01	-0.11	0.07	0.18	0	0.28	0.62	0	0	0.39	0.02
Sr-90 Inhalation	0.46	0.04	-0.17	0.01	0	0.67	---	---	---	---	---	---
SC1131_2	0.49	0.03	-0.19	---	---	---	0.01	0.02	0.28	0	0	1
CFRISK Thyroid	0.51	0.02	0.12	0.01	0.11	0	---	---	---	0	0.32	0.03
SC1141_2	0.52	0.01	-0.10	---	---	---	---	---	---	0	0.38	0.03
ESPEED	0.53	0.01	0.10	0.03	0	1	0.03	0.13	0.02	0	0.19	0.18
Ce-141 Inhalation	0.55	0.02	0.10	0	0.22	0	0	0	1	---	---	---
Pu-239 Inhalation	0.56	0.01	0.11	---	---	---	---	---	---	---	---	---
Cs-137 Inhalation	0.57	0.01	-0.08	0	0.06	0.19	0	0	1	0	0.54	0
RHONOM	---	---	---	0.03	0.08	0.13	---	---	---	---	---	---
SLCRFRAC	---	---	---	---	---	---	0.02	0.47	0	---	---	---
VDEPOS	---	---	---	---	---	---	0.02	0.17	0.01	0	0	1
DLTEVA Cohort 4	---	---	---	---	---	---	0	0	0.40	---	---	---
DLTEVA Cohort 3	---	---	---	---	---	---	0.03	0	1	---	---	---
Te-127m Inhalation	---	---	---	---	---	---	---	---	---	0	0	1
CSFACT Evacuation	---	---	---	---	---	---	---	---	---	0.37	0	1

Table 6.4-17 Conditional, mean, individual LCF risk (per event) regression of MACCS sensitivity HPS model at the 50-mile circular area

	Rank Regression			Quadratic			Recursive Partitioning			MARS		
Final R ²	0.56			0.82			0.70			0.86		
Input	R ² inc.	R ² cont.	SRRC	S _i	T _i	p-val	S _i	T _i	p-val	S _i	T _i	p-val
PROTIN Normal	0.10	0.10	-0.33	0.05	0	1	---	---	---	0	0.68	0
CFRISK Lung	0.22	0.12	0.33	0	0.08	0.02	---	---	---	0	0	1
SRVOAFRAC	0.34	0.12	-0.32	---	---	---	0.02	0	1	0	0.20	0.13
SRVLAM	0.40	0.06	0.21	0.09	0.33	0	0	0.10	0.07	0.48	1	0
Fuel failure criterion	0.40	0	0.08	0.04	0.07	0.03	---	---	---	---	---	---
BATTDUR	---	---	---	0	0.13	0.02	---	---	---	0	0.05	0.46
Sr-90 Inhalation	0.44	0.04	-0.16	---	---	---	0.03	0.08	0.1	---	---	---
SC1131_2	0.48	0.04	-0.20	---	---	---	0	0.01	0.32	0	0	1
CFRISK Thyroid	0.50	0.02	0.11	0	0.06	0.13	---	---	---	0	0.40	0
Ba-140 Inhalation	0.53	0.03	0.23	0.07	0.23	0	---	---	---	---	---	---
Te-127m Inhalation	0.55	0.02	-0.10	---	---	---	0.02	0.17	0.01	0	0	1
ESPEED	0.56	0.01	0.10	0	0	1	0	0	1	0	0.27	0.12
Sr-92 Inhalation	0.57	0.01	-0.11	0.06	0.21	0.01	0.05	0.60	0	0.06	0.78	0
Cs-137 Inhalation	0.59	0.02	-0.09	---	---	---	0.03	0.15	0	0	0.17	0.27
Pu-239 Inhalation	0.60	0.01	0.12	---	---	---	---	---	---	---	---	---
RHONOM	---	---	---	0	0.16	0	0.14	0.19	0.31	---	---	---
SC1141_2	---	---	---	0	0.15	0	0.03	0	1	0	0	1
DLTEVA Cohort 3	---	---	---	0.02	0.06	0.23	---	---	---	---	---	---
Ce-141 Inhalation	---	---	---	0	0.06	0.33	0.02	0	1	---	---	---
DLTEVA Cohort 1	---	---	---	0.01	0	1	---	---	---	---	---	---
SLCRFRAC	---	---	---	---	---	---	0.02	0.40	0	---	---	---
DLTEVA Cohort 3	---	---	---	---	---	---	0	0.12	0.01	---	---	---
VDEPOS	---	---	---	---	---	---	0	0.12	0.2	0	0.36	0
DLTEVA Cohort 4	---	---	---	---	---	---	0	0	1	---	---	---
CSFACT Evacuation	---	---	---	---	---	---	---	---	---	0	0	1

6.4.4 Habitability Criterion

Habitability is the consequence model parameter that is used to establish the dose level at which residents are allowed to return to their homes. Habitability applies to everyone, not just evacuees. During plume passage, hotspot and normal relocation criteria are applied to determine whether residents remain in their homes or not. After the emergency phase, the habitability criterion is applied to determine which residents can return home and which cannot. Site specific criterion are used to define the long-term habitability criterion; most states adhere to the EPA PAGs, which specify a dose of 2 rem in the first year and 500 mrem per year thereafter. This recommendation [63] has traditionally (e.g., NUREG-1150) been implemented as a cumulative 4 rem over the first five years (2 rem in the first year + 4 years x 0.5 rem/year) of exposure [16]. However, the State of Pennsylvania has a more restricted guideline of 0.5 rem/yr beginning in the first year. This criterion is expected to influence the consequence results because the long-term doses that residents receive typically exceed the emergency phase doses, as demonstrated in the SOARCA study. Because the definition of habitability is determined by the State of Pennsylvania, it was not considered to be uncertain in the uncertainty analysis.

Evacuees may not return and other residents are potentially relocated according to the hotspot or normal relocation parameters. The evacuees and relocated residents receive no additional emergency phase doses after they are modeled as moving out of the evacuation zone. MACCS implements user-defined habitability criterion to determine when residents may move back to their residence during the long-term phase. Any additional dose to these residents is calculated as long-term phase dose.

Habitability decision making in MACCS can result in four possible outcomes:

- (1). land is immediately habitable,
- (2). land is habitable immediately after decontamination,
- (3). land is habitable after decontamination followed by an additional period of interdiction, and
- (4). land is condemned and therefore not habitable for the entire calculation.

For the purpose of determining the habitability, dose is the sum of the doses from the groundshine and resuspension pathways. The user-specified value of DSCRLT is used to determine whether land is considered suitable for habitation during the long-term phase. This value is the maximum allowable direct exposure dose commitment to the critical organ during the long-term phase action period. If this dose criterion is exceeded in any spatial element during the long term action period, mitigative actions such as decontamination or decontamination followed by temporary interdiction are employed to limit the dose to the critical organ so that the allowable dose level is not exceeded in that spatial grid element. Usually, an effective dose is used to evaluate habitability. If the property cannot be made habitable within 30 years or if the cost of restoring habitability is greater than the cost of condemning it, the property is condemned and permanently withdrawn from use.

Five habitability sensitivity analyses were performed for each of the three dose-response models (i.e., LNT, USBGR, and HPS). For the Peach Bottom unmitigated LTSBO scenario, the conditional, mean, individual LCF risk (per event) (NUREG/CR-7110 Volume 1, Table 7-2) is compared for each of the variations considered. All the sensitivity analyses use the SOARCA uncertainty analysis base case MELCOR source term described in Appendix C.

All results are presented in conditional risk to a member of the public. The conditional risks assume that the accident occurs and indicate the risks to individuals as a result of the accident (e.g., latent cancer fatality (LCF) risk per event). The risk metrics used in this sensitivity study are conditional, mean, individual LCF risk (per event). There were no early-fatality risks observed in these analyses.

6.4.4.1 Habitability Sensitivity Inputs

The five habitability sensitivity simulations were based on the current State of Pennsylvania public radiation standard, EPA guidelines, NUREG-1150, and ICRP recommendations. The discussion below provides background information on the justification of the sensitivity cases analyzed.

SOARCA Estimate for Habitability: 0.5 rem/yr

Most states adhere to the EPA guidelines for habitability which specify a dose of 2 rem in the first year and 0.5 rem per year thereafter. However, the State of Pennsylvania guidance is for a stricter habitability criterion of 0.5 rem per year beginning in the first year, and this value was used in the NUREG/CR-7110 Volume 1 MACCS analyses [2].

EPA Habitability Criterion Interoperation: 5 rem over 7 years = 2 rem/yr (1st year) 0.5 rem/yr (2nd through 7th year)

The habitability criterion currently used by the EPA is 0.05 Sv (5 rem) over a 50 year period. For this implementation of the habitability criterion, the EPA recommendation is interpreted as a limit of 5 rem over 7 years (i.e., 2 rem in the first year + 6 years at 0.5 rem per year).

Based on EPA-400-R-92-001 [51] the following determines the EPA guidance habitability criterion:

From Section 4.2:

“PAGs for protection from deposited radioactivity during the intermediate phase are summarized in Table 4-1. The basis for these values is presented in detail in Appendix E. In summary, relocation is warranted when the projected sum of the dose equivalent from external gamma radiation and the committed effective dose equivalent from inhalation of resuspended radionuclides exceeds 2 rem in the first year. Relocation to avoid exposure of the skin to beta radiation is warranted at 50 times the numerical value of the relocation PAGs for effective dose equivalent.

From Section 4.2.1:

“It is an objective of these PAGs to assure that 1) doses in any single year after the first will not exceed 0.5 rem, and 2) the cumulative dose over 50 years (including the first and second years) will not exceed 5 rem. For the source terms from reactor incidents, the above PAGs of 2 rem projected dose in the first year is expected to meet both of these objectives through radioactive decay, weathering, and normal part time occupancy in structures.

NUREG-1150: 4 rem over 5 years = 2 rem/yr (1st year) 0.5 rem/yr (2nd through 5th year)

The habitability criterion used in NUREG-1150 was 0.04 Sv (4 rem) over a 5 year period [16]. The NUREG-1150 habitability criterion is the same as the value used for the Surry MACCS analyses in NUREG/CR-7110 Volume 2. NUREG-1150 was based on a draft EPA document [63] and has traditionally been implemented in MACCS¹⁶ as a cumulative 4 rem over the first 5 years (i.e., 2 rem in the first year + 4 years at 0.5 rem per year) of exposure.

ICRP: 0.1 rem/yr and 2 rem/yr

These two habitability criteria are consistent with ICRP 103 [64] and ICRP 111 [65] guidance. These reports serve as a guide for the protection of individuals living in contaminated areas for the long term after a nuclear accident or other situations involving dangerous levels of radiation. ICRP 103 suggests that appropriate reference levels should preferably be chosen in the 1-20 mSv (0.1–2 rem) band. As part of this sensitivity study, a lower bound of 0.1 rem per year and an upper bound of 2 rem per year were selected.

6.4.4.2 Habitability Sensitivity Results – LNT Dose-Response Model

A series of sensitivity analyses using the five habitability criteria was conducted for the LNT dose-response model. All the sensitivity simulations use the SOARCA uncertainty analysis base case source term described in Appendix C. As an additional comparison, the Peach Bottom unmitigated LTSBO scenario conditional, mean, individual LCF risk (per event) results from the SOARCA study (NUREG/CR-7110 Volume 1, Table 7-2) are also presented. All MACCS variables other than the habitability parameters remained fixed. Table 6.4-18 provides the results of the conditional, mean, individual LCF risk (per event) for specified circular areas and habitability parameters. As shown on Figure 6.4-4 and Table 6.4-18, a lower habitability limit results in a lower LCF risk, and a higher habitability limit results in a higher LCF risk. Table 6.4-19 shows the percent difference between the habitability sensitivities compared to the SOARCA uncertainty analysis base case with 0.5 rem/yr habitability at specified circular areas.

For this work, the emergency phase is defined as the first seven days following the initial release to the environment. The long-term phase is defined as a 50-year period immediately following the emergency phase (i.e., there is no intermediate phase). Figure 6.4-5 through Figure 6.4-9 show the emergency phase (red) and the long-term phase (blue) contributions to conditional, mean, individual LCF risk (per event) for each habitability criterion and at each specified circular area.

As shown on Figure 6.4-5, the majority of the LCF risk contribution within the EPZ results from the long-term phase for all of the habitability choices investigated. Thus the higher the habitability dose limit, the higher the LCF risk as a result of long-term dose within the EPZ. Figure 6.4-6 shows the majority of the LCF risk within 20 miles for the 0.1 rem/yr habitability criterion is from the emergency phase. While the emergency phase LCF risk for the 0.1 rem/yr habitability criterion is the same as the risk for all the habitability criteria, the low threshold reduces long-term LCF risk. All other habitability criteria have the majority of their respective

¹⁶ Note that in the MACCS implementation of 4 rem over 5 years, incurring a dose greater than 2 rem in the first year is possible as long as 4 rem is not exceeded in 5 years. Hence as reported in the sensitivity results, a habitability criterion of 2 rem/yr is actually more restrictive than 4 rem over 5 years in the MACCS implementation.

LCF risk from the long-term phase. The 30-mile, 40-mile, and 50-mile circular area results are similar in trend to the 20-mile circular area results shown on Figure 6.4-6.

Table 6.4-18 Habitability criterion comparison of conditional, mean, individual LCF risk (per event) for LNT dose-response model

Radius (mi)	SOARCA Estimate*	SOARCA Uncertainty Analysis Base Case Source Term				
		0.5 rem/yr*	0.1 rem/yr	2 rem/yr	4 rem/5 yrs	5 rem/7yrs
10	8.9×10^{-5}	9.0×10^{-5}	3.7×10^{-5}	1.6×10^{-4}	1.7×10^{-4}	1.8×10^{-4}
20	7.6×10^{-5}	8.3×10^{-5}	5.9×10^{-5}	1.1×10^{-4}	1.2×10^{-4}	1.2×10^{-4}
30	5.3×10^{-5}	5.8×10^{-5}	4.2×10^{-5}	7.4×10^{-5}	7.7×10^{-5}	7.8×10^{-5}
40	3.3×10^{-5}	3.7×10^{-5}	2.8×10^{-5}	4.6×10^{-5}	4.7×10^{-5}	4.8×10^{-5}
50	2.7×10^{-5}	3.0×10^{-5}	2.3×10^{-5}	3.7×10^{-5}	3.8×10^{-5}	3.9×10^{-5}

* The differences between the SOARCA estimate and the SOARCA uncertainty analysis base case with a habitability criterion of 0.5 rem/yr are discussed in Appendix C

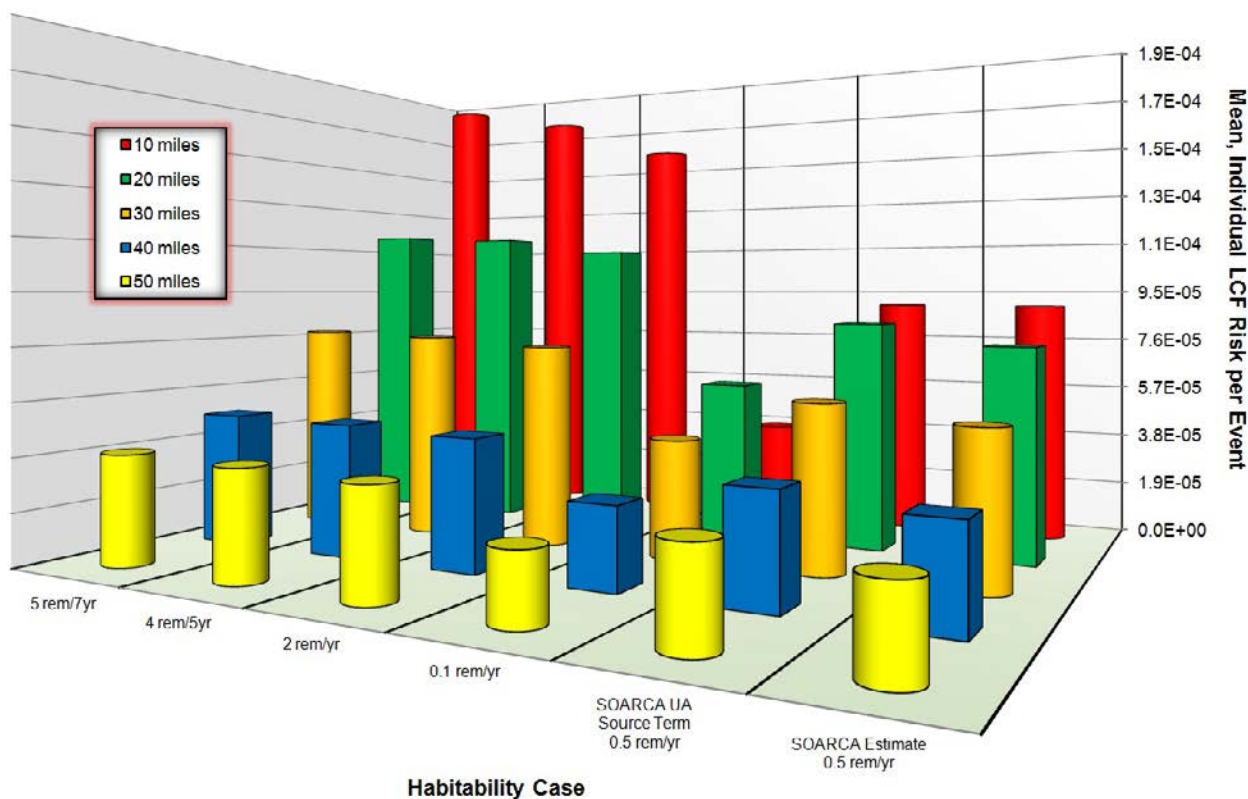


Figure 6.4-4 Habitability criterion comparison of conditional, mean, individual LCF risk (per event) for specified circular areas for the LNT dose-response model

Table 6.4-19 Percentage change in conditional, mean, individual LCF risk (per event) for the LNT dose-response model from variations in habitability criterion (reduction/increase (-/+))

Radius (mi)	SOARCA UA Base Case 0.5 rem/yr	0.1 rem/yr	2 rem/yr	4 rem/5yrs	5 rem/7yrs
10	0.0%	-59%	75%	93%	103%
20	0.0%	-30%	34%	41%	43%
30	0.0%	-27%	28%	33%	35%
40	0.0%	-25%	23%	27%	29%
50	0.0%	-25%	21%	25%	28%

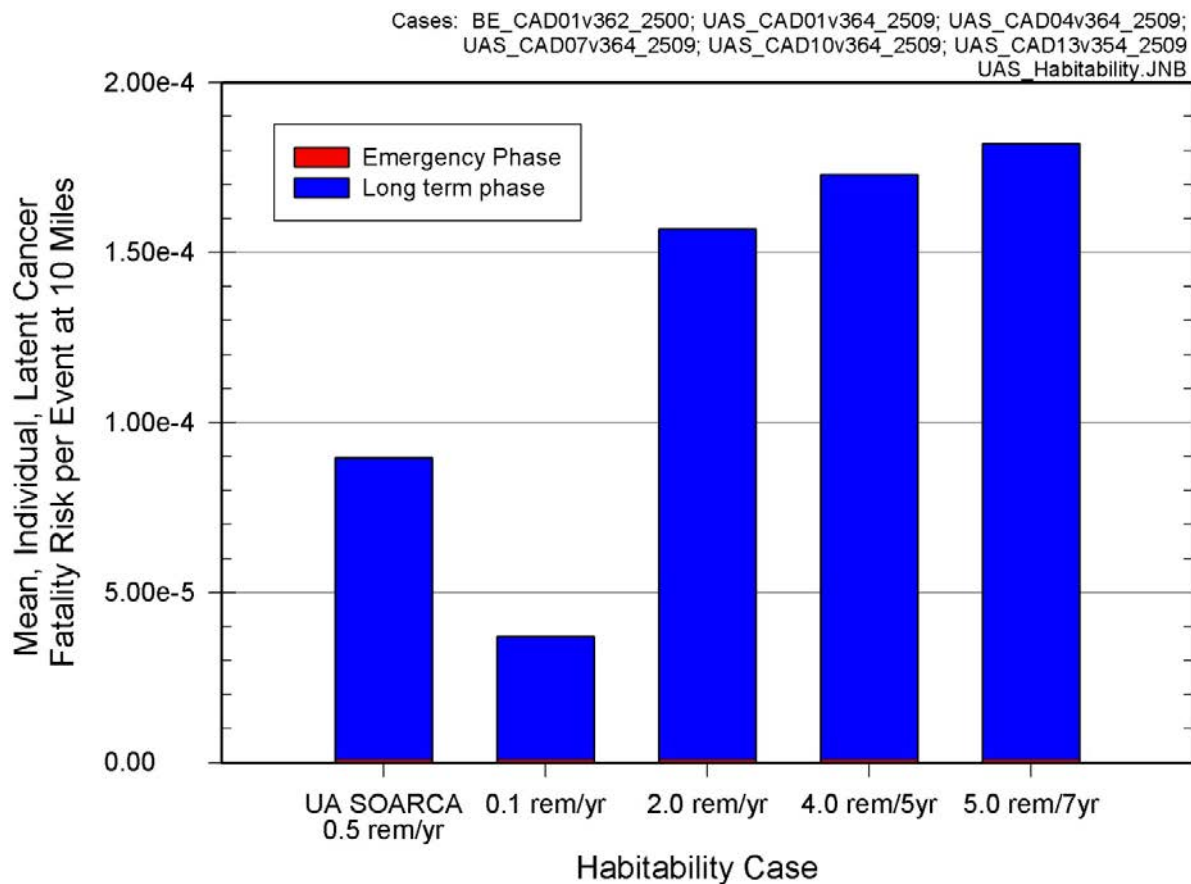


Figure 6.4-5 Habitability criterion comparison of conditional, mean, individual LCF risk (per event) for the 10-mile circular area for the LNT dose-response model

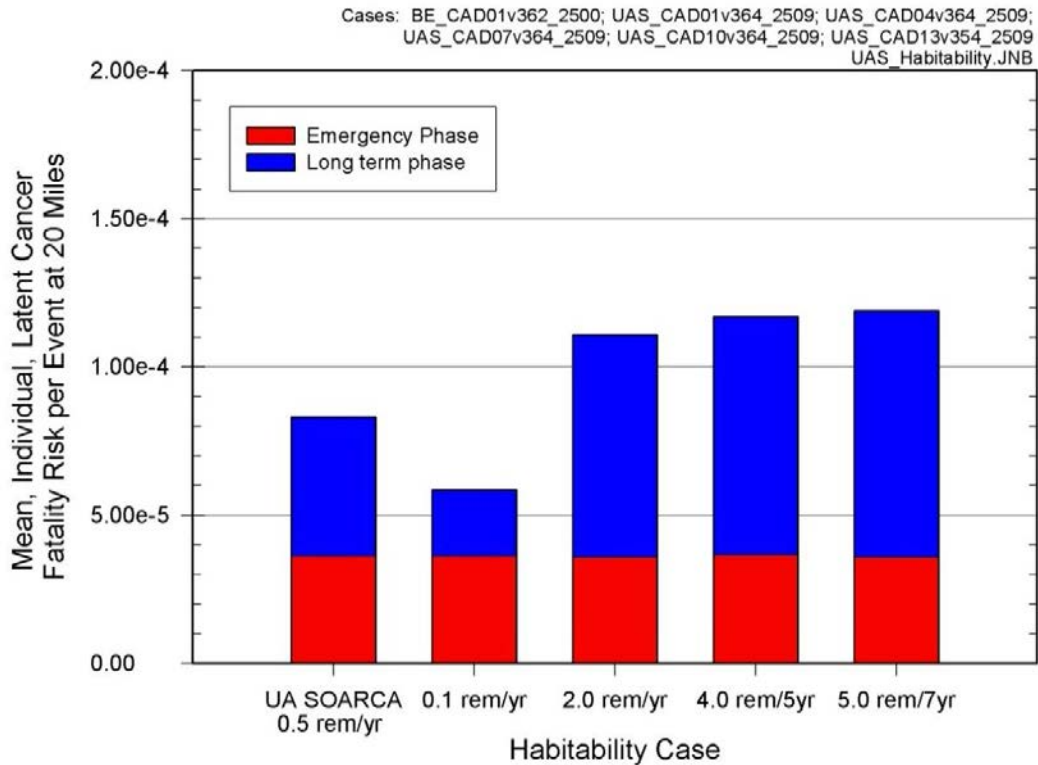


Figure 6.4-6 Habitability criterion comparison of conditional, mean, individual LCF risk (per event) for the 20-mile circular area for the LNT dose-response model

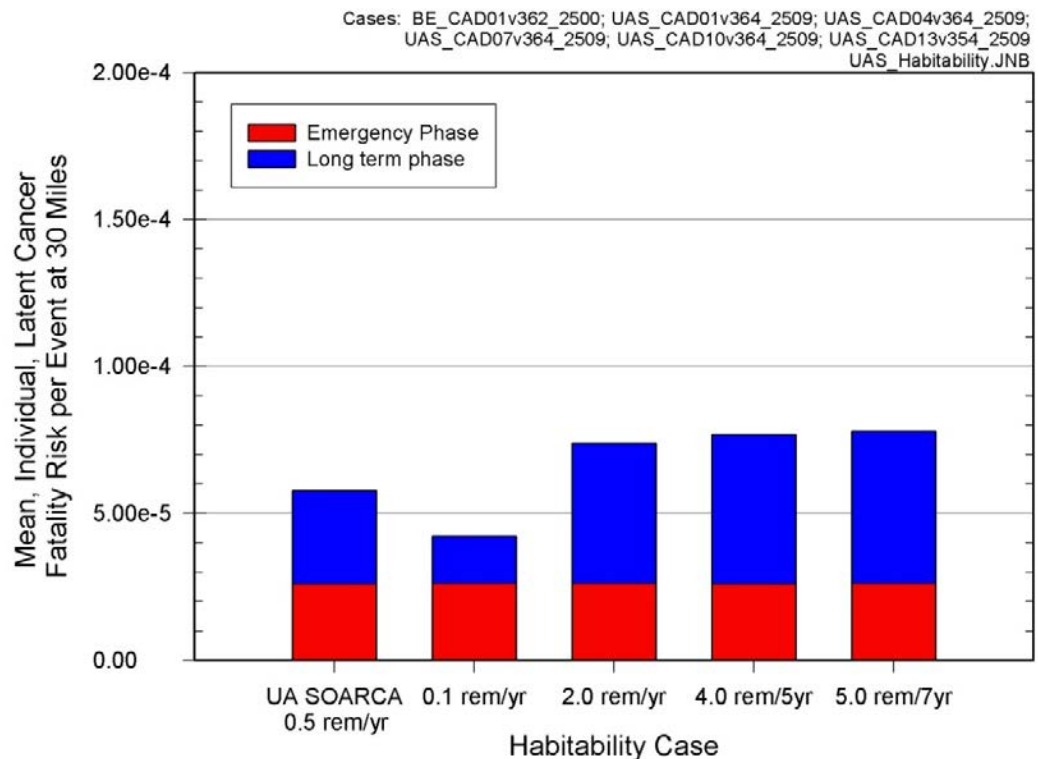


Figure 6.4-7 Habitability criterion comparison of conditional, mean, individual LCF risk (per event) for the 30-mile circular area for the LNT dose-response model

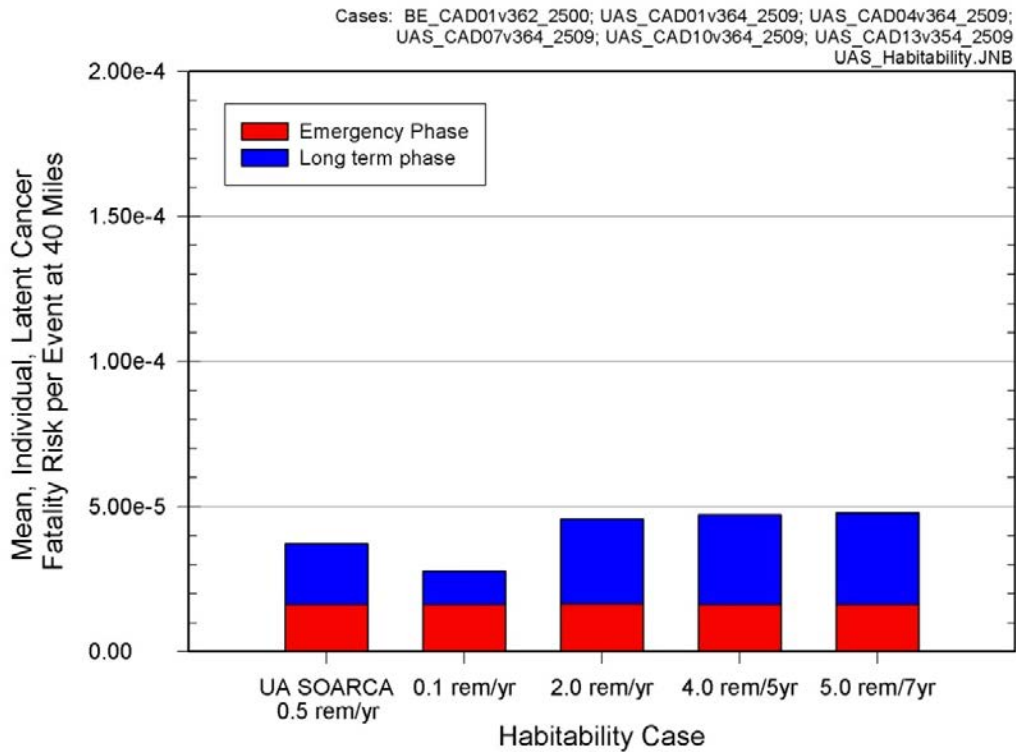


Figure 6.4-8 Habitability criterion comparison of conditional, mean, individual LCF risk (per event) for the 40-mile circular area for the LNT dose-response model

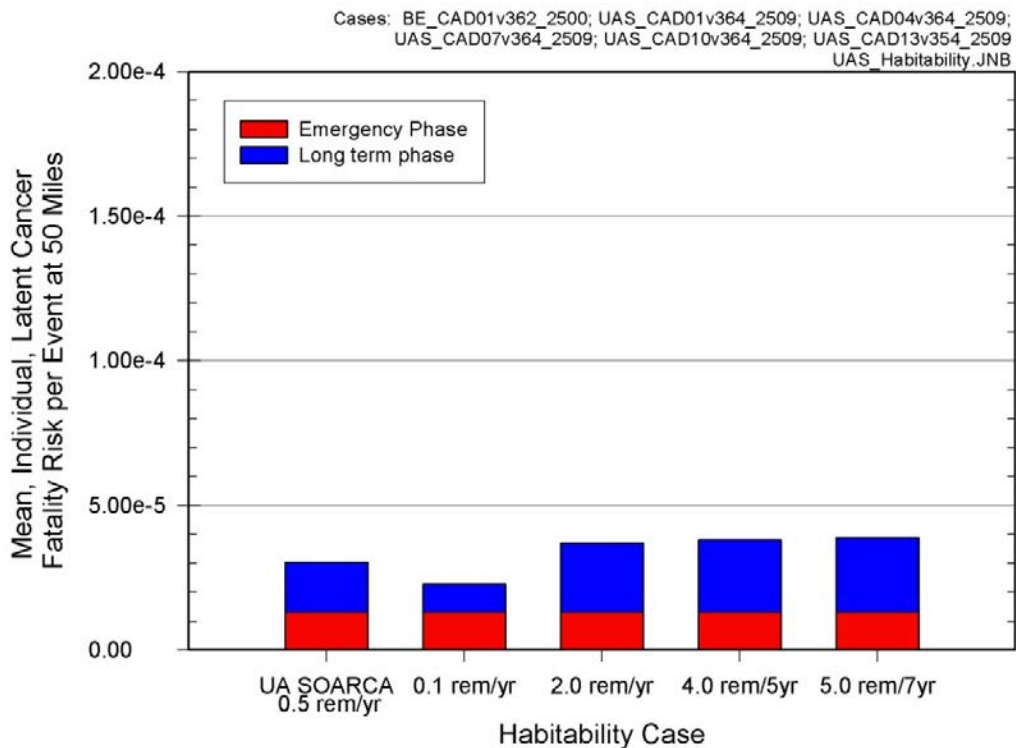


Figure 6.4-9 Habitability criterion comparison of conditional, mean, individual LCF risk (per event) for the 50-mile circular area for the LNT dose-response model

6.4.4.3 Habitability Sensitivity Results – Additional Dose-Response Models

A series of sensitivity analyses using the five habitability criteria were conducted for the USBGR and HPS dose-response models. All the sensitivity simulations use the SOARCA uncertainty analysis base case source term described in Appendix C. As an additional comparison, the Peach Bottom unmitigated LTSBO scenario, conditional, mean, individual LCF risk (per event) results from the SOARCA study (NUREG/CR-7110 Volume 1, Table 7-2) are also presented. All other MACCS variables other than the habitability parameters remained fixed. Table 6.4-20 provides the results of the conditional, mean, individual LCF risk (per event) at specified circular areas for the USBGR dose-response model and habitability parameters. As shown in Table 6.4-20 within the EPZ, when the dose rate for the habitability criterion is below the dose truncation level (0.62 rem/yr), LCF risks are two orders of magnitude lower than when the dose rate for the habitability criterion is above the dose truncation level. Table 6.4-21 shows the percent difference between each of the habitability criteria as compared with the SOARCA uncertainty analysis base case, which uses a 0.5 rem/yr habitability criterion. The percent differences are similar to those in Table 6.4-19 for the LNT dose-response model for distances beyond the EPZ.

Figures 6.4-10 through 6.4-14 show the LCF risk contribution for each habitability criterion at each specified circular area. Since there is no simple way to separate the LCF risks from the emergency phase and long-term phase, Figures 6.4-10 through 6.4-14 only show the total risk of both phases.

To better understand this inability to discern the LCF risk between the emergency and long-term phases, a discussion on the dose-response models is needed. The long-term phase risk dominates the total risk for the accident scenario when the LNT dose-response assumption is made. These long-term risks are controlled by the habitability (return) criterion, which is the dose rate at which residents are allowed to return to their homes following the emergency phase. For example, the Peach Bottom habitability criterion is a dose rate of 500 mrem/yr. This dose rate is below the truncation levels based on USBGR (620 mrem/yr) and based on the HPS position statement (5 rem/yr with 10 rem lifetime); therefore, most of the doses received during the long-term phase are below the dose truncation limit and are not counted toward health effects when using these criteria. Thus, most of the risks associated with either of the truncation levels are from doses received during the first year. The conditional, mean, individual LCF risk (per event) for these dose truncation models do not show separate risks for the emergency and long-term phases because those phases overlap, especially in the first year, and are not easily separated for purposes of evaluating the annual dose threshold.

Because the internal doses from inhalation diminish with time, most of the doses in the second and subsequent years are from the exposures during that year. But these doses are limited by the habitability criterion in any year. The habitability criterion limit is for all dose pathways, in this case groundshine and inhalation from resuspended aerosols. The inhalation dose used in this criterion is a committed dose (i.e., it accounts for doses received over the next 50 years). Because the annual doses allowed by the habitability criterion could be less than truncation levels based on USBGR and the HPS position statement, nearly all of the risk is from doses received during the first year. These doses include most of emergency phase doses and a fraction of the long-term phase doses. This explains the risk profiles for these dose-truncation criteria.

Figure 6.4-11 shows that the habitability sensitivities have little effect on the overall LCF risk when the USBGR dose-response model is applied beyond the EPZ. The risks are similar to those presented in the SOARCA study. The 30-mile, 40-mile, and 50-mile results are similar in trend to the 20-mile results shown on Figure 6.4-11.

Table 6.4-20 Habitability criterion comparison of conditional, mean, individual LCF risk (per event) for USBGR dose-response model

Radius (mi)	SOARCA Estimate*	SOARCA Uncertainty Analysis Base Case Source Term				
		0.5 rem/yr*	0.1 rem/yr	2 rem/yr	4 rem/5yrs	5 rem/7yrs
10	7.4×10^{-7}	8.9×10^{-7}	8.2×10^{-7}	2.5×10^{-5}	3.3×10^{-5}	3.8×10^{-5}
20	1.9×10^{-5}	2.6×10^{-5}	2.0×10^{-5}	3.9×10^{-5}	4.2×10^{-5}	4.3×10^{-5}
30	1.1×10^{-5}	1.6×10^{-5}	1.1×10^{-5}	2.3×10^{-5}	2.5×10^{-5}	2.5×10^{-5}
40	5.0×10^{-6}	7.7×10^{-6}	4.8×10^{-6}	1.2×10^{-5}	1.3×10^{-5}	1.3×10^{-5}
50	3.4×10^{-6}	5.2×10^{-6}	3.2×10^{-6}	8.7×10^{-6}	9.4×10^{-6}	9.7×10^{-6}

* The differences between the SOARCA estimate and the SOARCA uncertainty analysis base case with a habitability criterion of 0.5 rem/yr are discussed in Appendix C

Table 6.4-21 Percentage change in conditional, mean, individual LCF risk (per event) for the USBGR dose-response model from variations in habitability criterion (reduction/increase (-/+))

Radius (mi)	0.5 rem/yr	0.1 rem/yr	2 rem/yr	4 rem/5yrs	5 rem/7yrs
10	0.0%	-8.6%	2,600%	3,600%	4,100%
20	0.0%	-23%	49%	60%	65%
30	0.0%	-30%	50%	60%	64%
40	0.0%	-37%	57%	67%	72%
50	0.0%	-39%	66%	79%	86%

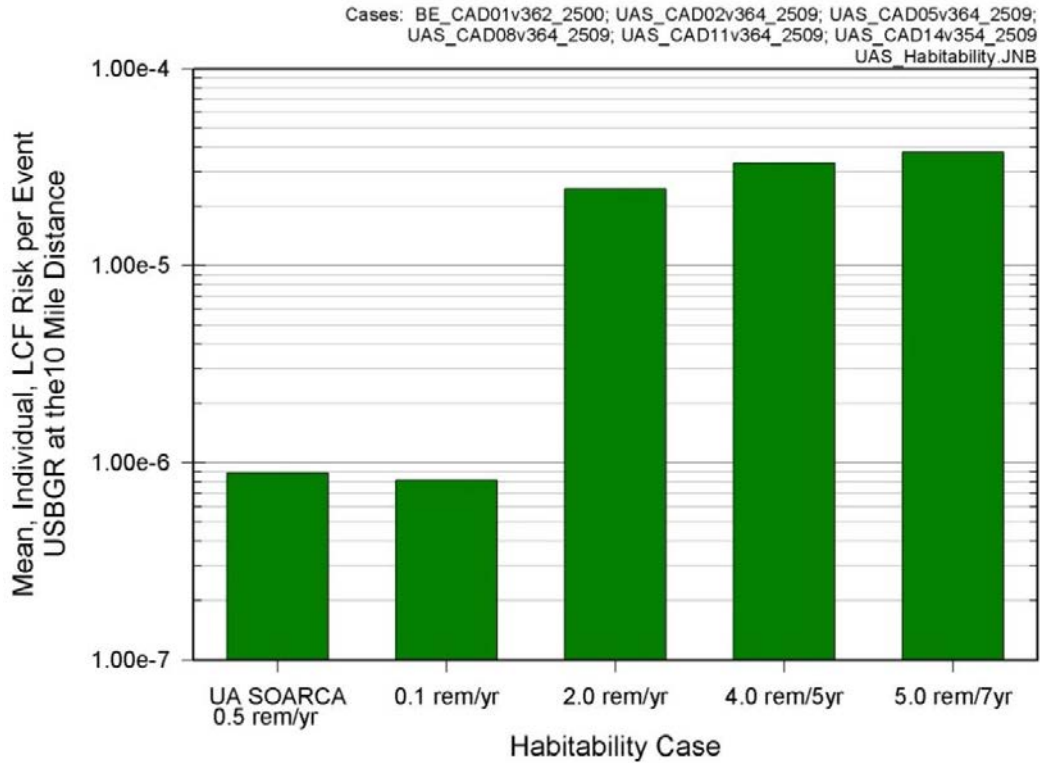


Figure 6.4-10 Habitability criterion comparison of conditional, mean, individual LCF risk (per event) for the 10-mile circular area for the USBGR dose-response model

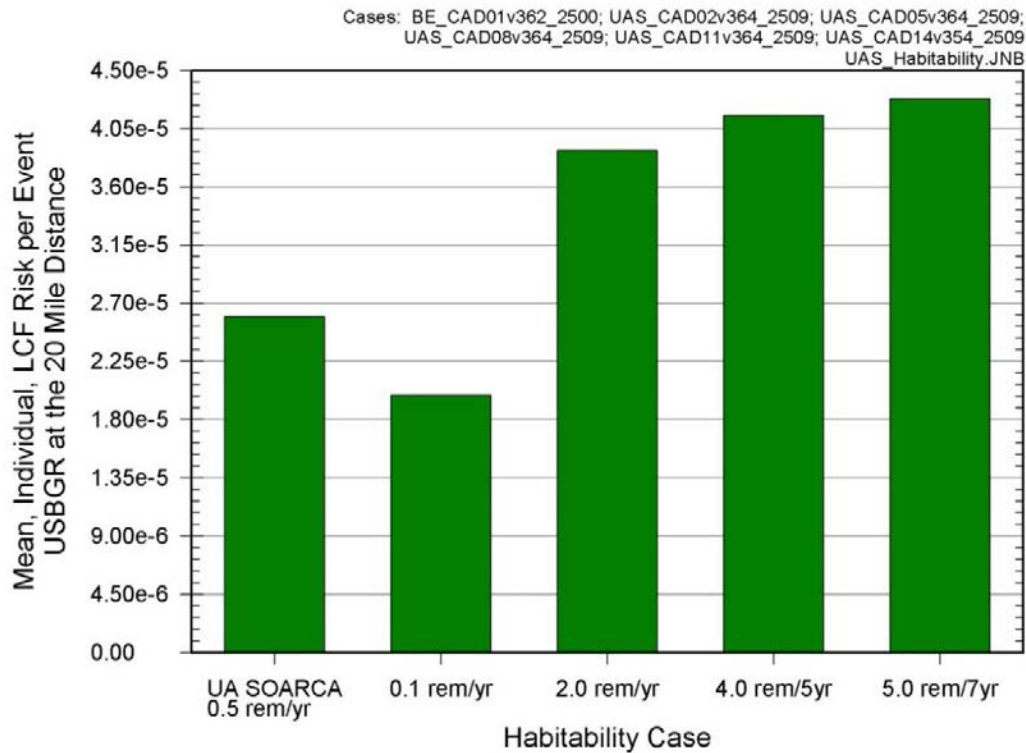


Figure 6.4-11 Habitability criterion comparison of conditional, mean, individual LCF risk (per event) for the 20-mile circular area for the USBGR dose-response model

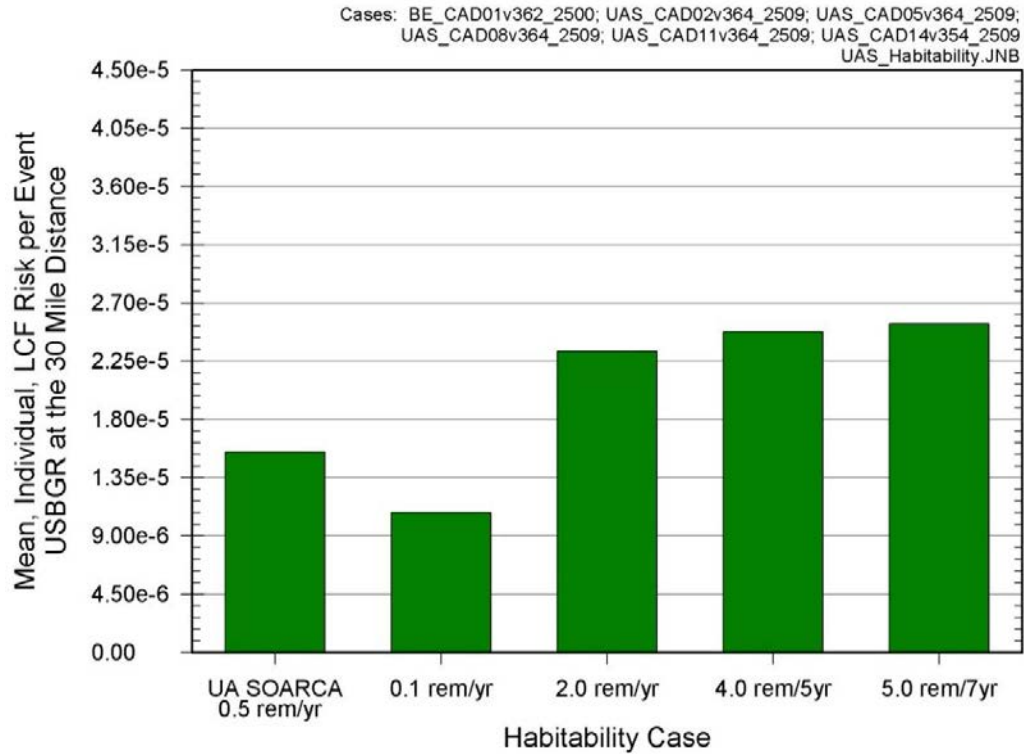


Figure 6.4-12 Habitability criterion comparison of conditional, mean, individual LCF risk (per event) for the 30-mile circular area for the USBGR dose-response model

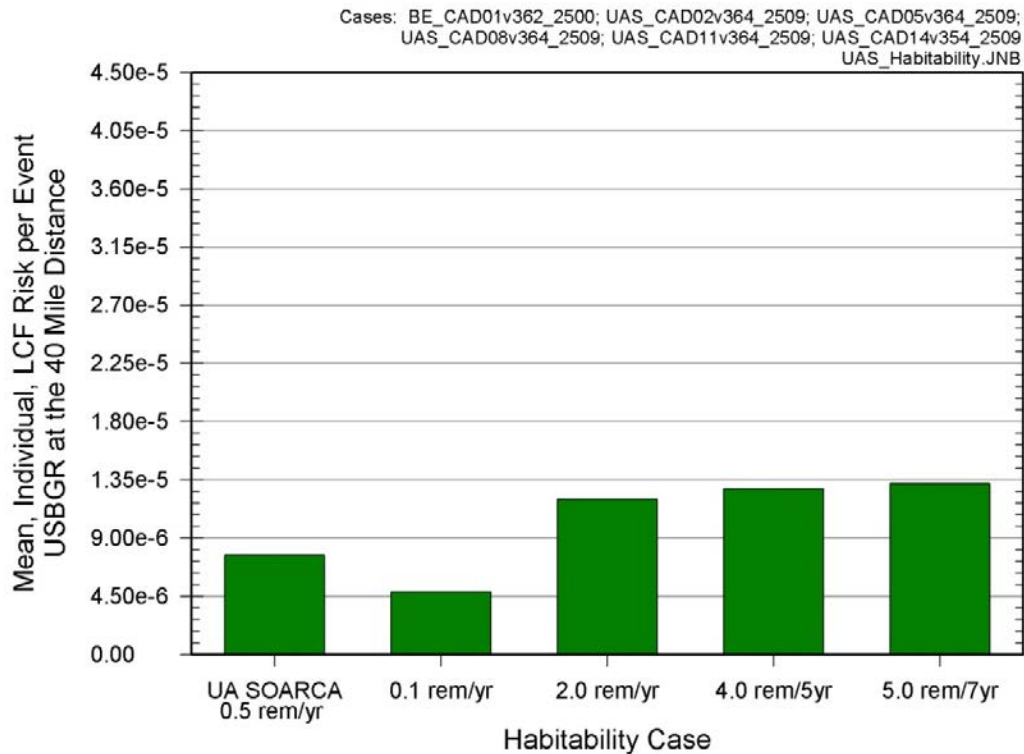


Figure 6.4-13 Habitability criterion comparison of conditional, mean, individual LCF risk (per event) for the 40-mile circular area for the USBGR dose-response model

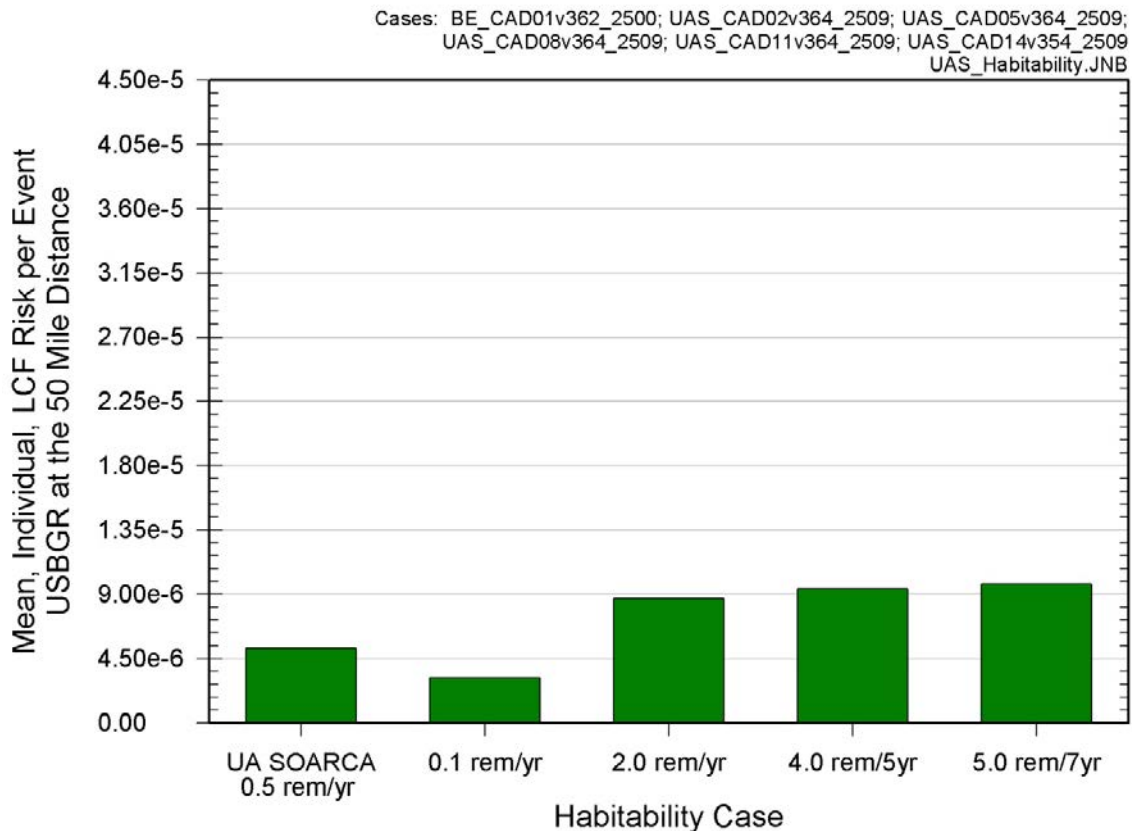


Figure 6.4-14 Habitability criterion comparison of conditional, mean, individual LCF risk (per event) for the 50-mile circular area for the USBGR dose-response model

Table 6.4-22 provides the results of the conditional, mean, individual LCF risk (per event) for specified circular areas for the HPS dose-response model. As shown in Table 6.4-22, the habitability criteria are all below the dose truncation level (5 rem/yr with 10 rem lifetime limit) and the results are similar to those for the SOARCA study. Table 6.4-23 shows the percent difference between the habitability criteria compared to the SOARCA uncertainty analysis base case with 0.5 rem/yr habitability. The percent differences are similar to those shown in Table 6.4-19 for the LNT dose-response model for specified circular areas.

Figures 6.4-15 through 6.4-19 show the conditional, mean, individual LCF risk (per event) contribution for each habitability criterion at each specified circular area. Since there is no simple way to separate the LCF risks from the emergency phase and long-term phase, Figures 6.4-15 through 6.4-17 only show the total risk of both phases. The inability to discern the emergency and long-term phase LCF risk is the same as that explained for the USBGR dose-response model. Figure 6.4-15 shows that the habitability criteria have little effect on the overall LCF risk when the HPS dose-response model is applied. The 20-mile, 30-mile, 40-mile, and 50-mile circular area results are similar in trend to the 10-mile circular area results shown on Figure 6.4-15.

Table 6.4-22 **Habitability criterion comparison of conditional, mean, individual LCF risk (per event) for HPS dose-response model**

Radius (mi)	SOARCA Estimate*	SOARCA Uncertainty Analysis Base Case Source Term				
		0.5 rem/yr*	0.1 rem/yr	2 rem/yr	4 rem/5 yrs	5 rem/7 yrs
10	3.7×10^{-7}	5.6×10^{-7}	5.3×10^{-7}	8.2×10^{-7}	8.3×10^{-7}	9.5×10^{-7}
20	2.2×10^{-6}	4.4×10^{-6}	3.8×10^{-6}	6.1×10^{-6}	8.2×10^{-6}	9.1×10^{-6}
30	8.9×10^{-7}	1.7×10^{-6}	1.5×10^{-6}	2.5×10^{-6}	3.5×10^{-6}	3.8×10^{-6}
40	3.7×10^{-7}	7.1×10^{-7}	6.2×10^{-7}	1.0×10^{-6}	1.4×10^{-6}	1.6×10^{-6}
50	2.4×10^{-7}	4.5×10^{-7}	3.9×10^{-7}	6.4×10^{-7}	9.0×10^{-7}	1.0×10^{-6}

* The differences between the SOARCA estimate and the SOARCA uncertainty analysis base case with a habitability criterion of 0.5 rem/yr are discussed in Appendix C

Table 6.4-23 **Percentage change in conditional, mean, individual LCF risk (per event) for the HPS dose-response model from variations in habitability criterion (reduction/increase (-/+))**

Radius (mi)	SOARCA UA Base Case with 0.5 rem/yr	0.1 rem/yr	2 rem/yr	4 rem/5yrs	5 rem/7yrs
10	0.0%	-5.7%	45%	48%	68%
20	0.0%	-12%	40%	89%	110%
30	0.0%	-13%	42%	99%	120%
40	0.0%	-13%	42%	99%	120%
50	0.0%	-13%	42%	98%	120%

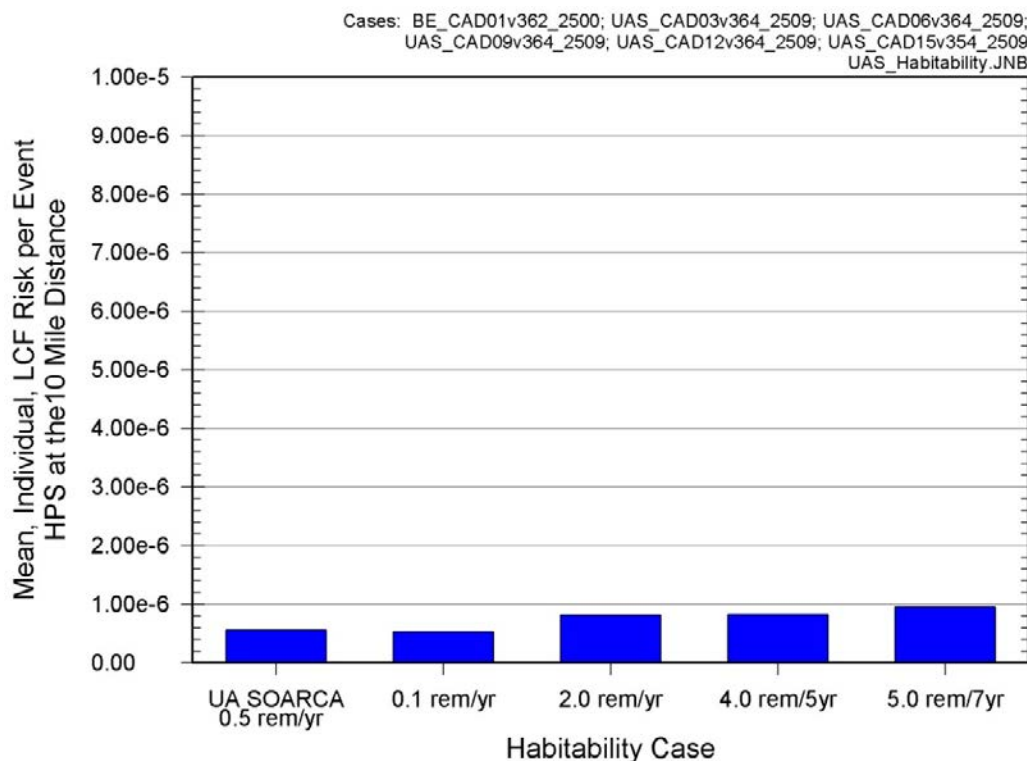


Figure 6.4-15 Habitability criterion comparison of conditional, mean, individual LCF risk (per event) for the 10-mile circular area for the HPS dose-response model

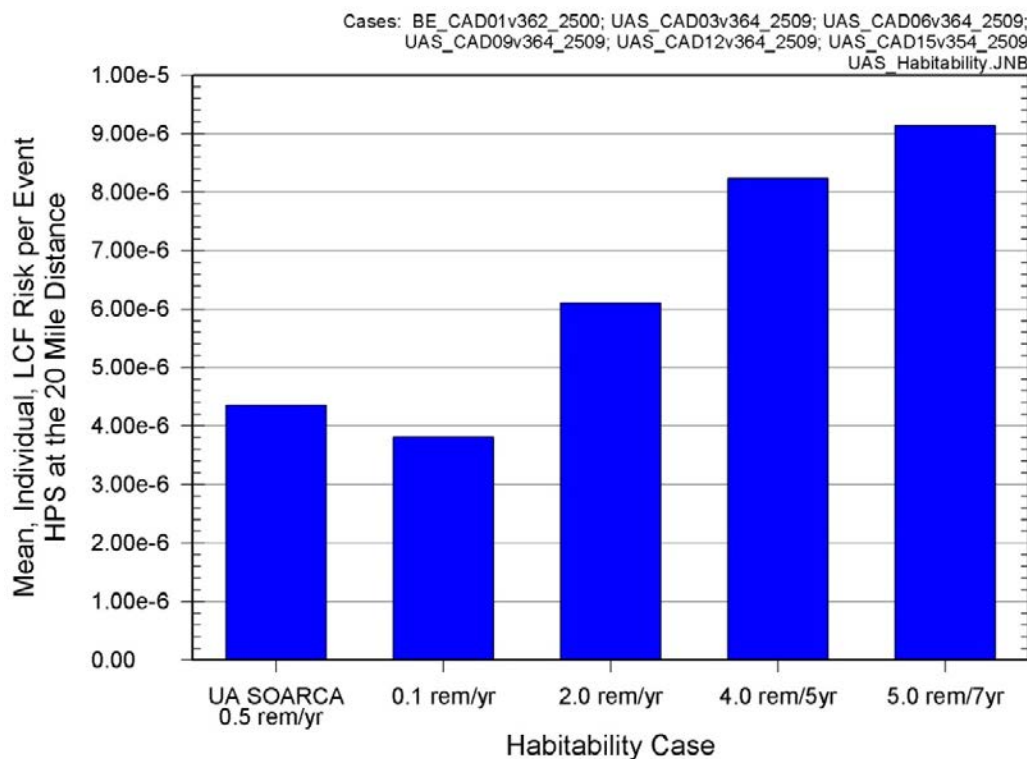


Figure 6.4-16 Habitability criterion comparison of conditional, mean, individual LCF risk (per event) for the 20-mile circular area for the HPS dose-response model

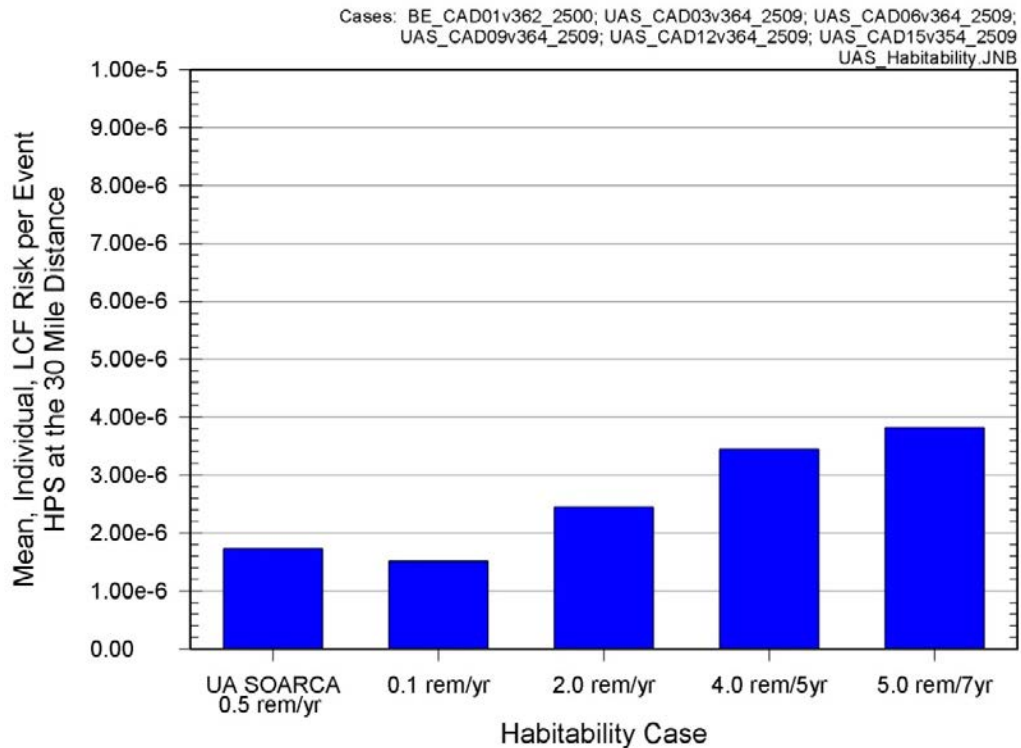


Figure 6.4-17 Habitability criterion comparison of conditional, mean, individual LCF risk (per event) for the 30-mile circular area for the HPS dose-response model

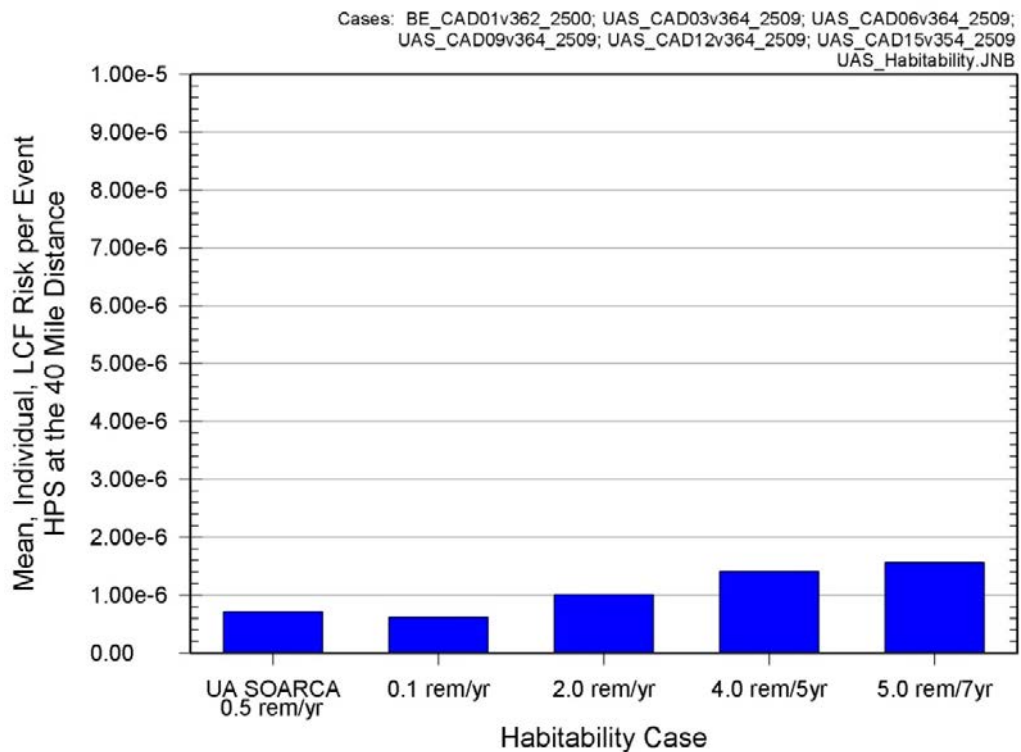


Figure 6.4-18 Habitability criterion comparison of conditional, mean, individual LCF risk (per event) for the 40-mile circular area for the HPS dose-response model

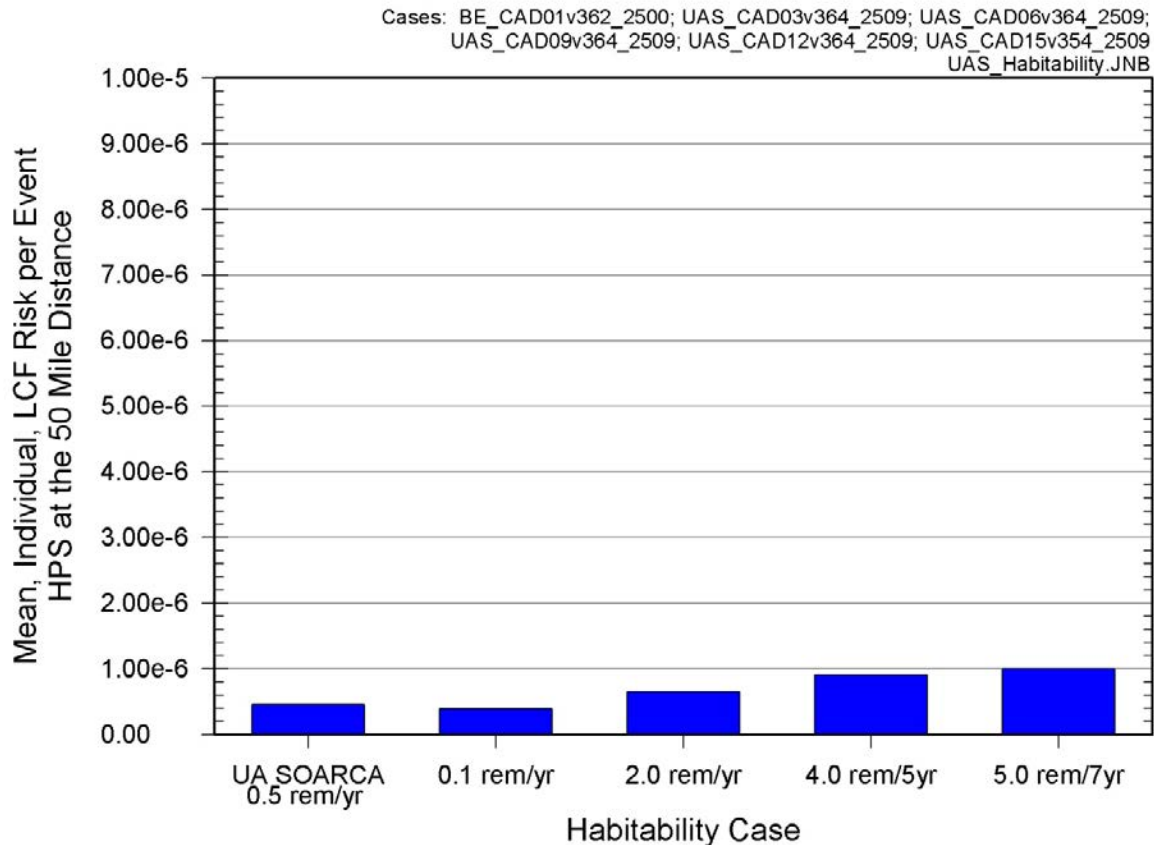


Figure 6.4-19 Habitability criterion comparison of conditional, mean, individual LCF risk (per event) for the 50-mile circular area for the HPS dose-response model

6.4.5 Weather Sampling Effects

In the foregoing sections, the uncertainty that has been addressed has been categorized as epistemic. In fact, each source of uncertainty has both an epistemic and aleatory component. For example, the conditions leading to failure of a SRV are currently poorly quantified. The lack of quantification results in epistemic uncertainty. However, if a large set of SRVs were tested to failure under accident-like conditions, the epistemic uncertainty would be diminished or even eliminated, but some aleatory uncertainty would remain. The source of the remaining aleatory uncertainty is sample-to-sample variations and manufacturing flaws. The effect of some of these flaws may not be able to be evaluated without testing a specific valve to failure, at which point it could no longer be used. Thus, in practice, all uncertainty has some aleatory component.

One large source of aleatory uncertainty in a probabilistic risk assessment is from the weather. In SOARCA, the aleatory uncertainties due to weather were characterized in terms of mean values. Unlike most of the other input parameters used in SOARCA or for any risk analysis, weather is inherently unknowable because of the exact time of an accident is unknowable. Because weather can have a significant impact on predicted consequences, it must be treated in a statistical fashion and the resulting uncertainty is clearly in the category of aleatory uncertainty. This section explores the sampling error associated with the aleatory uncertainty resulting from weather.

A set of sensitivity analyses to evaluate the SOARCA weather sampling technique was evaluated for the LNT, USBGR, and HPS dose-response models. All of the sensitivity simulations use the SOARCA uncertainty analysis base case source term described in Appendix C. The SOARCA weather sampling technique was compared to sampling the entire weather database used for Peach Bottom. All of the MACCS variables other than the sampled weather trials was held fixed.

For SOARCA, a structured Monte-Carlo sampling method was employed for weather sampling. This was done by random selection of a user-specified number of weather sequences (i.e., start times) from the set of sequences assigned to each user-specified weather category. This begins by sorting an annual weather file according to user specified criteria. Each MACCS analysis uses a user-specified random seed. This random seed was kept constant for all MACCS analysis and thus the same weather trials from the same meteorological data file were selected for all of the analyses.

When evaluating the consequences of a release, MACCS selects a set of weather trials (i.e., wind speeds, wind directions, stability classes, precipitation rates, and a diurnal seasonal mixing height). Each weather trial is characterized by a starting hour from a meteorological data file. Subsequent hours of the release use subsequent hours from the data file. Thus, each hour of the release uses weather inputs specific to an hour of weather data from the MACCS meteorological data file (PB MACCS 2006 Met Data 64WD.inp). However, while the data file contains data to perform 8,760 weather trials, only about 1,000 of them were sampled for SOARCA.

Weather binning is an approach used in MACCS to categorize similar sets of weather data based on wind speed, stability class, and the intensity of precipitation. The weather sampling strategy adopted for SOARCA uses the nonuniform weather-binning approach in MACCS. This approach, which allows the user to specify a different number of random samples for each bin, has been available since MACCS was first released [9] but was not used in previous studies.

The weather binning structure defined in SOARCA was used previously in NUREG-1150. This structure consists of 16 predefined bins for combinations of stability class and wind speed, and 20 user-defined bins for rain occurring before the plume travels 32 km (20 miles). The rain bins differentiate rain intensity and the distance the plume travels before rain begins. An approach called, uniform weather bin sampling was used in NUREG-1150. Four weather sequences were sampled per bin, resulting in a nominal 144 weather trials. In conjunction with this sampling method, an additional strategy called wind rotation was used. Wind rotation expands the set of weather trials by a factor of 16 (i.e., the number of compass sectors used in the analysis) by reevaluating the results for each weather trial assuming that the wind had blown in each of the other compass directions. The consequences for each wind direction are assigned a probability that accounts for the wind rose probability. In effect, this strategy results in $16 \times 144 = 2,304$ nominal weather trials.

A wind rose can be shown graphically using a wind rose diagram. A wind rose diagram schematically represents the wind direction and the frequency of occurrence for a particular wind direction. It can also differentiate other features of the weather, such as the intensity of the wind. Figure 6.4-20 provides an example of a wind rose diagram.

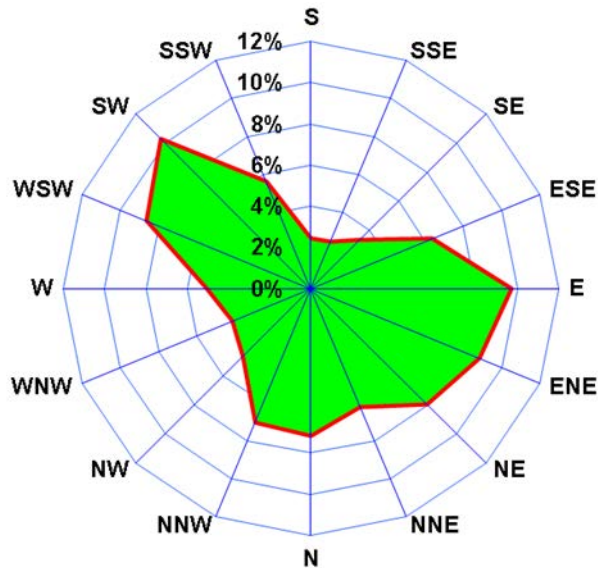


Figure 6.4-20 Example wind rose diagram

For the nonuniform weather sampling strategy approach adopted in SOARCA, the number of trials selected from each bin is the maximum of 12 trials and 10% of the number of trials in the bin. Some bins contain fewer than 12 trials. In those cases, all of the trials within the bin are used for sampling. This strategy results in 984 weather trials for Peach Bottom. Table 6.4-23 shows the weather sampling inputs used in SOARCA for Peach Bottom. MACCS does not allow wind rotation in conjunction with one of the other models used in SOARCA, network evacuation. Thus, expanding the number of weather trials by the number of compass sectors was not used in SOARCA, which is one of the main reasons that the number of weather trials was significantly increased from the number used in NUREG-1150.

Meteorological data used in the SOARCA project consisted of one year of hourly meteorological data (i.e., 8,760 hourly data points for each meteorological parameter). Stability class data were derived from temperature measurements at two elevations on the site meteorological towers. The specific year of data chosen was based on data recovery (e.g., greater than 90% being desirable) and proximity to the target year for SOARCA, which is 2005. Several trends (e.g., wind-rose pattern and hours of precipitation) between the years were evaluated and estimated to have a relatively minor (i.e., less than ± 10 percent) effect on the final results.

Data needed for MACCS, as used in the SOARCA project, includes: 10-meter wind speed, 10-meter wind direction in 64 compass directions, stability class (i.e., Pasquill-Gifford stability class using representative values of 1–6 for stability classes A–F/G), hourly precipitation, and diurnal (morning and afternoon) seasonal mixing heights.

Table 6.4-25 presents a summary of the meteorological data and shows that the annual average ground-level wind speeds were generally low at Peach Bottom. The atmospheric stability frequencies were found to be consistent with expected meteorological conditions. Neutral and slightly stable conditions predominated during the year, with stable and neutral conditions occurring at night and unstable and neutral conditions occurring during the day.

Table 6.4-24 Weather sampling inputs for Peach Bottom

MACCS Variable	Description	Peach Bottom LTSBO
INWGHT	Number of Samples for Each Bin Used for Nonuniform Weather Bin Sampling	
	Bin 1	71
	Bin 2	42
	Bin 3	12
	Bin 4	52
	Bin 5	57
	Bin 6	74
	Bin 7	21
	Bin 8	12
	Bin 9	49
	Bin 10	103
	Bin 11	77
	Bin 12	35
	Bin 13	51
	Bin 14	75
	Bin 15	14
	Bin 16	4
	Bin 17	44
	Bin 18	12
	Bin 19	17
	Bin 20	24
	Bin 21	24
	Bin 22	12
	Bin 23	4
	Bin 24	8
	Bin 25	12
	Bin 26	12
	Bin 27	12
	Bin 28	1
	Bin 29	3
	Bin 30	5
	Bin 31	4
	Bin 32	12
	Bin 33	1
	Bin 34	7
	Bin 35	9
	Bin 36	12

Table 6.4-25 Statistical summary of raw meteorological data

Parameter		Peach Bottom	
		Year 2005	Year 2006
Average Wind Speed (m/s)		2.17	2.12
Yearly Precipitation (hour) (% of Annual Weather)		588 (6.7%)	593 (6.8%)
Atmospheric Stability (%)	Unstable	21.43	20.56
	Neutral	63.97	62.34
	Stable	14.60	17.10
Joint Data Recovery (%)		97.53	99.25

Figure 6.4-21 shows the wind direction (i.e., wind rose) that the wind blows towards and atmospheric stability conditions (i.e., unstable, neutral, and stable) for two years, including the year that was used in the SOARCA consequence analyses for Peach Bottom (i.e., 2006). Figure 6.4-21 shows the Pasquill-Gifford stability categories in terms of stable conditions (categories A through C), neutral stability (category D), and stable conditions (categories E and F) for the weather year used in SOARCA on an hourly basis. The trends shown in the figure are expected, which are that unstable conditions occur during daylight hours, peaking around mid-day, and stable conditions primarily occur during nighttime hours.

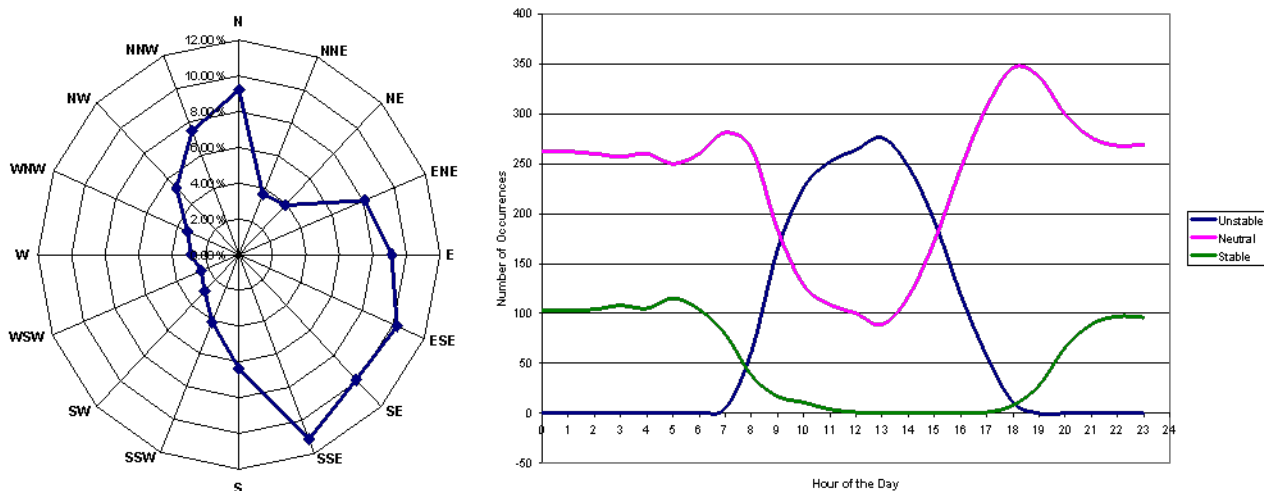


Figure 6.4-21 Peach Bottom wind rose and atmospheric stability chart, year 2006

For the sensitivity case, the SOARCA uncertainty analysis base case described in Appendix C was compared with the same MACCS analysis, except instead of using the SOARCA weather sampling technique; all 8,760 hourly weather data points were selected as the starting time for a weather trial.

Table 6.4-26 provides the results of the conditional, mean, individual LCF risk (per event) within specified circular areas for the LNT dose-response model. As shown in Table 6.4-26 the SOARCA weather sampling technique consistently produces slightly higher LCF risk results.

Table 6.4-26 Weather sampling comparison of the conditional, mean, individual LCF risk (per event) using the LNT dose-response mode

Distance	SOARCA UA Base Case	All Weather Trials	Difference (%)
10	9.0×10^{-5}	8.9×10^{-5}	0.8%
20	8.3×10^{-5}	8.1×10^{-5}	2.4%
30	5.8×10^{-5}	5.7×10^{-5}	1.7%
40	3.7×10^{-5}	3.7×10^{-5}	1.1%
50	3.0×10^{-5}	3.0×10^{-5}	1.3%

Figure 6.4-22 shows the conditional, mean, individual LCF risk (per event) within specified circular areas using the LNT dose-response model for the emergency phase risk contribution (red or green) and the long-term phase risk contribution (blue or orange). Both the emergency and long-term phase LCF risk results are consistently slightly higher for the SOARCA weather sampling technique (Base Case) than the sensitivity (All Weather Trials) case. Thus, the contribution from the change in the number of weather trials to either the long-term phase or the emergency phase does not dominate the overall LCF risk.

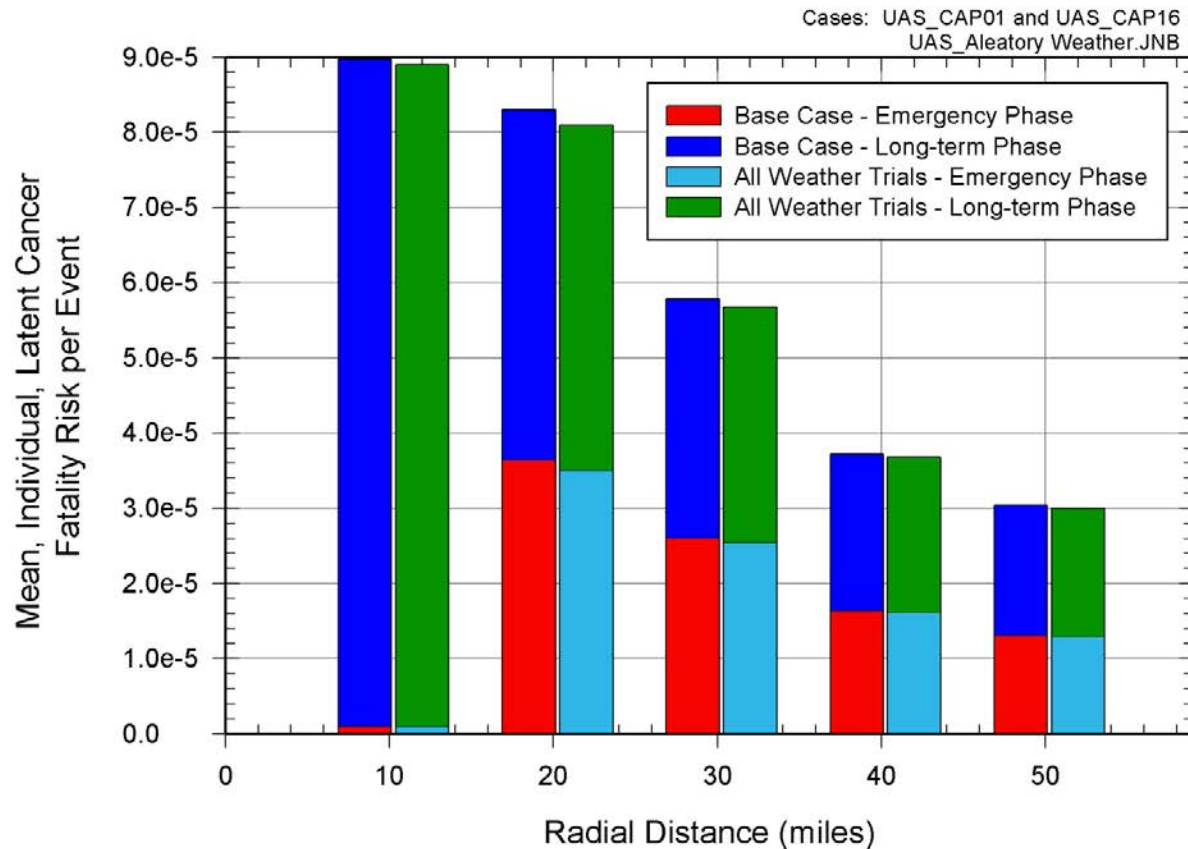


Figure 6.4-22 Weather sampling comparison of the conditional, mean, individual LCF risk (per event) using the LNT dose-response model within specified circular areas

Table 6.4-27 and Figure 6.4-23 provide the results of the conditional, mean, individual LCF risk (per event) within specified circular areas for the USBGR dose-response model. As shown in Table 6.4-27 the SOARCA weather sampling technique consistently produces slightly higher LCF risk results.

Beyond the EPZ, the SOARCA weather sampling technique produces larger differential results than those for the LNT dose-response model. Clearly, this nonlinear dose-response model is more sensitive to the specific selection of weather trials than the LNT dose-response model.

Table 6.4-27 Weather sampling comparison of the conditional, mean, individual LCF risk (per event) using the USBGR dose-response model

Distance	SOARCA UA Base Case	All Weather Trials	Difference (%)
10	8.9×10^{-7}	8.9×10^{-7}	0.8%
20	2.6×10^{-5}	2.5×10^{-5}	5.0%
30	1.6×10^{-5}	1.5×10^{-5}	5.2%
40	7.7×10^{-6}	7.2×10^{-6}	5.7%
50	5.2×10^{-6}	5.0×10^{-6}	5.5%

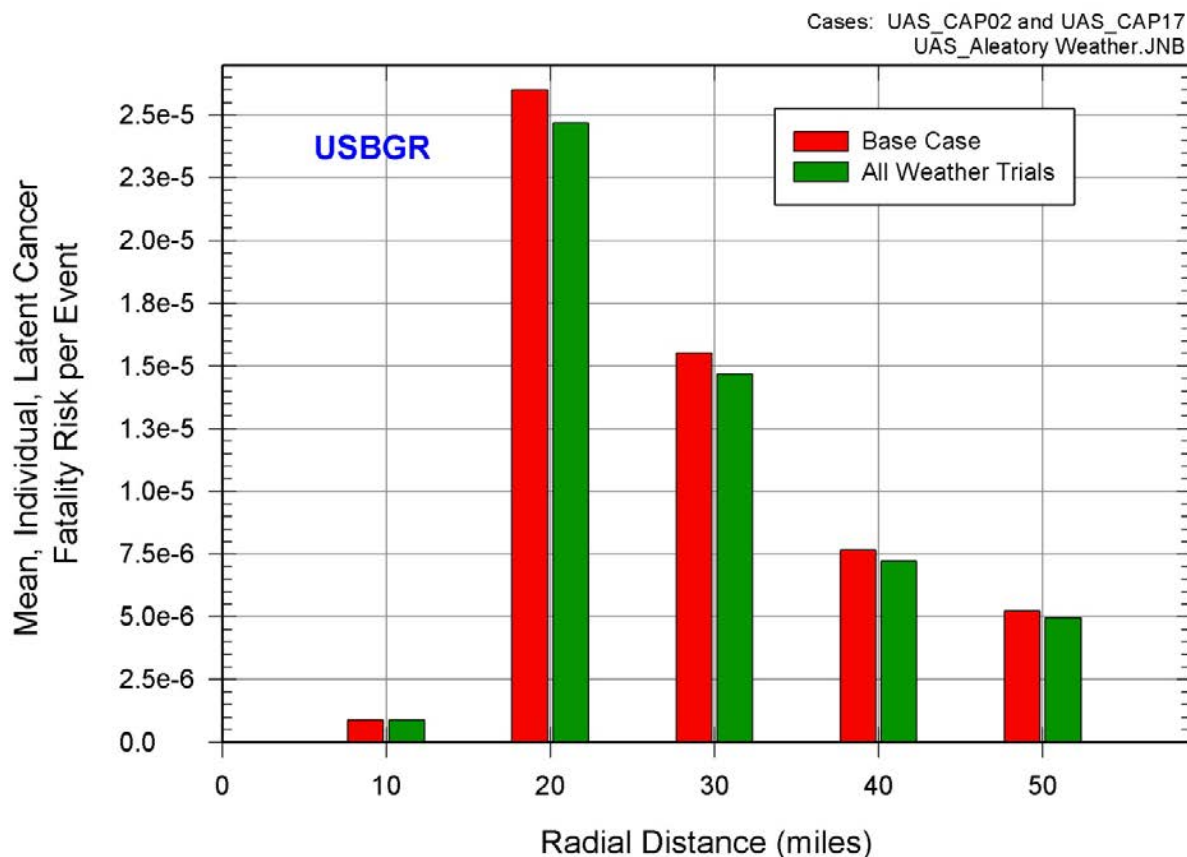


Figure 6.4-23 Weather sampling comparison of the conditional, mean, individual LCF risk (per event) using the USBGR dose-response model within specified circular areas

Table 6.4-28 and Figure 6.4-23 provide the results of the conditional, mean, individual LCF risk (per event) within specified circular areas for the HPS dose-response model. As shown in Table 6.4-28 the SOARCA weather sampling technique consistently produces higher LCF risk results.

Beyond the EPZ, the SOARCA weather sampling technique produces larger differential results than those for either the LNT or USBGR dose-response models. Clearly, this nonlinear dose-response model is more sensitive to the specific selection of weather trials than the LNT dose-response model.

Table 6.4-28 Weather sampling comparison of the conditional, mean, individual LCF risk (per event) using the HPS dose-response model

Distance	SOARCA UA Base Case	All Weather Trials	Difference (%)
10	5.6×10^{-7}	5.6×10^{-7}	0.9%
20	4.4×10^{-6}	3.9×10^{-6}	11.0%
30	1.7×10^{-6}	1.5×10^{-6}	11.6%
40	7.1×10^{-7}	6.3×10^{-7}	11.6%
50	4.5×10^{-7}	4.0×10^{-7}	11.7%

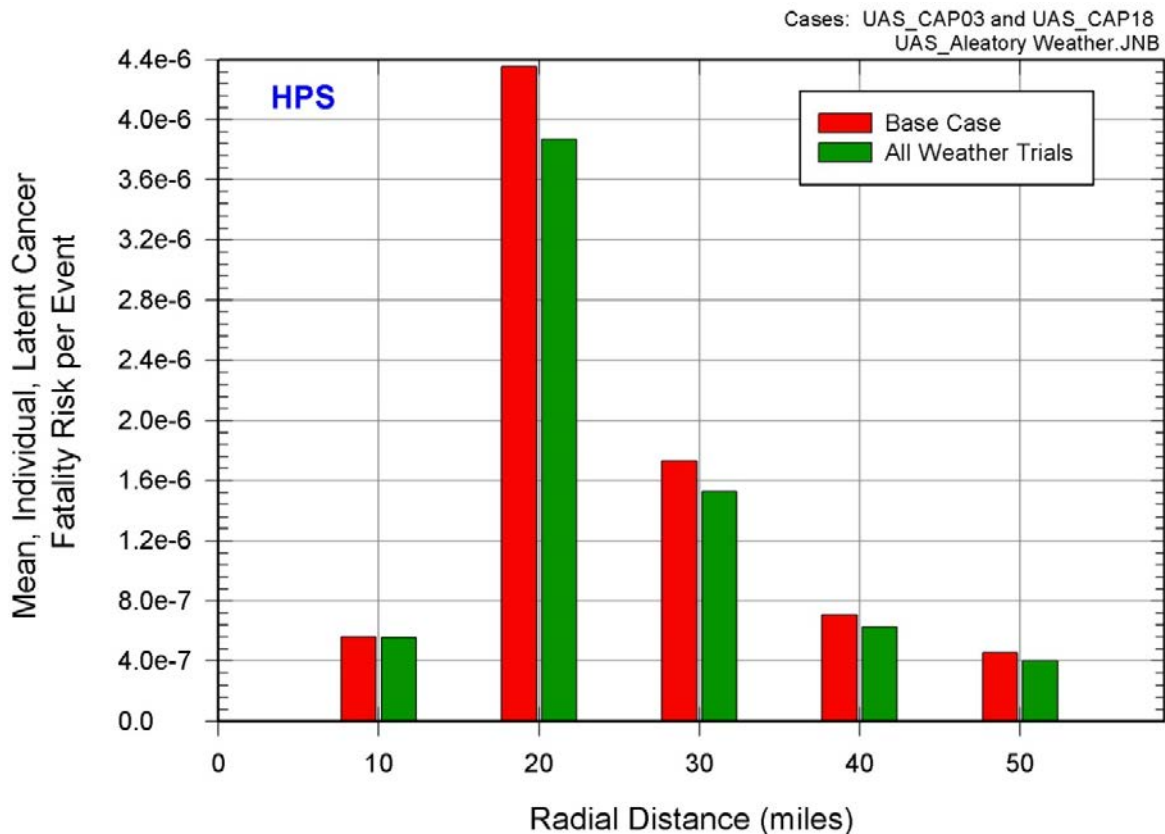


Figure 6.4-24 Weather sampling comparison of the conditional, mean, individual LCF risk (per event) using the HPS dose-response model within specified circular areas

The overall difference between the SOARCA weather sampling technique and sampling all 8,760 hourly data points is relatively small. However, the increase in computational time is eight fold. While this is not prohibitively long for the LNT dose-response model (i.e., ~1 hour to ~8 hours of run time for a single MACCS realization), the increase in computation time for the USBGR and HPS dose-response models would make uncertainty analysis applications less feasible (i.e., ~1 day to ~8 days of run time for a single MACCS realization).

6.4.5.1 Aleatory Weather Uncertainty

In SOARCA, the aleatory uncertainties due to weather were characterized in terms of mean values. However, a CCDF of aleatory uncertainties can be obtained using a single MACCS analysis for each source term. A set of sensitivity analyses to evaluate the aleatory weather uncertainty using the SOARCA weather sampling technique was evaluated for the LNT, USBGR, and HPS dose-response models.

Three source terms were selected, which provided insights into the overall distribution of LCF risk for the sensitivity simulations. The SOARCA uncertainty analysis base case source term described in Appendix C was used to represent the lower end of the conditional, mean, individual LCF risk distribution. Replicate 1 (STP08) Realization 170 source term described in Section 6.1.4 was chosen to represent the median of the conditional, mean, individual LCF risk distribution. Replicate 1 Realization 62 source term described in Section 6.1.4 was used to represent the upper end of the conditional, mean, individual LCF risk distribution. Table 6.4-29 provides a brief description of the three source terms. The SOARCA weather sampling

technique described earlier in this section was used for these analyses. All of the MACCS variables other than the sampled weather data were held fixed.

Table 6.4-29 Brief source term description for the single realizations selected from Replicate 1 (STP08) MELCOR Analyses for the aleatory weather uncertainty analyses

Scenario	Integral Release Fractions by Chemical Group									Atmospheric Release Timing	
	Xe	Cs	Ba	I	Te	Ru	Mo	Ce	La	Start (hr)	End (hr)
SOARCA UA Base Case	0.981	0.005	0.010	0.025	0.019	0	0	0	0	19.9	48
RLZ062	0.995	0.055	0.014	0.104	0.089	0	0.012	0	0	13.6	48
RLZ170	0.985	0.020	0.022	0.031	0.027	0	0	0.001	0	16.6	48

Two comparisons are presented to show the effects of aleatory weather uncertainty. The first shows the individual LCF risk results of the aleatory weather uncertainty for the three source terms using the LNT dose-response model with the conditional, mean, individual LCF risk results of the MACCS analysis for the combined MELCOR Replicates 1, 2, and 3 using the LNT dose-response model (CAP17) discussed in Section 6.2.1. Recall that the CAP17 MACCS analysis consists of 865 MELCOR source terms using 21 MELCOR epistemic uncertainty variables, and 350 MACCS epistemic uncertainty variables of which 338 variables apply to LCF risk.

The second comparison shows the individual LCF risk results of the aleatory weather uncertainty for the three source terms using the LNT, USBGR, and HPS dose-response models with the conditional, mean, individual LCF risk results of the MACCS analysis for MELCOR Replicate 1 using the LNT, USBGR, and HPS dose-response models (i.e., CAP14, CAP15, and CAP16, respectively) discussed in Section 6.4.3. Recall, the CAP14, CAP15, and CAP16 MACCS analyses consists of 284 MELCOR source terms using 21 MELCOR epistemic uncertainty variables, and 350 MACCS epistemic uncertainty variables of which 338 variables apply to LCF risk.

6.4.5.1.1 Aleatory Weather Uncertainty for LNT Dose Response

These analyses used the same 984 MACCS aleatory weather trials used for all other SOARCA analyses, except a CCDF of the aleatory weather trials was created for each of the three source terms. Table 6.4-30 shows the three source term's conditional, mean, individual LCF risk (per event) result with respect to the percentile of the CCDF for the conditional, mean, individual LCF risk (per event) results for the MACCS CAP17 analysis. Table 6.4-31 shows the three source term's conditional, mean, individual LCF risk (per event) results from the MACCS CAP 17 analysis with respect to the percentile of the CCDF. When Table 6.4-31 is compared with Table 6.4-30, the median individual LCF risk results for the three source terms in Table 6.4-30 do provide a good example of the median, lower, and upper bounds of the CAP17 conditional, mean, individual LCF risk (per event) CCDF distribution for all specified circular areas.

Table 6.4-30 MACCS aleatory uncertainty analyses conditional mean, individual LCF risk (per event) comparison of source terms to the conditional, mean, individual LCF risk (per event) CCDF of the MACCS CAP17 analysis for specified circular areas

Radius of Circular Area (miles)	SOARCA UA Base Case	Replicate 1 Realization 62	Replicate 1 Realization 170
10	32 nd	94 th	77 th
20	15 th	79 th	53 rd
30	15 th	81 st	52 nd
40	15 th	83 rd	52 nd
50	15 th	83 rd	53 rd

Table 6.4-31 The MACCS CAP17 analysis conditional, mean, individual LCF risk (per event) of the source terms for specified circular areas

Radius of Circular Area (miles)	SOARCA UA Base Case	Replicate 1 Realization 62	Replicate 1 Realization 170
10	32 nd	60 th	98 th
20	15 th	54 th	84 th
30	15 th	54 th	86 th
40	15 th	53 rd	88 th
50	15 th	52 nd	88 th

Figure 6.4-25 shows the CCDF of the aleatory weather uncertainty within the 10-mile circular area for the conditional, mean, individual LCF risk (per event) and CCDF of the conditional, mean, individual LCF risk (per event) results for the MACCS CAP17 analysis. Unlike the MACCS CAP17 analysis, the aleatory uncertainty analyses were bounded at the 99th and 1st percentiles. As shown in Figure 6.4-25, the conditional, mean, individual LCF risk (per event) for aleatory weather uncertainty is bounded for all analyses by the epistemic uncertainty for the conditional, mean, individual LCF risk (per event) results of the MACCS CAP17 analysis. This indicates that the epistemic uncertainties within the MACCS CAP17 analysis have a greater effect on the overall uncertainty than the aleatory weather uncertainty.

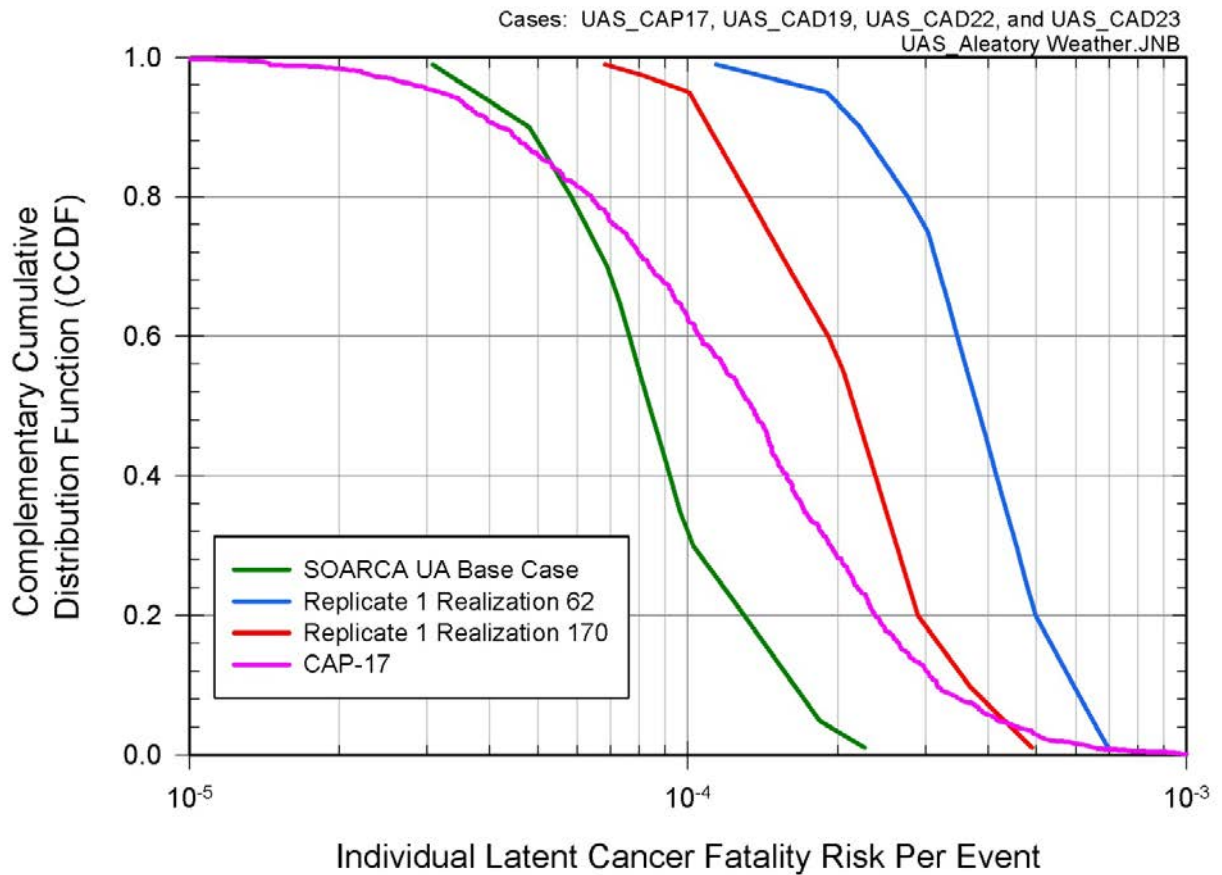


Figure 6.4-25 CCDF of conditional, mean, individual LCF risk (per event) within the 10-mile circular area for aleatory weather uncertainty and the MACCS CAP17 analysis

Figure 6.4-26 shows the CCDF of the aleatory weather uncertainty within the 20-mile circular area for the conditional, mean, individual LCF risk (per event) and CCDF of the conditional, mean, individual LCF risk (per event) results for the MACCS CAP17 analysis. Figure 6.4-26 shows similar results to those in Figure 6.4-25 and also indicates the epistemic uncertainties within the MACCS CAP17 analysis have a greater effect on the overall uncertainty than the aleatory weather uncertainty.

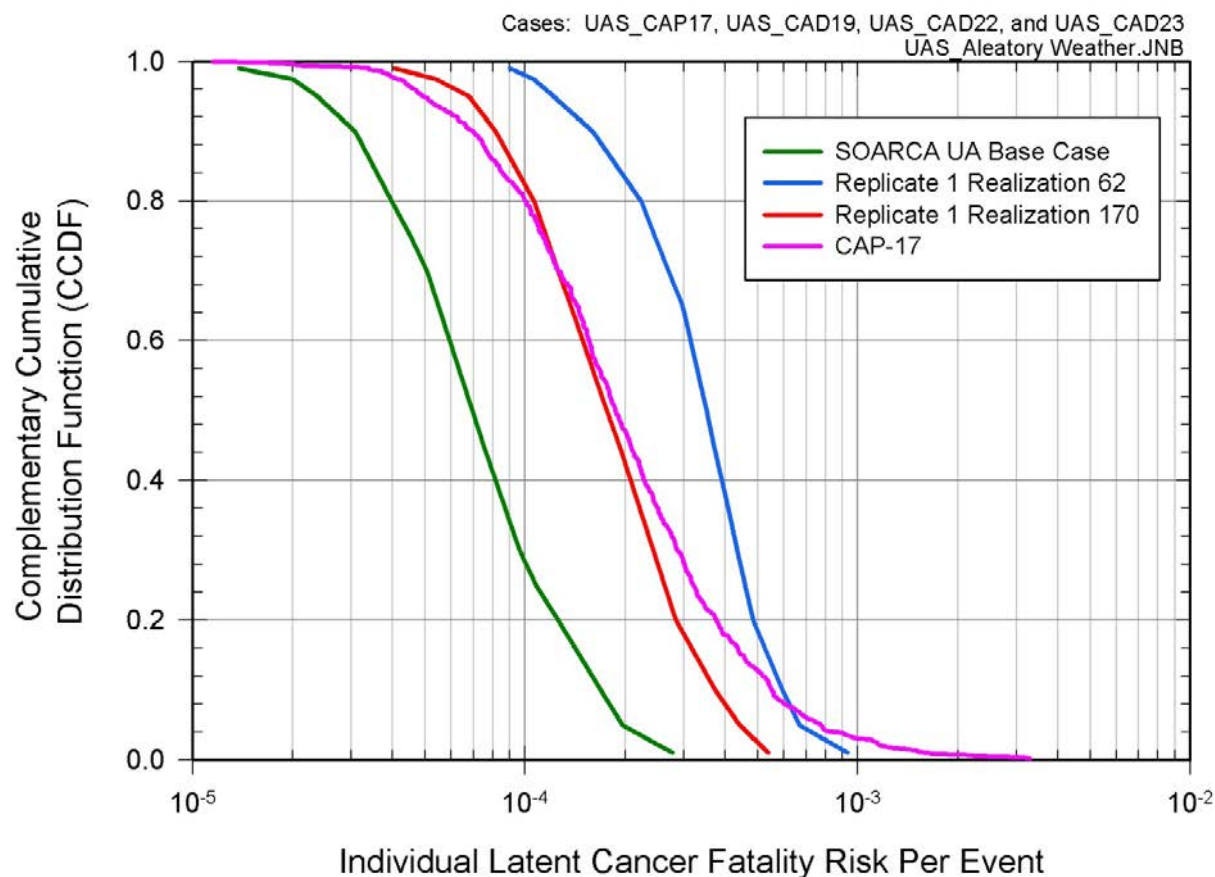


Figure 6.4-26 CCDF of conditional, mean, individual LCF risk (per event) within the 20-mile circular area for aleatory weather uncertainty and the MACCS CAP17 analysis

Figure 6.4-27 through Figure 6.2-29 show the CCDF of the aleatory weather uncertainty within the 30-mile, 40-mile, and 50-mile circular areas, respectively, for the conditional, mean, individual LCF risk (per event) and CCDF of the conditional, mean, individual LCF risk (per event) results for the MACCS CAP17 analysis. These figures show similar results to those in Figure 6.4-25 and also indicate the epistemic uncertainties within the MACCS CAP17 analysis have a greater effect on the overall uncertainty than the aleatory weather uncertainty.

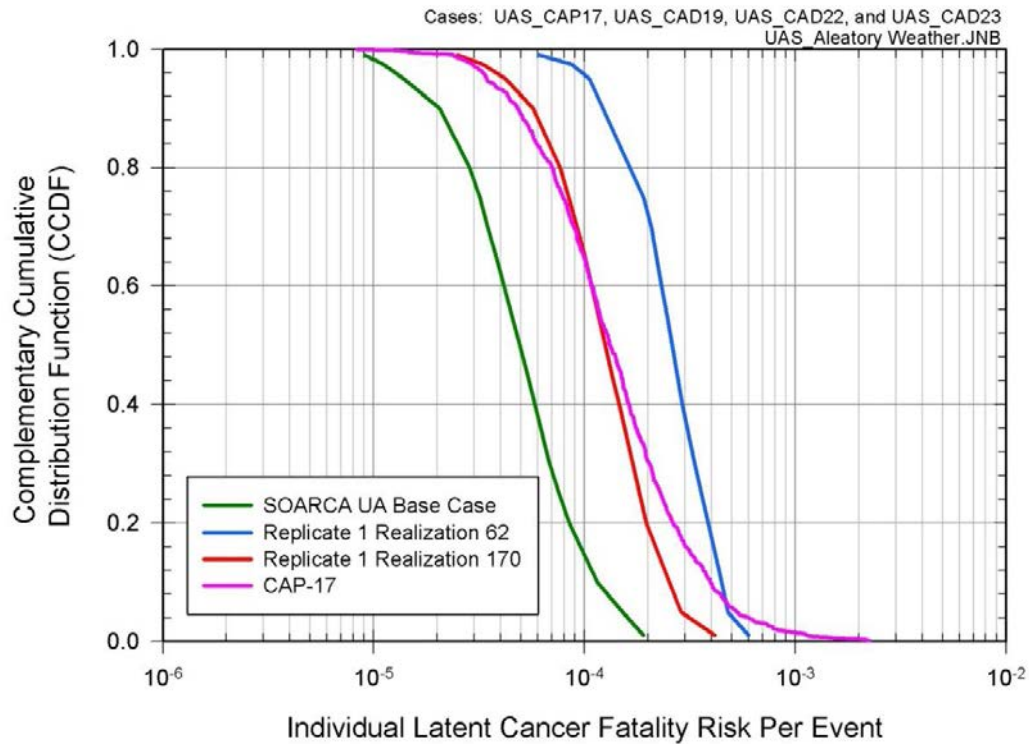


Figure 6.4-27 CCDF of conditional, mean, individual LCF risk (per event) within the 30-mile circular area for aleatory weather uncertainty and the MACCS CAP17 analysis

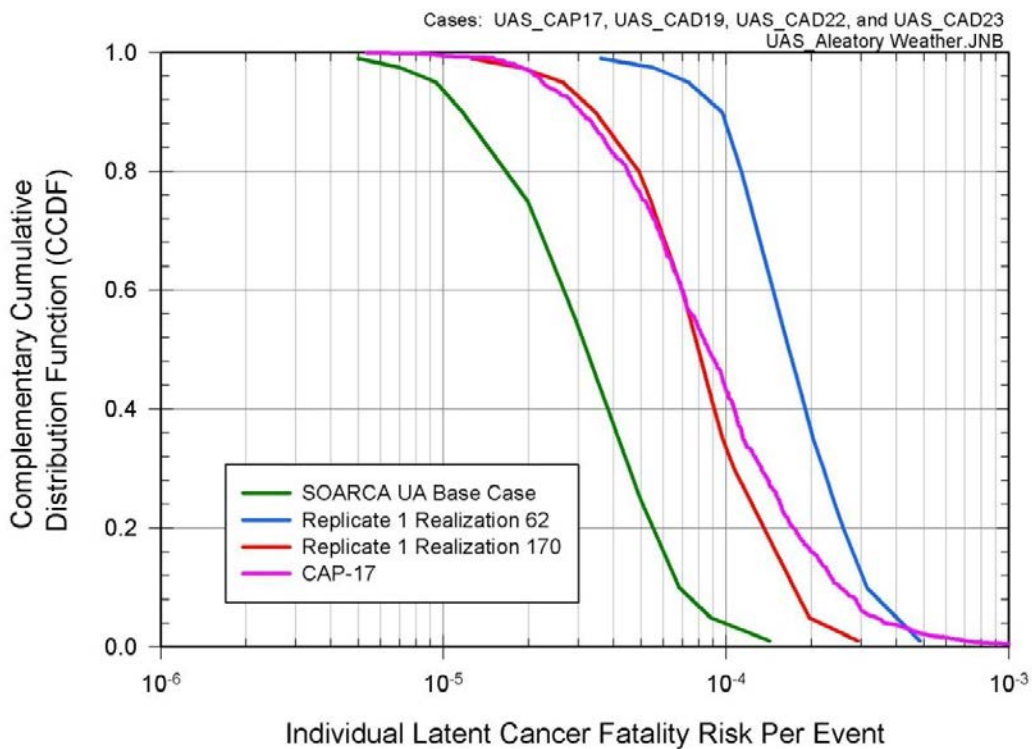


Figure 6.4-28 CCDF of conditional, mean, individual LCF risk (per event) within the 40-mile circular area for aleatory weather uncertainty and the MACCS CAP17 analysis

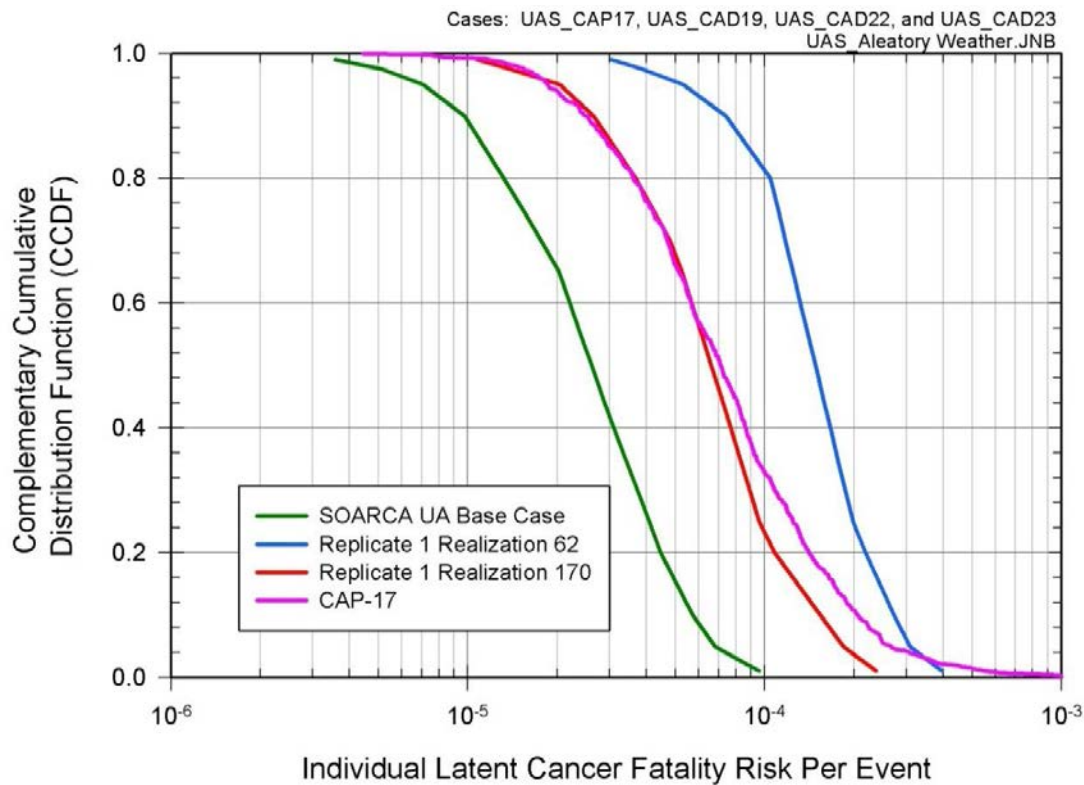


Figure 6.4-29 CCDF of conditional, mean, individual LCF risk (per event) within the 50-mile circular area for aleatory weather uncertainty and the MACCS CAP17 analysis.

Table 6.4-32 shows the ratio between the 5th and 95th percentile for the three source term's LCF risk per event results and the conditional, mean, individual LCF risk (per event) results for the MACCS CAP17 analysis. As shown in Table 6.4-32, the aleatory weather uncertainty individual LCF risk is narrower for all of the analyses than the epistemic uncertainty for the mean results of the MACCS CAP17 analysis within all circular areas. This again shows that the epistemic uncertainties within the MACCS CAP17 analysis have a greater effect on the overall uncertainty than the aleatory weather uncertainty.

Table 6.4-32 Conditional, mean, individual LCF risk (per event) ratio for the MACCS aleatory uncertainty analyses and the MACCS CAP17 analysis for specified circular areas

Radius of Circular Area (miles)	SOARCA UA Base Case	Replicate 1 Realization 62	Replicate 1 Realization 170	CAP17
10	4.9	3.4	4.3	13
20	8.3	5.5	6.5	15
30	11	4.5	6.8	15
40	9.4	5.4	7.4	15
50	9.6	5.8	9.0	14

6.4.5.1.2 Aleatory Weather Uncertainty for Dose-Truncation

The comparisons shown in this section use the same 984 MACCS aleatory weather trials as all other SOARCA analyses, except a CCDF of the aleatory weather trials was created for the three source terms using the LNT, USBGR, and HPS dose-response models. Table 6.4-33 through Table 6.4-35 show the three source term's median LCF risk per event result with respect to the percentile of the CCDF conditional, mean, individual LCF risk (per event) results for the MACCS CAP14 analysis for LNT, the MACCS CAP15 analysis for USBGR, and the MACCS CAP16 analysis for HPS dose-response models, respectively. For Table 6.4-33, the median LCF risk results for the three source terms do provide a good example of the median, lower, and upper bounds of the CAP14 CCDF distribution for all specified circular areas and are similar to those shown in Table 6.4-30 for the MACCS CAP17 analysis.

However, these three source terms only quantify the median and lower half of the CAP15 and CAP16 CCDF distributions of conditional, mean, individual LCF risk (per event) results for all specified circular areas. This is due to the dose-truncation models having more of the LCF risk contribution from the 1st year and thus a larger contribution from the emergency phase. The 2nd year and subsequent years have less of a contribution to the individual LCF risk than the LNT dose-response model because the majority of the doses in these years are below the truncation thresholds. Table 6.4-36 shows the percent contribution from each source term for the conditional, mean, individual LCF risk (per event) using the LNT dose-response model. Since none of the source terms selected for this sensitivity analyses have a large contribution from the emergency phase, the overall conditional, mean, individual LCF risks are at the lower end of the range for these dose-response models. Table 6.4-36 shows that the uncertainty analysis base case has a larger fractional contribution to the emergency phase than either of other realizations.

Table 6.4-33 MACCS aleatory uncertainty analyses median LCF risk per event comparison of source terms to the CCDF of the MACCS CAP14 analysis (LNT) for specified circular areas

Radius of Circular Area (miles)	SOARCA UA Base Case	Replicate 1 Realization 62	Replicate 1 Realization 170
10	28 th	94 th	76 th
20	9 th	80 th	45 th
30	9 th	81 st	46 th
40	9 th	80 th	45 th
50	9 th	82 nd	45 th

Table 6.4-34 MACCS aleatory uncertainty analyses median LCF risk per event comparison of source terms to the CCDF of the MACCS CAP15 analysis (USBGR) for specified circular areas

Radius of Circular Area (miles)	SOARCA UA Base Case	Replicate 1 Realization 62	Replicate 1 Realization 170
10	13 th	62 nd	32 nd
20	11 th	56 th	30 th
30	11 th	59 th	30 th
40	8 th	61 st	28 th
50	8 th	61 st	24 th

Table 6.4-35 MACCS aleatory uncertainty analyses median LCF risk per event comparison of source terms to the CCDF of the MACCS CAP16 analysis (HPS) for specified circular areas

Radius of Circular Area (miles)	SOARCA UA Base Case	Replicate 1 Realization 62	Replicate 1 Realization 170
10	7 th	58 th	25 th
20	5 th	27 th	8 th
30	6 th	27 th	8 th
40	6 th	29 th	8 th
50	5 th	29 th	8 th

Table 6.4-36 MACCS aleatory uncertainty analyses percent contribution of the emergency phase for the conditional, mean, individual LCF risk (per event) using the LNT dose-response model for specified circular areas

Radius of Circular Area (miles)	SOARCA UA Base Case	Replicate 1 Realization 62	Replicate 1 Realization 170
10	1.1%	1.0%	1.3%
20	44%	29%	36%
30	45%	28%	36%
40	44%	25%	34%
50	43%	23%	32%

Figure 6.4-30 through Figure 6.4-34 show a comparison of the CCDF distribution for conditional, mean, individual LCF risk (per event) results using the LNT, USBGR, and HPS dose-truncation models for aleatory weather uncertainty using the SOARCA uncertainty analysis base case source term within the 10-mile, 20-mile, 30-mile, 40-mile, and 50-mile circular areas, respectively. Unlike the MACCS CAP17 analysis, the aleatory uncertainty analyses were evaluated for the range between the 99th and 1st percentiles. As seen in these figures, the HPS dose-response model has the widest CCDF distribution of individual LCF risk per event for each of the circular areas and the LNT dose-response models has the narrowest CCDF distribution.

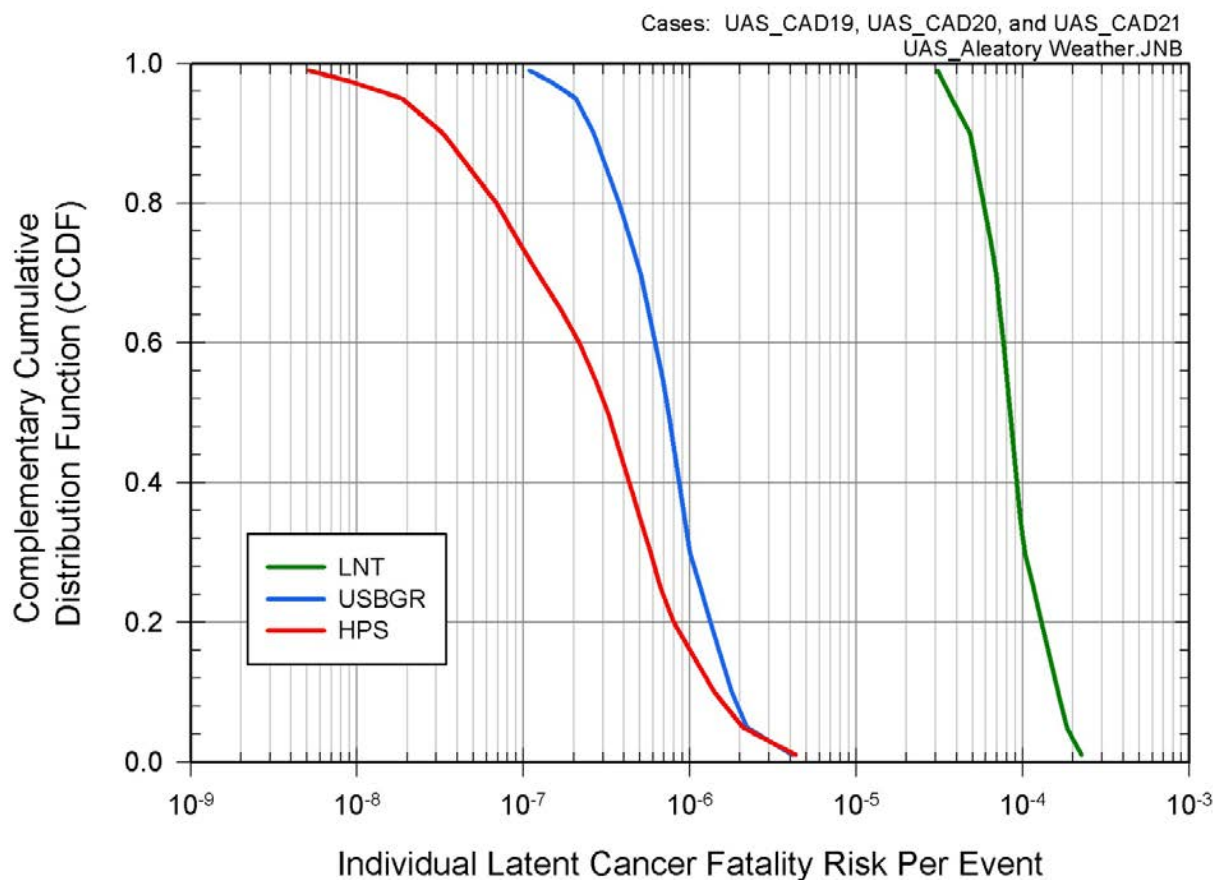


Figure 6.4-30 CCDF of conditional, mean, individual LCF risk (per event) within the 10-mile circular area for aleatory weather uncertainty for the LNT, USBGR, and HPS dose-response models using the SOARCA uncertainty analysis base case source term

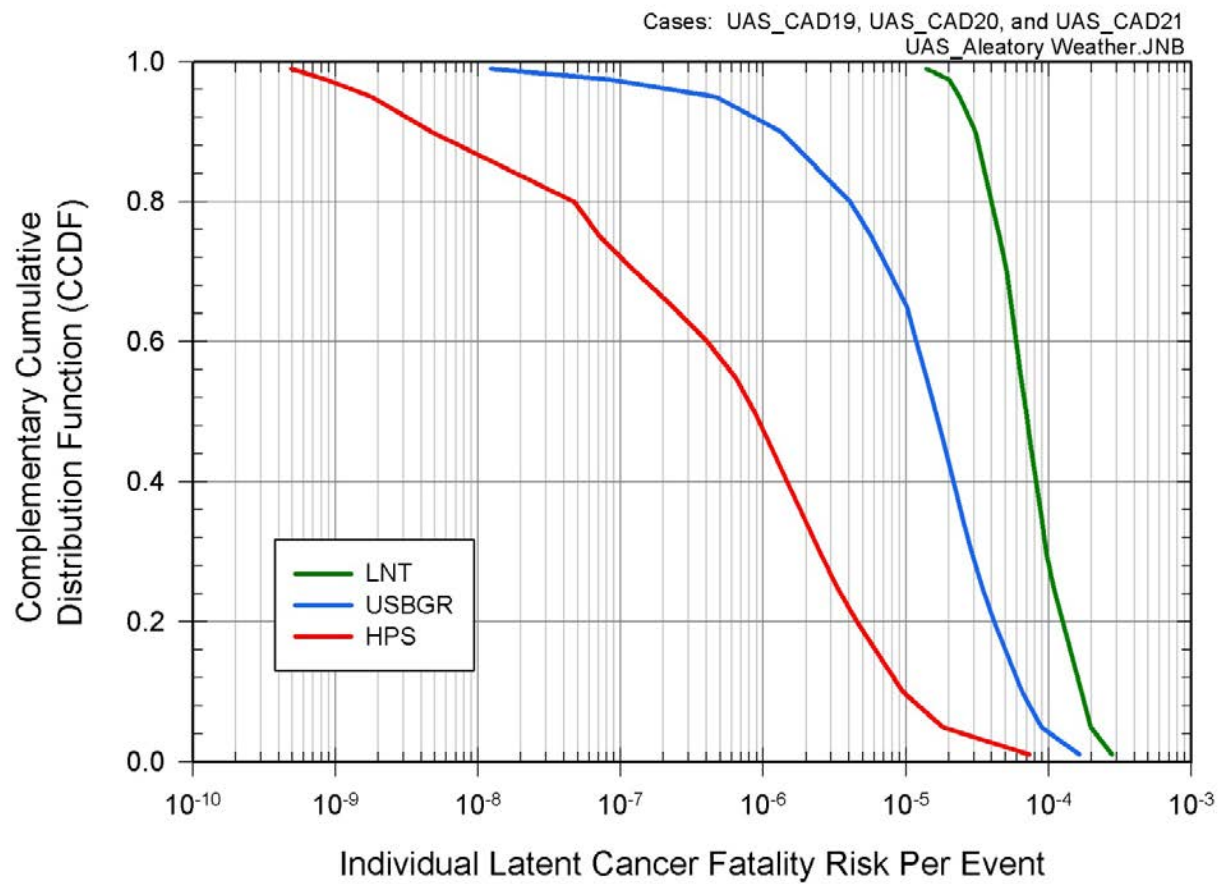


Figure 6.4-31 CCDF of conditional, mean, individual LCF risk (per event) within the 20-mile circular area for aleatory weather uncertainty for the LNT, USBGR, and HPS dose-response models using the SOARCA uncertainty analysis base case source term

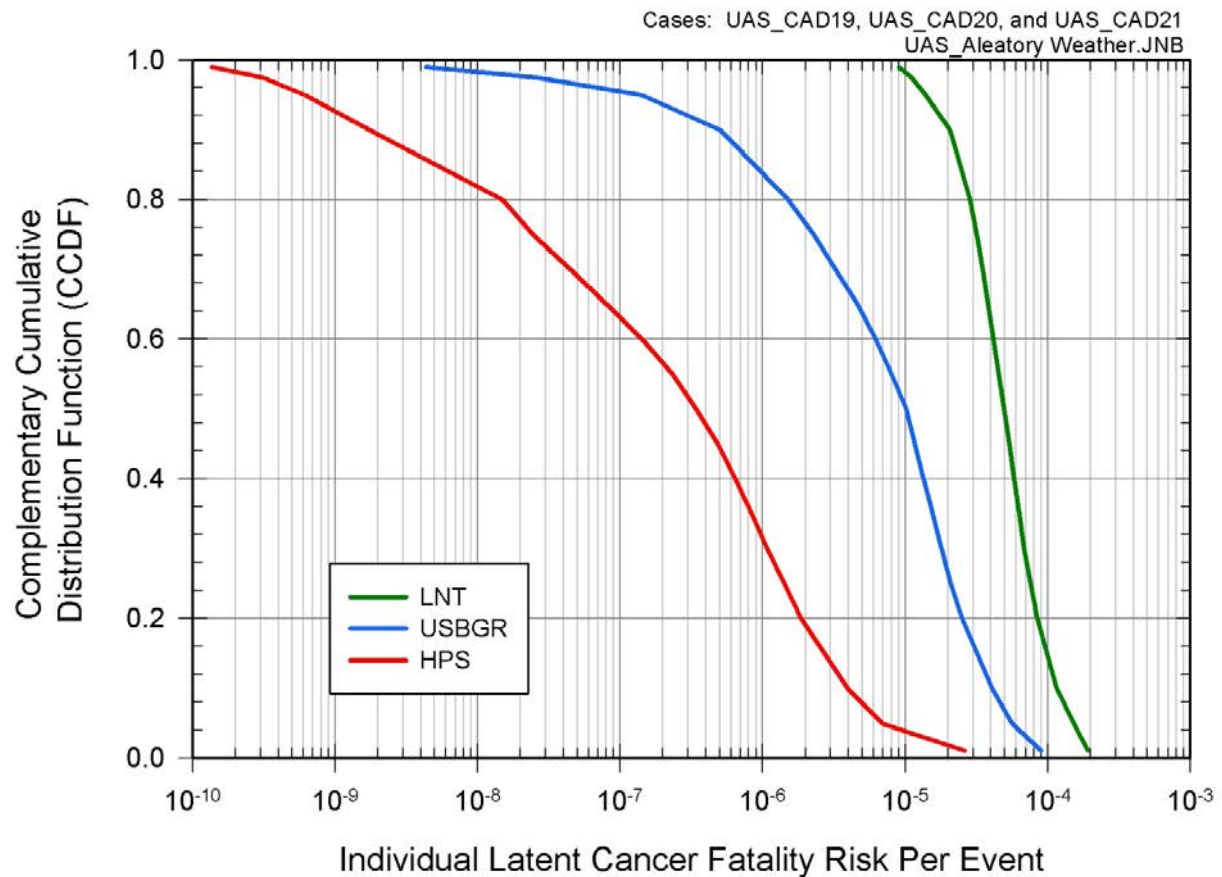


Figure 6.4-32 CCDF of conditional, mean, individual LCF risk (per event) within the 30-mile circular area for aleatory weather uncertainty for the LNT, USBGR, and HPS dose-response models using the SOARCA uncertainty analysis base case source term

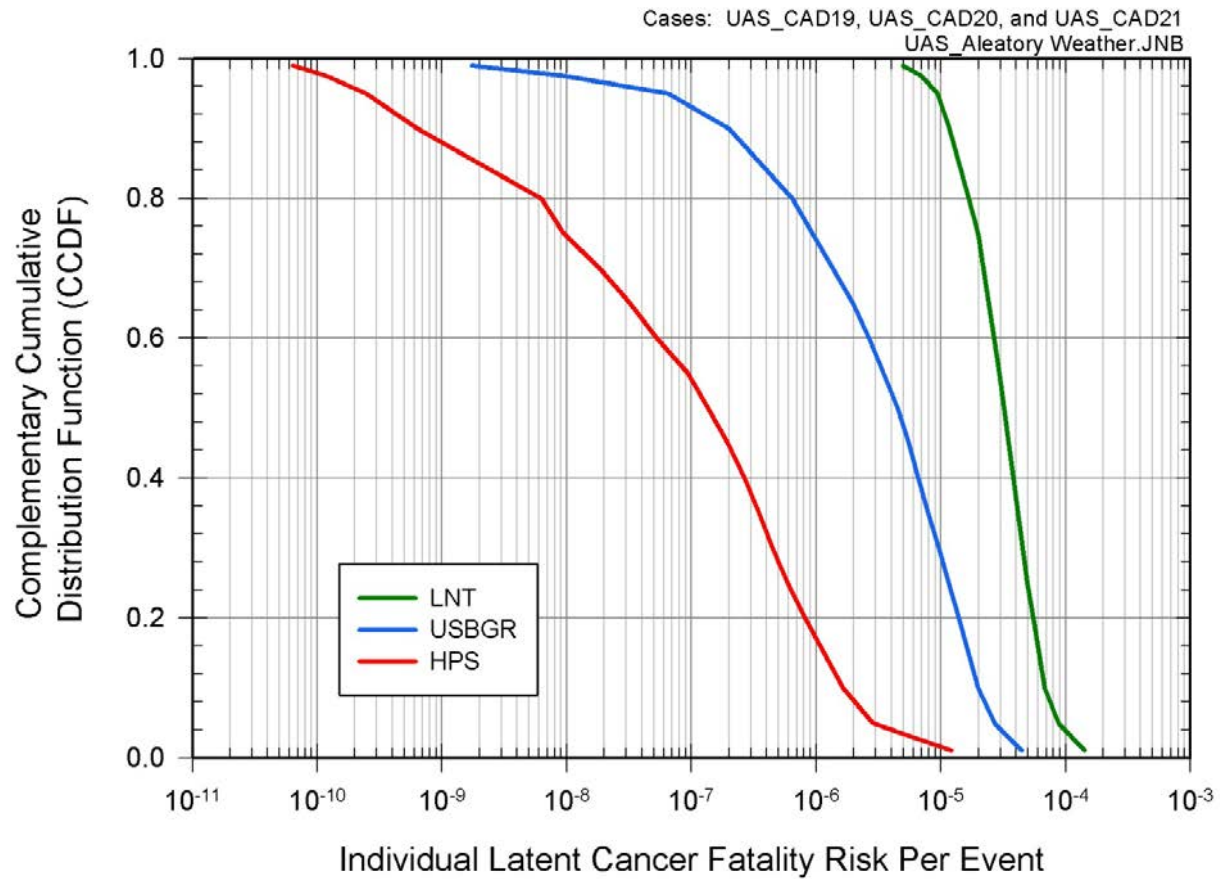


Figure 6.4-33 CCDF of conditional, mean, individual LCF risk (per event) within the 40-mile circular area for aleatory weather uncertainty for the LNT, USBGR, and HPS dose-response models using the SOARCA uncertainty analysis base case source term

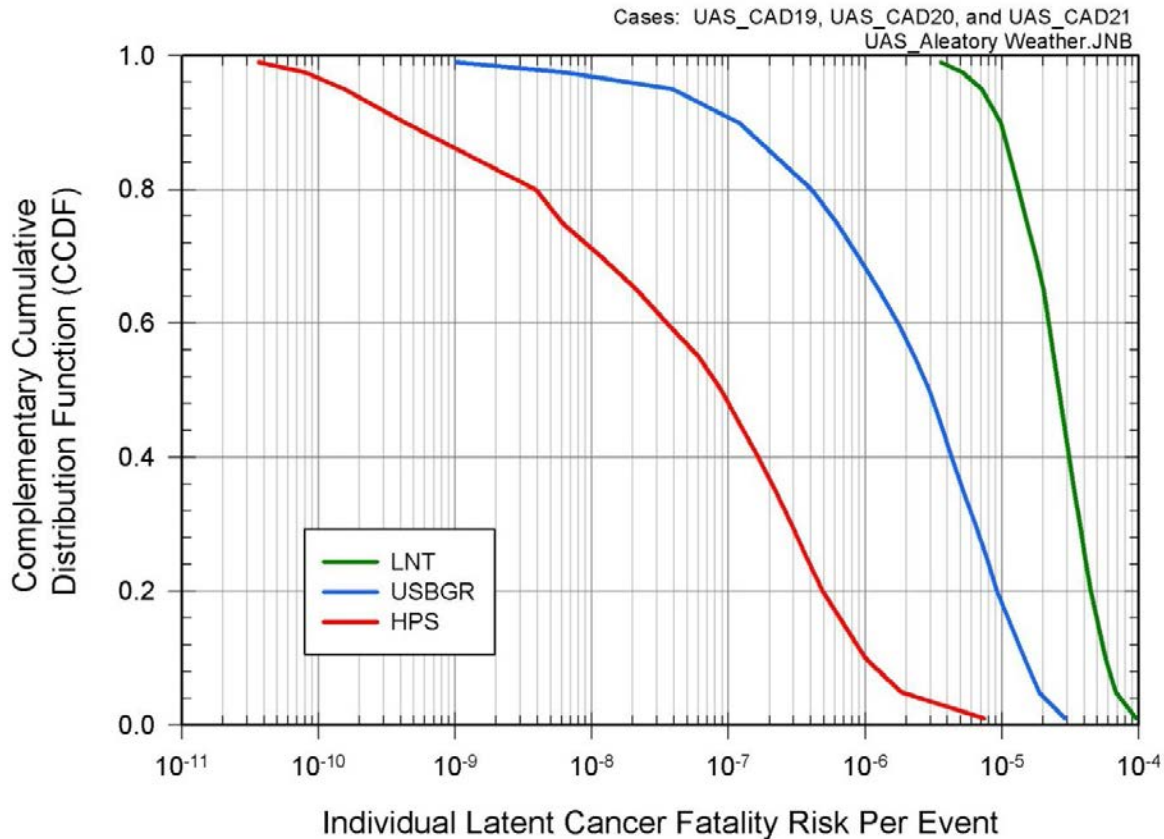


Figure 6.4-34 CCDF of conditional, mean, individual LCF risk (per event) within the 50-mile circular area for aleatory weather uncertainty for the LNT, USBGR, and HPS dose-response models using the SOARCA uncertainty analysis base case source term

Figure 6.4-35 through Figure 6.4-39 show the CCDF of aleatory weather uncertainty for the conditional, mean, individual LCF risk (per event) results using the USBRG dose-response model and the CCDF of the conditional, mean, individual LCF risk (per event) results for the MACCS CAP15 analysis within the 10-mile, 20-mile, 30-mile, 40-mile, and 50-mile circular areas, respectively. As seen in these figures, the aleatory weather uncertainty is bounded for the Replicate 1 Realization 62 and Replicate 1 Realization 170 source terms by the epistemic uncertainties within the MACCS CAP17 analysis, but not for the SOARCA uncertainty analysis base case source term. This indicates that the epistemic uncertainties for the conditional, mean, individual LCF risk results of the MACCS CAP15 analysis have a greater effect on the overall uncertainty than the aleatory weather uncertainty for the higher source term releases. The following trends are observed and are specific to the three source terms analyzed:

- The dose-truncation model has a larger contribution of the LCF risk from the emergency phase and earlier years of the long-term phase.
- The emergency phase risk for the smaller source term release has a larger effect on the overall LCF risk (see Table 6.4-36).

- The three source terms used in these analyses are bounded at the upper end of the CCDF individual LCF risk distribution for aleatory weather uncertainty by the epistemic uncertainties for the conditional, mean, individual LCF risk results of the MACCS CAP15 analysis, but are not bounded at the lower end of the distribution for individual LCF risk (see Figure 6.4-35 through Figure 6.4-39).

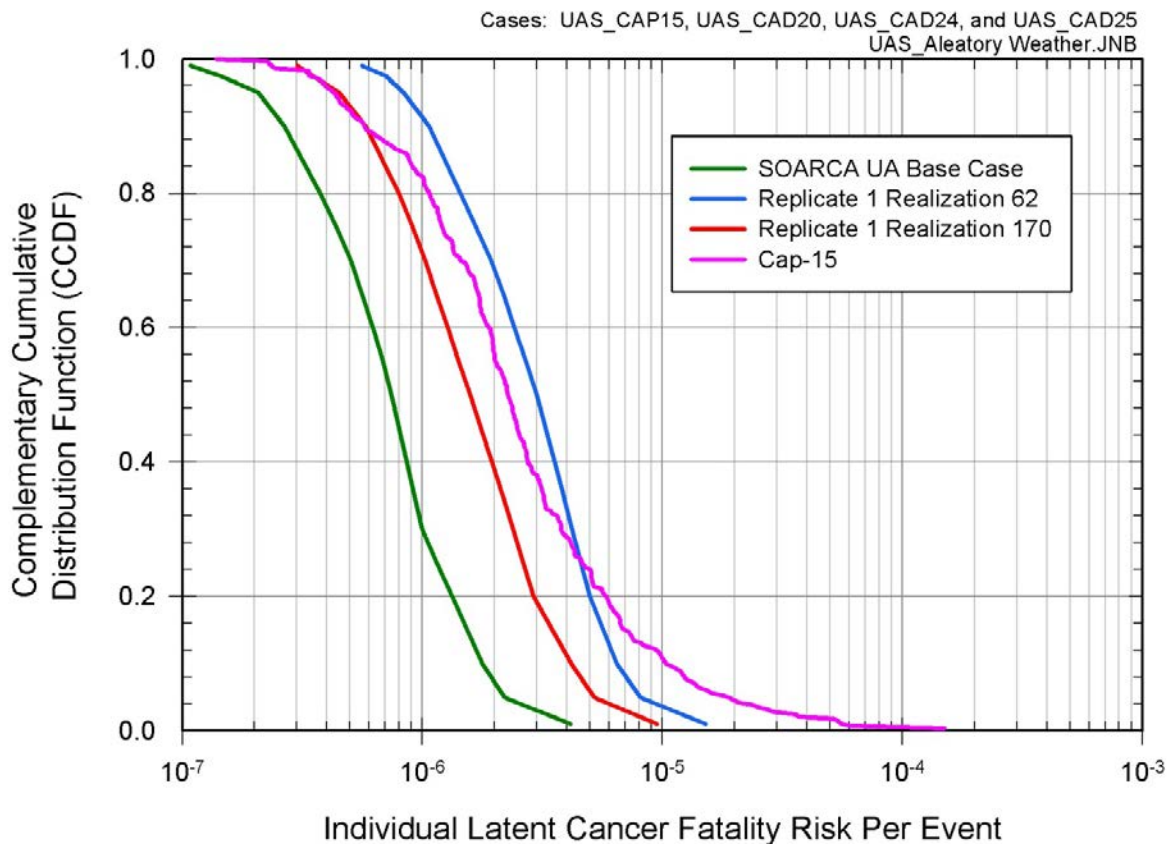


Figure 6.4-35 CCDF of conditional, mean, individual LCF risk (per event) within the 10-mile circular area for aleatory weather uncertainty using the USBGR dose-response model and the MACCS CAP15 analysis

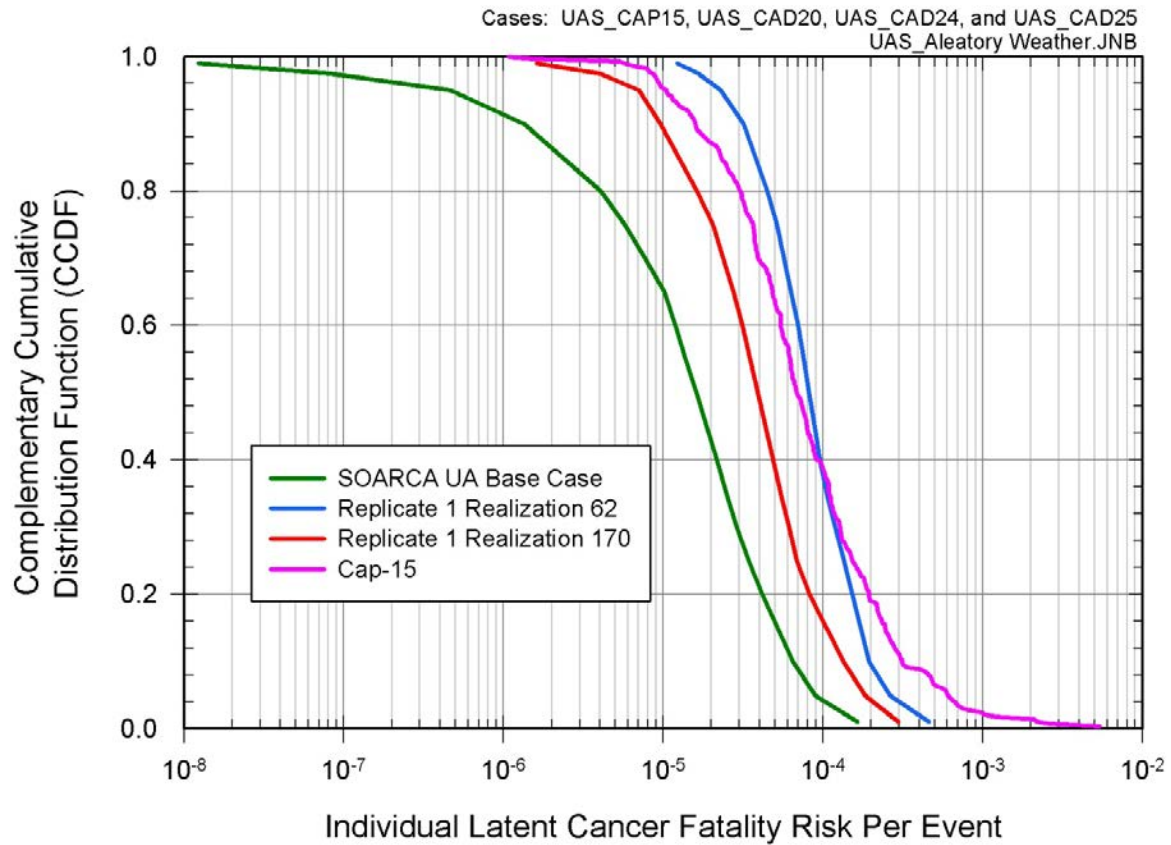


Figure 6.4-36 CCDF of conditional, mean, individual LCF risk (per event) within the 20-mile circular area for aleatory weather uncertainty using the USBGR dose-response model and the MACCS CAP15 analysis

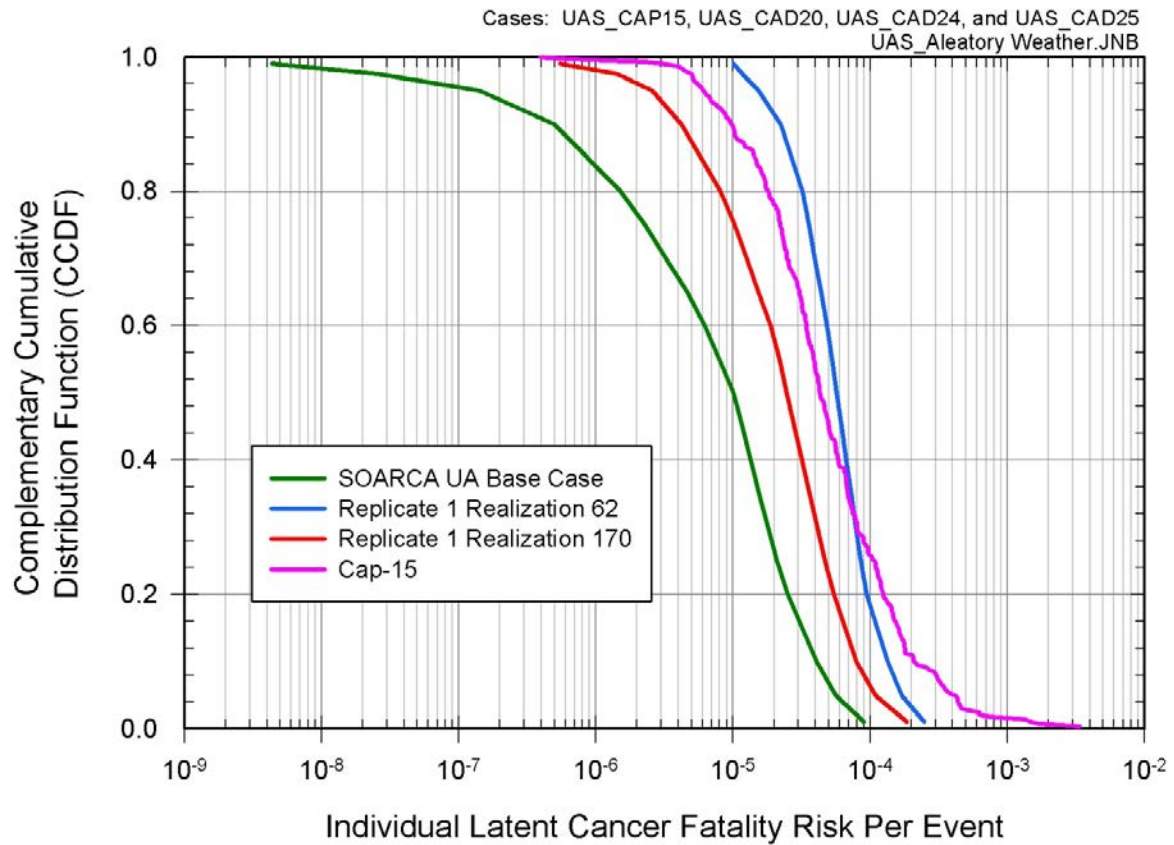


Figure 6.4-37 CCDF of conditional, mean, individual LCF risk (per event) within the 30-mile circular area for aleatory weather uncertainty using the USBGR dose-response model and the MACCS CAP15 analysis

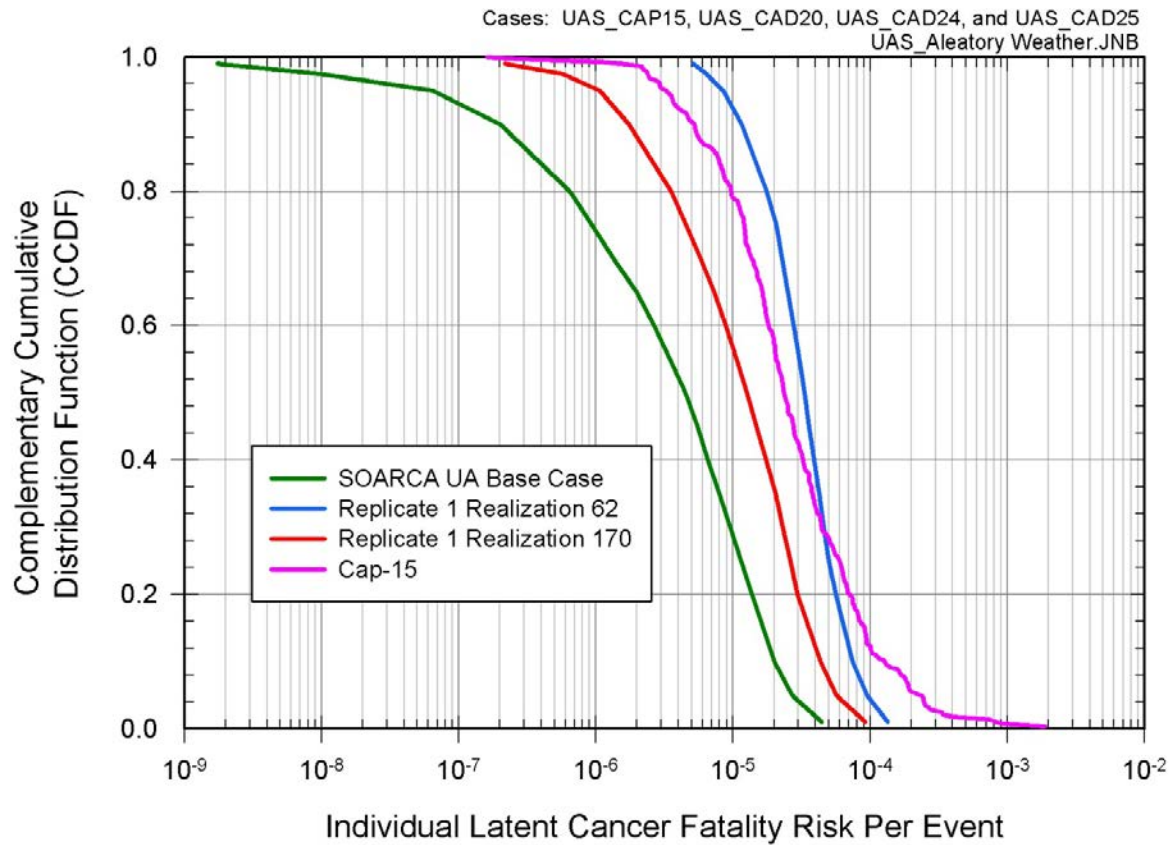


Figure 6.4-38 CCDF of conditional, mean, individual LCF risk (per event) within the 40-mile circular area for aleatory weather uncertainty using the USBGR dose-response model and the MACCS CAP15 analysis

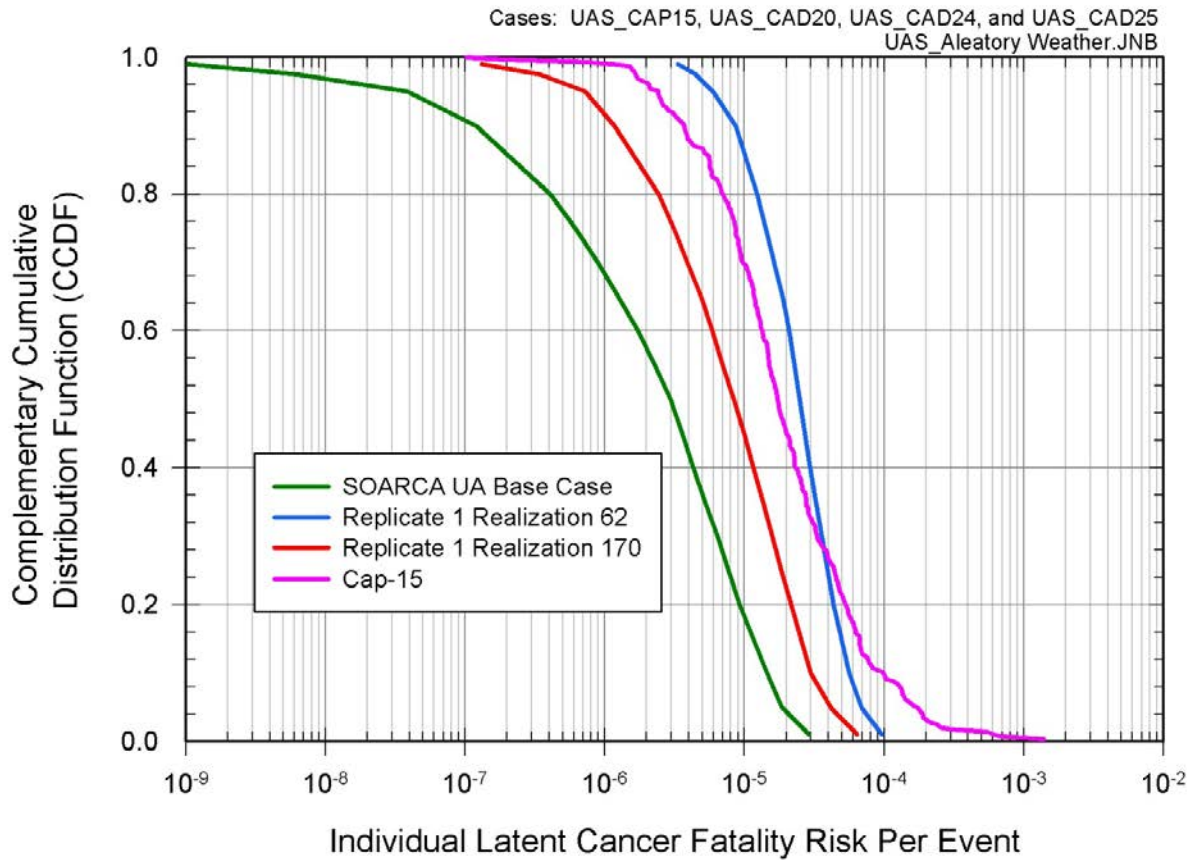


Figure 6.4-39 CCDF of conditional, mean, individual LCF risk (per event) within the 50-mile circular area for aleatory weather uncertainty using the USBGR dose-response model and the MACCS CAP15 analysis

Table 6.4-37 shows the ratio between the 5th and 95th percentile for the three source term's individual LCF risk per event results using the USBGR dose-response model and the conditional, mean, individual LCF risk (per event) results for the MACCS CAP15 analysis. As shown in Table 6.4-37, the aleatory weather uncertainty is narrower for all analyses than the epistemic uncertainty for the mean results of the MACCS CAP17 analysis within all circular areas for Replicate 1 Realization 62 and Replicate 1 Realization 170, but not for the SOARCA uncertainty analysis base case. From Figure 6.4-35 through Figure 6.4-39, the SOARCA uncertainty analysis base case source term consistently produced much lower individual LCF risk results than the conditional, mean, individual LCF risk results for the MACCS CAP15 analysis.

A determination of the upper bounding effects of aleatory weather uncertainty cannot be determined from these analyses. From Table 6.4-34, the selected source terms do not adequately represent the upper end of the range for the MACCS CAP15 analysis.

Table 6.4-37 Conditional, mean, individual LCF risk (per event) ratio for the MACCS aleatory uncertainty analyses using the USBGR dose-response model and the MACCS CAP15 analysis for specified circular areas

Radius of Circular Area (miles)	SOARCA UA Base Case	Replicate 1 Realization 62	Replicate 1 Realization 170	CAP15
10	11	10	12	45
20	190	12	26	58
30	400	11	43	70
40	420	11	53	73
50	480	12	58	72

Figure 6.4-40 through Figure 6.4-44 show the CCDF of aleatory weather uncertainty for the conditional, mean, individual LCF risk (per event) using the HPS dose-response model and the CCDF of the conditional, mean, individual LCF risk (per event) results for the MACCS CAP16 analysis within the 10-mile, 20-mile, 30-mile, 40-mile, and 50-mile circular areas, respectively. As shown in the figures, the aleatory weather uncertainty is bounded for the Replicate 1 Realization 62 source term by the epistemic uncertainties within the conditional, mean, individual LCF risk (per event) results for the MACCS CAP17 analysis, but not for the SOARCA uncertainty analysis base case and Replicate 1 Realization 170 source terms. This indicates that the epistemic uncertainties for the conditional, mean, individual LCF risk results of the MACCS CAP16 analysis have a greater effect on the overall uncertainty than the aleatory weather uncertainty for a larger release, but not for smaller ones. The trend observations are similar to those discussed for the USBGR dose-response model. However, these results also indicate that a higher dose-truncation threshold is more sensitive to aleatory weather uncertainty.

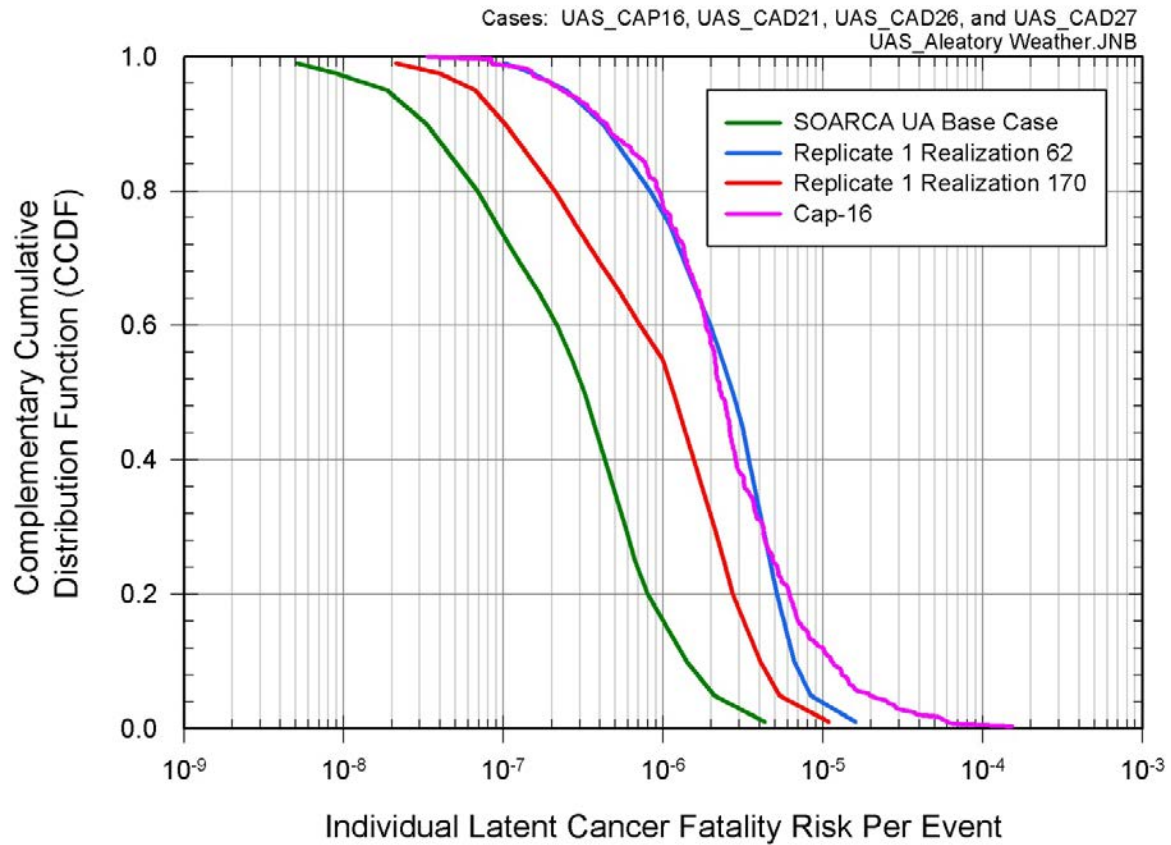


Figure 6.4-40 CCDF of conditional, mean, individual LCF risk (per event) within the 10-mile circular area for aleatory weather uncertainty using the HPS dose-response model and the MACCS CAP16 analysis

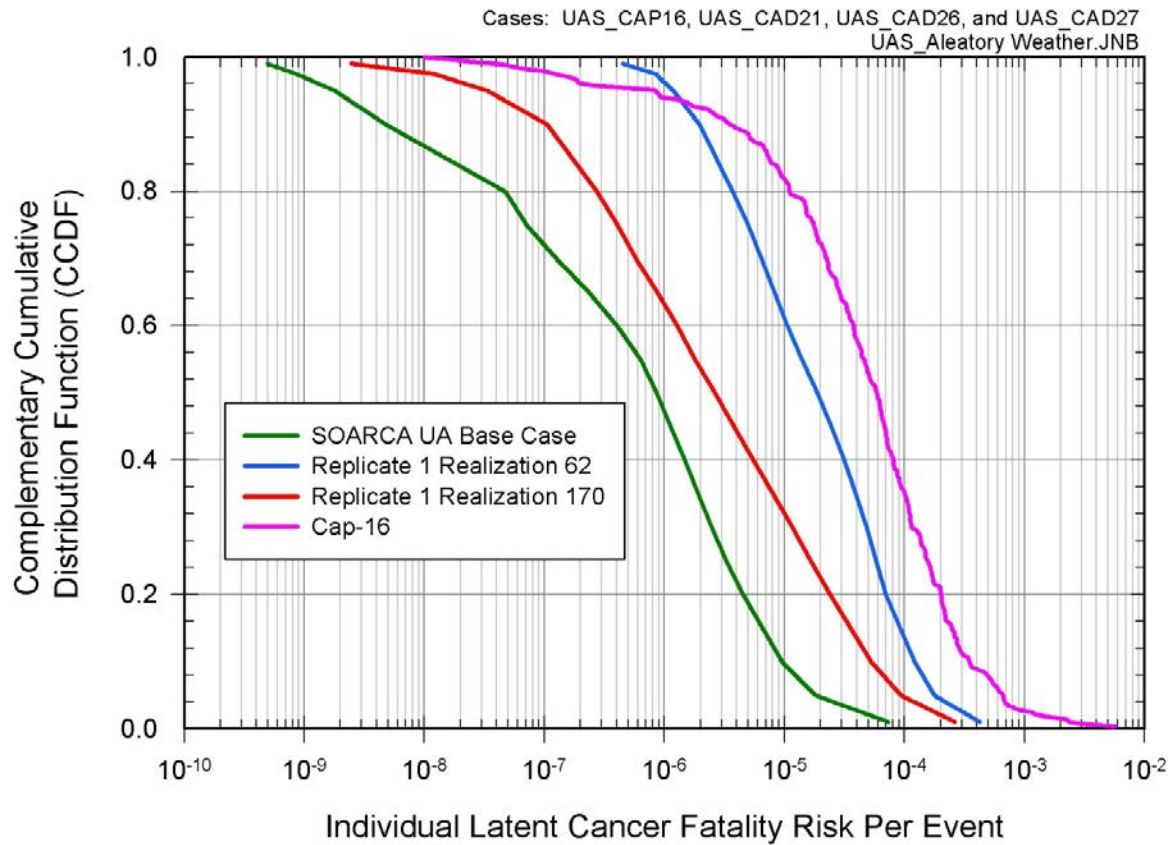


Figure 6.4-41 CCDF of conditional, mean, individual LCF risk (per event) within the 20-mile circular area for aleatory weather uncertainty using the HPS dose-response model and the MACCS CAP16 analysis.

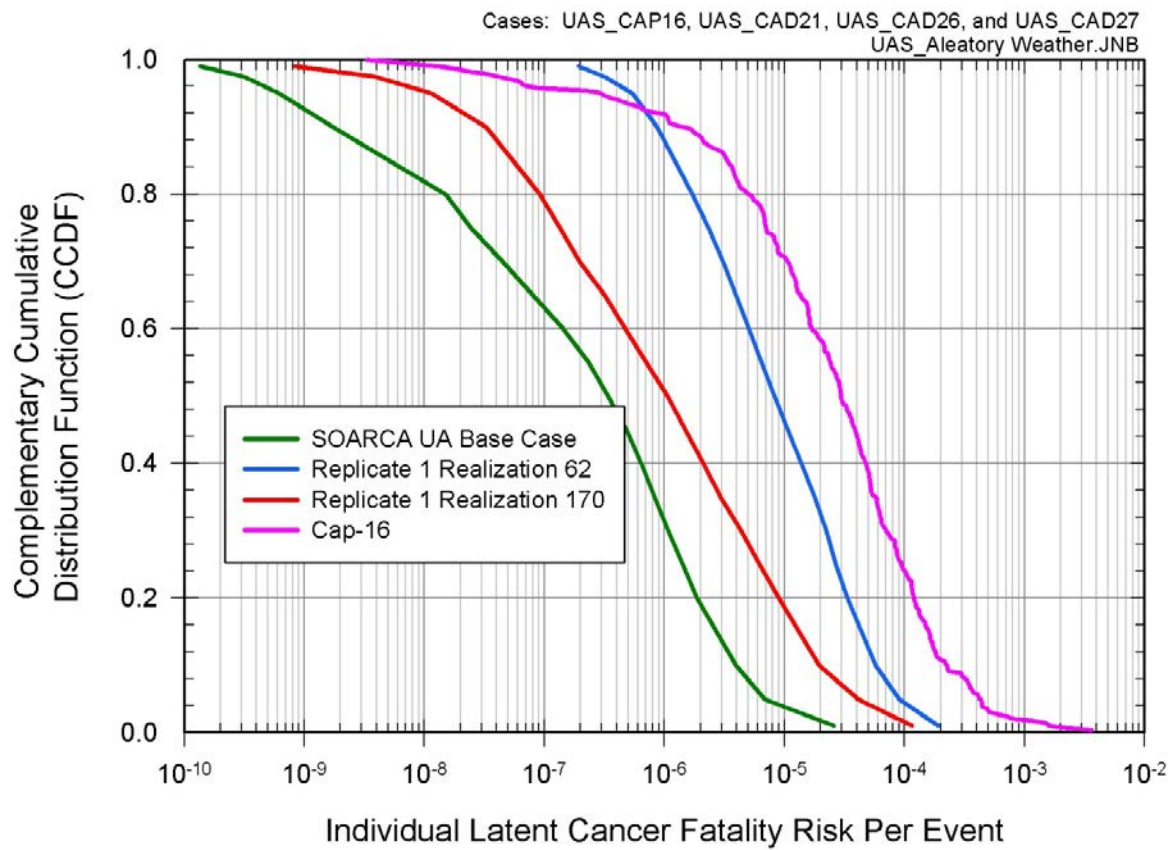


Figure 6.4-42 CCDF of conditional, mean, individual LCF risk (per event) within the 30-mile circular area for aleatory weather uncertainty using the HPS dose-response model and the MACCS CAP16 analysis

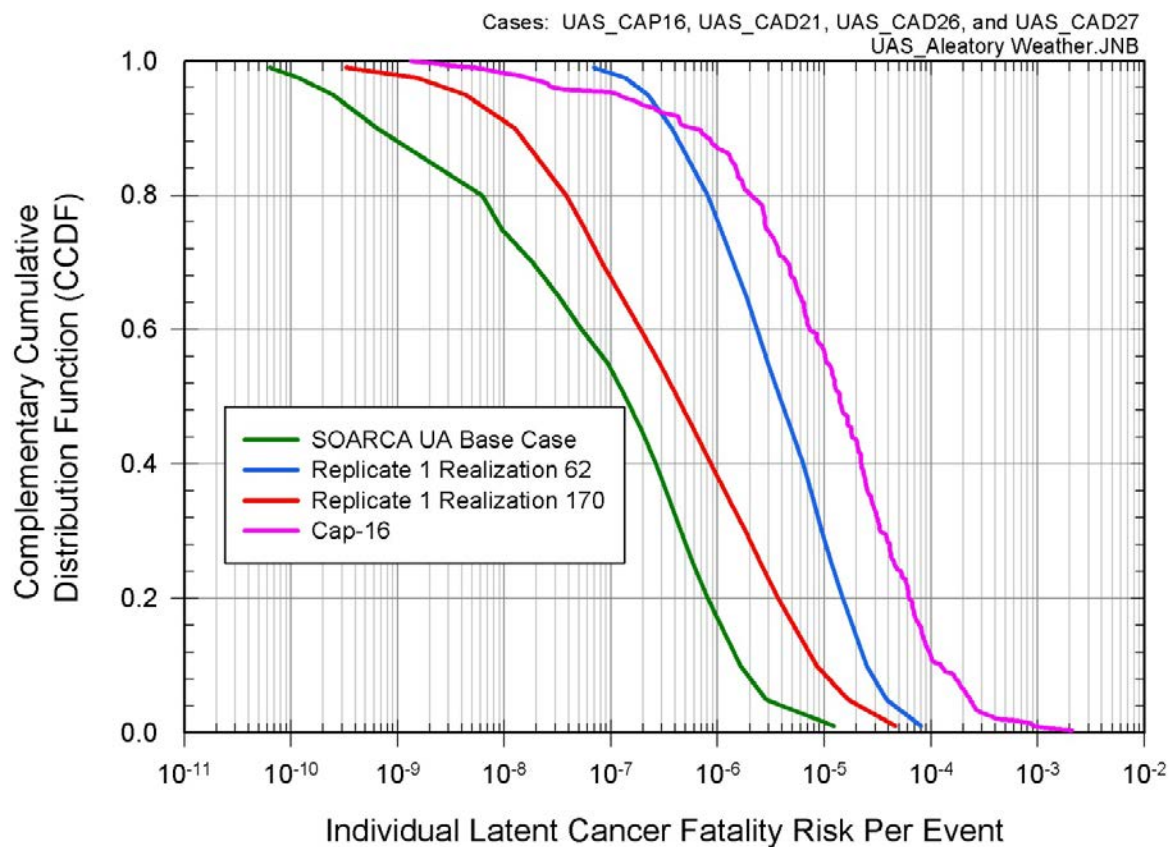


Figure 6.4-43 CCDF of conditional, mean, individual LCF risk (per event) within the 40-mile circular area for aleatory weather uncertainty using the HPS dose-response model and the MACCS CAP16 analysis

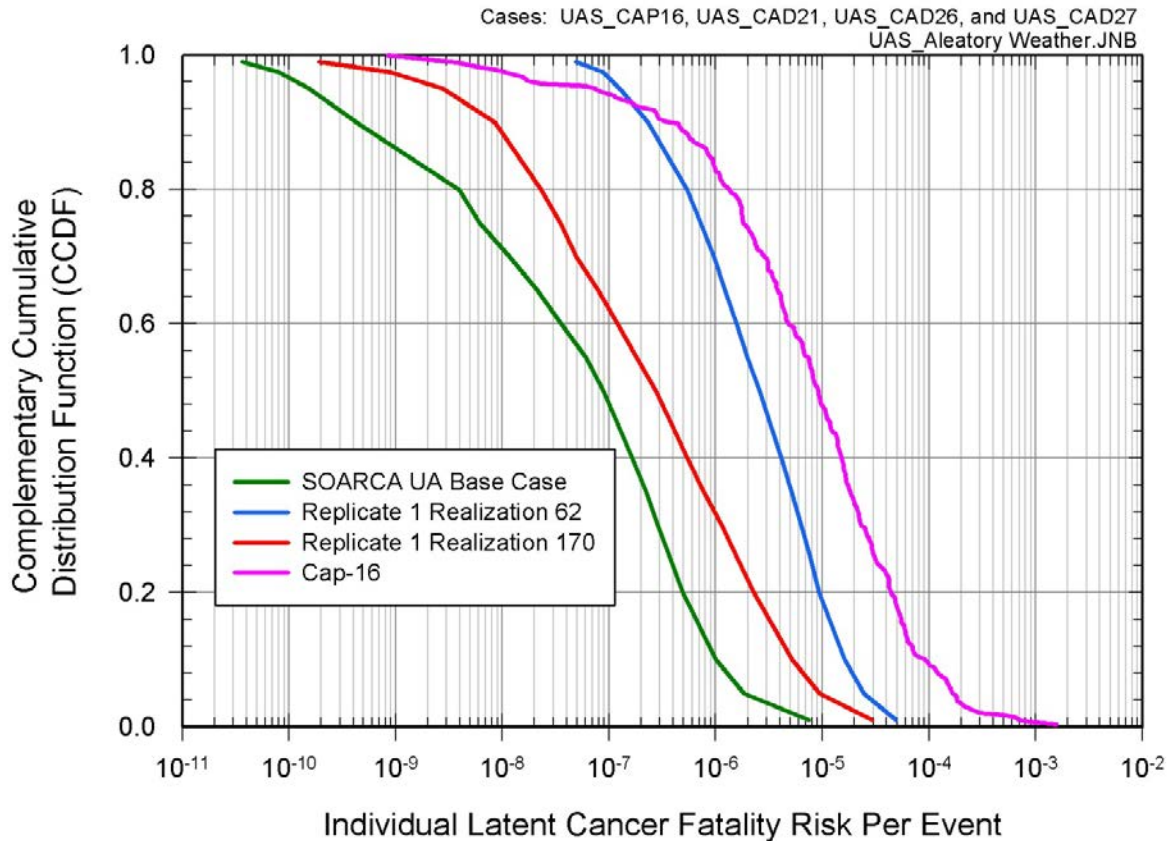


Figure 6.4-44 CCDF of conditional, mean, individual LCF risk (per event) within the 50-mile circular area for aleatory weather uncertainty using the HPS dose-response model and the MACCS CAP16 analysis.

Table 6.4-38 shows the ratio between the 5th and 95th percentile for the three source term's conditional, mean, individual LCF risk (per event) results using the HPS dose-response model and the MACCS CAP16 analysis. As shown in this table, the aleatory weather uncertainty for Replicate 1 Realization 62 is narrower than the epistemic uncertainty for the conditional, mean, individual LCF risk (per event) results of the MACCS CAP17 analysis within all circular areas, but this is not true for the SOARCA uncertainty analysis base case and Replicate 1 Realization 170. From Figure 6.4-40 through Figure 6.4-44, the SOARCA uncertainty analysis base case and Replicate 1 Realization 170 source terms consistently produced lower individual LCF risk results than the conditional, mean, individual LCF risk results for the MACCS CAP16 analysis.

A determination of the upper bounding effects of aleatory weather uncertainty cannot be determined from these analyses. From Table 6.4-35, the selected source terms do not adequately represent the upper end of the range for the MACCS CAP16 analysis.

Table 6.4-38 Conditional, mean, Individual LCF risk (per event) ratio for the MACCS aleatory uncertainty analyses using the HPS dose-response model and the MACCS CAP16 analysis for specified circular areas

Radius of Circular Area (miles)	SOARCA UA Base Case	Replicate 1 Realization 62	Replicate 1 Realization 170	CAP15
10	110	34	80	80
20	10,000	150	2,800	780
30	11,000	170	3,600	1,400
40	12,000	180	3,900	1,900
50	12,000	190	3,400	2,100

7. SUMMARY OF RESULTS AND CONCLUSIONS

This analysis is an integrated look at uncertainties in MELCOR accident progression and MACCS offsite consequence analyses for the SOARCA Peach Bottom unmitigated LTSBO scenario and demonstrates uncertainty analysis methodology that can be used in future source term, consequence, and Level 3 PRA studies. This work identified key uncertainties in the input parameters used in the SOARCA deterministic MELCOR and MACCS models and quantified the relative importance of each uncertain input on potential accident consequences. This quantitative uncertainty analysis provides measures of the effects, both individually and in interaction with other parameters, of each of the selected uncertain parameters. The study also provides phenomenological insights on the effects of important inputs and parameters used in the SOARCA calculations [1]. Specifically, this uncertainty analysis helps:

- Identify which uncertain important parameters and phenomena are driving the variability in SOARCA model results.
- Verify and validate the SOARCA models through exploration of unexpected or non-physical phenomena in the distributions of results.
- Provide an assessment of the regression techniques and uncertainty analysis approach.
- Provide a basis for future work.

This section summarizes the results of the uncertainty analyses including both the quantitative and qualitative insights with respect to the key uncertain parameters and phenomena influencing the source term and consequence analysis results.

7.1 Source Term Analyses

Performing the source term calculations of the Peach Bottom unmitigated LTSBO uncertainty analysis revealed three groups of similar accident progression within the Peach Bottom unmitigated LTSBO scenario: (1) early stochastic failure of the cycling SRV, which was the SOARCA scenario in NUREG-1935; (2) thermal failure of the SRV without MSL creep rupture; and (3) thermal failure of the SRV with MSL creep rupture. Several influences were found to strongly affect the magnitude and timing of fission product releases to the environment, as summarized below.

Most notably, with respect to the magnitude of the source term (i.e., the magnitude of cesium and/or iodine releases), the following were found to be influential:

- Whether the sticking open of the SRV (the lowest set-point SRV) occurs before or after the onset of core damage, with higher releases if after core damage,
- Whether a MSL creep rupture occurs, with higher releases if MSL rupture occurs due to fission products being vented straight to the drywell and bypassing wetwell scrubbing,
- The amount of cesium chemisorbed as CsOH onto the stainless steel of RPV internals; more chemisorption relating to less cesium release to the environment in high-temperature scenarios such as MSL rupture,

- Whether core debris relocates from the RPV to the reactor cavity all at once or over an extended period of time with relocation all at once leading to lower releases to the environment,
- The degree of oxidation, primarily fuel-cladding oxidation, occurring in-vessel with greater oxidation resulting in larger releases, and
- Whether a surge of water from the wetwell up onto the drywell floor occurs at drywell liner melt-through with the development of surge water leading to larger releases.

The sampled parameters shown to strongly or meaningfully influence the magnitude of the fission product releases, because they contribute to the important phenomena noted above, were:

- The expected number of cycles an SRV can undergo before failing to reclose (i.e., remain in the fully open position),
- The chemical form of cesium (i.e., the amount of cesium as CsOH opposed to as Cs_2MoO_4),
- The size of the breach in the drywell liner resulting from core debris contacting and melting through the liner,
- The fractional open area of an SRV after it has failed to reseal because of overheating,
- The time-at-temperature criterion specified for loss of “intact” fuel rod geometry, and
- The temperature at which oxidized cladding mechanically fails.

With respect to release timing, the strongest influences identified were:

- When the RCIC system failed,
- When the SRV failed to reseal, and
- What the open fraction of the SRV was when it failed to reseal given a thermally-induced failure.

The sampled parameters shown to strongly or meaningfully influence the timing of releases, by affecting the timing influences noted above, were:

- The time taken to exhaust the station batteries (i.e., the sole determinate of when the RCIC system fails),
- The number of cycles an SRV can undergo before failing to reclose (i.e., remain in the fully open position), and
- The fractional open area of an SRV after it has failed to reseal because of overheating.

The means by which fission products release to the environment in the MELCOR source term calculations are well characterized by what is observed for the release of cesium. Most of the cesium released to the environment in the calculations undergoes the following sequential processes:

- (1). Release from the dismantling core as CsOH, CsI, or Cs₂MoO₄ vapor.
- (2). Condensation into aerosols.
- (3). Gravitational settling onto reactor internals.
- (4). Re-vaporization after RPV lower head failure over approximately 24 hours.
- (5). Re-condensation into aerosols that are carried out a breach in the drywell liner resulting from core debris contacting and melting through the liner.

The most influential sampled parameter identified in the uncertainty analysis affecting the re-vaporization of cesium aerosols settled on reactor internals is the number of cycles an SRV can undergo before failing to reclose: a smaller number of cycles leading to less re-vaporization (and less release to the environment) and a larger number of cycles leading to more re-vaporization (and more release to the environment). While the importance of this parameter in determining whether or not MSL creep rupture occurs was not previously known, the dramatic influence of this parameter was not anticipated going into the uncertainty analysis.

An unexpected influence that arose in the analysis was that specifying the cesium inventory in the core in the form of CsOH (as opposed to Cs₂MoO₄) often led to smaller releases of cesium to the environment. This was surprising in that the lower vapor pressure dependence on temperature of CsOH than of Cs₂MoO₄ might intuitively suggest that CsOH would transport more readily. What led to a contradiction of intuition was the process of chemisorption where cesium bonds with impurities in the stainless steel of reactor internals. This process has a strong dependence on temperature, with higher temperatures yielding more chemisorption. In calculations where much of the reactor core degradation occurred with the reactor at pressure (i.e., where the lowest set-point SRV cycled as designed for a relatively long period before failing to reseal), temperatures in the RPV were higher and chemisorption potential was greater. In these calculations, if cesium were specified in the core predominantly as CsOH, more than half of the initial core inventory deposited on reactor internals through chemisorption. This deposition was permanent, making the absorbed cesium unavailable for transport and release to the environment. Previously, it was thought that cesium in the form of CsOH would lead to larger releases, but in fact for high temperature scenarios, CsOH resulted in smaller releases and thus limited the total effect of higher temperatures.

Another surprising influence in the analysis was the surging of water up from the wetwell to the drywell floor. This occurred in approximately half of the MELCOR calculations in association with large breaches¹⁷ (> 0.2 m²) in the drywell liner caused by core debris contacting the liner and melting through it. Large breaches resulted in larger depressurizations of the containment and a greater pressure differential between the drywell and the wetwell during the

¹⁷ Breach size is a user-specified input in the MELCOR model and this was included as an uncertain parameter in this study.

depressurizations. The suddenly superheated state of the water in the wetwell contributed to the pressure differentials in the presence of which some of the water flashed to steam. The pressure differentials overwhelmed the vacuum breakers between the wetwell and the drywell and contaminated water surged out of the wetwell. Most of the water surging from the wetwell flows from the drywell to the reactor building through the breach in the drywell liner.

In the SOARCA Peach Bottom unmitigated LTSBO scenario, two operator actions are credited: (1) the operators manually opening an SRV; and (2) the operators taking manual control of RCIC. Because there was no formal human reliability analysis for SOARCA, the timing¹⁸ of these operator actions were not included as uncertain inputs in the uncertainty analysis. Instead, the influence of the timing of the opening of an SRV was investigated through a separate sensitivity study. The influence on source term for operator action through the sensitivity calculations identified a significant importance for the only operator action considered; the time at which the operators manually opened an SRV. This manual action was assumed to occur at one hour in the SOARCA calculation [1]. Sensitivity calculations were carried out as part of the uncertainty analysis that varied this time the operator took action and included a calculation where the manual action was not taken at all. Substantial increases in iodine and cesium releases to the environment occurred in the 0.5-hr calculation. A significant increase in iodine release and a noticeable increase in cesium release also occurred for the calculation without the operator action to manually open the SRV. In both these cases, RCIC operation was negatively impacted early in the accident progression by a loss of sufficient steam to operate the RCIC turbine. In the 0.5-hr calculation, the RPV depressurized severely upon opening the SRV. In the calculation where the SRV was not opened, over-cycling of the SRV early in the accident sequence caused it to stick open and depressurize the RPV, which interrupted RCIC operation. The impacts to RCIC operation led to more extensive fuel-cladding oxidation in the RPV, elevated temperatures of reactor internals, and greater late revaporization from the hotter internals of previously accumulated deposits of iodine and cesium. It is worth noting that these sensitivity calculations may have led to unrealistic scenarios. For example, with respect to the calculation where the operators were assumed to open an SRV at 0.5 hours, it is unlikely that the operators would allow reactor pressure to drop sufficiently low to fail RCIC; instead, they would operate the valve so that sufficient steam pressure is maintained to drive the RCIC turbine. Similarly, given the known importance of manual depressurization in this scenario (i.e., identified as an important insight for BWRs in NUREG-1150 more than 20 years ago), the case where the SRV was not opened at all is likely to be a very low probability.

7.2 Consequence Analyses

The results of the consequence analyses are presented in terms of risk to the public for each of the realizations analyzed using the Peach Bottom unmitigated LTSBO MELCOR and MACCS models. All results are presented as conditional risk (i.e., assuming that the accident occurs), and show the conditional risks to individuals as a result of the accident (i.e., latent cancer fatality (LCF) risk per event or early-fatality risk per event).

The risk metrics are LCF risk and early-fatality risks to residents in circular regions surrounding the plant. The risks are mean values (i.e., expectation values) over sampled weather conditions representing a year of meteorological data and over the entire residential population within a

¹⁸ In the SOARCA best estimate study (NUREG-1935), the timing of these actions is based on emergency operating procedures and interviews with plant personnel.

circular region. The risk values represent the projected number of fatalities divided by the population, in other words, individual latent cancer fatality risk. LCF risks are calculated for a set of dose-response models, which are (1) LNT, (2) a linear with threshold dose-response model where the threshold is mean U.S. natural background plus mean medical radiation as a dose-truncation level (USBGR), and (3) a linear with threshold dose-response model where the threshold is based on an HPS Position Statement. The HPS Position Statement suggests that health effects not be quantified below an annual rate of 5 rem/yr provided that the total excess dose over a lifetime does not exceed 10 rem. These risk metrics account for the distribution of the population within the circular region and for the interplay between the population distribution and the wind rose probabilities.

For the LCF risk results, the emergency phase is defined as the first seven days following the initial release to the environment. The long-term phase is defined as the time following the emergency phase (i.e., there is no intermediate phase in the MACCS modeling). The long-term phase risk (i.e., the LCF risk contribution beyond the emergency phase) dominates the total risks (i.e., 100% of all realizations have a long-term risk contribution that is greater than 50% of the total risk) within the EPZ for the uncertainty analysis when the LNT dose-response assumption is made. No realization resulted in an emergency phase risk contribution greater than 48% of the total risk. The emergency phase risk within the EPZ is entirely to the 0.5% of the population who are assumed not to evacuate. These results further emphasize the benefits of evacuating the EPZ. The long-term risks are controlled by the habitability (return) criterion, which is the dose rate at which residents are allowed to return to their homes following the emergency phase. For Peach Bottom, the habitability criterion used is an annual dose rate of 500 mrem/yr¹⁹. For comparison, 55% of all realizations have a long-term risk contribution greater than 50% of the total risk within a 20-mile radius (i.e., 45% of the realizations have an emergency phase risk which contributes to greater than 50% of the total risk). Additionally, 53%, 48%, and 46% of all realizations have a long-term phase risk contribution greater than 50% of the total risk within a 30-mile, 40-mile, and 50-mile radius, respectively.

For the LCF risk results, when the 10-mile and 20-mile circular area statistics are compared, there is a larger influence of the emergency phase for the 20-mile region compared to the 10-mile region, for which nearly all of the population evacuated. This indicates that variations in doses during the emergency phase are greater than variations in dose during the long-term phase.

Unlike the SOARCA analyses in NUREG/CR-7110 Volume 1 and Volume 2, a non-zero early-fatality risk was calculated beyond 2.5 miles. 11% of the 865 MACCS realizations investigated resulted in a nonzero early-fatality risk per event out to 1.3 miles and 0.3% of the 865 realizations that resulted in a nonzero early-fatality risk per event out to 10 miles. In other words, a select few realizations result in a large enough source term that when combined with specific weather trials and LHS sampled uncertainties in the MACCS calculation result in calculable early-fatality risks out to the boundary of the EPZ. A more detailed discussion of this is provided in Section 6.2.4.

The early-fatality risks are zero for 87% of all realizations at all specified circular areas. This is because in most cases the release fractions are too low to produce doses large enough to exceed the dose thresholds for early fatalities, even for the 0.5% of the population that are

¹⁹ Per Pennsylvania State guidelines.

modeled as refusing to evacuate. The largest value of the mean, acute exposure for the closest resident (i.e., 1.6 to 2.1 kilometers from the plant) for many of these replicates is about 0.3 gray (Gy) to the red bone marrow, which is usually the most sensitive organ for early fatalities, but the minimum acute exposure that can cause a early fatality is about 2.3 Gy to the red bone marrow. The calculated exposures for these scenarios are all below this threshold.

At 2.5 miles and beyond the mean result is greater than the 95th percentile. This is due to the few number of nonzero early-fatality risks (i.e., less than 6% of the realizations) at these distances. In theory, a distribution can be skewed enough so that the mean is greater than the 95th percentile. An instance of this is an exponential of a value sample from a log-normal distribution. For these cases the mean may be higher than the 99th percentile, because it is driven by few nonzero values. This is the same thing that happens here in practice for early-fatality risk beyond 2.5 miles.

The nonzero early-fatality risk results decreases from 11% of the total early-fatality risk results at 1.3 miles to 4% of the total early-fatality risk results at 3.5 miles. Beyond the 3.5 mile circular area, the source terms that generate nonzero early-fatality risks drop below 2%. For distances beyond 2.5 miles, the 95th percentile statistics are not well converged (i.e., greater than an order of magnitude difference). Even at a 2-mile radius, the 95th percentiles differ up to 70%.

In the 865 realizations, the highest absolute early-fatality risk calculated is 10^{-10} pry²⁰ with a mean of 1.4×10^{-12} at 1.3 miles (i.e., recall the Peach Bottom LTSBO core damage frequency is 3×10^{-6} pry).

7.2.1 Regression Summary for LCF Risks

The regression techniques used to perform a sensitivity analysis for the consequence results were conducted with the 865 source terms evaluated with MELCOR using a set of 21 uncertain input variables and using 350 MACCS individual uncertain input variables in 20 parameter groups. The results of the regression analyses of mean, individual LCF are discussed in Section 6.2.3.1. Within the 10-mile circular area, the regression techniques indicate a confidence level >72%. Beyond the 10-mile circular area, each of the regression techniques indicate a confidence level ≥42% with the recursive partitioning analysis consistently being the highest with a confidence level of 71% to 64%.

Based on this, the statistical regression techniques used to determine the important input parameters for LCF risk are considered adequate for this work. While other regression techniques (e.g., ACOSSO or Gaussian process) not used in this study may provide additional insights, the four selected regression analyses cover a large spectrum of potential interactions and influences. Additional regression methods can be employed and may provide more insights in the analyses by confirming the influence of some parameters or perhaps capturing other kinds of interactions not considered in this work. However, since the monotonic (i.e., rank regression) and non-monotonic (i.e., quadratic, recursive partitioning, and MARS) regression techniques agree reasonably well, using more advanced methods was considered unnecessary.

²⁰ Estimated risks below 10^{-7} per reactor year should be viewed with caution because of the potential impact of events not studied in the analyses, and the inherent uncertainty in very small calculated numbers.

All regression methods at each of the circular areas consistently rank the following, respectively, as the most important input parameters:

- MACCS dry deposition velocity (VDEPOS), which involves a variety of mechanisms that cause aerosols to deposit, including gravitational settling, impaction onto terrain irregularities, including buildings and other manmade structures, and Brownian diffusion,
- the MELCOR SRV stochastic failure probability (SRVLAM), an important MELCOR parameter for source term determination, and
- the MACCS 'residual' cancer risk factor (CFRISK–Residual) which is used for estimating residual cancers not related to the seven organ-specific cancers that were used in SOARCA.

Some additional parameters also consistently show some level of importance at all circular areas. These are the following:

- The MELCOR fuel failure criterion, which is the time endurance of the upright, cylindrical configuration of fuel rod bundles,
- The MELCOR drywell liner melt-through open area flow path (FL904A), and
- The MACCS 'residual' dose and dose-rate effectiveness factor (DDREFA–Residual), which is based on BEIR V risk factors for estimating health effects to account for observed differences between low and high dose rates.

The three MELCOR uncertain parameters, SRVLAM, fuel failure criterion FL094A, ultimately account for the majority of the uncertainty in the source term inputs (release magnitude) for the consequence analysis.

7.2.2 Regression Summary for Early-Fatality Risk

The conditional, mean, individual early-fatality risk regression analyses are discussed in Section 6.2.3.2. Because fewer than 3% of all the MACCS uncertainty analysis realizations resulted in nonzero early-fatality risk at or beyond 5 miles, these circular areas are not included in the results. The regression did not produce any reliable results at these distances. On the other hand, the regression analyses produce non-monotonic confidence levels ($\geq 58\%$) at a distance at or within 2 miles. At these distances, approximately 13% of all MACCS realizations have a nonzero early-fatality risk, and the top one or two input parameters are correlated to a high confidence level. The rank regression analysis consistently produces a poor result, indicating that there is a non-linear relationship between the important input variables and early fatality risk.

Beyond 2 miles, at least one of the non-monotonic regression techniques produces poor results. Between the 2.5-mile and 3.5-mile circular areas, approximately 7% of all MACCS realizations produce nonzero early-fatality risks. This small amount of nonzero data produces a set of important input parameters with low confidence. Again, the rank regression analysis consistently produces a poor result, indicating that there is a non-linear relationship between the important input variables.

Based on these analyses, the statistical regression techniques used to determine the important input parameters for early-fatality risk are considered adequate for the distances reported in this work.

For the circular areas less than 2 miles, the non-rank regression methods consistently rank the following as the most important input variables, respectively:

- The MACCS wet deposition model (CWASH1), which is an important phenomenon that is very effective at rapidly depleting the plume and can produce concentrated deposits on the ground,
- the MELCOR SRV stochastic failure probability (SRVLAM), which is an important MELCOR parameter for source term determination,
- the MELCOR SRV open area fraction (SRVOAFRAC), which is an important MELCOR parameter for source term magnitude and timing,
- the MACCS early health effects threshold and beta (shape) factor for red bone marrow (EFFTHR-Red Marrow and EFFACB-Red Marrow), which is the most sensitive organ for the potential of early health effects, and
- the MACCS linear, crosswind dispersion coefficient (CYSIGA), which defines how concentrated the radionuclides are within the plume (i.e., the more concentrated the radionuclides are within the plume; the higher the possible dose to an individual within the plume).

Additional variables also consistently show some level of importance for circular areas less than 2 miles. These additional input variables include the following:

- The MACCS amount of shielding between an individual and the source of groundshine during normal activities for the non-evacuated residents (GSHFRAC-Normal),
- The MACCS evacuation delay for Cohort 5 (DELTVA-Cohort 5); Cohort 5 is the evacuation tail of the general public evacuation, and
- The MELCOR DC station battery duration (BATTDUR), which is important to release timing, which is more important to early fatality risk (than latent cancer fatality risk.)

For the circular areas between 2.5-miles and 3.5-miles, the regression methods consistently rank the MACCS crosswind dispersion coefficient (CYSIGA), the early health effects threshold for red bone marrow (EFFTHR-Red Marrow), the MELCOR SRV stochastic failure probability (SRVLAM), and the MELCOR SRV open area fraction (SRVOAFRAC), respectively, as the most important input parameters.

7.2.3 Regression Summary of LCF Risk using Dose Truncation

Additional regression analyses were conducted as a sensitivity analysis for the dose-response models considered in this report (i.e., linear no threshold, linear with a threshold of 0.62 rem/yr, and linear with a threshold of 5 rem/yr with 10 rem lifetime limit). The results are discussed in Section 6.4.3. The regression techniques were used with Replicate 1 that included 284 source terms with the MELCOR uncertain input variables and 350 MACCS uncertain input variables. The statistical regression techniques provided adequate results, as described below.

For the linear no-threshold sensitivity analysis, all circular areas for all regression methods consistently rank the MACCS dry deposition velocity (VDEPOS) and the MELCOR SRV stochastic failure probability (SRVLAM), respectively, as the most important input parameters. Some additional variables also consistently show some level of importance at all circular areas, including:

- The MELCOR fuel failure criterion, and
- The MELCOR SRV open area fraction (SRVOAFRAC),

Since this is a smaller subset of the MACCS uncertainty analysis and still ranks the same top two parameters as most important, this sensitivity analysis provides additional confidence in the regression analyses for parameters considered important.

For the alternative dose-response model (i.e., thresholds of 0.62 rem/yr and 5 rem/yr with a 10 rem lifetime limit) sensitivity analyses, the five circular areas for all regression methods consistently rank the MACCS inhalation protection factor for normal activity (PROTIN-Normal), the MACCS lung lifetime risk factor for cancer death (CFRISK-Lung), and the MELCOR SRV stochastic failure probability (SRVLAM) as the most important input variables. For the MACCS variables, the dose threshold models are those associated with doses received in the first year and not ones associated with the long-term phase risk beyond the first year. Because the internal doses from inhalation diminish with time, most of the doses in the second and subsequent years are from the exposures during that year. These doses are limited by the habitability criterion to be less than 500 mrem in any year. The inhalation dose used in this criterion is a committed dose (i.e., it accounts for doses received over the next 50 years). Because the annual doses allowed by the habitability criterion are less than the dose truncation levels, nearly all of the risk is from doses received during the first year. Additional variables also consistently show some level of importance at all circular areas, including:

- The MELCOR SRV open area fraction (SRVOAFRAC), and
- The MELCOR DC station battery duration (BATTDUR)

The important MELCOR input parameters are similar to those in the MACCS uncertainty regression analyses summarized in Section 7.2.1. However, the MACCS input variables are not the same. The use of either the 0.62 rem/yr dose truncation model or the 5 rem/yr with a 10 rem lifetime limit dose-response model has MACCS input variables associated with doses received in the first year and not MACCS input parameters associated with the long-term phase risk beyond the first year. Hence they show up as important for the threshold models and not for the LNT model where the more of the risk comes from the long-term phase.

For Peach Bottom, the habitability criterion used is an annual dose rate of 500 mrem/yr. This dose rate is below the threshold limit in both dose truncation models; therefore, most of the doses received during the long-term phase are below the dose truncation limit and are not counted toward health effects when using this criterion. Thus, most of the risks associated with either truncation level are from doses received during the first year²¹. The emergency and long-term phases are not easily separated in the first year for purposes of evaluating the annual dose threshold.

²¹ The total risk using the threshold models are substantially lower than the LNT model.

To better understand this explanation, it is important to understand the differences between exposure periods, commitment periods, and the periods of time when doses are actually received. For external dose pathways, the time over which doses are received is concurrent with the exposure period. External dose pathways include cloudshine and groundshine.

The exposure period for internal pathways, inhalation and ingestion, is the period of time when the inhalation or ingestion occurs; however, doses continue to be received over a person's entire lifetime following the exposure. The period of time over which doses are received from an internal pathway is accounted for in the construction of dose conversion factors by integrating the doses over a finite period called a dose commitment period, which is usually taken to be 50 years when calculating internal-pathway dose conversion factors for adults. The implicit assumption is that the average adult lives for an additional 50 years following the exposure, which is most likely a conservative assumption.

Since ingestion doses are taken to be negligible in SOARCA, inhalation is the only internal pathway that is treated. A significant portion of the exposures during the emergency phase are from inhalation. As explained above, these exposures are assumed to lead to doses over the commitment period, which is the next 50 years following the exposure. However, depending on the isotope inhaled, the doses received may diminish rapidly and become negligible for most of the dose commitment period.

Most of the exposures during the long-term phase are from groundshine, and a small fraction is from inhalation of resuspended aerosols. Since groundshine is an external pathway, doses received are concurrent with the exposure period, which is also taken to be 50 years in the SOARCA study. On the other hand, exposures from inhalation of resuspended material during each year of the long-term phase contribute to doses received over the subsequent 50-year commitment period.

Doses received in the first year thus correspond to:

- all of the dose from external exposure during the emergency phase,
- most of the dose from internal exposure during the emergency phase,
- all of the dose from external exposure during the first year of the long-term phase, and
- most of the dose from internal exposure during the first year of the long-term phase.

Doses received in the second and subsequent years correspond to:

- a fraction of the dose from internal exposure during all previous years plus most of the dose from internal exposure during that year, and
- all of the dose from external exposure during that year.

Because the internal doses from inhalation diminish with time, most of the doses in the second and subsequent years are from the exposures during that year. But these doses are limited by the habitability criterion to be less than 500 mrem in any year. The 500 mrem limit is for all dose pathways, except ingestion, in this case groundshine and inhalation from resuspended aerosols. The inhalation dose used in this criterion is a committed dose (i.e., it accounts for doses received over the next 50 years). Because the annual doses allowed by the habitability criterion are less than these truncation levels, nearly all of the risk is from doses received during the first year. These doses include most of emergency phase doses and a fraction of the long-term phase doses.

7.2.4 Habitability Sensitivity Study Summary

A series of sensitivity studies using five habitability criteria (i.e., 0.1 rem/yr, 0.5 rem/yr, 2 rem/yr²², 4 rem over 5 years, and 5 rem over 7 years) were conducted for the dose truncation models considered in this report (i.e., linear no threshold, threshold of 0.62 rem/yr, and threshold of 5 rem/yr with 10 rem lifetime limit). This sensitivity was performed to see how values of the habitability criterion might affect the results. The sensitivity results are discussed in Section 6.4.4.

Based on the linear no-threshold dose-response model, the majority of the LCF risk contribution within the EPZ resulted from the long-term phase for all habitability scenarios. Thus the higher the habitability criterion, the higher the LCF risk as a result of long-term dose within the EPZ. The majority of the LCF risk for the 0.1 rem/yr habitability criterion results from the emergency phase for all circular areas. While the emergency phase LCF risk for the 0.1 rem/yr habitability criterion is similar to all other emergency phase LCF risks for other habitability criteria, the low value significantly reduces long-term LCF risk, causing the emergency phase risk to exceed the long-term phase risk beyond the EPZ. Most of the risk corresponds to the long-term phase for all other choices of habitability criterion.

For the dose-truncation models, most of the doses received during the long-term phase are below the dose truncation limit and are not counted toward health effects. Thus, most of the risks associated with either of the truncation levels are from doses received during the first year.

When either of the dose-truncation models is used, the LCF risks within the EPZ are orders of magnitude lower when the habitability criterion is below the dose-truncation level, as compared with the cases when the habitability criterion is above the dose-truncation level. Beyond the EPZ, the habitability criterion has a smaller effect on the overall LCF risk when a dose-truncation model is applied, and yield similar results to those presented in the NUREG/CR-7110 Volume 1, Section 7, at the specified circular areas.

7.2.5 Weather Effects Summary

A set of sensitivity analyses to evaluate the SOARCA weather sampling technique was evaluated for the LNT, USBGR, and HPS dose-response models. All of the sensitivity simulations use the SOARCA uncertainty analysis base case source term. The SOARCA weather sampling technique was compared to sampling the entire weather database (i.e., 8,760 hourly weather samples) used for Peach Bottom. All MACCS variables other than the sampled weather trials were held fixed.

For SOARCA, a structured Monte-Carlo sampling method was employed for weather sampling. This was done by random selection of a user-specified number of weather sequences (i.e., start times) from the set of sequences assigned to each user-specified weather category. This begins by sorting an annual weather file according to user specified criteria. Each MACCS analysis uses a user-specified random seed. This random seed was kept constant for all MACCS analysis and thus the same weather trials from the same meteorological data file were selected for all of the analyses.

²² The way MACCS implements the habitability criterion, 2 rem/yr, is more restrictive than 4 rem over 5 years.

The overall difference between the SOARCA weather sampling technique and sampling all 8,760 hourly data points is relatively small, and the SOARCA weather sampling technique consistently produced higher LCF risk results. However, the increase in computational time is eight fold. While this is not prohibitively long for the LNT dose-response model (i.e., ~1 hour to ~8 hours of run time for a single MACCS realization), the increase in computation time for the USBGR and HPS dose-response models would make uncertainty analysis applications less feasible (i.e., ~1 day to ~8 days of run time for a single MACCS realization).

In SOARCA, the aleatory uncertainties due to weather were characterized in terms of mean values. However, a CCDF of aleatory uncertainties can be obtained using a single MACCS analysis for each source term. A set of sensitivity analyses to evaluate the aleatory weather uncertainty using the SOARCA weather sampling technique was evaluated for the LNT, USBGR, and HPS dose-response models.

Two comparisons are presented to show the effects of aleatory weather uncertainty. The first shows the individual LCF risk results of the aleatory weather uncertainty for three chosen source terms using the LNT dose-response model with the conditional, mean, individual LCF risk results of the MACCS analysis for the combined MELCOR Replicates 1, 2, and 3 using the LNT dose-response model (CAP17) discussed in Section 6.2.1. The second comparison shows the individual LCF risk results of the aleatory weather uncertainty for the three source terms using the LNT, USBGR, and HPS dose-response models with the conditional, mean, individual LCF risk results of the MACCS analysis for MELCOR Replicate 1 using the LNT, USBGR, and HPS dose-response models (i.e., CAP14, CAP15, and CAP16, respectively) discussed in Section 6.4.3. Recall that the CAP17 MACCS analysis consists of 865 MELCOR source terms using 21 MELCOR epistemic uncertainty variables, and 350 MACCS epistemic uncertainty variables of which 338 variables apply to LCF risk.

For the first comparison, the median individual LCF risk results for the three source terms analyzed do provide a good example of the median, lower, and upper bounds of the CAP17 conditional, mean, individual LCF risk (per event) CCDF distribution for all specified circular areas. For the aleatory weather uncertainty within the 10-mile, 20-mile, 30-mile, 40-mile, and 50-mile circular areas, the conditional, mean, individual LCF risk (per event) for aleatory weather uncertainty is bounded for all analyses by the epistemic uncertainty for the conditional, mean, individual LCF risk (per event) results of the MACCS CAP17 analysis. This indicates that the epistemic uncertainties within the MACCS CAP17 analysis have a greater effect on the overall uncertainty than the aleatory weather uncertainty.

For the second comparison, the median LCF risk results for the three source terms do provide a good example of the median, lower and upper bounds of the CAP14 CCDF distribution for all specified circular areas and are similar to those for the MACCS CAP17 analysis. However, these three source terms only quantify the median and lower half of the CAP15 and CAP16 CCDF distributions of conditional, mean, individual LCF risk (per event) results for all specified circular areas. This is due to the dose-truncation models having more of the LCF risk contribution from the 1st year and thus a larger contribution from the emergency phase. The 2nd year and subsequent years have less of a contribution to the individual LCF risk than the LNT dose-response model because the majority of the doses in these years are below the truncation thresholds. Since none of the source terms selected for this sensitivity analyses have a large contribution from the emergency phase, the overall conditional, mean, individual LCF risks are at the lower end of the range for these dose-response models.

For the conditional, mean, individual LCF risk (per event) results using the USBRG dose-response model and the CCDF of the conditional, mean, individual LCF risk (per event) results for the MACCS CAP15 analysis within the 10-mile, 20-mile, 30-mile, 40-mile, and 50-mile

circular areas, the epistemic uncertainties for the conditional, mean, individual LCF risk results of the MACCS CAP15 analysis have a greater effect on the overall uncertainty than the aleatory weather uncertainty for the higher source term releases. The following trends are observed and are specific to the three source terms analyzed:

- The dose-truncation model has a larger contribution of the LCF risk from the emergency phase and earlier years of the long-term phase.
- The emergency phase risk for the smaller source term release has a larger effect on the overall LCF risk.
- The three source terms used in these analyses are bounded at the upper end of the CCDF individual LCF risk distribution for aleatory weather uncertainty by the epistemic uncertainties for the conditional, mean, individual LCF risk results of the MACCS CAP15 analysis, but are not bounded at the lower end of the distribution for individual LCF risk.

Since the selected source terms do not adequately represent the upper end of the range for the MACCS CAP15 analysis, a determination of the upper bounding effects of aleatory weather uncertainty cannot be determined from these analyses.

For the conditional, mean, individual LCF risk (per event) using the HPS dose-response model and the CCDF of the conditional, mean, individual LCF risk (per event) results for the MACCS CAP16 analysis within the 10-mile, 20-mile, 30-mile, 40-mile, and 50-mile circular areas, the trend observations are similar to those discussed for the USBGR dose-response model. However, these results also indicate that a higher dose-truncation threshold is more sensitive to aleatory weather uncertainty.

Since the selected source terms do not adequately represent the upper end of the range for the MACCS CAP16 analysis, a determination of the upper bounding effects of aleatory weather uncertainty cannot be determined from these analyses.

Appendix E contains further analyses on the relative and combined contributions of weather and epistemic MELCOR and MACCS parameter uncertainty to uncertainty in consequence results.

7.2.6 Single Realization Summary

Select individual realizations from the uncertainty analysis were further investigated in greater detail to identify the influences affecting the predicted consequences. The cases investigated are broken into two groups, the MELCOR single realizations discussed in Section 6.1.4, and the MACCS Uncertainty Analysis single realizations that resulted in a nonzero early-fatality risk per event at the 10-mile circular area. These analyses were conducted from the results in the MACCS Uncertainty Analysis. The single realization results are discussed in Section 6.2.4.

For the MELCOR single realizations, when the fraction of cesium released to the environment is compared for all the realizations investigated, there is no direct relationship to the LCF risk in the long-term phase. However, when the cesium and cerium release fractions are both considered, a better relationship to long-term risk does appear.

For the MELCOR single realizations, the LCF risk results show emergency phase LCF risk and long-term phase LCF risk are dependent on the same input variables for all circular areas investigated (i.e., 10-, 20-, 30-, 40-, and 50-mile circular areas), and those dominated by the emergency phase LCF risk further emphasize the advantage of emergency phase evacuation within the EPZ.

For the MACCS Uncertainty Analysis single realizations, it was discovered that three of 865 realizations have a non-zero calculated conditional, mean, individual early-fatality risk (per event) out to the 10-mile circular area. Since this was not expected, a further investigation into these realizations was conducted. None of the realizations have a stochastic SRV failure, but for all three single realizations the accident progression is a SRV thermal failure followed by a main steam line creep rupture and ultimate containment failure due to wetwell rupture above the water line and drywell head flange failure. None of these realizations were selected for the MELCOR single realization analysis. As documented in Section 6.1.4, there are five factors found to strongly affect the amount of radionuclides released to the environment, namely:

- (1). Whether the SRV fails open before or after the onset of core damage,
- (2). Whether a main steam line creep rupture occurs,
- (3). The elapsed time between the onset of core damage and main steam line creep rupture,
- (4). Whether a surge of water from the wetwell goes up onto the drywell floor at drywell liner melt through, and
- (5). Whether an overpressure rupture of the wetwell occurs.

For one of the MACCS Uncertainty Analysis single realizations (i.e., only one of the 865 total realizations), there is a nonzero early fatality risk beyond the 10-mile circular area. A noticeable increase in early fatality risk beyond the 10-mile circular area was observed and is due to the population beyond 10 miles not evacuating, except for those in the 10-20 mile shadow evacuation for Cohort 2. As a result, the early fatality risk beyond 10 miles increases by two orders of magnitude in this realization. Also, 50% or greater of the weather trials result in a nonzero early fatality risk out to the 30-mile circular area in this realization.

While the early fatality risk results for this MACCS Uncertainty Analysis realization are extreme, further investigation into the parameters that affected these results does not indicate the source term as the predominant or only cause. Instead, the MELCOR source term and the MACCS parameters, which have a higher early fatality risk contribution for the red bone marrow, contribute to the early fatality risk beyond 10 miles. Specifically the following variables are at the upper/lower end (i.e., the worst end for consequence in each input variable) of their respective distributions, and hence indicate an extremely unlikely outcome:

- The early health effects threshold for red bone marrow (EFFTHR-Red Marrow) is near the 1st percentile of the distribution,
- The beta (shape) factor for red bone marrow (EFFACB-Red Marrow) is near the 10th percentile of the distribution,
- The crosswind dispersion coefficient (CYSIGA) is near the 5th percentile of the distribution,
- The vertical dispersion coefficient (CZSIGA) is near the 5th percentile of the distribution and,
- The MELCOR source term is near the 95th percentile of the distribution.

The first two relate to the most sensitive organ for the early health effects. The third and fourth parameters enable higher concentrations to reach individuals further from the plant due to a tighter plume.

For all single realizations analyzed, which have the overall LCF risk dominated by the emergency phase LCF risk beyond the 10 mile circular area, those realizations further emphasize the advantage of evacuation within the EPZ (i.e., the population of greatest risk) with significantly reduced emergency phase LCF risk within the EPZ (i.e., only the 0.5% of the population modeled as refusing to evacuate within the EPZ receive an emergency phase dose).

7.2.7 Importance Summary

All of the MACCS input parameters that were identified as being important are ones that were expected. A previous internal study at Sandia National Laboratories had identified a very similar set of important parameters [60]. In this earlier study, only the LNT dose-response model was considered, so the threshold-type dose-response models considered here are new and have no analog.

One parameter was identified for early-fatality risk in the earlier study that did not show up as important in this work, which was hotspot relocation time. This parameter clearly could be important for early-fatality risk, depending on the timing of the release compared with the timing of the relocation. Even when most of the release occurs before relocation, groundshine doses would be reduced by earlier relocation. One key difference is that the source term was based on one of the NUREG-1150 source terms in the previous study and was much larger than any of the source terms evaluated in this study. As a result, the number of realizations with nonzero early-fatality risk was much greater in the previous study, allowing for better statistics in the regression analysis.

Several parameters identified for LCF risk in the earlier study were not identified as important in this work. Two of these are protection factors for inhalation and groundshine during normal activities. Another key difference between the earlier study and this uncertainty analysis is that the earlier study only considered the emergency phase contributions to risk; no calculation was done for the long-term phase. This could explain why the inhalation protection factor was identified as important in the earlier study, since inhalation is usually the most important dose pathway for the emergency phase but is relatively unimportant for the long-term phase. The groundshine protection factor, on the other hand, is the dominant dose pathway for the long-term phase and is more important for that phase than it is for the emergency phase. This implies that the groundshine protection factor should have been identified to be important in the current study. In examining why it was not identified to be important, this study has varied source terms, a more detailed evacuation model, and approximately 300 more MACCS uncertainty variables

The third category of parameters that was found to be important in the earlier study was the vertical dispersion coefficients for stable atmospheric conditions. These parameters can affect doses at short distances; at longer distances the plume becomes well mixed within the mixing layer and additional vertical dispersion has no effect. The connection between dispersion and LCF risk tends to be much less than linear because less dispersion results in larger doses to fewer people while more dispersion results in smaller doses to more people. For linear no-threshold dose-response, this can result in a minimal dependence of LCF risk on dispersion, especially for crosswind dispersion. In practice, the influence of the dispersion parameters is somewhat site dependent and the earlier work was for a different site, Surry. Also, for this study the dispersion parameters for vertical and crosswind dispersion were correlated with each other and across the set of stability classes. This was not done in the earlier study, which most likely affected the evaluation of the dispersion parameters differently in the two studies.

7.3 Use of Multiple Regression Techniques

The SOARCA project [1] uses two complex codes to estimate the consequences of a severe nuclear accident: MELCOR and MACCS. Both of these codes involve complex physics phenomena and interactions. Past analyses (e.g., NUREG-1150) relied mostly on linear and rank regressions which suppose that the models are mostly additive (i.e., the variance in the results is driven by single effects from individual uncertain inputs) and the influences are linear or monotonic. Such an approach was valid for some of the MELCOR parameters analyzed, however the R^2 values (i.e., coefficient of determination) estimated by the regression models ranged from 0.42 to 0.69, meaning that between 30% and 60% of the variance was not explained. The rank regression analyses performed on selected MACCS results were even weaker. Latent cancer fatality analyses had an R^2 of 0.73 for a 10 miles radius and about 0.51 for larger radiuses (20, 30, 40, and 50 miles) indicating that most of the time, only half of the variance was explained. Rank analyses for early-fatality risk explained at best a quarter of the variance.

Such results are a clear indication that one cannot always rely on rank regression to provide a good indication of the effects of uncertainty in individual analysis inputs. While there are powerful techniques to fully decompose the variance of the selected results, such as Sobol decomposition or FAST, they can require such a large sample size that the cost of their implementation is prohibitive.

One of the major problems when trying to capture complex interactions is that so many different types of interactions are possible that a single parametric regression is often not effective in providing an adequate representation for model results. Some techniques, such as rank regression can be too restrictive, while others may be too broad and capture nonphysical interactions. This may happen, for instance with quadratic regression that incorporates for all 2nd-order interactions (influence of the type X_iX_j) as well as recursive partitioning. These limitations are increased when the sample size is relatively small compared to the number of input variables in consideration. As an example, 100 input variables were considered in the analyses for early fatalities, which leads to 10,000 possible regression terms analyzed with quadratic regression. LCF analyses considered 300 inputs parameters leading to 90,000 possible regression terms. In such conditions, it is likely that the regression technique will indicate some "important" relationships that are in fact due to spurious correlation, rather than actual importance.

For this reason, four regression techniques have been used for this study. Each has strengths and weaknesses. Some effects will be captured only by one or two of these techniques but the same techniques can ignore other kinds of interactions. The analysis of the resulting arrays is, consequently, not as straightforward. The confidence one has on the influence of a parameter is conditional on the number of techniques and the type of techniques capturing this influence. This analysis can only be done in conjunction with a careful physical interpretation and checking of the results. In this sense, the addition of sensitivity cases and study of selected deterministic cases provided information that was crucial in the interpretation of the results, as well as the subject matter experts' knowledge: any strange interaction (or non-interaction if one was expected) was double-checked in order to understand and explain it (or corrected if mistaken).

While the four selected regression analyses cover a large spectrum of potential interactions and influence, some other regression techniques (such as ACOSSE and Gaussian process for instance) have not been used in this study. They could bring more insights on the analysis by confirming the influence of some parameters (for which we were not completely confident) or capturing other kinds of interactions not considered by the original techniques.

The increased complexity of interpretation (compared to simple rank regression technique) derives from the complexity of the regression models and is necessary to increase the understanding with some confidence that the improvement in the R^2 is not spurious (and/or nonphysical) due to the large number of variables considered compared to the sample size. In the current analysis, the effort was fruitful as it allowed the achievement of an increase in the R^2 for all analyses such that approximately 80% or more of the variance in MELCOR results was captured, and approximately 40% to 85% for LCF and between 45% and 80% for early-fatality risk results from MACCS. The increase was confirmed by several techniques and via cross-validation of physical explanation of the results.

The use of multiple regressions techniques was beneficial in this study. While the R^2 associated with early-fatality risk results was low, the vast majority of the realizations had an estimated early-fatality risk of essentially zero. This tendency was even more pronounced when the circular area was increased beyond 1.3 to 2 miles (up to having only a handful of realizations from the set of 865 with nonzero values for a 10 miles radius). Statistical analysis of sparse data remains a complex domain of study and most methods are inefficient (either not finding any relation or over-fitting with spurious relations).

7.4 Conclusions

This uncertainty analysis corroborates the SOARCA project conclusions with the following:

- Public health consequences from severe nuclear accident scenarios modeled are smaller than NUREG/CR-2239, "Technical Guidance for Siting Criteria Development" [57].
- The delay in releases calculated provide more time for emergency response actions (i.e., evacuating or sheltering).
- The long-term phase dominates the overall health effect risk within the EPZ because the emergency response is faster than the onset of environmental release. More than half the time, the long-term phase is the larger contributor to overall health effect risk beyond the EPZ. Long-term health effect risk is largely controlled by the habitability criterion.
- "Essentially zero" absolute early fatality risk is projected:
 - The mean absolute early fatality risk is 1.4×10^{-12} per reactor year²³ within 1 mile of the EAB, and even this minute risk based on less than 13% of the 865 realizations having a non-zero risk; 87% had a zero risk.
 - This is orders of magnitude below the NRC quantitative health objective for early fatalities of 5×10^{-7} per reactor year
- A major determinant of source term magnitude is whether the sticking open of the SRV (i.e., lowest set-point SRV) occurs before or after the onset of core damage. Compounding this effect is whether or not main steam line creep rupture occurs (i.e., leads to higher consequences).

²³ Estimated risks below 10^{-7} per reactor year should be viewed with caution because of the potential impact of events not studied in the analyses, and the inherent uncertainty in very small calculated numbers.

- Health-effect risks vary sublinearly with source term because people are not allowed to return home until doses are below the habitability criterion.
- Analysis confirms known importance of some phenomena (e.g., dry deposition velocity), and reveals some new phenomenological insights (e.g., late phase revaporization of cesium and other fission products within the RPV).
- The use of multiple regression techniques, most of which include non-linear interactions between input variables, to post-process Monte Carlo and Latin Hypercube Sampling results provides better explanatory power of which input parameters are most important to uncertainty in results.

8. REFERENCES

- [1.] U.S. Nuclear Regulatory Commission, NUREG-1935, "State-of-the-Art Reactor Consequence Analyses (SOARCA) Report," Washington, DC, 2012.
- [2.] Sandia National Laboratories, NUREG/CR-7110, "State-of-the-Art Reactor Consequence Analyses Project Volume 1: Peach Bottom Integrated Analysis," U.S. Nuclear Regulatory Commission, Washington, DC, 2012.
- [3.] Gauntt, R.O., et al., SAND2012-6173, "Fukushima Daiichi Accident Study (Status as of April 2012)," Sandia National Laboratories, Albuquerque, NM, 2012.
- [4.] Helton, J.C., "Treatment of Uncertainty in Performance Assessments for Complex Systems," *Risk Analysis*, **14**(4): p. 483-511, 1994.
- [5.] Helton, J.C. and D.E. Burmaster, "Guest Editorial: Treatment of Aleatory and Epistemic Uncertainty in Performance Assessments for Complex Systems," *Reliability Engineering & System Safety*, **54**(2-3): p. 91-94, 1996.
- [6.] Kaplan, S. and B.J. Garrick, "On The Quantitative Definition of Risk," *Risk Analysis*, **1**(1): p. 11-27, 1981.
- [7.] Gauntt, R.O., et al., NUREG/CR-6119, "MELCOR Computer Code Manuals, Vol. 2: Reference Manuals, Version 1.8.6 (Vol. 2, Rev. 3)," U.S. Nuclear Regulatory Commission, Washington, D.C., 2005.
- [8.] McFadden, K., et al., "WinMAACS, a MACCS2 Interface for Calculating Health and Economic Consequences from Accidental Release of Radioactive Materials into the Atmosphere - User's Guide and Reference Manual - WinMACCS Version 3 - Draft," Sandia National Laboratories, Albuquerque, NM, 2007.
- [9.] Chanin, D.I. and M.L. Young, NUREG/CR-6613, "Code Manual for MACCS2: Volume 1, User's Guide," U.S. Nuclear Regulatory Commission, Washington, DC, 1997.
- [10.] U.S. Nuclear Regulatory Commission, Regulatory Guide 1.145, Revision 1, "Atmospheric Dispersion Models for Potential Accident Consequence Assessments at Nuclear Power Plants," Washington, DC, November 1982.
- [11.] Helton, J.C., et al., "Survey of Sampling-based Methods for Uncertainty and Sensitivity Analysis," *Reliability Engineering & System Safety*, **91**(10-11): p. 1175-1209, 2006.
- [12.] Storlie, C.B. and J.C. Helton, "Multiple predictor smoothing methods for sensitivity analysis: Description of techniques," *Reliability Engineering & System Safety*, **93**(1): p. 28-54, 2008.
- [13.] Storlie, C.B., et al., "Implementation and evaluation of nonparametric regression procedures for sensitivity analysis of computationally demanding models," *Reliability Engineering & System Safety*, **94**(11): p. 1735-1763, 2009.
- [14.] Eide, S.A., et al., NUREG/CR-6928, "Industry-Average Performance for Components and Initiating Events at U.S. Commercial Nuclear Power Plants," U.S. Nuclear Regulatory Commission, Washington, DC, 2007.

- [15.] Wierman, T.E., et al., NUREG/CR-7037, "Industry Performance of Relief Valves at U.S. Commercial Nuclear Power Plants through 2007," U.S. Nuclear Regulatory Commission, Washington, DC, 2011.
- [16.] U.S. Nuclear Regulatory Commission, NUREG-1150, "Severe Accident Risks: An Assessment for Five U.S. Nuclear Power Plants," Washington, DC, 1991.
- [17.] Gauntt, R.O., et al., NUREG/CR-6119, "MELCOR Computer Code Manuals, Vol. 1: Primer and User's Guide, Version 1.8.6 (Vol. 1, Rev. 3)," Sandia National Laboratories, Albuquerque, NM, 2005.
- [18.] Gauntt, R.O., N. Bixler, and K.C. Wagner, "An Uncertainty Analysis of the Hydrogen Source Term for a Station Blackout Accident in Sequoyah Using MELCOR 1.8.5 (Draft For Review)," Sandia National Laboratories, Albuquerque, NM, 2003.
- [19.] Hanniet-Girault, N. and G. Repetto, "PHEBUS FPT0 Final Report," Cadarache, France, 1998.
- [20.] Jacquemain, D., et al., "PHEBUS FPT1 Final Report," Cadarache, France, 2000.
- [21.] Gregoire, A.C., P. Chapelot, and G. Gregoire, "PHEBUS FPT4 Final Report," Cadarache, France, 2004.
- [22.] Gregoire, A.C., "PHEBUS FPT2 Final Report," Cadarache, France, 2008.
- [23.] Pavot, F., et. al., "PHEBUS FPT3 Final Report," Cadarache, France, 2010.
- [24.] Rathbun, H.J., "Three-Stage Target Rock Safety Relief Valve Performance and Reliability in Long-Term Station Blackout Accident Scenario for the State of the Art Reactor Consequence (SOARCA) Program," U.S. Nuclear Regulatory Commission, Washington, DC, 2012.
- [25.] DeGarmo, E.P., J.T. Black, and R.A. Kohser. *Materials and Processes in Manufacturing*. 9th ed. New Jersey: John Wiley & Sons, Inc., 2003.
- [26.] Maile, K., et al., "Load Carrying Behavior of the Primary System of Pwrs for Loads Beyond the Design Limits: Part 2: Creep and Failure Behavior of a Piping Section under Internal-Pressure and High-Temperature," *Nuclear Engineering and Design*, **119**(2-3): p. 131-137, 1990.
- [27.] Theofanous, T.G., et al., NUREG/CR-5423, "The Probability of Liner Failure in a Mark-I Containment," U.S. Nuclear Regulatory Commision, Washington, DC, 1989.
- [28.] HySafe, "Biennial Report on Hydrogen Safety (Version 1)," 2007.
- [29.] Laurendeau, N.M., "Thermal Ignition of Methane-Air Mixtures by Hot Surfaces: A Critical Examination," *Combustion and Flame*, **46**(1): p. 29-49, 1982.
- [30.] Lewis, B. and G. Von Elbe. *Combustion, Flames and Explosions of Gases*. Third ed. Orlando, FL: Academic Press, Inc., 1987.
- [31.] Astbury, G.R. and S.J. Hawksorth, "Spontaneous Ignition of Hydrogen Leaks: A Review of Postulated Mechanisms," *International Journal of Hydrogen Energy*, **32**(13): p. 2178-2185, 2007.

- [32.] Buckle, J.W. and S. Chandra, "Hot Wire Ignition of Hydrogen-Oxygen Mixtures," *International Journal of Hydrogen Energy*, **21**(1): p. 39-44, January 1996.
- [33.] Carleton, F.B., et al., "Prenormative research on the use of optics in potentially explosive atmospheres," 2000.
- [34.] Gilbert/Commonwealth, I., "Evaluation of Doors at Peach Bottom Atomic Power Station Units 2 and 3, Mod 2368 and 2489," 1990.
- [35.] Shigley, J.E. and C.R. Mischke. *Mechanical Engineering Design*. Third ed. New York: McGraw-Hill, Inc., 1977.
- [36.] Baumeister, T., E.A. Avallone, and T. Baumeister III. *Marks' Standard Handbook for Mechanical Engineers*. 8th ed. New York: McGraw-Hill Book Company, 1978.
- [37.] Kissane, M.P., "On the nature of aerosols produced during a severe accident of a water-cooled nuclear reactor," *Nuclear Engineering and Design*, **238**(10): p. 2792-2800, 2008.
- [38.] Lipinski, R.J., et al., "Uncertainty in Radionuclide Release Under Specific LWR Accident Conditions, Volume 2, TMLB' Analyses," Sandia National Laboratories, Albuquerque, NM, 1985.
- [39.] Hinds, W.C. *Aerosol Technology: Properties, Behavior, and Measurement of Airborne Particles*. New York, NY: John Wiley & Sons, Inc., 1982.
- [40.] Sandia National Laboratories, NUREG/CR-7110, "State-of-the-Art Reactor Consequence Analyses Project Volume 2: Surry Integrated Analysis," U.S. Nuclear Regulatory Commission, Washington, DC, 2012.
- [41.] Dotson, L.J. and J. Jones, NUREG/CR-6864, "Identification and Analysis of Factors Affecting Emergency Evacuations: Main Report (Volume 1) " Sandia National Laboratories, Albuquerque, NM, 2005.
- [42.] Jones, J., et al., NUREG/CR-6981, "Assessment of Emergency Response Planning and Implementation for Large Scale Evacuations," U.S. Nuclear Regulatory Commission, Washington, DC, 2008.
- [43.] Bixler, N., et al., "Synthesis of Distributions Representing Important Non-Site-Specific Parameters in Off-Site Consequence Analysis," Sandia National Laboratories, Albuquerque, NM, 2010.
- [44.] Harper, F.T., et al., NUREG/CR-6244, "Probabilistic Accident Consequence Uncertainty Analysis, Dispersion and Deposition Uncertainty Assessment," U.S. Nuclear Regulatory Commission, Washington DC, 1995.
- [45.] Goossens, L.H., et al., NUREG/CR-6526, "Probabilistic Accident Consequence Uncertainty Analysis, Uncertainty Assessment for Deposited Material and External Doses," U.S. Nuclear Regulatory Commission, Washington DC, 1997.
- [46.] Gregory, J.J., et al., "Task 5 Letter Report: MACCS2 Uncertainty Analysis of EARLY Exposure Results," Sandia National Laboratories, Albuquerque, NM, September 2000.
- [47.] Heames, T.J., M.L. Wilson, and N.E. Bixler, "Recommendations for MACCS2 Parameter Uncertainty Distributions," 2003.

- [48.] Haskin, F.E., et al., NUREG/CR-6545, "Probabilistic Accident Consequence Uncertainty Analysis, Early Health Effects Uncertainty Assessment " U.S. Nuclear Regulatory Commission, Washington, DC, 1997.
- [49.] Eckerman, K., "Radiation Dose and Health Risk Estimation: Technical Basis for the State-of-the-Art Reactor Consequence Analysis (SOARCA) Project," Oak Ridge National Laboratory, Oak Ridge, TN, 2011.
- [50.] Molenkamp, C.R., et al., NUREG/CR-6853, "Comparison of Average Transport and Dispersion Among a Gaussian, a Two-Dimensional, and a Three-Dimensional Model " U.S. Nuclear Regulatory Commission, Washington, DC, October 2004.
- [51.] Environmental Protection Agency, "Manual of Protective Action Guides and Protective Actions for Nuclear Incidents," U.S. Environmental Protection Agency, Office of Radiation Programs, Washington, DC, 1992.
- [52.] Sullivan, R., et al., NUREG/CR-6953, " Review of NUREG-0654, Supplement 3, "Criteria for Protective Action Recommendations for Severe Accidents" - Technical Basis for Protective Action Strategies (Vol. 3)," U.S. Nuclear Regulatory Commission, Washington, DC, 2010.
- [53.] Wolshon, B., J. Jones, and F. Walton, "The Evacuation Tail and Its Effect on Evacuation Decision Making," *Journal of Emergency Management*, **8**(1): p. 37-46, 2010.
- [54.] Rogers, G.O., et al., "Evaluating Protective Actions for Chemical Agent Emergencies," ORNL-6615, Oak Ridge National Laboratory, Oak Ridge, Tennessee, 1990.
- [55.] Jones, J., F. Walton, and R. Sullivan, NUREG/CR-6953, "Review of NUREG-0654, Supplement 3, 'Criteria for Protective Action Recommendations for Severe Accidents': Focus Groups and Telephone Survey (Vol. 2)," U.S. Nuclear Regulatory Commission, Washington, DC, 2008.
- [56.] Osborn, D.M., et al. "A Dynamic Level 2 PRA Using ADAPT-MELCOR." Paper presented at the European Safety and Reliability Conference, Troyes, France, September 2011.
- [57.] Aldrich, D.C., et al., NUREG/CR-2239, "Technical Guidance for Siting Criteria Development," U.S. Nuclear Regulatory Commission, Washington, DC, 1982.
- [58.] NRC Policy Statement, 10 CFR Part 50, "Safety Goals for the Operations of Nuclear Power Plants Policy Statement," 51 Federal Register pg. 33028, August 1986.
- [59.] U.S. Nuclear Regulatory Commission, NUREG-1860, "Feasibility Study for a Risk-Informed and Performance-Based Regulatory Structure for Future Plan Licensing, Volume 2," Washington, DC, December 2007.
- [60.] Gregory, J.J., et al., "Task 5 Letter Report: MACCS2 Uncertainty Analysis of EARLY Exposure Results," 2000.
- [61.] Pilch, M. and W.W. Tarbell, NUREG/CR-4383, "High Pressure Ejection of Melt from a Reactor Pressure Vessel: The Discharge Phase," Sandia National Laboratories, Albuquerque, NV, 1985.
- [62.] Armijo, J.S., *Letter from the Nuclear Regulatory Commission (NRC) Advisory Committee on Reactor Safeguards (ACRS)*, G. Jaczko, Editor May 15, 2012.

- [63.] Environmental Protection Agency, "Manual of Protective Action Guides and Protective Actions for Nuclear Incidents - DRAFT," U.S. Environmental Protection Agency, Washington, DC, 1989.
- [64.] ICRP. *The 2007 Recommendations of the International Commission on Radiological Protection*. Annals of the ICRP Publication 103. International Commission on Radiological Protection, Elsevier, March 2007.
- [65.] ICRP. *Application of the Commission's Recommendations to the Protection of People Living in Long-term Contaminated Areas After a Nuclear Accident or a Radiation Emergency*. Annals of the ICRP Publication 111. International Commission on Radiological Protection, Elsevier, April 2011.
- [66.] Helton, J.C., et al., "Conceptual Structure of the 1996 Performance Assessment for the Waste Isolation Plant," *Reliability Engineering & System Safety*, **69**(1-3): p. 151-165, 2000.
- [67.] Helton, J.C. *Mathematical and Numerical Approaches in Performance Assessment for Radioactive Waste Disposal: Dealing with Uncertainty*. New York, NY: Elsevier Science, 2003.
- [68.] Hora, S.C. and R.L. Iman, "Expert Opinion in Risk Analysis - The NUREG-1150 Methodology," *Nuclear Science and Engineering*, **102**(4): p. 323-331, 1989.
- [69.] Meyer, M.A. and J.M. Booker. *Eliciting and Analyzing Expert Judgement: A Practical Guide*. Society for Industrial and Applied Math, 2001.
- [70.] Thorne, M.C. and M.M.R. Williams, "A Review of Expert Judgment Techniques with Reference to Nuclear Safety," *Progress in Nuclear Safety*, **27**(2-3): p. 83-254, 1992.
- [71.] Helton, J.C. and F.J. Davis, "Latin Hypercube Sampling and the Propagation of Uncertainty in Analyses of Complex Systems," *Reliability Engineering & System Safety*, **81**(1): p. 23-69, 2003.
- [72.] McKay, M.D., R.J. Beckman, and W.J. Conover, "A Comparison of Three Methods for Selecting Values of Input Variables in the Analysis of Output from a Computer Code," *Technometrics*, **21**(2): p. 239-245, 1979.
- [73.] Saltelli, A., K. Chan, and E.M. Scott. *Sensitivity Analysis*. New York, NY: Wiley, 2000.
- [74.] Kleijnen, J.P.C. and J.C. Helton, "Statistical analyses of scatterplots to identify important factors in large-scale simulations, 1: Review and comparison of techniques," *Reliability Engineering & System Safety*, **65**(2): p. 147-185, 1999.
- [75.] Helton, J.C., et al., "Uncertainty and Sensitivity Analysis of a Model for Multicomponent Aerosol Dynamics," *Nuclear Technology*, **73**(3): p. 320-342, 1986.
- [76.] Helton, J.C., et al., "Uncertainty and Sensitivity Analysis of a Dry Containment Test Problem for the MAEROS Aerosol Model," *Nuclear Science and Engineering*, **102**(1): p. 22-42, 1989.
- [77.] Helton, J.C., et al., "An Exploratory Sensitivity Study With the MACCS Reactor Accident Consequence Model," *Reliability Engineering & System Safety*, **36**(2): p. 137-164, 1992.

- [78.] Helton, J.C., et al., "Robustness of an Uncertainty and Sensitivity Analysis of Early Exposure Results with the MACCS Reactor Accident Consequence Model," *Reliability Engineering & System Safety*, **48**(2): p. 129-148, 1995.
- [79.] Helton, J.C., et al., "Uncertainty and Sensitivity Analysis of Early Exposure Results With the MACCS Reactor Accident Consequence Model," *Reliability Engineering & System Safety*, **48**(2): p. 91-127, 1995.
- [80.] Helton, J.C., et al., "Uncertainty and Sensitivity Analysis of Food Pathway Results With the MACCS Reactor Accident Consequence Model," *Reliability Engineering & System Safety*, **49**(2): p. 109-144, 1995.
- [81.] Helton, J.C., et al., "Uncertainty and Sensitivity Analysis of Chronic Exposure Results With the MACCS Reactor Accident Consequence Model," *Reliability Engineering & System Safety*, **50**(2): p. 137-177, 1995.
- [82.] Hamby, D.M., "A Review of Techniques for Parameter Sensitivity Analysis of Environmental Models," *Environmental Monitoring and Assessment*, **32**(2): p. 135-154, 1994.
- [83.] Helton, J.C., "Uncertainty and Sensitivity Analysis Techniques for Use in Performance Assessment for Radioactive Waste Disposal," *Reliability Engineering & System Safety*, **42**(2-3): p. 327-367, 1993.
- [84.] Frey, H.C. and S.R. Patil, "Identification and Review of Sensitivity Analysis Methods," *Risk Analysis*, **22**(3): p. 553-578, 2002.
- [85.] National Council on Radiation Protection & Measurements (NRC), Repot No. 160, "Ionizing Radiation Exposure of the Population of the United States," NRC, Bethesda, MD, 2009.
- [86.] Health Physics Society (U.S.) (HPS), PS010-1, "Position Statement of the Health Physics Society - Radiation Risk in Perspective," HPS, McClean, VA, 2004.
- [87.] Turner, D.B. *Workbook of Atmospheric Dispersion Estimates*. 2nd ed.: Lewish Publishers, CRC Press, 1994.
- [88.] Chanin, D.I. and M.L. Young, NUREG/CR-6613, "Code Manual for MACCS2: Volume 2, Preprocessor Codes COMIDA2, FGRDCF, IDCF2," U.S. Nuclear Regulatory Commission, Washington, DC, 1998.
- [89.] Jow, H.N., et al., NUREG/CR-4691, "MELCOR Accident Consequence Code System (MACCS): Model Description," U.S. Nuclear Regulatory Commission, Washington, DC, 1990.
- [90.] Bixler, N. and et. al., "Software Regression Quality Assurance for MACCS2 Version 2.5.0.0 through Version 2.5.0.9," Sandia National Laboratories, Albuquerque, NM, July 2012.
- [91.] EPRI, "Modular Accident Analysis Program (MAAP) - MELCOR Crosswalk - Phase 1 Study," Prodcut ID: 3002004449, Electric Power Research Institute, Palo Alto, CA, November 2014.

- [92.] U.S. Nuclear Regulatory Commission, NUREG-2161, "Consequence Study of a Beyond-Design-Basis Earthquake Affecting the Spent Fuel Pool for a U.S. Mark I Boiling Water Reactor," Washington, DC, 2014.
- [93.] Sandia National Laboratories, NUREG/CR-7009, "MACCS Best Practices as Applied in the State-of-the-Art Reactor Consequence Analyses (SOARCA) Project," U.S. Nuclear Regulatory Commission, Washington, DC, 2014.
- [94.] U.S. Nuclear Regulatory Commission, Advisory Committee on Reactor Safeguards, "State-of-the-Art Reactor Consequence Analyses (SOARCA) Project May 15, 2012 letter report," ML12135A385, Washington D.C., 2012.

APPENDIX A
PROBABILISTIC ANALYSIS METHODOLOGY

A PROBABILISTIC ANALYSIS METHODOLOGY

A.1 Probabilistic Analysis Methodology

As described in Section 2.3, a consequence analysis for a NPP, or in general any type of engineered facility, is an analysis intended to answer three questions about the facility (i.e., Q1, Q2 and Q3) and one question about the analysis itself (i.e., Q4).

In turn, answering the four indicated questions leads to an analysis based on three basic mathematical structures or entities: (1) EN1, a probability space characterizing aleatory uncertainty; (2) EN2, a function that predicts the physical behavior of the facility under consideration; and (3) EN3, a probability space characterizing epistemic uncertainty [66, 67]. The probability space corresponding to EN1 characterizes aleatory uncertainty and provides the basis for answering Questions Q1 and Q2. In practice, the function corresponding to EN2 is one or more very complex numerical models and provides the basis for answering Question Q3. The probability space corresponding to EN3 characterizes epistemic uncertainty and provides the basis for answering Question Q4. The nature of the basic analysis components EN1, EN2 and EN3 in the context of the SOARCA Uncertainty Analysis is elaborated on in this section.

The first entity, EN1, corresponds to a probability space (A, \mathcal{A}, p_A) , where A is the set of everything that could occur in the particular universe under consideration (i.e., over some specified time period for the facility under analysis). \mathcal{A} is a suitably restricted set of subsets of A for which probability is defined, and p_A is the function that defines probability for elements of \mathcal{A} (i.e., if Σ is an element of \mathcal{A} , then $p_A(\Sigma)$ is the probability of Σ) (Ref 19). In the usual terminology of probability theory, A is called the sample space or sometimes the universal set; elements of \mathcal{A} are called elementary events; elements of A are called events; p_A is called a probability measure; and $p_A(\Sigma)$ is the probability of the event Σ . Elements of A are often called futures; elements of A are often called scenarios or scenario classes; and $p_A(\Sigma)$ is the probability of a scenario Σ .

For NPPs, the probability space (A, \mathcal{A}, p_A) for aleatory uncertainty is usually defined to characterize the occurrence of potential future events over some time period of interest (e.g., for a time period corresponding to one year plant operation or perhaps the intended operating life of the plant) that could affect the behavior/performance of the plant. Specifically, each element \mathbf{a} of the sample space A is a vector of the form $\mathbf{a} = [a_1, a_2, \dots, a_n]$, where the elements of \mathbf{a} characterize the properties of one potential sequence of occurrences over the time interval under consideration. The probability space (A, \mathcal{A}, p_A) , for aleatory uncertainty is typically developed with extensive use of fault and event trees to define the probabilities of all possible scenarios,

For the SOARCA analysis, A corresponds to the set of all possible five day sequences of weather conditions that could potentially occur at the Peach Bottom site. Specifically,

$$A = \{\mathbf{a} = \text{vector characterizing 5 day sequence of weather conditions at PB site}\}. \quad \text{Equation A-1}$$

In a full consequence analysis for a nuclear power station, the indicated vector of weather conditions would be only one of many components of each element of A (e.g., see summary of the NUREG-1150 reactor consequence analyses in [19]). In the SOARCA analyses, weather bins (i.e., sets of weather sequences with similar characteristics) correspond to elements of the

set A . Further, the probabilities that are defined by the function p_A are approximated on the basis on one year of hourly weather data collected at the Peach Bottom site (i.e., if ΩB is a weather bin, then $p_A(\Omega B)$ is the probability of this weather bin, with this probability being approximated on the basis of one year of weather data).

Although the concept of a probability space is important conceptually and convenient notationally, calculations involving a probability space (A, \mathcal{A}, p_A) are often described with a density function $d_A(\mathbf{a})$, where

$$p_A(S) = \int_S d_A(\mathbf{a}) dS \quad \text{Equation A-2}$$

for $\Sigma \in \mathcal{A}$, $\mathbf{a} \in \Sigma$, and dS corresponding to an increment of volume from Σ . Then, the expected value, variance, CDF, and CCDF at time τ (yr) associated with a real-valued function $y = f(\tau|\mathbf{a})$ defined on A are defined by

$$E_A[f(\tau|\mathbf{a})] = \int_A f(\tau|\mathbf{a}) d_A(\mathbf{a}) dA, \quad \text{Equation A-3}$$

$$V_A[f(\tau|\mathbf{a})] = \int_A \{f(\tau|\mathbf{a}) - E_A[f(\tau|\mathbf{a})]\}^2 d_A(\mathbf{a}) dA, \quad \text{Equation A-4}$$

$$p_A[f(\tau|\mathbf{a}) \leq y] = \int_A \underline{\delta}_y[f(\tau|\mathbf{a})] d_A(\mathbf{a}) dA, \quad \text{Equation A-5}$$

and

$$p_A[y \leq f(\tau|\mathbf{a})] = \int_A \bar{\delta}_y[f(\tau|\mathbf{a})] d_A(\mathbf{a}) dA, \quad \text{Equation A-6}$$

respectively, where

$$\underline{\delta}_y[f(\tau|\mathbf{a})] = \begin{cases} 1 & \text{if } f(\tau|\mathbf{a}) \leq y \\ 0 & \text{otherwise,} \end{cases} \quad \bar{\delta}_y[f(\tau|\mathbf{a})] = \begin{cases} 1 & \text{if } f(\tau|\mathbf{a}) > y \\ 0 & \text{otherwise,} \end{cases}$$

and dA represents an increment of volume from A .

The equalities in Equations A-5 and A-6 in effect define a CDF and a CCDF, respectively.

Specifically, if $[y_{mn}, y_{mx}]$ includes the range of possible values for y , then the plots defined by the points

$$\{y, p_A[f(\tau|\mathbf{a}) \leq y]\} \text{ and } \{y, p_A[y < f(\tau|\mathbf{a})]\} \quad \text{Equation A-7}$$

for $y_{mn} \leq y \leq y_{mx}$ correspond to the CDF and CCDF, respectively, for y . A CCDF is defined in Equation A-6 because of the typical usage of CCDFs to represent uncertainty in risk assessments. In particular, a CCDF answers the question “How likely is it to be this bad or worse?” which is usually the question asked with respect to individual consequences in a risk

assessment. In particular, CCDFs constitute the standard uncertainty structure used in the presentation of offsite consequence results calculated with MACCS.

The second entity, EN2, corresponds to a model, or more realistically a large system of interacting models, that predict the behavior of a NPP under accident conditions and various summary measures of this behavior (e.g., radionuclide release rates). Notationally, this model can be represented by a function of the form

$$\mathbf{f}(\tau | \mathbf{a}) = [f_1(\tau | \mathbf{a}), f_2(\tau | \mathbf{a}), \dots, f_m(\tau | \mathbf{a})], \quad \text{Equation A-8}$$

where τ corresponds to time (yr), each element $f(\tau | \mathbf{a})$ of $\mathbf{f}(\tau | \mathbf{a})$ is a specific calculated result, and \mathbf{a} is an element of the sample space A for aleatory uncertainty. In general, the value of $\mathbf{f}(\tau | \mathbf{a})$, and indeed the actual structure of the individual models that are combined to produce $\mathbf{f}(\tau | \mathbf{a})$, will change with changing values for \mathbf{a} . In the SOARCA Uncertainty Analysis, the function $\mathbf{f}(\tau | \mathbf{a})$ corresponds to combined calculations performed with models implemented within the MELCOR and MACCS programs. Consistent with the notation used in Equation A-8, the indicated models produce a large number of time dependent results.

In practice, functions of the form indicated in Equation A-8 are usually too complex for quadrature-based evaluations. This is certainly the case for results obtained with MACCS due to the complexity of the conditions associated with weather sequences and the extensive calculations that underlie the estimation of offsite consequences. As a consequence, results of the form indicated in Equations A-3 through A-6 are usually estimated with some form of sampling procedure. One possibility is to use simple random sampling from the sample space A for aleatory uncertainty. With this approach, a random sample

$$\mathbf{a}_j = [a_{1j}, a_{2j}, \dots, a_{nj}], j = 1, 2, \dots, nSA, \quad \text{Equation A-9}$$

is generated from A consistent with the defining probabilities for the probability space (A, \mathcal{A}, p_A) . Then, the results in Equations A-3 through A-6 are approximated on the basis of this sample. For example, the approximations to the expected value in Equation A-3 and the exceedance probability in Equation A-6 for an element $f(\tau | \mathbf{a})$ of the function $\mathbf{f}(\tau | \mathbf{a})$ in Equation A-8 are:

$$E_A[f(\tau | \mathbf{a})] \cong \sum_{j=1}^{nSA} f(\tau | \mathbf{a}_j) / nSA \quad \text{Equation A-10}$$

and

$$p_A[y \leq f(\tau | \mathbf{a})] \cong \sum_{j=1}^{nSA} \delta_y[f(\tau | \mathbf{a}_j)] / nSA, \quad \text{Equation A-11}$$

respectively.

An alternate procedure is to subdivide A into a sequence of disjoint subsets $A_j, j = 1, 2, \dots, nSA$, and randomly sample a single element \mathbf{a}_j from each set A_j . Then, the results in Equations A-3 through A-6 are approximated on the basis of the sets A_j and the sampled elements \mathbf{a}_j . For example, the resultant approximations to the expected value in Equation A-3 and the

exceedance probability in Equation A-6 for an element $f(\tau|\mathbf{a})$ of the function $\mathbf{f}(\tau|\mathbf{a})$ in Equation A-8 are:

$$E_A[f(\tau|\mathbf{a})] \cong \sum_{j=1}^{nSA} f(\tau|\mathbf{a}_j) p_A(\mathbf{A}_j) \quad \text{Equation A-12}$$

and

$$p_A[y \leq f(\tau|\mathbf{a})] \cong \sum_{j=1}^{nSA} \bar{\delta}_y[f(\tau|\mathbf{a}_j)] p_A(\mathbf{A}_j), \quad \text{Equation A-13}$$

respectively. This approach corresponds to use of the Kaplan-Garrick ordered triple representation for risk.

A variant of the approach indicated in the preceding paragraph is used with MACCS in the SOARCA analyses in the estimation of expected values and exceedance probabilities. In this variant, the sets \mathbf{A}_j , $j = 1, 2, \dots, nSA$, correspond to ΩB_j , $j = 1, 2, \dots, 36 = nWB$, weather bins (i.e., subsets of the set \mathbf{A} in Equation A-1), and \mathbf{a}_{jk} , $k = 1, 2, \dots, nWB_j$, elements are sampled from each weather bin ΩB_j . In the SOARCA uncertainty analyses, nWB_j is defined by

$$nWB_j = \begin{cases} [0.05 nWBT_j] & \text{if } 12 < 0.05 nWBT_j \\ 12 & \text{if } 0.05 nWBT_j < 12 < nWBT_j \\ nWBT_j & \text{if } nWBT_j \leq 12, \end{cases} \quad \text{Equation A-14}$$

where $nWBT_j$ is the number of elements in ΩB_j estimated on the basis of one year of weather data and $[~]$ corresponds to the greatest integer function. Then, the results in Equations A-3 through A-6 are approximated on the basis of the sets ΩB_j and the sampled elements \mathbf{a}_{jk} . For example, the resultant approximations to the expected value in Equation A-3 and the exceedance probability in Equation A-6 for an element $f(\tau|\mathbf{a})$ of the function $\mathbf{f}(\tau|\mathbf{a})$ in Equation A-8 are

$$E_A[f(\tau|\mathbf{a})] \cong \sum_{j=1}^{nWB} \left[\sum_{k=1}^{nWB_j} f(\tau|\mathbf{a}_{jk}) / nWB_j \right] p_A(\mathbf{WB}_j) \quad \text{Equation A-15}$$

and

$$p_A[y \leq f(\tau|\mathbf{a})] \cong \sum_{j=1}^{nWB} \left\{ \sum_{k=1}^{nWB_j} \bar{\delta}_y[f(\tau|\mathbf{a}_{jk})] / nWB_j \right\} p_A(\mathbf{WB}_j), \quad \text{Equation A-16}$$

respectively.

The third entity, EN3, corresponds to a probability space (E, E, p_E) for epistemic uncertainty. The conceptual properties associated with probability space (E, E, p_E) are the same as

indicated in Equations A-2 through A-6 for the probability space (A, \mathcal{A}, p_A) for aleatory uncertainty. In general, the elements of the sample space Ω are vectors of the form:

$$\begin{aligned}\mathbf{e} &= [\mathbf{e}_A, \mathbf{e}_M] \\ &= [e_{A1}, e_{A2}, \dots, e_{A,nEA}, e_{M1}, e_{M2}, \dots, e_{M,nEM}] \\ &= [e_1, e_2, \dots, e_{nE}], nE = nEA + nEM,\end{aligned}\tag{Equation A-17}$$

where $\mathbf{e}_A = [e_{A1}, e_{A2}, \dots, e_{A,nEA}]$ is a vector of epistemically uncertain quantities used in the characterization of aleatory uncertainty (not considered in this analysis as no aspect of the weather trials are treated as being epistemically uncertain) and $\mathbf{e}_M = [e_{M1}, e_{M2}, \dots, e_{M,nEM}]$ is a vector of epistemically uncertain quantities used in the evaluation of $\mathbf{f}(\tau|\mathbf{a})$.

In the SOARCA Uncertainty Analysis, the vector \mathbf{e}_M of epistemically uncertain model parameters has two components: a vector \mathbf{e}_{ME} of epistemically uncertain parameters used in MELCOR calculations and a vector \mathbf{e}_{MA} of epistemically uncertain parameters used in MACCS calculations (Table 2.2-1). Specifically, the form of \mathbf{e}_M in the SOARCA Uncertainty Analysis is

$$\begin{aligned}\mathbf{e}_M &= [\mathbf{e}_{ME}, \mathbf{e}_{MA}] \\ &= [e_{ME,1}, e_{ME,2}, \dots, e_{ME,nME}, e_{MA1}, e_{MA2}, \dots, e_{MA,nMA}] \\ &= [e_1, e_2, \dots, e_{nE}], nE = nME + nMA\end{aligned}\tag{Equation A-18}$$

with $nME = 12$ and $nMA = 9$.

In practice, the probability space (E, \mathcal{E}, p_E) is defined by assigning probability distributions to the individual elements of \mathbf{e} . In addition, correlations and other restrictions involving the elements of \mathbf{e} may also be specified. The specified distributions serve as mathematical summaries of all available information with respect to where the appropriate values for the elements of \mathbf{e} are located and are often developed through expert review processes [68, 69, and 70]. The development of the distributions characterizing epistemic uncertainty in the SOARCA Uncertainty Analysis, are discussed in Section 4.1.

With the introduction of the probability space (E, \mathcal{E}, p_E) for epistemic uncertainty, the representation for the system model in Equation A-8 becomes

$$\mathbf{f}(\tau|\mathbf{a}, \mathbf{e}_M) = [f_1(\tau|\mathbf{a}, \mathbf{e}_M), f_2(\tau|\mathbf{a}, \mathbf{e}_M), \dots, f_m(\tau|\mathbf{a}, \mathbf{e}_M)].\tag{Equation A-19}$$

Further, given that there is no uncertainty in the characterization of aleatory uncertainty as is the case in the SOARCA analysis, results of the form in Equations A-3, A-5, and A-6 become:

$$E_A[f(\tau|\mathbf{a}, \mathbf{e}_M)] = \int_A f(\tau|\mathbf{a}, \mathbf{e}_M) d_A(\mathbf{a}) dA,\tag{Equation A-20}$$

$$p_A[f(\tau|\mathbf{a}, \mathbf{e}_M) \leq y] = \int_A \delta_y[f(\tau|\mathbf{a}, \mathbf{e}_M)] d_A(\mathbf{a}) dA,\tag{Equation A-21}$$

and

$$p_A \left[y < f(\tau | \mathbf{a}, \mathbf{e}_M) \right] = \int_A \bar{\delta}_y \left[f(\tau | \mathbf{a}, \mathbf{e}_M) \right] d_A(\mathbf{a}) dA, \quad \text{Equation A-22}$$

where $f(\tau | \mathbf{a}, \mathbf{e}_M)$ corresponds to one of the functions $f_i(\tau | \mathbf{a}, \mathbf{e}_M)$ contained in $\mathbf{f}(\tau | \mathbf{a}, \mathbf{e}_M)$. As \mathbf{e}_M changes, each of the preceding quantities also changes and has a probability distribution that derives from the probability space (E, \mathcal{E}, p_E) for epistemic uncertainty.

In concept, probability distributions over epistemic uncertainty for quantities of the form defined in Equations A-20 through A-22 are defined by integrals over the sample space E for epistemic uncertainty. In practice, such integrals are too complex for quadrature approximations and, as a consequence, must be approximated with sampling-based procedures. Specifically, a random or Latin hypercube sample [71, 72]

$$\mathbf{e}_{Mi} = [e_{i1}, e_{i2}, \dots, e_{i,nE}], i = 1, 2, \dots, nSE, \quad \text{Equation A-23}$$

is generated from E in a manner consistent with the probability distributions that characterize epistemic uncertainty. Then, analysis results of interest (e.g., results of the form in Equations A-20 through A-22) are determined for each element \mathbf{e}_{Mi} of the indicated sample. For example, if random sampling is used to approximate integrals over aleatory uncertainty as in Equations A-10 and A-11, the approximations to the results in Equations A-20 and A-22 become:

$$\begin{aligned} E_A \left[f(\tau | \mathbf{a}, \mathbf{e}_{Mi}) \right] &= \int_A f(\tau | \mathbf{a}, \mathbf{e}_{Mi}) d_A(\mathbf{a}) dA \\ &\cong \sum_{j=1}^{nSA} f(\tau | \mathbf{a}_j, \mathbf{e}_{Mi}) / nSA \\ &= \tilde{E}_A \left[f(\tau | \mathbf{a}, \mathbf{e}_{Mi}) \right] \end{aligned} \quad \text{Equation A-24}$$

and

$$\begin{aligned} p_A \left[y < f(\tau | \mathbf{a}, \mathbf{e}_{Mi}) \right] &= \int_A \bar{\delta}_y \left[f(\tau | \mathbf{a}, \mathbf{e}_{Mi}) \right] d_A(\mathbf{a}) dA \\ &\cong \sum_{j=1}^{nSA} \bar{\delta}_y \left[f(\tau | \mathbf{a}_j, \mathbf{e}_{Mi}) \right] / nSA \\ &= \tilde{p}_A \left[y < f(\tau | \mathbf{a}, \mathbf{e}_{Mi}) \right] \end{aligned} \quad \text{Equation A-25}$$

for each element \mathbf{e}_{Mi} of the indicated sample. Approximations to distributions summarizing epistemic uncertainty can now be obtained from results of the form in Equations A-24 and A-25 with an equal weight of $1/nSE$ assigned to the results obtained with each sample element. Further, mappings of the form

$$[\mathbf{e}_{Mi}, \tilde{E}_A \left[f(\tau | \mathbf{a}, \mathbf{e}_{Mi}) \right]], i = 1, 2, \dots, nSE, \quad \text{Equation A-26}$$

and

$$\left[\mathbf{e}_{Mi}, \tilde{p}_A \left[y < f(\tau | \mathbf{a}, \mathbf{e}_{Mi}) \right] \right], i = 1, 2, \dots, nSE,$$

Equation A-27

form the basis for the application of a variety of sensitivity analysis procedures as discussed in Section 3.2.

In the SOARCA Uncertainty Analysis, a sample of size $nSE = 300$ is used to generate the sample indicated in Equation A-23. Specifically, the component \mathbf{e}_{ME} of \mathbf{e}_M will be sampled with random sampling and the component \mathbf{e}_{MA} of \mathbf{e}_M will be sampled with Latin hypercube sampling. In turn, SOARCA results of the form indicated in Equations A-15 and A-16 will be approximated by

$$\begin{aligned} E_A \left[f(\tau | \mathbf{a}, \mathbf{e}_{Mi}) \right] &\cong \sum_{j=1}^{nWB} \left[\sum_{k=1}^{nWB_j} f(\tau | \mathbf{a}_{jk}, \mathbf{e}_{Mi}) / nWB_j \right] p_A(WB_j) \\ &= \tilde{E}_A \left[f(\tau | \mathbf{a}, \mathbf{e}_{Mi}) \right] \end{aligned}$$

Equation A-28

and

$$\begin{aligned} p_A \left[y \leq f(\tau | \mathbf{a}, \mathbf{e}_{Mi}) \right] &\cong \sum_{j=1}^{nWB} \left\{ \sum_{k=1}^{nWB_j} \bar{\delta}_y \left[f(\tau | \mathbf{a}_{jk}, \mathbf{e}_{Mi}) \right] / nWB_j \right\} p_A(WB_j) \\ &= \tilde{p}_A \left[y \leq f(\tau | \mathbf{a}, \mathbf{e}_{Mi}) \right] \end{aligned}$$

Equation A-29

for each sample element \mathbf{e}_{Mi} . As discussed in the preceding paragraph, results of the form in Equations A-28 and A-29 provided the basis in SOARCA for assessing the effects and implications of epistemic uncertainty.

A.2 Parameter Sensitivity and Uncertainty Analysis Methodology

Closely associated with the characterization of epistemic uncertainty provided by the probability space corresponding to EN3 and the answering of Question Q4 (described in Section 2.3) are the concepts of uncertainty analysis and sensitivity analysis, where uncertainty analysis designates the determination of the epistemic uncertainty in analysis results that derives from epistemic uncertainty in analysis inputs and sensitivity analysis designates the determination of the contribution of the epistemic uncertainty in individual analysis inputs to the epistemic uncertainty in analysis results. Specifically, uncertainty analysis involves determining the range and distribution of an analysis result of interest that derive from the ranges and distributions of uncertain analysis inputs. The goal of uncertainty analysis is to determine the uncertainty in an analysis result that derives from the collective uncertainty in analysis inputs. In contrast, the goal of sensitivity analysis is to determine the extent to which the uncertainty in individual analysis inputs contributes to the uncertainty in an analysis result. Intuitively, sensitivity analysis corresponds to decomposing the uncertainty in an analysis result into the fractions of this uncertainty contributed by each uncertain analysis input. Commonly used sensitivity analysis procedures include scatterplots, correlation coefficients, partial correlation coefficients, stepwise regression with raw or rank transformed data, and a number of other techniques. General references on uncertainty and sensitivity analysis include [11-13, 71, 73, 74]. Example uncertainty and sensitivity analyses include studies of the MAEROS component of MELCOR model system for reactor accidents [75, 76] and the MACCS model system for offsite consequences of reactor accidents [77-80, and 81].

Basically, uncertainty and sensitivity analysis are the means by which EN3 gives rise to the answer to Question Q4. As an example, a parameter uncertainty analysis was conducted using the methods described below for both source term and radiological consequences to evaluate the effects of the uncertainty in key inputs on a selected accident scenario.

Several of the approaches to sensitivity analysis that can be used in conjunction with a sampling-based uncertainty analysis are listed and briefly summarized below. In this summary, (i) x_j is an element of a vector $\mathbf{x} = [x_1, x_2, \dots, x_{nX}]$ of epistemically uncertain analysis inputs, (ii) y_k is an element of $\mathbf{y}(\mathbf{x}) = [y_1(\mathbf{x}), y_2(\mathbf{x}), \dots, y_{nY}(\mathbf{x})]$, (iii) $\mathbf{x}_i = [x_{i1}, x_{i2}, \dots, x_{i,nX}]$, $i = 1, 2, \dots, nS$, is a random or Latin hypercube sample from the possible values for \mathbf{x} generated in consistency with the joint distribution assigned to the x_j , (iv) $\mathbf{y}_i = \mathbf{y}(\mathbf{x}_i)$ for $i = 1, 2, \dots, nS$, and (v) x_{ij} and y_{ik} are elements of \mathbf{x}_i and \mathbf{y}_i , respectively.

Scatterplots

Scatterplots are plots of the points $[x_{ij}, y_{ik}]$ for $i = 1, 2, \dots, nS$ and can reveal nonlinear or other unexpected relationships (Figure A-1). In many analyses, scatterplots provide all the information that is needed to understand the sensitivity of analysis results to the uncertainty in analysis inputs. Further, scatterplots constitute a natural starting point in a complex analysis that can help in the development of a sensitivity analysis strategy using one or more additional techniques [82, 83].

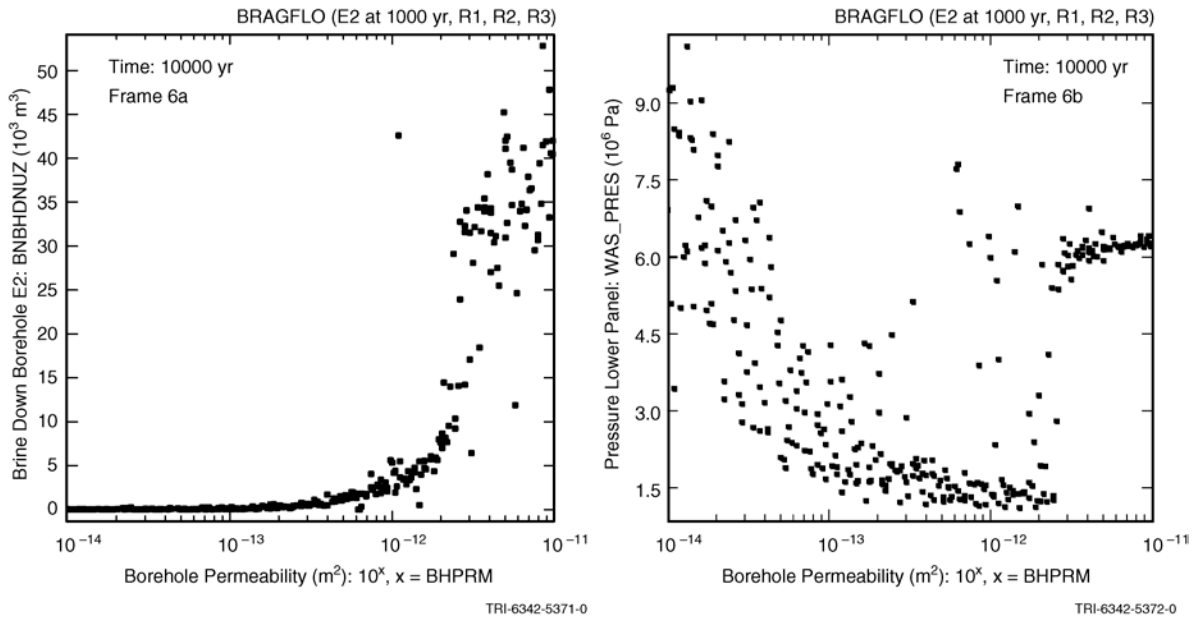


Figure A-1 Examples of scatterplots obtained in a sampling-based uncertainty /sensitivity analysis ([73], Fig. 8.2)

Correlation

A correlation coefficient (CC) provides a measure of the strength of the linear relationship between x_j and y_k . The CC between x_j and y_k is equal to the standardized regression coefficient (SRC) in a linear regression relating y_k to x_j and is also equal in absolute value to the square root of the R^2 value associated with the indicated regression. When calculated with raw (i.e., untransformed) data, the CC is often referred to as the Pearson CC [47, 82]

Regression Analysis

Regression analysis provides an algebraic representation of the relationships between y_k and one or more x_j 's. Regression analysis is usually performed in a stepwise fashion, with initial inclusion of most important x_j , then two most important x_j 's, and so on until no more x_j 's that significantly affect y_k can be identified. Variable importance is indicated by order of selection in the stepwise process, changes in R^2 values as additional variables are added to the regression model, and SRCs for the x_j 's in the final regression model (Table A-1). A display of regression results in the form shown in Table A-1 is very unwieldy when results at a sequence of times are under consideration. In this situation, a more compact display of regression results is provided by plotting time-dependent SRCs (Figure A-2) [82, 83].

Table A-1 Example of Stepwise Regression Analysis to Identify Uncertain Variables Affecting the Uncertainty in Pressure at 10,000 years on Figure 5a ([73], Table 8.6)

Step ^a	Variable ^b	SRC ^c	R^2 ^d
1	WMICDFLG	0.718	0.508
2	HALPOR	0.466	0.732
3	WGRCOR	0.246	0.792
4	ANHPRM	0.129	0.809
5	SHRGSSAT	0.070	0.814
6	SALPRES	0.063	0.818

^a Steps in stepwise regression analysis.

^b Variables listed in the order of selection in regression analysis.

^c SRCs for variables in final regression model.

^d Cumulative R^2 value with entry of each variable into regression model.

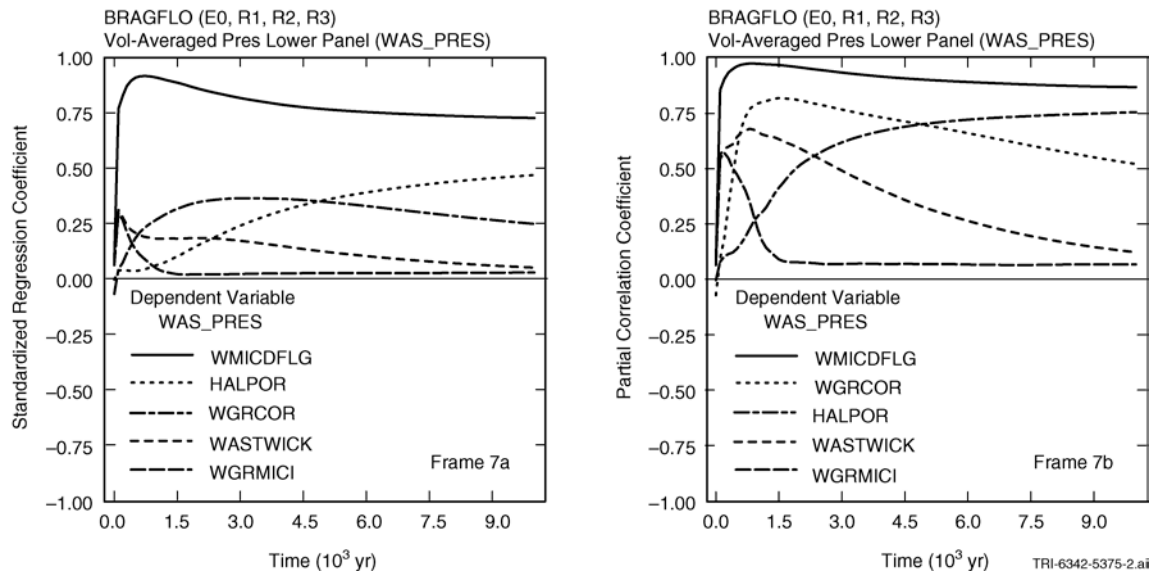


Figure A-2 Time-dependent sensitivity analysis results for uncertain pressure curves in Fig. 5a: (a) SRCs as a function of time, and (b) PCCs as a function of time ([73], Fig. 8.3)

Partial Correlation

A partial correlation coefficient (PCC) provides a measure of the strength of the linear relationship between y_k and x_j after the linear effects of all other elements of \mathbf{x} have been removed. Similarly to SRCs, PCCs can be determined as a function of time for time-dependent analysis results (Figure A-3) [82, 83].

Rank Transformations

A rank transformation replaces values for y_k and x_j with their corresponding ranks. Specifically, the smallest value for a variable is assigned a rank of 1; next largest value is assigned a rank of 2; tied values are assigned their average rank; and so on up to the largest value, which is assigned a rank of n . Use of the rank transformation converts a nonlinear but monotonic relationship between y_k and x_j to a linear relationship and produces rank (i.e., Spearman) correlations, rank regressions, SRRCs and partial rank correlation coefficients (PRCCs). In the presence of nonlinear but monotonic relationships between the x_j and y_k , the use of the rank transform can substantially improve the resolution of sensitivity analysis results (Table A-2) [and 82, 83, 84].

Table A-2 Comparison of Stepwise Regression Analyses with Raw and Rank-Transformed Data for Variable BRAALIC on Figure 4b ([73], Table 8.8)

Step ^a	Raw Data			Rank-Transformed Data		
	Variable ^b	SRC ^c	R^2 ^d	Variable ^b	SRRC ^e	R^2 ^d
1	ANHPRM	0.562	0.320	WMICDFLG	-0.656	0.425
2	WMICDFLG	-0.309	0.423	ANHPRM	0.593	0.766
3	WGRCOR	-0.164	0.449	HALPOR	-0.155	0.802
4	WASTWICK	-0.145	0.471	WGRCOR	-0.152	0.824
5	ANHBCEXP	-0.120	0.486	HALPRM	0.143	0.845
6	HALPOR	-0.101	0.496	SALPRES	0.120	0.860
7				WASTWICK	-0.010	0.869

^a Steps in stepwise regression analysis.

^b Variables listed in order of selection in regression analysis.

^c SRCs for variables in final regression model.

^d Cumulative R^2 value with entry of each variable into regression model.

^e SRRCs for variables in final regression model.

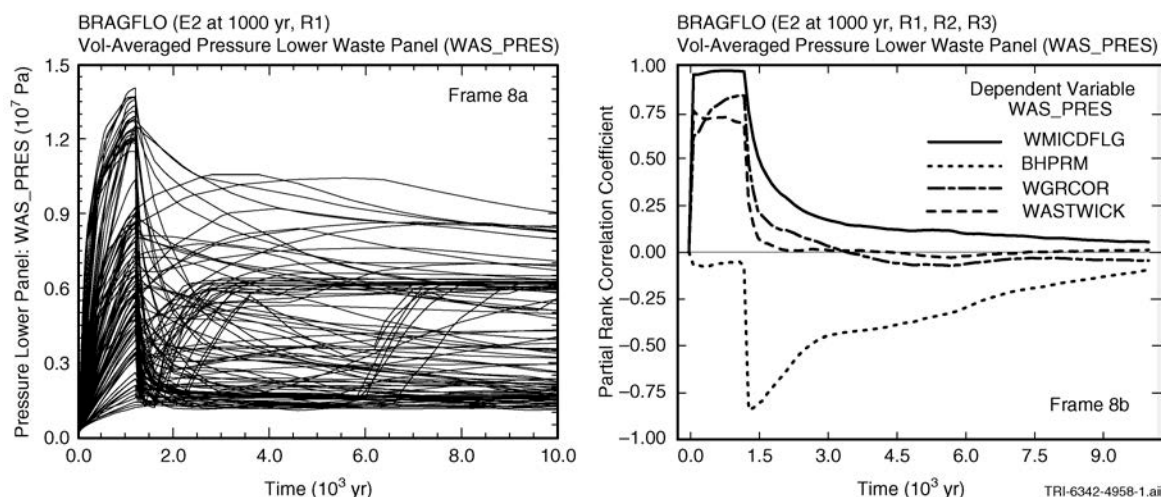


Figure A-3 Illustration of failure of a sensitivity analysis based on rank-transformed data: (a) Pressures as a function of time and (b) PRCCs as a function of time ([73], Figure 8.7)

For SOARCA the parameter uncertainty and sensitivity analysis will be based upon a mapping between uncertain inputs and analysis results using: (1) Stepwise rank regression analyses, and (2) Scatter plots.

Partial rank correlation coefficients provide a measure of the strength of the monotonic relationships between an independent variable and a dependent variable after a correction has been made to remove the monotonic effects of the other independent variables in the analysis. PRCCs involve the analysis of rank transformed data to transform monotonic relationships into linear relationships. In a stepwise rank regression, the single independent variable that makes the largest contribution to the uncertainty in the dependent variable is selected in the first step. This process continues until no additional variables are found that make identifiable

(i.e., significant) contributions to the uncertainty in the dependent variable. A significance level of 0.01 will be used as the criterion for terminating a stepwise regression analysis. In the context of stepwise regression analysis, variable importance is indicated by (1) order of selection in the stepwise selection process, (2) incremental changes in cumulative R^2 values, and (3) the sign and size of the standardized regression coefficients, (i.e., SRRCs, when rank regression is being used) in the final regression model. Results will be presented as a set of CCDFs. A calculation of the confidence bounds on the mean values for the CCDF and other result metrics (e.g., fraction of the cesium released to the environment) will be included.

Along with rank regression, quadratic, recursive partitioning, and multivariate adaptive regression splines (MARS) are the four regression techniques used to estimate the importance of the input parameters in the uncertainty of the output in consideration. A short description of each technique follows. A more detailed description of the techniques (with examples) can be found in [12] and [13].

Quadratic regression

Quadratic regression technique applies the same approach as linear regression, including individual input variables, the square of these variables and second order multiplicative interaction terms. The prediction model is of the form:

$$Y = a_0 + \sum_{i=1}^n a_i X_i + \sum_{i=1}^n b_i X_i^2 + \sum_{i=1}^n \sum_{j=i+1}^n c_{ij} X_i X_j + \varepsilon$$

Quadratic regression is not completely additive as it can capture 2nd order interactions. It can also capture the parabolic influence measured by the square of variables in the regression model. However, a complex relationship between variables and the output may still be hard to capture with this technique (asymptotic behavior for instance), and the method remains parametric which makes it sensitive to outliers. As quadratic regression can capture non-monotonic relationships, additional sets of metrics are displayed in the table of regression results from this method. S_i represents the first order sensitivity index and informs on how much of the variance of the selected output is explained by the input parameter in consideration by itself. This index is therefore very close in concept to the R^2_{cont} presented above for the rank regression technique and it is acceptable to compare the two metrics. The second metric, labeled T_i represents the total order sensitivity index and informs on how much of the variance of the selected output is explained by the input parameter in consideration by itself and its interaction with all of the other uncertain parameters. It has no equivalent in the rank regression model (as the additive model does not capture conjoint influences). The difference between T_i and S_i gives an estimate of the conjoint influence for this input on the output of consideration. Finally, a p-value is displayed as third metric, informing on how much confidence can be put in the results. A p-value equal or close to zero indicates that the influence is likely to be true (in the mathematical sense. It can still be unrealistic physically and due to the particularity of the sample), while a p-value equal or close to one indicates a relationship that is not real and due to spurious correlation.

Recursive partitioning

Recursive partitioning regression is also known as a regression tree. A regression tree splits the data into subgroups such as the values are more homogeneous in each subgroup. The regression function is constructed using the sample mean over each subgroup. This approach results in a piecewise constant function over the input space in consideration. Recursive partitioning handles conjoint influences. The predictive model is in the form of:

$$Y = \sum_{s=1}^{n^P} (d_s I_s(X_i))_{i=1, \dots, n} + \varepsilon$$

The same metrics used for quadratic regression are used for recursive partitioning, that is to say the first order sensitivity indices (S_i), total order sensitivity indices (T_i) and p-values.

Multivariate Adaptive Regression Splines (MARS)

MARS is a combination of (linear) spline regression, stepwise model fitting and recursive partitioning. A regression with a single input starts with a mean only model and adds basis functions in a stepwise manner adding first the overall linear trend. That creates a first model. A second model using linear regression via least square is fitted to the data. This model is then added to the basis functions in a way that reduce the SSE between observation and prediction. A fourth basis function is then added to minimize again the SSE. This process is repeated until 'M' basis functions have been added.

At this point, the MARS procedure will try to simplify the model using stepwise deletion of basis function, while keeping the y-intercept and linear trend. Over the 'M-2' candidates, the one leading to the smallest increase of SSE will be selected. This deletion will be applied until regressed to the original linear model.

Stepwise addition and deletion lead to the building of '2M-2' different models. The "best" model is chosen using generalized cross validation (GCV) score which corresponds to a SSE normalized by the number of basis functions considered. With multiple inputs, the basis functions will consists into main effects and multiple-way interactions. The options used for this analysis consider only two-way interaction to avoid exponential cost of considering more interactions. MARS are presented using the same metrics as quadratic regression and recursive partitioning in the summary tables.

APPENDIX B
SOFTWARE USED AND CODE INTEGRATION

B.1 SOFTWARE USED

To better understand the uses of computer codes that are discussed in this section, a brief overview is in order. MELCOR is a computer code that models the progression of severe accidents in PWRs and BWRs [7]. MELMACCS compiles MELCOR outputs for transition into part of a MACCS (MELCOR Accident Consequence Code System) input [8]. MACCS [9] can calculate the estimated consequences associated with a release of radioactive material into the environment. Detailed descriptions of the capabilities of the software used in this analysis can be found in the referenced user's manuals [7-9]. This section documents the process used including the inputs and outputs, information flow, and order of operation for each code used to conduct the integrated probabilistic analysis.

B.1.1 MELCOR

MELCOR was developed by SNL for the NRC to model the progression of accidents in a light water reactor. A broad spectrum of accident phenomena in both PWR and BWR are treated within the code. MELCOR can estimate the fission product source term and also apply sensitivity and uncertainty analysis for the estimated source term. For this work MELCOR Version 1.8.6 YV3780 was used to generate the source terms for the consequence and uncertainty analyses, respectively. MELCOR Version 1.8.6 YR549 was used for the Peach Bottom unmitigated LTSBO SOARCA estimate case presented in NUREG-1935. A comparison of the source term results between the two MELCOR versions is presented in Appendix C. However, both versions of MELCOR were used in NUREG-1935 while only MELCOR 1.8.6 YV3780 was used for the Surry ISLOCA scenario [40].

MELCOR is divided into 20 different packages and an execution primer. All of these packages are coupled within the code to model major reactor plant systems. The codes model response to accident conditions which include but are not limited to [7]:

- Thermal-hydraulic response of the primary reactor coolant system, the reactor cavity, the containment, and the confinement buildings;
- Core uncovering, fuel heatup, cladding oxidation, fuel degradation, and core material melting and relocation;
- Heatup of reactor vessel lower head from relocated fuel materials and the thermal and mechanical loading and failure of the vessel lower head and transfer of core materials to the reactor vessel cavity;
- Core-concrete attack and ensuing aerosol generation;
- In-vessel and ex-vessel hydrogen production, transport, and combustion;
- Fission product release, transport, and deposition;
- Behavior of radioactive aerosols in the reactor containment building; and
- Impact of engineered safety features on thermal-hydraulic and radionuclide behavior.

The MELCOR model uses a 'control volume' approach for describing and combining reactor plant systems (i.e., see Section 4.1 and 4.2 of Reference 2 for examples of MELCOR 'control volumes'). MELCOR can provide a detailed and unique reactor plant model for any type of PWR or BWR and has even been demonstrated to successfully model Russian VVER and RMBK-reactor classes [7].

The first part of the MELCOR execution is called MELGEN. MELGEN provides a starting point for MELCOR. The majority of the initial conditions are specified, processed, and checked for execution errors. Upon execution of MELGEN, a restart file for MELCOR is written. The MELCOR code is then executed using this restart file and advances the accident scenario through predetermined timesteps until a previously end time is achieved.

As part of the MELCOR/MELGEN output, a plot file (.PTF) is created. The MELCOR output variables are written to this plot file at time intervals predetermined by the user. Figure B.1-1 provides a graphic overview of the MELCOR code and the file relations.

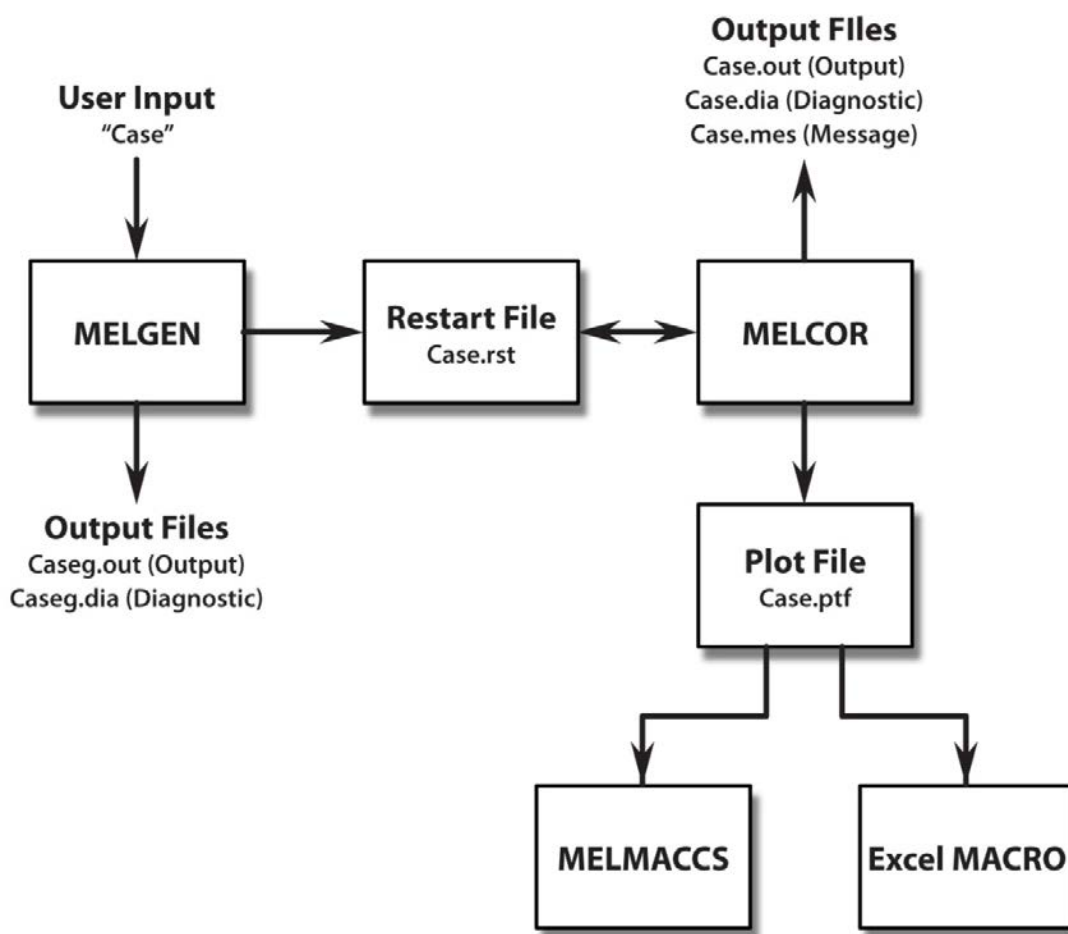


Figure B.1-1 MELCOR code and file relation

B.1.2 MELMACCS

The MELMACCS software is a Windows based program that is used to create a MELCOR Accident Consequence Code System, Version 2 (MACCS) input file from either a MELCOR Version 1.8.6 or Version 2.1 plot file (e.g., Case.ptf). The MELCOR plot files contain large amounts of data, only some of which is needed for MACCS calculations. The MELMACCS software was created to provide an interface utility between MELCOR and MACCS to integrate the required data.

MELMACCS obtains both time-independent and time-dependent data from the MELCOR plot files. Time independent data remains constant throughout the MELCOR calculation. Examples are radionuclide physical and chemical property classes and MELCOR flow paths to the environment. Time dependent data is written to the MELCOR plot file for each plot file timestep which has been determined by the user. Examples of this data are fluid temperature, flow rate through a MELCOR flow path to the environment, and the mass of each physical and chemical property class.

MELMACCS uses a graphical user interface (GUI) to allow the user to convert a MELCOR plot file into a radionuclide input file for MACCS. The inputs from the MELCOR plot file correspond to the radionuclide file inputs for the ATMOS portion of MACCS. The ATMOS portion of MACCS is discussed in Section B.1.3.1. MELMACCS can also be run in DOS to provide the user the ability to setup MELMACCS to convert multiple MELCOR plot files using a batch process. This batch process was used for this work. Each of the MELCOR plot files used in the batch process correspond with one radionuclide input file for MACCS.

Before converting the MELCOR plot file, the user must specify inputs that are needed for the MACCS radionuclide input file, but are not provided by MELCOR. These inputs are:

- Radionuclide classes,
- high/Medium/Low burnup fuel,
- time of accident initiation,
- MELCOR height associated with ground level,
- data for building height, initial plume width and height for wake calculations,
- deposition velocity information,
- mass thresholds fractions for released material, and
- time intervals for plume segments

Figure B.1-2 provides an example of a MELMACCS plume segment. A time-dependent segmented plume interval is done for each MELCOR release path to the environment. Some release paths may not contain all the radionuclides defined in MELCOR (e.g., only noble gases are released passed a failed door seal). On Figure B.1-2, the initial black vertical line shows the time of radionuclide release into the environment for this specified path, MELCOR Release Path 1. For this work, the plume release time intervals are 3,600 seconds (1 hour) as that is the minimum time interval which MACCS can incorporate into the analysis.

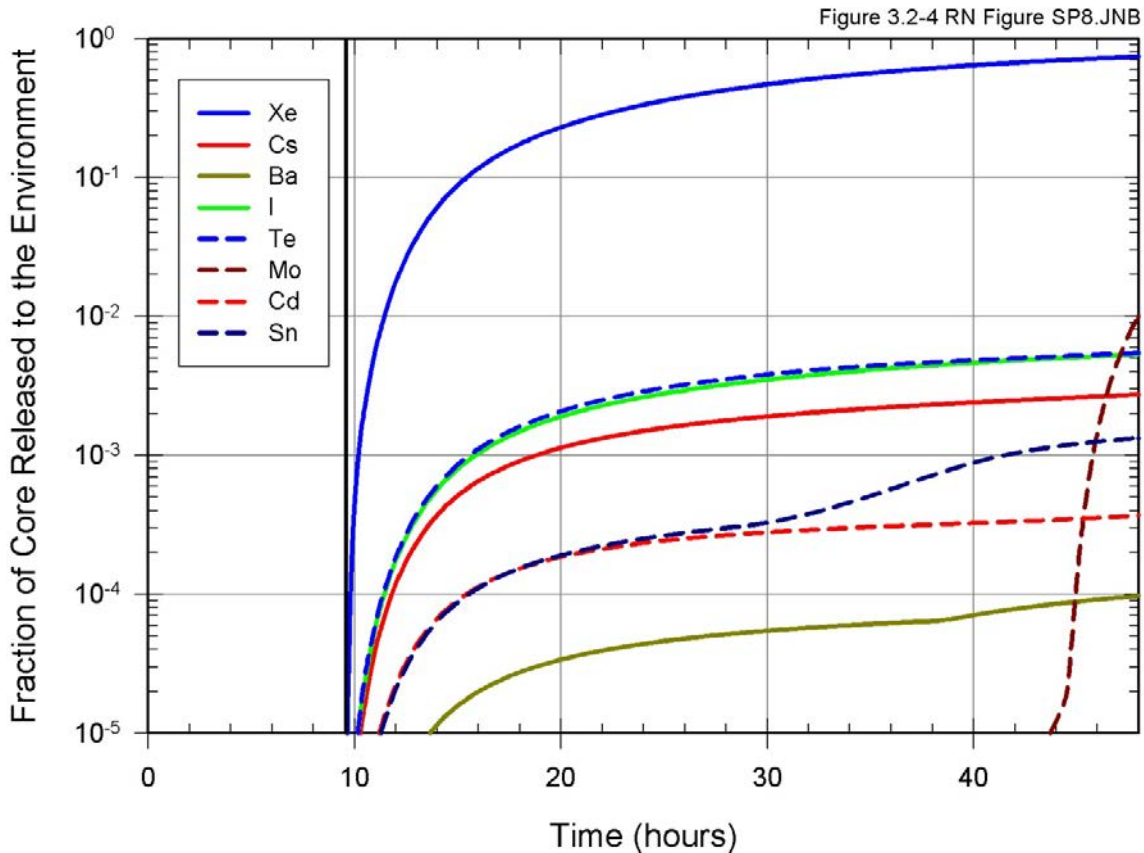


Figure B.1-2 MELMACCS plume segment

As shown on Figure B.1-2, not all radionuclide chemical/physical property classes are represented for a MELCOR release path (i.e., no uranium, U, class). Table B.1-1 lists the classes that are not represented in MELMACCS and are thus not carried over into the MACCS calculations. The user may also remove any of the 12 classes included in the MELMACCS as shown on Figure B.1-2. Class 13 through 16 are not included in the MELMACCS results because MACCS only reads the 12 radioactive radionuclide classes defined in MELCOR. Class 16 (CsI) is not a group that can be imported into MELMACCS. It is incorporated by carrying forward the activities and dose conversion factors for cesium and iodine separately, and therefore, is split accordingly into Class 2 (cesium) and Class 4 (halogens) fractions. Classes 13, 14, and 15 are nonradioactive. Figure B.1-2 does not show cerium, lanthanum, uranium, or ruthenium radionuclide classes as the release fractions of these radionuclides are less than 1.0×10^{-5} . MELMACCS does capture fractional releases below 1.0×10^{-5} ; however, for this work, a mass threshold fraction for a release path and a mass threshold fraction for plume segments to be used were set to 0.001 for MACCS inputs. These threshold limits are the same as those used in SOARCA calculations. The reason the thresholds are used is to keep the number of plume segments less than 200, which is the maximum number MACCS can analyze.

Table B.1-1 MELCOR radionuclide classes not included in MELMACCS

Class	Name	Representative	Member Elements
13	Boron	B	B, Si, P
14	Water	H ₂ O	H ₂ O
15	Concrete	--	--
16	Cesium Iodide	CsI	CsI

B.1.3 MACCS

MACCS was developed by SNL for the NRC to simulate the release of a radiological plume to the atmosphere and estimate the consequences associated with the release. The code uses a Gaussian plume dispersion model and incorporates plume depletion, exposure pathway assessment, and subsequent dose analysis. MACCS uses include PRA and radiological dose assessment for safety analyses and environmental studies such as NUREG-1150 [16]. The current version of MACCS 2.5.0.0 has a Windows based GUI called WinMACCS.

MACCS includes three primary models, ATMOS, EARLY, and CHRONC. Input files for these include the following parameter values [8]:

- ATMOS input: atmospheric transport, dispersion, and deposition parameters;
- EARLY input: parameters pertaining to the emergency phase, up to the first seven days after the accident, including mitigative actions such as evacuation, sheltering, and dose-dependent relocation; and
- CHRONC input: parameters pertaining to the intermediate and long-term phases.
- Additional auxiliary files are also required to run MACCS. These are a text file containing the path and names for the MACCS input files (MACCS.tmp), and an ASCII file containing decay-chain information (Indexr.dat). This ASCII file is included as part of the MACCS installation.

Optional data files may also be required by MACCS [8]:

- Meteorological file describing weather conditions for one or more years.
- Site files describing population, land use, and economic parameters.
- Dose conversion factor file used to calculate acute or latent health effects from various radionuclide exposures for each pathway.
- Comida2 binary file used to define food-chain doses.
- Dose threshold models

- LNT hypothesis;
- US average natural background dose rate combined with average annual medical exposure as a dose truncation level (USBGR), often cited as 620 mrem/yr [85]; and
- a dose truncation level based on the HPS that there is a dose below which, due to uncertainties, a quantified risk should not be assigned: 5 rem/yr with a lifetime limit of 10 rem [86].

All the optional files listed above were used for this analysis with the exception of the COMIDA2 binary file. The COMIDA2 binary file was not used since the ingestion pathway was not treated in SOARCA. An underlying assumption in SOARCA was uncontaminated food and water supplies are abundant within the United States, and it is unlikely that the public would eat radioactively contaminated food.

This section only discusses the three major models, ATMOS, EARLY, and CHRONC. For further information into the modeling packages described below or the auxiliary and optional data files not discussed, refer to NUREG/CR-6613 [9].

B.1.3.1 ATMOS Package

The Atmospheric Transport and Deposition (ATMOS) model uses a Gaussian plume model with Pasquill-Gifford dispersion parameters to determine the dispersion and deposition of radionuclides in the atmosphere as a function of downwind distance. The ATMOS model considers the following phenomena [9]:

- Building wake effects,
- buoyant plume rise,
- plume dispersion during transport,
- wet and dry deposition, and
- radioactive decay and ingrowth.

Figure B.1-3 provides a graphical representation of the Gaussian dispersion model along a Cartesian coordinate system.

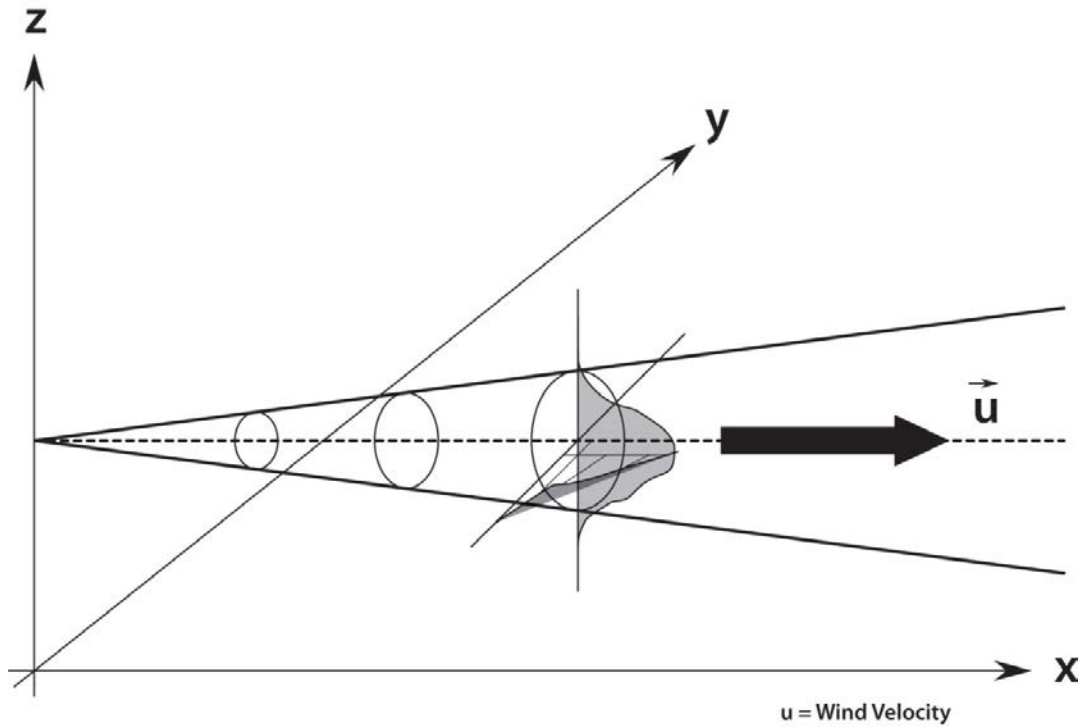


Figure B.1-3 Gaussian dispersion model

For the Gaussian puff dispersion model, isopleths of approximate equal pollutant concentrations can be created for downwind areas. Figure B.1-4 provides an example of this.

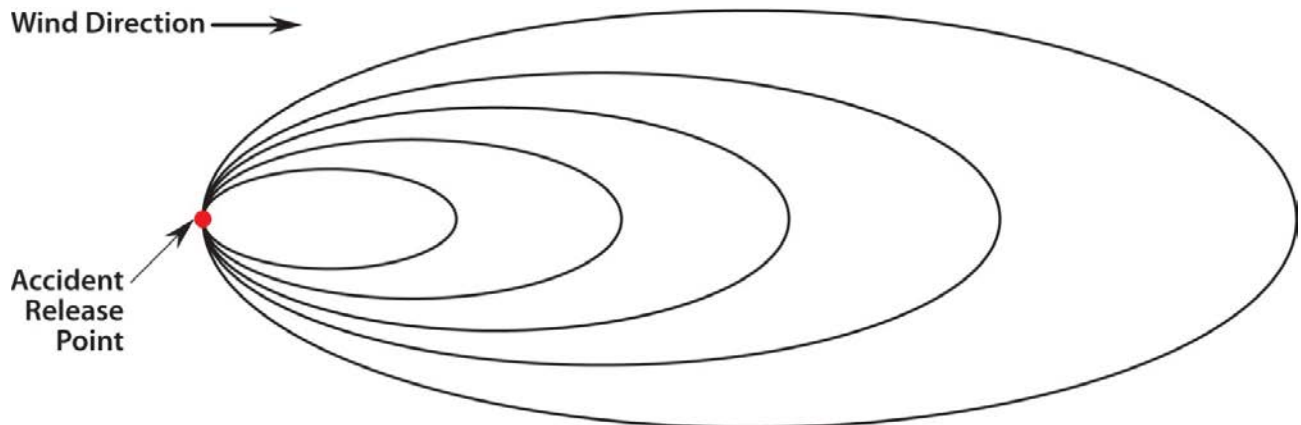


Figure B.1-4 Isopleths of equal pollutant concentration

For a Gaussian continuous source like that modeled in ATMOS, consider an infinite number of puffs, and assume the following:

- Along the x-axis as indicated on Figure B.1-3, the diffusion is negligible compared to advection thus, $\sigma_x = 0$.
- Slender plume approximation thus, $\frac{\sigma_z}{x} \gg 1$.
- The earth's surface is $z=0$ and this boundary is 'totally reflecting' the plume.

With the above assumptions, Equation B.1-1 shows a Gaussian continuous source:

$$\bar{X}(x, y, z, t) = \frac{Q}{2\pi\sigma_y\sigma_z\bar{u}} \cdot \exp\left[\left[-\frac{y^2}{2\sigma_y^2}\right] \cdot \left[\exp\left(-\frac{(z-H)^2}{2\sigma_z^2}\right) + \exp\left(-\frac{(z+H)^2}{2\sigma_z^2}\right)\right]\right] \quad \text{Equation B.1-1}$$

where:

\bar{X} = mean concentration of the pollutant

t = time

Q = emission strength of pollutant

x = x-direction on a Cartesian coordinate system

y = y-direction on a Cartesian coordinate system

z = z-direction on a Cartesian coordinate system

\bar{u} = wind velocity

H = effective elevation of source along the z-direction

The dispersion coefficients, σ_y and σ_z , depend on atmospheric stability conditions. These stability conditions vary from very stratified (Class A) to very unstable (Class B) to stable (Class F). The Pasquill-Gifford stability categories (stability classes) reflect the wind, turbulence, insolation, and other phenomena that determine dispersion of a pollutant plume in the troposphere [9]. Thus, the dispersion coefficients are the following [87]:

$$\sigma_y = \frac{k_1 x}{[1+(x/k_2)]^{k_3}} \quad \text{Equation B.1-2}$$

$$\sigma_z = \frac{k_4 x}{[1+(x/k_2)]^{k_5}} \quad \text{Equation B.1-3}$$

where:

x = downwind distance in meters from the source

k_{1-6} = constants determined as a function of the Pasquill-Gifford Stability Class

Isopleths (i.e., curves of equal concentration) can be created for downwind areas from a Gaussian continuous model. The isopleths shown on Figure B.1-4 can be applied to the continuous model. In the ATMOS model at the centerline midpoint of each isopleth, air and ground concentrations are determined for each radionuclide. Also, information about the plume size, height, and transport timing is determined for each isopleth. Concentrations are calculated along the plume centerline. The EARLY and CHRONC models make adjustments for off-centerline locations [9].

MACCS can include up to 150 radionuclides into the ATMOS model. This was expanded from the original MACCS database of 60 radionuclides used for the NUREG-1150 [16]. However, all the selected radionuclides must be present in the dose conversion file and the decay-chain database. The decay-chain database can include a maximum of six decay generations and using branch ratios will allow up to three different daughter products for each decay chain.

The ATMOS model can model up to 200 atmospheric dispersion plumes. Also, there are several different options for weather sampling within the ATMOS model. If the user supplies a one-year weather file, the ATMOS model can either sample the file using a weather category bin sampling method, or by a stratified random sampling method. However, if the user specifies a single weather trial, then the ATMOS model can either run the trial with [9]: (1) constant weather conditions, (2) fixed start time in the weather file, or (3) user-supplied 120-hr weather

sequence. Additionally, the ATMOS model can use multiple wind directions from a weather file. This can be graphically shown using a wind rose diagram. A wind rose diagram schematically represents the wind direction and the frequency of occurrence for a particular wind direction. Figure B.1-5 provides an example of a wind rose diagram.

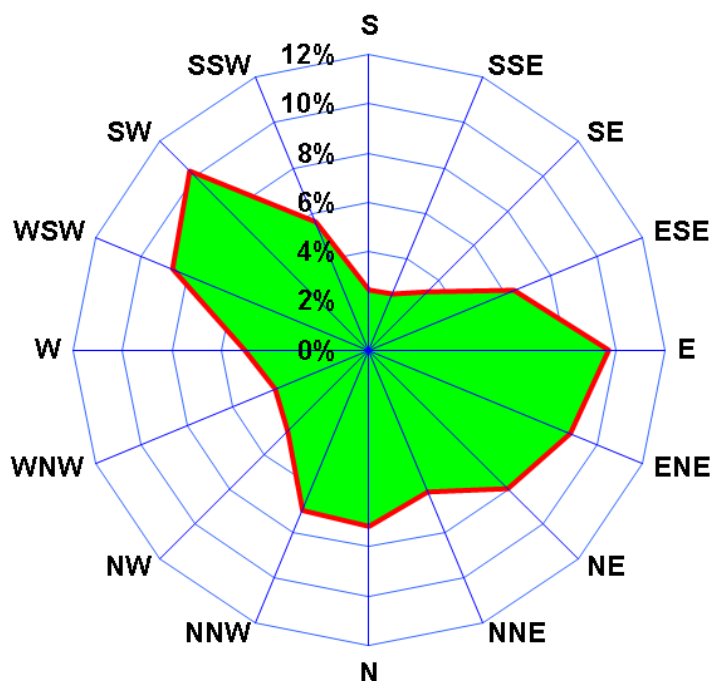


Figure B.1-5 Percent wind rose

B.1.3.2 EARLY Package

The emergency-phase (EARLY) model is the environmental consequence model for the time phase immediately following the radioactive release. This time phase can be up to one week following the arrival of the first radioactive plume. For longer time phases, the CHRONC model is used. The EARLY model time phase includes evacuation, sheltering, and dose-dependent relocation. The EARLY model can also combine up to 20 different emergency response scenarios (i.e., evacuation cohorts).

The EARLY model output is a weighted sum of the emergency-response scenarios. The scenarios may be combined using the following ways [9]:

- Time fractions (fraction of occurrence) or,
- population fractions (fraction of the population engaging in the specific behavior) for each scenario or,
- a sum of the results for each emergency-response scenario (when a unique population distribution is defined for each emergency-response scenario).

A CCDF is determined for each emergency-response scenario. The emergency-response scenarios are based on population fractions, the CCDFs are a function of the consequence for each meteorological trial or wind direction multiplied by the fraction of people assigned for that area for each scenario.

The EARLY model includes five exposure pathways for determining radiation dose. Figure B.1-6 provides an example of the five exposure pathways modeled. These five pathways are the following [9]:

1. Direct external exposure to radioactive material in the plume (cloudshine).
2. Exposure from inhalation of radionuclides in the cloud (cloud inhalation).
3. Exposure to radioactive material deposited on the ground (groundshine).
4. Inhalation of resuspended material (resuspension inhalation) and
5. Skin dose from material deposited on the skin.

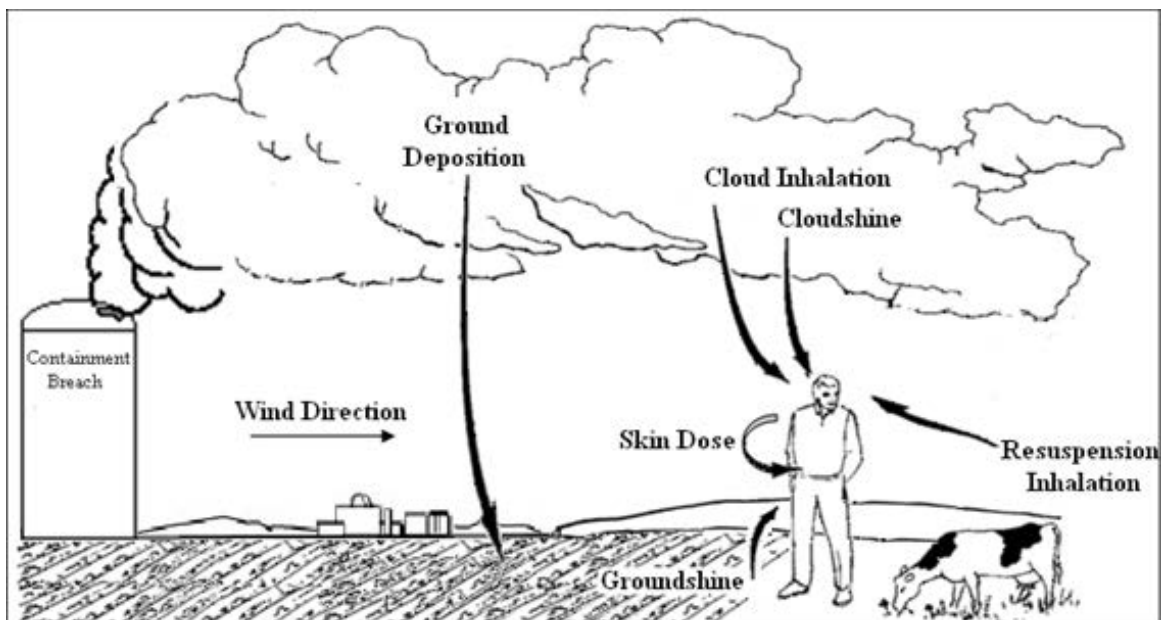


Figure B.1-6 Exposure pathways

The EARLY model calculates two kinds of doses [9]:

1. Acute doses used for calculating early fatalities, and
2. lifetime dose commitment used for calculating potential latent cancers resulting from the early exposure.

The doses calculated for early exposure are influenced by evacuation, sheltering, relocation dose threshold, and early relocation times. The cloudshine and cloud inhalation exposures are only determined for the time it takes the plume to pass, while the groundshine and resuspension inhalation exposures are calculated throughout the early phase time period (up to one week following the arrival of the first radioactive plume).

The EARLY model determines the dose to evacuees by adding the doses they received before evacuation and during evacuation. Once the evacuees are outside the evacuation zone, the model assumes no additional EARLY phase dose is received. However, the CHRONC model determines additional long-term doses to the evacuees.

B.1.3.3 CHRONC Package

The intermediate- and long-term phase (CHRONC) model calculates environmental consequences for the time phase following the emergency-phase modeled by the EARLY model. The intermediate-phase part of the CHRONC model is based on satisfying a dose criterion to the resident population. If the population radiation exposure from groundshine and the inhalation of resuspended radioactive material for the entire intermediate phase exceeds a predetermined threshold (e.g., habitability criterion), the population is assumed to be relocated to uncontaminated areas for the entire intermediate phase. The intermediate phase can be as short as zero (no intermediate phase, and thus the long-term phase begins immediately following the emergency phase) or as long as one year. The intermediate-phase only calculates the groundshine and resuspension inhalation exposure pathways to the effected population.

The long-term phase of the CHRONC model is based on two sets of independent actions [9]:

1. Decisions relating to whether or not land at a specific location and time is suitable for human habitation (i.e., habitability criterion), and
2. decisions relating to whether or not land at a specific location and time is suitable for agricultural production (i.e., farmability).

The CHRONC model determines doses to the population from direct exposure to groundshine and the inhalation of resuspended radioactive material as well as ingestion exposure by consumption of contaminated food and water. The ingestion exposure is not limited to the population within the contaminated areas. Both groundshine and resuspension inhalation exposure pathways can incorporate weathering data in the form of half-lives. The user must determine the relationship between the weathering coefficients and weathering half-lives.

In order to estimate doses from ingestion, mitigation of exposure effects are taken into account. Values for parameters like agricultural uses of land, whether land is immediately habitable after decontamination, or habitable after decontamination and interdiction are user defined. If radiation doses do not satisfy the criteria for habitability or for agricultural development after the maximum-duration of interdiction, then the land is considered condemned, or permanently interdicted. The ingestion pathway was not treated in the analyses reported here because uncontaminated food and water supplies are abundant within the United States and it is unlikely that the public would eat radioactively contaminated food.

B.2 Code Integration

In this section, a description of the elements and processes (e.g., codes and files) used to implement the integrated probabilistic analysis is provided. Figure B.2-1 shows the information flow of the SOARCA Uncertainty Analysis. A description of each item on Figure B.2-1 is described in this section.

- Uncertain MELCOR and MACCS parameters are sampled
- MELCOR is run for each set of its sampled values
- MACCS is run for each set of its sampled values in conjunction with the associated MELCOR source term outputs

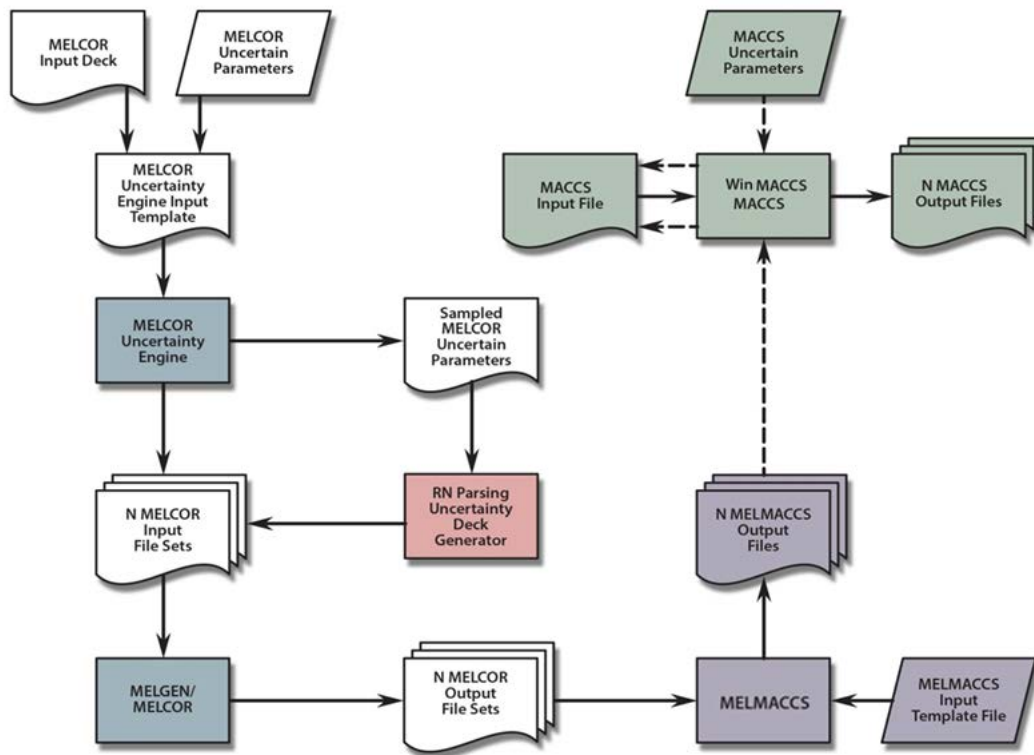


Figure B.2-1 Diagram of the information flow of the SOARCA Uncertainty Analysis

MELCOR Uncertain Parameters

The uncertain parameters selected from the MELCOR model for the Peach Bottom unmitigated LTSBO scenario are listed by their distribution types and associated parameters (e.g., uniform distribution with a lower and upper bound) in Section 4.1. These distributions are incorporated into the MELCOR Uncertainty Engine input template file.

MELCOR Input Deck

The input for the MELCOR model of the Peach Bottom unmitigated LTSBO scenario is divided into a set of input files. The files listed in Table B.2-1 contain the majority of the information that describes the model. The file `jelly_MScreep.gen` uses the MELCOR R*I*F feature to incorporate the individual input files in Table B.2-1 into a single MELGEN file. The file `jelly.cor` contains the MELCOR input information.

Table B.2-1 SOARCA Peach Bottom unmitigated long-term station blackout MELCOR Model input files

10x10-rn-set.gen	cont-cvh_mod.gen	rb-cvh.gen	rn.gen
10x10-rpv-cvh.gen	cont-hs.gen	rb-fl.gen	rpv-hs.gen
10x10-rpv-fl.gen	core-sc.gen	rb-hs-depos.gen	seq-trip.gen
10x10core.gen	cvtype.gen	rb-hs.gen	sloca-rcic.gen
burn.gen	dch-midcy.gen	rcic2.gen	sp-heatcap.gen
cav.gen	dw-liner-melt.gen	rscs-sys.gen	srv-fl3.gen
cf-midcy.gen	hpci.gen	recirc.gen	srv-tailpipe.gen
cf2.gen	hpci2.gen	rrh2.gen	Write_Output.gen
chex-layman-midcy.gen	lpcs.gen	rn-cor-struc.gen	MSLcreep.gen
cont-cvh.gen	mp.gen	rn-mass-midcy.gen	

MELCOR Uncertainty Engine Input Template

The MELGEN/MELCOR uncertainty engine template file consists of three sections. The first section contains the uncertain parameter definitions. Also, variables are defined for each uncertain parameter. The second section contains the model's MELGEN input records. These are incorporated by using the R*I*F feature to read in the jelly_DAK.gen file. The MELGEN records which contain uncertain parameters are also located in this section of the template file. The uncertain parameters in each record are replaced by their respective variables and are defined in the first section of the template file. The third section contains the model's MELCOR input records. These are incorporated by using the R*I*F feature to read in the jelly_DAK.cor file.

MELCOR Uncertainty Engine

Based on the input template, the MELCOR uncertainty engine creates N MELCOR input files (e.g., N = 300 realizations). Simple Monte Carlo sampling is used to generate N samples of the uncertain parameters. In each input file the uncertain parameter variables are replaced with their corresponding sampled value. In addition, an output file is created which contains the sampled values.

Sampled MELCOR Uncertain Parameters

The MELCOR Uncertainty Engine generates an Excel.csv file which contains the sampled uncertain parameter values.

RN Parsing Uncertainty Deck Generator

The uncertainty in the partitioning of the initial iodine core inventory between radionuclide Class 4 (Halogens - I) and radionuclide Class 16 (Cesium Iodide - CsI) cannot be directly implemented as a single sampled parameter value. Rather, that sampled value is an input into the core inventory calculation where it influences the distribution of the mass between the radionuclide Class 2 (Alkali Metals – Cs), Class 4, Class 7 (Early Transition Elements – Mo), Class 16, and Class 17 (Cesium Molybdate – Cs₂MoO₄) defined in Radionuclide Package Reference Manual, Section 2.1 and Table 2.1 [7]. The radionuclide parsing uncertainty deck

generator implements the inventory partitioning calculation as an Excel visual basic macro in an Excel workbook. The sampled value of the fraction of the initial iodine core inventory in radionuclide Class 4 is manually copied and pasted into the Excel workbook. The macro performs the partitioning calculation for each sampled value. The results of the calculation are incorporated into the appropriate records of the dch-mdcy_mod.gen and rn_mass_midcy_mod.gen files. A separate dch-mdcy_mod.gen and rn_mass_midcy_mod.gen is created for each sampled value.

N MELCOR Input File Sets

A MELCOR input file is created for each set of sampled values (i.e., realization). That file incorporates the original input deck with its uncertain parameters set equal to their sampled values. For uncertainties that cannot be directly implemented as a single parameter value (e.g., fraction of initial iodine core inventory partitioned into radionuclide Class 4) additional input files are generated, which are incorporated via the R*I*F feature (see Figure B.2-2).

MELGEN/MELCOR

The MELGEN and MELCOR executables are used to run the N MELCOR input files. Each run creates its own set of output files.

N MELCOR Output File Sets

Each MELCOR run has its own set of output files (Figure B.2-2).

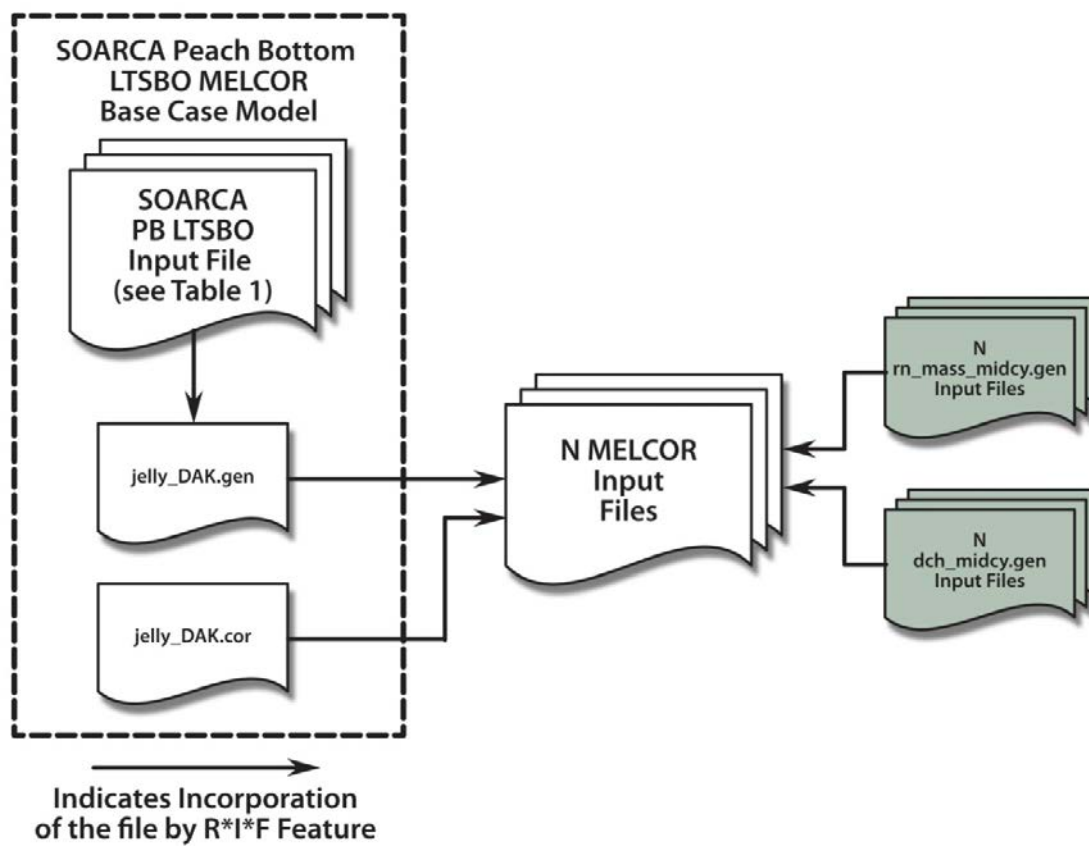


Figure B.2-2 MELCOR input files

MELMACCS Input Template File

The MELMACCS template file contains input needed by MELMACCS to extract the source term information from the MELCOR plot file (.ptf file) and generate the source term input files used by WinMACCS.

MELMACCS

The plot file from each MELCOR run is processed by MELMACCS to extract the information on the source term released to the environment and provide a radionuclide inventory input for a MACCS-compatible format.

N MELMACCS Output Files

A MELMACCS output file is created from each MELCOR plot output file.

MACCS Uncertain Parameters

The uncertain parameters in the MACCS model for the Peach Bottom unmitigated LTSBO scenario are defined by their distribution types and associated parameters (e.g., uniform distribution with a lower and upper bound) (see Section 4.2). These distributions are incorporated into MACCS using the WinMACCS GUI. The distributions are sampled using Latin Hypercube Sampling (LHS) when WinMACCS is run.

MACCS Input File

The WinMACCS input file contains input used by MACCS (e.g., weather and evacuation parameters) to perform consequence calculations.

MACCS

MACCS is used to calculate consequences for the *N* source term inputs (from the *N* MELMACCS radionuclide files) in conjunction with the uncertainty in the MACCS parameters. Weather uncertainty (i.e., weather bin sampling) is evaluated for each source term input and associated WinMACCS uncertain parameter sample.

N MACCS Output Files

A MACCS output file is generated for each source term input.

APPENDIX C
MODEL VERIFICATION AND CONVERGENCE

APPENDIX C – TABLE OF CONTENTS

<u>Section</u>	<u>Page</u>
C.1 SOURCE TERM MODEL	C-1
C.1.1 TEMPORAL AND NUMERICAL CONVERGENCE (DETERMINISTIC RUNS)	C-2
C.1.1.1 TEMPORAL CONVERGENCE (DTMAX, MELCOR 1.8.6 VERSION YR549.....	C-3
C.1.1.2 NUMERICAL CONVERGENCE	C-7
C.1.2 MODEL UPDATES (DETERMINISTIC RUNS)	C-13
C.1.2.1 UPDATES TO PEACH BOTTOM INPUT DECK.....	C-13
C.1.2.2 UPDATE TO INCLUDE PHEBUS TEST DATA	C-16
C.1.3 SOARCA UNCERTAINTY ANALYSIS BASE CASES (DETERMINISTIC) .	C-19
C.1.3.1 SOARCA UNCERTAINTY ANALYSIS BASE CASE ESTIMATE.....	C-19
C.1.3.2 SOARCA MAIN STEAM LINE CREEP SENSITIVITY	C-22
C.2 CONSEQUENCE MODEL.....	C-25
C.2.1 UPDATE TO MELMACCS PREPROCESSOR	C-26
C.2.2 UPDATE TO MELCOR SOURCE TERM	C-29
C.2.3 NUMERICAL CONVERGENCE – CODE UPDATES.....	C-35
C.2.4 SOARCA UNCERTAINTY ANALYSIS DETERMINISTIC BASE CASE	C-38
C.3 MODEL ERROR LOG	C-43
C.3.1 ERROR IN SAMPLED VALUES OF DRYWELL HEAD BOLD TORQUE COEFFICIENT	C-43
C.3.2 MISS ORDERING OF SAMPLED VALUES OF FUEL FAILURE CRITERION	C-43

APPENDIX C – TABLE OF FIGURES

<u>Figure</u>		<u>Page</u>
Figure C.1-1	Fraction of the core inventory released to the environment (a) Iodine and (b) Cesium temporal convergence comparisons for the Peach Bottom unmitigated LTSBO scenario.....	C-6
Figure C.1-2	Fraction of the core inventory released to the environment (a) Iodine and (b) Cesium numerical convergence comparisons for the Peach Bottom unmitigated LTSBO scenario.....	C-9
Figure C.1-3	Fraction of the core inventory released to the environment (a) Iodine and (b) Cesium with the revised treatment of the near equilibrium model disabled for the Peach Bottom unmitigated LTSBO scenario.....	C-12
Figure C.1-4	Fraction of the core inventory released to the environment (a) Iodine and (b) Cesium with model updates for the Peach Bottom unmitigated LTSBO scenario	C-15
Figure C.1-5	Fraction of the core inventory released to the environment (a) Iodine and (b) Cesium with CHEMFORM #5 for the Peach Bottom unmitigated LTSBO scenario	C-18
Figure C.1-6	Fraction of the core inventory released to the environment (a) Iodine and (b) Cesium for UA SOARCA for the Peach Bottom unmitigated LTSBO scenario	C-21
Figure C.1-7	Fraction of the core inventory released to the environment (a) Iodine and (b) Cesium for UA SOARCA MSL creep rupture for the Peach Bottom unmitigated LTSBO scenario.....	C-24
Figure C.2-1	MELMACCS plume segment	C-27
Figure C.2-2	Source term comparison of conditional, mean, individual LCF risk (per event) with LNT dose truncation for residents within a circular area of specified radius from the plant for emergency and long-term phases	C-32
Figure C.2-3	Source term comparison of conditional, mean, individual LCF risk (per event) with USBGR dose truncation for residents within a circular area of specified radius from the plant for emergency and long-term phases	C-33
Figure C.2-4	Source term comparison of conditional, mean, individual LCF risk (per event) with HPS dose truncation for residents within a circular area of specified radius from the plant for emergency and long-term phases	C-34
Figure C.2-5	SOARCA estimate and SOARCA UA base case comparison of conditional, mean, individual LCF risk (per event) with the LNT for residents within a circular area of specified radius from the plant for emergency and long-term phases.....	C-40
Figure C.2-6	SOARCA estimate and SOARCA UA base case comparison of conditional, mean, individual LCF risk (per event) with USBGR dose truncation for residents within a circular area of specified radius from the plant for emergency and long-term phases	C-41

Figure C.2-7 SOARCA estimate and SOARCA UA base case comparison of conditional, mean, individual LCF risk (per event) with HPS dose truncation for residents within a circular area of specified radius from the plant for emergency and long-term phases.....C-42

APPENDIX C – TABLE OF TABLES

<u>Table</u>	<u>Page</u>
Table C.1-1	Summary of MELCOR model changes to the SOARCA Peach Bottom unmitigated LTSBO scenario necessary to achieve UA Model convergence..... C-2
Table C.1-2	Time step definitions used in the probabilistic analysis..... C-3
Table C.1-3	Timing of key events for Peach Bottom LTSBO temporal convergence. C-4
Table C.1-4	Timing of key events for Peach Bottom LTSBO numerical convergence. C-8
Table C.1-5	Timing of key events for Peach Bottom LTSBO numerical convergence with near equilibrium model off.C-11
Table C.1-6	Timing of key events for Peach Bottom LTSBO Model updates.C-14
Table C.1-7	Timing of key events for Peach Bottom LTSBO with CHEMFORM #5.....C-17
Table C.1-8	Timing of key events for Peach Bottom LTSBO UA SOARCA Case.....C-20
Table C.1-9	Timing of key events for Peach Bottom LTSBO main steam line creep rupture.....C-23
Table C.2-1	Summary of consequence model changes to the Peach Bottom unmitigated LTSBO scenario used in the SOARCA Uncertainty Analysis.....C-25
Table C.2-2	MELCOR radionuclide classes not included in MELMACCS.C-27
Table C.2-3	Radionuclide classes used in SOARCA.....C-28
Table C.2-4	Brief source term description for the Peach Bottom unmitigated LTSBO.C-30
Table C.2-5	Source term comparison of conditional, mean, individual LCF risk (per event) for LNT dose truncation.C-31
Table C.2-6	Source term comparison of conditional, mean, individual LCF risk (per event) for USBGR dose truncation.C-31
Table C.2-7	Source term comparison of conditional, mean, individual LCF risk (per event) for dose truncation based on the HPS position statement.C-31
Table C.2-8	MACCS version comparison of conditional, mean, individual LCF risk (per event) for LNT dose truncation for the SOARCA estimate at specified circular areas.C-37
Table C.2-9	MACCS version comparison of conditional, mean, individual LCF risk (per event) for USBGR dose truncation for the SOARCA estimate at specified circular areas.....C-37
Table C.2-10	MACCS version comparison of conditional, mean, individual LCF risk (per event) for HPS dose truncation for the SOARCA estimate at specified circular areas.....C-37
Table C.2-11	SOARCA estimate and SOARCA UA base case comparison of conditional, mean, individual LCF risk (per event) for LNT dose truncation at specified circular areas.....C-38

Table C.2-12	SOARCA estimate and SOARCA UA base case comparison of conditional, mean, individual LCF risk (per event) for USBGR dose truncation at specified circular areas.	C-38
Table C.2-13	SOARCA estimate and SOARCA UA base case comparison of conditional, mean, individual LCF risk (per event) for HPS dose truncation at specified circular areas.....	C-39

C MODEL VERIFICATION AND CONVERGENCE

The intended purpose of the uncertainty analysis is to quantitatively evaluate the effects of selected key uncertain parameters on the estimation of the release of radionuclides to the environment and downstream consequences. Validation of a computer model for a physical system involves a series of activities designed to generate and enhance confidence in the model's conceptualization and results during and after model development. The SOARCA Peach Bottom unmitigated LTSBO model presented in NUREG/CR-7110 Volume I represents a complex system of the reactor core, pressure vessel, safety systems, environmental conditions, and downstream consequences including evacuation planning. In conventional modeling practice, model validation is achieved by comparing model results with experimental measurements. However, such measurements are impossible to obtain at the temporal and spatial scales of interest for a complex integrated level for reactor safety analyses. From a strictly computational perspective, a well-designed, correctly implemented numerical model should produce results that are explainable and appropriate for its intended purpose. Validation of the SOARCA model is a process to establish confidence that the model adequately represents with sufficient accuracy the accident scenario and satisfies its intended purpose. The SOARCA Peach Bottom LTSBO model presented in NUREG/CR-7110 Volume I included verification of the inputs and software and is considered valid for its intended use. Several computer software and associated electronic input files were used in the calculation as presented in Section 3.0 of this document. The software is verified for its intended use and has supporting documentation.

The results presented in this analysis were generated with an updated version of the SOARCA Peach Bottom unmitigated LTSBO model. The updated version primarily addresses issues identified during the development of the probabilistic analysis. For the uncertainty analysis, it is necessary to demonstrate the convergence of the probabilistic analysis, including both temporally and computationally. This section discusses the progression of the model changes including updated versions of the MELCOR and MACCS codes from those versions used in NUREG/CR-7110 Volume 1. A series of during development model verification and convergence activities presented in the following subsections document the MELCOR and MACCS model changes including: checking model changes and input verification, temporal and computational convergence testing. Model input parameter values and abstraction models, including their ranges of applicability, were reviewed and verified for accuracy (Section 4.0). Convergence tests were conducted to identify the impacts of timestep size (Section C.1.1.1), numerical accuracy (Section C.1.1.2 and C.2.3) and number of realizations (Section 5.1.1 and Section 5.2.1) to ensure that the model was converged.

C.1 Source Term Model

Early scoping analysis yielded a high number of failed realizations using MELCOR 1.8.6 code version YR549. Since the Peach Bottom unmitigated LTSBO scenario was developed in NUREG/CR-7110 Volume 1, developments to the MELCOR 1.8.6 code have improved the code convergence. In addition, several configuration inaccuracies in the Peach Bottom unmitigated LTSBO MELCOR model have been identified. It was necessary to take advantage of these advancements to generate converged probabilistic results for the uncertainty analysis. To enhance the convergence of the probabilistic analysis these issues were addressed in the updated SOARCA Peach Bottom LTSBO model used for the uncertainty analysis. Table C.1-1 summarizes the issues addressed. The overall impact of these updates is considered negligible on the results of the SOARCA analysis [1] and the SOARCA model [1] is considered adequate for the intended purpose.

Table C.1-1 Summary of MELCOR model changes to the SOARCA Peach Bottom unmitigated LTSBO scenario necessary to achieve UA Model convergence

SOARCA Model Issue	Issue Description	Addressed in Section
Variable timesteps	Variable timestep sizes optimized to the accident progression for SOARCA. This is done manually by stopping the analysis and restarting and over several iterations of the model calculation. A constant timestep size is needed to run the probabilistic case.	C.1.1.1
Numerical convergence	(i) MELCOR Code version 1.8.6 was updated from YR549 used in SOARA to YV3780. (ii) Disabling an instability in the revised near equilibrium model.	C.1.1.2
Configuration inaccuracies	Drywell liner open area rate, elevation of the lower separator control volume, check valve in the vacuum breaker.	C.1.2.1
Chemical forms of iodine and cesium	Include Phebus results including gaseous iodine and CsOH that were not used in the SOARCA calculations.	C.1.2.2

To ensure proper continuity between the SOARCA Peach Bottom unmitigated LTSBO and the modified Peach Bottom unmitigated LTSBO scenario used in this UA and for a comparison with the parametric uncertainty and sensitivity results, a series of 'one-off' MELCOR simulations were conducted. Section C.1 contains tables listing the calculated timing of key events that follow from key events in accident progression (as presented in NUREG/CR-7110 Volume I) as a quantitative comparison between the verification tests cases. In addition, a comparison of the fraction of cesium and iodine core inventory released to the environment is used to quantify the impact of each change. The only release pathways considered (i.e., refueling bay blowout panels and the equipment lock door at 135 feet above ground level) are those that are carried over into the MACCS analysis

C.1.1 Temporal and Numerical Convergence (Deterministic Runs)

To quantify the effects of the updates and advancements to the MELCOR 1.8.6 code implemented in the YV3780 version used in the probabilistic analysis, a series of deterministic MELCOR simulations were conducted to quantify the overall effects on the Peach Bottom unmitigated LTSBO scenario. Furthermore, the original Peach Bottom unmitigated LTSBO SOARCA simulation was completed using several restarts for timestep modifications whenever a MELCOR convergence error was encountered. Thus the exact same calculation is not recreated by simply rerunning the simulation with the optimized timestep input; slight differences in start and stop times (caused by MELCOR errors) relative to the user-specified timestep input can yield slight differences in the calculated results. The SOARCA Peach Bottom unmitigated LTSBO MELCOR simulation in Section 5.1 of NUREG/CR-7110 Volume 1 was conducted in September, 2010 and used MELCOR 1.8.6 code version YR549. The following sections outline the changes to the code and timesteps and quantify the resulting changes to the timeline of events and environmental releases.

C.1.1.1 Temporal Convergence (DTMAX, MELCOR 1.8.6 version YR549)

Temporal convergence refers to the use of an appropriate timestep size necessary to achieve a converged solution. The numerical solution presented in the SOARA analysis involves computations with discrete timesteps, referred to as temporal discretization. The temporal discretization may affect the accuracy of the solution to the differential equations, and thus affect the outputs.

The SOARCA Peach Bottom unmitigated LTSBO simulation encountered a few difficulties in obtaining a MELCOR solution during the core degradation portion of the calculation. To obtain a converged and more accurate solution the SOARCA MELCOR calculation used manual changes in the timestep size function during the core melt progression. A solution was obtained in an interactive manner—the simulation was restarted using smaller timesteps before the onset of code instabilities that lead to the calculation problems. A “hands-on” approach was employed, using a manual stopping and restarting of the simulation during run time to get the optimal timestep sizes over the defined time intervals. However, with the automated approach used in the probabilistic analysis (Section 3.0), it is not possible to interactively (i.e. manually) determine the optimal timestep scheme for each individual calculation and exactly replicate the changes completed in the SOARCA analysis to customize the timestep function. Rather, the final timestep definitions resulting from the SOARCA analyses were used (Table C.1-2).

Table C.1-2 Time step definitions used in the probabilistic analysis

	TIME (s)	DTMAX	DTMIN	DTEDT	DTPLT	DTRST
TIME1	-200	0.1	1.00×10^{-6}	600	10	600
TIME2	-135	0.05	1.00×10^{-6}	600	10	600
TIME3	0	0.1	1.00×10^{-6}	3600	2	600
TIME4	60	0.5	1.00×10^{-6}	3600	5	36,000
TIME5	600	1	1.00×10^{-7}	3600	10	36,000
TIME6	7,200	1	1.00×10^{-7}	3600	60	6,000
TIME7	28,000	1	1.00×10^{-7}	7200	60	36,000
TIME8	36,000	0.05	1.00×10^{-7}	7200	30	7,200
TIME9	72,000	0.01	1.00×10^{-7}	7200	60	7,200
TIME10	86,400	1	1.00×10^{-7}	7200	180	7,200
TIME11	172,800	2	1.00×10^{-7}	36000	600	36,000

Since the SOARCA analysis was never run from start to finish with the final timestep definitions defined in Table C.1-2, rather stopped at unequal time intervals, the SOARCA Peach Bottom unmitigated LTSBO model was re-run with the final SOARCA timestep definitions to assess the impact from using the steps defined in Table C.1-2. As shown in Table C.1-3, the timing of the core melt progression, lower head failure, and permanent containment failure (shell melt-through) have resulted in a slightly earlier releases of radionuclides to the environment. Most importantly, vessel breach and containment shell melt-through occur one hour earlier for the calculation run continuously with the final SOARCA timestep scheme. The two calculations exhibit negligible (<1 hour) variations in event timing for most of the other events listed in Table C.1-2.

Table C.1-3 Timing of key events for Peach Bottom LTSBO temporal convergence

Event	PB LTSBO w/ 4 hr DC power (time in hours unless noted)	
	SOARCA	Final Time Steps (UAS_STD06)
Station blackout loss of all onsite and offsite AC power	0	0
Low-level 2 and RCIC actuation signal	10 minutes	10 minutes
Operators manually open SRV to depressurize the reactor vessel	1	1
RPV pressure first drops below LPI set point (400 psig)	1.2	1.2
Battery depletion leads immediate SRV re-closure	4	4
RCIC steam line floods with water RCIC flow terminates	5.2	5.2
SRV sticks open because of excessive cycling	8.2	8.2
Downcomer water level reaches top of active fuel	8.4	8.4
First hydrogen production	8.9	8.5
First fuel-cladding gap release	9.1	9.1
First channel box failure	9.3	9.3
Reactor vessel water level reaches bottom of lower core plate	9.3	9.3
First localized failure of lower core plate	10.6	10.6
First core cell collapse because of time at temperature	9.8	10.1
Beginning of large-scale relocation of core debris to lower plenum	10.5	10.6
Lower head dries out	13.3	13
Ring 5 CRGT column collapse (failed at axial level 2)	15.8	16.1
Ring 1 CRGT column collapse (failed at axial level 2)	17.4	18.3
Ring 4 CRGT column collapse (failed at axial level 2)	17.4	17.7
Ring 3 CRGT column collapse (failed at axial level 2)	17.5	17.4
Ring 2 CRGT column collapse (failed at axial level 2)	18.6	18.7
Lower head failure	19.7	18.9
Drywell head flange leakage begins	19.9	19
Hydrogen burns initiated in drywell enclosure region of reactor building	20	19.1
Refueling bay to environment blowout panels open	20	19.1
Hydrogen burns initiated in reactor building refueling bay	20	19.1
Drywell shell melt-through initiated and drywell head flange re-closure	20	19.1
Hydrogen burns initiated in lower reactor building	20.1	19.1
Door to environment through railroad access opens because of overpressure	20.1	19.1
Equipment Lock Door at 135-ft fails due to overpressure	20.1	19.1
Refueling bay roof fails due to overpressure	20.2	-
Time iodine release to environment exceeds 1% of initial core inventory	23.6	23.0
Calculation terminated	48	48

BE_STD01v1.8.6YR549; UAS_STD06v1.8.6YR549

Figure C.1-1(a) depicts the fraction of iodine core inventory released to the environment as a function of time for the SOARCA estimate and the temporal convergence test scenarios. Similar information is shown on Figure C.1-1(b) for cesium. As shown on Figure C.1-1(a), the overall fraction of the iodine core inventory released to the environment is approximately 2×10^{-2} for both the final timestep case and the SOARCA estimate. As shown on Figure C.1-1(b), the overall environmental release fraction of cesium in the core is approximately 8×10^{-4} and 5×10^{-4} for the results using the final timesteps and the SOARCA estimate, respectively. This difference in cesium release is attributed to an increased release of cesium molybdate (Cs_2MoO_4) into the environment. The increased late phase release of cesium is caused by reheating of the heat structures in the upper and low reactor vessel, causing re-vaporization of radionuclide aerosols that were deposited on these surfaces. Overall, despite a slightly earlier release to the environment in the final timestep case, the magnitude and trend for the fractions released to the environment are closely represented. The timestep sizes can have a notable impact on the solution results for the fraction of the cesium core inventory released to the environment. The MELCOR simulation with the final timestep definitions (without restarts) calculated a 38% higher release fraction of cesium compared to the original SOARCA study; however, given the overall low magnitude of the cesium release fraction ($\sim 0.01\%$), this variability is a reasonable response to timestep changes in MELCOR.

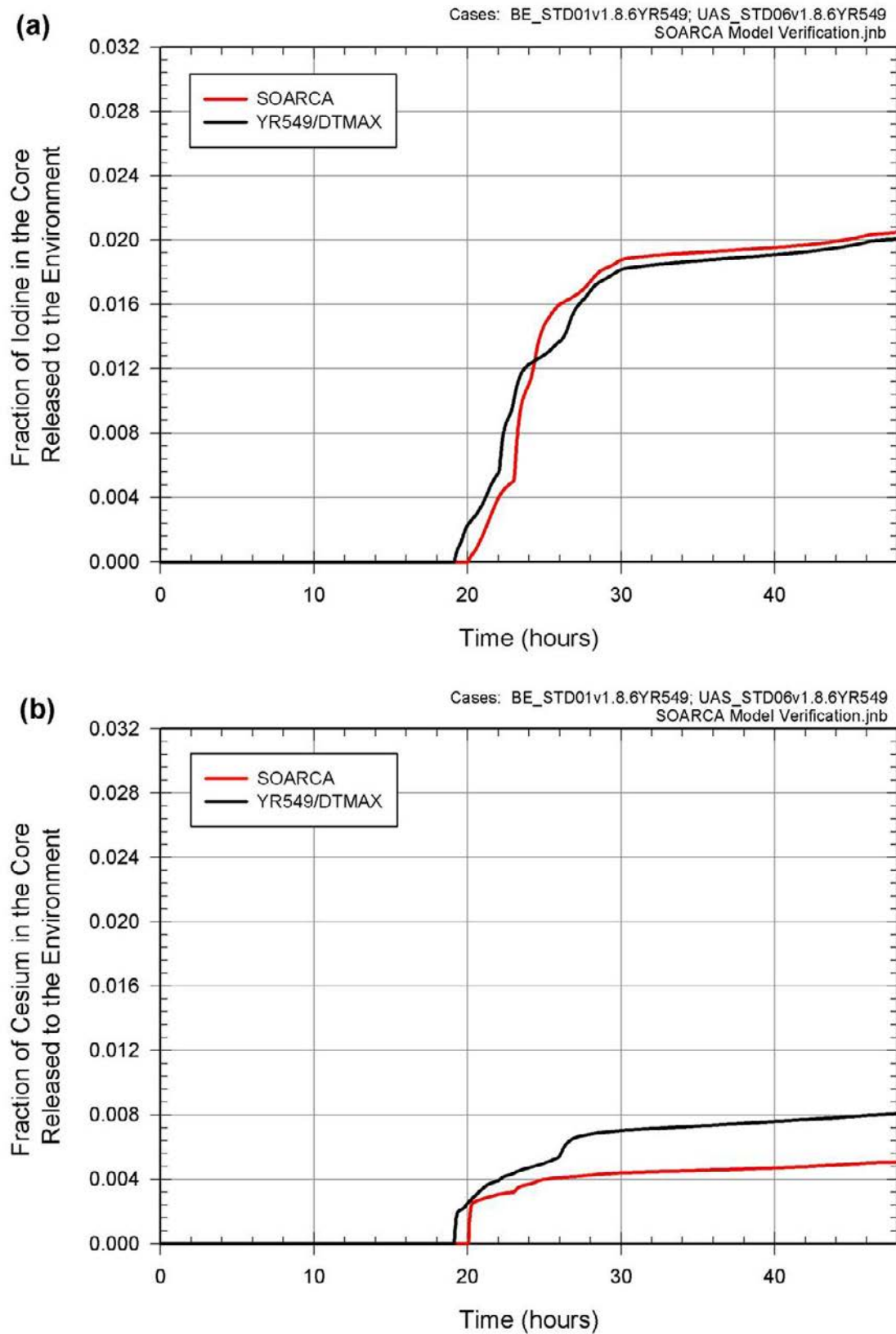


Figure C.1-1 Fraction of the core inventory released to the environment (a) iodine and (b) Cesium temporal convergence comparisons for the Peach Bottom unmitigated LTSBO scenario

C.1.1.2 Numerical Convergence

Since the SOARCA Peach Bottom LTSBO scenario was developed, MELCOR code advancements have been made that improve the numerical convergence of the physical models in MELCOR. The SOARCA estimate for the Peach Bottom unmitigated LTSBO scenario used MELCOR 1.8.6 Version YR549. For this study, MELCOR 1.8.6 Version YV3780 was used. This is the version used to analyze the Surry interfacing loss of coolant accident seen in Section 5.5 of NUREG/CR-7110 Volume 2. The improvement in the MELCOR 1.8.6 code between Versions YR549 and YV3780 resulted in reducing the number of failed UA realizations and decreased the individual run times. Typically, for a probabilistic simulation, 30% or more of the sample set would fail when using MELCOR 1.8.6 version YR549.

In addition, a revision to the MELCOR 1.8.6 near equilibrium model in a code version prior to YR549 resulted in a substantial increase in MELCOR CPU time for ISLOCA analyses of the SOARCA Surry model. During MELCOR development and verification testing conducted for MELCOR 2.0, this error was discovered and the near equilibrium model is disabled in all subsequent versions of MELCOR. Disabling the near equilibrium model increases the model convergence, improves the solution accuracy, and decreases run times. Using MELCOR 1.8.6 Version YV3780 with the near equilibrium model disabled, only two to four percent of the sample set failed.

C.1.1.2.1 MELCOR Code Version YV3780

Table C.1-4 shows a comparison of the results for the SOARCA model using MELCOR 1.8.6 Version YR549 for the Peach Bottom unmitigated LTSBO scenario versus the most recent MELCOR 1.8.6 Version YV3780. The same timestep function is used in both modeling cases (as detailed in Section C.1.1.1 and listed Table C.1-2).

The numerical convergence test shows differences in the timing of lower head failure with MELCOR 1.8.6 Version YV3780, predicting a time 1 hour 42 minutes later when compared to the YR549 version. This is attributed to hotter particulate debris temperature in the YR549 version due to a higher oxidation power and differences in the hydrogen production between the two code versions. The environmental release occurs earlier in the numerical convergence test and produces larger overall release of iodine to the environment. As shown on Figure C.1-2(a), the initial fraction of the iodine core inventory released to the environment is higher than the MELCOR 1.8.6 Version YR549 (SOARCA) cases.

Figure C.1-2(b) shows the fraction of the cesium core inventory released to the environment for the MELCOR 1.8.6 version YV3780 is slightly higher, yet closer, to the SOARCA solution than the MELCOR 1.8.6 version YR549 case with the final timesteps. Since the release of CsI is higher for the numerical convergence test, the overall difference in cesium release is attributed to the greater release of CsI, resulting in an increase in both cesium and iodine when compared to the SOARCA estimate.

Table C.1-4 Timing of key events for Peach Bottom LTSBO numerical convergence

Event	PB LTSBO w/4 hr DC power (time in hours unless noted)	
	Version YR549 (UAS_STD06)	Version YV3780 (UAS_STD08)
Station blackout loss of all onsite and offsite AC power	0	0
Low-level 2 and RCIC actuation signal	10 minutes	10 minutes
Operators manually open SRV to depressurize the reactor vessel	1	1
RPV pressure first drops below LPI setpoint (400 psig)	1.2	1.2
Battery depletion leads immediate SRV re-closure	4	4
RCIC steam line floods with water RCIC flow terminates	5.2	5.2
SRV sticks open because of excessive cycling	8.2	8.2
Downcomer water level reaches top of active fuel	8.4	8.4
First hydrogen production	8.5	8.6
First fuel-cladding gap release	9.1	9.1
First channel box failure	9.3	9.4
Reactor vessel water level reaches bottom of lower core plate	9.3	9.4
First localized failure of lower core plate	10.6	10.6
First core cell collapse because of time at temperature	10.1	9.9
Beginning of large-scale relocation of core debris to lower plenum	10.6	10.6
Lower head dries out	13	12.9
Ring 5 CRGT column collapse (failed at axial level 2)	16.1	16.9
Ring 3 CRGT column collapse (failed at axial level 2)	17.4	17.9
Ring 4 CRGT column collapse (failed at axial level 2)	17.7	18.2
Ring 1 CRGT column collapse (failed at axial level 2)	18.3	16.8
Ring 2 CRGT column collapse (failure occurs at different axial level)	18.7	18.5
Lower head failure	18.9	20.6
Drywell head flange leakage begins	19	20.7
Hydrogen burns initiated in drywell enclosure region of reactor building	19.1	20.7
Refueling bay to environment blowout panels open	19.1	20.7
Hydrogen burns initiated in reactor building refueling bay	19.1	20.9
Drywell shell melt-through initiated and drywell head flange re-closure	19.1	20.8
Hydrogen burns initiated in lower reactor building	19.1	20.9
Door to environment through railroad access opens because of overpressure	19.1	20.9
Equipment Lock Door at 135-ft fails due to overpressure	19.1	20.9
Time iodine release to environment exceeds 1% of initial core inventory	23.0	21.0
Calculation terminated	48	48

UAS_STD06v1.8.6YR549; UAS_STD08v1.8.6YV3780.

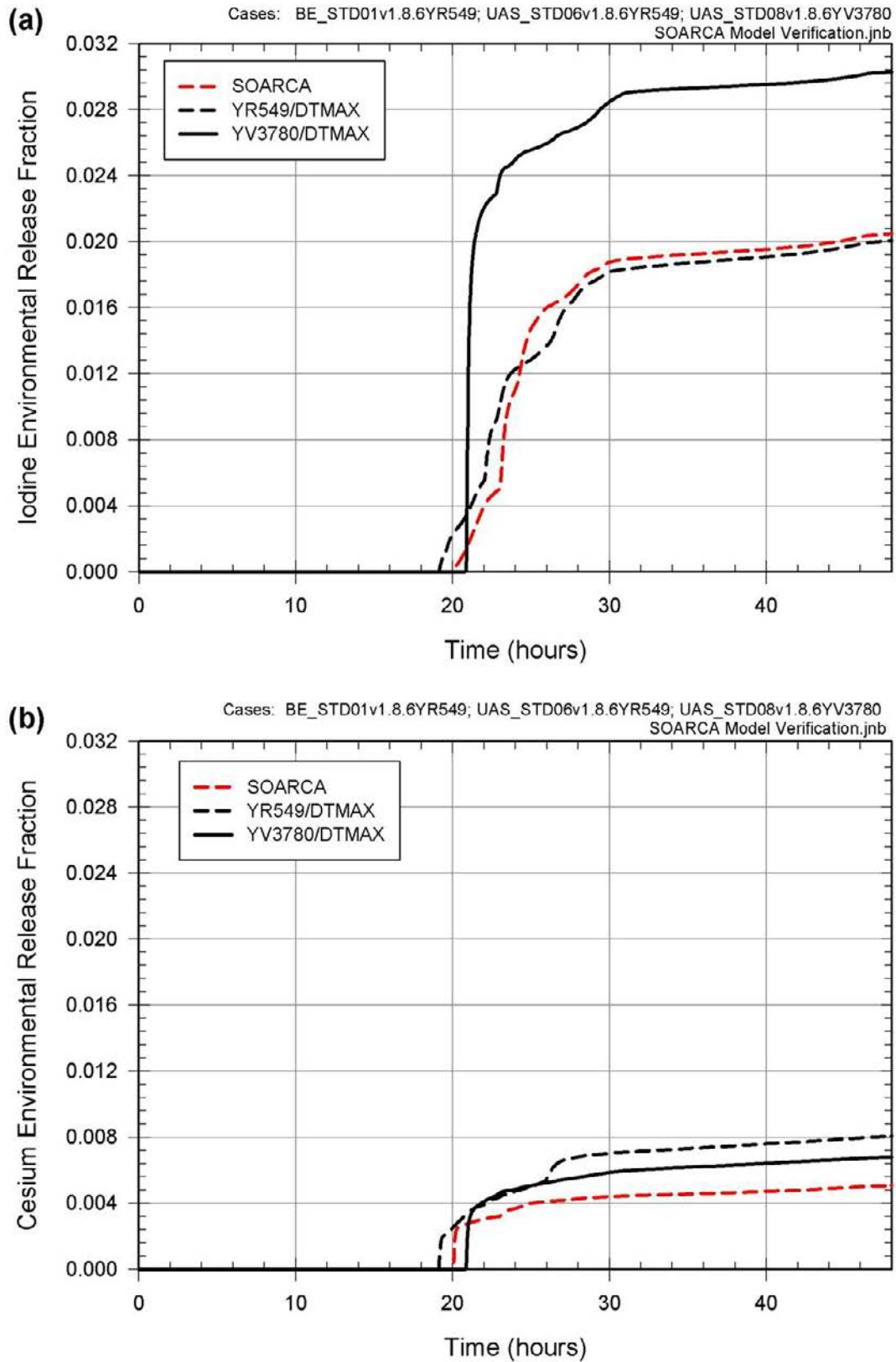


Figure C.1-2 Fraction of the core inventory released to the environment (a) Iodine and (b) Cesium numerical convergence comparisons for the Peach Bottom unmitigated LTSBO scenario

C.1.1.2.2 Disable the revised MELCOR Near Equilibrium Model

Table C.1-5 displays the results of the numerical convergence test conducted with MELCOR 1.8.6 Version YV3780 for the Peach Bottom unmitigated LTSBO scenario and the results for the MELCOR 1.8.6 Version YV3780 for the Peach Bottom unmitigated LTSBO scenario with the near equilibrium model turned off. The revised treatment of the near equilibrium model prevents the collapse of a boiled-up pool in a volume with a very small atmosphere and the possible revaporization of a very small pool. The same timestep function (Section C.1.1.1, Table C.1-2) is used for both cases.

The disabled near equilibrium model results in an earlier lower head failure (30 minutes) and earlier release of iodine to the environment (24 minutes) than when the model is not disabled. However, the lower head dryout occurs 36 minutes earlier (36 minutes) when the revised treatment of the near equilibrium model is used. The lower head failure is sooner in the disabled near equilibrium model because the particulate debris that has relocated is at higher temperatures, leading to an earlier failure time. The hotter temperatures are due to a larger oxidation power. As shown on Figure C.1-3(a), the iodine release fraction to the environment is higher for the case that disabled the revised treatment of the near equilibrium model case when compared to the SOARCA estimate. The divergence from the SOARCA values increases if the revised equilibrium model is used with MELCOR revision YV3780 (i.e. iodine release fraction is greater than the SOARCA values and the YV3780 calculation with the revised model disabled). The results with the disabled near equilibrium model are still higher than the SOARCA estimate. However, after this initial release, the rate of iodine released to the environment is similar to the SOARCA estimate.

Figure C.1-3(b) shows the cesium release fraction to the environment for the case that disabled the revised treatment of the near equilibrium is also slightly higher yet is closer to the SOARCA estimate than when the model is not disabled. Since the release of CsI for the disabled near equilibrium model is still higher than the SOARCA case, the overall difference in cesium release is attributed to the greater release of CsI, resulting in an increase in both cesium and iodine when compared to the SOARCA estimate.

Table C.1-5 Timing of key events for Peach Bottom LTSBO numerical convergence with near equilibrium model off

Event	PB LTSBO w/ 4 hr DC power (time in hours unless noted)	
	Version YV3780 (UAS_STD08)	Revised Near Equilibrium Model Off/ Version YV3780 (UAS_STD11)
Station blackout loss of all onsite and offsite AC power	0	0
Low-level 2 and RCIC actuation signal	10 minutes	10 minutes
Operators manually open SRV to depressurize the reactor vessel	1	1
RPV pressure first drops below LPI setpoint (400 psig)	1.2	1.2
Battery depletion leads immediate SRV re-closure	4	4
RCIC steam line floods with water RCIC flow terminates	5.2	5.2
SRV sticks open because of excessive cycling	8.2	8.2
Downcomer water level reaches top of active fuel	8.4	8.4
First hydrogen production	8.6	8.6
First fuel-cladding gap release	9.1	9.1
First channel box failure	9.4	9.4
Reactor vessel water level reaches bottom of lower core plate	9.4	9.3
First localized failure of lower core plate	10.6	10.6
First core cell collapse because of time at temperature	9.9	9.9
Beginning of large-scale relocation of core debris to lower plenum	10.6	10.6
Lower head dries out	12.9	12.3
Ring 5 CRGT column collapse	16.9	16.8
Ring 3 CRGT column collapse	17.9	16.8
Ring 4 CRGT column collapse	18.2	16.9
Ring 1 CRGT column collapse	16.8	17.5
Ring 2 CRGT column collapse	18.5	18.0
Lower head failure	20.6	20.1
Drywell head flange leakage begins	20.7	20.2
Hydrogen burns initiated in drywell enclosure region of reactor building	20.7	20.2
Refueling bay to environment blowout panels open	20.7	20.2
Hydrogen burns initiated in reactor building refueling bay	20.9	20.4
Drywell shell melt-through initiated and drywell head flange re-closure	20.8	20.3
Hydrogen burns initiated in lower reactor building	20.9	20.3
Door to environment through railroad access opens because of overpressure	20.9	20.3
Equipment Lock Door at 135-ft fails due to overpressure	20.9	20.3
Time iodine release to environment exceeds 1% of initial core inventory	21.0	20.6
Calculation terminated	48	48

UAS_STD08v1.8.6YV3780; UAS_STD11v1.8.6YV3780

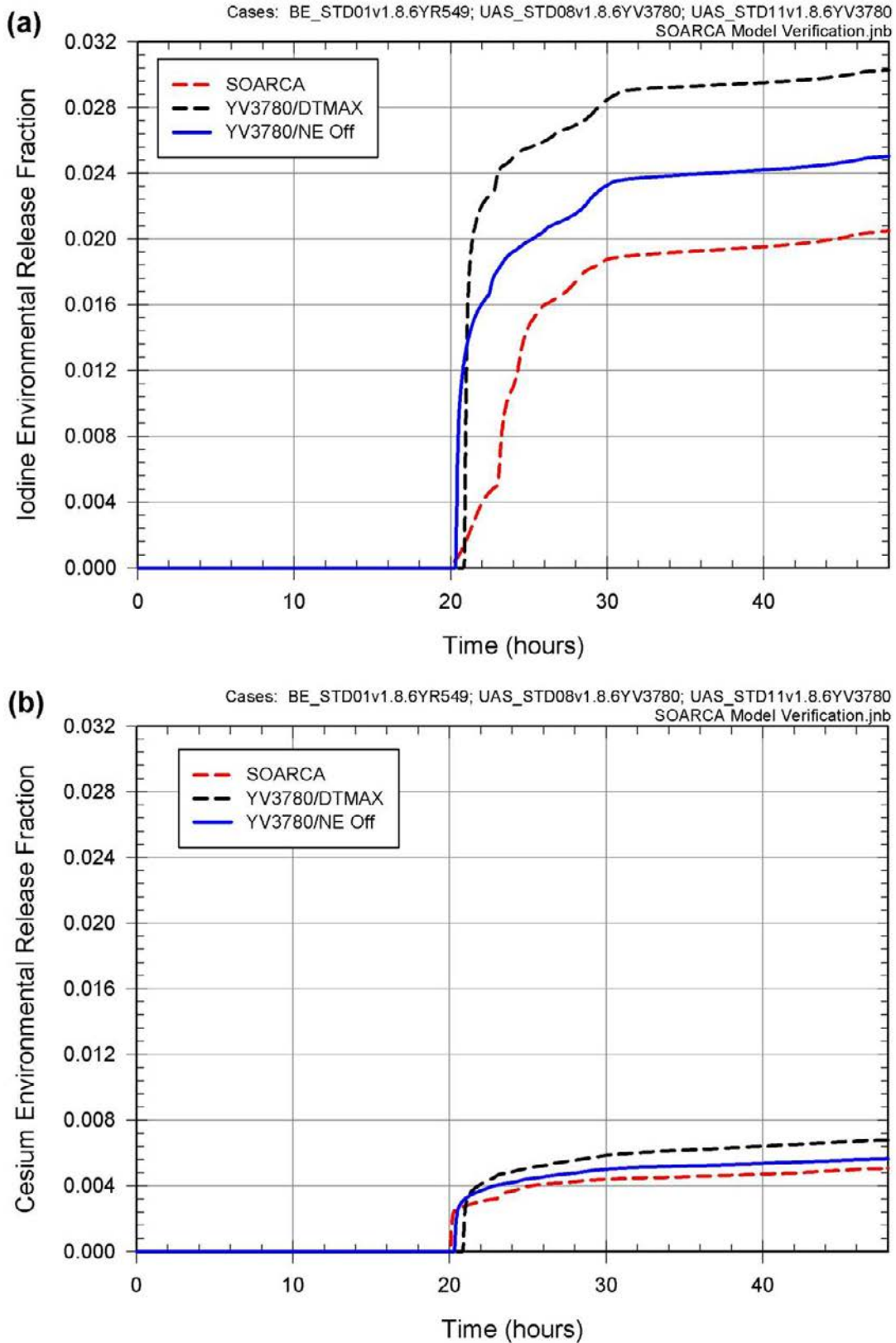


Figure C.1-3 Fraction of the core inventory released to the environment (a) Iodine and (b) Cesium with the revised treatment of the near equilibrium model disabled for the Peach Bottom unmitigated LTSBO scenario

C.1.2 Model Updates (Deterministic Runs)

C.1.2.1 Updates to Peach Bottom Input Deck

Model updates included defining the vacuum breakers between the drywell and wetwell to allow only forward flow, raising the bottom of the separator control volume to remove a nonphysical “bucket” for water to collect in, and slowing the drywell liner melt through (extending the time for the drywell breach to grow full open).

Table C.1-6 shows the results of the MELCOR 1.8.6 version YV3780 with the near equilibrium model disabled for the Peach Bottom unmitigated LTSBO scenario compared with the results when the model is updated to address configuration issues mentioned above. The updated model uses the same version of MELCOR 1.8.6 version YV3780 with the near equilibrium model disabled. The final timestep function (Section C.1.1.1, Table C.1-2) is used in both cases. The timing of key events for the updated model case is very similar to the previous test case without the updates. Most events occur within 30 minutes or less of each other. As seen by the comparison, these configuration errors would not be expected to impact the SOARCA results. However, during development of the probabilistic model, these inaccuracies in the model configuration contributed to some of the failed and inaccurate solutions.

As shown on Figure C.1-4(a), the initial fraction of the iodine core inventory released to the environment is slightly higher and yet again closer to the SOARCA estimate than the previous case using MELCOR 1.8.6 version YV3780 and the near equilibrium model disabled. The larger release in the previous case is due to the greater drywell head flange leakage, than in the updated model. The model updated to correct configuration inaccuracies results in a smaller leakage through the drywell head flange compared to the old model.

Figure C.1-4(b) shows the cesium release to the environment for the updated model is slightly higher, yet slightly closer, to the SOARCA estimate than the results previously shown on Figure C.1-3(b) without the model updates.

A noteworthy difference between MELCOR Versions YR549 and YV3780 related to cesium speciation is the default exchange of Cs_2MoO_4 between the radionuclide and cavity packages of the codes. In Version YR549, Cs_2MoO_4 was passed from radionuclide to cavity as cesium and cesium was passed from cavity to radionuclide as Cs_2MoO_4 . In Version YV3780, Cs_2MoO_4 is passed from radionuclide to cavity as cesium and molybdenum and cesium and molybdenum are passed from cavity to radionuclide as cesium and molybdenum. The change from Version YR549 to Version YV3780 was made to conserve mass. The inconsistency in the exchange of Cs_2MoO_4 between the radionuclide and cavity packages arises from the shortcoming in the cavity package wherein Cs_2MoO_4 is not a recognized compound. The impact of this difference between the code versions is thought to be insignificant given that most all of the Cs_2MoO_4 initialized in the core is released from the fuel in-vessel in the Peach Bottom LTSBO MELCOR calculations.

Table C.1-6 Timing of key events for Peach Bottom LTSBO Model updates

Event	PB LTSBO with 4 hr DC power (time in hours unless noted)	
	Revised Near Equilibrium Model Off/ Version YV3780 (UAS_STD11)	Model Updates MELCOR 1.8.6 Version YV3780
Station blackout loss of all onsite and offsite AC power	0	0
Low-level 2 and RCIC actuation signal	10 minutes	10 minutes
Operators manually open SRV to depressurize reactor vessel	1	1
RPV pressure first drops below LPI setpoint (400 psig)	1.2	1.2
Battery depletion leads immediate SRV re-closure	4	4
RCIC steam line floods with water RCIC flow terminates	5.2	5.2
SRV sticks open because of excessive cycling	8.2	8.2
Downcomer water level reaches top of active fuel	8.4	8.4
First hydrogen production	8.6	8.6
First fuel-cladding gap release	9.1	9.1
First channel box failure	9.4	9.4
Reactor vessel water level reaches bottom of lower core plate	9.3	9.4
First localized failure of lower core plate	10.6	10.7
First core cell collapse because of time at temperature	9.9	10.0
Beginning of large-scale relocation of core debris to lower plenum	10.6	10.7
Lower head dries out	12.3	12.6
Ring 5 CRGT column collapse	16.8	16.8
Ring 3 CRGT column collapse	16.8	16.8
Ring 4 CRGT column collapse	16.9	18.3
Ring 1 CRGT column collapse	17.5	16.5
Ring 2 CRGT column collapse	18.0	18.3
Lower head failure	20.1	20.2
Drywell head flange leakage begins	20.2	20.3
Hydrogen burns initiated in drywell enclosure region of reactor building	20.2	20.3
Refueling bay to environment blowout panels open	20.2	20.3
Hydrogen burns initiated in reactor building refueling bay	20.4	20.5
Drywell shell melt-through initiated and drywell head flange re-closure	20.3	20.4
Hydrogen burns initiated in lower reactor building	20.3	20.4
Door to environment through railroad access opens because of overpressure	20.3	20.4
Equipment Lock Door at 135-ft fails due to overpressure	20.3	20.4
Time iodine release to environment exceeds 1% of initial core inventory	20.6	21.1
Calculation terminated	48	48

UAS_STD11v1.8.6YV3780; UAS_STD12v1.8.6YV3780

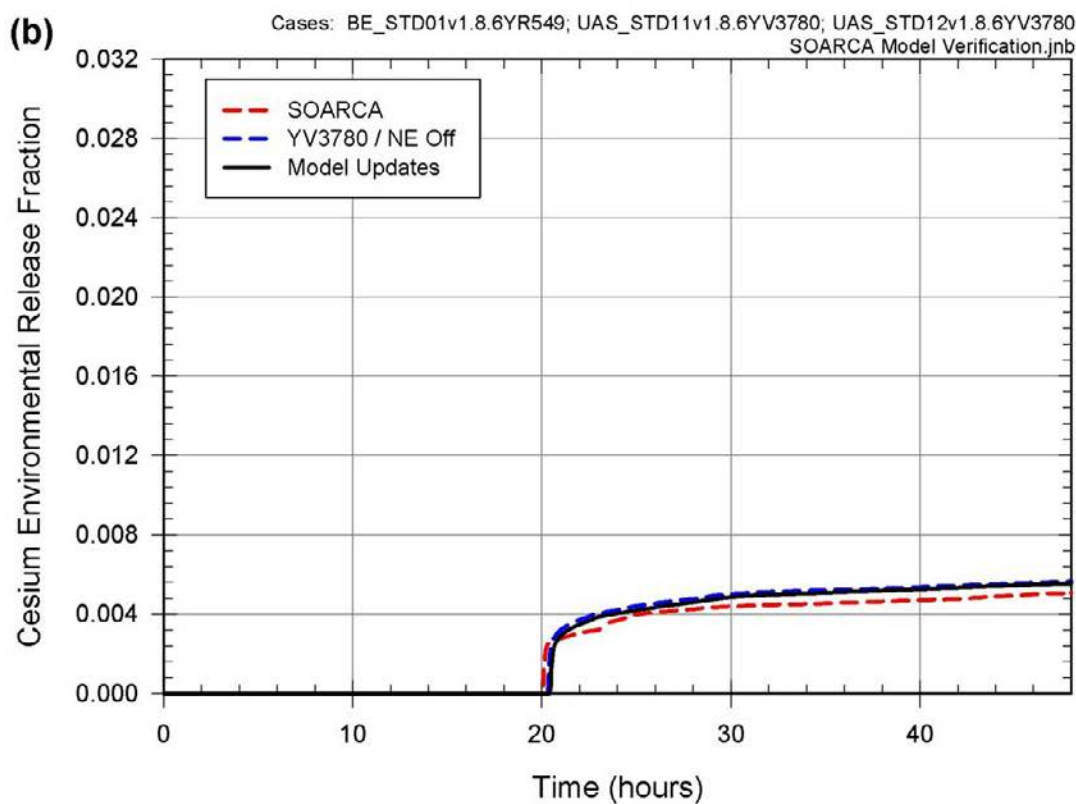
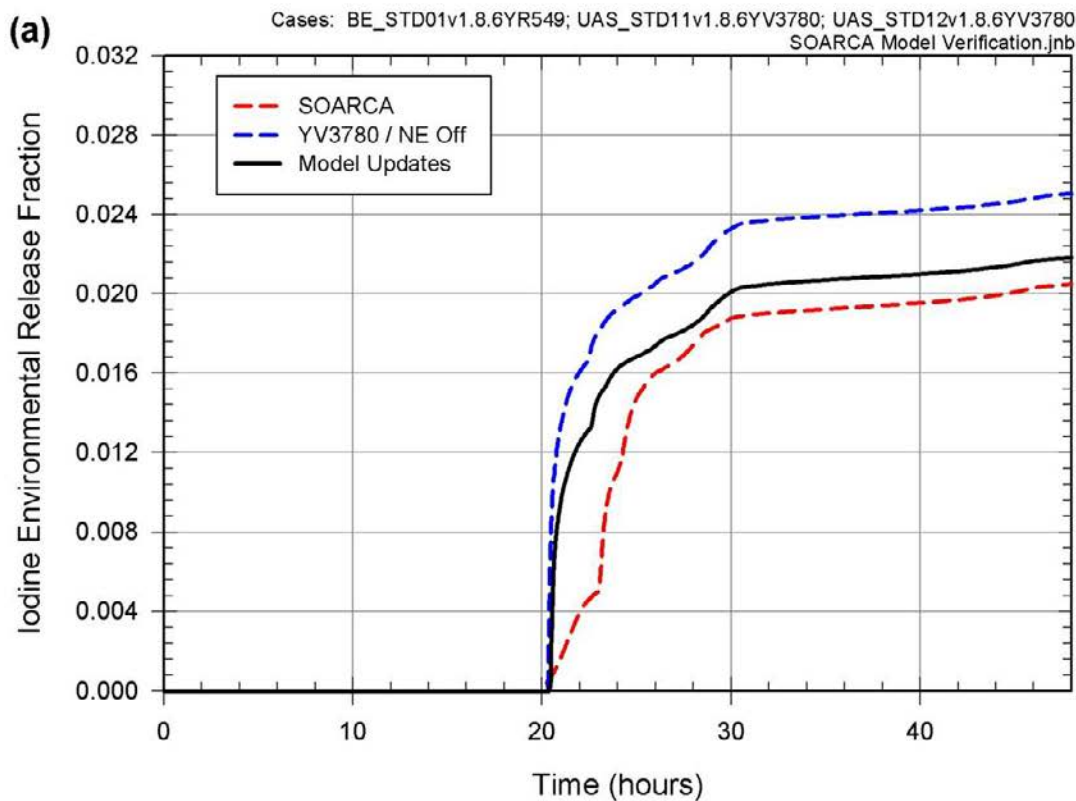


Figure C.1-4 Fraction of the core inventory released to the environment (a) Iodine and (b) Cesium with model updates for the Peach Bottom unmitigated LTSBO scenario

C.1.2.2 Update to Include Phebus Test Data

As discussed in Section 4.1.5, the predominant speciation of cesium described in NUREG/CR-7110 Volume 1 was based on detailed chemical analysis of the deposition and transport of the volatile fission products in the Phebus facility tests [19-23]. The chemical analysis revealed molybdenum combined with cesium and formed cesium molybdate. Prior to NUREG/CR-7110 Volume 1, the default assumed predominant chemical form of cesium was cesium hydroxide. Consistent with past studies, NUREG/CR-7110 Volume 1 assumed all released iodine combines with cesium. However, the Phebus facility tests show that gaseous iodine is found within containment [19-23]. Five alternative combinations of the four chemical groups are defined and each alternative has a probability of occurrence defined by a discrete distribution (Figure 4.1-20 and Table 4.1-7). Each of the five alternatives partitions the radionuclide mass of iodine and cesium between four radionuclide classes in the MELCOR model (radionuclide classes: 2 (CsOH), 4 (I₂), 16 (CsI), and 17 (Cs₂MoO₄), Table 4.1-7). The SOARCA values are not exactly represented in the uncertainty analysis due to the presence of gaseous iodine. To quantify this effect, the most likely combination was selected from the Phebus experiments [19, 20, 22, and 23] CHEMFORM #5, with an averaged peak gaseous iodine of 2.77% of the initial iodine inventory was assumed and like the SOARCA case the cesium is partitioned between CsI and Cs₂MoO₄.

Table C.1-7 shows the results with the MELCOR 1.8.6 version YV3780 with the revised near equilibrium model disabled for the Peach Bottom unmitigated LTSBO scenario compared with the results when Phebus results are incorporated into the analysis. The same final timestep function (Section C.1.1.1, Table C.1-2) is used in both cases.

The timing of key events for the model using CHEMFORM #5 is very similar to the results with the MELCOR 1.8.6 Version YV3780 with the near equilibrium model disabled until lower head failure. Lower head failure, and the events that occur after, occur roughly two hours earlier in the CHEMFORM #5 model.

As shown on Figure C.1-5(a), the initial iodine released to the environment is higher than the SOARCA estimate. This can be attributed to the presence of iodine gas for the CHEMFORM #5 case. 2.77% of the iodine core inventory is partitioned into iodine gas. However after this initial release, the rate of iodine released to the environment is similar to the SOARCA estimate.

Figure C.1-5(b) shows the cesium released to the environment for the CHEMFORM #5 case is higher than the SOARCA estimate. Since the release of CsI is higher for the CHEMFORM #5 case, the overall difference in cesium release is attributed to this when compared to the SOARCA estimate.

Table C.1-7 Timing of key events for Peach Bottom LTSBO with CHEMFORM #5

Event	PB LTSBO with 4 hr DC power (time in hours unless noted)	
	Revised Near Equilibrium Model Off/ Version YV3780 (UAS_STD11)	ChemForm #5 Version YV3780 (UAS_STD09)
Station blackout loss of all onsite and offsite AC power	0	0
Low-level 2 and RCIC actuation signal	10 minutes	10 minutes
Operators manually open SRV to depressurize reactor vessel	1	1
RPV pressure first drops below LPI setpoint (400 psig)	1.2	1.2
Battery depletion leads immediate SRV re-closure	4	4
RCIC steam line floods with water RCIC flow terminates	5.2	5.2
SRV sticks open because of excessive cycling	8.2	8.2
Downcomer water level reaches top of active fuel	8.4	8.4
First hydrogen production	8.6	8.5
First fuel-cladding gap release	9.1	9.1
First channel box failure	9.4	9.4
Reactor vessel water level reaches bottom of lower core plate	9.3	9.3
First localized failure of lower core plate	10.6	10.6
First core cell collapse because of time at temperature	9.9	9.9
Beginning of large-scale relocation of core debris to lower plenum	10.6	10.6
Lower head dries out	12.3	12.9
Ring 5 CRGT column collapse	16.8	17.3
Ring 3 CRGT column collapse	16.8	16.8
Ring 4 CRGT column collapse	16.9	18.2
Ring 1 CRGT column collapse	17.5	17.8
Ring 2 CRGT column collapse	18.0	18.4
Lower head failure	20.1	18.9
Drywell head flange leakage begins	20.2	19.0
Hydrogen burns initiated in drywell enclosure region of reactor building	20.2	19.0
Refueling bay to environment blowout panels open	20.2	19.0
Hydrogen burns initiated in reactor building refueling bay	20.4	--
Drywell shell melt-through initiated and drywell head flange re-closure	20.3	19.1
Hydrogen burns initiated in lower reactor building	20.3	19.1
Door to environment through railroad access opens because of overpressure	20.3	19.1
Equipment Lock Door at 135-ft fails due to overpressure	20.3	19.1
Time iodine release to environment exceeds 1% of initial core inventory	20.6	21.1
Calculation terminated	48	48

UAS_STD11v1.8.6YV3780; UAS_STD09v1.8.6YV3780

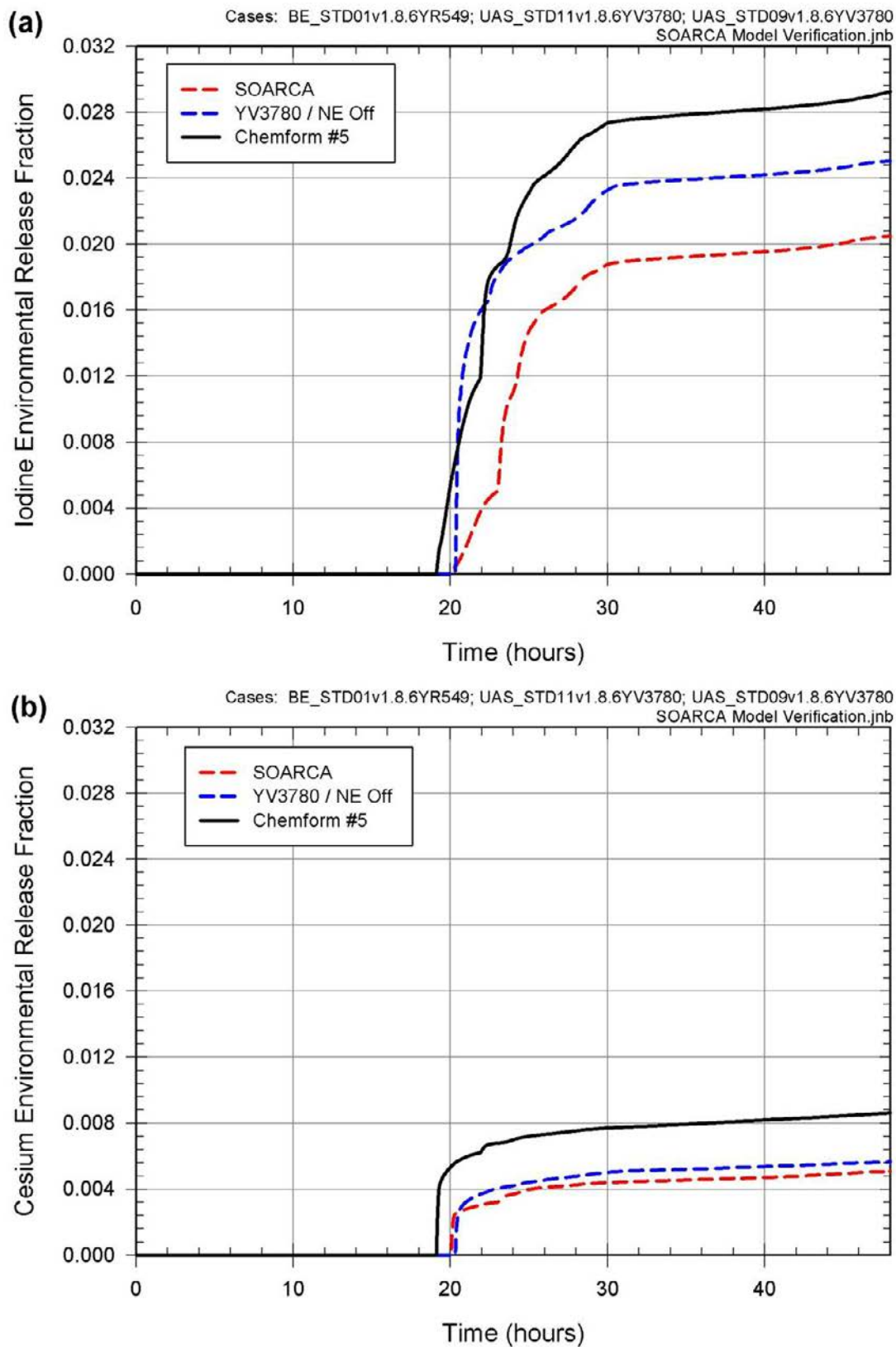


Figure C.1-5 Fraction of the core inventory released to the environment (a) Iodine and (b) Cesium with CHEMFORM #5 for the Peach Bottom unmitigated LTSBO scenario

C.1.3 SOARCA Uncertainty Analysis Base Cases (Deterministic)

The following two subsections present the results from the uncertainty analysis deterministic base case model for the SOARCA Peach Bottom unmitigated LTSBO scenario and an updated version of the MSL creep failure sensitivity case presented in NUREG/CR-7110 Volume 1. Both cases are used in the uncertainty analysis presented in Section 6.0.

C.1.3.1 SOARCA Uncertainty Analysis Base Case Estimate

Table C.1-8 shows the results with the MELCOR 1.8.6 Version YV3780 with the near equilibrium model disabled for the Peach Bottom unmitigated LTSBO scenario compared with the results of the UA SOARCA version of the same scenario using MELCOR 1.8.6 Version YV3780 including all of the updates and code changes summarized in Table C.1-1.

The timing of key events for the model using SOARCA Uncertainty Analysis model is very similar to the numerical convergence test up until lower head failure. Lower head failure, and the events that occur after, occur roughly one hour earlier in the SOARCA Uncertainty Analysis model. As shown on Figure C.1-6(a), the initial fraction of iodine core inventory released to the environment is higher than the SOARCA estimate due the presence of 2.77% of the iodine core inventory is partitioned into iodine gas as a result of incorporation of the Phebus test data (Section C.1.2.2). However after this initial release, the rate of iodine released to the environment is similar to the SOARCA estimate. Figure C.1-6(b) shows the fraction of cesium core inventory released to the environment for the SOARCA Uncertainty Analysis case is slightly higher than the SOARCA estimate.

Table C.1-8 Timing of key events for Peach Bottom LTSBO UA SOARCA Case

Event	PB LTSBO with 4 hr DC power (time in hours unless noted)	
	Revised Near Equilibrium Model Off/ Version YV3780 (UAS_STD11)	UA SOARCA MELCOR 1.8.6 Version YV3780 (UAS_STD13)
Station blackout loss of all onsite and offsite AC power	0	0
Low-level 2 and RCIC actuation signal	10 minutes	10 minutes
Operators manually open SRV to depressurize reactor vessel	1	1
RPV pressure first drops below LPI setpoint (400 psig)	1.2	1.2
Battery depletion leads immediate SRV re-closure	4	4
RCIC steam line floods with water RCIC flow terminates	5.2	5.2
SRV sticks open because of excessive cycling	8.2	8.2
Downcomer water level reaches top of active fuel	8.4	8.4
First hydrogen production	8.6	8.6
First fuel-cladding gap release	9.1	9.1
First channel box failure	9.4	9.4
Reactor vessel water level reaches bottom of lower core plate	9.3	9.4
First localized failure of lower core plate	10.6	10.7
First core cell collapse because of time at temperature	9.9	10.0
Beginning of large-scale relocation of core debris to lower plenum	10.6	10.7
Lower head dries out	12.3	12.1
Ring 5 CRGT column collapse	16.8	16.1
Ring 3 CRGT column collapse	16.8	16.9
Ring 4 CRGT column collapse	16.9	17.0
Ring 1 CRGT column collapse	17.5	17.4
Ring 2 CRGT column collapse	18.0	17.5
Lower head failure	20.1	19.8
Drywell head flange leakage begins	20.2	19.9
Hydrogen burns initiated in drywell enclosure region of reactor building	20.2	19.9
Refueling bay to environment blowout panels open	20.2	19.9
Hydrogen burns initiated in reactor building refueling bay	20.4	20.1
Drywell shell melt-through initiated and drywell head flange re-closure	20.3	20.0
Hydrogen burns initiated in lower reactor building	20.3	20.0
Door to environment through railroad access opens because of overpressure	20.3	20.0
Equipment Lock Door at 135-ft fails due to overpressure	20.3	20.0
Time iodine release to environment exceeds 1% of initial core inventory	20.6	22.8
Calculation terminated	48	48

UAS_STD11v1.8.6YV3780; UAS_STD13v1.8.6YV3780

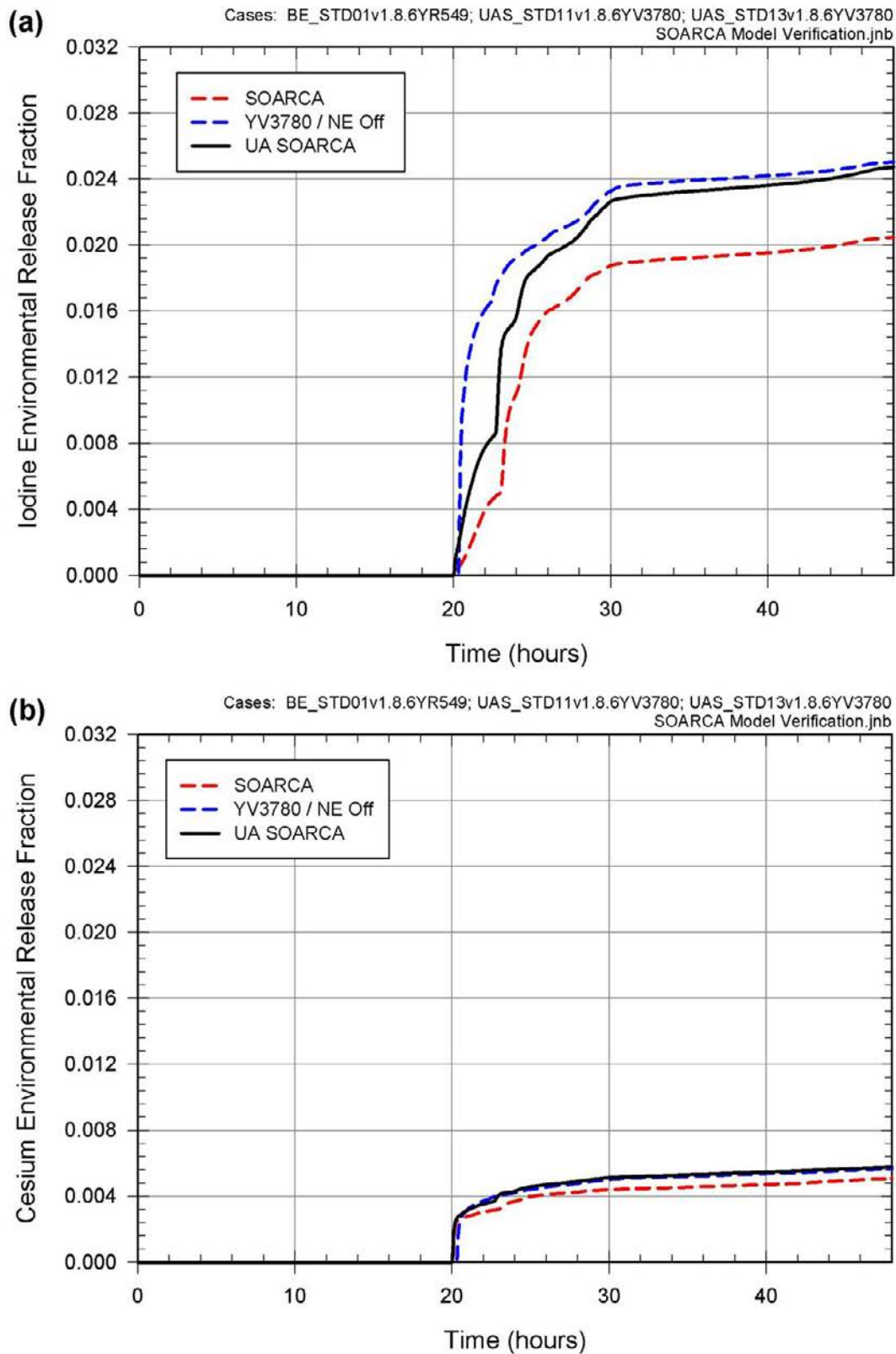


Figure C.1-6 Fraction of the core inventory released to the environment (a) Iodine and (b) Cesium for UA SOARCA for the Peach Bottom unmitigated LTSBO scenario

C.1.3.2 SOARCA Main Steam Line Creep Sensitivity

Table C.1-9 shows the results of the SOARCA Estimate SOARCA MSL Creep Rupture case using MELCOR 1.8.6 Version YR549 and the UA version of the same scenario using MELCOR 1.8.6 Version YV3780. The UA version of the MSL creep rupture case incorporates all of the changes documented in Table C.1-1, including the use of CHEMFORM #5 that contains a fraction of iodine as iodine gas (I_2).

The timing of key events for the model using UA MSL Creep Rupture model is very similar to the SOARCA MSL Creep Rupture model until lower core support plate failure and main steam line rupture. After this, the timing difference ranges from minutes to hours.

As shown on Figure C.1-7(a), the fraction of iodine core inventory released to the environment is higher than the SOARCA MSL Creep Rupture sensitivity analysis. The larger release in the UA SOARCA MSL Creep Rupture case is due to the drywell head flange leakage and the presence of 2.77% of the iodine core inventory is partitioned into iodine gas. This case includes the model updates (from Section C.1.2) and results in a much larger leakage through the drywell head flange compared to the old model. The fraction of iodine released in excess of the SOARCA MSL creep rupture sensitivity case is on the same order of magnitude as shown in the SOARCA base case comparison (Figure C.1-6). Figure C.1-7(b) shows the fraction of cesium core inventory released to the environment for the UA MSL Creep Rupture case is much higher than the SOARCA estimate.

Table C.1-9 Timing of key events for Peach Bottom LTSBO main steam line creep rupture

Event	PB LTSBO with 4 hr DC power (time in hours unless note)	
	SOARCA MSL Creep MELCOR 1.8.6 Version YR549	UA MSL Creep MELCOR 1.8.6 Version YV3780
Station blackout loss of all onsite and offsite AC power	0	0
Low-level 2 and RCIC actuation signal	10 minutes	10 minutes
Operators manually open SRV to depressurize the reactor vessel	1	1
RPV pressure first drops below LPI setpoint (400 psig)	1.2	1.2
Battery depletion leads immediate SRV re-closure	4	4
RCIC steam line floods with water RCIC flow terminates	5.2	5.2
SRV sticks open because of excessive cycling	11.8	--
Downcomer water level reaches top of active fuel	9.0	9.0
First hydrogen production	9.2	9.3
First fuel-cladding gap release	10.1	10.1
First channel box failure	10.6	10.7
Reactor vessel water level reaches bottom of lower core plate	11.6	11.7
First localized failure of lower core plate	12.5	13.1
First core cell collapse because of time at temperature	11.2	11.2
Main Steam Line Creep Rupture	11.9	11.9
Beginning of large-scale relocation of core debris to lower plenum	12.5	13.1
Lower head dries out	13.7	13.4
Ring 5 CRGT column collapse	17.8	14.8
Ring 3 CRGT column collapse	17.9	14.3
Ring 4 CRGT column collapse	18.4	14.6
Ring 1 CRGT column collapse	17.3	13.3
Ring 2 CRGT column collapse	16.3	13.3
Lower head failure	19.0	17.6
Drywell head flange leakage begins	11.9	11.9
Hydrogen burns initiated in drywell enclosure region of reactor building	--	--
Refueling bay to environment blowout panels open	11.9	11.9
Hydrogen burns initiated in reactor building refueling bay	19.1	11.9
Drywell shell melt-through initiated and drywell head flange re-closure	19.2	17.8
Hydrogen burns initiated in lower reactor building	19.2	11.9
Door to environment through railroad access opens because of overpressure	19.4	11.9
Equipment Lock Door at 135-ft fails due to overpressure	--	11.9
Time iodine release to environment exceeds 1% of initial core inventory	12.9	11.9
Calculation terminated	48	48

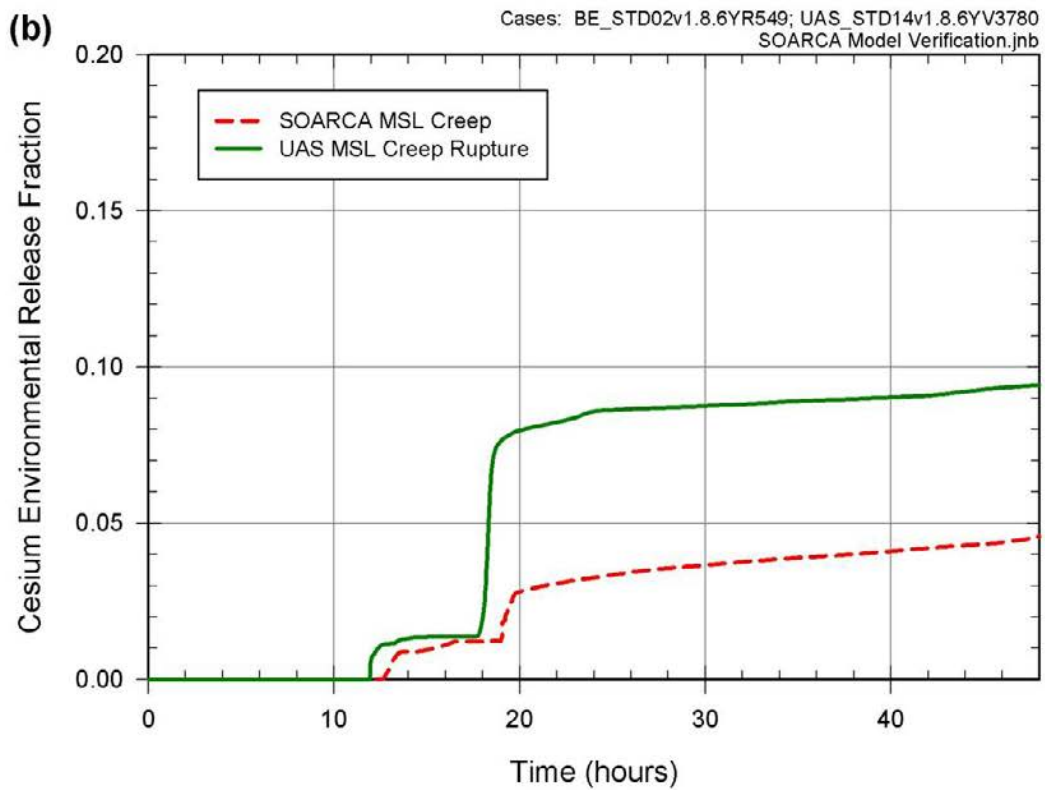
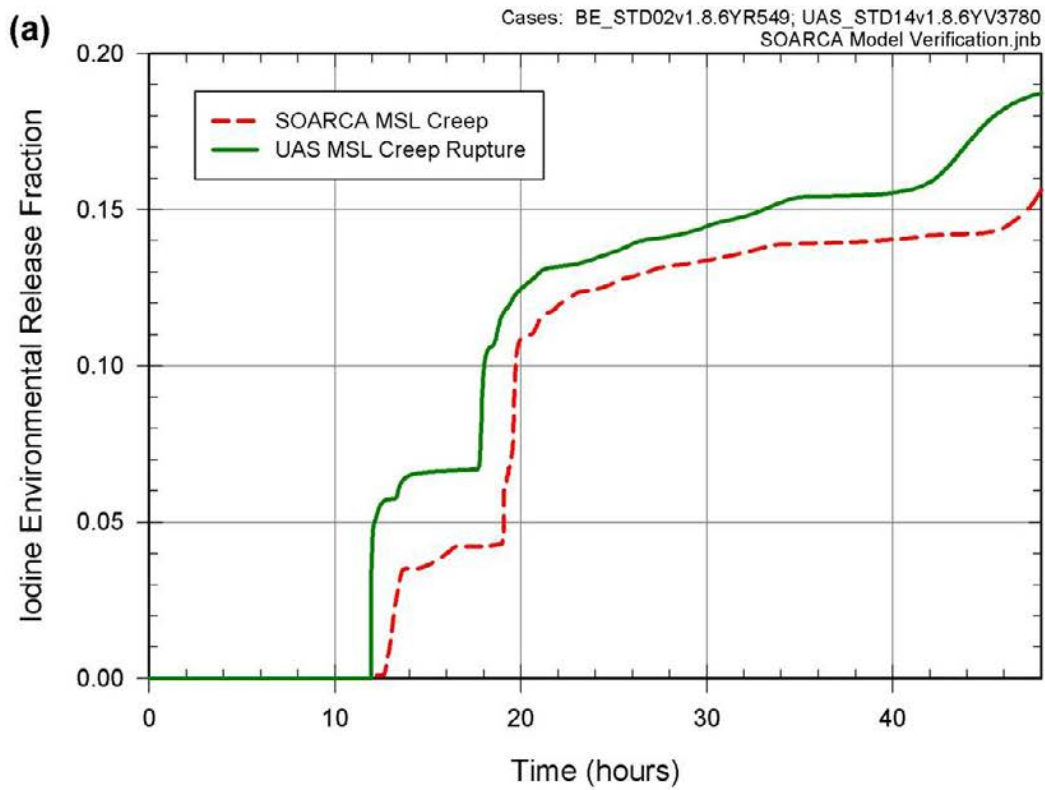


Figure C.1-7 Fraction of the core inventory released to the environment (a) Iodine and (b) Cesium for UA SOARCA MSL creep rupture for the Peach Bottom unmitigated LTSBO scenario

C.2 Consequence Model

Since the LTSBO scenario was developed in NUREG/CR-7110 Volume 1, improvements to the MACCS Version 2.5.0 code and updates to the WinMACCS Version 3.6 Peach Bottom LTSBO model have been made. Table C.2-1 summarizes the issues addressed. In order to take advantage of these improvements, but ensure proper continuity between the original LTSBO in SOARCA, and the LTSBO scenario used for a comparison with the parametric uncertainty and sensitivity results, a series of 'one-off' WinMACCS/MACCS simulations were conducted. The overall impact of these updates is considered negligible on the results of the SOARCA analysis, and the SOARCA model is considered adequate for the intended purpose.

Table C.2-1 Summary of consequence model changes to the Peach Bottom unmitigated LTSBO scenario used in the SOARCA Uncertainty Analysis

SOARCA Model Change	Issue Description	Addressed in Section
Updated MELMACCS Code	The MELMACCS pre-processor was updated to automate the processing of the probabilistic set of source terms generated by MELCOR for the uncertainty analysis	C.2.1
Updated MELCOR SOARCA source term	MELCOR code version and model updates as identified in Section C.1 resulted in an updated SOARCA source term	C.2.2
Numerical Convergence (WinMACCS)	WinMACCS Code version 3.6.2 was updated to version 3.6.4 to accommodate the large number of uncertain inputs evaluated in the uncertainty analysis.	C.2.3
Numerical Convergence (MACCS)	MACCS Code version 2.5.0.0 was updated to version 2.5.0.9 to increase convergence and numerical accuracy.	C.2.3

In addition to the items identified in Table C.2-1, to enhance the resolution of the statistical regression analysis used in the parameter uncertainty analysis, the initial set of uncertain parameters used in the MACCS uncertainty analysis base case analysis outlined in Section 4.2 was reduced. Section 5.2.1 documents the reduction in the number of uncertainty inputs for radionuclide inhalation DCFs. Originally, 69 radionuclides were selected to have uncertainty distributions applied to their respective DCFs (see Section 4.2.5) and have been reduced to 27 radionuclides.

As in presented in NUREG/CR-7110, Volume 1; the results of the consequence analyses are presented in terms of risk to the public for the Peach Bottom LTSBO scenario. For this work, conditional risk is tabulated. Conditional risk assumes that the accident occurred and shows the risk to individuals as a result of the accident (e.g., LCF risk per event). This is the same risk metric reported in NUREG/CR-7110 Volume 1.

Risk results are presented for three dose-response assumptions which are the following:

- (1). LNT hypothesis;
- (2). US average natural background dose rate combined with average annual medical exposure as a dose truncation level (USBGR), which is 620 mrem/yr; and
- (3). A dose truncation level based on the Health Physics Society's (HPS) position statement that there is a dose below which, due to uncertainties, a quantified risk should not be assigned, which is 5 rem/yr with a lifetime limit of 10 rem [86].

The results of the consequence analyses are presented in terms of risk to the public for each of the accident scenarios analyzed using the Peach Bottom LTSBO MELCOR model. All results are presented in terms of conditional, mean, individual risk (per event) (i.e., assuming that the accident occurs) and risk per year of reactor operation (i.e., accounting for the frequency of the accident) is discussed in certain instances within the text. The risks per event are conditional risks and show the risks to individuals as a result of the accident (i.e., latent cancer fatality (LCF) risk per event or early-fatality risk per event). The risks per year of reactor operation are absolute risks and are the product of the core damage frequency and the conditional risks. Absolute risk is the likelihood of receiving a latent fatal cancer or early fatality for an average individual living within a specified radius of the plant per year of plant operation (i.e., LCF risk per reactor year (pry) or early-fatality risk pry).

The risk metrics are LCF and early-fatality risks to residents in circular regions surrounding the plant. They are averaged over the entire residential population within the circular region. The LCF risk values represent the predicted number of fatalities divided by the population for three choices of dose truncation level. These risk metrics incorporate the distribution of the population within the circular region and the interplay between population distribution and the wind rose probabilities.

C.2.1 Update to MELMACCS preprocessor

The MELMACCS software is a Windows based program developed by to create a MACCS radionuclide file from the MELCOR output plot file. The MELCOR plot files contain large amounts of data, only some of which is needed for MACCS calculations. The MELMACCS software was created to provide an interface utility between MELCOR and MACCS to integrate the required data.

MELMACCS obtains two classes of data from the MELCOR plot files. The first is time independent data, which is data that remains constant throughout the MELCOR calculation. Examples of this would be radionuclide chemical/physical property classes and the flow paths to the environment. The second class is time dependent data, which is data that is written to the MELCOR plot file for each plot file timestep. The plot file timestep is determined by the user. Examples of this data would be fluid temperature and flow rate for a flow path to the environment and the mass of each chemical/physical property class.

MELMACCS uses a GUI to allow the user to convert one MELCOR plot file into radionuclide input file (.INP) for MACCS. The inputs from the MELCOR plot file correspond to the radionuclide file inputs for the ATMOS portion of MACCS.

Prior to MELMACCS converting the MELCOR plot file, the user must first specify specific inputs that are needed for the MACCS file, but are not provided by MELCOR. These inputs are:

- Radionuclide Classes,
- high/Medium/Low Burnup fuel,
- time of accident initiation,
- MELCOR height associated with ground level,
- data for building height, initial plume width and height for wake calculations,
- deposition velocity information,
- mass thresholds fractions for released material, and
- time intervals for plume segments

Figure C.2-1 provides an example of a MELMACCS plume segment. The plume segment time intervals are obtained for each MELCOR release path. Some release paths may not contain all the chemical/physical property classes defined in MELCOR. On Figure C.2-1, the initial black vertical line shows the time of radionuclide release into the environment for the specified path, MELCOR Release Path 1. For this work, the plume release time intervals are 3,600 seconds (1 hour) as that is the minimum time interval which MACCS can incorporate into the analysis.

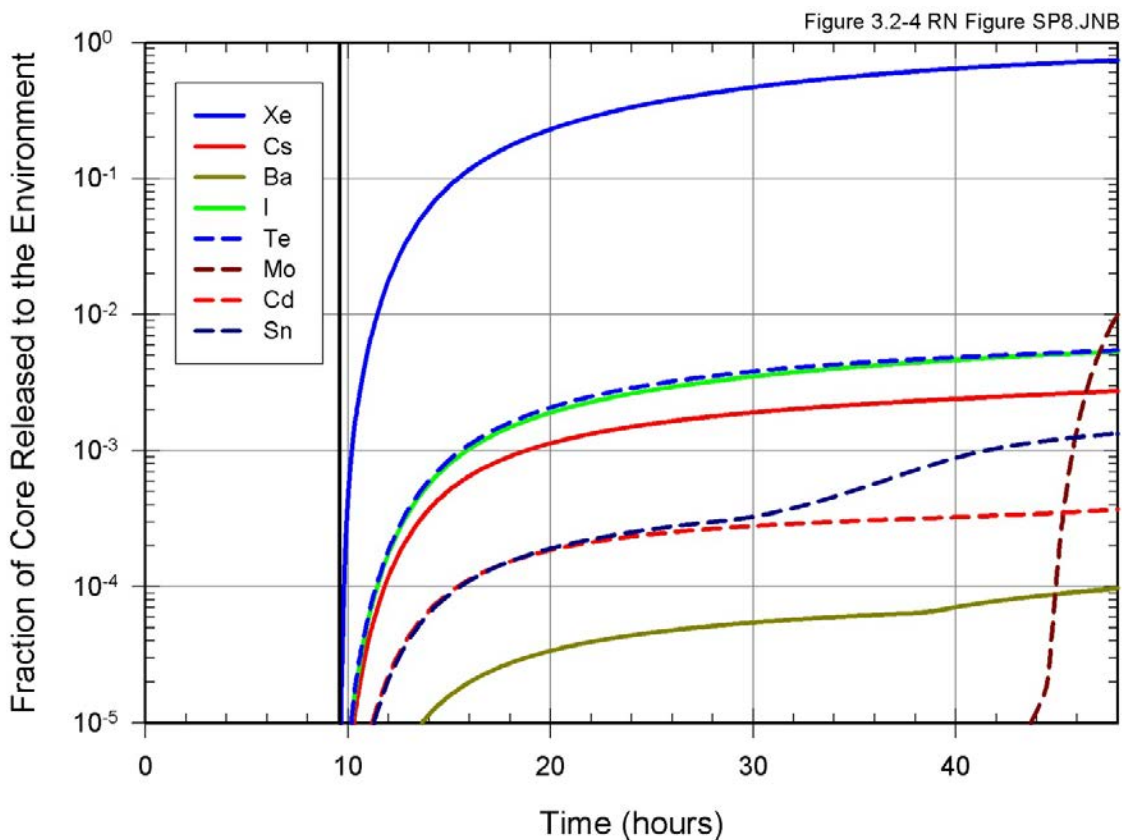


Figure C.2-1 MELMACCS plume segment

As shown on Figure C.2-1, not all radionuclide chemical/physical property classes are represented for a MELCOR release path. Table C.2-2 provides the classes which are not represented in MELMACCS and are thus not carried over into the MACCS model.

Table C.2-2 MELCOR radionuclide classes not included in MELMACCS

Class	Name	Representative	Member Elements
13	Boron	B	B, Si, P
14	Water	H ₂ O	H ₂ O
15	Concrete	--	--
16	Cesium Iodide	CsI	CsI
17	Cesium Molybdate	Cs ₂ MoO ₄	Cs ₂ MoO ₄

Class 13 through 16 are not included in the MELMACCS results because MACCS only reads the 12 radioactive radionuclide classes defined in MELCOR. Class 16 (Csl) is not a group that can be imported into MELMACCS. It is incorporated by carrying forward the activities and dose conversion factors for cesium and iodine separately, and therefore, is split accordingly into Class 2 (cesium) and Class 4 (halogens) fractions. Classes 13, 14, and 15 are nonradioactive. Figure C.2-1 does not show cerium, lanthanum, uranium, or ruthenium radionuclide classes as the release fractions of these radionuclides are less than 1.0×10^{-5} . MELMACCS does capture fractional releases below 1.0×10^{-5} ; however, for this work, a mass threshold fraction for a release path and a mass threshold fraction for plume segments to be used were set to 0.001 for MACCS inputs. These threshold limits are the same as those used in SOARCA calculations. The reason the thresholds are used is to keep the number of plume segments less than 200, which is the maximum number MACCS can analyze.

When the SOARCA scenarios were developed, the MELCOR output was converted to a MACCS radionuclide input file using MELMACCS Version 1.5.1. For the SOARCA scenarios only the radionuclide classes listed in Table C.2-3 were considered for environmental impacts. Class 10, uranium (U), Class 11, more volatile main group (Cd), and Class 12, less volatile main group (Sn), were not considered in the environmental impacts. For additional information regarding these radionuclide classes, see Table A-1 in NUREG/CR-7110 Volume 1.

Table C.2-3 Radionuclide classes used in SOARCA

Class	Name	Representative	Member Elements
1	Noble Gas	Xe	He, Ne, Ar, Kr, Xe, Rn, H, N
2	Alkali Metals	Cs	Li, Na, K, Rb, Cs, Fr, Cu
3	Alkali Earths	Ba	Be, Mg, Ca, Sr, Ba, Ra, Es, Fm
4	Halogens	I	F, Cl, Br, I, At
5	Chalcogens	Te	O, S, Se, Te, Po
6	Platinoids	Ru	Ru, Rh, Pd, Re, Os, Ir, Pt, Au, Ni
7	Early Transition Elements	Mo	V, Cr, Fe, Co, Mn, Nb, Mo, Tc, Ta, W
8	Tetravalent	Ce	Ti, Zr, Hf, Ce, Th, Pa, Np, Pu, C
9	Trivalent	La	Al, Sc, Y, La, Ac, Pr, Nd, Pm, Sm, Eu, Gd, Tb, Dy, Ho, Er, Tm, Yb, Lu, Am, Cm, Bk, Cf

The most current version of MELMACCS is Version 1.7.0. When Peach Bottom LTSBO scenario was developed in NUREG/CR-7110, the MELCOR output was converted to a MACCS radionuclide input file using MELMACCS 1.5.1. To ensure proper source term continuity between MELCOR and MACCS, a comparison of MELCOR source terms was conducted using MELMACCS Version 1.7.0 and MELMACCS Version 1.5.1. The upgrades to MELMACCS are attributed to the following:

- Allow the user incorporation of ORIGEN calculations into the MELMACCS initialization file. The Peach Bottom LTSBO ORIGEN calculation did not change (i.e., medium burnup, 49 MW-days/kg peak fuel rod at mid cycle Peach Bottom Unit 2),
- Provide a record of the user inputs and MELCOR plot file location in the MELMACCS output file,

- Implement batch processing, and
- Automation of the mass thresholds based on release path and plume segments.

The updated MELMACCS preprocessor includes an additional option that was applied as a mass-fraction threshold for release paths and plume segments. A value of 0.001 was given as the mass-fraction threshold for a given release path. This threshold is applied to the mass released from a radionuclide class for a given release path to the total mass released for that same class summed over all the release paths. If any radionuclide class released in a release path is equal to or exceeds this fraction, MELMACCS includes this release path in its evaluation of release fractions. If a release path falls below this threshold for every radionuclide class, MELMACCS does not include that release path in its evaluation of release fractions.

A value of 0.001 was also selected as the mass-fraction threshold for a plume segment. This threshold value is applied to the mass released from a radionuclide class for a given plume segment to the total mass released for that same class summed over all the release paths. If any radionuclide class in the plume segment exceeds this fraction, MELMACCS includes that plume segment in the results. If the plume segments fall below this threshold for every radionuclide class, then MELMACCS does not include that plume segment in the results. These two mass thresholds were applied to limit the number of 1-hour plume segments. A MACCS analysis is limited to a maximum of 200 plume segments.

A set of MELCOR plot files were converted to MACCS radionuclide input files using both versions of MELMACCS. A line by line comparison of the MELMACCS output files was conducted and no differences in the numerical values in the MACCS radionuclide input files were identified.

C.2.2 Update to MELCOR Source Term

To re-baseline the SOARCA uncertainty analysis base case and quantify any differences in the environmental impact from the changes to the updated MELCOR model for the Peach Bottom unmitigated LTSBO scenario discussed in Section C.1, a comparison of the two MELCOR source terms was conducted with WinMACCS Version 3.6.2 / MACCS Version 2.5.0.0 for the SOARCA estimate and SOARCA uncertainty analysis base case (see Section C.1.3.1). These versions of WinMACCS/MACCS were the same versions used for SOARCA to generate the results documented in Section 7 of NUREG/CR-7110 Volume 1.

A brief description of the Peach Bottom unmitigated LTSBO scenario for the two source terms are provided in Table C.2-4. The changes important to note are the 40% increase in the barium class and the 20% increase in the iodine class. These increases are expected to increase the early phase (i.e., primarily from iodine-131 and iodine-133) and long-term (i.e., primarily from barium-140 and strontium-89) risk. The other radionuclide classes that differ represent a small contribution to risk. Also, the change in initial release timing does not affect the contribution to early phase risk because evacuation is complete before the release begins.

Table C.2-4 Brief source term description for the Peach Bottom unmitigated LTSBO

Scenario	Core Damage Frequency (Events/yr)	Integral Release Fractions by Chemical Group									Atmospheric Release Timing	
		Xe	Cs	Ba	I	Te	Ru	Mo	Ce	La	Start (hr)	End (hr)
SOARCA Estimate	3×10^{-6}	0.978	0.005	0.006	0.020	0.022	0.0	0.001	0.0	0.0	20.0	48.0
SOARCA UA Base Case	3×10^{-6}	0.981	0.005	0.010	0.025	0.019	0.0	0.000	0.0	0.0	19.9	48.0
Percent Increase	N/A	0.3%	0.0%	40%	20%	-16%	0%	-176%	0%	0%	-0.5%	0.0%

As part of the source term comparison, the same methodology was applied to MELMACCS as that used to determine the NUREG/CR-7110 Volume 1 source terms. This means that only the radionuclide classes listed in Table C.2-3 are considered for environmental impacts. The uranium (U), more volatile main group (Cd), and less volatile main group (Sn) were not considered in the environmental impacts. For additional information regarding these classes, see Table A-1 in NUREG/CR-7110 Volume 1.

In this section, the risk tables represent rounded values obtained from the full data sets. The plots were developed from the full data sets and slight differences may be noticed due to rounding.

Tables C.2-5 through C.2-7 display the conditional, mean, individual LCF risk (per event) to residents within a set of concentric circular areas centered at the Peach Bottom site for the unmitigated LTSBO scenario presented in NUREG/CR-7110, Volume 1, and the SOARCA uncertainty analysis base case. Three values of dose truncation level are shown in the tables: LNT, USBGR, and HPS.

Dose-truncation based on the HPS position is more complex than the USBGR truncation because it involves both annual and lifetime limits. According to the recommendation, annual doses below the 5-rem truncation level do not need to be counted toward health effects; however, if the lifetime dose exceeds 10 rem, all annual doses, no matter how small, count toward health effects. Because of the 10 rem lifetime limit, risks predicted with the criterion based on the HPS position statement can sometimes exceed those using the USBGR truncation.

Table C.2-5 Source term comparison of conditional, mean, individual LCF risk (per event) for LNT dose truncation

Radius (mi)	SOARCA Estimate	SOARCA UA Base Case
10	8.9×10^{-5}	8.8×10^{-5}
20	7.6×10^{-5}	8.0×10^{-5}
30	5.3×10^{-5}	5.6×10^{-5}
40	3.3×10^{-5}	3.6×10^{-5}
50	2.7×10^{-5}	2.9×10^{-5}

Table C.2-6 Source term comparison of conditional, mean, individual LCF risk (per event) for USBGR dose truncation

Radius (mi)	SOARCA Estimate	SOARCA UA Base Case
10	7.4×10^{-7}	8.8×10^{-7}
20	1.9×10^{-5}	2.5×10^{-5}
30	1.1×10^{-5}	1.5×10^{-5}
40	5.0×10^{-6}	7.4×10^{-6}
50	3.4×10^{-6}	5.1×10^{-6}

Table C.2-7 Source term comparison of conditional, mean, individual LCF risk (per event) for dose truncation based on the HPS position statement

Radius (mi)	SOARCA Estimate	SOARCA UA Base Case
10	3.7×10^{-7}	5.6×10^{-7}
20	2.2×10^{-6}	3.7×10^{-6}
30	8.9×10^{-7}	1.5×10^{-6}
40	3.7×10^{-7}	6.1×10^{-7}
50	2.4×10^{-7}	3.9×10^{-7d}

Figure C.2-2 shows the conditional, mean, individual LCF risk (per event) using the LNT for the source term comparison. The figure shows the emergency and long-term phases. The emergency phase is defined as the first seven days following the initial release to the environment. The long-term phase is defined as the time following the emergency phase (i.e., there is no intermediate phase). The entire height of each column shows the combined (total) LCF risk for the two phases. The emergency response is very effective within the evacuation zone (10 miles) during the early phase, so those risks are very small and entirely represent the 0.5% of the population that are modeled as refusing to evacuate. The peak emergency-phase risk is at 20 miles, which is the first location in the plot outside of the evacuation zone. Comparing the two source terms, the differences in the long-term phase risk are trivial; the differences in the emergency-phase risks are small but meaningful and result from the differences in release fractions described.

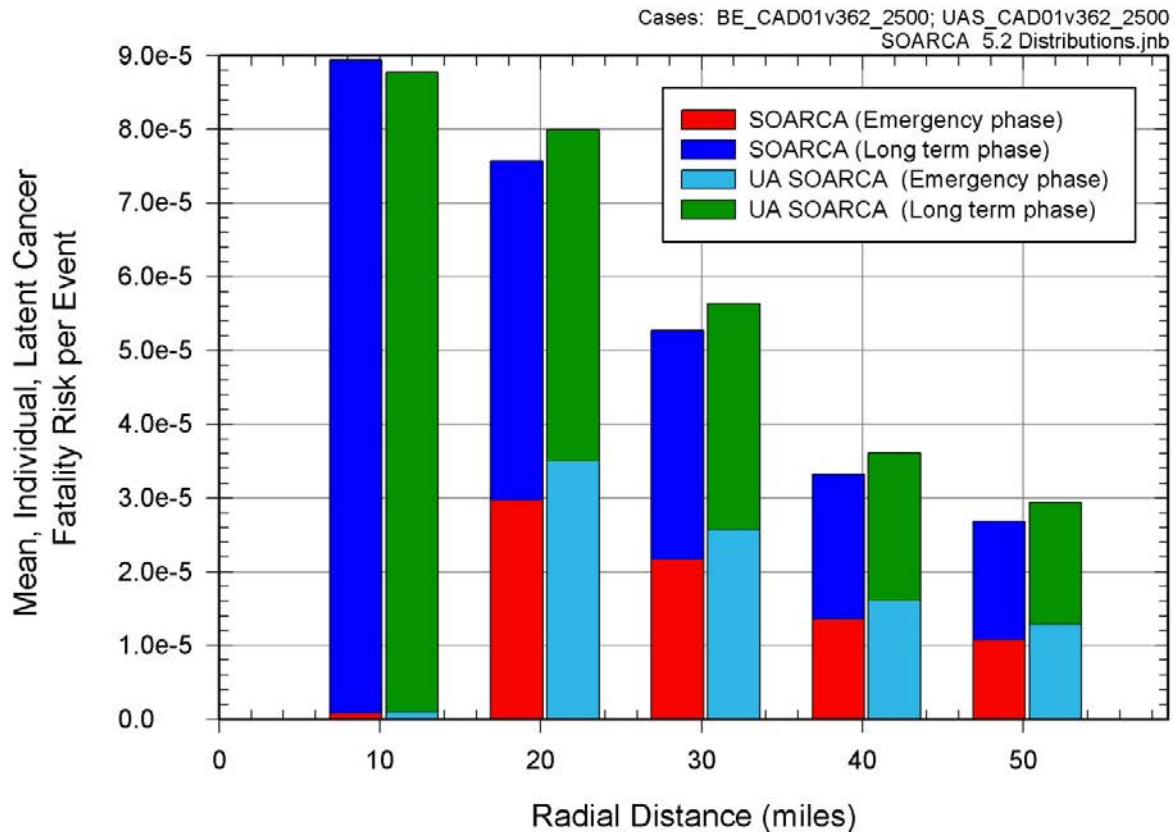


Figure C.2-2 Source term comparison of conditional, mean, individual LCF risk (per event) with LNT dose truncation for residents within a circular area of specified radius from the plant for emergency and long-term phases

The long-term phase risks dominate the total risks for the accident scenario when the LNT dose-response assumption is made. These long-term risks are controlled by the habitability (return) criterion, which is the dose rate at which residents are allowed to return to their homes following the emergency phase. For Peach Bottom, the habitability criterion is a dose rate of 500 mrem/yr. This dose rate is below the truncation levels of the USBGR (620 mrem/yr) and based on the HPS position statement; therefore, most of the doses received during the long-term phase are below the dose truncation limit and are not counted toward health effects when using these criteria. Most of the risks associated with either of the truncation levels are from doses received during the first year. The conditional, mean, individual LCF risk (per event) for these dose truncation models can be seen on Figure C.2-3 for the USBGR dose truncation model and Figure C.2-4 for the HPS dose truncation model.

Figure C.2-3 and Figure C.2-4 do not show separate risks for the emergency and long-term phases because those phases overlap, especially in the first year, and are not easily separated for purposes of evaluating the annual dose threshold. To better understand this explanation, it is important to understand the differences between exposure periods, commitment periods, and the periods of time when doses are actually received. For external dose pathways, the time over which doses are received is concurrent with the exposure period. External dose pathways include cloudshine and groundshine.

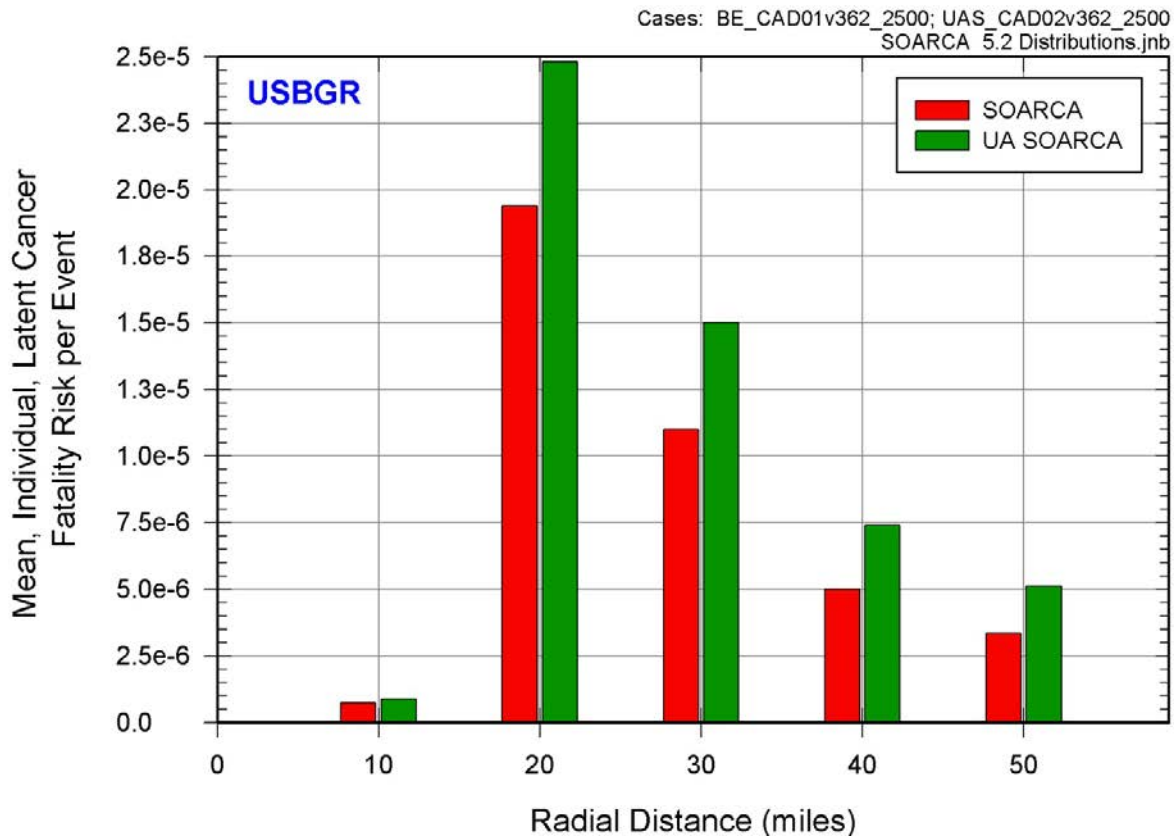


Figure C.2-3 Source term comparison of conditional, mean, individual LCF risk (per event) with USBGR dose truncation for residents within a circular area of specified radius from the plant for emergency and long-term phases

The exposure period for internal pathways, inhalation and ingestion, is the period of time when the inhalation or ingestion occurs; however, doses continue to be received over a person's entire lifetime following the exposure. A person's lifetime is variable, depending upon the age of the person at the time of exposure, among other things. The period of time over which doses are received from an internal pathway is accounted for in the construction of dose conversion factors by integrating the doses over a finite period called a dose commitment period, which is usually taken to be 50 years when calculating internal-pathway dose conversion factors for adults. An implicit assumption is that everyone in the analyses lives for an additional 50 years following the exposure, which is most likely a conservative assumption.

Most of the exposures during the long-term phase are from groundshine; a small fraction is from inhalation of resuspended aerosols. Since groundshine is an external pathway, doses received are concurrent with the exposure period, which is also taken to be 50 years in the SOARCA. On the other hand, exposures from inhalation of resuspended material during each year of the long-term phase contribute to doses received over the subsequent 50-year commitment period.

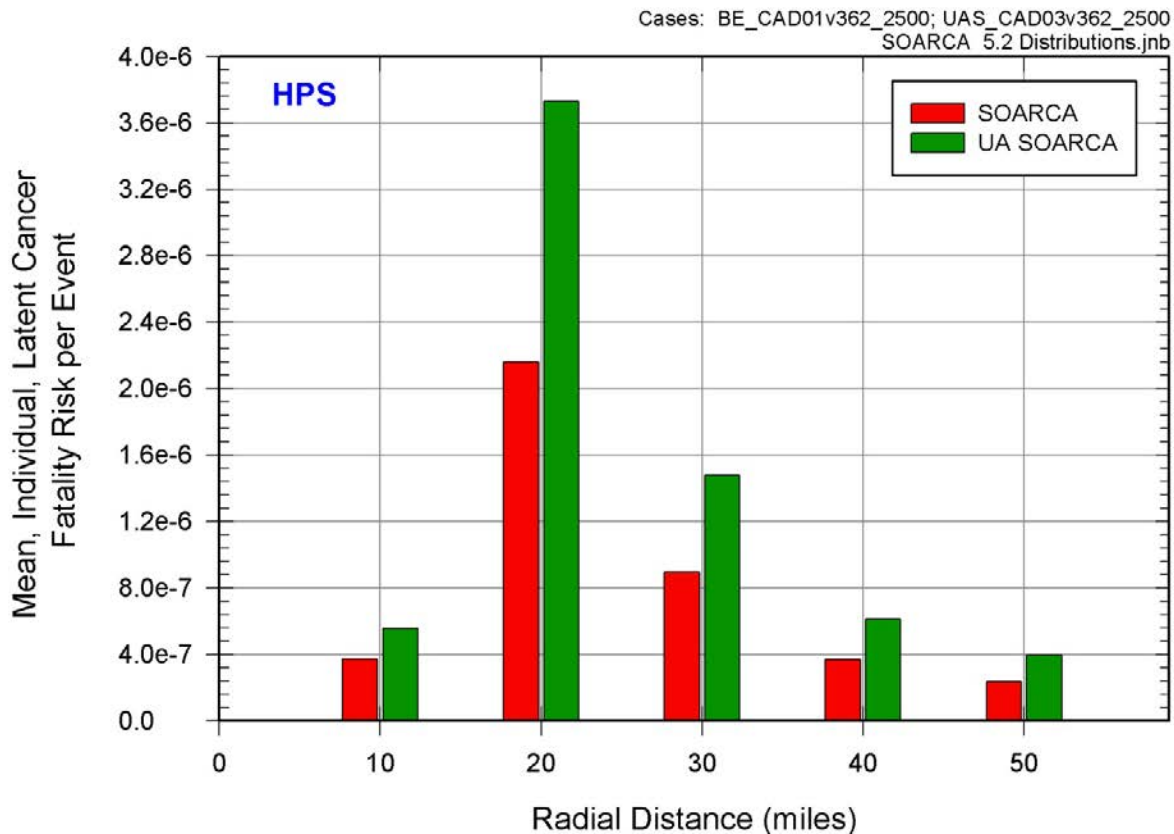


Figure C.2-4 Source term comparison of conditional, mean, individual LCF risk (per event) with HPS dose truncation for residents within a circular area of specified radius from the plant for emergency and long-term phases

Doses received in the first year thus correspond to:

- all of the dose from external exposure during the emergency phase,
- most of the dose from internal exposure during the emergency phase,
- all of the dose from external exposure during the first year of the long-term phase, and
- most of the dose from internal exposure during the first year of the long-term phase.

Doses received in the second and subsequent years correspond to:

- a fraction of the dose from internal exposure during all previous years plus most of the dose from internal exposure during that year, and
- all of the dose from external exposure during that year.

After a single exposure, internal doses decrease more slowly from one year to the next when the isotopic half-life is relatively long (i.e., on the order of a year or longer) and the solubility of the dominant chemical form of the isotope is low so that the removal rate from the human body is low (i.e., the biological half-life is long). A good example is ^{90}Sr , for which the second-year effective dose from inhalation is 60% of the first-year dose. The isotopic half-life is 29 years, so most of the reduction from year one to year two results from the biological half-life. The internal doses decrease more rapidly from one year to the next when either the isotopic half life is short or when the solubility of the dominant chemical form of the isotope is high so that the human

body tends to excrete it rapidly. A good example of this is ^{131}I , for which the second-year effective dose from inhalation is essentially zero. This isotope has a short isotopic half-life (i.e., 8 days) and a short biological half-life because of its high solubility. For comparison, the second-year effective dose from inhalation for ^{137}Cs is about 10% of the first-year dose, so it is intermediate between the previous examples.

The ingestion pathway was not treated in these SOARCA analyses because uncontaminated food and water supplies are abundant within the United States, and it is unlikely that the public would eat radioactively contaminated food. Since ingestion doses are taken to be negligible in SOARCA, inhalation is the only internal pathway that is treated. A significant portion of the exposures during the emergency phase are from inhalation. As explained above, these exposures are assumed to lead to doses over the commitment period, which is the 50 years following the exposure. However, depending on the isotope inhaled, the doses received may diminish rapidly and become negligible for most of the dose commitment period. Because the internal doses from inhalation diminish with time, most of the doses in the second and subsequent years are from the exposures during that year. But these doses are limited by the habitability criterion to be less than 500 mrem in any year. The 500 mrem limit is for all dose pathways except ingestion, in this case groundshine and inhalation from resuspended aerosols. The inhalation dose used in this criterion is a committed dose (i.e., it accounts for doses received over the next 50 years). Because the annual doses allowed by the habitability criterion are less than the truncation levels based on US background and the HPS position statement, nearly all of the risk is from doses received during the first year. These doses include most of emergency-phase doses and a fraction of the long-term phase doses. This explains the risk profiles for these dose-truncation criteria on Figure C.2-3 and Figure C.2-4.

The early-fatality risks are zero for both source terms. This is because the release fractions shown in Table C.2-4 are too low to produce doses large enough to exceed the dose thresholds for early fatalities, even for the 0.5% of the population that are modeled as refusing to evacuate. The largest value of the mean, acute dose for the closest resident (i.e., 0.5 to 1.2 kilometers from the plant) for this scenario is about 0.1 gray (Gy) to the red bone marrow, which is usually the most sensitive organ for early fatalities, but the minimum acute dose that can cause an early fatality is about 2.3 Gy to the red bone marrow. Clearly, the calculated doses are all well below this threshold.

In this comparison, the peak absolute risk is 2.7×10^{-10} per reactor year for the SOARCA estimate at the 10-mile circular area (i.e., see Table C.2-5, 10 mile circular area, and see Table C.2-4 for the LTSBO core damage frequency). Estimated LCF risks below 1×10^{-7} per reactor year should be viewed with caution because of the potential impact of events not studied in the analyses and the inherent uncertainty in very small calculated numbers.

C.2.3 Numerical Convergence – Code Updates

To reflect updates and advancements to the WinMACCS/MACCS code, a series of WinMACCS and MACCS simulations were conducted to see the overall effect on Peach Bottom LTSBO scenario. The original Peach Bottom LTSBO Unmitigated Response WinMACCS/MACCS simulation in Section 5.1 of NUREG/CR-7110 Volume 1 was conducted in November, 2010. In the past year and half, MACCS code changes have caused the numerical results for the Peach Bottom LTSBO scenario used in this study to change. These changes have resulted in changes to the conditional, mean, individual LCF risk.

WinMACCS

The updates in the MACCS graphic user interface, WinMACCS, from the version used in NUREG/CR-7110 Volume 1, WinMACCS Version 3.6.2, to the version used for this work, WinMACCS Version 3.6.4, deal with expanding the uncertainty engine. The older version of WinMACCS was not capable of handling the number of MACCS uncertainty distributions required for this study. Also, Version 3.6.2 did not allow certain DCF factors to be treated as uncertain. The newest version of WinMACCS, Version 3.6.4, has corrected these problems. These changes should not affect a deterministic calculation. To verify this, a series of WinMACCS/MACCS runs were conducted using the SOARCA estimate and SOARCA uncertainty analysis base case source terms (i.e., see Table C.2-4). The results yielded the same results shown in Tables C.2-8 through C.2-10 for the SOARCA estimate.

MACCS

The updates to MACCS from the version used in NUREG/CR-7110 Volume 1, MACCS Version 2.5.0.0, to the version used for this work, MACCS Version 2.5.0.9 deal with the following:

- Provide file locations on MACCS cyclical files (e.g., MELMACCS source term files) to provide enhances traceability between inputs and results,
- Lower plume density limit (PLMDEN) consistent with the MACCS User Manual [9],
- Change to a FORTRAN compiler compatible with the Windows 7 operating system, and
- Correction of the NRC Regulatory Guide 1.1.45 plume meander model [10], which is not used in the SOARCA scenarios.

The new compiler affects the way rounding is performed. The 'round off' changes the random values that are calculated, particularly the set of weather trials that are selected. These differences result from conversion of real numbers to integers, where the real numbers can be slightly greater than or less than the associated integer. This difference is considered acceptable and not an error because there is no reason to think that one set of random choices is better than another.

NUREG/CR-7110 Volume 1 and this work use 984 randomly selected weather trials selected from 36 bins used for nonuniform weather bin sampling. The random seed used to generate these weather trials is kept constant throughout the deterministic work in this study and is the same used in NUREG/CR-7110 Volume 1. This results in the same weather trials being sampled for all MACCS deterministic analysis using the same MACCS code version.

Since MACCS version 2.5.0.9 changes the weather trials sampled using the same random seed, the two MACCS versions were compared and the results are shown below. The change in weather trials results in about a 2-9% higher conditional, mean, individual LCF risk. Tables C.2-8 through C.2-10 show the differences in the SOARCA estimate LCF risk per event for the LNT, USBGR, and HPS dose truncation levels, respectively.

Table C.2-8 MACCS version comparison of conditional, mean, individual LCF risk (per event) for LNT dose truncation for the SOARCA estimate at specified circular areas

Radius (mi)	Version 2.5.0.0	Version 2.5.0.9
10	8.9×10^{-5}	9.2×10^{-5}
20	7.6×10^{-5}	7.9×10^{-5}
30	5.3×10^{-5}	5.4×10^{-5}
40	3.3×10^{-5}	3.4×10^{-5}
50	2.7×10^{-5}	2.8×10^{-5}

Table C.2-9 MACCS version comparison of conditional, mean, individual LCF risk (per event) for USBGR dose truncation for the SOARCA estimate at specified circular areas

Radius (mi)	Version 2.5.0.0	Version 2.5.0.9
10	7.4×10^{-7}	7.5×10^{-7}
20	1.9×10^{-5}	2.0×10^{-5}
30	1.1×10^{-5}	1.1×10^{-5}
40	5.0×10^{-6}	5.1×10^{-6}
50	3.4×10^{-6}	3.4×10^{-6}

Table C.2-10 MACCS version comparison of conditional, mean, individual LCF risk (per event) for HPS dose truncation for the SOARCA estimate at specified circular areas

Radius (mi)	Version 2.5.0.0	Version 2.5.0.9
10	3.7×10^{-7}	3.8×10^{-7}
20	2.2×10^{-6}	2.4×10^{-6}
30	8.9×10^{-7}	9.6×10^{-7}
40	3.7×10^{-7}	3.9×10^{-7}
50	2.4×10^{-7}	2.5×10^{-7}

The overall average difference between versions in terms of conditional, mean, individual LCF risk is less than 9%. The largest difference is noticed at the 20-mile radius in Table C.2-10 but is still less than 10%. A difference of less than 10% induced by weather sampling is considered small. The SORCA UA base case was also compared between versions and yielded similar results.

The WinMACCS/MACCS code behavior has been documented with a series of regression tests and expansion testing as new updates and models are added to the codes. Many WinMACCS/MACCS validation and verification analyses have been conducted. References [8, 9, 50, 88-90] provide the most current documentation for WinMACCS/MACCS.

C.2.4 SOARCA Uncertainty Analysis Deterministic Base Case

In this section, the risk tables represent rounded values obtained from the full data sets. The plots were developed from the full data sets and slight differences may be noticed due to this rounding.

Tables C.2-11 through Table C.2-13 display the conditional, mean, individual LCF risk (per event) to residents within a set of concentric circular areas centered at the Peach Bottom site for the unmitigated LTSBO scenario presented in NUREG/CR-7110, Volume 1, and the SOARCA uncertainty analysis base case source term using WinMACCS Version 3.6.4 and MACCS Version 2.5.0.9. Three values of dose truncation level are shown in the tables: LNT, USBGR, and HPS.

Table C.2-11 SOARCA estimate and SOARCA UA base case comparison of conditional, mean, individual LCF risk (per event) for LNT dose truncation at specified circular areas

Radius (mi)	SOARCA Estimate Version 2.5.0.9	SOARCA UA Base Case
10	9.2×10^{-5}	9.0×10^{-5}
20	7.9×10^{-5}	8.3×10^{-5}
30	5.4×10^{-5}	5.8×10^{-5}
40	3.4×10^{-5}	3.7×10^{-5}
50	2.8×10^{-5}	3.0×10^{-5}

Table C.2-12 SOARCA estimate and SOARCA UA base case comparison of conditional, mean, individual LCF risk (per event) for USBGR dose truncation at specified circular areas

Radius (mi)	SOARCA Estimate Version 2.5.0.9	SOARCA UA Base Case
10	7.5×10^{-7}	8.9×10^{-7}
20	2.0×10^{-5}	2.6×10^{-5}
30	1.1×10^{-5}	1.6×10^{-5}
40	5.1×10^{-6}	7.7×10^{-6}
50	3.4×10^{-6}	5.2×10^{-6}

Table C.2-13 SOARCA estimate and SOARCA UA base case comparison of conditional, mean, individual LCF risk (per event) for HPS dose truncation at specified circular areas

Radius (mi)	SOARCA Estimate Version 2.5.0.9	SOARCA UA Base Case
10	3.8×10^{-7}	5.6×10^{-7}
20	2.4×10^{-6}	4.4×10^{-6}
30	9.6×10^{-7}	1.7×10^{-6}
40	3.9×10^{-7}	7.1×10^{-7}
50	2.5×10^{-7}	4.5×10^{-7}

Figure C.2-5 shows the conditional, mean, individual LCF risk (per event) with the LNT for the SOARCA estimate and SOARCA uncertainty analysis base case comparison for the emergency and long term phases. The entire height of each column shows the combined (total) risk for the two phases. The emergency response is very effective within the evacuation zone (10 miles) during the early phase, so those risks are very small and entirely represent the 0.5% of the population that are modeled as refusing to evacuate. The peak emergency phase risk is at 20 miles, which is the first location in the plot outside of the evacuation zone. The differences in the long-term phases are trivial.

The SOARCA uncertainty analysis base case conditional, mean, individual LCF risks are greater for both phases for all circular areas. These higher results are attributed to the differences in the source term discussed in Section C.2.2 and the code changes discussed in Section C.2.3.

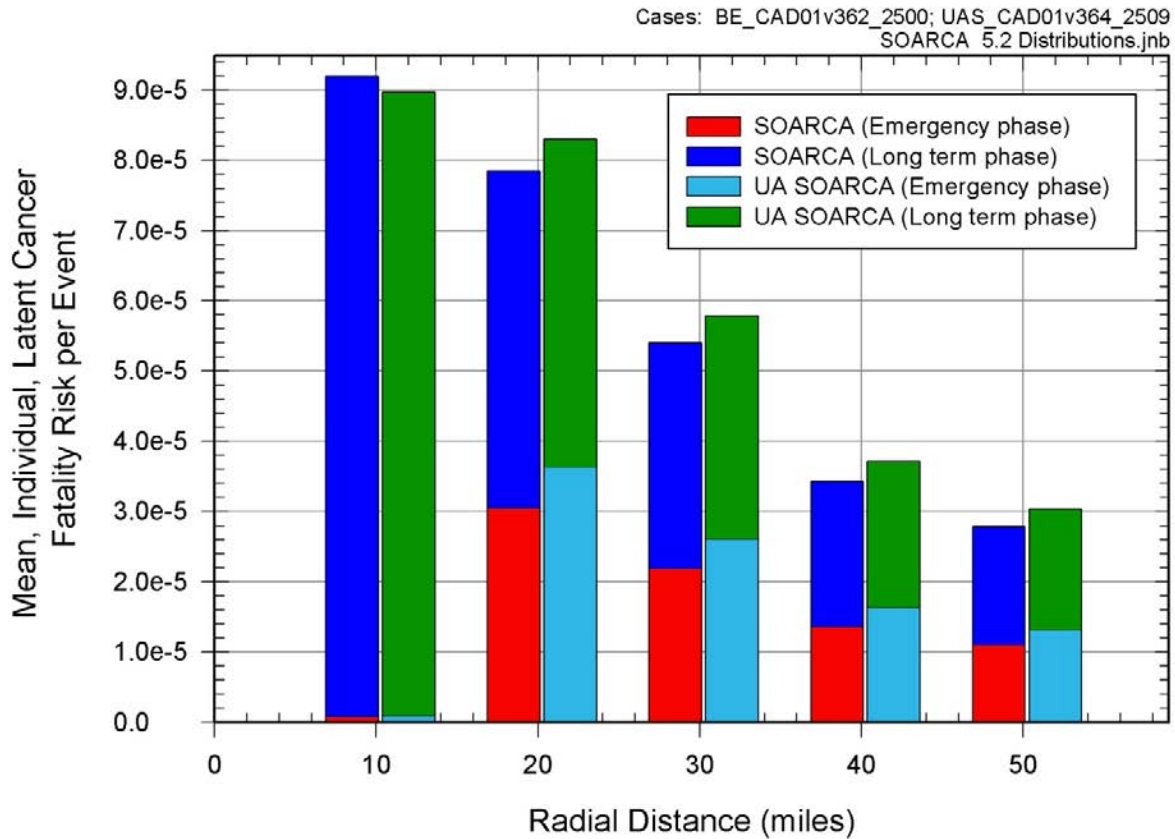


Figure C.2-5 SOARCA estimate and SOARCA UA base case comparison of conditional, mean, individual LCF risk (per event) with the LNT for residents within a circular area of specified radius from the plant for emergency and long-term phases

The long-term phase risk dominates the total risk for the accident scenario when the LNT dose-response assumption is made. These long-term risks are controlled by the habitability (return) criterion, which is the dose rate at which residents are allowed to return to their homes following the emergency phase. For Peach Bottom, the habitability criterion is a dose rate of 500 mrem/yr. This dose rate is below the truncation levels based on US background and based on the HPS position statement; therefore, most of the doses received during the long-term phase are below the dose truncation limit and are not counted toward health effects when using these criteria. Thus, most of the risks associated with either of the truncation levels are from doses received during the first year. The conditional, mean, individual LCF risk (per event) for these dose truncation models can be seen on Figure C.2-6 for the USBGR dose truncation model, and Figure C.2-7 for the HPS dose truncation model. Figure C.2-6 and Figure C.2-7 do not show separate risks for the emergency and long-term phases because those phases overlap, especially in the first year, and are not easily separated for purposes of evaluating the annual dose threshold.

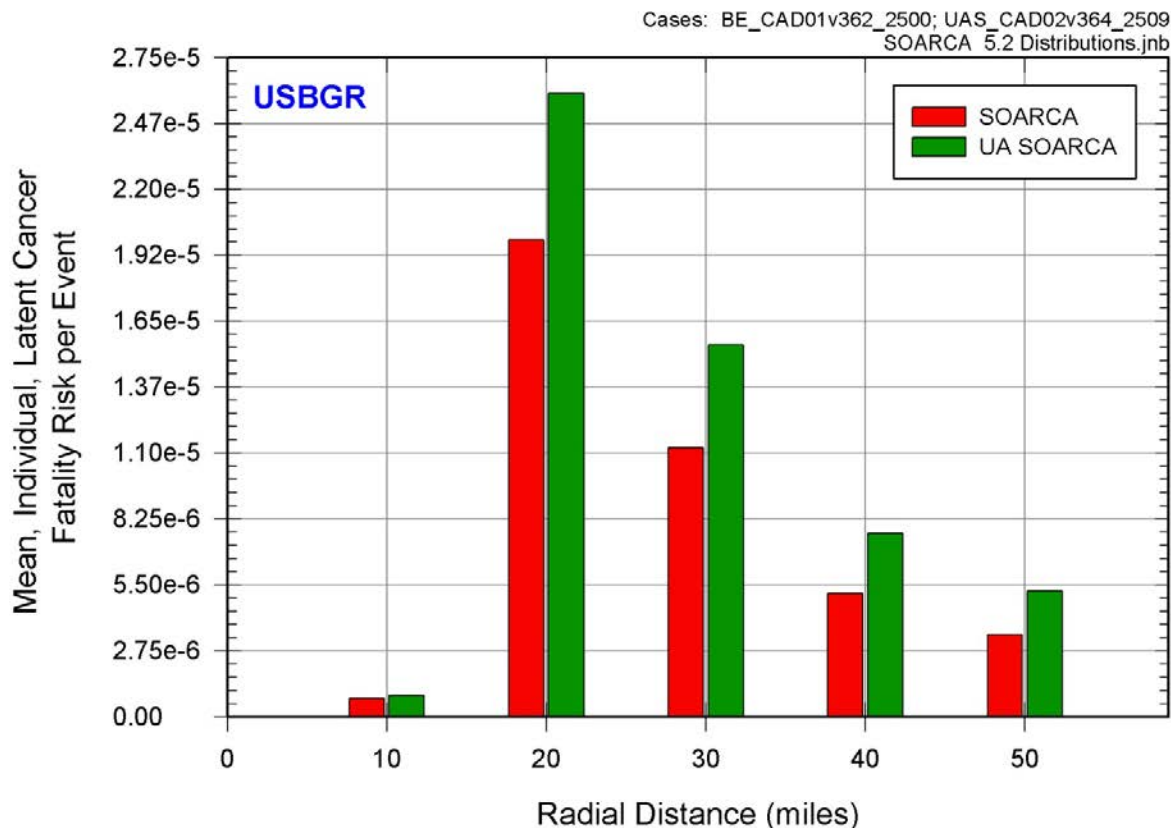


Figure C.2-6 SOARCA estimate and SOARCA UA base case comparison of conditional, mean, individual LCF risk (per event) with USBGR dose truncation for residents within a circular area of specified radius from the plant for emergency and long-term phases

Because the internal doses from inhalation diminish with time, most of the doses in the second and subsequent years are from the exposures during that year. But these doses are limited by the habitability criterion to be less than 500 mrem in any year. The 500 mrem limit is for all dose pathways, in this case groundshine and inhalation from resuspended aerosols. The inhalation dose used in this criterion is a committed dose (i.e., it accounts for doses received over the next 50 years). Because the annual doses allowed by the habitability criterion are less than truncation levels based on US background and the HPS position statement, nearly all of the risk is from doses received during the first year. These doses include most of emergency phase doses and a fraction of the long-term phase doses. This explains the risk profiles for these dose-truncation criteria on Figure C.2-6 and Figure C.2-7.

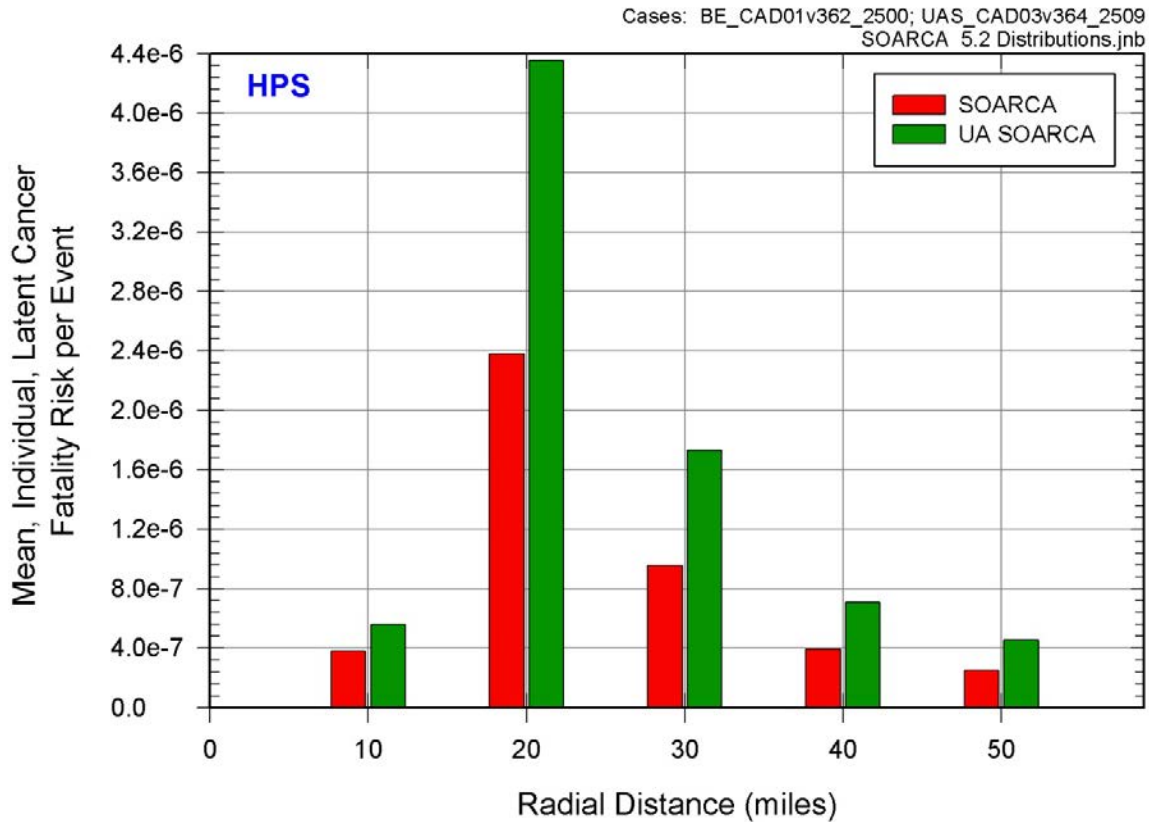


Figure C.2-7 SOARCA estimate and SOARCA UA base case comparison of conditional, mean, individual LCF risk (per event) with HPS dose truncation for residents within a circular area of specified radius from the plant for emergency and long-term phases

The early-fatality risks are zero for both source terms. This is because the release fractions shown in Table C.2-4 are too low to produce doses large enough to exceed the dose thresholds for early fatalities, even for the 0.5% of the population that are modeled as refusing to evacuate. The largest value of the mean, acute dose for the closest resident (i.e., 0.5 to 1.2 kilometers from the plant) for this scenario is about 0.1 gray (Gy) to the red bone marrow, which is usually the most sensitive organ for early fatalities, but the minimum acute dose that can cause an early fatality is about 2.3 Gy to the red bone marrow. Clearly, the calculated doses are all well below this threshold.

Estimated risks below 1×10^{-7} per reactor year should be viewed with caution because of the potential impact of events not studied in the analyses and the inherent uncertainty in very small calculated numbers. In this comparison, the peak absolute risk is 2.8×10^{-10} per reactor year for the SOARCA Estimate at the 10-mile circular area (i.e., see Table 5.2-1, 10 mile circular area, and see Table C.2-4 for the LTSBO core damage frequency).

C.3 Model Error Log

The post-model development activities following the completion of the SOARCA Peach Bottom unmitigated LTSBO uncertainty analysis identified several issues related to errors in implementation, identification of undocumented conservatisms, and/or updates to parameter values. These issues are addressed in this Appendix which includes an evaluation of the sensitivity of the error. Not all identified issues that are evaluated fall in the category of errors, as some of the issues are presented to only evaluate the degree of conservatism from the modeling choices made during the model development phase.

C.3.1 Error in Sampled Values of Drywell Head Bolt Torque Coefficient

Issue

The lower and upper bounds on the uncertainty distribution of torque coefficient K, used to determine the tensile force developed in the drywell head bolts during assembly, were specified incorrectly as 0.029 and 0.57 rather than as 0.050 and 0.00.

Description

This error effectively shifted the sampled variation in head flange leakage area with pressure such that pressures greater than SOARCA estimate were always necessary to initiate leakage. While it was desired to initiate leakage at between 46.87 psid and 109.26 psid (sampled around the SOARCA estimate of 81.88 psid), the error caused leakage to be initiated between 84.63 psid and 143.24 psid.

Impact

It is believed that what was most important to accomplish with respect to the sampling of torque coefficient was accomplished. The sampling allowed the effect of lifting the head flange earlier or later to be investigated. That the flange never lifted as early as desired and that it didn't lift in some calculations until later than desired seems less important than that the effect due to the flange lifting relatively early or relatively late was investigated.

C.3.2 Miss Ordering of Sampled Values of Fuel Failure Criterion

Issue

The three discrete sampling possibilities of fuel failure criterion were not defined to the statistics analysis in monotonic order.

Description

The sampled parameter of fuel failure criterion (FFC) had three possible outcomes. One of the outcomes (Outcome 1) was the SOARCA estimate time-at-temperature relationship for the collapse of fully oxidized fuel rods. Another of the outcomes (Outcome 2) was the SOARCA estimate relationship altered to cause earlier collapse. The remaining outcome (Outcome 3) was the SOARCA estimate altered to cause later collapse. To best analyze FFC for monotonic influences, the outcomes should have been defined to the statistics analysis in the order Outcome 2, Outcome 1, and Outcome 3. They were instead defined in the order Outcome 1, Outcome 2, and Outcome 3.

Impact

The significance of the miss ordering of FFC outcomes was investigated by righting the order and seeing if the statistical importance of FFC changed significantly with respect to the amount of cesium released to the environment in the Replicate 1 set of calculations. It did not suggest that the miss ordering was not important to the statistical analysis as a whole.

An additional analysis into the significance of FFC ordering on the LCF risk parameters for the 10-mile and 20-mile circular areas using the LNT dose-response model was conducted for all three replicates (CAP17). This analysis showed only a slight increase in the FFC contribution. The overall order of LCF risk parametric significance did not change.

APPENDIX D

PEER REVIEW/ACRS COMMENT RESOLUTION REPORT

Peer Review Comment Resolution Report

Uncertainty Analysis Plan

The purpose of this report is to provide the Peer Review Committee with the State-of-the-Art Reactor Consequence Analysis (SOARCA) team's resolution of each written peer review comment related to the uncertainty analysis (UA) plan in the December 22, 2010 and April 9, 2010 memoranda. This report is organized first by individual peer reviewers for comments in the December 22, 2010 memorandum, and then concludes with the joint comments in the April 9, 2010 Peer Review Guidance Memorandum (see the Contents below). Comments are extracted directly from the source documents with no changes. The report sections that are identified in the resolutions refer to the revised UA plan, as it is captured in Sections 1-4 of the draft NUREG/CR report that will document the UA.

Contents

Bernard Clément.....	D-2
Jeff Gabor.....	D-6
Robert Henry	D-9
David Leaver.....	D-10
Kevin O’Kula	D-17
John Stevenson	D-23
Karen Vierow	D-25
Jacquelyn Yanch.....	D-28
Peer Review Guidance Memo dated April 9, 2010.....	D-30
Advisory Committee on Reactor Safeguards.....	D-32

Note: Mr. Ken Canavan, Mr. Roger Kowieski, and Mr. Bruce Mrowca, did not provide individual written comments on the Uncertainty Analysis in the December 22, 2010 memorandum.

BERNARD CLÉMENT

**December 22, 2010 SOARCA Peer Review Memorandum, “Guidance on the SOARCA
Uncertainty Analysis Plan”**

1. Page 2

Comment:

General: As explained, the effort is limited due to time and resource constraints. This is understandable but will induce limitations in the conclusions that will be drawn from the exercise. It can be expected that the applicability of the methodology is, if not fully demonstrated, at least illustrated on the specific example that is treated. Concerning the specific sequence that will be treated it is expected that the exercise will show the effect of the most influential parameters. It will however not be possible to extrapolate in general the conclusions to other accidental sequences and other reactors.

The exercise is mainly based on a statistical treatment of the propagation of uncertainties of models parameters. This is probably the best way to proceed when using complex simulation tools such as MELCOR and MACCS. It should however be recognized that some epistemic uncertainties are not taken into account with this method, especially when some physical phenomena of potential importance are not modeled. When this is known, it should be clearly stated. An example is given in page 43 for CH3I.

Resolution:

The October 2010 draft UA plan did not fully document the technical basis for all chosen parameters. The documentation has been improved and Section 4 of the draft UA NUREG/CR report has been expanded to include the technical basis and justification of the parameters and distributions selected for this SOARCA UA study. The final SOARCA UA NUREG/CR report will contain a thorough discussion of the quantification of the uncertainty in the consequence results as driven by the uncertainty in the selected input parameters.

The scope of this uncertainty analysis indeed does not include all uncertainties. The effort is focused on capturing the effects of uncertainties in MELCOR and MACCS input parameters. Though some model uncertainties may be partially captured through surrogate input parameters, in general, the epistemic model uncertainties are not treated.

2. Page 2

Comment:

The Zr melt breakout temperature is certainly an important uncertain parameter. Its influence will be evaluated for the chosen scenario but it should be kept in mind that the relative influence of this parameter should largely differ for other scenarios.

Resolution:

Based on prior work on in-vessel melt progression, this parameter is expected to be among the more important uncertain parameters. The lower bound value is the zircaloy melting temperature, while the upper bound value is based on likely rod collapse temperature occurring within 15 minutes. The mode is the value used in the SOARCA deterministic analysis. The final SOARCA UA NUREG/CR report will contain a thorough discussion of the quantification of the uncertainty in the consequence results as driven by the uncertainty in the selected input parameters. See also response 4 below.

3. Page 2**Comment:**

Molten clad drainage rate: worthwhile to study, but probably less important than Zr melt breakout temperature.

Resolution:

The molten clad drainage rate has an impact on blockage on Top of Active Fuel melt to Bottom of Active fuel affecting material relocation. The Zr melt breakout can provide a surrogate for this parameter. Both have been included in the SOARCA uncertainty study; the Zr melt breakout temperature was added. See section 4.1.2 of the draft NUREG/CR.

4. Page 2**Comment:**

Fuel failure criterion is also an important parameter. There is certainly some correlation between its influence and the influence of Zr melt breakout temperature. The importance of fuel-cladding interactions will depend on the latter and in turn affect the temperature and time at which there will be transition from rod-like geometry to debris. A kind of correlation between the probability density functions of these parameters could in principle be established by looking at the results of MELCOR analyses of some experiments such as for instance Phebus FP. If this has not already been done, it should however be recognized that it would require quite a lot of work probably not manageable by the Project.

Resolution:

Fuel failure criterion represents complex phenomena and work has not been done in determining uncertainties within this parameter. Insights from the hydrogen uncertainty analysis completed in 2010 provide the principle basis for selecting Zr breakout temperature and clad drain rate as the two "surrogate" parameters for most in-vessel damage progression parameters.

The following discussion was added in the draft UA NUREG/CR report: "MELCOR lacks a deterministic model for evaluating fuel mechanical response to the effects of clad oxidation, material interactions (i.e., eutectic formation), zircaloy melting, fuel swelling and other processes that occur at very high temperatures. In lieu of detailed models in this area, a simple temperature-based criterion is used to define the threshold beyond which normal ("intact") fuel

rod geometry can no longer be maintained, and the core materials at a particular location collapse into particulate debris. The temperature-based criterion rolls up uncertainties in numerous physico-chemical processes that affect fuel rod integrity. The "time-at-temperature" criterion is the time endurance of the upright, cylindrical configuration of fuel rod bundles which decreases with increasing temperature. A temperature-based 'cumulative damage' criterion is used in the MELCOR model to define the remaining lifetime of normal fuel rod geometry (Table 4.1-2). The alternative functions represent shifts in temperature of +/- 100 K and fuel endurance times of +/- factor of 2.0 (Figure 4.1-9, Figure 4.1-10 and Table 4.1-3).

5. Page 2

Comment:

The wording about hydrogen ignition criteria is unclear as it is said both "no consideration currently given to possibility of the absence of an ignition source" and "accumulation of H₂ due to the absence of ignition source is credible".

Resolution:

Section 4.1.4 of the draft UA NUREG/CR report was updated with an initial attempt to clarify these points and to include a detailed discussion of most likely ignition sources with justification for the uncertain distribution. This section will likely be updated further to provide additional clarification.

6. Page 2

Comment:

Concerning chemical forms of iodine and cesium, the relative probability of the five different combinations is not justified. Concerning the fraction of gaseous iodine (that can be considered as I₂ as proposed) the value recommended by NUREG-1465, that is supposed to be best-estimate is 0.05. Unless there are good arguments, there should be the central value and not the upper bound. Concerning cesium, the partition between CsOH, CsI and Cs₂MoO₄ might have an impact on releases of both cesium and iodine. It is recommended to wait for the first results of the study to decide if other partitions (increased number of combinations) would be useful.

Resolution:

The SOARCA team reviewed NUREG-1465¹ recommendations; however, NUREG-1465 is not considered the current 'best estimate' source for iodine and cesium chemical forms. PHEBUS experimental results have been reviewed and incorporated instead. The gaseous iodine fractions in Section 4.1.5 of the draft UA NUREG/CR report have been updated to reflect PHEBUS experimental results and provide justification for each fraction. These are summarized in Table 4.1-7 (formerly Table 4.1-5 in the October 2010 plan).

¹ NUREG-1465 (1995) is under review and a proposal for revision is being considered.

7. Page 3

Comment:

Concerning the dynamic and agglomeration shape factors, not only the hygroscopic effects will cause the particles to tend towards being spherical but also the agglomeration processes (see e.g. M.P. Kissane: On the nature of aerosols produced during a severe accident of a water-cooled nuclear reactor, Nuclear Engineering and Design 238 (2008) 2792-2800).

Resolution:

The SOARCA team has updated the technical basis to include this reference and ensure the distribution is skewed towards spherical. The following text was added Section 4.1.6 of the draft UA NUREG/CR report: "For this work, it is assumed that hygroscopic effects during the accident sequence will induce some condensation of moisture on the aerosol particles causing the particles to tend towards being spherical and limit the degree of non-spherical shapes (i.e., 1.0 which is a perfectly spherical aerosol particle). Thus a beta distribution which produces a distribution that is biased towards 1.0 was selected. This specification expresses the belief that the shape factors lie closer to the range of 1.0 to 3.0 which diminishes the likelihood of having values approaching 5.0 (See Figure 4.1-18 and Table 4.1-8). The lower bound of 1.0 represents an aerosol particle having a perfectly spherical shape. The upper bound of 5.0 represents chains of particles which appear to be atypical during severe accident conditions (Ref. 77).

JEFF GABOR

December 22, 2010 SOARCA Peer Review Memorandum

8. Page 4

Comment:

Technical justification needs to be documented for the selection of each uncertainty parameter. Included should be a discussion of the best estimate value along with the basis for the range of uncertainty and the appropriate distribution. Technical references should be included for each parameter.

Resolution:

The October 2010 draft UA plan did not fully document the technical basis for all chosen parameters. The documentation has been improved and Section 4 of the draft UA NUREG/CR report has been expanded to include the technical basis and justification of the parameters and distributions selected for this SOARCA UA study, including identification of the SOARCA estimate values and technical references.

9. Page 4

Comment:

Many of the MELCOR uncertain parameters depend on one another. Correlations between various parameters should be developed to represent these dependencies.

Resolution:

As suggested by peer reviewers during the October 2010 meeting, the SOARCA team carefully deliberated on which MELCOR parameters should be correlated (MACCS parameter correlations were already included in the October 2010 draft UA plan). In addition, since the October 2010 meeting, the SOARCA team developed the capability to correlate input parameters in MELCOR. Appropriate correlations were identified and are now included for MELCOR parameters. Section 4 of the draft NUREG/CR has been updated to identify the correlated parameters.

10. Page 4

Comment:

- (1) In-core failures of instrument tubes have been raised by Dr. Henry and need to be addressed in the SOARCA documentation.
- (2) If uncertainties exist as to the potential for enhanced radionuclide release, these should be included in the uncertainty analysis.

Resolution:

The MELCOR model does not currently have the capability to consider the in-core failures of instrument tubes raised by Dr. Henry. However, the SOARCA team is currently further investigating these topics raised by Dr. Henry and the results will be documented in the Peach Bottom integrated analyses volume of the SOARCA reports (NUREG/CR-7110, Volume 1). In addition, a preview of insights from analyses to date was shared with peer reviewers at the December 2011 meeting, including the insight that the potential bypass pathway is not expected to be a concern based on the extremely low frequency of the vulnerability being present (i.e., low percentage of time that a bypass pathway is possible). We do not plan to further study this issue through inclusion of parameters in this UA, though the topic merits further consideration in future studies.

11. Page 4**Comment:**

The potential for Main Steam Line creep failure is not being considered as an uncertain parameter. The MSL rupture area for such a failure would likely be large and probably does not need to be evaluated as an uncertain parameter. I recommend that this uncertain parameter be replaced with a parameter that more directly relates to MSL creep failure.

Resolution:

The SOARCA team re-evaluated this phenomenon in regards to this comment. Our rationale is that the uncertainty in the parameters affecting the calculated potential for creep can be neglected in this assessment because prior experience (through sensitivity analyses) suggests the Larson-Miller (L-M) damage index transitions from zero to values well above unity within a very short time. The L-M parameter is not likely to be very sensitive because once the MSL enters creep conditions, the progression is very fast from 0 to 1.

On the other hand, we consider the area of the rupture as an important uncertain parameter because it relates to the more important factor of how we model flow to and through the MSL, and associated heat transfer to wall piping. And after the October 2010 and December 2011 peer review meetings and feedback, we have re-assessed the distribution for the MSL rupture area. It is now skewed heavily to large open areas, with only a small residual probability (0.01) of an open area less than 10%.

12. Page 4**Comment:**

Failure of both sets of railroad doors is included in the uncertainty, however, failure of the blowout panels at the top of the refueling floor are not included. Given the complexity of how the reactor building will respond to a containment failure, it is recommend that the RR door failure parameter be replaced with a more simplified parameter representing the potential decontamination factor for the entire reactor building.

Resolution:

In the MELCOR code the decontamination factor is a calculated result and not a parameter which can be given an uncertain value. However, as part of the overall integrated model, MELCOR calculates aerosol transport and retention in the reactor building using mechanistic models that account for the effects of changes in flow rates, flow paths and changing properties of deposition surfaces. Major uncertainties tend to lie in boundary conditions --- such as the criteria used to determine whether doors open and create new transport pathways.

Past calculations (NUREG/CR-7110, Vol. 1) have shown that hydrogen combustion leads to a nearly immediate opening of the refueling bay blow out panels and the railroad doorway at grade level. Blow-out panels into the turbine building and personnel access doorways out of the reactor building might also open. However, the dominant flow path for fission products to the environment is through the refueling bay blowout panels. A stable flow of air is calculated to enter the building through the open railroad doorway, rise upward through the open equipment hatches from grade level to the refueling bay and exit the building to the environment through the open blow-out panels. Failing the railroad doors will cause a 'chimney effect' and reduce the residence time for radionuclides within the reactor building. A smaller railroad door open area is credible and might reduce the airflow and increase residence time.

13. Page 4**Comment:**

The success and timing of operator actions should also be considered in the uncertainty analysis. These actions include opening of the SRVs earlier in the BWR event along with initial level control using RCIC.

Resolution:

As mentioned in the SOARCA documentation, a comprehensive human reliability assessment (HRA) was not conducted for operator actions. In the absence of an HRA, it is difficult to assign distributions to the timing of these two operator actions. Rather than include a distribution of times for these two operator actions in the integrated uncertainty analysis, we plan to explore the sensitivity of results to the timing of these two actions in a separate sensitivity study, planned to be documented in the UA NUREG/CR report. See also resolution 17 below.

ROBERT HENRY

December 22, 2010 SOARCA Peer Review Memorandum

14. Page 5

Comment:

My comments on the uncertainty study closely parallel my comments related to the information that we have yet to receive to quality the code.

(1) The uncertainty study only has substance when the variations in the mechanistic models are based on the uncertainty variations that have been derived by comparing the mechanistic models with various experiments. Without this, there is no technical basis for the variations that are used in the evaluations.

(2) In the framework of the uncertainty study that was sent to us, there were a number of parameters that were used to represent variations in the accident progression, but to date, no technical basis has been provided for any of these. Out of frustration, I Googled and found a presentation entitled "MELCOR Code Development Status, Code Assessment and QA". Under the heading of MELCOR 2.1 Assessment Matrix they discuss the TMI-2 accident as well as the following experiments: LOFT-FP2, PHEBUS, IIST, BACCHUS, LHF, OLHF, VERCORS, CVTR, HDR, NUPEC, Marviken, CSTF, PANDA, ABCOVE, SUPRA, and DEMONA. We have requested information relating to how the model parameters are varied as a function of these, or other benchmarks, if at all. More to the point, we have asked for these so that we can understand how the uncertainty variations are being quantified. The MELCOR best practices document that was given to the committee identifies MELCOR 1.8.6 as the code used to assess radiological releases to the environment. The assessment matrix that lists the experiments given above identifies MELCOR 2.1. Is this the difference that we are confronting? Have these benchmarks not been performed with 1.8.6 but are available for version 2.1? The committee somehow must be able to develop an appreciation of the extent of benchmarks that exist for the code that the NRC is using in this evaluation. Without the identification of the technical basis, neither the "best estimate" calculations nor the "uncertainty analysis" have any basis.

Resolution:

The October 2010 draft UA plan did not fully document the technical basis for all chosen parameters. The documentation has been improved and Section 4 of the draft UA NUREG/CR report has been expanded to include the technical basis and justification of the parameters and distributions selected for this SOARCA UA study. In addition:

(1) Some of the uncertainty variations are based directly on experimental results, for example, the PHEBUS Iodine distribution results. Other uncertainty distributions are based on expert judgment that is informed by knowledge of the relevant experiments and how they relate to MELCOR modeling. Section 4.0, introductory material has been added to the Draft NUREG/CR to clarify this.

(2) Many of the experiments listed and TMI-2 have been compared with MELCOR. The resolutions to comments 34, 35, 38, and 47 in the Peer Review Comment Resolution Report (available at NRC ADAMS number ML11118A0620) for the SOARCA estimate analysis include relevant discussions. In addition, the SOARCA team made a detailed presentation at the December 2011 peer review meeting on MELCOR validation and benchmarking activities to date.

DAVID LEAVER

December 22, 2010 SOARCA Peer Review Memorandum

15. Page 8

Comment:

Section 4 of the first report (UA Plan) notes that for some uncertain parameters there is a limited or in some cases no technical basis documented. This must be addressed in the final uncertainty report, even if the technical basis is qualitative and subjective. Some examples are discussed below. The basis should address the upper and lower bounds and the nature of the distribution.

Resolution:

The October 2010 draft UA plan did not fully document the technical basis for all chosen parameters. The documentation has been improved and Section 4 of the draft UA NUREG/CR report has been expanded to include the technical basis and justification of the parameters and distributions selected for this SOARCA UA study.

16. Page 8

Comment:

The uncertainty analysis methodology is attempting to address uncertainty in an integrated manner within the context of the core damage progression model and the consequence analysis. This is a worthwhile approach and it is innovative, but has the problem that dependencies among uncertain parameters may be hard to discern in some cases. The approach differs from traditional PRA-based approaches to uncertainty analysis which apply the Level 1 and Level 2 logic models, split fractions, and the like to identify these dependencies. In light of this, it is suggested that the SOARCA project consider use of traditional sensitivity studies as a supplement and sanity check for the integrated uncertainty analysis and as a way to provide insight on potential dependencies.

Resolution:

As suggested by peer reviewers during the October 2010 meeting, the SOARCA team carefully deliberated on which MELCOR parameters are dependent and should be correlated (MACCS parameter correlations were already included in the October 2010 draft UA plan). In addition, since the October 2010 meeting, the SOARCA team developed the capability to correlate input parameters in MELCOR. Appropriate correlations were identified and are now included for MELCOR parameters. Section 4.0 of the draft NUREG/CR has been updated to identify the correlated parameters. As part of the SOARCA study, numerous sensitivity studies were already completed. These sensitivity studies have informed the selection of important parameters and definition of their distributions for this UA study. Additional selected separate sensitivity studies will be considered and used as necessary to provide insight. For example, sensitivity of results to the timing of key operator actions is one study that is planned separate from the integrated analysis (see response 18).

17. Page 8

Comment:

Pg. 41 of Appendix A, "Peach Bottom Integrated Analysis," indicates that station blackout leads to loss of room cooling for the RCIC and HPCI corner rooms, and that the operators are directed to block open doors to these rooms to facilitate cross ventilation so as to slow the rate of room heat up. These actions were assumed to successfully prevent system isolation from high temperature for the maximum period of 4 hours of system operation. Thus there are two uncertain aspects to loss of room cooling: (1) the likelihood of successful operator action to block open the room doors; and (2) the likelihood that these actions prevent system isolation due to high temperature (note that apparently no modeling has been performed on the room heat up). Based on this, loss of room cooling should be considered as an uncertain parameter for the LTSBO uncertainty analysis.

Resolution:

The operator action to block open doors is directed by the relevant procedure for the LTSBO conditions, so it is expected that the operators would perform this action. From Section 5.1 of NUREG/CR-7110 Volume 1: "One consequence of station blackout is the loss of cooling to the RCIC and HPCI corner rooms. Heat losses from system piping and equipment to the room atmosphere would cause these areas to overheat. In such an event, step H 5 of Special Event Procedure SE 11 is applicable. It directs operators to block open doors to these rooms and facilitate cross ventilation, which would slow the rate of room heat up. These actions are assumed to successfully prevent system isolation from high room temperature for the entire period of system operation². Step H-6 of the procedure directs operators to defeat high torus temperature isolation signals for HPCI and RCIC (if operating). MELCOR calculations presented in Section 5.1.1 indicate these signals would not be received before the station batteries exhaust; therefore, these actions are not important for the LTSBO scenario."

While the loss of room cooling is not explicitly modeled or captured as a parameter in this UA study, battery duration, which is included as an uncertain parameter, is a good surrogate to capture the potential effect.

18. Page 9

Comment:

For the unmitigated LTSBO sequence, operator actions credited are opening one SRV (1 hour) and taking manual control of RCIC (2 hours) and as described on page 43 of Appendix A maintaining water level at 5 in to 35 in (i.e., 16 ft above TAF). These actions are uncertain (or rather, the time at which these actions are taken is uncertain) and thus should be included on the list of uncertain parameters.

² Heat loss from RCIC (or HPCI) systems to their enclosure corner rooms is not explicitly represented in the MELCOR model.

Resolution:

As mentioned in the SOARCA documentation, a comprehensive human reliability assessment (HRA) was not conducted for operator actions. In the absence of an HRA, it is difficult to assign distributions to the timing of these two operator actions. Rather than include a distribution of times for these two operator actions in the integrated uncertainty analysis, we plan to explore the sensitivity of results to the timing of these two actions in a separate sensitivity study, planned to be documented in the UA NUREG/CR report.

19. Page 9**Comment:**

In the paragraph on Main steam line creep rupture area, should the uncertainty in main steam line temperature be considered?

Resolution:

The main steam line structure temperature is calculated by the model and hence is not an uncertain input parameter. We consider the area of the rupture as an important uncertainty parameter. The rupture area is important because it affects containment response to MSL failure. Large areas generate relatively large pressure loads on the containment, and offer an opportunity for advancing the time of containment failure. The proposed SOARCA UA study considers the area of the rupture as an important uncertainty parameter because it relates to the more important factor of how we model flow to and through the MSL, and associated heat transfer to wall piping. After the October 2010 and December 2011 peer review meetings and feedback, we have re-assessed the distribution for the MSL rupture area. It is now skewed heavily to large open areas, with only a small residual probability (0.01) of an open area less than 10%.

In addition, uncertainty in the parameters affecting the calculated potential for creep is neglected in this assessment because prior experience (through sensitivity analyses) suggests the L-M damage index transitions from zero to values well above unity within a very short time. The L-M parameter is not likely to be very sensitive because once the MSL enters creep conditions, the progression is very fast from 0 to 1.

20. Page 9**Comment:**

Fuel failure criterion is an example of a parameter where there is lack of a basis for the characterization of the uncertainty (see general comment 1). The uncertainty proposed is not unreasonable, but some kind of basis is required, even if it is simply a qualitative discussion of how time at temperature can affect the various phenomena that impact fuel mechanical response as the fuel heats up.

Resolution:

A technical basis has been added to Section 4.1.2 of the draft NUREG/CR report. See also response 4 above.

21. Page 9

Comment:

Radial debris relocation time constants is another example of a parameter where there is no basis for the characterization of uncertainty. Also, there are two incomplete sentences at the bottom of this paragraph.

Resolution:

A technical basis has been added to Section 4.1.2 of the draft NUREG/CR report for this parameter and the editorial changes have been made.

The relocation time constant is meant to capture the rate of radial debris movement to the center and thus determine the time the debris moves to the lower plenum. This movement to the lower plenum then determines the time at which the lower plenum will fail. The distributions are based on expert judgment but are not based on TMI data since no data from TMI exists for radial debris relocation distribution. It is one of the few parameters to which a user has access to influence large scale movement and influences axial debris relocation as well. The time scale is a surrogate for the uncertainty in large scale movement. The range covers molten to solidus of core melt.

22. Page 9

Comment:

Why is Zr oxidation fraction and amount of H₂ generation not an uncertain parameter?

Resolution:

Zr oxidation fraction is a calculated result of in-vessel core damage progression and is not an input parameter; it is principally a result of the Zr melt breakout temperature.

H₂ generation is directly related to ZrO₂ production and thus is also result and not an input parameter. Both results are saved in the UA analysis and will be available for investigation and potential inclusion in the final NUREG/CR discussion of the results.

23. Page 9

Comment:

There should be a basis for the fraction of I₂. There is a lot of R&D going on regarding iodine chemistry that could be consulted.

Resolution:

The SOARCA team reviewed NUREG-1465³ recommendations; however, NUREG-1465 is not considered the current 'best estimate' source for iodine and cesium chemical forms. PHEBUS experimental results have been reviewed and incorporated instead. The gaseous iodine fractions in Section 4.1.5 of the draft UA NUREG/CR report have been updated to reflect PHEBUS experimental results and provide justification for each fraction. These are summarized in Table 4.1-7 (formerly Table 4.1-5 in the October 2010 plan).

24. Page 9**Comment:**

Indication of the MACCS values would be useful for comparison with Tables 4.2-3 and 4.2-4.

Resolution:

Tables 4.2-3 and 4.2-4 list the distributions selected for the MACCS shielding and inhalation and Early Health Effects parameters for this SOARCA UA study, respectively.

25. Page 9**Comment:**

What uncertainty is Figure 4.2-10 reflecting?

Table 4.2-10: dose threshold for what?

Resolution:

Figure 4.2-10 (in the October 2010 draft plan) is the uncertainty in the dose threshold parameter used in the MACCS model calculations for latent cancer fatality (LCF) risk. The dose threshold represents the threshold for a linear-threshold model (versus a LNT model), so that the LCF risk would be calculated only for those members of the population whose total dose exceeded the dose threshold. Note that this parameter has been removed in the updated uncertainty analysis plan and will no longer be sampled. Instead, the uncertainty analysis will use the same three dose models as the SOARCA study: LNT, "US background average threshold," and "Health Physics Society" models. The exploration of this model uncertainty will not be integrated with the other UA parameters, i.e., these three models will not be sampled along with the MACCS parameters. Rather, the three model results will be reported in parallel.

³ NUREG-1465 (1995) is under review and a proposal for revision is being considered.

26. Page 9

Comment:

The SOARCA report has 6 cohorts whereas Table 4.2-8 has 5. Perhaps Cohort 6 (non-evacuating public) was left off, but is there not some likelihood that they will actually evacuate with some delay?

Resolution:

Cohort 6 (non-evacuating public) is ultimately relocated, but by definition does not evacuate. Therefore we do not sample this cohort for evacuation.

27. Pages 8-9

Editorial Comments:

- (1) There are significant editorial errors in the first report (UA Plan).
- (2) Figure 4.1-7 has the wrong title.
- (3) The abscissa of Figure 4.1-15 should be labeled (H₂ mole fraction?).

Resolution:

- (1). The plan has been updated and incorporated within the draft NUREG/CR report that will document this SOARCA UA study and results. This initial draft has undergone a single round of technical editing with formal technical editing and review planned prior to the final release.
- (2). The Figure 4.1-7 caption is, "Cumulative distribution function of safety relief valve open area fraction after thermal seizure." It has been corrected and is included in the latest draft NUREG/CR report of this SOARCA UA Study.
- (3). Yes. The abscissa is hydrogen mole fraction for ignition. The caption is updated in the draft NUREG/CR report.

28. Pages 9-10

Comments on the Draft NUREG/CR Report, "Evaluation of Distributions Representing Important Non-Site-Specific Parameters in Off-Site Consequences":

- (1) The spread of dispersion estimates in Figures 2.47 through 2.54 are generally 1.5 to 2 orders of magnitude, and X/Q generally goes as $1/\sigma_y\sigma_z$. This spread is based on the 1995 – 1998 expert data cited in the report (references 1 to 6). This spread seems too high based on what was learned from the more recent comparisons of MACCS predicted X/Q with the LLNL detailed model (maybe a factor of 2 – 3 different). Why not adjust the older, subjective expert data to reflect the more rigorous and recent LLNL comparison?
- (2) To provide a comparison and sanity check on the correlations between dry deposition and wet deposition data, the deterministic particle velocity vs. particle size from the MACCS model should be displayed.
- (3) There should be some discussion and possibly adjustment regarding the fact that ICRP indicates $\sim 5 \times 10^{-4}$ fatality risk vs. $\sim 1 \times 10^{-3}$ for the 0.5 quantile in Table 5.1.
- (4) On page 89, what is the exposure time associated with the 100 Gy/hr?
- (5) Figure 6.1 is puzzling. Expert A has 0.0 – 0.05 quantile threshold dose of about 80 rem and Expert I has ~ 300 rem (seems more like it to me). How can these two "experts" not be at least somewhat close on the 0.0 – 0.05 quantile for threshold dose if the problem was well-posed and they are addressing the same problem? And how is it possible for ~ 0.8 Sv (80 rem) to cause an early fatality? Would this be for a non-healthy person?"

Resolution:

It should be noted that these comments, while relevant to the SOARCA UA study, are not specific to the October 2010 draft plan reviewed by the peer review team. Responses to these comments on the Draft NUREG/CR Report, "Evaluation of Distributions Representing Important Non-Site-Specific Parameters in Off-Site Consequences" are included herein for completeness.

- (1). The dispersion distributions have been updated, as documented in Section 4.2.6.
- (2). Through discussion with the peer reviewer, this comment was clarified to mean that the SOARCA estimate values should be displayed on the graphs showing the distribution. The graphs in Section 4.2.1 and Section 4.2.2 show the SOARCA estimate values.
- (3). The $\sim 5 \times 10^{-4}$ latent cancer fatality risk is per *rem*, which corresponds to $\sim 5 \times 10^{-2}$ per Sievert. The mode of the expert distributions is $\sim 7 \times 10^{-2}$ and the mean is $\sim 1 \times 10^{-1}$, which are a better match to the $\sim 5 \times 10^{-2}$ per Sievert.
- (4). The specified radiation rate is 100 Gy/hr. Table 6.1 provides a set of doses for thresholds, LD50s, etc. The dose divided by the dose rate would provide the exposure period for each of the doses in the table. The following errata in Table 6.1 will be fixed: the units were listed as Sv when they should have been Gy.
- (5). There is indeed a large difference of opinion between Expert A and Expert I for this parameter. We are unsure of the basis for this difference. For the purposes of this SOARCA UA, the early health effects parameters are not expected to be exercised. In all of the demonstration and test cases run to date for the PB LTSBO, early health effects have not been observed. We will revisit this issue if early health effects appear in the SOARCA UA.

KEVIN O’KULA
December 22, 2010 SOARCA Peer Review Memorandum

29. Page 11

Comment:

The set of consequence (MACCS analysis) uncertain parameters is appropriate considering their respective importance to the overall outcome. Of the set of eleven parameters to be included, i.e., dispersion parameters (σ_y and σ_z), washout model linear coefficient, *deposition velocity*, shielding parameters, early health effects, normal and hotspot relocation, evacuation delay and speed, *ground shine*, *habitability*, the three italicized parameters (deposition velocity, ground shine, and habitability) are expected to have large impacts (at least to this reviewer).

Resolution:

The updated UA plan continues to include 10 of the 11 parameters identified in the October 2010 draft plan. The habitability criterion is no longer included in the updated list of parameters. However, insights on the influence of the habitability criterion have been obtained through the UA demonstration and test cases that have been run, most recently with a sizable sample size of 263. We plan to include a discussion of the influence of the habitability criterion in an appendix to the UA NUREG/CR report, with a summary in the results section. The reason for removing it from the list of parameters is that the habitability criterion is a policy decision made by individual states, and hence may not be fully appropriate to make assumptions about what that decision may be as part of our study. This issue was discussed at the December 2012 peer review meeting.

30. Page 11

Comment:

Selection of Peach Bottom Unmitigated Long-Term Station Blackout (PB LTSBO) – This scenario is a reasonable choice to exercise appropriate parts of the source term – consequence methodology.

Resolution:

The updated UA plan continues to use the PB unmitigated LTSBO as the chosen scenario.

31. Page 11

Comment:

Bypassing a PIRT Process - Presentations and discussions made in March, and again in the October meetings noted that a PIRT process was not in the scope of work and subsequently, “a limited set of key parameters and their distributions was compiled that relies heavily on the best available data and expert judgment.” Given that the SOARCA uncertainty analysis will extend into the first half of CY2011, it is recommended that this position be revisited. In the long run, a targeted PIRT process would be a useful exercise to preclude inadvertent omission of parameters from the uncertainty analysis that later are deemed to be important. The PIRT process could be done in a short-term, expedited manner for both the source term phase and the consequence analysis phase, and documented as appendices to the final report.

Resolution:

The SOARCA project's subject matter experts have invested additional thought since the draft October 2010 UA plan and peer review meeting. While a formal PIRT process was not used, the SOARCA models and results are supported by years of extensive study. The detailed SOARCA Peach Bottom model was the basis of the expert judgment from informed subject matter experts who identified the key parameters and distributions for this UA study. In addition, the SOARCA team was fortunate to have the independent review and advice of the SOARCA peer review committee through the meetings and memoranda in 2010, and limited review by non-SOARCA staff at SNL and NRC who have specialized expertise in particular subject areas. Thus, the SOARCA team believes the UA approach is sound, without an exhaustive PIRT, given this UA study's focus on the uncertainty in the SOARCA estimate calculation. Additional rationale has been added to the introductory material of section 4.0 of the draft NUREG/CR report outlining our approach and identification of the parameters for study in the SOARCA UA, within the scope of the study to investigate the key parameters that most influence the uncertainty within the SOARCA estimate results.

32. Page 12

Comment:

Model Uncertainty – The uncertainty analysis as described by the SNL-NRC SOARCA project team is a parameter uncertainty analysis. It would be very informative to explore the uncertainty of several model options, or whether refinements in a base model helped reduce uncertainty in the overall analysis. NUREG-1855, Volume 1, and Regulatory Guide 1.174 are useful approaches to guide these types of analysis. The two categories that are of particular interest are:

Refinement of Polar Grid in ATMOS –The previous polar coordinate grid model in MACCS (Version 1.13.1) allowed 16 sectors. The new model in WinMACCS (V3.5.0 beta) uses 64, based on a suggestion made during the first round of SOARCA meetings in Albuquerque several years ago. It would be a valuable insight to understand if this helped reduce (1) the mean result; and (2) reduced uncertainty about the 50th percentile.

Latent health effect models – Four approaches have been applied in the SOARCA analysis for calculation of latent cancer fatality risk, LNT, ICRP 104 (truncation of 10 mrem/y), U.S. Background Average (truncation of 620 mrem/y), and the HPS (explanations provided in the SNL-NRC reports). It would be a significant milestone if a limited model uncertainty could be explored for LCF risk for both plants.

Resolution:

Model sensitivity analyses or 'one-off' calculations of the type you propose can be very informative and will be explored as part of the SOARCA UA, though the scope is not defined yet.

We currently do not have plans to further explore refinement of the polar grid in ATMOS, as comparisons completed as part of the SOARCA study showed that the refinement to 64 sectors did not make much difference to the mean result for latent health effects. This insight will be noted in the UA report.

As discussed with the peer review committee at the December 2011 meeting, the team's updated UA approach includes reporting the results for the three dose models that are used in the SOARCA study: LNT, "US background average threshold," and "Health Physics Society" models. The exploration of this model uncertainty will not be integrated with the other UA parameters, i.e., these three models will not be sampled along with the MACCS parameters. Rather, the three model results will be reported in parallel. This approach replaces the sampling of a dose threshold, which was a proposed parameter in the October 2010 draft UA plan.

33. Page 12

Comment:

Clarity of Discussion in Aleatory and Epistemic Uncertainty Results – This discussion is very good and needs to be repeated in summary at the end of the uncertainty analysis results. In addition, it is imperative that the study note an improvement in uncertainty with respect to results over earlier work, such as the Sandia Siting Study, and that is presented clearly without being hidden. If a comparison of overall uncertainty is not feasible, perhaps several important uncertain parameters can be compared in to what they were previously, then it would be key that these same parameters be compared.

Related Comment:

With the work that has been presented to the Peer Review Group since 2009, and progress in research and analytical methods since the Sandia Siting Study, the improvement in uncertainty in severe accident consequences should be as important as the reduction in the quantitative mean values obtained for specific risk metrics. The clarity of this message is important and must be made apparent in the final uncertainty analysis report.

Resolution:

The discussion of the UA results will summarize the concepts of aleatory and epistemic uncertainty with illustrations directly from the SOARCA UA results. A direct comparison to the Sandia Siting Study results would not be a feasible comparison because the same kind of aleatory and epistemic uncertainties were not included; although weather uncertainty was included. Discussion has been added in this draft NUREG/CR report comparing results to an earlier MACCS uncertainty analysis that was more similar to the scope of the current analysis.

34. Page 7

Comment:

Definition of Uncertainty Analysis and Sensitivity Analysis – Section 3.2 of the Uncertainty Analysis plan contains two definitions, i.e., that of uncertainty analysis and sensitivity analysis, that ought to be rewritten in simpler English for the final report. Although this content was in the draft uncertainty analysis plan, there is still too much importance of this section to leave as it stands. The sentence reads: "Closely associated with the characterization of epistemic uncertainty provided by the probability space corresponding to EN3 and the answering of Question Q4 are the concepts of uncertainty analysis and sensitivity analysis, where uncertainty analysis designates the determination of the epistemic uncertainty in analysis results that derives from epistemic uncertainty in analysis inputs and sensitivity analysis designates the determination of the contribution of the epistemic uncertainty in individual analysis inputs to the epistemic uncertainty in analysis results."

Resolution:

The following clarification text has been added to Section 3.4: “The goal of uncertainty analysis is to determine the uncertainty in an analysis result that derives from the collective uncertainty in analysis inputs. In contrast, the goal of sensitivity analysis is to determine the extent to which the uncertainty in individual analysis inputs contributes to the uncertainty in an analysis result. Intuitively, sensitivity analysis corresponds to decomposing the uncertainty in a result into the fractional contributions of each uncertain input. Commonly used sensitivity analysis procedures include scatterplots, correlation coefficients, partial correlation coefficients, stepwise regression with raw or rank transformed data, and a number of other techniques. General references on uncertainty and sensitivity analysis include [1-6]. Example past uncertainty and sensitivity analyses include studies of the MAEROS component of MELCOR model system for reactor accidents [7; 8] and the MACCS model system for off-site consequences of reactor accidents [9-13].” This draft discussion is likely to be clarified further into simpler English during technical editing prior to publication. Because it is at the same time important to maintain the technical clarity and rigor supporting the mathematical approach, the detailed discussion in Section 3.0 may be moved to an appendix.

35. Page 12**Comment:**

Section 2.4 Description of the Probabilistic Analysis Methodology for SOARCA - This information, while useful, should be published as an appendix in the final report.

Resolution:

The draft NUREG/CR document for the SOARCA UA has been reorganized. The material in question has been partitioned between two new sections, Sections 3.3 and 3.4. Additionally, a summary version is planned to replace the detailed discussion and the detailed discussion will be moved to an appendix.

36. Page 12**Comment:**

Percentile Bounds on Work – The briefing in October from Patrick Mattie noted that 25th/75th percentile bounds would be used on the CCDFs using the bootstrap method. There may have been a simple explanation for this set of bracketing bounds given during the discussion, such as a requirement on the number of simulations, or other limiting factor, but I don’t recall it and the more common set of bounds are 5th and 95th.

Resolution:

A confidence interval will be estimated using bootstrap methods. The validity and quality of the confidence interval depends on the original sample size. If the sample size in consideration is relatively small (as it was in the spring 2010 UA demonstration case) then it could be misleading to estimate a 90% confidence interval. For example, for a sample of size 50, quantiles $q=0.05$ and $q=0.95$ would be estimated by the bottom and top 2 values respectively. If the distribution is skewed and covers a large range, this estimate may not be accurate. Therefore, the confidence interval quantile values that can be supported are based on the sample size and the consideration that a Monte Carlo sample has an accuracy of $1/\sqrt{n}$ where n represents the sample size. The proposed sample size of $n=300$ for this UA, would be sufficient for the 5th and 95th percentile bounds.

37. Page 12-13

Comment:

Table and Figure Discussion – The importance of weather trials in the MACCS sampling methodology is known but inclusion of this term as an uncertainty parameter in Table 2.2-1 is not explained although several comments are made throughout Section 2.2. Please clarify in the final report. Examples of scatterplots, SRCs/PCCs as a function of time, and illustration of failure of a sensitivity analysis are illustrated in Figures 3.2.1, 3.2.2, and 3.2.2, respectively, are provided with little if any explanation. While these are meant to be illustrative in the plan, if they are used in the final report, please include sufficient discussion as to what is being shown in the figure of interest.

Resolution:

We acknowledge these deficiencies in the October 2010 draft, and will be adding explanatory text using the results of this study in the next version of the draft UA NUREG/CR report . These theoretical points will be easier to discuss in the presentation and discussion of UA analysis results, once they are available, in the UA NUREG/CR report.

38. Page 13

Comment:

Version of codes being applied – Mattie's presentation indicated the versions of MELCOR, MELGEN, and MACCS/WinMACCS being applied, but this is not documented consistently in the reports received to date. It is recommended that the final uncertainty analysis reports state directly the codes and versions being applied to support the final uncertainty study.

Resolution:

The final version of the UA NUREG/CR report, Section 3.1, will include the specific codes and versions used in the study, consistent with the codes used in the SOARCA estimate calculations.

Comment:

General Comment on “Evaluation of Distributions Representing Important Non-Site Specific Parameters in Off-Site Consequence Analyses” and Implementation in SOARCA – The manner in which deposition velocities are input for the nine physicochemical groups used in the MACCS Peach Bottom or Surry plant analysis is still unclear. Specifically, the manner in which each of the nine radionuclides groups is associated with a RDPSDIST00X bin and how the median diameter bins would be distributed for a given radionuclide group (example shown in Figure 1). While a brief discussion on this topic was given in the March briefing, this topic remains an issue because this SOARCA study apparently uses information from an updated expert elicitation, “Evaluation of Distributions Representing Important Non-Site-Specific Parameters in Off-Site Consequence Analysis”. Granted larger particle size deposition velocity will be site-independent and behavior should follow Stokes Law, the deposition velocity for smaller aerosol particle size groups (say for $d_p \lesssim 1 \mu\text{m}$) is site-dependent. This is because smaller particles will interact with regional ground cover such as the tree canopy and other vegetation. Consequently, field testing over forested sites typically shows higher deposition velocities compared to those with relatively little surface cover. Admittedly, this issue is perhaps a minor one for the SOARCA study as both sites are in the Eastern U.S. Nonetheless, a discussion on the specifics for implementation of final values of the deposition velocity by radionuclide bin should be provided in the final study as well as in the uncertainty analysis.

Resolution:

The NUREG/CR report discussed, "Evaluation of Distributions Representing Important Non-Site Specific Parameters in Off-Site Consequence Analyses" will be referenced in the UA report as the technical basis for those parameters whose distributions are based on that report. The effect of the surface roughness parameter has been analyzed and presented in NUREG/CR-7110, Volume 1 of the SOARCA report. This analysis addresses effects of regional ground cover and deposition velocities. Furthermore, the uncertainties in deposition velocity and dispersion, which are included in this uncertainty analysis, should capture the overall influence of surface roughness on the results.

JOHN STEVENSON

December 22, 2010 SOARCA Peer Review Memorandum

40. Page 14

Comment:

I would like to comment on the text of Section 2.1 of the "Uncertainty Analysis Plan Recommended by SANDIA Technical Staff," Draft dated 10/19/2010 which provides justification of the use of a seismic induced Station Beach Out, SBO as the scenario to be evaluated in the SOARCA as it relates to other NPP sites in the U.S.

With respect to seismic being the greatest natural hazard, there are a few NPP sites in Florida and along the Gulf of Mexico coast where the potential for a LOCA associated with a Category 5 hurricane and associated storm surge flooding may exceed the risk from an earthquake at the 10^{-6} to 10^{-7} /yr probability of exceedence level. Less than 10 percent of all NPP sites in the U.S. may be in this category leaving more than 90 percent of NPP sites being dominated by an earthquake.

With respect to those NPP sites dominated by earthquakes, perhaps 70 percent seismic induced SBO would dominate the risk of an unmitigated LOCA . The other 30 percent might be expected to be dominated by early containment failure as a result of seismic induced building foundation failure (i.e. liquification or consolidation) of the containment or adjacent structure foundation due to an earthquake at the 10^{-6} or 10^{-7} /yr probability of exceedence level.

Resolution:

The SOARCA analysis was completed for two pilot plants, Peach Bottom and Surry. Hence the analyses are specific to those two plants and sites. This UA study is also site-specific, plant-specific, and scenario-specific since it analyzes uncertainty in the model parameters in the long-term station blackout scenario for the Peach Bottom plant. As previously discussed, the appropriateness of applying individual SOARCA insights to other plants and sites should be evaluated on a case-by-case basis.

Comment:

I am also providing comments relative to the one and half day meeting held at NRC offices 26 and 27 October 2010. Again, the selected scenario for the limiting event discussed at the meeting was an extremely low probability of exceedence seismic event (i.e. less than 10^{-6} or 10^{-7} /yr probability of exceedence earthquake) causing a Station Blackout. This event would be applicable to most of the 70 plus NPP sites in the U.S., but as discussed in response to the SANDIA Uncertainty proposal, there are several sites where the wind and storm surge coming from a Level 5 hurricane would be at least as likely to cause an SBO as an earthquake 0.4 to 0.5g peak ground acceleration, pga for these sites at the 10^{-6} or 10^{-7} /yr probability of exceedence level. In a significant number of other NPP sites I believe such as is the case of the Surry NPP a 0.8 to 1.0g pga earthquake typical of a 10^{-6} to 10^{-7} /yr probability of exceedence level would more likely lead to an immediate gross loss of the containment leak tight integrity at penetrations resulting from differential settlement caused by foundation soil liquefaction or consolidation between the containment and adjacent safety related structures than would be caused by a longer term SBO.

Resolution:

The potential soil liquefaction issue was further evaluated for the Surry SOARCA report, and additional discussion is being added to the SOARCA report. This SOARCA UA study is specific to the Peach Bottom plant. Please see resolution to comment 40 above.

KAREN VIEROW

December 22, 2010 SOARCA Peer Review Memorandum

42. Page 15

Comment:

Similar to the SOARCA project, which was initially intended to evaluate a larger number of reactors than turned out to be feasible with the given time and resource restraints, the SOARCA Uncertainty Analysis effort must be justified as reasonable within the given programmatic restraints. Further, the sufficiency, or completeness, of the effort must be demonstrated.

A full level III PRA for each SOARCA scenario would require time and resources far beyond those which are available. The current effort will include one scenario for one reactor as a reasonable substitution approach. This approach has the merits of including establishment of the methodology for future Uncertainty Analyses and of allowing for depth of evaluation of the selected scenario. The definitions and detailed description of the methodologies in Section 2.4 are very helpful.

The case for completeness of the Peach Bottom Long Term Station Blackout Scenario must be made. That is, even though some low probability or low consequence aspects may be omitted, the high risk outcomes must be included.

Resolution:

The final NUREG/CR report for the UA study will include a more detailed justification of the scenario selection in Section 2.1, as well as more clarity in the intended objectives of the analysis. The SOARCA analysis evaluated the consequences of the most likely and important event sequences and current estimate inputs for the Peach Bottom and Surry sites. Thus the fundamental objective of this SOARCA uncertainty study is to quantify how uncertainty in the variation of the input parameters (e.g., in the selected SOARCA estimate values) affects the calculated consequences (e.g., source term releases and latent cancer fatality risk).

This systematic look at the uncertainty in the system, as detailed in Section 2.3, provides for the quantification of the confidence in the SOARCA result for one scenario in detail, as well as some useful insights for the SOARCA results in general. In addition, the uncertainty in the response can be quantified as a function of the uncertainty in the inputs. Section 3.0 of the Draft NUREG/CR outlines this in greater detail. Consideration of the low and high consequence results (e.g., variance) will be included with the discussion of the results of the UA study in the final UA NUREG/CR report. Through the integrated inclusion of uncertainty in important MELCOR and MACCS parameters, we expect to capture any potential high-risk outcomes (conditional on the scenario) that may be supported by the underlying distributions of uncertain parameters. This theoretical point will be easier to discuss in the presentation and discussion of UA analysis results, once they are available, in the UA NUREG/CR report.

43. Page 15

Comment:

The approach to not consider cross-correlation between uncertainty parameters needs to be justified or modified.

Resolution:

As suggested by peer reviewers during the October 2010 meeting, the SOARCA team carefully deliberated on which MELCOR parameters should be correlated (MACCS parameter correlations were already included in the October 2010 draft UA plan). In addition, since the October 2010 meeting, the SOARCA team developed the capability to correlate input parameters in MELCOR. Appropriate correlations were identified and are now included for MELCOR parameters. Section 4.0 of the draft NUREG/CR has been updated to identify the correlated parameters.

44. Page 15

Comment:

Several sections of the report describe the aspects of the Uncertainty Analysis effort but do not close the loop by relating these to the SOARCA Uncertainty Analysis objectives. Examples: - Section 2.3: the type of uncertainties targeted (aleatory and/or epistemic) should be stated up front.

- Section 2.3: How this approach enables one to validate the Best Estimate SOARCA calculations should be explained.

Resolution:

Section 2.2 has been updated to identify up front the uncertainty classification (epistemic or aleatory) selected for the study. In addition, the updated Section 2.3 contains some additional rationale for, and clarification of, the objectives of this study.

45. Page 15

Comment:

Section 2.1, item 5: consider rewording the “fewer failed MELCOR simulations” as this implied doubt about the robustness of the MELCOR code.

Resolution:

We are in the process of rewriting Section 2.1 of the draft NUREG/CR report to provide more thorough justification and background discussion for the selection of the PB LTSBO scenario for this study. The note on “fewer failed MELCOR simulations” has been deleted. That is no longer an issue, as the mechanics of the uncertainty engine execution have improved since October 2010. In addition, the robustness of the uncertainty calculation will be discussed in the results portion of the document.

46. Page 15

Comment:

Section 3.2, 1st sentence: This sentence seems essential to the report, however, this review is confused over the meaning. Please reword.

Resolution:

The draft NUREG/CR report has been reorganized to enhance the clarity of this discussion. While minor changes to the 1st sentence were made (now in Section 3.4), moving the discussion from Section 2.4 "Probabilistic Analysis Methodology" of the October UA draft Plan document to Section 3.3 of the draft NUREG/CR immediately preceding Section 3.4 (which is the section in question), should have a substantial benefit in adding clarity to the discussion.

47. Page 15

Comment:

Many sections of the report need better documentation of their justification, such as the selection of uncertainty parameters and/or their distributions. Under recommendation 2, the solicitation of these data from "senior SNL and NRC technical staff..." is needed to clarify that the effort is less than exhaustive due to programmatic constraints. However, also needed is an explanation that the value of the current effort is not compromised.

Resolution:

Section 4.0 of the draft NUREG/CR report has been expanded to include the technical basis and justification of the key parameters and distributions selected for the SOARCA UA study. While a formal PIRT process was not used, the SOARCA models and results are supported by years of extensive study. The detailed SOARCA Peach Bottom model was the basis of the expert judgment from informed subject matter experts who identified the key parameters and distributions for this UA study. In addition, the SOARCA team was fortunate to have the independent review and advice of the SOARCA peer review committee through the meetings and memoranda in 2010, and limited review by non-SOARCA staff at SNL and NRC who have specialized expertise in particular subject areas. Thus, the SOARCA team believes the UA approach is sound given this UA study's focus on the uncertainty in the SOARCA estimate calculation. In addition, the introductory material to Section 4.0 has been updated to document the approach used.

JACQUELYN YANCH

December 22, 2010 SOARCA Peer Review Memorandum

48. Page 16

Comment:

The main health impact of the severe reactor accident is predicted to be latent cancer fatalities. The main source of uncertainty associated with estimating the number of latent cancer fatalities arises from taking risk estimates originally generated for a situation involving rapid radiation exposure of people (total dose delivered in ≤ 1 minute) and applying these risk estimates to the post-reactor accident scenario where the total dose is delivered over a period of years to decades.

The SOARCA team plans to generate distributions to represent uncertainty in risk estimates in collaboration with Dr. Keith Eckerman. Their second (fallback) option [N. Bixler presentation, October 2010] is to use the spread of risk estimates generated via expert solicitation [NUREG/CR-6555, 1997] to represent uncertainty. Since the experts in this solicitation were asked to supply estimates of risk of a large dose (1 Gy) delivered rapidly (1 min), a dose rate effectiveness factor (DREF) must be used in order to make the risk estimates applicable to the prolonged exposure situation. The SOARCA team uses a value of 2 for the DREF and plans to sample this value, for determination of uncertainty, from a distribution provided by the EPA [EPA 402-R-99-003, 1999]. In my opinion the distribution function provided by the EPA is not applicable to the situation involving very prolonged exposures and a broader range of DREF values should be included in the uncertainty estimation.

In reviewing available data, the National Council on Radiation Protection and Measurements (NCRP) reports that the DREF depends very significantly on the duration of the radiation exposure [NCRP 64, 1980]. Short-term exposures, such as those representative of typical occupational radiation scenarios, require a smaller value of DREF than long term exposures such as those lasting years or decades. Since the radiation exposure represented by returning home to elevated radiation levels following a severe reactor accident involves years or decades of exposure, a DREF appropriate to this scenario should be used. This value, according to NCRP 64, ranges from 6.6 to 12.8 with a best estimate of 10. However, the distribution function of DREF values provided by the EPA peaks at a value of 2 and the probability of sampling a value of 10, the most likely applicable value for the post-accident scenario, is vanishingly small. Thus, while the EPA distribution may be relevant to the rapid exposure scenario (e.g., occupational radiation protection) it is not very relevant to the situation discussed here. This is echoed in BEIR V where it is stated that higher values of DREF reflect situations involving continuous irradiation until death. Therefore, in discussions with Dr. Eckerman, it is important that the more realistic DREF values be included in the estimate of uncertainty associated with latent cancer fatalities.

Resolution:

Since the October 2010 draft UA plan and peer review committee meeting, Dr. Keith Eckerman has provided recommendations to the SOARCA team on health effects parameters and distributions to include in the SOARCA UA. Dr. Eckerman's recommendations have been incorporated into section 4.2.5 of the draft UA NUREG/CR report. The variables that have been added to the updated plan include: (1) DDREFA, (2) uncertainty in the energy deposited within a human organ for a specified incident radiation using a multiplicative factor for GSHFAC, and

(3) uncertainty in the risk coefficients for each of the organs included in the SOARCA analyses for latent health effects.

For the DDREFA distribution, Dr. Eckerman's recommendations are based on Federal Guidance 13 (FGR 13), which the SOARCA team accepted. The NCRP 64 DREF values cited in the comment are based on animal studies. the final chapter of NCRP 64, Chapter 12 entitled "Summarizing Arguments; DREF Values", on page 174 states: "It follows from the indicated range of DDREFA values that if the linear hypothesis is applied to data on radiation effects observed in human beings obtained at high dose and dose rates, the resultant risk coefficient would be expected to overestimate the most realistic or correction value, for either single exposure to low doses or exposure to high doses delivered at low-dose rates, by a factor of between 2 and 10."

NCRP Report 64 was issued in April 1980 and in 1997 NCRP issued Report 126. Chapter 6 of that report entitled "Extrapolation to Low Dose or Dose Rate" reviews application of DREF and notes the NCRP position taken in Report 116 issued in 1993. On page 64 it states "The choice of DREF is somewhat arbitrary and the NCRP considered that it could reasonably range between two and three." The report then speaks to the uncertainty in the application of the DDREFA and suggest use of a piecewise linear distribution, peaked at 2.0 and spanning the interval from 1 to 5.

The current NCRP position on DDREFA seems to be reasonable consistent across Reports 64, 116 and 126 however the uncertainty domain has decreased over the last 30 years. The DDREFA assumed in FGR 13 and used in the SOARCA Project and its uncertainty distribution are consistent with current positions of NCRP, ICRP, and National Academy of Science BEIR reports.

49. Page 16

Comment:

Uncertainty in the shape of the risk/dose model also exists. This uncertainty is accounted for in the current SOARCA approach of incorporating different threshold values below which no cancer fatalities would be observed.

Resolution:

As discussed with the peer review committee at the December 2012 meeting, the team's updated UA plan includes reporting the results for the three dose models that are used in the SOARCA study, in short-hand: LNT, "US background average threshold", and "Health Physics Society" models. The exploration of this model uncertainty will not be integrated with the other UA parameters, i.e., these three models will not be sampled along with the MACCS parameters. Rather, the three model results will be reported in parallel. This approach replaces the sampling of a dose threshold, which was a proposed parameter in the October 2010 draft UA plan.

**April 9, 2010 SOARCA Peer Review Memorandum, “Guidance on the SOARCA
Uncertainty Quantification and Sensitivity Analysis”**

50. Page 1

Comment:

Of the two methods presented for quantifying uncertainty, the “Inner” Weather Loop method is the appropriate method for evaluating the SOARCA results and for comparing with the previous NRC studies. A few sequence results should be explored through the “Outer” Weather Loop method to illustrate the influence of uncertainty in weather conditions at the time of the release. The inner loop method preserves the perspective that the SOARCA source term is smaller and later in release to the environment than source terms used in previous risk work. In this manner, the modeling advancements and new insights from experimental testing of the past twenty years are reflected. The outer loop method provides results that are more influenced by the effects of site-specific weather. While the impact of site weather is important, it will statistically change little from year to year, and is not changeable through any SOARCA-based understanding or insights. Therefore, the inner loop method should better suit the objectives of the SOARCA project in discerning improved understanding of the risk from Nuclear Power Plant operation. The outer loop, however, provides a mechanism for looking at more limiting weather conditions. By performing a limited number of sensitivity analyses with the outer loop method in addition to analyses by the inner loop method, the SOARCA project can provide some insights when considering the uncertainty of both the source term and the weather.

Resolution:

The inner loop approach was selected as the appropriate approach for the SOARCA UA as documented in the Draft UA Plan (October 2010) presented to the peer review committee on 10/26/2010.

51. Page 2

Comment:

The Uncertainty Quantification and Sensitivity Analysis study is essential to the credibility of the SOARCA project and should be documented as part of the SOARCA NUREG report, or as a stand-alone supporting reference.

Resolution:

The SOARCA UA will be documented in a separate NUREG/CR report. At a minimum, a draft of the UA report is expected to be published at the same time that the final SOARCA reports (Summary and Peach Bottom and Surry detailed analyses) are published.

Comment:

The Uncertainty Quantification study is in its early stages of planning and was not available for Committee review. Nonetheless, the uncertainty analysis is an integral part of the SOARCA project, and the analysis could be regarded as incomplete if there is not an attempt to address uncertainty. The members of the Peer Review Committee concurring with this memo request the opportunity to review the uncertainty quantification effort. Parameter selection and parameter distributions require particular care. Updates as well as the final set to be used in the Uncertainty Quantification study are requested.

Resolution:

The SOARCA Draft UA Plan (October 2010) was presented to the peer review committee in October 2010. Comments were received from the committee in December 2010. A short update was presented to the committee on 12/7/11. A teleconference is scheduled in January 2012 to discuss resolution of peer review comments and the final parameters and distributions used in the study. The UA plan (which is now documented in the draft UA NUREG/CR report) has been and continues to be updated in response to peer reviewers' comments.

Advisory Committee on Reactor Safeguards Comment Resolution

Uncertainty Analysis Plan

The purpose of this section is to document the SOARCA team's resolution of each written comment related to the uncertainty analysis (UA) plan in the May 15, 2012 letter report of the NRC's Advisory Committee on Reactor Safeguards [D1, D2]. Comments are extracted directly from the letter report with no changes.

Comment:

The selection of parameters, their uncertainty distributions, and their correlations—as well as sensitivity studies to assess the impact of uncertainties that are difficult to quantify—are critical to the Peach Bottom and Surry uncertainty analyses. The uncertainty reports should describe the approaches used to identify the parameters, distributions, and sensitivity studies and justify the bases for omission of parameters or effects of interest not addressed in the uncertainty analyses. (p. 1)

The selection of parameters, their uncertainty distributions, and their correlations, as well as sensitivity studies to assess the impact of uncertainties that are difficult to quantify, are critical to the uncertainty analysis. The approach used to identify these parameters is not clear. In Section 2.2 of the draft NUREG/CR report on uncertainty analysis, it is stated that “the approach is based on a formalized PIRT (phenomena identification, and ranking table) process,” while in Section 4 it is stated that the “uncertain parameters and their distributions were identified/characterized through an informal elicitation of subject matter experts.” The report should be consistent and accurate in its description of the approach used to identify the parameters and distributions and the selection of sensitivity studies. (p.5)

Resolution:

The staff enhanced the documentation in Sections 2 and 4 of this NUREG/CR report to better describe the approaches for identifying parameters and distributions and parameters and effects not treated in the integrated UA. In addition, the UA team added section 4.3 to discuss some phenomena of interest that were not addressed in the uncertainty analysis.

Comment:

There are a number of physical processes involved during in-vessel and ex-vessel accident progression where uncertainties are large. Not all of these uncertainties can be represented by parameter distributions. One way to address such phenomenological uncertainties is sensitivity analyses for alternative models. For example, one area of uncertainty identified by the Peer Review Committee that the staff may have not explored sufficiently is lower head failure. MELCOR focuses on creep rupture as the dominant mechanism for lower head failure. The staff argues that this approach is supported by experimental results in NUREG/CR-5582, which were performed on one-fifth scale models representing PWR heads. They also argue that the timing differences between gross lower head failure and penetration failure with the available penetration model are not significant to the overall accident progression. The staff also notes that the penetration model is a simple lumped parameter model for bulk heat transfer and is not adequate to calculate molten material drainage into a BWR reactor pressure vessel drain line. More detailed analyses in NUREG/CR-5642 suggest that in certain scenarios failure of this penetration is more important than failure of other lower head penetrations or the vessel. Sensitivity studies could help to evaluate whether earlier failure of the drain line would have a significant impact on outcomes. (p. 6)

Resolution:

Staff added a sensitivity study of an alternate lower head failure mode in the MELCOR model, documented in Section 6.4.2.

References

- [D1.] U.S. Nuclear Regulatory Commission, Advisory Committee on Reactor Safeguards, "State-of-the-Art Reactor Consequence Analyses (SOARCA) Project May 15, 2012 letter report," ML12135A385, Washington D.C., 2012.
- [D2.] U.S. Nuclear Regulatory Commission, "Staff Response to the Advisory Committee on Reactor Safeguards (ACRS) May 15, 2012, memorandum, SUBJECT: State-of-the-Art Reactor Consequence Analyses (SOARCA) Project," ML12158A178, Washington D.C., 2012.

APPENDIX E

ADDITIONAL INFORMATION AND ANALYSES IN RESPONSE TO ACRS QUESTIONS

APPENDIX E – TABLE OF CONTENTS

<u>Section</u>	<u>Page</u>
E.1 Motivation.....	E-8
E.2 Discussion of MACCS Results.....	E-11
E.3 Selection of the Three Representative MELCOR Realizations.....	E-15
E.3.1 INTRODUCTION.....	E-15
E.3.2 METHODOLOGY.....	E-15
E.3.3 SELECTION OF THE WEIGHT.....	E-16
E.3.4 CHECKING OF RESULTS.....	E-16
E.3.5 USE OF THE EXCEL WORKBOOK.....	E-17
E.3.6 Results.....	E-20
E.4 Weather Uncertainty & MACCS Convergence.....	E-21
E.5 Conditional Mean, Individual LCF Risk and Prompt Fatality Risk Results & Model Convergence.....	E-29
E.6 SOARCA Uncertainty Analysis Results for Conditional Individual LCF Risk....	E-45
E.7 Stability Analysis Using Bootstrap Approach.....	E-47
E.7.1 Low, Medium, & High Source Term Combined Analysis.....	E-56
E.7.2 Bootstrap Comparison.....	E-58
E.8 MELCOR Parameters.....	E-65
E.8.1 Question 5.a.I – SRVLAM.....	E-65
E.8.2 Question 5.a.II – CHEMFORM.....	E-66
E.8.3 Question 5.a.III – FL904A.....	E-68
E.8.4 Question 5.a.IV – BATTDUR.....	E-69
E.8.5 Question 5.a.V – SRVOAFRAC.....	E-69
E.8.6 Question 5.a.VI – SLCRFRAC.....	E-70
E.8.7 Question 5.a.VII – RDMTC and RDSTC.....	E-71
E.8.8 Question 5.a.VIII – RRIDRFRAC and RODRFRAC.....	E-72
E.8.9 Question 5.a.X – RHONOM.....	E-72
E.8.10 Question 5.a.XI – FFC.....	E-72
E.8.11 Question 5.a.XII – SC1141(2).....	E-73
E.9 MACCS Parameters.....	E-73
E.9.1 Question 5.b.I and 5.b.II – DOSNRM, TIMNRM, DOSHOT, and TIMHOT.....	E-73
E.9.2 Question 5.b.III – ESPEED.....	E-74
E.9.3 Question 5.b.IV – GSHFAC.....	E-76
E.10 Other Issues.....	E-77
E.10.1 Question 6.a – Surrogate Parameters.....	E-77
E.10.2 Question 6.b – Lower Head Penetration Failures.....	E-77
E.10.3 Question 6.c – Drywell Liner Failure.....	E-78
E.10.4 Question 6.d – Operator Actions.....	E-79
E.11 References.....	E-80

APPENDIX E – LIST OF FIGURES

<u>Figure</u>	<u>Page</u>
Figure E-1	Run 1 Conditional Mean, Individual LCF Risk (per Event) CCDF for all Radial Distances Considered..... E-13
Figure E-2	Run 2 Conditional Mean, Individual LCF Risk (per Event) CCDF for all Radial Distances Considered..... E-14
Figure E-3	Example of CDFs Comparison in Linear Scale (left) and Semi-log Scale (right)..... E-17
Figure E-4	Example of Cobweb Plot Result..... E-18
Figure E-5	Screenshot of Data Sheet in the Excel Workbook..... E-19
Figure E-6	Screenshot of Main Sheet of Excel Workbook..... E-20
Figure E-7	Cobweb Graph for Selected Source Terms..... E-21
Figure E-8	Run 6-8 Combined Aleatory and Epistemic Uncertainty Conditional Individual LCF Risk (per Event) CCDF for the Radial Distances Considered..... E-23
Figure E-9	Run 3 Combined Aleatory and Epistemic Uncertainty Conditional Individual LCF Risk (per Event) CCDF and Run 1 Epistemic Uncertainty Conditional, Mean Individual LCF Risk (per Event) CCDF for the Radial Distances Considered..... E-24
Figure E-10	Run 6 Combined Aleatory and Epistemic Uncertainty Conditional Individual LCF Risk (per Event) CCDF and Run 1 Epistemic Uncertainty Conditional, Mean Individual LCF Risk (per Event) CCDF for the Radial Distances Considered..... E-25
Figure E-11	Run 9 Combined Aleatory and Epistemic Uncertainty Conditional Individual LCF Risk (per Event) CCDF and Run 1 Epistemic Uncertainty Conditional, Mean Individual LCF Risk (per Event) CCDF for the Radial Distances Considered..... E-26
Figure E-12	Run 12 Combined Aleatory and Epistemic Uncertainty Conditional Individual LCF Risk (per Event) CCDF and Run 1 Epistemic Uncertainty Conditional, Mean Individual LCF Risk (per Event) CCDF for the Radial Distances Considered..... E-27
Figure E-13	Run 15 Combined Aleatory and Epistemic Uncertainty Conditional Individual LCF Risk (per Event) CCDF and Run 1 Epistemic Uncertainty Conditional, Mean Individual LCF Risk (per Event) CCDF for the Radial Distances Considered..... E-28
Figure E-14	Runs 3-5 Epistemic Uncertainty Conditional, Mean, Individual LCF Risk (per Event) CCDFs and Run 1 Epistemic Uncertainty Conditional, Mean Individual LCF Risk (per Event) CCDF for the Radial Distances Considered..... E-33
Figure E-15	Runs 6-8 Epistemic Uncertainty Conditional, Mean, Individual LCF Risk (per Event) CCDFs and Run 1 Epistemic Uncertainty Conditional, Mean Individual LCF Risk (per Event) CCDF for the Radial Distances Considered..... E-34

Figure E-16	Runs 9-11 Epistemic Uncertainty Conditional, Mean, Individual LCF Risk (per Event) CCDFs and Run 1 Epistemic Uncertainty Conditional, Mean Individual LCF Risk (per Event) CCDF for the Radial Distances Considered.....	E-35
Figure E-17	Runs 12-14 Epistemic Uncertainty Conditional, Mean, Individual LCF Risk (per Event) CCDFs and Run 1 Epistemic Uncertainty Conditional, Mean Individual LCF Risk (per Event) CCDF for the Radial Distances Considered.....	E-36
Figure E-18	Runs 15-17 Epistemic Uncertainty Conditional, Mean, Individual LCF Risk (per Event) CCDFs and Run 1 Epistemic Uncertainty Conditional, Mean Individual LCF Risk (per Event) CCDF for the Radial Distances Considered.....	E-37
Figure E-19	Runs 3-5 Epistemic Uncertainty Conditional, Mean, Individual Prompt Fatality Risk (per Event) CCDFs and Run 1 Epistemic Uncertainty Conditional, Mean Individual Prompt Fatality Risk (per Event) CCDF for the Radial Distances Considered.....	E-41
Figure E-20	Runs 6-8 Epistemic Uncertainty Conditional, Mean, Individual Prompt Fatality Risk (per Event) CCDFs and Run 1 Epistemic Uncertainty Conditional, Mean Individual Prompt Fatality Risk (per Event) CCDF for the Radial Distances Considered.....	E-42
Figure E-21	Runs 9-11 Epistemic Uncertainty Conditional, Mean, Individual Prompt Fatality Risk (per Event) CCDFs and Run 1 Epistemic Uncertainty Conditional, Mean Individual Prompt Fatality Risk (per Event) CCDF for the Radial Distances Considered.....	E-43
Figure E-22	Runs 12-14 Epistemic Uncertainty Conditional, Mean, Individual Prompt Fatality Risk (per Event) CCDFs and Run 1 Epistemic Uncertainty Conditional, Mean Individual Prompt Fatality Risk (per Event) CCDF for the Radial Distances Considered.....	E-44
Figure E-23	Runs 15-17 Epistemic Uncertainty Conditional, Mean, Individual Prompt Fatality Risk (per Event) CCDFs and Run 1 Epistemic Uncertainty Conditional, Mean Individual Prompt Fatality Risk (per Event) CCDF for the Radial Distances Considered.....	E-45
Figure E-24	Run 1 Combined Aleatory and Epistemic Uncertainty Conditional Individual LCF Risk (per Event) CCDF and Run 1 Epistemic Uncertainty Conditional, Mean, Individual LCF Risk (per Event) CCDF for the Radial Distances Considered.....	E-46
Figure E-25	10-mile Conditional, Mean, Individual LCF Risk (per Event) CDF for Run 15 with SRS and 95% Confidence Interval Upper and Lower Bounds for Runs 16 & 17 with SRS.....	E-48
Figure E-26	10-mile Conditional, Mean, Individual LCF Risk (per Event) CDF for Run 16 with SRS and 95% Confidence Interval Upper and Lower Bounds for Runs 15 & 17 with SRS.....	E-49
Figure E-27	10-mile Conditional, Mean, Individual LCF Risk (per Event) CDF for Run 17 with SRS and 95% Confidence Interval Upper and Lower Bounds for Runs 15 & 16 with SRS.....	E-49

Figure E-28	50-mile Conditional, Mean, Individual LCF Risk (per Event) CDF for Run 15 with SRS and 95% Confidence Interval Upper and Lower Bounds for Runs 16 & 17 with SRS.....	E-50
Figure E-29	50-mile Conditional, Mean, Individual LCF Risk (per Event) CDF for Run 16 with SRS and 95% Confidence Interval Upper and Lower Bounds for Runs 15 & 17 with SRS.....	E-50
Figure E-30	50-mile Conditional, Mean, Individual LCF Risk (per Event) CDF for Run 17 with SRS and 95% Confidence Interval Upper and Lower Bounds for Runs 15 & 16 with SRS.....	E-51
Figure E-31	10-mile Conditional, Mean, Individual LCF Risk (per Event) CDFs for Runs 15-17 with SRS and the Density Function for Run 15 with SRS.....	E-51
Figure E-32	50-mile Conditional, Mean, Individual LCF Risk (per Event) CDFs for Runs 15-17 with SRS and the Density Function for Run 15 with SRS.....	E-52
Figure E-33	10-mile Conditional, Mean, Individual LCF Risk (per Event) CDF for Run 15 with LHS and 95% Confidence Interval Upper and Lower Bounds for Runs 16 & 17 with LHS.....	E-52
Figure E-34	10-mile Conditional, Mean, Individual LCF Risk (per Event) CDF for Run 16 with LHS and 95% Confidence Interval Upper and Lower Bounds for Runs 15 & 17 with LHS.....	E-53
Figure E-35	10-mile Conditional, Mean, Individual LCF Risk (per Event) CDF for Run 17 with LHS and 95% Confidence Interval Upper and Lower Bounds for Runs 15 & 16 with LHS.....	E-53
Figure E-36	50-mile Conditional, Mean, Individual LCF Risk (per Event) CDF for Run 15 with LHS and 95% Confidence Interval Upper and Lower Bounds for Runs 16 & 17 with LHS.....	E-54
Figure E-37	50-mile Conditional, Mean, Individual LCF Risk (per Event) CDF for Run 16 with LHS and 95% Confidence Interval Upper and Lower Bounds for Runs 15 & 17 with LHS.....	E-54
Figure E-38	50-mile Conditional, Mean, Individual LCF Risk (per Event) CDF for Run 17 with LHS and 95% Confidence Interval Upper and Lower Bounds for Runs 15 & 16 with LHS.....	E-55
Figure E-39	10-mile Conditional, Mean, Individual LCF Risk (per Event) CDFs for Runs 15-17 with LHS and the Density Function for Run 15 with LHS....	E-55
Figure E-40	50-mile Conditional, Mean, Individual LCF Risk (per Event) CDFs for Runs 15-17 with LHS and the Density Function for Run 15 with LHS....	E-56
Figure E-41	10-mile Conditional, Mean, Individual LCF Risk (per Event) CDFs for Low, Medium, and High Source Terms with LHS and the Conditional, Mean, Individual LCF Risk (per Event) CDF for the SOARCA UA with LHS Sampling.....	E-57
Figure E-42	50-mile Conditional, Mean, Individual LCF Risk (per Event) CDFs for Low, Medium, and High Source Terms with LHS and the Conditional, Mean, Individual LCF Risk (per Event) CDF for the SOARCA UA with LHS Sampling.....	E-58

Figure E-43	CAP17 Conditional, Mean, Individual LCF Risk (per Event) CCDF with LHS and MC Sampling for the Radial Distances Considered.....	E-60
Figure E-44	CAP17 Conditional, Mean, Individual Prompt Fatality Risk (per Event) CCDF with LHS and MC Sampling for the Radial Distances Considered.	E-62
Figure E-45	10-mile Conditional, Mean, Individual LCF Risk (per Event) CDF for CAP17, CAP40, and 95% Confidence Interval Upper and Lower Bounds for CAP17 and CAP40.....	E-63
Figure E-46	50-mile Conditional, Mean, Individual LCF Risk (per Event) CDF for CAP17, CAP40, and 95% Confidence Interval Upper and Lower Bounds for CAP17 and CAP40.....	E-63
Figure E-47	10-mile Conditional, Mean, Individual LCF Risk (per Event) CDFs for CAP17, CAP40 and the Density Function for CAP40.....	E-64
Figure E-48	50-mile Conditional, Mean, Individual LCF Risk (per Event) CDFs for CAP17, CAP40 and the Density Function for CAP40.....	E-64
Figure E-49	CDF of Failure Probability/Number of Valve Cycles.....	E-66
Figure E-50	Typical LTSBO Drywell Characteristics.....	E-69
Figure E-51	Peach Bottom Evacuation Routes.....	E-75

APPENDIX E – LIST OF TABLES

<u>Table</u>	<u>Page</u>
Table E-1	MACCS Runs to Source Term Crosswalk..... E-12
Table E-2	Run 1 Statistics..... E-13
Table E-3	Run 2 Statistics..... E-14
Table E-4	Parameters and Weighting (0.0 to 1.0) for Source Term Selection..... E-21
Table E-5	Average difference between the three separate LHS runs over all Aleatory Weather Distributions (1 st to 99 th percentile)..... E-22
Table E-6	Conditional, mean, individual LCF risk (per event) average statistics for the MACCS Uncertainty Analysis for five circular areas (Run 1)..... E-29
Table E-7	Runs 3-5 conditional, mean, individual LCF risk (per event) average statistics for five circular areas..... E-30
Table E-8	Runs 6-8 conditional, mean, individual LCF risk (per event) average statistics for five circular areas..... E-30
Table E-9	Runs 9-11 conditional, mean, individual LCF risk (per event) statistics for five circular areas..... E-31
Table E-10	Runs 12-14 conditional, mean, individual LCF risk (per event) average statistics for five circular areas..... E-31
Table E-11	Runs 15-17 conditional, mean, individual LCF risk (per event) average statistics for five circular areas..... E-32
Table E-12	Conditional, mean, individual prompt-fatality risk (per event) average statistics for the MACCS Uncertainty Analysis for specified circular areas (Run 1) E-38
Table E-13	Run 3-5 conditional, mean, individual prompt-fatality risk (per event) average statistics for specified circular areas..... E-38
Table E-14	Run 6-8 conditional, mean, individual prompt-fatality risk (per event) average statistics for specified circular areas..... E-39
Table E-15	Run 9-11 conditional, mean, individual prompt-fatality risk (per event) average statistics for specified circular areas..... E-39
Table E-16	Run 12-14 conditional, mean, individual prompt-fatality risk (per event) average statistics for specified circular areas..... E-40
Table E-17	Run 15-17 conditional, mean, individual prompt-fatality risk (per event) average statistics for specified circular areas..... E-40
Table E-18	Percent Difference in the CDF between the Combined Aleatory and Epistemic Uncertainty LCF Risk to Mean Aleatory Uncertainty LCF Risk for Specified Radial Distances..... E-47
Table E-19	Conditional, mean, individual LCF risk (per event) average statistics for the MACCS Uncertainty Analysis (CAP17) for five circular areas using LHS sampling..... E-59

Table E-20	Conditional, mean, individual LCF risk (per event) average statistics for the MACCS Uncertainty Analysis (CAP17) for five circular areas using SRS/MC sampling.....	E-60
Table E-21	Conditional, mean, individual prompt fatality risk (per event) average statistics for the MACCS Uncertainty Analysis (CAP17) for six circular areas using LHS.....	E-61
Table E-22	Conditional, mean, individual prompt fatality risk (per event) average statistics for the MACCS Uncertainty Analysis (CAP17) for six circular areas using MC.....	E-61

E.1 Motivation

As part of the NRC's 606th meeting of the Advisory Committee on Reactor Safeguards (ACRS), this uncertainty analysis was discussed by the ACRS, NRC staff, and Sandia staff. From this meeting a series of additional questions were submitted to the NRC staff from the ACRS. The NRC and Sandia staff addressed these questions, and the results were discussed with the ACRS Regulatory Policies and Practices Subcommittee on September 16, 2013. The following questions were submitted by the ACRS:

2. **MELCOR – MACCS¹ – Weather Uncertainty Integration:** For the combined MELCOR-MACCS results, the report currently presents only results averaged over the weather trials. At a minimum, the report should also present results that include and display the full weather aleatory uncertainty. We would also like to discuss the results from the following requested analyses.
3. **MACCS and Weather Uncertainties for Prompt² (Early) Fatalities:** Select the MELCOR realization that produced the largest conditional prompt fatality consequences in the current SOARCA uncertainty results. For that realization, sample from the 350 MACCS input parameters, and for each epistemic sample generate 984 weather cases to derive an uncertainty distribution for the conditional prompt fatality consequences at each distance. Demonstrate convergence of the combined MACCS-weather uncertainty analysis results. Present the results from this analysis in two forms:
 - Average over the weather samples as was done in the current report to show only the MACCS epistemic uncertainty.
 - Present results that retain the full combined MACCS epistemic and weather aleatory uncertainty.
4. **MACCS and Weather Uncertainties for Latent Cancer Fatalities 1:** Select the MELCOR realization that produced the largest conditional latent cancer fatality consequences in the current SOARCA uncertainty results. For that realization, sample from the 350 MACCS input parameters, and for each epistemic sample generate 984 weather cases to derive an uncertainty distribution for the conditional latent cancer fatality consequences at each distance. Demonstrate convergence of the combined MACCS weather uncertainty analysis results. Present the results from this analysis in two forms:
 - Average over the weather samples as was done in the current report to show only the MACCS epistemic uncertainty.
 - Present results that retain the full combined MACCS epistemic and weather aleatory uncertainty.

¹ Note that the time, NRC and SNL were calling the MACCS2 code, "MACCS." Subsequently the code is now simply being called "MACCS," as reflected in the body of the report.

² In this appendix, "prompt" and "early" are used interchangeably to describe early fatality risk.

5. **MACCS and Weather Uncertainties for Latent Cancer Fatalities 2:** Select a MELCOR realization that produced a small, but non-zero, contribution to the conditional latent cancer fatality consequences in the current SOARCA uncertainty results. For that realization, sample from the 350 MACCS input parameters, and for each epistemic sample generate 984 weather cases to derive an uncertainty distribution for the conditional latent cancer fatality consequences at each distance. Demonstrate convergence of the combined MACCS-weather uncertainty analysis results. Present the results from this analysis in two forms:

- Average over the weather samples as was done in the current report to show only the MACCS epistemic uncertainty.
- Present results that retain the full combined MACCS epistemic and weather aleatory uncertainty.

6. **Input Parameter Uncertainties:** We would like the staff to explain the technical justification for the uncertainties that are assigned for the following parameters. We would also like to understand the rationale for the type of distribution that is used to characterize the uncertainty. To facilitate planning, we have listed the parameters in the order of our general interests and priorities.

a. **MELCOR Parameters:**

- I. SRVLAM – SRV stochastic failure to reclose
- II. CHEMFORM – Iodine and cesium fraction
- III. FL904A – Drywell liner failure flow area
- IV. BATTDUR – Battery duration
- V. SRVOAFRAC – SRV open area fraction
- VI. SLCRFRAC – Main steam line creep rupture area fraction
- VII. RDMTC, RDSTC – Radial debris relocation time constants
- VIII. RRIDRFRAC, RODRFRAC – Railroad door open fraction
- IX. H2IGNC – Hydrogen ignition criteria
- X. RHONOM – Particle density
- XI. FFC – Fuel failure criterion
- XII. SC1141(2) – Molten clad drainage rate

b. **MACCS Parameters:**

- I. DOSNRM, TIMNRM – Normal relocation
- II. DOSHOT, TIMHOT – Hotspot relocation
- III. ESPEED – Evacuation speed
- IV. GSFAC – Shielding factor
- V. GSHFAC – Groundshine

7. **Other Issues:** We would like to discuss the following modeling and analysis issues.
- a. **Surrogate Parameters:** We would like to understand the technical bases for the selection of higher level "surrogate parameters" to account for the uncertainties and correlated effects from the lower level constituents that they represent in the models. In addition, we would like to understand how lower level parameters were combined to obtain an estimate and the uncertainty distribution for these lower level parameters. Should the MELCOR parameters for the in-core fuel degradation process be correlated and not independent?
 - b. **Lower Head Penetration Failures:** We would like to better understand why the sensitivity study in Section 6.4.2 provides a reasonable surrogate for understanding the effects from failure of the reactor vessel bottom head drain line.
 - c. **Drywell Liner Failure:** We would like to understand how the MELCOR drywell liner wall heatup and melt spreading model properly estimates the behavior of melt movement from the drywell pedestal leading to wall contact and failure. Is the presence of water considered in any way? If not, why not?
 - d. **Operator Actions:**
 - Operators manually open SRV: The base case model assumes that the operators open a SRV at 1 hour after the initiating event. The sensitivity study in Section 6.4.1 shows the effects from actions to open the valve at 0.5 hour, 2 hours, and 3 hours, and the effects if the operators do not open the valve. We would like to better understand the basis for the nominal 1-hour timing and how the open SRV is modeled in MELCOR for the base case model and the sensitivity study.
 - Operators shed DC loads: We would like to understand the bases and the timing for the operator actions that are needed to extend the battery life to the maximum modeled duration of 8 hours.

The rest of this section provides the written discussions the NRC and Sandia staff provided the ACRS subcommittee to support the September 16, 2013 subcommittee meeting (the transcript of this meeting is available in Reference [E.1]).

E.2 Discussion of MACCS Results

To address ACRS Questions 1 through 4, Sandia conducted a series of additional uncertainty MACCS analyses. Table E-1 provides a crosswalk of the MACCS analyses. Figure E-1 and Table E-2 show the Section 6.2 results. This figure and table is used as a comparison for the rest of this discussion. Figure E-2 and Table E-3 show a MACCS analysis using all 865 SOARCA Uncertainty Analysis source terms with the SOARCA (NUREG/CR-7110 Volume 1) point estimates. This analysis was used to select three representative MELCOR source terms for additional analyses.

Table E-1: MACCS Runs to Source Term Crosswalk

MACCS Analysis	Description	Source Term	Run Number
UAS_CAP17v364_2509	MACCS analysis with LHS inputs for combined MELCOR Replicates 1, 2, and 3 (SOARCA Uncertainty Analysis Section 6.2 results)	All 865 Source Terms	1
UAS_CAP20v364_2509	MACCS analysis with SOARCA Estimate inputs for combined MELCOR Replicates 1, 2, and 3	All 865 Source Terms	2
UAS_CAP22v364_2509	MACCS analysis with LHS inputs for highest Prompt Fatality Risk source term determined from CAP 17 (same LHS random seed as CAP 17)	Replicate 2 Realization 291	3
UAS_CAP23v364_2509	MACCS analysis with LHS inputs for highest Prompt Fatality Risk source term determined from CAP 17 (different LHS random seed than CAP 22)	Replicate 2 Realization 291	4
UAS_CAP24v364_2509	MACCS analysis with LHS inputs for highest Prompt Fatality Risk source term determined from CAP 17 (different LHS random seed than CAP 22 and CAP 23)	Replicate 2 Realization 291	5
UAS_CAP25v364_2509	MACCS analysis with LHS inputs for highest LCF Risk source term determined from CAP 17 (same LHS random seed as CAP 17)	Replicate 3 Realization 46	6
UAS_CAP26v364_2509	MACCS analysis with LHS inputs for highest LCF Risk source term determined from CAP 17 (different LHS random seed than CAP 25)	Replicate 3 Realization 46	7
UAS_CAP27v364_2509	MACCS analysis with LHS inputs for highest LCF Risk source term determined from CAP 17 (different LHS random seed than CAP 25 and CAP 26)	Replicate 3 Realization 46	8
UAS_CAP28v364_2509	MACCS analysis with LHS inputs for low LCF Risk source term determined from CAP 20 (same LHS random seed as CAP 17)	Replicate 3 Realization 187	9
UAS_CAP29v364_2509	MACCS analysis with LHS inputs for low LCF Risk source term determined from CAP 20 (different LHS random seed than CAP 28)	Replicate 3 Realization 187	10
UAS_CAP30v364_2509	MACCS analysis with LHS inputs for low LCF Risk source term determined from CAP 20 (different LHS random seed than CAP 28 and CAP 29)	Replicate 3 Realization 187	11
UAS_CAP31v364_2509	MACCS analysis with LHS inputs for medium LCF Risk source term determined from CAP 20 (same LHS random seed as CAP 17)	Replicate 1 Realization 75	12
UAS_CAP32v364_2509	MACCS analysis with LHS inputs for medium LCF Risk source term determined from CAP 20 (different LHS random seed than CAP 31)	Replicate 1 Realization 75	13
UAS_CAP33v364_2509	MACCS analysis with LHS inputs for medium LCF Risk source term determined from CAP 20 (different LHS random seed than CAP 31 and CAP 32)	Replicate 1 Realization 75	14
UAS_CAP34v364_2509	MACCS analysis with LHS inputs for high LCF Risk source term determined from CAP 20 (same LHS random seed as CAP 17)	Replicate 1 Realization 290	15
UAS_CAP35v364_2509	MACCS analysis with LHS inputs for high LCF Risk source term determined from CAP 20 (different LHS random seed than CAP 34)	Replicate 1 Realization 290	16
UAS_CAP36v364_2509	MACCS analysis with LHS inputs for high LCF Risk source term determined from CAP 20 (different LHS random seed than CAP 34 and CAP 35)	Replicate 1 Realization 290	17

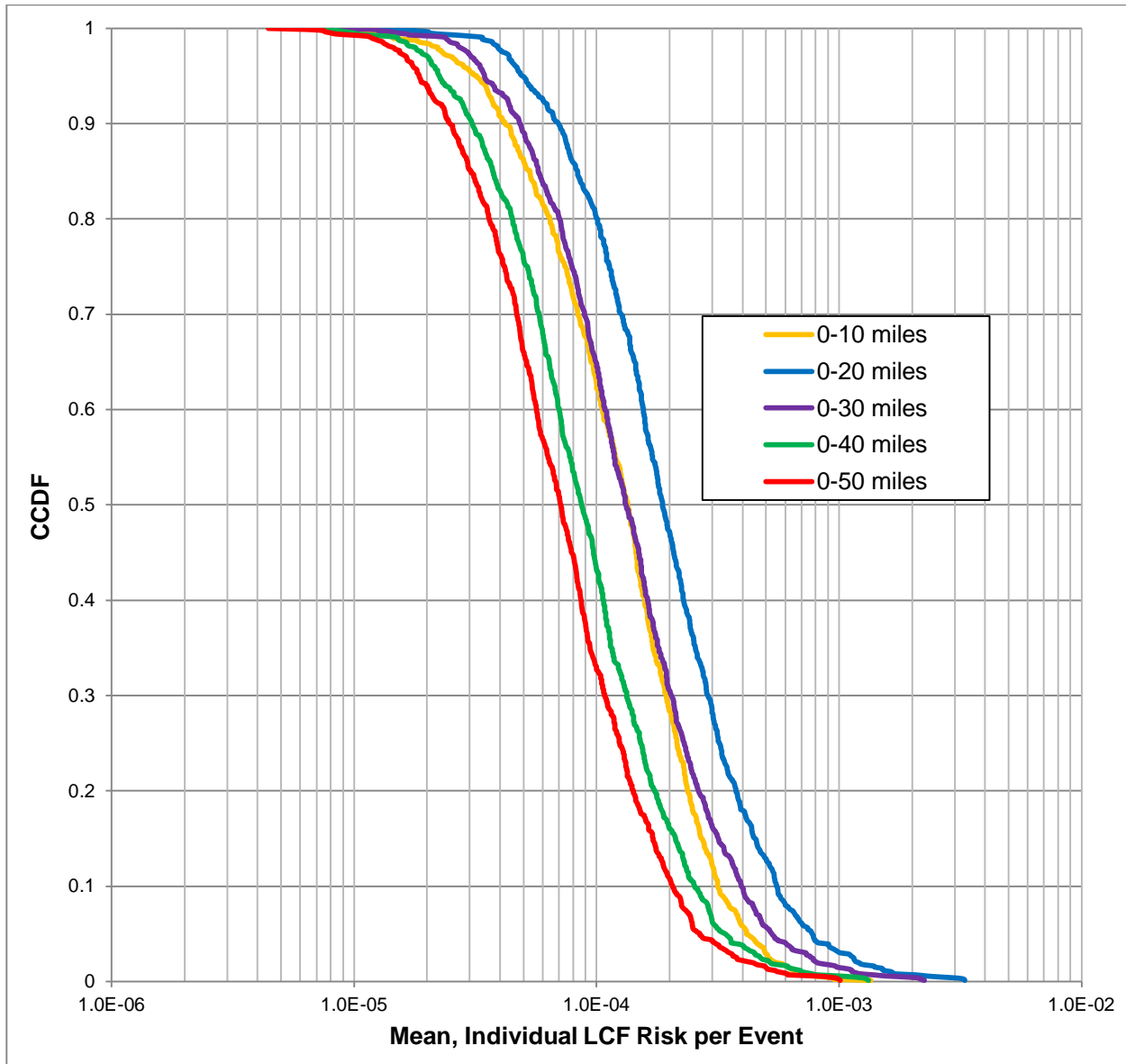


Figure E-1: Run 1 Conditional Mean, Individual LCF Risk (per Event) CCDF for all Radial Distances Considered

Table E-2: Run 1 Statistics

	0-10 miles	0-20 miles	0-30 miles	0-40 miles	0-50 miles
Mean	1.65E-04	2.79E-04	1.96E-04	1.26E-04	1.02E-04
Median	1.34E-04	1.87E-04	1.32E-04	8.67E-05	7.12E-05
5th Percentile	3.13E-05	4.89E-05	3.44E-05	2.24E-05	1.85E-05
95th Percentile	4.15E-04	7.73E-04	5.28E-04	3.38E-04	2.66E-04

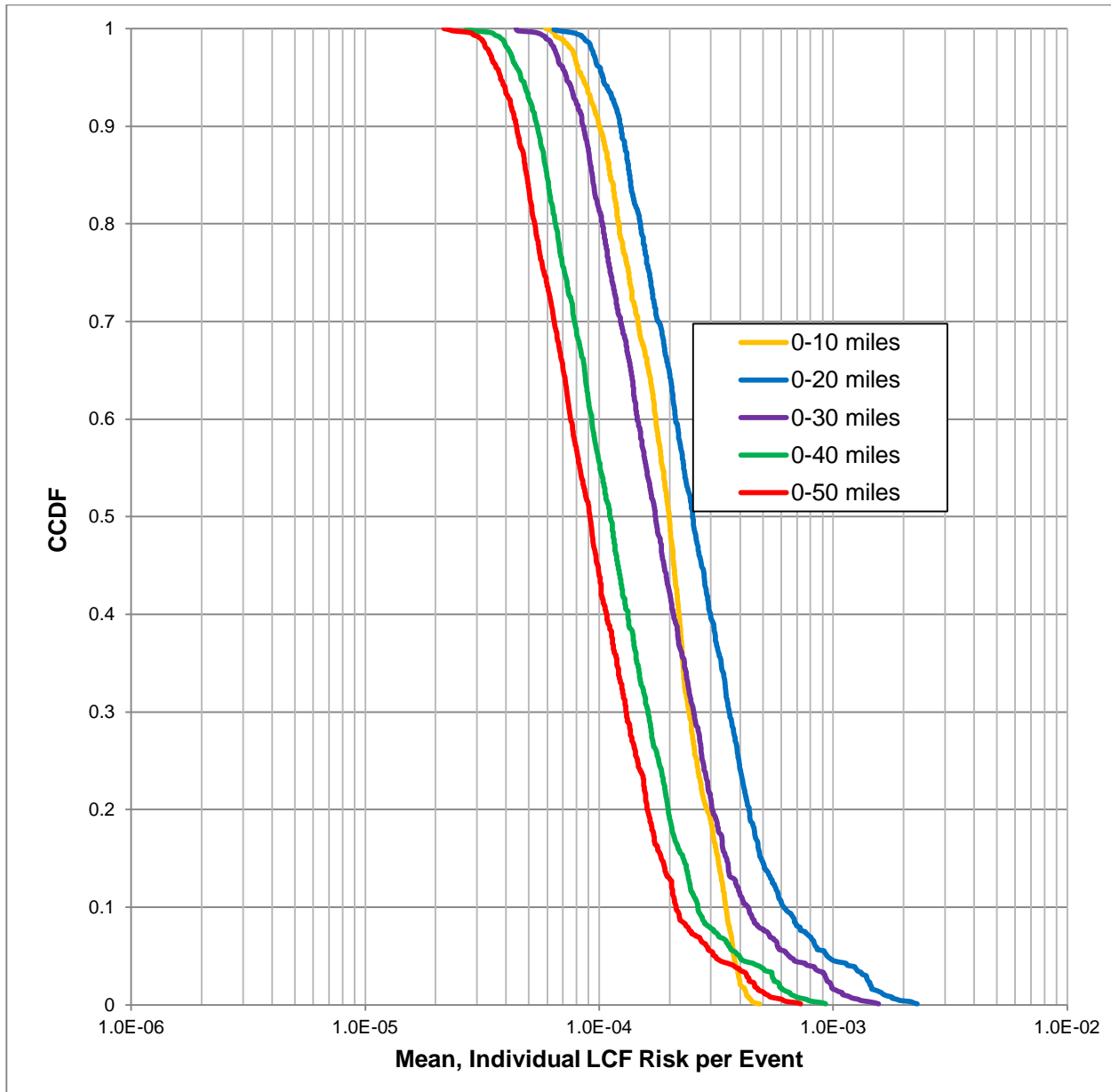


Figure E-2: Run 2 Conditional Mean, Individual LCF Risk (per Event) CCDF for all Radial Distances Considered

Table E-3: Run 2 Statistics

	0-10 miles	0-20 miles	0-30 miles	0-40 miles	0-50 miles
Mean	2.08E-04	3.42E-04	2.36E-04	1.49E-04	1.20E-04
Median	1.99E-04	2.50E-04	1.73E-04	1.11E-04	9.12E-05
5th Percentile	8.40E-05	1.03E-04	7.22E-05	4.62E-05	3.78E-05
95th Percentile	3.77E-04	9.41E-04	6.48E-04	3.98E-04	3.13E-04

E.3 Selection of the Three Representative MELCOR Realizations

E.3.1 INTRODUCTION

In order to test the influence of uncertain MACCS parameters by themselves to address ACRS Questions 1 through 4, three representative source terms needed to be selected. Each of them will be used as a reference source term on a Monte Carlo simulation in which only MACCS parameters will vary.

The selection of these source term required an initial MACCS run. In this run, all previously 865 source terms have been used, while all MACCS parameters have been set to nominal value (SOARCA point estimates). This way it was possible to assess the influence of the source term when MACCS parameters are fixed.

A set of 11 results have then been used as metrics to select the three representative source terms:

- Latent Cancer Fatality (LCF) at 5 different locations (10, 20, 30, 40 and 50 miles)
- Fraction of inventory released for 5 radionuclides (Cs, I, Ba, Ce, Te)
- Release time

As three values needed to be selected, the ensemble of possibility (prob=1) was decomposed into three equiprobable groups ($[0, 1/3]$, $[1/3, 2/3]$ and $[2/3, 1]$) and the mid-point quantile of each group was used as the ideal theoretical value (i.e., $q_1=1/6$, $q_2=1/2$ and $q_3=5/6$)

Amongst the 865 set of results generated, three results were selected, such that their quantile position for the considered metrics are the closest to the theoretical representative quantile.

In other words:

- One realization such as the difference between its quantile position for all the metrics and the theoretical value of $q_1=1/6$ is minimized
- One realization such as the difference between its quantile position for all the metrics and the theoretical value of $q_2=1/2$ is minimized
- One realization such as the difference between its quantile position for all the metrics and the theoretical value of $q_3=5/6$ is minimized

One additional constraint added to the problem is that the importance of the metrics is not equally likely. For instance, LCF results are considered more important (they are the final result of interest) than individual fraction of RN released and Release time is considered as the least important parameter. Furthermore, correlation amongst the outputs needs to be considered.

E.3.2 METHODOLOGY

Each of the 865 calculations performed generated a result for all the 11 metrics considered. For each realization the result for each metric was replaced by its quantile position, based on the 865 results. (The value was ranked with respect to the 864 other values and normalized by 865). Therefore, each realization was associated with 11 quantile positions (one for each metric).

$$Q_i = \{q_{1,i}, q_{2,i}, \dots, q_{10,i}, q_{11,i}^*\}, \quad i = 1, \dots, 865$$

Where i represents the realization number, Q_i the set of quantiles associated with realization i and $q_{j,i}$ the quantile associated with metric j for realization i .

As release time influence is inverse from the other metrics (the earlier the release time, the worse it is), a reverse quantile ($q^*=1-q$) has been used for this metric.

The importance of each metric is determined via a weight factor

$$W = \{w_1, w_2, \dots, w_{11}\}$$

Where W represents the set of weights and w_j the weight associated with metric j .

Three normalized distances (based on the L^2 norm) are estimated for each realization, one for each of the theoretical quantiles, via the following formula

$$d_{i,k} = \sqrt{\frac{\sum_{j=1}^{11} w_j (q_{j,i} - q_k)^2}{\sum_{j=1}^{11} w_j}}, \quad i = 1, \dots, 865 \text{ and } k = 1, 2 \text{ or } 3$$

Where k represents the theoretical quantile reference number, q_k the quantile for reference k

For each reference k the realization leading to the minimum of $d_{i,k}$ is selected as representative for the set. It will be the one that minimizes the difference between the theoretical quantile and actual quantile (in the L^2 norm sense) according to the weight of importance.

E.3.3 SELECTION OF THE WEIGHT

The weights are selected for each metric to represent the importance of the metric relative to the others according to the analyst. As the distance result is normalized, the range of values used is left open to the analyst (as long as it is positive or null). A weight of 0.0 will lead to the metric not being considered.

One important factor to consider, when the weights are chosen, is the eventual correlations amongst the results. LCF results will be correlated (and some more strongly than other). For strongly correlated results (beyond 0.9 for instance), the group can be considered as a single metric, and the weights associated to each member of the group will be added to the influence to the group. As an example, LCF at 50 miles and LCF at 40 miles results have a correlation of 0.999 (essentially correlation of 1). Associating a weight of 1 to both of these metric will be equivalent to associate a weight of 2 for the group consisting of these two metrics.

E.3.4 CHECKING OF RESULTS

Once the realizations are selected, one can check how good the selection is, with the selected set of weights. For this, two graphical methods are proposed.

The first one is a CDF comparison for each metric. The CDF resulting from the 865 values is plotted for each metric. On top, a CDF consisting of the three selected realizations is displayed. The analyst can then check how good the fit is between the two CDFs. A good fit will be obtained if the distance between the two CDFs is small. Another point of reference to evaluate

the goodness of fit is to check whether the CDFs cross at or close to the selected quantiles (1/6, 1/2 and 5/6). An example for LCF for a 50 miles radius is displayed in Figure E-3. The dashed lines indicate the quantiles position where the two CDFs are expected to cross.

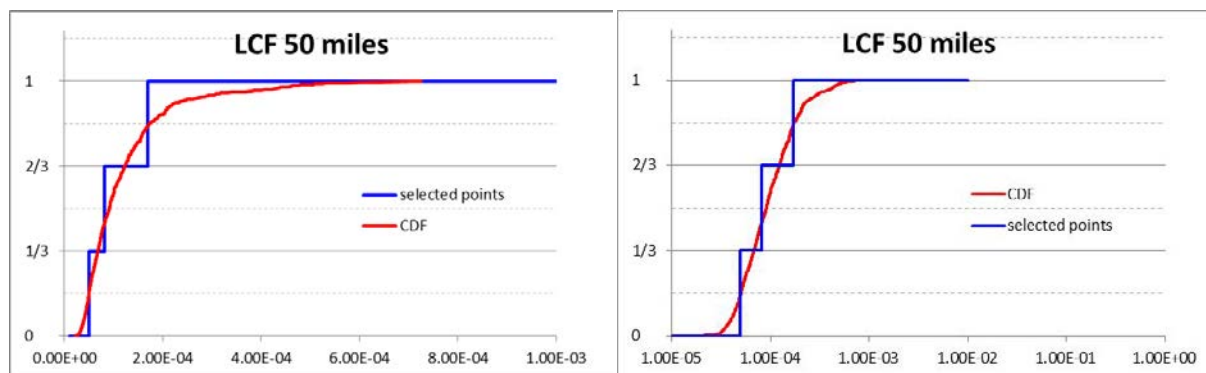


Figure E-3: Example of CDFs Comparison in Linear Scale (left) and Semi-log Scale (right)

The second one uses a Cobweb to represent how far from the selected realizations are from the theoretical quantiles. An example can be seen in Figure E-4. The three selected realizations' quantile curves are in color thick blue, green, and red lines, the theoretical quantiles in dot-dashed dark lines and a set of 150 realizations are displayed in thin gray lines as reference (not all 865 realizations are plotted as it would make the cobweb hard to read).

E.3.5 USE OF THE EXCEL WORKBOOK

An excel workbook has been developed to perform the minimization and select the realizations (Selection_curves_SOARCA_PB-UA_v1.3.xlsx). In the **Data** Spreadsheet, the analyst copies the results of the 11 metrics for the 865 results under column B to L (see screenshot in Figure E-5).

In **Main** spreadsheet (see Figure E-6) the analyst can select the quantile desired in cells D4 to D6 (by default 1/6, 1/2, and 5/6) and the weights to be used in row 4, column K to U. The calculations are performed automatically and the resulting CDFs are displayed (using linear and log-scale on the abscissa) below in the same sheet. A correlation matrix is displayed in the area AJ3-AU14 to help select the appropriate weights.

Finally, the cobweb plots are available in the sheet Cobweb (see Figure E-4 for an example). The metrics have been listed from left to right according to their decreasing order of importance following the weights selected.

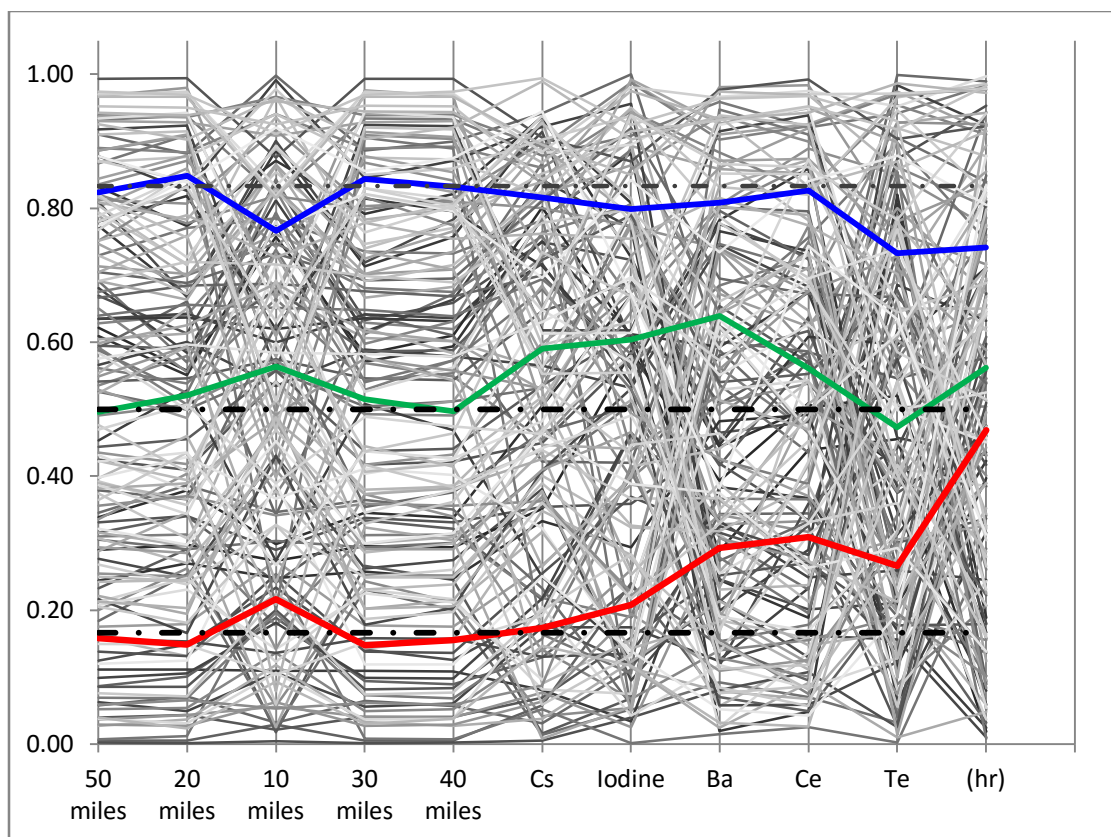


Figure E-4: Example of Cobweb Plot Result

	A	B	C	D	E	F	G	H	I	J	K	L	M
1			LCF Risk per Event				Radionuclides					Release Time	
2	Source Term	50 miles	20 miles	10 miles	30 miles	40 miles	Cs	Iodine	Ba	Ce	Te	(hr)	
3	1	1.09E-04	2.73E-04	2.71E-04	1.96E-04	1.30E-04	3.85E-02	9.96E-02	1.64E-02	4.39E-04	6.05E-02	19.73	
4	2	2.20E-04	5.66E-04	4.51E-04	3.97E-04	2.64E-04	8.06E-02	1.87E-01	3.01E-02	1.17E-03	1.77E-01	10.10	
5	3	6.17E-05	1.63E-04	1.82E-04	1.14E-04	7.47E-05	1.40E-02	1.94E-02	1.64E-02	4.75E-04	2.39E-02	17.73	
6	4	6.32E-05	1.76E-04	1.38E-04	1.22E-04	7.74E-05	1.26E-02	5.18E-02	2.19E-02	1.31E-03	3.17E-02	23.05	
7	5	7.86E-05	2.16E-04	2.07E-04	1.50E-04	9.58E-05	1.64E-02	5.06E-02	2.28E-02	7.53E-04	5.29E-02	20.85	
8	6	1.14E-04	3.23E-04	2.79E-04	2.18E-04	1.39E-04	3.23E-02	8.67E-02	2.58E-02	1.66E-03	7.12E-02	14.63	
9	7	1.55E-04	3.43E-04	3.41E-04	2.58E-04	1.82E-04	7.42E-02	8.68E-02	7.15E-03	2.30E-04	6.21E-02	19.95	
10	8	1.29E-04	2.82E-04	3.17E-04	2.13E-04	1.51E-04	5.88E-02	1.59E-02	1.04E-02	2.67E-04	1.36E-02	18.59	
11	9	1.23E-04	3.08E-04	3.13E-04	2.19E-04	1.48E-04	3.38E-02	7.46E-02	2.49E-02	1.22E-03	7.35E-02	11.68	
12	10	1.13E-04	2.79E-04	2.63E-04	2.01E-04	1.34E-04	4.07E-02	5.45E-02	1.79E-02	1.07E-03	3.37E-02	21.40	
13	11	6.60E-05	1.94E-04	1.31E-04	1.32E-04	8.21E-05	8.63E-03	3.57E-02	2.99E-02	1.87E-03	2.71E-02	18.63	
14	12	5.30E-05	1.66E-04	8.62E-05	1.10E-04	6.66E-05	4.54E-03	1.63E-02	3.59E-02	1.62E-03	1.25E-02	16.12	
15	13	4.51E-05	1.25E-04	1.03E-04	8.66E-05	5.53E-05	5.66E-03	1.48E-02	2.16E-02	8.60E-04	2.20E-02	22.68	
16	14	2.68E-04	8.26E-04	3.04E-04	5.56E-04	3.39E-04	6.20E-02	1.07E-01	1.34E-01	9.22E-03	9.86E-02	10.52	
17	15	6.77E-05	1.94E-04	1.43E-04	1.33E-04	8.36E-05	1.28E-02	3.31E-02	2.41E-02	1.99E-03	1.92E-02	14.53	
18	16	6.87E-05	2.06E-04	1.46E-04	1.35E-04	8.45E-05	1.95E-02	6.57E-02	2.39E-02	1.29E-03	3.78E-02	19.89	
19	17	4.29E-05	1.23E-04	1.19E-04	8.41E-05	5.30E-05	6.65E-03	2.76E-02	1.26E-02	2.90E-04	5.78E-02	20.72	
20	18	8.04E-05	2.18E-04	2.07E-04	1.50E-04	9.75E-05	2.42E-02	6.91E-02	1.95E-02	7.53E-04	4.20E-02	16.21	
21	19	1.26E-04	2.90E-04	3.00E-04	2.15E-04	1.49E-04	5.13E-02	8.13E-02	1.17E-02	5.52E-04	4.85E-02	16.28	
22	20	6.53E-05	1.85E-04	1.17E-04	1.26E-04	8.02E-05	8.66E-03	2.52E-02	2.85E-02	1.17E-03	5.50E-02	19.22	
23	21	5.58E-05	1.74E-04	7.28E-05	1.15E-04	7.02E-05	3.80E-03	1.75E-02	3.43E-02	1.60E-03	2.53E-02	14.95	
24	22	5.72E-05	1.68E-04	1.33E-04	1.13E-04	7.08E-05	1.18E-02	2.97E-02	2.53E-02	1.25E-03	2.00E-02	18.22	
25	23	3.88E-05	1.13E-04	7.89E-05	7.65E-05	4.79E-05	4.28E-03	2.03E-02	1.98E-02	7.79E-04	2.30E-02	20.10	
26	24	5.06E-05	1.41E-04	1.38E-04	9.74E-05	6.21E-05	9.83E-03	3.50E-02	2.07E-02	6.20E-04	2.72E-02	18.70	
27	25	2.33E-04	7.22E-04	2.10E-04	5.03E-04	3.00E-04	2.52E-02	5.55E-02	7.19E-02	1.06E-02	3.37E-02	17.93	
28	26	9.57E-05	2.87E-04	1.69E-04	1.95E-04	1.20E-04	1.66E-02	5.33E-02	2.81E-02	3.02E-03	3.70E-02	17.39	
29	27	9.69E-05	2.71E-04	2.14E-04	1.87E-04	1.19E-04	2.66E-02	6.91E-02	2.65E-02	1.67E-03	3.89E-02	16.80	
30	28	1.72E-04	4.10E-04	3.33E-04	3.00E-04	2.05E-04	7.71E-02	7.52E-02	2.39E-02	1.81E-03	4.26E-02	15.52	
31	29	5.15E-05	1.64E-04	7.68E-05	1.08E-04	6.51E-05	3.75E-03	1.59E-02	3.08E-02	1.68E-03	1.50E-02	17.08	
32	30	1.61E-04	5.06E-04	2.15E-04	3.45E-04	2.06E-04	2.35E-02	1.03E-01	5.61E-02	5.60E-03	4.65E-02	17.57	
33	31	3.97E-05	1.03E-04	1.02E-04	7.33E-05	4.83E-05	7.67E-03	2.45E-02	1.17E-02	3.91E-04	2.15E-02	23.62	
34	32	9.03E-05	2.52E-04	2.13E-04	1.72E-04	1.10E-04	2.41E-02	3.56E-02	2.65E-02	1.46E-03	2.41E-02	16.90	
35	33	2.85E-05	7.86E-05	7.84E-05	5.46E-05	3.51E-05	5.08E-03	2.79E-02	9.25E-03	2.33E-04	2.42E-02	22.40	
36	34	1.56E-04	4.55E-04	2.23E-04	3.18E-04	1.96E-04	3.08E-02	4.87E-02	4.36E-02	5.84E-03	2.38E-02	18.00	
37	35	6.46E-05	1.74E-04	1.47E-04	1.21E-04	7.86E-05	1.47E-02	4.36E-02	1.88E-02	5.51E-04	6.44E-02	16.92	
38	36	1.08E-04	3.08E-04	2.32E-04	2.09E-04	1.33E-04	2.22E-02	2.87E-02	4.04E-02	1.91E-03	4.90E-02	13.34	
39	37	1.64E-04	3.42E-04	3.48E-04	2.64E-04	1.92E-04	7.07E-02	5.40E-02	1.14E-02	8.24E-04	3.33E-02	15.58	
40	38	1.73E-04	5.37E-04	2.56E-04	3.59E-04	2.18E-04	2.25E-02	6.63E-02	4.65E-02	7.84E-03	6.79E-02	14.92	
41	39	1.05E-04	3.38E-04	1.60E-04	2.25E-04	1.34E-04	1.53E-02	3.72E-02	4.63E-02	3.80E-03	2.57E-02	16.53	
42	40	1.15E-04	3.20E-04	2.23E-04	2.21E-04	1.41E-04	3.39E-02	5.47E-02	3.05E-02	2.22E-03	2.87E-02	20.95	
43	41	1.38E-04	4.08E-04	2.76E-04	2.71E-04	1.70E-04	3.81E-02	1.01E-01	3.37E-02	3.13E-03	8.16E-02	15.03	
44	42	6.60E-05	1.75E-04	2.19E-04	1.23E-04	8.00E-05	1.60E-02	2.03E-02	9.67E-03	2.58E-04	2.41E-02	21.40	
45	43	4.67E-05	1.34E-04	1.29E-04	9.16E-05	5.76E-05	8.17E-03	4.02E-02	1.54E-02	3.51E-04	4.41E-02	18.08	
46	44	5.85E-05	1.63E-04	1.76E-04	1.12E-04	7.15E-05	1.35E-02	2.70E-02	1.97E-02	7.10E-04	2.13E-02	17.03	
47	45	7.33E-05	2.03E-04	2.24E-04	1.37E-04	8.95E-05	1.72E-02	4.35E-02	1.75E-02	7.51E-04	4.09E-02	11.98	
48	46	8.31E-05	2.61E-04	1.38E-04	1.75E-04	1.05E-04	9.35E-03	2.18E-02	4.25E-02	2.84E-03	1.65E-02	18.83	
49	47	1.25E-04	3.58E-04	2.59E-04	2.42E-04	1.53E-04	3.56E-02	4.93E-02	3.62E-02	2.74E-03	2.64E-02	15.74	
50	48	4.96E-05	1.31E-04	1.26E-04	9.21E-05	6.04E-05	1.23E-02	2.92E-02	8.75E-03	3.48E-04	3.87E-02	16.39	
51	49	2.29E-05	6.41E-05	6.32E-05	4.41E-05	2.81E-05	3.20E-03	1.53E-02	9.69E-03	3.17E-04	1.27E-02	17.37	
52	50	4.18E-04	1.43E-03	2.30E-04	9.37E-04	5.47E-04	2.13E-02	8.22E-02	1.65E-01	2.35E-02	5.64E-02	14.26	
	Data	CDFs	Main	Cobweb									
	Ready												

Figure E-5: Screenshot of Data Sheet in the Excel Workbook

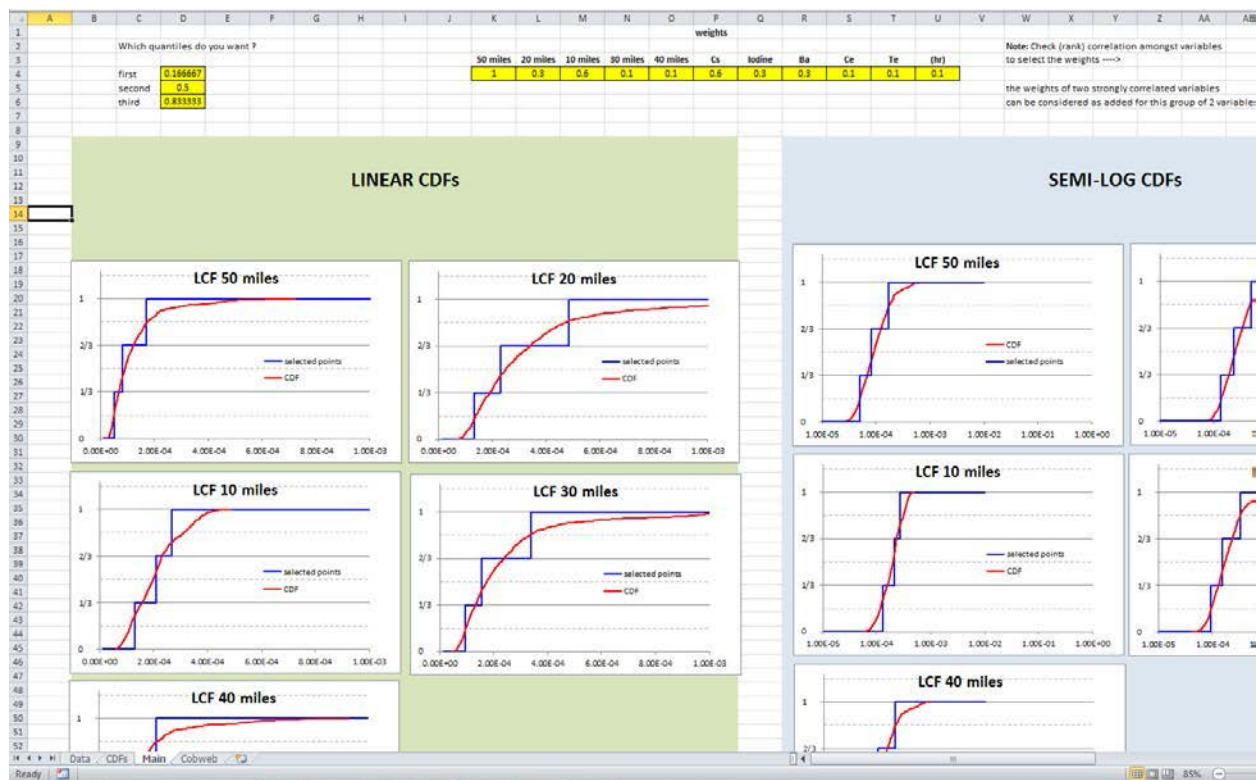


Figure E-6: Screenshot of Main Sheet of Excel Workbook

E.3.6 Results

The selection of these three source terms are based on the Run 2 results for 11 input and output parameters. Each of these 11 parameters is assigned an importance factor based on their respective CDFs (i.e., conditional LCF risk, radionuclides, and release timing). The 11 parameters are shown in Table E-4 with their respective weighting factor.

Conditional LCF risk at 50 miles was considered the most important metric and was associated with a value of 1.0. As 20-, 30- and 40-miles results are strongly correlated to this metric; their weight was fixed to a low value (0.3, 0.1, and 0.1, respectively). Result at 10-miles tends to be different so a higher weight (0.6) was associated to this metric.

With respect to radionuclides releases, Cesium was considered as the most important (weight of 0.6), followed by Iodine and Barium (weight of 0.3 each). Cerium and Tellurium releases were considered less important (weight of 0.1 each).

Finally, environmental release time was considered to have a small effect (weight of 0.1).

The source terms selected try to best represent 1/3 of the total CDF's considered. The source terms selected try to best correspond to the 17th, 50th, and 83rd percentiles for each of the 11 parameters considered. Figure E-7 shows a cobweb graph for the low (red line), medium (green line), and high (blue line) source terms selected. In Figure E-7, each of the source terms shows its respective representation to the parameters considered and its corresponding CDF information.

Table E-4: Parameters and Weighting (0.0 to 1.0) for Source Term Selection

Conditional, Mean, Individual LCF Risk (per Event) at:				
50 miles	20 miles	10 miles	30 miles	40 miles
1.0	0.3	0.6	0.1	0.1
Radionuclide Group				
Cesium	Iodine	Barium	Cerium	Tellurium
0.6	0.3	0.3	0.1	0.1
Environmental Release Time (hour)				
0.1				

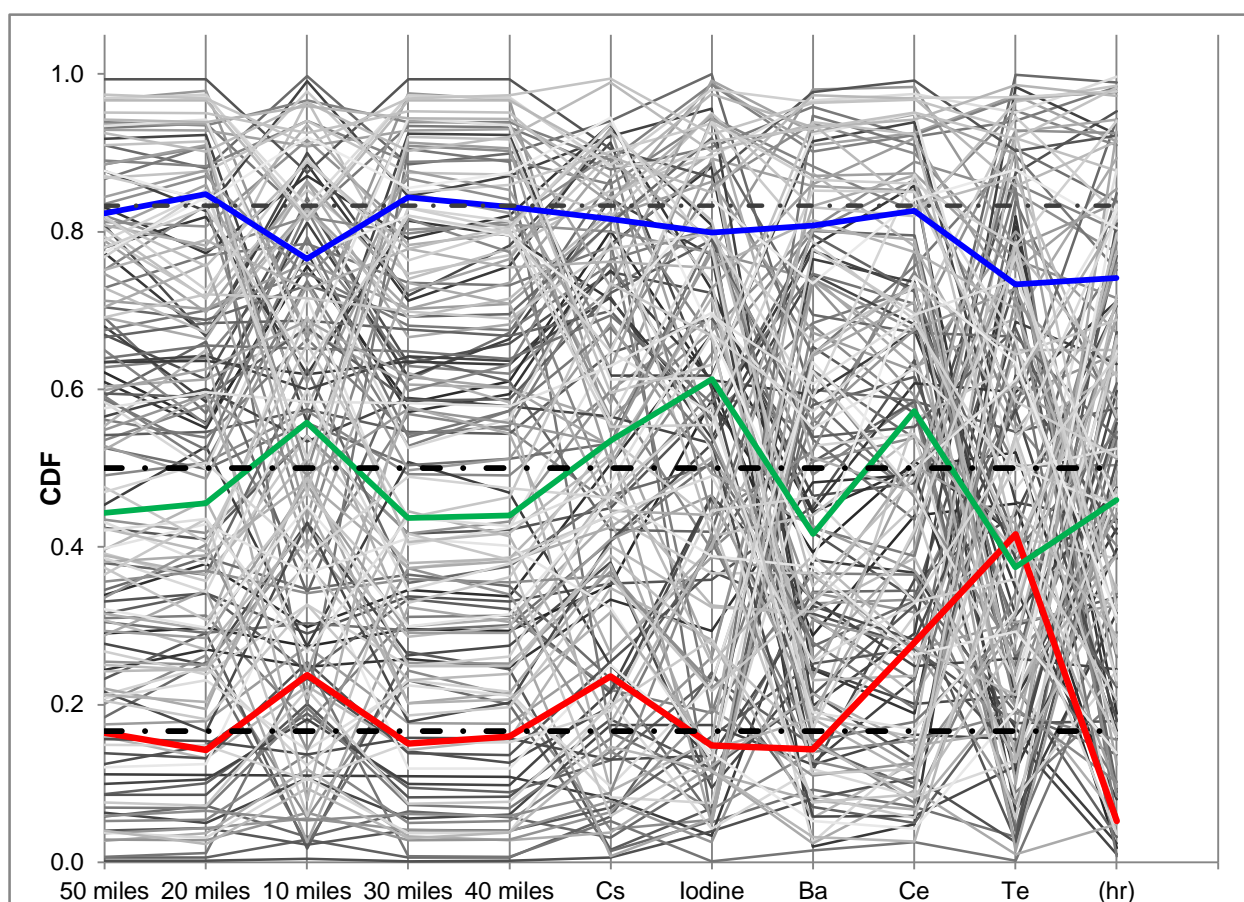


Figure E-7: Cobweb Graph for Selected Source Terms

E.4 Weather Uncertainty & MACCS Convergence

To answer ACRS Questions 1 through 4 for the five source terms considered (highest prompt fatality risk source term, highest LCF risk source term, and three high/medium/low source terms selected by the methodology described in Section E.1), three Latin Hypercube Sampling (LHS) runs of 1,000 samples varying all 350 MACCS uncertain input variables were conducted. As part of this analysis, the distribution across the sampled weather is considered. Table E-5 provides the average percent difference in results across the weather distribution for each of the

source terms considered and their associated Runs (i.e., see Table E-1 for a more detailed description of each Run). The largest deviation between the three LHS runs is observed for the 0-10 mile radial distance to be the 'low' source term (4.5%) at the 99th percentile, and for the 0-50 mile radial distance it is observed for the 'medium' source term (8.5%) at the 99th percentile.

Figure E-8 shows an example of the Table E-5 results for Run 6, 7, and 8 combined aleatory and epistemic uncertainty conditional individual LCF risk (per event) CCDFs for the 10- and 50-mile radial distances. This figure further emphasizes how well converged the MACCS results are for the source terms and sampled weather considered.

Figure E-9 through Figure E-13 show the 10- and 50-mile combined aleatory and epistemic uncertainty conditional LCF risk (per event) CCDFs for specified Runs compared to the epistemic uncertainty conditional, mean LCF risk (per event) CCDFs for Run 1. Based on these figures, the combined aleatory and epistemic results are similar to those from the SOARCA Uncertainty Analysis for the 'medium' source term determined from Section 2 (i.e., 5% average error between Run 1 and Runs 12-14 for the 0-10 mile radial distance (24% peak error at 99th percentile), and 32% average error between Run 1 and Runs 12-14 for the 0-50 mile radial distance (72% peak error at 99th percentile)).

Based on these analyses, it is judged that the MACCS model is well converged with respect to weather uncertainty for conditional LCF risk.

Table E-5: Average difference between the three separate LHS runs over all Aleatory Weather Distributions (1st to 99th percentile)

Source Term	Conditional LCF Risk 0-10 miles	Conditional LCF Risk 0-50 miles
Highest Prompt Fatality Risk – Runs 3-5	0.8%	0.8%
Highest LCF Risk – Runs 6-8	0.8%	0.9%
Low – Runs 9-11	0.9%	0.8%
Medium – Runs 12-14	0.8%	0.9%
High – Runs 15-17	1.0%	0.6%
Overall Average	0.9%	0.8%

Prompt fatality risk was not able to be determined for the combined aleatory and epistemic results uncertainties because the large number of 'zero' risk results prevents the MACCS post-processor from generating the convoluted CCDF.

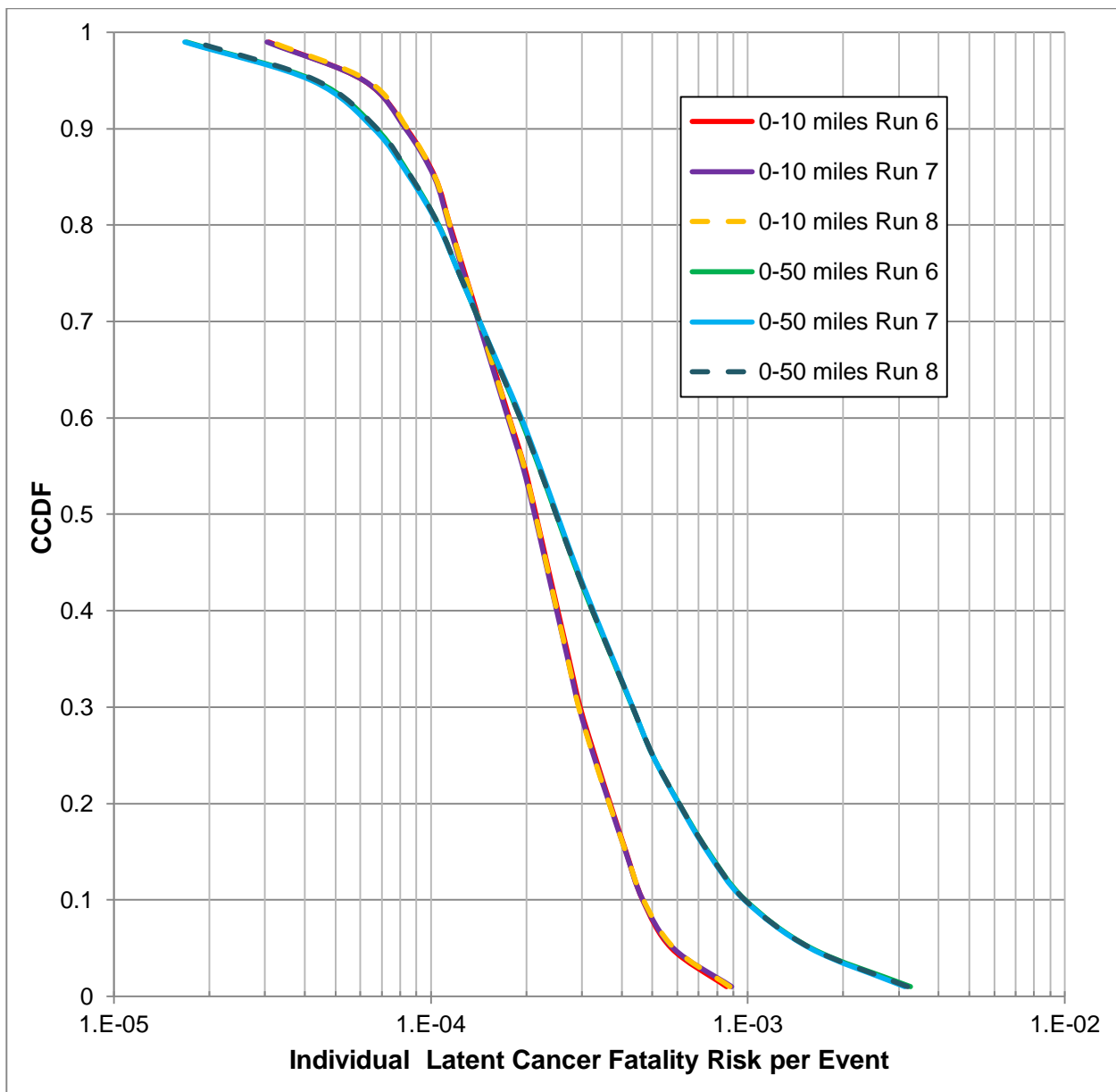


Figure E-8: Run 6-8 Combined Aleatory and Epistemic Uncertainty Conditional Individual LCF Risk (per Event) CCDF for the Radial Distances Considered

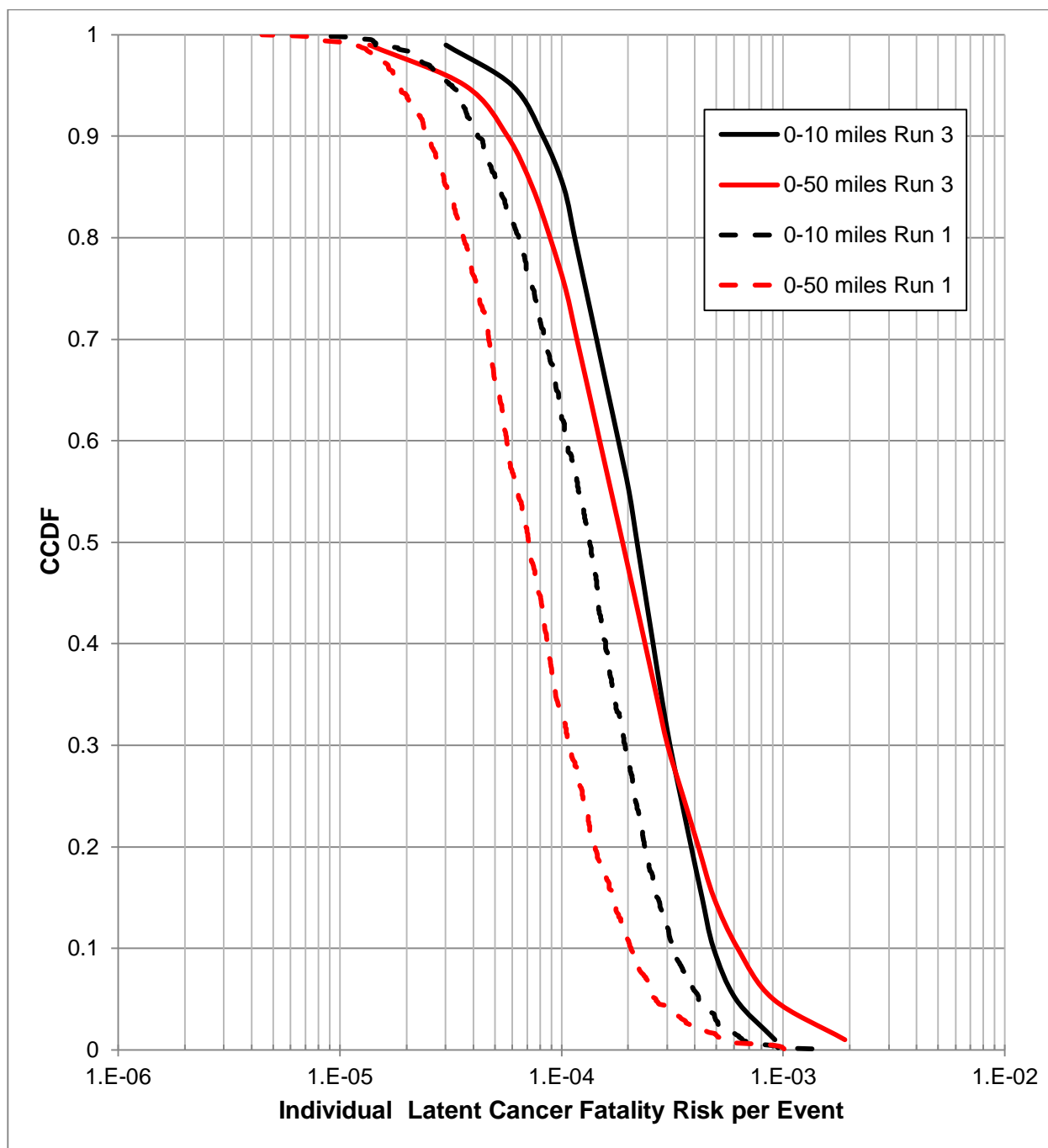


Figure E-9: Run 3 Combined Aleatory and Epistemic Uncertainty Conditional Individual LCF Risk (per Event) CCDF and Run 1 Epistemic Uncertainty Conditional, Mean Individual LCF Risk (per Event) CCDF for the Radial Distances Considered

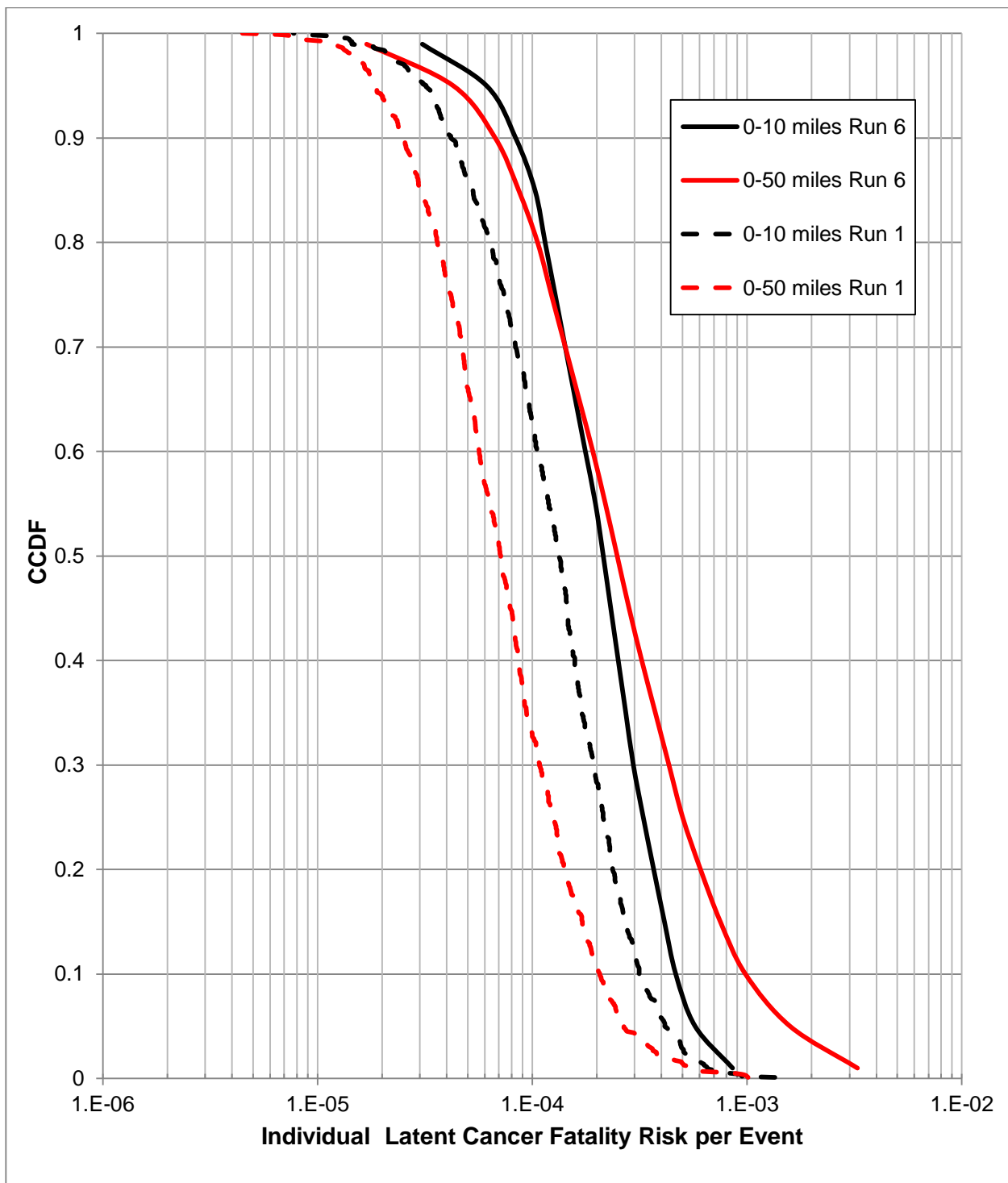


Figure E-10: Run 6 Combined Aleatory and Epistemic Uncertainty Conditional Individual LCF Risk (per Event) CCDF and Run 1 Epistemic Uncertainty Conditional, Mean Individual LCF Risk (per Event) CCDF for the Radial Distances Considered

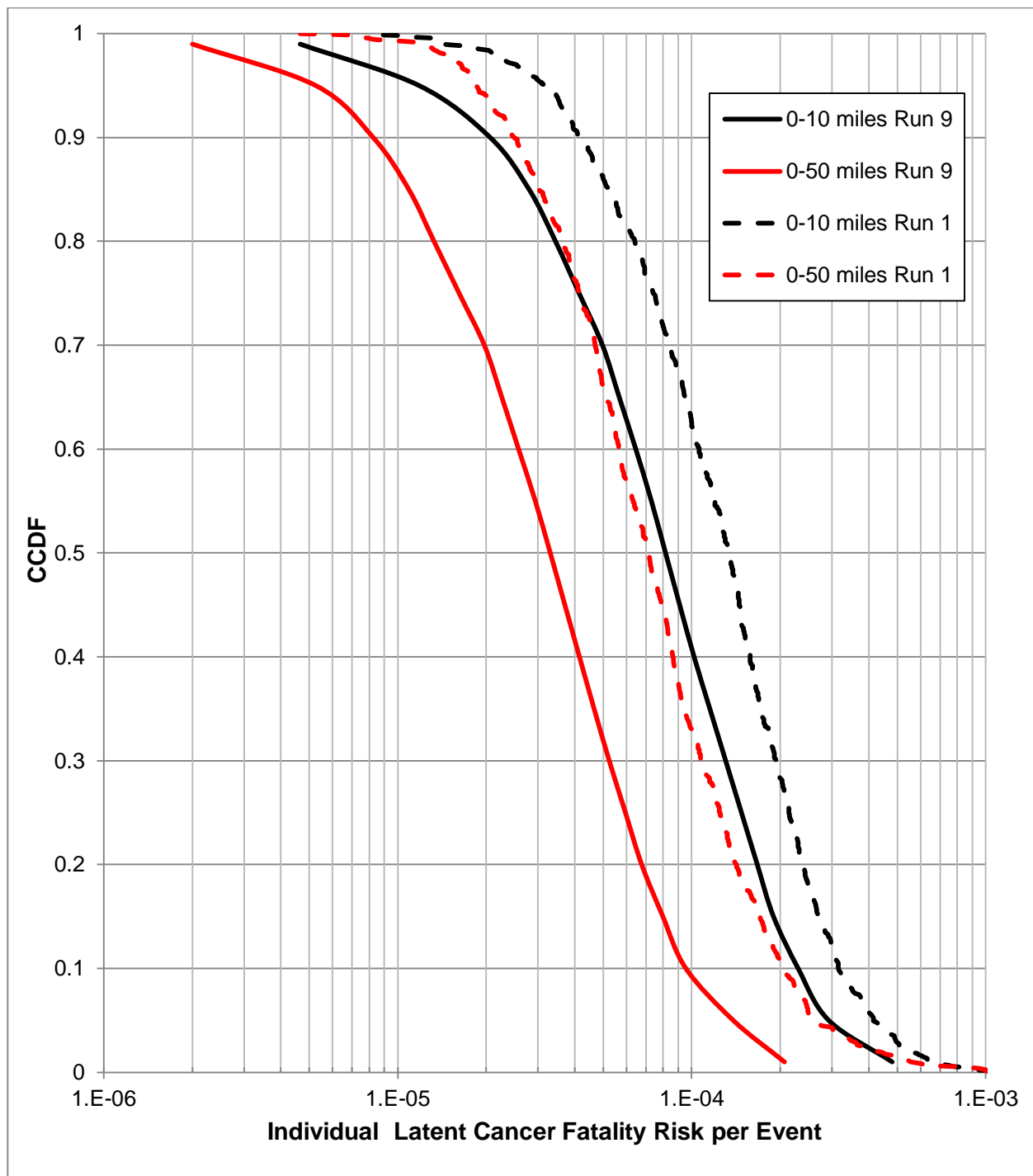


Figure E-11: Run 9 Combined Aleatory and Epistemic Uncertainty Conditional Individual LCF Risk (per Event) CCDF and Run 1 Epistemic Uncertainty Conditional, Mean Individual LCF Risk (per Event) CCDF for the Radial Distances Considered

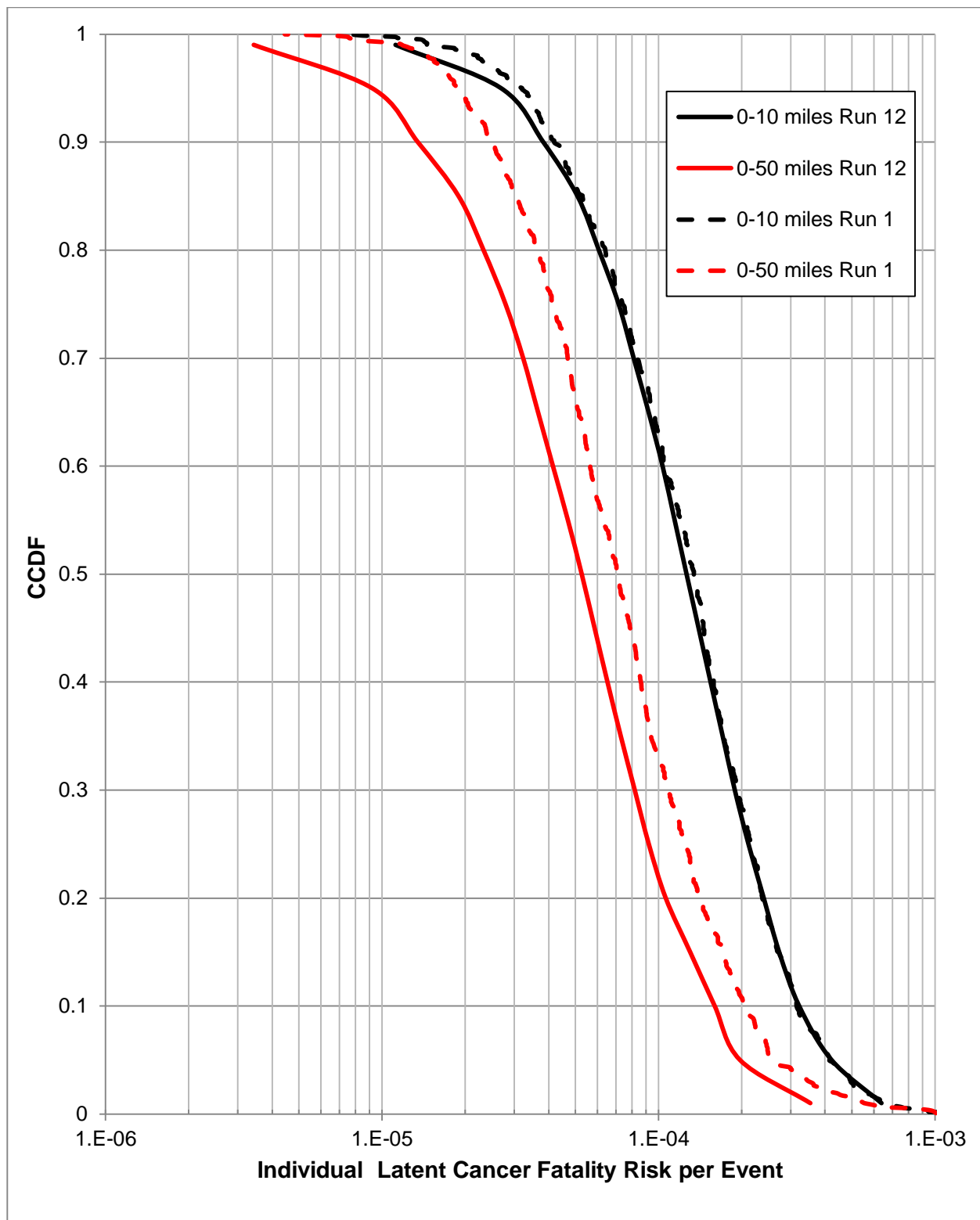


Figure E-12: Run 12 Combined Aleatory and Epistemic Uncertainty Conditional Individual LCF Risk (per Event) CCDF and Run 1 Epistemic Uncertainty Conditional, Mean Individual LCF Risk (per Event) CCDF for the Radial Distances Considered

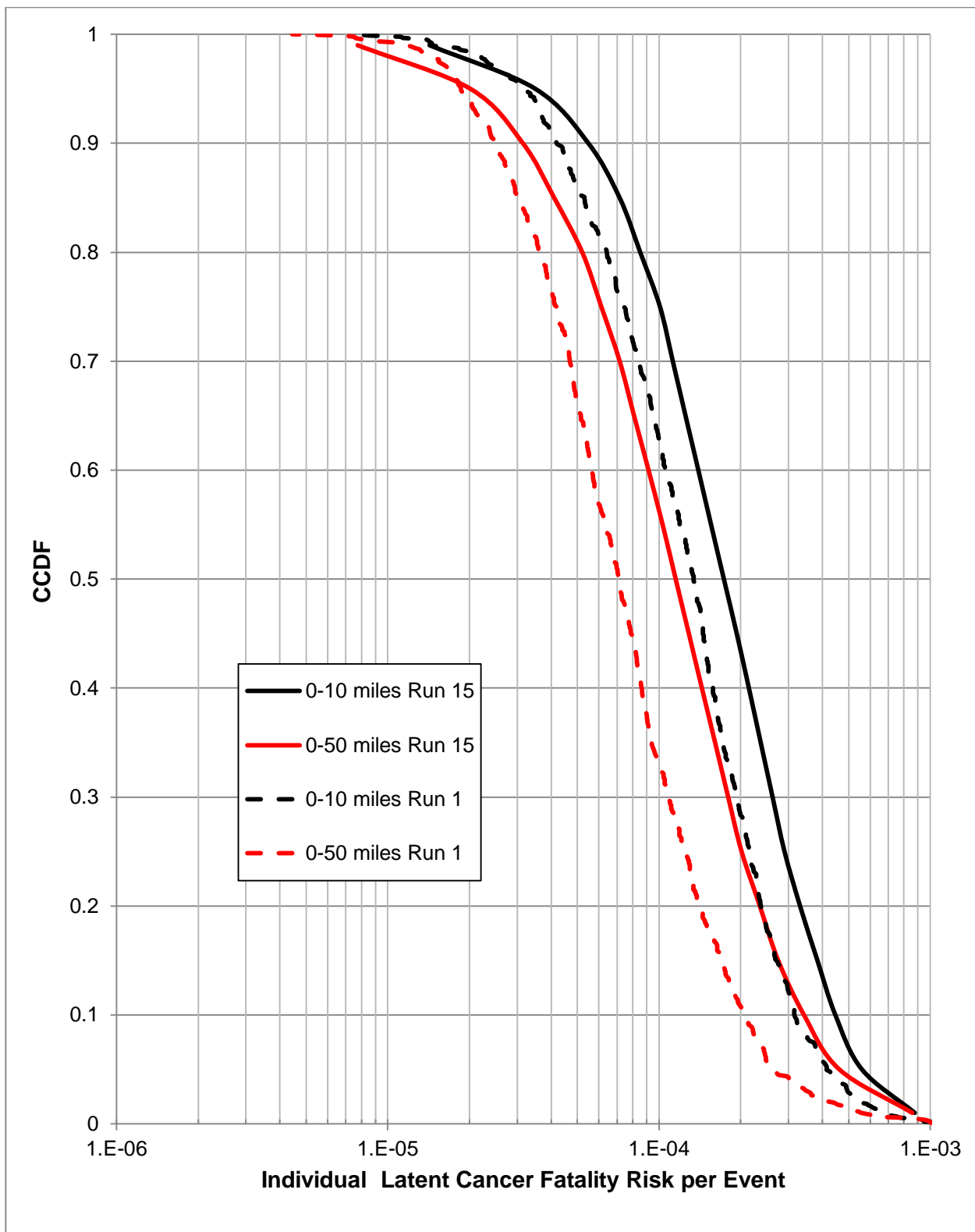


Figure E-13: Run 15 Combined Aleatory and Epistemic Uncertainty Conditional Individual LCF Risk (per Event) CCDF and Run 1 Epistemic Uncertainty Conditional, Mean Individual LCF Risk (per Event) CCDF for the Radial Distances Considered

E.5 Conditional Mean, Individual LCF Risk and Prompt Fatality Risk Results & Model Convergence

To answer ACRS Questions 1 through 4 for the five source terms considered, three LHS runs of 1,000 samples varying all 350 MACCS uncertain input variables were conducted. Table E-6 through Table E-11 provides the mean, conditional LCF risk (per event) statistical results for each of the source terms considered and their associated Runs (i.e., see Table E-1 for a more detailed description of each Run) for all radial distances considered. Figure E-14 through Figure E-18 show the 10- and 50-mile mean, conditional LCF risk (per event) CCDFs for the each source term considered. Again, these figures and tables show that the MACCS results are well converged for the source terms and for the three LHS sets considered. Based on these analyses and those discussed in Section E.4, it is determined that the MACCS model for the SOARCA Uncertainty Analysis for the Peach Bottom LTSBO is convergent with regards to conditional LCF risk for the uncertain inputs considered with respect to mean, conditional LCF risk.

Table E-12 through Table E-17 provides the mean, conditional prompt fatality risk (per event) statistical results for each of the source terms considered and their associated Runs (i.e., see Table E-1 for a more detailed description of each Run) for all radial distances considered. Figure E-19 through Figure E-23 show the 3.5-mile mean, conditional prompt fatality risk (per event) CCDFs for the each source term considered. For Table E-15 and Figure E-21, there is only one non-zero conditional, mean, individual prompt fatality risk data point for Run 9; all other data points for Runs 9-11 are zero. Again, these figures show convergence the MACCS results are for the source terms and for the three LHS sets considered. However, for some of the results (e.g., Runs 12-14) the limited number of non-zero conditional prompt fatality risk samples results in poor statistics and thus do not show a good convergence for the MACCS model. Yet, for the higher source terms considered (e.g., Runs 6-8), there are a sufficient number of non-zero prompt fatality risk results to provide a high confidence in the convergence of the MACCS model for the SOARCA Uncertainty Analysis for the Peach Bottom LTSBO for the uncertain inputs considered with respect to mean, conditional prompt fatality risk.

Table E-6: Conditional, mean, individual LCF risk (per event) average statistics for the MACCS Uncertainty Analysis for five circular areas (Run 1)

	0-10 miles	0-20 miles	0-30 miles	0-40 miles	0-50 miles
Mean	1.7×10^{-4}	2.8×10^{-4}	2.0×10^{-4}	1.3×10^{-4}	1.0×10^{-4}
Median	1.3×10^{-4}	1.9×10^{-4}	1.3×10^{-4}	8.7×10^{-5}	7.1×10^{-5}
5th percentile	3.1×10^{-5}	4.9×10^{-5}	3.4×10^{-5}	2.2×10^{-5}	1.9×10^{-5}
95th percentile	4.2×10^{-4}	7.7×10^{-4}	5.3×10^{-4}	3.4×10^{-4}	2.7×10^{-4}

Table E-7: Runs 3-5 conditional, mean, individual LCF risk (per event) average statistics for five circular areas

Run 3	0-10 miles	0-20 miles	0-30 miles	0-40 miles	0-50 miles
Mean	2.60E-04	8.70E-04	5.93E-04	3.65E-04	2.88E-04
Median	2.29E-04	6.91E-04	4.67E-04	2.91E-04	2.30E-04
5 th percentile	9.08E-05	2.22E-04	1.56E-04	1.04E-04	8.51E-05
95 th percentile	5.19E-04	2.07E-03	1.38E-03	8.22E-04	6.39E-04
Run 4	0-10 miles	0-20 miles	0-30 miles	0-40 miles	0-50 miles
Mean	2.60E-04	8.67E-04	5.89E-04	3.62E-04	2.86E-04
Median	2.24E-04	7.13E-04	4.84E-04	3.02E-04	2.42E-04
5 th percentile	8.77E-05	2.11E-04	1.50E-04	1.00E-04	8.25E-05
95 th percentile	5.50E-04	2.08E-03	1.42E-03	8.51E-04	6.65E-04
Run 5	0-10 miles	0-20 miles	0-30 miles	0-40 miles	0-50 miles
Mean	2.61E-04	8.68E-04	5.91E-04	3.64E-04	2.88E-04
Median	2.27E-04	6.85E-04	4.68E-04	2.95E-04	2.34E-04
5 th percentile	9.18E-05	2.32E-04	1.61E-04	1.04E-04	8.66E-05
95 th percentile	5.62E-04	2.08E-03	1.42E-03	8.32E-04	6.40E-04

Table E-8: Runs 6-8 conditional, mean, individual LCF risk (per event) average statistics for five circular areas

Run 6	0-10 miles	0-20 miles	0-30 miles	0-40 miles	0-50 miles
Mean	2.50E-04	1.33E-03	9.09E-04	5.51E-04	4.30E-04
Median	2.24E-04	1.05E-03	7.12E-04	4.32E-04	3.34E-04
5 th percentile	9.57E-05	2.80E-04	1.95E-04	1.22E-04	9.79E-05
95 th percentile	4.92E-04	3.35E-03	2.28E-03	1.36E-03	1.06E-03
Run 7	0-10 miles	0-20 miles	0-30 miles	0-40 miles	0-50 miles
Mean	2.50E-04	1.33E-03	9.04E-04	5.47E-04	4.27E-04
Median	2.20E-04	1.08E-03	7.30E-04	4.43E-04	3.45E-04
5 th percentile	9.00E-05	2.73E-04	1.87E-04	1.21E-04	9.81E-05
95 th percentile	5.10E-04	3.36E-03	2.32E-03	1.39E-03	1.07E-03
Run 8	0-10 miles	0-20 miles	0-30 miles	0-40 miles	0-50 miles
Mean	2.50E-04	1.33E-03	9.07E-04	5.50E-04	4.29E-04
Median	2.19E-04	1.01E-03	6.89E-04	4.16E-04	3.27E-04
5 th percentile	9.33E-05	2.95E-04	1.99E-04	1.32E-04	1.05E-04
95 th percentile	5.23E-04	3.26E-03	2.26E-03	1.35E-03	1.04E-03

Table E-9: Runs 9-11 conditional, mean, individual LCF risk (per event) statistics for five circular areas

Run 9	0-10 miles	0-20 miles	0-30 miles	0-40 miles	0-50 miles
Mean	1.07E-04	1.18E-04	8.26E-05	5.41E-05	4.44E-05
Median	8.75E-05	1.03E-04	7.21E-05	4.73E-05	3.85E-05
5 th percentile	2.34E-05	3.78E-05	2.68E-05	1.74E-05	1.36E-05
95 th percentile	2.52E-04	2.40E-04	1.69E-04	1.10E-04	8.89E-05

Run 10	0-10 miles	0-20 miles	0-30 miles	0-40 miles	0-50 miles
Mean	1.07E-04	1.18E-04	8.25E-05	5.40E-05	4.43E-05
Median	8.57E-05	1.05E-04	7.36E-05	4.82E-05	3.93E-05
5 th percentile	2.24E-05	3.78E-05	2.65E-05	1.71E-05	1.39E-05
95 th percentile	2.58E-04	2.41E-04	1.71E-04	1.16E-04	9.51E-05

Run 11	0-10 miles	0-20 miles	0-30 miles	0-40 miles	0-50 miles
Mean	1.07E-04	1.18E-04	8.27E-05	5.41E-05	4.44E-05
Median	8.75E-05	1.03E-04	7.22E-05	4.68E-05	3.85E-05
5 th percentile	2.30E-05	3.98E-05	2.72E-05	1.78E-05	1.42E-05
95 th percentile	2.67E-04	2.39E-04	1.70E-04	1.13E-04	9.38E-05

Table E-10: Runs 12-14 conditional, mean, individual LCF risk (per event) average statistics for five circular areas

Run 12	0-10 miles	0-20 miles	0-30 miles	0-40 miles	0-50 miles
Mean	1.58E-04	1.92E-04	1.33E-04	8.59E-05	7.01E-05
Median	1.35E-04	1.69E-04	1.17E-04	7.53E-05	6.13E-05
5 th percentile	4.10E-05	6.52E-05	4.55E-05	2.88E-05	2.38E-05
95 th percentile	3.43E-04	3.95E-04	2.73E-04	1.80E-04	1.44E-04

Run 13	0-10 miles	0-20 miles	0-30 miles	0-40 miles	0-50 miles
Mean	1.59E-04	1.93E-04	1.33E-04	8.60E-05	7.01E-05
Median	1.31E-04	1.72E-04	1.18E-04	7.69E-05	6.24E-05
5 th percentile	4.10E-05	6.56E-05	4.59E-05	2.91E-05	2.40E-05
95 th percentile	3.64E-04	3.91E-04	2.69E-04	1.76E-04	1.46E-04

Run 14	0-10 miles	0-20 miles	0-30 miles	0-40 miles	0-50 miles
Mean	1.59E-04	1.92E-04	1.33E-04	8.61E-05	7.03E-05
Median	1.35E-04	1.69E-04	1.16E-04	7.53E-05	6.15E-05
5 th percentile	4.18E-05	6.71E-05	4.54E-05	2.88E-05	2.38E-05
95 th percentile	3.63E-04	3.93E-04	2.73E-04	1.75E-04	1.44E-04

Table E-11: Runs 15-17 conditional, mean, individual LCF risk (per event) average statistics for five circular areas

Run 15	0-10 miles	0-20 miles	0-30 miles	0-40 miles	0-50 miles
Mean	2.19E-04	4.18E-04	3.01E-04	1.94E-04	1.57E-04
Median	1.85E-04	3.57E-04	2.59E-04	1.70E-04	1.38E-04
5th percentile	5.86E-05	1.41E-04	1.00E-04	6.42E-05	5.30E-05
95th percentile	4.72E-04	8.87E-04	6.44E-04	4.15E-04	3.37E-04

Run 16	0-10 miles	0-20 miles	0-30 miles	0-40 miles	0-50 miles
Mean	2.19E-04	4.17E-04	3.00E-04	1.94E-04	1.57E-04
Median	1.82E-04	3.71E-04	2.65E-04	1.72E-04	1.38E-04
5th percentile	5.94E-05	1.34E-04	9.63E-05	6.18E-05	5.10E-05
95th percentile	4.93E-04	8.59E-04	6.32E-04	3.98E-04	3.22E-04

Run 17	0-10 miles	0-20 miles	0-30 miles	0-40 miles	0-50 miles
Mean	2.19E-04	4.17E-04	3.01E-04	1.94E-04	1.57E-04
Median	1.86E-04	3.64E-04	2.59E-04	1.68E-04	1.37E-04
5th percentile	5.95E-05	1.39E-04	1.00E-04	6.28E-05	5.08E-05
95th percentile	5.04E-04	8.55E-04	6.25E-04	4.05E-04	3.27E-04

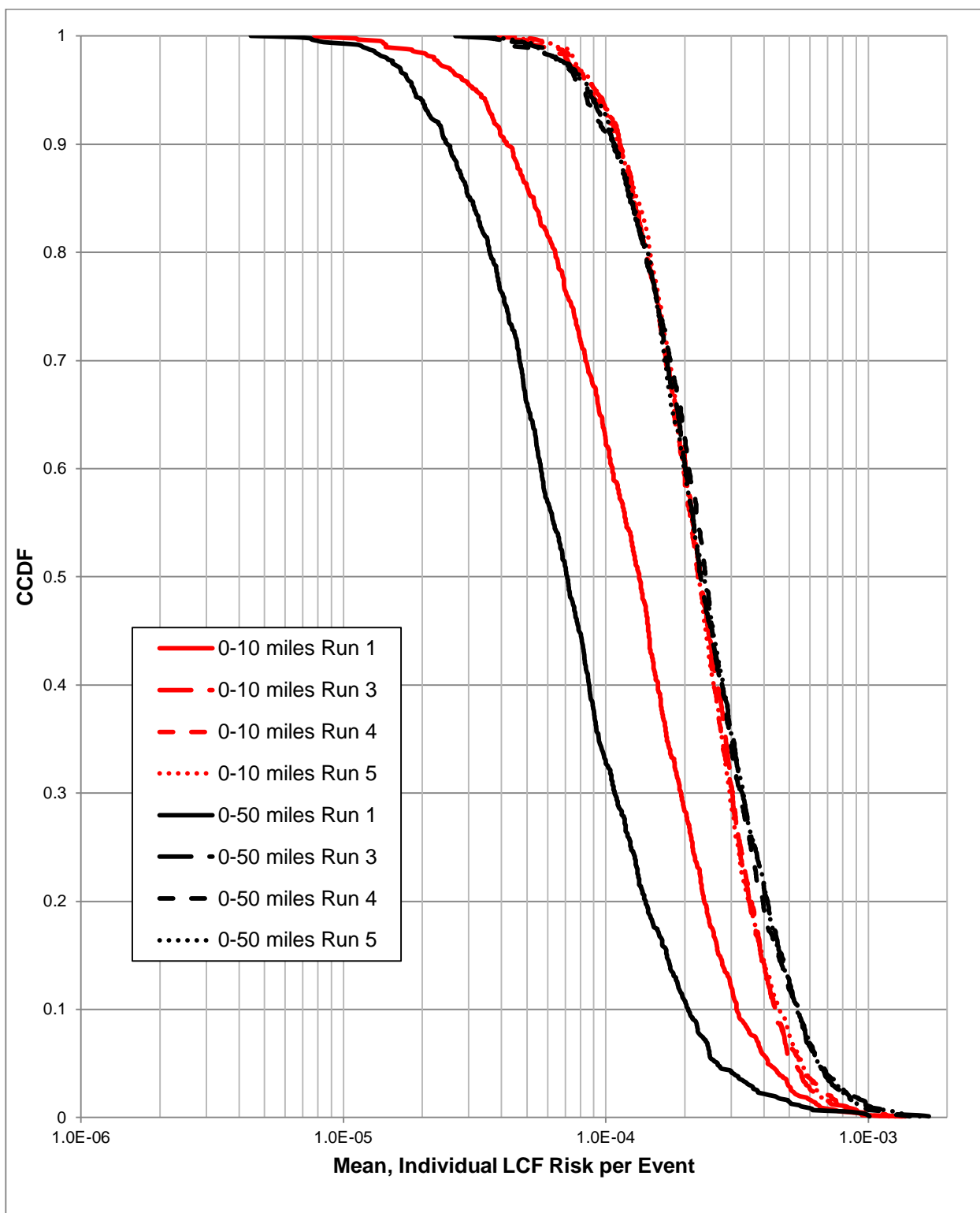


Figure E-14: Runs 3-5 Epistemic Uncertainty Conditional, Mean, Individual LCF Risk (per Event) CCDFs and Run 1 Epistemic Uncertainty Conditional, Mean Individual LCF Risk (per Event) CCDF for the Radial Distances Considered

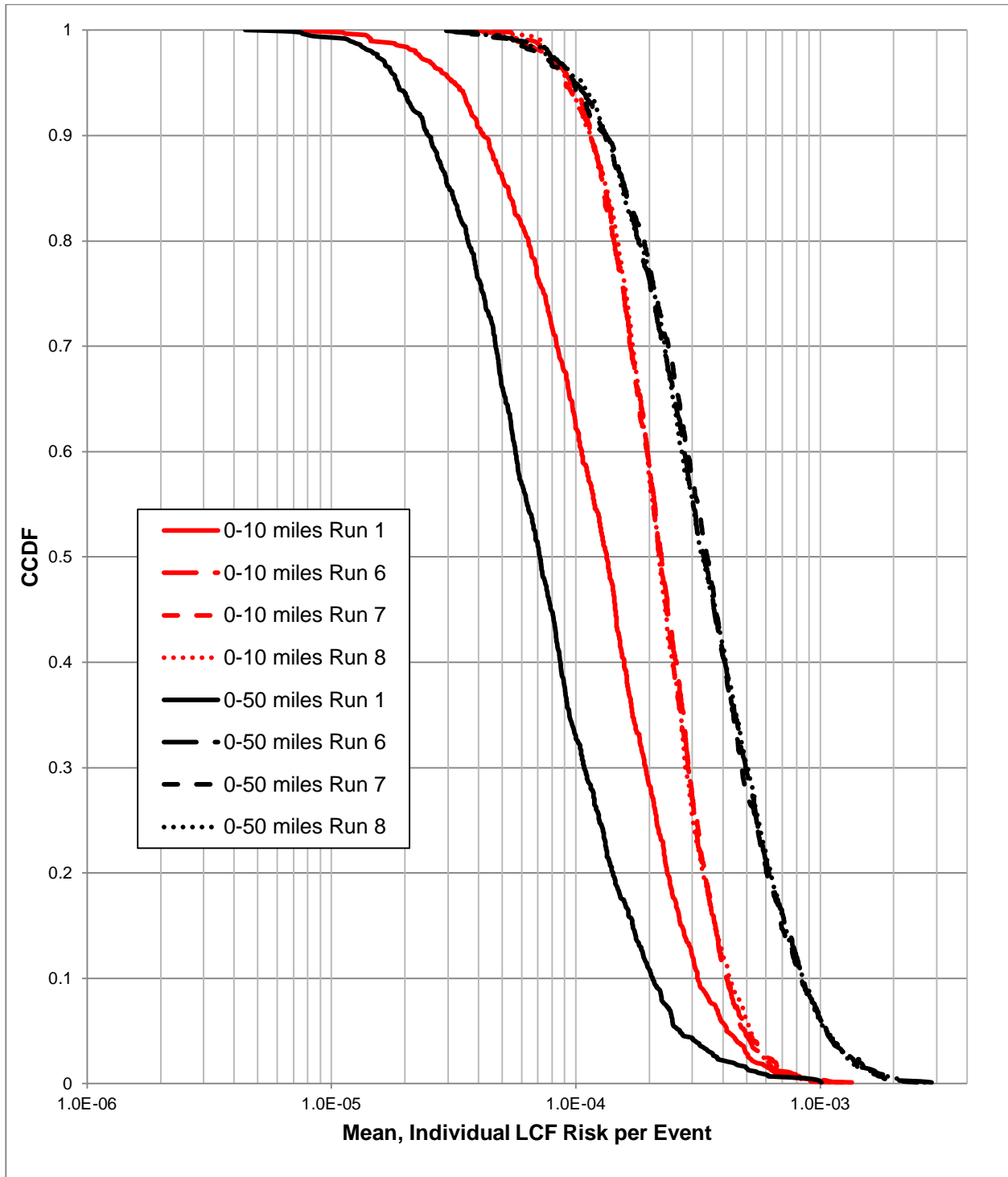


Figure E-15: Runs 6-8 Epistemic Uncertainty Conditional, Mean, Individual LCF Risk (per Event) CCDFs and Run 1 Epistemic Uncertainty Conditional, Mean Individual LCF Risk (per Event) CCDF for the Radial Distances Considered

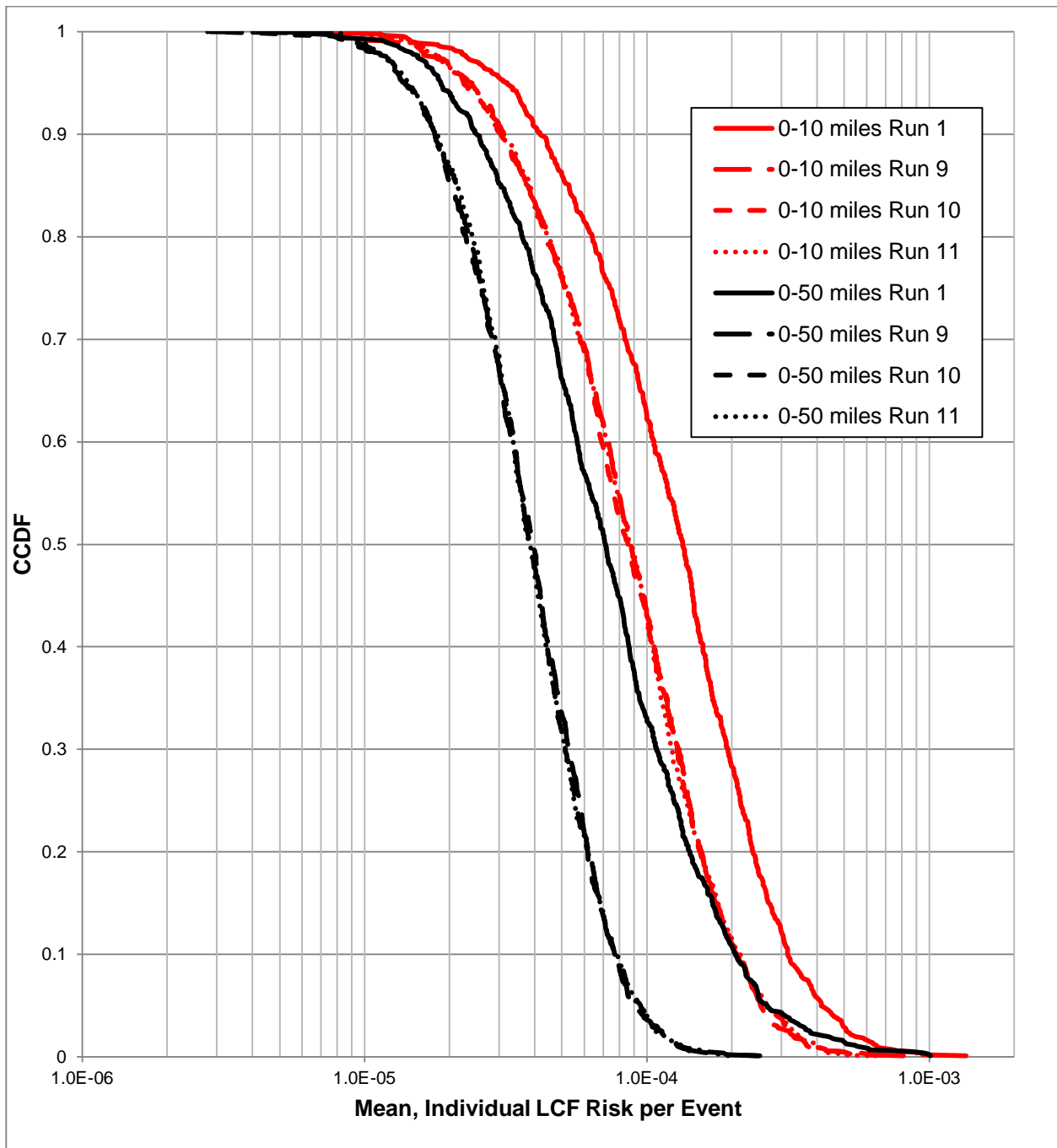


Figure E-16: Runs 9-11 Epistemic Uncertainty Conditional, Mean, Individual LCF Risk (per Event) CCDFs and Run 1 Epistemic Uncertainty Conditional, Mean Individual LCF Risk (per Event) CCDF for the Radial Distances Considered

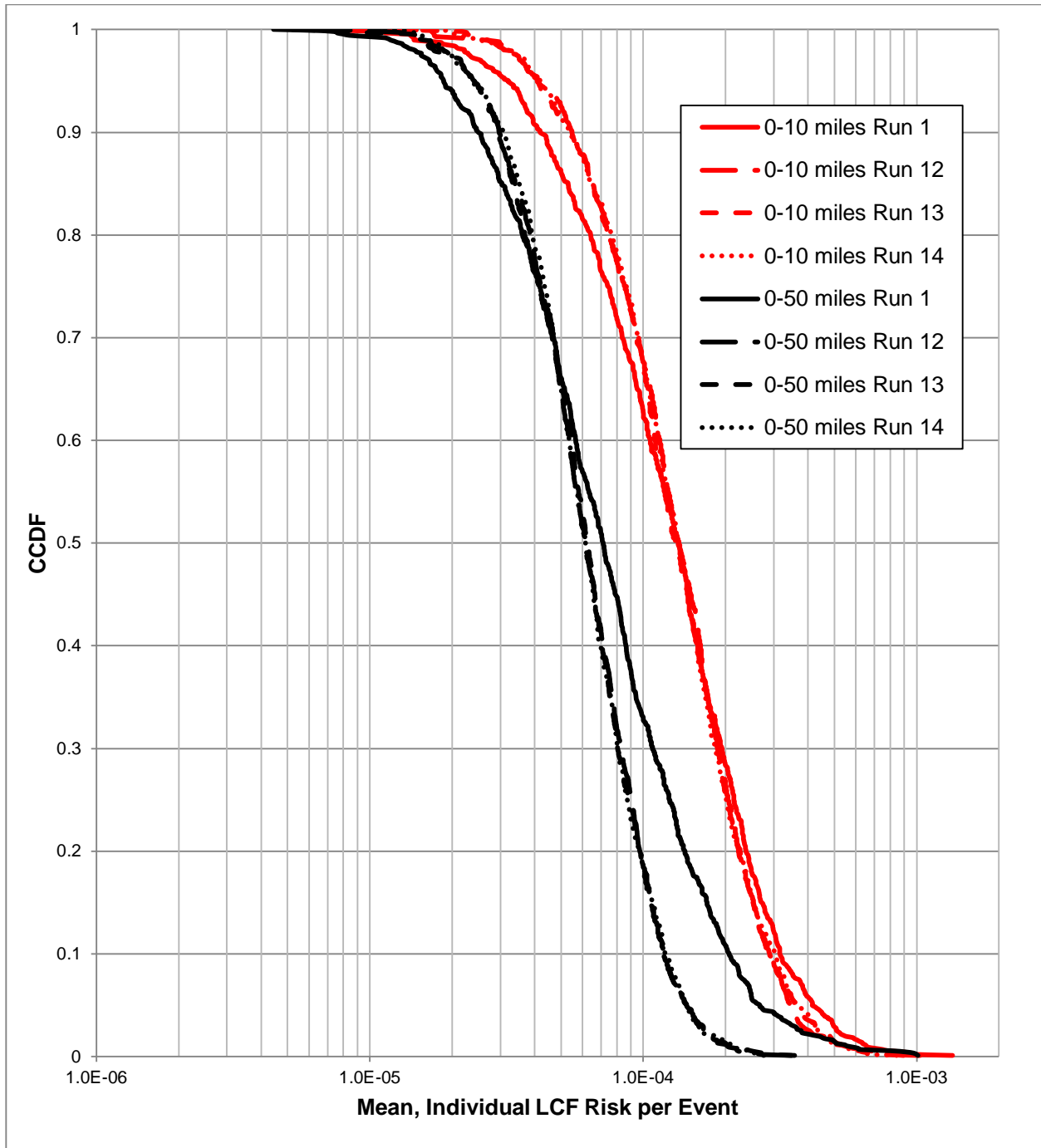


Figure E-17: Runs 12-14 Epistemic Uncertainty Conditional, Mean, Individual LCF Risk (per Event) CCDFs and Run 1 Epistemic Uncertainty Conditional, Mean Individual LCF Risk (per Event) CCDF for the Radial Distances Considered

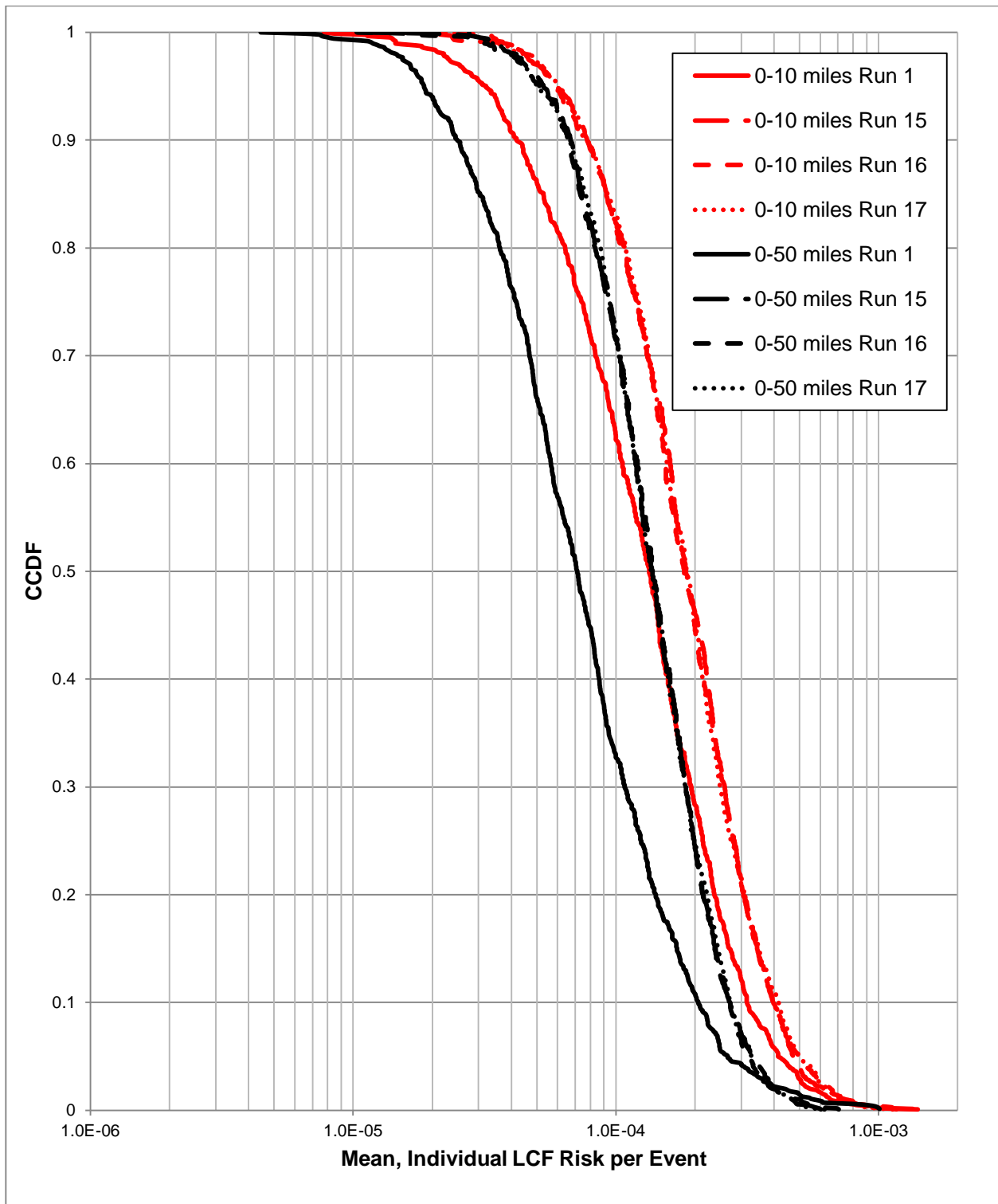


Figure E-18: Runs 15-17 Epistemic Uncertainty Conditional, Mean, Individual LCF Risk (per Event) CCDFs and Run 1 Epistemic Uncertainty Conditional, Mean Individual LCF Risk (per Event) CCDF for the Radial Distances Considered

Table E-12: Conditional, mean, individual prompt-fatality risk (per event) average statistics for the MACCS Uncertainty Analysis for specified circular areas (Run 1)

	0-3.5 miles	0-7 miles	0-10 miles
Mean	3.5x10 ⁻⁸	8.3x10 ⁻⁹	4.8x10 ⁻⁹
Median	0.0	0.0	0.0
75 th percentile	0.0	0.0	0.0
95 th percentile	0.0	0.0	0.0

Table E-13: Run 3-5 conditional, mean, individual prompt-fatality risk (per event) average statistics for specified circular areas

Run 3	0-3.5 miles	0-7 miles	0-10 miles
Mean	3.42E-07	4.69E-08	9.53E-09
Median	0.0	0.0	0.0
75 th percentile	2.02E-07	3.84E-09	0.0
95 th percentile	1.53E-06	2.13E-07	1.24E-08
Run 4	0-3.5 miles	0-7 miles	0-10 miles
Mean	2.98E-07	4.18E-08	8.86E-09
Median	0.0	0.0	0.0
75 th percentile	2.22E-07	1.11E-08	0.0
95 th percentile	1.75E-06	2.33E-07	0.0
Run 5	0-3.5 miles	0-7 miles	0-10 miles
Mean	3.04E-07	4.67E-08	1.25E-08
Median	0.0	0.0	0.0
75 th percentile	1.94E-07	8.17E-09	0.0
95 th percentile	1.59E-06	2.06E-07	0.0

Table E-14: Run 6-8 conditional, mean, individual prompt-fatality risk (per event) average statistics for specified circular areas

Run 6	0-3.5 miles	0-7 miles	0-10 miles
Mean	7.44E-07	1.25E-07	3.12E-08
Median	1.25E-07	0.0	0.0
75th percentile	8.56E-07	9.84E-08	0.0
95th percentile	3.01E-06	5.52E-07	1.74E-07
Run 7	0-3.5 miles	0-7 miles	0-10 miles
Mean	6.68E-07	1.12E-07	2.92E-08
Median	1.30E-07	0.0	0.0
75th percentile	7.95E-07	9.42E-08	0.0
95th percentile	3.11E-06	5.50E-07	1.84E-07
Run 8	0-3.5 miles	0-7 miles	0-10 miles
Mean	6.99E-07	1.29E-07	4.08E-08
Median	1.25E-07	0.0	0.0
75th percentile	7.96E-07	8.64E-08	0.0
95th percentile	3.34E-06	5.37E-07	1.65E-07

Table E-15: Run 9-11 conditional, mean, individual prompt-fatality risk (per event) average statistics for specified circular areas

Run 9	0-3.5 miles	0-7 miles	0-10 miles
Mean	5.38E-11	0.0	0.0
Median	0.0	0.0	0.0
75th percentile	0.0	0.0	0.0
95th percentile	0.0	0.0	0.0
Run 10	0-3.5 miles	0-7 miles	0-10 miles
Mean	0.0	0.0	0.0
Median	0.0	0.0	0.0
75th percentile	0.0	0.0	0.0
95th percentile	0.0	0.0	0.0
Run 11	0-3.5 miles	0-7 miles	0-10 miles
Mean	0.0	0.0	0.0
Median	0.0	0.0	0.0
75th percentile	0.0	0.0	0.0
95th percentile	0.0	0.0	0.0

Table E-16: Run 12-14 conditional, mean, individual prompt-fatality risk (per event) average statistics for specified circular areas

Run 12	0-3.5 miles	0-7 miles	0-10 miles
Mean	1.67E-09	3.49E-10	0.0
Median	0.0	0.0	0.0
75th percentile	0.0	0.0	0.0
95th percentile	0.0	0.0	0.0
Run 13	0-3.5 miles	0-7 miles	0-10 miles
Mean	1.28E-11	3.24E-10	0.0
Median	0.0	0.0	0.0
75th percentile	0.0	0.0	0.0
95th percentile	0.0	0.0	0.0
Run 14	0-3.5 miles	0-7 miles	0-10 miles
Mean	7.48E-10	1.84E-10	0.0
Median	0.0	0.0	0.0
75th percentile	0.0	0.0	0.0
95th percentile	0.0	0.0	0.0

Table E-17: Run 15-17 conditional, mean, individual prompt-fatality risk (per event) average statistics for specified circular areas

Run 15	0-3.5 miles	0-7 miles	0-10 miles
Mean	1.87E-08	2.19E-09	2.66E-10
Median	0.0	0.0	0.0
75th percentile	0.0	0.0	0.0
95th percentile	0.0	0.0	0.0
Run 16	0-3.5 miles	0-7 miles	0-10 miles
Mean	2.24E-08	2.44E-09	2.79E-10
Median	0.0	0.0	0.0
75th percentile	0.0	0.0	0.0
95th percentile	0.0	0.0	0.0
Run 17	0-3.5 miles	0-7 miles	0-10 miles
Mean	1.33E-08	1.26E-09	7.09E-11
Median	0.0	0.0	0.0
75th percentile	0.0	0.0	0.0
95th percentile	0.0	0.0	0.0

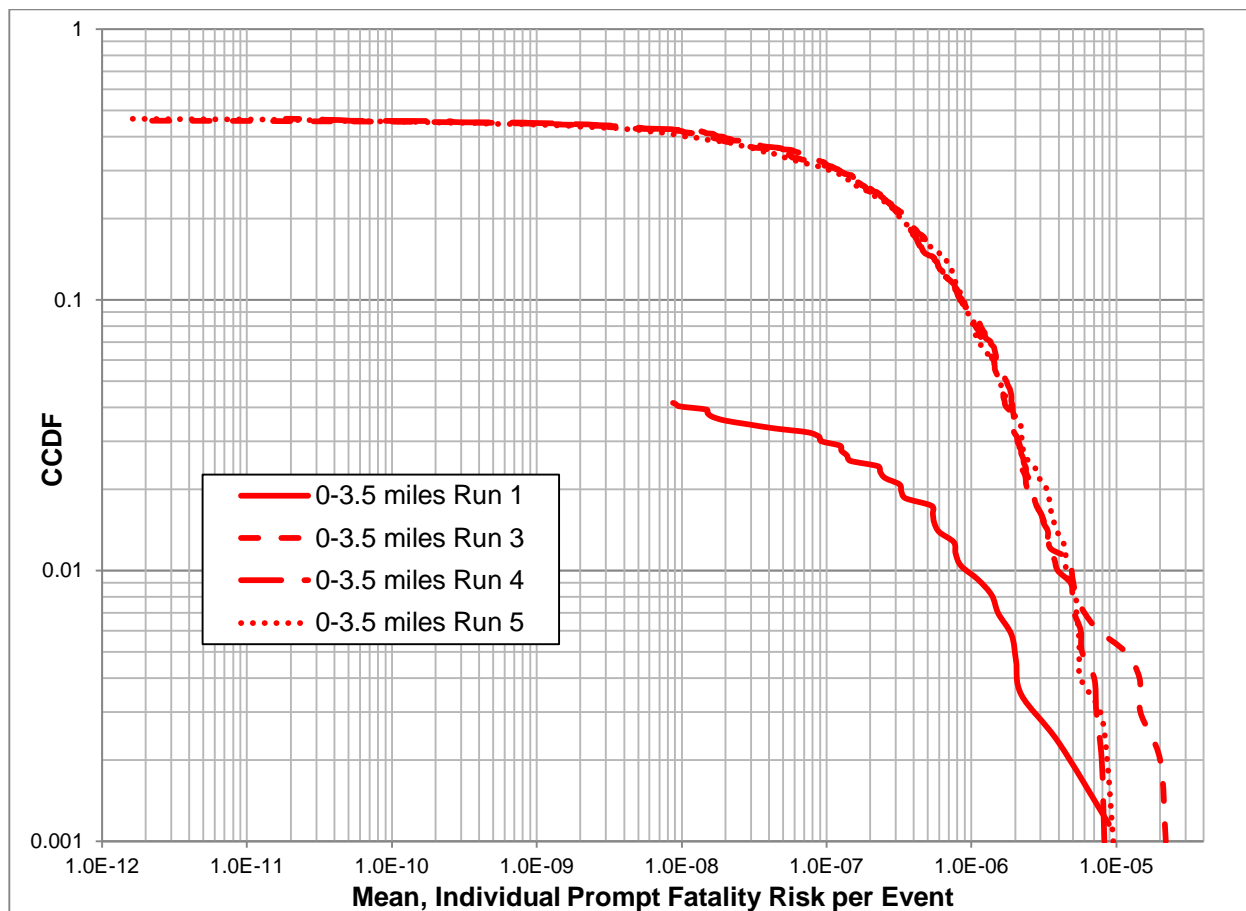


Figure E-19: Runs 3-5 Epistemic Uncertainty Conditional, Mean, Individual Prompt Fatality Risk (per Event) CCDFs and Run 1 Epistemic Uncertainty Conditional, Mean Individual Prompt Fatality Risk (per Event) CCDF for the Radial Distances Considered

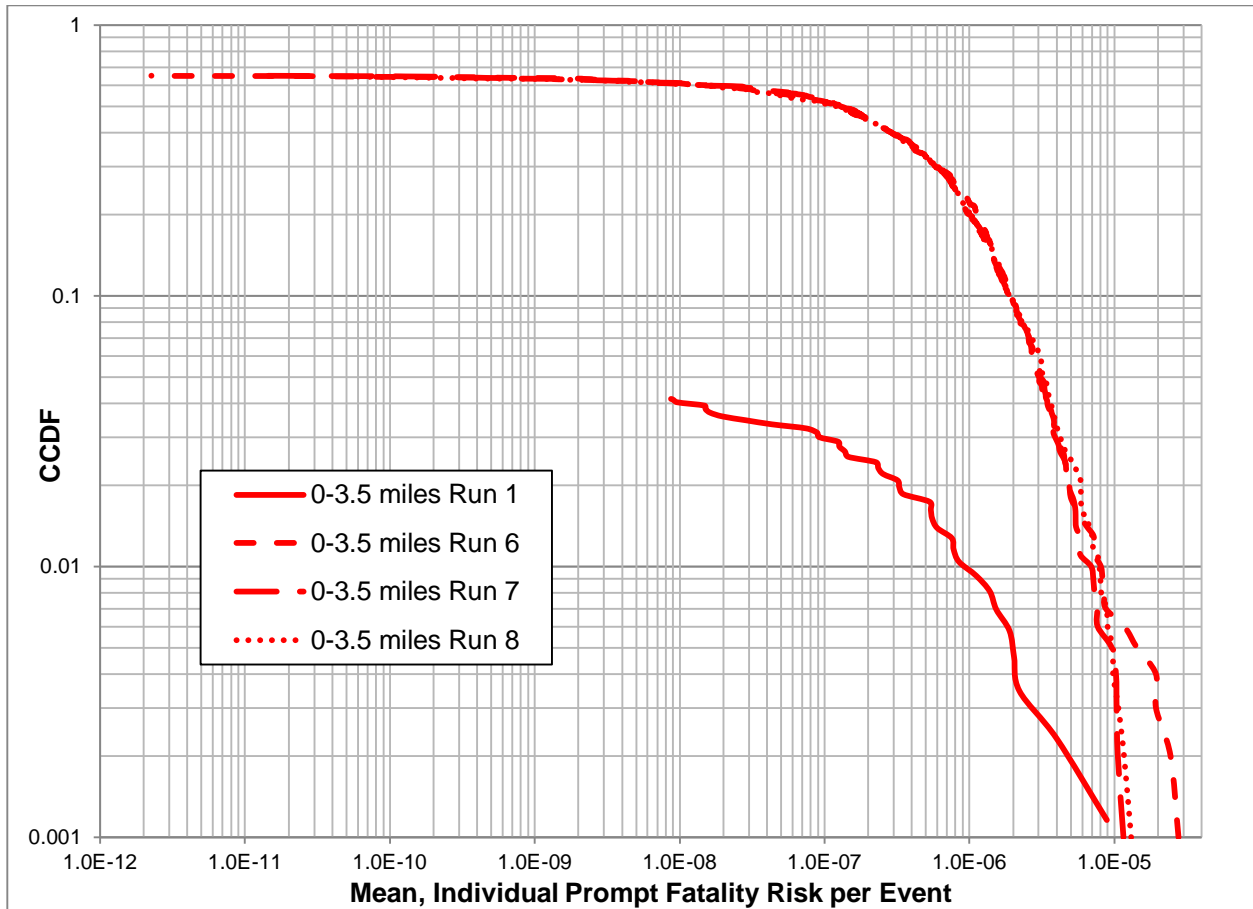


Figure E-20: Runs 6-8 Epistemic Uncertainty Conditional, Mean, Individual Prompt Fatality Risk (per Event) CCDFs and Run 1 Epistemic Uncertainty Conditional, Mean Individual Prompt Fatality Risk (per Event) CCDF for the Radial Distances Considered

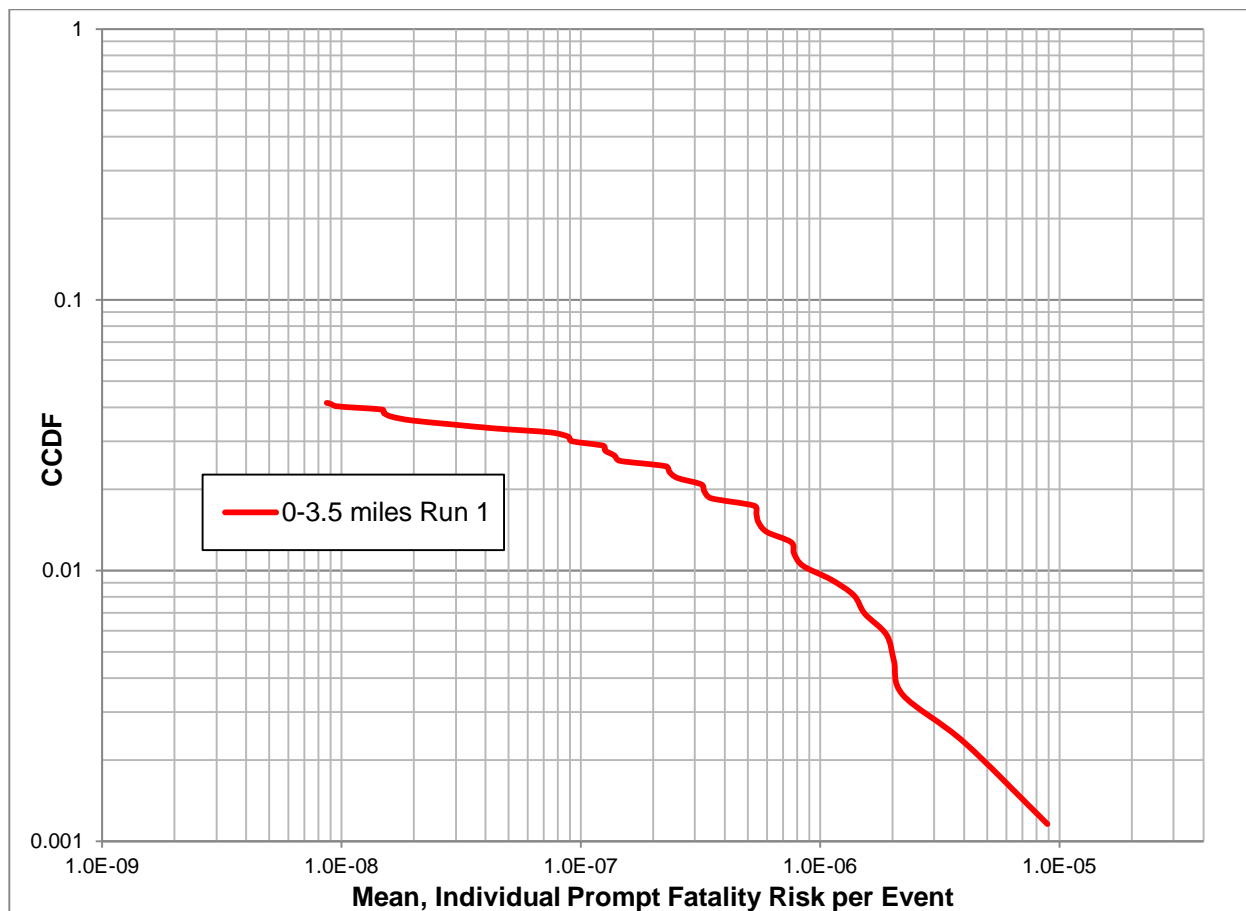


Figure E-21: Runs 9-11 Epistemic Uncertainty Conditional, Mean, Individual Prompt Fatality Risk (per Event) CCDFs and Run 1 Epistemic Uncertainty Conditional, Mean Individual Prompt Fatality Risk (per Event) CCDF for the Radial Distances Considered

Note: There is only one non-zero conditional, mean, individual prompt fatality risk data point for Run 9; all other data points for Runs 9-11 are zero.

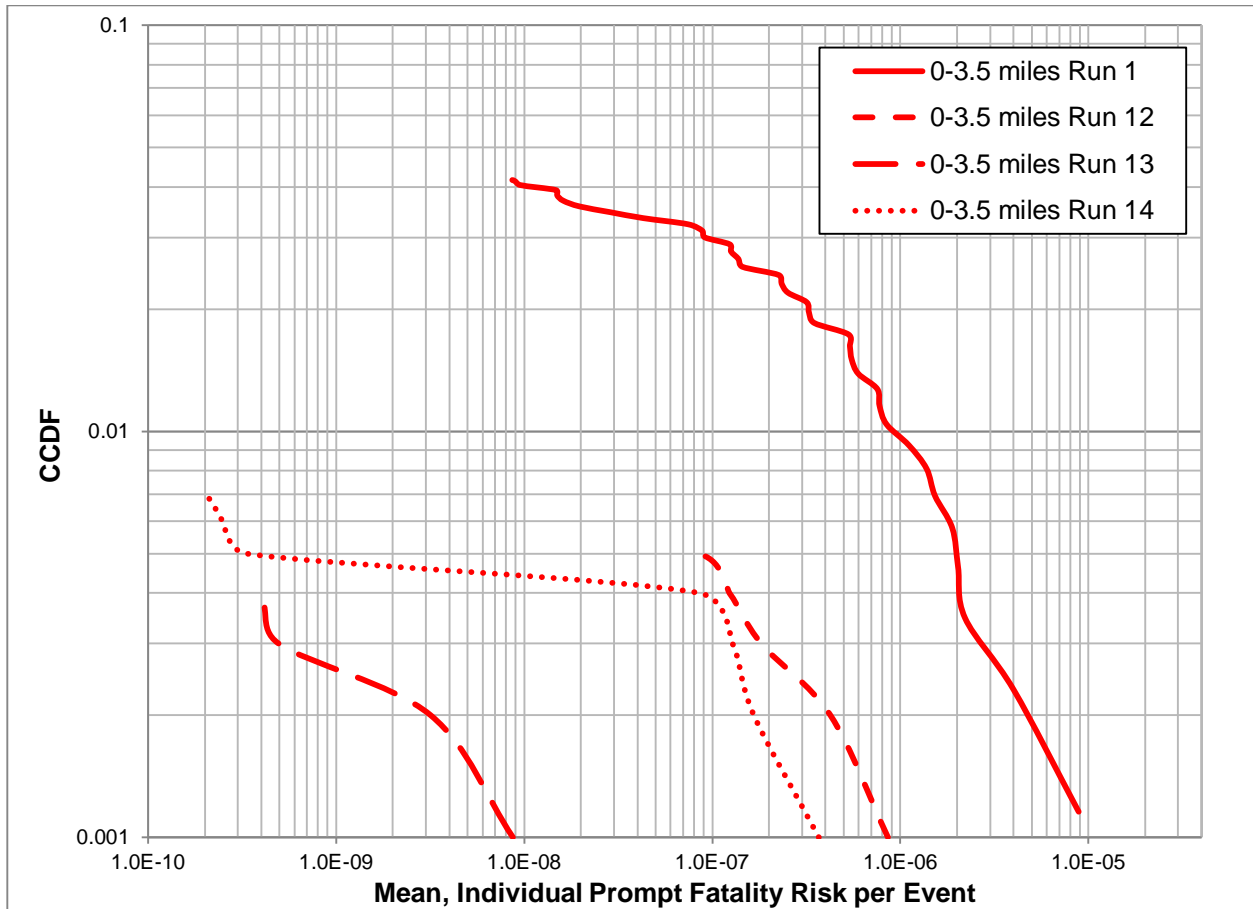


Figure E-22: Runs 12-14 Epistemic Uncertainty Conditional, Mean, Individual Prompt Fatality Risk (per Event) CCDFs and Run 1 Epistemic Uncertainty Conditional, Mean Individual Prompt Fatality Risk (per Event) CCDF for the Radial Distances Considered

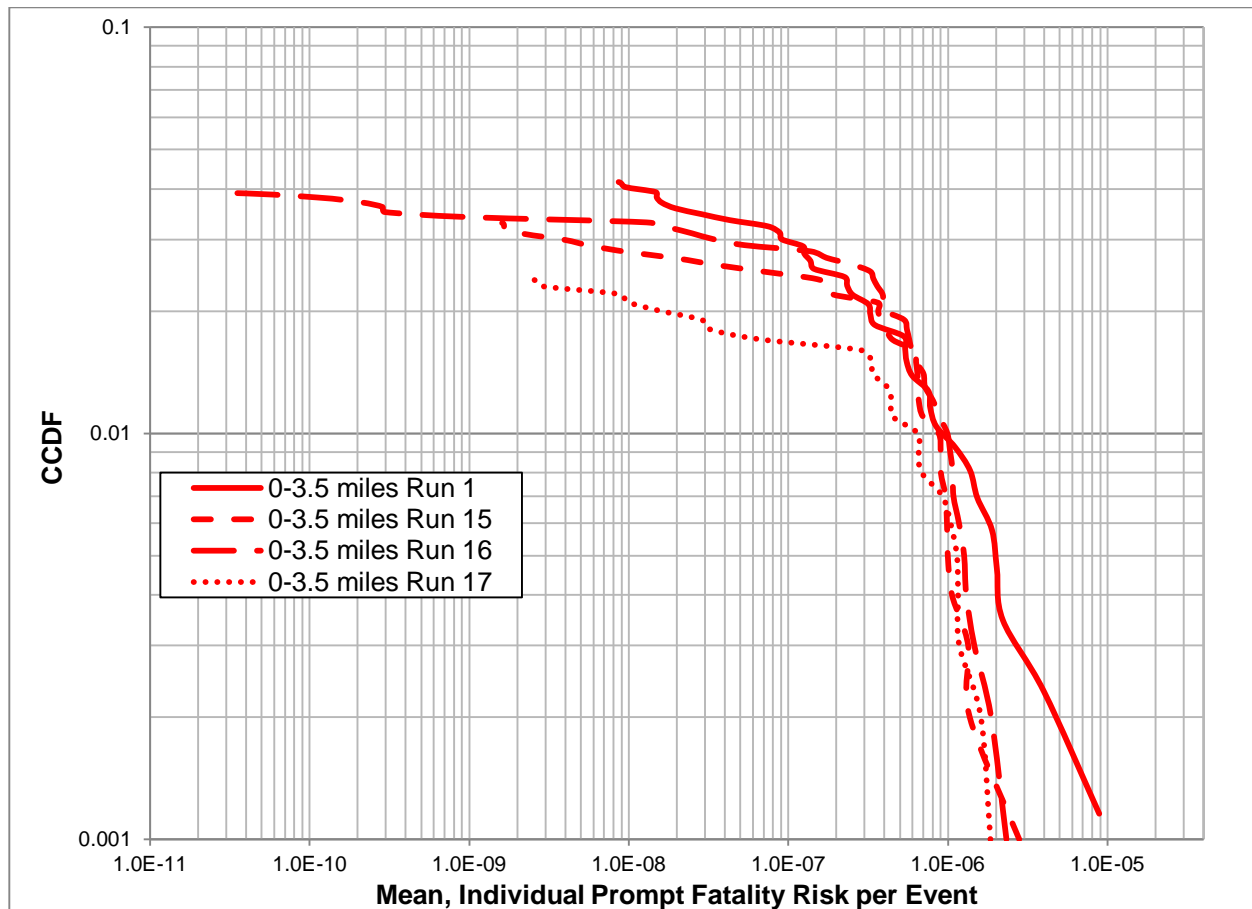


Figure E-23: Runs 15-17 Epistemic Uncertainty Conditional, Mean, Individual Prompt Fatality Risk (per Event) CCDFs and Run 1 Epistemic Uncertainty Conditional, Mean Individual Prompt Fatality Risk (per Event) CCDF for the Radial Distances Considered

E.6 SOARCA Uncertainty Analysis Results for Conditional Individual LCF Risk

Figure E-24 shows Section 6.2 results (i.e., solid lines) for mean, individual LCF risk, and the combined aleatory and epistemic uncertainty (i.e., dashed lines) between the 1st and 99th percentile for individual LCF risk at the 10-, 20-, and 50-mile radial distances. Table E-18 shows the percent difference between the results presented in Figure E-24 at specified percentiles for the radial distances considered. In Figure E-24 for solid lines, what is displayed is an expected value over aleatory results, and for the dashed line, it is not.

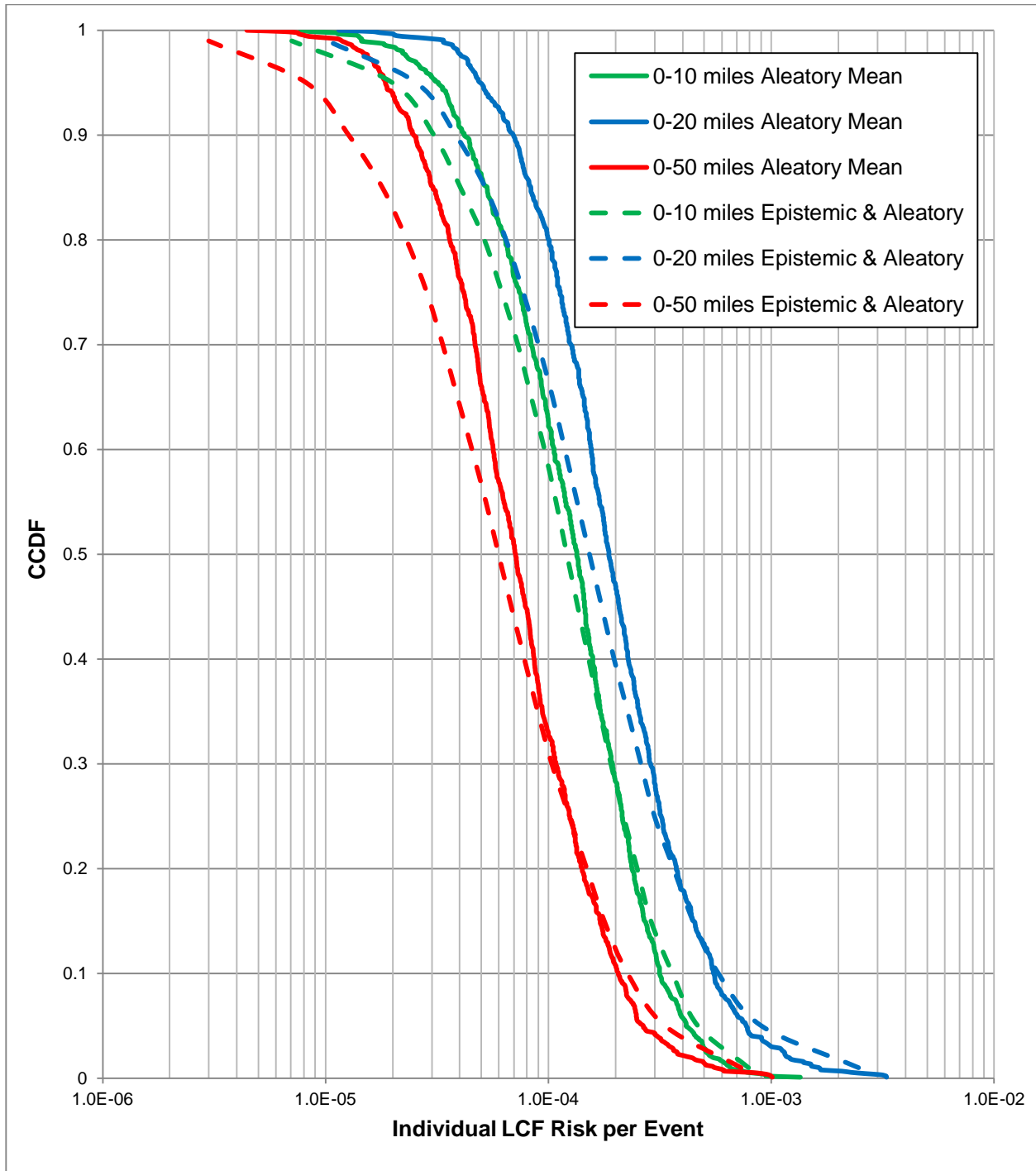


Figure E-24: Run 1 Combined Aleatory and Epistemic Uncertainty Conditional Individual LCF Risk (per Event) CCDF and Run 1 Epistemic Uncertainty Conditional, Mean, Individual LCF Risk (per Event) CCDF for the Radial Distances Considered

Table E-18: Percent Difference in the CDF between the Combined Aleatory and Epistemic Uncertainty LCF Risk to Mean Aleatory Uncertainty LCF Risk for Specified Radial Distances

Percentile	0-10 miles	0-20 miles	0-50 miles
99 th	17%	34%	24%
95 th	11%	14%	20%
80 th	5%	3%	4%
60 th	4%	14%	10%
50 th	10%	18%	16%
40 th	9%	24%	20%
20 th	19%	36%	36%
5 th	38%	48%	56%
1 st	51%	70%	74%

E.7 Stability Analysis Using Bootstrap Approach

The 'high' source term (i.e., Replicate 1 Realization 290) has been selected to be used for a comparison between Simple Random Sampling (SRS) and Latin Hypercube Sampling (LHS) in order to validate the use of LHS. In addition to the three MACCS runs replicates of size 1000 each using LHS (i.e., Runs 15-17 in Table E-1), another set of three replicates has been run using same sample size and random seed, but with SRS.

Conditional, mean, individual LCF risks (per event) for the 10-mile the 50-mile radial distance have been considered for this analysis. Each CDF has been estimated three times using a different random seed (i.e., Runs 15-17 in Table E-1 using SRS). Bootstrapping has been used on each of the three replicated CDFs, and for each distance radius considered, to generate a distribution of 1000 possible CDFs. This set of CDFs was used to estimate a 95% confidence interval (the confidence interval being centered, the 2.5th and 97.5th percentiles were used) for each replicate. These results are presented in Figure E-25 through Figure E-30 (note for these figures CAP 37 is Run 15 with SRS, CAP 38 is Run 16 with SRS, and CAP 39 is Run 17 with SRS).

In order to estimate the stability of results, one replicate's CDF is displayed along with the confidence intervals for the two other replicates. Having the replicate CDF within the confidence interval defined by two other replicates (i.e., the other two replicates used a different random seed) can be considered a good test of stability.

Furthermore, the distribution of mean value based on bootstrap has been displayed for all three replicates, with the density estimated via binning for one of the replicates (Run 15 with SRS). This is presented in Figure E-31 and Figure E-32 for the 10-mile and 50-mile radial distances, respectively. This comparison also informs on the stability of the mean result for a sample of size 1000. Two things are considered at this level:

1. How close are the means, and
2. How close to a normal distribution is the density function, as the distribution of mean should tend to normal according to central limit theorem.

Several analyses have demonstrated the faster convergence of LHS results compared to SRS (i.e., see Reference [E.2] for an example). One of the limitations of LHS compared to SRS is, however, with respect to the use of bootstrapping to estimate confidence intervals over estimators. Bootstrapping assumes that the set of observations used is from an independent and identically distributed population. While the LHS stratification enforces the identical distribution, it violates the independency statement; as each stratum is only used once. This means that each stratum already used cannot be used again and such action creates dependency in the sampling.

While it would be hard to prove theoretically that the use of bootstrapping on LHS results is appropriate, an original sample size of 1000 can be considered large enough so that a selection of values (with replacement) will still lead to a good representation of the uncertainty in the CDF. Thus, bootstrapping has been used on the LHS results for Runs 15-17 in the same way it was used on SRS results in order to compare the stability and check if indeed the LHS results look more stable than conditional, mean, individual, LCF risk (per event) results when the same sample size is used. These results are presented in Figure E-33 through Figure E-38 for the 10-mile and 50-mile radial distances (recall from Table E-1 CAP 34 is Run 15, CAP 35 is Run 16, and CAP 36 is Run 17).

The distribution of mean value based on bootstrap has been displayed for all three replicates, with the density estimated via binning for one of the replicates (Run 15 with LHS). This is presented in Figure E-39 and Figure E-40 for the 10-mile and 50-mile radial distances, respectively.

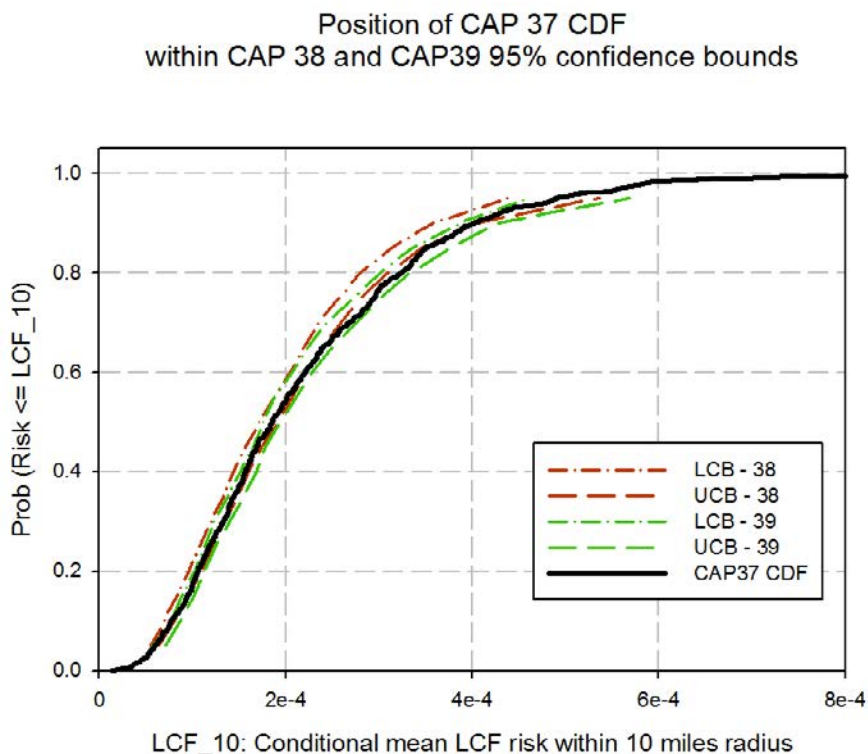
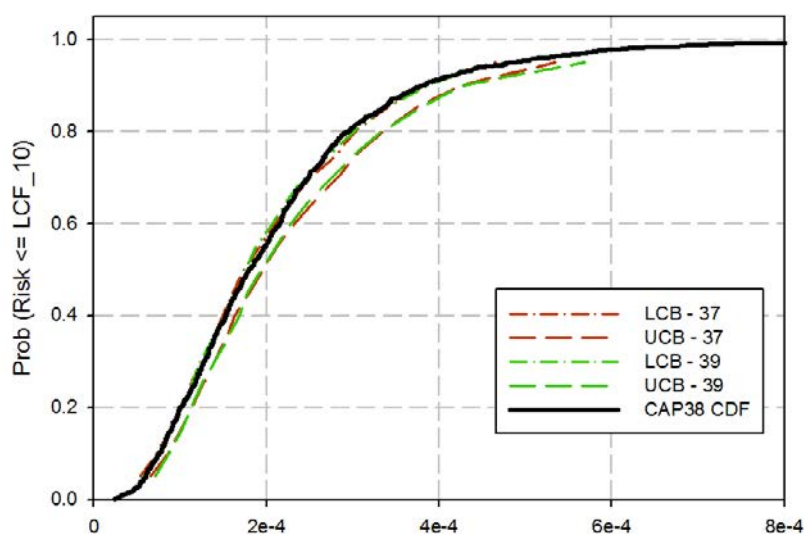


Figure E-25: 10-mile Conditional, Mean, Individual LCF Risk (per Event) CDF for Run 15 with SRS and 95% Confidence Interval Upper and Lower Bounds for Runs 16 & 17 with SRS

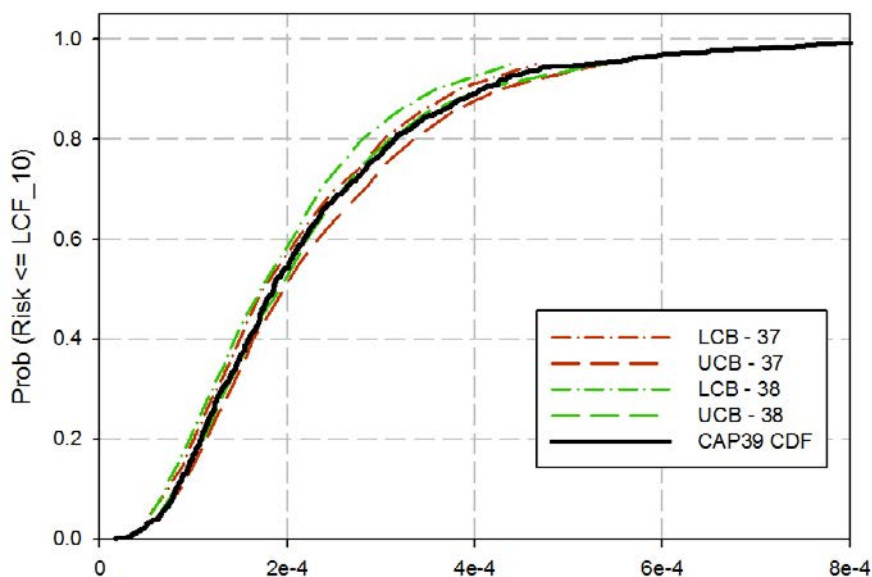
Position of CAP 38 CDF
within CAP 37 and CAP39 95% confidence bounds



LCF_10: Conditional mean LCF risk within 10 miles radius

Figure E-26: 10-mile Conditional, Mean, Individual LCF Risk (per Event) CDF for Run 16 with SRS and 95% Confidence Interval Upper and Lower Bounds for Runs 15 & 17 with SRS

Position of CAP 39 CDF
within CAP 37 and CAP38 95% confidence bounds



LCF_10: Conditional mean LCF risk within 10 miles radius

Figure E-27: 10-mile Conditional, Mean, Individual LCF Risk (per Event) CDF for Run 17 with SRS and 95% Confidence Interval Upper and Lower Bounds for Runs 15 & 16 with SRS

Position of CAP 37 CDF
within CAP 38 and CAP39 95% confidence bounds

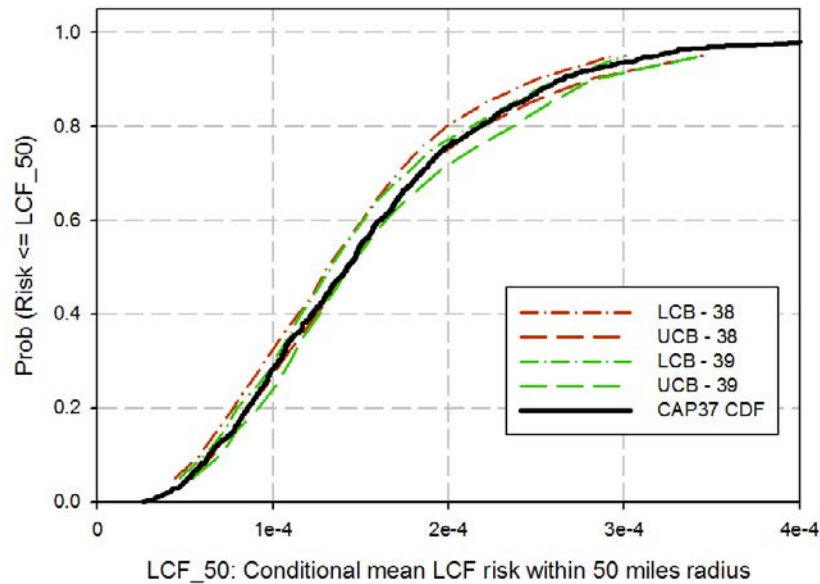


Figure E-28: 50-mile Conditional, Mean, Individual LCF Risk (per Event) CDF for Run 15 with SRS and 95% Confidence Interval Upper and Lower Bounds for Runs 16 & 17 with SRS

Position of CAP 38 CDF
within CAP 37 and CAP39 95% confidence bounds

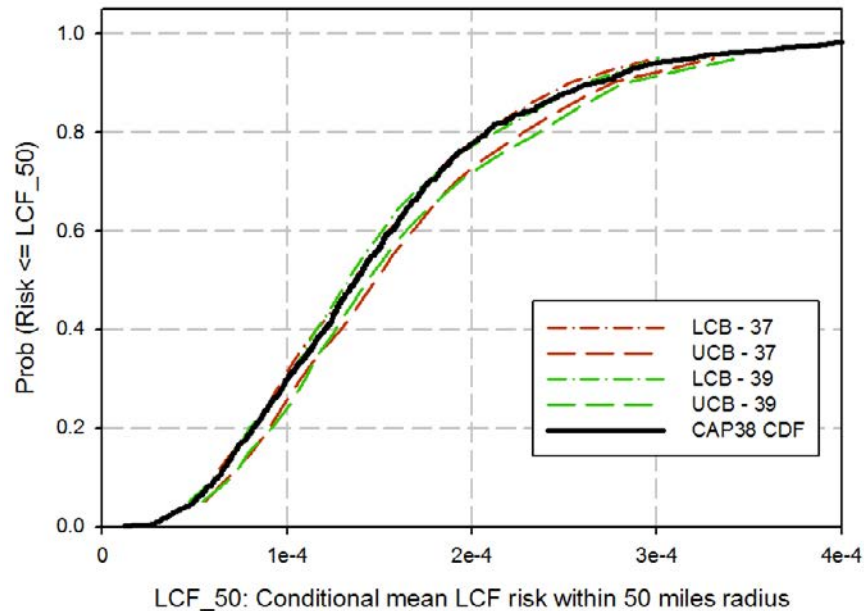


Figure E-29: 50-mile Conditional, Mean, Individual LCF Risk (per Event) CDF for Run 16 with SRS and 95% Confidence Interval Upper and Lower Bounds for Runs 15 & 17 with SRS

Position of CAP 39 CDF
within CAP 37 and CAP38 95% confidence bounds

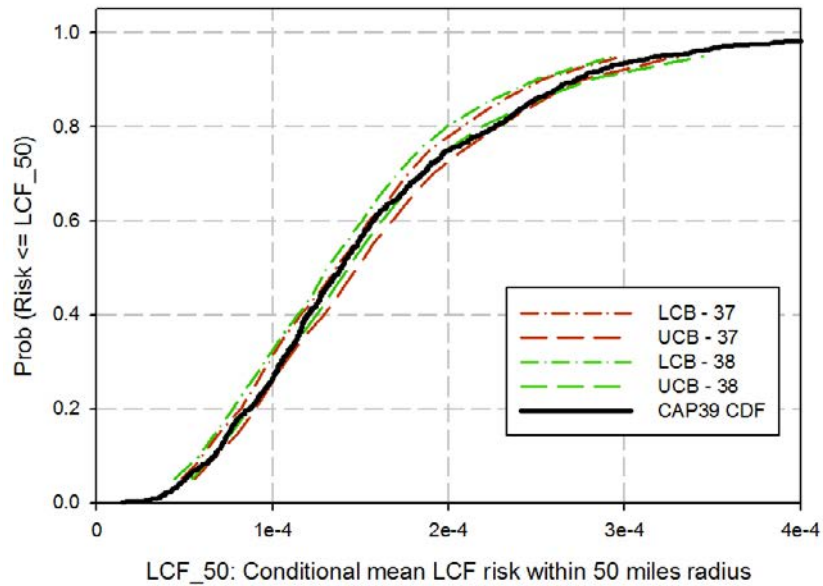


Figure E-30: 50-mile Conditional, Mean, Individual LCF Risk (per Event) CDF for Run 17 with SRS and 95% Confidence Interval Upper and Lower Bounds for Runs 15 & 16 with SRS

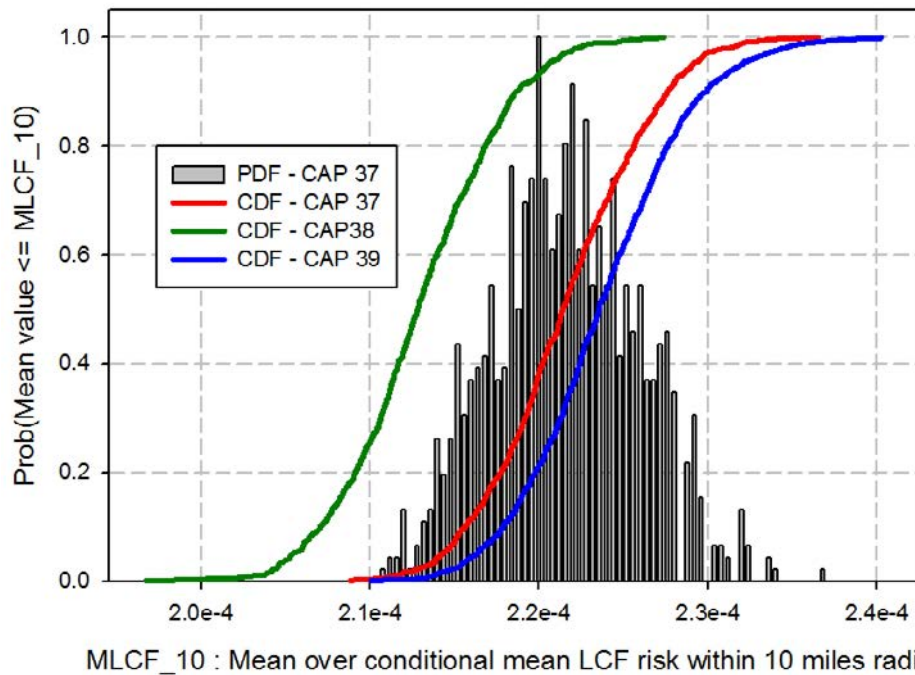
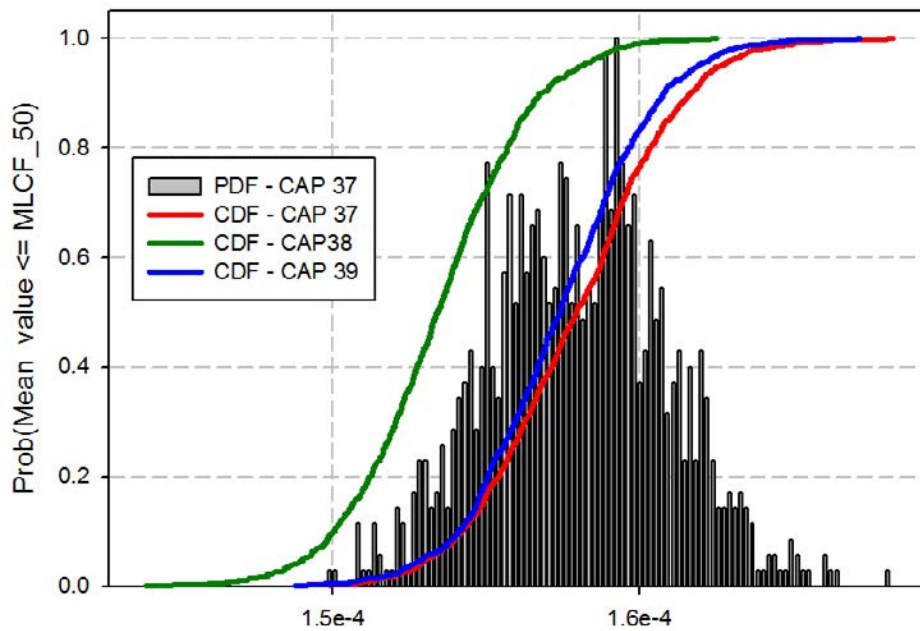


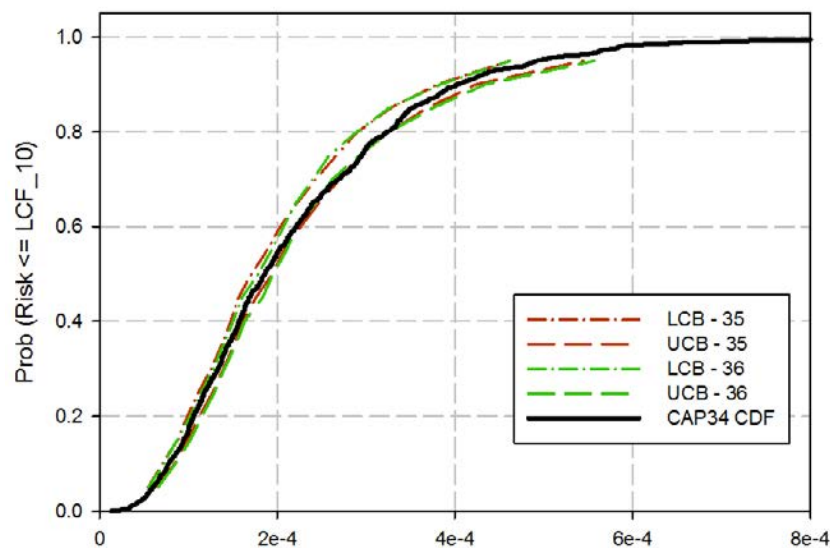
Figure E-31: 10-mile Conditional, Mean, Individual LCF Risk (per Event) CDFs for Runs 15-17 with SRS and the Density Function for Run 15 with SRS



MLCF_50 : Mean over conditional mean LCF risk within 50 miles radius

Figure E-32: 50-mile Conditional, Mean, Individual LCF Risk (per Event) CDFs for Runs 15-17 with SRS and the Density Function for Run 15 with SRS

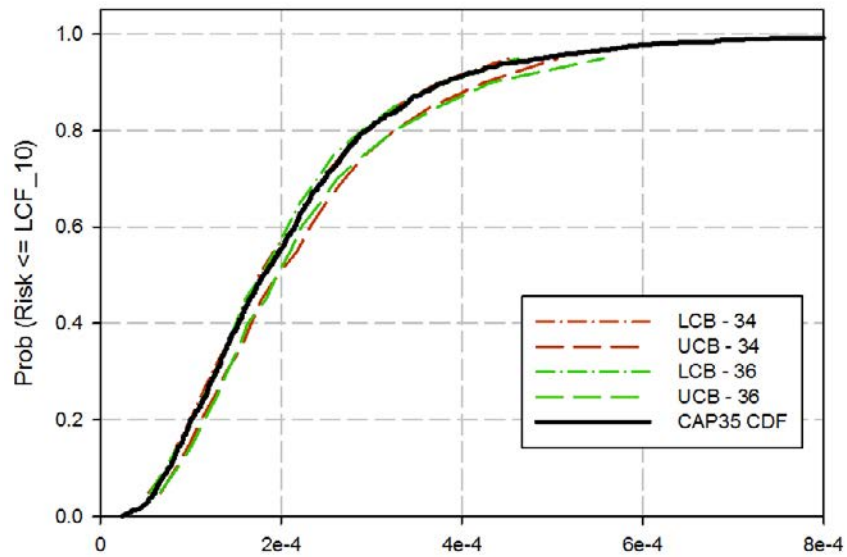
Position of CAP 34 CDF
within CAP 35 and CAP36 95% confidence bounds



LCF_10: Conditional mean LCF risk within 10 miles radius

Figure E-33: 10-mile Conditional, Mean, Individual LCF Risk (per Event) CDF for Run 15 with LHS and 95% Confidence Interval Upper and Lower Bounds for Runs 16 & 17 with LHS

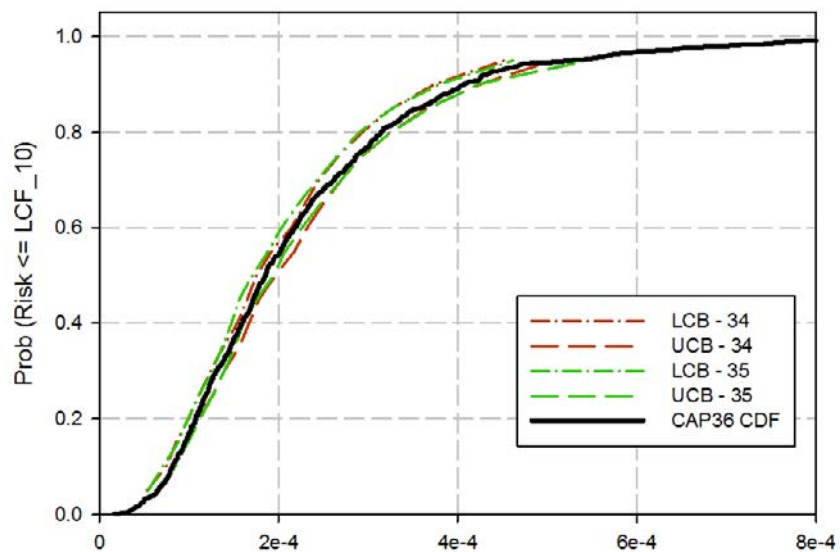
Position of CAP 35 CDF
within CAP 34 and CAP 36 95% confidence bounds



LCF_10: Conditional mean LCF risk within 10 miles radius

Figure E-34: 10-mile Conditional, Mean, Individual LCF Risk (per Event) CDF for Run 16 with LHS and 95% Confidence Interval Upper and Lower Bounds for Runs 15 & 17 with LHS

Position of CAP 36 CDF
within CAP 34 and CAP 35 95% confidence bounds



LCF_10: Conditional mean LCF risk within 10 miles radius

Figure E-35: 10-mile Conditional, Mean, Individual LCF Risk (per Event) CDF for Run 17 with LHS and 95% Confidence Interval Upper and Lower Bounds for Runs 15 & 16 with LHS

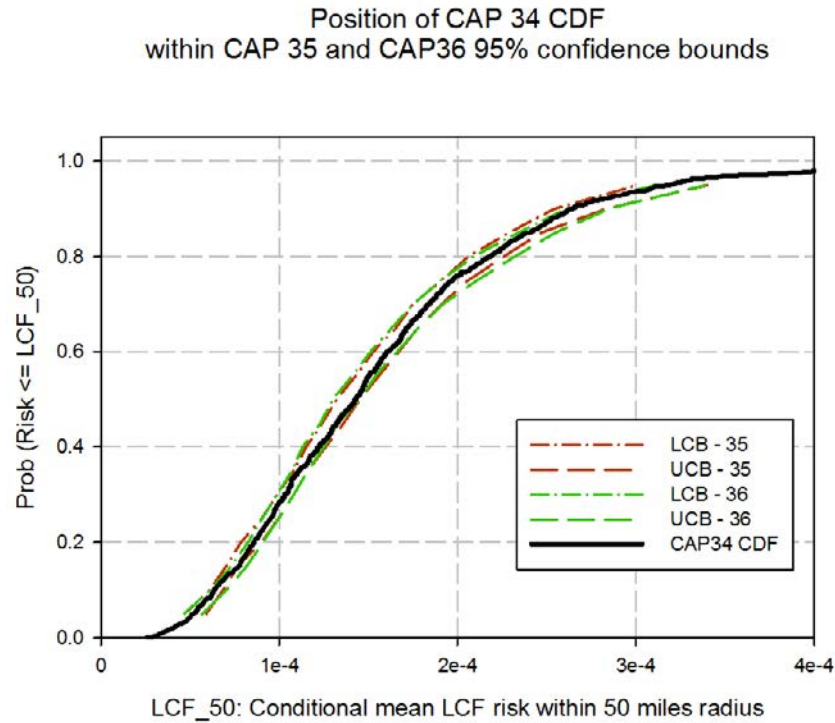


Figure E-36: 50-mile Conditional, Mean, Individual LCF Risk (per Event) CDF for Run 15 with LHS and 95% Confidence Interval Upper and Lower Bounds for Runs 16 & 17 with LHS

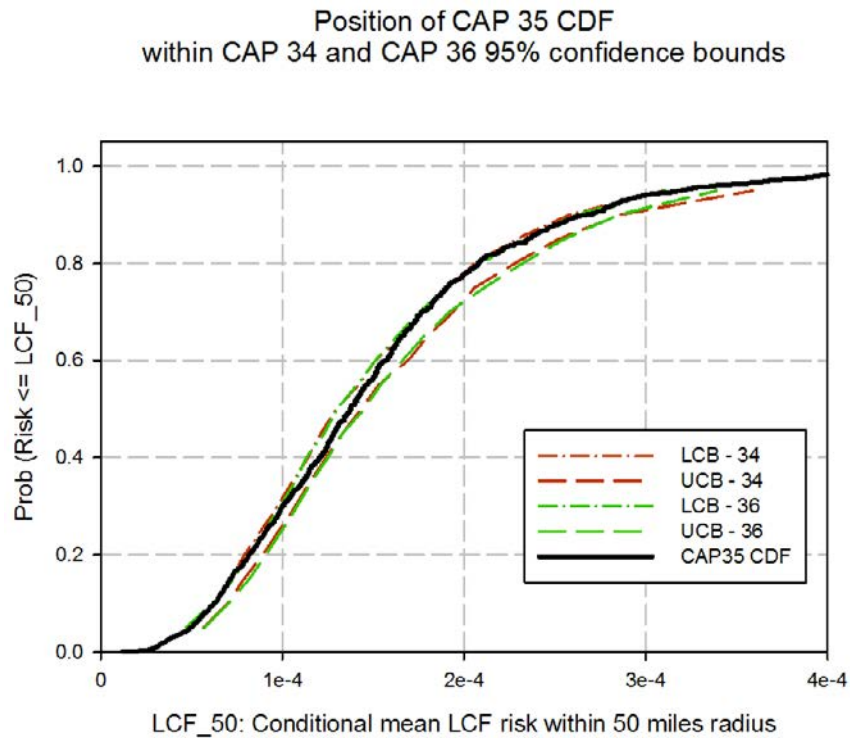


Figure E-37: 50-mile Conditional, Mean, Individual LCF Risk (per Event) CDF for Run 16 with LHS and 95% Confidence Interval Upper and Lower Bounds for Runs 15 & 17 with LHS

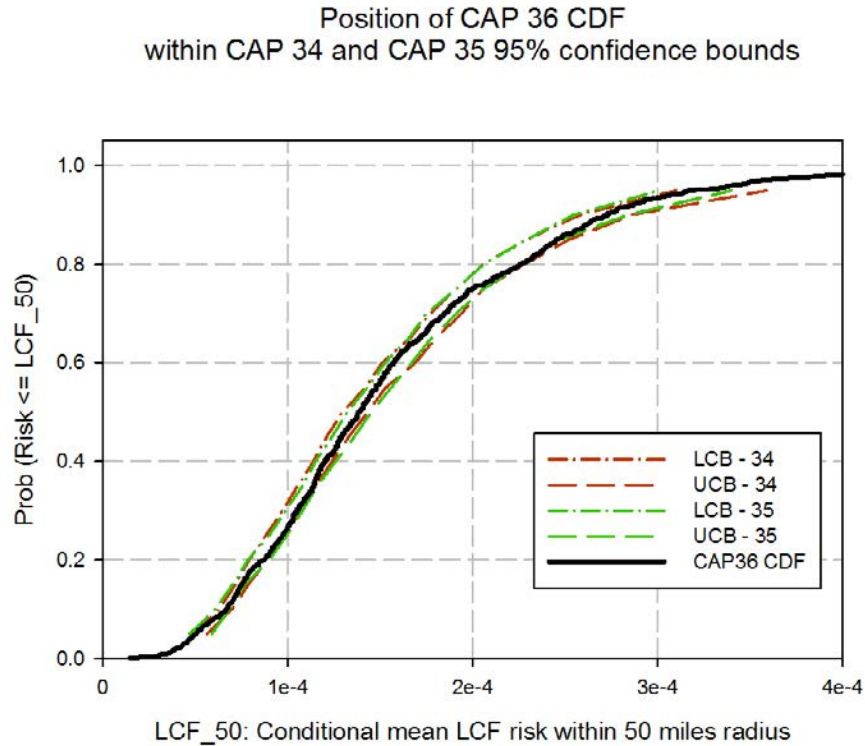


Figure E-38: 50-mile Conditional, Mean, Individual LCF Risk (per Event) CDF for Run 17 with LHS and 95% Confidence Interval Upper and Lower Bounds for Runs 15 & 16 with LHS

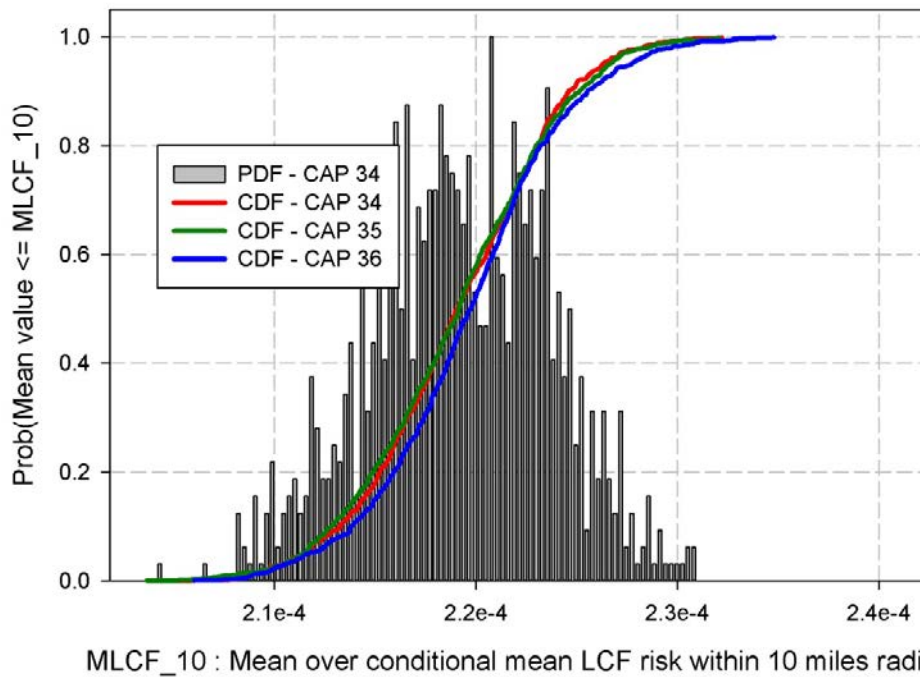
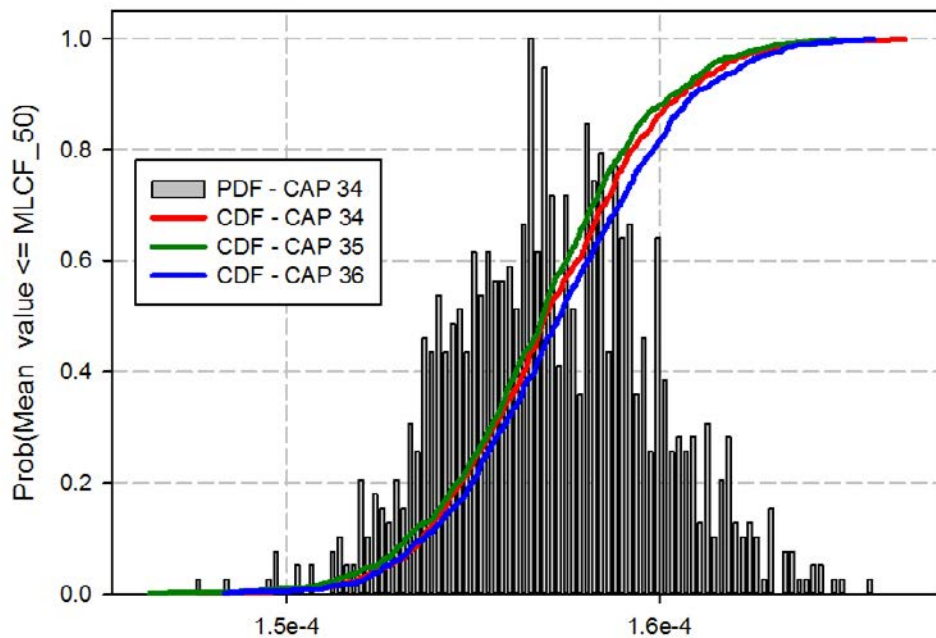


Figure E-39: 10-mile Conditional, Mean, Individual LCF Risk (per Event) CDFs for Runs 15-17 with LHS and the Density Function for Run 15 with LHS



MLCF_50 : Mean over conditional mean LCF risk within 50 miles radius

Figure E-40: 50-mile Conditional, Mean, Individual LCF Risk (per Event) CDFs for Runs 15-17 with LHS and the Density Function for Run 15 with LHS

E.7.1 Low, Medium, & High Source Term Combined Analysis

From Section E.3, three source terms were selected to test the influence of uncertain MACCS parameters by themselves. A comparison of these source terms' conditional, mean, individual LCF risk results was conducted by weighting the three source terms' LCF risks by 1/3 (i.e., each represents 1/3 of the source term uncertainty) to the SOARCA UA LCF risk results. Figure E-41 and Figure E-42 show the comparison for the low source term (CAP29), medium source term (CAP32), and high source term (CAP35) with the SOARCA UA results (CAP17) at the 10- and 50-mile radial distances, respectively. As seen in these figures, the source terms selected are a good representation of the 10-mile radial distance and of the 50-mile radial distance to ~80th percentile where the 'averaged' estimate under predicts the LCF risk when compared to the SOARCA UA.

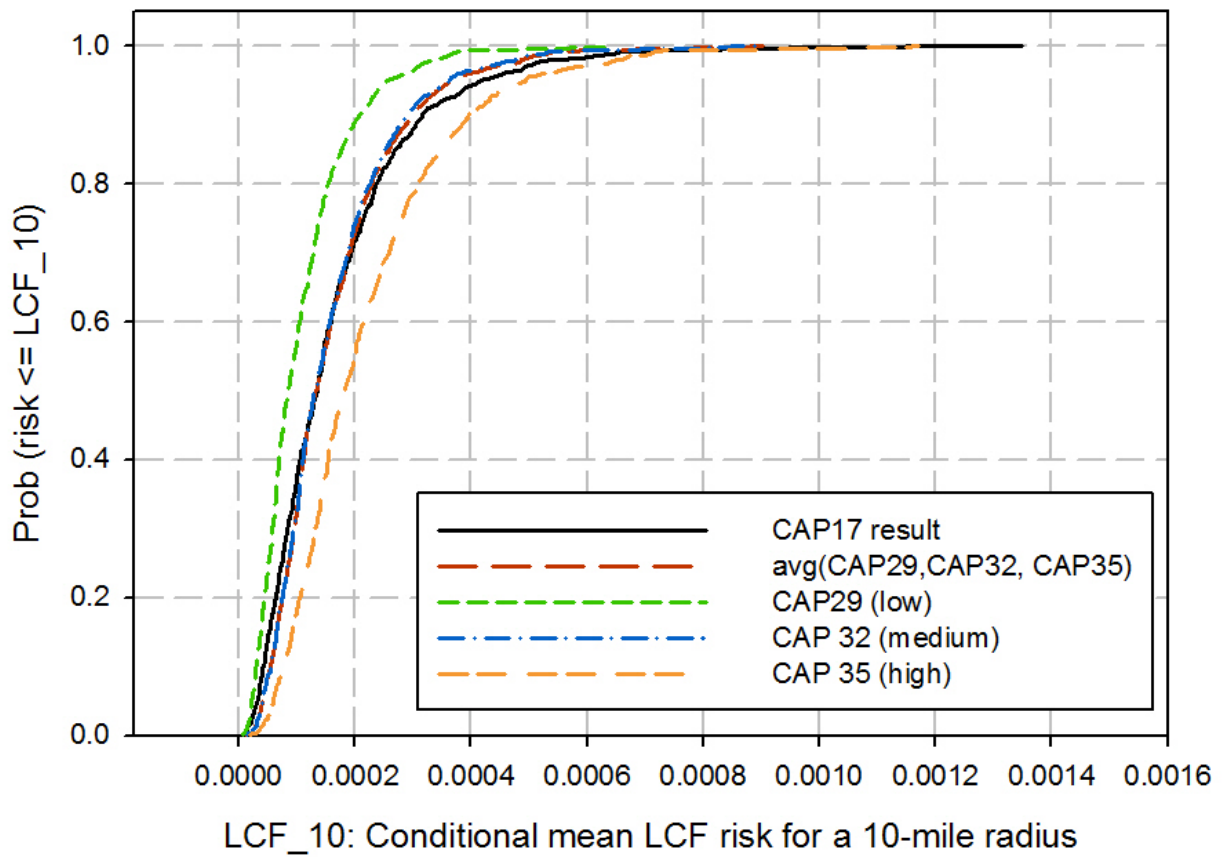


Figure E-41: 10-mile Conditional, Mean, Individual LCF Risk (per Event) CDFs for Low, Medium, and High Source Terms with LHS and the Conditional, Mean, Individual LCF Risk (per Event) CDF for the SOARCA UA with LHS Sampling

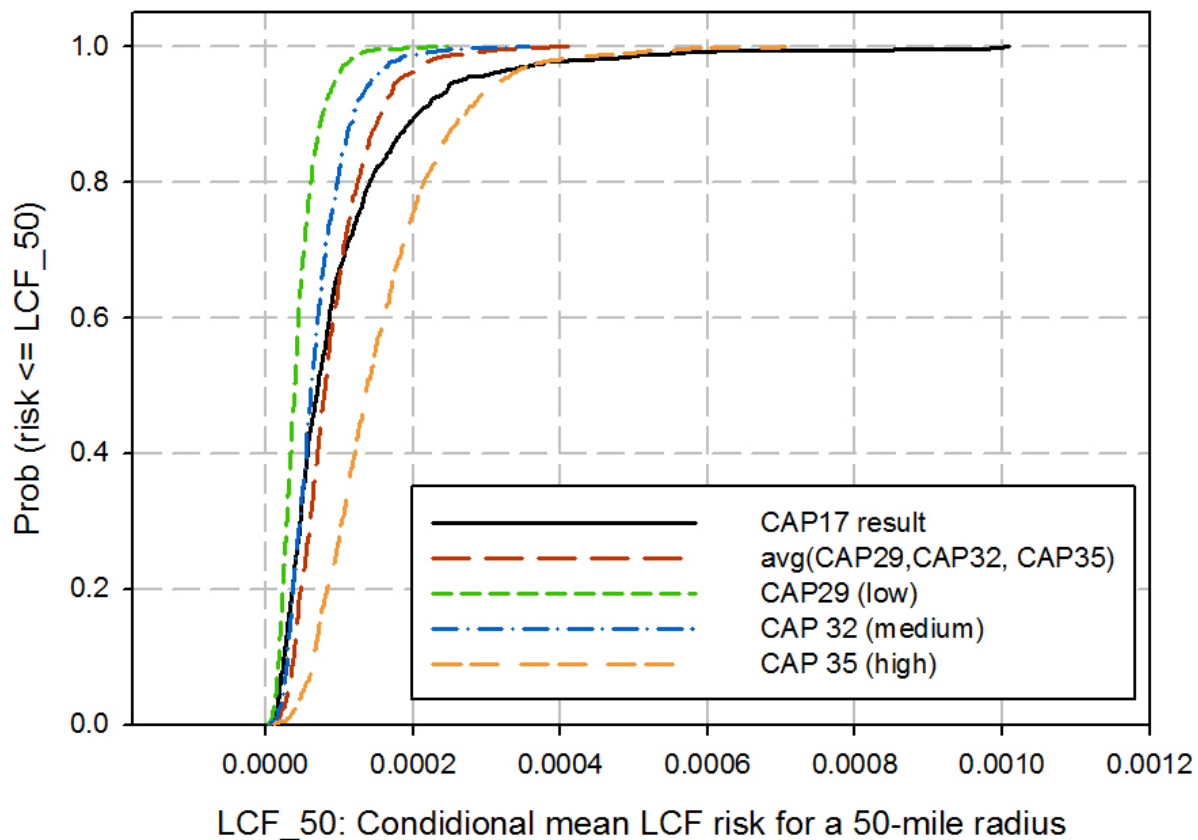


Figure E-42: 50-mile Conditional, Mean, Individual LCF Risk (per Event) CDFs for Low, Medium, and High Source Terms with LHS and the Conditional, Mean, Individual LCF Risk (per Event) CDF for the SOARCA UA with LHS Sampling

E.7.2 Bootstrap Comparison

During the July 10, 2013 ACRS meeting, an ACRS member asked why the NRC/SNL didn't use simple random/Monte-Carlo (MC) sampling for the MACCS portion of the uncertainty analysis. Staff responded with the reasons why an LHS is traditionally preferred. But in addition, the MACCS code did not have the capability to do a simple random/MC sampling (abbreviated as MC in the figure legends). Current updates to the MACCS uncertainty code allow simple random sampling (SRS). Thus, a comparison of the SOARCA UA results (CAP17) to the CAP17 analysis using SRS/MC was conducted. Table E-19 and Table E-20 show the statistics for the conditional, mean, individual LCF risk (per event) results at specified radial distances for LHS and MC uncertainty sampling, respectively. Figure E-43 shows the comparison of CAP17 CCDF LCF risk for LHS and MC results for the 10- and 50-mile radial distances. As seen from both the tables and figure, the LHS and MC results are very similar and would be considered in good agreement for conditional LCF risk.

Table E-21 and Table E-22 show the statistics for the conditional, mean, individual prompt fatality risk (per event) results at specified radial distances for LHS and MC uncertainty

sampling, respectively. Figure E-44 shows the comparison of CAP17 CCDF prompt fatality risk for LHS and MC results for the 1.3-, 2-, and 3.5-mile radial distances. As seen from both the tables and figure, the LHS and MC results are very similar and would be considered in good agreement for conditional prompt fatality risk for the 1.3-mile and 2-mile radial distances. This is because there are a sufficient number of realizations that have a non-zero prompt fatality risk to provide a statistical comparison. Beyond 2 miles, there are few realizations that calculate a non-zero result and the statistics are less reliable.

For CAP17, the distribution of mean value based on bootstrap has been displayed for MC sampling (i.e., CAP40) and is presented in Figure E-45 and Figure E-46 for the 10-mile and 50-mile radial distances, respectively. Additionally, Figure E-47 and Figure E-48 show the distribution of the mean values based on bootstrap with the density estimated via binning for CAP40. This comparison informs on the stability of the mean result for a sample of size 865. Two things are considered at this level:

1. How close are the means, and
2. How close to a normal distribution is the density function.

An original sample size of 865 can be considered large enough so that a selection of values (with replacement) from a LHS sample will still lead to a good representation of the uncertainty in the CDF. Thus, bootstrapping has been used on the LHS results for CAP17 in the same way it was used on SRS results in order to compare the stability and check if indeed the LHS results look more stable than conditional, mean, individual, LCF risk (per event) results when the same sample size is used. These results are presented in Figure E-45 and Figure E-46 for the 10-mile and 50-mile radial distances (i.e., recall from CAP17 is the Uncertainty Analysis results with LHS sampling and CAP40 is the Uncertainty Analysis results with MC sampling).

The distribution of mean value based on bootstrap has been displayed for CAP17 and CAP40, with the density estimated via binning for CAP40. This is presented in Figure E-47 and Figure E-48 for the 10-mile and 50-mile radial distances, respectively.

As seen from Figure E-45 through Figure E-48, a reduction of variance in the mean for LHS sampling is seen (compared to SRS/MC); this is expected.

Table E-19: Conditional, mean, individual LCF risk (per event) average statistics for the MACCS Uncertainty Analysis (CAP17) for five circular areas using LHS sampling

	0-10 miles	0-20 miles	0-30 miles	0-40 miles	0-50 miles
Mean	1.7×10^{-4}	2.8×10^{-4}	2.0×10^{-4}	1.3×10^{-4}	1.0×10^{-4}
Median	1.3×10^{-4}	1.9×10^{-4}	1.3×10^{-4}	8.7×10^{-5}	7.1×10^{-5}
5th percentile	3.1×10^{-5}	4.9×10^{-5}	3.4×10^{-5}	2.2×10^{-5}	1.9×10^{-5}
95th percentile	4.2×10^{-4}	7.7×10^{-4}	5.3×10^{-4}	3.4×10^{-4}	2.7×10^{-4}

Table E-20: Conditional, mean, individual LCF risk (per event) average statistics for the MACCS Uncertainty Analysis (CAP17) for five circular areas using SRS/MC sampling

	0-10 miles	0-20 miles	0-30 miles	0-40 miles	0-50 miles
Mean	1.7E-04	2.9E-04	2.0E-04	1.3E-04	1.0E-04
Median	1.3E-04	1.9E-04	1.3E-04	8.7E-05	7.1E-05
5th percentile	3.0E-05	4.9E-05	3.4E-05	2.2E-05	1.8E-05
95th percentile	4.5E-04	8.8E-04	5.8E-04	3.8E-04	3.0E-04

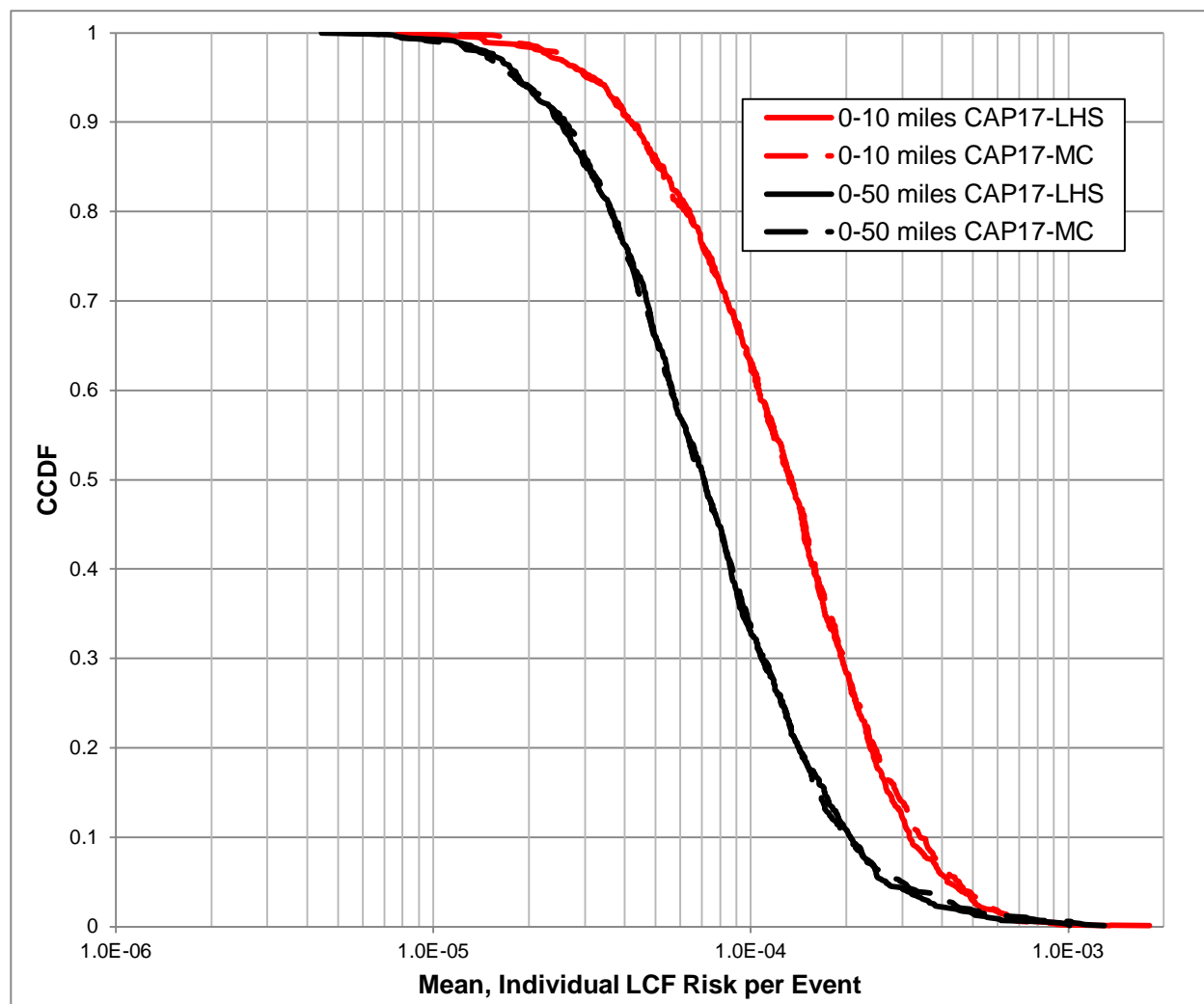


Figure E-43: CAP17 Conditional, Mean, Individual LCF Risk (per Event) CCDF with LHS and MC Sampling for the Radial Distances Considered

Table E-21: Conditional, mean, individual prompt fatality risk (per event) average statistics for the MACCS Uncertainty Analysis (CAP17) for six circular areas using LHS

	0-1.3 miles	0-2 miles	0-3 miles	0-3.5 miles	0-7 miles	0-10 miles
Mean	4.5×10^{-7}	1.8×10^{-7}	6.4×10^{-8}	3.5×10^{-8}	8.3×10^{-9}	4.8×10^{-9}
Median	0.0	0.0	0.0	0.0	0.0	0.0
75th percentile	0.0	0.0	0.0	0.0	0.0	0.0
95th percentile	1.9×10^{-6}	7.4×10^{-7}	5.3×10^{-10}	0.0	0.0	0.0

Table E-22: Conditional, mean, individual prompt fatality risk (per event) average statistics for the MACCS Uncertainty Analysis (CAP17) for six circular areas using MC

	0-1.3 miles	0-2 miles	0-3 miles	0-3.5 miles	0-7 miles	0-10 miles
Mean	4.6E-07	1.5E-07	5.6E-08	2.8E-09	2.4E-09	4.9E-10
Median	0.0	0.0	0.0	0.0	0.0	0.0
75th percentile	0.0	0.0	0.0	0.0	0.0	0.0
95th percentile	2.3E-06	5.6E-07	8.0E-08	0.0	0.0	0.0

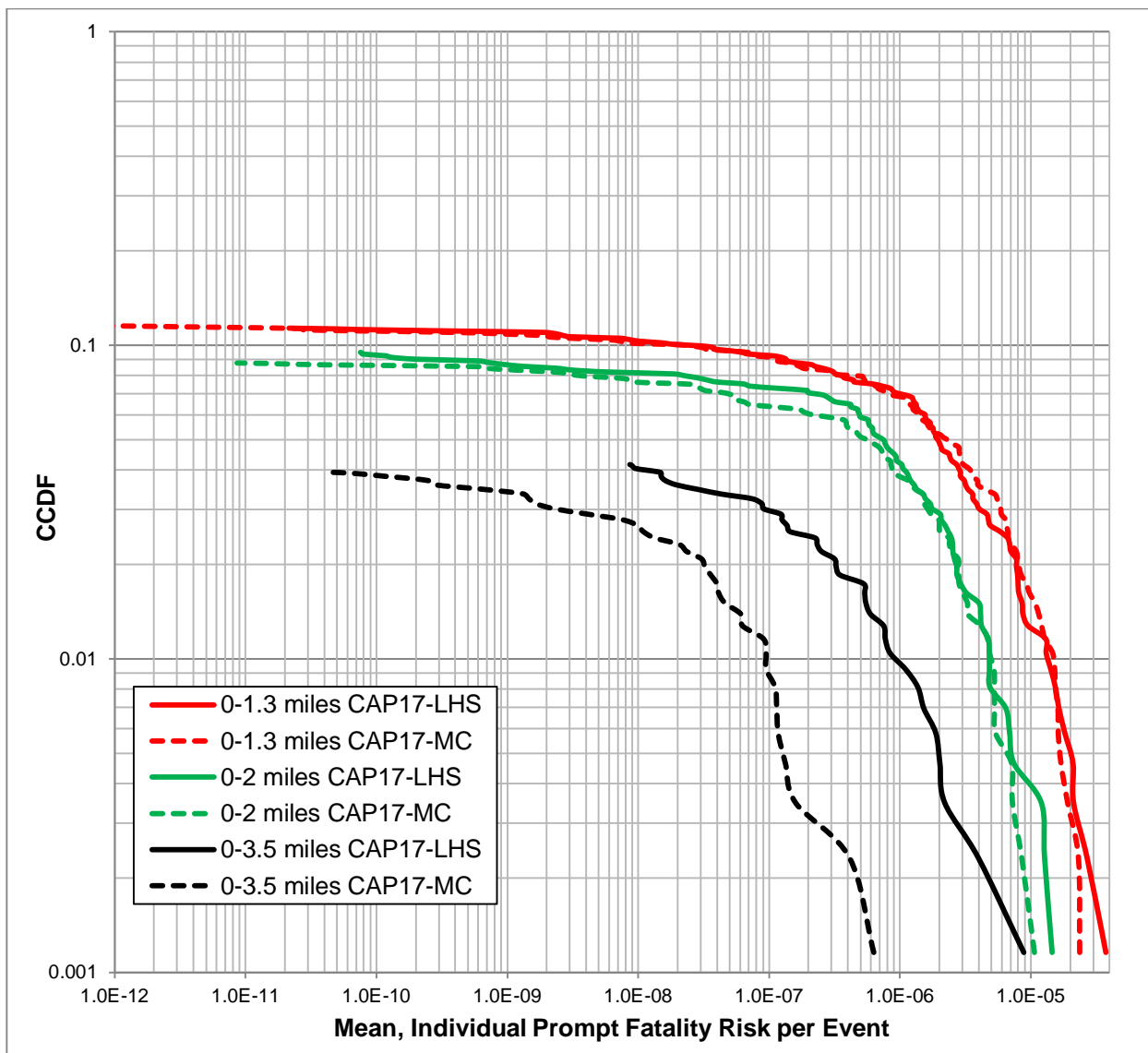


Figure E-44: CAP17 Conditional, Mean, Individual Prompt Fatality Risk (per Event) CCDF with LHS and MC Sampling for the Radial Distances Considered

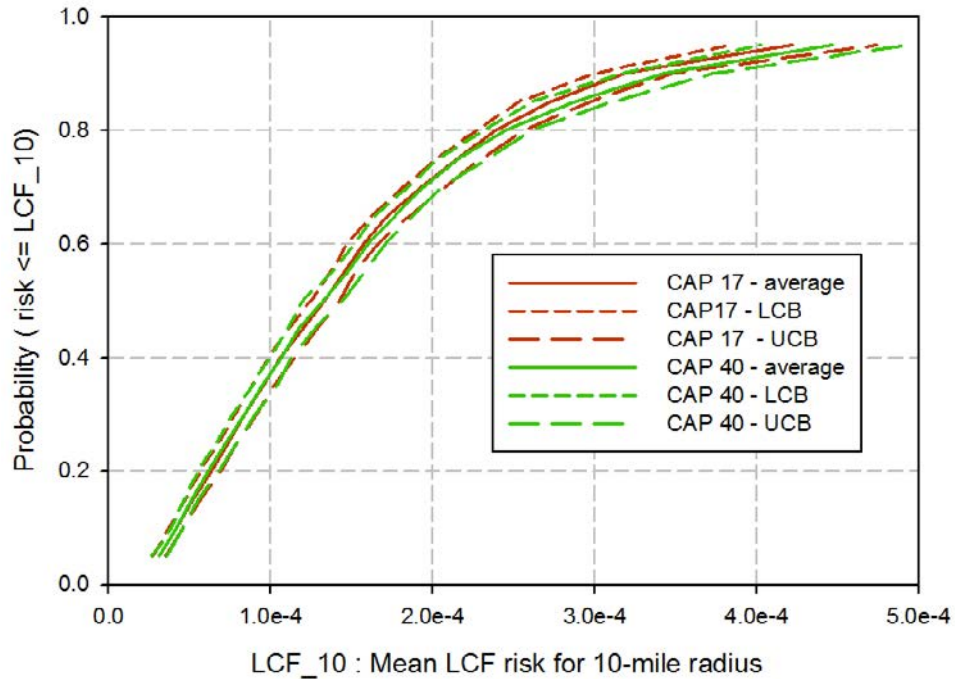


Figure E-45: 10-mile Conditional, Mean, Individual LCF Risk (per Event) CDF for CAP17, CAP40, and 95% Confidence Interval Upper and Lower Bounds for CAP17 and CAP40

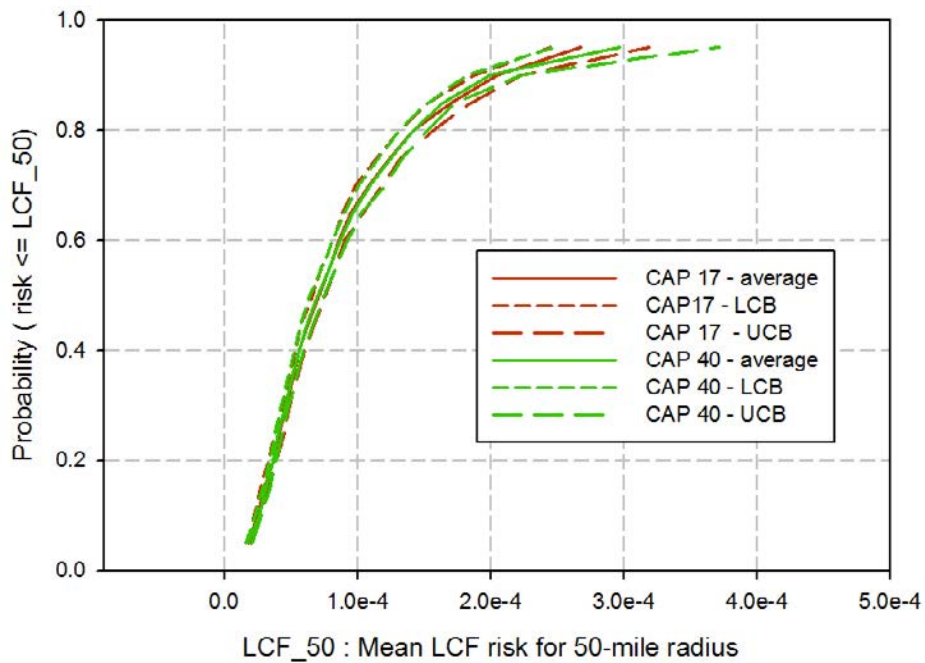


Figure E-46: 50-mile Conditional, Mean, Individual LCF Risk (per Event) CDF for CAP17, CAP40, and 95% Confidence Interval Upper and Lower Bounds for CAP17 and CAP40

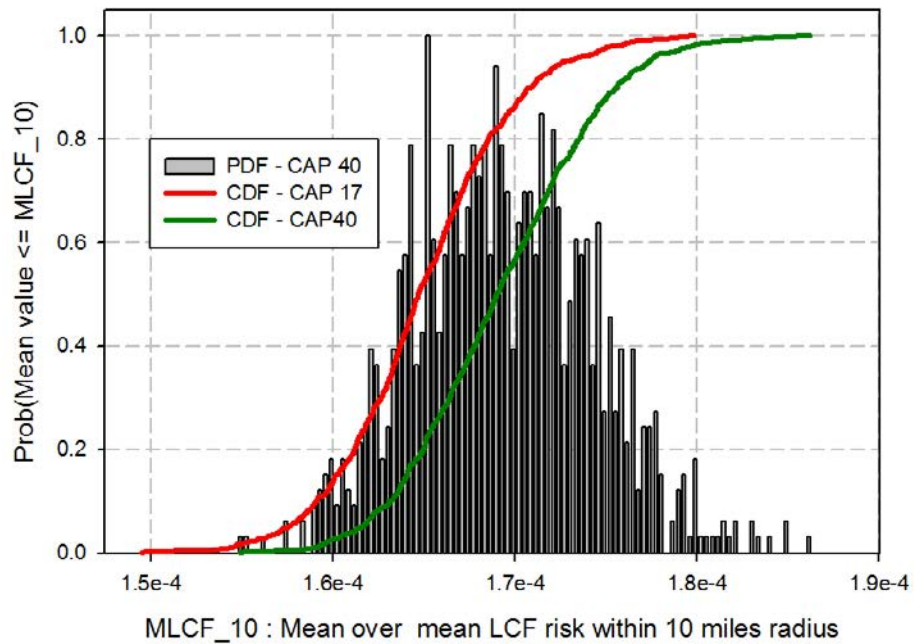


Figure E-47: 10-mile Conditional, Mean, Individual LCF Risk (per Event) CDFs for CAP17, CAP40 and the Density Function for CAP40

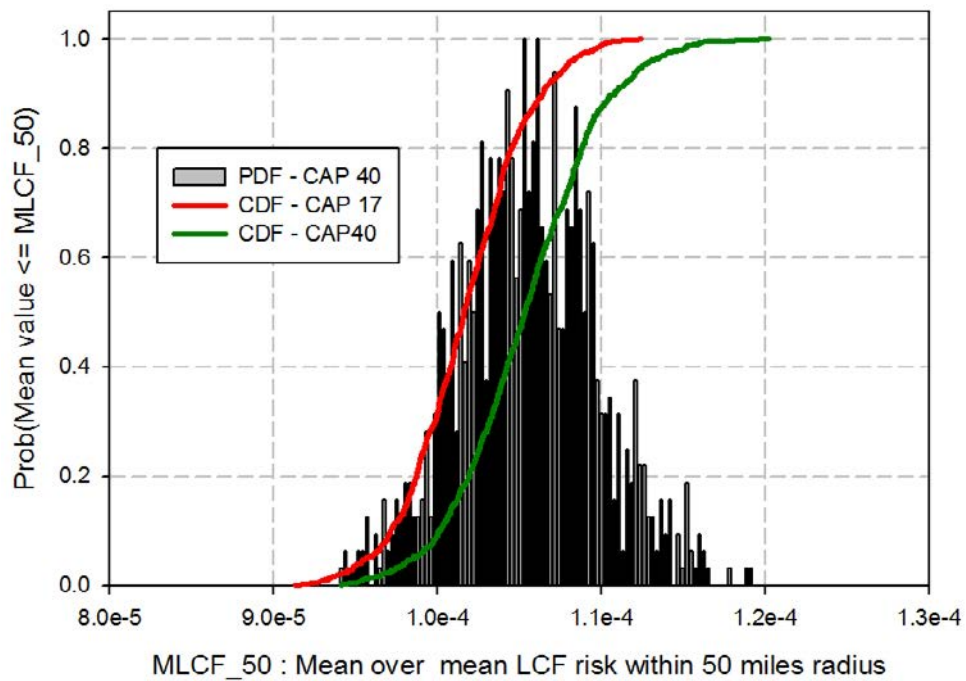


Figure E-48: 50-mile Conditional, Mean, Individual LCF Risk (per Event) CDFs for CAP17, CAP40 and the Density Function for CAP40

E.8 MELCOR Parameters

To address ACRS Question 5.a, NRC and Sandia staff conducted a thorough search through previous studies and lessons learned. The information provided in this section was complimentary to the discussions NRC and Sandia staff provided to the ACRS subcommittee on September 16, 2013. A detailed transcript of the verbal discussions can be found in the official transcript of the proceedings (ML14014A383).

E.8.1 Question 5.a.I – SRVLAM

1. Very limited data exists on the probability of an SRV to fail to reclose; what little testing data is available is not thought to be representative of the environmental conditions that the SRV would experience in a severe accident progression. So the associated stochastic failure distribution in the uncertainty analysis is known to be uncertain. However, it is evidenced in documented SOARCA uncertainty calculations and in the results of the uncertainty analysis that the range of the distribution specified leads on one end to cases where the lowest setpoint SRV fails open quite early (before the onset of core damage) and on the other end to cases quite late (such that a MSL rupture results). The fact that these extremes are captured is thought to be a good indication that the stochastic failure distribution specified in the uncertainty analysis is inclusive of the possible meaningful over-cycle failures that an SRV might suffer.
2. The SOARCA probability for SRV stochastic failure to reclose was adopted from the Peach Bottom IPE as 3.7×10^{-3} per demand which relates to failure after 270 cycles.
3. A beta distribution with mean equal to the SOARCA failure-to-close probability of 3.7×10^{-3} per demand was applied in the uncertainty analysis sampling of SRV stochastic failure criterion. The beta distribution is typically used to represent uncertainty in stochastic failure-on-demand parameters. The sampling resulted in a distribution skewed towards more cycles to failure relative to the SOARCA estimate as illustrated in the Figure E-49.
4. As noted in Section 4.1.1, a stochastic failure rate of 9×10^{-3} per demand or below; the SRV will fail from thermal seizure and/or MSL creep rupture and the shape of the distribution below this value has no bearing on results.
5. Stochastic failures are treated as fully separable from elevated temperature effects in the uncertainty analysis as in the NUREG/CR-7110 Volume 1 Peach Bottom LTSBO MELCOR model.
6. Differential thermal expansion of adjacent moving parts resulting in seizure, at temperatures exceeding design, is categorized as a 'thermal' failure in the uncertainty analysis.
7. Failure due to plastic deformation of valve parts at severe temperatures is also categorized as a 'thermal' failure in the uncertainty analysis.
8. The uncertainty analysis assumes a stochastic SRV failure to reclose always results in a fully open valve.
9. If an SRV were to fail closed, pressure relief would move up to the SRV with the next lowest pressure setpoint. Peach Bottom has 11 SRVs. The possibility that all of the SRVs could fail closed is considered remote and so is not addressed in the uncertainty analysis.

10. Similarly, if an SRV were not to open on demand, pressure relief would move up to the SRV with the next lowest pressure setpoint. The possibility that all of the SRVs could fail to open is considered remote and so is not addressed in the uncertainty analysis.

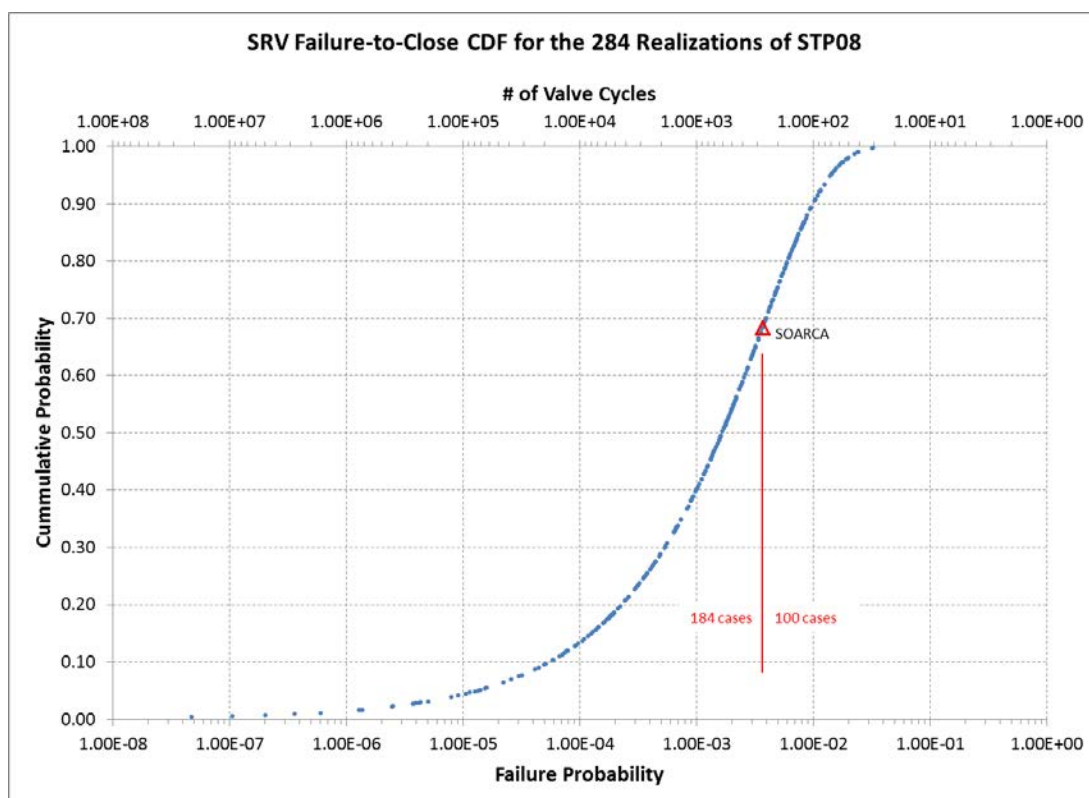


Figure E-49: CDF of Failure Probability/Number of Valve Cycles

E.8.2 Question 5.a.II – CHEMFORM

1. The peak gaseous iodine amounts recorded in four different Phebus experiments were fundamental in defining the five speciation combinations of cesium and iodine considered in the uncertainty analysis. A combination was devoted to each of the four recorded amounts and a 5th combination was formed by averaging the four recorded amounts of iodine together. Equal weighting in the parameter sampling was given to all but the 5th combination which was weighted four times greater than the other combinations reflecting that it was jointly formed from the iodine recorded in the four experiments.
2. With gaseous iodine (fraction of initial core inventory) defined for the five combinations, enough cesium was defined as CsI to involve all of the iodine not defined as gaseous (i.e., most all of the iodine).
3. Remaining cesium was defined in the different combinations to be either in the form of all CsOH, all Cs₂MoO₄, or half CsOH and half Cs₂MoO₄.
4. With respect to cesium speciation, Combinations 3 and 5 closely match the SOARCA calculation. In the sampling of the chemical form of iodine and cesium, Combination 3 results once in every eight realizations while Combination 5 results four times in every eight

realizations. In five of every eight realizations then, the cesium speciation closely resembles the cesium speciation in the SOARCA calculation.

5. There is no speciation combination that matches the iodine and cesium speciation of the SOARCA calculation identically. Combination 3 comes closest with the smallest fraction of gaseous iodine (~0.3%) and 100% Cs_2MoO_4 . SOARCA did not include any gaseous iodine.
6. In all cases, including the SOARCA case, 1% of the initial cesium inventory is defined to be elemental cesium residing in the fuel-cladding gap.
7. The discussion below are results of the Phebus studies that were used to inform the gaseous iodine used for this work:

a. Phebus FPT-0

- Gaseous iodine:
 - 3% +/- 1.1% of initial iodine inventory (33% +/- 12.1% of the total iodine found in containment during 13500 ~ 13700 sec, following first zircaloy oxidation phase)
 - The gaseous iodine concentration level drops after the main zircaloy oxidation phase in few hours (2.5% of the initial bundle inventory, 0.039% of the total iodine in containment after core shutdown and 0.32+/-0.16% of the bundle inventory after containment isolation), due to steam condensation on the painted condenser and/or adsorption process on other containment surfaces.
- References: FPT0 Final Report Part D, 3-3 and FPT1 Final Report Section 5, 5.4.4.4

b. Phebus FPT-1

- Gaseous iodine fraction:
 - At first oxidation phase: At least 0.2 +/- 0.045% bundle inventory (corresponds to 4.05 +/- 0.9% of the containment inventory)
 - After two oxidation phases, level drops to about 0.07+/-0.016% of the initial bundle inventory due to similar reasons as in FPT0.
- Reference: FPT1 Final Report Section 5, 5.4.4.4

c. Phebus FPT-2

- Unlike the previous two tests, the gaseous iodine concentration in containment is minimum during or following the main oxidation phase. The gaseous iodine fraction was determined from the following table:

Time (sec)	% gaseous iodine of the initial bundle inventory	% gaseous iodine of the total found in containment
10322-10387	0.011	0.209
13742-13848	0.128	0.392
16267-16453	0.298	0.615
16878-16918	0.196	0.375
20281-20583	0.083	0.146

- Reference: FPT2 Final Report Section 5, 5.4

d. Phebus FPT-3

- Sharp increase of gaseous iodine and the peak observed at about ~ 14000 sec, just after the main oxidation phase (~9700 sec to ~11000 sec). Iodine concentration then drops due to depositions onto surfaces. The gaseous iodine fraction was determined from the following table:

Time (sec)	% gaseous Iodine of the initial bundle inventory	% gaseous Iodine of the total found in containment
9894-10208	0.28	63.11
10387-10512	0.42	32.91
10389-10703	1.49	98.79
11795-12097	7.57	60.4
15028-15135	7.26	22.83
17038-17210	2.85	8.6
18692-18963	2.12	6.22

- Reference: FPT3 Final Report 5.4, Table 5.4.2.10

e. Phebus FPT-4

- The FPT4 test objectives didn't include the study of iodine behavior in containment.

E.8.3 Question 5.a.III – FL904A

1. Drywell liner shell melt-through occurs in the MELCOR model when molten-core debris contacts the drywell liner with a temperature of 1,700 K or higher (the melting temperature of carbon steel) for a period of five minutes. Stress induced in the liner due to pressurization of the drywell is not considered in the shell melt-through determination.
2. All of the uncertainty analysis realizations suffered a drywell liner melt-through as did the SOARCA calculation.
3. The drywell floor is characteristically dry in the LTSBO scenario (see the Figure E-50 for an example).
4. Upon drywell shell liner melt-through in the SOARCA calculation, a 1.667-m long by 6-cm high (0.1-m² area) slit was opened between the lower drywell and the main torus room at the elevation of the drywell floor.
5. In the uncertainty analysis sampling of melt-through size, the lower bound of 0.05 m² (\approx 10 inch diameter hole) is half the SOARCA estimate and is the minimum observed critical zone determined for a damage index profile at 1143°C (2090°F) in NUREG/CR-6025. The upper bound (1.0 m² \approx 44-inch diameter hole) is determined as a sufficient flow area to provide containment depressurization within a few minutes, and is 14% greater than the maximum observed critical zone (0.88 m²) determined for a damage index profile at 1260°C (2300°F) in NUREG/CR-6025.

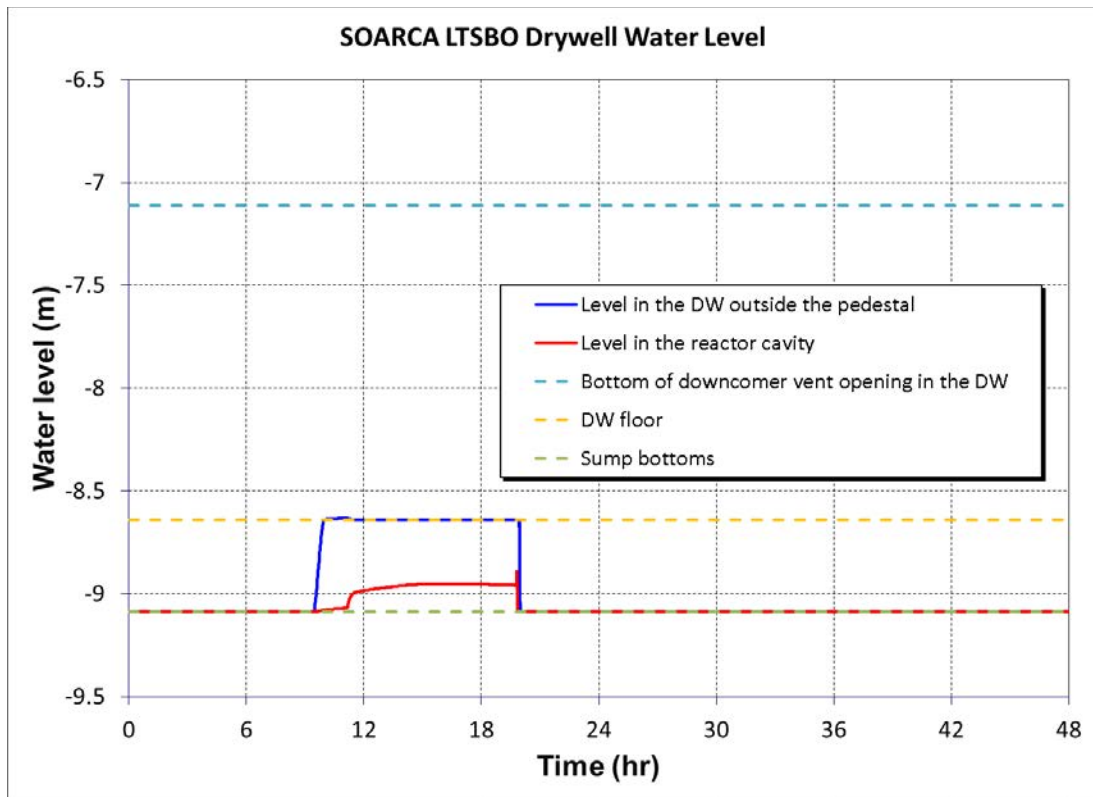


Figure E-50: Typical LTSBO Drywell Characteristics

6. The hole opened in the drywell shell in the uncertainty analysis realizations, like in the SOARCA calculation, was 6 cm tall. It was as long as necessary to develop the sampled value of area. The hole was opened at a rate reflecting core-concrete debris moving as a stream to the liner and then along the liner in both directions at 0.72 m/min. The 0.72 m/min is the velocity observed in preliminary LTSBO calculations of core-concrete debris spreading on the drywell floor. At this velocity, it would take 35 sec to open a 0.05-m² hole and 11.57 minutes to open a 1-m² hole.
7. Originally a uniform distribution was applied between these bounds, but the team felt this distribution did sample lower values often enough, and such as values closer the SOARCA value which is still thought to be the 'best-practice' nominal value. The team settled on applying a log-uniform distribution in the sampling of melt-through area, which still resulted in a distribution skewed towards larger areas relative to the SOARCA estimate.

E.8.4 Question 5.a.IV – BATTDUR

See Section E.10.4 for further discussions regarding operator actions.

E.8.5 Question 5.a.V – SRVOAFRAC

1. This parameter is the open area fraction of the lowest-setpoint SRV in the MELCOR model subsequent to it overheating to failure. This open fraction only applies to an overheating (thermal) failure of the valve to reclose (i.e., it does not apply to an over-cycling (stochastic) failure of the valve to reclose). Over-cycling failures are assumed to leave the valve in a fully open position.

2. Since heating of an SRV would predominately occur when it is flowing (i.e., when it is open), it seems plausible that seizure of adjacent moving parts or deformation of valve parts would occur with the valve at least partway open.
3. A log-uniform distribution was employed in the sampling of SRVOAFRAC with mode 1.0, a minimum value of 0.1, and maximum value of 1.0. This sampling weighted larger area fractions more heavily than smaller fractions.
4. Sampling was skewed to higher values because the geometry of the SRV is such that it does not have to vertically traverse much of its stem length before reaching an open area close to fully open.
5. The possibility of an over-heating failure that leaves an SRV fully closed was not considered. If such were to happen, pressure relief would move on to the SRV with the next lowest pressure setpoint. There are 11 SRVs at Peach Bottom so the likelihood of all the SRVs failing closed seems remote.

E.8.6 Question 5.a.VI – SLCRFRAC

1. The intent in the uncertainty analysis was to open the MSL to the containment through an area equivalent to the full cross-sectional area of the pipe 85% of the time. However, the means through which the MSL rupture is accomplished in the Peach Bottom MELCOR model (i.e., adjusting the flow area of 3 junctions), leads to an effective break area equal to the full area of the pipe for any value of SLCFRAC greater than or equal to 0.5. So, the MSL was actually opened fully to containment 96% of the time in the UA.
2. Applicable SOARCA Peer Review comments and resolutions are provided below:

a. Jeff Gabor – December 22, 2010 SOARCA Peer Review Memorandum

- **Comment:** The potential for Main Steam Line creep failure is not being considered as an uncertain parameter. The MSL rupture area for such a failure would likely be large and probably does not need to be evaluated as an uncertain parameter. I recommend that this uncertain parameter be replaced with a parameter that more directly relates to MSL creep failure.
- **Resolution:** The SOARCA team re-evaluated this phenomenon in regards to this comment. Our rationale is that the uncertainty in the parameters affecting the calculated potential for creep can be neglected in this assessment because prior experience (through sensitivity analyses) suggests the Larson-Miller (L-M) damage index transitions from zero to values well above unity within a very short time. The L-M parameter is not likely to be very sensitive because once the MSL enters creep conditions, the progression is very fast from 0 to 1.

On the other hand, we consider the area of the rupture as an important uncertain parameter because it relates to the more important factor of how we model flow to and through the MSL, and associated heat transfer to wall piping. And after the October 2010 and December 2011 Peer Review meetings and feedback, we have re-assessed the distribution for the MSL rupture area. It is now skewed heavily to large open areas, with only a small residual probability (0.01) of an open area less than 10%.

b. David Leaver – December 22, 2010 SOARCA Peer Review Memorandum

- **Comment:** In the paragraph on Main steam line creep rupture area, should the uncertainty in the main steam line temperature be considered?
- **Resolution:** The main steam line structure temperature is calculated by the model and hence is not an uncertain input parameter. We consider the area of the rupture as an important uncertainty parameter. The rupture area is important because it affects containment response to MSL failure. Large areas generate relatively large pressure loads on the containment, and offer an opportunity for advancing the time of containment failure. The proposed SOARCA UA study considers the area of the rupture as an important uncertainty parameter because it relates to the more important factor of how we model flow to and through the MSL, and associated heat transfer to wall piping. After the October 2010 and December 2011 Peer Review meetings and feedback, we have re-assessed the distribution for the MSL rupture area. It is now skewed heavily to large open areas, with only a small residual probability (0.01) of an open area less than 10%.

In addition, uncertainty in the parameters affecting the calculated potential for creep is neglected in this assessment because prior experience (through sensitivity analyses) suggests the L-M damage index transitions from zero to values well above unity within a very short time. The L-M parameter is not likely to be very sensitive because once the MSL enters creep conditions, the progression is very fast from 0.0 to 1.0.

E.8.7 Question 5.a.VII – RDMTC and RDSTC

1. The improvements to fuel degradation modeling and 2-dimensional core modeling show a delayed heat-up followed by accelerated oxidation. The accelerated oxidation phase ends following molten Zircaloy breakout. Without Zircaloy, the subsequent heatup is primarily controlled by decay heat. The best-practice modeling of Zircaloy-oxide collapse creates a debris bed similar to TMI-2. The debris bed slows oxidation by creating blockages and inhibiting natural circulation. The debris bed gradually grows axially and radially, which eventually leads to core plate failure
2. These affect the rate of radial relocation from ring to ring of either solid debris material or molten materials that may be supported by complete underlying blockages. Significant changes (upwards) in the default values for these parameters were made in the Version 1.8.5 release of MELCOR, based mostly on recommendations from ORNL and on intuitive reasoning with respect to smooth behavior in the melt progression. The previous values (short time constants) produced sometimes-erratic behavior that did not seem physically reasonable. Siemens uncovered sensitivities here and explored ranges below those currently recommended in the MELCOR 1.8.5 defaults. At this point, we do not recommend varying these parameters for this study as sensitivities to hydrogen are not expected from variations about the currently used values. Additionally, the basis for variation of this parameter would be difficult to rationalize.
3. Applicable SOARCA Peer Review comment and resolution is provided below:
 - a. David Leaver – December 22, 2010 SOARCA Peer Review Memorandum

- **Comment:** Radial debris relocation time constants are another example of a parameter where there is no basis for the characterization of uncertainty. Also, there are two incomplete sentences at the bottom of the paragraph.
- **Resolution:** A technical basis has been added to Section 4.1.2 of the draft NUREG/CR report for this parameter and the editorial changes have been made.

The relocation time constant is meant to capture the rate of radial debris movement to the center and thus determine the time the debris moves to the lower plenum. This movement to the lower plenum then determines the time at which the lower plenum will fail. The distributions are based on expert judgment but are not based on TMI data since no data from TMI exists for radial debris relocation distribution. It is one of the few parameters to which a user has access to influence large scale movement and influences axial debris relocation as well. The time scale is a surrogate for the uncertainty in large scale movement. The range covers molten to solidus of core melt.

E.8.8 Question 5.a.VIII – RRIDRFRAC and RODRFRAC

1. Sampling of railroad door open fraction was bound between something relatively small and something relatively large. The doors are large, and so even the smallest open fraction in the sampling related to a fairly large hole (4'-10" square). Sampling was done uniformly for lack any knowledge of whether small or large openings are most likely. What showed to matter in the uncertainty calculations was whether these doorways opened; rather than how much they opened. Thus, the exact distributions were unimportant to the results.

E.8.9 Question 5.a.X – RHONOM

1. The average material density of the particulate released to the environment in the SOARCA LTSBO MELCOR calculation ($6.45\text{E}+03 \text{ kg/m}^3$) served as the basis for the sampling of particle density in the uncertainty analysis calculations. Packing factors of 0.18 minus 25% variance ($= 0.135$) and 0.5 plus 25% variance ($= 0.626$) were applied to the average from the SOARCA calculation to define the lower and upper bounds of the sampling as 870 kg/m^3 and $4,037 \text{ kg/m}^3$, respectively. A triangular distribution was invoked with mode equal to the MELCOR default density of $1,000 \text{ kg/m}^3$ lending somewhat of a bias toward smaller densities in the sampling. At first, DASF was also identified as an uncertain parameter for sampling, but there was a worry about simultaneous varying both variables potentially leading to the modeling of unphysical conditions. After further deliberation and consultation with experts, the team concluded that assuming a DASF of 1 (perfectly spherical) and varying RHONOM should capture the effects of uncertainty stemming from both these related parameters.

E.8.10 Question 5.a.XI – FFC

1. The hydrogen uncertainty analysis done at Sandia in 2002 didn't make use of a time-at-temperature consideration for fuel rod collapse. It instead prescribed collapse at a threshold temperature considered to be distributed normally about a best-estimate value of 2,575 K with upper and lower bounds of 2,400 K and 2,700 K, respectively. The distribution was based on interpretations of results from the Phebus FPT-1 and FPT-2 tests. Further discussion will be provided by Sandia about why the team incorporated a time-at-

temperature collapse criteria for oxidized fuel rods at the ACRS subcommittee meeting. Maybe his explanation with a mentioning of the Phebus temperatures will satisfy the ACRS.

E.8.11 Question 5.a.XII – SC1141(2)

1. SOARCA best practices for the value of SC1141(2) (the maximum melt flow rate per unit width after breakthrough) has been adjusted to 0.2 kg/m-s to yield an effective velocity of 2 mm/s which reflects observations made in CORA experiments.
2. The hydrogen uncertainty analysis done at Sandia in 2002 did not address SC1141(2). It does state that measurements taken from video observation of CORA experiments revealed that while some free-falling molten droplets relocate very rapidly, most of the downward draining melt moves more on the order of millimeters per second.

E.9 MACCS Parameters

To address ACRS Question 5.b, NRC and Sandia staff conducted a thorough search through previous studies and lessons learned. The information provided in this section was complimentary to the discussions NRC and Sandia staff provided to the ACRS subcommittee on September 16, 2013. A detailed transcript of the verbal discussions can be found in the official transcript of the proceedings (ML14014A383).

E.9.1 Question 5.b.I and 5.b.II – DOSNRM, TIMNRM, DOSHOT, and TIMHOT

Hotspot and normal relocation of the public are additional protective measures that may be modeled in the MACCS code. These are implemented after the initial evacuation and after plume arrival. The EPA Manual of Protective Action Guides (PAGs) (EPA 400: Table 2-1) recommends evacuation of the public if the projected dose range is from 1 to 5 rem, calculated as the projected sum of the effective dose over the early phase. These EPA PAGs have traditionally been implemented in MACCS as hotspot and normal relocation with hotspot set at 5 rem and normal at 1 rem and typically apply to residents in areas beyond the emergency planning zone (EPZ). This is because the EPZ has been evacuated. However, the State or local authorities make the protective action decisions and can follow EPA PAGs or use different values.

There are many opportunities for uncertainty in the dose and time values used in the analysis. In addition to authorities potentially selecting different values, the dose can be influenced by meteorology, shielding, infiltration of contamination indoors, and other factors.

The initial projected dose would typically be based on a dose model that includes atmospheric modeling, while later in the event, field surveys would provide actual data. The source of the model data is the site meteorological tower, which is located at least 10 miles from the relocated population who reside beyond the EPZ. There is uncertainty in applying calculating the relocation dose using meteorological data from a source 10 miles away.

Dose to the public also depends on the shielding factors used in the analysis. MACCS allows a single value for sheltering which is intended to represent the typical shielding capacity of housing within the region. However, an average value may not be representative because housing types are not uniformly distributed. For instance, trailer parks and brick housing are not typically intermixed. The variation in housing stock and the distribution of types of housing are not standard introducing uncertainty when an average value is applied. Furthermore, the dose

projection is calculated assuming the residents stay indoors for the entire time and does not consider the potential for equilibration of contamination indoors and outdoors through infiltration into the homes. This is another introduction of uncertainty.

The selection of 0.5 rem for the normal relocation was based on input from the State; therefore, this value has high confidence. The 5 rem hotspot relocation is established from the EPA PAGs. There was an interest in understanding the sensitivity of hotspot and normal relocation. Thus, we only needed to establish a reasonable range to determine the contribution of these parameters to the risk. With the modes established, the team selected the upper and lower bounds shown in Table 4.2-14.

The relocation times also do not need to be precise to identify the contribution to risk. Relocation is typically implemented beyond the EPZ and after plume arrival. A release of sufficient size such that relocation is required, has broad impacts in the area, and response agencies would have competing priorities. For Peach Bottom, evacuation of the EPZ has been completed for almost 50,000 people. Congregate care centers (Shelters) have been established, traffic control is in place, people are being monitored, field teams are confirming on ground doses, and Federal resources have arrived to support the local agencies. The timing of the relocation is important at this point, but not urgent, because this is a 4 day integrated dose. A few hours delay in relocation would not be expected to increase risk to residents beyond 10 miles to a significant degree. Therefore, reasonable ranges were established based on when offsite resources would likely be available to implement relocation. The hotspot value of 12 hours (after plume arrival) considers that the Federal Radiological Monitoring and Assessment Center (FRMAC) would be in place (or nearly in place) at this time and DOE resources could help with definition of hotspot areas and relocation of individuals. The State and county resources would have completed evacuation activities within the EPZ and could support relocation efforts beyond the EPZ. Hotspot relocation is completed first. The normal relocation value of 24 hours was established to provide ample time to complete the hotspot relocation recognizing the normal relocation for dose of 0.5 rem is not urgent. The upper and lower bounds were set at 200% and 50% of the mode of the relocation times to identify any sensitivity in the timing.

A triangle distribution was selected because the team had a mode (the nominal, most likely value) and upper and lower bounds. A normal distribution could have been applied, but was not selected because we had a nominal, most likely value for the mode.

E.9.2 Question 5.b.III – ESPEED

Evacuation speeds are developed using a traffic simulation model that analyzes the travel of vehicles over a roadway segment under specified conditions. Generally speaking, a roadway segment has a maximum capacity that may be calculated using Highway Capacity Manual methods based on the roadway characteristics (i.e., number of lanes, width of lanes, free-flow speed, intersection control, etc.) As the number of evacuating vehicles exceed the capacity, congestion occurs.

There are three speeds assigned for each cohort including ESPEED early, ESPEED mid, and ESPEED late. ESPEED early reflects the initial speed of the cohort when they begin their evacuation. ESPEED late is the speed of the cohorts typically after they have exited the EPZ. ESPEED mid was the parameter evaluated in the uncertainty analysis because this represents the cohorts as they travel within the EPZ at times when congestion is present, specifically for the general public, which is the largest population group.

The evacuating speed on any given roadway within the Peach Bottom EPZ is primarily influenced by the roadway (and intersection) capacity and the number of vehicles. As shown in Figure E-51, there are multiple evacuation routes, each of which may have a different evacuation speed. The MACCS model allows a single speed value for ESPEED mid for each cohort.



Figure E-51: Peach Bottom Evacuation Routes

For the general public cohort (Cohort 1 in Table 4.2-16), the team developed the average evacuation speed for the entire EPZ of 3 mph, based on the traffic simulation model output and mobilization activities described in the ETE study. The team did not consider uncertainty in the traffic model. The team can establish an initial bound knowing the speed must be greater than 0.0 and less than the evacuation roadway speed limits which range from 20 to 55 mph (an average of about 35 mph). Therefore, the initial range is 0.0 to 35 mph with a mode of 3 mph. The team refined the bounds by using information from the ETE study, which describes congestion along the evacuation routes. For congestion to occur, the upper bound must be less than the average speed of 35 mph. The ETE study indicates that the evacuation speed in select areas is twice the average evacuation speed, or about 6 mph. For the upper bound the team rounded this value to 10 mph. To establish a lower bound, the team needed a value between 0.0 and 3 mph. It is not an option to select 0.0 mph, because this would effectively be a shelter in place. The team selected 1 mph to provide the greatest chance of observing an increase in risk. The speeds for the remaining cohorts were developed with similar rationale, and also considered when the cohort enters the roadway network.

A triangular distribution was applied because the team has confidence in the mode and the team was able to define upper and lower bounds with some confidence. A normal distribution was considered but discounted because it is less likely speeds would be slower than the mode and more likely they would be greater than the mode. A discrete distribution is possible for evacuation speeds and could have been applied had the raw output from the traffic simulation model been available. However, even if the data were available, a distribution would have been developed for each evacuation route and then would have been averaged because MACCS only allows one ESPEED and value for each cohort.

E.9.3 Question 5.b.IV – GSHFAC

In MACCS, shielding and protection factors are specified for each dose pathway and directly affect the dose received by individuals at each location. The shielding factors are used as multipliers on the dose that a person would receive if there were no shielding or protection. Thus, a shielding factor of one represents the limiting case of a person receiving the full dose (i.e., standing outdoors and completely unprotected from exposure); a shielding factor of zero represents the limiting case of complete shielding from the exposure. The shielding factors used in the MACCS calculation are clearly important because the doses received are directly proportional to these factors. As shown in Figure 4.2-3, the range of uncertainty of the shielding factors would be expected to have a significant impact on the overall outcome of a consequence analysis.

While shielding factors for three dose pathways, groundshine, cloudshine, and inhalation, were treated as uncertain in the uncertainty analysis, groundshine is usually the most important of these pathways because of the dominant contribution of gamma radiation from the decay of Cs-137 (actually from its daughter, Ba-137m) during the long-term phase. Thus, it is important to treat the uncertainty of GSHFAC in the MACCS model in this uncertainty analysis. GSHFAC for the emergency phase was taken to be rank correlated with a similar parameter used in the long-term phase. This assumption makes sense because we also assume that the same building structures continue to be used (unless they are condemned) following the emergency phase.

Three types of activity, normal, sheltering, and evacuation, are evaluated for each dose pathway, resulting in nine sets of shielding factors. Normal activity refers to a combination of activities that are averaged over a week and over the population, including being indoors at home, commuting, being indoors at work, and being outdoors at home or at work.

Values for GSHFAC are provided in Table 4.2-3b. Groundshine shielding factors are taken from a joint NRC/CEC study and were compiled by Bixler in NUREG/CR-7161. The values in Table 4.2-3b are taken directly from this NUREG/CR report, which faithfully represents the expert elicitation data.

Values for GSHFAC are used in the uncertainty analysis with the further assumption that the distributions for normal activity and sheltering are correlated with a rank correlation coefficient (RCC) of 0.75. This correlation is applied for normal and sheltering activities for each of the dose pathways, including groundshine. There is no correlation between the three pathways. Each parameter (CSFACT, GSHFAC, PROTIN) can be specified for each of the six cohorts in WinMACCS. In the SOARCA analysis, the values listed in Table 1 were used. GSHFAC values for Cohorts 1, 2, 3, 5, and 6 were chosen to be identical. Cohort 4 is special facilities, which was assigned different shielding values in the SOARCA study. For this study, a single distribution was sampled and applied to all of the cohorts for simplicity.

Uncertainty in groundshine doses has two components: uncertainty in the amount of shielding between an individual and the source of the groundshine (GSHFAC) and uncertainty in the energy deposited within a human organ for specified incident radiation. Distributions representing the uncertainty in the groundshine shielding factors (GSHFAC) are presented in Table 4.2-3b. Additional uncertainties of the deposition of radiation in individual organs stem from age, height, and weight variations of the population exposed to the radiation. Eckerman [E.3] recommended that a triangular distribution be used to represent uncertainty in dose coefficients. The parameters for that distribution are presented in Table 4.2-5.

To simplify the implementation of uncertainty in the energy deposited within a human organ for a specified incident radiation, Eckerman [E.3] recommended that a single uncertainty distribution be applied as a multiplicative factor for all radionuclides and for all organs. Furthermore, Eckerman suggested that the uncertainty in groundshine dose coefficients are highly correlated over the set of human all organs. As a result, it is possible to combine the uncertainty in the groundshine shielding factor and the uncertainty in the dose coefficients into a single uncertainty factor, which can be implemented as an overall uncertainty in the groundshine shielding factor (GSHFAC). Further, Eckerman recommended that the uncertainties in the groundshine shielding factor and in the groundshine dose coefficients should be treated as uncorrelated.

The distribution for groundshine shielding factor is presented in Table 4.2-3b. The parameters for the triangular distribution used to represent uncertainty in the dose coefficients for groundshine radiation are presented in Table 4.2.5. Piecewise uniform distributions for the overall uncertainty in GSHFAC are provided in Table 4.2-6 and plotted in Figure 4.2-5. These distributions are the ones used in the uncertainty analysis. The resulting rank correlation for the combined groundshine shielding factors were implemented using 0.76 for normal and sheltering, 0.2 for normal and evacuation, and 0.15 for sheltering and evacuation.

E.10 Other Issues

To address ACRS Question 6, NRC and Sandia staff conducted a thorough search through previous studies and lessons learned. The information provided in this section was complimentary to the discussions NRC and Sandia staff provided to the ACRS subcommittee on September 16, 2013. A detailed transcript of the verbal discussions can be found in the official transcript of the proceedings (ML14014A383).

E.10.1 Question 6.a – Surrogate Parameters

1. **Zr breakout temperature:** From the Sandia hydrogen uncertainty study conducted in 2002, “The MELCOR parameter that controls the retention of molten zircaloy within the outer ZrO₂ shell is probably the most important factor affecting the total amount of hydrogen produced in the early stage of core degradation. The default value is 2400K, considered to be a most likely value based upon assessment of many experimental studies, including the Phebus FPT-1 test. Highly reducing (H₂) conditions could encourage melt breakout at a lower temperature, as could protracted time encountered in the 2200K-2400K temperature range, owing to effects of oxygen profiles in the cladding oxide phase layers and on kinetics respectively. It is not considered likely that breakout could be delayed to temperatures higher than ~2500K owing to the strong tendency for Zr metal to dissolve its oxide and due to the fact that complete rod collapse by slumping and/or liquefaction seems to begin at about this temperature as evidenced from Phebus tests. A reasonable range for parameter variation is considered to be 2250K to 2550K, with a most probable value of 2400K. The Siemens report is consistent with this determination.”
2. **In-vessel radial relocation time constants for molten and particulate debris:** Certain parameters were correlated in the uncertainty analysis sampling. RDMTC and RDSTC, the time constants for radial relocation of molten and solid debris within the RPV, respectively, were correlated to prohibit combinations where solid debris relocated faster than liquid debris. Similarly, DHEADLIQ and DHEADSOL, the debris height required for lateral movement of core-concrete debris at the liquidus and solidus temperatures (of concrete),

respectively, were correlated so that cooler debris never moved more readily than hotter debris.

E.10.2 Question 6.b – Lower Head Penetration Failures

The lower head penetration model in MELCOR is largely parametric but does employ important mechanistic heat transfer considerations. The model considers the limited contact area available for conduction between, for example, a guide tube and the lower head, i.e., the area of the circumferential weld securing and sealing the tube to the head. It also considers the surface area of the tube available for contact with core debris relocated to the lower plenum as well as the user-definable heat transfer coefficient between the tube and the debris. The mass of the tube is accounted for in calculating its heating. The temperature associated with failure of the tube/penetration is defined by the user.

The input specified to the penetration model in the standalone calculations of Section 6.4.2 was descriptive of instrument guide tubes and their associated penetrations. Given that a drain line is of somewhat different construct than an instrument guide tube, the calculations probably do not best address the specific interest the ACRS has expressed in the susceptibility and ramifications of the drain line overheating to failure. However, the construct and size of a guide tube penetration (1.5-in inner-diameter) and the 2-in drain line are not so different and the sampling of the number of penetrations enabled to fail resulted in a number of cases with initial leakage areas similar to the area of the 2-in drain line (i.e., leakage areas that were small). Little enough material passed through the small breaches in these cases that the calculations progressed to gross failure of the lower head. Key to the progression in these calculations to gross lower head failure may be that little ablation of the failed penetrations occurred likely due to the low-pressure situation of the RPV. Higher pressures would drive more material through the breach aggravating the ablation. SNL argues then that the stand-alone calculations undertaken to investigate the susceptibility of lower head penetrations to failure and the ramifications of their failure address the drain line fairly well.

E.10.3 Question 6.c – Drywell Liner Failure

Neither the drywell liner melt-through nor the core-concrete spreading models are mechanistic enough to claim that the phenomena they represent are accurately simulated. Both models are largely parametric and uncertainty exists in the key parameters. However, the dependencies within the models are understandable and the uncertain parameters serve as a means to investigate the importance of the phenomena relative to the metrics of the uncertainty analysis (e.g., relative to iodine and cesium releases to the environment).

The presence of water in contact with the core-concrete debris is inherently considered in both models in that water would serve to cool the debris. Cool enough debris is prohibited from failing the drywell liner and the movement of core-concrete debris is slowed or stopped dependent upon how cool the debris becomes. However, the LTSBO scenario does not result in amounts of water making it to the drywell floor that quench or even significantly cool the debris. Consequently, the potential benefits of water interacting with the debris are not realized.

E.10.4 Question 6.d – Operator Actions

1. Operators manually open SRV:

- When plant conditions stabilized in a LTSBO, Special Event Procedure SE-11 would call for a controlled depressurization of the RPV to 125 psig using the instructions in the RC/P Leg of Trip Procedure T-101. Depressurization would be accomplished by opening one or more SRVs or, if necessary, by manually opening other steam vent pathways, such as main steam line drains. The cooldown rate would be limited to less than 100°F per hour. In the SOARCA calculation, conditions were judged to be stable 1.0 hours into the blackout, and a controlled depressurization was initiated by opening a single SRV. Variations about the 1-hr timing in the SOARCA calculation were investigated in the uncertainty analysis that were simply considered to be reasonable.

2. Operators shed DC loads:

- The load shedding is expected to extend battery life from 2 hours (with no load shedding) to 4 hours (with load shedding). This information was obtained through SOARCA-initiated communication with Peach Bottom system engineers. The action to shed loads is directed by applicable Special Event Procedure SE-11.
- As noted in Section 4.1.1, an upper limit of 8 hours was chosen based on input from the licensee. In 2008 to most recently in 2011, NRC staff had informal discussions with knowledgeable Peach Bottom personnel on what the range of battery duration may truly be. In some plant calculations, battery durations were shown to possibly last up to 12 hours. However, plant personnel felt strongly that our public uncertainty analysis should not credit anything higher than 8 hours in the unmitigated LTSBO scenario. Staff explained the interpretation of higher percentiles (e.g., asked, as an example, whether they felt that there was truly less than one-in-a-hundred chance that the battery could last more than 8 hours). Even faced with this formulation, plant personnel were unwilling to place an upper bound at anything higher than 8 hours.

The unmitigated case credits automatic system responses and manual actions that would be directed by plant EOPs, such as operator reactor vessel depressurization and intervention to control RCIC injection flow (after its automatic actuation) to stabilize and maintain the level within a target range. The unmitigated case did not credit operator actions that are beyond the scope of EOPs – primarily, the mitigation measures installed in response to 10CFR50.54(hh).

The following is the timeline of events and operator actions that were credited in the LTSBO unmitigated case with SE-11 procedures only:

Event Initiation and Initial Plant Response

- Control room receives indication that plant is in a station blackout condition requiring the operator to enter Special Event Procedure SE-11, “Station Blackout Procedure.” RCIC automatically starts when level drops to low-level setpoint with suction aligned to the CST.

10-15 minutes

- In accordance with SE-11, plant operations personnel initiate the following mitigation measures:
 - Attempt to line up the Conowingo hydroelectric dam (i.e., station blackout line) as an alternative offsite power source, but the line is not available.
 - Attempt manual start of emergency diesel generators, but none is available.
 - Begin to shed non-essential loads from the emergency DC bus.

1 hour

- Actions to shed non-essential loads from DC bus is complete, battery life extended to an estimated 4 hours.

2 hours

- Operator assumes remote manual control of RCIC flow.

4 hours

- DC power from station batteries is exhausted. The consequences of a loss of DC power are:
 - Open SRV closes.
 - Remote control of RCIC flow terminates. The system is assumed to continue operate at the conditions it experienced immediately prior to battery exhaustion. This effectively assumes the RCIC pump continues to operate at a constant rate, ultimately flooding the main steam line causing delayed termination of RCIC.

E.11 References

- E.1 Nuclear Regulatory Commission, Official Transcript of Proceedings, Advisory Committee of Reactor Safeguards Regulatory Policies and Practices, September 16, 2013, Rockville, MD.
- E.2 Helton, J.C., F.J. Davis, and J.D. Johnson, "A comparison of uncertainty and sensitivity analysis results obtained with random and Latin hypercube sampling," Rel. Eng. & Sys. Safety 89(3), pages 305-330 (2005).
- E.3 Eckerman, K., "Radiation Dose and Health Risk Estimation: Technical Basis for the State-of-the-Art Reactor Consequence Analysis (SOARCA) Project," Oak Ridge National Laboratory, Oak Ridge, TN, 2011.

APPENDIX F
GLOSSARY OF UNCERTAINTY ANALYSIS TERMS

This appendix is glossary defines terms as they are used in this study, and the same terms may be used differently in other studies. Note also that Appendix A in this report provides a description of probabilistic analysis methodology, including regression techniques, used in this study.

Additive Model – A regression technique where an estimation of the regression line is formed by a summation of a collection of one-dimensional arbitrary basis functions. An additive model considers the influence of the variables themselves and does not consider any possible interaction.

Aleatory – Inherent randomness in the properties or behavior of the system under study. Aleatory uncertainty cannot be reduced based on increased knowledge of the system under study.

Basis Function – Elementary elements used in the decomposition of a function in a specific space. Every continuous function can be constructed as a linear combination of basis functions. For example, a quadratic polynomial has basis functions of $\{1, x, x^2\}$. Every quadratic polynomial has the form:

$$y = a * 1 + b * x + c * x^2$$

where 1, x , and x^2 are the basis functions and a , b , and c are coefficients of the basis functions that define the unique polynomial.

Beta Distribution – A family of continuous probability distributions defined on the interval [0,1] parameterized by two positive shape parameters (α and β) that control the shape of the distribution. Its probability density function is expressed as follow:

$$f(t) = \frac{\Gamma(\alpha + \beta)}{\Gamma(\alpha)\Gamma(\beta)} t^{\alpha-1} (1 - t)^{\beta-1}$$

where Γ represents the gamma function:

$$\Gamma(w) = \int_0^{\infty} x^{w-1} e^{-x} dx$$

Beta distributions can serve as a model for the probability that a system or component is in operation for at least t units of time. Sometimes, two parameters (min and max) are added to the beta function parameters. These parameters scale the domain of definition from [0,1] to [min,max]. See illustrations below.

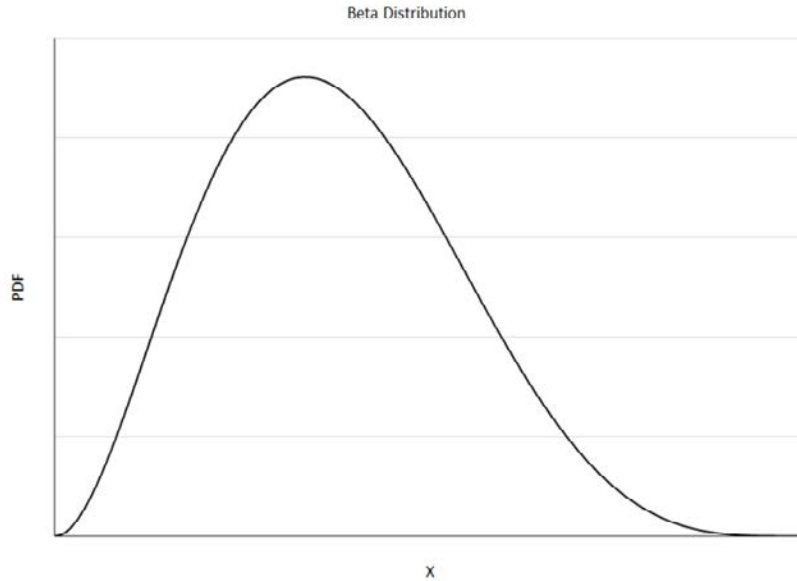


Figure F-1: Example of Beta Probability Distribution Function

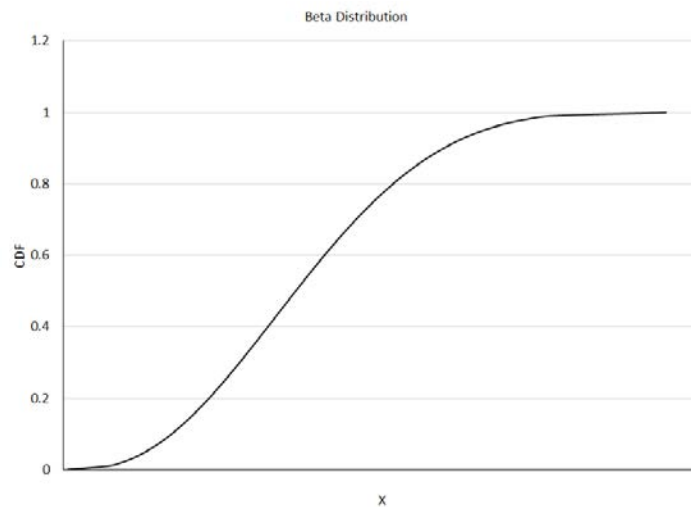


Figure F-2: Example of Beta Cumulative Distribution Function

Cliff-edge Effects – An instance in which a small change in an input can lead to a large change in the response of the system.

Coefficient of Determination – This coefficient (noted as R^2) estimates the proportion of the variance of the output that is explained by the regression model under consideration. Thus, this coefficient provides an indication of how well a regression model replicates the observed outcomes.

Complementary Cumulative Distribution Function (CCDF) – This function represents the probability for a value sampled from a probability distribution to be greater than a given quantile value. Given a real-valued random variable X and a threshold value x for a metric of interest, the complementary cumulative distribution function $\bar{F}(x)$ is defined as:

$$\bar{F}(x) = P(X > x) = 1 - F(x)$$

where $F(x)$ is the cumulative distribution function (CDF) defined by $F(x) = P(X \leq x)$.

Conjoint Influence – The influence of two or more input parameters acting together. This influence may have synergistic effects that would not be uncovered by studying the influence of each parameter individually.

Correlation – A possible dependence between two random variables. Positive correlation between two variables implies that a high value (or low value) for one variable is more likely to be associated with a respectively high value (low value) for the other. Negative correlation will reverse this relation, meaning that low values of one variable will be associated with high values of the other. Correlation does not imply causation. Correlation determines the existence of a trend but does not assess the magnitude of the change in output with respect to the change in input.

Cumulative Distribution Function (CDF)¹ - This function represents the probability for a value sampled from a probability distribution to be equal to or less than a given quantile value. For continuous variables, this function is the integral of the probability density function and is given by:

$$F(x) = \int_{-\infty}^x f(x)dx$$

where $F(x)$ is the cumulative distribution function and $F(x) = P(X \leq x)$.

Deterministic – Describing a system in which no randomness is involved in the calculation of a given response. A set of constant inputs definitively predict the output.

Discrete Distribution – A probability distribution where the random variable can have a set of distinct, finite values.

Epistemic – Uncertainty related to the lack of knowledge or confidence about the system under analysis. This type of uncertainty is produced by a lack of knowledge regarding the inputs or models under consideration. Epistemic uncertainty is usually considered as reducible uncertainty because increased knowledge should reduce it. Also called “state-of-knowledge” uncertainty.

Kaplan/Garrick ordered triplet representation for risk – This representation of risk poses three questions:

- 1) What can go wrong?
- 2) How likely is it to go wrong?
- 3) What are the consequences if the event occurs?

¹ Not to be confused with core damage frequency (CDF) from a level 1 probabilistic risk assessment.

This representation is used to assess inherent randomness in the system (i.e., aleatory uncertainty). Potential lack of knowledge (i.e., epistemic uncertainty) adds a fourth question to the original triplet which is:

4) How much confidence do we have in the answers to the first three questions?

The exploration of these questions is the basis for Probabilistic Risk Assessment (PRA) (see 'Probabilistic Risk Assessment' below.) The Kaplan/Garrick ordered triplet representation is typically the NRC's definition of the term "risk."

Latin Hypercube Sampling (LHS) – A sampling technique in which each input variable is sampled in a stratified way in order to guarantee that all portions of the range of the variable's distribution are represented. LHS samples a probability density function (PDF) by first dividing the PDF of each variable into N bins of equal probability where N is the sample size per variable chosen ahead of time. One value is then sampled from the random variable's PDF in each of the N bins. Thus, if there are n random input variables, the input space is partitioned into $n \times N$ hypercubes from which N will be selected such that each variable will have exactly one value sampled in each of its defined strata (PDF interval). See illustrations below for one (x) and two (x, y) variables, where the red marks on the 2nd illustration represent one possible Latin Hypercube Sample of size $N = 6$.

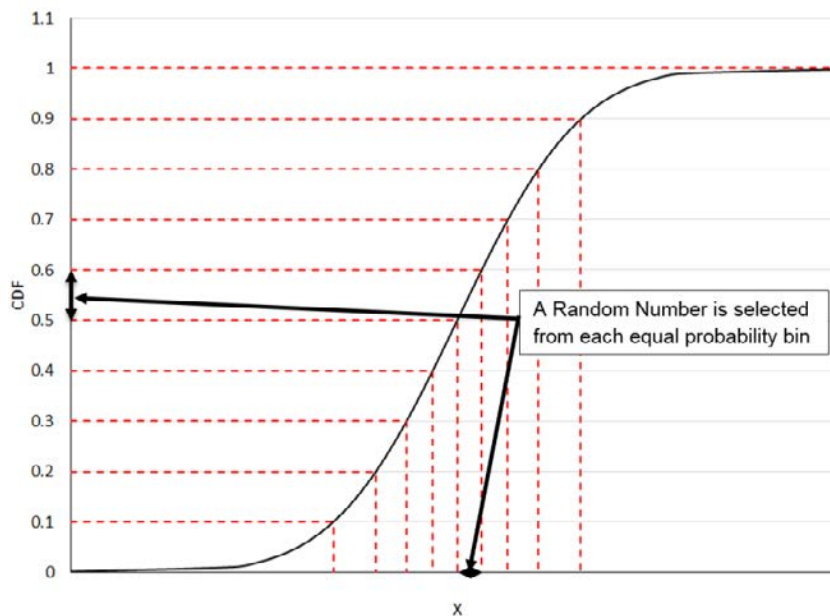


Figure F-3: Example of One-variable LHS Sample Technique

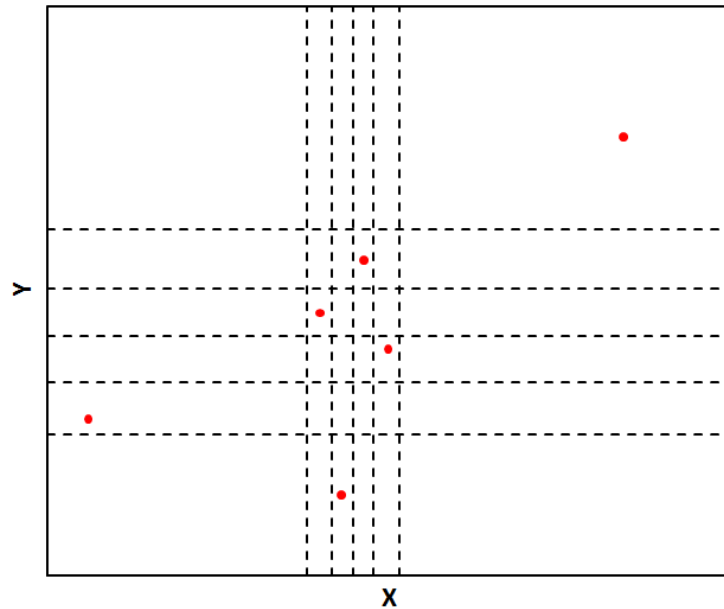


Figure F-4: Example of Two-variable LHS Sample Technique

Least Squares – An optimization technique that select the parameters of a model such that the difference between the estimation and empirical values (derived from observations or another model) is minimized according to the L^2 -norm (i.e., the square root of the sum of square differences is minimized).

Lognormal Distribution – A normal distribution over the logarithm of the random variable.

Log Triangular Distribution – A triangular distribution over the logarithm of the random variable. See illustrations under '**Triangular Distribution**' below, where the only difference is that " $\log(x)$ " replaces " x " on the x axis.

Log Uniform Distribution – A uniform distribution over the logarithm of the random variable. See illustrations under '**Uniform Distribution**' below, where the only difference is that " $\log(x)$ " replaces " x " on the x axis.

Mean – Estimates the expected value of a distribution of values. The mean value of a random variable is the arithmetic average of possible values as described by its probability density function. See illustration below for '**mean**,' '**median**,' and '**mode**,' all of which are measures of central tendency, though they are all different.

Median – The median of a probability distribution corresponds to the middle value that separates a sample or a distribution into halves of equal likelihood. A random variable is equally likely to take on a value greater than the median or less than the median. In other words, the $CDF(\text{Median value}) = CCDF(\text{Median value}) = 0.5$. See illustration below for '**mean**,' '**median**,' and '**mode**,' all of which are measures of central tendency, though they are all different.

Mode – The most likely value for an uncertain variable. For a discrete distribution, the mode represents the most common (most likely) value in a set of n values. For a continuous distribution, the mode represents the value at which the probability density function reaches its

maximum. See illustration below for ‘**mean**,’ ‘**median**,’ and ‘**mode**,’ all of which are measures of central tendency, though they are all different.

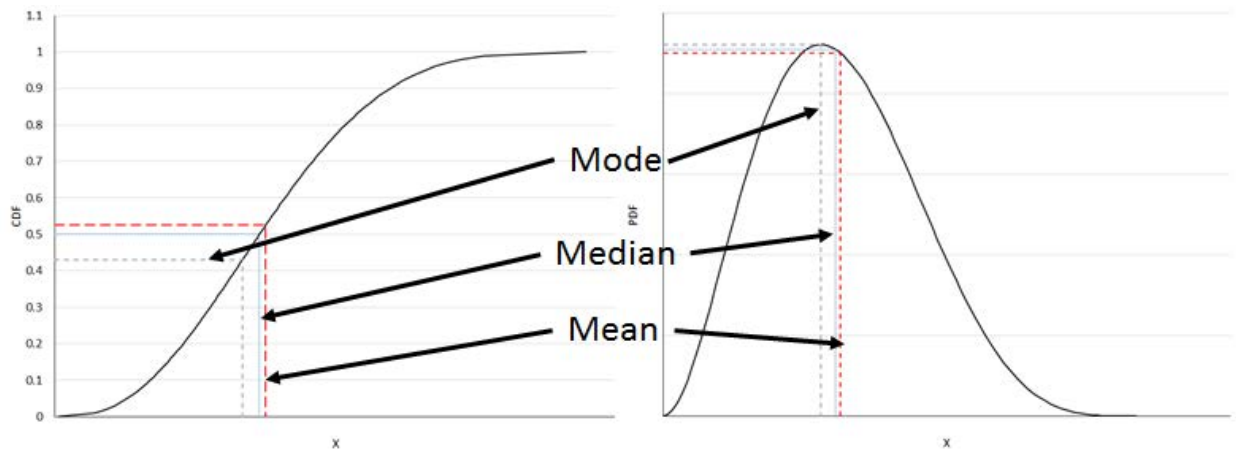


Figure F-5; Example of Mode/Median/Mean Differences

Monotonic – A monotonic function is a function which is either solely non-increasing or solely non-decreasing. A monotonic function cannot increase with increasing values of a dependent variable in one range and then decrease with increasing values of a dependent variable in a different range.

Monte Carlo simulation – A numerical technique that covers the uncertain input space (multidimensional space where each dimension represents a different random variable with its associated distribution) by sampling each probability distribution using random, or pseudo-random, numbers. This method is preferred over a direct discretization when the number of inputs is large because a regular discretization in each direction would lead to an impractically large number of simulations. The system model is then run repeatedly using a single set of values for the input variable vector at each repetition. With this process, Monte Carlo simulation produces a distribution of system model outputs (results) based on the input variable uncertainty as described by the input space.

(Multiplicative) Interaction Term – In regression models, interaction (or higher order) terms are basis functions that do not solely depend on one parameter. They can involve interactions amongst just two parameters up to interactions that involve all parameters under study. They can be as simple as a multiplication of two parameters or fairly complex (division, power, log, etc.). These terms are ignored by additive regression models.

Normal distribution – The normal distribution is one of the most common probability distributions. As demonstrated by the central limit theorem, the normal distribution can be used to represent the distribution of the sum of random variables (if they follow the same distribution) or the distribution of the mean value. The normal distribution’s probability density function is defined from $-\infty$ to $+\infty$ and has a bell shape:

$$f(x|\mu, \sigma) = \frac{1}{\sigma\sqrt{2\pi}} e^{-\frac{(x-\mu)^2}{2\sigma^2}}$$

Where μ and σ represent respectively the mean and standard distribution and are the traditional parameters used to define a normal distribution.

Percentile – Specific form of quantile for which the value is reported as a percentage (e.g. the 0.01 quantile is the same as the 1st percentile). See ‘**quantile**’ for additional description.

Piecewise Uniform Distribution – A distribution formed by distinct uniform distributions over intervals of the range of the probability density function. See illustration below.

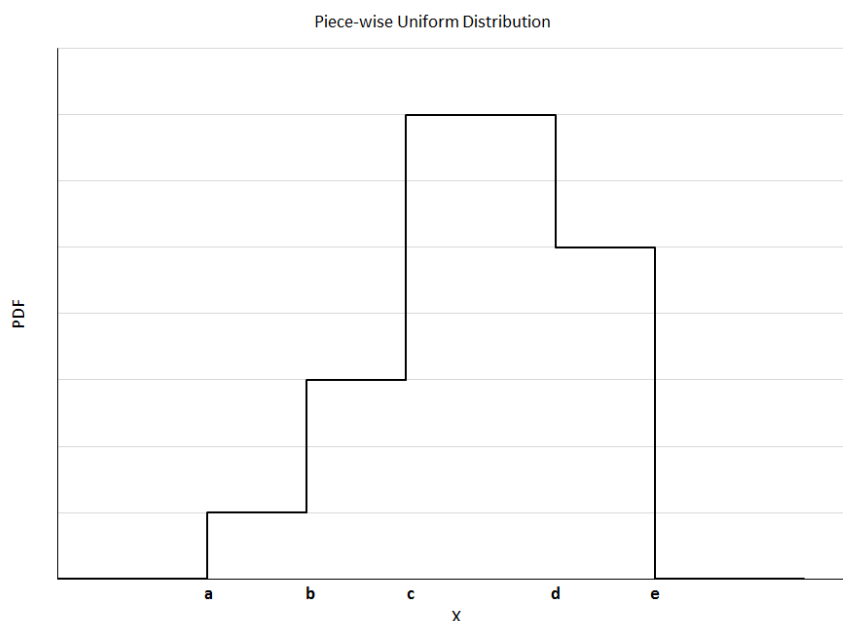


Figure F-6: Example of Piecewise Uniform Probability Mass Function

Probabilistic Risk Assessment (PRA) – A systematic method for assessing three questions that the NRC uses to define "risk." These questions consider (1) what can go wrong, (2) how likely it is, and (3) what its consequences might be. (see **Kaplan/Garrick ordered triplet representation for risk**) These questions allow the NRC to understand likely outcomes, sensitivities, areas of importance, system interactions, and areas of uncertainty, which the staff can use to identify risk-significant scenarios. The NRC uses PRA to determine a numeric estimate of risk to provide insights into the strengths and weaknesses of the design and operation of a nuclear power plant.

Probability Density Function (PDF) – A function that describes the likelihood that a continuous random variable takes on a value in an interval. A PDF has the properties that 1) a value on the function is greater than or equal to 0 and 2) the total integral probability is 1.

$$\begin{aligned} f(t) &\geq 0 \\ \int_{-\infty}^{\infty} f(t) dt &= 1 \end{aligned}$$

Probability Distribution – A mathematical representation of the uncertainty of a random variable in a probabilistic framework. Specification of a probability distribution can be done via probability density (or mass for discrete variable) function or a cumulative distribution function for instance.

Probability Mass Function (PMF) – A function that is equivalent to the probability density function for discrete variables (and for which integral is replaced with a regular sum).

Quantile – A quantile x_q is the value of a random variable such that there is a probability q that a sampled value will be equal or lower to x_q . Specific quantiles include the median (for which $q = 0.5$), quartiles (where $q = 0.25$ and 0.75 and represents the 1st and 3rd quartiles, respectively) and percentiles (in which q is expressed as a percent from 0 to 100 instead of a probability between 0 and 1).

Random Seed – An integer value (or vector) used to initialize the random number sequence of a pseudo random number generator. Random seeds are used so that the same sequences can be reproduced when the same random number generator is used. The use of different random seeds, even those close to each other, should lead to completely different and uncorrelated random number sequences.

Rank Correlation Coefficient – Also known as Spearman Correlation Coefficient, the rank correlation coefficient measures the degree of linearity in the relationship between two random variables after they have been rank-transformed (see ‘rank transformation’).

Rank Regression – Rank regression is a linear regression applied to rank values. The linear regression builds a linear function model between outputs and inputs using a least squares approach. Often, linear and rank regressions use a stepwise approach such that new parameters are added to the model only if they increase the strength of the regression model significantly enough such that the complexity of adding a parameter is overcome by the increase in variance explained. Rank Regression is solely used to estimate the influence of uncertainty in the input parameters on the output uncertainty and is not used for prediction.

Rank Transformation – Rank transformation consists of replacing the actual value of a random variable by its rank in the total sample. Regression methods become non-parametric when working with rank values instead of with raw data. This allows for monotonic relations to be captured instead of simple linear relations and reduces the effect of outliers.

Realization – An individual calculation using one sample of values for the input variable vector in Monte Carlo simulation. In other words, a Monte Carlo simulation where the system model is run N times has N realizations. Within a realization, the model is usually run deterministically and returns a unique set of output values

Regression – A measure of the relation between one variable (e.g., output or results of a model) and corresponding values of other variables (e.g., inputs to a model). Regression methods attempt to find a mathematical relationship between input variables and the output variable(s) of interest.

Replicates – A set of Monte Carlo simulations on the same system model, usually of the same sample size, that use different random numbers generated using a different random seed. For Monte Carlo simulations using simple random sampling, the results of replicates can be combined to form one larger data set for better statistics because all random samples are independent.

Sensitivity Study – A set of studies that exercise a complex system under different conditions in order to 1) validate some assumptions, 2) explore alternative conceptual models or address differences in opinion, or 3) study one particular aspect of the complex system in greater detail. These studies are different from Monte Carlo simulations in that they require changing some options that have been considered to be constants in the study of reference and may study only

one variable or conceptual model in isolation. Such studies can be completed through either deterministic or probabilistic means.

Sensitivity Analysis – An analysis that determines how sensitive an output is to a given input or set of inputs. Sensitivity analysis can be conducted using a deterministic set of model calculations (through a sensitivity study), or can be conducted probabilistically using Monte Carlo simulation and regression results that quantify how much the uncertainty in each analysis input contributes to the variance in the output under consideration. In this document, “sensitivity analysis” refers to the latter usage.

Simple Random Sampling (SRS) – A random sampling technique where for each time sampled, the probability that a particular value of a variable is chosen is proportional to the probability density function of the variable at that particular value. No further requirements are imposed on the sampling (unlike Latin Hypercube Sampling).

Stochastic – A random occurrence. A stochastic simulation refers to a simulation in which randomness in uncertain input variables is used to calculate a system response.

Stochastic Failure – A failure that is caused by random processes.

Sum of Square Error (SSE) – The total sum of the squares of the differences between estimated and empirical values (i.e., observations, measurements, or an empirical model).

$$SSE = \sum_i (y_i - f(x_i))^2$$

A small SSE indicates a good fit between the predicted and observed values.

t-distribution – A probability distribution that can be used when determining the mean when the sample size is small and the data is normally distributed with an unknown standard deviation. The t-distribution describes samples drawn from a full data set. It can be used to assess the statistical difference between two means, confidence intervals in linear regressions.

Triangular distribution – A continuous distribution that takes the form of a triangle. The probability density for the range $[a,b]$ reaches its mode at the location c and form a triangular shape:

$$f(x) = \begin{cases} 0 & \text{for } x < a \\ \frac{2(x-a)}{(b-a)(c-a)} & \text{for } a \leq x < c \\ \frac{2}{b-a} & \text{for } x = c \\ \frac{2(b-x)}{(b-a)(b-c)} & \text{for } c < x \leq b \\ 0 & \text{for } x > b \end{cases}$$

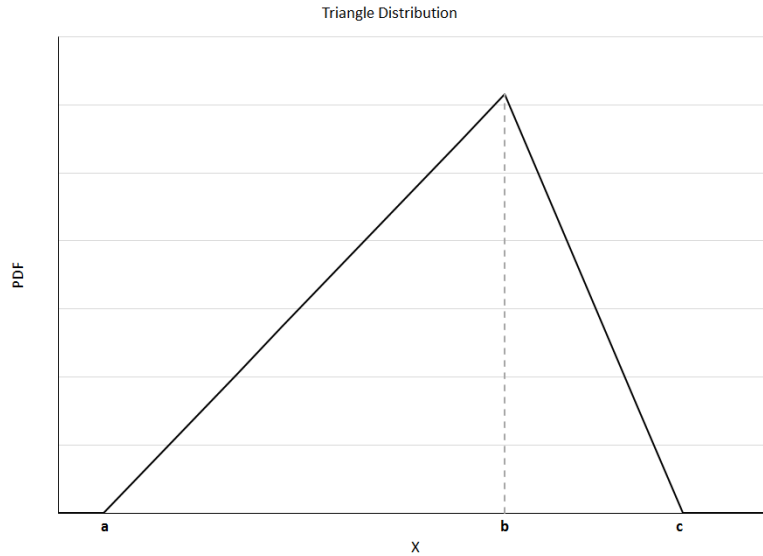


Figure F-7: Example of Triangle Probability Distribution Function

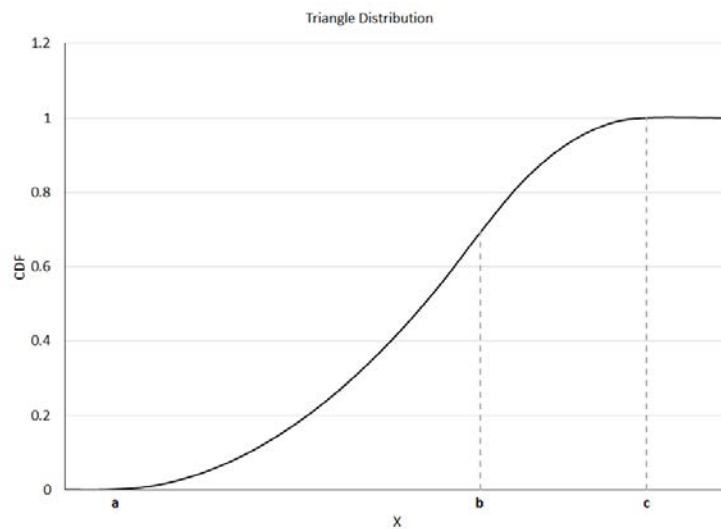


Figure F-8: Example of Triangle Cumulative Distribution Function

Uncorrelated – A situation in which no linear dependence between sampled values for two variables is observed.

Uniform Distribution – A distribution used when any value for a random variable defined on a range $[a,b]$ is equally likely. The uniform probability density function forms a rectangle and is given by:

$$f(x) = \begin{cases} \frac{1}{b-a} & \text{for } x \in [a, b] \\ 0 & \text{otherwise} \end{cases}$$

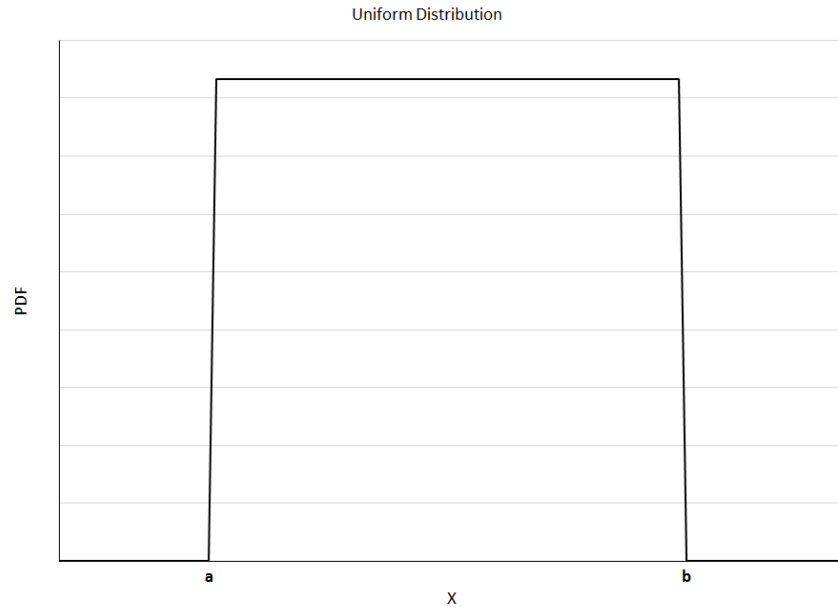


Figure F-9: Example of Uniform Probability Distribution Function

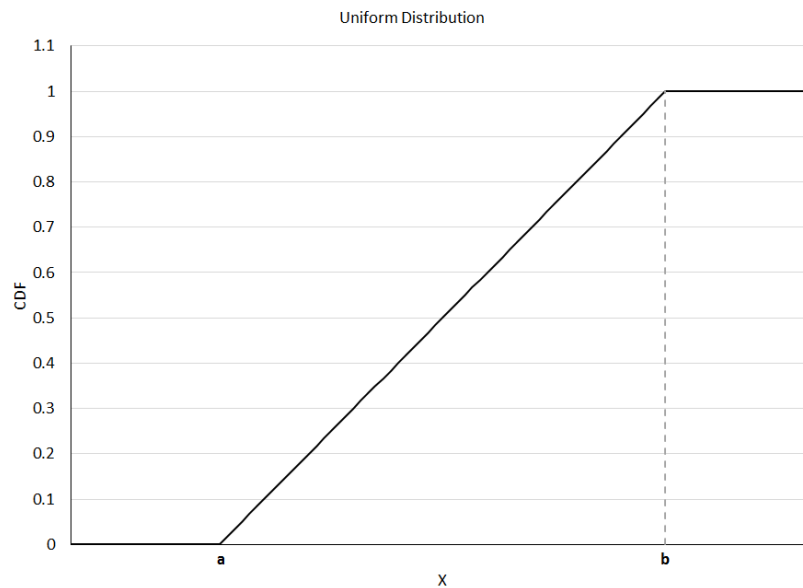


Figure F-10: Example of Uniform Cumulative Distribution Function

Variance – A measure of the dispersion of data about a mean, given by:

$$V = \sigma^2 = \frac{\sum_{i=1}^N (Y_i - \mu)^2}{N}$$

where Y_i is a particular data point, μ is the mean, and N is the number of data points. The variance characterizes the average spread squared of the data set.

NRC FORM 335 (12-2010) NRCMD 3.7		U.S. NUCLEAR REGULATORY COMMISSION		1. REPORT NUMBER (Assigned by NRC, Add Vol., Supp., Rev., and Addendum Numbers, if any.) NUREG/CR-7155					
BIBLIOGRAPHIC DATA SHEET (See instructions on the reverse)				2. TITLE AND SUBTITLE State-of-the-Art Reactor Consequence Analyses Project: Uncertainty Analysis of the Unmitigated Long-Term Station Blackout of the Peach Bottom Atomic Power Station					
				3. DATE REPORT PUBLISHED <table border="1"> <tr> <td>MONTH</td> <td>YEAR</td> </tr> <tr> <td>May</td> <td>2016</td> </tr> </table>		MONTH	YEAR	May	2016
				MONTH	YEAR				
May	2016								
4. FIN OR GRANT NUMBER									
5. AUTHOR(S) P. Mattie, R. Gauntt, K. Ross, N. Bixler, D. Osborn, C. Sallaberry, J. Jones (SNL); and T. Ghosh (NRC)				6. TYPE OF REPORT Technical					
				7. PERIOD COVERED (Inclusive Dates)					
8. PERFORMING ORGANIZATION - NAME AND ADDRESS (If NRC, provide Division, Office or Region, U. S. Nuclear Regulatory Commission, and mailing address; if contractor, provide name and mailing address.) Sandia National Laboratories Severe Accident Analysis Dept. 6232 Albuquerque, NM 87185-0748									
9. SPONSORING ORGANIZATION - NAME AND ADDRESS (If NRC, type "Same as above", if contractor, provide NRC Division, Office or Region, U. S. Nuclear Regulatory Commission, and mailing address.) Division of Systems Analysis Office of Nuclear Regulatory Research U.S. Nuclear Regulatory Commission Washington, DC 20555-0001									
10. SUPPLEMENTARY NOTES									
11. ABSTRACT (200 words or less) This document describes the U.S. Nuclear Regulatory Commission's (NRC's) uncertainty analysis of the accident progression, radiological releases, and offsite consequences for the State-of-the-Art Reactor Consequence Analyses (SOARCA) unmitigated long-term station blackout (LTSBO) severe accident scenario at the Peach Bottom Atomic Power Station. The SOARCA project is a program that estimates the outcomes of postulated severe accident scenarios which could result in release of radioactive material from a nuclear power plant (NPP) into the environment. SOARCA couples the deterministic "best estimate" modeling of accident progression (i.e., reactor and containment thermal-hydraulic and fission product response), embodied in the MELCOR code with modeling of offsite consequences in the MELCOR Accident Consequence Code System (MACCS). This uncertainty analysis presents the results of an analysis of epistemic uncertainty associated with the accident progression and offsite consequence modeling.									
12. KEY WORDS/DESCRIPTORS (List words or phrases that will assist researchers in locating the report.) Uncertainty Analysis, State-of-the-Art Reactor Consequence Analyses (SOARCA)				13. AVAILABILITY STATEMENT unlimited					
				14. SECURITY CLASSIFICATION (This Page) unclassified					
				(This Report) unclassified					
				15. NUMBER OF PAGES					
				16. PRICE					



Federal Recycling Program



**UNITED STATES
NUCLEAR REGULATORY COMMISSION**
WASHINGTON, DC 20555-0001

OFFICIAL BUSINESS



NUREG/CR-7155

**State-of-the-Art Reactor Consequence Analyses Project: Uncertainty analysis of the
Unmitigated Long-term Station Blackout of the Peach Bottom Atomic Power Station**

May 2016